PROCEEDINGS
OF THE
WEDNESDAY SLIDE
CONFERENCE 2025-2026

JOINT PATHOLOGY CENTER
VETERINARY PATHOLOGY SERVICE
SILVER SPRING, MD 20910

On behalf of the Joint Pathology Center, I would like to extend sincere gratitude to the contributors who submitted cases to the 2025-2026 Wednesday Slide Conference. We received many outstanding submissions this year from all over the world. At a time when our nation's international relationships feel tenuous, the opportunity to engage with each of you served as a poignant reminder of how essential our connections are and how much stronger we are when we foster collaboration at every level. Ours is a truly global profession and our community is at its best when we work together.

This conference year would not have been possible without the expertise, time, and dedication of our moderators. I am deeply appreciative of Drs. Sharon Daye, Bruce Williams, Jeremy Bearss, Tom Cecere, William Baskerville, Katie Scott, Erica Barkei, Lou Huzella, Julie Engiles, Cory Brayton, Paco Uzal, Elise LaDouceur, Sarah Sulkosky, Kim Whitten, Patty Pesavento, Tony Alves, Corrie Brown, Jey Koehler, Francisco Carvallo, and Kali Holder for taking time from their busy schedules to engage in thoughtful academic discussions and education of the greater veterinary pathology community.

It cannot be overstated how integral our staff is to the success of the WSC. I would like to personally thank Dr. Bruce Williams for his leadership and support of the program; Ms. Kenenya Gathers and Ms. LaKindra Peirce for accessioning and organizing WSC cases; Ms. Stacey Tamer for her exceptional immunohistochemical and special stain support; MAJ Judy Kovach-Zukin for assisting with process improvements; and our newest team member, Ms. Katherine Maye, for her enthusiasm and willingness to jump in as we begin preparations for the 2026–2027 conference year. Your efforts are sincerely appreciated.

In developing the JPC comments this year, I aimed to emphasize disease pathogenesis and focus on topics I felt would be most relevant to fellow pathology residents worldwide. I firmly believe that a touch of humor can make complex or potentially dry material more approachable, and while I make no claims at comedic prowess, I did my best to keep the content engaging where appropriate. I hope these efforts brought a smile to our readers along the way.

Finally, I would like to thank my friends, family, and mentors for their support throughout the past year as I navigated this challenging and rewarding role. I am grateful for your guidance and advice. To my fellow residents, thank you for your enthusiasm, dedication, and understanding throughout this conference year. It is truly a privilege to work alongside you, and I look forward to stepping further into the world of veterinary pathology with each of you as my colleagues.

MAJ Caitlin M. Culligan, DVM
2025-2026 WSC Coordinator

Case	Species	Tissue	Lesion/condition	Page
Conference 1 - August 20, 2025				
1	Horse (foal)	Thyroid	Thyroid hyperplasia and musculoskeletal deformities syndrome (TH-MSD)	8
2	Horse	Cerebrum	Fungal encephalitis	11
3	Horse	Small colon	Idiopathic focal eosinophilic enteritis (IFEE)	17
4	Horse	Spinal cord	Western equine encephalitis virus (WEEV)	21
Conference 2 - August 27, 2025				
1	Pony	Skeletal muscle	Necrotizing myositis (amoebiasis)	28
2	Rhesus macaque	Prostatic urethra	Retrograde ejaculation cystolithiasis	35
3	African pygmy hedgehog	Liver, lung, kidney	Myeloproliferative neoplasm (favor chronic eosinophilic leukemia)	41
4	Cat	Conjunctiva	Feline lipogranulomatous conjunctivitis	47
Conference 3 -September 3, 2025				
1	Cat	Lung	Parapneumonic disease with bronchopneumonia	50
2	Pig	Haired skin	*Staphylococcus hyicus* epidermitis (“Greasy pig disease”) and sarcoptic mange	56
3	Dog	Lung	Eosinophilic bronchopneumonopathy	61
4	Dog	Kidney	Glomerulocystic disease	65
Conference 4 – September17, 2025				
1	Black-tailed prairie dog	Lung	Multinucleated giant cell pneumonia	69
2	Goat	Thoracic mass	Malignant thymoma	73
3	Sheep	Cerebrum, lung	Fungal meningoencephalitis and pneumonia	78
4	Goat	Kidney	Immune-complex glomerulonephritis	86
Conference 5 - September 24, 2025				
1	Dog	Heart	*T. cruzi* pancarditis	95
2	Cynomolgus macaque	Heart, lung	Bacterial endocarditis and embolic pneumonia	100
3	Dog	Eye	Ocular onchocerciasis	105
4	Cat	Eye	Traumatic endophthalmitis	109
Conference 6 - October 1, 2025				
1	Dog	Small intestine	*Spirocerca lupi* enteritis	114

Case	Species	Tissue	Lesion/condition	Page
2	Dog	Brain, frontal cortex	Neuronal ceroid lipofuscinosis	119
3	Cat	Lung	Feline Pulmonary Langhans Cell Histiocytosis	124
4	Camel	Lung, lymph node	B-cell lymphoma	129
Conference 7 - October 8, 2025				
1	Horse	Suspensory ligament	Chronic suspensory desmitis	137
2	Pig	Ileum, colon, lymph node	PRRSV with *Cystoisospora, Cryptosporidium*, and Trichomonads	143
3	Cat	Mandibular lymph node	Primary nodal angiosarcoma	151
4	Dog	Skin	Basosquamous carcinoma	158
Conference 8 - October 15, 2025				
1	Cat	Eye	Medulloepithelioma	164
2	Dog	Femoral head	Avascular femoral head necrosis (Legg-Calves-Perthes disease)	170
3	Cat	Eye	Intraocular metastatic carcinoma	174
4	Dog	Lung	*Babesia canis* alveolitis	181
Conference 9 – October 22, 2025				
1	Pig	Haired skin	Cutaneous apocrine cystomatosis	187
2	Dog	Haired skin	Hyperkeratotic erythema multiforme	192
3	Horse	Haired skin (coronary band)	Equine multi-systemic eosinophilic epitheliotropic disease	197
4	Pig	Haired skin	Congenital swinepox	204
Conference 10 – November 5, 2025				
1	Dog	Adrenal gland	Adrenal gland arteriosclerosis + hypertensive vasculopathy	211
2	Dog	Colon, duodenum	Intestinal pythiosis	216
3	Golden lion tamarin	Liver, spleen	Hepatic and splenic listeriosis	222
4	Sprague Dawley rat	Skeletal muscle	Rhabdomyosarcoma	227
Conference 11 – November 12, 2025				
1	Chicken	Liver, spleen	*E. faecalis* hepatitis and splenitis	233
2	Chicken	Liver	Erythroblastosis	239
3	Cow	Heart, skeletal muscle	Reactive angioendotheliomatosis-like syndrome	244
4	Cow (calf)	Abomasum	Bovine adenovirus-5 abomasitis	250

Case	Species	Tissue	Lesion/condition	Page
Conference 12 – November 19, 2025				
1	Sheep	Placenta	Placental toxoplasmosis	255
2	Dog	Lymph node	Mammary carcinoma and malignant myoepithelioma (CAMM)	259
3	Cynomolgus macaque	Ovary, uterus	Uterine choriocarcinoma	265
4	Rabbit	Uterus	Uterine deciduate reaction	269
Conference 13 - November 26, 2025				
1	Rabbit	Liver	Hepatic steatosis	277
2	Pig	Large intestine, mandibular lymph node	Salmonellosis secondary to PCV-2	281
3	Bald eagle	Heart	West Nile Virus (WNV) and protozoal myocarditis	286
4	Greater sandhill crane	Liver	*Pasteurella multocida* hepatitis (Fowl cholera)	290
Conference 14 – January 7, 2026				
1	Horse	Liver	Zinc phosphide toxicosis	295
2	Horse	Kidney	*Halicephalobus gingivalis* nephritis	300
3	Donkey	Omentum	Mesothelioma	305
4	Sheep	Large intestine	Intestinal adenocarcinoma	311
Conference 15 - January 14, 2026				
1	C57BL/6 mouse	Kidney	Tubulointerstitial nephritis from adenine metabolism	316
2	Rhesus macaque	Stomach	Gastric carcinoid	322
3	Wild mouse	Salivary gland	Cytomegalovirus	328
4	B6 mouse	Kidney	Renal dysplasia	332
Conference 16 - January 21, 2026				
1	Horse	Colon	*Clostridioides difficile* + *Salmonella typhimurium* colitis	340
2	Cat	Skeletal muscle	*Clostridium novyi* myositis	345
3	Dog	Jejunum	Chronic intestinal pseudo-obstruction (CIPO)	350
4	Rabbit	Cecum	*Clostridioides difficile* ulcerative typhlocolitis	355
Conference 17 – January 28, 2026				
1	Indian ringneck parrot	Lung	Psittacid herpesvirus-5	360
2	Duck	Eye	Highly pathogenic avian influenza (HPAI)	365
3	Carrion crow	Liver	Mycobacterium avium spp. avium + *Lyperosomum longicauda* hepatitis	369
4	Oriental magpie robin	Wing, cross-section	*Yersinia pseudotuberculosis* osteomyelitis	376

Conference 18 – February 4, 2026				
1	Sheep	Cerebellum, brainstem, spinal cord	*Listeria spp.* meningoencephalitis	381
2	Dog	Cerebrum	CaAV-2 meningitis and vasculitis	386
3	Dog	Brain	*Toxoplasma gondii* meningoencephalitis	390
4	Cow	Cerebellum	Alpha-mannosidosis	396
Conference 19 – February 11, 2026				
1	Fischer 344 rat	Liver	Large granulocytic lymphocyte (LGL) leukemia	402
2	Cynomolgus macaque	Kidney	Acute tubulonephritis from tacrolimus toxicity	406
3	Dog	Liver	Hepatic necrosis due to cycad palm toxicity	410
4	129S/SvEv mouse	Skull with eye	Blepharoconjunctivitis	416
Conference 20 – March 25, 2026				
1	Donkey	Lung	Equine influenza	421
2	Cat	Lymph node	Feline infectious peritonitis	426
3	Black-winged starling	Liver, duodenum, cloaca, bursa of Fabricius, colon	Isosporosis + tetratrichomonads	430
4	Dog	Brain	Canine distemper virus (CDV)	436
Conference 21 – April 8, 2026				
1	Ferret	T11 vertebra	Multiple myeloma	441
2	Rat	Kidney	Urothelial cell carcinoma + hydronephrosis	452
3	Marmoset	Gallbladder and liver	Bacterial cholangiohepatitis and cholecystitis	456
4	African green monkey	Subcutis and skeletal muscle	Calcinosis circumscripta	463
Conference 22 – April 16, 2026				
1	Cow	Mammary gland	*Klebsiella spp*. mastitis	469
2	Cow	Heart, lung	*Helcococcus ovis* endocarditis + thromboembolic pneumonia	475
3	Cow	Lung	Atypical interstitial pneumonia	480
4	Sheep	Cerebrum	Maedi-Visna viral encephalitis	483
Conference 23 – April 22, 2026				
1	Dog	Spinal cord	Spinal ganglioradiculitis	489
2	Badger	Cerebrum	Mustelid gammaherpesvirus-1 meningoencephalitis	494
3	Horse	Cervical spinal cord	Wobbler's disease	498
4	Dog	Cerebrum	Suprasellar germ cell tumor	502

Conference 24 – April 29, 2026				
1	Cat	Trachea	Adenosquamous carcinoma	509
2	Cat	Lung	Lung lobe torsion secondary to chronic chylothorax	513
3	Dog	Cervical spinal cord	Disseminated canine herpesvirus-1 (CaHV-1)	517
4	Bighorn sheep	Spinal cord	Bronchopneumonia due to *Mycoplasma ovipneumoniae, Bibersteinia trehalosi,* and *Protostrongylus spp*.	521
Conference 25 – May 6, 2026				
1	Blue-tongued skink	Colon	Colonic adenosquamous carcinoma	527
2	Striped skunk (juvenile)	Lung	Canine morbillivirus (Distemper) pneumonia + pulmonary larval nematodiasis	532
3	Stingray	Pectoral fin	Pectoral fin soft tissue mineralization (tumoral calcinosis)	538
4	Philippine crocodile	Eye	Ocular mycosis (*Purpureocillium lilacinum*)	542

Joint Pathology Center
Veterinary Pathology Services

WEDNESDAY SLIDE CONFERENCE 2025-2026

Conference #1 — 20 August 2025

CASE I:

Signalment:
Equine Standardbred. Female, 2 days.

History:
Filly foal born with angular limb deformities of the all limbs, worse in the hind limbs. Foal had a fever, leukocytosis and neutrophilia.

Gross Pathology:
The crown rump length of this foal was 112 cm, Bilaterally, the tarsal joints were fixed in extension. The left fetlock has a 15 degree lateral deviation. The right tarsus was deviated about 30% and the fetlock a further 15 degrees medially. Eponychia were on all 4 hooves. The thyroid was normal in appearance. Bone marrow appeared to be normal also.

Laboratory Results:
Leukocytosis, neutrophilia, hypoproteinemia, hypoalbuminemia, severe hypoglobulinemia, azotemia, increased bilirubin, cholesterol, GLDH, Alk Phos, and CK.

Microscopic Description:
About 20% of follicles have colloid in the lumen and even those had a small diameter. The majority of follicles have no colloid or lumens. The thyroid follicular cells are tall cuboidal to columnar with abundant cytoplasm. Thyroid medullary cells are inapparent.

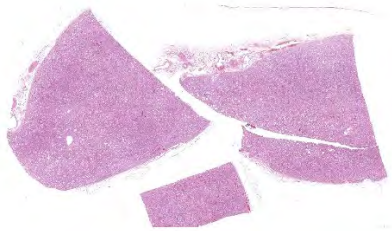

Figure 1-1: Thyroid gland, foal. Multiple sections of thyroid gland are submitted for examination. A few ectatic follicles are visible at subgross examination. (HE, 5X)

Contributor's Morphologic Diagnoses:
Thyroid follicular cell hypertrophy and hyperplasia, with minimal colloid.

Contributor's Comment:
This foal has the macroscopic and microscopic changes of the syndrome of horses known as thyroid hyperplasia and musculoskeletal deformities (TH-MSD) or congenital hypothyroidism-dysmaturity syndrome. Foals with or without musculoskeletal deformities may have microscopic thyroid hyperplasia yet no clinically visible goitre. A variety of musculoskeletal deformities occur.

Affected horses are newborn or are aborted. Foals have microscopic hyperplasia of the thyroid gland and may have multiple congenital musculoskeletal deformities. The thyroid gland are usually of normal size macroscopically.

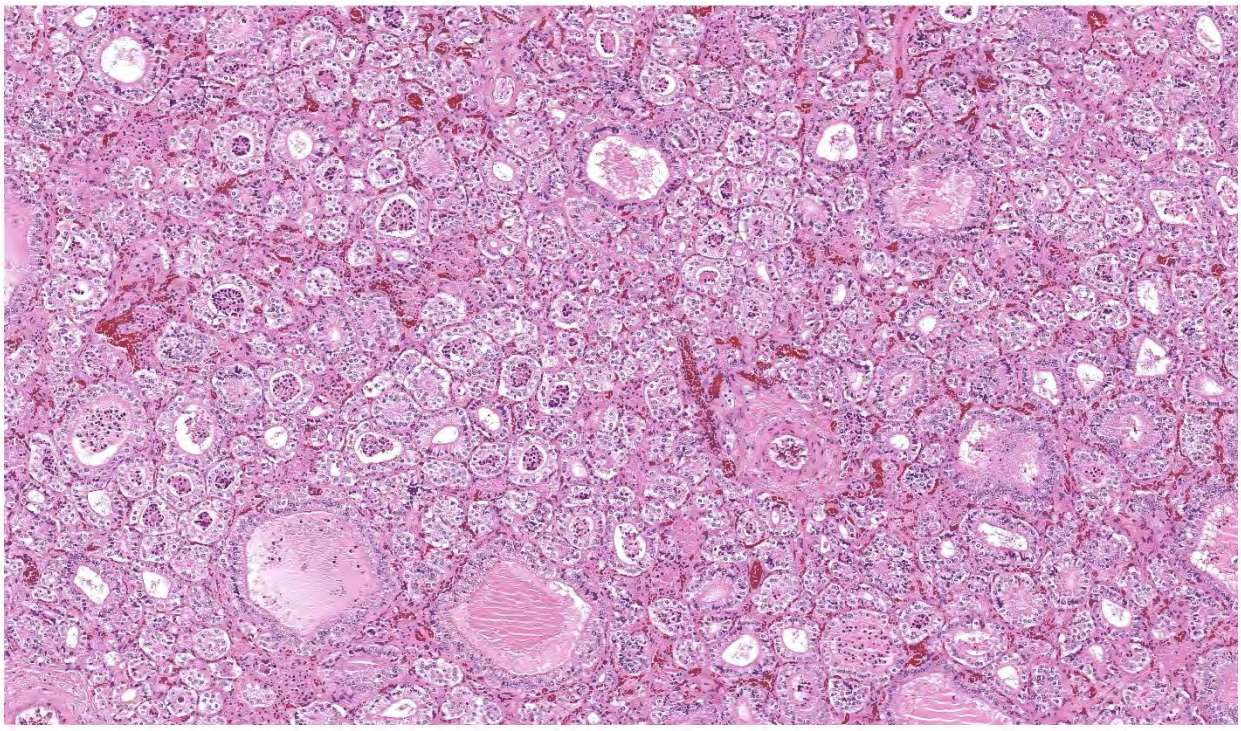

Figure 1-2: Thyroid gland, foal. There is wide variation in the size of follicles. Some are collapsed, some are dilated up to 0.2mm. Few have any colloid. (HE, 136X)

Musculoskeletal lesions include mandibular prognathia, inappropriately ossified carpal and tarsal bones, flexural deformities of the forelimbs and ruptured tendons of the common digital extensor muscles. Foals have either normal or lengthened gestation, and they show signs of immaturity including a short soft coat and lax joints. Aborted foals may have osteopetrosis. It is attributed to micronutrient deficiency including iodine deficiency of the mare. Cases were initially reported in Western Canada but have been found in a variety of other locations in Canada and internationally including Europe. Unless the thyroid gland is examined histologically, the diagnosis will be missed.

Contributing Institution:
Department of Pathobiology, Ontario Veterinary College, University of Guelph

JPC Diagnoses:
Thyroid gland: Follicular hyperplasia,diffuse, marked.

JPC Comment:
And…they're off! Conference is breaking out of the starting gate of the 2025-2026 Wednesday Slide Conference with an equine-centric lineup moderated by the Director of the Joint Pathology Center, COL Sherri Daye. This first case stimulated excellent discussion of a syndrome that is making its debut appearance in the WSC. There have been some great cases of goiter over the years (most recently, WSC 2017-2018, Conf 19, Case 4), but never an equine thyroid hyperplasia and musculoskeletal dysmaturity syndrome (THMSD). Many thanks to the contributor for this unique case. Conference discussion was based largely around the pathogenesis of this condition and potential causes of iodine imbalance in pregnant mares, including consumption of too much or too little iodine or the ingestion of goitrogenic plants (Brassica spp, clover, soybeans, sorghum, etc.). The lack of thyroid C-

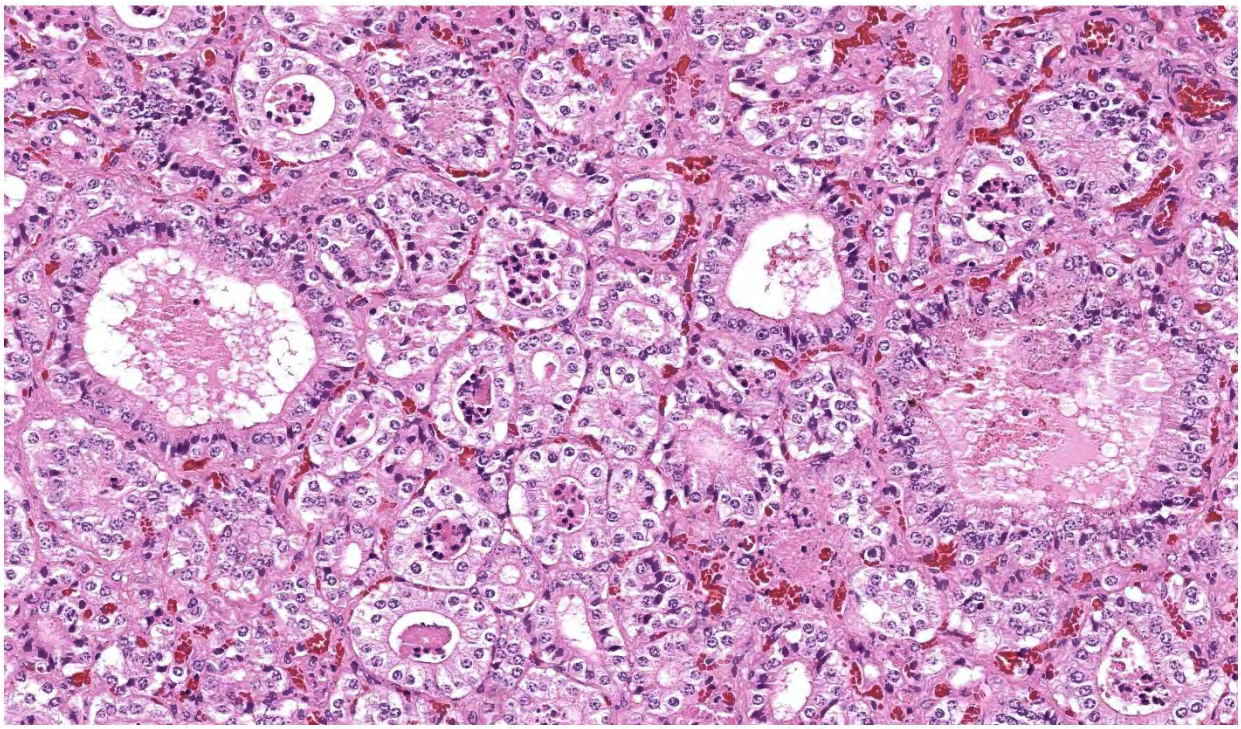

Figure 1-3: Thyroid gland, foal. Follicles are lined by a single layer of hypertrophiccolumnar epithelium. Few follicles contain any colloid. In numerous follicles, the follicular epithelium is apoptotic and sloughed into the lumen. There are few totally collapsed and necrotic follicles and a single ectatic follicle at right. (HE, 381X)

cells in this condition provided a good exercise for participants in evaluating what is not present and how that is often just as important as seeing what is.

Equine THMSD was first described in 1981 in Western Canada when 7 foals were submitted to the Western College of Veterinary Medicine for numerous musculoskeletal deformities, where it was determined that all foals also had evident goiter. Since these cases were reported, this syndrome has been described in thousands of foals across Canada, Europe, and the United States. As the contributor stated, many of the foals affected by this syndrome have grossly normal thyroid glands and a range of congenital deformities of variable severity, but all have had histologic evidence of thyroid hyperplasia. Although no exact cause has been decided on, the most widely accepted risk factors include nutritional iodine deficiency and/or high dietary nitrate in the dam leading to the congenital changes in the fetus. In humans, low selenium can also contribute to the development of a similar condition4. Ensuring adequate nutrition of the dam throughout pregnancy is the best prevention. You know what people say…an ounce of a balanced diet is worth of a pound of appropriately functioning thyroids…or something like that.

A quick review of thyroid physiology is warranted to understand the proposed pathogenesis of THMSD. The thyroid gland is responsible for several physiologic functions, including metabolism, thermogenesis, gluconeogenesis, cardiovascular support, neuronal development, and musculoskeletal development. Thyroid hormone production starts with the hypothalamus, which produces thyrotropin-releasing hormone (TRH). TRH acts on the anterior pituitary to stimulate release of thyroid-stimulating hormone (TSH), which is the major regulator of thyroid hormone synthesis in the thyroid gland. These three organs make

up the hypothalamic-pituitary-thyroid axis, which allows for negative feedback control of thyroid hormone production. When functioning appropriately, the thyroid gland produces thyroxine (T4) and triiodothyronine (T3), with T3 being the bioactive form. Although low levels of T3 are produced directly, most T3 must be converted within the target cell from T4. That's where the iodine comes in, because conversion of T4 to T3 requires iodine! When there is a lack of iodine, there will not enough bioavailable thyroid hormone being produced. In cases of low thyroid hormone levels, TSH will continue to be produced by the anterior pituitary to stimulate the thyroid glands to produce thyroid hormone. This results in hyperplasia of the thyroid gland, which can become severe enough to cause goiter.

How does this tie in to the musculoskeletal deformities? Thyroid hormone is a critical regulator of energy availability and consumption within the musculoskeletal system6. While the hypothalamus has mostly thyroid hormone receptor (TR) β, TRα is the main receptor expressed in the skeleton and mediates T3 action in bone and cartilage7. Chondrocytes and osteoblasts are directly responsive to thyroid hormone and osteoclastic activity is sensitive to changes in thyroid hormone availability. It's not clear whether osteoclasts are direct target cells of T3 or if the effects on bone resorption are indirect and mediated by primary thyroid hormone actions in other cells7. Via its action on these cells of the skeleton, thyroid hormone works to regulate intramembranous and endochondral ossification, control the rate of linear growth and bone maturation, and ensure appropriate skeletal mineralization. In an absence of thyroid hormone, these processes are delayed, which can result in the variety of dysmaturities seen in THMSD-affected foals.

References:

1. Allen AL. Hyperplasia of the thyroid gland and musculoskeletal deformities in two equine abortuses. *Can Vet J.* 1995;36: 234-236.
2. Allen AL, Doige CE, Fretz PB, Townsend HG. Hyperplasia of the thyroid gland and concurrent musculoskeletal deformities in western Canadian foals: reexamination of a previously described syndrome. *Can Vet J.* 1994; 35: 31-38.
3. Allen AL, Townsend HG, Doige CE, Fretz PB. A case-control study of the congenital hypothyroidism and dysmaturity syndrome of foals. Can Vet J. 1996; 37: 349-351; 354-358.
4. Chanoine JP. Selenium and thyroid function in infants, children and adolescents. Biofactors. 2003;19(3-4):137-43.
5. Koikkalainen K, Knuuttila A, Karikoski N, Syrja P, Hewetson M. Congenital hypothyroidism and dysmaturity syndrome in foals: First reported cases in Europe. Equ Vet Educat. 2014; 26: 181-189.
6. Sindoni A, Rodolico C, Pappalardo MA, Portaro S, Benvenga S. Hypothyroid myopathy: A peculiar clinical presentation of thyroid failure. Review of the literature. Rev Endocr Metab Disord. 2016 Dec;17(4):499-519.
7. Williams GR, Bassett JHD. Thyroid diseases and bone health. J Endocrinol Invest. 2018 Jan;41(1):99-109.

CASE II:

Signalment:

19-year-old, American miniature stallion.

History:

The horse presented with a 24-hour history of lethargy and possible neurologic signs. Circling to the left had been noted the day prior to admission, and the horse was frequently seen standing quietly with his head lowered. During physical examination, the horse was quiet, yet alert and responsive. A cranial nerve exam was within normal limits. quiet,

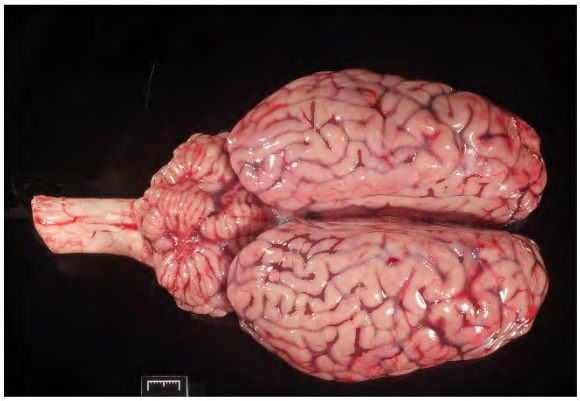

Figure 2-1: Brain, horse. The right frontal lobe is assymetrically enlarged. (Photo courtesy of: Department of Veterinary Pathobiology, College of Veterinary Medicine, Texas A&M University, https://vtpb.tamu.edu).

yet alert and responsive. A cranial nerve exam was within normal limits. Blood work, including bile acids and ammonia levels, was unremarkable as were cervical spinal radiographs. The horse was treated with flunixin meglumine, Vitamin E, Marquis®, and intramuscular dexamethasone injections. Despite treatment for 4 days, the horse developed an intermittently absent menace of the left eye, a left head tilt, compulsive walking in the right direction, and a medial strabismus of the left eye. These signs progressed to full body muscle fasciculations, fixed dilated pupils, absent pupillary light reflex and menace bilaterally, head pressing, of the left eye. These signs progressed to full body muscle fasciculations, fixed dilated pupils, absent pupillary light reflex and menace bilaterally, head pressing, and a rising body temperature. Due to the horse's worsening condition, humane euthanasia was elected.

Gross Pathology:

The right frontal lobe was slightly enlarged (asymmetry) (Fig.1). On cut surface, the white matter was mildy expanded and yellow (edema). A 1.1x0.5 cm, soft, red-brown area was within the right thalamus (malacia).

Laboratory Results:

Rabies fluorescent antibody testing: negative; Eastern Equine Encephalitis virus RT-PCR: negative; Western Equine Encephalitis virus RT-PCR: negative; West Nile virus RT-PCR: negative; St. Louis Encephalitis virus RT-PCR: negative.
(https://tvmdl.tamu.edu/tests/panfungal-pcr/)

Panfungal PCR targeting the internal transcribed spacer (ITS) region and agarose gel electrophoresis yielded 2 bands of DNA at approximately 350bp and 450bp. DNA was purified from the gel and sequenced. The resulting 119bp and 295bp sequences were analyzed with the NCBI BLAST database. The sequence matched *Chaetomium strumarium* and *Malassezia restricta* with 100% identity.

Microscopic Description:

Cerebrum: Multifocally and randomly infiltrating the neuroparenchyma are numerous distinct accumulations of inflammatory cells composed of epithelioid macrophages and neutrophils with fewer lymphocytes, multinucleated giant cells (Langhans and foreign body type), and plasma cells. Inflammatory cells also frequently and moderately expand

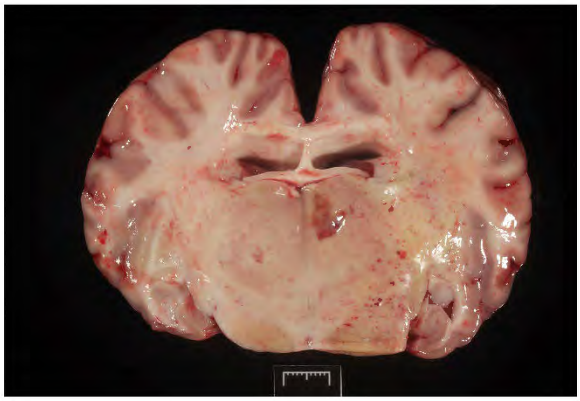

Figure 2-2 Brain, horse. A 1.1x0.5 cm, soft, red-brown area of malacia is present within the right thalamus . (Photo courtesy of: Department of Veterinary Pathobiology, College of Veterinary Medicine, Texas A&M University, https://vtpb.tamu.edu).

Virchow-Robins' spaces. Admixed extracellularly with inflammatory cells and phagocytosed within macrophages and multinucleated giant cells are sections of golden-brown, 7-10 µm pigmented fungal hyphae characterized by frequent septation, dichotomous branching, and terminal bulbous swellings. The section also exhibits multifocal areas of cavitation with loss of neuroparenchyma and replacement by numerous foamy macrophages (gitter cells) accompanied by increased numbers of astrocytes and microglia (gliosis) with increased clear space (edema) and areas of hemorrhage. Neurons in these areas are multifocally shrunken and hypereosinophilic with pyknotic nuclei (necrosis) and axons are frequently swollen and hypereosinophilic and surrounded by dilated myelin sheaths (spheroids).

Contributor's Morphologic Diagnoses:
Cerebrum: Marked, multifocal to coalescing, chronic, pyogranulomatous encephalitis with extracellular and intrahistiocytic fungal hyphae.

Contributor's Comment:
Histologic evaluation identified fungal encephalitis as the cause of the horse's neurologic signs with PCR results identifying the dematiaceous fungus, *Chaetomium sp.*, as the cause. Meningoencephalitis associated with dematiaceous fungi has been previously described in horses[10].

The term "dematiaceous" has been used to describe fungi that are olivaceous, dark brown, or black due to the presence of melanin or melanin-like pigment within the cellular walls13. It has been suggested that the term "dematiaceous" is not appropriate given its etymologic derivation from the Greek "deme," meaning "bundle." The term "melanized" has been used more recently to describe pigmented fungi[11]. Melanized fungi are responsible for causing a wide range of diseases including

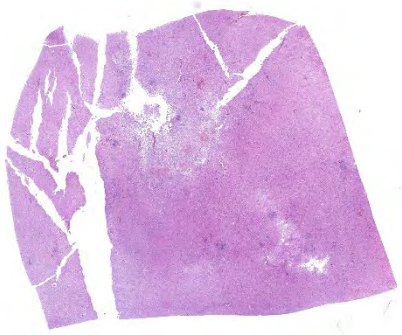

Figure 2-3: Cerebrum, horse: One section of cerebrum is submitted for examination. There are multifocal to coalescing areas of necrosis within this section, and cuffed vessels are visible at the periphery. (HE, 10X)

chromoblastomycosis and phaeohyphomycosis. Chromoblastomycosis is a chronic infection of the skin and subcutaneous tissues, characterized by muriform bodies or sclerotic bodies, and typically caused by *Fonsecaea pedrosoi, Fonsecaea compacta, Phialophora verrucosa,* or *Cladosporium carrionii*[13].

The name "phaeohyphomycosis" is derived from the Greek word "phaeo" meaning "dusky" or "grey." In phaeohyphomycosis, the tissue morphology of the fungus is predominantly composed of hyphae (mycelial). Although the agents of phaeohyphomycosis may exhibit a dark coloration in culture and the gross appearance of these lesions may be partially pigmented, these organisms appear non-pigmented in histologic sections stained with using H&E. In such cases, Fontana-Masson may be helpful in identifying the pigmented hyphae, while Gomori methenamine silver (GMS) and periodic acid-Schiff (PAS) usually obscure the pigment[13].

In humans, phaeohyphomycosis causes opportunistic infections in the cornea, sinus, skin, and lungs of immunocompromised patients, with the exception of central nervous system infections, which tend to affect immunocompetent individuals. Genera involved with phaeohyphomycosis in humans include: *Alternaria, Bipolaris, Chaetomium, Clado-*

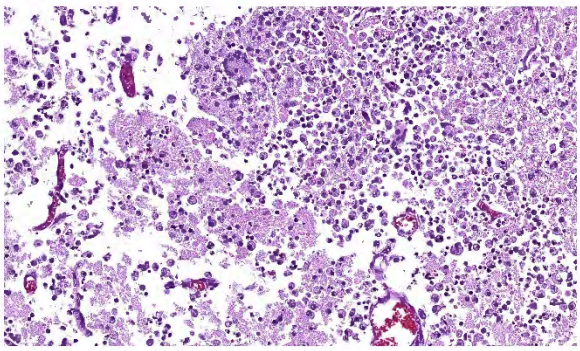

Figure 2-4: Cerebrum, horse. Areas of necrosis contain numerous Gitter cells, viable and necrotic neutrophils, rare multinucleated foreign body giant cells, and in areas of neuroparenchymal loss, gliovascular strands (bottom left). (HE, 332X)

phialophora, Curvularia, Exophiala, Exserohilum, Lasiodiplodia, Lecythophora, Ochroconis, Phaeoacremonium Pseudallescheria, Rhinocladiella, and *Scedosporium*, among others[13].

Fungi of the members of the orders Chaetothyriales, Pleosporales, Ochroconiales, and Capnodiales are involved in phaeohyphomycosis in a wide range of cold-blooded vertebrates, such as crustaceans, captive and farmed fish, amphibians, and aquarium animals. Phaeohyphomycosis is less prevalent or less recognized in warm-blooded animals[12]. Cats appear to be more susceptible with case reports of this infection documenting nasal, renal, cutaneous, subcutaneous, ocular, cerebellar and systemic involvement[12,14]. Members of the family Chaetomiaceae are ubiquitous fungi which reside in soil enriched with manure or cellulosis-decaying materials[1,2]. A certain prevalence of chaetomium-like species was noted in desert soil subjected to conditions of dryness and extremely variable temperatures[2]. *Chaetomium atrobrunneum*, *C. perlucidum*, and *C. strumarium* are neurotropic species causing serious and life-threatening infections in people[1,3].

Mycotic encephalitis is rare in horses. Reported cases include aspergillosis[4], one of which presented with concurrent Mucor sp. infection, and cryptococcosis. Recently, phaeohyphomycosis within the Chaetomiaceae family, including *Acrophialophora fusispora*, *Acrophialophora levis*, and *Chaetomium strumarium* has been described as novel causes of equine neurotropic mycosis. Affected animals ranged from 8 to 22 years of age. The most common central nervous system location was the cerebrum[10].

Panfungal PCR on formalin-fixed paraffin-embedded (FFPE) tissues targeting the ribosomal RNA large subunit coding region and the noncoding internal transcribed spacer-2 region is a useful technique when fresh tissue is not available for culture. Although pigmented fungi may appear to be a straightforward identification on H&E sections, variability exists in the amount of melanin produced by a genotypic variant, and thus these fungi could be confused with other hyaline hyphae. Additionally, pigmented fungi cannot be identified to the genus level using histologic evaluation alone[5]. In this case, the amplified *Malassezia restricta* sequence is a common contaminant in paraffin blocks and unrelated to the cause of the fungal infection in this case. Panfungal PCR and sequencing results should always be correlated with the assessment of fungal morphology.

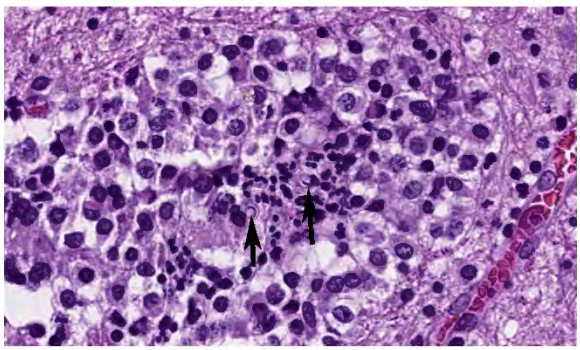

Figure 2-5: Cerebrum, horse. Fungal hyphae are difficult to visualize on HE section. Cross sections of hyphae may be seen within foreign body-type giant cell macrophages. (HE, 526X)

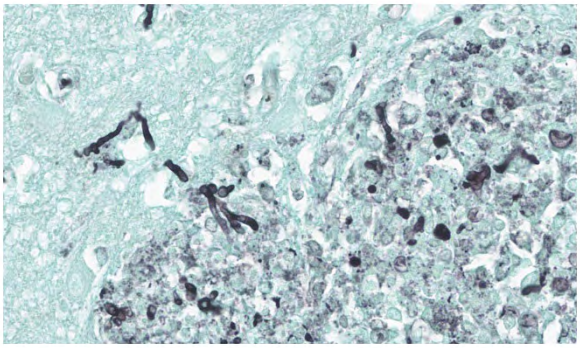

Figure 2-6: Cerebrum, horse. A silver stain demonstrates the morphology of the fungal hyphae with elongate 4-10um pauciseptate hyphae. (GMS 600X)

Contributing Institution:
Department of Veterinary Pathobiology
College of Veterinary Medicine and Biomedical Sciences, Texas A&M University
https://vtpb.tamu.edu

JPC Diagnoses:
Cerebrum: Encephalitis, necrotizing and pyogranulomatous, focally extensive, severe, with vasculitis and rare pigmented fungal hyphae.

JPC Comment:
This is a excellent case of a fungal encephalitis in a horse caused by a unique mycotic pathogen. The contributor gives a thorough overview of this condition and other relevant fungi in their comment. While it is well-established that the brain and retina of horses, as well as the nervous system and skin of cats, are frequent targets of dematiaceous fungi in veterinary species, this particular pathogen is rarely isolated from infections in animals.

This conference case stimulated discussion on how, despite the challenge of finding the hyphae on the H&E slide, the type of inflammation (pyogranulomatous) should make the pathologist suspicious for particular types of pathogens and stimulate careful search in affected areas for those agents. A GMS stain readily revealed the fungal hyphae within the affected neuropil and was shown to conference participants following the H&E description. A great review of microglia and their roles followed case presentation, including the differences between resting microglia, gitter cells, multinucleated giant cells, and "rod" cells. A brief review of the necessary fungal features to mention in a slide description was covered and included: size, branching (acute vs right angle, dichotomous vs irregular, and frequency), parallel vs. non-parallel walls, septation, pigmented or non-pigmented, and mention of whether the fungus is angioinvasive or not. One conference participant also made an excellent point that, after others questioned the pigmentation of the fungi outside of that seen in histiocytes, that pigmented fungi are classified as such based on their appearance on a growth plate and not on an H&E slide.

A closer look at *Chaetomium* sp fungi helps elucidate how they cause illness. *Chaetomium* sp are well-documented neurotropic fungal pathogens of humans, but until recently, were not associated with disease in veterinary species11. "Chaeto-" comes from the Greek word "chaitē", meaning "long hair" in reference to the filamentous setae covering the fruiting bodies of these fungi. These setae are considered one of the defining morphologic features of this fungal genus, and differing setae characteristics within the genus can assist in speciation.

These opportunistic fungi, when in an environment that enables their growth, produce a variety of mycotoxins, including several types of chaetoglobosins. Chaetoglobosins are a type of cytochalasin fungal metabolite that binds to and prevents the polymerization of actin filaments in animal cells, inhibiting cellular movement, changing cellular morphology, and hindering mitosis, ultimately resulting in apoptosis of the affected cell[5]. Chaetoglobosin A, in particular, is highly toxic to

mammalian cells and, even at low doses, has been demonstrated to be acutely fatal in laboratory rats and mice[9]. Other produced toxins, such as chaetoviridins, have antimicrobial and antifungal properties against other fungi, enabling the *Chaetomium* sp to thrive while inhibiting the growth of competitors[4].

Chaetoviridins have also been shown to inhibit tumor development in carcinogenic mice models via targeted cytotoxic effects. As such, chaetoglobosins and chaetoviridins are currently being studied for their use as potential antimicrobial and chemotherapeutic agents6. *Chaetomiaciae* sp are yet another excellent example of the natural world enabling biochemists and pharmacologists to walk the fine line between therapeutic dosage and toxicity.

References:

1. Abbott SP, Sigler L, McAleer R, et al. Fatal cerebral mycoses caused by the ascomycete Chaetomium strumarium. *J Clin Microbiol*. 1995;33(10): 2692–2698.
2. Ahmed SA, Ziauddin K, Wang X, et al. Chaetomium-like fungi causing opportunistic infections in humans: a possible role for extremotolerance. Fungal Diversity. 2016:76:11–26.
3. Barron MA, Sutton DA, Veve R, et al. Invasive mycotic infections caused by Chaetomium perlucidum, a new agent of cerebral phaeohyphomycosis. J Clin Microbiol. 2003;41(11):5302–5307.
4. Elkhateeb WA, Kolaibe AG, Elnahas MO, Daba GM. Highlights on Chaetomium morphology, secondary metabolites and biological activates. J Pharmaceutics and Pharmacology Research. 2021;4(1).
5. Fogle MR, Douglas DR, Jumper CA, Straus DC. Growth and mycotoxin production by Chaetomium globosum is favored in a neutral pH. Int J Mol Sci. 2008;9(12):2357-2365.
6. Goda MS, El-Kattan N, Abdel-Azeem MA, Allam KAM, Badr JM, Nassar NA, Almalki AJ, Alharbi M, Elhady SS, Eltamany EE. Antimicrobial Potential of Different Isolates of Chaetomium globosum Combined with Liquid Chromatography Tandem Mass Spectrometry Chemical Profiling. Biomolecules. 2023 Nov 21;13(12):1683.
7. Hunter B, Nation PN. Mycotic encephalitis, sinus osteomyelitis, and guttural pouch mycosis in a 3-year-old Arabian colt. Can Vet J. 2011;52(12):1339–1341.
8. Meason-Smith C, Edwards EE, Older CE, et al. Panfungal polymerase chain reaction for identification of fungal pathogens in formalin-fixed animal tissues. Vet Pathol. 2017;54(5):640–648.
9. Ohtsubo K, Saito M, Sekita S, Yoshihira K, Natori S. Acute toxic effects of chaetoglobosin A, a new cytochalasan compound produced by Chaetomium globosum, on mice and rats. Jpn J Exp Med. 1978 Apr;48(2):105-10.
10. Plumlee P, Meason-Smith C, Dieterly, et al. Chaetomiaceae Fungi, Novel Pathogens of Equine Neurotropic Phaeohyphomycosis. Vet Pathol. 2017;54(5):813-819.
11. Revankar SG, Sutton DA. Melanized Fungi in Human Disease. Clin Microbiol Rev. 2010:884-928.
12. Seyedmousavi S, Guillot J, de Hoog GS. Phaeohyphomycoses, emerging opportunistic diseases in animals. *Clin Microbiol Rev*. 2013;26(1):19–35.
13. Schmitt BH, Pritt B. Dematiaceous Fungal Infections. In: Procop GW, Pritt BS,

ed. Pathology of Infectious Diseases. 1st ed. Saunder; 2014: 516-530.
14. Velazquez-Jimenez Y, Hernandez-Castro R, Romero-Romero R. Feline phaeohyphomycotic cerebellitis caused by Cladosporium cladosporioides-complex: case report and review of literature. J Comp Path. 2019:170:78-85.

CASE III:

Signalment:
10 yr Gypsy Vanner mare, *Equus caballus*, horse.

History:
Tissue from a 10-year-old Gypsy Vanner mare with a 24-hour history of colic. On presentation, the horse was tachycardic with decreased borborygmi in all quadrants. An abdominal ultrasound was performed that identified increased motility on the right side, decreased motility on the left side, and severely thickened sections of intestine. An abdominocentesis found increased lactate (4.0 mmol/L). Peripheral lactate was in the normal range (1.5 mmol/L). The mare was taken into surgery where a focal area of thickened small colon was identified, and a resection and anastomosis was performed along with biopsy of the affected site. Ultimately the mare did poorly following surgery, and was euthanized; a postmortem examination was not performed, and examination was limited to biopsy tissues removed during surgery.

Figure 3-1: Colon, horse. A segment of opened small colon was submitted for histologic evaluation. On the mucosal surface, there is a focal, well demarcated, irregularly marginated tan to brown plaque rimmed in dark red that measures 8x9cm. (Photo courtesy of: The Ohio State University College of Veterinary Medicine, Department of Veterinary Biosciences, https://vet.osu.edu/biosciences).

Gross Pathology:
A segment of opened small colon measuring 16cm in length and 17cm in width was submitted for histologic evaluation. The segment is 1cm thick on the margins, narrowing to 0.4cm thick in the center of the section. On the mucosal surface, there is a focal, well demarcated, irregularly marginated tan to brown plaque rimmed in dark red that measures 8x9cm.

Laboratory Results:
Peripheral lactate: 1.5 mmol/L
Abdominal effusion lactate: 4.0 mmol/L

Microscopic Description:
Small colon: Markedly, transmurally expanding the bowel wall, with the submucosa and muscularis layers most prominently affected, are numerous eosinophils, macrophages, and fewer lymphocytes, plasma cells, and neutrophils. The mucosa is mildly expanded by described inflammatory infiltrates, and vessels within the mucosa are congested with multifocal, variably minimal to moderate numbers of extravasated red blood cells (hemorrhage). Segmentally, approximately 50% of the mucosa has relatively sharply-demarcated loss of differential staining with variable retention of

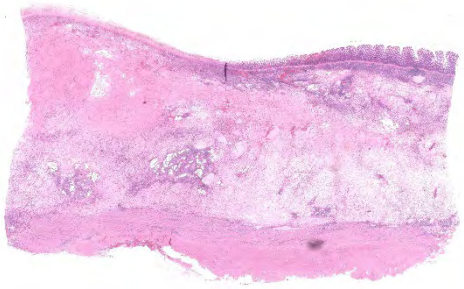

Figure 3-2: Colon, horse. One section of severely inflamed colon is submitted for wzmination. At subgross, mucosal necrosis (top left) and marked expansión of the submucosa are evident (HE, 10X)

cellular architecture (coagulative necrosis) in termixed with foci comprised of karyorrhectic nuclear debris and granular eosinophilic material (lytic necrosis). Necrosis extends regionally into the superficial underlying submucosa. Beyond described inflammatory cells, the submucosa is further severely expanded by abundant homogenous pale eosinophilic fluid (edema), resulting in the submucosa comprising approximately 70% of the entire thickness of the bowel wall. Within the tunica muscularis, described inflammatory cells infiltrate between and separate branching bundles of smooth muscle, often loosely associated with small caliber vessels lined by hypertrophied endothelial cells. Within both the submucosa and muscularis, inflammatory cells are multifocally accompanied by mild proliferation of plump spindle cells (fibroblasts). The serosa is mildly affected by inflammation with associated multifocal vascular congestion and patchy hemorrhage. Grocott methenamine silver (GMS) stain is performed on tissues, and no etiologic agents are identified.

Contributor's Morphologic Diagnoses:
Small Colon: Marked, multifocal to coalescing, subacute, submucosal and tunica muscularis-focused, eosinophilic, histiocytic, and neutrophilic colitis with marked diffuse edema and regional acute necrosis

Contributor's Comment:
The key histologic findings in this lesion are 1) the marked transmural infiltration of eosinophils within the segment of thickened bowel and 2) the particular concentration of eosinophils within the submucosa and muscularis of the affected bowel. In the horse, scattered eosinophils are commonly found within normal tissues of the gastrointestinal tract, but recruitment of eosinophils in diseased states are less common and most frequently attributed to parasitic migration, pythiosis, type I hypersensitivity, or idiopathic inflammatory conditions[10,17]. The eosinophilic inflammatory conditions with unknown causes have been categorized as part of an inflammatory bowel disease (IBD) complex[14]. Two distinct idiopathic causes will be discussed in detail: idiopathic focal eosinophilic enteritis (IFEE) and chronic eosinophilic enteritis (part of the multisystemic epitheliotropic eosinophilic disease, MEED). Idiopathic eosinophilic enterocolitis, or diffuse eosinophilic enteritis as proposed by Makinen *et al*., is a third idiopathic condition grouped into the IBD complex that is localized to the alimentary tract and consists of diffuse infiltrates of eosinophils with fewer macrophages than IFEE lesions and no obstructive disease, but with an otherwise similar histologic appearance[2,9,14,17].

IFEE was first identified in the early 1990s and since then has been documented in the United Kingdom, Republic of Ireland, United States and South Africa[1,12]. Archer *et al*. found IFEE to be an emerging disease with an increased incidence of cases from 2002 to 2010 in addition to possible seasonal and geographic correlations when cases are compared to control colic patients[1]. Clinical signs consist of acute colic, and focal circumferential thickening of the intestines can be identified on rectal palpation or by ultrasound[1]. The focal lesions are most often identified within the small intestine but have also been noted in the dorsal

left colon and can result in obstructive disease[4,12,16,17]. Surgical resection of the affected segments of bowel is thought to be curative[1,2]. Histologically, the lesions consist of focal infiltrations of eosinophils and macrophages within the submucosa and tunica muscularis with increased numbers of mononuclear cells[2,9,17]. The lamina propria is typically expanded with fewer eosinophils and abundant lymphocytes, plasma cells, and macrophages[2,9,17]. A causative agent has not been identified, but exposure to stagnant water has been a proposed contributor[1]. A type I hypersensitivity or parasitism cannot be ruled out given the nature of the disease.

Chronic eosinophilic enteritis has been documented in conjunction with MEED since the early 1980's[11,19]. Young horses are most at risk for developing the disease[14,18]. Clinical symptoms typically develop over a period of months with eosinophilic and granulomatous lesions noted most often in the skin, biliary ducts, pancreas, lung, salivary glands, and mesenteric lymph nodes[15,17]. Clinical presentation often consists of severe weight loss that develops over months and pitting edema attributed to enteric loss of plasma protein from chronic inflammation[3]. With colonic involvement, horses will develop diarrhea[17]. The intestinal histologic lesions consist of mucosaI, submucosal, and often transmural eosinophilic infiltrates accompanied by mast cells, macrophages, lymphocytes, and plasma cells[3,17,18]. In the author's experience, this will often include formation of discrete eosinophilic granulomas, which is in contrast to IFEE. Often lesions will contain extensive fibrosis, villous atrophy, and muscularis mucosa hypertrophy[17]. Proposed pathogeneses include a type I hypersensitivity to migration of enteric parasite larva or ingested allergens, or undetected IL-5 secreting T-cell lymphoma as supported by a documented case of CD3+ intestinal lymphosarcoma with concurrent MEED in the horse[8,17].

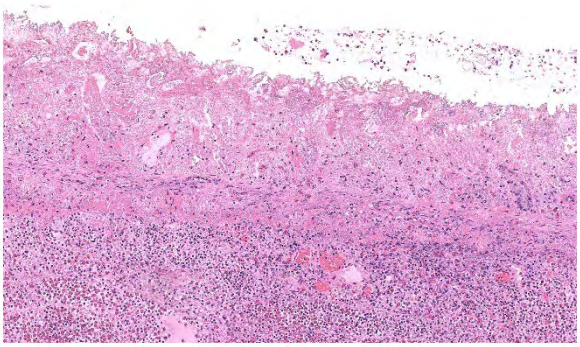

Figure 3-3: Colon, horse. There is segmental necrosis of the colonic mucosa; necrosis extends into the underlying muscularis mucosae. (HE, 215X)

In other species, eosinophilic enterocolitis entities attributed to a variety of causes has been identified in humans, dogs, cats, ferrets, and cattle either alone or with multisystemic inflammation[5,6,7,13].

Collectively, while occurring in an unreported location (small colon), the clinical presentation, gross finding of focal thickening of the bowel, and histologic appearance of this case support a diagnosis of IFEE. Histologically, there is extensive submucosal and tunica muscularis infiltration by predominantly eosinophils and macrophages, with fewer numbers of neutrophils, lymphocytes, plasma cells. While neutrophils are not commonly described in IFEE lesions, we attribute the presence of neutrophils to regional necrosis of the bowel, which we suspect is secondary to obstruction. The concentration of inflammatory cells within the submucosa and muscularis is reportedly a key feature of IFEE, supporting this diagnosis. The differential diagnosis of chronic eosinophilic enteritis as a component of MEED is not favored in this case due to the absence of eosinophilic granulomas, lesion distribution in the bowel wall, and absence of other known affected systems, although lack of postmortem examination precludes true evaluation of the latter point. Lastly, idiopathic eosinophilic enterocolitis/diffuse eosinophilic enteritis is not favored in this case due to the focal and obstructive nature of the le-

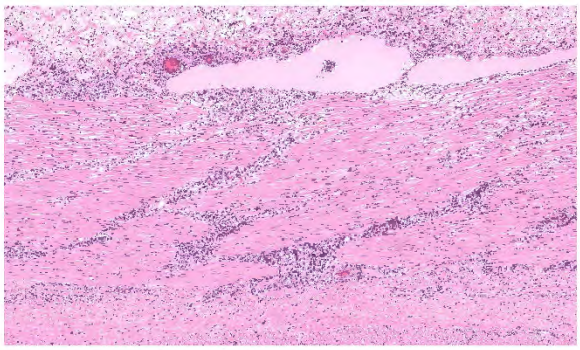

Figure 3-5: Colon, horse. The mixed inflamamtion extends from the dematous submucosa down into the muscularis, infiltrating along perivascular áreas and between muscle fibers. (HE, 115X)

sion, as well as the abundance of macrophages. Despite our preference for this lesion representing IFEE, we recognize that these conditions are not extensively characterized within veterinary pathology literature, so we cannot fully rule out that this lesion may reflect a variant of one of these other idiopathic conditions. In this case, infectious agents (i.e. fungal or fungal-like organisms, e.g. *Pythium* spp.) were not identified via H&E and GMS evaluation, but we cannot rule out that undetected agents may be inciting this lesion. Overall, this case highlights the need for further investigation and characterization of equine idiopathic eosinophilic inflammatory bowel conditions.

Contributing Institution:
The Ohio State University College of Veterinary Medicine, Department of Veterinary Biosciences
https://vet.osu.edu/biosciences

JPC Diagnoses:
Colon: Colitis, eosinophilic, subacute, focally extensive and transmural, severe, with segmental necrosis and marked edema.

JPC Comment:
The contributor provided a thorough comment comparing two entities that share many similarities yet have some distinct differences. Conference discussion was largely centered around comparing idiopathic focal eosinophilic enteritis (IFEE) and multisystemic epitheliotropic eosinophilic disease (MEED), with the clearest differences being the distribution of lesions and histologic presence of eosinophilic granulomas in MEED. However, it was also stated that the lack of eosinophilic granulomas does not rule out MEED and attention should be given more so to distribution and clinical history due to the similarities in these conditions. There was also special attention given to the segmental coagulative necrosis in this case, which conference participants largely attributed to the histologically evident vasculitis. Ultimately, in light of the clinical and histologic findings in this case, conference participants agreed with the contributor's diagnosis of IFEE. Grocott's methenamine silver (GMS) and periodic acid-Schiff (PAS) stains were run on this case and did not reveal any infectious agents, which is consistent with what the contributor reported in their own work-up.

References:

1. Archer DC, Costain DA, Sherlock C. Idiopathic focal eosinophilic enteritis (IFEE), an emerging cause of abdominal pain in horses: the effect of age, time and geographic location on risk. PloS One. 2014;9(12):e112072.
2. Archer DC, Edwards GB, Kelly OF, et al. Obstruction of equine small intestine associated with focal idiopathic eosinophilic enteritis: An emerging disease? Vet J. 2006;171 :504-512.
3. Bosseler L, Verryken K, Bauwens C, et al. Equine multisystemic eosinophilic epithelotropic disease: a case report and review of literature. NZ Vet J. 2013;61 :177-182.

4. Edwards GB, Kelly DF, Proud man CJ. Segmental eosinophilic colitis: a review of 22 cases. Equine Vet J. 2000;32:86-93.
5. Fox JG, Palley LS, Rose R. Eosinophilic Gastroenteritis with Splendor-Hoeppli Material in the Ferret. Vet Pathol. 1992;29:21-26.
6. Fushimi Y, Takagi M, Kawaguchi H, et al. Three cases of idiopathic eosinophilic enteritis with chronic obstinate diarrhea in Japanese Black fattening cattle. J Vet Med Sci. 2015;77(3):337-340.
7. Hendrick M. A spectrum of hypereosinophilic syndromes exemplified by six cats with eosinophilic enteritis. Vet Pathol. 1981 ;18:188-200.
8. La Perle KM, Piercy RJ, Long JF, et al. Multisystemic, eosinophilic, epitheliotropic disease with intestinal lymphosarcoma in a horse. Vet Pathol. 1998;35(2):144-6.
9. Makinen P, Archer DC, Baptiste KE, et al. Characterization of the inflammatory reaction in equine idiopathic focal eosinophilic enteritis and diffuse eosinophilic enteritis. Equine Vet J. 2008;40:386-392.
10. Morton LD, Morton DG, Baker GJ, et al. Chronic eosinophilic enteritis attributed to Pythium sp. in a horse. Vet Pathol. 1991;28:542-544.
11. Pass DA, Bolton JR. Chronic Eosinophilic Gastroenteritis in the Horse. Vet Pathol. 1982;19:486-496.
12. Piketh G, Henning A, Smit Y. Idiopathic focal eosinophilic enteritis associated with ileocaecal and ileal obstruction in a 10-year-old warmblood gelding. Vet Rec. 2022;1 0:e421.
13. Quigley PJ, Henry K. Eosinophilic enteritis in the dog: A case report with a brief Review of the Literature. J Comp Path. 1981 ;91 :387-392.
14. Schumacher J, Edwards JF, Cohen ND. Chronic idiopathic inflammatory bowel diseases of the horse. J Vet Intern Med. 2000;14(3):258-65.
15. Singh K, Holbrook TC, Gilliam LL, et al. Severe pulmonary disease due to multisystemic eosinophilic epitheliotropic disease in a horse. Vet Pathol. 2006;43: 189-193.
16. Swain JM, Licka T, Rh ind SM, et al. Multifocally eosinophilic enteritis associated with a small intestinal obstruction in a standard bred horse. Vet Rec. 2003;152:648-651.
17. Uzal FA, Plattner BL, Hostetter JM. Alimentary system. In: Maxie MG, ed. Jubb, Kennedy and Palmer's Pathology of Domestic Animals. Vol 2. 6th ed.St. Louis, MO: Elsevier Saunders; 2015:96.
18. Villagran CC, Vogt D, Gupta A, et al. Inflammatory bowel disease characterized by multisystemic eosinophilic epitheliotropic disease (MEED) in a horse in Saskatchewan, Canada. Can VetJ. 2021;62:1190-1194.
19. Wilkie JSN, Yager JA, Nation PN, et al. Chronic eosinophilic dermatitis: a manifestation of a multisystemic, eosinophilic, epitheliotropic disease in five horses. Vet Pathol. 1985;22:297-305.

CASE IV:

Signalment:
5-year-old, intact male, Criollo horse (Equus caballus)

History:
The horse had a 3-day history of progressive

Figure 4-1: Cervical spinal cord, horse. A section of cervical spinal cord is submitted for examination. At this magnification, small foci of hemorrhage are visible throughout the gray and white matter. (HE, 10X).

neurological signs including lethargy, circling, recumbency, paralysis, and occasional seizures, and was humanely euthanized due to severe clinical deterioration and poor prognosis.

Gross Pathology:
Gross findings included flattening of gyri in the cerebral hemispheres, diffuse hyperemia of the cerebral leptomeninges, and scattered foci of hemorrhage in the gray matter of the spinal cord.

Laboratory Results:
Samples of brain and spinal cord were positive for Western equine encephalitis virus (WEEV) by RT-PCR.

Microscopic Description:
Spinal cord (C1): multifocally the perivascular spaces are expanded and infiltrated by lymphocytes, histiocytes and fewer plasma cells forming layers of up to 7 cell thick (perivascular cuffing), with occasional accumulation of perivascular eosinophilic homogeneous finely granular material (protein-rich edema fluid. Similar inflammatory cells multifocally infiltrate the adjacent neuropil and/or white matter, occasionally forming discrete nodular aggregates. Rarely, multinucleated cells with abundant eosinophilic cytoplasm (interpreted as multinucleated astrocytes) are admixed with the inflammatory infiltrates. There is mild to moderate erythrocyte extravasation into the neuroparenchyma (hemorrhage). The inflammation, edema and hemorrhages are more frequent and severe in the gray than the white matter, with hemorrhages being particularly prominent in the dorsal horns. Scattered neurons depict chromatolysis (neuronal necrosis) and are either surrounded by inflammatory/glial cells (satellitosis) or invaded by them (neuronophagia) (not present in all sections). Capillaries are frequently hyperemic and lined by plump endothelial cells. Few swollen axons within dilated myelin sheaths (spheroids) are observed in the white matter. The leptomeninges are multifocally infiltrated by lymphocytes, histiocytes and fewer plasma cells.

Contributor's Morphologic Diagnoses:
Spinal cord (C1): Meningomyelitis, lymphocytic, histiocytic and plasmacytic, multifocal, moderate, with neuronal necrosis and hemorrhage, horse.

Contributor's Comment:
Differential diagnoses for non-suppurative

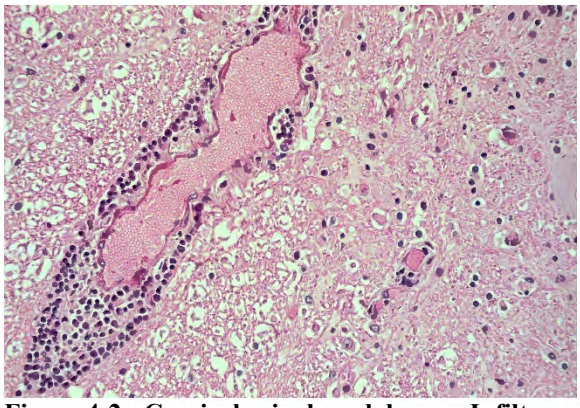

Figure 4-2: Cervical spinal cord, horse: Infiltration of lymphocytes, histiocytes and plasma cells in the perivascular space of a venule located in the junction between the white and gray matter. (HE, 400X). (Photo courtesy of: Instituto Nacional de Investigació Agropecuaria (INIA), La Estanzuela, Uruguay. www.inia.uy)

encephalitis/encephalomyelitis in horses include viruses [neuropathogenic strains of Equine herpesvirus 1 (EHV 1), rabies virus, several viruses in the Flavivirus genus such as West Nile virus (WNV), Japanese encephalitis virus (JEV), Saint Luis encephalitis virus (SLEV), and alphaviruses (Eastern, Western and Venezuelan equine encephalitis viruses: EEEV, WEEV and VEEV, respectively)], as well as protozoal diseases (Sarcocystis neurona, Neospora hughesi)[4,9,10,15].

Given that most viral causes of encephalitis in horses are zoonotic and/or notifiable to the World Organization for Animal Health, rapid confirmation of the etiologic diagnosis is crucial. This can be achieved by PCR, immunohistochemistry, or in situ hybridization targeting specifically the different viruses, by virus isolation, next generation sequencing, and/or by fluorescent antibody testing in the case of rabies.

While JEV is exotic in South America, neuropathic EHV 1, WNV, SLEV, WEEV, EEEV, and rabies are endemic or sporadically reported[1,5,6,11-13]. In the spring of 2023 and summer of 2024, a large epizootic outbreak of WEE affecting primarily horses and to a lesser extent humans occurred in South America, notably in Argentina,[16] Uruguay,[17] and southern Brazil[3]. The case presented here was the first equine case investigated in Uruguay during this epizootic in the summer of 2024. The epidemiological, clinical, and histopathologic findings lead to the suspicion of a viral encephalitis, and WEE was highly suspected as cases had recently been confirmed in neighboring areas of Argentina. WEEV was detected by reverse transcriptase PCR in samples of spinal cord and brain from this horse submitted to the

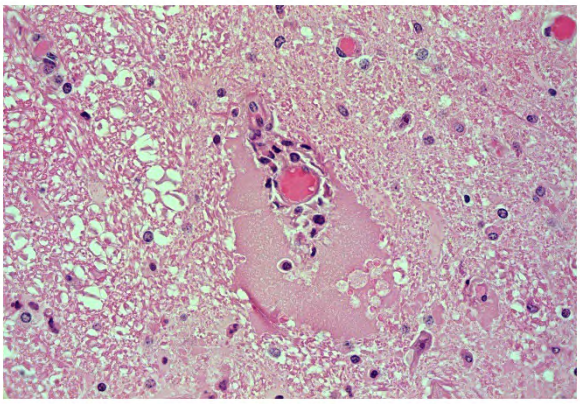

Figure 4-3: Cervical spinal cord, horse. The perivascular space of this capillary is infiltrated by a few lymphocytes and histiocytes and expanded by protein-rich edema fluid.

laboratory of the national sanitary authority ("Ministerio de Ganadería, Agricultura y Pesca" (MGAP), confirming the etiologic diagnosis.

Besides WEEV, VEEV and EEEV are other important alphaviruses (Togaviridae family), WEEV being the less virulent for horses of the three. Reservoir hosts are mainly birds (WEEV, EEEV), and rodents (VEEV)13. WEEV is transmitted primarily by *Culex* and *Aedes* mosquitoes from reservoir hosts to horses and humans, which are considered dead-end hosts.

The pathogenesis of alphavirus infection and encephalitis is complex and involves viremia after replication in peripheral tissues, neuroinvasion, and viral spread within the central nervous system. The initial viremia often goes unnoticed (subclinical), or manifests as fever and depression. If the animal fails to recover, neuroinvasion occurs, after which the virus replicates in neurons, glial cells, and blood vessels of the central nervous system. At this stage, the animal usually exhibits neurological clinical signs such as circling, cen

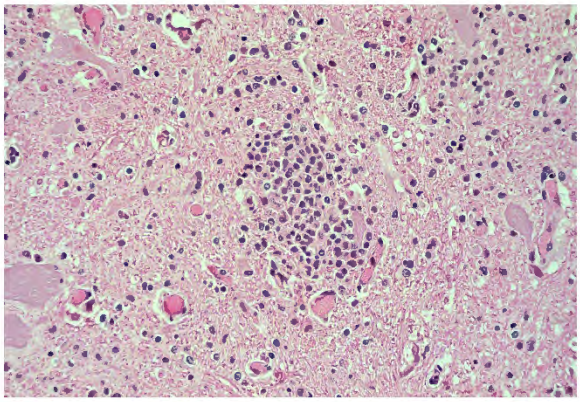

Figure 4-4: Cervical spinal cord, horse. Inflammatory infiltrates occasionally form discrete nodular aggregates adjacent to degenerating neurons in the gray matter (HE, 400X). (Photo courtesy of: Instituto Nacional de Investigación Agropecuaria (INIA), La Estanzuela, Uruguay. www.inia.uy

tral blindness, seizures, and terminal paralysis[14]. There are usually no gross changes, while histologic lesions frequently localize in the cerebral cortex and are almost limited to

the gray matter, typically with prominent neutrophil infiltration when the course is short or lymphoplasmacytic infiltration after a couple of days. Other common findings are neuronal degeneration, neuronophagia, gliosis, edema, and hemorrhage[4]. The histologic lesions caused by these three alphaviruses are similar in nature and distributions. For this reason, specific testing (i.e. PCR, IHC, ISH, and/or virus isolation) is required to confirm the etiologic diagnosis.

Outbreaks of arboviral-encephalitis usually affect non-vaccinated horses10. As vaccination is not mandatory in South America, many horses are not routinely vaccinated against these diseases.

Contributing Institution:
Instituto Nacional de Investigacion Agropecuaria (INIA), Uruguay. Avenida Italia 6201, Edificio Los Guayabos, Parque Technologico del LATU, Montevideo, Uruguay, www.inia.uy

JPC Diagnoses:
Cervical spinal cord: Poliomyelitis, lymphohistiocytic, diffuse, mild, with multifocal neuronal degeneration.

JPC Comment:
Last year's WSC coordinator, MAJ James Gaffney, adorned in a black cowboy hat provided by COL Daye for case presenters, grabbed this spinal cord case by the dorsal horns and proclaimed, "Pardner, this slide ain't big enough for the two of us." In the end, the slide was wrassled and conference participants branded this a "poliomyelitis" due to the focus of the inflammation being within the grey matter of the spinal cord. This case stimulated great discussion about the need for pathologists and clinicians alike to pay special attention to equine neurologic cases for which viral differentials are considered, as every virus on the differentials list is reportable and almost all are zoonotic. This list included flaviviruses (West Nile virus, Japanese encephalitis virus, Saint Louis encephalitis virus), the equine alphaviral encephalidities (WEEV, EEEV, and VEEV), equine herpesvirus-1, and

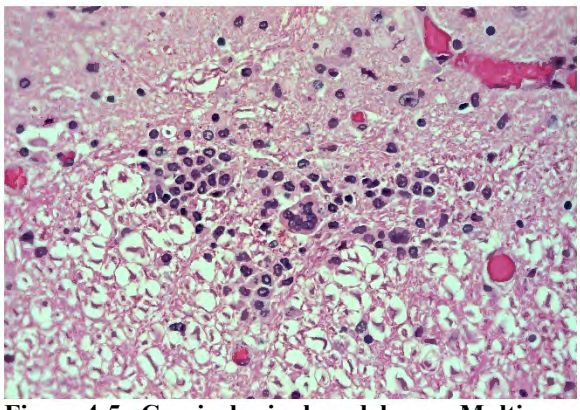

Figure 4-5: Cervical spinal cord, horse. Multinucleated cells interpreted as multinucleated astrocytes (center) occasionally admix with the inflammatory infiltrates in the gray-white matter junction. (HE, 400X). (Photo courtesy of: Instituto Nacional de Investigación Agropecuaria (INIA), La Estanzuela, Uruguay. www.inia.uy

rabies virus. In cases where any of these viral etiologies is suspected, rapid reporting and confirmatory diagnosis are crucial.

WEEV is widely considered to have arisen from a recombination event between Eastern equine encephalitis virus (EEEV) and a Sindbis-like alphavirus that resulted in a viral chimera. This recombinant virus ultimately diversified into WEEV, Highlands J Virus (HJV) and Fort Morgan virus (FMV), all of which are considered part of the WEEV antigenic complex. All three of these WEEV strains are considered endemic to North America2.

The first major outbreak of WEEV in the United States occurred in the 1940s with approximately 500,000 equine cases and several thousand human infections. The disease resurged with an additional outbreak in the United States and Canada the 1980s. Since then, cases in the United States have dropped significantly. However, Uruguay and Argentina experienced another outbreak of WEEV in 2024, with both equines and humans affected, bringing WEEV back to the forefront of disease surveillance.

WEEV causes disease through a variety of factors. Its structural proteins play significant roles in its survivability and pathogenesis and include a capsid protein, a signal peptide (E3), an envelope glycoprotein (E2) that binds target receptors, another envelope glycoprotein (E1) that primarily functions to fuse the virus with the cellular membrane of the target cell, and a signaling peptide (6K) that may also function as a viroporin6. These structural proteins continue to be targets in WEEV vaccine research.

Target cell receptors of WEEV have historically included protocadherin 10 (PCDH10), Very Low-Density Lipoprotein Receptor (VLDLR), and apolipoprotein E receptor 2 (ApoER2), all of which are expressed by neurons in the CNS7. However, the binding affinity for these receptors has changed significantly over time and has played a role in the submergence of WEEV in North America. A newer strain of WEEV has, for example, lost the ability to bind mammalian PCDH10, but continues to bind avian PCDH107. This changing affinity for receptors across species keeps those that study WEEV on their toes and provides a sentinel for potential re-emergence of WEEV.

Conference discussion touched on some of these evolutions as part of the viral ecology that led to the 2024 resurgence of WEEV in South America. Rapid genetic changes, in concert with increased rainfall leading to booming mosquito populations, bird migrations providing ample reservoirs, lower vaccination rates against WEEV in horses, and surveillance gaps due to the disease being considered historic in South America all likely

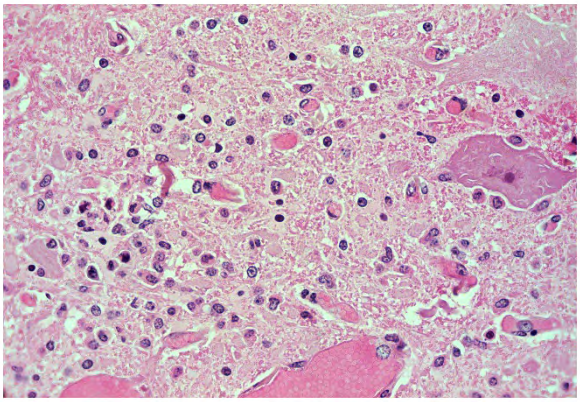

Figure 4-6: Cervical spinal cord, horse: The neuron to the right side of the image is shrunken, has angular cell borders and fading nucleus, and is surrounded by phagocytes that are in close contact to the cell body (satellitosis / early neuronophagia). There is increased cellularity due to inflammatory cell infiltration and gliosis in the adjacent neuropil. (HE, 400X). (Photo courtesy of: Instituto Nacional de Investigación Agropecuaria (INIA), La Estanzuela, Uruguay. www.inia.uy)

contributed to the outbreak and are a prime example of how rapidly deadly viruses can re-emerge in the face of ideal ecologic conditions.

References:

1. Albrieu-Llinás G, Gallardo R, Konigheim BS, et al. Arbovirus serosurvey (Orthobunyavirus, Flavivirus, and Alphavirus) in a draft horse population from Santa Fe, Argentina (2013-2016). *Arch Virol*. 2021;166(3):881–884.

2. Allison AB, Stallknecht DE, Holmes EC. Evolutionary genetics and vector adaptation of recombinant viruses of the western equine encephalitis antigenic complex provides new insights into alphavirus diversity and host switching. *Virology*. 2015;474:154-62.

3. Campos AS, Franco AC, Godinho F, et al. Molecular epidemiology of Western equine encephalitis virus in Brazil, 2023-2024. Version 1. medRxiv. Preprint 2024 Apr 18.

4. Cantile C, Youssef S. Nervous system. In: Maxie M.G., ed. Jubb, Kennedy, and Palmer's Pathology of Domestic Animals. Vol 1. 6th ed. St. Elsevier; 2016.

5. Delfraro A, Burgueño A, Morel N, et al. Fatal human case of Western equine encephalitis, Uruguay. *Emerg Infect Dis*. 2011;17(5):952–954.

6. Gauci PJ, Wu JQ, Rayner GA, Barabé ND, Nagata LP, Proll DF. Identification of Western equine encephalitis virus structural proteins that confer protection after DNA vaccination. *Clin Vaccine Immunol*. 2010;17(1):176-9.

7. Li W, Plante JA, Lin C. et al. Shifts in receptors during submergence of an encephalitic arbovirus. *Nature*. 2024;632: 614–621.

8. Mori E, Borges AS, Delfiol DJZ, et al. First detection of the equine herpesvirus 1 neuropathogenic variant in Brazil. *Rev Sci Tech Off Int Epiz*. 2011;30(3):949–954.

9. Rech R, Barros C. Neurologic diseases in horses. *Vet Clin North Am Equine Pract*. 2015;31(2):281–306.

10. Rosa R, Costa EA, Marques RE, et al. Isolation of Saint Louis encephalitis virus from a horse with neurological disease in Brazil. *PLoS Negl Trop Dis*. 2013;7(11):e2537.

11. Silva ASG, Matos ACD, da Cunha MACR, et al. West Nile virus associated with equid encephalitis in Brazil. *Transbound Emerg Dis*. 2019;66(1):445–453.

12. Silva ML, Galiza GJ, Dantas AF, Oliveira RN, Iamamoto K, Achkar SM, Riet-Correa F. Outbreaks of Eastern equine encephalitis in northeastern Brazil. *J Vet Diagn Invest*. 2011;23(3):570–575.

13. Silva Oliveira FA, Souza Castro RJ, de Oliveira JF, et al. Geographical and temporal spread of equine rabies in Brazil. *Acta Trop*. 2022;227:106302.

14. Steele KE, Twenhafel NA. Review Paper: Pathology of animal models of alphavirus encephalitis. *Vet Pathol*. 2010;47:790.

15. Wobeser BK, Godson DL, Rejmanek D, Dowling P. Equine protozoal myeloencephalitis caused by *Neospora hughesi* in an adult horse in Saskatchewan. *Can Vet J*. 2009;50(8):851–853.

16. World Health Organization. Disease outbreak news. Western equine encephalitis - Argentina. December 28, 2023. Accessed June 5, 2024.

17. World Health Organization. Disease outbreaks news. Western equine encephalitis - Uruguay. February 8, 2024. Accessed June 5, 2024.

Joint Pathology Center
Veterinary Pathology Services

WEDNESDAY SLIDE CONFERENCE 2025-2026

Conference #2 27 August 2025

CASE I:

Signalment:
28-year-old male castrated domestic pony *(Equus ferus caballus)*

History:
A pony from a zoo in Michigan was diagnosed with choke on January 17th, 2020. On January 22nd, endoscopy was performed, an esophageal tear was suspected, and the animal was treated with Uniprim, procaine penicillin G, and phenylbutazone. The pony became febrile with a 103˚F temperature and had multiple abscesses in the cervical area on ultrasound exam. The pony died with respiratory distress on January 28th when loaded on to the trailer for travel for repeat endoscopy.

Gross Pathology:
There was a 3 cm x 1.5 cm x 3.5 cm focal concretion of caseous material in the right serratus ventralis cervicis muscle. Fifteen to twenty multifocal similar lesions ranging from 6 cm x 0.75 cm x 0.5 cm to 2 mm x 2 mm x 1 mm were scattered throughout the cervical musculature. A 60 cm segment of serosa and tunica muscularis of the mid-esophagus was mottled black to purple. In the center of this affected area was a large cavitary space that extended approximately 10 cm into the surrounding cervical musculature and contained approximately 2 L of a suppurative exudate. The muscle surrounding the cavitary space was multifocally dark black and necrotic. There was no gross evidence of mucosal alterations in the esophagus, and no exudate was observed.

Laboratory Results:
PCR *for Acanthamoeba sp., Balamuthia mandrillaris*, and *Naegleria fowleri* were negative. Aerobic culture yielded growth of moderate

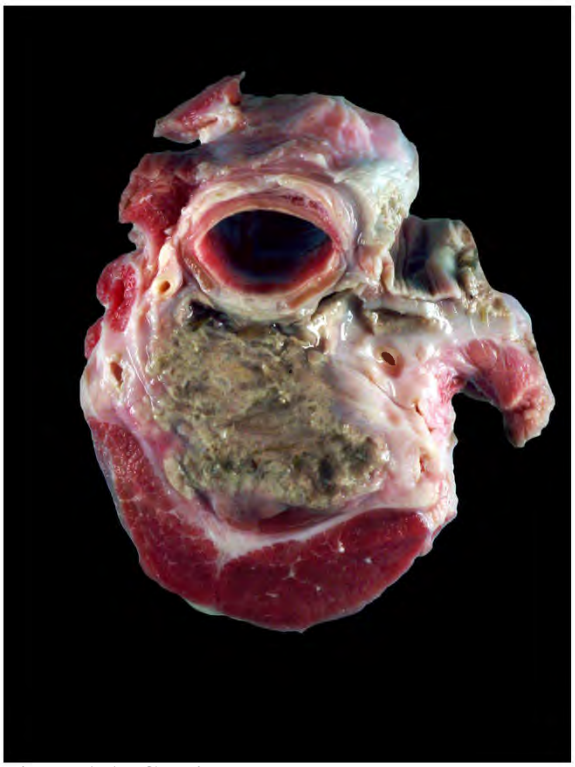

Figure 1-1: Cervical skeletal muscle, pony. There was a 3 cm x 1.5 cm x 3.5 cm focal concretion of caseous material in the right serratus ventralis cervicis muscle. (Photo courtesy of: Michigan State University, Veterinary Diagnostic Laboratory - Michigan State University, https://cvm.msu.edu/pdi; Veterinary Diagnostic Laboratory, https://cvm.msu.edu/vdl).

Actinobacillus spp, few *Escherichia coli*, and numerous *Actinomyces spp*. Anaerobic culture yielded numerous *Bacteroides pyogenes*, moderate *Fusobacterium necrophorum*, and numerous *Porphyromonas sp*. PCR for *Streptococcus equi* was negative.

On cytology, there were large numbers of degenerate neutrophils. A heterogeneous population of extracellular bacterial rods and cocci, including some long filamentous rods, were either individualized or arranged in large aggregates. There were few round to oval organisms measuring approximately 1.5-2X the diameter of a neutrophil with a small purple eccentric nucleus and lightly to moderately basophilic cytoplasm that contained few clear vacuoles.

Microscopic Description:
In multiple sections of cervical skeletal muscle, there were vast areas of liquefactive necrosis comprised of eosinophilic amorphous material, degenerated neutrophils and karyorrhectic debris. Within areas of necrosis were myriads of round amoebic trophozoites that were approximately 15um in diameter with a pale finely vacuolated to granular basophilic cytoplasm and eccentric eosinophilic 2-3um in diameter nucleus with a central karyosome and peripheralized chromatin. These organisms were variably degenerated. There were also numerous colonies of bacterial cocci and bacterial rods. Rimming these areas of necrosis was a band of degenerate neutrophils surrounded by a dense band of mature granulating fibrosis with fewer admixed lymphocytes, plasma cells, and histiocytes. Vessels in these areas were lined by plump reactive endothelium. Bands of fibrosis and lymphoplasmacytic inflammation extended into the skeletal muscle separating myofibers. Myocytes were multifocally shrunken and hypereosinophilic with loss of cross striation.

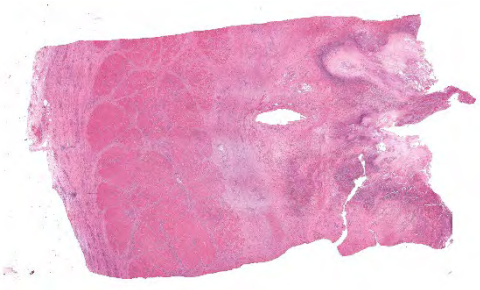

Figure 1-2: Cervical skeletal muscle, pony. A section of skeletal muscle is submitted for examination. There is a large area of coagulative necrosis with viable but highly inflamed necrotic muscle surrounded by a dense fibrous capsular. (HE, 10X)

Contributor's Morphologic Diagnoses:
Cervical muscle: Subacute, severe, locally extensive, necrotizing myositis with intralesional extracellular trophozoites, bacterial cocci, and bacterial rods.

Contributor's Comment:
Amoebic myositis has rarely been reported in humans and animals and has only been associated with *Entamoeba sp*.[2,4,12,16] In the two human cases, rupture of liver abscesses, perforation of intestines, or hematogenous or lymphatic spread of the organisms was the suspected route of infection.[12,16] In these two cases, the amoebic myositis was caused by infections with *Entamoeba histolytica*, and in a single case in a monitor lizard, myositis was caused by *Entamoeba invadens*.[2,12,16] In the monitor lizard, direct infection of a wound and hematogenous spread were determined to be the source of infection.[2] Primary amoebic myositis has not previously been reported in horses and *Entamoeba sp.* has not been demonstrated as a primary pathogen in horses.[3,6]

Entamoeba sp. generally are a nonpathogenic commensal organism; however, they occasionally cause disease in animals that are immune suppressed, have concurrent disease, or experience a dramatic change in their intestinal flora.[16] *Entamoeba equi* has been identified in the intestines of horses; but has not

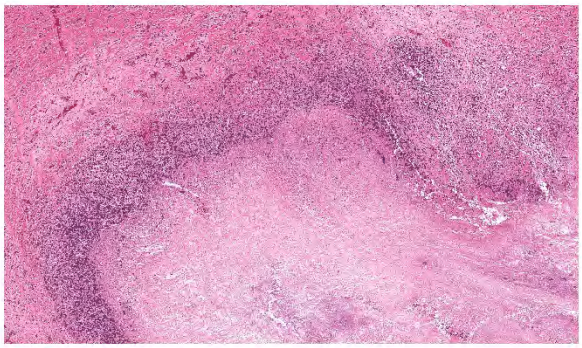

Figure 1-3: Cervical skeletal muscle, pony. An area of coagulative necrosis (right) is surrounded by a dense band of viable and necrotic neutrophils admixed with cellular debris. (HE, 61X)

been associated with clinical disease.[3,6] In animal species, the most commonly reported pathogenic entamoeba species are *Entamoeba histolytica* in primates and rarely dogs and cats, and *Entamoeba invadens* in reptiles.[11,12,17]

In humans and primates, *Entamoeba histolytica* is considered a primary pathogen that causes gastrointestinal disease and is spread via the fecal-oral route.[5] Clinical signs include bloody diarrhea, and the disease is responsible for 70 thousand human deaths a year.[5] The trophozoites are located in the large intestine, and can spread through the intestinal wall leading to hematogenous spread.[5] Entamoebic cysts are excreted in stool, and are ingested by the new host via contaminated food or water.[5] Similarly, *Entamoeba invadens* is a major pathogen in reptilian species and can cause severe necrotizing hepatitis and enterocolitis in various snake species and chelonians.[11,12]

The pathophysiology of Entamoeba-associated diseases is linked to the important virulence factor in *Entamoeba sp.,* the galactose and *N*-acetyl D-galactosamine (Gal-GalNAc) adherence lectin. This lectin allows the parasite to bind to the exposed Gal-GalNAc residues on the target cell glycoproteins.[5] *Entamoeba sp.* also form an amebapore, which is a channel-forming peptide.[5] Once inserted into the target cell, this pore allows water and ions to enter the cell leading to lysis. *Entamoeba sp.* also produces cysteine proteases,[5] which break down the extracellular matrix allowing for invasion of the organism.[5]

The suspected source of infection in the submitted case is a contaminated wound or injection site. The grossly observed white, inspissated material in multifocal areas of cervical muscle appeared microscopically as pools of pale eosinophilic crystalline material and most likely represent old injection sites. Clinically, an esophageal tear secondary to choke was suspected which may have represented a possible site of infection; however, no evidence of an acute or healing tear was observed grossly. Opportunistic infections of free-living amoeba have been reported in horses causing pneumonia, encephalitis, and placentitis.[1,7,8] Considering the unusual location of the infection, a free-living amoeba was suspected as the cause of myositis; however, *Acanthamoeba sp.*, *Balamuthia mandrillaris*, and *Naegleria fowleri* were excluded by PCR on formalin fixed paraffin embedded tissue.[10] The water from the facility was also tested for free-living amoeba as there was concern for potential infections of other exotic species. No organisms were found in the tested water sample. Regardless, the histologic appearance of the trophozoites is most consistent with *Entamoeba sp.* as the nuclei have a central karyosome and peripheralized chromatin clumps.[17] We were unable to confirm this by PCR as the available test was limited to fresh material due to the large size of

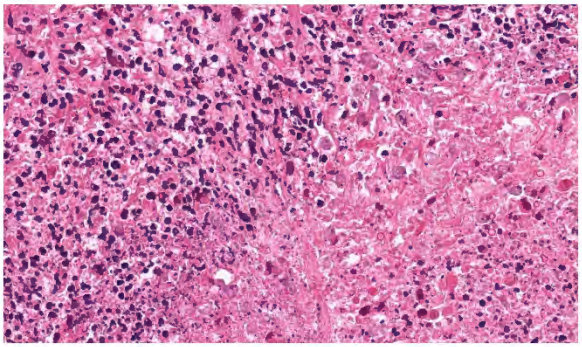

Figure 1-4: Cervical skeletal muscle, pony. Within the area of coagulative necrosis, there are numerous amebic trophozoites (arrows). (HE, 766X)

the PCR target. Further characterization with additional primers or submission of fresh material for additional testing could not be performed due to the COVID-19 pandemic. A large component of the infection in this case was also bacterial. Organisms cultured in this case such as *Fusobacterium sp., Bacteroides sp. and Actinomyces sp.* are commonly associated with necrotizing myositis.[4] Overall, the necrotizing myositis is suspected to be due to a combination of the effects of these bacteria and the *Entamoeba sp.*

Contributing Institution:
Michigan State University
Veterinary Diagnostic Laboratory
4125 Beaumont Road
Lansing MI 48910

JPC Diagnoses:
Skeletal muscle: Rhabdomyositis, necrotizing, chronic-active, focally extensive, severe, with numerous amoebic trophozoites.

JPC Comment:
Kicking off the second conference in this year's lineup is the Joint Pathology Center's very own Dr. Bruce Williams! (Please hold your applause until the end.) Supplemented by an excellent contributor write-up and an AI-generated image of a psychedelic "ant-amoeba" (courtesy of Dr. Williams; please don't hesitate to contact him for this image as it is truly… something), this case made for a tough diagnostic challenge for conference participants. Who would have thought *Entamoeba sp.* in a pony's neck!?

Conference discussion focused on the five "famous amoebae" that pathologists should have mentally filed away for a rainy day, which are *Entamoeba histolytica*, *Entamoeba invadens*, *Balamuthia mandrillaris, Naegleria fowleri*, and *Acanthamoeba spp*. In addition, participants were put through their paces to name the primary species affected, organs affected, and diseases caused by these five. The main morphologic differences between a protozoal trophozoite and a protozoal cyst were covered and can be distilled down to trophozoites having more indistinct cell borders, a single nucleus, and exhibiting phagocytosis whereas cysts are round with distinct borders and 4+ nuclei. A rather unfortunate reference was made to the fact that, in humans, amoebic abscesses used to be called "anchovy paste abscesses", which is something that absolutely no one needed to be informed of…. ever. The last point of discussion was generated by a question from a conference participant asking why a karyosome is called such when it so closely resembles a nucleolus? To answer that inquiry, a nucleolus is a membrane-bound organelle in the nucleus of a cell responsible for making ribosomal RNA (rRNA) and producing ribosomes. A karyosome, by contrast, is a clustered bunch of chromatin and protein found within the nucleus and is often associated with the nucleolus. Hypothetically, they should sometimes both be able to be seen histologically within amoebic trophozoites.

There are scattered reports of amoebic infection in horses primarily involving "free-living" amoeba species, in particular *Acanthamoeba* and *Balamuthia* spp.[8] However, *Entamoeba histolytica* and *E. moshkovskii* have also been reported to cause severe disease, and these have both been isolated in rare cases from horses. *E. histolytica*, the most widely studied member of its species

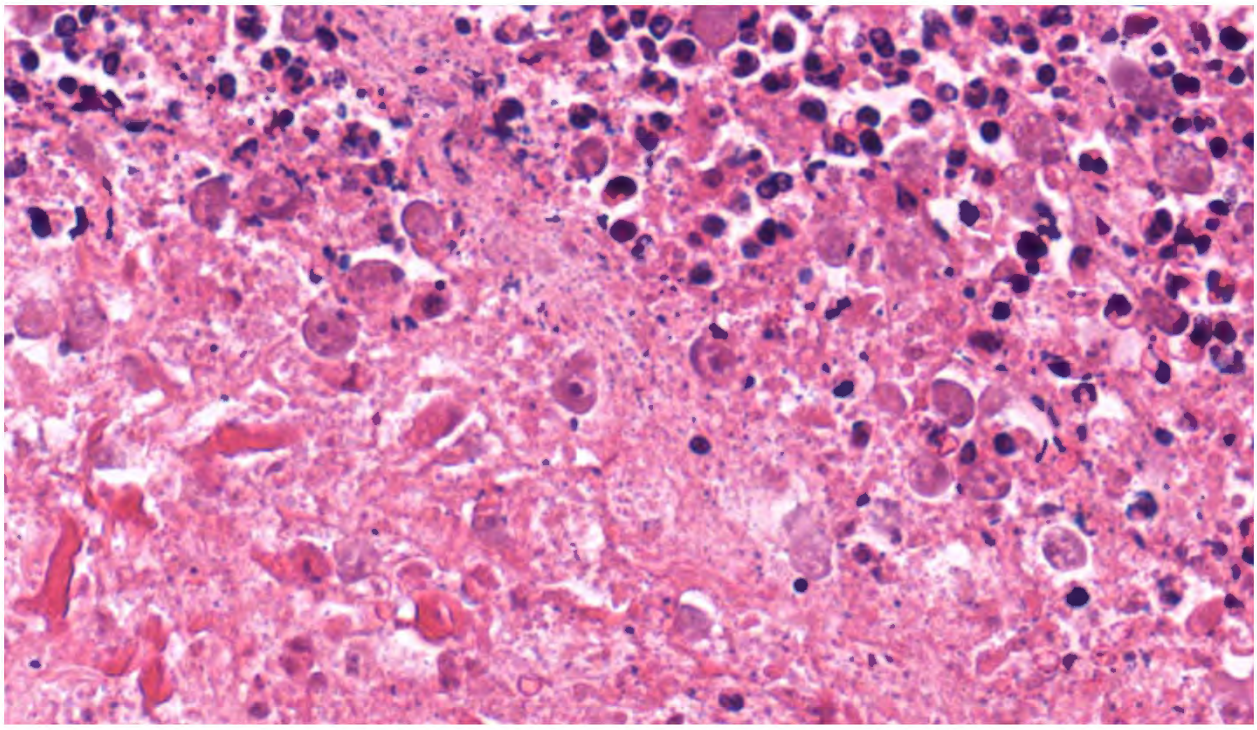

Figure 1-5: Cervical skeletal muscle, pony. High magnification of amebic trophozoites within the area of necrosis. (HE, 1316X

that most notably affects humans and non-human primates, is equipped with a variety of nasty virulence factors that enable it to cause devastating disease in its host. As a generality, most *Entamoeba sp.* are non-pathogenic, lacking the same virulence factors as pathogenic *Entamoeba sp*. Even pathogenic *Entamoeba sp*. don't generally cause issues unless there is a drastic change in the host's gastrointestinal microflora, which are the primary nutrient source for *Entamoeba sp.* within the host. If that happens, all bets are off. Think of these pathogenic *Entamoeba sp.* as tiny, living bombs with anger management problems that are kept docile only by giving them their favorite foods to eat…if they no longer can feed on those preferred bacteria, they exist the GI lumen by invading the intestinal walls and, in a blind rage, start blowing up everything in their paths. From there, they can go wherever the vascular system takes them.

The virulence factors that allow them to do so include the Gal/GalNAc lectin, which is a protein that allows the *Entamoeba* to adhere to host cells, including erythrocytes and GI epithelial cells, and the protective mucus layer of the GI tract.[17] The Gal/GalNAc lectin is the primary determinant in *Entamoeba*'s ability to invade tissues[9]. Additionally, it has pore-forming peptides known as "amoebapores" that the *Entamoeba* shoves into 7host cell membranes, resulting in cell lysis.[9,17] Amoebapores are basically the offensive, single-protein, protozoal version of our own multi-protein, defensive complement cascade. This amoebapore enables the *Entamoeba* to kill host cells and invade tissues.[9] Once within the

tissue, *E. histolytica* secretes a variety of cysteine protease (CPs) enzymes that degrade host tissue components, including intestinal mucus and extracellular matrix.[9] Specific CPs have been linked to pathogenicity, such as CP5 in humans, which enables the induction of apoptosis in host target cells. In the face of all this destruction, the host immune system utilizes, among other things, oxidative stress to try and fight off the invaders. However, *Entamoeba histolytica* has an uncanny ability to resist oxidative stress by using a combination of antioxidant enzymes, such as peroxiredoxin and superoxide dismutase, and by making metabolic shifts towards glycerol and chitin biosynthesis, both of which are additionally protective against free O_2 radicals[13]. Finally, as if this protozoon needed any additional advantages, *Entamoeba histolytica* engages in "trogocytosis", in which the trophozoite ingests small "bites" of living host cells. It then processes and displays host cell membrane proteins on its own surface, which function like a cloaking device and gives the *Entamoeba* a +10 stealth boost against host immune cells. With all these virulence factors primed for pure devastation, it should come as no surprise

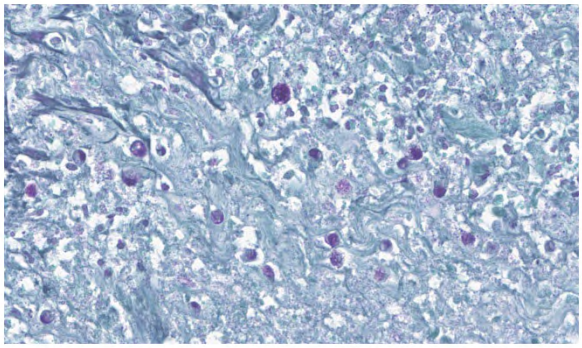

Figure 1-6: Cerebrum, horse: A PAS stain helps to highlight the location of amebic trophozoites. (PAS with malachite green counterstain (PASG), 1271X)

that the National Institute of Allergy and Infectious Diseases (NIAID) classifies *E. histo lytica* as a category B priority biodefense pathogen.

The contributor made note that they also cultured three different bacteria from this case: *Fusobacterium necrophorum, Actinomyces sp.,* and *Bacillus fragilis*. Each of these bacteria is considered an opportunistic commensal, and conference participants largely regarded them and their potential effects as secondary to the damage wrought by the *Entamoeba*. However, they're worth briefly discussing.

F. necrophorum, once inoculated into an anaerobic environment (such as an area of necrosis), can cause devastating lesions via multiple virulence factors, including a leukotoxin, endotoxin, haemolysin, haemagglutinin, and adhesin. Among these, leukotoxin and endotoxin are believed to be the more important toxins in overcoming the host's defenses[15]. *F. necrophorum* is frequently seen in mixed infections and synergisms between it and other pathogens are considered important in causing disease. *Bacillus fragilis*, now known as *Bacteroides fragilis*, which usually resides in the intestines, is a common cause of peritonitis and sepsis from intestinal integrity issues or diseases, including post-operative complications.[19] It, too, has multiple virulence factors at its disposal, such as fragilysin (also known as BFT, or *Bacteroides fragilis* toxin), capsular polysaccharides that promote abscess formation, make the bacteria more resistant to degradation, and increasing bacterial aggregation, as well as several enzymes, including hyaluronidase, chondroitin sulfatase, deoxyribonuclease, proteases, phosphatases, and lipases, which allow attack and penetration of the

host's extracellular matrix.[19] The production of hemolysins is thought to facilitate access of *B. fragilis* to iron and heme *in vivo* via damaged host cells and erythrocytes. Lastly, and showing up empty-handed to the community potluck of devastation, is *Actinomyces sp*. *Actinomycosis* infections are usually polymicrobial and they are generally considered opportunistic bystanders, with few notable exceptions, who don't really contribute much but get to reap the benefits of just being there. All in all, it was the opinion of conference participants that *Entamoeba* was the star of this show, followed around by three enthusiastic bacterial groupies to cause the worst case of "not-actually-choke" choke ever.

References:

1. Begg AP, Todhunter K, Donahue SL, Krockenberger M, Slapeta J. Severe amoebic placentitis in a horse caused by an *Acanthamoeba hatchetti* isolate identified using next-generation sequencing. *J Clin Microbiol.* 2014:52(8):3103-3104.
2. Chia MY, Jeng CR, Hsiao SH, Lee AH, Chen CY, Pang VF. *Entamoeba invadens* myositis in a common water monitor lizard (*Varanus salvator)*. *Vet Pathol.* 2009; 46:6733-676.
3. Clark CG, Kaffashian F, Tawari B, et al. New insights into the phylogeny of Entamoeba species provided by analysis of four new small-subunit rRNA genes. International Journal of Systemic and Evolutionary Microbiology. 2006;56:2235-2239.
4. Crum-Cianflone NF. Bacterial, fungal, parasitic, and viral myositis. Clin Microbiol Rev. 2008;21(3)473-494.
5. Espinosa-Cantellano M and Martinez-Palomo A. Pathogenesis of intestinal amebiasis: From molecules to Disease. Clin Microbiol Rev. 2000; 13(2)318-331.
6. Jacob AS, Busby EJ, Levy AD, Komm N, Clark CG. Expanding the Entamoeba universe: New hosts yield novel ribosomal lineages. J Eukaryot Microbiol. 2016;63:69-78.
7. Kinde H, Read DH, Daft BM, et al. Infections caused by pathogenic free-living amebas (Balamuthia mandrillaris and Acanthamoeba sp.) in horses. J Vet Diagn Invest. 2007;19:317-322.
8. Kinde H, Visvesvara GS, Barr BC, Nordhausen RW, Chiu PWH. Amebic meningoencephalitis caused by Balamuthia mandrillaris (leptomyxoid ameba) in a horse. J Vet Diagn Invest. 1998;10:378-381.
9. Nakada-Tsukui K, Nozaki T. Immune Response of Amebiasis and Immune Evasion by Entamoeba histolytica. Front Immunol. 2016 May 12;7:175.
10. Norgan AP, Sloan LM, Pritt BS. Detection of Naegleria fowleri, Acanthomoeba spp, and Balamuthia mandrillaris in formalin-fixed, paraffin-embedded tissues by real-time multiplex polymeras chain reacton. Am J Clin Pathol. 2019;152:799-807.
11. Ossiboff RJ. Serpentes. In: Terio KA, McAloose D, St. Leger J, ed. Pathology of Wildlife and Zoo Animals. 1st ed. London, UK: Academic Press.
12. O'Leary C and Finch R. Amoebic psoas and liver abscesses. Postgrad Med J. 1992;68:972-973.
13. Rastew E, Vicente JB, Singh U. Oxidative stress resistance genes contribute to the pathogenic potential of the anaerobic protozoan parasite, Entamoeba histolytica. Int J Parasitol. 2012;42(11):1007-15.
14. Rodriguez CE, Duque AMH, Steinberg J, Woodburn DB. Chelonia. In: Terio KA, McAloose D, St. Leger J, ed. Pathology of Wildlife and Zoo Animals. 1st ed. London, UK: Academic Press.
15. Tan ZL, Nagaraja TG, Chengappa MM. Fusobacterium necrophorum infections: virulence factors, pathogenic mechanism

and control measures. Vet Res Commun. 1996;20(2):113-40.
16. Tetiker T, Sert M, Tuncer I, et al. An unusual amebic localization on the right hip. Infection. 1995; 23:124-125.
17. Uzal FA, Plattner BL, Hostetter JM. Alimentary system. In: Maxie MG, ed. Jubb, Kennedy and Palmer's Pathology of Domestic Animals. 6th ed. Vol 2. St. Louis, MO: Elsevier
18. Yanagawa Y, Sharma M, Izumiyama S, Singh U. Exploring virulence and stress response in *Entamoeba histolytica*: insights from clinical strains. *Microbiol Spectr*. 2025;13(7):e0050625
19. Yekani M, Baghi HB, Naghili B, Vahed SZ, Sóki J, Memar MY. To resist and persist: Important factors in the pathogenesis of Bacteroides fragilis. *Microb Pathog*. 2020;149:104506.

CASE II:

Signalment:
10 year old male rhesus macaque (*Macaca mulatta*)

History:
This animal was received from a U.C. Davis colony in October of 2018, and was subsequently used on malaria and dengue studies. The last routine physical performed in December 2023, where it was noted that this animal was missing the tips of the left and right pinna, and there was unspecified dental disease.

During 02 February 2024 cage-side rounds examination, this animal was noted to be staring at a resident too intently, and a sedated exam was elected to investigate further. Moderate abdominal distention was noted when the animal was placed in dorsal recumbency. A firm bladder was palpated on physical exam, and animal caretakers noted that there was low urine production for this animal. Ultrasound and radiographs showed a large bladder with no obvious blockage, and medical management was elected over the weekend.

Figure 2-1: Presentation, rhesus macaque. The animal had significant abdominal distention. (Photo courtesy of: Walter Reed Army Institute of Research).

On 05 February 2024, this animal's clinical signs persisted, and a cystotomy was performed. A large amount of friable, tan-brown irregularly shaped to molded round material was removed from the urinary bladder. The material had a foul odor and was suspected to have a significant bacterial component. The luminal material was sent for culture and sensitivity, a section was used to make a smear cytology, and H&E slides. The results of preliminary diagnostics are below.

This animal recovered, and approximately one month later was euthanized as part of a protocol and was submitted for necropsy. The submitted slides were created from materials collected at necropsy.

Gross Pathology:
There is moderate abdominal distension in dorsal recumbency. Lateral radiographs show a moderate amount of heterogenous material at the cranial aspect of the urinary bladder, having irregular margins and poor contrast against surrounding tissue. Urinary catheter placement was difficult due to suspected narrowing of the urethra. Contrast material

Figure 2-2: Urinary bladder, rhesus macaque. At cystotomy, a large amount of friable material was removed from the bladder. (Photo courtesy of: Walter Reed Army Institute of Research).

did not uniformly highlight the margins of the urinary bladder. A 60 cc syringe was used to remove normal colored urine from the distended urinary bladder.

Gross examination of the urinary bladder during exploratory surgery revealed congested serosal vessels, and mild erythema of the detrusor muscle. The urinary bladder wall is markedly thickened at approximately 1 cm thickness. There is multifocal friable, irregularly tan-brown material in the lumen of the urinary bladder, which emits an odor consistent with bacterial infection.

On subsequent necropsy, there is approximately 20 mL of blood in the abdomen. There are multifocal adhesions from the lateral and ventral aspect of the urinary bladder to the body wall. The urinary bladder appears mildly thickened. There is tan-brown irregular friable material within the lumen of the urinary bladder, and the urothelial mucosa is characterized by mild multifocal petechial hemorrhage.

Laboratory Results:

Cytology: These good quality, moderately cellular cytologic specimens contain mature sperm, rafts of 1-2 µm basophilic cocci, 1-2 µm x 1 µm bacilli, aggregates of extracellular matrix, infrequent macrophages, and necrotic material, overlying a faintly basophilic proteinaceous background. Sperm most often consist of only the head, with acrosome surrounding a variably intact nucleus, and measuring approximately 3 µm x 4 µm, with a polar oriented basophilia. Numerous sperm also contain the centriole and tail intact. Macrophages most often have abundant cytoplasm densely packed with cocci and bacilli, and few have multiple peripheralized nuclei (multinucleated giant cells).

A coagulum of material was processed for routine H&E evaluation. Multifocal colonies

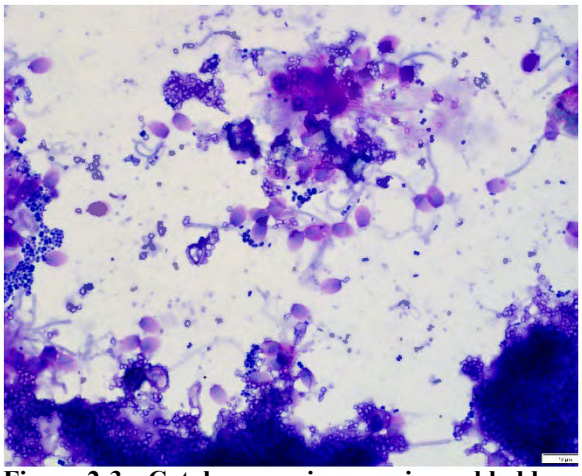

Figure 2-3: Cytology specimen, urinary bladder contents, rhesus macaque. Specimens contain mature sperm, rafts of 1-2 µm basophilic cocci, 1-2 µm x 1 µm bacilli, aggregates of extracellular matrix, infrequent macrophages, and necrotic material, ona a faintly basophilic proteinaceous background. Sperm most often consist of only the head. (*Photo courtesy of:* WRAIR).

of gram-positive coccobacilli are visualized embedded in the extracellular proteinaceous material.

Culture and initial identification was performed using MALDI. The isolate was small, pleomorphic, gram positive bacilli that are catalase positive and oxidase negative. An initial identification of *Corynebacterium confusum* was made.

Sensitivity testing indicated the following:

Antimicrobial	Result
Tetracycline	S
Levofloxacin	R
Amoxicillin Clavulanic Acid	S
Erythromycin	S
Chloramphenicol	NA
Nitrofurantoin	NA
Sulfamethoxazole Trimethoprim	NA
Oxacillin	R
Ciprofloxacin	R
Vancomycin	S
Cefazolin	S
Clindamycin	NA
Gentamicin	S
Polymyxin B	I

S: Sensitive; I: Intermediate; R: Resistant

After whole genome sequencing, the isolate was identified as *Corynebacterium renale*.

Microscopic Description:
Occupying approximately 90% of the markedly dilated prostatic urethra is a round, 13 mm diameter cross section of a heterogenous plug, composed of eosinophilic extracellular protein, variably mature fibrin, collagen, and numerous macrophages surrounding or centered on spermatids. The fibrin and collagen vary from compact, to basketweave appearance, and there is multifocal mineralization.

The prostatic urothelium is attenuated, with multifocal ulceration. Multifocal degenerating urothelial cells are characterized by moderate to marked cytoplasmic vacuolation, with neutrophils transmigrating the urothelium. The underlying lamina propria has multifocal to coalescing hemorrhage, edema, and perivascular to diffuse neutrophilic urethritis. Multifocal myocytes are characterized by hypereosinophilia, sarcoplasmic vacuolation, and/or pyknotic nuclei.

The glands of the ventral prostate are multifocally ectatic, occasionally filled with eosinophilic proteinaceous material admixed with necrotic neutrophils and macrophages. Glandular epithelial cells are multifocally attenuated, vacuolated (degenerate), or necrotic, with multifocal neutrophilic inflammation surrounding glands and overlying regions of increased fibrosis. There are multiple corpora amylacea within glands.

Contributor's Morphologic Diagnoses:
1. Prostatic urethra: Plug, proteinaceous, with urethral dilatation, moderate neutrophilic urethritis, moderate multifocal hemorrhage, and smooth muscle degeneration and necrosis.
2. (Not submitted) Urinary bladder: Cystitis, neutrophilic and eosinophilic, multifocal to coalescing, acute, mild, with urothelial de

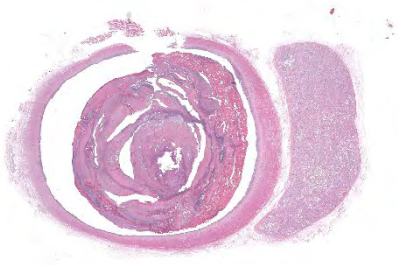

Figure 2-4: Prostatic urethra, rhesus macaque. The prostatic urethra is markedly dilated and occluded by a non-adherent lamellated proteinaceous plug. (HE, 8X)

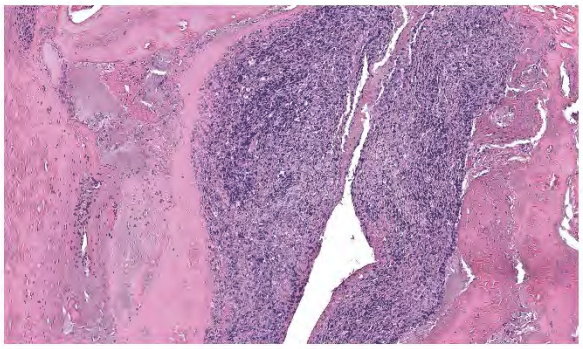

Figure 2-5: Prostatic urethra, rhesus macaque: The plug is composed of islands of intact and degenerating spermatids, inflammatory cells and abundant eosinophilic protein and fibrin. (HE, 311X)

generation and erosion, edema, and retrograde ejaculation coagulum.
3. (Not submitted) Seminal vesicle: Dilation, multifocal, mild, with multifocal aggregates of sperm.
4. (Not submitted) Kidney, left; kidney, right: Dilation, renal pelvis, moderate, with papillary necrosis, tubular epithelial necrosis, and dilation of Bowman's space.
5. Ventral prostate: Prostatitis, lymphocytic and neutrophilic, multifocal, moderate, with multifocal corpora amylacea, and regional glandular ectasia.
6. (Not submitted) Testis, seminiferous tubules: Degeneration, multifocal, moderate, with moderate ectasia.

Contributor's Comment:

Retrograde ejaculation cystolithiasis is an uncommon, but previously reported, affliction of nonhuman primates. This condition has been associated with repeated electroejaculation events; however, spontaneous disease has also been reported, as in this case.[3] In most cases, clinical signs include stranguria, dysuria, hematuria, lethargy, and distended abdomen. This animal was fortunate to have forged a close relationship with the residents and communicated his distress non-verbally.

In the 1985 seminal work on electrostimulation and penile erection, it was shown that in canines and macaques (pigtail and Rhesus) the spinal nucleus responsible for erection is the mediolateral autonomic neurons in the T_{12}-L_3, and S_1-S_3 locations. However, stimulation of these nerves does not generally result in ejaculation.[5] During normal ejaculation, there are two physiologically synchronized events controlled by sympathetic nerves. Emission and expulsion of ejaculate are distinct processes, and even minor alterations may adversely affect the animal. The expulsion process requires both urethral and penile muscle tissue to contract, allowing for the correct flow of fluid. If the internal urethral sphincter in the urinary bladder does not contract completely, reflux of fluid may occur and is called retrograde ejaculation. Retrograde ejaculation has been reported in numerous domestic species, as well as non-human primates. However, in non-human primates, the condition has most often been associated with electroejaculation, likely caused by asynchronous stimulation of nerve bundles. In these primates, the deposition of coagulum in the posterior urethra results in continued retrograde flow of semen into the urinary bladder. This has been reported in Rhesus macaques (*Macaca mulatta*) and cynomolgus macaques (*Macaca fascicularis*)[1], though usually without cystolithiasis in cynomolgus monkeys.[4]

The composition of semen impacts the possible degree of compromise in these cases. Ejaculate is comprised of sperm suspended in a fibrinous material produced by the accessory sex glands. The consistency of ejaculate changes based on the balance of coagulation and fibrinolytic factors present, and different ratios exist for different species. In humans,

the balance of fibrinogen, factor VIII:c, plasminogen, antithrombin III, fibrin monomers, and plasminogen activator inhibitor-1 is critical, and altered ratios of D-dimer/thrombin-antithrombin-III ratios have been detected post-vasectomy and in some cases of involuntary infertility.[8] For the human patient, after discharge from the urethra, semen normally takes on a gelatinous consistency, but will turn to liquid again after 3 to 30 minutes.[7] This is due to fibrinolysin contributed by the prostate, and this degradation does not occur in Rhesus macaques due to lower fibrinolytic activity and no fibrinolysin.[3]

In this animal, there was no history of electroejaculation. However, also considered were conditions that affect the competency of the urethral sphincter, and included congenital malformation, spinal cord damage or disease, previous urinary bladder surgery, or chronic inflammation. This event appears to be idiopathic, with no predisposing cause identified.

Unfortunately for this animal, a concurrent bacterial infection colonized the proteinaceous coagulum. There was spirited debate about the order in which events took place, and a primary bacterial infection leading to retrograde ejaculation cystolithiasis cannot be definitively excluded. However, the specific location of the plug and accompanying clinical signs support a primary retrograde ejaculation cystolithiasis with secondary bacterial infection. Regardless of event order, the observed cystitis and hydronephrosis are common findings accompanying cystolithiasis and urinary obstruction.

Contributing Institution:
Walter Reed Army Institute of Research
Silver Spring, MD

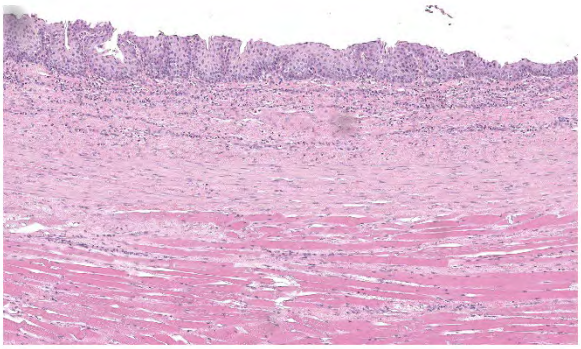

Figure 2-6: Prostatic urethra, rhesus macaque. High magnification of spermatozoa embedded within the urethral plug. (HE, 1500)

JPC Diagnoses:
Prostatic urethra: Seminal plug, chronic, with diffuse, mild, neutrophilic and eosinophilic urethritis and skeletal muscle atrophy.

JPC Comment:
The contributor provides a thorough overview of this entity in non-human primates in their comment! Conference discussion touched on several important topics mentioned in the contributor's write-up, as well as provided a review of the differences in terminology between spermatids, spermatozoa, and sperm. Spermatids are the developing, immature form of spermatozoa. Spermatozoa are the mature form that has an acrosome and a tail. The term "sperm" refers to the whole ejaculate that contains spermatozoa and other fluid components.

Another species in which a similar condition occurs is mice. Known as Mouse Urologic Syndrome (MUS), it is characterized as an obstructive genitourinary condition in male mice resulting from a urethral blockage composed of a white-yellow protein-rich plug resembling seminal vesicular gland secretions (the copulatory plug). Histologically, these plugs are composed of a proteinaceous coagulum with mixed inflammatory cells, spermatozoa,

and sloughed urothelial cells, which can become impacted within the urethral bulb, urethra, or urinary bladder. This can lead to urinary bladder distension, edema, complete pelvic or penile urethral blockage, paraphimosis, penile ulceration, and/or lethal hydronephrosis.[6]

The flexed anatomy of the penis in male mice, along with the pressure placed on the urethra from surrounding tissues and the ability of the seminal fluids to rapidly coagulate to form the copulatory plug, are thought to be contributory to the formation of MUS.[6] Histologically, seminal coagulum plugs have been associated with urothelial erosion, congestion, and inflammation, which are consistent with prolonged pressure injury.[9] Certain strains of mice are more predisposed to the development of MUS than others, including the male epileptic EL strain, STR/1N[10] strain, and obese diabetic KK-A^{y} strain.[9] This study also found that there was an increased incidence of MUS with medetomidine-ketamine anesthesia in C57/B6 and mixed genetic background strains due to the release of seminal fluids during anesthetic events with these medications. When their protocol was altered to xylazine-ketamine, the mice did not develop MUS.[9]

Something to be aware of when diagnosing MUS is that careful consideration must be given to the presence of other confirmatory lesions outside of the presence of a urethral plug. It is well known that mice will also release agonal nonobstructive plugs during death, so differentiating these from obstructive antemortem plugs is crucial in the diagnosis of MUS.[6,9] In an effort to standardize their criteria, one study utilized the presence of histologic urethritis, clinical azotemia, and gross/histologic hydronephrosis or renal cortical dilation to help them diagnose MUS vs agonal secretion.[9]

As a closing "fun fact", one of Dr. Williams' rules of engagement for today's conference was that each case presenter had to bring him a fact about their assigned entity that he did not know. The presenter for this case successfully found such a fact and stated that other species that produce a copulatory plug include butterflies, spiders, scorpions, cats, kangaroos, and Madagascar hissing cockroaches. The more you know…

References:

1. Chandolia RK, Luetjens CM, Wistuba J, Semjonow A, Puhse G, Nieschlag E. Blockage of urine by intravesical ejaculate in cynomolgus monkeys. *J Med Promatol*. 2007;36:21-24.
2. Cline JM, Brignolo L, Ford EW. Urogenital System. In: Abee CR, Mansfield K, Tardiff S, Morris T, eds. *Nonhuman primates in medical research, Vol. 2*, 2nd Ed. San Diego, CA: Academic Press; 2012:p 494.
3. Colman K, Andrews RN, Atkins H, et al. International Harmonization of Nomenclature and Diagnostic Criteria (INHAND): Non-proliferative and proliferative lesions of the non-human primate (M. fascicularis). J Toxicol Pathol. 2021;34(3 Suppl):1S-182S.
4. Gumber S, Courtney CL, Strait KR, Sharma P, Freebersyser JE, Crane MM. Retrograde ejaculation associated spontaneous sperm cystolithiasis in four Rhesus Macaques (Macaca mulatta). Exp Toxicol Pathol. 2013. 65(0):1121-1125.
5. Lue TF, Schmidt RA, Tanagho EA. Electrostimulation and penile erection. Urol. Int. 1985;40:60-64.

6. Ninomiya H, Inomata T, Ogihara K. Obstructive uropathy and hydronephrosis in male KK-Ay mice: a report of cases. J Vet Med Sci. 1999 Jan;61(1):53-7.
7. Rasmussen J, Albrechtsen OK. Fibrinolytic activity in human seminal plasma. Fertility and Sterility. 1960;11(3):264-277.
8. van Wersch JW, de Vries-Hanje JC, Ubachs JM. Coagulation and fibrinolysis markers in seminal plasma of patients under evaluation for involuntary childlessness. Eur I Clin Chem Clin Biochem. 1992;30(8):467-71.
9. Wells S, Trower C, Hough TA, Stewart M, Cheeseman MT. Urethral obstruction by seminal coagulum is associated with medetomidine-ketamine anesthesia in male mice on C57BL/6J and mixed genetic backgrounds. J Am Assoc Lab Anim Sci. 2009;48(3):296-9.

CASE III:

Signalment:
3-year-old, male, African hedgehog, *Atelerix albiventris*

History:
The hedgehog was lethargic, with a history of decrease in water intake, respiratory distress, and anorexia. At clinical examination, the hedgehog was bradycardic, hypothermic, and with agonal breathing. Supportive care and treatment, including external warming, subcutaneous fluids and atropine, were given, without success. The hedgehog died of cardiac arrest and was submitted for postmortem examination.

Gross Pathology:
The hedgehog was in good body condition, with pale mucous membranes and distended abdomen. The spleen was severely enlarged, measuring 7.0 x 3.5 x 2.0 cm and weighing 6.52% of total body weight (reference interval: 0.1-2.47% of the body weight)[3], with multifocal to coalescent pale yellow to green areas (necrosis) interspersed with dark red areas (hemorrhage). The liver was also enlarged, with round borders, diffuse pale-yellow discoloration, and accentuated lobular pattern . The liver samples floated in 10% formalin. The kidneys exhibited multifocal well delimited and irregular tan

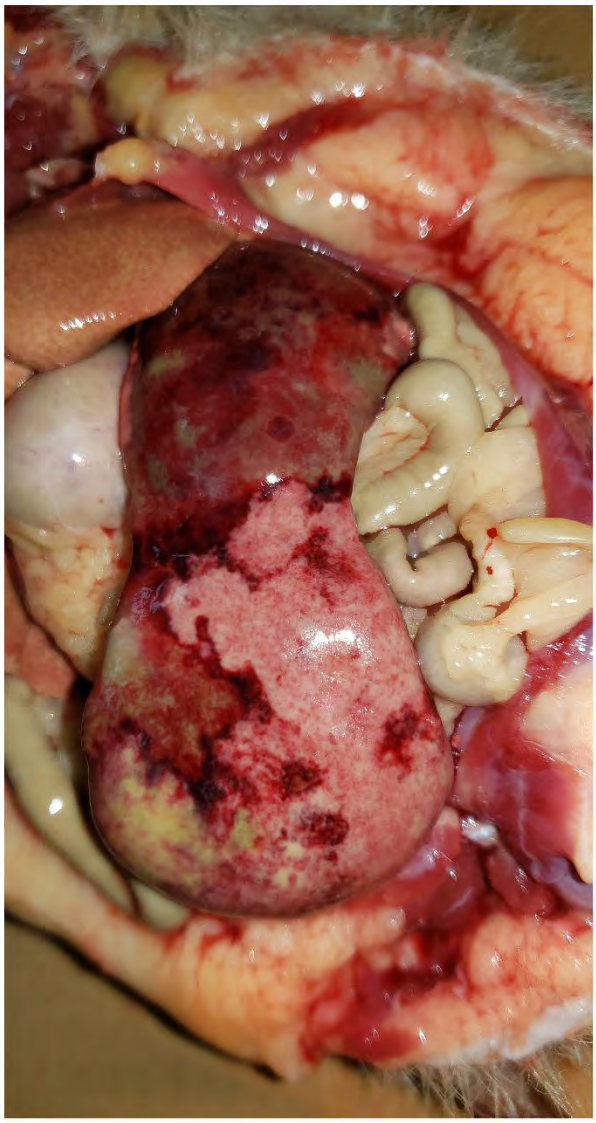

Figure 3-1: Abdominal viscera, hedgehog. The spleen is severely enlarged, weighing 6.52% of total body weight (reference interval: 0.1-2.47% BW), and pale with multifocal hemorrhage. (Photo courtesy of: Louisiana Animal Disease Diagnostic Laboratory (LAD

areas. In the distal region of the colon, a 2 mm diameter ulcer was observed in the mucosa, at 5 cm from the rectum.

Laboratory Results:
N/A

Microscopic Description:
The submitted slide has a section of lung, a section of kidney, and a section of liver. In the lung, a neoplastic population of immature and mature eosinophils expands the peribronchiolar and perivascular interstitial tissue and is present in the lumen of blood vessels including both larger vessels and capillaries in the alveolar septa. The neoplastic cells are of intermediate size, measuring approximately 1.5 to 2 times the size of erythrocytes, and have abundant lightly basophilic cytoplasm containing variable quantities of small, round, eosinophilic granules. The nucleus of the immature eosinophils ranges from round to reniform, with open chromatin and one prominent nucleolus. The mature eosinophils have similar cytoplasm, multilobulated nuclei, and inconspicuous nucleoli. There is mild anisocytosis and anisokaryosis. Mitoses are rare (1 to 2 figures per high power field). The pleura is lined by mildly hypertrophic mesothelial cells. In the renal interstitium, there are multifocal to coalescing, predominantly perivascular sheets of immature eosinophils and fewer mature eosinophils like those described in the lung. A few immature eosinophils are entrapped in glomerular capillaries. The renal tubules have occasionally attenuated epithelium and intraluminal eosinophilic proteinaceous fluid or casts. Multifocal mineral deposits are present in renal medullary tubules. An aggregate of immature and mature eosinophils is seen in the perirenal adipose tissue. In the liver, hepatocytes are diffusely swollen, with clear cytoplasmic vacuoles (lipid-type vacuolar degeneration). The sinusoids are often expanded by predominantly immature and fewer mature eosinophils like those present in the lung and kidney. Perivascular areas (predominantly in the portal regions) have aggregates of similar cells, which also infiltrate multiple other tissues, including the bone marrow (sections not submitted). The cytoplasmic granules in both the immature and mature eosinophils stain strongly with the Luna stain.

Contributor's Morphologic Diagnoses:
Lung, kidney, and liver: Eosinophilic leukemia

Liver: Lipidosis, diffuse, severe

Contributor's Comment:
Spontaneous neoplasia is common in adult African hedgehogs without sex predilection. The median age of affected animals is 3.5 years.[11] The most common sites of tumor development in these animals are skin (especially mammary gland), lymphoid, gastrointestinal, endocrine, and reproductive systems. Most of these tumors are malignant and tend to have a poor prognosis.[11] Hematopoietic tumors can account for up to 11% of the tumors in hedgehogs. Lymphoma is the most common of this type of tumor, predominantly of the multicentric and alimentary forms, while leukemia in hedgehogs is considered rare.[9,11] Leukemias in hedgehogs include eosinophilic leukemia and acute leukemia/lymphoma.[7,9,10]

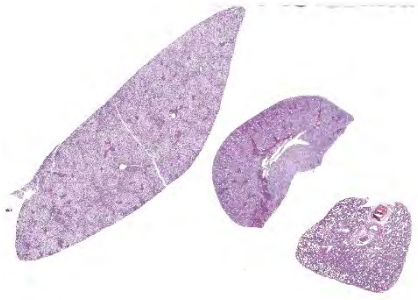

Figure 3-2: Liver, kidney, lung, hedgehog. One section of each tissue is submitted for examination. At subgross magnification, marked hepatocellular lipidosis can be discerned. (HE, 10X)

Eosinophilic leukemia is a variant of granulocytic leukemia and has been described in cats and humans.[3,4] This type of neoplasm is considered to be chronic with an indolent course, and the cells are usually immature with eosinophilic differentiation. Some reports suggest that hedgehogs may have a unique genetic susceptibility to this specific type of leukemia, and that the behavior of the neoplasm is more aggressive in this species.[9] Differential diagnoses include idiopathic hypereosinophilic syndrome and paraneoplastic hypereosinophilia, both described as increase of solely mature eosinophils in blood and tissues.[4,7,9] The diagnosis of idiopathic hypereosinophilic syndrome is made by exclusion, in the absence of an eosinophilic neoplasm, like leukemia, or by determining primary causes of reactive increase of eosinophils, such as allergies, autoimmune disease, or parasitic infestation.[7,9,10]

The diagnosis of leukemia can be performed through clinical pathologic findings, especially marked leukocytosis, composed mostly of immature eosinophils, which can be observed in the peripheral blood smear. Animals with myelogenous leukemia can present concurrent cytopenias, like non-regenerative anemia and thrombocytopenia. Serum biochemistry findings depend on the organs affected by the neoplastic cells. The literature describes a predominance of liver injury, leading to hypoalbuminemia.[9] Histologically, it is common to visualize neoplastic cell infiltrate in multiple organs, including the bone marrow, pancreas, liver, kidney, gastrointestinal tract, lungs, lymph nodes, heart, and spleen.[7,9] Although eosinophils can be easily recognized cytologically or histologically, the identification of immature cells can be a challenge. Histochemistry and/or immunohistochemistry may be

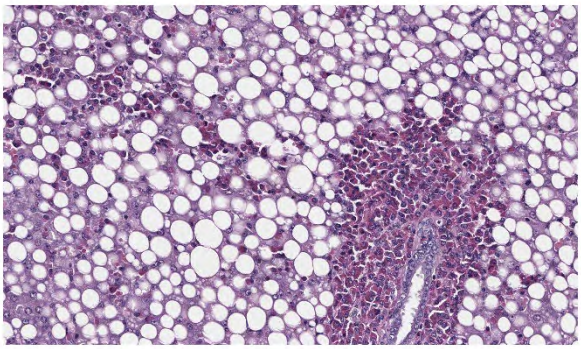

Figure 3-3: Liver, hedgehog. Neoplastic eosinophilis form aggregates within portal áreas and within sinusoids. Diffusely, hepatocytes contain large cytoplasmic lipid droplets. (HE, 318X)

helpful in these cases to confirm the lineage of the leukemia cells. In cases of eosinophilic leukemia, Luna stain is the most consistent stain utilized to highlight the granules of both immature and mature eosinophils.[10] Cytochemical staining for myeloperoxidase (MPO), alkaline phosphatase (ALP), and Sudan Black B can also be performed to demonstrate the granules of eosinophils in blood smears.[9]

In the current case, variable degrees of neoplastic cell infiltrate were observed in the bone marrow, lungs, trachea, nasal cavity, heart, kidneys, liver, spleen, pancreas, gastrointestinal tract, mesenteric lymph node, skin, eyes, eyelids, lacrimal glands, sciatic nerve, and cerebral meninges. Blood vessels were filled with immature eosinophils, which indicates abundant neoplastic eosinophils were in circulation, consistent with leukemia. Causes of hypereosinophilia, such as parasitism or allergy, were ruled out based on the history and lack of gross or microscopic evidence. The severely enlarged spleen (6.52% of total body weight; reference interval: 0.1-2.47% body weight)[5] had multifocal to coalescent, large areas of necrosis within extensive sheets of neoplastic cell infiltrate; little of the normal parenchyma

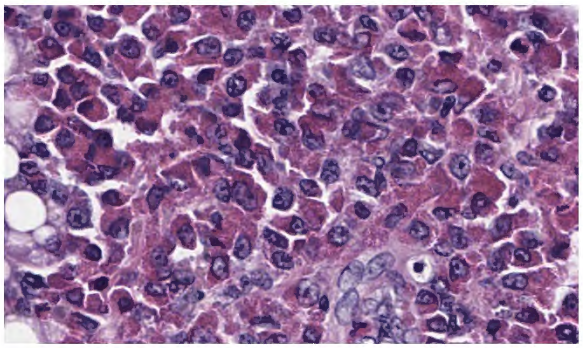

Figure 3-4: Liver, hedgehog. High magnification of neoplastic eosinophils. While some mature mature forms are bilobed, the majority have large round nuclei. (HE, 1450X)

remained. The bone marrow was markedly hypercellular; 70-80% of the cellularity was composed of immature forms of eosinophils, with 2 mitotic figures per 10 high power fields. Megakaryocytes and erythroid precursor cells were markedly reduced in numbers. The cause of death was presumed to be from multiorgan dysfunction due to the severe neoplastic cell infiltrate in all organs, further complicated by the severe hepatic lipidosis.

There is no scientific evidence of the efficacy of chemotherapy for the treatment of eosinophilic leukemia in hedgehogs. Drugs like cytarabine, used for the treatment of cats and dogs with hypereosinophilic syndrome, were tested in hedgehogs.[10] No treatment has been successfully established for this condition in hedgehogs, however. Affected animals usually die shortly after diagnosis.[8-10]

Contributing Institution:
Louisiana Animal Disease Diagnostic Laboratory (LADDL), School of Veterinary Medicine, Louisiana State University (http://www1.vetmed.lsu.edu/laddl/index.html)

JPC Diagnoses:
1. Liver, kidney, lung: Myeloproliferative neoplasm, favor chronic eosinophilic leukemia.
2. Liver, hepatocytes: Lipidosis, diffuse, severe.

JPC Comment:
Of the four entities seen in today's conference, this is the only one that has been seen in a Wednesday Slide Conference before (WSC 2020-2021, Conf 19, Case 2). In what initially was thought to be a straightforward case, some conference participants engaged in a spirited debate about whether to call this acute vs chronic eosinophilic leukemia and if it also classified as an eosinophilic sarcoma due to extravasation of the neoplastic epithelial cells into the surrounding tissues. As such, a CD34 immunohistochemical marker was performed post-conference to determine maturity of the eosinophils, which revealed that the neoplastic cells were not immunoreactive to CD34. This allowed participants to conclude that the leukemic portion of the diagnosis was chronic. Additionally, this case was sent for human hematopathology consult with the Walter Reed National Military Medical Center, who expressed that they would diagnose this case as chronic eosinophilic leukemia based on the degree of granularity of the eosinophils, which they stated is a feature of maturity. However, they also mentioned that "myeloproliferative neoplasm" would be a more appropriate term according to the WHO, as there was no clinical documentation to demonstrate a peripheral eosinophilia over time in this patient and there was no clonality performed. Both of these are considered diagnostic criteria according to the most updated World Health Organization classification for leukemias.[2] All factors considered, conference participants agreed with the diagnosis of "myeloproliferative neoplasm, favor chronic eosinophilic leukemia" in line with the WHO classification.

The eosinophil was discovered by Paul Erlich in 1879 when he found distinctive properties of a particular subset of leukocytes that exhibited a pink color when stained with eosin dye.[1] Eosin dye is made from fluorescein, which is a coal tar derivative, that is treated in an ethanol solution with bromine to form tetrabromofluorescein.[8] This compound, which is acidic, is then neutralized into a salt, resulting in a water (or ethanol) soluble dye. Eosin is negatively charged, and thus stains positively charged tissues, including cytoplasmic elements, extracellular matrix, and connective tissues such as collagen.[8] Additionally, it stains basic proteins, including Major Basic Protein found in the granules of eosinophils, which is what causes them to stain so strongly with eosin and gives them their characteristic name.[8]

Eosinophils originate in the bone marrow from multipotent hematopoietic stem cells (HSC) that differentiate down the myeloid lineage. The common CD34+ myeloid progenitor (CMP) gives rise to myeloblasts, which are enter granulopoiesis towards one of three cell types: neutrophils, basophils, and eosinophils. The differentiation and maturation of eosinophils through eosinophilic lineage are dependent on timely expression and presence of several transcription factors and cytokines, such as interleukin-5 (IL-5).[12] IL-5 is the most important factor promoting eosinophil differentiation, maturation, and survival. Other cytokines, including IL-3 and granulocyte-macrophage colony-stimulating factor (GM-CSF) also contribute to this process.[12]

Mature eosinophils contain granules rich in major basic protein (MBP), eosinophil cationic protein (ECP), eosinophil peroxidase

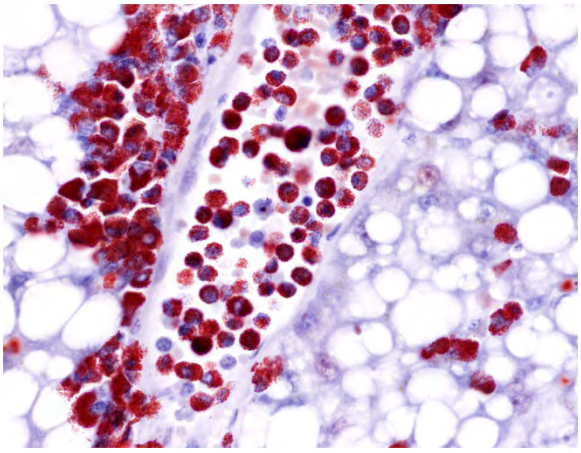

Figure 3-5: Liver, hedgehog. A Luna mast cell stain highlights the eosinophlic granules within the cytoplasm. Additionally numerous neoplastic eosinophils are present within vessels. (Luna mast, 1000X) (Photo courtesy of: Louisiana Animal Disease Diagnos

(EPO/EPX), and eosinophil-derived neurotoxin (EDN), among other things.[12] Eosinophil granules are cytotoxic and are released in response to a variety of infections, particularly parasitic infection, as well as to allergen exposure. Normally, in response to infection or allergen, Type 2 inflammatory (Th2) cells that are in proximity to the stressor produce high levels of IL-5, which triggers eosinophil infiltration into tissues and activation.[12] Activated eosinophils release a variety of substances, including cytokines, chemokines, and granule proteins such as those mentioned above. These mediators, if not regulated, contribute to the tissue damage and dysfunction seen in the affected organs. Eosinophil peroxidase, in particular, impart a characteristic green hue to tissues it affects due to it's high iron concentration, which at one point led to the use of the now-retired terms "chloroleukemia" and "chloroma" to describe associated lesions of eosinophilic leukemias grossly.

Now that some basics eosinophil origin and function have been discussed, what about eosinophilic leukemias? Specific mutations in the CD34+ myeloid progenitor cells can lead to primary eosinophilic disorders, including leukemias and hypereosinophilic syndromes, where eosinophils are part of the clonal expansion. The FIP1L1-PDGFRA fusion gene is a well-studied example of such a mutation associated with chronic eosinophilic leukemia (CEL) in humans.[6] This gene is not normally present and arises from a chromosomal deletion that results in the production of an activated tyrosine kinase that drives uncontrolled growth and division of myeloid cells, particularly eosinophils.[6]

In veterinary species, this disease is rare with only scattered reports in African pygmy hedgehogs, cats, dogs, and one report in a tiger salamander. Despite the growing body of information that exists about this entity in humans, studying the lineage and genetics of eosinophilic leukemia in veterinary species has proven to be challenging due to the lack of cross-reactive or species-specific reagents and immunohistochemical markers.[9] Until that changes and someone develops species-specific reagents to study eosinophilic leukemia in African pygmy hedgehogs (or other affected species, I'm sure there's a Ph.D. niche there), further understanding of this disease in animals will come with time....and funding.

References:

1. Aoki A, Hirahara K, Kiuchi M, Nakayama T. Eosinophils: Cells known for over 140 years with broad and new functions. *Allergol Int*. 2021;70(1):3-8.
2. Barbui T, Thiele J, Gisslinger H, Kvasnicka HM, Vannucchi AM, Guglielmelli P, Orazi A, Tefferi A. The 2016 WHO classification and diagnostic criteria for myeloproliferative neoplasms: document summary and in-depth discussion. Blood Cancer J. 2018;8(2):15.
3. Bain BJ, Fletcher SH: Chronic Eosinophilic Leukemias and the Myeloproliferative Variant of the Hypereosinophilic Syndrome. Immunol Allergy Clin. 2007;27:377-388.
4. Gelain ME, Antoniazzi E, Bertazzolo W, Zaccolo M, Comazzi S: Chronic eosinophilic leukemia in a cat: cytochemical and immunophenotypical features. Vet Clin Pathol. 2006;35:454-459.
5. Girgiri IA, Gambo BG, Ibrahim B, Bwala A: Morphometric studies of some visceral organs and gastrointestinal tract of four-toed African hedgehog (Atelerix albiventris). J Morphol Sci. 2015;32(1):29-32.
6. Haydon SJ, Ross DE, Caucci S, Clark S, Hrinczenko B. Chronic Eosinophilic Leukemia Positive for FIP1L1-PDGFRa. Cureus. 2025;17(2)
7. Higbie CT, Eshar D, Choudhary S, Pohlman LM, Ganta CR, Andrews G: Eosinophilic leukemia in a pet African hedgehog (Atelerix Albiventris). J Exot Pet Med. 2016;25:65-71.
8. Kay AB. The early history of the eosinophil. Clin Exp Allergy. 2015;45(3):575-82.
9. Koizumi I, Hernandez-Muguiro D, Chu SAA, Stokol T, Asakawa MG: Clinicopathologic findings of spontaneous leukemia in 9 pet African hedgehogs (Atelerix albiventris). Front Vet Sci. 2020;7(54):1-10.
10. Martinez-Jimenez D, Garner B, Coutermarsh-Ott S, et al. Eosinophilic leukemia in three African pygmy hedgehogs

(Atelerix albiventris) and validation of Luna stain. J Vet Diag Invest. 2017;29(2):217-223.
11. Raymond JT, Garner MM: Spontaneous tumors in captive African hedgehogs (Atelerix albiventris): A retrospective study. J Comp Pathol. 2001;124:128-133.
12. Rosenberg HF, Dyer KD, Foster PS. Eosinophils: changing perspectives in health and disease. Nat Rev Immunol. 2013;13(1):9-22.

CASE IV:

Signalment:
7 year old male neutered Domestic Shorthair Cat.

History:
A red plaque from the right upper conjunctiva was submitted for biopsy.

Gross Pathology:
One irregular piece of pale tan, soft to firm tissue with no natural borders was received.

Laboratory Results:
N/A

Figure 4-1: Eyelid, cat. Two sections of eyelid are submitted for examination. At this magnification, marked inflammation of the dermis is evident, as is significant expansion of the underlying tissue by numerous variably sized clear spaces. (HE, 10X)

Microscopic Description:
Skin (right upper palpebral conjunctiva). One bisected tissue is examined. The substantia propria is markedly expanded by coalescing, variably sized clear spaces (presumptive lipid), occasionally containing low numbers of macrophages, and surrounded by a small amount of fibrosis, few macrophages, and rare multinucleated giant cells. Larger aggregates of macrophages are present superficially. The superficial substantia propria is moderately expanded by low numbers of lymphocytes and few plasma cells.

Contributor's Morphologic Diagnoses:
Skin (right upper palpebral conjunctiva):
Marked chronic lipogranulomatous conjunctivitis

Contributor's Comment:
These findings are consistent with the uncommon condition known as Feline Lipogranulomatous Conjunctivitis. This condition results in nodular lesions, most commonly affecting the palpebral conjunctiva, and it occurs secondary to leakage of lipid-rich material into the tissue. Cats with sparse periocular pigment (such as white or orange cats) may be predisposed. One source reports that nearly a quarter of cats with this condition also had concurrent periocular neoplasia; there was no evidence of neoplasia in these sections. Complete excision is expected to be curative for this benign lesion.

Contributing Institution:
University of Tennessee College of Veterinary Medicine
Department of Biomedical and Diagnostic Sciences
https://vetmed.tennessee.edu/academics/biomedical-and-diagnostic-sciences/

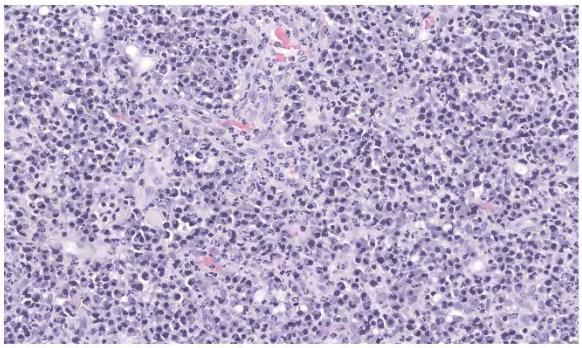

Figure 4-2: Eyelid, cat. The superficial dermis, particularly that underneath the ulcerated mucosal epithelium is infiltration by large number of plasma cells, with fewer lymphocytes, neutrophils, and macrophages. HE, 522X)

JPC Diagnoses:
Conjunctiva: Conjunctivitis, lipogranulomatous and lymphoplasmacytic, chronic, diffuse, severe.

JPC Comment:
The last conference case of the day represented a unique feline entity that lent itself to a difficult tissue ID for conference participants. Many thanks to our contributor for this unique case! Conference participants waffled on anatomic location initially but eventually settled on either conjunctiva or mucocutaneous junction of some kind. Dr. Williams steered participants in the right direction to conjunctiva and drew special attention to the large lakes of clear space within the subconjunctival tissues. He turned those lakes into yet another lesson about paying special attention to what is NOT present. He stated that, when there is clear space, it should make the pathologist consider, "Is this air (emphysema), clear fluid, or fat?" In this case, those clear spaces were what was left of large lakes of lipid, characteristic in this condition, following tissue processing.

Feline lipogranulomatous conjunctivitis includes characteristic non-ulcerated, smooth, white, conjunctival nodules within the palpebral conjunctiva. These are almost always adjacent to the eyelid margin and usually involve the meibomian glands.[1,3] These nodules often cluster, are usually bilateral, and may be present on both upper and lower eyelids.[1,3] However, lesions are usually more severe on the upper lid than the lower. This condition doesn't generally respond well to treatment and surgery is usually recommended if there is irritation. Luckily, these cats typically have a good prognosis post-op. Feline lipogranulomatous conjunctivitis is similar to chalazia in dogs, except that chalazia are usually the result of Meibomian gland neoplasia and do not tend to cluster.[3] Differential diagnoses for conjunctival inflammation with nodule formation in cats should include meibomian gland infections (i.e. marginal blepharitis or styes), eosinophilic keratoconjunctivitis, feline herpesvirus 1 (FHV-1), *Chlamydia felis*, feline calicivirus (FCV), and *Mycoplasma spp*. Conjunctival neoplasia should also be considered in these cases, as approximately 25% of cats with lipogranulomatous conjunctivitis have had concurrent neoplasms, usually squamous cell carcinomas.[2,3]

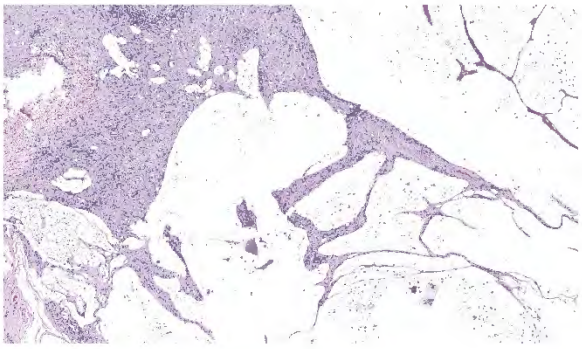

Figure 4-3: Eyelid, cat. Deeper areas of the dermis are expanded by large, irregularly shaped clear spances which are separated by fibrous stroma that is infiltrated by regionally variable numbers of vacuolated epithelioid macrophages. (HE, 106X)

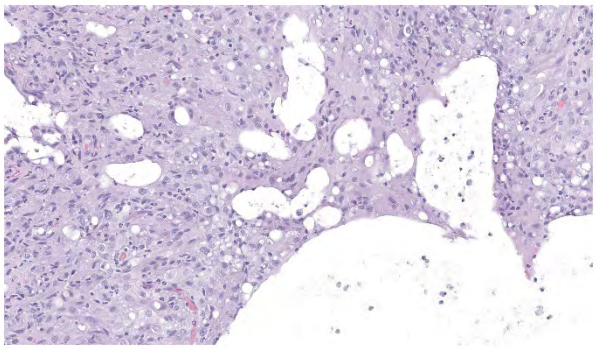

Figure 4-4: Eyelid, cat. Higher magnification of the infiltrate of vacuolated macrophages which border clear spaces. The clear spaces contain few macrophages as well. (HE, 381X)

Inflammation within the Meibomian glands is usually minimal, but abnormal squamous epithelium may be seen within ducts. Usually, there is fibrosis surrounding the gland.[3]

The pathogenesis is currently thought to involve actinic (UV or solar) radiation-induced damage to the Meibomian glands, resulting in blockage of normal glandular secretion and leakage of sebaceous material into the surrounding tissues, which incites a granulomatous inflammatory response.

It is thought that the UV radiation leads to DNA damage and oxidative stress, followed by cytokine release and immune activation with subsequent damage to the gland. This might help explain why cats with low levels of periocular pigment are more susceptible to the condition, as well as why a quarter of these cats also have concurrent UV-related neoplasms.

On microscopic examination, the nodules are characterized by variably sized lipid lakes within the submucosal connective tissue. These lakes are usually surrounded by macrophages, multinucleated giant cells, and low numbers of plasma cells and lymphocytes.[3] Macrophages frequently will have phagocytosed lipid droplets and/or cholesterol crystals.

References:

1. Dubielzig, RR, Ketring, K, McLellen, GJ, Albert, DM. Veterinary Ocular Pathology. Elsevier; 2010. pp. 174, 179.
2. Foster TM, Newbold GM, Miller EJ, Jeong YJ, Premanandan C, Husbands BD. Periocular fibrosarcoma with lipogranulomatous conjunctivitis in a cat. Vet Ophthalmol. 2025;28(3):646-650.
3. Read, RA, Lucas, J. Lipogranulomatous conjunctivitis: clinical findings from 21 eyes in 13 cats. Veterinary Ophthalmology. 2001;4:93-98.

Joint Pathology Center
Veterinary Pathology Services

WEDNESDAY SLIDE CONFERENCE 2025-2026

Conference #3 — 03 September 2025

CASE I:

Signalment:
5.5-year-old, male castrated, domestic short-hair cat (*Felis catus*)

History:
The cat was presented to the emergency service for a two-day history of lethargy and anorexia and a one-day history of labored breathing. The cat was reportedly indoor-only with no other animals in the house, had no history of illness, and had not been given any medications or preventatives. Thoracic auscultation revealed muffled heart sounds, decreased ventral lung sounds, and harsh dorsal lung sounds. The cat's pulses were strong and synchronous, and no murmur or arrhythmias were appreciated. A brief thoracic ultrasound revealed a large amount of pleural effusion. Following a discussion about differentials and prognosis, the owner elected humane euthanasia with necropsy.

Gross Pathology:
The thoracic cavity contained 180 mL of malodorous, tan to dark yellow to pale green, opaque effusion with free-floating aggregates of yellow to pale green friable material admixed. The same material covered the pericardium and multifocally covered the parietal and visceral pleura throughout the thoracic cavity, with the right side more severely affected than the left. The lung lobes were diffusely mildly

Figure 1-1 The pleura and pericardium are covered by aggregates of yellow to pale green friable material. (Photo courtesy of: UPenn School of Veterinary Medicine, Dept. of Pathobiology, https://www.vet.upenn.edu/).

rubbery and collapsed. The cranial aspect of the right caudal lung lobe was expanded by multiple, coalescing, approximately 0.3 cm diameter, tan to yellow nodules that oozed opaque, mucoid, yellow to gray exudate on cut section. Sections of the cranial portion of the

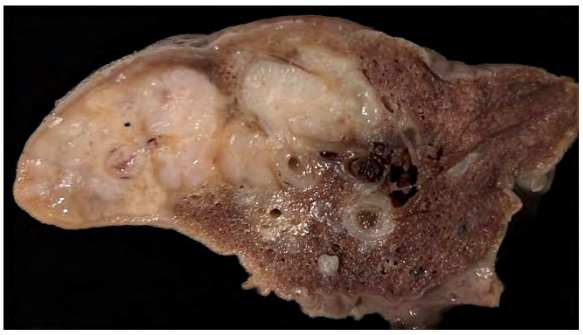

Figure 1-2: Lung, cat. There is marked consolidation of an apical section of formalin-fixed lung. (Photo courtesy of: UPenn School of Veterinary Medicine, Dept. of Pathobiology, https://www.vet.upenn.edu/).

right caudal lung lobe hovered below the surface in 10% formalin, while sections from the other lung lobes floated in 10% formalin.

There was no evidence of thoracic trauma or migrating foreign material on gross postmortem examination.

Laboratory Results:

Aerobic culture of the pleural fluid isolated *Escherichia coli*, *Actinomyces* sp. (suspect *Canibacter oris*), and *Staphylococcus aureus*. Aerobic culture of fresh lung tissue isolated *Escherichia coli*. Anaerobic culture of both the pleural fluid and lung tissue had no growth.

Microscopic Description:

One section each of the right caudal lung lobe and pericardium are examined. The parenchyma of the right caudal lung lobe is severely expanded by coalescing aggregates of viable and nonviable neutrophils amidst abundant fibrin and cellular debris, admixed with fewer epithelioid macrophages and occasional multinucleated giant cells. These aggregates are further encircled by a ring of maturing fibrous connective tissue with few admixed lymphocytes and plasma cells. These foci of inflammation are centered on large airways and rarely contain fragments of bronchiolar walls that have been effaced. Less affected bronchi and bronchioles occasionally have eroded to ulcerated epithelium with intraluminal coagula of fibrin, neutrophils, foamy macrophages, erythrocytes, and proteinaceous fluid. The visceral pleura is covered by a mat of viable and nonviable neutrophils with fewer epithelioid macrophages enmeshed in abundant fibrin, cellular debris, and mixed bacteria comprising cocci and short to filamentous bacilli. The underlying pleural connective tissue is diffusely thickened by granulation tissue with infiltrating epithelioid macrophages, lymphocytes, and plasma cells. The pericardial pleura is similarly affected.

Gram-stained sections of the right caudal lung lobe and pericardium demonstrate myriad gram-positive and gram-negative filamentous and short bacilli bacteria, both extracellular and within the cytoplasm of macrophages associated with the parietal pericardium, pulmonary visceral pleura, and pulmonary parenchymal lesions. An acid-fast-stained section (Ziehl-Neelsen) of the pericardium demonstrates that the filamentous and bacilli bacteria are uniformly acid-fast negative.

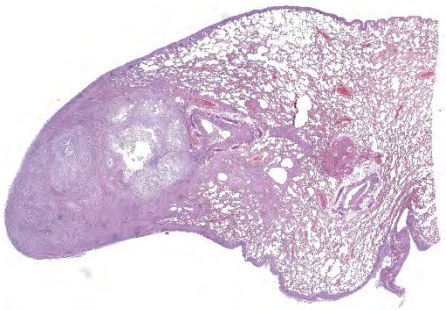

Figure 1-3. Lung, cat. At subgross magnification, the apex of the lung and a thin rim immediately beneath the pleura is consolidated. At the tip of the section, airways are filled and effaced with abundant inflammatory infiltrate which extends into the surrounding parenchyma. (HE, 10X).

Contributor's Morphologic Diagnoses:
Cat, right caudal lung lobe: severe regionally extensive chronic fibrinosuppurative and pyogranulomatous bronchopneumonia and pleuritis with bronchiectasis, granulation tissue, fibrosis, and bacilli and filamentous bacteria.

Cat, pericardium: severe diffuse chronic fibrinosuppurative and pyogranulomatous pericarditis with granulation tissue and bacilli and filamentous bacteria.

Contributor's Comment:
Pyothorax, or thoracic empyema, is characterized by accumulation of suppurative exudate within the pleural space.[1] Cats between 4-6 years old are predominantly affected, and no sex or breed predispositions have been identified.[2–4] More than 80% of feline pyothoraces are associated with a mix of obligate anaerobes (e.g., *Clostridium*, *Fusobacterium*, and *Bacteroides* sp.) and facultative aerobic bacteria (e.g., *Pasteurella* and *Actinomyces* sp.) which are reported constituents of the normal feline oropharyngeal flora, though non-oropharyngeal bacteria (including *Staphylococcus aureus* and *Escherichia coli*) have been isolated in a smaller percentage of cases.[4-9] It follows that pyothorax has frequently been associated with bite trauma which, by direct penetration of the thorax or by local extension of a subcutaneous abscess, can inoculate the pleural space with oropharyngeal bacteria.[2,3,10] Other reported routes of infection in cases of pyothorax include esophageal rupture, inhaled or migrating foreign bodies, larval migrans, therapeutic thoracic interventions (e.g., thoracocentesis or thoracic surgery), and spread of inflammation from a distant site.[3] While chest bite trauma remains an important risk factor for pyothorax, current evidence suggests that aspiration of oropharyngeal bacteria, leading to colonization of the lower respiratory tract and subsequent parapneumonic spread, is a more likely source of pleural infection in cats.[3,4,11] This mechanism of infection is also the most common mechanism of infection in human anaerobic pyothorax and equine pleuropneumonia.[4,12,13]

In this case, the distribution of lung lesions, i.e. a focal parenchymal lesion in the right caudal lobe as well as pleural lesions throughout all lobes, in context with the absence of chest trauma, is most suggestive of parapneumonic spread from bronchopneumonia arising from aspirated oropharyngeal bacteria. The bacterial isolates from the lung and pleural effusion are consistent with the findings in the gram- and acid-fast-stained sections of tissue and correspond to organisms reported in the feline pyothorax literature.

Contributing Institution:
University of Pennsylvania School of Veterinary Medicine
Department of Pathobiology
https://www.vet.upenn.edu/

JPC Diagnoses:
Lung: Bronchopneumonia, necrotizing and pyogranulomatous, chronic-active, focally extensive, severe, with pleural granulation tissue, bronchiectasis, and mixed bacteria.

JPC Comment:
COL (Retired) Jeremy Bearrs, former director of the Joint Pathology Center, spearheaded today's conference with a case that ended up as a staff favorite! This case's discussion started off with some clarifying definitions of pneumonia-related terms that are used ubiquitously by the pathologist that have specific meanings and should be used accurately. These included: "bronchopneumonia", referring to an exudative pulmonary lesion originating at the

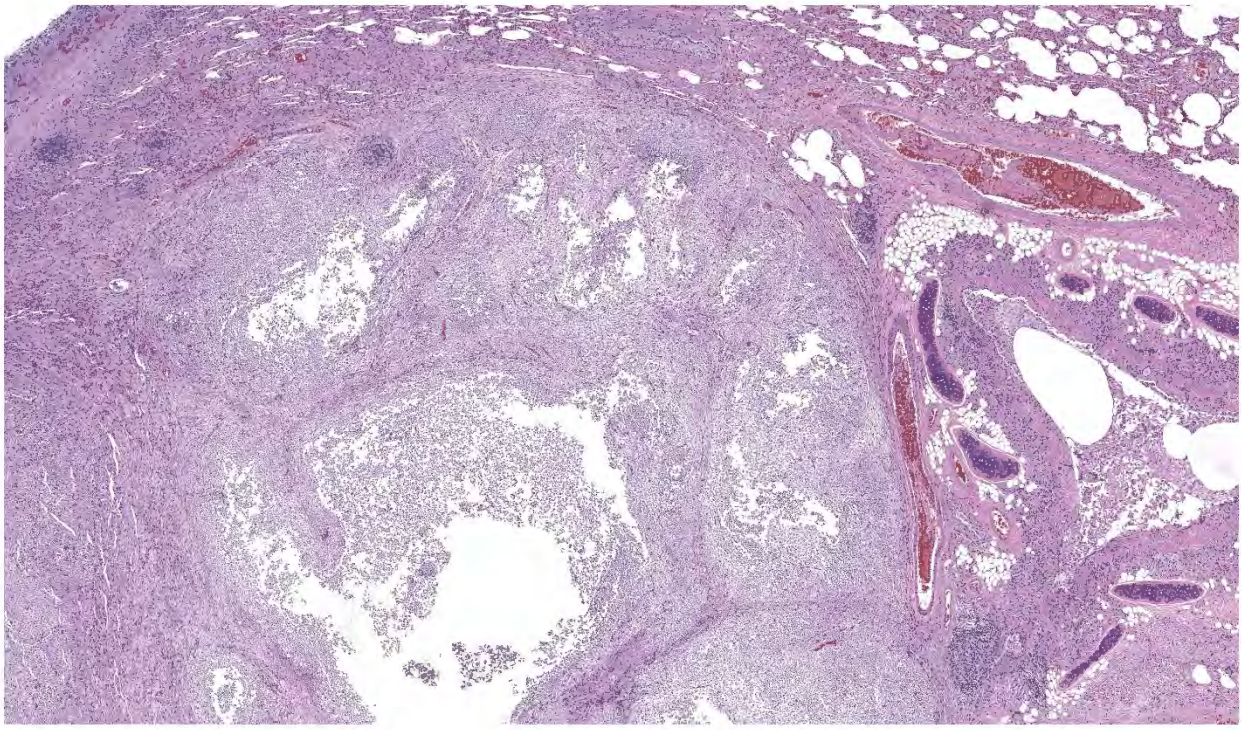

Figure 1-4: Lung, cat. A bronchiole is filled with an exudate of innumerable neutrophils and foamy macrophages which efface the wall and extends into the submucosa and fills the adjacent alveolar parenchyma. (HE, 33X).

bronchiolar-alveolar junction; bronchopneumonias usually start via airborne entry to the respiratory tract, are most often seen in the cranioventral lung lobes grossly, and often have an inflammatory exudate filling airways; "interstitial pneumonia", referring to generally diffuse destruction and inflammation centered upon the three components of the alveolar wall, frequently undergoing exudative, proliferative, and fibrosing phases, and typically enters the lung via bloodborne route of entry (think "viral") or secondary to toxins; "bronchointerstitial pneumonia", defined as the destruction of both bronchiolar and alveolar epithelium, typically via an airborne route of entry; "bronchitis", defined as a type of pulmonary inflammation that affects the bronchi specifically (note that "bronchopneumonia" does NOT, by definition, include the bronchi); and "bronchiectasis/bronchiolectasis", meaning a bronchus or bronchiole, respectively, is irreversibly expanded by inflammation and/or inspissated material as a sequela to loss of elastin and increased fibrosis from a chronic inflammatory response. These terms laid the groundwork for more descriptive accuracy and conversation by the conference participants. Among other notable points of discussion was a challenge to participants to name the major large colony-forming bacteria, which was prompted by the presence of sizeable bacterial colonies in the case slide. These bacteria include *Yersinia, Actinomyces, Actinobacillus, Campylobacter, Corynebacterium, Staphylococcus, Streptococcus, Nocardia,* and *Trueperella* (YAACCSS-NT). On a final note, Dr. Bearrs made an important point to mention knowing which bacteria are excep-

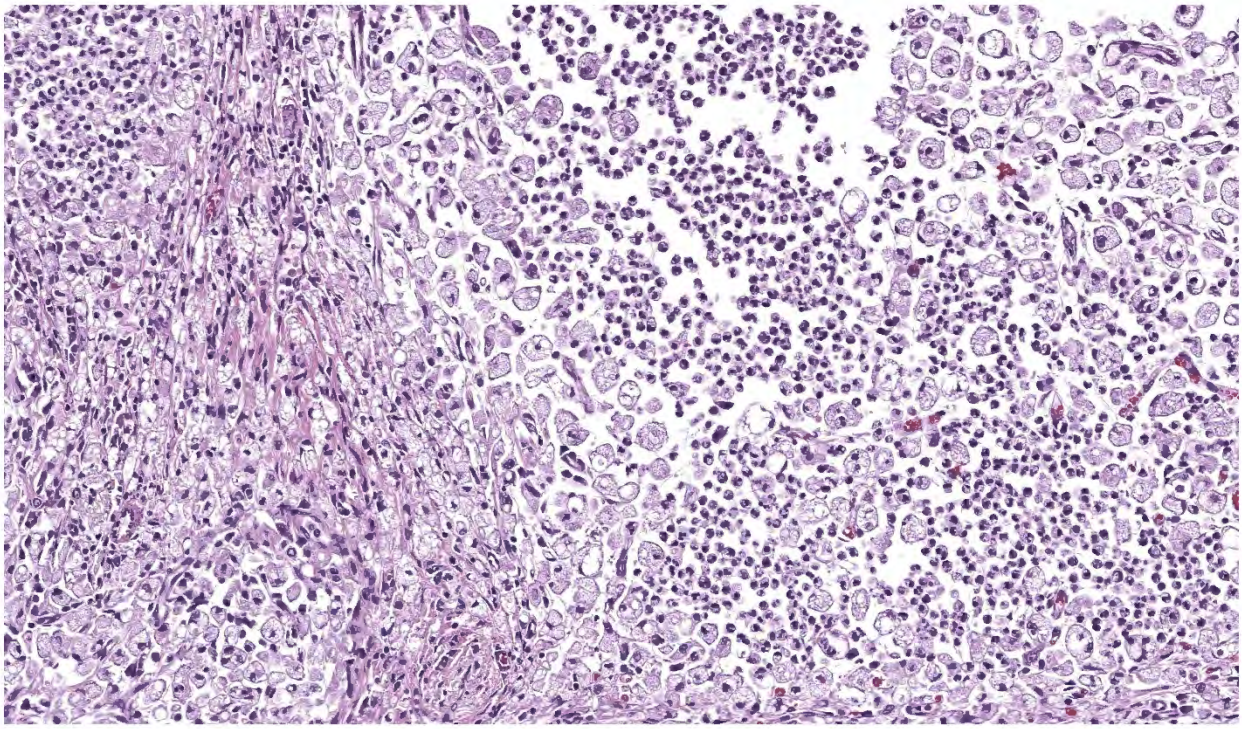

Figure 1-5: Lung, cat. Higher magnification of the inflammatory exudate. (HE, 363X)

tions to general rules, such as *Clostridium piliforme*, which is one of very few Clostridial species that are gram-negative.

Feline infectious peritonitis (FIP), congestive heart failure (CHF), pyothorax, and neoplasia represent the overwhelming majority of cases of pleural effusion in cats.[4] In an elegantly succinct manner, the contributor wrote a terrific comment about routine causes of pyothorax in cats. The possibility of aspiration from a regurgitation that the owners may not have been aware of (because, you know, cats) is certainly worth considering given the presence of E. coli. While the pathogenesis of an aspiration pneumonia with pleural spread might be considered reasonably straightforward, understanding how any form of pulmonary inoculation, including aspiration, leads to pneumonia and parapneumonic disease is worth reviewing.

Normal bacterial flora can be symbiotic with their host when they stay where they're supposed to be, but can become dangerous pathogens when they go where they aren't. Considering the bacteria cultured from this case (*E. coli, S. aureus*, and *Actinomyces* spp), *E. coli* will be used as an example. There are a variety of non-pathogenic *E. coli* strains that reside in the GI tract of cats (and most mammals) that are generally considered beneficial. However, they can also be opportunistic when they end up in, say, the lungs because some kid thought it was funny to make their cat gag at the sound of tape being ripped and it threw up its breakfast. Any event of vomiting or regurgitation can result in an aspiration, though this is most commonly seen during sedation or anesthesia.

Those beneficial gut bacteria, having been forcibly ejected from their home and sucked into the respiratory tract along with other bacteria from the oropharynx, find themselves in a strange and foreign place full of opportunity, far beyond the normal protective mechanisms of the coughing reflex and the mucociliary apparatus. Thus, the party begins. The presence of bacteria in the airways causes inflammation and it's not long before the "cops" show up to try and handle the wayward bacteria. Alveolar macrophages, being the resident neighborhood watch, show up first, having been summoned to the scene by pro-inflammatory cytokines such as IL-1, IL-6, IL-8, and TNFα. However, these cells can only do much, so they start calling in additional support in the form of neutrophils. With all these inflammatory cells and their myeloperoxidases showing up, there is rapid accumulation of pus full of bacteria, dead cells, fibrin, fluid, and damaged tissue. That's the short version of how a suppurative aspiration pneumonia is born.

As the bacteria continue to grow and translocate throughout the lungs, they eventually reach the pleural surface. From there, it's just a hop, skip, and a jump into the pleural cavity. This is usually a potential space with just a minute amount of fluid within it to allow for lubrication during respiration, but the inflammation from the raging pneumonia can result in additional fluid accumulation and edema around the lungs.[4] Bacteria can move out into that fluid and, where they go, neutrophils will follow and do what they do…kill things and make pus. In cats (and dogs), the mediastinum is fenestrated, so there is frequently bilateral accumulation of fluid.[4] That suppurative pneumonia has now graduated to a pyothorax.

Pyothoraces can be notoriously challenging to treat and most require aggressive medical management +/- surgery. In cats, survival rates from pyothorax are reported to be only 62%, with a 58% complication rate with thoracotomy tube placement.[11] Post-treatment complications are common and include pleural adhesions, pulmonary fibrosis, abscesses, sepsis, cardiac disease, recurrent infections, bronchopleural fistulas, and even death. However, parapneumonic disease in indoor cats from single-cat households is rare. The moral of the story? Keep your "murder mittens" in the house and, aside from the good that it would do for songbird populations, reduce their risk of pyothorax!

References:

1. Barrs VR, Allan GS, Martin P, Beatty JA, Malik R. Feline pyothorax: a retrospective study of 27 cases in Australia. *J Feline Med Surg*. 2005;7:211–222.
2. Barrs VR, Beatty JA. Feline pyothorax - new insights into an old problem: part 1. Aetiopathogenesis and diagnostic investigation. Vet J Lond Engl. 2009;179:163–170.
3. Bartlett JG. Anaerobic Bacterial Infections of the Lung and Pleural Space. Clin Infect Dis. 1993;16:S248–S255.
4. Beatty J, Barrs V. Pleural effusion in the cat: a practical approach to determining aetiology. J Feline Med Surg. 2010;12(9):693-707.
5. Heier E, Wurtinger G, Hassdenteufel E, Schneider M. Therapy of Pyothorax in Cats via Small-Bore Thoracostomy Tube in Terms of Efficacy, Complications and Outcomes. Animals. 2022;12:107.
6. Johnson LR, Epstein SE, Reagan KL. Etiology and effusion characteristics in 29

cats and 60 dogs with pyothorax (2010-2020). J Vet Intern Med. 2023;37:1155–1165.
7. Lopez A, Martinson SA. Chapter 9: Respiratory System, Thoracic Cavities, Mediastinum, and Pleurae. In: Zachary, JF, ed. Pathologic basis of veterinary disease. 7th ed. Elsevier; 2022.
8. Love DN, Jones RF, Bailey M, Johnson RS, Gamble N. Isolation and characterization of bacteria from pyothorax (empyema) in cats. Vet Microbiol. 1982;7:455–461.
9. Love DN, Vekselstein R, Collings S. The obligate and facultatively anaerobic bacterial flora of the normal feline gingival margin. Vet Microbiol. 1990;22:267–275.
10. Racklyeft D, Raidal S, Love D. Towards an understanding of equine pleuropneumonia: factors relevant for control. Aust Vet J. 2000;78:334–338.
11. Sim JJ, Lau SF, Omar S, Watanabe M, Aslam MW. A Retrospective Study on Bacteriology, Clinicopathologic and Radiographic Features in 28 Cats Diagnosed with Pyothorax. Animals. 2021;11: 2286.
12. Stillion JR, Letendre J. A clinical review of the pathophysiology, diagnosis, and treatment of pyothorax in dogs and cats. J Vet Emerg Crit Care. 2015;25:113–129.
13. Waddell LS, Brady CA, Drobatz KJ. Risk factors, prognostic indicators, and outcome of pyothorax in cats: 80 cases (1986-1999). J Am Vet Med Assoc. 2002;221:819–824.
14. Walker AL, Jang SS, Hirsh DC. Bacteria associated with pyothorax of dogs and cats: 98 cases (1989-1998). J Am Vet Med Assoc. 2000;216:359–363.

CASE II:

Signalment:
2-month-old, female, Yorkshire swine *(Sus scrofa domesticus*).

History:
This animal was found dead after exhibiting coughing and poor appetite for an unknown duration. It came from a group of 30 pigs, many of which had pruritus and black "greasy" exudate of the extremities. These animals had been purchased from multiple sources and introduced to the property within the last six weeks. This pig, and several others had areas of pruritic skin with black, "greasy" exudate, most severely on the distal extremities. Previous bacterial culture of these lesions had identified *Staphylococcus hyicus*.

Gross Pathology:
Distal extremities: The dorsal aspects of the pasterns of all four limbs are carpeted with dark brown, crusty, raised plaques. The lesions are most severe on the forelimbs (Fig 1).
Thorax: Multifocal strands of tan to yellow friable material (fibrin) are loosely adhered between the pleural surfaces of the lungs and the

Figure 2-1: Haired skin, pig. The dorsal aspects of the pasterns of all four limbs are covered with dark brown, crusty, raised plaques. The lesions are most severe on the forelimbs. (Photo courtesy of: University of Missouri Veterinary Medical Diagnostic Laboratory https://vmdl.missouri.edu/).

body wall. The lungs are diffusely wet, heavy, soft, pink and exude dark red fluid on cut section. All examined sections float in formalin. The pericardium contains ~5 mL of pink, clear, watery fluid. The hilar lymph nodes are mildly enlarged to 1.5 - 2x normal size.
Abdomen: The abdomen contains approximately 50 mL of dark red, clear, watery peritoneal fluid. There are multifocal strands fibrin adhered between visceral organs. The stomach contains bright yellow to green semiliquid ingesta. The descending colon contains formed feces. There is mild congestion in the liver, and black, round, flat spots on the left lateral lobe of the liver. The remainder of the gross examination is unremarkable.

Laboratory Results:
Bacteriology: *Staphylococcus hyicus* was cultured from the liver.

Microscopic Description:
Skin: In the dermis, there is marked parakeratotic hyperkeratosis, with numerous colonies of extracellular cocci, and intracorneal arthropod mites. The mites are up to 300-400 µm in diameter, have a chitinous exoskeleton with dorsal spines, short jointed appendages, striated skeletal muscles, and internal gastrointestinal and reproductive tracts. The mites often contain birefringent internal crystalline material, suspected to be scybala. The epidermis is hyperplastic with prominent rete pegs, and the superficial dermis is infiltrated by marked numbers of lymphocytes, plasma cells, macrophages, and fewer eosinophils.

Contributor's Morphologic Diagnoses:
Haired skin: Severe, locally extensive, chronic, lymphoplasmacytic and histiocytic hyperplastic dermatitis with hyperkeratosis, intralesional arthropods (*Sarcoptes scabiei* presumed), and numerous colonies of extracellular cocci.

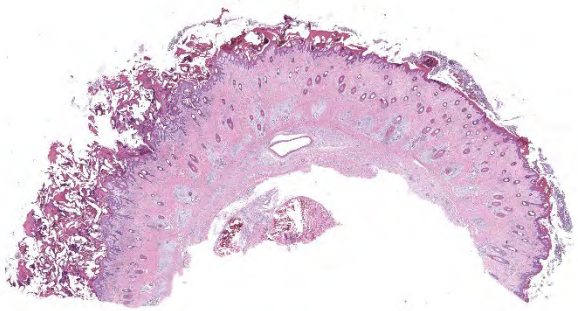

Figure 2-2: Haired skin, pig. At subgross magnification, there is severe hyperkeratosis overlying a hyperplastic epidermis. There is moderate inflammation of the underlying dermis. (HE, 10X)

Contributor's Comment:
Microscopic evaluation revealed two concurrent pathogenic processes within the exudative skin lesions observed grossly: exudative epidermitis (greasy pig disease) caused by *Staphylococcus hyicus*, and sarcoptic mange, caused by *Sarcoptes scabiei*.

Staphylococcus hyicus is a Gram-positive, coagulase-variable, facultatively anaerobic bacterium which typically causes disease in piglets between 5 and 60 days old. The most common clinical finding is greasy, often crusting exudate widely dispersed over the body, but most severely affecting the feet. It is typically transmitted from animal to animal, or is sometimes acquired from the environment, and enters the skin through penetrating wounds.[3] Strains of *S. hyicus* that have the potential to cause clinical disease do so by producing exfoliative toxins. These toxins, including ExhA, ExhB, ExhC, ExhD, SHETA, and SHETB, are thought to cause exfoliation of the epidermis through the cleavage of porcine desmoglein 1, an integral component of the epidermal desmosomes.[9] Infections are often introduced into herds by new animals, and morbidity and mortality rates can be high in

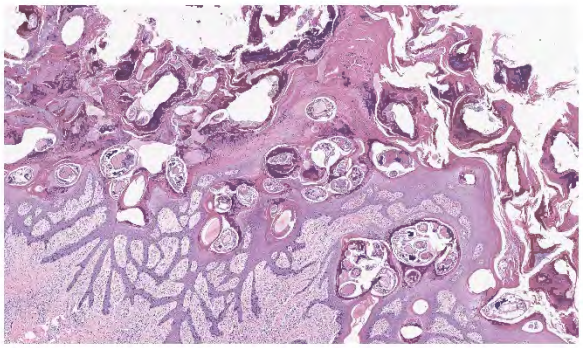

Figure 2-3: Haired skin, pig. There are numerous cross- and tangential sections of adult and nymphal mites within the lamellar keratin and rarely in the underlying epidermis. There are numerous pustules within the hyperkeratotic plaque. (HE, 65X)

younger piglets.[3] In addition to abrasions and wounds from rough surfaces and fighting, additional predisposing factors for infection are infestation with ectoparasites such as mites.[4,7,8] The isolation of *Staphylococcus hyicus* from the liver in this case suggests the animal developed bacteremia.

Sarcoptes scabiei var *suis* is a specific variety of *Sarcoptes scabiei* mite which is globally endemic in swine and is the causative agent of Sarcoptic mange. It is typically transmitted by direct contact, but it may also be spread by fomites and can be easily introduced into a naïve herd by a single infected animal or contaminated equipment. This disease is most prevalent in younger animals, and typically manifests as papules which progress to scaling, oozing, crusts, and alopecia, and often progresses to lichenification in chronic cases. Affected areas are afflicted with severe pruritus. The mechanism of injury to the skin is a combination of mechanical trauma caused by the mite's feeding and burrowing behavior, chemical irritation from ectoparasite saliva and feces, and a hypersensitivity reaction to Sarcoptes antigens.[1]

Contributing Institution:

University of Missouri Veterinary
Medical Diagnostic Laboratory
https://vmdl.missouri.edu/

JPC Diagnoses:

1. Haired skin: Epidermal hyperplasia and hyperkeratosis, diffuse, severe, with mild lymphoplasmacytic dermatitis, intracorneal adult and nymphal mites and eggs.

2. Haired skin: Epidermitis, pustular, subacute, regionally extensive, moderate with extracellular cocci.

JPC Comment:

"Greasy pig disease" has been covered several times in the Wednesday Slide Conference, including as recently as last year (Case 1, Conference 4, 2024-2025, Case 1, Conference 9, 2008-2009, and Case 3, Conference 8, 2009-2010). It always provides a solid descriptive opportunity for conference participants and is truly a classic entity. This year's case, though, had additional guests on the slide in the form of *Sarcoptes scabiei* var *suis*, making this a great "two-fer" case. The slides provided by the contributor were simply beautiful; you

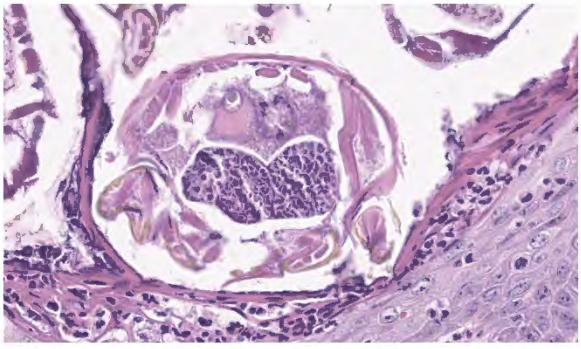

Figure 2-4: Haired skin, pig. Cross sections of adult arthropods demonstrate a brown, spiked chitinous exoskeleton, jointed appendages with skeletal muscle, a hemocoel, and a densely cellular nervous system. (HE, 900X)

could almost draw a line right down the middle of the tissue to demarcate the more routine lesions from *Staphylococcus hyicus* on the right side compared to the far more severe lesions on the left from both the mites and the bacteria together. Many thanks to the contributor for an excellent submission of these two infectious dermatologic entities.

Conference discussion focused on the virulence factors of *S. hyicus* that enable it to cause the exudative epidermitis it is famous for. This bacterium has a variety of exfoliative toxins, such as ExhA, ExhB, ExhC, ExhD, *S. hyicus* exfoliative toxin A (SHETA), and SHETB. These toxins selectively digest desmoglein-1 in porcine skin.[4] Desmoglein-1 is a tight junctional adhesion molecule that is primarily expressed in the superficial epithelium of the skin, playing a critical role in maintaining cell–to-cell adhesion and tissue integrity. When broken down, the cells stop "holding hands" and separate from one another. Coupled with sebaceous hyperplasia within the dermis as a sequela of inflammation, these broken cell junctions enable leakage of sebaceous material onto the surface of the skin, thus the name "greasy pig disease." Conference participants were also quizzed about other commonly encountered desmogleins, including desmoglein-2 (found in desmosomes in skin, cardiomyocytes, and intestines), desmoglein-3 (found between basilar epithelial cells and their basement membranes in the skin; also the known target of pemphigus vulgaris), and desmoglein-4 (found in desmosomes between epithelial cells both in the epithelium of the skin and in hair follicles, and helps to anchor the hair follicle into the dermis).

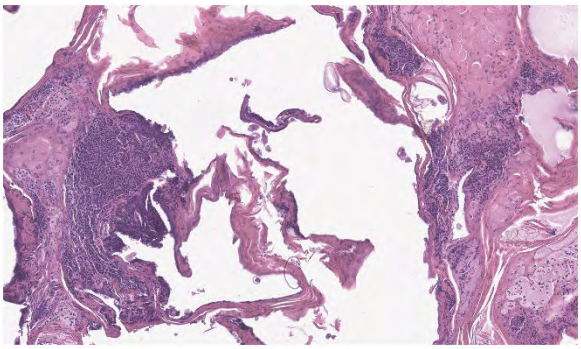

Figure 2-5: Haired skin, pig. There are numerous pustules within the hyperkeratotic crust. (HE, 311X)

Shifting now to the maddeningly itchy *Sarcoptes scabiei* mite, "scabies" or "sarcoptic mange" is caused by *Sarcoptes scabiei,* a burrowing mite, of which there are numerous subspecies that are host specific. Female mites invade the stratum corneum of their selected host and create cozy homes for themselves in the form of tunnels, where they live, move, feed, defecate, and lay eggs.[7] Upon locating a host, the mite secretes saliva that lyses the epithelium of the stratum corneum. As the mite works its way deeper with its cutting mouthparts, it uses its two anterior-most pairs of legs to "swim" forward and create a tunnel. The mite intakes water and nutrients from the host's extracellular fluid and lymph that leaks into the space around the mite's mouthparts while they dig.[7] The females, once mated, will lay their eggs in a burrow that offshoots from their tunnel. The eggs hatch into larvae, which channel their way out of their nursery burrow within the stratum corneum and grow into two subsequent nymphal stages: protonymphs and tritonymphs.[7] The tritonymphs mature into adults on the skin and males will roam about looking for unmated females to repeat the life cycle with.

Scabies is most common in tropical countries, but is ubiquitous and can be seen anywhere,

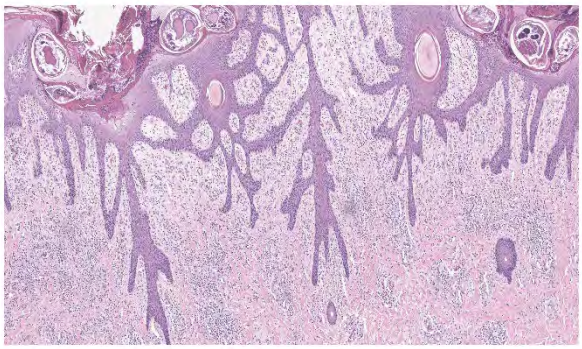

Figure 2-6: Haired skin, pig. The epidermis is markedly hyperplastic, forming deep rete ridges into the underlying moderately inflamed dermis. (HE, 105X)

including cold regions where people (and animals) will huddle together for warmth, as prolonged physical contact is the main mode of mite transmission between hosts.[7] Transmission can occur indirectly on contaminated fomites, but environmental temperature plays a strong role in mite survivability while off-host. Mites don't survive long in warmer climates, regardless of humidity, due to being unable to maintain water balance, but have increased survivability in cooler temperatures with high humidity.[7]

So, which came first, the chicken or the egg? It is the opinion of conference participants that, in the case of this particular young pig, the *Sarcoptes scabiei suis* mites likely set up shop first, causing superficial trauma to the skin of the pig and inducing severe itch, which would have resulted in additional self-trauma from scratching. As a result, the *Staphylococcus hyicus*, seeing as how they are opportunistic commensals, would have had an easy time infecting the skin further and causing additional dermatologic insult. Talk about an itchy one-two punch.

References:

1. Davis DP, Moon RD. Density of itch mite, Sarcoptes scabiei (Acari: Sarcoptidae) and temporal development of cutaneous hypersensitivity in swine mange. *Vet Parasitol*. 1990;36(3–4):285–293.
2. Foo CW, Florell SR, Bowen AR. Polarizable elements in scabies infestation: a clue to diagnosis. J Cutan Pathol. 2012;40(1):6–10.
3. Foster AP. Staphylococcal skin disease in livestock. Vet Dermatol. 2012;23(4):342.
4. Fudaba Y, Nishifuji K, Andresen LO, Yamaguchi T, Komatsuzawa H, Amagai M, Sugai M. Staphylococcus hyicus exfoliative toxins selectively digest porcine desmoglein 1. Microb Pathog. 2005;39(5-6):171-6.
5. Kim J, Chae C. Concurrent presence of porcine circovirus type 2 and porcine parvovirus in retrospective cases of exudative epidermitis in pigs. Vet J. 2003;167(1):104–106.
6. Maes D, Vandersmissen T, De Jong E, Boyen F, Haesebrouck F. Staphylococcus hyicus-infecties bij varkens. Vlaams Diergeneeskd Tijdschr. 2013;82(5).
7. Sharaf MS. Scabies: Immunopathogenesis and pathological changes. Parasitol Res. 2024;123(3):149.
8. Wattrang E, McNeilly F, Allan GM, Greko C, Fossum C, Wallgren P. Exudative epidermitis and porcine circovirus-2 infection in a Swedish SPF-herd. Vet Microbiol. 2002;86(4):281–293.
9. Yun CS, Kang S, Kwon DH, et al. Characterization and antimicrobial resistance of Staphylococcus hyicus from swine exudative epidermitis in South Korea. BMC Vet Res. 2024;20(1).

CASE III:

Signalment:
5-year-old, male castrated, Rottweiler, canine.

History:
The dog was presented to the Auburn University Bailey small animal teaching hospital with one week history of a wet productive cough. Thoracic radiographs showed pneumonia and CBC revealed eosinophilia. On thoracic CT, there was severe bronchiectasis within the accessory lung lobe and mild focal bronchiectasis within the left caudal lung lobe. Bacterial and fungal culture were negative on bronchoalveolar lavage fluid. The patient was sent home on marbofloxacin and prednisone. The owners have noted the cough has approved with treatment but still not ideal. Three months later, the dog returned to the teaching hospital and the right caudal, right accessory, and left caudal lung lobes were removed and submitted for histopathological examination.

Gross Pathology:
Right caudal, right accessory, and left caudal lung lobes had multiple, markedly dilated bronchi or bronchioles filled with light pink to brown inspissated material. The walls of several bronchi was markedly thickened and the intervening lung parenchyma was multifocally collapsed.

Laboratory Results:
Bronchoalveolar lavage fluid submitted for bacterial and fungal cultures was negative.

Microscopic Description:
Diffusely, bronchioles and bronchi are markedly ectatic and filled with large amount of inspissated material composed of larger numbers of eosinophils, degenerate neutrophils, admixed with macrophages, mucin, serum, sloughed epithelial cells and eosinophilic cellular and basophilic nuclear debris. Large

Figure 3-1: Lung, dog. The bronchi and bronchioles are markedly dilated, have a thickened wall and are filled with a pale tan, firm, dry exudate. In some sections, the adjacent pulmonary parenchyma is consolidated and pale tan. (Photo courtesy of: Auburn University http://www.vetmed.auburn.edu/academic-departments/dept-of-pathobiology/).

numbers of similar inflammatory cells also infiltrate the bronchial wall. The lining mucosal epithelium is diffusely moderately hyperplastic or occasionally eroded or ulcerated. Multifocally, bronchi and bronchioles are also surrounded by moderate numbers of eosinophils, neutrophils and macrophages. There is moderate hyperplasia of bronchus-associated lymphoid tissue. Inflammatory exudate multifocally extends into the adjacent alveolar lumina. The adjacent normal alveoli contain moderate numbers of neutrophils, eosinophils and intraalveolar macrophages. The lung parenchyma surrounding the markedly expanded bronchi is multifocally collapsed with closely apposed alveolar septa. Multifocally, there is mild pleural fibrosis. Occasionally, there is mild smooth muscle hypertrophy of bronchioles and tunica media of small caliber blood vessels. Bacterial and fungal organisms are not observed by Gram and GMS stains, respectively.

Contributor's Morphologic Diagnoses:
Lung; right caudal lung lobe, right accessory and left caudal lung lobes: Severe, chronic, multifocal bronchiectasis and bronchiolectasis

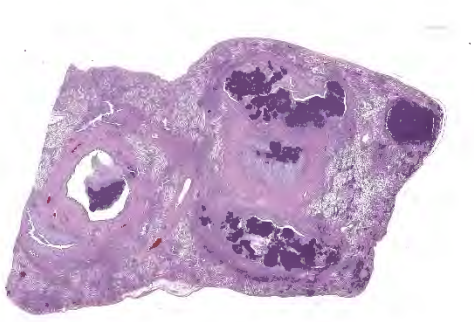

Figure 3-2: Lung, dog. Approximately 66% of the lung is consolidated by inflammation. Airways are ectatic and filled with a densely cellular luminal exudate which extends into the adjacent parenchyma . (HE, 10X).

with marked eosinophilic, suppurative bronchitis and bronchiolitis.

Contributor's Comment:

Eosinophilic bronchopneumopathy (EBP) is an uncommon, chronic, usually steroid-responsive condition of young adult dogs. EBP has been described in several breeds of dogs with Siberian huskies and Alaskan malamutes being overrepresented.[5] The presentation varies from mild to severe, intermittent to chronic, and self-limiting to sometimes fatal. The most common clinical sign is persistent cough, followed by gagging and retching. Other common clinical symptoms include dyspnea, exercise intolerance and nasal discharge that is usually yellow-green to mucopurulent. Radiographic findings include diffuse bronchointerstitial pattern, peribronchial cuffing with or without bronchiectasis.[5] Approximately 50% of the dogs have peripheral eosinophilia[2]. The disease is characterized by eosinophilic infiltration of the lung and bronchial mucosa with epithelial hyperplasia, ulceration or squamous metaplasia. The destruction of the walls of the airways leading to bronchiectasis has also been reported.[5]

The cause of EBP is unknown, however it is thought to be due to hypersensitization to aeroallergens. Immunological and immunohistochemical studies show that bronchoalveolar (BAL) fluid contains decreased numbers of CD8+ T cells, while CD4+ T cell number is increased in the bronchial mucosa and pulmonary interstitium. The predominance of CD4+ T cells supports the role of a dominant Th2 immune response in the affected dogs.[4] The dog in the current case was presented with characteristic clinical signs and blood eosinophilia. Based on the imaging findings of bronchiectasis with negative bacterial and fungal culture, EBP was the primary differential. In most cases, the cytological evaluation of BAL fluid usually reveals marked eosinophilia, which along with imaging findings is sufficient to confirm the diagnosis of EBP. The macroscopic lesions vary from no discharge to the presence of abundant yellow-green mucopurulent material within bronchi or bronchioles, thickening of bronchial and bronchiolar walls, bronchiectasis and consolidation of adjacent parenchyma. Typical histologic findings include eosinophilic infiltrate beneath or within the mucosal epithelium and varying degrees of

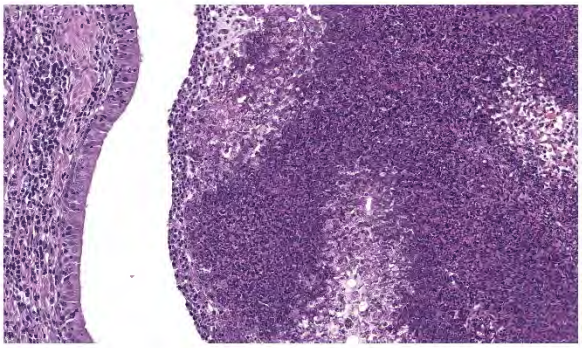

Figure 3-3: Lung, dog. The exudate in the airway lumina is predominantly composed of degenerating eosinophils admixed with fewer macrophages and neutrophils. (HE, 370X).

mucosal thickening, infiltration by other inflammatory cell types, collagenolysis, and fibrosis. In cases of extensive involvement of lung parenchyma, there is diffuse eosinophilic and granulomatous infiltrate, with focal eosinophilic granulomas centered on necrotic tissues can be present.[3] The diagnosis of EBP was confirmed only after ruling out other causes of eosinophilic infiltrate in the lung and negative bacterial and fungal culture. The tracheobronchial parasites *Crenosoma vulpis*, *Eucoleus aerophilus, Oslerus osleri*; the lungworm *Angiostrongylus vasorum* and *Filaroides hirthi*; occult *Dirofillaria immitis* infection are the main differential diagnosis.[2] There was no evidence of parasite eggs, larvae or adults in the examined sections. The lesions were primarily centered on bronchioles and bronchi, with mild to moderate involvement of the pulmonary parenchyma. A rare condition called eosinophilic pulmonary granulomatosis is also characterized by similar clinical signs including blood eosinophilia should be included in the differential diagnoses list, but in this condition, there are nodular necrotizing lesions formed by eosinophils, epithelioid macrophages, type II pneumocyte proliferation, which were absent in this case.[3] Other causes of eosinophilic infiltrate in the lung parenchyma include lymphomatoid granulomatosis, carcinomas and lymphomas. The mainstay of treatment for EBP is the long-term administration of corticosteroids such as prednisolone.[1] In summary, the clinical diagnosis relies on a typical history of chronic respiratory distress, demonstration of bronchopulmonary eosinophilia by cytology or histopathologic examination, and exclusion of known causes of lower airway eosinophilia.

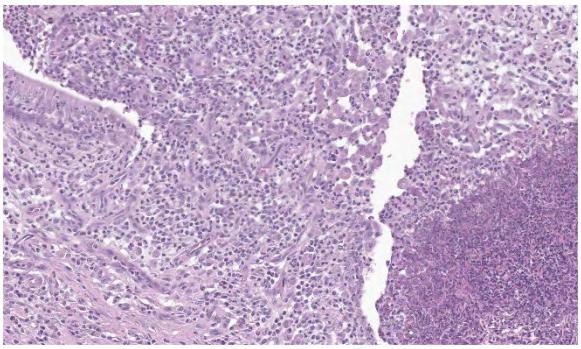

Figure 3-4: Lung, dog. There is multifocal necrosis of airway epithelium with infiltration of the airway wall and adjacent parenchyma by inflammatory cells. (HE, 381X).

Contributing Institution:
Auburn University http://www.vetmed.auburn.edu/academic-departments/dept-of-pathobiology/

JPC Diagnoses:
Lung: Bronchiolitis, eosinophilic and granulomatous, chronic, multifocal to coalescing, severe, with bronchiolectasis, necrotizing alveolitis, and Type II pneumocyte hyperplasia.

JPC Comment:
Today's third case took conference participants on another "Magic School Bus"-esque trip into the lungs in the form of a disease that has more names than it knows what to do with: eosinophilic bronchopneumonopathy. Conference discussion started off with a brief nod to the Rottweiler breed and its storied history as descendants from Roman dogs that moved with their humans across the Alps and ultimately into Rottweil, Germany. The dogs ultimately became known as "Rottweiler metzgerhunds", and were common companions of butchers, where these stocky canines would be seen pulling carts of meat for sale through the streets of Rottweil. Despite this case of eosinophilic bronchopneumonopathy being in a Rottweiler, however, they are not considered

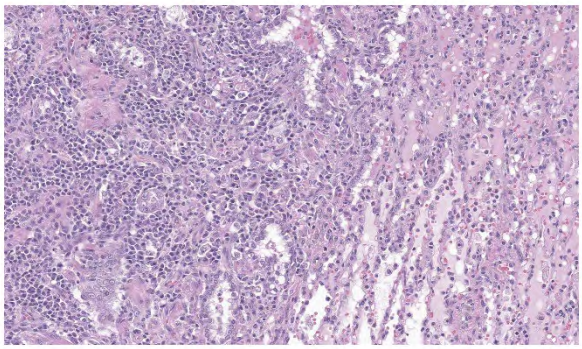

Figure 3-5: Lung, dog. Alveolar parenchyma adjacent to affected airways demonstrates one or more of the following: filling of alveoli and expansion of alveolar septa by eosinophils, macrophages and neutrophils, lymphocytes, and plasma cells admixed with edema and cellular debris, septal fibrosis, and type II pneumocyte hyperplasia. (HE, 381X).

a predisposed breed. Alaskan Malamutes and Siberian Huskies, however, are.

This case provided a fantastic example of true bronchiectasis with abundant inflammation and debris filling the larger airways in section. Eosinophilic bronchopneumopathy is one of the most common diseases associated with bronchiectasis in dogs, with over a quarter There was some discussion about the brightly eosinophilic material admixed with the eosinophils filling these airways, which was interpreted as likely to be a combination of necrotic eosinophils and major basic protein. A more substantial review of eosinophils was covered in last week's conference (Conf 2, Case 3), so that topic won't be belabored further today.

This condition is considered to be both "eosinophilic" and "granulomatous" due to the profound presence of both eosinophils and macrophages. In the course of this disease, there is an upregulated Th2 response, favoring CD4+ T-helper cells over those that are CD8+. The Th2 response is important for fighting extracellular parasites and allergens via production of cytokines like IL-4, IL-5 (chemotactic for eosinophils), and IL-13.[6] These cytokines trigger IgE antibody production, recruit and activate cells such as eosinophils and mast cells, increase mucus production, and promote tissue healing. While protective against parasites and involved in wound healing, an overactive Th2 response can cause chronic inflammatory conditions.[6] Despite being a common condition in dogs, the exact cause of eosinophilic bronchopneumonopathy in dogs is not known. There are conflicting papers that argue for or against an association with heartworm disease, although there isn't much argument that heartworm disease is not the *only* cause of this condition, and it is ultimately suspected that EBP is due to a hypersensitivity reaction of some kind.[3,4,5]

References:

1. Canonne AM, Bolen G, Peeters D, Billen F, Clercx C. Long-term follow-up in dogs with idiopathic eosinophilic bronchopneumopathy treated with inhaled steroid therapy. *J Small Anim Pract*. 2016; 57(10):537-542.
2. Caswell JF, Williams KJ. Respiratory system. In: Maxie MG, ed. Jubb, Kennedy, and Palmer's Pathology of Domestic Animals. Vol 2. 6th ed. Philadelphia, PA: Elsevier Saunders; 2016: 465-590.
3. Clercx C, Peeters D. Canine eosinophilic bronchopneumopathy. Vet Clin North Am Small Anim Pract. 2007;37(5):917-935.
4. Clercx C, Peeters D, German AJ, Khelil Y, McEntee K, Vanderplasschen A, Schynts F, Hansen P, Detilleux J, Day MJ. An immunologic investigation of canine eosinophilic bronchopneumopathy. J Vet Intern Med. 2002;16(3):229-237.
5. Clercx C, Peeters D, Snaps F, Hansen P, McEntee K, Detilleux J, Henroteaux M,

Day M. Eosinophilic bronchopneumopathy in dogs. J Vet Intern Med. 2000; 14(3):282-291.
6. Kokubo K, Onodera A, Kiuchi M, Tsuji K, Hirahara K, Nakayama T. Conventional and pathogenic Th2 cells in inflammation, tissue repair, and fibrosis. Front Immunol. 2022;13:945063.

CASE IV:

Signalment:
5 year old, neutered male, Shetland sheepdog, dog (*Canis familiaris*).

History:
This 5-year-old Shetland sheepdog had a history of anorexia, diarrhea, vomiting and anuria of 4 days duration. Blood chemistry values were consistent with renal failure (exact values not reported). The dog was treated with intravenous fluids and diuretics, with no improvement in its condition. Due to the progression of the clinical signs and poor prognosis (without treatment), the owner elected for euthanasia. The dog was sent to our diagnostic laboratory, and a complete necropsy was performed.

Gross Pathology:
The dog was in good body condition. There were 10 and 20 ml of serous yellowish fluid in the pericardial sac and peritoneal cavity, respectively. Both kidneys showed a slightly irregular/pitted and mottled surface; on cut section, the cortex appeared slightly granular, and the medulla pale and firm. The stomach was empty, with a few shallow ulcers of varying size in the fundus.

Laboratory Results:
N/A

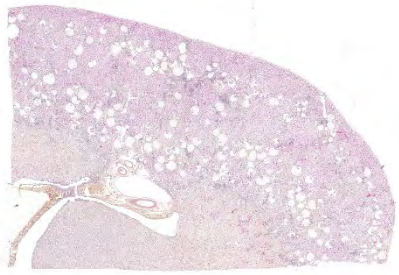

Figure 4-1: Kidney, dog. At subgross magnification, Bowman's spaces are diffusely dilated up 500um. (HE, 10X)

Microscopic Description:
Both kidneys presented similar lesions. Almost all glomerular chambers (Bowman's spaces) are variably dilated, often markedly (cystic dilation, up to about 500 μm), with a thickened/sclerotic, undulating and often mineralized Bowman's capsule (basement membrane) Most glomerular tufts are either absent or shrunken and sclerotic with occasional synechiae. In the cortex, there is a moderate multifocal chronic tubulointerstitial nephritis with tubular atrophy and loss, peritubular sclerosis (thickened basement membrane) and occasional luminal crystals; tubular dilation is present but mild and multifocal. Several tubular basement membranes are diffusely mineralized. In the medulla there is a mild to moderate fibrosis with scant inflammation; rarely, dilated tubular structures lined by a simple columnar eosinophilic or stratified cubic/columnar amphophilic epithelium are present.

Other significant changes in other organs (not submitted) included gastric mucosal mineralization and submucosal vasculopathy ("*uremic gastritis*"), and changes suggestive of bilateral parathyroid chief cell hyperplasia, consistent with renal secondary hyperparathyroidism.

Contributor's Morphologic Diagnoses:
1) Kidney: Glomerular chamber (Bowman's space) dilation, diffuse, moderate to marked

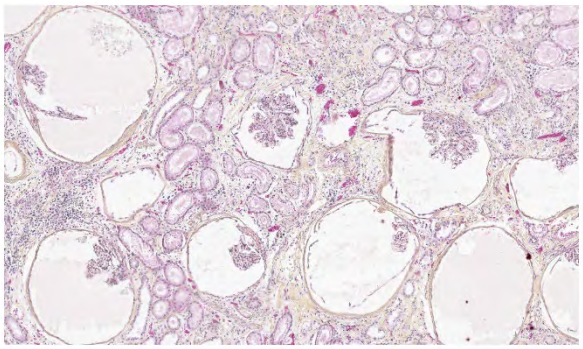

Figure 4-2: Kidney, dog. Within dilated Bowman's spaces, glomerular tufts are small and often adherent to the inner aspect of Bowman's capsule. At this (HE, 140X)

(cystic glomeruli), with moderate multifocal tubulointerstitial nephritis, consistent with glomerulocystic kidney disease

2) Multifocal glomerular and tubular basement membrane (metastatic) mineralization

Contributor's Comment:

Glomerulocystic kidney disease (GCKD) is a rare disease reported mostly in humans, and also in 3 dogs and a single stillborn foal; it is part of the polycystic kidney disease (PKD) complex.[1-7] In dogs, the disease has been described in a Shiba, a Belgian Malinois, and a Blue merle collie.[3,6-7] In humans, GCKD is mostly observed in infants and young children, but adults may be affected.[2,6] The canine cases involved adult animals, with ages ranging from 11 months to 5 years, as in our case. Diseases of the PKD complex are well described in humans and, to a lesser degree, in animals.[1,4] They are part of the larger group of renal cystic diseases that include multiple hereditary, nonhereditary and acquired conditions.[1,4] In diseases of the PKD complex, there is a progressive dilation of different portions of the nephron or collecting duct with the eventual formation of cysts.[4,6] In GCKD, it is the glomerular chambers (Bowman's spaces) that are cystic; in humans, the adjacent portion of the proximal convoluted tubules is also dilated.[1] A glomerular cyst has been defined as a glomerulus with a 2- to 3-fold dilatation of its Bowman's space.[2]

Although periglomerular fibrosis and proximal tubular obstruction due to ischemic changes have been suggested as a possible mechanisms,[4,7] the pathogenesis remains largely unknown in animals. In humans, the pathogenesis is still unclear, but there have been some advances in the understanding of the pathophysiology. For instance, it has been proposed that a ciliopathy may be involved, similarly to other renal cystic diseases; several genes involved in renal development are also under investigation (GCKD can develop due to changes in Wnt or hedgehog signaling).[2] In humans, GCKD is often associated with other lesions or diseases, including autosomal dominant polycystic kidney disease (ADPKD) and the tuberous sclerosis complex.[1,2] Three clinical variants have been originally described: malformation syndrome-associated GCKD, renal dysplasia-associated GCKD, and primary GCKD (heritable and sporadic).[2,6] A more recent classification of GCKD has been published in 2007: 1) familial nonsyndromic (e.g. ADPKD in infants), 2) associated with inheritable malformation syndromes (e.g. tuberous sclerosis complex), 3) syndromic, non-Mendelian (e.g. trisomy 9, 13 or 18), 4) sporadic (new mutations), and 5) acquired and dysplastic kidneys (e.g. hemolytic uremic syndrome and obstructive uropathy).[2] There are mouse models of GCKD that are relevant to the human disease.[2]

As with other chronic glomerular diseases, secondary chronic tubulointerstitial nephritis will develop in time.[3] Glomerulocystic disease

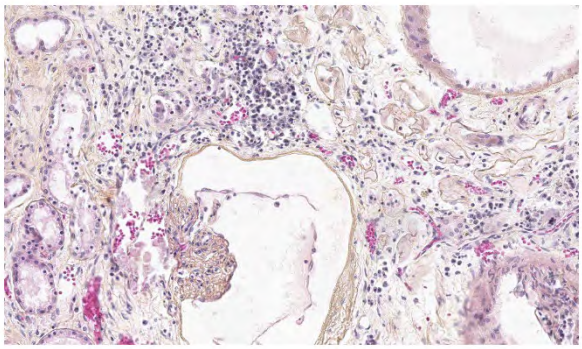

Figure 4-3: Kidney, dog. Occasional glomeruli are sclerotic, with marked fibrosis of the glomerular tufts. There is also diffuse interstitial fibrosis with marked atrophy of entrapped tubules and scattered aggregates of lymphocytes and plasma cells. (HE, 380X)

(GCKD) must be differentiated from "glomerulocystic change", in which cystic glomeruli are secondary to renal scarring from different renal pathologies.[3] In the present case, the chronic tubulointerstitial nephritis is considered to be secondary to the glomerular pathology.

Contributing Institution:
Faculty of veterinary medicine, Université de Montréal, St-Hyacinthe, Quebec, Canada:
http://www.medvet.umontreal.ca

JPC Diagnoses:
Kidney: Glomerulocystic atrophy, chronic, diffuse, severe, with tubular degeneration and necrosis, basement membrane mineralization, and multifocal lymphocytic interstitial nephritis and fibrosis.

JPC Comment:
The last case for today's conference represented a condition so uncommonly encountered that there was prolonged discussion about differential diagnoses and why this condition was not those things. Differentials included Lyme disease, which would have tubular degeneration, lymphoplasmacytic interstitial nephritis, and glomerulonephritis; Renal dysplasia, which has a trifecta of findings including fetal glomeruli, primitive tubules, and fetal mesenchyme; and urolithiasis leading to hydronephrosis, which would have dilation/ectasia of tubules at all levels, renal pelvic dilation, and would likely have protein casts within tubules. The defining features of glomerulocystic disease that separate it from these other conditions are dilation of the glomerular tuft with cystic expansion of Bowman's space and glomerular atrophy with no concurrent glomerulonephritis. Additionally, the proximal convoluted tubules (PCTs) closest to the glomeruli are the most affected and may also demonstrate a degree of dilation due to stenosis between the glomeruli and the PCTs. There may also be a lymphoplasmacytic interstitial nephritis, which was seen in this case.

An interesting feature of this condition is that the basement membranes of multiple tubules and glomeruli were mineralizing, even in the absence of obvious degeneration. Hmm! A review of clinical pathology data from a pair of 2008 case reports in dogs with glomerulocystic disease was conducted during conference and revealed that dogs affected with this condition can have an abnormal Calcium/Phosphorus ratio secondary to their renal disease, so much so that metastatic mineralization can occur.[5]

Additionally, the dogs in the case report had low hematocrit, low hemoglobin, and low reticulocyte count.[5] All three of these can be explained by the loss of the renal juxtaglomerular apparatus in this disease that is responsible for sensing feedback on erythrocyte concentrations within the blood and subsequently

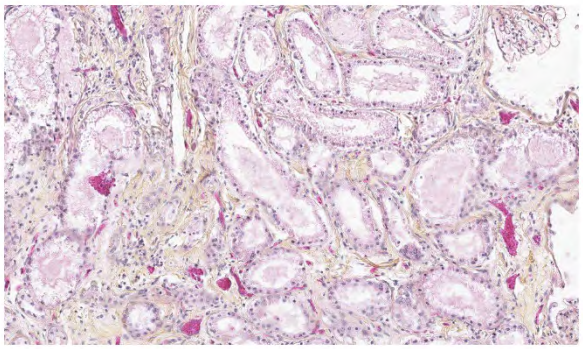

Figure 4-4: Kidney. Tubules demonstrate a range of changes within the fibrotic interstitium: cell swelling and vacuolation, necrosis and sloughing, and accumulation of protein within the lumen. (HE, 400X).

stimulating erythropoietin production when needed. If there's no stimulus to make more red blood cells, of course your HCT, Hbg, and reticulocytes are going to be lacking and an anemia will result.

Lastly worth nothing is that the dogs in the case report were also azotemic and acidotic.[5] The metabolic acidosis in these cases is due to a combination of the azotemia and anemia. Fewer red blood cells to transport oxygen leads to tissue hypoxia and an increase in anaerobic glycolysis, which produces lactic acid. Azotemia causes acidosis due to the kidneys being unable to properly excrete waste products that generate acid, such as phosphates and sulfates, and they lose the ability to regenerate and resorb bicarbonate, which is a vital buffer of acids in the bloodstream. Understanding how these clinical findings translate to the lesions pathologists see is critical to being able to logically follow a disease pathogenesis, to know where to look for lesions in particular diseases, and to understand how to make sense of pathophysiology. As such, the clin path review during this conference case was well-received by all participants and much appreciated.

References:

1. Bisceglia M, Galliani CA, Senger C, Stallone C, Sessa A. Renal cystic diseases: a review. *Adv Anat Pathol*. 2006;13:26-56.
2. Bissler JJ, Siroky BJ, Yin H. Glomerulocystic kidney disease. Pediatr Nephrol. 2010;25:2049-56.
3. Chalifoux A, Phaneuf J-B, Olivieri M, et al. Glomerular polycystic kidney disease in a dog (blue merle collie). Can Vet J. 1982;23:365-368.
4. Maxie, MG, Newman SJ. Urinary system. In: Jubb, Kennedy and Palmer's Pathology of domestic animals, vol.2. Fifth Edition. Elsevier Saunders. Philadelphia, PA, 2007:281-458.
5. Morales E, Montesinos-Ramirez LI, Garcia-Ortuno LE, and Nunez-Diaz AC. Glomerulocystic kidney disease in two dogs with renal failure. Veterinaria Mexico. 2008:39(1):97-110.
6. Ramos-Vara JA, Miller MA, Ojeda JL, et al. Glomerulocystic kidney disease in a Belgian malinois dog, an ultrastructural, immunohistochemical, and lectin-binding study. Ultrastruct Pathol. 2004;28:33-42.
7. Takahashi M, Morita T, Sawada M, et al. Glomerulocystic kidney in a domestic dog. J Comp Path. 2005;133:205-208.

Joint Pathology Center
Veterinary Pathology Services

WEDNESDAY SLIDE CONFERENCE 2025-2026

Conference #4 — 17 September 2025

CASE I:

Signalment:
Unknown age, male, black-tailed prairie dog, *Cynomys ludovicianus*

History:
Prairie dog sourced from a zoologic collection. Clinical presentation for acute ptyalism, easily captured, poor vision. Clinical examination noted superficial healing wounds on bilateral forearms, facial scarring with intermittent swellings, incisor malocclusion, elongate buccal aspects of mandibular molars, bilateral tongue ulceration.

Gross Pathology:
External examination of the lungs was normal. On serial sectioning and trimming in representative sections of lung a single small sample of lung tissue was noted as floating low in formalin solution; on examination of one aspect of the cut section the lung was pale tan and consolidated with multifocal pale tan, circular, soft foci (exudate filling bronchi). The total volume of affected lung mass was less than 10%.

Laboratory Results:
Initial Gram, GMS, and acid-fast stains of affected lung tissue did not identify bacterial or fungal microorganisms. Please see comments below for details on follow-up ancillary diagnostics.

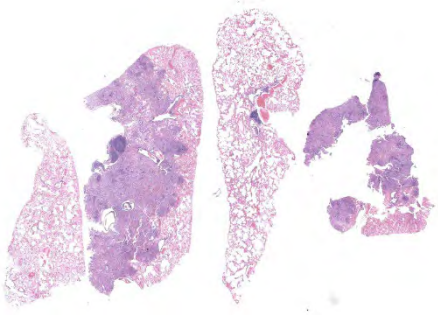

Figure 1-1: Lung, prairie dog. Four sections of lung are submitted for examination, with two sections demonstrating marked consolidation. (HE, 10X)

Microscopic Description:
Lung, multiple sections. Within a single section of lung, approximately 75% of the bronchial, bronchiolar, and alveolar lumina contain overall large numbers of neutrophils, macrophages, large multinucleated cells, cellular debris, homogenous eosinophilic material, fibrillary eosinophilic material, and occasionally scattered erythrocytes. The multinucleated cells are often large and bizarre in appearance, some containing approximately 40 nuclei. The cytoplasm of these multinucleated cells is eosinophilic and variably granular to homogenous. A subset of these multinucleated cells contains few distinct optically clear vacuoles, while others demonstrate phagocytosis of few neutrophils. There is mild vascular congestion throughout, and there are small clusters of lymphocytes cuffing airways multifocally.

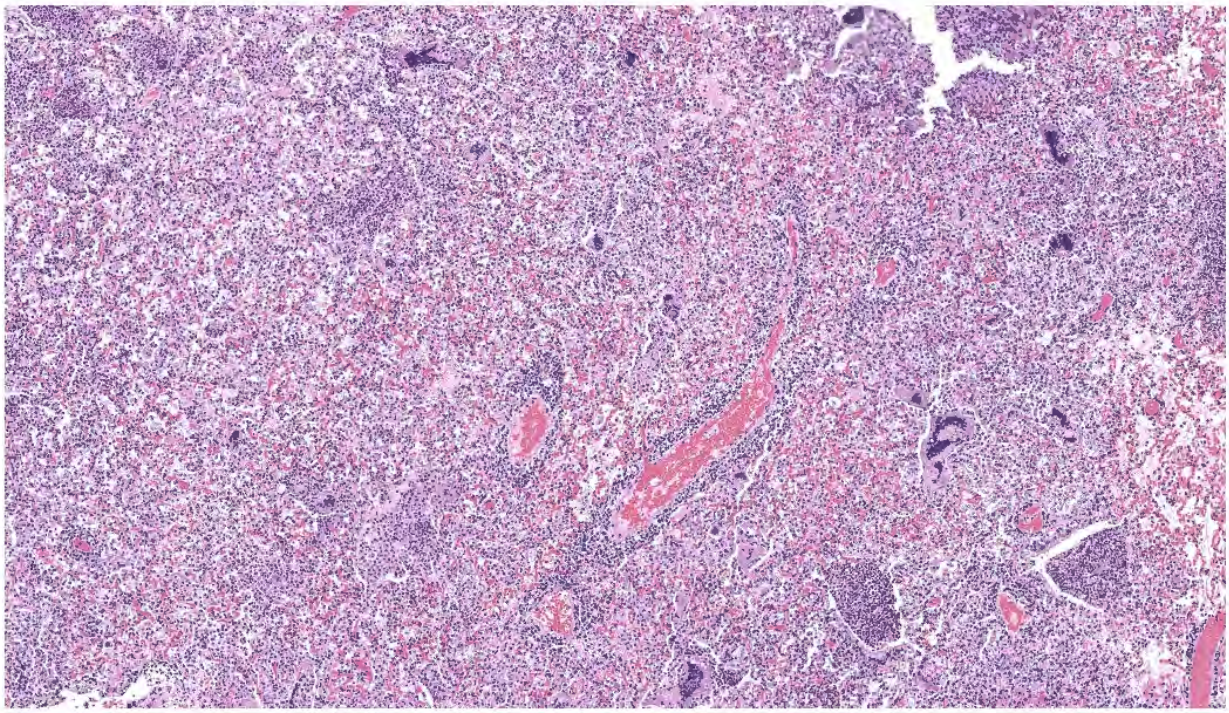

Figure 1-2: Lung, prairie dog. Within affected sections, normal pulmonary architecture is effaced by a dense inflammatory infiltrate expanding alveolar septa and filling alveolar spaces and airways. At this magnification, large multinucleated giant cells and BALT hyperplasia is visible. (HE, 103X)

Contributor's Morphologic Diagnoses:
Pneumonia, bronchoalveolar, suppurative, histiocytic, focal, subacute, severe with intraluminal multinucleated giant cells.

Contributor's Comment:
Initial Gram, GMS, and acid-fast stains of affected lung tissue did not identify bacterial or fungal microorganisms. Viral inclusions were not evident on H&E-stained sections of the affected lung and other tissues evaluated during necropsy evaluation.

Pathologists reviewing the case considered the possibility of multinucleated giant cells versus syncytia. Pulmonary syncytia in mammalian species may be seen with orthopoxviruses, herpesviruses, and respiratory syncytial viruses.[5] Among the orthopoxviruses, monkeypox virus would be a possible differential that must be considered given this species' vulnerability to the virus and the zoonotic potential.[2,7] Necrotizing bronchopneumonia has been reported in prairie dogs with monkeypox viral infection, and histologic descriptions have included syncytia and poorly discernible eosinophilic intracytoplasmic inclusions.[4,6]

Formalin-fixed, paraffin-embedded lung tissue was submitted to the Center for Disease Control and Prevention (CDC) for further evaluation. Immunohistochemical staining for orthopoxviruses was not detected. Additional immunohistochemical stains for canine distemper virus, measles virus, and respiratory syncytial virus were reported negative. PCR testing for human parainfluenza virus (1-4) and respiratory syncytial virus were also reported negative.

Transmission electron microscopy provided ultrastructural evidence of bacteria within giant cells, with no viral particles identified.

The sample was immunoreactive on a polybacterial immunohistochemical assay, but negative for select gram-negative bacteria on a separate immunohistochemical assay. PCR

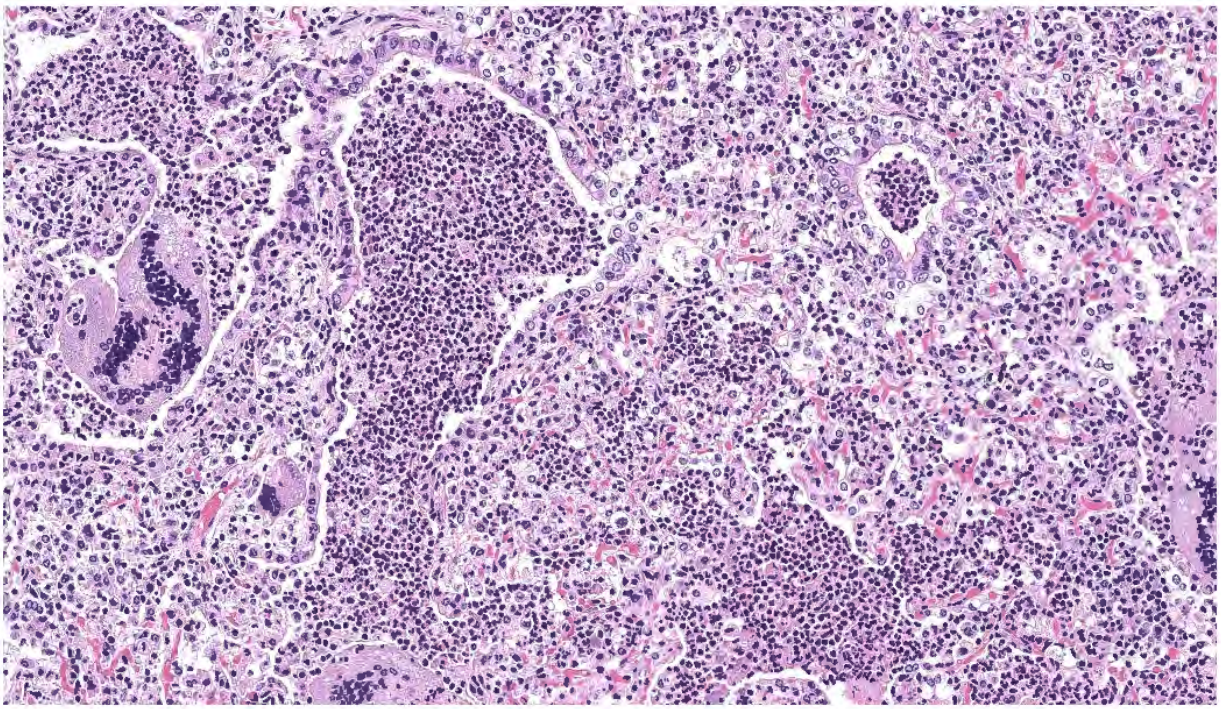

Figure 1-3: Lung, prairie dog. Higher magnification of pulmonary consolidation with expansion of septa by numerous foamy macrophages and fewer neutrophils and scattered multinucleated giant cells with up to twenty nuclei. Airways are filled with similar cells with a higher percentage of neutrophils, and there is multifocal necrosis and loss of airway epithelium. (HE, 285X)

testing for the groEL gene of mycobacteria and *Nocardia* spp. was positive, with subsequent sequencing identifying *Nocardia* spp. PCR testing for gram-negative bacteria specific 16S rRNA gene was positive for Pasteurellaceae. Immunohistochemical staining for *Pasteurella multocida* was negative. PCR testing for gram-positive bacteria specific 16S rRNA gene was indeterminate. Repeat acid fast staining (Fite's stain) identified long filamentous rods within the giant cells.

Contributing Institution:
Arizona Veterinary Diagnostic Laboratory
https://azvdl.arizona.edu

JPC Diagnosis:
Lung: Bronchopneumonia, histiocytic and neutrophilic, chronic, multifocal to coalescing, severe, with numerous multinucleated giant cells.

JPC Comment:
Our fourth conference this year was moderated by the esteemed Dr. Thomas Cecere from Virgina Tech. The JPC team was thrilled to have him back for the second year in a row. This first case provided a great discussion on diagnostic workups and the processes that the pathologist should consider when choosing next steps in a case. Here, the lungs were "chock-a-block" full with histiocytic and neutrophilic inflammation with numerous giant cells that one participant remarked as having "a million nuclei." These were some of the most impressive giant cells that many participants had seen. The bacteria were very difficult to see on the H&E, but the pattern of inflammation and presence of such robust giant cells should clue one into the presence of infectious organisms. As such, next steps should

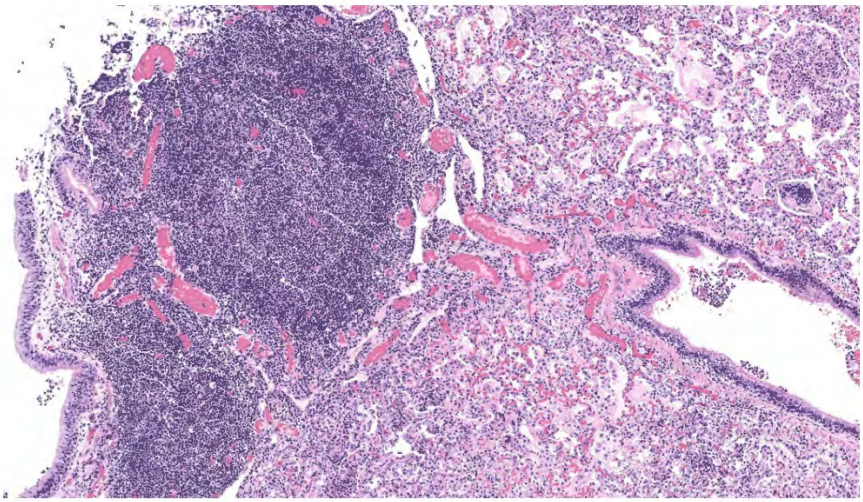

Figure 1-4: Lung, prairie dog. There is significant BALT hyperplasia. (HE, 131X)

include a full gamut of routine infectious organism stains, including gram stains, acid fast stains, and fungal stains (GMS, PAS). Given that these were performed by the contributor, only confirmatory GMS and Fite-Faraco (FF) stains were performed in house, which revealed weakly acid-fast, GMS-positive organisms within multinucleated giant cells. This is consistent with the *Nocardia spp.* that were identified by the contributor. Those "chef's kiss" multinucleated giant cells, though, deserve some recognition here.

The multinucleated giant cell macrophage is a truly remarkable physiologic phenomenon. How they are formed is poorly understood. The current understanding is that macrophages need to be present in chronic inflammation, where they are constantly exposed to pro-inflammatory cytokines, such as IFN-γ, IL-3, IL-4, IL-13, and GM-CSF, as well as pathogen-associated molecular patterns (PAMPs) and other mediators of inflammation.[1] A common setting in which these "ingredients" are found is in fungal infections or when dealing with foreign bodies, both of which can sometimes be too large for inflammatory cells to phagocytose and handle on their own. In this environment, macrophages will be in close association with one another and will begin to express molecules on their cell surface that enable fusion with one another, including dendritic cell-specific transmembrane protein (DC-STAMP; major driver of fusion), β1 and β2 integrins, CD44 (hyaluronic acid receptor), CD47 (integrin-associated protein), macrophage fusion protein receptor (MFPR), fusion regulatory protein (FRP-1, also known as CD98), and P2X7 (an ATP-activated ion channel that results in pore formation).[1]

Now that the involved macrophages have fused together into their version of Infinity Man, they are better equipped with their combined powers to engulf larger threats. One of the mechanisms that multinucleated giant cells have at their disposal to combat pathogens is to produce abundant amounts of nitric

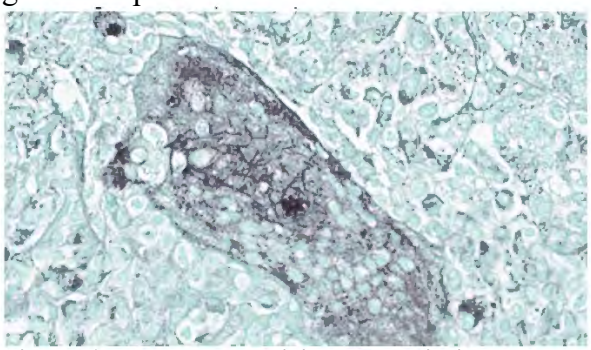

Figure 1-5: Lung, prairie dog. Within the cytoplasm of multinucleated giant cell macrophages, a silver stain demonstrates moderate numbers of haphazardly arranged filamentous bacilli. (GMS, 1189X)

oxide (NO), which is generally microbicidal via induced oxidative stress.[3] However, *Mycobacterium spp.* and *Nocardia spp.* target macrophages as their preferred home within the body and are able to survive intracellularly by preventing fusion of the phagosome and lysosome. Additionally, they produce enzymes to help them combat the damaging effects of NO and other reactive oxygen species produced by macrophages. Multinucleated giant cells are, for all their pathogen-fighting abilities, rather permissive to the persistence of *Mycobacterium spp.* and *Nocardia spp.* within them.[3] With multinucleated giant cells pumping out a ton of NO, other macrophages are additionally induced to fuse and become multinucleated giant cells, which further perpetuates mycobacterial survival and can contribute to the chronic nature of *Mycobacterium spp*. and/or *Nocardia spp*. infections.[3]

References:

1. Ackermann MR. Inflammation and Healing. In: Zachary JF, ed. *Pathologic Basis of Veterinary Disease*. 7th ed. St. Louis, MO: Elsevier; 2022:104-170.
2. Essbauer S, Pfeffer M, Meyer H. Zoonotic poxviruses. Vet Micro. 2010;140:229-236.
3. Gharun K, Senges J, Seidl M, Lösslein A, Kolter J, Lohrmann F, Fliegauf M, Elgizouli M, Alber M, Vavra M, Schachtrup K, Illert AL, Gilleron M, Kirschning CJ, Triantafyllopoulou A, Henneke P. Mycobacteria exploit nitric oxide-induced transformation of macrophages into permissive giant cells. EMBO Rep. 2017;18(12):2144-2159.
4. Guarner J, Johnson BJ, Paddock CD, Shieh WJ, et al. Monkeypox transmission and pathogenesis in prairie dogs. Emerg Inf Dis. 2004;10(3):426-431.
5. Hughes L, Olson VA, Damon IK. Poxviruses. In: Jorgensen JH, ed. Manual of Clinical Micrology. 11th ed. ASM Press; 2015.
6. Langohr IM, Stevenson GW, Thacker HL, Regnery RL. Extensive lesions of monkeypox in a prairie dog (Cynomys sp.). Vet Pathol. 2004;41(6):702-707.
7. Yarto-Jaramillo E. Rodentia. In: Miller RE ed. Fowler's Zoo and Wild Animal Medicine. Vol 8. Saunders; 2015.

CASE II:

Signalment:

12-year-old, female, mixed breed, domestic goat, *Capra aegagrus hircus*

History:

The owners report weight loss and cough for a few weeks. When auscultated, muffled heart sounds were heard on the right side, but no heart sounds were heard on the left side. Crackling sounds were heard in the dorsal lung fields but lungs sounds were absent ventrally. The owners elected for euthanasia and the goat was sent for a postmortem.

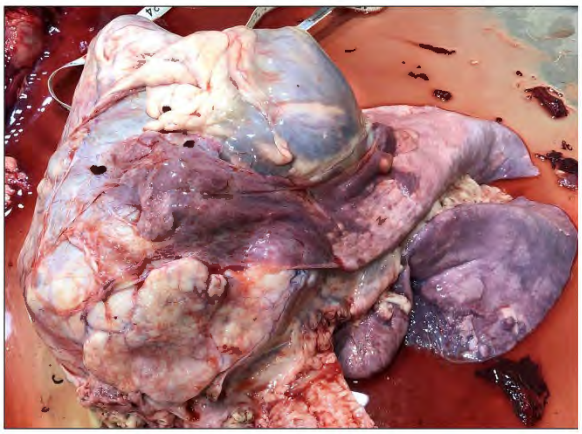

Figure 2-1: Thoracic viscera, goat. There is a large mediastinal mas. Cranioventral lung lobes are multifocally firmly adhered to the outer surface of the mass. Multifocal small nodules are scattered within the lung parenchyma (Photo courtesy of: Atlantic

Gross Pathology:
The goat was thin with small visceral and subcutaneous body fat stores. Moderate clear edema expanded the subcutis and deeper soft tissues along the ventral aspect of the mandibles, the ventral neck and the ventral trunk (dependent edema). Approximately 500 mls of orange-tinged fluid containing a few strands of fibrin was present in both the thoracic and abdominal cavities. Approximately 500 mls of similar fluid also distended the pericardial sac. An approximately 24cm mass expanded the cranial mediastinum and filled the cranioventral thorax, displacing and compressing the lungs caudodorsally. When sectioned, much of the center of this mass was brown, necrotic and composed of many cystic pockets filled with yellow-brown clear fluid intermingled with pale yellow-tan, friable, debris. A thin peripheral layer of relatively intact tissue was generally present just beneath the variably thick layer of dense fibrous tissue which surrounded the mass. Portions of the cranioventral lung lobes were attached by extensive fibrous pleural adhesions to the outer surface of the mass. The pulmonary parenchyma was pale pink, partially collapsed and contained numerous, firm, randomly scattered, nodules ranging in size from 0.7-2.5 cm in greatest diameter. The base of the pulmonary trunk was markedly dilated just proximal to where it entered and passed through the large mediastinal mass. The right ventricular lumen and the right atrium were also markedly dilated. Mediastinal lymph nodes were unremarkable. The liver was diffusely dark red, moderately enlarged and when sectioned had a prominent red brown to tan, reticular (or nutmeg) pattern.

Laboratory Results:
Immunohistochemistry on sections of the mediastinal mass was performed; see microscopic description.

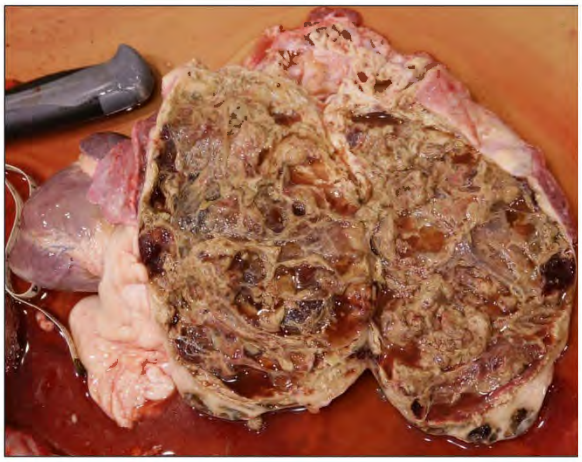

Figure 2-2: Mediastinum, goat. Cut section of the mediastinal mass with a large necrotic center. (Photo courtesy of: Atlantic Veterinary College, University of Prince Edward Island; www.upei.ca/avc).

Microscopic Description:
Much of the center of this mediastinal mass is effaced by extensive areas of necrosis and cystic degeneration. Sections were taken from the remaining thin peripheral rim of intact tissue that is surrounded by a variably thick, dense fibrous capsule. Neoplastic tissue is composed of highly cellular, infiltrates of plump spindled to polygonal cells which are arranged in coalescing trabeculae and sheets and are intermingled with moderate to large numbers of small lymphocytes. These infiltrates multifocally infiltrate the surrounding capsule and are supported by small amounts of fine fibrovascular stroma which often forms dissecting thick bands and thinner septa. Frequently scattered within these infiltrates are small clusters of pale, polygonal, epithelial cells with glassy, keratinized, cytoplasm that are sometimes partially mineralized (Hassall's corpuscles). The interstitium within the mass is also multifocally, mildly to moderately, expanded by pale poorly cellular fine fibrous stroma which often contains variably sized, deposits of basophilic, granular mineral. The majority of neoplastic polygonal to spindloid cells exhibit strong cytoplasmic staining with

Figure 2-3: Thymus, goat. A section of a mediastinal neoplasm is submitted for examination. There is multifocal capsular invasion. (HE, 10X)

cytokeratin. Most of the small lymphocytes scattered within the mass were CD3 positive.

The masses noted in the lung consist of similar, nodular mixed infiltrates of pale polygonal to spindloid cells intermingled with numerous small lymphocytes. These mixed infiltrates often dilated and fill pulmonary arteries and veins. Frequent scattered small deposits of mineral, foci of lytic and coagulative necrosis are also often scattered within these metastatic nodules.

Contributor's Morphologic Diagnoses:
Malignant thymoma/thymic carcinoma with pulmonary metastasis

Contributor's Comment:
In general, thymic epithelial tumors are considered uncommon tumors in veterinary medicine and have been reported in humans and in a wide range of animals including(but not limited to) dogs, cats, rabbits, cattle, horses and sheep. The exception appears to be in older goats where, although neoplasia is generally uncommon, thymoma was reported as the third most common tumor in a retrospective study involving 100 goats.[5] One report involving a herd of dairy goats (mainly of Saanens or Saanen mixed breeds) found thymomas in 17 of 67 (25.3%) necropsied goats over 2 years of age.[2] Other reports have suggested that pygmy goats may also have a high incidence of thymomas.[3]

In goats, thymomas are often considered benign, slow growing tumors and many are incidental findings at necropsy or slaughter of mature animals. In most species, including goats, thymomas largely reside in the cranial mediastinum. However, due to the anatomy and development of the thymus in ruminants, whereby portions of this large lobulated organ in young animals may extend from the larynx to the cranial aspect of the pericardium, thymomas may form in ventral cervical region, the mediastinum, or involve both locations.[4] When large, as in this case, mediastinal thymomas may result in clinical signs such as respiratory distress and coughing due to compression and displacement of the lung, and trachea. Dependent edema in this goat was attributed to right heart failure caused by compression of the pulmonary trunk as it passed through this large mediastinal mass.

Histologically, thymomas can vary greatly in appearance and in composition. Neoplastic

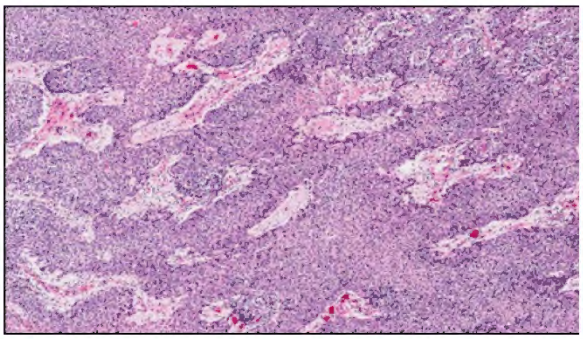

Figure 2-4: Thymus, goat. The neoplasm is composed of coalescing trabeculae and sheets of plump spindled to polygonal tumor cells intermingled with many small lymphocytes. (HE, 4X) (Photo courtesy of: Atlantic Veterinary College, University of Prince Edward Island; www.upei.ca/avc

cells are epithelial and originated from endoderm of the third pharyngeal pouch in the fetus.[2] Tumor cells may appear polygonal and/or spindled, and are accompanied by variable, sometimes large, numbers of mature, non-neoplastic lymphocytes. As in this case, neoplastic cells exhibit cytoplasmic staining with cytokeratins and most of the small lymphocytes present within the tumor are small CD3+ T cells. Thymomas have been subcategorized, based on cellular composition as lymphocyte-predominant, epithelial-predominat, or mixed. A variety of subtypes have also been identified (clear cell, spindle cell, pigmented).[9] A clear association with prognosis and these subtypes has not been identified in veterinary medicine. In human medicine, the 2004 World Health Organization (WHO) classification scheme of thymic epithelial tumors was created to better correlate histologic findings with the clinical behavior of these tumors. This system is also based on the cell morphology of neoplastic epithelial cells and the relative proportion of non-neoplastic lymphocytes present and appears to be applicable to canine thymomas.[10]

Malignant thymomas, or thymic carcinomas, are very rare but have been reported in a variety of species, including goats.[7] As in this case, the previously reported malignant thymoma involved a very large thymoma that had likely been present for a prolonged period and had many small pulmonary metastases. Thoracic lymph nodes were unaffected in the reported case, and in our goat.

A high incidence of paraneoplastic conditions is reported in association with thymomas in both human and veterinary medicine. In dogs, hypercalcemia due to production of PTH-rP is commonly associated with thymomas.[9] Autoimmune paraneoplastic conditions are also commonly associated with thymomas. Most thymomas exhibit varying, and sometimes marked, degrees of lymphopoiesis resulting in the proliferation of polyclonal CD4+ and CD8+ T cells. Normally in humans and animals, naïve T lymphocytes in the thymus interact with thymic epithelial cells which express high levels of MHC I and II molecules. This interaction results in the selection and weeding out of auto-reactive T cells that recognize both MHC molecules and self-antigens.[2] In animals with thymomas, aberrant expression by neoplastic epithelial cells of MHC molecules, autoantigens, and other critical receptors in this selection process, is thought to allow release of CD4+ and CD8+ T cells into systemic circulation which may then react with a wide variety of self-antigens. CD4+ T lymphocytes that recognize self-antigens (such as acetylcholine receptors) stimulate proliferation and differentiation of B lymphocytes with subsequent autoantibody production (resulting in myasthenia gravis and megaesophagus). In some conditions, such as thymoma-associated exfoliative dermatitis (which shares many clinical and histologic

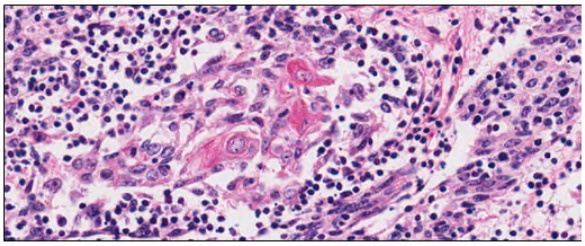

Figure 2-5: Thymus, goat. The neoplasm is composed of coalescing trabeculae and sheets of plump spindled to polygonal tumor cells intermingled with many small lymphocytes. (HE, 4X) (Photo courtesy of: Atlantic Veterinary College, University of Prince Edward I

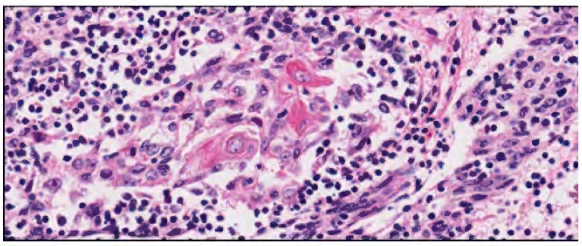

Figure 2-6: Thymus, goat. Small clusters of pale, polygonal, epithelial cells with glassy, often keratinized, cytoplasm (Hassall's corpuscles) are scattered throughout the neoplasm. (HE, 20X) (Photo courtesy of: Atlantic Veterinary College, University of Prince Edward Island; www.upei.ca/avc).

features with erythema multiforme), autoreactive lymphocytes bind directly to keratinocytes and induce apoptosis.[1] A wide variety of additional autoimmune diseases have been reported in animals in association with thymomas including polymyositis, thrombocytopenia, anemia, and granulocytopenia.[9] Paraneoplastic disease in goats with thymomas is extremely rare but megaesophagus and ruminal tympany attributed to esophageal compression by a large mediastinal mass, and thymoma-associated exfoliative dermatitis have both been described in domestic goats.[1,8]

Contributing Institution:
Atlantic Veterinary College, University of Prince Edward Island; www.upei.ca/avc

JPC Diagnosis:
Thymus: Thymoma.

JPC Comment:
The contributor provided an excellent, thorough explanation of thymomas, the paraneoplastic syndromes seen with this neoplasm, and the pathogeneses of how thymomas cause these syndromes. These topics were central to the conference discussion of this case, as well as to the types of questions that were asked of participants about thymomas. As such, the contributor's comment is well-worth a complete read.

Another topic discussed was of the differing types of thymomas classified in human patients and how applicable these are to veterinary medicine. The major thymoma classifications according to the World Health Organization are Types A, A/B, B1, B2, and B3.[6] Type A thymomas are defined by their predominance of spindle-shaped epithelial cells and lack of T-cells.[6] Type A/Bs, also known as "mixed" thymomas, have similar epithelial cell morphology but have an abundance of T-cells throughout.[6] Type B1 has abundant immature T-cells, areas of medullary differentiation, and few epithelial cells.[6] Type B2 is described as having abundant immature T-cells with greater numbers of singular or clustered epithelial cells dispersed throughout the lymphocytes.[6] Lastly, Type B3 has sheets of epithelial cells with rare intercellular bridging and a paucity of T-cells.[6]

Thymoma classification has been discussed in dogs, goats, and sheep predominantly, and there seems to be a shift towards trying to

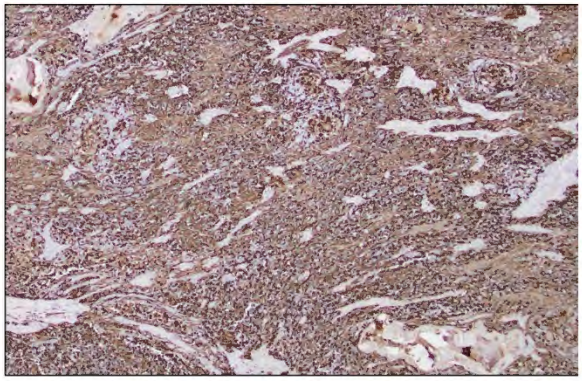

Figure 2-7: Thymus, goat. Neoplastic cells demonstrated strong cytokeratin immunopositivity. (anti-cytokeratin, 40X) (Photo courtesy of: Atlantic Veterinary College, University of Prince Edward Island; www.upei.ca/avc).

align thymoma diagnoses in veterinary species with the classification system that the WHO utilizes for humans. Although it has yet to be fully elucidated whether these classifications are truly comparable in veterinary medi

cine, current literature states that approximately 15% of canine thymomas, as well as the overwhelming majority of thymomas in goats and sheep, are most consistent with Type A/B, although other types have been reported.[10]

References:

1. Byas AD, Applegate TJ, Stuart A, Byers S, Frank CB. Thymoma-associated exfoliative dermatitis in a goat: case report and brief literature review. *J Vet Diagn Invest*, 2019;31(6):905-908.
2. Boes KM, Durham AC. Bone marrow, blood cells and the lymphoid/lymphatic system. In: Zachery JF, ed. Pathologic Basis of Veterinary Disease, 6th ed. St' Louis, Missouri: Elsevier; 2017: 761-764.
3. Hadlow WJ. High Prevalence of thymoma in the dairy goat: report of 17 cases. *Vet Pathol*, 1978;15:153-169.
4. Hill JA, Fubini SL, Hackett RP. Clinical features, treatment, and outcome in goats with thymomas: 13 cases (1990-2014). *JAVMA*; 2017;251(7):829-834.
5. Lohr CV. One hundred two tumors in 100 goats. *Vet Pathol*, 2012; 50(4):668-675.
6. Marx A, Chan JKC, Chalabreysse L, Dacic S, Detterbeck F, French CA, Hornick JL, Inagaki H, Jain D, Lazar AJ, Marino M, Marom EM, Moreira AL, Nicholson AG, Noguchi M, Nonaka D, Papotti MG, Porubsky S, Sholl LM, Tateyama H, Thomas de Montpréville V, Travis WD, Rajan A, Roden AC, Ströbel P. The 2021 WHO Classification of Tumors of the Thymus and Mediastinum: What Is New in Thymic Epithelial, Germ Cell, and Mesenchymal Tumors? *J Thorac Oncol*. 2022;17(2):200-213.
7. Olchowy TWJ, Toal RL, Brenneman KA, Slauson DO, McEntee MF. Metastatic thymoma in a goat. *Can Vet J*, 1996; 37:165-167.
8. Parish SM, Middleton JR, Baldwin TJ. Clinical megaesophagus in a goat with thymoma. *Vet Rec*, 1996; 139:94.
9. Valli VE, Bienzle D, Meuton DJ. Tumors of the Hemolymphatic System. In: Meuton DJ, ed. *Tumors in Domestic Animals*, 5th ed. Ames, Iowa; Wiley Blackwell; 2017: 305-307.
10. Valli VEO, Kiupel M, Bienzle, D, Wood RD. Hematopoietic System. In: Maxie MG, ed. *Jubb, Kennedy, and Palmer's Pathology of Domestic Animals*, 6th ed. St' Louis, Missouri: Elsevier; 2016: Vol 3; 150-158.

CASE III:

Signalment:
Adult, female, Pantaneira, *Ovis aries*, sheep.

History:
On July 24, 2018, the ewe presented with a mild nasal mucohemorrhagic discharge. When rechecked on July 28, 2018 the discharge had become more severe and the ewe was dyspneic and gasping. There was cranium facial asymmetry of the right eye due to exophthalmos. The protrusion of the eyeball resulted in keratitis and corneal ulceration. The ewe was treated with homeopathy with no success. Due to poor prognosis, the ewe was euthanized 34 days after the onset of clinical signs. During July-August 2018, two more cases of the same disease occurred on the premises.

Gross Pathology:
The cadaver denoted poor nutritional status. In the right orbital region, there was a severe increase in periocular volume caused by exophthalmos and resulting in marked cranial asymmetry.

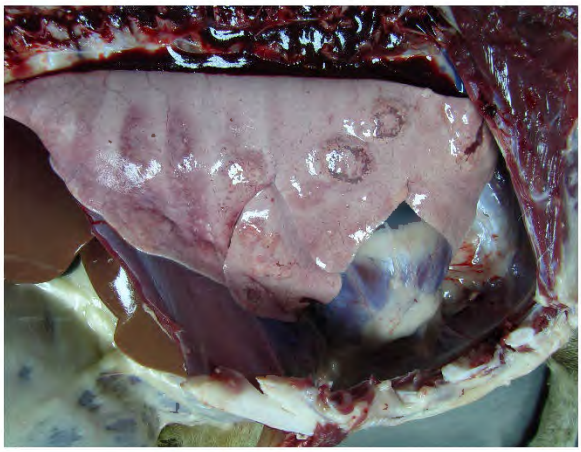

Figure 3-1: Lung, sheep. There are numerous raised nodules, which range up to 2cm and are often surrounded by a red rim scattered throughout the lung. (Photo courtesy of: Universidad Federal de Mato Grosso do Sul, https://www.ufms.br/).

The eyeball was not visible since it was covered by reddish, swollen, ulcerated mucosa. At the cut surface, it was evident that the eyeball had been replaced by a white irregularly outlined mass that was sparsely sprinkled with red spots, with a greyish granular center (caseous material). In the subcutaneous region of the right nasal bone, there was a mass of 2x0.5 cm, the cut surface of which looked similar to that of the ocular mass, but without caseous spots. There was moderate to marked edema throughout the right periocular region.

In the lung, there were several soft, yellowish subpleural nodules of variable sizes (0.5-2cm) and surrounded by a red rim.

The omentum had fair adipose tissue depots, but the serosa of intestines was pale. There were moderate numbers of small hard grey nodules in the serosal aspects of some intestinal loops (calcified nodules of *Oesophagostomum* sp. larvae). The liver was moderately pale, with evidence of the lobular pattern; in the left lobe, there was a firm-to-hard grey nodule interpreted as a calcified hydatid. In both kidneys, irregular pale areas were observed in the natural surface which extended to the cortical region, and in some points reaching the limit of the corticomedullary junction.

On mid-sagittal section of the head, the right side was completely destroyed with loss of nasal conchae which are replaced by a large firm-to-soft, focally friable mass with irregular contours. The mass extended to the pharyngeal region and invaded the cranial cavity, destroying the turbinates and striking the frontal lobe of the brain. After the removal of the cartilage, it was observed that the conchae on the left side were intact but had moderate congestion. After removal of the right hemisphere, an increase in the volume of the olfactory bulb was observed, which was swollen, dark and with a caseous lesion at its junction with the frontal lobe. In the frontal portion of the right cerebral hemisphere, the meninges were thickened, and there was a focal loss of gray matter.

Laboratory Results:

N/A

Figure 3-2: Cerebrum, sheep. A friable mass extends from the nasopharynx through the cribriform plate into the cerebrum. (Photo courtesy of: Universidad Federal de Mato Grosso do Sul, https://www.ufms.br/).

Microscopic Description:
Brain, right frontal lobe: The leptomeninges are focally extensive and moderately expanded by pyogranulomatous exudate. The exudate is formed by nodular to coalescent (mild slide variation) collections of epithelioid macrophages, lesser eosinophils, lymphocytes and plasma cells and few Langhans giant cells. The granulomatous component is admixed with plump fibroblasts, thin bundles of fibrous tissue, and multifocal aggregates of granular, deep basophilic and dense material (mineral). Among the cell debris or in the cytoplasm of the multinucleated cells there are tubularly elongated (when longitudinally sectioned), circular or oval (when transversally sectioned) structures barely stained and hard to visualize in hematoxylin and eosin (HE) stained slide ("negative" images of fungal hyphae). The hyphae are characterized by a body that is hollow or filled with eosinophilic or basophilic granular material and surrounded by varying, but mostly scarce, amounts of strongly eosinophilic, smooth or granular material (Splendore-Hoeppli reaction). The wall of medium-sized arteries in the affected areas is segmentally or cincunferentially expanded by acellular, bright eosinophilic and homogeneous material (fibrinoid necrosis) and occasionally there are hyphae infiltrating the vessel wall or associated with thrombosis in the vessel lumen. There is a focally extensive area of necrosis of liquefaction, swelling of astrocytes and cavitation of nervous tissue, where the parenchyma has been replaced by proliferating microglial cells, many of which already differentiate into foamy macrophages (Gitter cells).

Figure 3-3: Cerebrum and lung, sheep. An inflammatory mass infiltrates the cerebrum at left, and a focally extensive area of consolidation is present in the lung at right. (HE, 10X).

Perivascular cuffs containing up to three layers of lymphocytes are also observed. The organisms stain well by the GMS method as slightly branched hyphae with an irregular diameter of 7-10 μm, associated with foci of necrosis. Occasionally there is a rounded structure of larger diameter (up to approximately 15 μm) at the end of the hyphae.

Lung: There are focal to coalescent areas of consolidation consisting of nodules or sheets of large numbers of epithelioid macrophages and Langhans giant cells admixed with numerous eosinophils and surrounded by fibroblasts and fibrous tissue. The macrophages encircle hyphae similar to that described in the brain that are surrounded by moderate to abundant Splendore-Hoeppli material. Throughout the lung parenchyma there are also small multifocal areas of necrosis containing hyphae. Mineralization is sparsely observed amid necrosis and inflammation. Diffusely, the reminiscent alveolar septa are mildly infiltrated by neutrophils and eosinophils.

Not submitted:

Pyogranulomatous inflammation associated with intralesional hyphae are also observed in

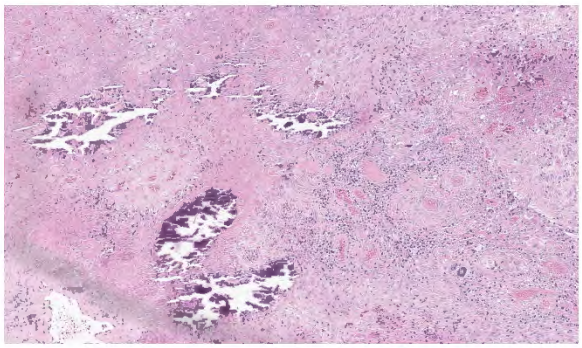

Figure 3-4: Cerebrum, sheep. There is a focally extensive área of coagulative necrosis of the cerebral gray matter (left) with significant pyogranulomatous inflammation with astrocytosis and microgliosis at its periphery. There are scattered aggregates of mineralized debris within the necrotic neuroparenchyma. (HE, 140X).

the nasal conchae, multifocally in the kidneys and expanding eyelids, sclera and periocular tissues.

In the intestinal lamina propria there are small sparsely distributed foci of mineralization, probably mineralized nodules of *Oesophagostomum* sp.

The centrilobular hepatocytes have distended cytoplasm by a sizeable solitary vacuole that pushes the nucleus peripherally (centrilobular lipidosis).

The cytoplasm of the cardiomyocytes is expanded by single, oval structures up to 300 µm in length, filled with elongate banana-like organisms (tachyzoites) consistent with protozoal cysts (*Sarcocystis* sp., most likely *S. bovis*).

Other sections of the brain, spleen, rumen, omasum, and reticulum have no histopathological changes.

Contributor's Morphologic Diagnoses:
Brain, pyogranulomatous meningoencephalitis, focally extensive, with fibrinoid vasculitis and trombi, associated with intralesional fungal hyphae, morphology consistent with *Conidiobolus* sp.

Lung, pyogranulomatous pneumonia, multifocal to coalescent, associated with intralesional fungal hyphae, morphology consistent with *Conidiobolus* sp.

Contributor's Comment:
The lesions presented by this ewe are consistent with nasal zygomycosis of sheep which is a common disease in the semiarid Region of Northeastern and Midwestern Brazil.

The fungi of phylum Zygomycota (zygomycetes) that are of importance as cause of animal disease belong to three orders; Mucorales, Mortierellales, and Entomophtorales.[19] Zygomycetes include widely distributed saprophytes capable of producing opportunistic diseases in animals, and the term zygomycosis is used to describe the illnesses caused by these fungi. Fungi within the order Entomophtorales (entomophthoromycosis) causing animal diseases include (1) *Basidiobolus* spp. reported as a cause of cutaneous granulomas in horses and dogs and (2) *Conidiobolus* spp. reported as responsible for granulomatous inflammation in the subcutaneous tissue of horses; subcutaneous, gastrointestinal and pulmonary granulomas in dogs and nasal granulomas in sheep and horses.[4,5,9,10,12,13,15,16]

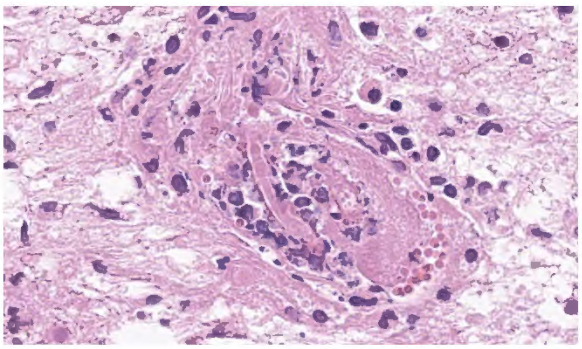

Figure 3-5: Cerebrum, sheep. Thrombosed vessels in the área of necrotic gray matter occasionally contain tangential sections of 6-8um fungal hyphae seen in negative relief. (HE 1400X)

The term zygomycosis is used to describe the diseases caused by fungi mentioned above. In the past, the term phycomycosis was used to refer to infections induced both by zygomycetes and by the fungus-like organism *Pythium insidiosum*, now classified as an Oomycete from the kingdom Chromista.[5,15,16,19] *P. insidiosum* is a well-known cause of eosinophilic subcutaneous and pulmonary granulomas in horses and of similar lesions in several other anatomical sites, including granulomatous rhinitis in sheep and horses.[1,7,14,19,21,24]

In Brazil, granulomatous rhinitis produced by *Conidiobolus* spp. is a common affection of sheep with the highest prevalence in the Northeast and Midwest, but also occurring, although less frequently, in the South.[2,3,6,8,17,18,20,22,23,27,28] The disease can cause significant losses in sheep due to its high lethality rate, that can reach 100%.[2,3]

Infection may occur through spore implantation in the nasal cavity by small traumas as insect bites, as was described in *C. coronatus* infection.[11] Inhalation of fungal conidia from the pasture or possibly inoculation by the sharp-pointed plant parts is the presumed means of infection of the nasal cavity. From there, the microorganism invades adjacent tissues by direct dissemination.[13,27] The extension of the inflammatory reaction to the orbit causes exophthalmia and other injuries of the eye.[1]

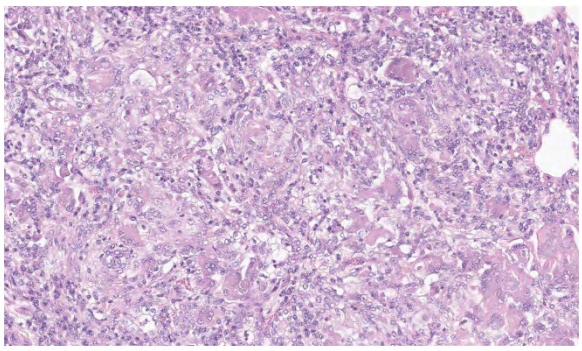

Figure 3-6: Lung, sheep. Within approximately 33% of the section, normal pulmonary parenchyma is effaced by chronic pyogranulomatous inflammation with large numbers of multinucleated foreign body type macrophages. (HE, 381X).

The invasion of the olfactory bulb and frontal lobe of the brain occurs through destruction of the ethmoid bone by the inflammatory process. This has been reported in relation to the rhinopharyngeal form of *Conidiobolus* spp. infection with a prevalence of about 20% to 40 %.[2,13,22,27] In this report the spread also occurred to the lungs, which occurs in this disease with a prevalence of about 15% of the cases, and probably due to aspiration.[8,20,27] The strong effort to breathe may cause fragments of the granulomatous mass to detach and lodge in the lungs, developing new granulomatous foci there.[22] However, dissemination to distant organs such as the kidney, which is reported here, has probably occurred by lymphatic or hematogenous spread. There is evidence for hematogenous dissemination, including mycotic lesions in the vessel walls and invasion of the lumen of vessels associated with thrombosis.

The fungal or fungal-like produced granulomatous rhinitis in sheep occurs in two forms: (1) rhinofacial presentation that affects the nose and the entrance of the nasal fossae and the upper lip,and (2) rhinopharyngeal presentation that affects the turbinates, paranasal sinuses hard, and soft palates and pharynx.[20,21,22,23,27] Over 85% of cases of rhinofacial presentation are caused by *P. insidiosum* and over 90% of the cases of rhinopharyngeal presentation are caused by *Conidiobolus*

spp.[27] In Brazil, *C. lamprauges* and *C. coronatus* have been isolated from these rhinopharyngeal conidiobolomycosis.[3,6,8,22,27,28]

Clinical signs consist of serous nasal discharge that evolves to mucous or mucohemorrhagic; the disease is associated with difficult breathing with stridor, anorexia, and swollen of the anterior or posterior nasal cavity.[4,13]

The tissues of the case reported here were formalin-fixed when they arrived at the laboratory, precluding fungal cultures. Immunohistochemistry and PCR would be the best options to confirm the diagnosis.[27] They were not available to us at the time. So, we had to engage in a diagnostic exercise the allowed us to reach etiology with a reasonably good margin of certainty. A comprehensive review of the lesions affecting the nasal cavity of ruminants in Brazil listed the following five in small ruminants: rhinopharyngeal conidiobolomycosis, rhinofacial pythiosis, aspergillosis, protothecosis and neoplasia (myxoma and enzootic intranasal tumors). After the histopathological examination, only the first two diseases presented a challenge in the differential diagnosis.[18] However, there are significant clinical and pathological differences between rhinopharyngeal conidiobolomycosis and rhinofacial pythiosis that will allow one to reach a final diagnosis. The clinical sign of exophthalmos, due to the presence of retrobulbar granuloma, is a useful indication of rhinopharyngeal zygomycosis.[2,3,4,8,13,17,20,22,27] Although both causal agents may be associated with rhinopharyngeal or rhinofacial presentation of rhinitis in sheep, the location of gross lesions provides a good indicator for the for diagnosis. Disease produced by infection of

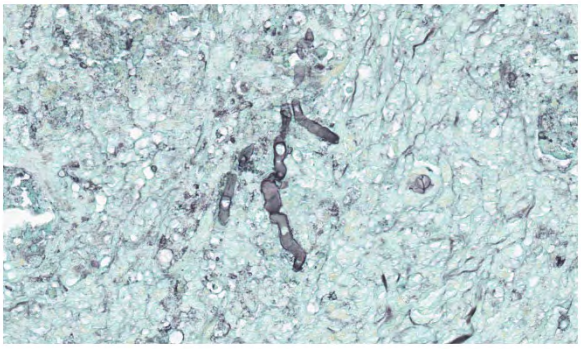

Figure 3-7: Lung, sheep. A GMS stain demonstrates pauciseptate fungal hyphae with non-parallel walls, non-dichotomous branching, and a diameter of 6-8um. (GMS, 674X)

Conidiobolus spp. are almost always rhinopharyngeal and appear as a firm yellow or white mass; pythiosis, almost always located in the rhinofacial region producing a necrotic and friable cellular exudate. Histologically, important morphological differences between the two diseases include the morphology of the two microorganisms. The hyphae in pythiosis have thick walls, almost parallel, and sparsely septate. The hyphae of *Conidiobolus* spp. are thin-walled, non-parallel, and sparsely septate, with ballooning dilations in their extremities.

Enzootic intranasal tumors of ruminants are occasionally diagnosed in cattle and sheep in Brazil, and rhinopharyngitis caused by *Conidiobolus* spp. infection has been mistakenly diagnosed as enzootic intranasal tumor.[18] Although these two conditions have some similar aspects, they can be easily differentiated on histological examination.[26]

Contributing Institution:
Laboratory of Anatomic Pathology, Universidade Federal de Mato Grosso do Sul,
https://www.ufms.br/

JPC Diagnoses:

1. Cerebrum:Meningoencephalitis, pyogranulomatous and necrotizing, chronic, focally extensive, severe, with vasculitis, thrombosis, and numerous intravascular and intrahistiocytic fungal hyphae.
2. Lung: Pneumonia, interstitial, pyogranulomatous, chronic, multifocal to coalescing, severe, with vasculitis and intrahistiocytic fungal hyphae.

JPC Comment:

This is an exceptional write-up by the contributor for this conference. Despite not having ancillary diagnostics available to them, they took on this challenge and presented a clear, concise, and well-organized argument for their diagnosis of *Conidiobolus spp.* as the causative agent in this case. The pathologist will not always have additional diagnostics at their disposal in real-world situations, so being able to reason through a case, reach a logical conclusion, and present differentials given the case findings is critical to the profession. Additionally, they provided a succinct overview of the pathogenesis of *Conidiobolus spp*. infections. As far as the case goes, it's almost as if it read the textbook for lesions while providing a diagnostic challenge to conference-goers.

Participants experienced a wide range of emotions during this case presentation due to the difficulty in locating the fungal hyphae on H&E. They are certainly there, but required some squinting to locate and were best found in the sections of cerebrum. Upon revealing the cause, some participants were high-fiving one another out of mutual success while others audibly groaned in dismay.

Discussion focused on indicative features of a zygomycete histologically, which include a broad diameter ranging from 5-15um, non-parallel thin walls, rare septations, asymmetric acute-angle branching, and potentially a terminal bulb. Zygomycetes are typically weakly PAS-positive and more strongly GMS-positive. This correlated nicely with the PAS and GMS stains run in-house. Other differentials mirrored those discussed by the contributor, including oomycetes like *Pythium insidiosum*, which would be PAS-negative and GMS-positive, as well as *Basidiobolus spp.*, another member of the Entomophthoramycota family alongside *Conidiobolus*. However, *Basidiobolus spp.* typically affect the thorax, trunk, limbs, intestinal tract, and, in atypical cases, can cause systemic infection.[28] *Conidiobolus* is far more commonly seen localized to face and nostrils. Using a variety of proteases (including elastase and collagenase), lipases, esterases, and glycoside hydrolases at their disposal, *Conidiobolus spp.* can wreak havoc to the nasal and facial bones and surrounding soft tissues[24]. Ultimately, they may eat through the cribriform plate and enter the brain.[28,29] It's pretty much "game over" at that point.

References:

1. Bianchi MV, Mello LS, De Lorenzo C, et al. Lung lesions of slaughtered horses in southern Brazil. *Pesq Vet Bras*. 2018;38(11):2056-2064.
2. Boabaid FM, Ferreira EV, Arruda LP, et al. Conidiobolomicose em ovinos no Estado de Mato Grosso [Conidiobolomycosis in sheep in the state of Mato Grosso, Brazil]. *Pesq Vet Bras*. 2008;28(1):77-81.

3. Câmara ACL, Soto-Blanco B, Batista JS, Vale AM, Feijó FMC, Olinda RG. Rhinocerebral and rhinopharyngeal conidiobolomycosis in sheep. *Cienc Rural*. 2011;41(5):862-868.
4. Carrigan MJ, Small AC, Perry GH. Ovine nasal zygomycosis caused by *Conidiobolus incongruous*. *Aust Vet J*. 1992;69(10):237-240.
5. Connole MD. Equine phycomycosis. *Aust Vet J*. 1973;49:215-216.
6. de Paula DAJ, Oliveira-Filho JX, Silva MC, et al. Molecular characterization of ovine zygomycosis in central western Brazil. *J Vet Diagn Invest*. 2010;22:274–277.
7. Frade MTS, Diniz PVN, Olinda RG, et al. Pythiosis in dogs in the semiarid region of Northeast Brazil. *Pesq Vet Bras*. 2017;37(5):485-490.
8. Furlan FH, Lucioli J, Veronezi LO, et al. Conidiobolomicose causada por *Conidiobolus lamprauges* em ovinos no Estado de Santa Catarina [Conidiobolomycosis caused by *Conidiobolus lamprauges* in sheep in the state of Santa Catarina, Brazil]. *Pesq Vet Bras*. 2010;30(7):529-532.
9. Greene CE, Brockus CW, Currin MP, Jones CJ. Infection by *Basidiobolus ranarum* in two dogs. *J Am Vet Med Assoc*. 2002;221:528-532.
10. Grooters AM. Pythiosis, lagenidiosis, and zygomicosis in small animals. *Vet Clin North Am Small Anim Pract*. 2003;33:695-720.
11. Gugnani H. Entomophthoromycosis due to *Conidiobolus*. *Eur J Epidemiol*. 1992;8:391-396.
12. Humber RA, Brown CC, Kornegay RW. Equine zygomycosis caused by *Conidiobolus lamprauges*. *J Clin Microbiol*. 1989;27:573-576.
13. Ketterer PJ, Kelly MA, Connole MD, Ajello L. Rhinocerebral and nasal zygomycosis in sheep caused by *Conidiobolus incongruus*. *Aust Vet J*. 1992;69:85-87.
14. Martins TB, Kommers GD, Trost ME, Inkelmann MA, Fighera RA, Schild AL. A comparative study of the histopathology and immunohistochemistry of pythiosis in horses, dogs and cattle. *J Comp Pathol*. 2012;146(2-3):122-131.
15. Miller R, Campbell RSF. The comparative pathology of equine cutaneous phycomycosis. *Vet Pathol*. 1984;21:325-332.
16. Miller R, Pott B. Phycomycosis of the horse caused by *Basidiobolus haptosporus*. *Aust Vet J*. 1980;56:224-227.
17. Pedroso PMO, Dalto AGC, Raymundo DL, et al. Rinite micótica nasofaríngea em um ovino Texel no Rio Grande do Sul [Rhinopharyngeal mycotic rhinitis in a Texel sheep in Rio Grande do Sul]. *Acta Sci Vet*. 2009;37(2):181-185.
18. Portela RA, Riet-Correa F, Garino-Junior F, Dantas AFM, Simões SVD, Silva SMS. Doenças da cavidade nasal em ruminantes no Brasil [Diseases of the nasal cavity of ruminants in Brazil]. *Pesq Vet Bras*. 2010;30(10):844-854.
19. Quinn PJ, Markey BK, Leonard FC, Fitz-Patrick ES, Fanning S, Hartigan PJ. Zygomycetes of veterinary importance. In: *Veterinary Microbiology and Microbial Diseases*. 2nd ed. Oxford, UK: Wiley Blackwell; 2011:466-451.
20. Riet-Correa F, Dantas AFM, Azevedo EO, et al. Outbreaks of rhinofacial and

rhinopharingeal zygomycosis in sheep in Paraíba, northeastern Brazil. *Pesq Vet Bras*. 2008;28(1): 29-35.
21. Santurio JM, Argenta JS, Schwendler SE, et al. Granulomatous rhinitis associated with *Pythium insidiosum* infection in sheep. *Vet Rec*. 2008;163(9):276-277.
22. Silva SMMS, Castro RS, Costa FAL, et al. Conidiobolomycosis in sheep in Brazil. *Vet Pathol*. 2007a;44:314-319.
23. Silva SMMS, Castro SC, Costa FAL, et al. Epidemiologia e sinais clínicos da conidiobolomicose em ovinos no Estado do Piauí [Epidemiology and symptoms of conidiobolomycosis in sheep in the State of Piauí, Brazil]. *Pesq Vet Bras*. 2007b;27(4):184-190.
24. Shaikh N, Hussain KA, Petraitiene R, Schuetz AN, Walsh TJ. Entomophthoramycosis: a neglected tropical mycosis. *Clin Microbiol Infect*. 2016;22(8):688-94.
25. Tabosa IM, Riet-Correa F, Nobre VMT, Azevedo EO, Reis-Junior JL, Medeiros RM. Outbreaks of pythiosis in two flocks of sheep in northeastern Brazil. *Vet Pathol*. 2004;41:412-415.
26. Teifke JP, Klopfleisch R, Czerwinski G, et al. Morphologische, immunhistologische und molekulare Untersuchungen zur Pathogenese der enzootischen Nasentumoren beim Schaf. *Tierärztl Prax*. 2007;35:264-272.
27. Ubiali DG, Cruz RAS, de Paula DAJ, et al. Pathology of nasal infection caused by *Conidioboulus lamprauges* and *Pythium insidiosum* in sheep. *J Comp Pathol*. 2013;149:137-145.
28. Vilela R, Mendoza L. Human Pathogenic Entomophthorales. *Clin Microbiol Rev.* 2018 ;31(4):e00014-18.
29. Vilela R, Silva SMS, Riet-Correa F, Dominguez E, Mendoza L. Morphologic and phylogenetic characterization of *Conidiobolus lamprauges* recovered from infected sheep. *J Clin Microbiol*. 2010;48(2): 427-432.

CASE IV:

Signalment:
5 year old castrated male Nubian goat (*Capra aegagrus hircus*).

History:
The goat presented to Ohio State Large Animal Services with a 10-day history of lethargy, depression and difficulty standing. Previously he had a wet cough that resolved with Nuflor by the rDVM, though he continued to have mucopurulent discharge and a mild cough. Upon presentation, he was quiet, alert, responsive, and in sternal recumbency. Bloodwork suggested renal disease based on azotemia and metabolic acidosis (see laboratory results below), with an unremarkable urinary bladder and small hypoechoic region in the renal medulla on ultrasound. He received a blood transfusion and fluid therapy, but was not observed to urinate. He continued to decline clinically, and was humanely euthanized.

Gross Pathology:

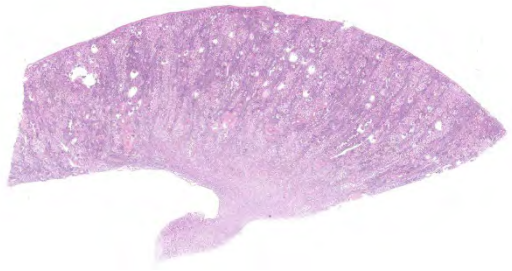

Figure 4-1: Kidney, goat. A single section of kidney is submitted for examination. (HE, 10X)

On gross examination, there was mild serosanguineous pericardial effusion, similar fluid within the entire length of the trachea as well as pulmonary edema. The urogenital tract was unremarkable.

Laboratory Results:

PCV/TP:

- Pre-transfusion = 11/ 7.4
- Post-transfusion = 17/ 6.4

NOVA Panel:

- pH = 7.467
- BUN = 303mg/dL
- Creatinine = 15.5mg/dL
- pCO_2 = 31.4mmHg
- HCO_3 = 22.9mmol/L

Biochemistry Profile:

- BUN = 380mg/dL
- Creatinine = 17.8mg/dL
- Phosphorous = 4.5mg/dL
- Calcium (total) = 7.7mg/dL
- Sodium = 138meq/dL
- Potassium = 3.73meq/dL
- Chloride = 86.7meq/dL
- Anion Gap = 39meq/dL
- Total protein = 5.8g/dL
- Albumin = 3.1g/dL
- Globulin = 2.7g/dL

Hemogram/ CBC:

- Plasma protein = 7.8g/dL
- HCT = 15%
- Hemoglobin = 3.8g/dL
- RBC = 7.3x10^12/L
- MCHC = 25.7g/dL
- Retic absolute = 32.1x10^9/L
- Total leukocytes = 19.9x10^9/L
- Seg neutrophils = 16.9x10^9/L
- Lymphocytes = 3.0x10^9/L

Parasitology (McMaster's Fecal Float):

- Few strongyles and occasional Eimeria were detected in post-mortem colonic contents. No parasites were detectable in the posts-mortem abomasal contents.

Microscopic Description:

There are multiple sections of kidney that include cortex, medulla, and papilla. All of the glomeruli are affected to varying degrees of severity. The glomeruli are globally hypercellular, within both the endocapillary and mesangial compartments. Capillary walls are markedly thickened by eosinophilic matrix. There is frequent dilation of Bowman's capsules and segmental collapsed glomerular tufts/ capillaries with expansion of mesangium with eosinophilic matrix (segmental sclerosis). Less than 25% of the glomeruli are globally sclerotic. Occasionally glomerular tufts are segmentally to globally effaced by eosinophilic mesangial matrix, and mesangial and intracapillary dark brown (hemosiderin) and yellow (hematoidin) pigment with scattered hemosiderin laden macrophages within Bowman's space. There is infrequent segmental loss of podocytes with proliferation of eosinophilic matrix and cells that adhere the glomerular tuft to Bowman's capsule (crescents). Several glomerular capillary loops are filled with fibrin thrombi.

Over half of the tubules are characterized by attenuated epithelium, sloughed hypereosinophilic necrotic intraluminal epithelium, and/or piling of basophilic tubular ep

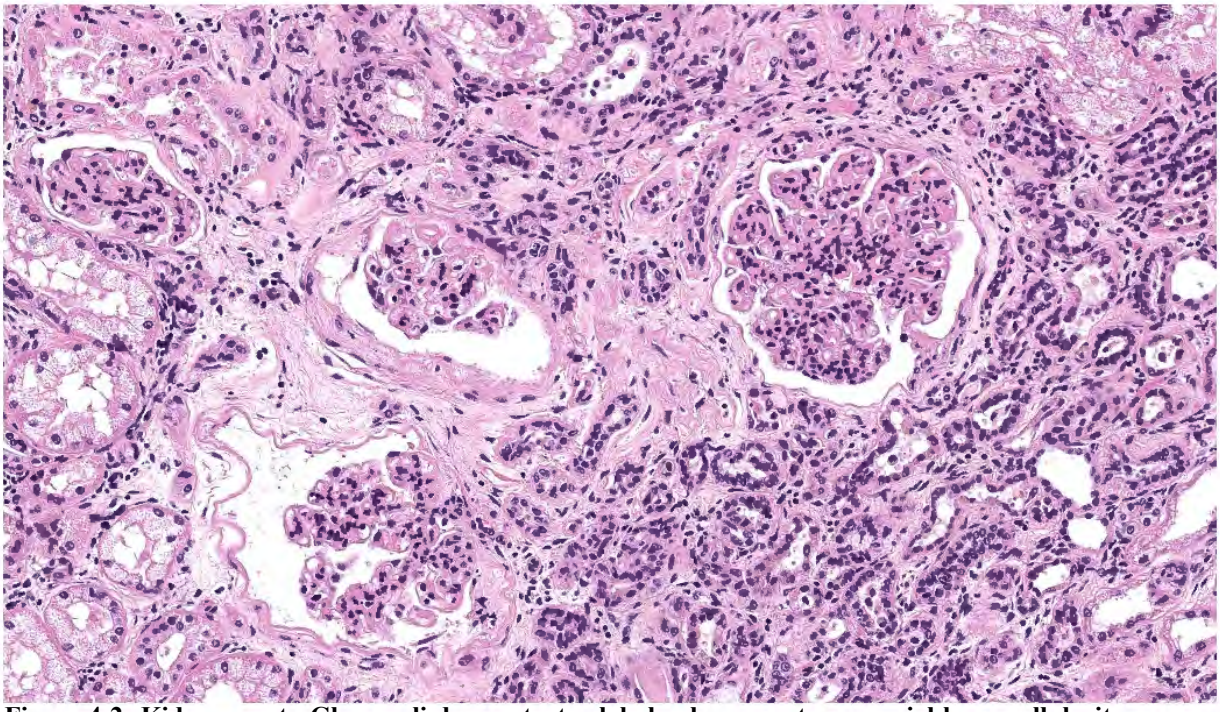

Figure 4-2: Kidney, goat. Glomeruli demonstrate global enlargement, mesangial hypercellularity, expansion of capillary loops, thickening of Bowman's capsule and periglomerular fibrosis. The interstitium is expanded by fibrous connective tissue with entrapped and atrophic tubules. (HE, 381X)

ithelium (regeneration). Often tubules are dilated with eosinophilic proteinaceous material (hyaline casts), and contain intraluminal basophilic refractile material (mineralization). Infrequently, tubules are filled with degenerate neutrophils. There is a mild loss of tubules with expansion of the interstitium by fibrous matrix and aggregates of lymphocytes with fewer plasma cells. There are multiple arcuate arteries with an expanded tunica intima by increased numbers of smooth muscle cells and fibrous matrix, and/or thickened and hypercellular tunica medias (arteriosclerosis).

Special stains included Masson's trichrome, periodicacid-Schiff (PAS), and Jones methenamine silver (JMS). The PAS demonstrated that the thickened mesangium and glomerular capillary loops were expanded by PAS positive material that often-formed double contours, spike-like projections and encircled bright magenta deposits using the Trichrome stain. Both the PAS and trichrome highlight the collapsed capillary loops of the globally sclerotic glomeruli with expansion of Trichrome and PAS-positive matrix.

Three glomeruli were available for ultrastructural evaluation by transmission electron microscopy (TEM). One glomerulus had collapsed capillary loops and fibrillary material in Bowman's space. All glomeruli had numerous large electron dense deposits within the capillary walls in intramembranous, subendothelial, mesangial, and subepithelial locations. Subepithelial deposits were associated with spike-like projections and circulations of glomerular basement membrane material. One glomerulus is segmentally sclerotic with loss of podocytes and denuded capillary walls. The afferent/ efferent arterioles have severely hypertrophied endothelial cells with markedly narrow lumens. In one of the arterioles the circulating erythrocytes are distorted.

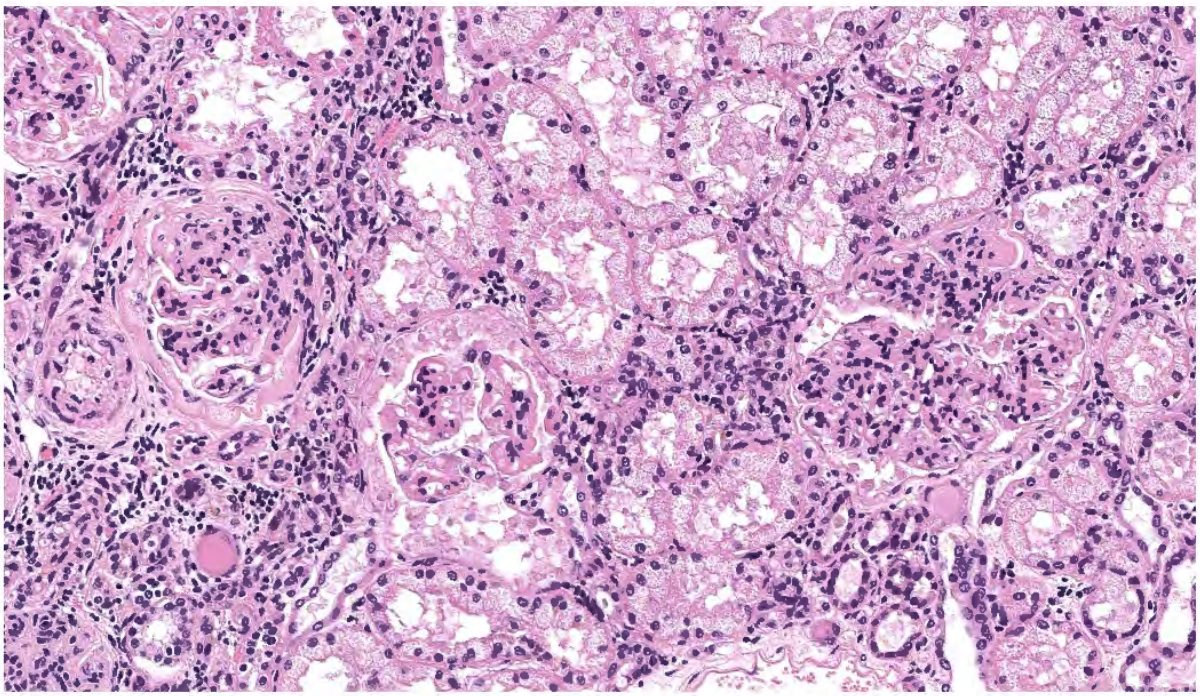

Figure 4-3: Kidney, goat. In this field, glomeruli demonstrate segmental sclerosis as well as synechia formation (glomerulus), mesangial hypercellularity, expansion of capillary loops, thickening of Bowman's capsule and periglomerular fibrosis. Tubular epithelium is degenerative with cell swelling and vacuolation, and there are numerous individualized and aggregated lymphocytes and plasma cells. The interstitial is expanded by fibrous connective tissue with entrapped and atrophic tubules. (HE, 381X)

Contributor's Morphologic Diagnoses:
Kidney: Diffuse global to segmental marked chronic active immune complex mediated membranoproliferative glomerulonephritis with superimposed thrombotic microangiopathy, tubular necrosis and atrophy, interstitial fibrosis and lymphoplasmacytic interstitial nephritis

Contributor's Comment:
Immune complex (IC) glomerulonephritis (GN) is classified as membranous, proliferative, mesangioproliferative, and membranoproliferative. Membranous glomerulonephritis is characterized by a remodeled basement membrane secondary to IC deposition on the abluminal surface of the glomerular basement membrane leading to normocellularity to mild hypercellularity. Proliferative glomerulonephritis histologically has increased cellularity without alterations to the glomerular basement membranes and may be associated with IC deposition. Histologically, mesangioproliferative glomerulonephritis has increased cellularity within the mesangium with IC deposition usually between the endothelium and the glomerular basement membrane. Membranoproliferative glomerulonephritis (MPGN) is characterized by endocapillary and mesangial cell proliferation with remodeling of the capillary loop due to IC deposition usually between the endothelium and the glomerular basement membrane[4]. In the present case, the immune complexes were present in multiple locations hence the use of "mixed MPGN".

ICGN results from circulating antigen-antibody complexes of non-glomerular origin

that localize in the glomerulus and are able to be detected via immunofluorescence or TEM

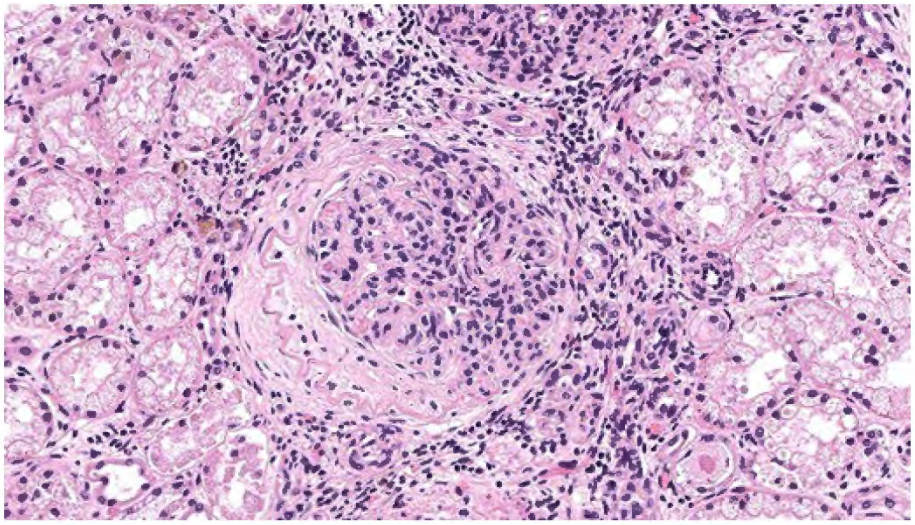

Figure 4-4: Kidney, goat. A hypercellular glomerulus with marked expansion of capillary loops and synechiae formation. (HE, 576X)

as electron-dense deposits. The immune complexes often contain complement, as well. IC deposition is thought to occur when concentrations of antigen and antibody are equal, or when antigens are in slight excess in comparison to antibody concentrations.[4] Another hypothesis is that some antigens, such as those derived from viruses like feline leukemia virus, bacteria, and parasites, such as *Dirofilaria,* can lead to immune complex deposi tion.[4,2] Experimentally, chronic antigenemia leading to ICGN is modeled by repeatedly injecting small doses of endogenous or exogenous antigens. Although caprine arthritis and encephalitis virus (CAEV) has not been previously reported to cause ICGN in goats, the herd of the present case was positive for CAEV and is thought to be the source of consistent antigen stimulation. There was a study on naturally infected sheep with Maedi-visna virus and associated glomerular lesions; however, there was lack of TEM and glomerular staining (PAS, JMS, and Trichrome) to fully characterize the lesions of ICGN.[1]

Thrombotic microangiopathy is characterized by endothelial cell damage that potentially produces thrombocytopenia and hyaline thrombi.[3,6] Causes include genetic factors, malignant hypertension, pregnancy, drugs, transplantation, and infections.[3] TMA is the lesion in greyhounds with idiopathic cutaneous and renal glomerular vasculopathy, as well as the well-characterized hemolytic uremic syndrome in humans associated with shiga or shiga-like exotoxin of *Escherichia coli* O157:H7.[3,4] In humans there are also several viruses associated with and thought to cause TMA.[3,6] Therefore, in the present case, the superimposed lesion of TMA is likely related to CAEV infection and/or hypertension. The acute tubular necrosis in this case is likely

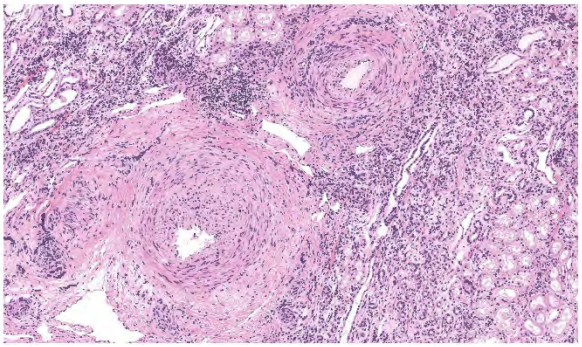

Figure 4-5: Kidney, goat. There is asymmetric mural hyperplasia and tortuosity of arcuate arterioles. There is loss of the inner elastic lamina for mural proliferation of smooth muscle cells and fibroblasts, and circumferential lamellations of collagen and fibroblasts within the adventitia. (HE, 400X).

related to ischemia possibly related to the vasculopathy as indicated by the arcuate arteriosclerosis and TMA lesions.

Contributing Institution:
The Ohio State University, Department of Veterinary Biosciences, Columbus Oh. www.vet.osu.edu

JPC Diagnoses:
Kidney: Glomerulonephritis, membranoproliferative, chronic, diffuse, severe, with glomerulosclerosis, lymphoplasmacytic interstitial nephritis, tubular degeneration, necrosis, and regeneration, and arteriolar fibrointimal hyperplasia and sclerosis.

JPC Comment:
Closing out our fourth conference, this case graced participants with an opportunity to see a lovely correlation between light microscopy and electron microscopy (EM) findings. It's not often that EM images are sent in as part of Wednesday Slide Conference submissions, but it's always a treat when they are! Many thanks to the contributor for providing both a wonderful slide and beautiful EM images. Together, they truly did paint the whole picture for this EM-worthy condition.

Because the EM images were provided, a review of the ultrastructural anatomy of a glomerular capillary profile and its surrounding structures ensued, with focus on the primary and secondary foot processes of the visible podocyte and the different layers of the glomerulus. However, the main show was the electron-dense, granular, irregularly shaped clumps of immune complexes (IC) within subepithelial, intramembranous, and subendothelial spaces of the glomerular tuft. Having IC deposition demonstrably in all three of those locations within the glomerulus assisted with the determination of the "mixed" type of glomerulonephritis in this case. Conference participants favored "membranoproliferative" based on the H&E slide, but acknowledged that this case did not fit 100% into that box upon review of the EM images and accepted the use of the term "mixed" in discussion. Typing of glomerulonephritis is more difficult to do with light microscopy alone due to some histologic similarities between the types, bringing home the point that, for definitive characterization of glomerulonephritis, EM is indispensable.

There was discourse on differentiating membranoproliferative from membranous glomerulonephritis based on histologic features, as some conference participants went one way or the other in their morphologic diagnoses. To summarize, membranoproliferative glomerulonephritis will have an increased number of nuclei within the glomerular tuft, mesangial cell proliferation, and often, the presence of recruited neutrophils. Membranous glomerulonephritis typically just has an increased amount (thickening) of basement membranes with little cellular proliferation within the glomerular tuft. One conference participant inquired on the histologic differences between synechiae and crescents in the glomerulus. Synechiae were described as the touching of the visceral layer of Bowman's capsule to the parietal layer without fibrosis, whereas crescents have a fibrous component and demonstrate full adhesion of the glomerulus to the capsule. Conference participants did not think there was enough histologic evidence of thrombotic microangiopathy include it in the morphologic diagnosis in this particular case.

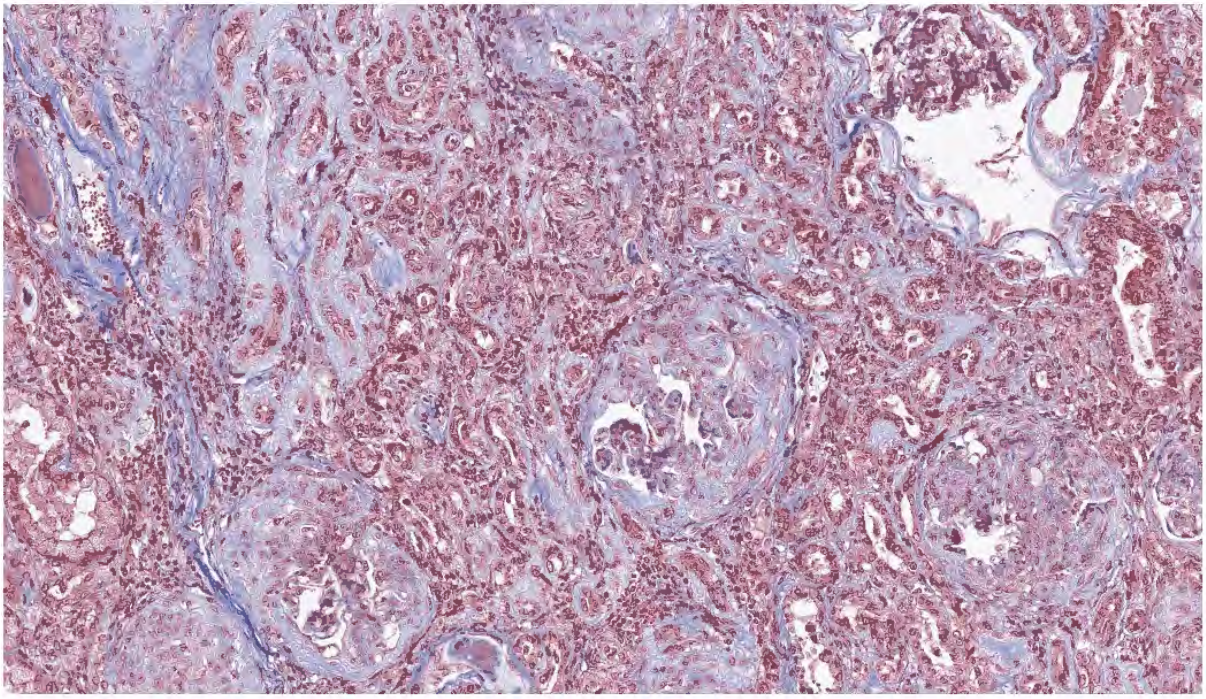

Figure 4-6: Kidney, goat. A Masson's stain demonstrates the amount of collagen within the glomerular mesangium associated with segmental sclerosis, the periglomerular fibrosis, and the interstitial expansion by collagen. (Masson's trichrome, 545X)

So, the renal glomerulus…what a champion. The glomerulus is a physiologic heavy lifter made up of three distinct layers: fenestrated endothelium, basement membrane, and podocytes. These layers enable the glomerulus to fulfill its destiny as a highly selective filter of blood based on compound size and charge, ridding the body of wastes while retaining essential materials. Glomerular filtrate is passed into the surrounding Bowman's capsule before moving into the proximal convoluted tubules to continue its journey. For all its hard work and contributions to the bodily society, glomeruli are relatively fragile and prone to injury. Immune-complex glomerulonephritis occurs when the concentration of antigen-antibody complexes within the body becomes too high for the body to clear in a timely fashion. The size, charge, and insolubility of ICs, along with excessive complement activation secondary to their deposition, can overwhelm the body's clearance mechanisms and result in deposition into the glomerulus.

Complexes are deposited into glomerular capillaries due to the basement membrane's negative charge. The basement membrane will attract positively charged pre-formed complexes, but can also form IC complexes on itself if a positively charged antigen binds to the glomerulus directly and is then tagged by an antibody.[5] The ICs trigger an immune response by either calling in inflammatory cells via their sheer presence or by activating resident glomerular cells to release cytokines, vasoactive substances, and prothrombotic compounds. Either way, this ultimately damages the endothelium, epithelium, and mesangium of the affected glomerulus, resulting in glomerulonephritis.[5]

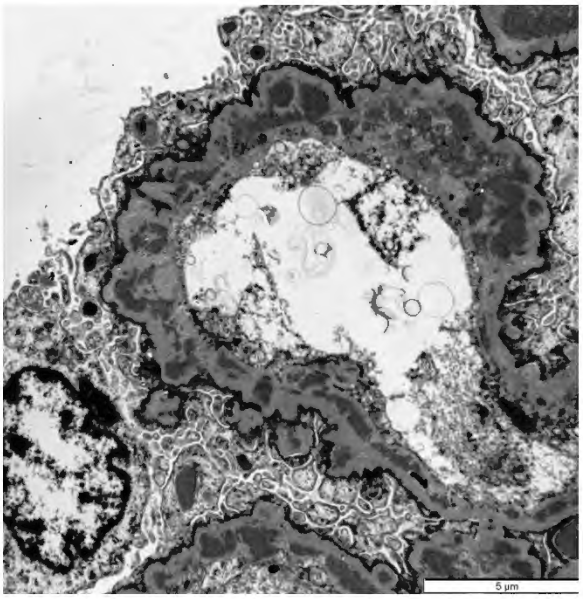

Figure 4-7: Kidney, goat. All glomeruli had numerous large electron dense deposits within the capillary walls in intramembranous, subendothelial, mesangial, and subepithelial locations. Subepithelial deposits were associated with spike-like projections and circulations of glomerular basement membrane material. (Photo courtesy of: The Ohio State University, Department of Veterinary Biosciences, Columbus Oh. www.vet.osu.edu)

The primary mediator of IC glomerulonephritis is the complement system, specifically the membrane attack complex (MAC), which is made up of complement components C5b complexed with C6-9 to create C5b6789. The MAC generally does not achieve sufficient quantities to result in cell lysis in this IC glomerulonephritis, but inserts into the membranes of glomerular cells and causes their conversion into resident inflammatory effector cells that then damage the glomerulus.[5]

Couple this process with the lymphocytes and plasma cells that show up in response, the poor affected glomerulus is set on a course of irreversible damage. Mesangial cells and capillary endothelial cells try their best to combat the glomerular destruction by proliferating and remodeling, hence the "proliferative" part of this diagnosis, but this can only do so much if the antigen-antibody complexes continue to circulate in high numbers and continuously deposit into glomeruli.

All in all, this case was easily the most heavily discussed both during conference and the morphologic diagnosis session, where there was highly spirited discussion between staff on the most appropriate morphologic diagnosis. The attending residents were able to hear a variety of opinions on these lesions and, ultimately, consensus (more or less) was reached. Many thanks again to this contributor for a truly high-value learning case!

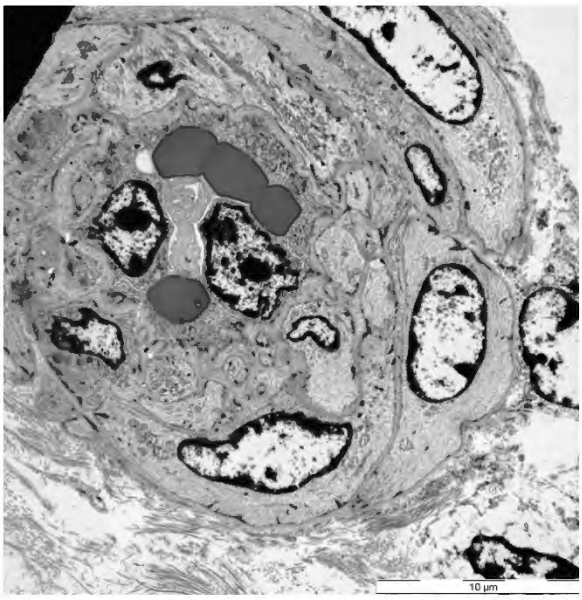

Figure 4-8: Kidney, goat. In sclerotic glomeruli, the afferent/ efferent arterioles have severely hypertrophied endothelial cells with markedly narrow lumens. (Photo courtesy of: The Ohio State University, Department of Veterinary Biosciences, Columbus Oh. www.vet.osu.edu)

References:

1. Angelopoulou K, Brellou GD, Vlemmas I. Detection of maedi-visna virus in the kidneys of naturally infected sheep. *Journal of comparative pathology*. 2006;134: 329-335.
2. Long JD, Rutledge SM, Sise ME. Autoimmune Kidney Diseases Associated with Chronic Viral Infections. *Rheumatic diseases clinics of North America*. 2018;44: 675-698.
3. Lopes da Silva R. Viral-associated thrombotic microangiopathies. *Hematology/oncology and stem cell therapy*. 2011;4: 51-59.
4. Maxie MG. *Jubb, Kennedy, and Palmer's pathology of domestic animals*, Sixth ed., vol. 2. St. Louis (MO): Elsevier; 2016.
5. Nangaku M, Couser WG. Mechanisms of immune-deposit formation and the mediation of immune renal injury. *Clin Exp Nephrol*. 2005;9(3):183-91.
6. Salter T, Burton H, Douthwaite S, Newsholme W, Horsfield C, Hilton R. Immune Complex Mediated Glomerulonephritis with Acute Thrombotic Microangiopathy following Newly Detected Hepatitis B Virus Infection in a Kidney Transplant Recipient. *Case reports in transplantation*. 2016;2016**:** 3152495.
7. Sementilli A, Moura LA, Franco MF. The role of electron microscopy for the diagnosis of glomerulopathies. *Sao Paulo Med J.* 2004;122(3):104-9.

Joint Pathology Center
Veterinary Pathology Services

WEDNESDAY SLIDE CONFERENCE 2025-2026

Conference #5 — 24 September 2025

CASE I:

Signalment:
10-week-old, female intact, mixed breed, *Canis lupus familiaris,* canine.

History:
The submitted dog was from a litter of puppies that was found living underneath a shed in Texas. A rescue organization acquired the puppies, and the dog was later adopted by a family in Colorado. The dog was apparently healthy up until 10 weeks of age when she suddenly developed a bloated appearance and began vomiting. The animal's condition worsened overnight, becoming lethargic and not acting herself. The next morning, the dog went outside and tried to vomit but subsequently collapsed and died.

Gross Pathology:
A 7.55 kg, intact female, mixed breed puppy was submitted for necropsy, one day post-mortem, and in good condition. The lungs and heart were grossly unremarkable. The peritoneal cavity contained approximately 400 ml of serosanguinous fluid. All liver lobes had numerous, multifocal to coalescing, pinpoint, flat, tan foci that extended into the hepatic parenchyma on cut section. The stomach contained a black plastic clothing hook and yellow to green mucoid material. The small intestines contained yellow to tan liquid material and the large intestines had no intraluminal contents.

Laboratory Results:
N/A

Microscopic Description:
Expanding and infiltrating all layers of the heart, with the greatest severity in the myocardium, are large numbers of plasma cells, lymphocytes, and macrophages. Cardiomyocytes in areas of inflammation are multifocally hypereosinophilic, shrunken, and have striation loss with fragmented to absent nuclei (necrosis). There is mild, multifocal, interstitial fibrosis often associated with cardiomyocyte degeneration and inflammation. Throughout the myocardium, there are occasional cardiomyocytes that contain intrasarcoplasmic, variably sized (up to 100 µm in length) pseudocysts with numerous, 2-3 µm, round protozoal amastigotes.

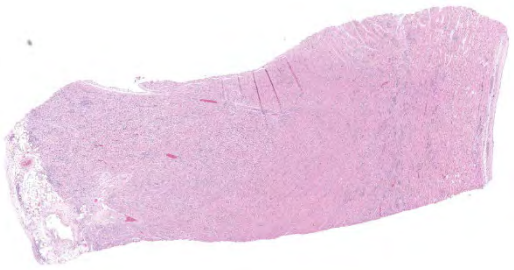

Figure 1-1: Heart, dog. A section of heart is submitted for examination. Numerous hypercellular foci within the myocardium are visible at subgross magnification. (HE, 10X)

Contributor's Morphologic Diagnoses:
Heart: Severe, multifocal, chronic-active, lymphoplasmacytic and histiocytic pancarditis with intrasarcoplasmic pseudocysts containing amastigotes

Contributor's Comment:
The histologic findings within the heart are most consistent with the protozoal organism, *Trypanosoma cruzi*, also known as Chagas disease or American trypanosomiasis. *Trypanosoma cruzi* is a flagellate protozoan organism that primarily harbors in an insect vector of the *Triatominae* family, most commonly the kissing bug or triatomine bug.[5,8-10] It affects a variety of mammalian species across South, Central, and North America, including humans, domestic animals, and non-human primates.[5,8-10] It is estimated that approximately 8 million people worldwide have this disease, and around 280,000 reside within the United States.[5] Between 60 to 70% of people infected with *T. cruzi* will never develop clinical signs or symptoms, the remaining 30-40% will develop chronic symptomatic forms within 10 to 30 years.[8]

The life cycle of *T. cruzi* is complex and begins when the triatomine bug feeds on a host's blood infected with trypomastigotes. Once in the insect's midgut, the trypomastigotes differentiate into the epimastigote form where they later become the infective metacyclic trypomastigotes at the rectal ampulla.[5] The infective trypomastigotes are then excreted into the feces. As the now-infected bug moves on to its next victim, it will take a blood meal from the host and subsequently defecate near the bite wound. In humans, triatomine bugs will frequently bite along the face and near the mouth, hence their name "kissing bug", due to their attraction to the carbon dioxide and warmth produced by the face. The parasites can then enter through the mucous membranes, the bite wound, or a cut/abrasion to the skin, as infected hosts will often scratch at the time of

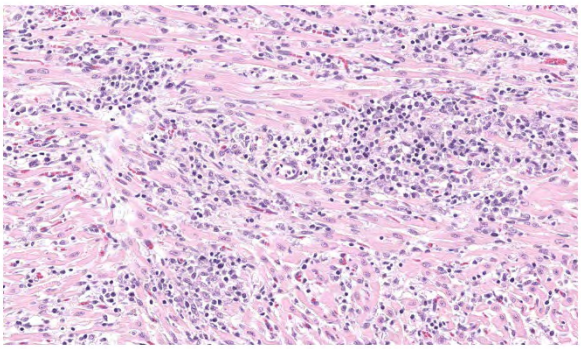

Figure 1-2: Heart, dog. Hypercellular foci consist of numerous lymphocytes and plasma cells within the myocardial interstitium which multifocally efface cardiomyocytes. (HE, 315X)

the bite. Once in the bloodstream, the metacyclic trypomastigotes will invade the host cells and begin the intracellular transition to amastigotes. Amastigotes will replicate by binary fission differentiating back to metacyclic trypomastigotes and rupturing the cell making their way back into the bloodstream.

T. cruzi can infect myocytes, endothelial cells, fibroblasts, and adipocytes, but has a tropism for cardiac muscle tissue.[11] Grossly, there are no pathognomonic lesions for Chagas disease. Histologically, the cardiomyocytes will be expanded by a pseudocyst containing amastigotes. While best observed ultramicroscopically, the amastigotes will have a large nucleus and an adjacent rod-shaped kinetoplast, like *Leishmania* spp. Unlike the defined perpendicular orientation of the kinetoplast in *Leishmania*, the location of the kinetoplast relative to the nucleus changes during the life cycle and cannot be a diagnostic feature in Chagas disease.[10] Unfortunately, additional diagnostics including PCR, culture, and serology were not performed so leishmaniasis cannot be completely ruled out, but the geographic and anatomic location of the organism along with the histologic appearance is most likely consistent with *T. cruzi*. Infection results in marked inflammation of the heart, often not associated with the intracellular pseudocysts. Myocarditis can lead to heart failure with cardiac arrest and potentially fatal arrhythmias. In this case, there was multi-organ evidence of

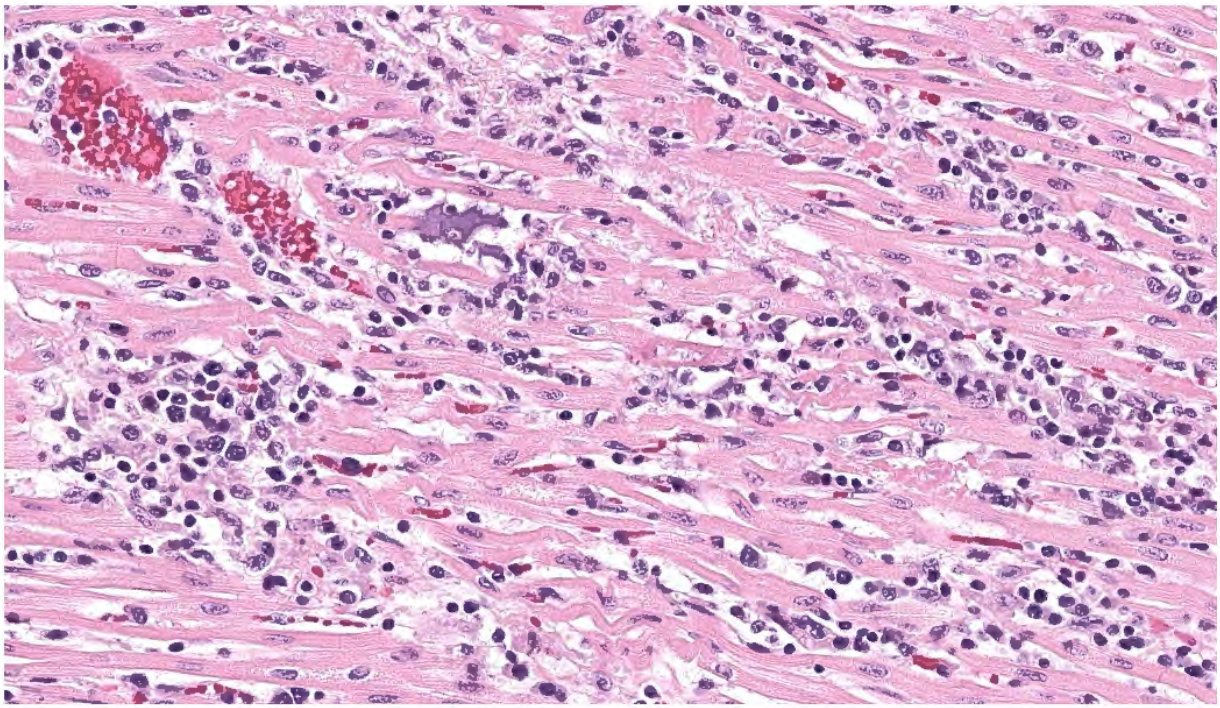

Figure 1-3: Heart, dog. In areas of dense inflammatory infiltration of the myocardium, cardiomyocytes multifocal are lost, fragmented, atrophic and hypereosinophilic, and rarely mineralized. (HE, 600X)

heart failure including ascites (abdominal effusion) and centrilobular hepatocyte necrosis due to hypoxia.

Dogs play a crucial role in the domestic life cycle and are excellent reservoir hosts to continue parasite transmission. Cases have been reported in domestic and working dogs in South America and the southern United States, especially Texas and Gulf Coast states. Interestingly, the vectorial transmission that occurs in humans is less likely in dogs. Transmission is suspected to occur orally through ingestion of the infected vectors, ingestion of meat from infected mammals, or through ingestion of milk from infected lactating bitches.[5,11] The human-companion animal relationship has become increasingly more important, and it is proposed that dogs could act as a sentinel for human exposure, environmental risks, and continued surveillance.[5] Shelter and stray dogs with greater exposure to the outdoors are more likely to encounter *T. cruzi* and with increased human encroachment the interactions with wildlife reservoirs will also likely increase.[3] There are no commercially available vaccines for dogs but potential vaccines are being tested including live-attenuated vaccines, recombinant protein and vector vaccines, and DNA and mRNA vaccines.[3] Current prevention strategies include vector control methods and prophylactic treatment options.[3]

Contributing Institution:
Colorado State University Veterinary Diagnostic Laboratory
https://vetmedbiosci.colostate.edu/vdl/

JPC Diagnoses:
Heart: Pancarditis, lymphoplasmacytic and histiocytic, subacute, multifocal to coalescing, marked, with numerous sarcoplasmic amastigotes.

JPC Comment:
Moderated by MAJ William Baskerville, the 5th WSC of the year started off with a great

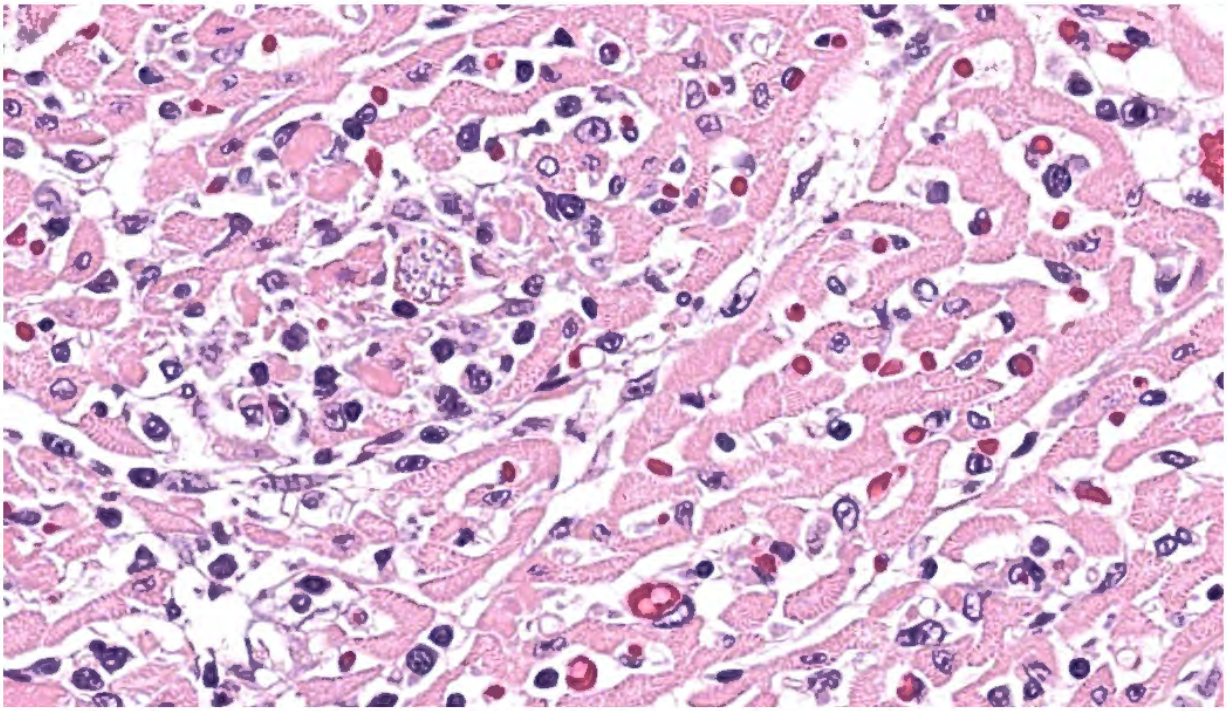

Figure 1-4: Heart, dog. Cardiomyocytes occasionally contain sarcoplasmic pseudocysts contain numerous round 2-4um amastigotes compatible with *Trypanosoma cruzi*. (HE, 1400X)

case of a relevant infectious disease that is gathering more attention as it spreads within the United States: American trypanosomiasis (Chagas disease). Chagas disease was recently designated as endemic in the southern United States.[5] Current data also indicate that, as temperatures continue to trend warmer, the triatome vectors of Chagas are increasing and expanding their range further north in the United States. Conference discussion largely centered on this being a growing health concern within the US for both humans and veterinary species, especially domestic dogs that are housed outdoors in kennel situations and have higher rates of exposure to insect vectors. This has been exceptionally relevant for military working dogs (MWDs) housed in Texas kennels, where there has been a disproportionally high number of MWDs contracting Chagas Disease compared to other locations within the US. Due to the likelihood of contact with vectors in these housing situations, dogs are currently being looked at as a sentinel species for this condition.

The causative protozoa's tropism for specific tissues can result in fatal chronic disease in the heart, esophagus, and/or colon.[6] While most infections are asymptomatic, in humans, approximately 30% of chronically infected people will develop cardiomyopathy, megacolon, or megaesophagus with chronic Chagas disease.[5] In fact, this condition is the current leading cause of infectious myocarditis in humans and most robust blood-banking operations are now testing for *Trypanosoma cruzi* before administering blood to patients. Trypomastigotes of *T. cruzi* detect and subsequently alter their movement in the presence of mammalian cells and, in the presence of specific cell types, will respond more strongly to and invade these cells over alternative cell lineages.[2]

Across multiple studies, it has been demonstrated that *T. cruzi* shows particular tropism for cardiomyocytes.[1,2,6,13] Studies in rats have demonstrated that cardiomyocytes infected with *T. cruzi* lose their gap junctional commu-

nication, which results in decreased automaticity of the cardiac muscle with subsequent electrical alterations.[7] Gap junction proteins (connexins) enable transmission of ions and signaling molecules between cells, making them critical to proper cardiac function.[6] Similarly, mouse cardiac myocytes infected with *T. cruzi* trypomastigotes had significant alterations in connexin43 (Cx43) distribution with an initial increase in their expression in peracute infection followed by a marked decrease in acute and chronic infections. These gap junction disruptions are thought to contribute to the heart's electrical dysregulation observed in some *T. cruzi* infections.[1]

It has also been suggested that *T. cruzi* exploits a HIF-1α-dependent, stress-related activation of glycolysis that is intrinsic to cardiomyocytes, further promoting intracellular infection and replication.[15] These chronic stress responses by cardiomyocytes lead to dysfunction, cell death, and, ultimately, development of cardiac disease. More recently, in vitro studies have demonstrated possible cell-to-cell transfer of the parasite between cardiomyocytes, although the mechanism by which this occurs is not yet known.[5]

Along with exploiting cellular pathways, *T. cruzi* also utilizes a handful of virulence factors to invade host cells, including a trans-sialidase to allow the parasite to bind to host cells, a penetrin to mediate invasion into a host cell, neuraminidase and hemolysins to destabilize and disrupt lysosomes, and galectin-3 (gal-3).[10] Gal-3 in particular is being studied as a potential target for therapeutics, as it is involved in the stimulation of cardiac fibroblasts to synthesize Type I collagen and resultant cardiac fibrosis. One study found, in vivo, that mice infected with *T. cruzi* that were subsequently treated with a gal-3 blocker had significantly reduced cardiac fibrosis and inflammation.[10] With this disease on the rise in the Southern U.S. and South American nations, the growing body of research on Chagas disease will become ever more important as scientists and medical professionals attempt to further the development of treatments and preventatives for this condition.

References:

1. Adesse D, Garzoni LR, Huang H, Tanowitz HB, de Nazareth Meirelles M, Spray DC. Trypanosoma cruzi induces changes in cardiac connexin43 expression. *Microbes Infect.* 2008;10(1):21-8.
2. Arias-Del-Angel JA, Santana-Solano J, Santillán M, Manning-Cela RG. Motility patterns of Trypanosoma cruzi trypomastigotes correlate with the efficiency of parasite invasion in vitro. Sci Rep. 2020;10(1):15894.
3. Barr SC. Canine Chagas' Disease (American Trypanosomiasis) in North America. Veterinary Clinics: Small Animal Practice. 2009;39(6):1055-1064.
4. Busselman RE, Meyers AC, Zecca IB, et al. High incidence of Trypanosoma cruzi infections in dogs directly detected through longitudinal tracking at 10 multi-dog kennels, Texas, USA. PLoS Negl Trop Dis. 2021;15(11):e0009935.
5. CDC. About Chagas Disease. Chagas Disease. September 4, 2024. Accessed June 16, 2025. https://www.cdc.gov/chagas/about/index.html.
6. Contreras-Ortiz JME, Hernández-Mendoza D, Márquez-Dueñas C, Manning-Cela R, Santillán M. In vitro characterization of Trypanosoma cruzi infection dynamics in skeletal and cardiac myotubes models suggests a potential cell-to-cell transmission in mediating cardiac

pathology. PLoS Negl Trop Dis. 2024;18(6):e0012288.
7. de Carvalho AC, Tanowitz HB, Wittner M, Dermietzel R, Roy C, Hertzberg EL, Spray DC. Gap junction distribution is altered between cardiac myocytes infected with Trypanosoma cruzi. Circ Res. 1992;70(4):733-42.
8. Durães-Oliveira J, Palma-Marques J, Moreno C, et al. Chagas Disease: A Silent Threat for Dogs and Humans. International Journal of Molecular Sciences. 2024;25(7):3840.
9. Sousa AS de, Vermeij D, Ramos AN, Luquetti AO. Chagas disease. The Lancet. 2024;403(10422):203-218.
10. Souza BSF, Silva DN, Carvalho RH, Sampaio GLA, Paredes BD, Aragão França L, Azevedo CM, Vasconcelos JF, Meira CS, Neto PC, Macambira SG, da Silva KN, Allahdadi KJ, Tavora F, de Souza Neto JD, Dos Santos RR, Soares MBP. Association of Cardiac Galectin-3 Expression, Myocarditis, and Fibrosis in Chronic Chagas Disease Cardiomyopathy. Am J Pathol. 2017;187(5):1134-1146.
11. Rassi A, Marin-Neto JA. Chagas disease. The Lancet. 2010;375(9723):1388-1402.
12. Hodo CL, Wilkerson GK, Birkner EC, Gray SB, Hamer SA. Trypanosoma cruzi Transmission Among Captive Nonhuman Primates, Wildlife, and Vectors. Ecohealth. 2018;15(2):426-436.
13. Montalvo-Ocotoxtle IG, Rojas-Velasco G, Rodríguez-Morales O, et al. Chagas Heart Disease: Beyond a Single Complication, from Asymptomatic Disease to Heart Failure. Journal of Clinical Medicine. 2022;11(24):7262.
14. Teixeira ARL, Hecht MM, Guimaro MC, Sousa AO, Nitz N. Pathogenesis of Chagas' Disease: Parasite Persistence and Autoimmunity. Clin Microbiol Rev. 2011;24(3):592-630.
15. Venturini G, Alvim JM, Padilha K, Toepfer CN, Gorham JM, Wasson LK, Biagi D, Schenkman S, Carvalho VM, Salgueiro JS, Cardozo KHM, Krieger JE, Pereira AC, Seidman JG, Seidman CE. Cardiomyocyte infection by Trypanosoma cruzi promotes innate immune response and glycolysis activation. Front Cell Infect Microbiol. 2023;13:1098457.

CASE II:

Signalment:
5 years old, male intact, cynomolgus macaque (*Macaca fascicularis*)

History:
A 5-year-old training animal from the stock colony, not actively enrolled in a study presented with decreased activity and reactivity and was emaciated, pale, dehydrated, and hypothermic. Cardiothoracic examination revealed increased respiratory effort, muffled

Figure 2-1: Right ventricle and atrioventricular valve, cynomolgus macaque. There is a large septic thrombus attached to the right AV valve. (HE, 10X)

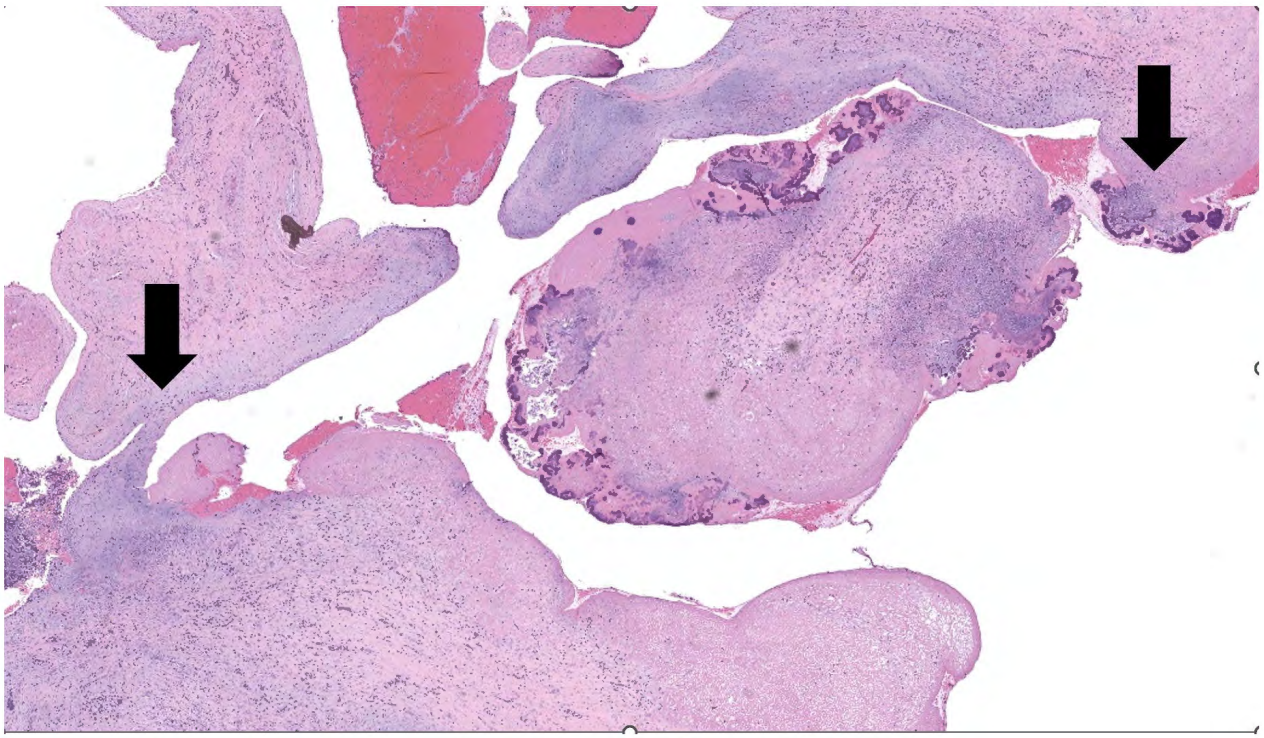

Figure 2-2. Right atrioventricular valve, cynomolgus macaque: The septic thrombus is multifocally attached to the AV valve (arrows). (HE, 35X)

cardiac sounds with a suspected systolic murmur, and thoracic edema. The animal was euthanized *in extremis*.

Gross Pathology:
Lung: Discoloration, dark, brown, diffuse
Heart: Irregular surface, right AV valve, 100% affected

Laboratory Results:
Aerobic bacterial culture, heart: Moderate *Escherichia coli*, Few *Staphylococcus warneri*, Few *Streptococcus mitis*

Microscopic Description:
Representative sections of heart and lungs are examined.

In the heart, the right atrioventricular valve is extensively overlain by large mats of fibrin, admixed with numerous degenerate and viable neutrophils and multiple coccobacilli bacterial colonies. The valvular stroma is diffusely expanded by moderate myxedema and there are moderate numbers of neutrophils and lesser numbers of hemosiderin-laden macrophages, plasma cells and lymphocytes scattered throughout the valvular stroma and expanding the endocardium of the adjacent papillary muscles. The epicardium and surrounding adipose tissue are mildly infiltrated by small numbers of neutrophils, lymphocytes, and plasma cells.

Regionally, sharply demarcated areas of the pulmonary parenchyma are markedly necrotic and replaced by abundant hemorrhage, fibrin, inflammatory infiltrates composed mainly of neutrophils and macrophages, and necrotic cellular debris. In these areas, multiple blood vessels contain thrombi consisting of large numbers of degenerate neutrophils, organizing fibrin, occasional colonies of bacterial coccobacilli, and necrotic cellular debris that variably obscure the lumen and vessel walls. Affected vessels often have smudgy, hypereo-

sinophilic walls that are transmurally infiltrated by neutrophils, lymphocytes, and macrophages. In less affected regions, the alveolar spaces contain a small amount of fibrin, numerous foamy alveolar macrophages (some of which contain brown granular hemosiderin pigment), and fewer neutrophils and erythrocytes. There are moderate numbers of hemosiderin-laden macrophages mostly concentrated around pulmonary arteries, multifocally. Regionally, along the pleural surface there is a large amount of fibrin admixed with numerous degenerate neutrophils and necrotic cellular debris. The pleura itself is mildly thickened by fibrous connective tissue and edema and is multifocally lined by markedly

reactive mesothelium, characterized by plump, rounded mesothelial cells.

Contributor's Morphologic Diagnoses:
Heart, right atrioventricular valve: Marked, chronic, fibrinosuppurative valvular endocarditis with intralesional bacterial colonies; Mild, multifocal, suppurative epicarditis

Lungs: Marked, regional, suppurative, necrotizing embolic pneumonia with vascular thrombosis and intrathrombotic bacteria; Marked, regional, fibrinosuppurative pleuritis

Contributor's Comment:
Endocarditis refers to the inflammation of the endocardium, primarily of the heart valves, and can affect most animal species.[7] Mechanistically, endothelial lesions tend to start at areas of highest trauma, particularly the lines of apposition of the valvular surface exposed towards the direction of blood flow.[2,5] Bloodborne microorganisms may become adhered to these regions, resulting in a localized infection, which can cause valvular injury and subsequent insufficiency.[2,5] Infectious causes are

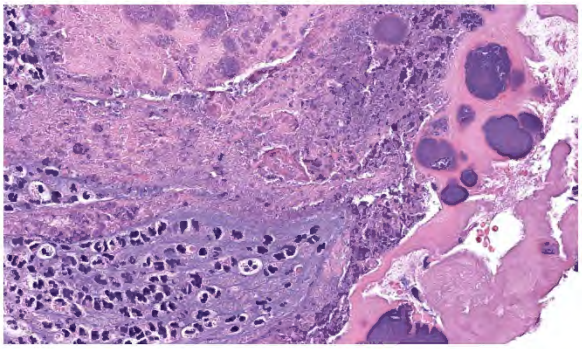

Figure 2-3: Right atrioventricular valve, cynomolgus macaque. The septic thrombus contains numerous dispersed bacilli and colonies of cocci. (HE, 748X)

usually of bacterial origin, usually from systemic infection, but can also be of mycotic or parasitic origin.[5] The bacteria most commonly involved in valvular endocarditis varies among species, but *Streptococcus* sp., *Staphylococcus* sp., and *Enterococcus* sp. have been implicated in endocarditis in humans and most animal species.[5] In cattle, *Trueperella pyogenes* is the most common agent involved in bacterial endocarditis, whereas in pigs, *Erysipelothrix rhusiopathiae* is most common. Bacterial endocarditis is less common in horses, dogs, and cats.[5]

Valvular endocarditis usually involves the left atrioventricular valve, followed by the aortic valve, right atrioventricular valve, and pulmonic valve.[5] In non-human primates, valvular endocarditis is an uncommon spontaneous finding, with an incidence of 0.6% of all spontaneous cardiovascular lesions observed.[1] Endocarditis can be associated with systemic bacterial infections or, particularly in the laboratory environment, contaminated venous indwelling catheters, the latter more commonly affecting the right atrioventricular valve.[6] Interestingly, in cattle, the right atrioventricular valve is mostly affected, most

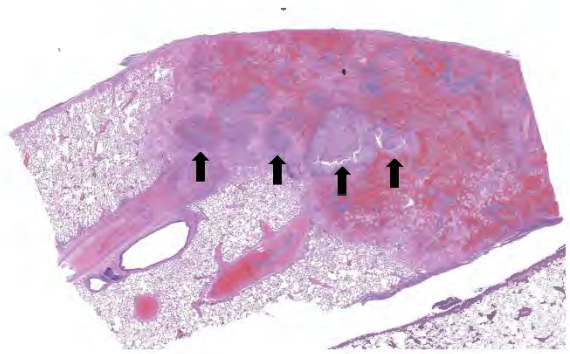

Figure 2-4: Lung, cynomolgus macaque. Multiple branches of the pulmonary artery contain septic thrombi (arrows) (HE, 14X)

likely due to the increased incidence of liver abscesses and subsequent bacterial venous spread to the caudal vena cava and right side of the heart.[4]

As the adherence of bacteria and blood components to the valve leaflets progresses, irregular, raised vegetations replace the smooth valvular surface.[5] Portions of such vegetations may become detached and travel throughout the body as septic emboli.[5] Emboli arising from the right side mainly affects the lungs, while emboli from the left side may dislocate and travel to distant organs, such as kidney and spleen.[5]

In the current case, right-sided valvular endocarditis was observed, most likely a consequence of a contaminated venous injection. Septic emboli translocated to the lungs, causing pulmonary thrombosis and infarction. Bacterial cultures of the heart and lungs revealed large numbers of *E. coli* and fewer *Staphylococcus* sp.

Contributing Institution:
Charles River Laboratories Mattawan
(criver.com/products-services/safety-assessment/preclinical-facilites/Mattawan-michigan)

JPC Diagnoses:
1. Heart, right AV valve: Valvulitis, fibrinosuppurative, chronic, focally extensive, severe, with valvular remodeling and numerous colonies of coccobacilli.

2. Lung: Pneumonia, embolic, necrotizing and suppurative, chronic, multifocal to coalescing, severe, with septic arterial thrombi and suppurative pleuritis.

JPC Comment:
This second case provides a beautiful example of an infective endocarditis with subsequent embolic bacterial pneumonia, stimulating value-added educational discussion of a classic pathogenesis that the contributor sums up nicely in their comment. Other major points of discussion included clinical signs associated with either right or left-sided emboli and associated gross lesions with endocarditis, including those seen in acute cases where only irregular ulcerations on swollen valve leaflets may be seen instead of the more classic irregular "vegetations" on affected valves.

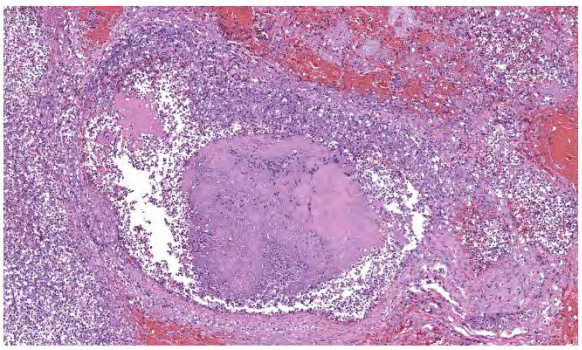

Figure 2-5: Lung, cynomolgus macaque. Higher magnification of septic thrombus within the pulmonary artery, with numerous neutrophils effacing the arterial wall. (HE, 150X)

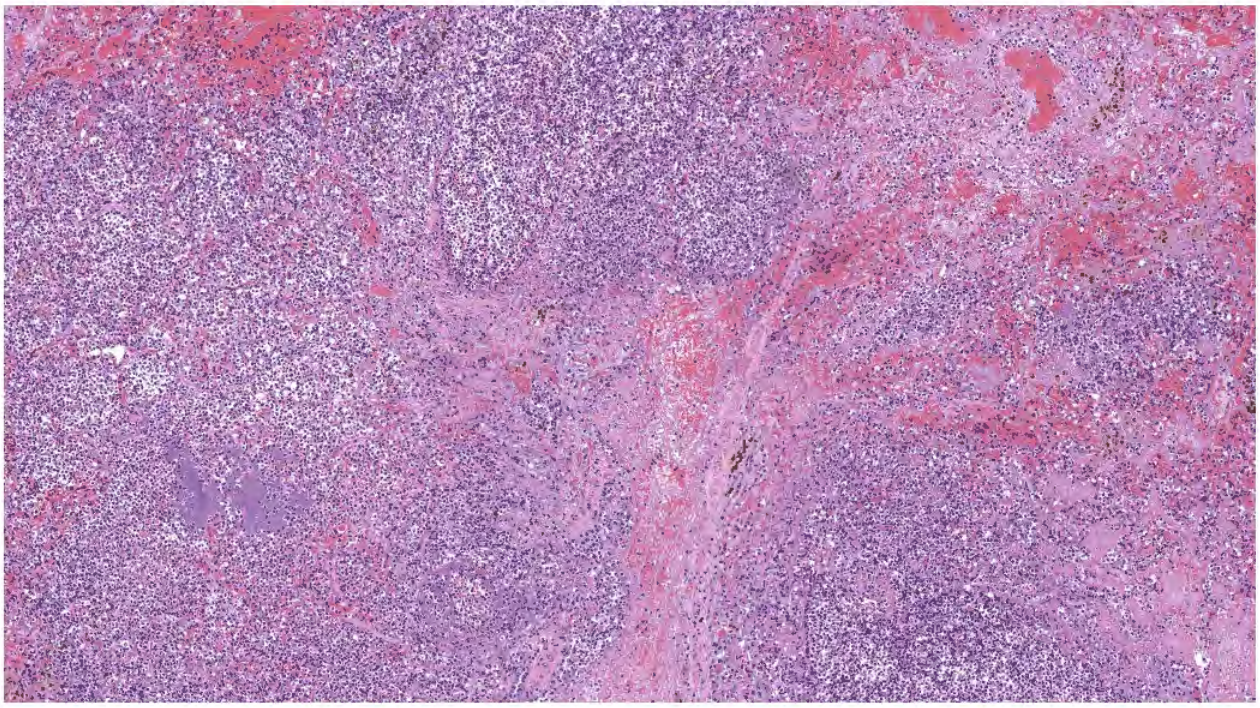

Figure 2-6: Lung, cynomolgus macaque. Suppurative inflammation and colonies of bacteria extend into the pulmonary parenchyma adjacent to effaced pulmonary arterial branches. (HE, 150X)

Conference participants were again asked to recall the "YAACSS-NT" acronym of large colony-forming bacteria, which was previously spelled out in this year's Conference 3, if a refresher is needed. (Repetition is key!) To drive home the dramatic degree of valvular expansion seen in the heart in this case, a review of valvular anatomy followed and included discussion of the normal composition of valves, which are made up of collagen, ground substance (proteoglycans and elastin fibers), and endothelium lining both sides of the valve leaflets.

Endocarditis was first documented almost 350 years ago.[3] The term "vegetative" in the term "vegetative valvular endocarditis" refers to the clumps of bacteria, fibrin, platelets, and other cellular material that adhere to a damaged heart valve. This conglomeration has traditionally been referred to as a "vegetation".

This term was first used by French physician Jean-Nicolas Corvisart in 1806 to describe "wart-like growths" he observed on the heart valves of patients with endocarditis at autopsy, stating that they appeared to resemble natural plant life.[3] Considering this information, one must wonder of Dr. Corvisart had, in fact, ever seen a plant in his own natural life to have named it thus. Despite its historical use, the medical community as a whole is has moved away from that term in favor of either "infective endocarditis" when microorganisms are present, or "nonbacterial thrombotic endocarditis" when the lesion is sterile.

References:

1. Chamanza R, Parry NM, Rogerson P, Nicol JR, Bradley AE. Spontaneous lesions of the cardiovascular system in purpose-bred laboratory nonhuman primates. *Toxicol Pathol*. 2006;34:357-363.

2. Chorianopoulos E, Bea F, Katus HA, Frey N. The role of endothelial cell biology in endocarditis. *Cell Tissue Res*. 2009;335**:**153-163.
3. Geller SA. Infective endocarditis: a history of the development of its understanding. *Autops Case Rep*. 2013;3(4):5-12.
4. Gudmundson J, Radostits OM, Doige CE. Pulmonary thromboembolism in cattle due to thrombosis of the posterior vena cava associated with hepatic abscessation. *Can Vet J*. 1978;19**:**304-309.
5. Robinson WF, Robinson NA. Chapter 1 - Cardiovascular System. In: Maxie MG, ed. *Jubb, Kennedy & Palmer's Pathology of Domestic Animals: Volume 3 (Sixth Edition)*. W.B. Saunders; 2016:1-101.e101.
6. Saravanan C, Flandre T, Hodo CL, et al. Research Relevant Conditions and Pathology in Nonhuman Primates. *ILAR Journal*. 2020;61**:**139-166.
7. Vilcant V, Hai O. *Bacterial Endocarditis*-StatPearls Publishing, Treasure Island (FL);2023.

CASE III:

Signalment:
11-years-old, male, mixed breed canine, *Canis familiaris*.

History:
"Enucleated right eye**".** No other history was provided.

Gross Pathology:
An entire formalin-fixed eye was submitted for histopathology.

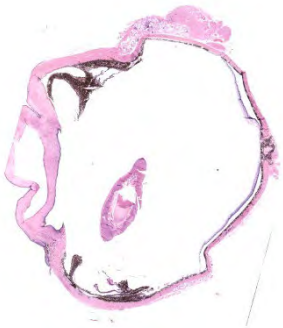

Figure 3-1: Eye, dog. A cross -section of the globe is submitted for examination. There are cross-sections of larval nematodes embedded in the sclera on both sides of the globe. (HE 5X).

Laboratory Results:
N/A

Microscopic Description:
Enucleated right eye: Expanding and infiltrating the sclera, and occasionally extending to and dissecting the periocular skeletal muscle, are multiple cross and oblique sections of nematode parasites. Nematodes are characterized by a thick cuticle with annular ridges seen as raised areas in oblique sections, coelomyarian/polymyarian musculature that is atrophied and multifocally replaced by hypodermal tissue, a very small intestinal cross section, and reproductive organs. Mild hemorrhage, fibrin, and edema are present in affected sclera, and occasional nematode cross sections are surrounded by epithelioid macrophages. The cornea is hypercellular with low numbers of neutrophils and areas of neovascularization.

Contributor's Morphologic Diagnoses:
Granulomatous scleritis and myositis with intralesional *Onchocerca lupi*

Contributor's Comment:
Onchocerca lupi is a parasitic, filarid nematode that is the causative agent of ocular onchocerciasis in domestic dogs.[1] Cases have also been described in cats, one case was reported in a wolf, and coyotes in the southwestern United States have been reported to be

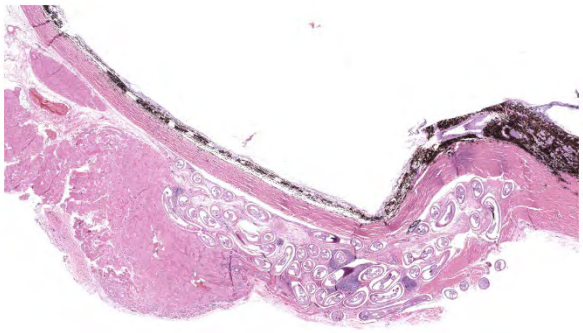

Figure 3-2: Eye, dog. On one side of the globe, cross-sections of one or more larval nematodes are embedded in an inflammatory nodule in the sclera and adjacent orbital skeletal muscle. (HE 28X).

probable reservoirs.[1,2,3] Canine infections with *Onchocerca lupi* have been reported in Europe, North America, and in Asia.[1,3,4,5] *Onchocerca lupi* is also zoonotic, and human cases of *Onchocerca lupi* have been reported in the United States, Europe, North Africa, and in the Middle.[4,6,7] Outside of the United States, reported human cases are mostly in adults, manifesting as localized ocular disease, however, human cases in the southwestern United States have been predominately seen in children, including at least 4 neuroinvasive cases.[7,8]

The life cycle of *Onchocerca lupi* has not been completely described, but it is thought to be similar to that of other filarid nematodes. Canids are described as definitive hosts.[4] Adult male and female nematodes develop within canine periocular tissues, and, after mating, females release microfilariae, which travel to the subcutaneous tissues, especially of the head, and the inter-scapular and lumbar areas.[4] Rare cases of intraocular onchocerciasis, and of extensive aberrant migration of onchocerciasis have been reported in domestic dogs.[9,10] *Wolbachia* spp. have been described in adult *Onchocerca lupi*, and this bacteria is necessary for the reproduction and survival of other *Onchocerca* species, as well as of *Dirofilaria immitis* , another filarid nematode.[8] Presumably, the intermediate host becomes infected with microfilaria while feeding on the definitive host. The exact intermediate host is unknown, but is thought to be a species of black fly (*Simulium* spp), as is the case in other *Onchocerca* species, and *Onchocerca lupi* DNA has been isolated from *Simulium tribulatum* in California, USA.[11] *Onchocerca lupi* DNA has also been found within *Ceratopogonidae* sp. (biting midges) in Northern Arizona and New Mexico, USA.[12] Presumably, the larvae develop into infective L3s within the intermediate host, which then infects the definitive host during feeding.[4]

Clinically, canine cases of *Onchocerca lupi* may present with single or multiple, variably sized nodules on the bulbar conjunctiva, conjunctival hyperemia, episcleral injection, chemosis, periocular swelling, retinal detachment, and corneal edema.[13,14] Typical gross lesions include nodules affecting the conjunctiva, episcleral tissue, and periorbital soft tissues.[13] Some cases do not have reported clinical signs directly attributable to Onchocerciasis, and are diagnosed as an incidental lesion on biopsy secondary to other presenting causes like neoplasia.[13] Bilateral involvement is described.[14]

Onchocerca lupi is typically diagnosed via histopathology, and to our knowledge no commercially available polymerase chain reaction (PCR) tests is available, although PCR assays have been described in the peer reviewed literature.[7,14] Typical histologic lesions include nematodes with very small intestinal cross sections, atrophied coelomyarian/polymyarian musculature, and annular cuticular ridges that can be seen in longitudinal or oblique sections. Microfilaria may be seen within female worms. Variable amounts of inflammation

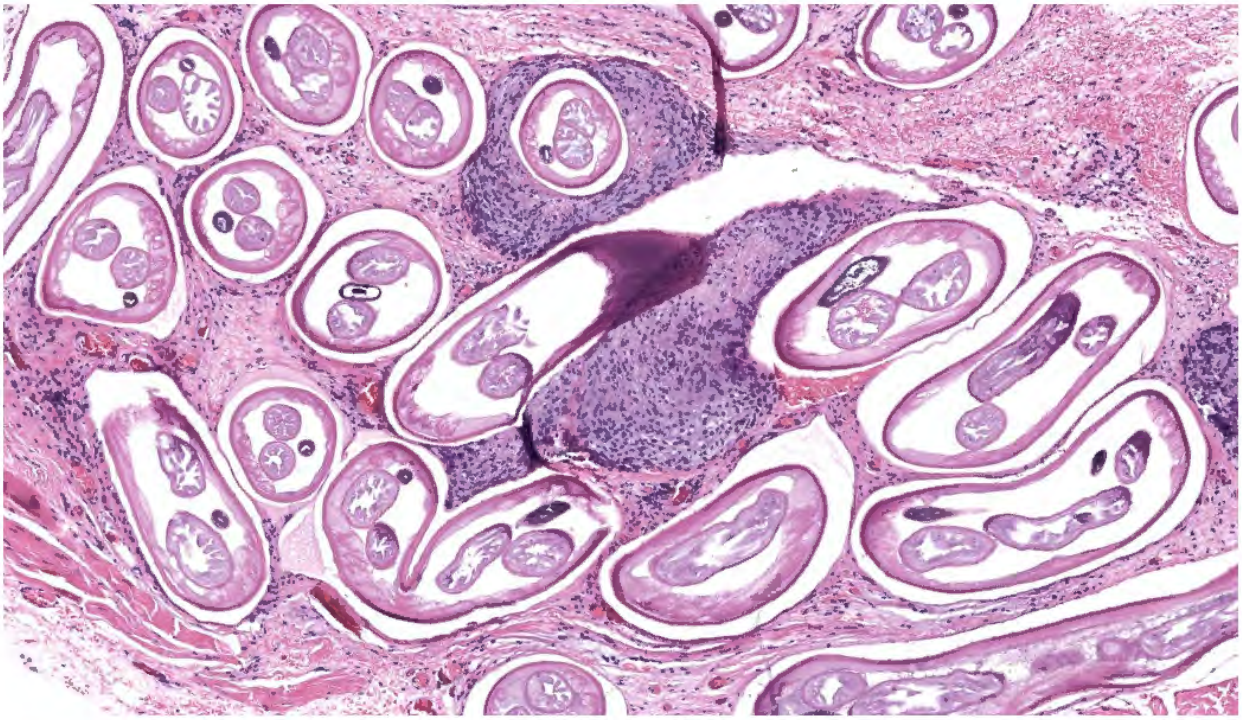

Figure 3-3: Eye, dog. Higher magnification of the mass of nematode larvae within the sclera. Some of the larvae are surrounded by granulomatous inflammation. At the periphery of the nodule, larvae extend into the adjacent atrophic orbital skeletal muscle. (HE 131X)

ranging from mild to severe, and including macrophages, lymphocytes, and eosinophils may be seen, as can fibroplasia. We have seen pyogranulomatous inflammation as well in our laboratory. Currently, a commercially available serology test is not available, although serologic tests are in development.[15]

Contributing Institution:
NMDA Veterinary Diagnostic Services, 1101 Camino de Salud NE, Alberquerquw, NM 87102,
https://nmdeptag.nmsu.edu/labs/veterinary-diagnostic-services.html

JPC Diagnoses:
1. Globe and periocular tissue: Scleritis and orbital rhabdomyositis, granulomatous, chronic, multifocal, moderate, with adult filarids.
2. Retina, ganglion cell layer: Degeneration and atrophy, chronic, diffuse, severe.
3. Globe, lens: Cataract.
4. Globe, cornea: Keratitis, neutrophilic and histiocytic, chronic, multifocal, moderate.

JPC Comment:
This third case stimulated excellent discourse on ocular pathology and the associated changes seen in this eye. While the nematodes in the periocular tissues were striking, the other ocular lesions were a point of discussion focus for conference participants to ensure residents in attendance understood the importance of not latching on to one lesion ("search satisfaction") before examining the tissues in their entirety. This eye had multiple other lesions, some of which were subtle, and these caught the attention of the more experienced participants in the room. The keratitis in this eye served as a springboard to discuss the other changes, and conference participants suspect the keratitis was secondary to melanosis and inflammation causing occlusion of the drainage angle in this case, resulting in secondary glaucoma (as evidenced

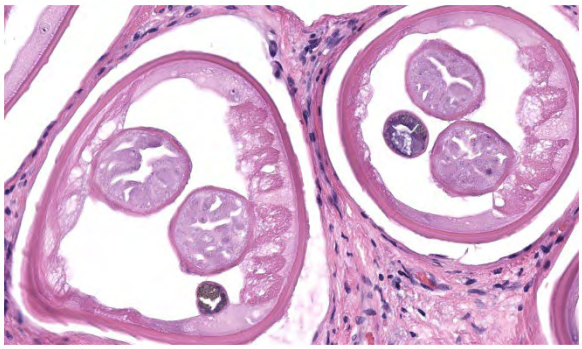

Figure 3-4: Eye, dog. Higher magnification of a larva in cross section. Larvae have no developed reproductive tracts. The nematodes have a tegument with thin spikes, coelomyarian-polymyarian musculature which is interrupted by a hypodermis, a small triradiate esophagus, and sections of a small multinucleated intestine.

by degeneration of inner retinal cells and retinal ganglion cell loss) and subsequent buphthalmia. One of the more common sequelae to buphthalmia is an exposure keratitis due to inability of the eyelids to completely close over the enlarged eye. Coupled with possible irritation from the nematodes, participants felt that the keratitis and precluding factors were important features to discuss in this case.

Conference participants unanimously agreed that the nematodes in section were consistent with *Onchocerca lupi*. For the sake of educational discussion, differentials for ocular nematodes in a dog were: *Toxacara canis* (ascarid), *Onchocerca lupi* (spirurid), *Angiostrongylus vasorum* (metastrongylid), *Dirofilaria immitis* (spirurid), *Ancylostoma caninum* (strongylid), *Trichinella spiralis* (aphasmid), and *Thelazia spp.* (spirurids). Of these, *Thelazia spp.* are the true ocular parasite and tend to reside in the conjunctival sacs and lacrimal ducts of infected animals. *Onchocerca spp*. in other species were briefly discussed, and honorable mentions included *O. cervicalis*, which sets up shop in the nuchal ligament of horses, *O. gutturosa* and *O. lienalis*, both of which invade the nuchal and gastrosplenic ligaments of cattle, and O. volvulus, the causative agent of "river blindness" in humans.

References:

1. Labelle AL, Maddox CW, Daniels JB et al. Canine ocular onchocercosis in the United States is associated with *Onchocerca lupi*. *Vet Parasitol*. 2013;193(1-3):297-301.
2. Tudor P, Ionașcu I, Mateescu CI, Bezerra-Santos MA et al. Feline ocular onchocercosis by *Onchocerca lupi*: Phylogenetic insights and implication for veterinary health. *Acta Trop*. 2023; 237:106723.
3. Roe CC, Yaglom H, Howard A, et al. Coyotes as Reservoirs for *Onchocerca lupi*, United States, 2015-2018. *Emerg Infect Dis*. 2020 Dec;26(12):2989-2993.
4. Rojas A, Morales-Calvo F, Salant H, Otranto D, Baneth G. Zoonotic Ocular Onchocercosis by *Onchocerca lupi. Yale J Biol Med*. 2021;94(2):331-34
5. McGarry JW, Carrozza R, Bradley C, Latrofa MS, Makepeace BL, Otranto D. *Onchocerca lupi* in imported dogs in the UK: implications for animal and public health. *BMC Vet Res*. 2022 Feb;18(1):66.
6. Otranto D, Sakru N, Testini G, Gürlü VP, Yakar K, Lia RP, Dantas-Torres F, Bain O. Case report: First evidence of human zoonotic infection by Onchocerca lupi (Spirurida, Onchocercidae). *Am J Trop Med Hyg*. 2011;84(1):55-8.
7. Bowers Wu D, Ko B, Lopez Hernandez G, et al. Neuroinvasive *Onchocerca lupi* Infection in a Ten-Year-Old Girl. *Case Rep Infect Dis*. 2022; 2022:9773058
8. Cantey PT, Weeks J, Edwards M, et al. The Emergence of Zoonotic Onchocerca lupi Infection in the United States--A Case-Series. *Clin Infect Dis.* 2016 15;62(6):778-83
9. Komnenou AT, Thomas AL, Papadopoulos E, Koutinas AF. Intraocular

localization of *Onchocerca lupi* adult worm in a dog with anterior uveitis: A case report. *Vet Ophthalmol.* 2016 ;19(3):245-249.
10. Wallitsch K, Jaffey JA, Ferguson S, et al. Extensive Aberrant Migration of *Onchocerca lupi* in a Dog. *Top Companion Anim Med.* 2022;49:
11. Hassan HK, Bolcen S, Kubofcik J, et al. Isolation of *Onchocerca lupi* in Dogs and Black Flies, California, USA. *Emerg Infect Dis*. 2015;21(5):789-96.
12. Roe CC, Holiday O, Upshaw-Bia K, et al. Biting midges (Diptera: Ceratopogonidae) as putative vectors of zoonotic *Onchocerca lupi* (Nematoda: Onchocercidae) in northern Arizona and New Mexico, southwestern United States. *Front Vet Sci*. 2023 15;10:1167070.
13. Dubielzig RR, Ketring KL, McLellan GJ, Albert DM. Veterinary Ocular Pathology: A comparative review. Saunders Elsevier; 2010.
14. McLean NJ, Newkirk K, Adema CM. Canine ocular onchocerciasis: a retrospective review of the diagnosis, treatment, and outcome of 16 cases in New Mexico (2011-2015). *Vet Ophthalmol.* 2017;20(4):349-356.
15. Latrofa MS, Louzada-Flores VN, Maia C, et al. Development of an indirect ELISA for the serodiagnosis of canine infection by *Onchocerca lupi*. *Sci Rep*. 2024;14(1):3348

CASE IV:

Signalment:
2.5-year-old spayed female domestic shorthair cat (*Felis catus*)

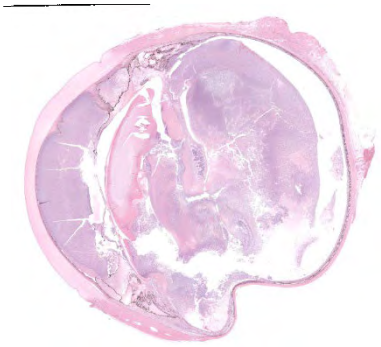

Figure 4-1: Eye, cat. There are profound inflammatory changes in all segments of the eye. (HE, 10X)

History:
Dental procedure performed 6 weeks prior with multiple extractions, including right maxillary arcade. Right eye discomfort was noted by the owner one day post-surgery. Medical management (full details not available) was attempted by the primary veterinarian, but the patient was refractory to treatment. The cat was referred to an ophthalmologist who documented severe anterior uveitis, iris bombe, and lens capsule rupture via ultrasound. Enucleation was performed due to suspicion of septic endophthalmitis secondary to dentistry-related ocular trauma.

Gross Pathology:
Submitted fixed in 10% neutral buffered formalin for evaluation is an enucleated eye (diameter: 31mm; cornea diameter: 18mm; axial length: 22mm) with a less than 1mm segment of optic nerve. On section of the eye, the ocular chambers contain abundant amounts of thick off-white purulent material.

Laboratory Results:
N/A

Microscopic Description:
Filling all ocular chambers and coating the surfaces of intraocular structures are vast accumulations of exudate consisting of myriad

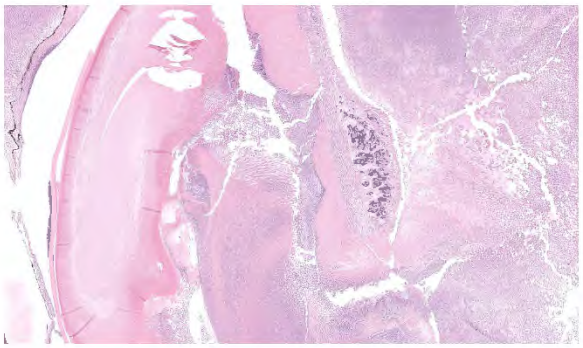

Figure 4-2: Eye, cat. The lens is ruptured. HE, 25X)

degenerate and intact neutrophils, many macrophages, abundant amounts of fibrinous to proteinic material, abundant necrotic cellular debris, occasional pools of extravasated erythrocytes, and multifocal colonies of mixed bacteria (rods and coccobacilli). Centrally incorporated into the inflammatory exudates is a ruptured lens which lacks a capsule in many areas and has highly undulating free capsule margins regionally. The lenticular stroma is variably vacuolated with the following features: streaks of pallor, Morgagnian globules, many infiltrating leukocytes (mostly neutrophils), and occasional pockets of similar bacteria. The retina is diffusely detached and largely inapparent apart from remnant segments of atrophied and degenerate retina enmeshed within the exudate. Suppurative to pyogranulomatous inflammatory infiltrates multifocally extend into the iris, ciliary body, choroid, optic nerve which is significantly gliotic with rarefied neuropil, and optic nerve meninges. The iris is displaced anteriorly and multifocally abuts the posterior aspect of the cornea. The anterior chamber is severely narrow, and the drainage angle is collapsed and inapparent. The corneal stroma is moderately to markedly oedematous and contains small to moderate numbers of scattered neutrophils. The anterior corneal epithelium appears attenuated in areas. The sclera is variably thinned with multifocal often perivascular infiltrates of lymphocytes and plasma cells with variable numbers of admixed neutrophils and occasional macrophages. There are increased numbers of perilimbal pigmented cells. A thin to moderately thick layer of oedematous and inflamed granulation tissue regionally lines the mid and posterior scleral margins outside the globe and extends into a bundle of periocular skeletal muscle. In addition to infiltrates of the aforementioned inflammatory cells, the granulation tissue also contains many golden-brown pigmented macrophages (siderophages) which are concentrated at the level of the ciliary body. There is abundant haemorrhage in the retrobulbar loose connective tissue.

Contributor's Morphologic Diagnoses:
Endophthalmitis, diffuse, suppurative to pyogranulomatous, severe, with lens rupture, retinal detachment and degeneration/atrophy with intraocular exudation and intralesional mixed bacteria, drainage angle collapse, keratitis, corneal oedema, scleritis and regional periscleral fibrosis

Contributor's Comment:
Ophthalmic complications associated with scleral penetrating injuries are infrequently reported in dogs and cats with a recent history of dental procedures. Iatrogenic globe trauma as

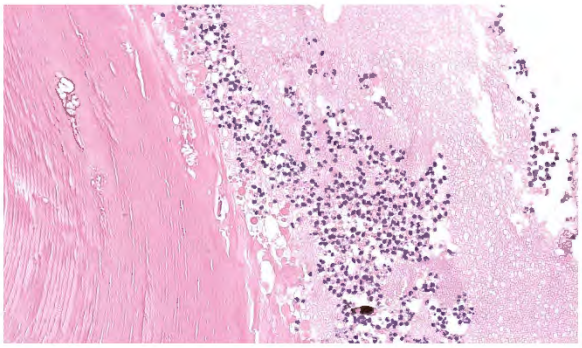

Figure 4-3: Eye, cat. The ruptured lens is infiltrated by numerous neutrophils which are attracted to lens protein. The posterior lens capsule is at right. (HE, 457X)

a complication of routine dentistry may occur secondary to slippage of dental instruments during maxillary tooth extraction or inadvertent needle perforation of the globe when placing infra-orbital and maxillary nerve blocks. Endophthalmitis is a common sequela of dental-associated globe penetration due to implantation of bacteria and/or lens rupture. Medical management is often poor and most cases of post-dentistry endophthalmitis lead to palliative and diagnostic enucleation.

Compared with other species, cats may be at increased risk of traumatic globe injury during exodontic procedures due to a large globe size that nearly fills the orbit, lack of bony orbital floor, and close proximity of maxillary tooth roots (especially PM4 and M1) to the ventral orbit. Bone resorption associated with periodontal and endodontic disease may further compromise the narrow rim of alveolar bone surrounding the roots of the maxillary premolars and molars, increasing vulnerability to iatrogenic ocular trauma. Older cats may be at increased risk of penetrating ocular trauma during dental procedures compared with younger cats due to age-associated atrophy of orbital fat pads and closer globe position to the oral cavity.

Clinical findings in animals following orbital penetration during a dental procedure include vision loss, epiphora, mucopurulent ocular discharge, blepharospasm, exophthalmos, buphthalmos, glaucoma, hyphema, hypopyon, miosis, iris bombe, cataract, and orbital cellulitis. Gross examination of the globe commonly demonstrates opacification of the aqueous and vitreous humor and may reveal a site of scleral penetration. Histopathologic lesions include severe suppurative endophthalmitis or panophthalmitis, varying degrees of orbital cellulitis and episcleral fibrosis of the ventral

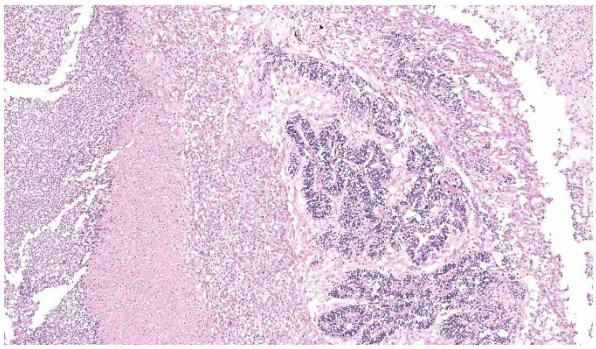

Figure 4-4: Eye, cat. The markedly atrophic and coiled retina is floating free within a mass of fibrinosuppurative inflammation within the vitreous behind the ruptured lens. (HE, 121X)

aspect of the globe, and in some instances rupture of the posterior or equatorial lens capsule and/or presence of intraocular bacteria. Ventral scleral perforation may be appreciated in some cases, but a site of penetrating injury is not always detected. In this case, a scleral penetration site was not appreciated grossly or histologically despite review of multiple step sections.

Contributing Institution:
University of Sydney
https://sydney.edu.au/science/schools/sydney-school-of-veterinary-science/veterinary-science-services.html

JPC Diagnoses:
Globe: Endophthalmitis, fibrinosuppurative, subacute, diffuse, severe, with lens rupture, synechiae, fibrovascular membranes, retinal detachment and atrophy, and bacterial colonies.

JPC Comment:
Talk about a descriptive case that made, for obvious reasons, an excellent sales pitch on why pathology is the best profession! This case provides an excellent opportunity for participants to push themselves on their ocular descriptive abilities. Many thanks to this contributor for a fantastic case! Much like the previous eye case in this conference,

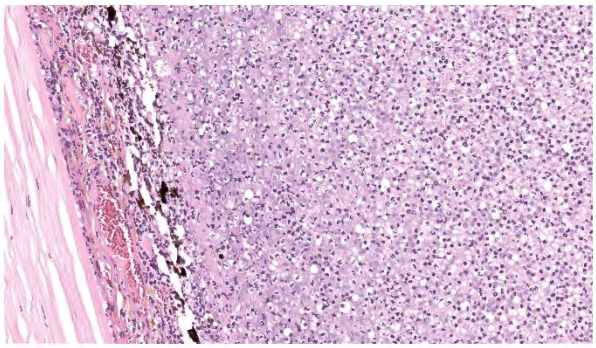

Figure 4-5: Eye, cat. The iris is adhered to the posterior of the cornea (anterior synechia) and expanded by pre- and post-iridal fibrovascular membranes. The anterior segment is filled with neutrophils. (HE, 379X)

there was substantial discussion on ocular pathology. The most informative nuggets from that conversation included utilizing the lens capsule, which is an easily identifiable structure in the eye, to assist with orientation in a busy ocular slide such as this one. The pigmented irideal stroma, as well as the "golden" fibers of the iris, can also be used to help identify structures that might otherwise be difficult to ascertain due to the degree of damage and/or inflammation.

This case had beautiful examples of iris bombe (iris pushed forward into the anterior chamber and adhered to the back of the cornea), numerous types of fibrovascular membranes (retrocorneal, preiridial, cyclitic, etc.), and a fantastic phakoclastic panuveitis from lens rupture. The six types of uveitis and their definitions were discussed and included: 1) anterior uveitis (inflammation of the iris and ciliary body), 2) posterior uveitis (inflammation of the ciliary body and choroid), 3) panuveitis (iris, ciliary body, and choroid affected), 4) chorioretinitis (inflammation of the choroid and retina), 5) endophthalmitis (inflammation of uvea, retina, and ocular cavities), and 6) panophthalmitis (all ocular structures are affected, including sclera). Being able to recognize and accurately use these terms as pathologists can provide crucial information to ophthalmologists when it comes to treating these patients.

As anyone who has owned a cat will tell you, cats are no strangers to ocular trauma. Common causes include fights (especially with claws), foreign bodies, blunt trauma, chemical burns, and, less commonly, iatrogenic (such as dental work or local nerve blocks). Of the frequently encountered domestic species in veterinary medicine, cats are more likely to end up with traumatic globe injury following dental procedures due to their complete lack of a bony orbital floor, their objectively massive eyes that stare straight into the void, and the close proximity of their maxillary roots (PM4 and M1) to their ventral orbit. Additionally, they get a fair amount of periodontal disease, which can lead to bone resorption and thinning of the alveolar bone around the tooth roots. Older cats, as if they needed any additional help getting their eyeballs stabbed, also have age-associated atrophy of their orbital fat pad, putting their globes in even closer proximity to the oral cavity.

An unfortunate possible sequela to chronic ocular trauma in cats is the development of feline post-traumatic ocular sarcoma (FPTOS), which is an aggressive malignant neoplasm of the eye in cats and the third most common primary intraocular tumor in feline patients.[6] It can take up to seven years for these sarcomas to develop following ocular trauma or disease, and they are thought to arise from malignant transformation of lens

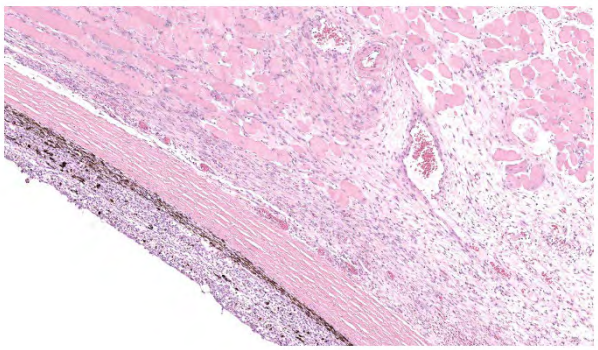

Figure 4-6: Eye, cat. The retina is detached and the choroid is expanded by moderate numbers of infiltrating neutrophils. The sclera is thinned. The periorbital fat and atrophic orbital skeletal muscle are infiltrated by edematous fibrous connective tissue.

epithelium, as there is a history of lens rupture is almost all cases of FPTOS.[6] Most of these tumors look very similar to fibrosarcomas, but there can be variation in their morphology; some may look like osteosarcomas, others like giant cell neoplasms.[6] Recently, there has been a link established between the development of FPTOS and the use of intravitreal gentamicin injections used to ablate the ciliary body in cases of unresolving glaucoma.[6] Medicine is ever-evolving, and one of the great burdens of clinicians is making treatment decisions that carry risk knowing that, for some patients, the benefit of such treatment outweighs that risk. For cats afflicted with these aforementioned conditions, though, it seems that all roads lead to enucleation.

References:

1. Dubielzig RR, Ketring KL, McLellan GJ, Albert DM. *Veterinary Ocular Pathology, a Comparative Review*. Philadelphia, PA: Elsevier; 2010:330-336.
2. Duke FD, Snyder CJ, Bentley E, Dubielzig RR. Ocular trauma originating from within the oral cavity: clinical relevance and histologic findings in 10 cases (2003-2013). *J Vet Dent.* 2014;31(4):245-248.
3. Perry R, Moor D, Scurrell E. Globe penetration in a cat following maxillary nerve block for dental surgery. *J Feline Med Surg*. 2015;17(1):66-72.
4. Smith MM, Smith EM, La Croix N, Mould J. Orbital Penetration Associated with Tooth Extraction. *J Vet Dent.* 2003;20(1):8-17.
5. Volk HA, Bayley KD, Fiani N, Bilson FM. Ophthalmic complications following ocular penetration during routine dentistry in 13 cats. *N Z Vet J.* 2019;67(1):46-51.
6. Wood C, Scott EM. Feline ocular post-traumatic sarcomas: Current understanding, treatment and monitoring. *J Feline Med Surg.* 2019;21(9):835-842.

Joint Pathology Center
Veterinary Pathology Services

WEDNESDAY SLIDE CONFERENCE 2025-2026

Conference #6 — 1 October 2025

CASE I:

Signalment:
Two year and nine month-old, male castrated, mixed breed, canine
Three year-old, male intact, Golden retriever, canine
Eight year-old, male castrated, mixed breed, canine
Fifteen year-old, male castrated, Labrador, canine

History:
Acute onset of vomiting and collapse.

Gross Pathology:
Segmental hemorrhagic necrosis of the bowel with perforation and peritonitis

Laboratory Results:
N/A

Microscopic Description:
Findings are very similar in all cases that were submitted to the diagnostic laboratory.

In all samples from the grossly discolored and swollen segment there was transmural necrosis of the intestine with extensive hemorrhage extending into the mesenteric fat. In the adjacent viable intestine there was eosinophilic infiltration of variable intensity. There was multifocal necrosis of mesenteric fat and, in some sections, diffuse eosinophilic infiltration.

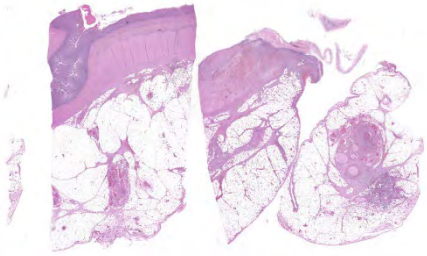

Figure 1-1: Intestine and mesentery. Three sections of intestine and mesentery are submitted for examination. At this magnification, the vessels of the mesentery and septa between lobules of mesenteric fat is expanded in each section. (HE, 10X)

Large vessels were dilated and many contained thrombi.

Within the media of medium to small sized arteries there were sections (not present in all slides due to the small size of the parasite – but see photomicrographs) of a nematode larva, approximately 100-200 µm in diameter with lateral allae and central digestive tract. These features are consistent with a spirurid of which *Spirocerca* is the most likely in our region. Foci of necrosis with hemorrhage were observed in the media of some arteries, where no larvae were identified.

Contributor's Morphologic Diagnoses:
Acute transmural necrotizing eosinophilic enteritis and eosinophilic peritonitis with arterial mesenteric thrombi and rare intralesional nematode larvae (spirurid)

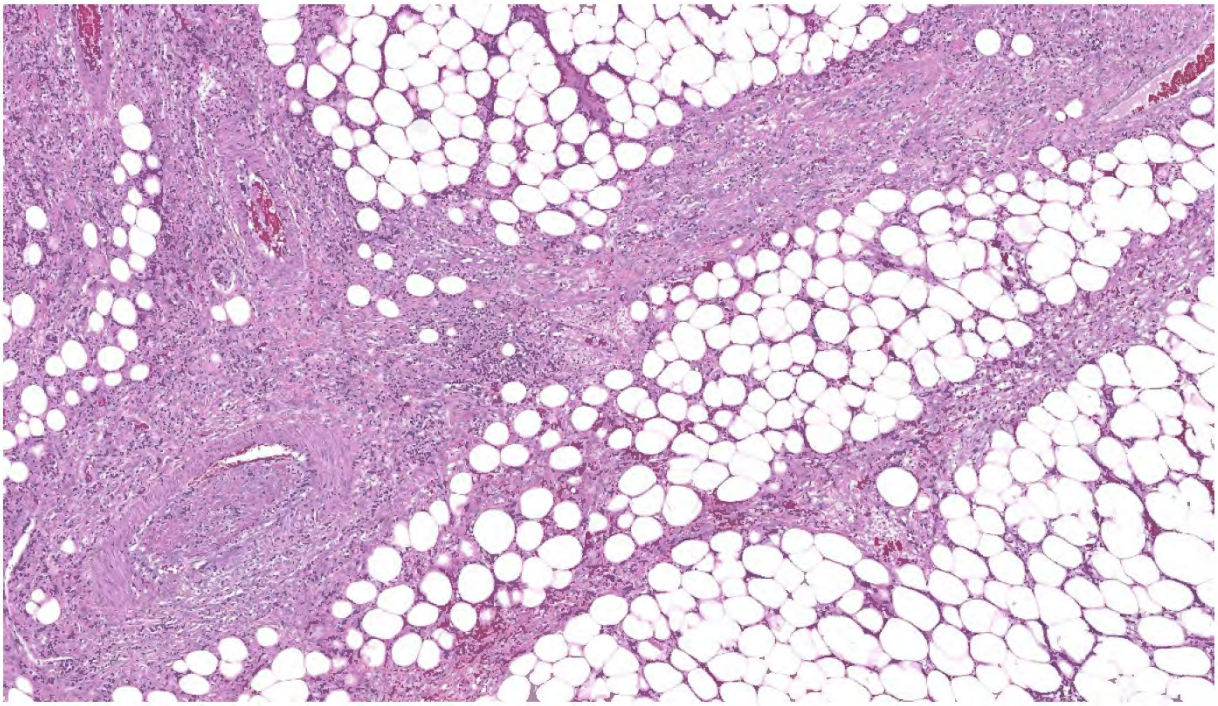

Figure 1-2: Mesentery, dog. Granulation tissue and eosinophilic inflammation expand the interlobular septa between lobules of mesenteric fat. A recanalized arteriole is present at bottom left. (HE, 80X)

Contributor's Comment:

Several cases of this condition were diagnosed in the last few years in Israel, where incidence of *Spirocerca* infection is high.[1,7] We have not observed breed or age predilection. The presenting history is usually that of intestinal infarction, with or without peritonitis. Clinical DDs are volvulus or intussusception.

Heavy eosinophilic infiltration of mesenteric fat and thrombi are a common histologic finding in all samples in addition to acute transmural intestinal necrosis. In only a few of the samples intralesional larvae have been observed.

Some samples with similar history which were received in the past, before we became aware of this condition, were evaluated retrospectively. Although no parasites were found, we considered the presence of heavy eosinophilic infiltration and thrombi to be highly suggestive of aberrant larval migration of *Spirocerca*.

Follow up information was available for some of these dogs. The vets described recurrent intestinal infarction and peritonitis with or without perforation.

Spirocerca lupi is a spirurid nematode that parasitizes the esophageal wall of dogs and

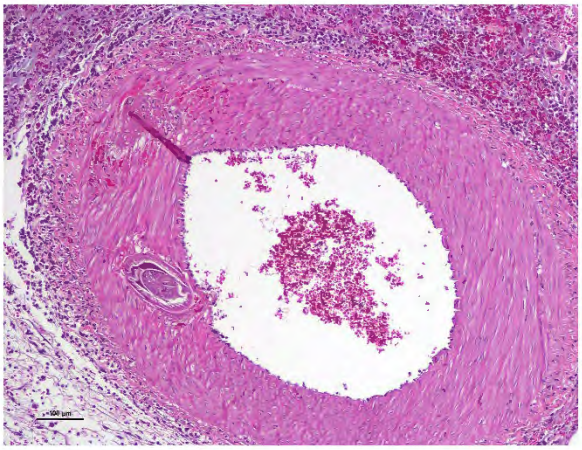

Figure 1-3: Mesentery, dog. A tangential section of a larval nematode is present in he wall of a mesenteric artery. (HE, 100X) (Photo courtesy of: The Weizmann Institute of Science, http://www.weizmann.ac.il/)

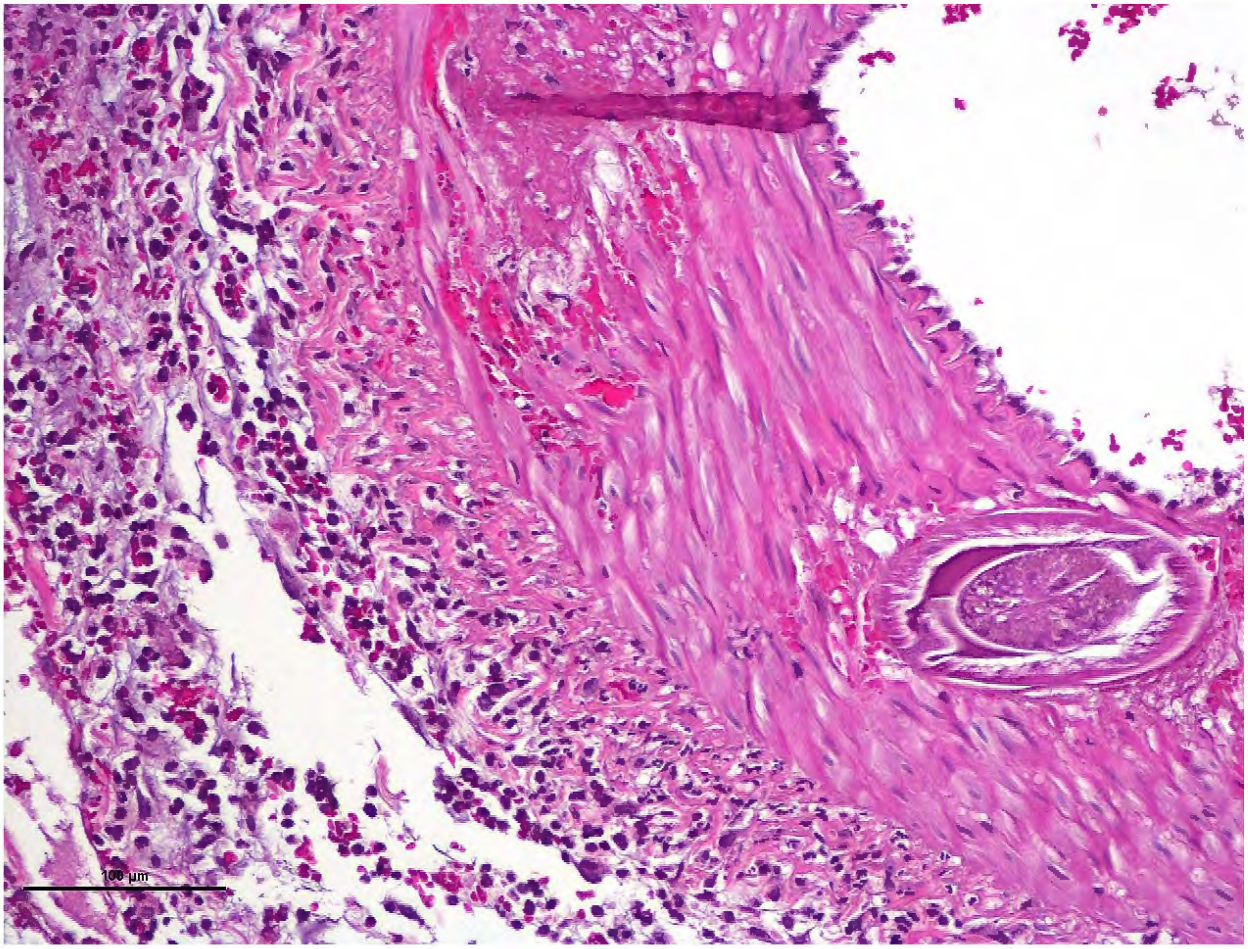

Figure 1-4: Mesentery, dog. Higher magnification of a tangential section of a larval nematode within the wall of a mesenteric artery. (HE, 400X) (Photo courtesy of: The Weizmann Institute of Science, http://www.weizmann.ac.il/)

other carnivores. It is most common in warm climates where beetles act as intermediate hosts.[1,2,7] The normal site for the adult nematode is the distal region of the esophageal submucosa or the proximal stomach, where they are found in a cystic granulomatous lesion.[2]

Third stage larvae of *Spirocerca* are ingested with beetles and penetrate the gastric mucosa. They move along arteries to the aorta and migrate in its wall to the thoracic region where they are found several weeks after ingestion. They incite granulomatous inflammation in the aorta and stay there for 2-4 months. Later, the larvae migrate to the esophagus where they mature in the submucosa and perforate the epithelium.[2,7]

Larvae that follow aberrant migratory pathways may be found in granulomas in subcutaneous tissue, bladder, kidney, spinal cord and intrathoracic locations.[2,3,9] To our knowledge, there are no descriptions of Spirocerca in mesenteric blood vessels.

Aortic lesions associated with *Spirocerca* include intimal and medial hemorrhage and necrosis with eosinophilic inflammation, thrombus formation and rarely rupture of the aortic wall.[1,2,7]

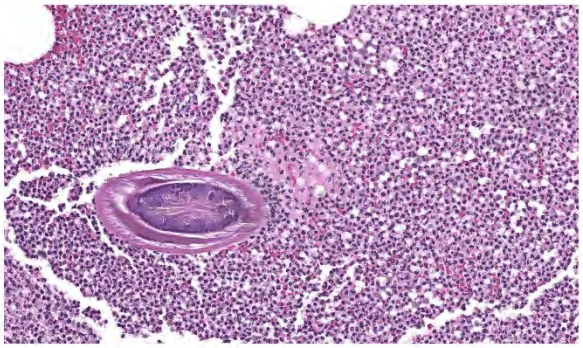

Figure 1-5: Mesentery, dog. A tangential section of a larval nematode in an area of eosinophilic inflammation demonstrates a smooth cuticle, polymyarian-coelomyarian musculature, a pseudocoelom containing bright red material (characteristic of spirurids) and and a single cross section of a large intestine. (HE, 800X) (*Photo courtesy of:* The Weizmann Institute of Science, http://www.weizmann.ac.il/)

Contributing Institution:
The Weizmann Institute of Science
http://www.weizmann.ac.il/

JPC Diagnoses:
1. Mesentery: Arteritis and periarteritis, necrotizing and eosinophilic, chronic, multifocal, severe, with arterial thrombi and rare larval spirurids.
2. Small intestine: Enteritis and peritonitis, necrotizing and eosinophilic, chronic, regionally extensive, severe.

JPC Comment:
The JPC's own MAJ Katie Scott moderated Conference 6 and took participants on a journey of cases from around the world; each one was from somewhere outside of the continental U.S., highlighting the truly global nature of the WSC and the importance of international contributions to pathology education. This first case provided an excellent opportunity to review of the pathogenesis and life cycle of *Spirocerca lupi*, both of which are well-covered in the contributor's comment. Additionally, the lesions of spirocercosis that are considered pathognomonic in the dog were covered and include aortic scarring with aneurysms, thoracic spondylitis, and caudal esophageal nodules. Special attention was paid to the chronic arterial thrombi present in numerous arteries in this case, which are a classic part of the pathogenesis of this parasite due to its arterial migratory routes and chronic intimal irritation. Participants were also reminded of the importance of specifying what type of vessels (arteries, arterioles, veins, lymphatics, etc.) are affected when giving a description, as this can provide important clues towards pathogenesis of some diseases that may preferentially affect a specific vessel type.

Spirocerca lupi is one of a handful of helminths that are classified as Group I carcinogens by the International Agency for Research on Cancer (IARC) due to the well-documented malignant transformation of S. *lupi* esophageal nodules into esophageal fibrosarcomas or osteosarcomas in up to 25% of infected dogs.[6] Less commonly, chondrosarcomas or undifferentiated pleomorphic sarcomas can also be seen.[6] Metastasis to multiple locations throughout the body, including the lungs, kidneys, stomach, spleen, heart, and tongue, occurs frequently.[6,7] Significantly higher levels of interleukin-8 (IL-8) have been documented in dogs with malignant esophageal nodules.[4] IL-8 is released by activated fibroblasts in pre-neoplastic nodules and is chemotactic for neutrophils. IL-8 is also involved in the tumor progression of human herpesvirus-4 (Epstein–Barr virus)-induced carcinomas.[4]

Other unwanted guests that no one invited to the party due to their classification as Group I carcinogens include *Clonorchis sinensis,*

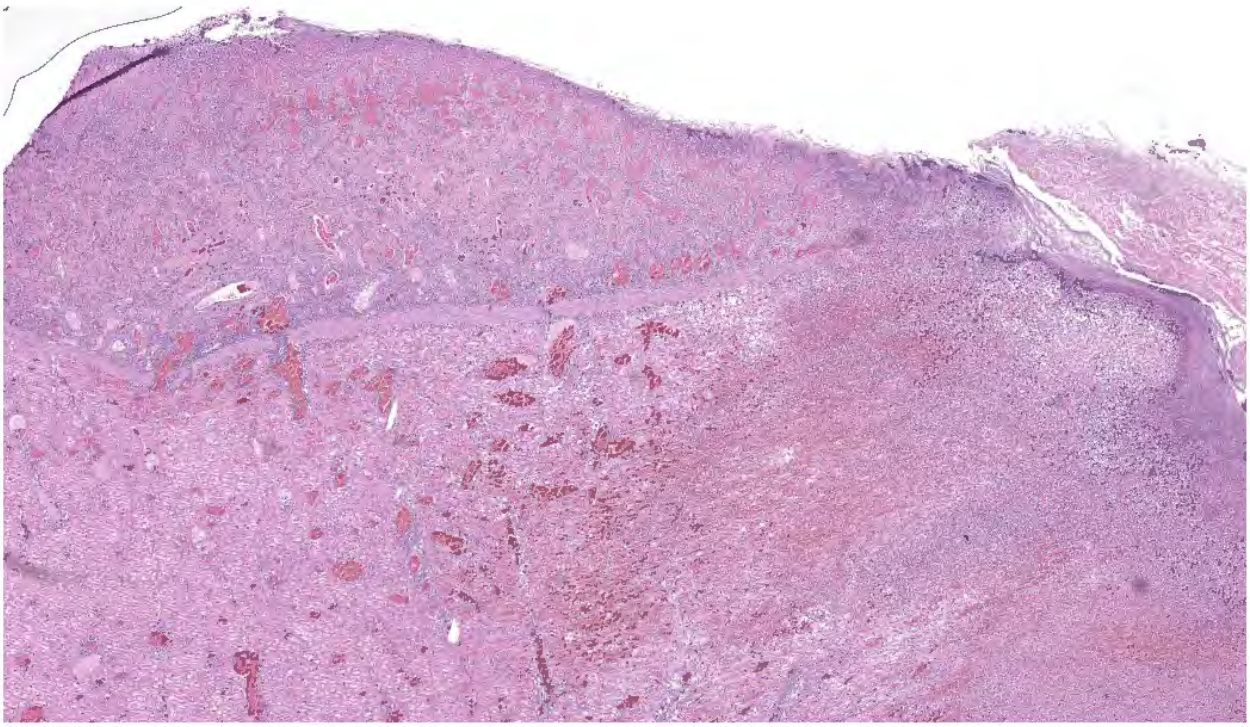

Figure 1-6: Jejunum, dog. There is full thickness necrosis of the mucosa and effacement of the normal architecture of the muscular tunics by granulation tissue in segments supplied by affected arterioles. (HE, 46X)

Opisthorchis viverrine, and *Schistosoma haematobium*. *Clonorchis sinensis*, a liver fluke transmitted via ingestion of undercooked fish hosting the parasitic metacercariae, can induce hepatocellular carcinomas or cholangiocarcinomas via mechanical damage to bile duct epithelial cells and suppression of biliary epithelial apoptosis via a wide range of excretory and secretory products (ESP).[6] *Opisthorchis viverrine,* another liver fluke ingested from raw fish, also induces cholangiocarcinoma through similar mechanisms to *C. sinensis*. *Schistosoma haematobium*, another trematode, causes squamous cell neoplasms within the urinary bladder and is the only human schistosome directly associated with cancer. *S. japonicum* and *S. mansoni* are also classified as carcinogens, but as Groups 2B and 3, respectively.[6]

Yet another parasite within veterinary species that is well-known to induce malignant neoplasms is *Cysticercus fasciolaris*, the larval form of the cestode *Taenia taeniaformis*. This larval tapeworm can induce the formation of fibrosarcomas in the liver of infected rats.[5] There is a short list of additional parasites associated with the development of neoplasia, but the body of literature has not yet established a direct causal link between these neoplasms and the parasites themselves. These include: *Trichosomoides crassicauda*, the urinary bladder threadworm of rats that, although not directly carcinogenic in and of itself, is associated with the development of urothelial carcinomas via the creation of a chronically irritated environment within the urinary bladder that may be more receptive to the effects of external carcinogens; *Heterakis gallinarum* and *H. isolonche*, cecal nematodes of avian

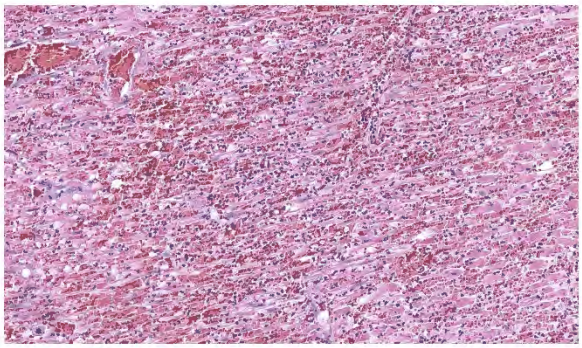

Figure 1-7: Jejunum. High magnification of the muscular tunic of the affected segment of intestine with degeneration, necrosis and atrophy of smooth muscle and proliferation of granulation tissue. (HE, 304X)

species, induce granulomatous nodule formation that can eventually progress to leiomyomas; and *Trichuris muris*, an intestinal-dwelling nematode of mice, can induce chronic cecal irritation that can develop into intestinal neoplasms.[5,8] Keeping these tiny not-friends on a short list of carcinogenic or cancer-associated parasites is crucial to the pathologist's differentials list when faced with cases where their consideration is warranted.

References:

1. Aroch I et al. Spirocercosis in dogs in Israel: A retrospective case-control study (2004-2009). *Vet Parasitol.* 2005;211:234-40.
2. Brown CC et al. Alimentary system. In: Jubb, Kennedy, and Palmer's Pathology of Domestic Animals, 5th edition; Maxie MG ed., Academic Press, Inc. Vol 2, 2007 pp. 97-98.
3. Du Plessis CJ et al. Aberrant extradural spinal migration of Spirocerca lupi: four dogs. J Small Anim Pract. 2007;48:275-8 (2007).
4. Long X, Ye Y, Zhang L, Liu P, Yu W, Wei F, Ren X, Yu J. IL-8, a novel messenger to cross-link inflammation and tumor EMT via autocrine and paracrine pathways (Review). Int J Oncol. 2016;48(1):5-12
5. Mahesh Kumar J, Reddy PL, Aparna V, Srinivas G, Nagarajan P, Venkatesan R, Sreekumar C, Sesikaran B. Strobilocercus fasciolaris infection with hepatic sarcoma and gastroenteropathy in a Wistar colony. Vet Parasitol. 2006;141(3-4):362-7.
6. Porras-Silesky C, Mejías-Alpízar MJ, Mora J, Baneth G, Rojas A. Spirocerca lupi Proteomics and Its Role in Cancer Development: An Overview of Spirocercosis-Induced Sarcomas and Revision of Helminth-Induced Carcinomas. Pathogens. 2021;10(2):124.
7. Sasani F et al. The evaluation of retrospective pathological lesions on spirocercosis (Spirocerca lupi) in dogs. J Parasit Dis. 2014;38:170–173.
8. Serakides R, Michel AF, de Lima Santos R, and Silva SM. Proliferative and inflammatory changes in the urinary bladder of female rats naturally infected with Trichosomoides crassicauda: Report of 48 cases. Arq Bras Med Vet Zootec. 2001;53(2).
9. Tudury EA et al. Spirocerca lupi-induced acute myelomalacia in the dog. A case report. Braz J Vet Res Anim Sci. 1995;32:22.

CASE II:

Signalment:

18 months old ewe, Merino, *Ovis aries*

History:

An experimental Merino CLN6 research flock was maintained at University of Sydney Farms, Camden, which was based on affected and carrier sheep that were sourced from two medium-wool Merino flocks in northern New South Wales.

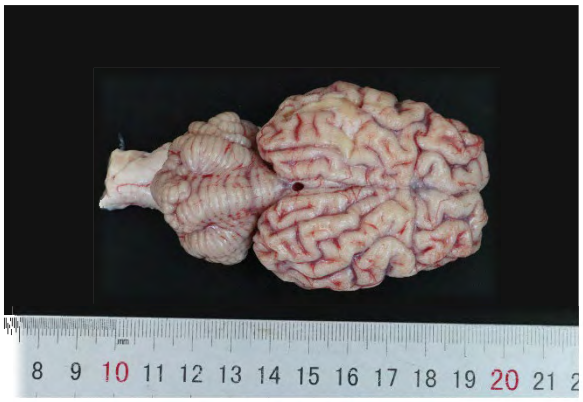

Figure 2-1: Brain, sheep. The cerebral hemispheres are small, firm and flattened dorsoventrally. The sulci are wider, and gyri were narrower than normal. There is diffuse, mild to moderate yellow discoloration (The University of Sydney, Veterinary Pathology Diagnostic Services http://sydney.edu.au/vetscience/vpds/)

This ewe developed clinical signs including decreased menace response, visual impairment, motor deficit and reduced herding instinct. The animal was euthanized.

Gross Pathology:
At postmortem examination the cerebral hemispheres were small, firm and flattened dorsoventrally. The sulci were wider, gyri were narrower than normal. There was diffuse, mild to moderate yellow discoloration.

Laboratory Results:
Missense mutation (c.184C > T; p.Arg62Cys) in ovine CLN6 gene detected by single nucleotide polymorphism (SNP) genotyping using a commercial SNP-Chip panel.

Microscopic Description:
Brain, frontal cortex: There is diffuse disruption of the laminar cortical architecture and diffuse atrophy of all layers, most apparent in the granular, pyramidal and ganglionic cell layers (mid-layers atrophy). The grey matter shows neuronal loss and diffuse moderate gliosis with increased numbers of astrocytes. The remaining neurons frequently contain variable numbers of up to 5 µm diameter, granular to globular, glassy, eosinophilic, intraneuronal bodies displacing large and often vesicular nuclei. Small neurons show hypereosinophilic cytoplasmic and pyknotic nuclei (necrosis).

Luxol fast blue (LFB): Intraneuronal storage material is LFB positive.

Periodic acid-Schiff (PAS): Intraneuronal storage material is PAS positive.

Contributor's Morphologic Diagnoses:
Brain, frontal cortex: Neuronal degeneration and loss, diffuse, moderate with intracytoplasmic ceroid accumulation and moderate astrocytosis, Merino, ovine.

Neuronal ceroid lipofuscinosis

Contributor's Comment:
Neuronal ceroid-lipofuscinoses are a heterogenous group of recessively inherited lysosomal storage diseases. In human medicine this neurodegenerative disease is referred to as Batten's disease and affects children.[1] This disease is characterized by atrophy of cerebral cortex, retina and cerebellar Purkinje system and accumulation of autofluorescent pigment in neurons and other cells. The pathogenesis

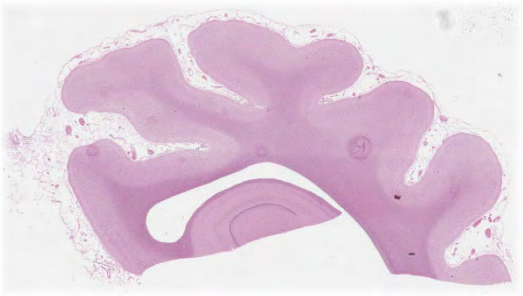

Figure 2-2: Diencephalon, sheep. There is diffuse separation and thinning of the cerebral gyri and dilation of the lateral ventricle (hydrocephalus ex vacuo) (HE, 10X)

of at least some forms of NCL may involve a defect in mitochondria rather than a defect in lysosomal catabolism and may involve accumulation of hydrophobic protein.[2]

Studies show that functional neuron loss is related to selective loss of specific neuron populations that is preceded by localized glial activation, and synaptic alterations. Rather than storage material accumulation, localized activation of glia is a better predictor of the distribution of subsequent neuron loss.[5,7] It is not clear whether this glial activation contributes to neuron loss or is a protective response, nevertheless it appears that neuroinflammation is a key part of the pathogenesis in many, if not all, forms of NCL.[10]

NCLs have been documented in a number of domestic animal species, including dogs, cats, cattle, and several breeds of sheep such as Merino, South Hampshire, Rambouillet and White Swedish Landrace.[3,6,9,11] Affected Merino sheep developed clinical signs between 7 months and a year of age. The ovine gene organization in this breed is very similar to that of human CLN6 (late infantile variant) and there is a high degree of homology between species along the whole coding length.[4] Active research studies utilize sheep flocks containing affected animals deliberately bred and maintained for studies relevant to human disease.

Contributing Institution:
The University of Sydney
University Veterinary Teaching Hospital Camden
https://www.univetscamden.com.au/
Veterinary Pathology Diagnostic Services
http://sydney.edu.au/vetscience/vpds/

JPC Diagnoses:
Cerebrum: Neuronal degeneration and loss, chronic, diffuse, severe, with cortical atrophy, neuronal intracytoplasmic pigment, mild astrocytosis, and hydrocephalus ex vacuo.

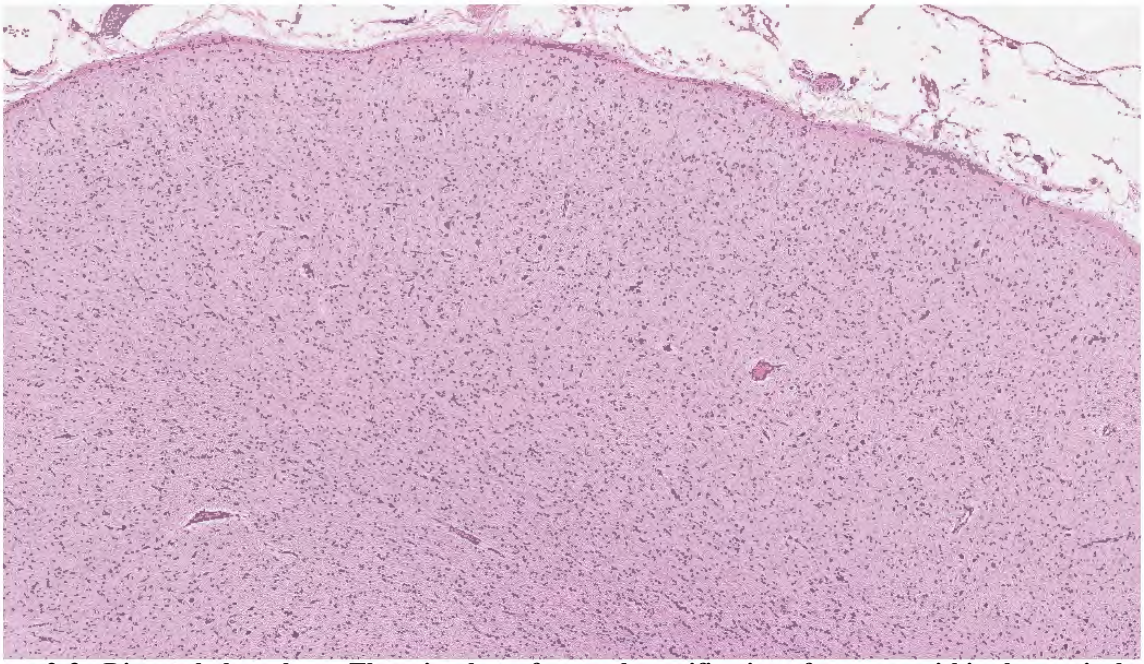

Figure 2-3: Diencephalon, sheep. There is a loss of normal stratification of neurons within the cortical gray matter. (HE, 65X)

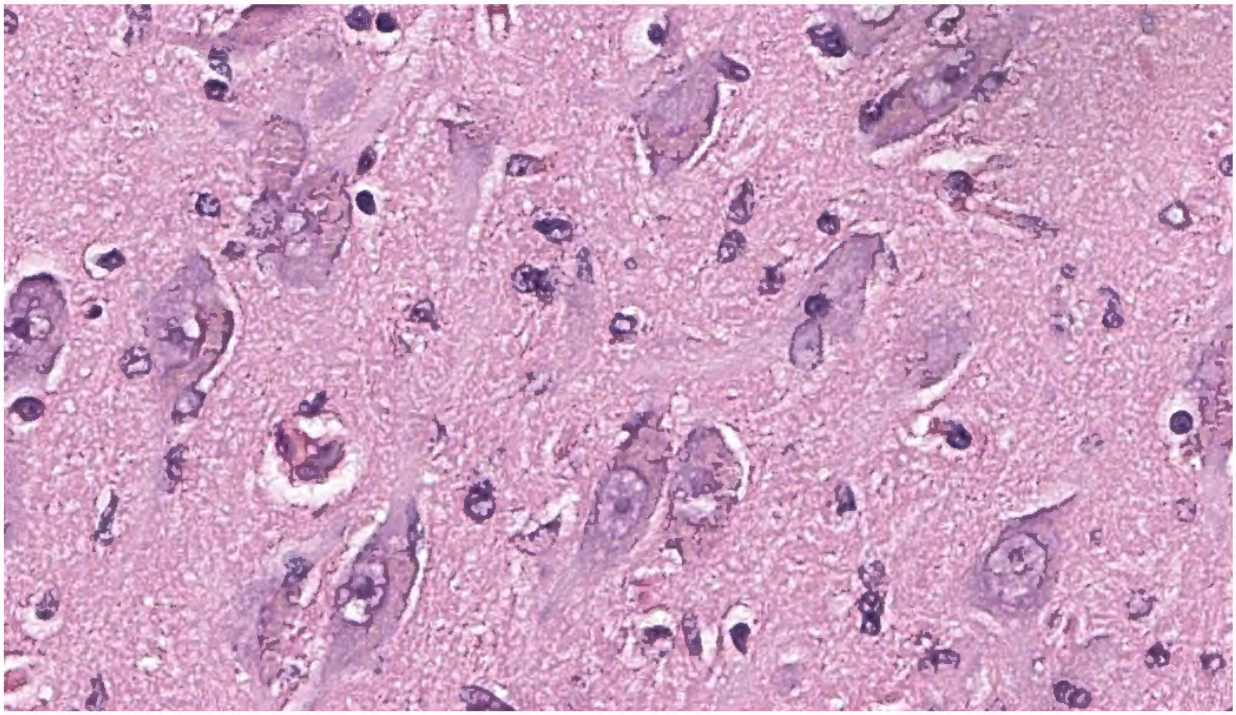

Figure 2-4: Diencephalon, sheep. Neuronal cytoplasm contains numerous amphophilic to brown 2um ceroid granules. (HE, 650X)

JPC Comment:

This classic case of ovine neuronal ceroid lipofuscinosis (NCL) stimulated great discussion on some of the histologic changes seen in the conference slide. It was the opinion of conference participants that there was true ventricular dilation evident histologically, likely secondary to the cerebral atrophy and parenchymal loss that is characteristic in this condition, leading to the development of a hydrocephalus *ex vacuo.* This brand of hydrocephalus is characterized by the ventricles filling with additional cerebrospinal fluid (CSF) in response to a vacuum created by the extra space from parenchymal loss. As the pathogenesis would imply, there is no accompanying increase in CSF pressure with this type of hydrocephalus as there is in other types.

One participant remarked that there was an increased number of visible axons within the affected grey matter. This posed the question of whether the increased visibility of axons was secondary to the neuronal loss from NCL or if there was true disorganization of the axons from the outset. The jury was split on this one, but the majority thought it was likely due to the former. A discussion on the intracytoplasmic storage material within neurons in this condition followed, including a review of the difference between lipofuscin and ceroid. Lipofuscin is considered a normal "wear and tear" pigment seen in long-lived cells and is not considered to be related to pathologic processes. Ceroid, however, is only seen in disease states and accumulates secondary to oxidative stress. The autofluorescent proteins in these cases are stored within lysosomes, which are unable to further break them down due to an endo-lysosome defect. In this case, in-house Luxol fast blue and PAS stains were performed, which nicely highlighted the intracytoplasmic accumulations.

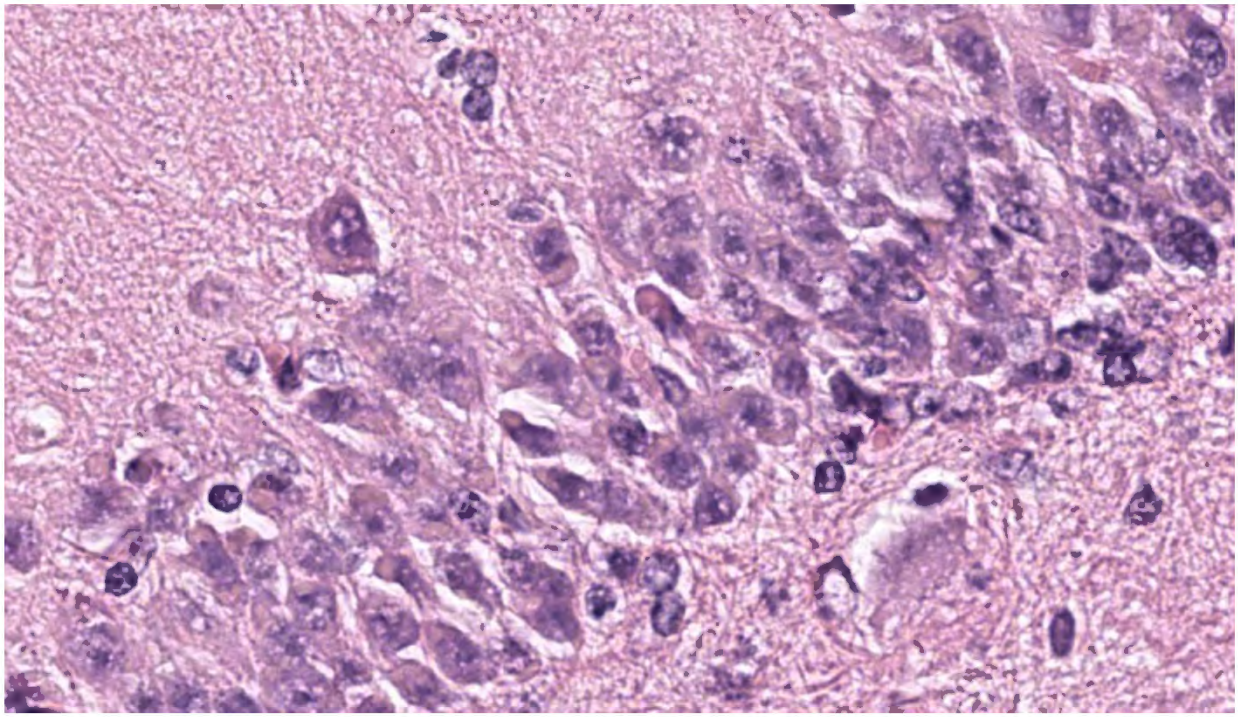

Figure 2-5: Diencephalon, sheep. Hippocampal neurons contains numerous amphophilic to brown 2um ceroid granules. (HE, 650X)

Currently, there are 13 different forms of NCLs documented in humans.[9] Each one has a distinct single-gene defect that affects the encoding of proteins in the endolysosomal system. These forms are generally classified into either soluble lysosomal enzyme/cytosolic protein deficiencies or insoluble transmembrane protein defects.[9] The lysosome is traditionally viewed as the 'waste-disposal' unit of the cell, but recent studies on NCLs has shown that the lysosomal system also plays critical roles in nutrient sensing and cellular homeostasis. This indicates that NCL mutations have wide effects on cellular functions in multiple organ systems, including autophagy and synaptic dysfunctions.[9] The use of animal models for NCLs has enabled researchers to identify the most susceptible neuronal populations and has demonstrated that glial cells are both negatively affected by and actively contribute to disease progression.[9]

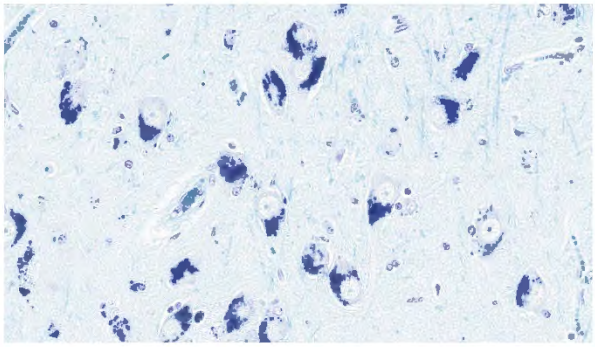

Figure 2-6: Diencephalon, sheep. A Luxol fast blue demonstrates the ceroid granules within neuronal cytoplasm. (Luxol fast blue, 650X).

References:

1. Anderson G, Elleder M, Goebel HH. Morphological diagnostic and pathological considerations. In: In: Mole SE, Williams RE, Goebel HH, ed. The Neuronal Ceroid Lipofuscinoses (Batten Disease). 2nd ed. New York, NY: Oxford University Press; 2011:35-36.
2. Cantile C, Youssef, S. Nervous system. In: Maxie MG, ed. Jubb, Kennedy, and

Palmer's Pathology of Domestic Animals. Vol 1. 6th ed. St. Louis, MO: Saunders Elsevier; 2016:290-291

3. Chalkley MD, et al. Characterization of neuronal ceroid-lipofuscinosis in 3 cats. *Vet Pathol*. 2014;51(4):796-804.
4. Chalkley MD, et al. Characterization of neuronal ceroid-lipofuscinosis in 3 cats. *Vet Pathol*. 2014;51(4):796-804.
5. Cook RW, Jolly RD, Palmer DN, Tammen I, Broom MF, McKinnon R. Neuronal ceroid lipofuscinosis in Merino sheep. *Aust Vet J*. 2002;80:292–297.
6. Cooper JD, Russell C, Mitchison HM. Progress towards understanding disease mechanisms in small vertebrate models of neuronal ceroid lipofuscinosis. *Biochim Biophys Acta.* 2006;1762(10):873-889.
7. Jolly RD, Martinus RD, Palmer DN. Sheep and other animals with ceroid-lipofuscinoses: their relevance to Batten disease. *Am J Med Genet*. 1992;42(4):609–614.
8. Kay GW, Palmer DN, Rezaie P, Cooper JD. Activation of non-neuronal cells within the prenatal developing brain of sheep with neuronal ceroid lipofuscinosis. *Brain Pathol*. 2006;16(2):110-116.
9. Nelvagal HR, Lange J, Takahashi K, Tarczyluk-Wells MA, Cooper JD. Pathomechanisms in the neuronal ceroid lipofuscinoses. *Biochim Biophys Acta Mol Basis Dis*. 2020;1866(9):165570.
10. O'Brien DP, Katz ML. Neuronal ceroid lipofuscinosis in 3 Australian Shepherd littermates. *J Vet Intern Med.* 2008;22(2):472–475.
11. Palmer DN, Barry LA, Tyynelä J, Cooper JD. NCL disease mechanisms. *Biochim Biophys Acta.* 2013;1832(11):1882-93.
12. Palmer DN, Tammen I, Drogemuller C, et al. Large animal models. In: Mole SE, Williams RE, Goebel HH, ed. The Neuronal Ceroid Lipofuscinoses (Batten Disease). 2nd ed. New York, NY: Oxford University Press;2011:284–320.

CASE III:

Signalment:
9 year 7 months old, male neutered, domestic short haired cat, Felis Cattus.

History:
Presented in March for progressive lethargy, anaemia and thrombocytopenia. CT scan showed lung and splenic abnormalities. A splenectomy was performed and histology

Figure 3-1: Lung, cat. Diffusely, all lung lobes are markedly expanded by moderately firm red-cream tissue. The pleural surfaces are smooth despite the lungs being expanded. (Photo courtesy of: Department of Veterinary Medicine, University of Cambridge, www. vet.cam.ac.uk)

(external laboratory) was suggestive of histiocytic disease. Lomustine treatment was started, and the animal was euthanised in May after progressing to respiratory distress.

Gross Pathology:
Diffusely all lung lobes were markedly expanded by moderately firm red-cream tissue. The pleural surfaces were smooth despite the lungs being expanded.

The pericardial sac contained approximately 2mL of serosanguinous fluid. The heart weighed 28 g (cardiomegaly, <20g is considered normal). Cross section of the left ventricular free wall, interventricular septum, and right ventricular free wall measured 6 mm, 6 mm, 3 mm respectively (cardiac hypertrophy with right ventricular free wall most prominently affected). This results in a ratio between the chamber widths of 2:2:1. The left and right auricles were approximately 15 mm in length and width, and 5-10 mm in depth, and were both similar sizes (bilateral auricular dilation).

Laboratory Results:
Anaemia and thrombocytopenia diagnosed on haematology at first presentation in March to the referring vet practice.

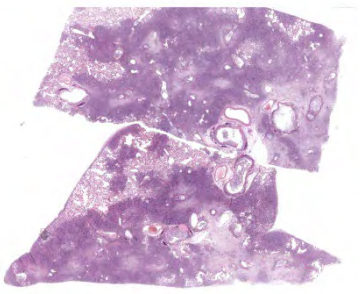

Figure 3-2: Lung, cat. Two sections of consolidated lung are submitted for examination. There is an extensive alveolar infiltrate which affects approximately 90% of the section. (HE 10X).

Microscopic Description:
Expanding the airway and alveolar interstitium, subpleural spaces and also filling alveolar spaces, there is a proliferation of large numbers of round-polygonal cells. The proliferative round cell population have a moderate amount of eosinophilic cytoplasm and a reniform nucleus that contains coarsely stippled chromatin and a single nucleolus. There is mild anisocytosis and anisokaryosis, and there are occasional multinucleated cells. There is one mitotic figure per 2.37 square mm. Within the pleural, peribronchiolar interstitium and alveolar septa, the proliferative cells are accompanied by fine strands of collagen, resulting in further expansion of those structures, and in some areas, complete effacement of the normal pulmonary architecture with obliteration of air spaces. In non-consolidated areas, alveolar septa are multifocally ruptured (microscopic emphysema). There is multifocal, moderate, hyperplasia of bronchiolar smooth muscle, and occasionally, especially in subpleural areas, there is type 2 pneumocyte hyperplasia. Medium-sized pulmonary arteries demonstrate hyperplasia of the tunica media. Airway epithelium is frequently sloughed (post-mortem artefact). Gram, Ziehl-Neelson and PAS-stained sections do not highlight micro-organisms.

Contributor's Morphologic Diagnoses:
Lung, feline pulmonary histiocytosis

Etiological diagnosis: Feline pulmonary Langerhans cells histiocytosis

Contributor's Comment:
Feline pulmonary Langerhans cell histiocytosis is a proliferative disorder of Langerhans cells predominantly affecting the lung. The process is progressive, with animals ultimately developing fatal respiratory compromise. The condition has been reported to have

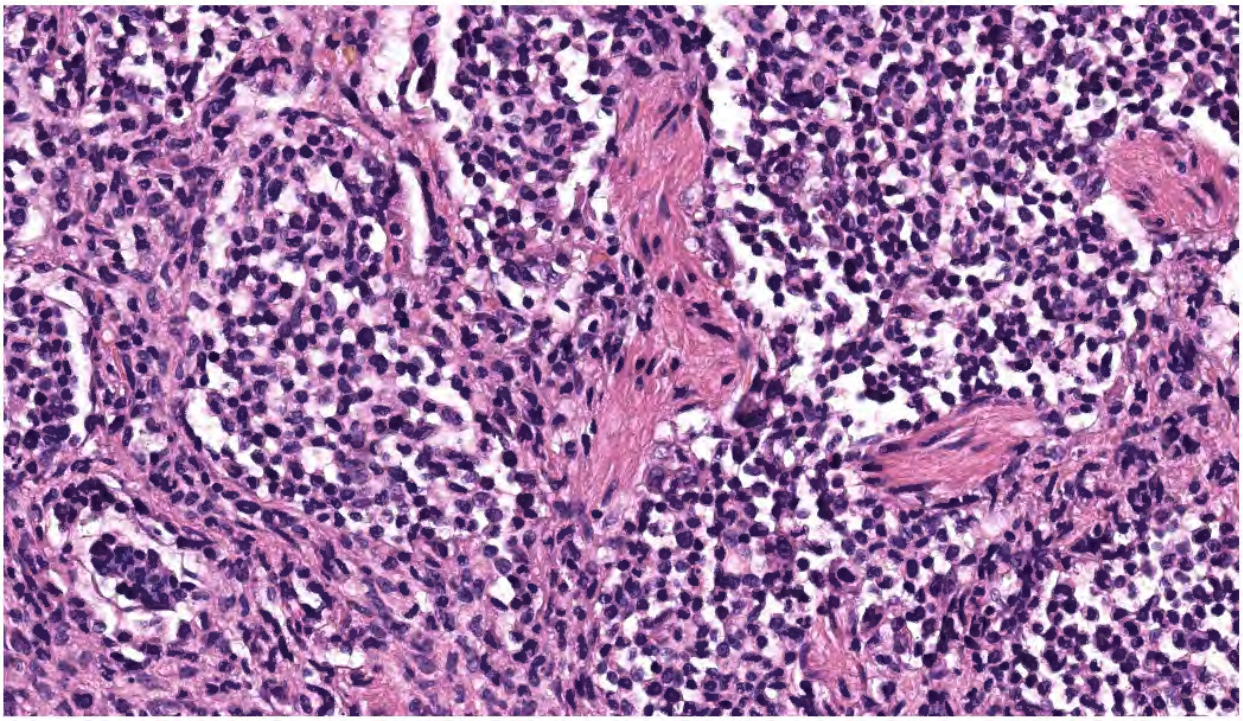

Figure 3-3: Lung, cat. In affected areas, alveoli are filled by sheets of histiocytes. Intervening septa are expanded by congestion, edema, fibrous connective tissue, and there is smooth muscle hyperplasia. (HE 597X).

multi-organ involvement and may affect the spleen, as in this case.[3]

Initial clinical signs of feline pulmonary Langerhans cell histiocytosis are variable but ultimately progress to a restrictive dyspnoea.[1] The insidious onset and unspecific clinical signs means that definitive diagnosis in live patients is challenging. Langerhans cells express CD1a, MHC-class 2, langerin (CD207) and E-cadherin.[6,8]

In humans, the condition is associated with young adults who smoke. The exact pathogenesis of the condition is uncertain.[3] Current evidence from human medicine suggests the underlying process is a myeloid neoplasm with inflammatory properties, which may regress or progress in response to cessation of smoking.[13] In cats, reactivity or neoplastic has not been defined.

The condition generally affects middle aged to older cats, with an interstitial and alveolar pattern on lung imaging.[1] Similar to the eccentric cardiac hypertrophy in this case, occasionally cats with Feline progressive pulmonary histiocytosis develop right ventricular hypertrophy and right auricle dilation due to the increase in pulmonary pressure.[14]

Grossly, lungs have an expanded non-collapsing texture and contain multifocal pale red-cream coalescing masses, which can be very extensive in distribution. In advanced cases the entire lung lobes can be affected, with extension of masses into the pleura.[12] The pancreas, kidney, liver and local or remote lymph nodes may also contain similar mass lesions.[2]

Typical microscopic findings include pleomorphic histiocytic cells that target terminal and respiratory bronchioles and extend into

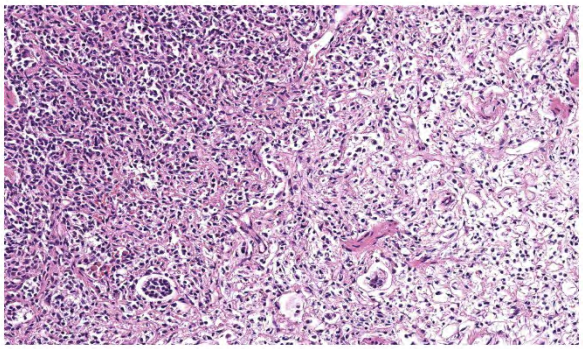

Figure 3-4: Lung, cat. In less affected areas (at right), there are fewer histiocytes, and alveolar parenchyma is effaced by edema and fibrosis. (HE, 333X).

adjacent alveoli.[3] Affected bronchioles undergo smooth muscle hyperplasia and there is fibrosis of the alveolar septa. The Langerhans cells demonstrate CD18 and E-cadherin, vimentin and IBA-1positive immunoreactivity.[1] In addition, feline Langerhans cells do not react to CD204.[7]

The presence of Birbeck granules in the cytoplasm ultrastructurally is characteristic of the Langhans cell phenotype in cats.[3,4] Birbeck granules are the langerin (CD207) receptor cross-linked to antibody and subsequently internalised from the cell surface membrane.[9] Canine Langerhans cells do not contain Birbeck granules.[12]

Feline pulmonary Langerhans cell histiocytosis has been diagnosed on the basis of BAL cytology and pulmonary radiographs.[9] Thoracic radiographs have miliary to nodular radiodense foci in a bronchointerstitial pattern.[10]

Other progressive histiocytic diseases that affect the lungs include progressive histiocytosis in cats, and cutaneous Langerhans histiocytosis or systemic histiocytosis in dogs.[10] The microscopic appearance between canine and feline Langerhans histiocytosis in the lungs is similar, with a primary focus on terminal bronchioles.[12] Feline progressive pulmonary histiocytosis has been reported in a lion,[14] and focal Langerhans cell histiocytosis, without lung involvement, has been reported in the pancreas of a cat.[11]

Contributing Institution:
University of Cambridge, Madingley Road, Cambridge UK

JPC Diagnoses:
Lung: Histiocytosis, alveolar, chronic, diffuse, severe, with fibrosis and smooth muscle hyperplasia.

JPC Comment:
The contributor does an excellent job of summarizing this condition in cats and cross-comparing with a few other species affected by a similar process (including humans). Many of the topics mentioned in their write-up were focal points of discussion during conference, including key histologic features, IHC immunoreactivity profile, and ultrastructural findings.

Langerhans cells are antigen-presenting dendritic cells (DC) derived from CD34+ precursors in the bone marrow. They eventually make their way to and reside in the epidermis and epithelium of the oral cavity, vagina, and bronchial mucosa of the lung.[3] Upon contacting and internalizing an antigen, Langerhans cells will migrate to regional lymph nodes and present their cool find (the antigen) to naïve CD4+ T-cells using major histocompatibility complex (MHC) class II. The characteristic "Birbeck's granules" seen on electron microscopy (EM) are five-layered, rod-shaped cytoplasmic organelles that kind of resemble hot dogs on a bun and are present only within Langerhans cells. These granules are formed by the internalization of CD207, normally found on the surface of Langerhans cell.

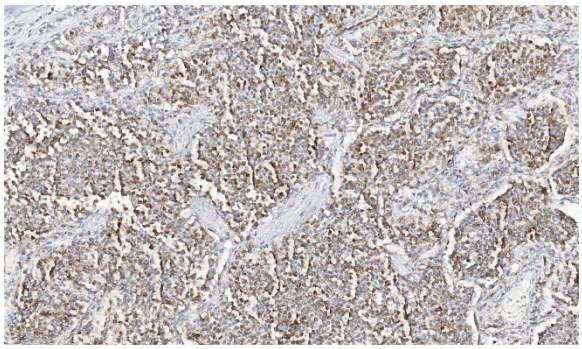

Figure 3-5: Lung, cat. Histiocytes within alveoli demonstrate strong cytoplasmic immunoreactivity for IBA-1) (anti-IBA1, 328X).

CD207 is a C-type lectin also known as "langerin" that assists with recognition of pathogen-associated molecular patterns (PAMPs), internalization of an antigen, and further stimulating an immune response as described above.[3]

While the pathogenesis of feline pulmonary Langerhans cell histiocytosis is not yet fully understood, in humans, one of the main hypotheses for pulmonary Langerhans cell histiocytosis is that of the "cytokine storm".[3,5] This hypothesis suggests that T-lymphocytes and Langerhans cells within the lungs produce a mutually amplifying cytokine cascade that drives recruitment, maturation, and proliferation of Langerhans cells in this condition.[5] Whether or not this fits within a reactive or neoplastic process remains to be seen, and some studies suggest assessing the clonality of the Langerhans cells in future research to try and make that distinction.[3]

References:

1. Argenta FF, de Britto FC, Pereira PR, et al. Pulmonary Langerhans cell histiocytosis in cats and a literature review of feline histiocytic diseases. *J Feline Med Surg*. 2020;22(4):305-312.
2. Bellamy E, Di Palma S, Ressel L, et al. Disseminated Langerhans cell histiocytosis presenting as oesophageal disease in a cat. JFMS Open Rep. 2019;5(2):2055116919874902.
3. Busch MD, Reilly CM, Luff JA, et al. Feline pulmonary Langerhans cell histiocytosis with multiorgan involvement. Vet Pathol. 2008;45(6):816-24.
4. Caswell JL, Williams KJ. Respiratory System. In: Maxie MG, ed. Jubb, Kennedy, and Palmer's Pathology of Domestic Animals. Vol 2. 6th ed. Philadelphia, PA: Elsevier Ltd. 2016:499.
5. Egeler RM, Favara BE, van Meurs M, Laman JD, Claassen E. Differential In situ cytokine profiles of Langerhans-like cells and T cells in Langerhans cell histiocytosis: abundant expression of cytokines relevant to disease and treatment. Blood. 1999;94(12):4195-201.
6. Fulmer AK, Mauldin GE. Canine histiocytic neoplasia: an overview. Can Vet J. 2007;48(10):1041-3,1046-50.
7. Hirabayashi M, Chambers JK, Sumi A, et al. Immunophenotyping of nonneoplastic and neoplastic histiocytes in cats and characterization of a novel cell line derived from feline progressive histiocytosis. Vet Pathol. 2020;57(6):758-773.
8. Laman JD, Leenen PJ, Annels NE, et al. Langerhans-cell histiocytosis 'insight into DC biology'. Trends Immunol. 2003;24(4):190-6.

9. Mau A, Chiu ES, Armien A, et al. Antemortem cytologic diagnosis of pulmonary Langerhans cell histiocytosis in a cat. Vet Clin Pathol. 2023;52(4):691-697.

10. Moore PF. A review of histiocytic diseases of dogs and cats. Vet Pathol. 2014;51(1):167-84.

11. Rissi DR, Brown CA, Gendron K, et al. Pancreatic Langerhans cell histiocytosis in a cat. J Vet Diagn Invest. 2019;31(6):859-863.

12. Valli VEO, Kiupel M, Bienzle D. Hematopoietic System. In: Maxie MG, ed. Jubb, Kennedy, and Palmer's Pathology of Domestic Animals. Vol 3. 6th ed. Philadelphia, PA: Elsevier Ltd. 2016 245-247.

13. Vassallo R, Harari S, Tazi A Current understanding and management of pulmonary Langerhans cell histiocytosis Thorax 2017;72:937-945.

14. Zhang L, Chen H, Ding Y, et al. Pulmonary Langerhans Cell Histiocytosis in an African Lion: A Rare Case Report. Animals (Basel). 2024;14(7):1011.

CASE IV:

Signalment:
Dromedary camel (*Camelus dromedarius*), adult female

History:
A lactating adult dromedary camel was one of two breeding females which had been recumbent for the last 2 to 4 days; both were in poor body condition. Other camels in the breeding herd were also in low body condition. Both recumbent animals were eating, drinking and were up to date with vaccinations. There had been no change in condition in response to worming and anticoccidial treatments. A pasture assessment was conducted, and the amount of feed available was determined to be inadequate for the lactating camels. Bloods were taken from both camels and supplementary feeding initiated.

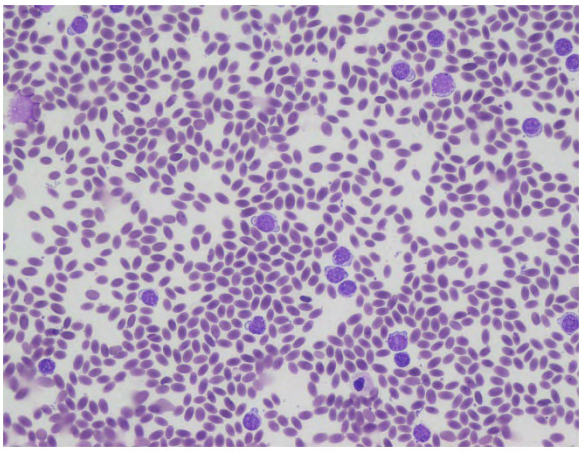

Figure 4-1: Blood smear, camel. Numerous atypical lymphocytes were present in the blood smear (Diff Quik, 400X). (Photo courtesy of: New South Wales Department of Primary Industries, Menangle,NSW2568 https://www.dpi.nsw.gov.au/about-us/science-and-research)

The second camel began to put on weight and became ambulatory after supplementary feeding, however the first female camel was unable to rise without assistance and continued to loose condition. The animal was euthanized and a post mortem conducted.

Gross Pathology:
Necropsy examination revealed that the ventral 40-50% of both lungs were pale-pink to white with a firm consistency and smooth surface on cross section. The paratracheal and parabronchial lymph nodes were diffusely markedly enlarged and were white on the cut surface. Other viscera appeared grossly normal.

Laboratory Results:

Hematology

On the blood smear collected during the initial clinical exam, numerous large atypical lymphocytes were observed throughout the smear.

Test	Normals	Units	Female camel 1 (euthanized)	Female camel 2 (recovered)
PCV (%)	27-45	%	24	22
RBC	10.5-17.2	10^{12}/L	6.32	5.76
Hemoglobin	11.3-19.0	g/dL	11.0	9.2
MCV	22-29.5	fL	38	38
MCHC	38-46	g/dL	46	42
MCH	9.6-12	pg	17	16
WBC	6.0-20.9	10^9/L	194.6	19.3
Neutrophils	2.0-13.3	10^9/L	21.41	17.18
Band Neutrophils	0.0-2.9	10^9/L	0	0
Lymphocytes	2.1-6.8	10^9/L	173.19	2.12
Monocytes	0.0-0.6	10^9/L	0.0	0.0
Eosinophils	0.0-3.0	10^9/L	0.0	0.0
Basophils	0.0-0.3	10^9/L	0.0	0.0
Nucleated RBC		/100wbc	0	Occasional
Reticulocytes		%	0	1
Platelets			Adequate	Adequate

Serum Biochemistry

Test	Normals	Units	Female camel 1 (euthanized)	Female camel 2 (recovered)
GGT	0-60	U/L	19	17
GLDH	0-20	U/L	4	4
AST	0-320	U/L	123	150
Bilirubin	0.1-3.2	µmol/L	2.0	3.1
CK	0-750	U/L	423	1693
Urea	5.0-12.4	mmol/L	11.1	9.4
Creatinine	0-288	µmol/L	101	119
Phos	1.5-3.4	mmol/L	1.2	1.98
Urea/Creatinine	0.00-0.07		0.11	0.08
Protein	54.0-75.0	g/L	53.8	48.1

Test	Normals	Units	Female camel 1 (euthanized)	Female camel 2 (recovered)
Albumin	25.0-45.0	g/L	16.2	20.4
Globulins	15.9-41.0	g/L	37.6	27.7
Albumin/Globulins	1.3-3.3		0.4	0.7
β-Hydroxybutyrate	0.00-0.50	mmol/L	0.02	0.01
Calcium	1.9-2.7	mmol/L	2.1	2.11
Magnesium	0.7-1.3	mmol/L	0.96	0.92
Haptoglobin	1.0-2.0	g/L	0.69	0.58
Serum Hemoglobin	0.0-0.2	g/dL	0.04	0.04
Glutathione Peroxidase	15-200	U/gHb	69	170

Bacterial Culture, Lungs
Moderate pure growth of *Streptococcus agalactiae*
Enzootic Bovine Leukosis ELISA
Camel 1 seronegative

Immunohistochemical markers

Marker	Cell type	Tissue	Number of positive cells	Positive cell distribution
CD79b	B Cell	Lung	+++	Majority of cells within neoplastic infiltrate, scattered cells within peribronchial and peribronchiolar spaces, interlobular and alveolar septae and alveolar lumen
		Lymph node	+++	The majority of cells within the cortex and moderate numbers (30-50% of cells) within the medulla
		Spleen	+++	Majority of cells within red and white pulp
CD3	T Cell	Lung	+	Scattered throughout parenchyma, and small numbers accompanying neoplastic infiltrate
		Lymph node	++	Moderate numbers multifocally throughout the medulla
		Spleen	+	Predominantly around blood vessels

Microscopic Description:
Camel; Lung
Description Multifocally throughout the section, expanding the lamina propria of larger airways, multifocally invading the airway epithelium, expanding numerous alveolar septae and infiltrating into interlobular septae and the pleural space, there is a densely cellular lymphoid neoplasm. The neoplasm is made up of sheets and rows of closely packed round cells supported by a fine pre-existing fibrous stroma. The neoplastic cells contain nuclei 5-7µm in diameter and have indistinct cytoplasmic borders, scant amphophilic cytoplasm, round to ovoid paracentral nuclei with coarsely clumped chromatin with moderate numbers of cells possessing a single nucleolus. Throughout the neoplastic cells there is mild anisokaryosis and anisocytosis. Mitotic figures numbering 5 per 2.37mm^2 with occasional bizarre mitoses. Multifocally the neoplastic cells closely surround and infiltrate the tunica media of small blood vessels. Numerous alveolar spaces are filled with eosinophilic

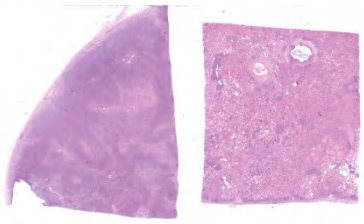

Figure 4-2: Lymph node, lung, camel. At subgross magnification, there is an cellular infiltrate in both organs which effaces normal architecture. (HE, 5X)

fibrillar material (fibrin) admixed with abundant neutrophils and foamy macrophages, while others contain large amounts of homogenous eosinophilic material (edema). Multifocally some alveolar spaces are expanded and ruptured (emphysema). Bronchioles contain moderate numbers of neutrophils and macrophages admixed with strands of hypereosinophilic fibrillar material (fibrin) with neutrophils transmigrating across the respiratory epithelium. There is occasional loss of type I pneumocytes with replacement by type II pneumocytes.

Camel; Paratracheal Lymph Node
Description Multifocally the normal architecture of the cortex, paracortex and medulla is disrupted and replaced by a densely cellular neoplasm composed of lymphoid cells. The neoplasm is comprised of sheets of closely packed small round cells with nuclei 5-7µm in diameter. Cells are mostly round with indistinct cytoplasmic margins, scant basophilic or eosinophilic cytoplasm, high nuclear to cytoplasmic ratio, and a paracentric nucleus with coarsely clumped chromatin. There is mild anisocytosis and anisokaryosis. There is an average of 12 mitoses per 2.37mm^2. Within the capsule of the lymph node there are small aggregates of neoplastic cells organized into sheets.

Contributor's Morphologic Diagnoses:
Lung and Lymph node; B-cell lymphoma
Lung; bronchopneumonia, fibrinosuppurative, multifocal, severe, subacute, with type II pneumocyte hyperplasia.

Contributor's Comment:
In this case, neoplastic cells were also found in the liver, spleen and heart of the camel. No neoplastic cells were found in the kidneys or in two sections of bone marrow (rib and sternum). The presence of atypical lymphocytes within the peripheral blood collected at the initial clinical examination greatly aided the diagnosis of lymphoma or leukemia in this case (Figure 1) and allowed the clinician to understand why this animal did not improve like the others in the herd once nutrition was improved. The neoplastic cells observed in the peripheral blood was suspected to be secondary to the lymphoma, given that no neoplastic cells were found within the bone marrow of the bones examined histopathologically. Leukemia is a feature of less than 20% of lymphomas in animals and is more commonly a feature of T-cell lymphomas.[9] Leukemia is most likely observed when the lymphoma invades the bone marrow or spleen, the latter of which contained neoplastic cells in this case.[9] In this

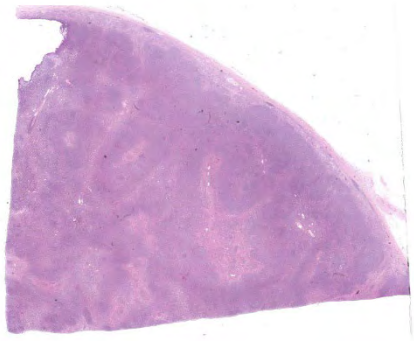

Figure 4-3: Lymph node, camel. The nodal architecture to include the cortex, paracortex, and medullary sinuses are expanded and/ effaced by a round cell neoplasm. (HE, 10X)

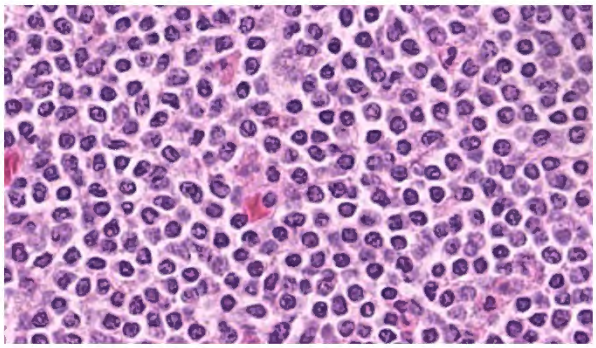

Figure 4-4: Lymph node, camel. High magnification of neoplastic lymphocytes. (HE, 1800X)

case a B-cell phenotype was confirmed via immunohistochemistry (Figures 7-11).

There are only a few reports in the literature describing lymphoma in dromedary camels. Similar to this case, the disease is typically reported in adult animals (>7 years) and has been reported in both male and female camels. Common clinical presentations include weight loss, anorexia, polyuria and polydipsia, with one report also describing peripheral lymphadenopathy and bilateral masses in the conjunctiva of one animal.[3,4,6] Peripheral lymphocytosis, sometimes with significant atypia in circulating lymphocytes and lymphoblasts, has been reported occasionally but is not always a feature of the disease in dromedary camls.[3,7]

Necropsy findings typically include disseminated nodules which can be found in various organs including the liver, spleen, lungs, kidneys, bladder and intestines. Often multiple mesenteric and/or mediastinal lymph nodes are enlarged.[3,4,6]

Histologically, lymphomas in dromedary camels are described as a highly cellular neoplasm often effacing the normal architecture of the tissues, made up of sheets of lymphoid cells with scant cytoplasm and distinct cell margins. There is some variability in the cellular morphology including anisocytosis and anisokaryosis, indistinct nucleoli to multiple nucleoli present and in one case multinucleated cells were observed.[3,4,6]

In contrast to this case, all cases in the literature from dromedary camels were identified as T-cell lymphomas. In those cases, lymphocyte lineage identification was performed using immunohistochemistry and identified the neoplastic cells as CD3 (pan T-cell) positive and either CD20 or CD79a (pan B-cell markers) negative.[3,4] More recently, flow cytometry has been used to further classify a multicentric T-cell lymphoma as a gd T-cell lymphoma and a combination of CD4 and WC-1 markers.[4] Other markers which have been used in the literature to differentiate round cell neoplasms in camelids include PAX-5, CD79b (B-cell markers), CD5 (T-cell marker), MUM1 (plasma cell marker), CD18 and CD68 (histiocyte markers).[1,4,6,8]

In other camelids (llamas and alpacas), lymphoma is identified as one of the most common types of neoplasia, and both T-cell and B-cell as well as non-T and non-B cell lympho

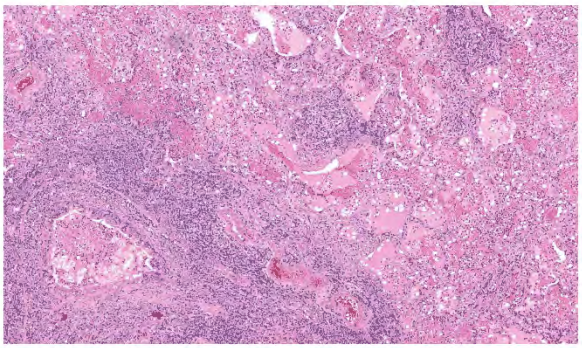

Figure 4-5: Lung, camel. Neoplastic lymphocytes infiltrate the walls of airways, efface BALT, surround vessels, and markedly expand alveolar septa (HE, 152X)

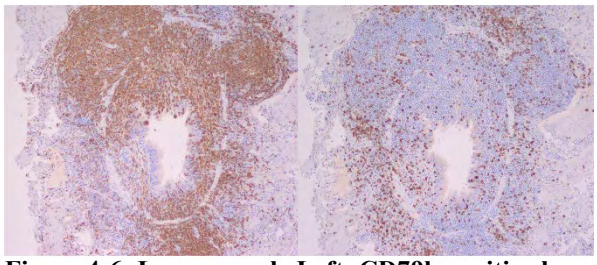

Figure 4-6: Lung, camel. Left: CD79b-positive lymphocytes surrounding and infiltrating into the epithelium of an airway (anti-CD79b, 100x). Right: Only relatively low numbers of CD3 positive lymphocytes are scattered throughout the lung (anti-CD3, 100x). (Photo courtesy of: New South Wales Department of Primary Industries, Menangle, NSW, 2568 https://www.dpi.nsw.gov.au/about-us/science-and-research/centres/emai)

mas have been reported.[1,8] Disseminated lymphoma has been reported in juvenile alpacas[1]

and lymphoma of the liver has been reported in a juvenile llama.[8] Multicentric lymphoma has been reported in both adult alpacas and llamas and the distribution of lesions in organs is similar to that described for dromedary camels with lesions also seen in the spleen, stomach, trachea and bone marrow.[1,8]

Contributing Institution:
Elizabeth Macarthur Agricultural Institute
New South Wales Department of Primary Industries,
Woodbridge Road, Menangle, NSW, 2568

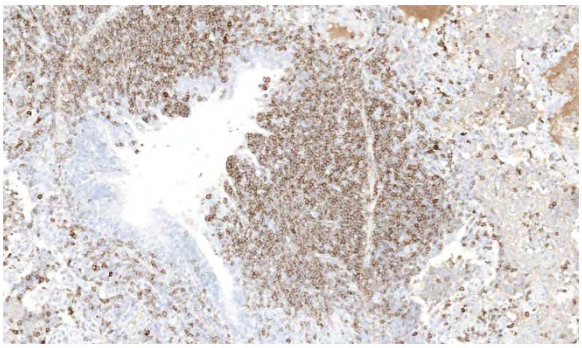

Figure 4-7: Lung, camel. Neoplastic cells infiltrating an airway demonstrate strong membranous immunoreactivity for CD20, a B-cell marker. (anti-CD20, 263X)

https://www.dpi.nsw.gov.au/dpi/about-us/research-and-development

JPC Diagnoses:
1. Lymph node and lung: Lymphoma.
2. Lung:Bronchopneumonia, fibrinosuppurative, subacute, multifocal, severe, with type II pneumocyte hyperplasia.

JPC Comment:
This camel just had to be contrarian in that it had a lymphoma of B-cell origin instead of T-cell like almost every other camel lymphoma out there. This case provided a great two-fer of a late-stage lymphoma and bronchopneumonia, and the contributor provides a thorough and well-written comment on lymphomas in camels.

Another primary point of discussion, and one that was briefly mentioned by the contributor, was the classification of this case as a lymphoma a leukemia given that there were intravascular atypical lymphocytes. Given that there was no bone marrow involvement, though, a lymphoma was the consensus. According to the WHO guidelines in dogs, a stage 5 lymphoma is characterized as generalized lymphadenopathy (involving both thoracic and abdominal nodes) with hepatosplenomegaly and involvement of either bone marrow, the CNS, or another extranodal site (such as the lungs).[10] This stage would best fit with the histologic findings in this case, as there was multiorgan involvement. Stage V is further classified into 5a or 5b, with either no clinical signs or apparent clinical illness, respectively, which would classify this camel's lymphoma as a stage 5b due to the obvious clinical signs described in her case. In human medicine, the fifth stage is not utilized; their

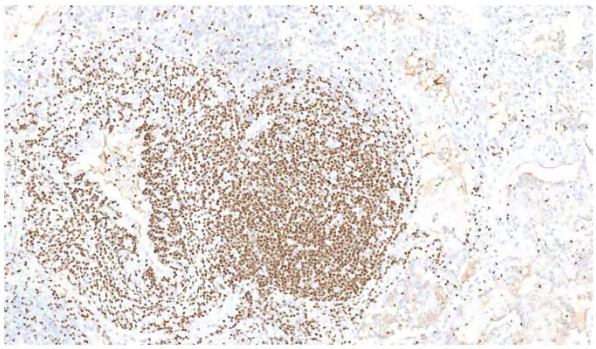

Figure 4-8: Lung, camel. Neoplastic cells infiltrating an airway demonstrate strong nuclear immunoreactivity for PAX5, a B-cell marker. (anti-PAX5, 263X)

grading scheme ends at stage 4.[5] Whether either (or neither) of these classification schemes fits with lymphoma in camelids, however, is currently unknown and will require additional studies.

References:

15. Aboellail TA. Pathologic and immunophenotypic characterization of 26 camelid malignant round cell tumors. J Vet Diagn Invest. 2013;25(1):168–172.

16. Desmirean M, Deak D, Rus I, Dima D, Iluta S, Preda A, Moldovan T, Roman A, Tomuleasa C, Petrushev B. Paraneoplastic hypereosinophilia in a patient with peripheral T cell lymphoma, not otherwise specified. Med Pharm Rep. 2019;92(4):421-426.

17. Heather A. Simmons, Scott D. Fitzgerald, Matti Kiupel, David R. Rost, Robert W. Emery. Multicentric T Cell Lymphoma in a Dromedary Camel (Camelus dromedarius). Journal of Zoo and Wildlife Medicine. 2005;36(4):727–729.

18. Ibrahim A, Hussen J, Shawaf T, Al-Hizab FA, Kiupel M. Disseminated gamma-delta T-cell lymphoma in a dromedary camel. Veterinary Record Case Reports. 2023;n/a(n/a):e650.

19. Khoury JD, Solary E, Abla O, Akkari Y, Alaggio R, Apperley JF, Bejar R, Berti E, Busque L, Chan JKC, Chen W, Chen X, Chng WJ, Choi JK, Colmenero I, Coupland SE, Cross NCP, De Jong D, Elghetany MT, Takahashi E, Emile JF, Ferry J, Fogelstrand L, Fontenay M, Germing U, Gujral S, Haferlach T, Harrison C, Hodge JC, Hu S, Jansen JH, Kanagal-Shamanna R, Kantarjian HM, Kratz CP, Li XQ, Lim MS, Loeb K, Loghavi S, Marcogliese A, Meshinchi S, Michaels P, Naresh KN, Natkunam Y, Nejati R, Ott G, Padron E, Patel KP, Patkar N, Picarsic J, Platzbecker U, Roberts I, Schuh A, Sewell W, Siebert R, Tembhare P, Tyner J, Verstovsek S, Wang W, Wood B, Xiao W, Yeung C, Hochhaus A. The 5th edition of the World Health Organization Classification of Haematolymphoid Tumours: Myeloid and Histiocytic/Dendritic Neoplasms. Leukemia. 2022;36(7):1703-1719.

20. Raval SH, Joshi DV, Patel BJ, Patel JG, Bhatt NG. Histological and immunohistochemical characterisation of T-Cell Lymphoma in A Camel. J Camel Pract and Res. 2015;22(2):247–250.

21. Tageldin MH, al Sumry HS, Zakia AM, Fayza AO. Suspicion of a case of lymphocytic leukaemia in a camel (Camelus dromedarius) in Sultanate of Oman. Rev Elev Med Vet Pays Trop. 1994;47(2):157–158.

22. Twomey DF, Barlow AM, Hemsley S. Immunophenotyping of lymphosarcoma

in South American camelids on six British premises. Vet J. 2008;175(1):133–135.

23. Valli VE, Bienzle D, Meuten DJ. Tumors of the Hemolymphatic System. In: Tumors in Domestic Animals. 2016:203–321.

24. Valli VE, Myint MS, Barthel A, et al. Classification of Canine Malignant Lymphomas According to the World Health Organization Criteria. Veterinary Pathology. 2010;48(1):198-211.

Joint Pathology Center
Veterinary Pathology Services

WEDNESDAY SLIDE CONFERENCE 2025-2026

Conference #7 — 8 October 2025

CASE I:

Signalment:
21-year old, female intact, Trakehner horse (*Equus caballus*)

History:
The mare had a ten-year history of bilateral rear limb suspensory ligament degeneration. She was euthanized due to acute onset of fever and recumbency, which were later attributed to a pheochromocytoma and multifocal myocardial necrosis.

Gross Pathology:
Both rear metacarpophalangeal joints are enlarged with thick, fibrous joint capsules but no effusion. The branches of the rear suspensory ligaments are enlarged to approximately twice the diameter of the front suspensory ligament branches, and they are mottled yellow, tan, and white on cut section.

Laboratory Results:
N/A

Microscopic Description:
Suspensory ligament, right rear branch. Compared to a branch of the clinically normal right front suspensory ligament, collagen fibers are irregular and often form intersecting or divergent bundles. In many areas, there are fewer fibroblasts among collagen fibers than in the normal control. Throughout the tissue, wavy

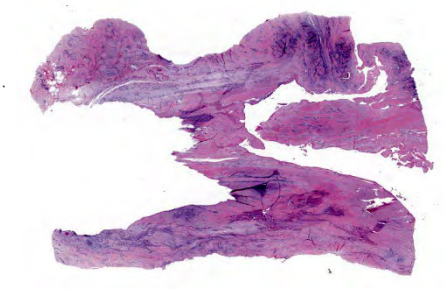

Figure 1-1: Tendon, horse. One section of the suspensory apparatus is submitted for examination and the normal eosinophilic color is interspersed with areas of basophilic ground substance. (HE, 10X)

tendrils of pale basophilic, Alcian blue-positive matrix dissect between collagen bundles. Similar material surrounds increased numbers of variably sized, dilated and tortuous blood vessels. These vessels have thin walls and are lined by plump endothelial cells, and are often surrounded by loosely arranged stellate cells. In other areas, there is chondroid metaplasia, with clustered and individual chondrocyte-like cells in lacunae surrounded by amorphous, pale basophilic matrix, which is sometimes faintly mineralized. There is rare hemorrhage.

Contributor's Morphologic Diagnoses:
Severe chronic extensive suspensory ligament degeneration with chondroid metaplasia and vascular proliferation

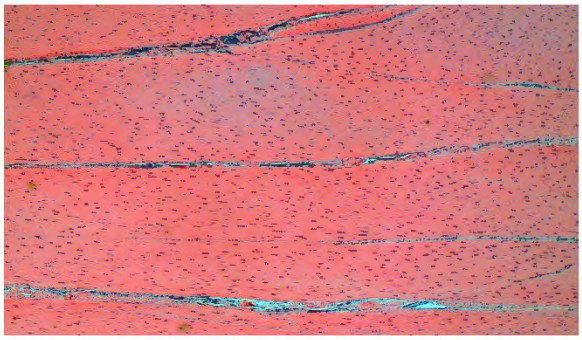

Figure 1-2: Tendon, horse. Histology of a normal equine tendon with eosinophilic collagen fibers arranged linearly and in register, with collagen fibers separated by thin capillaries. (HE,400X) (Photo courtesy of: University of Tennessee College of Veterinary Medicine, https://vetmed.tennessee.edu/academics/biomedical-and-diagnostic-sciences/)

Contributor's Comment:

The terms "degenerative suspensory ligament desmitis (DSLD)" and "suspensory ligament degeneration (SLD)" are used somewhat synonymously, with DSLD often used to describe horses with a clinical diagnosis of suspensory ligament degeneration, and SLD used to describe histologic findings in the suspensory ligaments of horses that may or may not have a clinical diagnosis of DSLD. DSLD causes chronic, progressive multi-limb lameness of variable severity, often recognized by enlarged, hyperextended or "dropped" fetlocks.[8] The rear limbs are typically more affected.[3,8] In addition, the terms "suspensory ligament desmitis" or "suspensory ligament desmopathy" may be used to describe any of a variety of clinically or ultrasonographically detected injuries anywhere along the length of the suspensory ligament.[3] Histology is rarely performed in these cases, especially in the acute phase, and it is unclear if these injuries are related to degenerative changes.[3]

Histologic changes in SLD/DSLD include loss of longitudinal arrangement of collagen fibers, proteoglycan accumulation, presence of chondrocytes, hemorrhage, vascular proliferation, and widened interstitial connective tissue septa.[4,6] Despite the use of the term "desmitis," inflammatory cells are not present.[4] These changes are reported to be more severe in the branches of the suspensory ligament than in the body or origin of the ligament.[3,5]

The pathogenesis of SLD/DSLD is incompletely understood. It has been associated with athletic function, broodmare status, and old age, but strong breed predispositions to DSLD, particularly in the Peruvian Paso, suggest a hereditary basis in many cases.[8] In one recent genome-wide association study of single nucleotide polymorphisms in different breeds of horse, several candidate loci were identified among genes which are related to collagen synthesis, tendon aging, mechanotransduction, signaling, and metabolism.[9] However, a single gene has not been identified as causative, and the disease is assumed to be polygenic and multifactorial.[9]

One avenue of investigation also suggests an association between SLD and pituitary pars intermedia dysfunction (PPID), which may be similar to the Achilles tendinopathy that rarely

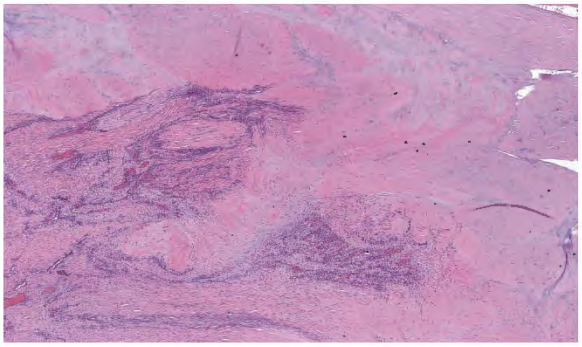

Figure 1-3: Tendon, horse. The normal linear array of collagen bundles within the tendon is lost and there are areas of basophilic ground substance between and within fibers. Collagen bundles are also separated by proliferating and tortuous capillaries. (HE, 33X)

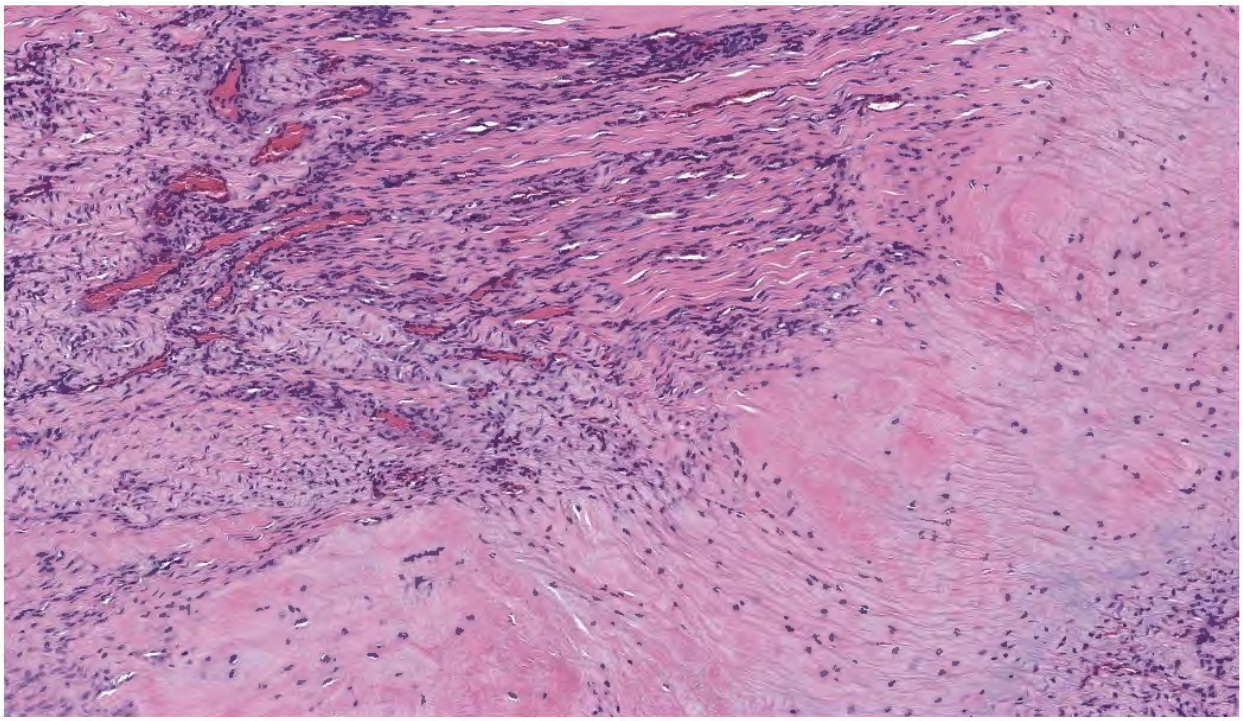

Figure 1-4: Tendon, horse. Collagen bundles are separated by numerous tortuous capillary profiles surrounded by amphophilic ground substance. (HE, 131X)

occurs in humans with Cushing's syndrome.[1,5,6] Endogenous or exogenous glucocorticoid excess can lead to various changes in collagen, proteoglycans, and matrix metalloproteinases and result in connective tissue weakness.[1,5,6] The exact mechanisms in affected humans and horses are unknown; however, horses with PPID have increased numbers of glucocorticoid receptors and increased 11β-hydroxysteroid dehydrogenase type 1 in the suspensory ligament compared to unaffected horses, suggesting a role for abnormal local cortisol metabolism.[6]

Some older studies posit that abnormal proteoglycan deposition and turnover is the primary cause of the functional and structural changes.[4,7,10] Affected horses have an atypical isoform of the proteoglycan decorin,[7] and affected ligaments have markedly increased amounts of the proteoglycan aggrecan, as well as increased amounts of aggrecan degradation products and enzymes.[10] One report suggested that abnormal proteoglycan accumulation may be systemic in affected horses,[4] but the findings could not be reproduced.[11] The cause of the altered proteoglycan milieu is unknown; however, the more recent genome-wide association study failed to identify any alterations in the genes responsible for proteoglycan turnover.[9]

Despite the lack of inflammatory cells in affected ligaments, there are increased levels of inter-alpha-trypsin-inhibitor components, which are associated with multiple inflammatory conditions.[10] In addition, some of the candidate genes identified in the genome-wide association study are associated with inflammatory pathways.[9] The complete role of inflammatory processes in disease progression is unknown.

Finally, true suspensory ligament desmitis with degeneration has been rarely reported in

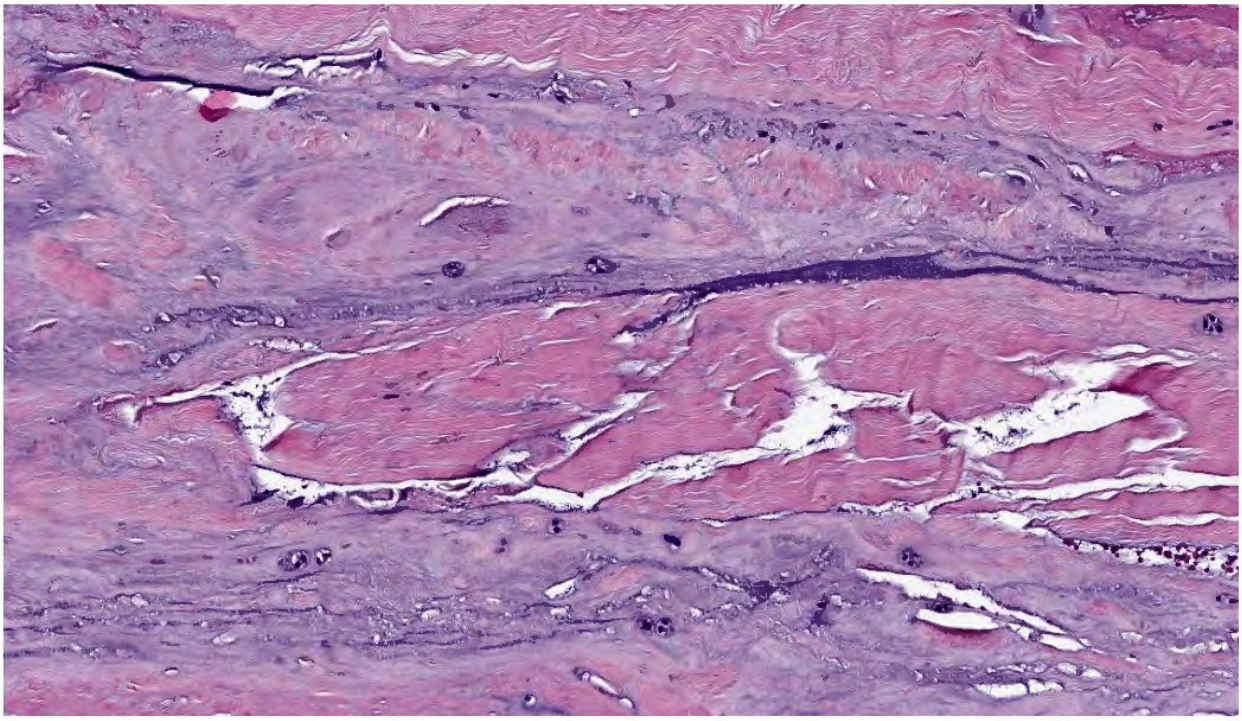

Figure 1-5: Tendon, horse. Collagen bundles are also separated and/or expanded by abundant basophilic ground substance. Within the ground substance, there are foci of cartilaginous metaplasia with individualized chondrocytes within lacunae.

horses and donkeys as a result of onchocerciasis.[2] Degenerative lesions of the ligament are similar, but they are accompanied by eosinophilic granulomas with encysted nematodes.[2]

Contributing Institution:
Biomedical and Diagnostic Sciences
University of Tennessee College of Veterinary Medicine
https://vetmed.tennessee.edu/academics/biomedical-and-diagnostic-sciences/

JPC Diagnoses:
Ligament: Degeneration, chronic, diffuse, marked, with increased ground substance, vascular proliferation, loss of ligamentocytes, and cartilaginous metaplasia.

JPC Comment:
The JPC's own LTC Erica Barkei moderated this week's conference and chose a variety of fascinating entities, three of which that have never been seen before in the Wednesday Slide Conference (WSC). She tends to look specifically for cases that are either novel to the WSC, are within residents' 5-year reading windows, or will stimulate great discussion amongst participants. She was certainly successful in that mission this year!

This case, coupled with a well-written and thorough comment from the contributor on this challenging clinical condition, gifted participants with a beautiful slide of an oft-forgotten organ (tendon/ligament) with all the classic features of suspensory ligament degeneration (SLD). The WSC team is grateful to the contributor for this case and the excellent educational value it brought to the conference.

Conference discussion focused on the proposed pathogeneses of this condition (genetic vs. metabolic vs. athletic) in horses and its likely multifactorial origins (see contributor comment). A key feature of SLD/DSLD is

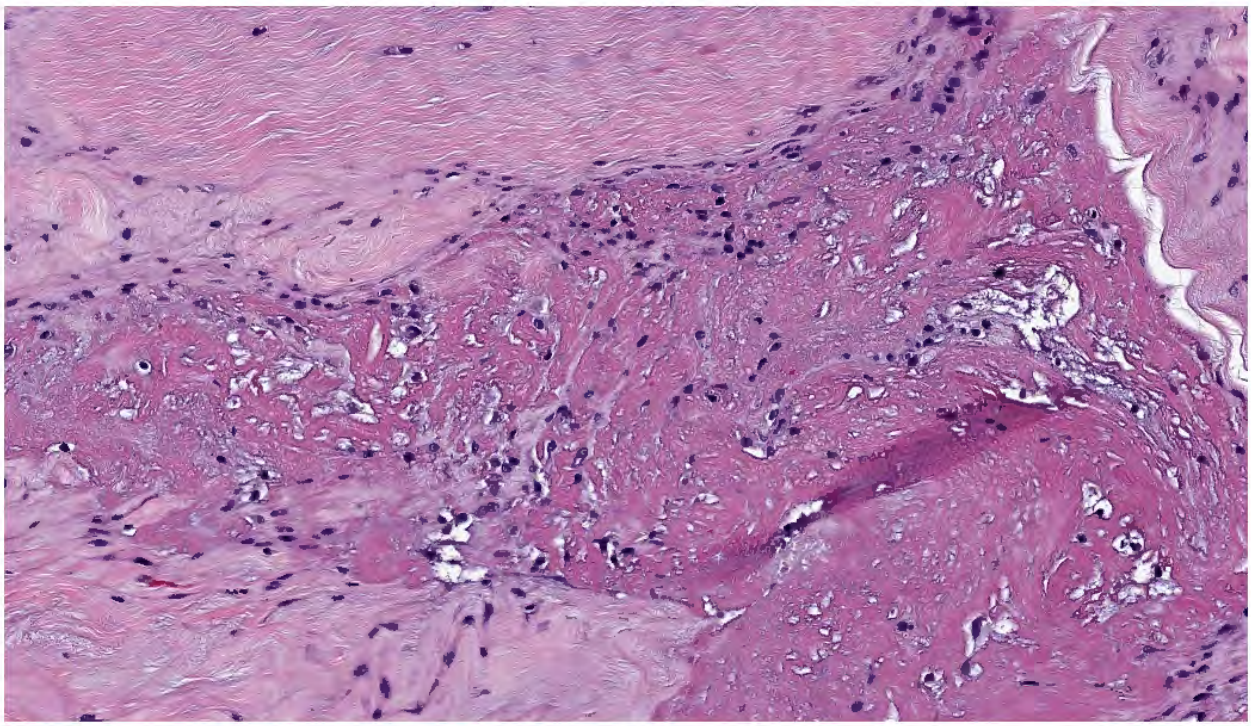

Figure 1-6: Tendon, horse. Collagen bundles are occasionally hypereosinophilic and fragmented.

acellular accumulation of proteoglycans, including decorin and aggrecan, replacing cells and collagen bundles.[10] This suggests a disturbance to matrix homeostasis where the responses of the matrix to mechanical loading are disrupted. As the contributor stated in their comment, there have been numerous genes found to be associated with SLD/DSLD, including those involved in tendon aging (PIN1), mechanotransduction (KANK1, KANK2, JUNB, SEMA7A), collagen synthesis (COL4A1, COL5A2, COL5A3, COL6A5), matrix response to hypoxia (PRDX2), and lipid metabolism (LDLR, VLDLR).[8,9] These features parallel the changes seen in humans with similar tendinopathies. There are currently conflicting articles within the literature on if the proteoglycan accumulation seen in SLD is systemic or localized, and more research is needed to determine this.[4,11]

There were a few important "buzzwords" or phrases mentioned during conference that are important to include in a histologic description of an SLD case and include some form of "collagen fiber disorganization" and "loss of tenocytes/ligamentocytes." (If anyone is wondering, "What the heck are tenocytes and ligamentocytes?", they are, quite simply, fibroblasts respectively within a tendon or ligament.) The different types of collagens within tendons and ligaments were also reviewed and include: Type I collagen, which is the most prevalent within the normal flexor tendons; Type II collagen, which is found within enthesis insertions and areas where a tendon changes directions around a bony prominence; and, lastly, type III collagen, which is one of the first collagens synthesized within tendons at sites of injury.

The major histologic findings within ligaments suffering from SLD include loss of longitudinal arrangement of collagen fibers (disorganization), proteoglycan accumulation (increased ground substance), presence of chondrocytes (chondroid metaplasia), hemorrhage, vascular proliferation, widened interstitial connective tissue septae, and a lack of inflammatory cells.[8] As this disease develops, regardless of cause, degenerating collagen fascicles blend together and there is either death of the tenocytes/ligamentocytes or metaplasia of tenocytes/ligamentocytes into chondrocytes. Fibrosis develops within and around the ligament and is usually associated with hypertrophied tenocytes/ligamentocytes. These areas are generally interpreted as failed attempts at repair.

As these changes progress, the suspensory ligament (SL) progressively thickens, weakens, and ultimately ruptures, resulting in the classic dropped fetlocks seen in affected horses.[8,9] Some horses may also have neurogenic muscular atrophy secondary to either nerve entrapment within areas of fibrosis or due to nerve compression from a thickened and enlarged SL. SLD is typically more evident in the pelvic limbs and is usually bilateral, although some horses have all four limbs affected.[3,8,9]

The last major discussion point in conference related to the use of the term "desmitis" vs. "degeneration." In a true SLD/DSLD case, there should be no inflammatory cells within the tendon/ligament, so conference participants favored "degeneration" over "desmitis." The exception to this would be in cases of ligamentous Onchocerciasis, where an eosinophilic and granulomatous inflammatory infiltrate could be expected.[2] In addition to morphing "degeneration" for this case, a few "withs" were added to the JPC morph to better define the typical findings associated with the degeneration in a case of SLD. Participants thought it was academically pertinent to ensure those were part of the morph for the purposes of resident education and encompass the primary histologic changes of this condition.

References:

1. Batisse M, Somda F, Delorme JP, Desbiez F, Thieblot P, Tauveron I. Spontaneous rupture of Achilles tendon and Cushing's disease. Case report. *Ann Endocrinol* (Paris). 2008;69:530-531.
2. Brown KA, Johnson AL, Bender SJ, et al. (2023). Onchocerca sp. in an imported Zangersheide gelding causing suspensory ligament desmitis. *J Vet Intern Med.* 2023;37:735-739.
3. Dyson S. Clinical commentary: Is degenerative change within hindlimb suspensory ligaments a prelude to all types of injury? *Equine Vet. Educ.* 2010;22(6):271-274.
4. Halper J, Kim B, Khan A, Yoon JH, Mueller POE. Degenerative suspensory ligament desmitis as a systemic disorder characterized by proteoglycan accumulation. *BMC Vet Res.* April 12, 2006.
5. Hofberger S, Gauff F, Licka T. Suspensory ligament degeneration associated with pituitary pars intermedia dysfunction in horses. *Vet J.* 2015;203:348–350.
6. Hofberger S, Gauff F, Thaller D, Morgan R, Keen J, Licka T. Assessment of tissue-specific cortisol activity with regard to degeneration of the suspensory ligaments in

horses with pituitary pars intermedia dysfunction. *Am J Vet Res.* 2018;79(2):199–210.
7. Kim B, Yoon JH, Zhang J, Mueller POE, Halper, J. Glycan profiling of a defect in decorin glycosylation in equine systemic proteoglycan accumulation, a potential model of progeroid form of Ehlers-Danlos syndrome. *Arch Biochem Biophys.* 2010;501:221–231.
8. Mero J, Pool RR. Twenty cases of degenerative suspensory ligament desmitis in Peruvian Paso horses. *AAEP Proceedings*. 2002;48:329-334.
9. Momen M, Brounts SH, Binversie EE, et al. Selection signature analyses and genome-wide association reveal genomic hotspot regions that reflect differences between breeds of horse with contrasting risk of degenerative suspensory ligament desmitis. *G3-Genes Genom Genet*. 2022;12(10).
10. Plaas A, Sandy JD, Liu H, et al. Biochemical identification and immunolocalization of aggrecan, ADAMTS5 and inter-alpha-trypsin-inhibitor in equine degenerative suspensory ligament desmitis. *J Orthop Res.* 2011;29(6): 900–906.
11. Schenkman, Daniel et al. Systemic proteoglycan deposition is not a characteristic of equine degenerative suspensory ligament desmitis (DSLD). *J Equine Vet Sci.* 2009;29(10): 748–752.

CASE II:

Signalment:
Three-week-old castrated male PIC Camborough ® x PIC 800 ® cross bred pig (*Sus scrofa*).

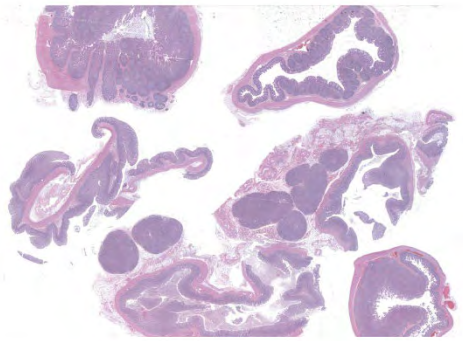

Figure 2-1: Ileum and colon, piglet. Multiple sections of ileum, colon, and attached mesenteric lymph nodes are submitted for examination. (HE, 6X)

History:
Enteric, respiratory, CNS, and systemic signs reported in 3-week-old pigs from a wean-to-finish barn in Iowa.

Gross Pathology:
This pig exhibited significant ataxia and paresis, and would "high-step" if made to walk. It would often become laterally recumbent but typically stayed centrally aware. Eye movement was normal. The piglet was thin and gaunt, with a raised coarse hair coat. All lung lobes were diffusely tan, rubbery, and non-collapsing with multifocal lobules in the cranial and middle lung lobes that were diffusely dark red and firm. Colon content was green-brown and watery, but the associated tissue was grossly unremarkable. The stomach of this animal was full of feed, and no ulcers were apparent. Tracheobronchial and ileac lymph nodes were enlarged.

Laboratory Results:
- PRRSV PCR (lung): Positive (Ct = 11.1)
- IAV PCR (lung): Negative
- PCV 2/3 Differential PCR (spleen): Negative
- TGEV/PEDV/PDCoV Differential PCR: Negative
- PRRSV IHC (intestine/colon): Abundant strong punctate intracytoplasmic staining in mononuclear cells with morphology similar to macrophages in the mediastinal

lymph node, Peyer's patches, and lamina propria.

- Bacterial culture: Low growth from both the intestine and colon of *Salmonella enterica* ssp *enterica* serovar Heidelberg.

Microscopic Description:

Ileum: In several sections, there is moderate multifocal blunting and fusion of villi with a crypt: villus ratio of 1:1. Apical enterocytes are often moderately attenuated with loss of the brush border and reduced apical cytoplasm. In some sections, these cells have a profound number of intracellular but extracytoplasmic 1-2 um circular eosinophilic apicomplexan organisms with 0.5 um basophilic nuclei (*Cryptosporidium* sp.). In other sections, these cells contain numerous larger apicomplexans with varied life-stages apparent including: 10 x 5 um curvilinear binucleate meronts (type I meronts), 4 x 12 um curvilinear uninucleate merozoites (type I merozoites), 9 x 6 um ovoid multinucleate meronts (type II meronts), multiple 3 x 12 um curvilinear uninucleate merozoites joined at their base by a residual body (type II merozoites), a 12um diameter circular lightly basophilic microgamont filled with numerous peripheral uninucleate deeply basophilic microgametes, or a 18 um diameter circular lightly basophilic macrogamont with a 8 um granular circular nucleus (macrogamont) (*Cystoisospora suis*). Rare crypts are ectatic, lined by moderately flattened, attenuated epithelium, and filled with cellular and karyorrhectic debris admixed with rare degenerate neutrophils (crypt abscesses). The associated lamina propria is often infiltrated by numerous eosinophils admixed with a few neutrophils. In one section, there is profound necrosis in Peyer's patches, characterized by abundant karyorrhectic and cellular debris admixed with rare neutrophils, that often obscures typical follicular architecture. Similar changes are occasionally present

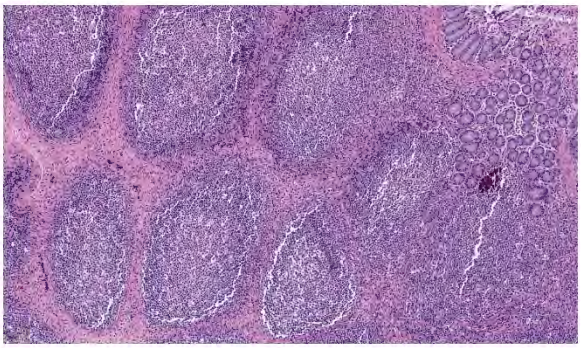

Figure 2-2: Ileum, piglet. Peyer's patches are depleted and lack normal architecture. (HE, 121X)

in the overlying lamina propria, with marked lymphocytolysis and loss of proprial architecture. Vascular structures in all tunics are moderately congested, and macrophages occasionally aggregate around medium-caliber vessels in the submucosa.

Spiral Colon: In both sections, there is moderate multifocal ulceration of the colonic mucosa characterized by loss of apical colonocytes with abundant cellular and karyorrhectic debris admixed with minimal fibrin and extravasated erythrocytes adhered to the exposed lamina propria. Adjacent colonocytes are often flattened, irregularly spaced, with reduced apical cytoplasm (attenuation). The associated lamina propria is often infiltrated by neutrophils and eosinophils admixed with necrotic debris and a few macrophages. Crypts within these areas are often ectatic, lined by mildly attenuated epithelium, and filled with either cellular and karyorrhectic debris admixed with degenerate neutrophils (crypt abscesses) or numerous eosinophils. Several other crypts are filled with up to 15 5 x 7 um pyriform to crescent-shaped protozoa with lightly basophilic cytoplasm and a faint nucleus (Suspect Trichomonads). The colonic lumen contains abundant cellular debris admixed with numerous colonies of basophilic bacteria with morphology ranging from coccoid to bacillary to filamentous, as well as rare 80 um circular flagellated protozoa with a prominent bean-

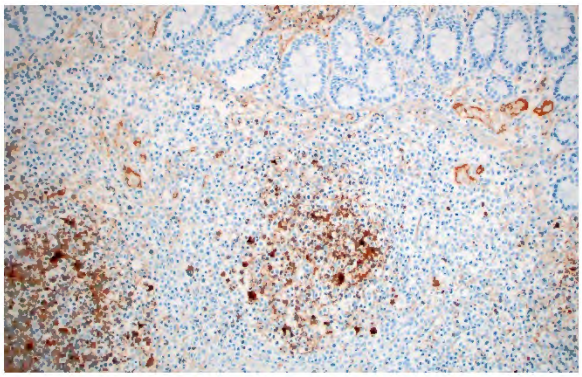

Figure 2-3: Ileum, piglet. Macrophages within Peyer's patches demonstrate strong labeling for PRRSV antigen. (anti-PRRSV, 400X) (Photo courtesy of: Department of Veterinary Pathology, Iowa State University CVM, https://vetmed.iastate.edu/vpath)

shaped nucleus and a large cytoplasmic vacuole and abundant phagocytosed cellular debris (Suspect *Balantidium coli*). The submucosa is multifocally infiltrated by numerous macrophages admixed with lymphocytes and a small amount of karyorrhectic debris and these cells often aggregate around medium to large caliber vessels. Multifocally the cortical and medullary architecture of the mesenteric lymph node is effaced by abundant cellular and karyorrhectic debris (lymphocytolysis) admixed with rare infiltrating neutrophils and macrophages.

Contributor's Morphologic Diagnoses:

Ileum and colon (mediastinal lymph node, Peyer's patches, and lamina propria): Lymphoid necrosis, multifocal, profound, subacute.

Ileum: Atrophic enteritis, necrosuppurative and eosinophilic segmental, marked, subacute, with crypt abscesses and numerous intralesional apicomplexans with morphology consistent with *Cryptosporidium spp*. and *Cystoisospora suis*

Colon: Ulcerative colitis, segmental, marked, subacute, with crypt abscesses and numerous intralesional protozoans with morphology consistent with *Balantidium coli*, and Trichomonads.

Contributor's Comment:

This is great example of a real-world production animal diagnostic case. It's also a great reminder to look for a primary etiology when there are multiple organisms/changes present in a piece of tissue that aren't typically seen together. *Cryptosporidium suis* and *scrofarum* are present in many commercial pigs but typically do not cause clinical disease and are generally not histologically apparent.[8,13] The presence of such profound quantities of *Cryptosporidium* spp. in this case suggests primary immune suppression. The larger apicomplexan present in this slide has life stages that are morphologically consistent with *Cystoisospora suis*. While this organism can act as a primary enteric pathogen in pigs, it is also present at low levels in many commercial swine post-weaning without causing clinical disease, often with few if any histologically apparent life-stages. The presence of both types of meronts, both types of merozoites, as well as microgamonts and macrogamonts in a single section of tissue is unusual

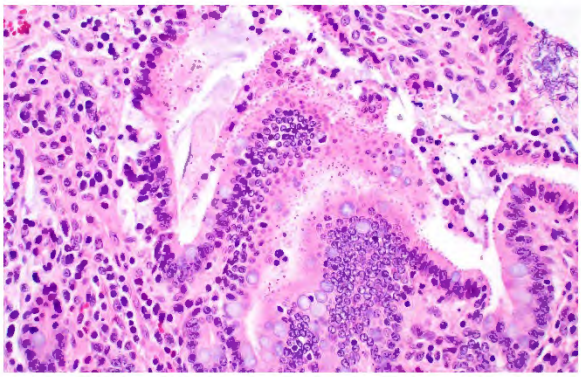

Figure 2-4: Ileum, piglet. Numerous cryptosporidium meronts and gamonts line the attenuated ileal villi. (Photo courtesy of: Department of Veterinary Pathology, Iowa State University CVM, https://vetmed.iastate.edu/vpath)

and also suggests that primary immune suppression may be at play. Lindsay *et al.* did a great job describing these life stages in a in 1980 *Journal of Parasitology* paper.[7] The moderate ulcerative colitis in this animal is typical of a *Salmonella* spp. It's also common to have *Balantidium coli* find their way into these colonic lesions, often phagocytosing necrotic debris.[9,13] The pyriform organisms in the colonic crypts are morphologically consistent with trichomonads. *Tetratrichomanas foetus*, *suis, buttreyi*, and *Pentatrichomonas hominis* have all been described as inhabitants of the porcine digestive tract. Others are likely present in pigs, and there have been increased efforts, especially in China, to better characterize these organisms.[6] They are commonly seen in higher numbers in porcine colonic crypts during disease or dysbiosis.

PCV-2 parasitizes lymphocytes and is a common cause of immune suppression in commercial pigs. However, this virus typically causes lymphoid depletion with granulomatous inflammation and rarely intracytoplasmic botryoid inclusion bodies. PCV-2/3 differential PCR was negative in this animal. The massive amount of karyorrhectic debris in the lymphoid tissue is more in line with PRRSV infection, which was detected at a very low CT in lung, and colocalized to the lesioned enteric lymphoid tissue by IHC. PRRSV is a member of the family *Arteriviridae*, which together with *Coronaviridae, Roniviridae, and Mesonoviridae* form the order Nidovirales, a contemporarily relevant viral order that has evolved a unique replication strategy utilizing discontinuous extension and a set of nested subgenomic mRNAs. The economic impact of

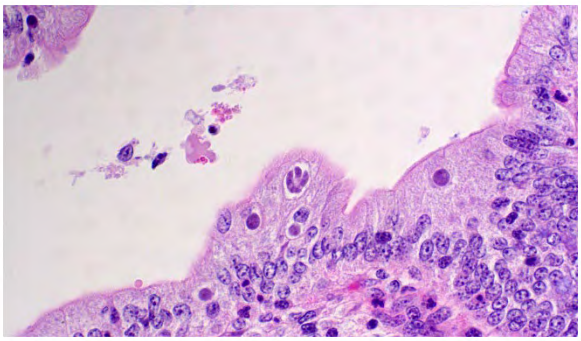

Figure 2-5: Ileum, piglet. Numerous life stages of Cystoisospora suis are present within ileal epithelium. This field contains, several primary meronts and a schizont in which merozoites are connected by a residual body. (Photo courtesy of: Department of Veterinary Pathology, Iowa State University CVM, https://vetmed.iastate.edu/vpath)

PRRSV in the US is estimated to be $660 million annually, and a reasonable case could be made that this is the most economically important virus of any domestic species in the US.[3] PRRSV replicates in macrophages and, to a lesser extent, dendritic cells. There was much historical controversy about the receptor utilized by this virus for cell entry. In a landmark paper, Prather et al. were able to demonstrate complete resistance to the virus by knocking out CD163 in commercial pigs with CRISPR/Cas9 methods.[11] CD163 (HbSR) is a hemoglobin scavenger receptor that is expressed in cells of the monocyte-macrophage lineage.[1] Currently, CD163 knock-out pigs are working their way through the federal regulatory system, with the genetics company involved hoping to market a completely PRRSV resistant animal. This may have huge economic implications given the limited success of commercial vaccines against this phylogenetically diverse virus. While this virus is classically associated with interstitial pneumonia with intralesional "necrotic macrophages", it's a systemic pathogen that can infect macro

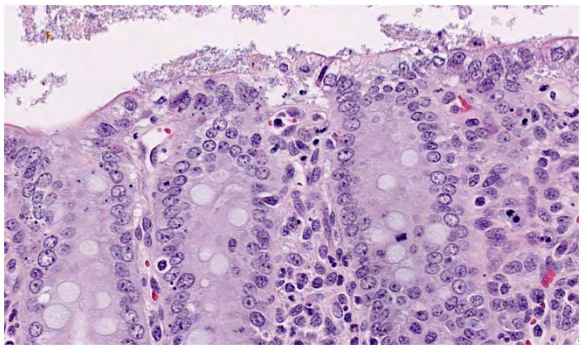

Figure 2-6: Colon, piglet. There is multifocal ulceration of the colonic epithelium with few neutrophils infiltrating the lamina propria. (HE, 455X).

phages in any body system, especially lymphoid tissue. The terms "necrotic macrophages" and "lymphoid necrosis" are somewhat controversial in PRRSV infection. An early paper utilizing tunnel assays, demonstrated widespread apoptosis of noninfected cells in the lung, testes, and lymphoid tissue, giving rise to the idea of "bystander-apoptosis" involvement in the pathogenesis of this virus.[10] Subsequent papers further characterizing the involvement of intrinsic/extrinsic/other apoptotic pathways in infected and uninfected cells are conflicting.[2] At the very least it can be stated that much of the cell death in a PRRSV infection occurs in uninfected cells, and a significant proportion of those cells are likely apoptotic as opposed to necrotic.

PRRSV-associated lesions and IHC staining were also present in the lung, brain, spleen, and tracheobronchial lymph nodes of this animal (not included on this slide).

In this case, the clinical signs in the population are not the result of a lateral introduction of any of the 4 protozoans described or the *Salmonella* sp. isolated. Rather, all of these organisms were endemic in this population and caused no clinically apparent disease. The introduction of a new PRRSV strain into the sow farm resulted in significant immune suppression in weaned pigs, disrupting the balance of the enteric ecosystem, culminating in enhanced replication of *Cryptosporidium* spp, *Cystoisospora suis and* several trichomonads.

Contributing Institution:
Department of Veterinary Pathology
College of Veterinary medicine
Iowa State University
1800 Christensen Drive
Ames, Iowa 50011-1134
https://vetmed.iastate.edu/vpath

JPC Diagnoses:

1. Ileal Peyer's patches and mesenteric lymph nodes: Lymphoid depletion, chronic, diffuse, marked, with lymphocytolysis.
2. Ileum: Villar blunting, diffuse, marked with numerous intracytoplasmic, extracellular apicomplexan schizonts and gamonts consistent with *Cryptosporidium sp*., and intracytoplasmic, intracellular apicomplexan meronts, schizonts, and gamonts consistent with coccidiosis.
3. Colon: Colitis, ulcerative, multifocal, mild to moderate with crypt abscesses and intraglandular flagellates.

JPC Comment:
The good folks at Iowa State provide a great write-up that touches on some very diagnostically relevant topics and stimulated excellent pathogenesis discussion during conference. The #1 take-home lesson in this case for participants was, "Don't stop looking just because you found one cause" – a common diagnostic pitfall referred to as "search satisfaction". As in this case, there were many, many

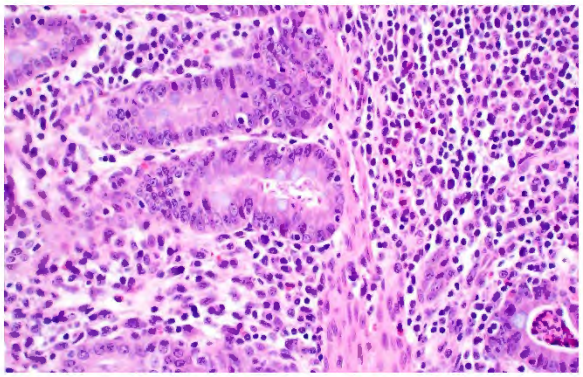

Figure 2-7: Colon, piglet. Occasional colonic glands contain numerous trichomonads. (Photo courtesy of: Department of Veterinary Pathology, Iowa State University CVM, https://vetmed.iastate.edu/vpath)

organisms present in far greater numbers than normal as a result of virally-induced immune suppression.

If you see infectious agents, think about how that organism interacts with the host animal. Then, think about if that organism should or should not be present and, if they are expected, are they present in expected numbers? If there are multiple species of agent, and they are in higher numbers than expected, a primary immune suppression should rise to the top of the list. In this case, *Cryptosporidium spp, Balantidium coli*, and trichomonads are found in many commercial pigs and do not typically cause disease. *Cystoisospora suis* can be a primary enteric pathogen of swine but may also be present in low levels in post-weaning commercial pigs without issue. However, the presence of both types of meronts, both types of merozoites, and both micro- and macrogamonts in one tissue section should raise red flags and make the pathologist look for an underlying cause that might explain the lack of immune regulation of commensals.

Other honorable mentions discussed in conference included the other members of the porcine respiratory disease complex, which are PRRSV, PCV2, *Pasteurella multocida*, swine influenza A, and *Mycoplasma hyopneumoniae*, and a quick mention of other relevant arteriviruses within veterinary species, such as equine Arterivirus (equine viral arteritis), Simian hemorrhagic fever virus in non-human primates, and lactate dehydrogenase-elevating virus in mice (although this one is pretty laid back, all things considered).

This case provides an excellent opportunity to review relevant general pathology of viral infections. One of the most critical players in innate viral defense is type I interferon (IFN-I). The initiation of IFN-I production is dependent on host pathogen recognition receptors (PRRs) that recognize pathogen-associated molecular patterns (PAMPs), which is where the whole process starts. The body must be able to recognize the "bad guy" before it can mount an appropriate response to handle it.

Certain classes of PRRs, such as the membrane-bound Toll-like receptors (TLR), specifically TLR3, TLR7/8 and TLR9, detect viral PAMPs and foreign nucleic acids within cellular endosomes and help upregulate the production of IFN-1 and pro-inflammatory cytokines. Once one of these endosomal TLRs has bound and recognized a viral PAMP, the TLR recruits the adaptor molecule TIR-containing adaptor-inducing IFN-β (TRIF). TRIF then binds Tumor Necrosis Factor Receptor Associated Factor 6 (TRAF6) and activates transforming growth factor β (TGF-β)-activated kinase-1 (TAK1) and TAK1-binding proteins (TABs).[4,5] This complicated cascade

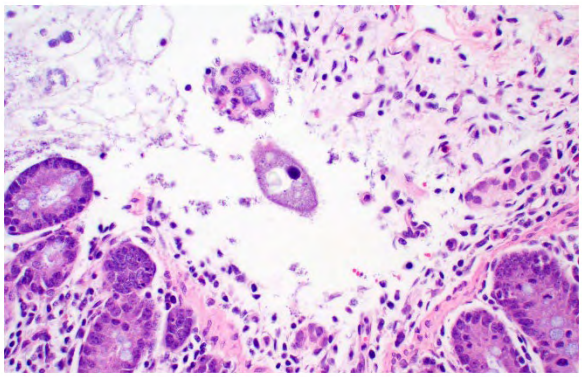

Figure 2-8: Colon, piglet. Rare Balantidium coli are present within the colonic lumen. (Photo courtesy of: Department of Veterinary Pathology, Iowa State University CVM, https://vetmed.iastate.edu/vpath)

results in the phosphorylation of NF-κB essential modulator (NEMO) and the activation of an IKK complex. IκBα, which is bound to and inhibits the transcription factor NF-κB, is phosphorylated and degraded by the proteosome. Upon release from its inhibitor, NF-κB translocates to the nucleus and upregulates the expression of IFN-β and inflammatory cytokines.[4,5,12]

Working in concert with the TLRs are cytoplasmic RIG-I-like receptors (RLRs), another class of PRR that includes retinoic acid-induced gene I (RIG-I) and melanoma differentiation associated gene 5 (MDA5), among others.[4,5] These RLRs recognize viral nucleic acid in the cytosol of the affected cell. RIG-I and MDA5 both have a feature called the "caspase activation and recruitment domain" (CARD) which, upon activation, interacts with virus-induced signaling adaptor (VISA), the primary (and necessary) signaling adapter protein of the cytosolic RLRs.[4,5,12] These interactions allow RLRs to relocate to mitochondrial membranes and initiate the formation of the VISA signalosome, which basically functions as a scaffold to which other proteins can stick.[4] The assembled VISA signalosome recruits TNF receptor-associated factors (TRAFs) or Fas-associated death domain protein (FADD), which activate caspases 8 and 10.[4,5] These caspases then stimulate NF-κB activation. Once activated, NF-κB translocates to the nucleus to its job of upregulating production of IFN-1 and other cytokines as described above.

Now the body has IFN-1 circulating about. Now what? IFN-I binds to its receptor, appropriately named type I IFN receptor, and initiates the Janus kinase signal transducer and activator of transcription (JAK-STAT) pathway, thereby resulting in the expression of numerous IFN-1 stimulated genes that ultimately rev up the anti-viral adaptive immune response.[4,5] Several arteriviruses, including PRRSV, cleave signaling molecules of IFN-I responses.[4] A recent study demonstrated that highly pathogenic PRRSV and its nsp4 protein antagonize IFN-1 expression by cleaving VISA and NEMO to block NF-κB signaling pathways.[4] (Cue some commentary about evolution being an arms race…)

PRRSV infection occurs primarily through alveolar macrophages in the lung of infected pigs. On top of its anti-IFN-1 actions, PRRSV primarily utilizes a CD163 receptor, especially the scavenger receptor cysteine-rich domain 5 (SRCR5) of the receptor, to infect macrophages.[1,2,5] The interaction between the PRRSV minor envelope glycoproteins (GP2a and GP4) and the CD163 SRCR5 domain facilitates the release of genetic material from the virus, thereby enabling viral replication within the infected cell.[1,2,5]

As mentioned by the contributor in their excellent write-up, targeting this interaction by blocking viral binding or removing CD163 from the cell surface is a promising strategy

for controlling PRRSV. Currently, ABS, one of the premier genetics companies for livestock, is developing a CD163-knockout pig strain that is resistant to PRRSV.[11] Long story short, no receptor for PRRSV to bind equals no PRRSV infection. This has massive implications for both commercial pig operations and research labs. Research is generally reliant upon smaller, younger pigs. PRRSV has been a challenging confounder of research findings in these pigs, as they are transported in from commercial farms and can develop respiratory disease secondary to transport stress. If a pig has PRRSV and is then utilized for a study, who's to say what lesions are due to PRRSV and what lesions are due to the agent of study interest? Although many institutes are actively looking to reduce the use of animals, some studies are still reliant upon live animal models. Being able to utilize PRRSV-resistant pigs could be a huge leap forward for such studies and would very likely reduce the overall number of animals needed for study completion.

References:

1. Etzerodt A. and Moestrup SK. CD163 and inflammation: biological, diagnostic, and therapeutic aspects. *Antioxid Redox Signal*. 2013. 18(17):2352-63.
2. Fan L. Signaling pathways involved in regulating apoptosis induction in host cells upon PRRSV infection. *Virus Genes*. 2019. 55(4):433-439.
3. Holtkamp DJ, et al. Assessment of the economic impact of porcine reproductive and respiratory syndrome virus on United States pork producers. *Journal of Swine Health and Production*. 2013. 21(2):72-84.
4. Huang C, Du Y, Yu Z, Zhang Q, Liu Y, Tang J, Shi J, and Feng W. Highly pathogenic porcine reproductive and respiratory syndrome virus nsp4 cleaves VISA to impair antiviral responses mediated by RIG-1-like receptors. *Scientific Reports.* 2016;6(1):28497.
5. Huang C, Zhang Q, Guo XK, Yu ZB, Xu AT, Tang J, Feng WH. Porcine reproductive and respiratory syndrome virus nonstructural protein 4 antagonizes beta interferon expression by targeting the NF-κB essential modulator. *J Virol.* 2014;88(18):10934-45.
6. Li W, et al., The prevalence of intestinal trichomonads in Chinese pigs. *Veterinary Parasitology*. 2015. 211(1):12-15.
7. Lindsay, DS, et al. Endogenous development of the swine coccidium, Isospora suis Biester 1934. *J Parasitol*. 1980. 66(5):771-9.
8. Pettersson E, et al. Detection and molecular characterisation of Cryptosporidium spp. in Swedish pigs. *Acta Veterinaria Scandinavica*. 2020. 62(1):40.
9. Schuster FL and Ramirez-Avila L. Current world status of Balantidium coli. *Clin Microbiol Rev.* 2008. 21(4):626-38.
10. Sur JH, Doster AR, and Osorio FA. Apoptosis induced in vivo during acute infection by porcine reproductive and respiratory syndrome virus. *Vet Pathol*. 1998. 35(6):506-14.
11. Whitworth, KM, et al. Gene-edited pigs are protected from porcine reproductive and respiratory syndrome virus. *Nature Biotechnology*. 2016. 34(1):20-22.

12. Xu LG, Wang YY, Han KJ, Li LY, Zhai Z, Shu HB. VISA is an adapter protein required for virus-triggered IFN-beta signaling. *Mol Cell.* 2005;19(6):727-40.
13. Zimmerman JJ. Diseases of Swine. 11th edition. ed. 2019. Hoboken, NJ: Wiley-Blackwell.

CASE III:

Signalment:
12-year-old, neutered male, European, cat (*Felis catus*)

History:
The cat was presented to our institution for a right subcutaneous cervical mass that was noticed by the owner 2 months ago. The cat had no general signs and there was no significant clinical history. The cat lived exclusively indoor with no other animals.

Clinical examination revealed an ovoid, 4 x 6 x 6 cm, firm, well-demarcated, non-painful and non-adherent mass in the cranial right ventro-lateral part of neck. Based on location, a right mandibular lymphadenopathy was suspected and a fine-needle aspiration was performed.

Cytological examination revealed a reactive lymphoid population (non-specific hyperplasia) admixed with numerous aggregates of plump and pleomorphic spindle to epithelioid cells that were occasionally separated by a delicate eosinophilic extracellular matrix (Figures 1-3). Atypia were severe with macrokaryosis and irregular macronucleoli but mitoses were not observed. Some siderophages were present. A diagnosis of malignant anaplastic tumor, primary or metastatic, of the right mandibular lymph node was made.

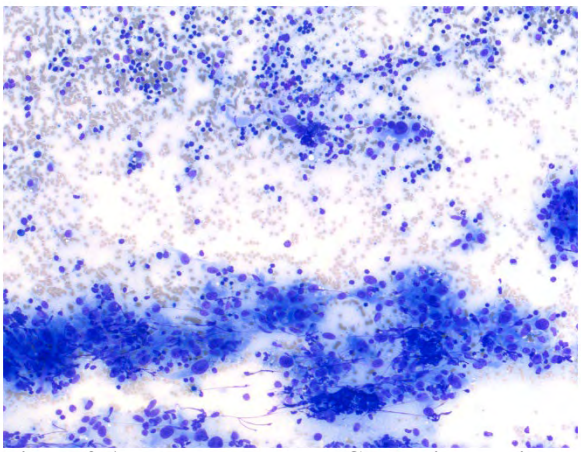

Figure 3-1: Lymph node, cat. Cytologic examination of the cervical mass: mixture of a reactive lymphoid population and atypical spindle to epithelioid cells with malignant features. (May-Grünwald & Giemsa.400X) (Photo courtesy of: Ecole Nationale Vétérinaire d'Alfort, Unité d'Histologie et d'Anatomie Pathologique, www.vet-alfort.fr)

Complete staging, including oral cavity and eyes, did not reveal any other mass and a primary sarcoma of the right lymph node was considered. A needle biopsy was made and revealed a sarcomatous proliferation highly suggestive of hemangiosarcoma. Considering the results of the staging, a primary nodal hemangiosarcoma was considered.

The lymph node was surgically removed and submitted for histopathological examination.

Gross Pathology:
A 4 x 6 x 6 cm lymph node was submitted (Figures 4-6). On cut section (after fixation), the lymphoid tissue was severely compressed and atrophic due to a rather well demarcated, white to dark red, firm to spongy proliferation that occupied 90% of the section. Some cavitary dark foci were present. The proliferation was limited by the nodal capsule and there was no sign of capsular effraction.

Laboratory Results:
Complete blood count revealed a mild macrocytic hypochromic and regenerative anemia with poikilocytosis. Numerous schistocytes

Figure 3-2: Lymph node , cat. This is the fixed section of mandibular lymph node. The nodal parenchyma is atrophic and compressed by a heterogenous neoplasm with white-tan to dark areas. The neoplasm is well demarcated and encapsulated. Some spongy/cavitary foci are present (Photo courtesy of: Ecole Nationale Vétérinaire d'Alfort, Unité d'Histologie et d'Anatomie Pathologique, www.vet-alfort.fr).

were observed suggesting a mechanical anemia (fragmentation anemia). Thrombocytosis and moderate neutrophilic leukocytosis were also observed.

Microscopic Description:
The remaining nodal tissue was atrophic, congested and severely compressed by a densely cellular, well-demarcated, encapsulated neoplasm composed of compact intermingled bundles of spindle to epithelioid cells associated to a delicate fibrous stroma. Neoplastic cells often delineated vascular lumens filled with red blood cells. They measured 50-100 µm, had distinct cell borders, a moderately abundant eosinophilic cytoplasm and a round vesicular nucleus with a large eosinophilic nucleolus. Some cells contained intracytoplasmic red blood cells.

Pleomorphism and atypical were marked: macrokaryosis, macronucleoli, irregular nuclei, nuclear hyperchromasia etc. Mitotic count was 6 mitoses per HPF (field surface = 0.307 mm^2).

The neoplasm incorporated many remaining lymphoid follicles, some of which were hyperplastic. There was also diffuse lymphocytic and plasmacytic infiltration as well as some siderophages and macrophages showing prominent erythrophagocytosis.

Immunohistochemical staining showed marked positive labelling for vimentin (cytoplasm) and CD31 (membrane) of neoplastic cells. Regarding CD31, normal sinus-lining endothelial cells were also positive.

Contributor's Morphologic Diagnoses:
Right mandibular lymph node: Primary nodal hemangiosarcoma (likely corresponding to malignant transformation of feline plexiform vascularization of cervical lymph nodes).

Contributor's Comment:
There are several descriptions of distinctive vascular lesions in cervical lymph nodes of cats.[7,8,13,15] They represent a morphologic spectrum ranging from benign lesions (plexiform vasculopathy/vascularization) to clearly malignant neoplasms (hemangiosarcomas).[13]

Feline plexiform vasculopathy/vascularization of lymph nodes (FPVLN) has first been

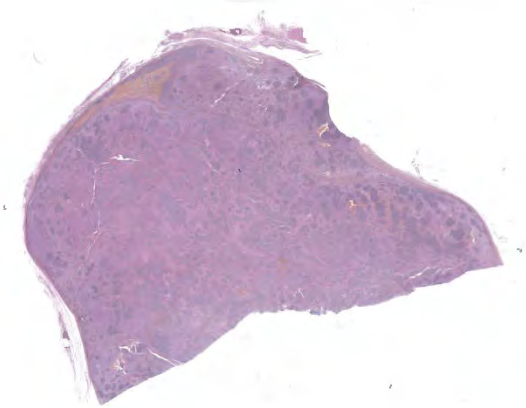

Figure 3-3: Lymph node, cat. A section of lymph node is submitted for examination. At subgross magnification, there is loss of normal nodal architecture. (HE 9X).

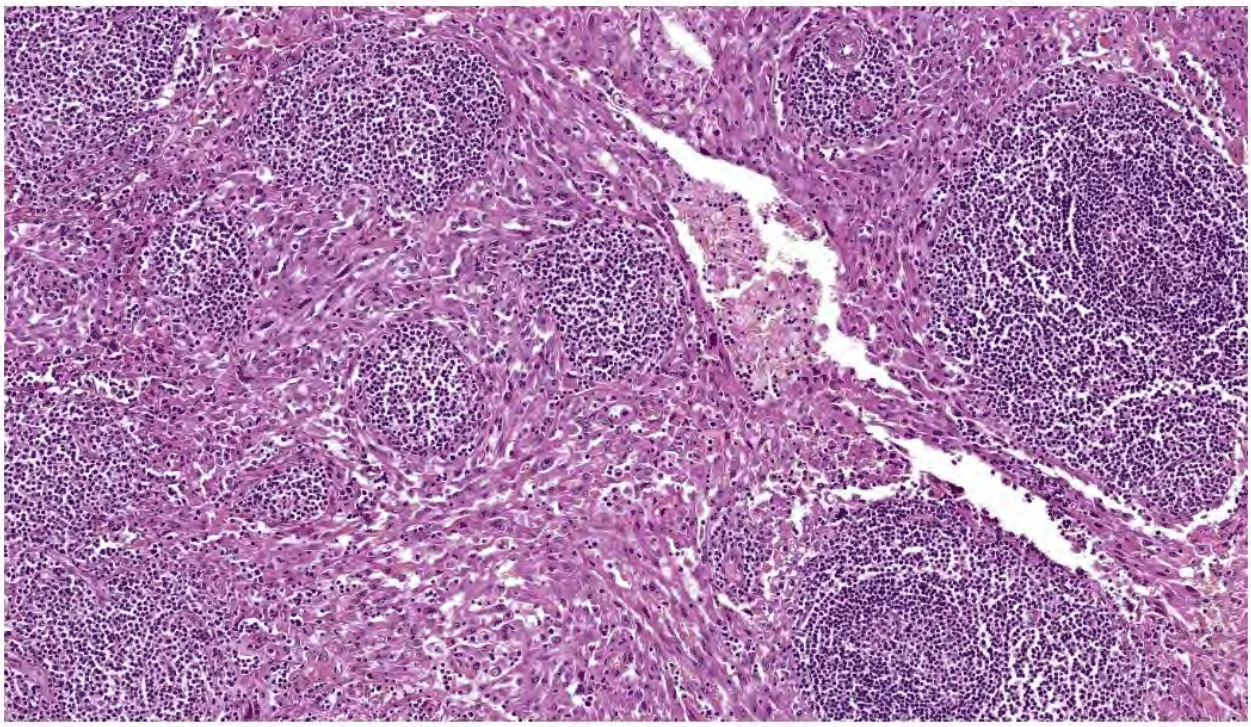

Figure 3-4: Lymph node , cat. Lymph node remnants are separated, surrounded and replaced by neoplastic endothelial cells arranged in sheets and forming small blood-filled spaces. (HE 201X).

described by Lucke *et al*. in 1987 and corresponds to nodal capillary vasoproliferation and lymphoid atrophy.[8] These lesions have been compared to vascular transformation of lymph node sinuses in humans, a conversion of nodal sinuses to capillary-like channels accompanied by fibrosis.[8,10,13] Such lesions have also been described in a dog.[5] In humans, such changes are believed to be secondary to occlusion of efferent lymphatics and/or sluggish venous blood flow due to thrombotic obstruction, heart failure, or other conditions leading to venous stasis.[10] The etiology of FPVLN remains uncertain.

FPVLN has a wide range of age (3 to 16 years old).[8,13] As in the single canine case, it mostly affects the cervical lymph nodes, which is different from vascular transformation of lymph node sinuses in humans that is predominantly observed in intra-abdominal lymph nodes.[8,10,13,15] FPVLN involving inguinal lymph nodes has also been described and other lymph nodes may rarely be affected (axillary lymph node for example).[8,13] Lesions are most often solitary but may also be multiple/bilateral. Generally, affected cats are otherwise clinically normal and prognosis after complete surgical excision is usually considered to be excellent with no recurrence or progression.[8,13,15]

Grossly, lymph nodes are enlarged, up to 5-6cm. On cut section, lymph nodes are heterogeneous and appear tan to purple, reflecting follicular structures and congestion respectively.[8,13] Histologically, there is lymphoid atrophy and a proliferation of capillary-like vessels lined by a single layer of flattened endothelial cells without atypia. The lumen may contain red blood cells or appear empty. Hyperplastic lymphoid follicles may also be observed.[8,13]

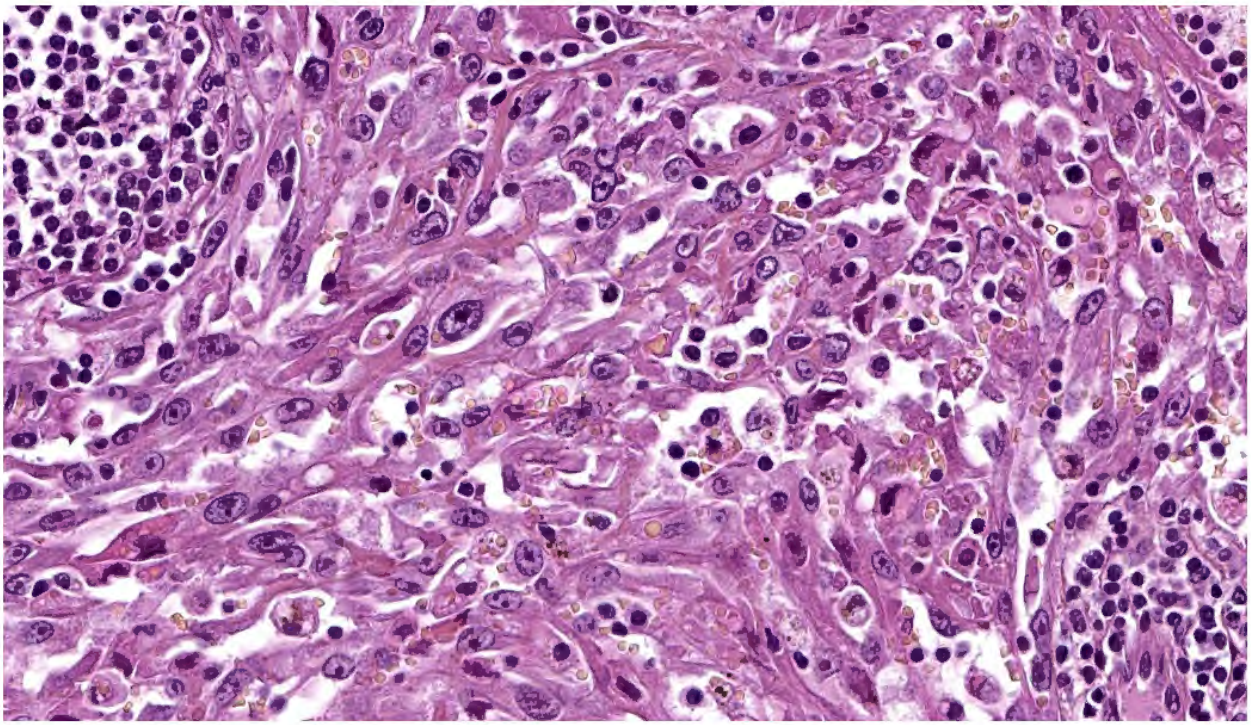

Figure 3-5: Lymph node , cat. Neoplastic endothelial cells demonstrate marked anisokaryosis and nuclear pleomorphism (HE 744X).

Recently, the endothelial cells in FPVLN have been proposed to be of lymphatic origin based on their expression of Prox-1 (nuclear labelling) in addition to CD31 and factor VIII-related antigen, the former being specific of lymphatic endothelial cells. LyVe-1 is another specific marker for the lymphatic endothelium.[7]

In 2015, primary hemangiosarcomas of feline cervical lymph nodes were reported in 12 cats.[13] Some cats also had typical lesions of FPVLN suggesting that there is a pathogenic and pathologic continuum between FPVLN and primary nodal hemangiosarcomas, similar to the continuum that exists between injection-associated panniculitis and injection site sarcomas in cats.[13] Clinical and gross findings appear similar to FPVLN, indicating that histopathological examination is essential to distinguish both entities. This is all the more important given that the prognosis of primary nodal hemangiosarcoma appears different from FPVLN as recurrence and suspected metastases were reported in some animals.[13]

Histologically, the proliferation has the classical appearance of malignant vascular neoplasms.[13] Although initially considered to be hemangiosarcomas based on the presence of red blood cells within the vascular channels, the recent demonstration that FPVLN arises from lymphatic endothelium suggests that these tumors may actually be lymphangiosarcomas.[7] The association of red blood cells with lymphatic endothelial proliferation is also found in Kaposi's sarcoma, a distinct low-grade vascular sarcoma in humans associated with human herpesvirus 8 (HHV8). There are several forms of Kaposi sarcoma (classic, African, AIDS-associated and iatrogenic). Interestingly, it has been shown that infection with HHV8 reprograms blood endothelial cells to make them upregulate several

lymphatic-associated genes such as lymphatic vessel endothelial receptor 1 (LYVE1), podoplanin, and vascular endothelial growth factor receptor 3 (VEGFR3), so that, in the end, they resemble lymphatic endothelial cells, at least immunohistochemically (Kaposi's sarcoma is very different histologically from lymphangiosarcoma).[12] This example nicely illustrates that, in oncology, the phenotype of neoplastic cells may not accurately reflect the cell of origin. To date, the cause of FPVLN and FPVLN-associated hemangiosarcomas remains unknown and a viral etiology/contribution may be considered.

So far, FPVLN-associated hemangiosarcomas have not been further characterized immunohistochemically so we do not actually know if they also express markers of lymphatic endothelial cells (in this case, LyVe-1/Prox-1 immunohistochemical labelling was not performed). In such conditions, it might be better, regarding the terminology, pathogenesis and nomenclature, to rather name these distinctive lesions "FPVLN-associated angiosarcomas" or to refer to them as "benign vs. malignant forms of FPVLN".

Other malignant vascular neoplasms in cats include feline ventral abdominal lymphangiosarcoma (a distinctive cutaneous neoplasm previously termed feline ventral abdominal angiosarcoma) and hemangiosarcomas at other sites.[4,6,9,11,14] Contrary to dogs, hemangiosarcomas are uncommon in cats, accounting for 0.5% of cases at necropsy.[13] Most feline hemangiosarcomas are cutaneous and subcutaneous, with subcutaneous forms being more aggressive.[6] Some cutaneous hemangiosarcomas may develop secondary to chronic UV exposure on hypopigmented skin, as in dogs. Corneal and conjunctival hemangiosarcomas have also been described and appear to be associated with a good prognosis if completely excised.[11,14] Feline visceral hemangiosarcomas are rare and have a poor prognosis.[6] Finally, feline reactive systemic angioendotheliomatosis is a rare, multisystemic intravascular proliferative disorder of cats that most commonly affects the heart. Lymph nodes may occasionally be involved.[3]

This case represents a typical example of primary nodal hemangiosarcoma in the setting of FPVLN (although typical foci of FPVLN may be difficult to demonstrate in this case due to the extent of the hemangiosarcoma). Cytologic diagnosis yielded a diagnosis of malignant neoplasm, prompting for a complete staging in the search of a primary tumor. As no primary tumor was found and the morphology was not typical of lymphoma, FPVLN-associated hemangiosarcoma was suspected and subsequently confirmed by histological examination. Interestingly, hemangiosarcoma could have also been suggested by the finding of regenerative anemia with numerous schistocytes on hematological examination.

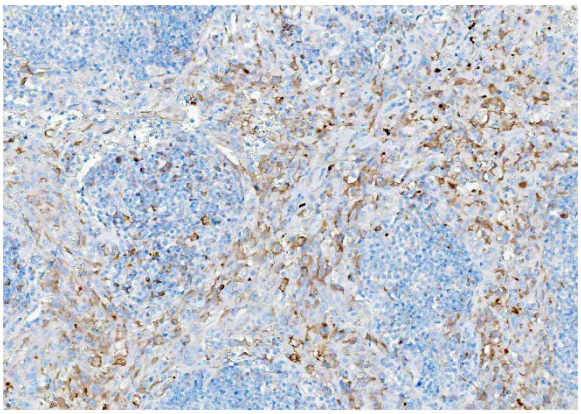

Figure 3-6: Lymph node, cat. Neoplastic endothelial cells demonstrate moderate cytoplasmic immunoreactivity for podoplanin) (anti-podoplanin, 175X).

Schistocytes usually result from the fragmentation of red blood cells in abnormal small vessels (fragmentation anemia). They are observed mostly in dogs with disseminated intravascular coagulation, hemangiosarcoma, myelofibrosis, glomerulonephritis etc. They are also described in cats with hepatic disease.[2] Following the complete excision of the affected lymph node, schistocytes were not found on subsequent blood smears and the animal completely recovered from its anemia.

As a conclusion, differential diagnosis for enlarged cervical lymph nodes in cats should include lymphadenitis, lymphoma (non-Hodgkin and Hodgkin-like), metastases, lymphoid hyperplasia, distinctive peripheral lymph node hyperplasia of young cats, plexiform vascularization and primary (hem)angiosarcoma.[13]

Contributing Institution:
Ecole Nationale Vétérinaire d'Alfort
Unité d'Histologie et d'Anatomie Pathologique, BioPôle Alfort
Département des Sciences Biologiques et Pharmaceutiques
7 avenue du Général De Gaulle
94704 Maisons Alfort Cedex
FRANCE
www.vet-alfort.fr

JPC Diagnoses:
Lymph node: Angiosarcoma.

JPC Comment:
This case proved to be a real diagnostic challenge for participants. Much of the discussion of this entity happened in real-time during conference, as most participants were unclear on the diagnosis in this case. The contributor

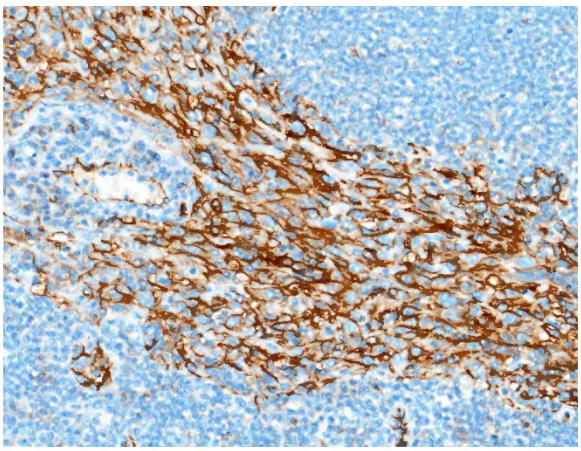

Figure 3-7: Lymph node, cat. Neoplastic endothelial cells demonstrate strong membranous immunoreactivity for CD31) (anti-CD31, 400X). (Photo courtesy of: Ecole Nationale Vétérinaire d'Alfort, Unité d'Histologie et d'Anatomie Pathologique, www.vet-alfort.f

provided an exceptional write-up on this enigmatic entity and makes numerous excellent points for consideration. Their comment is well worth the read and covers most of what was discussed in conference. Participants were initially unsure on tissue identification given the degree of parenchymal effacement by the neoplasm, with some getting to lymph node, but most thinking spleen. There were a few subtle clues to help participants get to the right organ, the most useful of which is the distribution of the extracapsular adipose tissue. Lymph nodes tend to be embedded in and surrounded by adipose tissue, whereas the spleen has only a strip of adipose tissue along its mesenteric side where vasculature enters the splenic body. In addition to covering much of what was stated by the contributor, differential diagnoses for vascular proliferations in feline patients were discussed and included hemangioma, hemangiosarcoma, lymphangioma, lymphangiosarcoma (especially on the inguinal skin), and systemic reactive angioendotheliomatosis.

As is the nature of science, despite most of the historical literature calling these neoplasms "primary nodal hemangiosarcomas," there is an increasing body of evidence that the neoplastic cells are immunoreactive for lymphatic endothelial markers (D2-40, Prox-1, LyVe-1).[7] The most popular arising school of thought regarding this neoplasm in the context of feline plexiform vasculopathy/vascularization of lymph nodes (FPVLN) is that it is most likely of lymphatic endothelial origin and is part of a continuum of FVPLN, where the proliferating benign vasculature undergoes malignant transformation secondary to obstruction of the efferent hilar lymphatics of the lymph node.[7] There is a similar condition to FPVLN that can occur in the mesenteric lymph nodes of rats, and neoplasms arising from affected lymph nodes in these animals have also been immunoreactive to Prox-1 and VEGF.[1]

In an effort to further contribute information to the speculative origins of this neoplasm, a podoplanin was performed in-house at the Joint Pathology Center (JPC) to try and tease out any lymphatic origin in the neoplastic cells in this case (LyVe-1 or Prox-1 are not available for use at the JPC). Approximately 60% of the neoplastic cells had moderate cytoplasmic immunoreactivity to D2-40 (podoplanin) in this case, which correlates with a lymphatic endothelial origin. CD31, Factor VIII, CD20, and CD3 were also performed. The Factor VIII demonstrated diffuse, strong cytoplasmic immunoreactivity within neoplastic cells, while the CD31 had moderate membranous immunoreactivity in approximately 65% of neoplastic cells. Both blood vessel and lymphatic endothelial neoplasms can be immunoreactive to these IHCs. CD3 and CD20 nicely showed the dispersed follicular architecture of the lymph node, with follicular T-cells and parafollicular B cells demonstrating strong membranous immunoreactivity to CD3 and CD20, respectively. Putting everything in context, conference participants favored the diagnosis of angiosarcoma for this neoplasm.

References:

1. Awazuhara Y, Tomonari Y, Kokoshima H, Wako Y, Doi T. Lymphangiomas with the presence of erythrocytes in mesenteric lymph nodes of Wistar Hannover rats. *J Toxicol Pathol.* 2025;38(1):37-42.
2. Barger AM. Erythrocyte morphology. In: *Schalm's Veterinary Hematology*. Ames, Iowa: Weiss DJ & Wardrop KJ; 2010:148.
3. Fuji RN, Patton KM, Steinbach TJ, et al. Feline systemic reactive angioendotheliomatosis: eight cases and literature review. *Vet Pathol*. 2005;42:608–617.
4. Galeotti F, Barzagli F, Vercelli A, et al. Feline lymphangiosarcoma--definitive identification using a lymphatic vascular marker. *Vet Dermatol*. 2004;15:13–18.
5. Gelberg HB, Valentine BA. Lymphadenopathy associated with a thyroid carcinoma in a dog. *Vet Pathol*. 2011;48:530–534.
6. Johannes CM, Henry CJ, Turnquist SE, et al. Hemangiosarcoma in cats: 53 cases (1992-2002). *J Am Vet Med Assoc*. 2007;231:1851–1856.
7. Jungwirth N, Junginger J, Andrijczuk C, Baumgärtner W, Wohlsein P. Plexiform Vasculopathy in Feline Cervical Lymph Nodes. *Vet Pathol*. 2018;55:453–456.
8. Lucke VM, Davies JD, Wood CM, Whitbread TJ. Plexiform vascularization of lymph nodes: an unusual but distinctive

lymphadenopathy in cats. *J Comp Pathol*. 1987;97:109–119.
9. McAbee KP, Ludwig LL, Bergman PJ, Newman SJ. Feline cutaneous hemangiosarcoma: a retrospective study of 18 cases (1998-2003). *J Am Anim Hosp Assoc*. 2005;41:110–116.
10. Miranda RN, Khoury JD, Medeiros LJ. Vascular transformation of lymph node sinus. In: Vol. 2, *Atlas of Lymph Node Pathology*. New York: Cheng L; 2013:493–494.
11. Pirie CG, Dubielzig RR. Feline conjunctival hemangioma and hemangiosarcoma: a retrospective evaluation of eight cases (1993-2004). *Vet Ophthalmol*. 2006;9:227–231.
12. Radu O, Pantanowitz L. Kaposi sarcoma. *Arch Pathol Lab Med*. 2013;137:289–294.
13. Roof-Wages E, Spangler T, Spangler WL, Siedlecki CT. Histology and clinical outcome of benign and malignant vascular lesions primary to feline cervical lymph nodes. *Vet Pathol*. 2015;52:331–337.
14. Shank AMM, Teixeria LBC, Dubielzig RR. Canine, feline, and equine corneal vascular neoplasia: A retrospective study (2007-2015). *Vet Ophthalmol*. 2019;22:76–87.
15. Welsh EM, Griffon D, Whitbread TJ. Plexiform vascularisation of a retropharyngeal lymph node in a cat. *J Small Anim Pract*. 1999;40:291–293.

CASE IV:

Signalment:
3-year-old male beagle (*Canis lupus familiaris*) dog

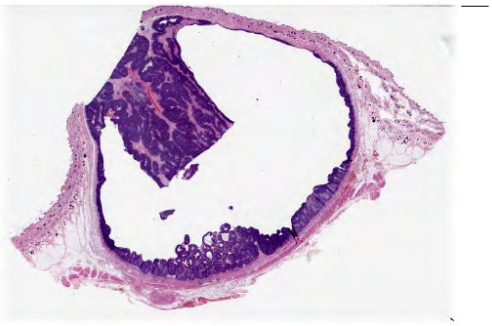

Figure 4-1: Haired skin, dog. A well demarcated cystic neoplasm is present within the dermis. The interaction with the overlying epidermis cannot be assessed based on this section. (HE, 8X)

History:
A 3-year-old male beagle dog was presented to staff veterinarians for the evaluation of a fluctuant mass present on the left caudolateral thorax. A fine needle aspirate was performed; red-tinged fluid was obtained. There was no resolution after 5 weeks. The mass was surgically excised on October 21, 2022, and submitted for histologic evaluation.

All procedures performed on animals were in accordance with regulations and established guidelines and were reviewed and approved by an Institutional

Animal Care and Use Committee or through an ethical review process.

Gross Pathology:
N/A

Laboratory Results:
N/A

Microscopic Description:
Haired skin: Extending from the dermis deep into the subcutis is an approximately 2 x 2 cm well-demarcated cystic mass lined by neoplastic undifferentiated basaloid epithelial

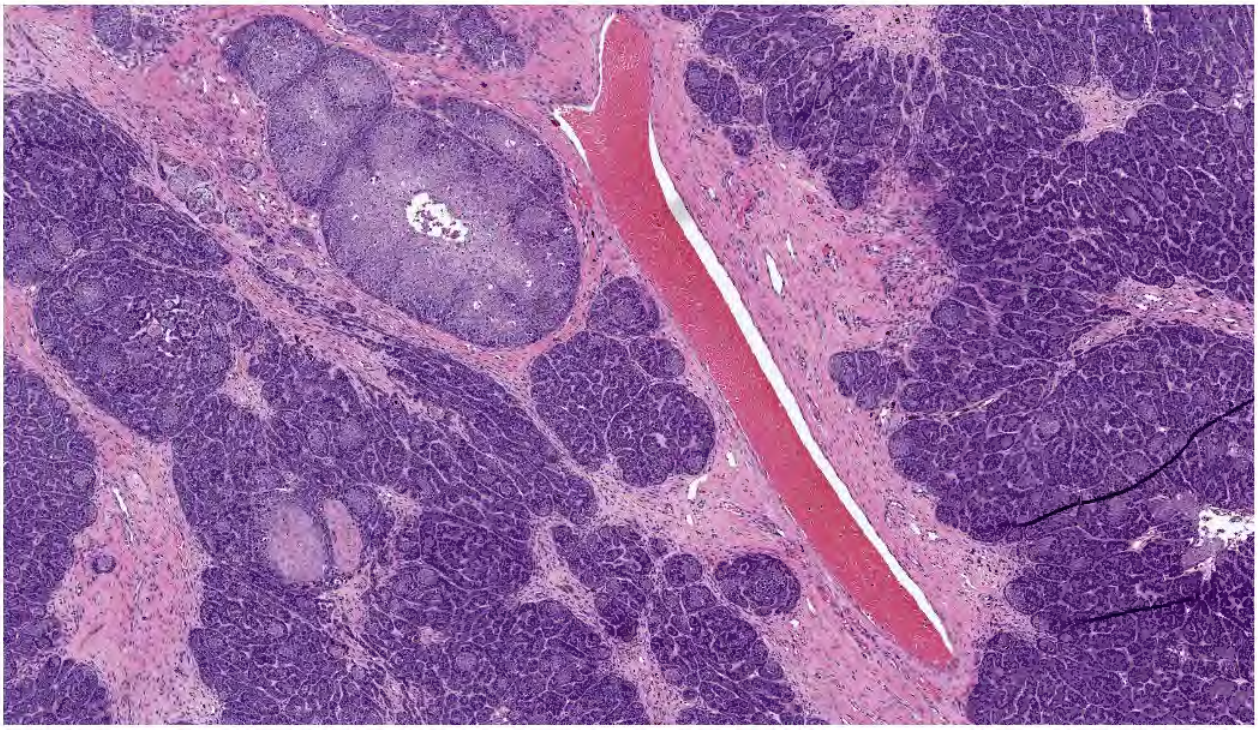

Figure 4-2: Haired skin, dog. Neoplastic basal cells are arranged in variably broad trabeculae and large islands and central areas of islands and trabeculae contain cells undergoing squamous differentiation which basal cells palisade along the outside. (HE, 81X)

cells. The neoplastic cells are arranged in lobules of dense anastomosing and palisading cords or small tightly packed nests, supported by scant fibrovascular stroma. There are multifocal papillary projections of neoplastic lobules into the lumen of the large cystic cavity. Multifocai lobules have smaller central cyst formation. The neoplastic basaloid cells are cuboidal with scant basophilic cytoplasm and round to oval, hyperchromatic nuclei, with two or more prominent nucleoli. There is minimal anisocytosis and moderate anisokaryosis. There is multifocal abrupt squamous differentiation and necrosis and approximately 5 mitotic figures per high power field. Brown granular pigment, most consistent with melanin, is present throughout the periphery of the mass; multifocal melanomacrophages infiltrate neoplastic lobules. Neoplastic cells extend to within 2mm of the surgical margin; however, there are multifocal foci suspicious for local invasion.

Contributor's Morphologic Diagnoses:
Haired skin: Basosquamous cell carcinoma

Contributor's Comment:
In dogs and cats, cutaneous neoplasms are common. Some of the most common tumor types reported in canine patients include mast cell tumors, lipomas, hair follicular and/or sebaceous gland tumors, histiocytomas, soft tissue sarcomas, and melanocytic tumors.[2,5,10] However in cats, basal cell tumors, mast cell tumors, squamous cell carcinoma, and fibrosarcomas are the most common skin tumors reported.[6] Tumors of the epidermis include

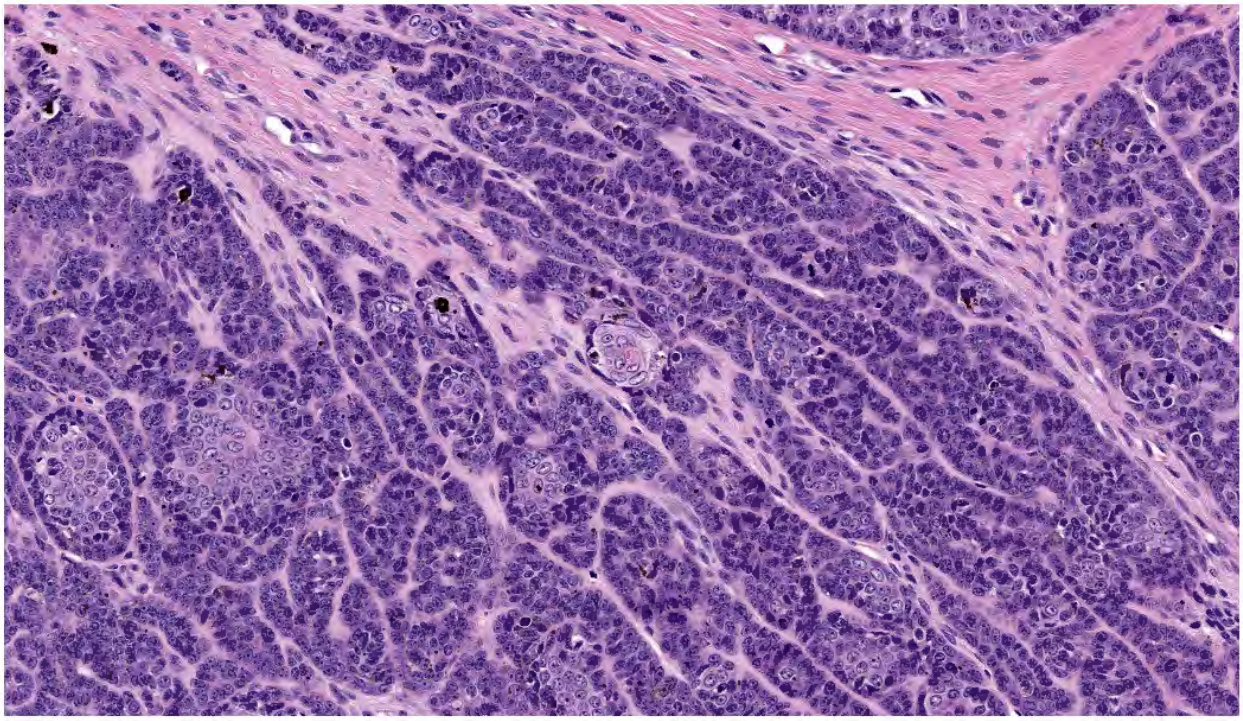

Figure 4-3: Haired skin, dog. Higher magnification of trabeculae of neoplastic epithelial cells. The basal-like cells palisade along the basement membrane, and central areas of trabeculae demonstrate squamous differentiation and keratinization. (HE, 381X)

papillomas and papillomavirus-induced tumors/tumor-like lesions, squamous cell carcinoma, basal cell carcinomas, and basosquamous carcinomas.[4]

Arising from epidermal basal cells, basosquamous carcinomas share features with squamous cell carcinomas and basal cell carcinomas and are considered low-grade malignancies.[4] Although rare in dogs and cats, along with other domestic animals, these tumors are more commonly reported in dogs.[1] Canine breeds reported to have an increased risk of developing basosquamous carcinomas, include Saint Bernard, bloodhound, Samoyed, and old English sheepdog.[1] These tumors are more likely found on the head, neck, and limbs.[1]

Histologically, basosquamous carcinomas are predominately composed of intradermal to subcutaneous lobules of undifferentiated basal cells with central foci of abrupt squamous differentiation.[1] Keratinocytes at the center of neoplastic lobules have mild "nuclear pleomorphism, mitotic activity and dyskeratosis."[1] Unlike other epidermal neoplasms, connection to the overlying epidermis is not a consistent diagnostic feature.[4] However, cyst formation and melanization, as seen in this case, are common and can often be appreciated grossly.[1,4] Keratinocytes, present in the foci of abrupt and atypical keratinization, that display features of malignancy, along with "the lack differentiation of the follicular isthmus or bulb are features that help differentiate basosquamous carcinomas" from other tumors.[4]

As basosquamous carcinomas share features with squamous cell carcinomas and basal cell carcinomas, these neoplasms represent possible differential diagnoses for basosquamous carcinomas.[1,4] Adequate surgical excision is

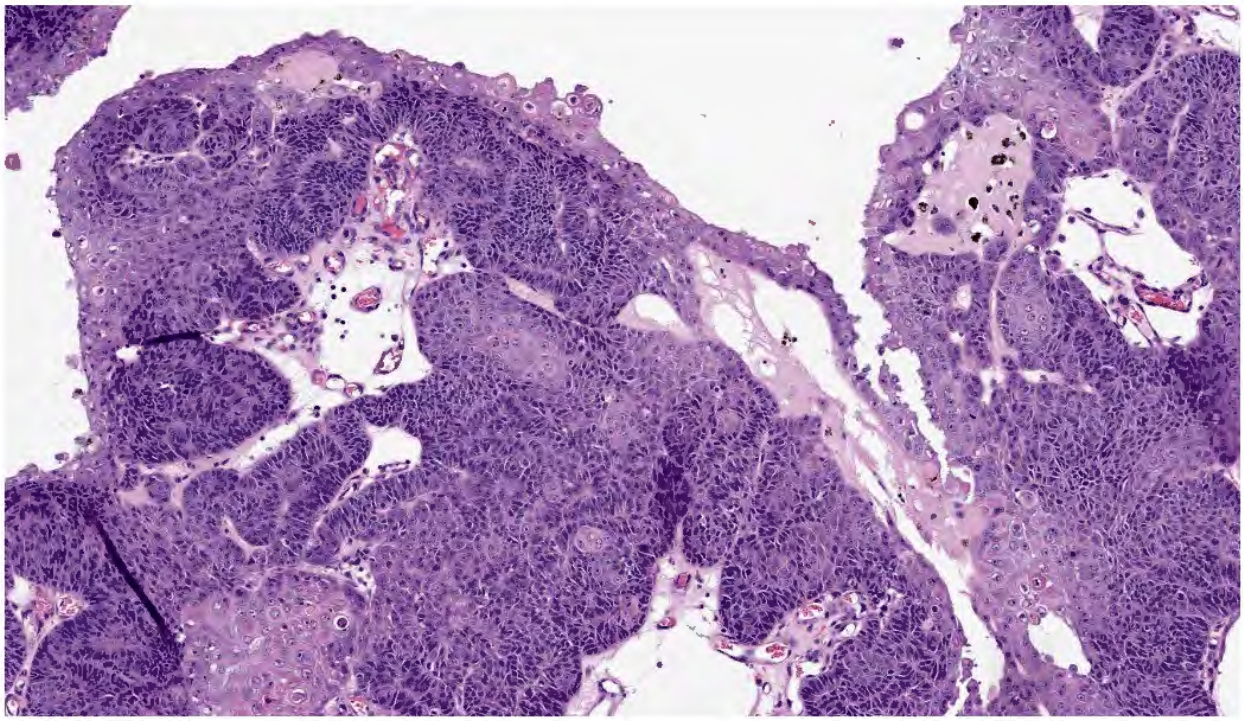

Figure 4-4: Haired skin, dog. Along the central space of this cystic neoplasm, there is more extensive squamous differentiation, and the cystic papillary projections into the central space are lined with several layers of squamous epithelium. (HE, 203X)

usually curative for these slow growing malignancies.[1]

Contributing Institution:
Pfizer Research and Development
455 Eastern Point Rd., Groton, CT 06340
www.pfizer.com

JPC Diagnoses:
Haired skin: Basosquamous carcinoma.

JPC Comment:
Basosquamous carcinoma (BSC) was first described in 1910 by Dr. Henry MacCormac.[10] He called this particular type of growth, which he astutely related to squamous cell carcinoma, a "rodent ulcer", which was a once-popular term used to describe ulcerative growths that had a "rat bite" appearance. Although this term has long since fallen out of use, BSC remains a controversial entity that has histologic features of both squamous cell carcinoma (SCC) and basal cell carcinoma (BCC) yet represents its own diagnosis. Whether or not this diagnosis is part of a continuum of changes seen in various stages of either BCC or SCC is currently unclear, and the diagnoses of BSC is highly contested within both human and veterinary medical circles.

In the current academic and clinical environment, BSCs are considered rare cutaneous neoplasms in both humans and veterinary species. While thought of as a low-grade malignancy with low metastatic potential in dogs and cats, this is not the case in humans, where basosquamous carcinomas are considered aggressive with more common metastases and a high rate of recurrence, even with wide surgical margins.[3] Behaviorally, BSC is more akin to SCC than to BCC in humans. There are rare reports of metastatic BSC in dogs, as well, but

this incredibly uncommon for this entity in dogs and cats.[9]

In human literature, it is currently believed that the BSC initially arises as a BCC that then undergoes genetic and epigenetic alterations, ultimately leading to squamous differentiation through basal-to-squamous transition (BST). As such, the BSC was classified as a BCC variant by the WHO in 2023.[7] To further complicate matters, there are also "basaloid SCC" and "keratotic BCC" diagnoses in humans, as well as BCC/SCC collision tumors.[7] Participants were shown histologic images of what the moderator currently uses to differentiate between a keratinizing BCC, a basaloid SCC, and a BSC. The basaloid SCC is typically described as having comedonecrosis with squamous differentiation at the edges of lobules and is NOT classified as a skin tumor. Rather, it is found in the oral cavity, cervix, lung, etc.[7] The keratotic BCC variant is composed of horn cysts, parakeratotic cells, and abrupt keratinization.[7] BSC is identified by abrupt squamous differentiation (not abrupt keratinization) with dyskeratotic squamous cells within the center of lobules of basal cells.[7] Both the basal cells and keratinocytes have mitotic activity. Considering these factors, a diagnosis of BSC was favored by participants. Ultimately, though, there seems to be substantial disagreement on how to define the BSC in veterinary literature, even between prominent tumor texts and fascicles.

To throw yet another wrench in this entity, it is well-known that papillomaviruses can induce squamous cell neoplasms in numerous species. Common examples include bovine papillomaviruses 1 and 2 causing equine sarcoids, bovine papillomavirus-4 resulting in squamous neoplasms of the alimentary tract in cattle, and canine papillomavirus-2 causing cutaneous papillomas in dogs.[4] Any of these can undergo malignant transformation when the right conditions occur. In recent years, *Felis catus* papillomavirus-2 (FcaPV-2) was detected within neoplastic cells of a multicentric cutaneous basosquamous carcinoma in a cat.[8] Although not generally thought to be associated with a papillomavirus, this was the first case report of a BSC associated with FcaPV-2.[8] Although better understood in humans, much has yet to be elucidated about this rare neoplasm in veterinary species and its clinical behavior, survivability, and potential correlations to papillomaviruses in certain cases.

References:

1. Goldschmidt MH and Goldschmidt KH, Epithelial and Melanocytic Tumors of the Skin. In: Meuten DJ, ed. *Tumors in Domestic Animals*, *5th ed*. 2017; Ames, IA, John Wiley & Sons, Inc., p.88-141.

2. Graf R, Pospischil A, Guscetti F, et al. Cutaneous Tumors in Swiss Dogs: Retrospective Data from the Swiss Canine Cancer Registry, 2008-2013. *Vet Pathol.* 2018;55(6):809-820.

3. Lima NL, Verli FD, de Miranda JL, Marinho SA. Basosquamous carcinoma: histopathological features. *Indian J Dermatol.* 2012;57(5):382-3.

4. Mauldin EA and Peters-Kennedy J, Integumentary System. In: Maxie MG, ed. *Jubb Kennedy and Palmer's Pathology of Domestic Animals*, *6th ed*. 2016; St. Louis MO, Elsevier Press, vol 1, p.703-736.

5. Martins AL, Canadas-Sousa A, Mesquita JR et al. Retrospective study of canine cutaneous tumors submitted to a diagnostic

pathology laboratory in Norther Portugal (2014-2020). *Canine Medicine and Genetics.* 2022;9(1):2.

6. Miller MA, Nelson JR, Turk L, et al. Cutaneous Neoplasia in 340 Cats. *Vet Pathol.* 1991;28:389-395.

7. Murgia G, Denaro N, Boggio F, Nazzaro G, Benzecry V, Bortoluzzi P, Passoni E, Garrone O, Marzano A. Basosquamous Carcinoma: Comprehensive Clinical and Histopathological Aspects, Novel Imaging Tools, and Therapeutic Approaches. *Cells*. 2023;12(23):2737.

8. Oh YI, Cheon DS, Lee JK, Choi MH, Hwang SY, Kim HW, Kang BJ, Youn HY. Detection of Felis catus papillomavirus type 2 within multicentric basosquamous carcinoma in a domestic cat. *J Vet Med Sci.* 2018;80(9):1445-1449.

9. Shin SK, Kim TW, Youm SY, Kim G, Na KJ, Chang D, Ahn B. Basosquamous carcinoma with systemic metastasis in a miniature Pinscher. *Jpn J Vet Res*. 2011;59(4):173-9.

10. Villamil JA, Henry CJ, Bryan JN, et al. Identification of the most common cutaneous neoplasms in dogs and evaluation of breed and age distributions for selected neoplasms. *JAVMA*. 2011;239(7):960-965.

11. Wermker K, Roknic N, Goessling K, Klein M, Schulze HJ, Hallermann C. Basosquamous carcinoma of the head and neck: clinical and histologic characteristics and their impact on disease progression. *Neoplasia*. 2015;17(3):301-5.

Joint Pathology Center
Veterinary Pathology Services

WEDNESDAY SLIDE CONFERENCE 2025-2026

Conference #8 — 15 October 2025

CASE I:

Signalment:
1.7-year-old, female spayed, domestic short-hair cat

History:
This animal presented for a large, intraocular mass occupying approximately 80% of the volume of the globe. Corneal opacification and secondary glaucoma were also noted.

Gross Pathology:
On external examination, the eye is notably buphthalmic. The cornea is centrally ulcerated and opaque. On cut surface, a tan, soft mass with multifocal cystic spaces extends from the ventral choroid, protrudes into the anterior and posterior chambers, and abuts and minimally displaces the lens dorsally. The ventral iris is not observed.

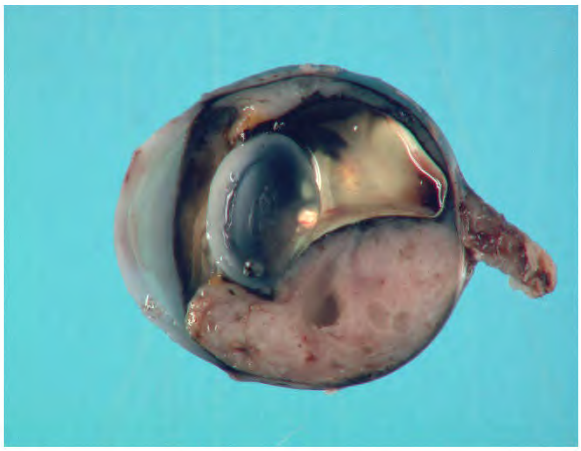

Figure 1-1: Globe, cat. On cut surface, a tan soft mass with multifocal cystic spaces extends from the ventral choroid, protrudes into the anterior and posterior chambers, and abuts and minimally displaces the lens dorsally. The ventral iris is not evident. (Photo courtesy of: National Institutes of Health, https://nih-cbstp.nci.nih.gov/)

Laboratory Results:
N/A

Microscopic Description:
Expanding the anterior uvea, effacing the iris, and markedly expanding the suprachoroidal space is a densely cellular, unencapsulated neoplasm of neuroepithelial cells. Neoplastic cells are arranged in variably dense sheets and as palisading columnar cells surrounding a central lumen (Flexner-Wintersteiner rosettes) or surrounding eosinophilic fibrillar material (Homer-Wright rosettes) surrounded by collagenous and occasionally myxomatous stroma. Neoplastic cells are polygonal to fusiform, have a high nuclear to cytoplasmic ratio, and have distinct cell borders. The nuclei are round to ovoid, finely stippled, and have indistinct nucleoli. There are 16 mitoses in 10 high power fields and anisokaryosis is mild. The neoplastic cells are impinging upon the optic nerve, which has multifocal axonal degeneration and is infiltrated by a population of histiocytes, lymphocytes, and plasma cells, as well as scattered foci of hemorrhage. The retina has multifocal, disorderly components of viable photoreceptor and retinal ganglion cells, dense necrosis, glial scarring, and

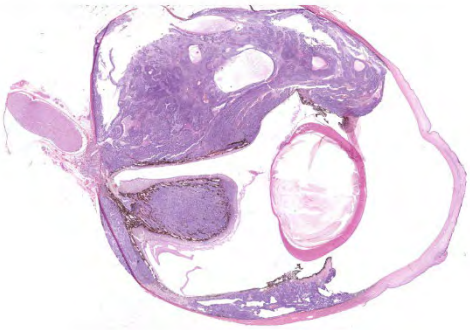

Figure 1-2: Globe, cat. A densely cellular neoplasm expands and effaces the choroid, uvea, and infiltrates the ciliary body and iris. (HE, 10X)

presumed Mueller cells. The retina is diffusely detached and lacks apparent retinal vessels. The retinal pigment epithelial cells have multifocally migrated through to the inner layers of the retina. The cortical lens fibers are moderately liquefied and homogenous and there is posterior migration of the lens epithelium, consistent with cataractous change. The corneal epithelium has marked, segmental ulceration and the outer corneal stroma in this area is mineralized with occasional breaks and is densely compact with fibrosis. Multifocally throughout the corneal stroma are areas of fibrosis, vascularization, and scattered neutrophils.

Contributor's Morphologic Diagnoses:
Eye: Medulloepithelioma, Cataractous change, Ulcerative and neutrophilic keratitis, Stromal fibrosis and mineralization, Diffuse, severe retinal atrophy, Suspect avascular retina, Moderate optic nerve degeneration and necrosis

Contributor's Comment:
Medulloepitheliomas are congenital neoplasms classified as primitive neuroectodermal tumors. They are derived from embryonal neural tissue, the tissue that forms the inner layer of the neural cup. Medulloepitheliomas are categorized into teratoid and nonteratoid forms and further categorized into benign and malignant.[8]

The most common presentation for this tumor is a young animal with a clinically identified intraocular mass. Despite their embryological etiology, medulloepitheliomas have been identified in older animals and age alone is not a disqualifying feature. They have been described primarily in dogs and horses and rarely in other species, including cats, rabbits, and llamas.[2,3,4]

Medulloepitheliomas classically present grossly as white to tan masses that fill the posterior chamber. The hallmark feature of primitive neuroectodermal tumors is the formation of rosettes. This tumor forms both Flexner-Wintersteiner rosettes (characterized by the formation of a central lumen) and Homer-Wright rosettes (characterized by the lack of central lumen and may surround eosinophilic fibrillar material).[10] Importantly, the formation of both rosettes is found in other primitive neuroectoderm tumors and is not unique for medulloepitheliomas. Retinoblastoma is a similar primitive neuroectodermal tumor and must be differentiated histologically from medulloepitheliomas. In retinoblastomas, although they may occasionally have both types of rosettes, Flexner-Wintersteiner rosettes are often the dominant type. While retinoblastomas are common ocular tumors in young children, there are very few accounts of this diagnosis in veterinary species.[5] Characteristically, rosettes in a medulloepithelioma are often large, multi-layered and lined by cuboidal cells arranged in a right angle to the lumen. There is pronounced neuroepithelial tubule formation, a distinguishing characteristic not found retinoblastomas. Medulloepitheliomas have been described more robustly in veterinary species, and the presence of large, multilayered, Flexner-Wintersteiner and Homer-Wright rosettes ultimately led to the diagnosis of medulloepithelioma in this case.

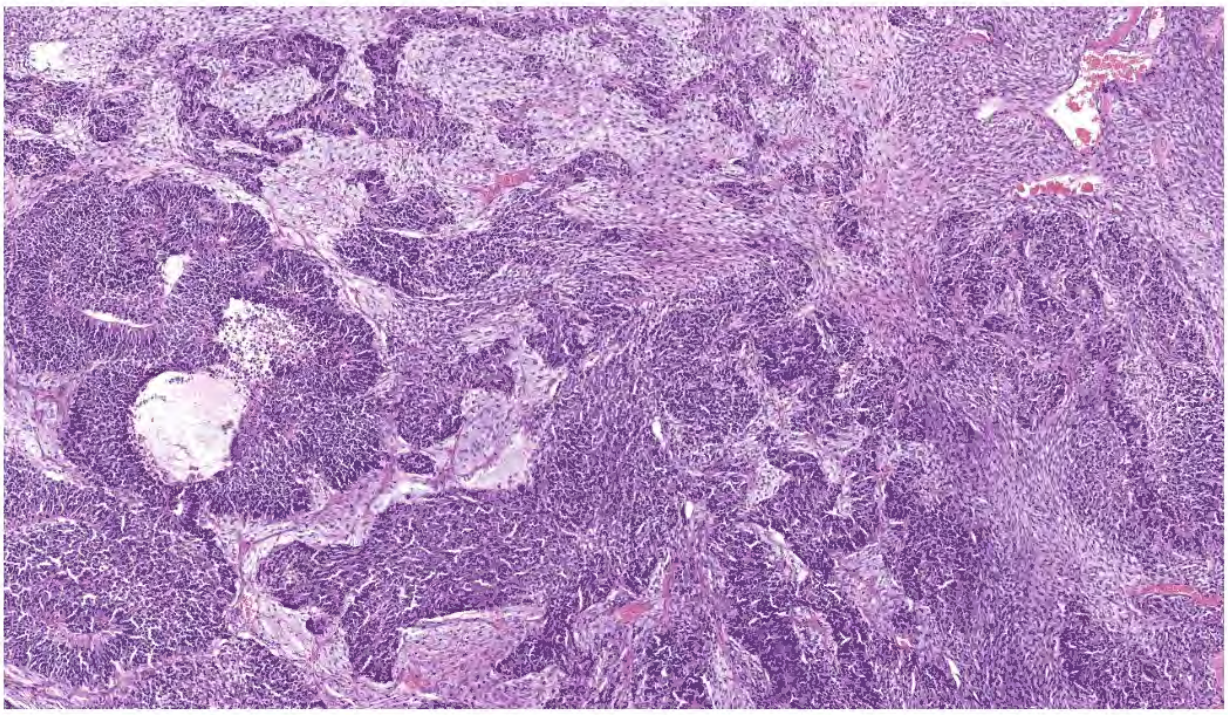

Figure 1-3: Globe, cat. The neoplasm is composed of sheets and trabeculae of palisading neuroepithelial cells which often are separated by loosely arranged myxomatous stroma. (HE, 105X)

Medulloepitheliomas are classified as benign or malignant. Criteria for malignancy set forth by Zimmerman *et al.* include poor differentiation, sarcomatous change, increased mitotic rate or nuclear pleomorphism, and invasion into other structures such as the sclera or uveal stroma.[1] In most veterinary cases with continued follow-up, malignancy was rare. In all cases, enucleation is the preferred treatment method.

Contributing Institution:
National Institutes of Health, Comparative Biomedical Scientist Training Program (CBSTP), 37 Convent Drive, Bldg. 37, Rm. 2002, Bethesda, MD 20892
https://nih-cbstp.nci.nih.gov/

JPC Diagnoses:
Globe, choroid, ciliary body, and iris: Medulloepithelioma.

JPC Comment:
This week's conference was moderated by MAJ Kelsey Fiddes, former Training Officer at the Joint Pathology Center. Two of today's entities (Cases 1 and 2) are new to the Wednesday Slide Conference and provided excellent discussion amongst participants. The conference kicked off with a review of the gross orientation of the eye and how to determine which aspect of the eye contains a lesion (i.e. dorsal, ventral, lateral, medial, etc. A few key features to assess for orientation are the position of the optic nerve, which tends to exit the eye in a ventromedial direction the location of the tapetum lucidum, which is located in the dorsal fundus in dogs, the location of the ciliary arteries (located dorsolaterally and ventromedially from the optic nerve), the dorsal oblique muscle , which is located dorsally and exiting medially from the globe, and the ventral oblique muscle, which is ventrolateral on the globe and exits medially.

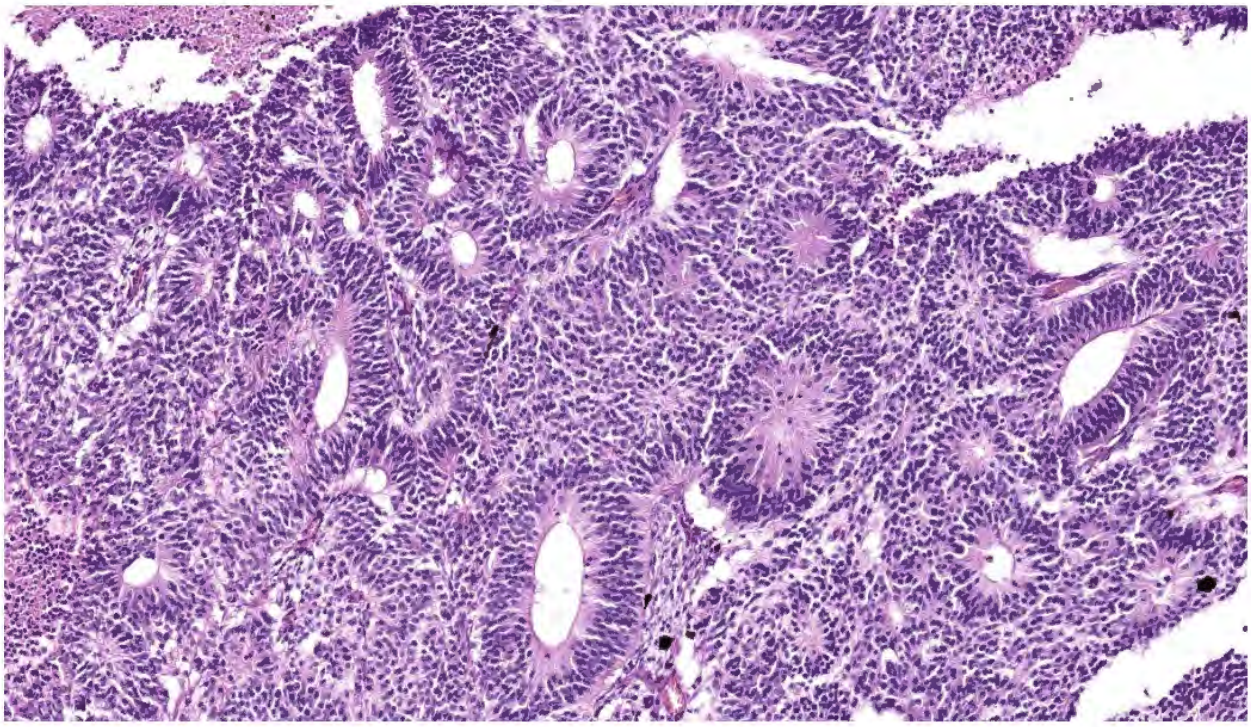

Figure 1-4: Globe, cat. Neoplastic cells form numerous rosettes, some with empty lumina (Flexner-Wintersteiner) and some with lumina that contain neurofilaments (Homer-Wright). (HE, 233X)

Gross preparation of an eye for histopathology was also reviewed and can be summarized as, for standard eye preparation, a vertical cut perpendicular to the ciliary arteries just offset from the optic nerve will provide the best cut for evaluating both tapetal and non-tapetal sides of the choroid. This is especially important for the evaluation of some disease processes, such as tapetal-sparing glaucoma. However, some species require a horizontally oriented cut to ensure that certain structures, such as the pectin in birds or the fovea and macula in some non-human primates, are included in section.

A review of the most pertinent, "board-worthy" basics of feline intraocular neoplasms was performed in the form of a "Jeopardy!" with some feline-centric, pun-based category titles, such as "Meow-lignancy" and "Pathology Purr-view." The major takeaways are: iridociliary tumors can co-express both vimentin and cytokeratin; the most common intraocular malignancy of cats is feline diffuse iris melanoma; neoplastic transformation of lens epithelium, as well as the migration of neoplastic cells to cover the inner circumference of the globe, occurs in feline post-traumatic ocular sarcoma; and the most frequently diagnosed orbital tumor of cats is the feline restrictive orbital myofibroblastic sarcoma.

Lastly, there was much discussion on the extensive secondary changes seen in this eye histologically, including keratitis and panuveitis. It is the opinion of conference participants that these changes were likely secondary to the medulloepithelioma and, as such, favored a traditional JPC morphologic diagnosis in such cases which is limited to the tumor and anatomic locations within the globe. This is not to say that the secondary changes are unimportant or should not be listed, but in true JPC

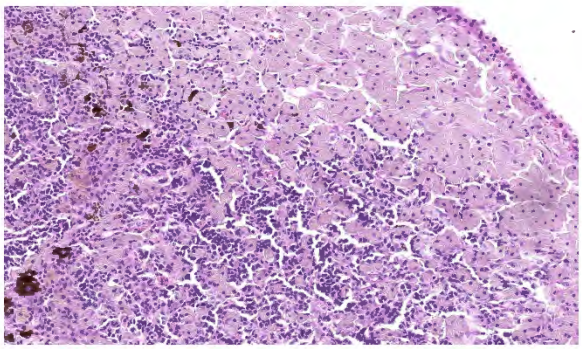

Figure 1-5: Globe, cat. The neoplasm elevates and infiltrates the tapetum lucidum; reflective rodlets are entrapped within the neoplasm. (HE, 305X)

tradition, changes secondary to a tumor are not included in the morphologic diagnosis.

The naming of the medulloepithelioma has a rather storied history. It was first called "carcinome primitif" by French doctors A. Badel and F. Lagrange in their 1892 article titled, "Carcinome primitif des procès et du corps ciliaire" (meaning "Primitive carcinoma of the processes and ciliary body"). These two individuals are credited with the first description of this neoplasm and are considered foundational in ophthalmologic and embryologic pathology. In 1904, a doctor named F. Verhoeff renamed it "teratoneuroma" due to the various tissues seen within the neoplasm in some cases.[9] In 1908, Dr. E. Fuchs decided to call it "diktyoma" after the Greek word "*diktyon*", meaning "net", secondary to the interlacing bands of neuroepithelial cells and meshwork of medullary epithelial cords seen histologically.[9] It wasn't until 1931 that the term "medulloepithelioma" made its way to the scene, coined by Dr. R. Grinker, in reference to the histological resemblance of the tumor to the neuroepithelium of the embryonic neural tube, which is now considered one of the main diagnostic features of this neoplasm.[9]

Intraocular medulloepitheliomas arise from the primitive medullary epithelium of the inner layer of the optic cup. This structure normally develops into the retina, iris, and ciliary body epithelium. This neoplasm most commonly forms in the non-pigmented epithelium of the ciliary body but can rarely originate from the retina or optic nerve. In dogs and cats, intraocular medulloepitheliomas most often follow the playbook and arise from the ciliary body neuroepithelium, but in horses, they tend to go off-book and originate from the optic nerve head.[7] Medulloepitheliomas are classified as either benign or malignant, and teratoid or non-teratoid. The teratoid form, as the name would imply, contains tissues that are not present within the normal eye (e.g., cartilage, bone, brain tissue, or muscle). In the conference case, due to the presence of primitive retinal tissue and neuropil within the neoplasm, conference participants favored a "teratoid" classification for this neoplasm.

Each of the common locations of the intraocular medulloepithelioma represents places where the closure of the optic cup and choroid fissure (also known as the optic stalk fetal fissure) last occur and where the final differentiation of the last multipotent neuroepithelial

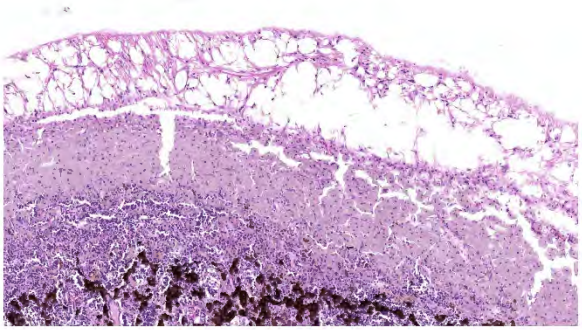

Figure 1-6: Globe, cat. The retina is detached and severely atrophic, with severe loss of nuclei in all layers of the retina, marked loss of nerve fibers and retinoschisis. (HE, 315X)

progenitor cells happens.[6] The optic cup forms from invagination of the optic vesicle, which buds from the developing diencephalon. When the optic vesicle contacts the overlying surface ectoderm, this induces the surface ectoderm to thicken and form the lens placode.[6] Both the lens placode and the underlying optic vesicle begin to invaginate. The invaginating optic vesicle collapses in on its internal space, forming a two-layered optic cup. The outer layer of this optic cup develops into the retinal pigment epithelium (RPE), while the inner layer differentiates into the neural retina, eventually forming the light-sensing rods and cones.[6] The invagination progresses dorsally to ventrally, creating a gap on the ventral surface of the optic cup and stalk called the optic fissure, which is crucial for the development of the optic nerve and other structures. Mesenchymal tissue, mostly from neural crest cells, enters the developing eye through the optic fissure and forms the hyaloid artery, which provides crucial blood supply.[6] The two edges of the optic fissure then fuse together, a process that starts near the optic stalk and moves cranially.[6] This closure is critical for normal

eye development and generally occurs around day 25 in fetal dogs and day 21 in fetal cats under normal conditions. Failure of the optic fissure to close can result in conditions such as coloboma formation.

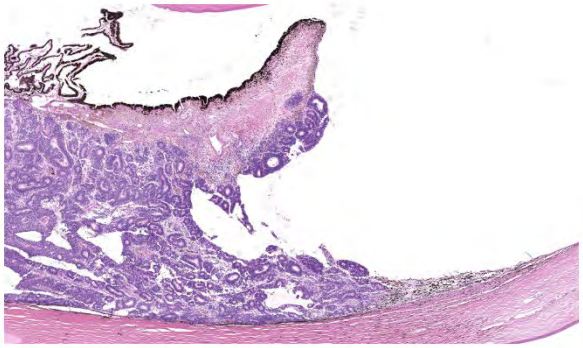

Figure 1-7: Globe, cat. The neoplasms efface the drainage angle and carpets and infiltrates the anterior surface of the iris. (HE, 43X)

Although not considered hereditary, current studies indicate that medulloepitheliomas may be linked to certain genetic mutations that disrupt embryonic development. In some cases, medulloepithelioma formation has been associated with germline mutations in the DICER1 gene, which is involved in microRNA processing (hello, Gen Path).[9] Others may feature somatic mutations in the KMT2D gene, which plays an important role in histone methylation.[9] These genetic changes interfere with the normal differentiation of primitive neuroectodermal stem cells, causing them to develop into a neoplasm instead of their mature, specialized tissues.

References:

1. Broughton WL, Zimmerman LE. A Clinicopathologic Study of 56 Cases of Intraocular Medulloepitheliomas. *American Journal of Ophthalmology*. 1978; 85(3):407-418.
2. Eagle RC Jr, Font RL, Swerczek TW. Malignant medulloepithelioma of the optic nerve in a horse. *Vet Pathol.* 1978;15(4):488-94.
3. Langloss JM, Zimmerman LE, Krehibiel JD. Malignant intraocular teratoid medulloepithelioma in three dogs. *Vet Pathol.* 1976;13(5):343-52.
4. Monk CS, Craft WF, Abbott JR, et al. Clinical behavior of intraocular teratoid medulloepithelioma in two-related Quarter Horses. *Vet Ophthalmol*. 2017;20(6):551-559.
5. Peiffer RLJr, Simons KB. Ocular Tumors in Animal and Humans. Iowa State University Press, 2002, 1st Edition.

6. Rosen D, Mahabadi N. Embryology, Optic Cup. [Updated 2023 May 1]. *StatPearls*. Treasure Island (FL): StatPearls Publishing; 2025. Available from: https://www.ncbi.nlm.nih.gov/books/NBK545150/.
7. Salih A, Moore D, Giannikaki S, Scurrell E. Malignant ocular teratoid medulloepithelioma in two cats. *J Comp Pathol.* 2023;201:10-12.
8. Saunders T, Margo CE. Intraocular medulloepithelioma. *Arch Pathol Lab Med*. 2012;136(2):212-216.
9. Tadepalli SH, Shields CL, Shields JA, Honavar SG. Intraocular medulloepithelioma - A review of clinical features, DICER 1 mutation, and management. *Indian J Ophthalmol*. 2019;67(6):755-762.
10. Wippold FJ 2nd, Perry A. Neuropathology for the neuroradiologist: rosettes and pseudorosettes. *AJNR Am J Neuroradiol*. 2006;27(3):488-92

CASE II:

Signalment:
11-month-old Toy Poodle, Female Spayed

History:
The patient presented for left hindlimb lameness which was localized to the left hip. Radiographs were most consistent with a diagnosis of Legg–Calvé–Perthes disease. The patient underwent a femoral head osteotomy, and the tissue was submitted for histopathology.

Gross Pathology:
A photograph of the femoral head taken immediately post operatively. The femoral head is misshapen with a focal region of flattening and indentation adjacent to the ligamentum capitis

Figure 2-1: Pelvic radiograph, dog. Pre-operative ventrodorsal radiograph of the hips showing bone loss, osteolysis and a severely misshapen left femoral head. (Photograph courtesy of: Murdoch University, www.murdoch.edu.au/theanimalhospital/services/pathol

femoris. Orientation was not provided with the gross image.

Laboratory Results:
Pre-operative VD radiograph of the hips showing bone loss, osteolysis and a severely misshapen left femoral head.

Microscopic Description:
Femoral head: Affecting approximately 30-50% of the epiphysis from the subchondral aspect of the articular cartilage to the physis, there is a focally extensive area of osteonecrosis characterized by bony trabeculae which are irregular and brightly eosinophilic with loss of differential staining. There is loss of both osteocytes within lacunae and osteoblasts lining trabeculae in this region. Along the margins of the necrotic area, multiple bone trabeculae are fragmented and/or have scalloped margins with osteoclasts in Howship's lacunae (osteolysis). The intertrabecular spaces within and at the periphery of the necrotic area contain variably amounts of amorphous eosinophilic matrix (fibrin), occasional neutrophils and mac-

rophages and/or loosely arranged myxomatous to collagenous matrix with variable numbers of plump spindle cells and capillaries (fibroplasia). Occasionally, there are also finer, irregular trabeculae of paler staining or partially mineralized bone (woven bone). Adjacent viable trabeculae are lined by numerous active osteoblasts (remodeling) and are sometimes laced with wavy basophilic lines (resting / resorption lines). The articular cartilage is fragmented (likely artifact).

Contributor's Morphologic Diagnoses:
Osteonecrosis, focally extensive, chronic with fibroplasia and bone remodeling; femoral head.

Contributor's Comment:
The signalment, clinical history, radiographic findings and histopathology are most consistent with a diagnosis of avascular necrosis of the femoral head, also known as Legg-Calvé-Perthes Disease or Osteonecrosis of the femoral head.

Avascular necrosis of the femoral head (ANFH) is a well-recognized condition which occurs most frequently in small breed dogs, including miniature poodles, West Highland White terriers and Yorkshire terriers.[3] This condition is heritable in these breeds and there is evidence to support an autosomal recessive mode of inheritance.[2,3] Most affected individuals present between 3 and 13 months of age with unilateral hindlimb lameness.[2] The condition is bilateral in approximately 12-17% of cases.[2] A significant percentage of dogs have concurrent patellar luxation which can complicate diagnosis, particularly as radiography lacks sensitivity in detecting early cases.[2,7]

Figure 2-2: Femoral head, dog. The femoral head is misshapen with a focal areas of flattening and indentation adjacent to the ligamentum capitis femoris. (Photograph courtesy of: Murdoch University, www.murdoch.edu.au/theanimalhospital/services/pathology-services)

ANFH is not always a heritable condition. In humans and dogs ANFH can be broadly categorized as non-traumatic or traumatic, and within those categories, as pediatric or adult.[5] Traumatic cases are typically associated with femoral neck fractures; this should be excluded clinically in affected dogs.[3,5] In humans, although most 'non-traumatic' cases of ANFH are deemed idiopathic, there is typically some metabolic disorder which underpins the disease, with alcoholism and steroid administration among the most common in adults.[5] A number of experimental animal models have examined the pathophysiology of

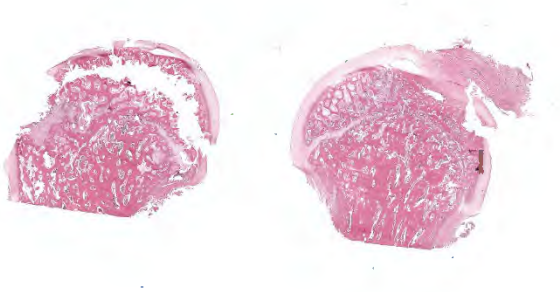

Figure 2-3: Femoral head, dog. Two sections of the femoral head are submitted for examination. (HE, 12X)

osteonecrosis because there remains no consensus on an optimal approach for treatment in humans.[4]

Although ANFH is often labelled 'idiopathic', it is well understood that vascular compromise and subsequent ischemia of the bone are involved in the pathogenesis in both humans and animals.[3,4,5,6] The underlying cause or trigger of vascular compromise is varied, particularly in affected human adults with underlying metabolic disease.[5] In young, small breed dogs with heritable ANFH it is postulated that the development of the vascular supply of the femoral head contributes to the condition.[3] In normal, crossbred dogs the blood vessels supplying the femoral head are gradually incorporated into fibro-osseous canals during development and as such are well protected by the surrounding bone.[3] In Miniature poodles, which are highly susceptible to the heritable, juvenile form of ANFH, the incorporation of these vessels is delayed or does not occur completely.[3] As a result, even a slight increase in intraarticular pressure can result in venous occlusion and subsequent ischemic injury.[3] Joint effusion due to transient episodes of synovitis or minor trauma could trigger the condition in predisposed individuals.[2,3]

The gross and microscopic pathology varies depending on the chronicity of the disease at the time of diagnosis.[1,3] Early on, the shape and structure of the femoral head are grossly and radiographically normal. Histologically, there may be evidence of osteonecrosis predominantly within the subchondral bone at this stage.[1] With chronicity, if the area of necrosis is large enough, the necrotic bone collapses which causes flattening of the femoral head (Figure 1) which eventually results in a degenerative arthropathy.[1,3]

Contributing Institution:
Murdoch University Pathology Services.
www.murdoch.edu.au

JPC Diagnoses:
Femur, epiphysis: Osteonecrosis, chronic, focally extensive, moderate, with osteolysis, woven bone, fibrosis, and bony remodeling.

JPC Comment:
The contributor of this case gives an excellent overview of this condition.

Most of conference discussion was centered on pathogenesis and key histologic features of

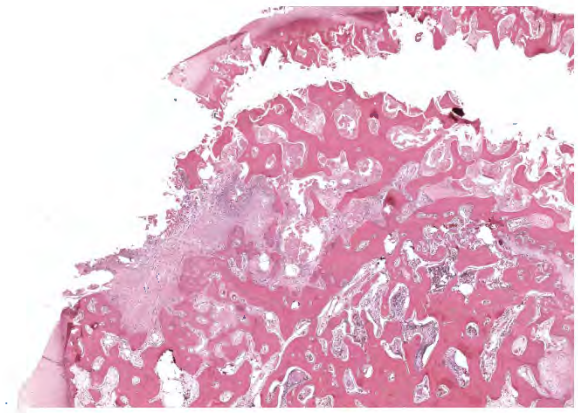

Figure 2-4: Femoral head, dog. There is a focally extensive area of bone loss within the femoral epiphysis. Peripheral to the area of osteonecrosis, trabeculae spaces are filled with variably cellular areas of fibrosis. (HE, 27X)

this condition. This disease can be, as stated by the contributor, either hereditary or secondary to trauma or other ischemic event.[1,3,4,5,6] The hereditary form is most often seen in young, small breed dogs, such as terriers, dachshunds, pugs, Chihuahuas, and toy poodles. When looking at this case, there are a few histologic clues that can assist in determining the age of this animal, which can help with reaching the correct diagnosis. These include the presence of discontinuous physeal cartilage and the horizontal orientation of the bony spicules deep to the physis. In dogs, physes typically close around 10 months of age. Physis closure in Legg-Calves-Perthes disease (LCPD) is typically delayed secondary to ischemia of the physeal cartilage and the subchondral bone, which can result in a malformed or improperly angled femoral head.[1] Additionally, in young animals, the bony spicules that extend into the metaphysis from the developing stages of the growth plate are oriented vertically (perpendicular) to the growth plate to facilitate the elongation of the bone. In older animals that have closed physes, the bone below the growth plate becomes oriented horizontally (parallel) to the growth plate, effectively "capping" it to facilitate closure of the physes. In this case, the bone has become horizontally oriented below the growth plate, indicating that this animal should have closed physes at this stage, but the presence of and discontinuity of the lingering growth plate indicate that this young animal is likely experiencing delayed physeal closure.

There are three recognized grades of LCPD and include: Grade 1, defined as necrosis of bone with empty lacunae, lack of viable bone marrow, and normal articular chondrocytes.

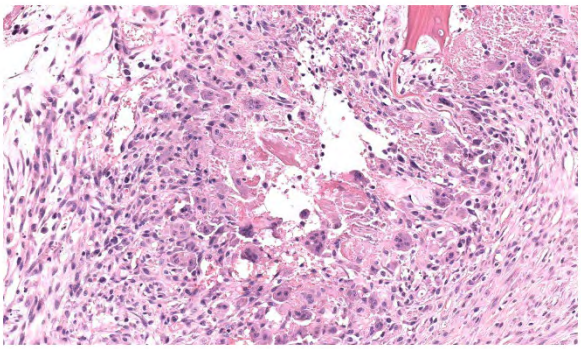

Figure 2-5: Femoral head, dog. In areas of osteonecrosis, fragmented and hypereosinophilic fragments of necrotic bone are surrounded by numerous macrophages, osteoclasts, and cellular debris against a background of fibroblasts and maturing collagen. (HE, 312X)

Grade II, characterized by cracks in the articular cartilage, subchondral bone collapse, and flattening of the femoral head with re-vascularization coming in from the periphery of the epiphysis +/- granulation tissue development; and Grade III, in which the articular cartilage is highly deformed with folds and cracks and the femoral head loses its shape.[1]

In the early stages (Grade I) of LCPD, the articular cartilage is spared because of its avascular nature.[1,3,5] The subchondral bone, however, will become necrotic, and there is frequently a characteristic "tideline" of hypereosinphilia between the unaffected articular cartilage and the affected subchondral bone.[3,5] As the condition progresses, however, the joint is subjected to altered conductive forces from abnormal weight-bearing, which places excessive pressure upon the articular surface and ultimately results in articular cartilage loss.[1,5] This results in both the flattening of the femoral head from mechanical collapse and in asymmetrical growth between the affected limb and unaffected limb, as this disease is usually unilateral.[5] Additionally, secondary to the altered conductive forces through the joint,

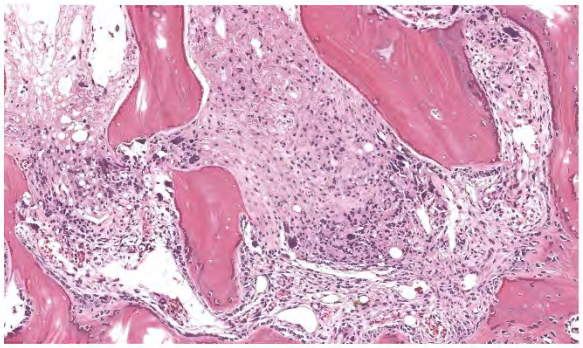

Figure 2-6: Femoral head, dog. Peripheral to the areas of osteonecrosis, there is loss of osteoclasts lining remnant bony trabeculae, and intertrabecular spaces contain abundant variably mature fibrous connective tissue populated with fibroblasts, macrophages, and scattered osteoclasts. (HE, 202X)

new woven bone begins proliferating in an attempt to re-stabilize the bone and adjust for the altered force conduction.[1] This woven bone is usually seen flanking either side of an area of lamellar bone to create a "sandwich" effect.

Differentiating necrotic bone from normal bone can be challenging, but one of the key features to look for is the loss of osteocytes from lacunae.[5] Osteocytes either become pyknotic and hypereosinophilic or disappear entirely, and you can best convince yourself this is a real change (and not just a staining artifact) by comparing an area of suspected necrosis to an area of less affected or normal bone where the osteocytes will still be in their lacunae and have a nice, basophilic nucleus. Another useful way to determine osteonecrosis is to assess the bone marrow. In necrotic bone, there is usually histologic loss of marrow elements secondary to ischemia, which will manifest as a loss of differential staining with retention of architecture within the marrow.

References:

1. Aguado E, Goyenvalle E. Legg Calvé Perthes disease in the dog. *Morphologie*. 2021;105:143-147.
2. Cardoso CB, Rahal SC, Mamprim MJ, Oliveira HS, Merlchert A, Coris JGF, dos Reis Mesquita L. Avascular necrosis of the femoral head in dogs-retrospective study. *Acta Scientiae Veterinariae*. 2018;46:5-5.
3. Craig LE, Dittmer KE, Thompson KG. Bones and joints. Jubb, Kennedy & Palmer's pathology of domestic animals. 2015;1:16-163.
4. Fan M, Peng J, Qin L, Lu S. Experimental animal models of osteonecrosis. *Rheumatology International.* 2011;31:983-994.
5. Guerado E, Caso E. The physiopathology of avascular necrosis of the femoral head: an update. *Injury*. 2016;47:S16-S26.
6. Kerachian MA, Harvey EJ, Cournoyer D, Chow TY, Séguin C. Avascular necrosis of the femoral head: vascular hypotheses. *Endothelium*. 2006;13:237-244.
7. Mapuvire T. Legg-Calvé-Perthes Disease in the Dog: A Case-Based Review. *South African Veterinary Association*. 2023.
8. Vasseur PB, Foley P, Stevenson S, Heitter D. Mode of inheritance of Perthes' disease in Manchester terriers. *Clinical Orthopaedics and Related Research*. 1989;244:281-292.

CASE III:

Signalment:

17-year-old, female (spayed), domestic long hair, Felis catus, feline.

History:

Patient presented with uveitis OU, OD greater than OS. Significant corneal edema and increased intraocular pressure (IOP) recorded

OD. Uveitis seemed to respond to medical therapy, but IOP did not. Enucleation performed OD and submitted for determination of etiology of uveitis.

Gross Pathology:
Intact globe OD submitted with no gross evidence of intraocular neoplasm.

Laboratory Results:
N/A

Microscopic Description:
Eye: Overlying the corneal endothelium, anterior and posterior iris, portions of the lens epithelium, and the inner surface of the retina, as well as effacing and replacing the ciliary body, and occluding the drainage angle is an unencapsulated, densely cellular, infiltrative, neoplasm composed of epithelial cells arranged in broad dense cords on a moderate fibrovascular stroma. Neoplastic cells are polygonal with distinct cell borders, pronounced intercellular bridging, a moderate amount of pale eosinophilic cytoplasm, and irregularly round to vesiculate nuclei, with up to three distinct nucleoli. Anisocytosis and anisokaryosis is moderate. The mitotic rate is high with up to 12 mitotic figures per ten 40x HPF. Multifocally, neoplastic cells exhibit squamous differentiation. Near the optic nerve, the neoplastic cells invade the vascular and fibrous tunics, elevating and dissecting beneath the retinal pigment epithelium under a detached and coiled degenerate retina. At the caudal interior surface of the globe, there are numerous neutrophils admixed with abundant eosinophilic cellular and karyorrhectic debris and neoplastic cells infiltrate into the retinal vasculature.

Contributor's Morphologic Diagnoses:
Eye: Squamous cell carcinoma, domestic long hair, *Felis catus*, feline.

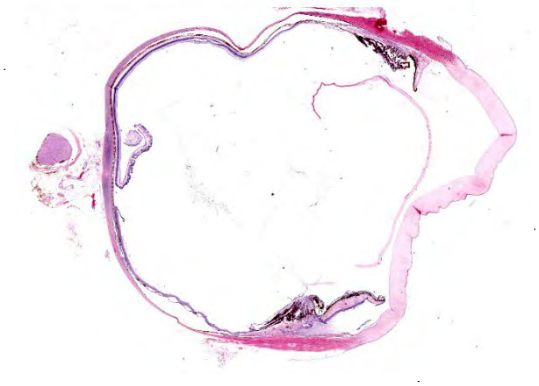

Figure 3-1: Globe, cat. At subgross magnification, the globe appears subjectively enlarged with thinned fibrous tunics. Most of the lens is missing, with only the anterior capsule in section. (HE, 7X)

Contributor's Comment:

Generally, neoplasms within the globe may be (1) primary (arising from one of the intraocular tissues), (2) secondary (invading the globe from an adjacent tissue), or (3) metastatic (arising via hematogenous dissemination of a distant malignancy).[2] Many ophthalmic tumors are histologically benign but are locally invasive and, within the confined space of the eye or orbit, can produce significant tissue distortion.[5]

Surgical definitions which may be relevant when communicating with clinicians include: *evisceration*, which is the removal of the cornea and the internal contents of the eye while leaving the scleral shell of the globe and eye muscles behind; *enucleation*, which is the removal of the entire globe while leaving muscles that control eye movement and other orbital contents intact; and *exenteration*, which is the total removal of the globe and all surrounding tissues including eyelids, muscles, nerves and fatty tissues from the orbit.

Primary intraocular neoplasia. Uveal melanocytic neoplasia ("diffuse iris melanoma" in

Figure 3-2: Globe, cat. The choroid and ciliary body are expanded and infiltrated, the drainage angle is effaced, and both the anterior and posterior aspects of the iris are carpeted by a moderately cellular epithelial neoplasm. (HE, 55X)

cats and "canine anterior uveal and epibulbar melanoma/melanocytoma" in dogs) is the most common primary intraocular neoplasm, occurring roughly three times as frequently as ciliary body epithelial neoplasms in dogs and ten times as frequently as ciliary body epithelial neoplasms in cats.[1-2,5] This neoplasm typically originates on the anterior surface of the iris, producing multifocal areas of pigmentation with a high potential for local invasion into the ciliary body and the iridocorneal angle.[5] Common presenting clinical signs in affected cats includes hyperpigmentation of the iris, pupillary deficits, buphthalmia resulting from secondary glaucoma, and evidence of uveitis.[5] Extension posteriorly to affect the choroid is rare.[5] Anterior uveal melanocytomas and melanomas may extend along the anterior or posterior scleral emissaria into and through the sclera to involve the periocular tissues, and the optic nerve provides routes of egress for neoplasms in the posterior pole, but extraocular extension does not always correlate with a poor prognosis.[2] Only malignant uveal melanomas and schwannomas in dogs and diffuse iris melanoma and ocular sarcomas in cats carry significant metastatic risk.[2] The regional lymph nodes, liver, and lungs are the principal sites for melanoma metastasis.[5] Other primary intraocular neoplasms are uncommon and include posttraumatic sarcomas of cats and rarely other species such as the rabbit, schwannomas of blue eyed dogs, astrocytomas, and primary neuroectodermal neoplasms including medulloepitheliomas and retinoblastomas in varied animal species.[2] With few exceptions, the majority of primary intraocular neoplasms remain restricted to the globe and timely enucleation is curative.[2] As the globe lacks lymphatics, metastasis from the intraocular tissues will be hematogenous and occurs either through the scleral venous

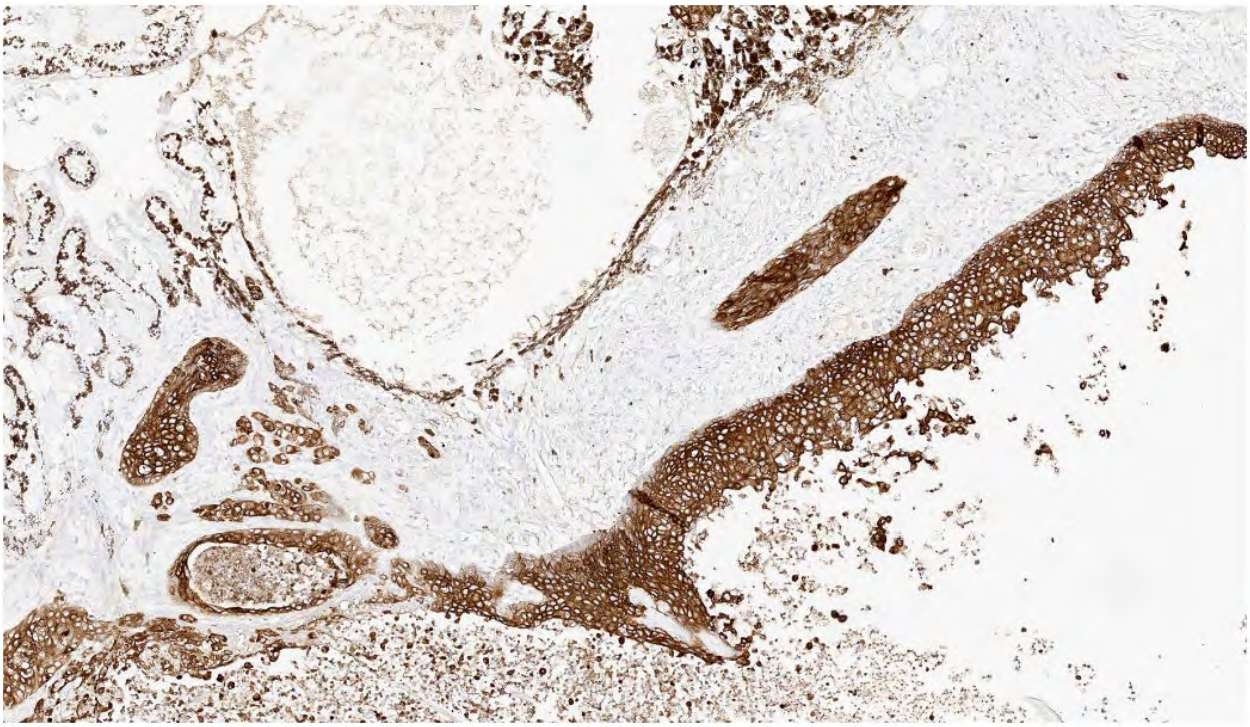

Figure 3-3: Globe, cat. Neoplastic epithelial cells demonstrate strong cytoplasmic positivity for cytokeratin. (anti-AE1/AE3, 55X)

plexus subsequent to invasion of the trabecular meshwork and sclera, or tumor invasion of the uveal and retinal vasculature.[1-2]

Secondary intraocular neoplasia. Aggressive malignancies of adjacent tissues may invade the eye and uvea through the cornea, sclera, or optic nerve.[2] Scant descriptive literature is available; secondary neoplasia is most commonly encountered with squamous cell carcinoma of cow, horse, and cat, and nasal adenocarcinomas with orbital extension in dogs.[2,4] A myxosarcoma involving the optic disc was most likely an extension from the orbit and optic nerve.[2] Meningiomas of the optic nerve may extend through the lamina cribrosa into the globe.[2] Other feline orbital neoplasms include zygomatic osteoma, parosteal osteoma, osteosarcoma, fibrosarcoma, undifferentiated sarcoma, and rhabdomyosarcoma.[4]

Metastatic intraocular neoplasia. It is not surprising that the extensive vascular network of the uvea renders it a prime site for metastatic disease from primary malignancies elsewhere; incidence of metastasis to the eye is less than primary uveal neoplasms but more frequent than implied by the scant literature as the majority of animals dying of widespread metastatic disease are not subjected to thorough ophthalmic clinical, postmortem, and histopathologic examinations.[2] Intraocular lymphosarcoma is the most common metastatic neoplasm in the dog and cat, with shared clinical and histopathologic presentations.[1,2,4] In dogs, these neoplasms occurred bilaterally, predominantly in the anterior uvea, and were diffuse large B-cell, T-lymphoblastic, peripheral T-cell not otherwise specified, and lymphocytic B-cell lymphomas.[1] In cats, feline leukemia virus (FeLV)-associated T-cell lymphoma was the most common.[1] Mammary carcinoma was the second most common ocular metastatic neoplasm in bitches, with a predominantly unilateral involvement of the

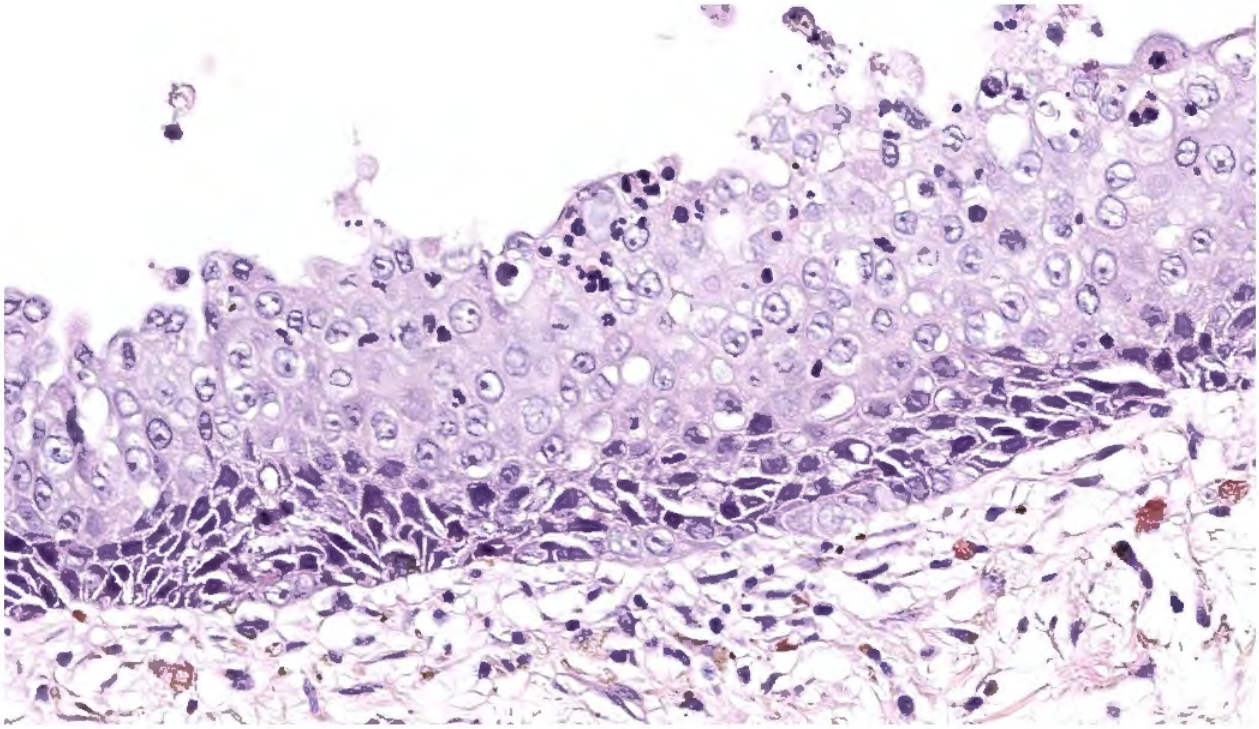

Figure 3-4: Globe, cat. On the anterior surface of the iris, neoplastic squamous epithelium vaguely recapitulates normal maturation with a basal-like layer and multiple layers of additional non-keratinizing squamous epithelium on top. Few neutrophils infiltrate the neoplasm. (HE 730X).

uveal tract.[1] Clinically and by gross examination, intraocular lymphosarcoma is a masquerader and may manifest as unilateral or bilateral uveitis, keratitis, retinal detachment, intraocular hemorrhage, and glaucoma, with or without observable proliferative lesions.[2,4] Not uncommonly, the ocular manifestations may be the presenting sign of occult systemic disease and globes are frequently enucleated due to complicating factors but with a suspicion of intraocular neoplasia.[2,4] Typical ocular presentation of lymphosarcoma in cats is a nodular iridal mass.[3] The question "does unicentric intraocular lymphoma exist" often has been asked, and the response is "probably not," with disease developing elsewhere over time.[2] Additional feline tumors that are known to metastasize to the eye include fibrosarcoma, squamous cell carcinoma, mammary adenocarcinoma, uterine adenosarcoma, and adenocarcinomas of undetermined origin.[4] In cats, following lymphoma, pulmonary and squamous cell carcinomas were the most common multicentric/metastatic neoplasms of the eyes.[1] Pulmonary carcinoma is unusual in its capacity to colonize the vascular endothelium of choroidal retinal arteries.[4] Individual cases of cholangiocarcinoma, hemangiosarcoma, and chemodectoma in the dog, as well as individual cases of mammary gland cribriform carcinoma, salivary gland carcinoma, and histiocytic sarcoma in the cat have been reported.[1]

Conclusion. It is a common belief among specialists in veterinary and human ocular pathology that squamous cell carcinoma cannot originate from within the globe. (J.S. Estep, personal communication; December 26, 2019) Therefore, finding squamous cell carcinoma within the globe of a living patient should prompt the pathologist to warn clinicians to

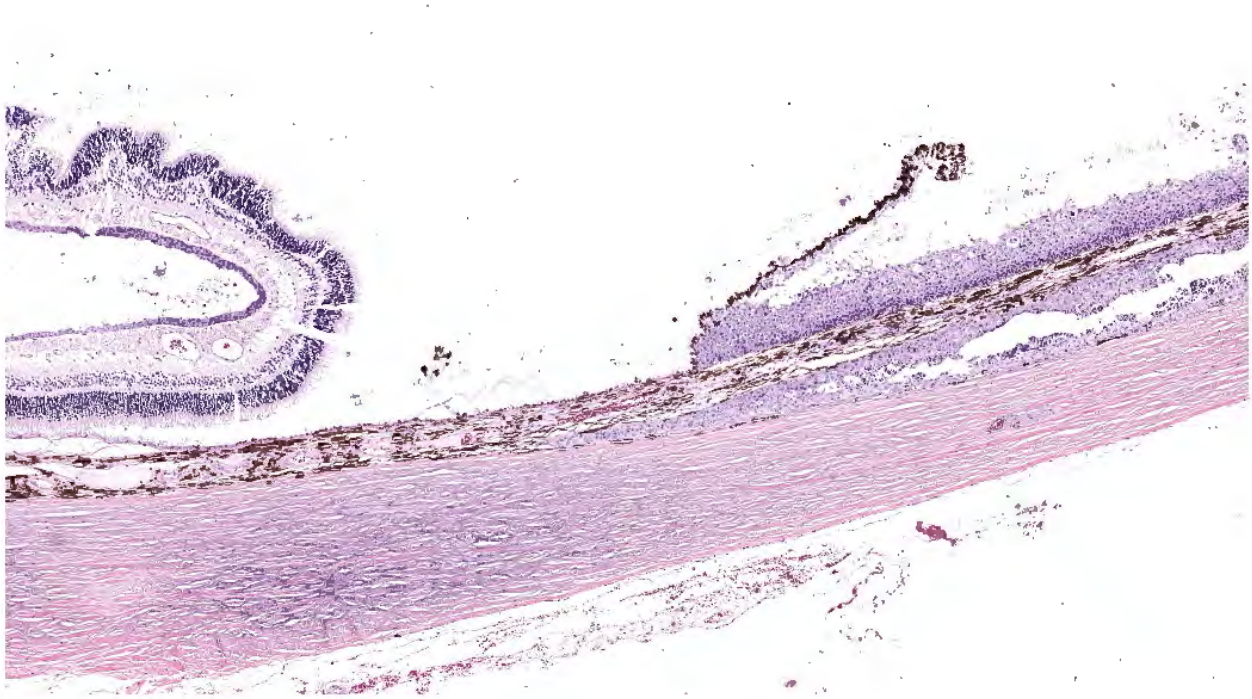

Figure 3-5: Globe, cat. At the back of the eye, the neoplasm infiltrates the choroid and beneath the retinal pigmented epithelium (right), and the retia. (HE 730X).

perform a thorough search for the primary neoplasm elsewhere.

Contributing Institution:
Texas Veterinary Pathology Associates
https://texasvetpath.com/index.htm

JPC Diagnoses:
Globe: Metastatic carcinoma.

JPC Comment:
This case contributor gives a thorough review of intraocular neoplasms in cats, touching on many major points of discussion during review of this case. Conference participants were readily able to reach a diagnosis of metastatic carcinoma, but not all were convinced that this was a metastatic squamous cell carcinoma (SCC) due to the lack of dyskeratosis within neoplastic epithelial cells, coupled with the lack of a primary mass found during workup. The prominent intercellular bridging between the neoplastic cells was noted by all, which can be a major feature of SCC; and squamous cell carcinomas are common tumors of the feline head; however other participants felt strongly that they could not rule out a carcinoma of other origin based on histology alone. For this reason, a morphologic diagnosis of "metastatic carcinoma" was ultimately favored by participants in this case due to the lack of clear-cut evidence of a squamous cell carcinoma on the H&E.

There was no argument to be found on whether this was primary or metastatic, as the histologic evidence was strongly supportive of a metastatic process (i.e., the neoplasm primarily found within the highly vascular choroid and uvea, intravascular neoplastic cell emboli, etc.). The secondary changes in the eye were also discussed and it was concluded that this eye had glaucoma secondary to the neoplasm, evidenced by the retinal ganglion cell degeneration and loss with tapetal sparing,

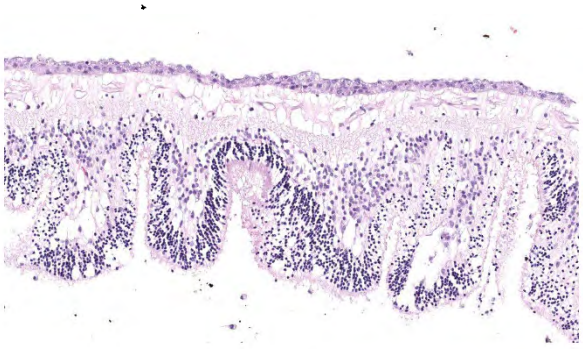

Figure 3-8: Globe, cat. The detached area of the retina demonstrates marked atrophy with almost total loss of ganglion cells, loss of nuclei in the inner and outer nuclear layers, and loss of nerve fibers and photoreceptors. The inner surface of the retina is carpeted with multiple layers of neoplastic squamous epithelium. (HE 307X).

occlusion of the drainage angles by both the neoplasm and inflammation, buphthalmia (enlarged globe, attenuated and degenerative corneal epithelium, scleral thinning), and perivascular edema of the aqueous veins that drain the trabecular meshwork of the drainage angle.

During conference, yet another opportunity arose to briefly discuss common intraocular neoplasms of cats. Key nuggets from this discussion include the fact that cats can develop primary uveal schwannomas similar to those seen in blue-eyed dogs, the most common metastatic neoplasm of the eye in cats is lymphoma, and most other metastatic tumors to the eye in cats are carcinomas that most often affect the posterior uvea.[1,2]

In keeping with her "games" theme, MAJ Fiddes put participants through a few rounds of "I Spy" during this case, focused entirely on the pancytokeratin (AE1/AE3) immunohistochemical stain run on this case and a few issues spotted therein. The first issue was that, while the neoplastic cells had strong cytoplasmic immunoreactivity to pancytokeratin, the retinal pigmented epithelium (RPE) was diffusely unreactive. As it turns out, RPE is specifically reactive for CK8/18, and the pancytokeratin cocktail used by the JPC does not include these. Instead, CK8/18 is offered as a stand-alone IHC here, and its absence in the pancytokeratin would explain why the RPE was not reactive. The second issue was that the neural fibers of the optic nerve had diffuse reactivity to pancytokeratin. That's weird, why would neural tissue be reactive to cytokeratins? Well, as fate would have it, it's not. Pancytokeratin and GFAP are cross-reactive. GFAP is not cross-reactive with most individual cytokeratins, but is to pancytokeratin, making neural tissue appear immunoreactive to AE1/AE3![3] Between AE1 and AE3, it is the AE3 component specifically that contributes to this cross-reactivity.[3] This has been demonstrated in brain and glial tissues, as well as in some retroperitoneal schwannomas. As such, interpretation of cytokeratin expression in neural tissue, including neoplasms of neural origins, should be cautiously interpreted.[3] This "I Spy" game was a poignant reminder that pathologists should scrutinize IHCs and ensure good external and internal control prior to reading them out, and knowledge of what reacts to what can be critical to appropriate interpretation.

References:

1. Bandinelli MB, Viezzer Bianchi M, Wronski JG, et al. Ophthalmopathologic characterization of multicentric or metastatic neoplasms with an extraocular origin in dogs and cats. *Vet Ophthalmol*. 2020;23(5):814-827.
2. Grahn B, Peiffer R, Wilcock B. Intraocular neoplasia. In: *Histologic Basis of Ocular Disease in Animals*. 1st ed. Hoboken, NJ: Wiley-Blackwell; 2019:409,433,435-436.

3. Kriho VK, Yang HY, Moskal JR, Skalli O. Keratin expression in astrocytomas: an immunofluorescent and biochemical reassessment. *Virchows Arch.* 1997;431(2):139-47.
4. La Croix NC. Ocular manifestations of systemic disease in cats. *Clin Tech Small Anim Pract*. 2005;20(2):121-128.
5. Willis AM, Wilkie DA. Ocular oncology. *Clin Tech Small Anim Pract*. 2001;16(1):77-85.

CASE IV:

Signalment:
10-week-old male mixed-breed puppy (*Canis familiaris*, dog)

History:
The body of a 10-week-old mixed breed puppy was received for post-mortem examination. The pup died unexpectedly on a commercial airline flight from the Dominican Republic to Canada. The pup was travelling in a cage in the passenger cabin.

Gross Pathology:
There was mild generalized icterus of mucous membranes and soft tissues. The spleen was enlarged and meaty in texture on cut section. The liver was pale. The renal cortices were dark red-grey, and the urinary bladder contained red-tinged urine.

Laboratory Results:
Fresh-frozen lung was submitted to the Vector-Borne Disease Lab at North Carolina State University for PCR analysis for *Babesia, Anaplasma, Bartonella, Ehrlichia, Rickettsia,* and Hemotropic *Mycoplasma spp.* PCR was positive for *Babesia vogeli*.

Microscopic Description:
Alveolar septa are mildly thickened and hypercellular, and contain increased numbers of macrophages, rare neutrophils, and small

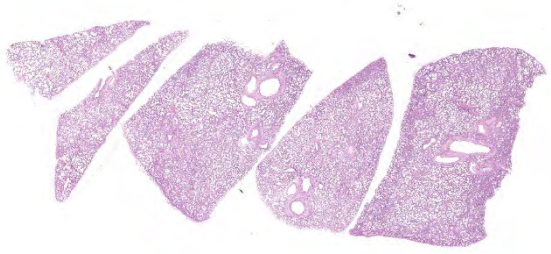

Figure 4-1: Lung, dog. Five sections of lung are submitted for examination. At subgross magnification, the lungs are mildly atelectatic and alveolar septa are thickened and hypercellular. (HE, 8X)

quantities of fibrin (occasionally suspicious for capillary fibrin thrombi). Alveolar lumens contain increased numbers of free-floating macrophages, very rare neutrophils, and protein-rich fluid. Most intravascular erythrocytes contain small (1-3 micron) intracytoplasmic basophilic bodies, most visible in alveolar capillaries around the periphery of the histologic sections. Giemsa stains accentuate these small round faintly vacuolated organisms within erythrocytes.

Contributor's Morphologic Diagnoses:
Generalized histiocytic and neutrophilic alveolitis with multifocal capillary thrombosis and intravascular, intraerythrocytic parasites (Babesia vogeli)

Contributor's Comment:
Babesia spp. are tick-transmitted, apicomplexan, hemoprotozoan parasites. They are closely related to *Cytauxzoon spp*. and *Theileria spp*., and these three genera are termed piroplasmids. *Babesia spp*. was initially identified as a hemoparasite of cattle in Romania in 1888, causing hemoglobinuria, a syndrome termed "Red Water Fever". Soon after, similar organisms were identified in cattle in Texas, and today *Babesia spp*. are recognized worldwide as tick-borne parasites of wild and domestic ruminants, equids, pigs, dogs, and

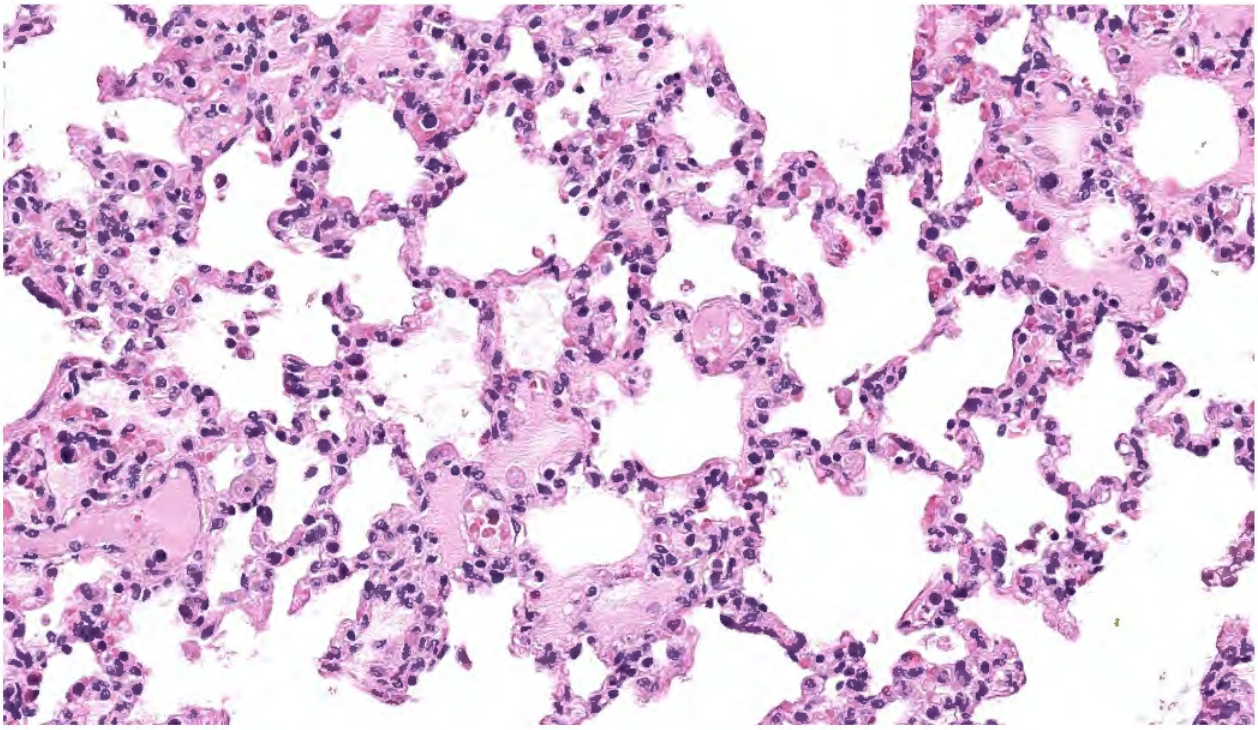

Figure 4-2: Lung, dog. Alveolar septa are markedly thickened by congestion, edema, and fibrin, and are hypercellular as a result of hypertrophy of septal macrophages, circulating neutrophils, and infiltration of the septa by additional macrophages and neutrophils. Alveoli contain edema fluid, protein, and foamy macrophages. (HE, 476X)

cats[8]. Internationally, these parasites are of economic concern due to their impact on livestock health and productivity. Humans are also susceptible to *Babesia spp*., including *B. microti, B. venatorum, B. divergens, B. duncani, B. divergens*, and other unnamed *Babesia spp.*, and human transmission has also been documented horizontally, or via blood transfusion[7].

Dogs have been reportedly infected with *B. vogeli, B. conradae, B. gibsoni, B. vitali, B. rossi, B. canis*, and unspeciated *Babesia* spp[7]. Original studies classified canine *Babesia spp*. based on morphology, with larger (3-5 micron) forms named *B. canis*, and smaller (1-3 micron) forms named *B. gibsoni*. However, it was suspected based on differences in pathogenicity that *B. canis* was heterogeneous, and with the advent of molecular diagnostic techniques, at least four small and four large *Babesia* parasites have been identified. *B. canis* was reclassified into three separate species (*B. canis, B. vogeli, B. rossi*)[5]. *Babesia vogeli* is transmitted by the Brown Dog tick (*Rhipicephalus sanguineus*) and has a wide endemic range throughout tropical and subtropical regions of the world, occasionally extending into cooler latitudes[5].

In dogs, clinical babesiosis varies from mild to severe forms, manifesting as hemolysis and secondary systemic hypoxic and inflammatory organ injury, organ dysfunction, shock, and death[1]. The severity of clinical disease varies with a number of factors, including parasite species, and host age, immune status, and the presence of concurrent infection. The least pathogenic species recognized is *B. vogeli*, the

most virulent is *B. rossi*. While *B. vogeli* more frequently subclinical, it is notably more pathogenic in puppies younger than 3-4 months[5]. A number of mechanisms have been implicated for the parasite-mediate hemolysis, including direct parasite-mediated injury, osmotic fragility of infected erythrocytes, oxidative stress, and secondary immune-mediated cell membrane injury, resulting in mixed intravascular and extravascular hemolysis[5].

Common hematologic abnormalities include anemia, thrombocytopenia, and variable leukopenia or leukocytosis. Serum biochemical abnormalities include increased activity of aspartate aminotransferase and alanine aminotransferase, hyperbilirubinemia, hypoalbuminemia, and variable electrolyte and acid-base imbalances. Eichenberger *et al.* reported that the prognosis of clinically ill dogs infected with *Babesia canis* was negatively impacted by hyperlactatemia, leukopenia, hyperphosphatemia, hypertriglyceridemia, and hypoproteinemia[1]. Similarly, prognosis for *B. rossi* infection has been found to be impacted by hyperlactatemia, hypoglycemia, clinically compromised circulation/consumptive coagulopathy, and increased serum cortisol[1].

Preliminary diagnosis of acute clinical Babesiosis typically requires evaluation of blood smears, usually using Giemsa or Wright's stain. The likelihood of diagnosis, particularly with large *Babesia* spp., may be improved through specific evaluation of blood smears from capillary beds (ear tips, toenail) or evaluation of cells beneath the buffy coat of a hematocrit tube. In chronic cases, parasitemia may be minor and intermittent, making blood smear diagnosis more challenging[5].

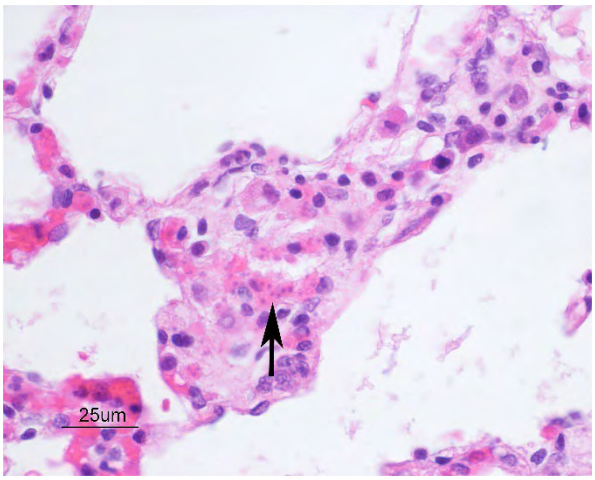

Figure 4-3: Lung, dog. Erythrocytes contain small (1-3 micron) intracytoplasmic basophilic bodies (arrow).(Photo courtesy of: Animal Health Laboratory, University of Guelph, http://www.guelphlabservices.com/AHL/) (HE, 600X)

PCR, immunofluorescence, and ELISA testing have also improved the rate of diagnosis of babesiosis, and PCR testing has become the principle means of diagnosis and species determination[5]. However, false negative results may be seen in cases of chronic babesiosis because of limitations similar those of blood smear diagnosis, and detection of chronic/carrier animals often requires repeated testing and use of complimentary testing methods[2,6].

Importation of domestic dogs to Canada from other countries is becoming more common, though this is not well-tracked and reliable statistics are not available. This pattern of importation provides a risk of infectious diseases being imported along with them, and because some of these pathogens depend on environments or vectors not found in Canada, recognition may be delayed. However, because of the presence of competent tick vectors in some regions of Canada, the importation of dogs with babesiosis may provide a risk for disease

transmission to local dog populations. Hemotropic parasites such as *Babesia, Anaplasma, Mycoplasma, Bartonella, Ehrlichia*, and *Rickettsia* spp. should be considered as possibly subclinical infections in imported dogs, and blood testing (including review of blood smears) prior to importation of dogs from endemic areas is recommended to reduce the risk of establishing infection within Canadian tick populations.

Contributing Institution:
Animal Health Laboratory, University of Guelph, Guelph, Ontario, Canada
http://www.guelphlabservices.com/AHL/

JPC Diagnoses:
Lung: Pneumonia, interstitial, histiocytic and neutrophilic, subacute, diffuse, moderate, with intraerythrocytic piroplasms.

JPC Comment:
MAJ Fiddes chose this case specifically because it was going to be a diagnostic challenge. The intraerythrocytic piroplasms of *Babesia sp.* are quite difficult to see until you find one and got an eye for them within erythrocytes; then, they were much easier to spot. A few participants were successful in finding these small parasite. Along with discussion on the basics and life cycle of *Babesia sp.*, which the contributor's comment beautifully covers, conference goers participated in a matching game of other boards-worthy infectious hemotropic agents of note. These agents and their matching facts included *Anaplasma sp.*, which may infect platelets, *Theileria sp.*, which infect leukocytes and are another genus of piroplasm, *Mycoplasma sp.*, which tend to reside in an epicellular location, and *Cytauxzoon felis,* yet another piroplasmid and one that has a bobcat reservoir host.

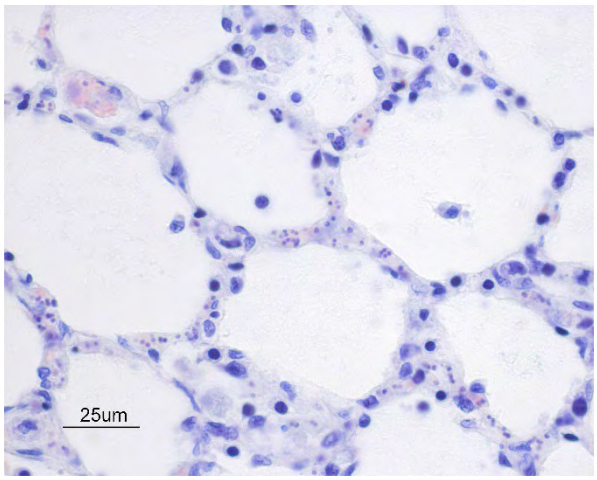

Figure 4-4: Lung, dog. A Giemsa stain helps delineate the punctate intracytoplasmic intraerythrocytic inclusions.(Photo courtesy of: Animal Health Laboratory, University of Guelph, http://www.guelphlabservices.com/AHL/) (Giemsa, 600X)

Babesia sp. are apicomplexan piroplasmid protozoans that infect erythrocytes in numerous species, ultimately lysing infected red blood cells (RBCs) and resulting in intravascular hemolysis within the host. As mentioned,

by the contributor, there are several species of *Babesia* that infect dogs, and there is a wide range of severity in the clinical manifestations amongst these. The focus here will primarily be on *Babesia canis,* which infects dogs, and *Babesia bovis*, the species responsible for most *Babesia* infections in cattle and has a substantial amount of research behind it.

Most of the virulence factors that *Babesia* is equipped with are responsible for survival and pathogenicity. Like other apicomplexans, *Babesia's* virulence factors are generally secreted to the host cell surface, where they structurally remodel and biochemically modify the infected RBC's ability to interact with specific host proteins in an effort to promote their own survivability. The most notable of

these numerous virulence factors is the Virulence, Evasion, and Secretion-associated (VESA) proteins. VESA is responsible for inhibiting the binding of infected erythrocytes to endothelial cells, as well as reversing the binding of already-adhered erythrocytes.[3,7] This ensures that, when the piroplasms have reproduced via binary fission and are ready to lyse the infected red cell, that they will remain within the vasculature to be picked up by a tick vector.

VESA proteins cluster on the surface of erythrocyte within ridges that are structurally induced by *Babesia*.[3] The number of ridges increases as the piroplasmids grow and multiply within the erythrocyte.[3] With VESA being expressed on the surface of infected red cells, the immune system should be able to locate and target those cells for antibody-mediated immune response, right? Yes, but no. *Babesia bovis* has demonstrated that it can express antigenic variants of VESA through epigenetic alterations and/or genomic recombination at the locus of active transcription that is responsible for the production of VESA proteins.[3,7] This alters the VESA protein enough antigenically to become a constant moving target for immune cells, contributing to the chronic and recurrent nature of babesiosis.[3] It is yet another prime example of the evolutionary arms race between infectious agents and immune cells, and it is currently speculated that many other virulent *Babesia sp* can perform the same epigenetic alterations to their VESA antigens.

There was some discussion on the presence of megakaryocytes within the affected lung sections in this case. Megakaryocytes can be present normally in low numbers in the lungs or can be seen in increased numbers secondary to an immune response. Megakaryocytes normally function to produce platelets, and a single megakaryocyte can make them by the thousands. In an immune response, though, megakaryocytes display an impressive range of functions related to pathogen recognition, antigen presentation, and inflammatory modulation.[4] Lung megakaryocytes, specifically, express higher levels of pathogen recognition receptors (PRRs), specifically, toll-like receptors (TLRs) and C-type lectin-like receptor (CLEC). Lung megakaryocytes also sense and uptake pathogens, can release a gamut of inflammatory cytokines, function as antigen-presenting cells, and participate in immune responses against pathogen invasion.[4] Because of their wide range of functions and key physiologic roles, megakaryocytes are sometimes referred to as an "omnipotent" cell type.[4] In this case, it was the opinion of conference participants that the megakaryocytes were likely present due to the inflammation and protozoal infection due to the higher-than-expected number seen within section.

References:

1. Eichenberger RM, Riond B, Willi B, Hofmann-Lehman R, Deplazes P. Prognostic markers in acute Babesia canis infections. J Vet Intern Med. 2016;30:174-182.
2. Goo Y, Jia H, Aboge GO, et al.. Babesia gibsoni: Serodiagnosis of infection in dogs by an enzyme-linked immunosorbent assay with recombinant BgTRAP. *Exp Parasitol.* 2008;118:555-560.
3. Hakimi H, Yamagishi J, Sakaguchi M, Fathi A, Lee JS, Verocai GG, Kawazu SI, Asada M. ves1α genes expression is the major determinant of Babesia bovis-infected erythrocytes cytoadhesion to endothelial cells. *PLoS Pathog*. 2025; 21(4):e1012583.

4. Hua T, Yao F, Wang H, Liu W, Zhu X, Yao Y. Megakaryocyte in sepsis: the trinity of coagulation, inflammation and immunity. *Crit Care.* 2024;28(1):442.
5. Irwin PJ. Canine babesiosis: from molecular taxonomy to control. *Parasit Vectors*. 2009;2(suppl 1):1-9.
6. Jefferies R, Ryan UM, Jardine J, et al. Babesia gibsoni: Detection during experimental infections and after combined atovaquone and azithromycin therapy. *Exp Parasitol.* 2007;117:115-123.
7. Schetters T. Mechanisms Involved in the Persistence of *Babesia canis* Infection in Dogs. *Pathogens*. 2019;8(3):94.
8. Schnittger L, Rodriguez AE, Florin-Christensen M, Morrison DA. Babesia: A world emerging. *Infect. Genet Evol*. 2012;12:1788-1809.
9. Uilenberg G. *Babesia* – A historical perspective. *Vet Parasitol*. 2006;138:3-10.

Joint Pathology Center
Veterinary Pathology Services

WEDNESDAY SLIDE CONFERENCE 2025-2026

Conference #9 — 22 October 2025

CASE I:

Signalment:
3 months-old, female, Piétrain x Large White, pig, *Sus scrofa domesticus*

History:
Two pigs were purchased from a commercial pig breeder and housed in a research facility where a planned necropsy was carried out as part of an experimental procedure. Both animals showed skin lesions unrelated to the experimental design.

Gross Pathology:
Multiple, 1-2 mm in diameter, non-raised, red to blue, irregular lesions were found diffusely distributed through the skin of the ventral and inguinal regions well as the head, nose and ears. Upon incision, lesions were localized at the dermal/subcutaneous junction.

Laboratory Results:
Cells lining cystic cavities immunohistochemically stained positive with pan-cytokeratin and negative with CD31. Immunohistochemistry with Ki67 and alpha-SMA revealed a low proliferative index in the apocrine epithelial cells and strong positivity for alpha-SMA in the basal area of the cystic lesions.

Microscopic Description:
Haired skin (dorsal nose, three sections):

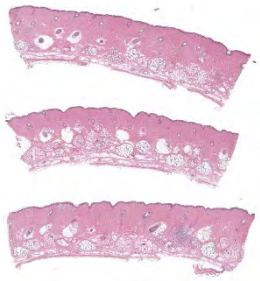

Figure 1-1: Haired skin, pig. Three sections of haired skin are submitted for examination. (HE, 7X)

Within the deep dermis and subcutis there are multiple well delineated clusters of variably distended apocrine glands with sinuous cystic cavities and partial tubular folding, which expand and replace dermal adipose tissue and muscle. Most of the clustered cysts are lined by a single layer of flattened columnar epithelial cells without apical blebbing. Adjacent smaller clusters of lesser distended glands exhibit one to several layers of more cuboidal epithelium. The outer layer of the cyst wall consists of thin layers of myoepithelial cells. Many gland lumina contain pale eosinophilic secretory products. Surrounding tissue and stroma comprise mild lymphoplasmacytic infiltrates.

Focally in the mid dermis and associated with a hair follicle there is a localized, well demarcated focus of moderate mixed cellular in-

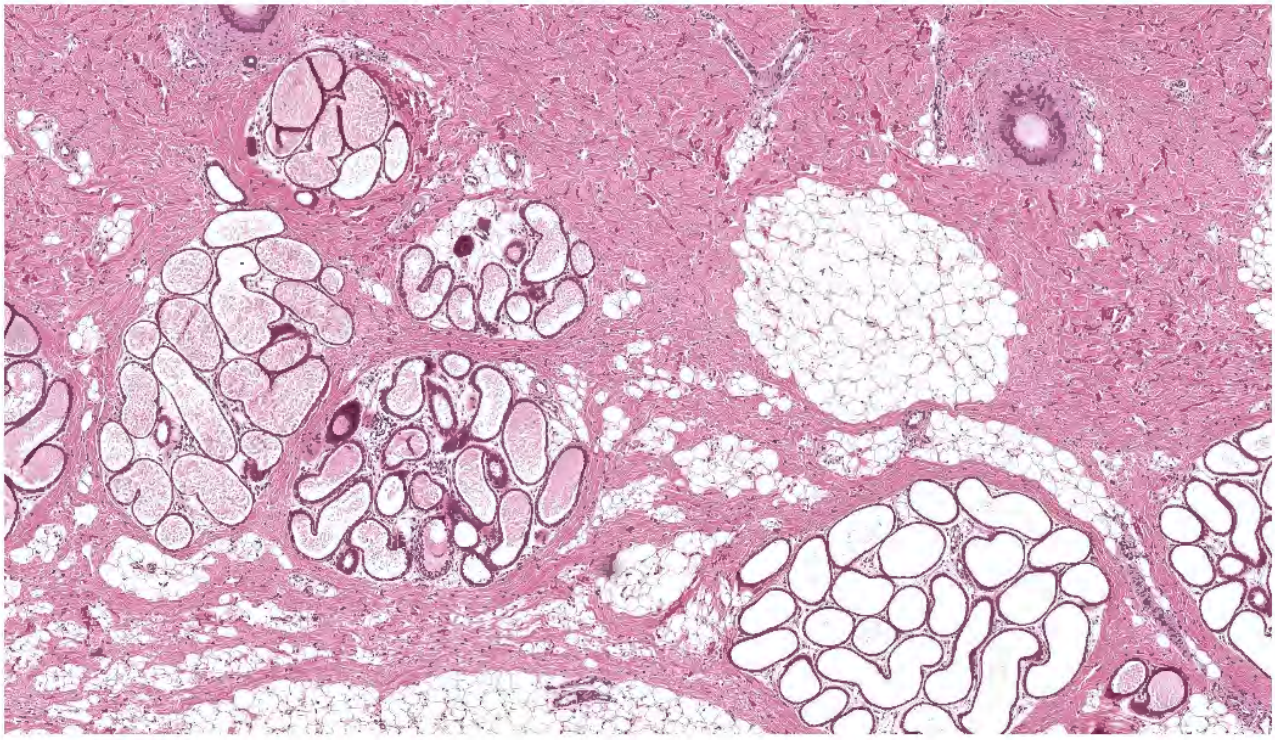

Figure 1-2: Haired skin, pig. Apocrine glands are diffusely and markedly dilated, some with retention of eosinophilic secretory product. (HE, 53X)

flammation composed of macrophages, neutrophils and lesser lymphocytes and plasma cells. These encase numerous distorted and/or ruptured apocrine glands, infiltrate their epithelium and are present within the lumen of remaining glandular structures (foreign body type reaction). Macrophages frequently contain cellular debris.

The remaining epidermis and dermis are unremarkable.

Contributor's Morphologic Diagnoses:
Skin: cystic distention of apocrine glands, diffuse, severe, with compression of adjacent muscle tissue consistent with cutaneous apocrine cystomatosis.

Skin: hidradenitis and dermatitis, focally extensive, moderate, chronic, mixed cellular with apocrine gland rupture (foreign body type reaction).

Contributor's Comment:
Cutaneous apocrine cystomatosis is an uncommon non-neoplastic condition, which has been first reported in three pigs from three different abattoirs in Spain in 2020.[6] There, the lesions appeared as brown, non-prominent nodules within the subcutaneous fat distributed over the entire dorsal region. Microscopically, the authors' findings correspond to results reported here. Ki67 immunohistochemistry showed only few glands with single cells of positive stained epithelium indicating a low proliferative index. In addition to the findings of Lopez-Figueroa et al. an inflammatory site was present in the case described here. This possibly occurs due to rupture of an adjacent dilated gland.

Cutaneous apocrine cystomatosis has also been reported in dogs and cats[4,9,10]. In dogs, it is mainly distributed over the head and neck

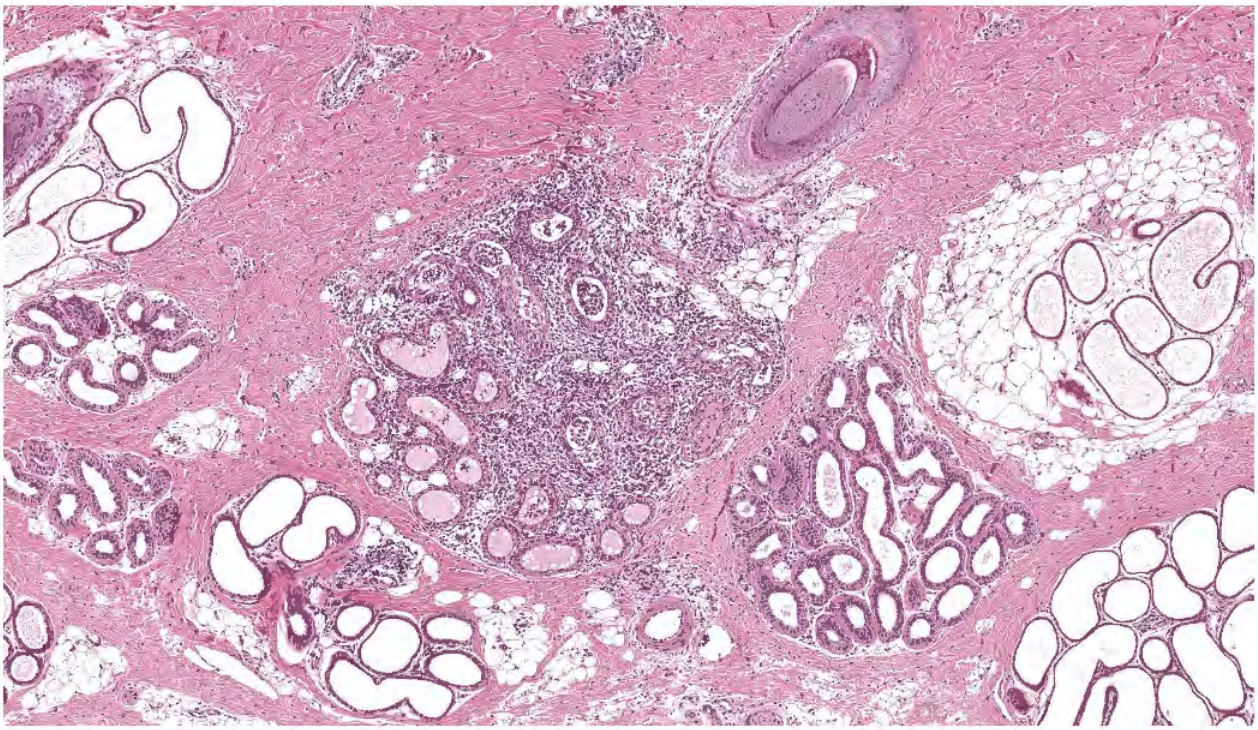

Figure 1-3. Haired skin, pig: Occasionally, rupture of dilated apocrine glands results in infiltration of moderate numbers of lymphocytes, plasma cells, macrophages, and neutrophils, which are often present within the lumina of dilated glands. (HE, 7X)

but was also described at the dorsal trunk and flanks as well as solitary at the cheeks. Microscopically, the lesions are described as multiple clusters of cystically dilated sweat glands, but, in contrast to the lesions in the pigs, show the same morphology as normal apocrine glands with a single layer of cuboidal to columnar epithelium with dome-shaped apical surface. In addition, the epithelial cells of the cyst wall in dogs show some pseudo-papillary projections protruding into the lumen. Inflammation and fibrosis in the surrounding tissue is rare and mild. In case of cyst rupture, moderate inflammation can occur comprising plasma cells, neutrophils and lymphocytes. Pale siderophages, which contain pigment from the iron content of apocrine secretions, may be found.

Feline ceruminous cystomatosis is the corresponding disorder described in cats.[4] The lesion develops from the ceruminous glands and occurs in the external ear and the inner pinna.[5] Microscopically, the cysts are lined by a single layer epithelium that varies from attenuated to cuboidal to columnar. In contrast to dogs and pigs, the surrounding dermis often shows mild fibrosis with detection of inflammatory cells like lymphocytes, neutrophils, mast cells and pigmented macrophages.

The etiology of cutaneous apocrine cystomatosis is uncertain. For dogs, a senile degenerative change has been discussed because affected animals were middle-aged or older. The average age in affected cats has been reported between 8 and 9.5 years, but animals as young as one year can be affected.[4] As all described cases in pigs were from abattoirs or, in our case, from experimental studies, and therefore

comparatively young (3 to 6 months), the disease in pigs seems to be unrelated to the aging process. A congenital origin is also discussed as normal apocrine glands are absent and no other alterations in the surrounding tissue are detectable.[6] Whether there is a genetic origin in dogs and cats is unknown.

In cats, there seems to be a breeding predisposition in Persian and Abyssinian cats with a slight male predominance, whereas in dogs and pigs no over-representation in certain breeds or sex predilection is described to date.[3]

The differential diagnosis of cutaneous apocrine cystomatosis includes apocrine hidrocystoma/cystadenoma, particularly described in cats, where it is predominantly located in the eyelid.[1,2] It is a benign neoplasm characterized by cysts with a single or multilayered cuboidal to columnar epithelium and true papillary projections into the cavity. These neoplasms usually show a higher proliferative index.

In humans, cutaneous apocrine cystomatosis has not been described. The related benign neoplasm is, corresponding to the differential diagnosis in animals, the apocrine hidrocystoma/cystadenoma, which includes a spectrum of benign cystic lesions of ductal sweat gland origin, with architecture ranging from simple cystic (hidrocystoma) to more complex (cystadenoma).[7]

Contributing Institution:
Ludwig-Maximilians-Universität München (LMU)
Institute of Veterinary Pathology
Veterinärstr. 13
80539 Munich
Germany
www.patho.vetmed.uni-muenchen.de

in cooperation with:

Technical University of Munich (TUM)
Institute of Pathology
Comparative Experimental Pathology (CEP)
Trogerstr. 18
81675 Munich
Germany
web.med.tum.de/path/vergleichende-experimentelle-pathologie

JPC Diagnoses:
Haired skin, apocrine glands: Dilation, chronic, diffuse, marked.

JPC Comment:
The JPC was fortunate enough to host Dr. Charles Bradley again this year for an excellent dermatopathology-focused conference that was preceded by his highly educational and forever crowd-pleasing "Approach to a Case Using Pattern Analysis" lecture. This first case was a great exercise in reminding the pathologist to not overinterpret histological findings. Participants are, rightfully so, primed to expect description-heavy cases in conferences. Every once in a while, though, a moderator selects a case that is on the leaner descriptive side to make this point: don't make a mountain out of a molehill and only describe what you see, not what you want to see. Participants did an excellent job adhering to this principle, and most were able to reach the correct diagnosis. The contributor in this case provided an excellent write-up of this lesion across species and it is well-worth the read.

Conference discussion for this case covered numerous topics, including the specific histologic findings that can assist the pathologist in

species identification based on skin. Dr. Bradley insists on this as part of his dermatopathology diagnostic process: look at the slide first, try to identify the species you have, and then check the case information. If they don't seem to match up, a call to the submitting clinician might be in order. For most porcine skin, the epidermis is thicker than other common species, usually 5-7 nucleated cells thick, and forms papillary, shallow rete pegs that project into and interdigitate with the superficial dermis.[8] This papillary epidermis is also a feature of human skin. Porcine skin is especially thick on the dorsum. Additionally, pig sebaceous glands are sparse and typically associated with hair follicles. Porcine hair follicles are, generally, large and far apart from one another.

Participants were asked to describe the difference between apocrine and eccrine glands and why they chose apocrine cystomatosis over eccrine cystomatosis. Histologically, apocrine and eccrine glands are indistinguishable, but location, which varies by species, can help with differentiation. In humans, eccrine glands are all over the body and responsible for sweat production, which aids in thermoregulation, whereas apocrine glands are restricted to the axilla and groin regions. In pigs, eccrine glands are restricted to the tip of the snout and to the carpal regions and serve no thermoregulatory function.[5] In dogs, eccrine glands are restricted to the paw pads and nose, and have limited sweating function.[5] Apocrine glands, however, are everywhere in pig skin and are, like the sebaceous glands, associated with hair follicles. The skin samples in this case were from the abdomen and dorsal nose, neither of which is an eccrine gland location in pigs. Differentiating between the two can be diagnostically important, especially in cases of neoplasia, as eccrine adenocarcinomas are considered more aggressive than apocrine adenocarcinomas.

There was brief discussion on the inflammatory component in this case. Mild inflammation of apocrine glands, known as hidradenitis, is a common background lesion in many species that is usually associated with folliculitis. In this case, the focus of inflammation was severe enough that it was unanimously thought by conference participants to be due to a ruptured apocrine gland secondary to dilation. There was a question posed to participants regarding possible other differentials based on gross images in other species, and included apocrine cystadenoma, basal cell adenoma, sebaceous adenoma, or melanocytic neoplasms. Of these, apocrine cystadenoma vs. apocrine cystomatosis was discussed most heavily for educational purposes, the main differences being that this lesion was diffuse throughout the skin, which is more common with cystomatosis, and there are no papillary projections into the lumens of affected glands. Papillary projections of epithelial cells into the cystic glandular lumen are a common finding in apocrine cystadenomas, but not in cystomatosis.[7] Wrapping up conference discussion of this case was a brief review of apocrine cystomatosis lesions in other species, which are discussed by the contributor in their comment.

Apocrine gland cystomatosis is also known as epitrichial sweat gland cystomatosis, apocrine cystic hyperplasia, and cystic hyperplasia of apocrine sweat glands (human and canine term).[6,10] When initially described in the medical literature, it was proposed that cyst formation might be due to the occlusion of excre-

tory ducts.[7,9] Later, it was suggested that apocrine cysts result from episodes of glandular hyperplasia followed by an involution phase and inability of the body to reabsorb the contents of the dilated glands.[7,9] More recently, though, single or multiple apocrine cysts have been described as either benign sweat gland tumors, as idiopathic, non-neoplastic, senile degenerative changes or, such as in this pig's case, as a congenital condition.[6,7,9]

References:

1. Cantaloube B, Raymond-Letron I, Regnier A. Multiple eyelid apocrine hidrocystomas in two Persian cats. *Vet Ophthalmol*. 2004;7:121-125.
2. Chaitman J, van der Woerdt A, Bartick TE. Multiple eyelid cysts resembling apocrine hidrocystomas in three Persian cats and one Himalayan cat. *Vet Pathol*. 1999;36:474-476.
3. Goldschmidt MH, Shofer FS. *Skin Tumors of the Dog and Cat*. Pp 280-283. Oxford: Pergamon Press;1992.
4. Gross TL. Sweat gland tumors. In: Gross TL, Ihrke PJ, Walder EJ. *Skin Diseases of the Dog and Cat: Cinical and Histopathologic Diagnosis*. 2nd ed., pp. 666-674. Oxford: Wiley-Blackwell 2008.
5. Jubb KVF, Kennedy PC, Palmer NC. *Pathology of Domestic Animals*. 6th ed., vol. 1, p718. Elsevier;2015.
6. Lopez-Figueroa C, Domingo M, Marti B, Vidal E, Segales J. Cutaneous apocrine cystomatosis in three slaughter-aged pigs. *J Vet Diagn Invest*. 2020;32:159-161.
7. Sangüeza OP, Cassarino DS, Glusac EJ. Benign tumours with apocrine and eccrine differentiation: Hidrocystoma/cystadenoma. In: Elder DE, Massi D, Scolyer RA. *WHO Classification of Tumours: Skin Tumours.* 4th ed.;2018.
8. Skydsgaard M, Dincer Z, Haschek WM, Helke K, Jacob B, Jacobsen B, Jeppesen G, Kato A, Kawaguchi H, McKeag S, Nelson K, Rittinghausen S, Schaudien D, Vemireddi V, Wojcinski ZW. International Harmonization of Nomenclature and Diagnostic Criteria (INHAND): Nonproliferative and Proliferative Lesions of the Minipig. *Toxicol Pathol*. 2021;49(1):110-228.
9. Stazi M, Silvestri S, Mechelli L, Brachelente C. A case of generalised cutaneous apocrine cystomatosis in a Pekingese dog. *Vet Med Sci*. 2022;8:450-453.
10. Vilafranca M, Domingo M , Roura X. Generalized Apocrine Cystomatosis in an Old English Sheepdog. *Veterinary Dermatology*. 1994;5:83-87.

CASE II:

Signalment:
12-year-old neutered male Pomeranian dog (*Canis lupus familiaris)*

History:
The patient has been presented for a specialistic dermatological examination due to the presence of blackish skin lesions scattered throughout the body, particularly severe in the abdomen, thigh, neck, and chest. Multifocal areas were characterized by severe alopecia. Licking of the groin area was reported. The patient has been treated with levothyroxine.

Gross Pathology:
Four skin biopsy punches from the abdomen, thigh, neck, and chest were received and processed.

Laboratory Results:
N/A

Microscopic Description:
Haired skin. All the biopsies are histologically similar. The superficial and mid dermis are obscured by a moderate to severe inflammatory infiltrate, often obscuring the dermo-epidermal junction. The inflammatory infiltrate is represented by a prevalence of lymphocytes and plasma cells, macrophages occasionally engulfing melanin (melanophages), and rare neutrophils. The epidermis is moderately thickened (irregular hyperplasia), with mild intercellular edema (spongiosis) and severe thickening of the stratum corneum by predominantly nucleated (parakeratotic hyperkeratosis) or less frequently non-nucleated keratin (orthokeratotic hyperkeratosis). Numerous apoptotic figures are observed throughout the epidermis, occasionally surrounded by lymphocytic satellitosis. Similar lesions are observed in the hair follicles. There is multifocal erosion or ulceration of the epidermis; the ulcerated areas are obscured by serocellular crusts.

Contributor's Morphologic Diagnoses:
MD: Haired skin. Lymphoplasmacytic interface dermatitis, diffuse moderate chronic, with epidermal hyperplasia, numerous suprabasal apoptosis with lymphocytic satellitosis, parakeratosis

ND: Hyperkeratotic erythema multiforme

Contributor's Comment:
Erythema multiforme (EM) denotes a disease histologically characterized by keratinocyte death (apoptosis) with lymphocytes satellitosis.[3] Historically, veterinary EM has been compared to human EM, thus been considered as one end of the spectrum of diseases including Stevens-Johnson Syndrome (SJS) and toxic epidermal necrolysis (TEN).[5,6] The

Figure 2-1. Haired skin, dog. Alopecic, ulcerated skin lesions are scattered throughout the body, particularly severe in the abdomen, thigh, neck, and chest. (Photograph courtesy of: San Marco Veterinary Clinic and Laboratory, https://www.clinicaveterinari

terms, 'erythema multiforme minor' (EM minor) and 'erythema multiforme major' (EM major) have been previously adopted to describe entities with significant differences in the severity of involvement, expressed as percentage of body surface.[3] Respectively, EM minor is characterized by target lesions, affecting maximum one mucosal surface, and less than 10% of body surface; EM major involves more than one mucosal surface affected, between 10% and 50% of body surface, with less than 10% epithelial detachment.[3] SJS involves more than 50% of body surface, with an epithelial detachment of 10%-30%; TEN is characterized by a generalized disease and more than 30% epithelial detachment.[3]

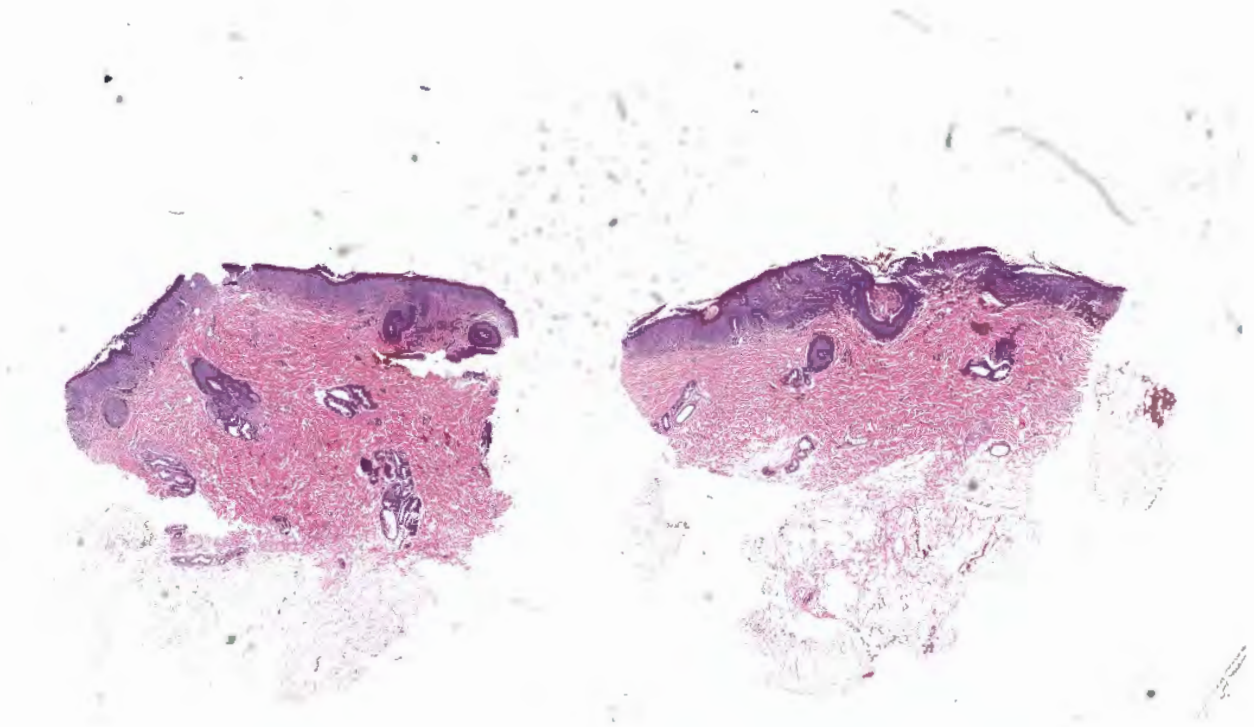

Figure 2-3. Haired skin, dog. The epidermis is hyperplastic, hyperkeratotic, and multifocally ulcerated with pustule formation. There is interface dermatitis with numerous lymphocytes, plasma cells, and macrophages, which often migrate into the epidermis and follicular epidermis. There is moderate pigmentary incontinence. (HE, 158X)

However, nowadays in human medicine, EM and SJS/TEN are considered different entities, and not a spectrum: EM is considered a separate disease, mostly associated with herpes simplex virus, while SJS and TEN are mostly drug-induced. [5,6] Unfortunately, there is no consensus about the criteria for the differentiation of these diseases in veterinary medicine.[5,6]

EM is a rare disease and has been reported in dogs, cats, horses, cattle, swine, and a ferret.[3,5] EM is a multi-factorial disease: adverse drug reaction is traditionally considered the most common cause, but also other triggers have been reported, including neoplasia, parvovirus infection and commercial dog food preservatives, and also idiopathic cases are reported.[2-6] EM is presumably a host-specific T cell-mediated hypersensitivity phenomenon directed towards different keratinocyte-associated antigens, thus eliciting the death of the keratinocytes through apoptosis.[3]

Grossly, EM is frequently characterized by erythematous macules, papules, and plaques with central clearing, usually with acute onset.[3.5.6] In later phases, there could be crusts, with a more targetoid appearance, arciform and serpiginous patterns.[3] Mucosal lesions include vesicles, bullae, and ulcers.[3] Fever and pain may be present. Lesions most commonly involve trunk, groin, and axillae, but may be present anywhere.[3]

Histologically, EM has the features of a cytotoxic (interface) dermatitis. Necrotic keratinocytes are present throughout the epidermis and the adnexal epithelia, often associated with lymphocytic satellitosis. The dermo-epidermal junction is obscured by lymphocytes and

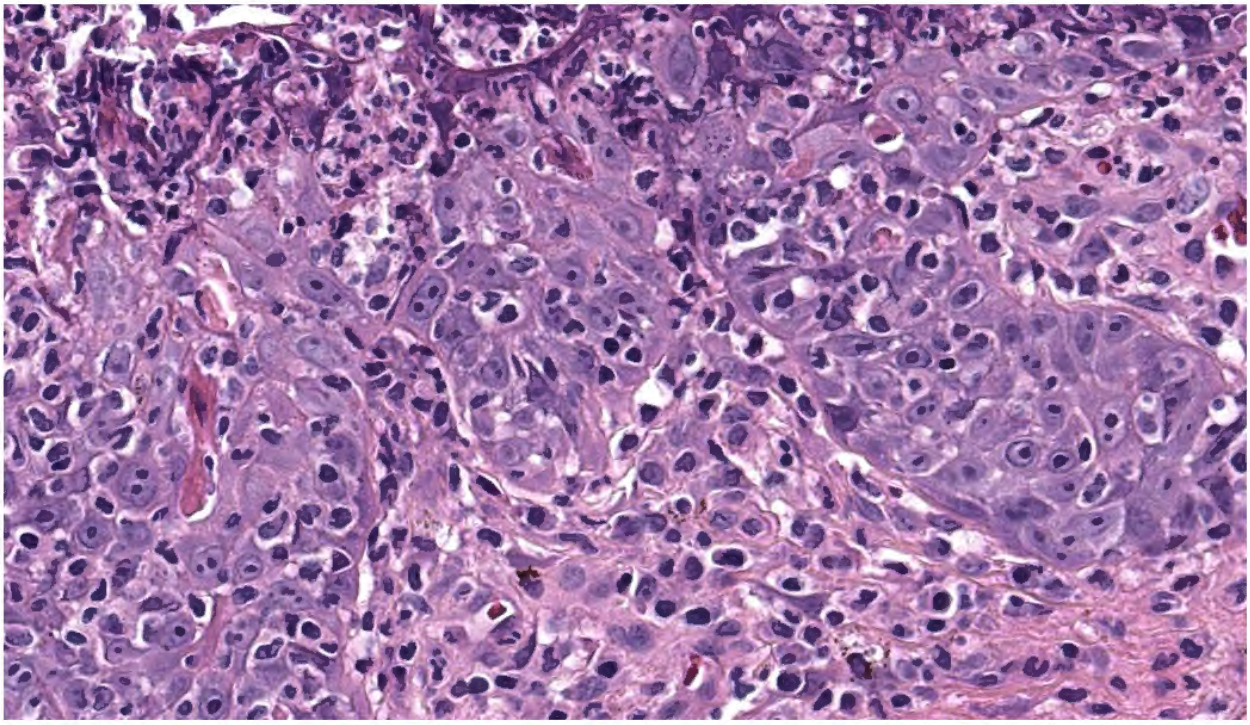

Figure 2-4. Haired skin, dog. There are numerous individualized and small aggregates of eosinophilic apoptotic keratinocytes at all levels of the epidermis. Numerous lymphocytes migrate into the inflamed epidermis. (HE, 960X)

macrophages. Basal keratinocytes could be degenerated.[3,5,6] Hyperkeratosis and parakeratosis are commonly seen in canine EM, as opposed to human EM, and may be severe in persistent forms of EM.[6] This latter form is called "hyperkeratotic EM".[1]

Based on the morphological features, the differential diagnoses include cutaneous lupus erythematosus, thermal or caustic burns, epitheliotropic lymphoma.[3,5]

Contributing Institution:
San Marco Veterinary Clinic and Laboratory Pathology division
Viale dell'Industria 3, 35030
Veggiano (PD), Italy
https://www.clinicaveterinariasanmarco.it/

JPC Diagnoses:
Haired skin: Dermatitis, cytotoxic-interface, lymphocytic, chronic, marked, with transepidermal keratinocyte apoptosis and parakeratotic hyperkeratosis.

JPC Comment:
This classic case of erythema multiforme (EM) was much appreciated by participants as it stimulated great discussion on EM and other top differentials, cytotoxic dermatitis pathogenesis, and a handful of "boards-worthy" information. The contributor's well-written and thorough comment covers much of what was discussed in conference related to the differences between the human and canine manifestations of EM, so focus will be placed on other major discussion points.

The major histologic features to help differentiate EM from other conditions are the presence of suprabasilar and transepidermal apoptosis of keratinocytes and satellitosis of lymphocytes around affected keratinocytes.[5]

Note, however, that if lymphocytes are instead aggregating in and near the epidermis rather than just hovering around affected keratinocytes, epitheliotropic T-cell lymphoma should rise on the differential list. In EM, epithelial dysplasia may also be seen secondary to the concurrent inflammation and necrosis. The same features of transepidermal apoptosis and lymphocyte satellitosis can also be seen in the follicular epithelium, not just in the epidermis! Follicular epithelium may also exhibit hyperpigmentation and vacuolation secondary to inflammation. Parakeratotic hyperkeratosis is often seen in the hyperkeratotic form of EM but is not considered a key diagnostic feature of EM in general.[1,5]

Two other top differentials to consider when looking at a case of hyperkeratotic EM (HKEM) are exfoliative cutaneous lupus erythematosus (CLE) and generalized discoid lupus erythematosus (GDLE). CLE can look similar histologically, but will not have transepidermal keratinocyte apoptosis, will lack lymphocyte satellitosis, and won't have as much hyperkeratosis. GDLE is less proliferative than HKEM with scarring and skin atrophy, neither of which are seen in HKEM. GDLE will also lack the prominent suprabasilar and transepidermal apoptosis and lymphocytic satellitosis seen in HKEM.[1] Other diseases that can more closely mimic EM histologically (i.e. have transepidermal apoptosis, lymphocyte satellitosis, etc.) include SJS/TEN, which is typically acute, severe, and may present as diffuse necrosis, and cutaneous drug reactions, which can honestly look like anything.[6]

Clinical photographs and a thorough history are crucial to dermatopathology cases as a whole and, when it comes to hyperkeratotic EM, can significantly help with diagnosis. Grossly, canine EM typically appears as red papules to plaques that are centrally cyanotic and present on the trunk, groin, and axilla. Hyperkeratotic canine EM, however, can look like raised, hyperpigmented, lichenified plaques in similar locations, but predominantly affects the face and ears. The current school of thought is that hyperkeratotic EM is idiopathic and may target suprabasilar keratinocytes with subsequent proliferation of basilar cells that results in the parakeratotic hyperkeratosis seen histologically.[1,6]

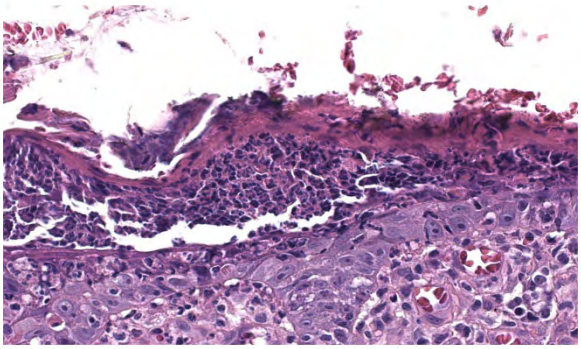

Figure 2-5. Haired skin, dog. Corneal pustules contain large numbers of necrotic neutrophils admixed with cellular debris and edema fluid. (HE, 960X)

In keeping with current dermatopathology terminology, EM is classified as a cytotoxic dermatitis. Other entities that fall under this designation include SJS/TEN, graft-vs-host disease, and cutaneous viral infections (i.e. poxvirus). Both EM and SJS/TEN are mediated by cytotoxic CD3+/CD8+ lymphocyte responses against keratinocytes that have been altered either due to infectious agents or drugs.[6] Apoptosis results from either direct cytotoxicity or through soluble mediators such as Fas ligand, granzymes, perforin, and granulysin.[1,6] For those taking the Phase I exam

soon, Fas ligand should ring a bell as the ligand that binds to the Fas death receptor in extrinsic apoptosis.

Although the pathogenesis of EM is not yet fully understood, CD3+/CD8+ lymphocytic cytotoxic responses against keratinocytes are seen in both human and canine EM diseases. In human EM, a recent study found that T-lymphocyte/NK cell cytotoxicity and Janus kinase (JAK)-signal transducer and activator of transcription (STAT) signaling were highly upregulated.[1] As such, JAK inhibitors have become a promising source of treatment modality for EM patients, both human and canine. If JAK is inhibited, STAT cannot be phosphorylated and cannot translocate to the nucleus to upregulate target gene transcription. Interferon genes can be targets of the JAK/STAT pathway, so the effectiveness of JAK inhibitors in EM cases may be related to the inhibition of interferon-y and type I interferon production.[1]

References:

1. Banovic et al. "Hyperkeratotic erythema multiforme variant in 17 dogs". *Vet Dermatol*. 2023;34(2):125-133
2. Favrot C, Olivry T, Dunston SM, Degorce-Rubiales F, Guy JS. Parvovirus infection of keratinocytes as a cause of canine erythema multiforme. *Vet Pathol*. 2000 Nov;37(6):647-9.
3. Gross TL et al. *Skin diseases of the dog and cat*. Second edition. Blackwell Publishing; 2005; 65-68.
4. Itoh T, Nibe K, Kojimoto A, et al. Erythema multiforme possibly triggered by food substances in a dog. *J Vet Med Sci.* 2006;68(8):869-71.
5. Mauldin EA, Peters-Kennedy J. Integumentary System. In: Grant Maxie M, ed. *Jubb, Kennedy and Palmer's Pathology of domestic animals*. 6th ed. St. Louis, USA: Elsevier;2016;609-10.
6. Yager JA. Erythema multiforme, Stevens–Johnson syndrome and toxic epidermal necrolysis: a comparative review. *Vet Dermatol*. 2014;25(5):406-e64.

CASE III:

Signalment:

1 year and 11 months old, Mare, Standardbred Horse (Equus cabal/us)

History:

The horse was referred to the large animal university hospital due to watery diarrhea, loss of weight and intermittent fever since 1 week. On presentation at the clinic, the horse had a decreased general condition. A sternal subcutaneous edema and swollen legs with crusting and small hemorrhages in the skin, especially on the distal extremities and around the coronary bands, were noted. There was multifocal alopecia on ventral neck, abdomen and distal extremities. In addition, the chestnuts on the legs were easily peeled off. Rectal examination was normal, but ascites (a clear transudate) was evident on abdominocentesis. Lactate level in the abdominal fluid was 5.1 mmol/L (normal ref:< 2 mmol/L). On blood gas analysis, acidosis was evident (pH 7.12).

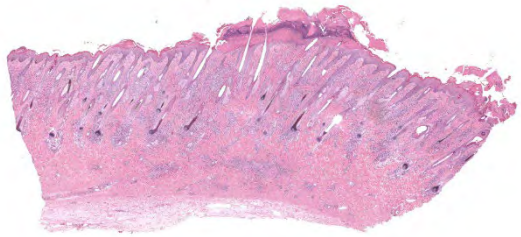

Figure 3-1. Haired skin, horse: At subgross magnification, there is a diffuse perivascular and periadnexal cellular infiltrated. The overlying epidermis is hyperplastic and there is an area of partial thickness epidermal necrosis which is covered by a serocellular crust. (HE, 7X)

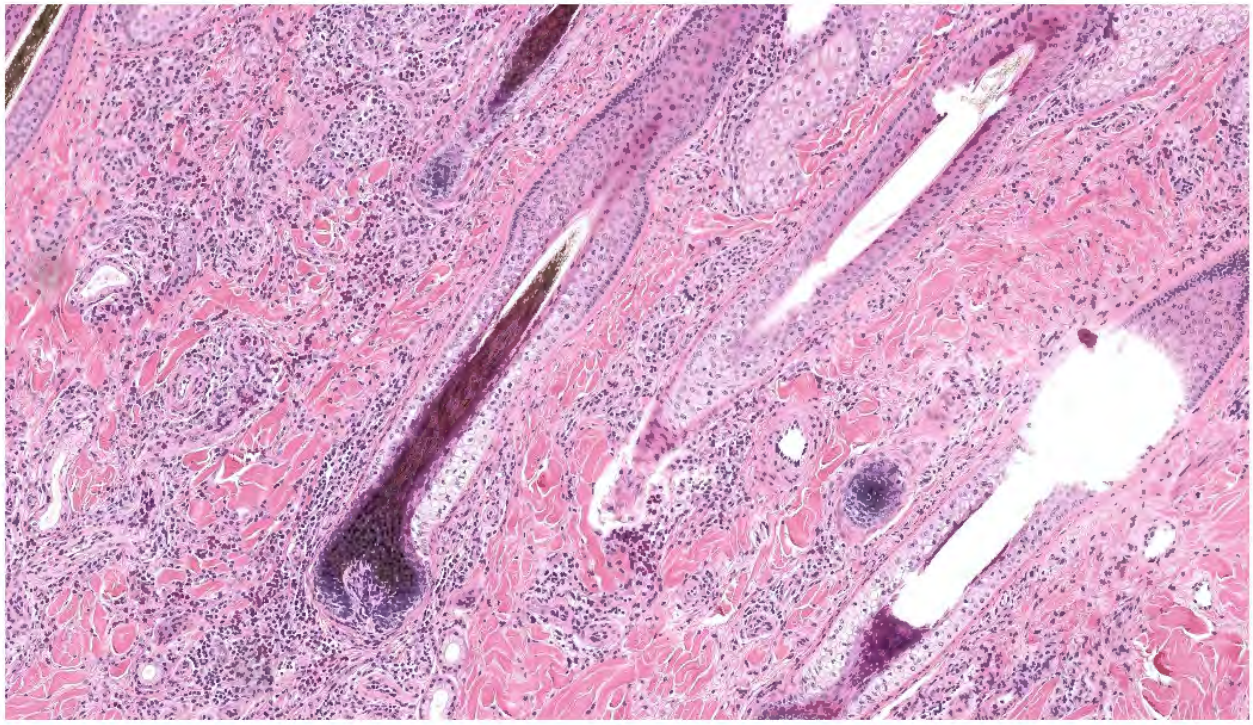

Figure 3-2. Haired skin, horse: Higher magnification of the perivascular chronic inflammation within the dermis. (HE, 154X)

Hematology and total protein values were within normal reference range. Further blood works and diagnostics were declined by the owner, and the horse was euthanized and subsequently submitted for necropsy.

Gross Pathology:
The horse was in slightly poor body condition, with a mild generalized muscle atrophy and dull hair coat with multifocal alopecia, most evident on the ventral neck, abdomen and distal extremities. On closer inspection of the alopecic areas, there were abundant crusting, erosions and ulcerations of the skin, especially around the coronary bands and pastern on all four limbs. A moderate subcutaneous edema was evident on ventral abdomen and distal extremities. Free within the abdominal and thoracic cavity respectively, there were 2 liters of a straw-colored transudate. In the mucosa of the small intestine, large intestine and cecum, there were multifocal to coalescing, variably brownish colored, round "button like" ulcers of approximately 0.5-4 cm in diameter, with elevated borders of firm consistency. The ulcers were often covered by light, dry, fibrinonecrotic material. There was also a diffuse, mild to moderate submucosal edema. In the non-glandular parts of stomach, there was severe hyperkeratosis. The liver was slightly decreased in size with a firm consistency, and on cut surface abundant fibrous streaks were evident, especially dissecting along bile ducts. The pancreas was moderately enlarged, firm in consistency and diffusely light in color. Visceral and peripheral and lymph nodes varied from mildly to moderately enlarged, were slightly edematous, and varied in appearance; some showed distinct follicle formation and some were more homogenously light on cut surface. The bone marrow was light to dark red in color.

Laboratory Results:
N/A

Microscopic Description:
Haired skin, coronary band. Expanding and

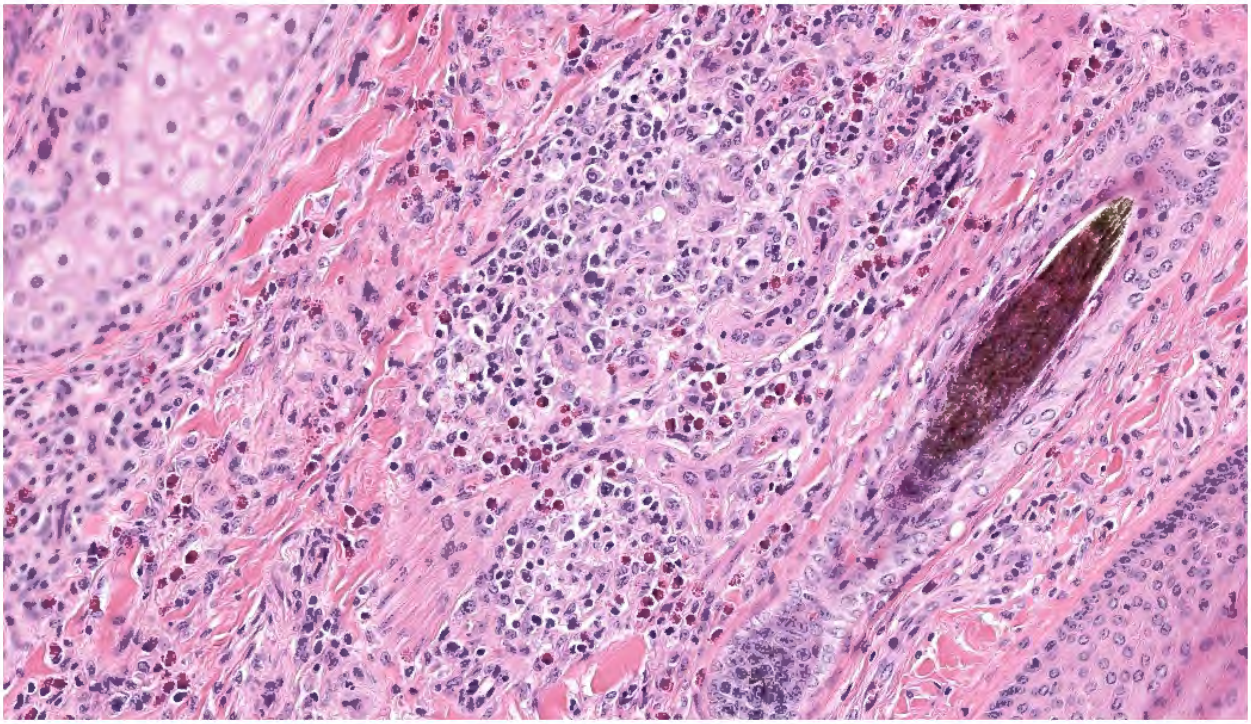

Figure 3-3. Haired skin, horse: Eosinophils are a prominent component of the inflammatory infiltrate (HE, 154X)

infiltrating the entire dermis are multifocal to coalescing perivascular, periadnexal and interstitial aggregates of moderate numbers of lymphocytes, eosinophils and histiocytes, fewer plasma cells and occasional neutrophils. Multifocally within dermis are few small areas of intensely eosinophilic, fragmented collagen fibers admixed with eosinophilic cellular- and basophilic nuclear debris, surrounded by epithelioid macrophages and multinucleated giant cells (eosinophilic granulomas). Intramurally and intraluminally within multiple hair follicles are moderate numbers of eosinophils, lymphocytes and histiocytes and few multinucleated giant cells (mural and luminal folliculitis), and adjacent follicular epithelium display moderate spongiosis. In the dermal-epidermal interface, there is a multifocal mild edema. The epidermis shows mild lymphocytic infiltration, mild spongiosis and occasional apoptotic keratinocyte, diffuse mild acanthosis and mild rete ridge formation (epidermal hyperplasia), moderate parakeratotic and orthokeratotic hyperkeratosis and multifocal erosions and ulcerations, the latter being covered by large serocellular crusts spanning over several adnexal units. Serocellular crusts show abundant viable and degenerated neutrophils, occasional eosinophil, cellular debris, fibrin, free keratin and hair fragments and occasional small basophilic bacterial colonies. There are also small epidermal intracorneal pustules multifocally. Several arteriolar walls in deep dermis show infiltration of few eosinophils and lymphocytes (vasculitis). The deep dermis displays mild diffuse edema.

Contributor's Morphologic Diagnoses:
Haired skin, coronary band: Dermatitis and folliculitis, lymphoplasmacytic, histiocytic and eosinophilic, multifocal to coalescing, moderate, with eosinophilic granulomas, epidermal intracorneal pustules, serocellular crusts and orthokeratotic and parakeratotic hyperkeratosis

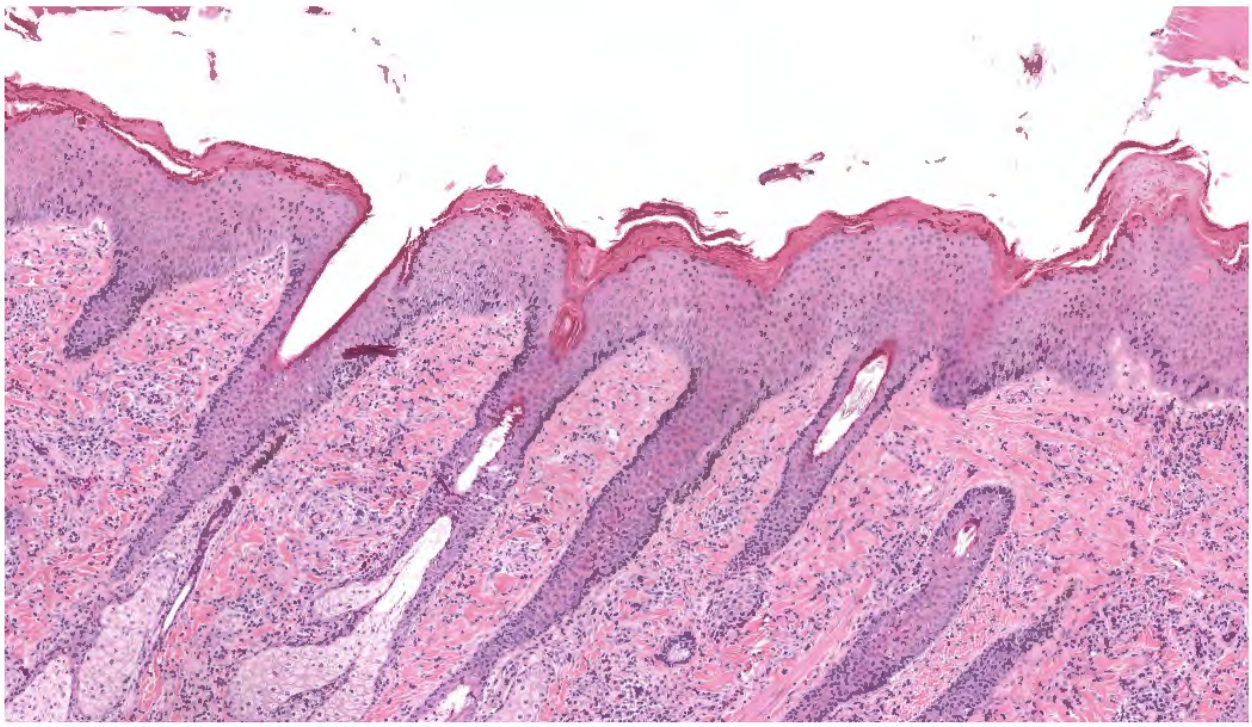

Figure 3-4. Haired skin, horse: There is moderate parakeratotic hyperkeratosis of the hyperplastic epidermis. (HE, 154X)

Equine multisystemic eosinophilic epitheliotropic disease (MEED)

Contributor's Comment:

Equine multisystemic eosinophilic epitheliotropic disease (MEED) is a rare chronic disease and constitutes part of inflammatory bowel disease (IBD) in horses.[13,15,17] MEED typically affects young Standardbred and Thoroughbred horses even though horses of older age and other breeds also may be affected.[3,8,9,10,11,13,14,18,19,24] Seasonality with cases occurring in spring or summer is reported in some studies.[11,14] Clinically, horses with MEED present with progressive weight loss, pitting edema, alopecia and exudative, exfoliative dermatitis characterized by scaling, crusting and skin ulcerations.[3,6,10,11,13,14] Lesions often originate around coronary bands, sometimes with associated loss of chestnuts, and progressively becomes more generalized to also include head and the rest of the body.[3,11,13,14] Most affected horses die or are euthanized within 8 months of diagnosis.[13] In clinical cases described in the literature, pruritus is variably evident, as well as fever, diarrhea and peripheral eosinophilia.[3,6,10,11,13,14,19] Peripheral eosinophilia is reported in approximately 14% of cases.[3,13] Serum biochemical evidence of liver disease and/or hypoproteinemia may also be seen, and in a few cases, respiratory symptoms have been noted.[3,6,8,9-11,18,19] In our case, there was no peripheral eosinophilia and no hypoproteinemia present at clinical work-up. Serum biochemistry was not investigated; hence, liver values were unknown.

On postmortem examination, several organs are commonly affected in cases of MEED, including skin, pancreas, liver, common bile duct, gastrointestinal tract and lungs.[13] Histologically, the disease is characterized by eosinophilic and lymphoplasmacytic infiltration, sometimes with eosinophilic granuloma formation.[13] In the skin, various inflammatory

patterns have been reported in MEED, including perivascular, lichenoid interface, interstitial, diffuse, and granulomatous.[13,14] Eosinophils, lymphocytes and plasma cells are the main cellular elements.[13,14] Other histological findings in the skin include epidermal hyperplasia, orthokeratotic and parakeratotic hyperkeratosis, epitheliotropic infiltration of eosinophils and lymphocytes, apoptotic keratinocytes, eosinophilic folliculitis, furunculosis, eosinophilic granulomas, and lymphoid nodules.[13] Coagulated protein and collagen degeneration may be seen within deep dermal vessel walls.[14] In our case, most of these lesions were present in examined sections of the skin. Within the gastrointestinal tract, lesions include ulcers on the tongue and/or within oral cavity, hyperkeratosis of the esophagus and non-glandular stomach, and mucosal ulcerations within the small and/or large intestine, as well as marked fibrosis in some organs, such as pancreas and liver; in the liver especially dissecting along bile ducts.[11,14] Fibrosis may be so severe that loss of exocrine tissue is evident within pancreas, and in the liver, there may also be biliary hyperplasia.[11,14] Lymph nodes may be enlarged due to eosinophilic infiltration, and increased numbers of eosinophils can be seen in bone marrow.[6,9,13,14,18,19] In our case, all of these findings were present except oral ulcerations.

Cases of equine MEED has been reported since 1960's in Sweden, and was in 1985 described under the name of eosinophilic granulomatosis (EG).[11] A case series was also reported from Canada the same year.[14] Since then, various case reports of MEED have been published from around the world, including the US, Germany, Ireland, Belgium, Brazil, Italy and Spain.[3,6,8,9,10,18,19,24] Systemic eosinophilic disorders, often referred to as hypereosinophilic syndrome (HES), have also been described in other species, such as dogs, cats, ferrets, donkeys, and humans.[4,5,7,16,20]

The underlying cause of MEED is yet unknown.[13] For equine IBD, a delayed hypersensitivity reaction has been proposed.[15] For MEED specifically, recurrent type I hypersensitivity reactions caused by dietary, inhaled, or parasitic antigens have been suggested.[11,13] In one recently published report, authors suggest that larval migrans seen in their case could have contributed to development of MEED.[24] In our case, there was no evidence of ecto- or endoparasitism on either gross or histological examination. A genetic cause of MEED has been discussed, since Standardbreds and Thoroughbreds are over-represented in MEED cases.[13] Another hypothesis is that clonal proliferation of T-lymphocytes trigger eosinophil proliferation through secretion of cytokines such as interleukin-5, which has been proposed as an underlying cause for HES in humans.[4] In the horse, MEED has been seen concurrently with intestinal T cell lymphoma, which may support this theory. Also in other species, such as the cat, dog and ferret, hypereosinophilic syndromes have been reported together with various T cell neoplasms. [1,2,9,12] In our case, there was no evidence of concurrent lymphoma.

Our case fits well with a diagnosis of MEED with regards to both clinical picture, gross findings, and histological findings. Differential diagnoses for lesions in the skin include autoimmune disorders, such as pemphigus foliaceus (PF), equine sarcoidosis, hairy vetch *(Vicia villosa*) intoxication, and insect bite hypersensitivity. PF presents with a similar clinical picture of crusting of the skin; however, on histopathological examination, consistent findings in PF patients are serocellular crusts or intraepidermal pustules and vesicles containing rafts of, or individualized, acantholytic

cells, which were not seen in our case.[13,22] In equine sarcoidosis, a nodular to diffuse lymphogranulomatous dermatitis with multinucleated giant cells and vasculitis is commonly seen.[13] Hairy vetch toxicosis is mainly seen in cattle, but may also occur in horses.[13] In horses, it is characterized by a nodular, granulomatous dermatitis. Eosinophilic infiltration may be seen in cattle with hairy vetch toxicosis but it is rarely seen in horses.[13] Insect bite hypersensitivity, commonly caused by *Culicoides* spp in horses, is usually severely pruritic and presents as a superficial or superficial to deep perivascular dermatitis, dominated by eosinophils and lymphocytes. Eosinophilic folliculitis, erosions and ulcerations may also be seen as a result of self-trauma.[13] Another differential diagnosis discussed for this case, mainly based on the ulcerative lesions within the intestine, was *Rhodococcus equi* infection. However, no pyogranulomatous lesions supporting *Rhodococcus equi* infection were present in the lymph nodes. Infection by *Salmonella enterica* ssp. *enterica* serovar t*yphimurium* may as well give rise to button like ulcers within the large intestine, but taken all together, the combined clinical, gross and histological picture in this case supported a diagnosis of MEED.[21]

Contributing Institution:
Swedish University of Agricultural Sciences Department of Animal Biosciences, Section of Pathology Box 7023 SE 750 07, Uppsala, Sweden
https://www.slu.se/enldepartments/Animal-Biosciencesf

JPC Diagnoses:
Haired skin: Dermatitis, perivascular, lymphohistiocytic and eosinophilic, chronic, moderate, with epidermal hyperplasia and parakeratotic hyperkeratosis.

JPC Comment:
The contributor's comment in this case provides an exceptional overview of multisystemic epitheliotropic eosinophilic disease (MEED) in horses and its major differentials, all of which were discussed during conference. MEED is currently considered to be an abnormal manifestation of inflammatory bowel disease (IBD) in horses. The cutaneous manifestation of MEED classifies as a perivascular dermatitis pattern, and the depth of inflammation and affected vasculature can assist with the diagnosis of MEED compared to others that would be confined more to the superficial dermis (i.e. insect bite hypersensitivity). Conference participants ultimately all agreed with the contributor's diagnosis of MEED in this case.

If lesions are restricted to the GI tract, other causes of inflammatory bowel disease, intestinal parasitism, and idiopathic focal eosinophilic enteritis (IFEE) should rise higher on the differentials list. There was an excellent case of IFEE seen earlier this year in Conference 1, Case 3, the contributor of which provided a fantastic comparison between IFEE and MEED in their comment. Additionally, a thorough overview of eosinophils was covered in the JPC comment for Conference 2, Case 3 this year as well, and those two comments are great supplementals to this case.

As a quick refresher, the differentiation and maturation of eosinophils are dependent on expression and presence of certain transcription factors and cytokines, such as interleukin-5 (IL-5). IL-5 is the most important of these in eosinophil differentiation, maturation, and survival. As referenced by the contributor, there is a case report of MEED with concurrent GI lymphoma in a horse, contributing to

the hypothesis that clonal expansion of T-lymphocytes may contribute to eosinophil proliferation via secretion of eosinophil-promoting cytokines, such as IL-5, in cases of hypereosinophilia seen in some lymphomas.[4] Mature eosinophils contain granules that are full of cytotoxic compounds that are released in response to stimuli (i.e. certain infectious agents, allergens). Normally, T-helper type 2 (Th2) cells that are in proximity to the stressor produce high levels of IL-5, triggering eosinophil infiltration, activation, and subsequent release of additional cytokines, chemokines, and eosinophil granules. There is still substantial speculation on the cause(s) of MEED, but current literature suggests that it is likely a multifactorial, systemic presentation of a hypersensitivity reaction and that causes may vary between affected individuals, although parasites seem to be overrepresented in case reports.[23]

References:

1. Barrs VR, Beatty JA, Mccandlish IA, Kipar, A. Hypereosinophilic paraneoplastic syndrome in a cat with intestinal T cell lymphosarcoma. *J Small Anim Pract*. 2002;43:401-405.
2. Blomme EAG, Foy SH, Chappell KH, La Perle KMD. Hypereosinophilic syndrome with Hodgkin's-like lymphoma in a ferret. J Comp Pathol. 1999;120:211-217.
3. Bosseler L, Verryken K, Bauwens C, et al. Equine multisystemic eosinophilic epitheliotropic disease: A case report and review of literature. NZ Vet J. 2013;61 (3):177-182.
4. Curtis C, Ogbogu P. Hypereosinophilic syndrome. Clin Rev Allergy lmmunol. 2016;50:240-251.
5. Fox JG, Palley LS, Rose R. Eosinophilic gastroenteritis with Splendore-Hoeppli material in the ferret (Mustela putoris furo). Vet Pathol. 1992;29:21-26.
6. Gehlen H, Cehak A, Bag6 Z, Stadler P. Multisystemic eosinophilic disease in a Standardbred mare combined with generalized lymphadenitis. J Equine Vet Sci. 2003;23(5):216-219.
7. Hendrick M. A spectrum of hypereosinophilic syndromes exemplified by six cats with eosinophilic enteritis. Vet Pathol. 1981; 18: 188-200.
8. Horan EM, Metcalfe LVA, de Swarte M, Cahalan SD, Katz LM. Pulmonary and hepatic eosinophilic granulomas and epistaxis in a horse suggestive of multisystemic eosinophilic epitheliotropic disease. Equine Vet Educ. 2013;25(12):607-613.
9. La Perle KMD, Piercy RJ, Long JF, Blomme EAG. Multisystemic, eosinophilic, epitheliotropic disease with intestinal lymphosarcoma in a horse. Vet Pathol. 1998;35: 144-146.
10. Laisse CJM, Castro do Nascimento L, Panziera W, et al. Multisystemic eosinophilic epitheliotropic disease in a horse in Brazil. Cienc Rural. 2017;47(5):e20160896.
11. Lindberg R, Persson SGB, Jones B, Thoren-Tolling K, Ederoth M. Clinical and pathophysiological features of granulomatous enteritis and eosinophilic granulomatosis in the horse. Zentralbl Veterinarmed A. 1985;32:526-539.
12. Marchetti V, Benetti C, Citi S, Taccini V. Paraneoplastic hypereosinophilia in a dog with intestinal T-cell lymphoma. Vet Clin Pathol. 2005;34:259-263.
13. Mauldin EA., Peters-Kennedy J. lntegumentary System. In: Maxie MG, ed. Jubb, Kennedy and Palmers, Pathology of Domestic Animals. Vol. 1. 6th ed. Elsevier; 2016.
14. Nimmo Wilkie JS, Yager JA, Nation PN, Clark EG, Townsend HGG, Baird JD. Chronic eosinophilic dermatitis: A manifestation of a multisystemic, eosinophilic, epitheliotropic disease in five horses. Vet Pathol. 1985;22:297-305.

15. Olofsson KM. lmmunopathological aspects of equine inflammatory bowel disease. Swedish University of Agricultural Sciences; 2016.
16. Paraschou G, Vogel PE, Lee AM, Trawford RF, Priestnall SL. Multisystemic eosinophilic epitheliotropic disease in three donkeys. J Comp Pathol. 2023;201:105-108.
17. Schumacher J, Edwards JF, Cohen ND. Chronic idiopathic inflammatory bowel disease of the horse. J Vet Intern Med. 2000; 14:258-265.
18. Singh K, Holbrook TC, Gilliam LL, Cruz RJ, Duffy J, Confer AW. Severe pulmonary disease due to multisystemic eosinophilic epitheliotropic disease in a horse. Vet Pathol. 2006;43:189-193.
19. Stucchi L, Lo Feudo CM, Valli C, et al. Equine multisystemic eosinophilic epitheliotropic disease in two horses in Italy. Equine Vet Educ. 2022;34(10):413-417.
20. Sykes JE, Weiss DJ, Buoen LC, Blauvelt MM, Hayden OW. Idiopathic hypereosinophilic syndrome in 3 Rottweilers. J Vet Intern Med. 2001;15:162-166.
21. Uzal, FA., Plattner, BL., Hostetter, JM. Alimentary System. In: Maxie MG, ed. Jubb, Kennedy and Palmers, Pathology of Domestic Animals. Vol. 2. 6th ed. Elsevier;2016.
22. Vandenabeele SI, White SD, Affolter VK, Kass PH, Ihrke PJ. Pemphigus foliaceus in the horse: a retrospective study of 20 cases. Vet Dermatol. 2004;15:381-388.
23. Villagrán CC, Vogt D, Gupta A, Fernández EA. Inflammatory bowel disease characterized by multisystemic eosinophilic epitheliotropic disease (MEED) in a horse in Saskatchewan, Canada. Can Vet J. 2021;62(11):1190-1194.
24. Vitale V, Troya-Portillo L, Corradini I, Serrano B, Armengou L. Multisystemic eosinophilic epitheliotropic disease subsequent to parasitic lymphadenopathy in a mare. Vet Rec Case Rep. 2023;11:e711.

CASE IV:

Signalment:
Six day-old piglet, male, cross-breed (*Sus scrofa domestica*)

History:
Sow farm where six weeks before the submission of this case, the herd experienced four litters with abortions and few newborn animals with cutaneous problems. All affected litters corresponded to multiparous sows. In each litter there was 3 or 4 affected piglets, except in the last one, which 7 out of 8 newborn piglets displayed cutaneous lesions. The affected newborn piglets usually died during the first week of life. This case corresponds to a lactating piglet of 6 days of age with generalized cutaneous lesions from last litter, which died naturally.

Figure 4-1. Haired skin, pig. Multiple sections of haired skin, to include the pinna, the prepuce and two unlabeled sections of skin are submitted for examination. (HE, 8X)

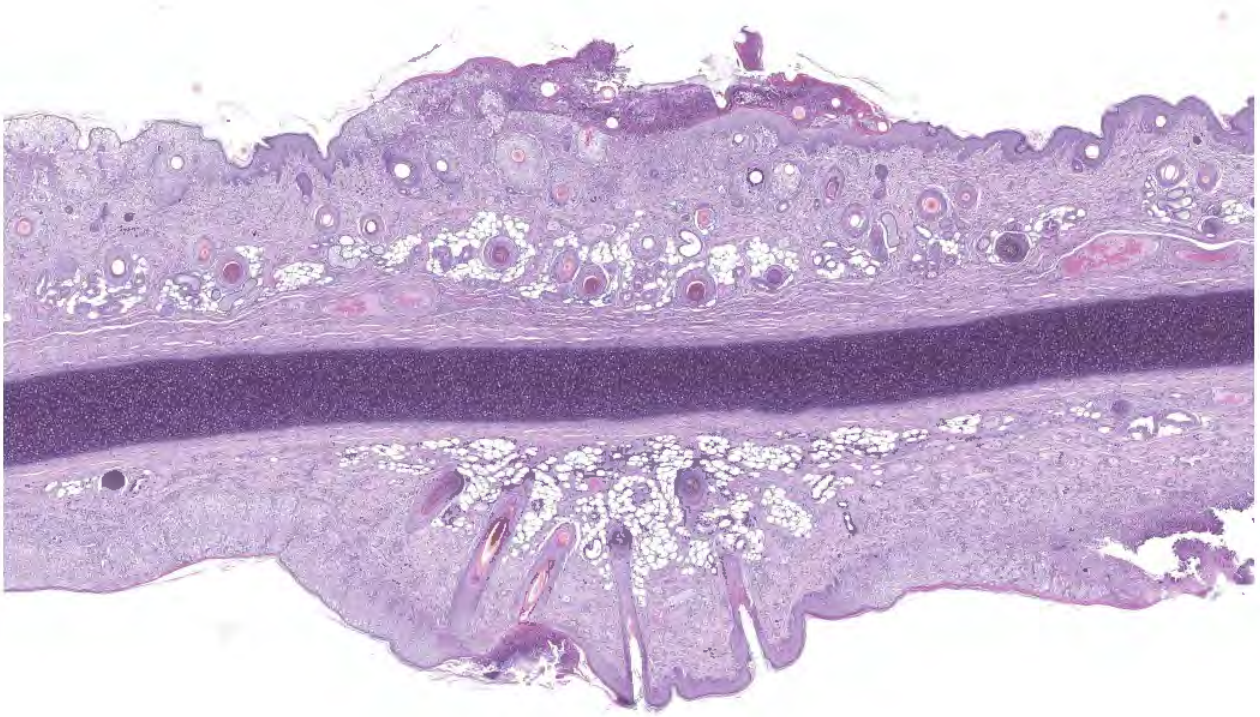

Figure 4-2. Pinna, pig. There is diffuse epidermal hyperplasia with ballooning edema, necrosis, and overlying serocellular crust. (HE, 125X)

Gross Pathology:
Six-day-old piglet of 1.16 kg weight with poor body condition and prominent bone protuberances. In a multifocal to generalized pattern throughout the skin and tongue, there were circular 0.1 to 0.5 cm in diameter lesions characterized by slightly prominent, firm, and well circumscribed aspect (papules and pustules); most of them were brownish in color with central umbilication and crusted. Significant lesions were not found in internal organs or in the subcutaneous tissue.

Laboratory Results:
N/A

Microscopic Description:
Haired skin (ear, prepuce, and inguinal area): affecting 20% of the evaluated section there is a proliferative and necrotizing process that mainly affects the epidermis. The epidermis and hair follicle epithelium show the following features: stratum corneum with diffuse mild compact hyperkeratotic orthokeratosis with multifocally serocellular crusts composed by cellular debris, degenerated keratin, degenerated neutrophils, and multiple superficial coccoid bacterial colonies (secondary contamination). Also, stratum spinosum shows multifocal marked thickening (acanthosis), and numerous keratinocytes display ballooning degeneration and intracytoplasmic perinuclear 2-5 µm eosinophilic inclusion bodies. Multifocally, in the most affected areas, there is marked neutrophilic exocytosis, and numerous keratinocytes lost intercellular connections and undergo lytic necrosis. Superficial and mid dermis show perivascular to diffuse, moderate to severe inflammatory infiltrates composed by viable and degenerated neutrophils, macrophages, and lesser numbers of lymphocytes and plasma cells. Significant lesions were not seen in the hypodermis.

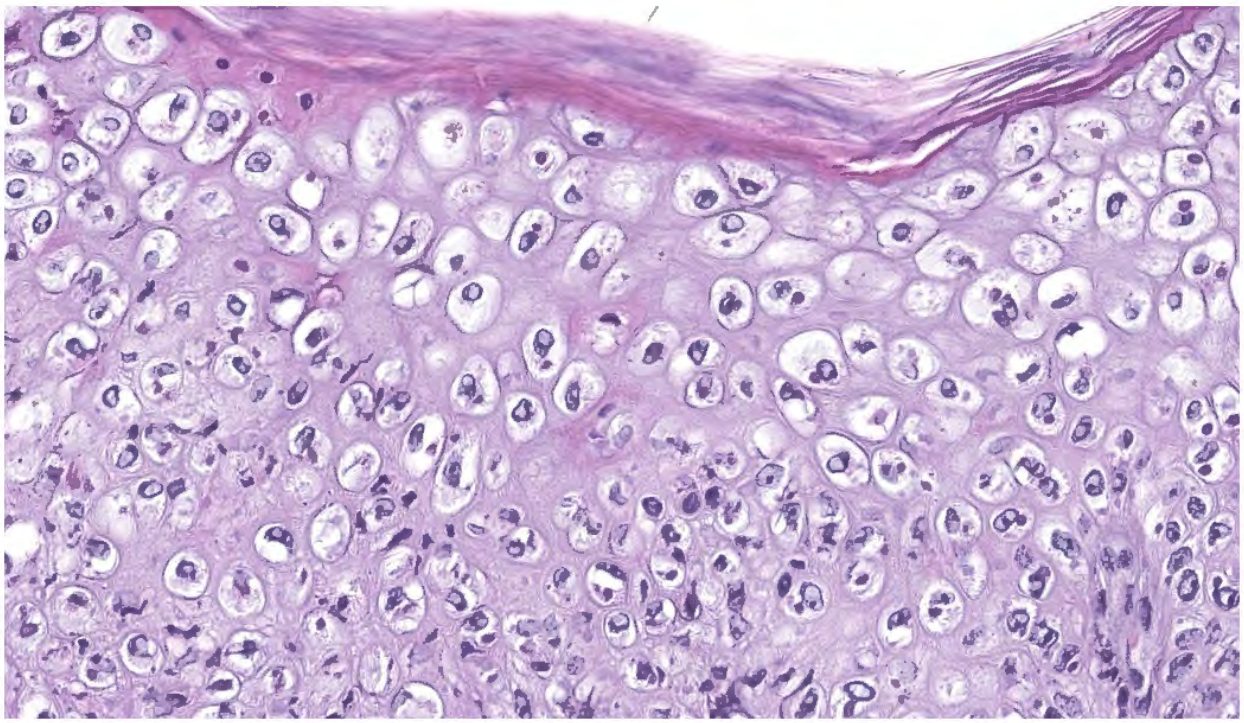

Figure 4-3. Pinna, pig. Within the proliferative epidermis, keratinocytes within the stratum spongiosum are expanded by abundant intracellular edema ("ballooning degeneration") and contain one or more irregularly round intracytoplasmic viral inclusions.

Contributor's Morphologic Diagnoses:
Morphologic diagnosis: Haired skin; severe, subacute, proliferative, necrotizing, and crusting dermatitis with intracytoplasmic eosinophilic inclusion bodies. Etiologic diagnosis: Poxviral dermatitis. Etiology: Swine poxvirus.

Contributor's Comment:
The clinical case reflects typical clinical signs and lesions of congenital swine poxvirus infection. Swine pox (SwP) is a sporadic disease of pigs caused by swine pox virus (SwPV) belonging to the *Poxviridae* family. SwP is a skin disease of worldwide distribution, generally associated with poor sanitary status of herds, and can be vectored by pig lice (*Haematopinus suis*) and domestic flies (*Musca domestica*).[4,8] The disease is pathologically characterized by the formation of pustular/papular skin lesions in different regions of the body, with more severe forms in young pigs (<3-4 months), including neonates with the condition (congenital SwP).[6,7]

SwPV is the only member of the genus *Suipoxvirus* in the subfamily *Chordopoxvirinae*. As all poxviruses, it has a DNA genome that replicates in the host cell cytoplasm. SwPV has a linear double-stranded DNA molecule with 150 genes, of which 146 conserved genes encode proteins essential for survival in the host cell.[1,7] SwPV replication in infected cells can generate two forms of virions: 1) mature virions (MV), which are the vast majority, and are released by budding or after cell lysis, and 2) extracellular enveloped virions (EEV), which leave the cell by exocytosis.[7] The difference between the two forms is the stability in the ambient, being MVs very stable and EEVs relatively fragile.[7]

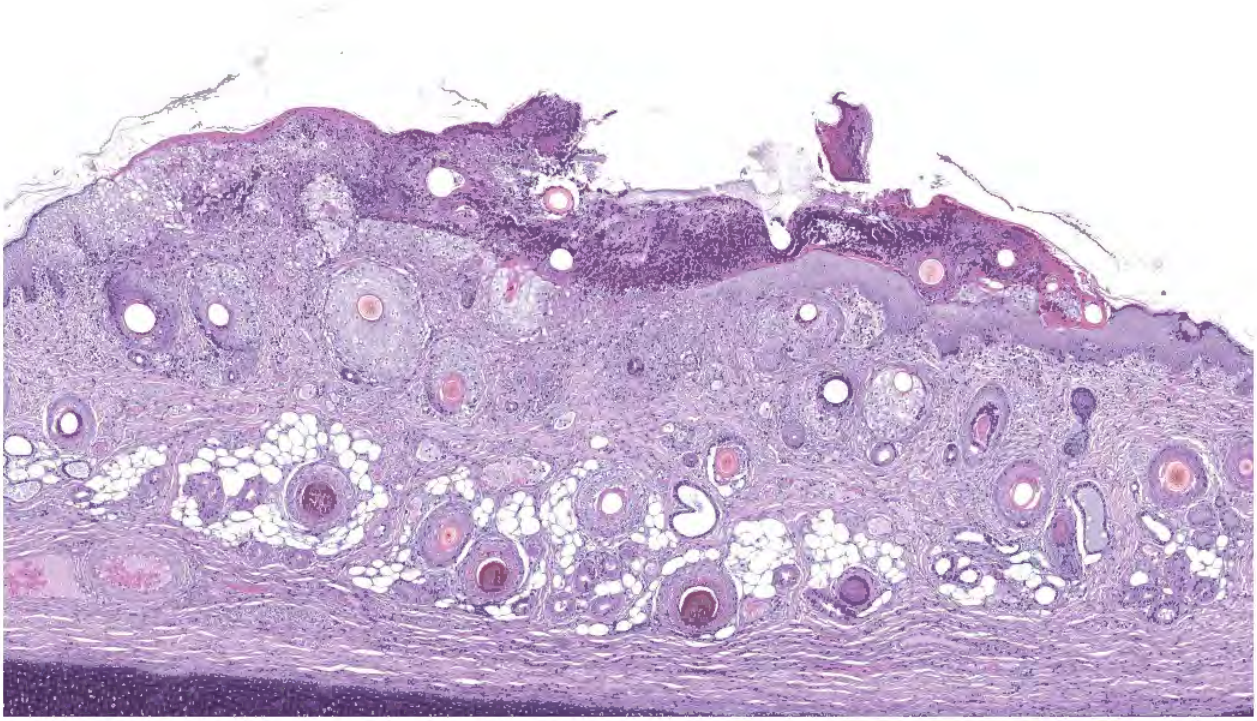

Figure 4-4 Pinna, pig. There is focal partial thickness necrosis of the virally infected hyperplastic epithelium. (HE, 125X)

The clinical signs associated with SwPV infection are directly related to age and viral load. The most affected animals are relatively young (<3-4 months of age), and the condition has high morbidity at the herd level, although mortality is usually very low.[4,7] In contrast, SwPV infection in adult animals is usually mild/subclinical and self-limiting. It has been suggested that congenital infections may result from infected and viremic sows during gestation, causing fetal membrane infection.[6] The pathogenesis of congenital SwPV infection in pigs has not been completely elucidated; however, compartmentalization of placental membranes in swine probably explains why some fetuses are affected and others are not.[4,6,7]

The topography of the skin lesions is commonly found throughout the body but more evident on the flanks, ventral abdomen, legs, inguinal areas, and ears. The incubation period of SwPV infection ranges from 4 to 14 days and the lesions evolve from macules, papules, and vesicles to umbilicated lesions with purulent contents, followed by crusting. Congenitally affected piglets usually have cutaneous lesions at birth, being stillborn or dying within a few days. Lesser affected animals can survive and heal the cutaneous lesions.

The typical histological features of SwPV infection comprises hydropic degeneration of keratinocytes of the epidermal stratum spinosum and follicular epithelium during the papular phase. As a result, thickening of the epidermis due to mild spongiosis can be observed; however, epidermal hyperplasia caused by SwPV is usually less prominent than that caused by the other poxviruses.[7] Other finding are eosinophilic inclusion bodies in the cytoplasm of infected cells.[7] Regarding inflammation, the damage caused by virus

replication on keratinocytes causes recruitment of neutrophils, eosinophils, lymphocytes and histiocytes, forming intraepithelial pustules, as well as in the superficial and mid-dermis.[4,6,7]

The presumptive diagnosis of SwP is based on the observation of typical macroscopic skin lesions and the presence of epidermal hyperplasia with ballooning degeneration of keratinocytes and inclusion bodies on histopathology. Differential diagnoses of SwPV infection are infectious diseases such as vesicular diseases (foot-and-mouth disease, vesicular exanthema of swine, vesicular stomatitis, swine vesicular disease and Seneca virus A infection), early stages of ringworm, localized streptococcal and staphylococcal epidermitis, and non-infectious diseases such as pityriasis rosea, allergic skin lesions, and sunburn.[6,7]

Contributing Institution:
Veterinary Pathology Department Veterinary Faculty, Autonomous University of Barcelona, 08193 Bellaterra, Barcelona, Spain. https://www.uab.cat/web/els-serveis/-servei-diagnostic-de-patologiaveterinaria1297063220061.html

JPC Diagnoses:
Haired skin: Dermatitis, necrotizing and proliferative, subacute, multifocal, severe, with ballooning degeneration and intracytoplasmic viral inclusions.

JPC Comment:
This was a truly phenomenal case of congenital swinepox, complete with clear viral inclusions and all the classic histologic features of the disease. The JPC extends sincere gratitude to the contributor of this case for providing such an exceptional example of this entity for the Wednesday Slide Conference!

One of the very first questions posed to conference participants was, “If poxvirus is a dsDNA virus, why are the inclusions cytoplasmic instead of intranuclear?” This is because poxviruses are unique among DNA viruses in that they possess all their own required machinery, including their own DNA-dependent RNA polymerase, to carry out replication and transcription independent of the host cell nucleus.[9] Poxviruses can even go so far as to form their own membrane-bound "mini-nuclei" within the cytoplasm, derived from rough endoplasmic reticulum.[9] These cytoplasmic sites contain all the components needed for viral DNA replication and protein synthesis. As such, poxviral inclusions will be seen in the cytoplasm of infected keratinocytes instead of in the nucleus.

The contributor lists some great differentials to consider for swinepox in pigs where the condition is not thought to be congenital. For congenital cutaneous conditions, however, only swinepox virus and parvovirus are reported to cause lesions in neonatal pigs.[6] In conference, it was also mentioned that vaccinia virus, another poxvirus that was previously used for smallpox vaccination in humans, was once considered a cause of poxviral dermatitis in pigs due to its broader species tropism, but this is no longer seen due to the cessation of the use of vaccinia virus for smallpox vaccines. Congenital swinepox is thought to occur via intrauterine infection resulting in a low-level viremia within the sow that allows the virus to spread to the fetal membranes.[6] Swine placental membranes are

compartmentalized, so while some fetuses are affected, others may not be. [6]

The pathogenesis of poxviruses involves the inhibition of a cytosolic pathogen recognition receptor (PRR) known as protein kinase R (PKR), which is a crucial part of the host immune system that limits viral replication in an infected cell via phosphorylation of eukaryotic initiation factor 2α (eIF2α).[3] PKR recognizes double-stranded RNA (dsRNA) produced during viral replication and helps control major signaling pathways involved in the immune response, such as the integrated stress response (ISR), mitogen-activated protein kinases (MAPKs), and the NF-κB pathway.[2] During the poxviral replication process, long dsRNAs are generated as intermediates for translation of the viral genome. When a dsRNA fragment is longer than 33 base pairs (bp), two PKR molecules bind to the RNA and become dimerized, followed by autophosphorylation to become an active kinase.[2] Once activated, PKR can then either undergo nuclear translocation to act on the above-listed transcription factors or it can phosphorylate cytoplasmic eIF2α, which is a competitive inhibitor of eIF2B, the factor that recycles eIF2 for subsequent rounds of translation.[2,5] This inhibition globally halts new protein synthesis for both host and viral mRNA.[5] Poxviruses produce a pair of proteins, known as E3 and K3, that antagonize PKR and enable viral activity within cells.[3] Protein E3 binds dsDNA and inhibits PKR activation, while protein K3 acts as an eIF2α analog for PKR, limiting activation of eIF2α by making less PKR available for eIF2α binding.[3]

Conference discussion concluded with a review of other significant poxviruses in veterinary species, of which the most notable were cowpox, due to its wider species tropism and penchant to use rodents as reservoir hosts, monkeypox, due to its current relevance in the U.S., and Ectromelia virus in mice, also known as mousepox. To wrap everything up with a bow, participants reviewed what poxviral virions look like on electron microscopy, which Dr. Bradley, promptly tossing the stereotypical dumbbell reference out the window, affectionally refers to as "tater tots" or "squished tater tots." Conference participants unanimously agreed that "tater tots" needs to catch on pronto.

References:

1. Afonso CL, Delhon G, Tulman E R, Lu Z, Zsak A, Becerra VM, Zsak L, Kutish GF, & Rock DL. Genome of deerpox virus. *Journal of Virology.* 2005;79(2):966–977.
2. Chung J, Lee Y, Yoon J, Kim Y. Deciphering the multifaceted role of double-stranded RNA sensor protein kinase R: pathophysiological function beyond the antiviral response. *RNA Biol.* 2025;22(1):1-14.
3. Haller SL, Park C, Bruneau RC, Megawati D, Zhang C, Vipat S, Peng C, Senkevich TG, Brennan G, Tazi L, Rothenburg S. Host species-specific activity of the poxvirus PKR inhibitors E3 and K3 mediate host range function. *J Virol.* 2024;98(11):e0133124.
4. Mech P, Bora DP, Neher S, Barman NN, Borah P, Tamuly S, Dutta LJ, & Das SK. Identification of swinepox virus from natural outbreaks in pig population of Assam. *Virus disease.* 2018;29(3):395–399.

5. Taylor SS, Haste NM, Ghosh G. PKR and eIF2alpha: integration of kinase dimerization, activation, and substrate docking. *Cell*. 2005;122(6):823-5.
6. Thibault S, Drolet R, Alain R, et al. Congenital swine pox: a sporadic skin disorder in nursing piglets. *Swine Health and Production.* 1998;6(6):276–278.
7. Freitas TRP. Swinepox Virus. In *Diseases of Swine*, 11th edition. Edited by JJ Zimmerman, LA Karriker, A Ramirez, KJ Schwartz, GW Stevenson, and J Zhang. 2019; 709-714.
8. Kagira, JM, Kanyari PN, Maingi N, Githigia SM, Ng'ang'a C, & Gachohi J. Relationship between the Prevalence of Ectoparasites and Associated Risk Factors in Free-Range Pigs in Kenya. *ISRN Veterinary Science.* 2013:650890.
9. Schramm B, Locker JK. Cytoplasmic organization of POXvirus DNA replication. *Traffic*. 2005;6(10):839-46.

Joint Pathology Center
Veterinary Pathology Services

WEDNESDAY SLIDE CONFERENCE 2025-2026

Conference #10 — 5 November 2025

CASE I:

Signalment:
8-year-old female spayed wire-haired terrier (*Canis familiaris*)

History:
The dog had history of acute glaucoma with bullous retinal detachment, kidney disease, and recent seizures. This animal was treated with fortekor and diethylstilbestrol.

Gross Pathology:
The dog had moderate amounts of body fat stores and normal muscle mass. The thoracic cavity contained approximately 40 ml of red-tinged, watery fluid. The lungs were mottled dark and bright red, heavy, wet, and non-collapsed; abundant pink foamy fluid oozed from the cut surface. The heart was rounded; the left ventricular free wall was 22 mm thick, and the right ventricular free wall was 5 mm thick (left ventricular hypertrophy). The left atrium was mildly dilated. The leaflets of the mitral valve were shrunken, thickened, and nodular (myxomatous valvular degeneration or endocardiosis). The right ventricle had multifocal, slightly raised, areas of subendocardial hemorrhage. In the abdominal cavity, the stomach contained moderate amounts of clear mucoid material. The intestinal tract showed multifocal areas of mucosal congestion. The pancreas had a diffuse nodular surface (nodular hyperplasia). The spleen had multifocal, small, dark-red nodules scattered throughout the surface.

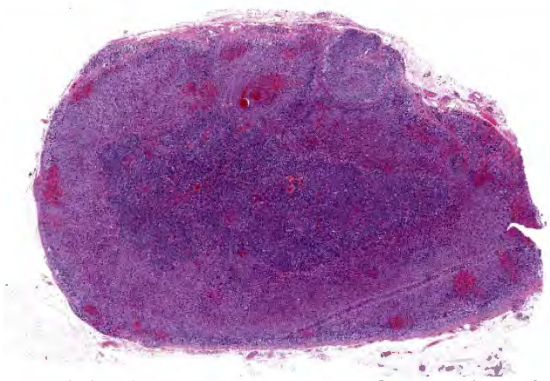

Figure 1-1: Adrenal gland, dog. One section of adrenal gland is submitted for examination. There is a focal cortical nodule and intracapsular hyperplasia of zona-glomerulosa cells. There is multifocal hemorrhage randomly scattered throughout the cortex and medulla.. (HE, 10X)

Multifocal areas of mucosal hemorrhage were noted in the trigone of the urinary bladder. The brain showed multifocal areas of meningeal hemorrhage over the occipital lobes. No gross abnormalities were observed in the rest of the carcass.

Laboratory Results:
N/A

Microscopic Description:
Adrenal glands: Multifocally, the small arteries and arterioles within the cortex and medulla show marked thickening of their walls, and narrowing or obliteration of their lumen, by intramural deposition of plasma proteins (consistent with hyaline arteriolosclerosis).

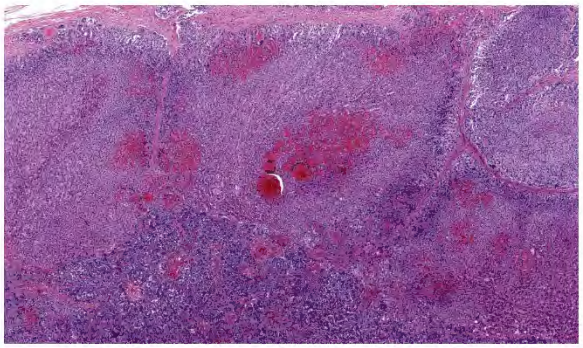

Figure 1-2: Adrenal gland, dog. There are numerous areas of sinusoidal congestion and hemorrhage scattered throughout the cortex and medulla. (HE, 52X)

Some vessels show intramural laminar deposits of plasma proteins (onion-skinning). Many sinusoidal vessels in the medulla are occluded by fibrin thrombi and are frequently effaced by hyaline material.

Contributor's Morphologic Diagnoses:
Adrenal glands: Multifocal hyaline arteriolosclerosis.
Condition: Hypertensive vasculopathy.
Other diagnoses (tissues not included in the submission):
Kidneys: Glomerulonephritis, diffuse, global, severe, subacute to chronic.
Eye globes: Bilateral retinal detachment with hyaline arteriolosclerosis, subretinal hemorrhage, and retinal atrophy (secondary glaucoma).
Heart, brain (choroid plexus), and spleen: Multifocal hyaline arteriolosclerosis.
Heart, right ventricle: Myocardial infarction, multifocal, acute.
Heart, mitral valve: Myxomatous valvular degeneration (endocardiosis).
Heart: Left ventricular hypertrophy.
Stomach: Mucosal necrosis and mineralization (uremic gastropathy).

Contributor's Comment:
Arteriolosclerosis is defined as "hardening of small arterial vessels" and consists of a group of arteriolar lesions often characterized as either predominantly hyaline or predominantly hyperplastic.[4] Hyaline degeneration (intimal hyalinosis), such as that seen in this case, refers to the histologic observation of amorphous, brightly eosinophilic material in vessel walls. This material stains magenta with periodic acid-Shiff (PAS) and often appears glassy.[4,5] It is a common vascular lesion resulting from accumulation of various serum plasma components in the subendothelial space and often extends into the media.[5] This lesion can be seen in various conditions, such as hypertension, diabetes mellitus, and focal segmental glomerulosclerosis (FSGS).[5] Thickening of the arteriolar wall due to accumulation of plasma proteins may lead to luminal narrowing and local ischemia.[4]

In humans, the most common inciting cause is hypertension. The pathogenesis in domestic animals is often not confirmed; most of the postmortem findings in the present case were consistent with systemic hypertension secondary to renal disease.[4] Although both primary and secondary hypertension have been reported in dogs, the latter is more common.[4]

Renal disease, such as in this case, is likely the most common cause of hypertension in dogs; however, since renal disease can be both the cause and consequence of systemic hypertension, it can be challenging to discern whether hypertensive vascular lesions are the result of primary or secondary hypertension.[4] Primary hypertensive lesions can lead to renal hypoperfusion, which activates the renin-angiotensin-aldosterone system, leading to more hypertension.[4] On the other hand, chronic renal disease often results in unbalanced excretion/retention of sodium and water, which

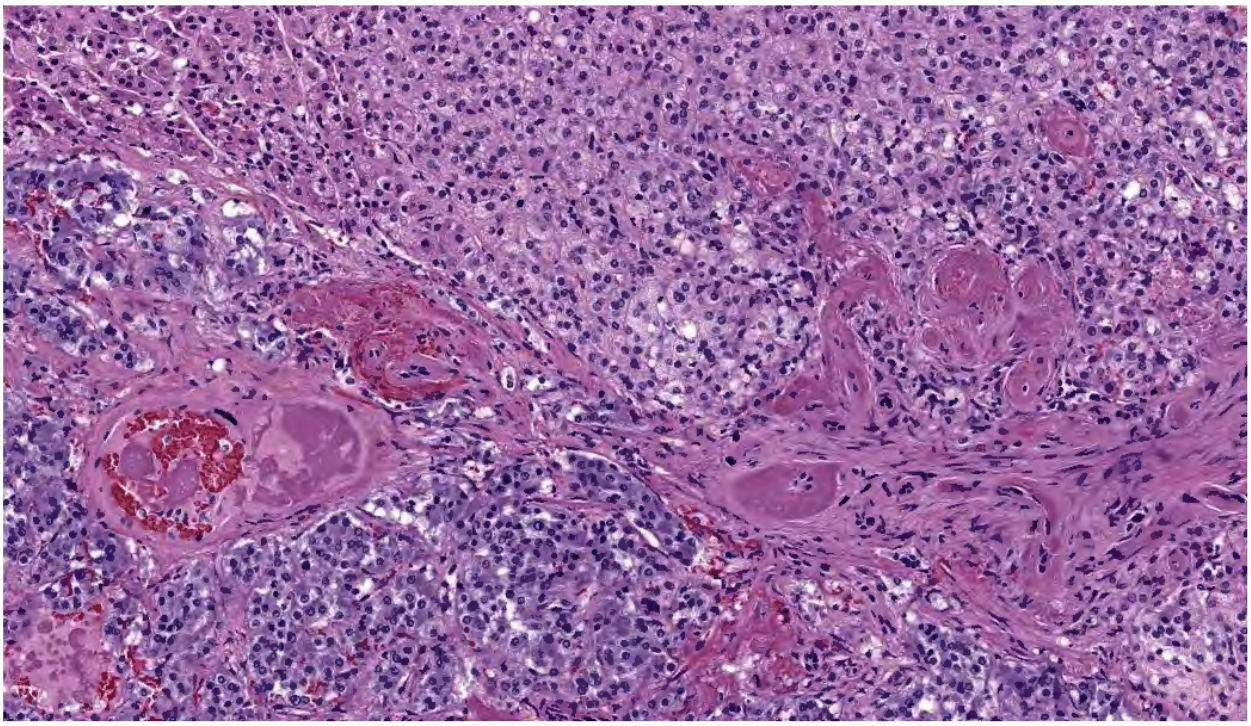

Figure 1-3: Adrenal gland, dog. Throughout the section (here at the corticomedullary junction), arteriolar profiles are tortuous, and the walls of arterioles are expanded by an accumulation of protein which expands the wall, effaces the tunica intima and smooth muscle cells, and compromises the lumen. There is periarteriolar hemorrhage. (HE, 261X)

leads to blood volume expansion and secondary hypertension.[4] Regardless of the initial inciting cause, hypertension becomes self-perpetuating as medial hypertrophy and hyalinization of arteries lead to hypoperfusion of organs, such as the kidney, and promotes additional hypertension and vascular damage.[4] Other lesions associated with secondary hypertension include hypertensive retinopathy with retinal detachment and left ventricular hypertrophy, which were also seen in this case.

Contributing Institution:
Veterinary Pathology – Western College of Veterinary Medicine
(https://wcvm.usask.ca/departments/vet-pathology.php)

JPC Diagnoses:
Adrenal gland, arterioles: Fibrinoid necrosis, chronic, diffuse, moderate, with fibrin thrombi and hemorrhage.

JPC Comment:
Conference 10 was moderated by the steadfast former Training Officer (and former WSC Coordinator) of the JPC, LTC Sarah Cudd! She chose to focus her conference cases on board-worthy entities and critical concept discussions for residents. This first case was challenging for participants and served as an excellent segway into a review of hypertension and atherosclerosis.

Discussion began with the differences between arteriosclerosis and atherosclerosis. Arteriosclerosis, meaning "hardening of arter-

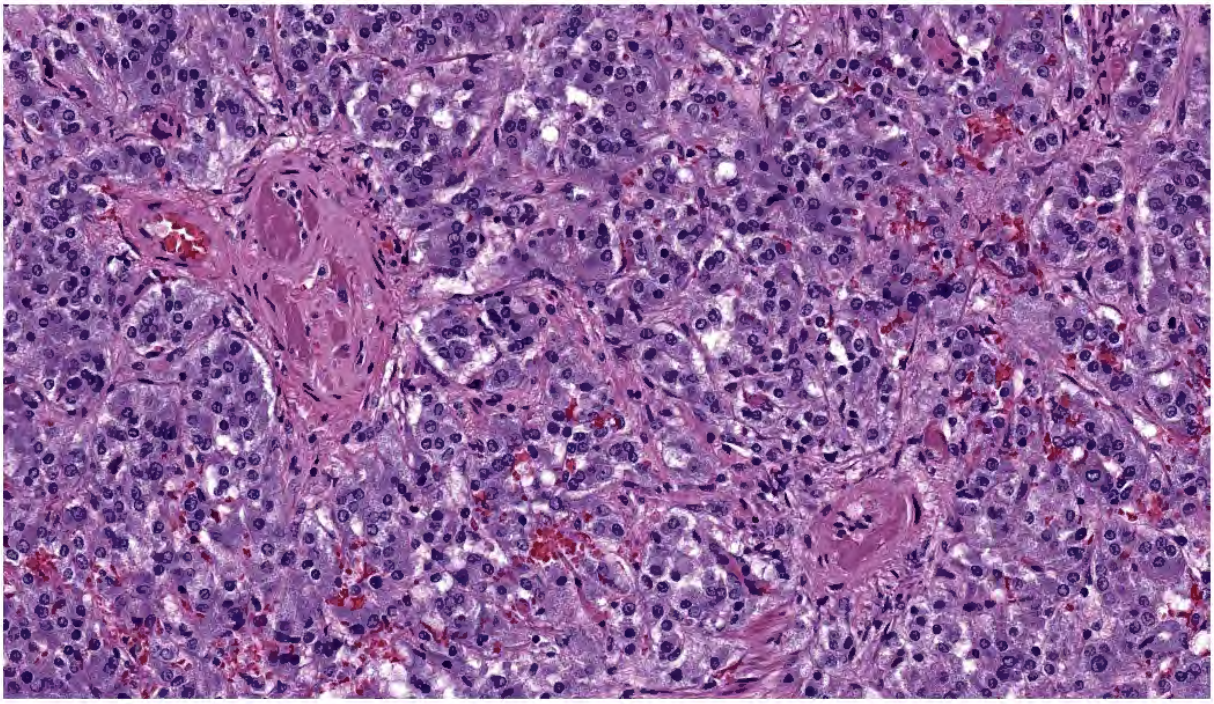

Figure 1-4: Adrenal gland, dog. Affected arterioles often contain fibrin thrombi. (HE, 451X)

ies", is characterized as a proliferative and degenerative arterial change in the absence of inflammation with thickening of the tunicas media and intima. Smooth muscle cells from the tunica media migrate to the tunica intima under the influence of platelet-derived growth factor PDGF), which stimulates smooth muscle cell migration and growth by binding to its receptors on the muscle cell surface. This triggers a series of internal signaling pathways that promote cell proliferation and migration, such as the PI3K/Akt/mTOR cascade. This pathway ultimately activates transcription factors that cause changes in gene expression and cell cycle progression via the activation of receptor tyrosine kinases. Atherosclerosis, on the other hand, is a subset of arteriosclerosis and is characterized histologically by degenerative fatty changes with cholesterol clefts, foam cells (which can be either macrophages or smooth muscle cells), and extra cellular lipid within arterial walls. Atherosclerosis is the most common type of arteriosclerosis in humans and is rarely seen in dogs except in cases of hypothyroidism or diabetes mellitus that contribute to hyperlipidemia. Miniature Schnauzers are genetically predisposed to atherosclerosis due to idiopathic hyperlipoproteinemia. Watanabe rabbits are also predisposed to and used as a research model for atherosclerosis due to a genetic mutation in their LDL receptors.

So, what about arteriolosclerosis? How does that compare to arteriosclerosis? Arteriosclerosis usually affects large arteries, such as the abdominal aorta in horses, ruminants, and carnivores, and is an aging change. Arteriolosclerosis affects small arterioles and is largely due to endothelial damage secondary to hypertension. There are two types of arteriolosclerosis: hyaline and hyperplastic. The hyaline form is considered the acute stage. In the hyperplastic form, proliferation of smooth muscle cells

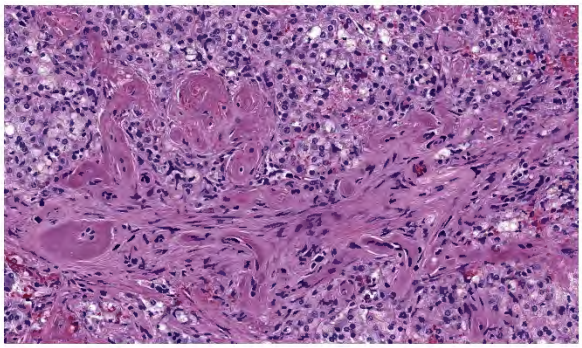

Figure 1-5: Adrenal gland, dog. Effete arterioles are surrounded by abundant fibroblasts and mature collagen, often giving cross sections of arterioles an "onion-skinned" appearance. (HE, 381X)

within the tunica intima, coupled with concentric fibrosis, can lead to a characteristic "onion-skinning" appearance of the affected vessels with chronicity.

Wrapping up conference discussion was a review of primary vs. secondary hypertension, which the contributor did an excellent job of covering in their comment. Hypertension causes hyaline arteriolosclerosis by causing endothelial damage, which then forces serum proteins from the blood out into the arteriolar walls where they accumulate and form deposits. This is traditionally referred to as "fibrinoid necrosis", and conference participants elected to use this term for the morphologic diagnosis. Additionally, the damage to the vessel walls from the increased pressure causes them to become tortuous and stimulates them to thicken and harden via smooth muscle proliferation and fibrosis as previously mentioned, reducing their elasticity and narrowing the lumen. This impairs blood flow and may result in thrombosis.[3] In cases of hypertension, the most common presenting clinical sign in affected animals is acute blindness secondary to hypertensive retinopathy.

With renal disease being one of the key drivers of hypertension in many species, a quick review of this pathogenesis is warranted. Renal disease causes secondary hypertension primarily through fluid retention. Injured kidneys are less able to remove excess fluid and sodium, which leads to an increased blood volume and, subsequently, an increased blood pressure. In primary hypertension leading to renal hypoperfusion, there is activation of the renin-angiotensin-aldosterone system (RAAS), which unfortunately only exacerbates the problem.

The RAAS first came under study in 1898 with the discovery of renin by Drs. Tigerstedt and Bergman when they found that renal extracts produced a vasopressor effect on tissue.[1] It wasn't until many years later that angiotensin and aldosterone were discovered and described, ultimately resulting in the RAAS we understand today.[1] RAAS becomes activated following an initial drop in blood pressure, during which less sodium is flowing through the kidneys.[1,2,3] The macula densa cells within the juxtaglomerular apparatus of

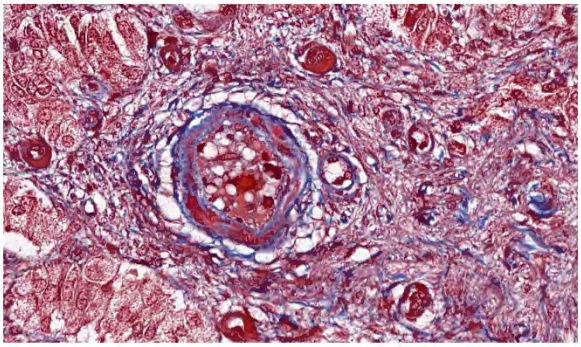

Figure 1-6: Adrenal gland, dog. A Masson's trichrome demonstrates the presence of mural collagen as well as protein deposits within the wall of affected arterioles. (Masson's trichrome, 581X).

the kidneys detect lower sodium levels within the proximal convoluted tubules and subsequently release prostaglandin E2 (PGE2).[2]

PGE2 then acts on juxtaglomerular cells within the afferent arterioles of the kidneys and causes them to release renin. From there, renin stimulates conversion of liver-produced angiotensinogen in the blood to angiotensin I within the kidneys.[2] Angiotensin-converting enzyme (ACE) then converts angiotensin I to active angiotensin II, which is a potent vasoconstrictor. Constriction of blood vessels subsequently stimulates the adrenal cortices to synthesize and release aldosterone, which then signals the kidneys to retain water and sodium from the distal convoluted tubules and collecting ducts, thereby increasing both blood volume and blood pressure.[2,3]

Angiotensin II also stimulates secretion of antidiuretic hormone (ADH) from the posterior pituitary, which increases the glomerular filtration rate by increasing water resorption from the kidneys.[2] It does this via the insertion of aquaporin-2 channels in the collecting duct.[2,3] It's not difficult to see from here how activation of RAAS makes a hypertensive problem worse. When coupled with a chronic arteriolosclerosis, it has been suggested that autoregulation of these systems becomes even further impaired and may result in additional increased systemic pressure to the glomerulus, further perpetuating renal disease and contributing to the vicious cycle of hypertension.[2]

References:

1. Basso N, Terragno NA. History about the discovery of the renin-angiotensin system. *Hypertension*. 2001;38(6):1246-9.
2. Manrique C, Lastra G, Gardner M, Sowers JR. The renin angiotensin aldosterone system in hypertension: roles of insulin resistance and oxidative stress. *Med Clin North Am*. 2009;93(3):569-82.
3. Nair R, Vaqar S. Renovascular Hypertension. [Updated 2023 May 22]. In: StatPearls [Internet]. Treasure Island (FL): StatPearls Publishing; 2025.
4. Robinson WF, Robinson NA. Cardiovascular system. In: Maxie MG, ed. Jubb, Kennedy, and Palmer's Pathology of Domestic Animals. Vol 3. – 6th ed. Philadelphia, PA: Elsevier; 2016: 59-60.
5. Olson JL. Hyaline arteriolosclerosis: New meaning for an old lesion. *Kidney International*. 2009;63:1162–1163.

CASE II:

Signalment:
2-month-old, male-intact, French bulldog, *Canis familiaris*, dog

History:
2-week history of vomiting, diarrhea, hyporexia, and lethargy. Generalized subcutaneous edema on presentation. Parvovirus snap test negative. Fecal culture:

Figure 2-1: Colon, dog. The serosal surface of the distal colon contains two, 10 x 15 x 4mm, ovoid, expansile, targetoid lesions (pale pink center surrounded by a hyperemic rim). (Photograph courtesy of: University of California, Davis School of Veterinary Medicine, Anatomic Pathology service https://www.vetmed.ucdavis.edu/hospital/support-services/lab-services/anatomic-pathology-service)

Figure 2-2: Colon, dog. The corresponding colonic mucosa of these foci is friable, thickened up to 8 mm thick, with an irregular corrugated mucosal surface that is mottled tan to brown, with a central area of pasty, white exudate. (Photograph courtesy of: University of California, Davis School of Veterinary Medicine, Anatomic Pathology service https://www.vetmed.ucdavis.edu/hospital/support-services/lab-services/anatomic-pathology-service)

negative for Salmonella sp., C. difficile, C. perfringens.

Gross Pathology:

The subcutis is diffusely expanded by up to 1 cm of gelatinous, translucent, pale yellow material (edema).

On the serosal surface of the distal colon are two, 10 x 15 x 4mm, ovoid, expansile, targetoid (pale pink center surrounded by a hyperemic rim) foci, located 15mm apart and approximately 2cm orad from the anus. The corresponding colonic mucosa of these foci is friable thickened up to 8 mm thick, with an irregular corrugated mucosal surface that is mottled tan to brown, with a central area of pasty, white exudate (pus, ulceration and necrosis).

Laboratory Results:

Parvovirus antigen SNAP test: negative (premortem

Fecal culture: negative for Salmonella sp., C. difficile, C. perfringens.

Pan-fungal PCR (through UGA) negative

Oomycete PCR (through UGA), positive for Pythium spp.

Microscopic Description:

This slide consists of three sections of segmentally ulcerated and necrotic colon and one section of less severely affected duodenum with attached pancreas. Within the colonic sections the mucosa is segmentally necrotic with loss of cellular architecture and replacement with amorphous to fibrillary eosinophilic material (fibrin, proteinaceous exudate), scattered karyorrhectic debris, and frequent 4 to 9 um wide, hyphal elements that have 1um wide, bright eosinophilic cell walls that are nonparallel, and demonstrate irregular, non-dichotomous, lateral branching and rare septation. The underlying submucosa, muscular layers, and occasionally the serosa (transmural), are infiltrated by the previously described hyphal structures, scattered karyorrhectic debris, mixed, swollen leukocytes (neutrophils, histiocytes, lymphocytes, and rare eosinophils), and extravasated erythrocytes (hemorrhage). The intestinal wall is variably necrotic, with loss of cellular detail and loss of differential staining. Medium sized arteries within the submucosa frequently contain dense mats of hyphal structures, with individual hyphae present within the vessel walls. In segments of mucosa adjacent to the completely ulcerated regions, fibrin thrombi are frequently present within lamina propria vessels. The necrotic luminal surface is lined by dense sheets of ovoid, bright eosinophilic, 5 x 5 to 5 x 8 um structures with a thin cell wall, and irregular, pale eosinophilic, internal vacuoles (zoospores), as well as loosely clustered dark basophilic, 1 to 2 um diameter, round structures (bacteria).

The section of duodenum demonstrates multifocal ulceration down to the submucosa, with replacement by fibrin and swollen leukocytes. Clusters of the previously described yeast

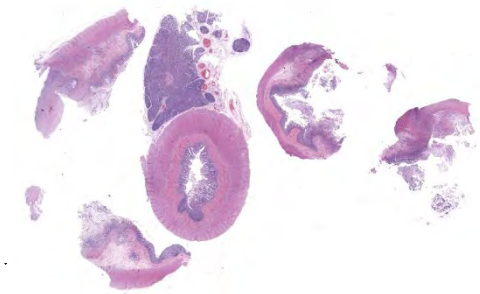

Figure 2-3: Colon, duodenum and attached pancreas, dog. Multiple ulcerated sections of colon, and an ulcerated section of duodenum with attached pancreas are submitted for examination. (HE, 10X)

structures are present within the fibrinous, luminal exudate. Villi are diffusely, markedly blunted (crypt: villous ratio ~ 1:1), fused, and the lamina propria is markedly expanded by densely packed mixed leukocytes, that include mainly lymphocytes and histiocytes, with fewer multinucleated giant cells, plasma cells, and granulocytes.

The interstitium of the pancreas is moderately to markedly expanded by dense streams of lymphocytes, plasma cells, histiocytes, and rare, fragmented neutrophils.

Contributor's Morphologic Diagnoses:

1. Colon: Fibrinonecrotizing and ulcerative, granulomatous and neutrophilic, transmural colitis, multifocal to segmental, severe, acute on chronic, with fibrin thrombi, intralesional hyphae, and intraluminal zoospores, and coccobaccili
2. Duodenum: Lymphoplasmacytic and fibrinonecrotizing duodenitis, moderate to marked, chronic, segmental with villous fusion, blunting, and intraluminal zoospores
3. Pancreas: Lymphoplasmacytic and histiocytic pancreatitis, marked, multifocal to coalescing

Contributor's Comment:

This case represents a florid case of intestinal pythiosis. The etiologic agent of pythiosis in mammals is *Pythium insidiosum*, which causes cutaneous, intestinal, and occasionally upper respiratory infections in a wide variety of species. *P. insidiosum* is an aquatic oomycete (clade Stramenopila/ heterokonts, class Oomycetes, order Pythiales, family *Pythiaceae*), with many of its closest relatives being plant pathogens that are the cause of what is colloquially known as "root rot". *Pythium* spp. are closer relatives to algae than fungi, and care should be taken to not miscategorize these organisms into the kingdom Fungi.

These water molds, unsurprisingly, preferentially grow in aquatic, warm environments. The preferable temperature range for growth ranges from 34 to 36C (93 to 97F) but growth is still possible in temperatures up to 45C (113F).[2] Historically, the distribution of this organism has been limited to tropical and subtropical environments, and in recent years (starting in 2003) increasing numbers of cases have been reported in higher latitude regions, such as Northern California and the Chincoteague national wildlife refuge in Virginia.[1,5,6] Speculation about the cause for the expansion in the geographic range of this or

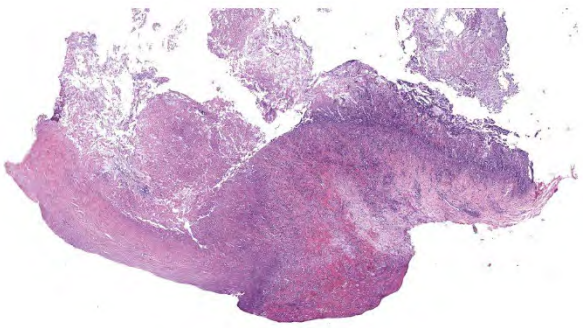

Figure 2-4: Colon, dog. Biopsy from one of the colonic lesions with full-thickness necrosis and abundant necrotic debris within the lumen (HE, 38X)

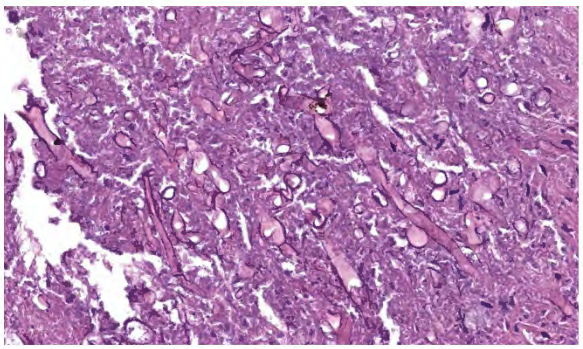

Figure 2-5: Colon, dog. The necrotic mucosa (left) contains numerous cross and tangential sections of pauciseptate 8-16um hyphae with non-parallel walls (HE, 778X)

ganism includes the adoption of environmental modifications such as rice field flooding in Northern California.[1]

Intestinal infection typically occurs through ingestion of contaminated water. Though typically not seen in tissue sections, this case included abundant intraluminal zoospores, which are the infective stage of this organism.[2] Motile zoospores are produced asexually from the bulbous sporangia formed at the terminal ends of the organism's hyphae.[4] Sexual reproduction resulting in oogonia also may occur, but the size of the intraluminal structures in this case was not consistent with oogonia, which measure 23 to 30 microns in diameter.[4] Oogonia/ oospores, unlike zoospores, can persist in sub-optimal environmental conditions and may survive for months to years.[1]

Infection of the digestive tract is the most common form of pythiosis in the dog; infections of young, large-breed dogs are most commonly reported, but have also been reported in female and small-breed dogs.[1,5] Digestive tract pythiosis has also been reported in small ruminants, and horses.[2,11] Cutaneous pythiosis occurs in dogs, horses, cats, humans, cattle, as well as a number of exotic species.[1,7] Additionally, rhinofacial pythiosis ("bullnose") has been reported in sheep in Brazil.[2]

The intestinal form of pythiosis typically involves segmental thickening with associated ulceration of any portion for the gastrointestinal tract wall, from stomach to colon with variable enlargement of associated lymph nodes.[11] Occasionally a distinct mass-like lesion composed of granulomatous and fibrous tissue will form; necrotic coagula known as "leeches" or "kunkers" can be embedded within the granulation tissue.[11] Histologically, intestinal infections consist of mural to transmural pyogranulomatous inflammation with concurrent lymphadenitis, lymphangitis, and in severe cases, peritonitis. Eosinophils, though not a prominent feature in this case, are frequently present in addition to pyogranulomatous inflammation; this is presumably due to a Th2 shifted immune response that has been associated with documented increased serum concentrations of Il-4, Il-5, and IgE.[9] In contrast to the presently discussed case, hyphal structures (as described above) are frequently difficult to discern with hematoxylin and eosin staining alone, and silver staining is often needed for visualization of the organism.[11] PAS staining is frequently poor to entirely ineffective due to lack of chitin production by the organism.[11]

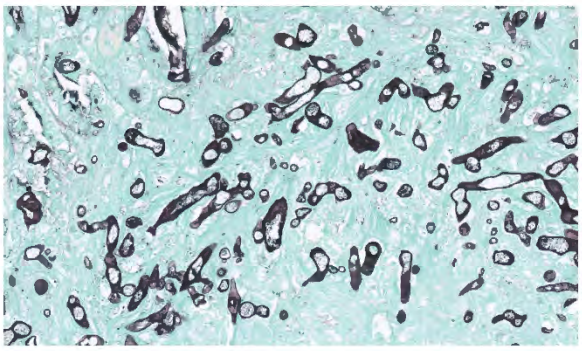

Figure 2-6: Colon, dog. A Gridley's methenamine silver bests demonstrates the morphology of the hyphae in section. (GMS, 594X)

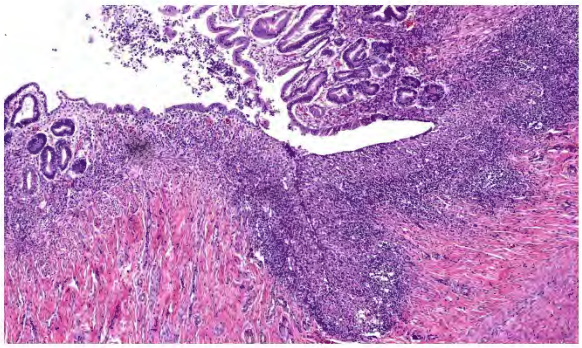

Figure 2-7: Duodenum, dog. There is a segmental duodenal ulcer extending downward into the underlying Peyer's patch. There is no evidence of fungal hyphae in this section. (HE, 124X)

The histologic lesions of intestinal pythiosis are not unique, and differential diagnoses based on histology include *Lagenidium* spp. (another oomycete), as well as a number of fungi, including zygomycetes, most notably *Conidiobolus* spp., and *Basidiobolus* spp.[2,11] Culture, serology, or molecular techniques (PCR, as used in this case) are needed for definitive diagnosis; interestingly, some panfungal PCR tests have been reported to amplify *Pythium* spp., likely due to the reliance on amplification of the internal transcribed spacer region, which is a pan-eukaryotic, non-coding segment of DNA.[8]

Unfortunately, intestinal infection with this organism can frequently be fatal. Treatment with antifungal agents is largely unsuccessful; it has been hypothesized that this may be due to the lack of ergosterol (the target of -conazole drugs) in oomycete cytoplasmic membranes.[9] Surgery to remove infected tissue is frequently the treatment of choice, and various immunotherapies have also been pursued with mixed success.[9]

Contributing Institution:
University of California, Davis School of Veterinary Medicine, Anatomic Pathology service
https://www.vetmed.ucdavis.edu/hospital/support-services/lab-services/anatomic-pathology-service

JPC Diagnoses:
1. Colon: Colitis, necrotizing and pyogranulomatous, subacute, multifocal, severe, with numerous hyphae, zoospores, and hyphal vascular invasion.
2. Duodenum: Duodenitis, ulcerative, subacute, multifocal, moderate.
3. Pancreas: Pancreatitis, lymphoplasmacytic and histiocytic, subacute, diffuse, marked, with acinar atrophy.

JPC Comment:
This was a truly phenomenal case of pythiosis and conference participants felt spoiled with how visible the hyphae and zoospores were on the slide. Oomycetes usually are much more challenging to find and tend to appear as "hyphal ghosts" from The Great Beyond, only visible with use of special paranormal photography...or a GMS stain. A classic entity, the contributor of this case provided an exceptional write-up on *Pythium insidiosum* and other major differentials in this case.

Conference discussion largely focused on a review of oomycete characteristics, most of which were covered by the contributor, as well as a few interesting facts about them that were not in the contributor's write-up. For one, infective *Pythium insidiosum* zoospores display chemotaxis towards animal hairs, intestinal mucosa, and wounded tissue. How neat is that? *Pythium* is also equipped with some impressive virulence factors that enable it to cause death and destruction regardless of it ends up in the intestinal tract or in the skin. Its cell wall components include cellulose and β-1,3-glucan. Beta-glucan, in particular, can be a target for host immune cells. [3,10] Despite

these being literal components of its own cell wall, *Pythium* comes equipped with a glucan 1,3-beta glucosidase, which breaks down β-1,3-glucan. While that may seem a bit counterintuitive, glucan 1,3-beta glucosidase acts as a virulence factor for *Pythium* by breaking down β-1,3-glucan from the cell wall, allowing the pathogen to dampen the host's immune responses and enable it to invade tissues.[3,10] This enzyme is identified as an "immunodominant" protein and is upregulated by *Pythium* during infection, suggesting it plays a key role in both disease progression and in triggering host immunity.[10]

Pythium also sports virulence factors such as has heat shock protein 70, chaperone proteins, enolase, elicitins, and urease. Much like it does in mammalian cells, heat shock protein 70 (HSP70) and other chaperone proteins protect *Pythium* from damage by binding to and stabilizing stress-induced misfolded proteins, preventing their aggregation and degradation and facilitating proper folding. HSP70 is induced under stressful conditions, such as heat (mammalian body temperature is pretty spicy if you're an oomycete), cold, infection, and inflammation. Another virulence factor, enolase, is primarily a glycolytic enzyme that catalyzes a crucial step in glycolysis to generate ATP. Enolase is also considered an immunodominant antigen.

Elicitins are proteins that are secreted by oomycetes, especially in those that infect plants, but are also seen in *Pythium insidiosum* and have dual functions. Elicitins can act as pathogen-associated molecular patterns (PAMPs) to trigger host defense responses, or they can act as virulence factors by manipulating host

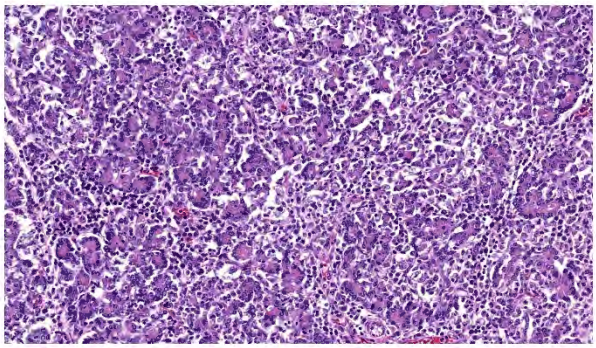

Figure 2-8: Pancreas, dog. There is marked interstitial inflammation within the pancreatic stroma by large numbers of lymphocytes and macrophages with fewer lymphocytes. There is marked atrophy of pancreatic acini. (HE, 348X).

defenses. They also act as sterol carriers, binding and transporting sterols that are essential for their growth and invasion. The dual role of elicitins makes their function context-dependent and varies based on the host and specific oomycete.

Lastly, the *P. insidiosum* urease, Ure1, hydrolyzes urea to produce nitrogen, which aids the organism's survival. Fun fact: *P. insidiosum's* urease shares similarity with the virulence factor urease, URE1, of *Cryptococcus neoformans*. In cases of pythiosis, urease is striding to the forefront as a potential diagnostic and therapeutic target because humans, as well as many domestic species, do not produce their own form of this enzyme.

References:

1. Berryessa, N., Marks, S., Pesavento, P., Krasnansky, T., Yoshimoto, S., Johnson, E. and Grooters, A.. Gastrointestinal Pythiosis in 10 Dogs from California. *Journal of Veterinary Internal Medicine*. 2008;22:1065-1069.

2. Carmo PMS, Uzal FA, Riet-Correa F. Diseases caused by *Pythium insidiosum* in sheep and goats: a review. *JVDI*. 2021;33(1):20-24.

3. Chechi JL, Franckin T, Barbosa LN, Alves FCB, Leite AL, Buzalaf MAR, Delazari Dos Santos L, Bosco SMG. Inferring putative virulence factors for *Pythium insidiosum* by proteomic approach. *Med Mycol*. 2019;57(1):92-100.

4. De Cock AW, Mendoza L, Padhye AA, Ajello L, Kaufman L. *Pythium insidiosum* sp. nov., the etiologic agent of pythiosis. *Journal of Clinical Microbiology.* 1987 Feb;25(2):344-9.

5. Fischer JR, Pace LW, Turk JR, Kreeger JM, Miller MA, Gosser HS. Gastrointestinal Pythiosis in Missouri Dogs: Eleven Cases. *JVDI*. 1994;6(3):380-382.

6. Jara M, Holcomb K, Wang X, et al. The Potential Distribution of *Pythium insidiosum* in the Chincoteague National Wildlife Refuge, Virginia. *Frontiers in Veterinary Science.* 2022;8.

7. Mauldin EA, Peters-Kennedy J. Chapter 6 - Integumentary System In: Maxie MG, ed. Jubb, Kennedy & Palmer's Pathology of Domestic Animals: Volume 1 (Sixth Edition): W.B. Saunders, 2016;509-736.

8. Meason-Smith C, Edwards EE, Older CE, et al. Panfungal Polymerase Chain Reaction for Identification of Fungal Pathogens in Formalin-Fixed Animal Tissues. *Veterinary Pathology.* 2017;54(4):640-648.

9. Mendoza L, Newton JC. Immunology and immunotherapy of the infections caused by *Pythium insidiosum*. *Med Mycol.* 2005;43(6):477-486.

10. Rujirawat T, Patumcharoenpol P, Lohnoo T, Yingyong W, Kumsang Y, Payattikul P, Tangphatsornruang S, Suriyaphol P, Reamtong O, Garg G, Kittichotirat W, Krajaejun T. Probing the phylogenomics and putative pathogenicity genes of *Pythium insidiosum* by oomycete genome analyses. *Sci Rep*. 2018;8(1):4135.

11. Uzal FA, Plattner BL, Hostetter JM. Chapter 1 - Alimentary System In: Maxie MG, ed. Jubb, Kennedy & Palmer's Pathology of Domestic Animals: Volume 2 (Sixth Edition): W.B. Saunders, 2016;1-257.e252.

CASE III:

Signalment:
14-year-old male intact Golden lion tamarin (*Leontopithecus rosalia)*

History:
The tamarin was housed in a zoo and had a chronic history (unknown duration) of waxing and waning diarrhea which was occasionally responsive to probiotics. The tamarin had a three-month history of increased symmetric dimethylarginine (SDMA) and blood urea nitrogen (BUN) that initially improved with antibiotics, but then continued to progress. Multiple renal cysts were noted on abdominal ultrasound. There was an additional two-month

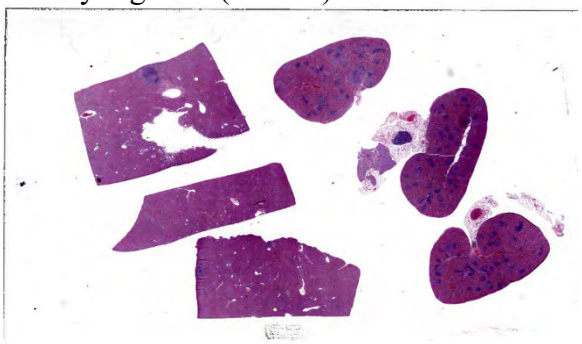

Figure 3-1: Liver and spleen, marmoset. The sections each of liver and spleen (and one section of pancreas and lymph node) are submitted for examination. AT subgross magnification, multiple foci of necrosis are visible within both the liver and splenic splenic parenchyma. (HE, 12X)

history of waxing and waning hyporexia and weight loss. Three days prior to euthanasia, the tamarin was progressively weak, lethargic, and ataxic. The tamarin was euthanized with pentobarbital following isoflurane anesthesia due to poor quality of life and prognosis.

Gross Pathology:
Approximately 20% of the hepatic and splenic parenchyma was effaced by approximately 30-40 pale tan, soft, well-demarcated foci ranging from pinpoint to 3 mm in diameter. The moderately distended gall bladder contained eight dark green choleliths ranging from 1 mm to 3 mm in diameter. Multiple lymph nodes (right mandibular, mesenteric, hepatic) were enlarged and oozed abundant pale tan purulent material on cut surface. Both kidneys had 10-15 multifocal to coalescing cystic dilations in the corticomedullary junction and medulla ranging from 2 to 5 mm in diameter. The cortex and medulla had approximately 20 multifocal punctate tan foci.

Laboratory Results:
Postmortem aerobic culture of pooled mandibular lymph node and liver grew *Listeria monocytogenes.*

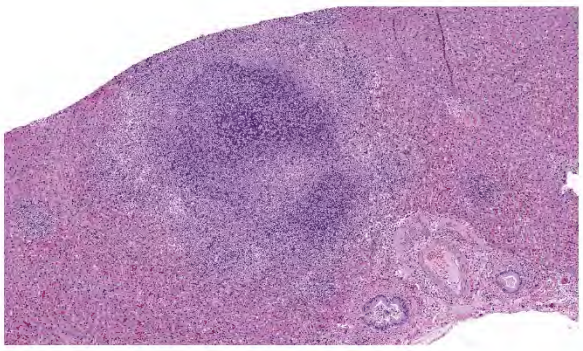

Figure 3-2: Liver, marmoset. Multiple foci of lytic necrosis ranging up to 1.5mm in diameter are scattered multifocally within the hepatic parenchyma.

Microscopic Description:
Liver: Approximately 40% of the hepatic lobular architecture is effaced by multifocal periportal to random discrete foci of lytic necrosis. Foci are composed of cellular debris, fibrin, myriad intact and fragmented neutrophils and moderate numbers of macrophages. There are small numbers of macrophages with tan to brown cytoplasmic pigment (hemosiderin vs. lipofuscin). Portal triads contain up

to four biliary duct profiles (biliary hyperplasia) and are surrounded by moderate numbers of lymphocytes, plasma cells, and macrophages. Moderate numbers of scattered hepatocytes contain brown granular cytoplasmic pigment (lipofuscin vs. hemosiderin) and cytoplasmic large discrete vacuoles. Multifocally, small hepatic vessels are partially occluded by aggregates of eosinophilic homogenous material interspersed with pyknotic debris, fragmented neutrophils, and macrophages (fibrin thrombi). Hepatic sinusoids are variably expanded with moderate numbers of erythrocytes (congestion), similar inflammatory infiltrates, and fibrin thrombi.

Spleen: Approximately 20% of the splenic parenchyma is effaced by multifocal to coalescing foci of necrosis and inflammation (similar to those described in the liver). Multifocally, the center of lymphoid follicles is hypocellular with eosinophilic karyorrhectic debris, extracellular yellow brown pigment globules (hematoidin), and moderate numbers of macrophages containing yellow brown cytoplasmic pigment (suspect hemosiderin). Splenic vessels are multifocally partially occluded by fibrin thrombi.

Contributor's Morphologic Diagnoses:
1. Liver: Moderate subacute multifocal random necrosuppurative hepatitis with periportal lymphoplasmacytic and histiocytic

cholangiohepatitis and mild biliary hyperplasia
2. Spleen: Moderate subacute multifocal necrosuppurative splenitis with lymphoid necrosis

Slides not submitted:

1. Kidney: Moderate acute multifocal suppurative nephritis, severe chronic diffuse cystic nephropathy and glomerulosclerosis with tubular proteinosis and mineralization
2. Gallbladder: Moderate cholelithiasis with mixed bacteria
3. Lymph node, mesenteric: Severe acute subacute multifocal necrosuppurative lymphadenitis

Contributor's Comment:
The combined gross findings, aerobic culture results, and histologic changes are consistent with necrotizing hepatitis, splenitis, nephritis, and lymphadenitis secondary to *Listeria monocytogenes* (sections of kidney and lymph node not included in submission). *Listeria monocytogenes* is a gram-positive, facultative anaerobic, bacillary bacterium that is abundant in soil and an opportunistic foodborne pathogen. In humans, common sources of infection include dairy products and processed fruits and vegetables. In this tamarin, contaminated fruit is postulated as the source of infection.

Infection in susceptible species can lead to various clinical syndromes, including gastroenteritis, septicemia, meningoencephalitis, abortion, and conjunctivitis. Reports of listeriosis in nonhuman primates are primarily focused on animal models of human abortion and fetal infection.[5] Spontaneous listeriosis is rarely reported.[2,6]

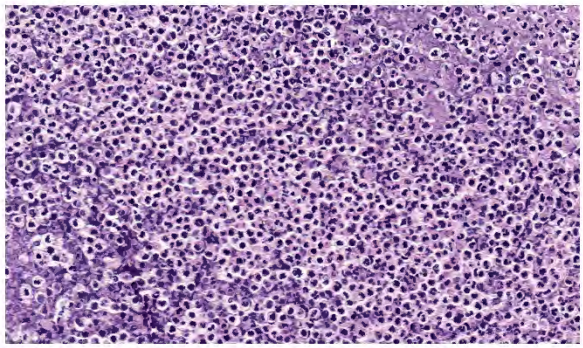

Figure 3-3: Liver, marmoset. Foci of lytic necrosis contain large numbers of viable and necrotic neutrophils admixed with fewer macrophages and abundant cellular debris. (HE, 660X)

Necrotizing hepatitis has been reported in a free-ranging Kenyan colubus monkey, and more recently, septicemic listeriosis was reported in a captive white-faced saki, which resulted in meningoencephalitis and hepatitis.[2,6] Similarly, *Listeria*-associated hepatitis is rarely reported in humans.[8] When reported in both humans and nonhuman primates, gross and histologic findings are similar to those described here. Grossly, the liver has multifocal pinpoint tan foci, which histologically correlate to multifocal areas of hepatic necrosis with infiltration of large numbers of neutrophils. Bacteria are not always histologically evident; therefore, culture is necessary for confirmatory diagnosis.[2,6,8]

As *L. monocytogenes* is an opportunistic pathogen, most infections are mild or subclinical. Multiple host risk factors contribute to severity of clinical disease. Neonates, pregnant animals, aged animals, and immunocompromised animals are most at risk for clinically significant disease. Chronic disease, including renal disease (as in this patient), liver disease, diabetes, and concurrent neoplasia all contribute to a poorer clinical presentation and prognosis.[9]

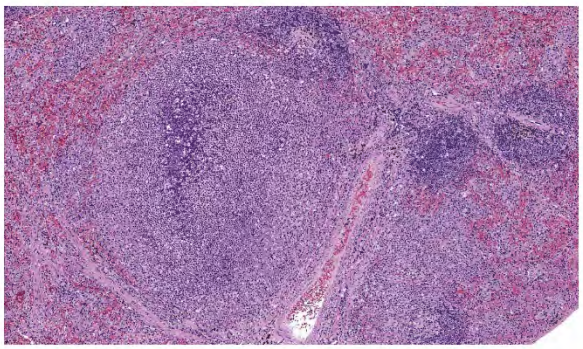

Figure 3-4: Spleen, marmoset. Similar foci of lytic necrosis ranging up to 1mm in diameter are scattered multifocally within the splenic parenchyma as well.

Infection occurs through ingestion and direct infection of enterocytes or invasion through Peyer's patches.[7] Gastroenteritis is a possible consequence of intestinal colonization, but not essential for systemic infection to occur. Rodent studies demonstrate that bacteria can cross the intestinal barrier within minutes of infection, and systemic infection can occur without histologically evident gastroenteritis.[3,4] Following intestinal infection, *L. monocytogenes* spreads to the liver through portal circulation, where it infects and proliferates within Kupffer cells and hepatocytes. In immunocompetent patients, infection is usually limited in the liver by activated macrophages and cytotoxic T-cells.[9] In acute infection, NK cells produce INF-γ, activating macrophages, which act to eliminate bacteria. In chronic infection, cytotoxic T-cells act to eliminate cells infected with *L. monocytogenes*.[1] In immunocompromised patients, infection can persist, and in some cases, become multisystemic through bacteremia and subsequent septicemia, as reported here.

Listeria monocytogenes has multiple key virulence factors involved in epithelial cell invasion (Internalin1A and Internalin1B), intracellular survival (hemolysin/lysteriolysin O), and cell-to-cell spread (ActA).[9,10] Internalin1A and Internalin 1B allows *L. monocytogenes* to infect non-phagocytic cells by interacting with lysteriolysin O to form a membrane pore through which the bacteria can enter the cell.[1,10] When engulfed by phagocytic cells, *L. monocytogenes* evades destruction by escaping the phagolysosome with listeriolysin O and phospholipases.[1,10] Once the bacteria are cytoplasmic, replication can occur. The virulence factor ActA then aids in cell-cell transfer by altering the cell cytoskeleton (actin filaments) to facilitate transfer of bacteria between cells.[1,10] In addition to aiding in phagolysosome escape, listeriolysin O and phospholipases aid in formation of bacteria-filled extracellular vesicles, which can be phagocytized by neighboring cells, leading to infection.[1,10]

Contributing Institution:
University of Wisconsin – Madison
School of Veterinary Medicine
Department of Pathobiological Sciences

JPC Diagnoses:
1. Liver: Hepatitis, necrosuppurative, acute, multifocal, moderate, with fibrin thrombi.
2. Spleen: Splenitis, necrosuppurative, acute, multifocal, moderate, with fibrin thrombi.

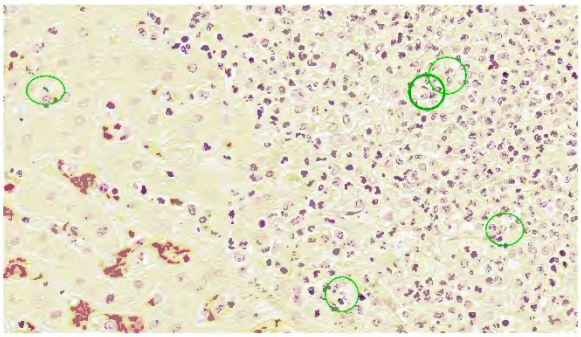

Figure 3-5.: Liver, marmoset. Rare gram-positive bacilli are present within areas of necrosis. (Brown-Brenn, 400X)

JPC Comment:

The contributor of this case wrote an excellent comment about *Listeria monocytogenes;* many topics of conference discussion focused on points from their write-up. Because the organisms were not visible without gram staining, this case proved challenging for conference participants, which some wondering about a protozoal cause for the lesions and others tentatively speculating about bacterial sepsis. Gram stains were performed in house at the JPC and revealed scattered, usually individualized, gram-positive bacilli, consistent with the *Listeria monocytogenes* identified by the contributor in this case.

Listeria monocytogenes is a resistant creature that is capable of withstanding harsh environments. It is not an organism one ever hopes to encounter in real life, but nevertheless, it occasionally finds a way to make headlines. *Listeria* is an intracellular pathogen that, as participants found, is very difficult to see on routine H&E staining. It is known to cause encephalitis and abortions but can also cause septicemia in some affected animals. It has an arsenal of virulence factors at its disposal that were nicely covered by the contributor and could make for easy boards-fodder.

LTC Cudd recounted a story about one of these virulence factors that may assist other residents in committing it to memory. She said that, during her residency, a resident-mate of hers found a video on YouTube of *Listeria monocytogenes* bacteria moving around within a cell using their ActA protein, which co-opts host cell actin to facilitate intracellular movement of the bacterium, as well as to transfer bacteria from cell to cell. The polymerized actin tails look like tiny "comets" or "rockets." In light of this, they adopted the term "Actin-A rockets" for *Listeria*. Having since watched this video, the bacteria do, in fact, look like microscopic rockets complete with fiery tails shooting around inside of the infected host cell. For educational (and entertainment) purposes alike, consider it recommended to go watch the video.

References:

1. Coelho C, Brown L, Maryam M, et al. *Listeria monocytogenes* virulence factors, including listeriolysin O, are secreted in biologically active extracellular vesicles. *J Biol Chem.* 2019;294(4):1202-1217.

2. Kock ND, Kock RA, Wambua E, et al. Listeriosis in a free-ranging colobus monkey (*Colubus guereza caudatus)* in Kenya. *The Vet Rec*. 2003:152:141-142.

3. Marco AJ, Prats N, Ramos JA, et al. A microbiological, histopathological and immunohistological study of the intragastric inoculation of *Listeria monocytogenes* in mice. *J Comp Pathol.* 1992;107(1):1-9.

4. Pron B, Boumalia C, Jaubert F, et al. Comprehensive study of the intestinal stage of listeriosis in a rat ligated ileal loop system. *Infect Immun.* 1998;66(2):747-755.

5. Schuppler M, Loessner M. The Opportunistic Pathogen *Listeria monocytogenes*: Pathogenicity and Interaction with the Mucosal Immune System. *Int J Inflam.* 2010:704321.

6. Smith MA, Takeuchi K, Brackett RE, et al. Nonhuman primate model for *Listeria monocytogenes*-induced stillbirths. *Infect Immun*. 2003;71(3):1574-1579.

7. Struthers JD, Kucerova Z, Finley A, Goe A, Huffman J, Phair K. Septicaemic Listeriosis in a White-Faced Saki (*Pithecia pithecia*). *J Comp Pathol.* 2022;194:7-13.

8. Vargas V, Alemán C, de Torres I, et al. *Listeria monocytogenes*-associated acute hepatitis in a liver transplant recipient. *Liver*. 1998;18(3):213-215.

9. Vazquez-Boland JA, Kuhn M, Berche P, et al. *Listeria* Pathogenesis and Molecular Virulence Determinants. *Clin Microbiol Rev.* 2001;14(3):584-640.

10. Zachary JF. Mechanisms of Microbial Infections. In: Zachary JF, ed. Pathologic Basis of Veterinary Disease. 7th ed. Elsevier; 2022.

CASE IV:

Signalment:
13-month-old, male, Sprague Dawley rat, *Rattus norvegicus*

History:
The animal was part of a colony of Dystrophin-deficient Sprague Dawley rats with a deletion within the exon 52 of the Dystrophin gene (R-DMDdel52 rats). These rats are used as a model for Duchenne muscular dystrophy. The rat was euthanized due to a masse on the left cheek.

Gross Pathology:
A 2-cm in diameter, well-demarcated, firm, tan mass with a central area of necrosis was observed within the left masseter muscle of the rat.

Laboratory Results:
N/A

Figure 4-1: Skeletal muscle, rat. A 2-cm in diameter, well-demarcated, firm, tan mass with a central area of necrosis was observed within the left masseter muscle. (Photo courtesy of: Unité d'Histologie et d'Anatomie Pathologique, BioPôle Alfort, Département des Sciences Biologiques et Pharmaceutiques, https://www.vet-alfort.fr)

Microscopic Description:
Left masseter muscle: Expanding and replacing up to 95% of the striated muscle on the tissue section, is a well-circumscribed, unencapsulated, highly cellular and heterogeneous neoplasm. The tumor is composed of tightly packed to loosely arranged round to elongated cells, haphazardly arranged or sometimes forming streams and bundles, separated by a moderate fibrovascular stroma. Some areas have a lower cellular density with increased amount of dense fibrous stroma.

Neoplastic cells have rather distinct cell borders, a plump appearance, variable amount of an intensely eosinophilic cytoplasm, oval to elongate paracentral nuclei with finely stippled chromatin and prominent nucleoli. Round to racket-shaped or tadpod shapes cells (rhabdomyoblasts) are observed. Some cells have moreover an intensely eosinophilic appearance with a central acidophilic inclusion-like structure peripherizing the nucleus (rhabdoid cells). Numerous and scattered multinucleated giant cells are also observed.

Figure 4-2: Skeletal muscle, rat. The mass from the masseter muscle, dissected and bisected. (Photo courtesy of: Unité d'Histologie et d'Anatomie Pathologique, BioPôle Alfort, Département des Sciences Biologiques et Pharmaceutiques, https://www.vet-alfort.fr)

There is marked cytologic atypia, namely anisocytosis, anisokaryosis, karyomegaly, macronucleolation, multinucleation, and bizarre mitotic figures. Mitotic figures average 10 per 10 high power fields and are often atypical.

Some preexisting dissected muscle fibers and adipocytes are present within the tumor.

Within the mass, there are several randomly distributed necrotic areas composed of eosinophilic cellular debris, viable and degenerate neutrophils. There are also lymphocytes, plasma cells and mast cells scattered among and at the periphery of the neoplasm. Surrounding tissue is compressed and neoplastic cells infiltrate the peripheral muscle fibers.

PTAH coloration was performed and showed very subtle striations in the tumor cells.

Immunohistochemistry was also performed for vimentin, myogenin and desmin. Tumor cells were strongly vimentin positive (intense cytoplasmic staining), and most cells were positive for myogenin (nuclear staining) and/or desmin (cytoplasmic staining).

Micrometastasis was observed in the associated lymph node and in the lungs (not present on slides)

Contributor's Morphologic Diagnoses:
Left masseter muscle: Rhabdomyosarcoma, pleomorphic type.

Contributor's Comment:
Rhabdomyosarcomas (RMS) are relatively rare mesenchymal neoplasms of skeletal muscle origin with varying myogenic differentiation that develop among several domestic animal species and in humans.[3,5,8,9,15] RMS can encompass a variety of gross and histologic aspects.[3] This tumor may be underdiagnosed due to these extreme variations in phenotype, age of onset, and cellular morphology that hinder diagnosis and classification.[3]

The most aggressive forms of RMS have been described in juvenile dogs younger than 2 years and include alveolar RMS and embryonal RMS.[3] Canine RMS has been described most commonly in the larynx and urogenital tract and were less frequently documented in the head, neck, and face.[3,9] Gross findings include firm, tan to white, multilobular masses with varying degrees of hemorrhage and necrosis.[3,9]

Figure 4-3: Skeletal muscle, rat. One section of the multilobular mass from the skeletal muscle is submitted for examination (normal skeletal muscle at right). (HE, 10X).

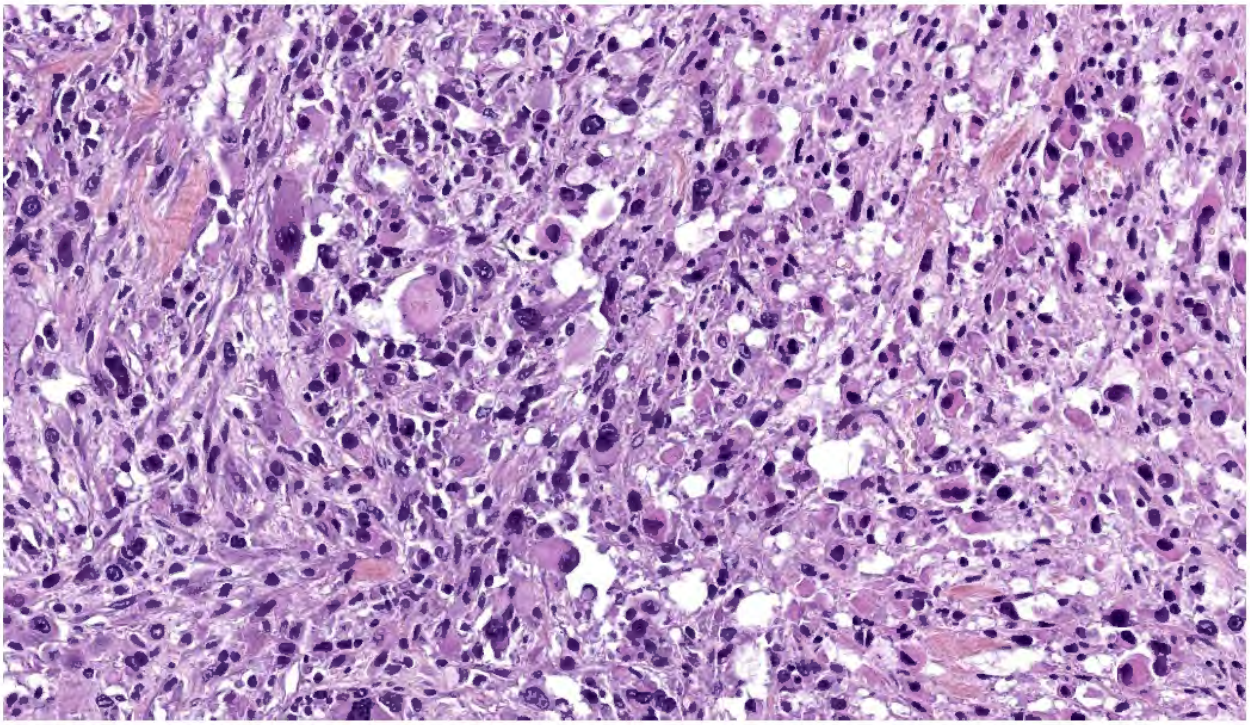

Figure 4-4: Skeletal muscle, rat. Pleomorphic polygonal to spindle cells comprise the neoplasm. (HE, 511X)

Common histologic subtypes include embryonal, botryoid, alveolar, and pleomorphic RMS.[1,3] Embryonal RMS and botryoid RMS are the most common forms in people and, seemingly, also in animals.[5,8,15]

Immunohistochemical (IHC) diagnosis of RMS in humans and dogs relies on detection of at least one muscle-specific marker (in particular, positive IHC labeling for desmin) and absence of smooth muscle markers.[1,3,14] It was recently suggested MyoD1 and myogenin should be included with desmin as part of a diagnostic IHC panel for canine RMS.[14]

Embryonal RMS is composed of either round cells or cells that exhibit different stages of development from myoblast-like and elongated cells to myotube-like ("strap") cells, that can be mononuclear or multinucleated in a myxoid stroma, with the majority of described cases arising from the head.[3,15]

Botryoid RMS is characterized by its submucosal location and its "grape-like" gross appearance. Histologically, it comprises mixed round and myotubular cells in mucinous stroma. It occurs most often in the trigone area of the urinary bladder in young large breed dogs.[3,15]

Alveolar RMS displays fibrous bands that divide small round cells into clusters and/or loose aggregates and can form thin fibrous septa.[3]

Pleomorphic RMS consists of haphazardly arranged plump spindle cells that may be admixed with scattered multinucleated cells, strap cells, racket-shaped cells, and large, round rhabdomyoblasts. Some pleomorphic RMS display cells with a rhabdoid morphology characterized by a peripherally located vesicular nucleus, prominent nucleolus, and intracytoplasmic eosinophilic hyaline

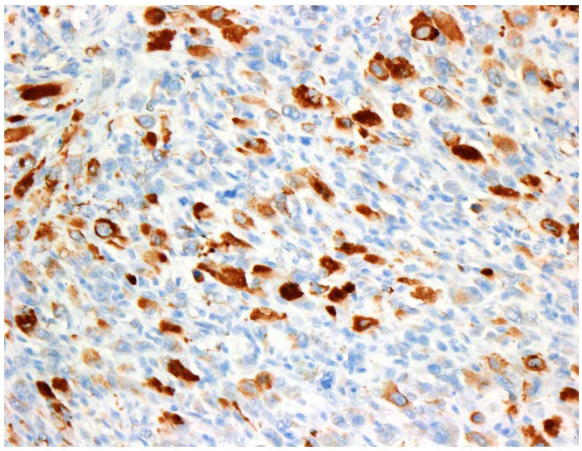

Figure 4-5: Skeletal muscle rat. Neoplastic cells demonstrate strong cytoplasmic immunopositivity for desmin. (anti-desmin, 400X) (Photo courtesy of: Unité d'Histologie et d'Anatomie Pathologique, BioPôle Alfort, Département des Sciences Biologiques et Pharmaceutiques, https://www.vet-alfort.fr)

inclusion-like structures.[5] Cells exhibit marked anisocytosis and anisokaryosis and bizarre mitotic figures.[3,15] Diagnosis of pleomorphic RMS is generally made when the whole tumor is pleomorphic, areas with embryonal or alveolar morphology are absent, and myogenic differentiation has been confirmed by immunohistochemistry.[3,15] This subclass can cause confusion since histologic evidence of skeletal muscle differentiation might not be obvious. Without immunohistochemical confirmation, such neoplasms may be diagnosed as anaplastic sarcomas.[3]

Pleomorphic rhabdomyosarcoma has been reported in dogs, cats, cows, horses, mice and rats. [2,3,4,6,9,10,13,15] It occurs less frequently than alveolar and embryonal RMS in humans. It is found more often in adult humans and animals and arises almost exclusively within skeletal muscle.[3] Noteworthy, development of pleomorphic RMS was described in a rat model of Duchenne muscular dystrophy (as in this case) following double knock-out of p16, a tumor suppressor gene, and dystrophin protein.[13]

Contributing Institution:
Ecole Nationale Veterinaire Alfort, Paris France, 7 avenue due General de Gaulle, 94700 Maisons-Alfort – 01 43 96 71 00
https://www.vet-alfort.fr

JPC Diagnoses:
Skeletal muscle: Rhabdomyosarcoma.

JPC Comment:
Although it provided a relatively straightforward diagnosis, this case stimulated great discussion in conference on subtyping of rhabdomyosarcomas, which the contributor also did an excellent job of writing about in their comment. Participants were split on what to classify this particular rhabdomyosarcoma as and, while most felt it was more likely an embryonal subtype rather than a pleomorphic due to the presence of myoblast-looking cells and strap cells, participants ultimately decided to forgo a subtype in the final morphologic diagnosis as there is currently no reported difference in clinical outcome with the different subtypes.

Other key points of conference discussion included a quick review of main sites for rhabdomyosarcoma development in other species. In dogs, these tumors often arise in the trigone of the urinary bladder, where they are usually

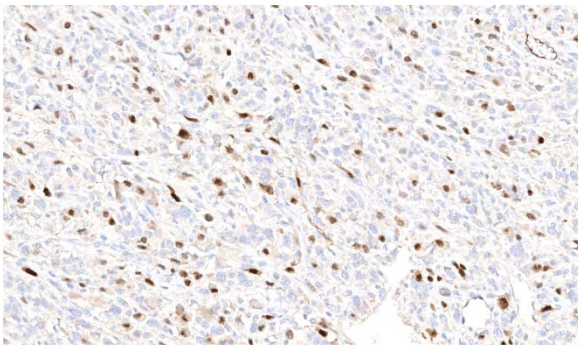

Figure 4-6: Skeletal muscle, rat. Neoplastic cells demonstrate strong regional nuclear immunoreactivity for myogenin. (anti-myogenin, 459X)

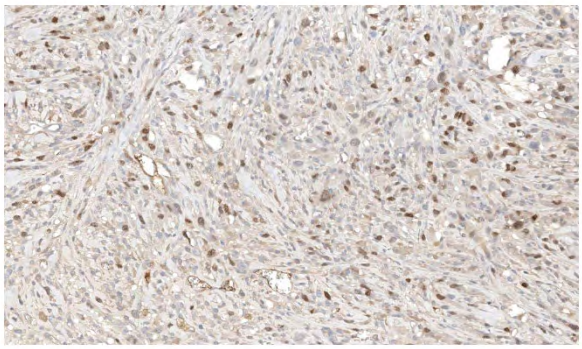

Figure 4-7: Skeletal muscle, rat. Neoplastic cells demonstrate strong regional nuclear immunoreactivity for myoD1. (anti-myoD1, 459X)

of the embryonal subtype, and in the larynx. Although rhabdomyosarcomas frequently occur in places that lack skeletal muscle (i.e. the urinary bladder), it is important to remember that they arise from myogenic precursors, which are stem cells, and stem cells can do whatever they want.

This conference case is from a dystrophin-deficient Sprague-Dawley (SD) rat, a strain of SDs used to study Duchenne muscular dystrophy of humans. Muscular dystrophy patients are predisposed to the development of rhabdomyosarcoma due to the loss of dystrophin.[7,13] Dystrophin normally functions to strengthen and stabilize muscle fibers via linking the actin cytoskeleton to the outer cell membrane and extracellular matrix. Loss of dystrophin leads to chronic damage of muscle cells and an increased rate of regeneration, which provides more chances for genetic mutations to occur.[7] Dystrophin is also a tumor suppressor gene, and its loss can result in an increased rate of not just myogenic neoplasms, but in cancer overall, especially carcinomas of the head and neck.[7]

The rhabdomyosarcoma was first described by German physician Dr. Weber in 1854 as a malignancy of striated muscle. There is some speculation on this, but he may have first described this lesion in a human tongue.[12] A more complete histologic definition was made in 1946 by Dr. Arthur Stout when he described distinct features of rhabdomyoblasts, which he stated appeared in “round, strap, racquet, and spider” shapes.[12] The current classification system for rhabdomyosarcoma was introduced in 1958 by Drs. Horn and Enterline.

Rhabdomyosarcomas are neoplasms of skeletal muscle, which is a type of striated muscle. Skeletal muscle striations are composed of alternating dark and light bands (A and I bands) that result from the highly organized, repeating arrangement of myosin and actin filaments within sarcomeres. I-bands are separated by a dark line called a Z-band, so named from the German word "zwischen" for their dark, zigzagging linear appearance. In contrast, according to Disney, “Z-bands” are “bracelets that all zombies are equipped with that send doses of electromagnetic pulses into the body, keeping the wearers from returning to their former brain-eating state. If the Z-band goes offline, the zombies revert.” So, there’s that.

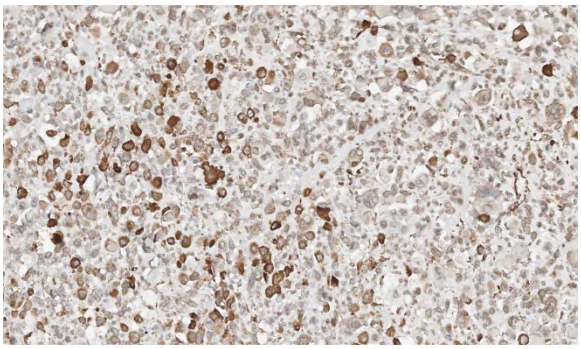

Figure 4-8: Skeletal muscle, rat. Neoplastic cells demonstrate strong regional cytoplasmic immunoreactivity for smooth muscle actin. (anti-SMA, 381X)

References:

1. Agaram NP. Evolving classification of rhabdomyosarcoma. *Histopathology*. 2022;80(1):98–108.
2. Aoyagi T, Saruta K, Asahi I, Hojo H, Shibahara T, Kadota K. Pleomorphic Rhabdomyosarcoma in a Cow. *J Vet Med Sci*. 2001;63(1):107–110.
3. Caserto BG. A Comparative Review of Canine and Human Rhabdomyosarcoma With Emphasis on Classification and Pathogenesis. *Vet Pathol*. 2013;50(5):806–826.
4. Castleman WL, Toplon DE, Clark CK, et al. Rhabdomyosarcoma in 8 Horses. *Vet Pathol*. 2011;48(6):1144–1150.
5. Goldblum JR, Folpe AL, Weiss SW. Rhabdomyosarcoma, in: Enzinger and Weiss's Soft Tissue Tumors. 2020, Mosby Elsevier, Philadelphia, PA, p. 652 696.
6. Inoue K, Yoshida M, Takahashi M, Cho Y-M, Takami S, Nishikawa A. Rhabdomyosarcoma in the Abdominal Cavity of a 12-Month-Old Female Donryu Rat. *J Toxicol Pathol*. 2009;22(3):195–197.
7. Jones L, Divakar S, Collins L, *et al.* Duchenne muscular dystrophy gene product expression is associated with survival in head and neck squamous cell carcinoma. *Sci Rep.* 2025;15:10754.
8. Meuten DJ., Cooper BJ., Valentine BA. Tumors of muscle, in: Tumors in Domestic Animals. p. 425-466. Wiley Blackwell 2017.
9. Scott EM, Teixeira LBC, Flanders DJ, Dubielzig RR, McLellan GJ. Canine orbital rhabdomyosarcoma: a report of 18 cases. *Vet Ophthalmol*. 2016;19(2):130–137.
10. Sher RB, Cox GA, Mills KD, Sundberg JP. Rhabdomyosarcomas in Aging A/J Mice. McNeil P, ed. *PLoS ONE*. 2011;6(8):e23498.
11. Spugnini EP, Filipponi M, Romani L, et al. Electrochemotherapy treatment for bilateral pleomorphic rhabdomyosarcoma in a cat. *J Small Anim Pract*. 2010;51(6):330–332.
12. Tandon A, Sethi K, Pratap Singh A. Oral rhabdomyosarcoma: A review. *J Clin Exp Dent*. 2012;4(5):e302-8.
13. Teramoto N, Ikeda M, Sugihara H, et al. Loss of p16/Ink4a drives high frequency of rhabdomyosarcoma in a rat model of Duchenne muscular dystrophy. *J Vet Med Sci*. 2021;83(9):1416–1424.
14. Tuohy JL, Byer BJ, Royer S, et al. Evaluation of Myogenin and MyoD1 as Immunohistochemical Markers of Canine Rhabdomyosarcoma. *Vet Pathol*. 2021;58(3):516–526.
15. Maxie MG, editor. Jubb, Kennedy, and Palmer's pathology of domestic animals. Elsevier 2016.

Joint Pathology Center
Veterinary Pathology Services

WEDNESDAY SLIDE CONFERENCE 2025-2026

Conference #11 — 12 November 2025

CASE I:

Signalment:
1-year-old, female, Brahma chicken (*Gallus gallus*)

History:
Found dead in the coop after sudden onset of inability to move with eyes closed and purple comb and wattle two days prior.

Gross Pathology:
The hen was covered in innumerable presumed mites. The heart had multifocal to coalescing regions of pallor. The liver had multifocal to coalescing regions of pallor with a focus of yellow, caseous material surrounded by green discoloration on the left lobe. The kidneys bilaterally had multifocal to coalescing regions of pallor.

Laboratory Results:
Aerobic bacterial culture of the liver: *Enterococcus faecalis*

Twort's tissue Gram stain: Cocci were gram-positive.

Microscopic Description:
Liver: Three sections of liver are examined. Within one section, there are multiple and coalescent, irregularly shaped granulomas replacing up to 60% of the tissue, multifocally blending in with the fibrous connective tissue of portal areas. Granulomas center around hypereosinophilic necrotic material mixed with

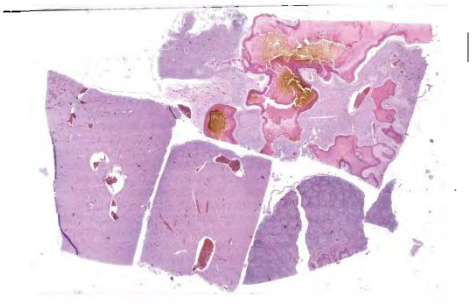

Figure 1-1: Liver and spleen, chicken. Three sections of liver and one section of spleen are submitted for examination. One section of liver demonstrates large geographic areas of necrosis. Similar but much smaller areas of necrosis are present at the bottom edge of the section of spleen. (HE, 10X)

relatively low to medium numbers of degenerate heterophils and cellular debris and multiple clusters of coccoid bacteria. Bordering the necrotic center is a layer of palisading macrophages with abundant eosinophilic and frequently vacuolated cytoplasm (epithelioid macrophages) and occasional multinucleated giant cells, which are further outlined by a robust layer of fibroblasts and collagen. Portal areas are variably expanded by medium to high numbers of lymphocytes, plasma cells, macrophages, including many laden with brown cytoplasmic granules, intermingled with numerous bile ducts (biliary hyperplasia), which extend into the adjacent parenchyma. In some portal areas, there are higher numbers of granulocytes with large, indented, vesiculate nuclei (interpreted as myeloid pre-

cursor cells and extramedullary hematopoiesis). Throughout all three sections of liver are individual necrotic hepatocytes to large regions of coagulative necrosis often centered around centrilobular veins, characterized by hepatocytes with shrunken, angular cell borders, hypereosinophilic cytoplasm and a pyknotic to karyorrhectic nucleus; larger areas of coagulative necrosis are frequently infiltrated by viable and non-viable heterophils. Within areas of necrosis and areas of viable hepatocytes are small clusters of coccoid bacteria within sinusoids.

Spleen: The splenic parenchyma is interrupted by a few, relatively smaller, coalescing granulomas centered around numerous viable and non-viable heterophils, pyknotic nuclei and cellular and karyorrhectic debris, which is separated by a collar of collagen and macrophages with the occasional multinucleated giant cells. Within these regions, there are multifocal cocci bacteria colonies. There are deposits of fibrin and serum protein present throughout the sinuses and around ellipsoids. Within these foci are few reticuloendothelial cells, red cells, low numbers of lymphocytes and macrophages, as well as pyknotic nuclei and karyorrhectic and cellular debris and colonies of coccoid bacteria.

Contributor's Morphologic Diagnoses:
Liver: granulomatous and necrotizing hepatitis, multifocal to coalescing, severe, with intralesional cocci and biliary hyperplasia

Spleen: granulomas, multifocal, marked, with intralesional and embolic cocci

Contributor's Comment:
Enterococci are non-motile, gram-positive, facultative anaerobic cocci bacteria that can appear in short and medium chains.[6] Unlike staphylococci and streptococci, toxins are not produced. Surface components that allow success for *Enterococci* include a polysaccharide capsule, adhesins, pili, and aggregation substance. *Enterococci* are able to produce biofilms, which allows for adherence, especially in nosocomial infections and contributes to antibiotic resistance. Virulence factors include bacteriocins, hemolysins, gelatinases, and serine proteases. Cell injury has been induced via production of toxic oxygen metabolites.[7] Unlike *Streptococcus* sp., these bacteria can tolerate bile salts and grow on MacConkey agar.[9]

Enterococcus sp. are considered normal flora in the gastrointestinal tract of poultry and other bird.[3,5,8] However, certain species that have been isolated in clinical disease include *E. avium, E. cecorum, E. durans, E. faecalis, E. faecium,* and *E. hirae*. Enterococcosis is a bacterial septicemia that has been reported in a variety of avian species. Birds can be afflicted via oral or aerosol routes (bedding, water, hatchery fluff) but can also arise from skin wounds.[5,8] There have been reports of vertical transmission through hens with salpingitis or peritonitis that continue to lay.[5] However, *Enterococcus faecium* has the potential to be a useful probiotic against other detrimental gastrointestinal disease in birds, such as colibacillosis, and improve feed efficiency.[3,10]

Across all ages, *Enterococcus faecalis* affects birds of all ages just as in this hen in this case, followed by *faecium*. Many birds die due to the rapid progression of disease and have vague clinical signs to include depression, lethargy, ruffled feathers, diarrhea, and decrease in egg production. Virulence factors that allow for infection include the collagen-binding protein (ace), aggregation substances

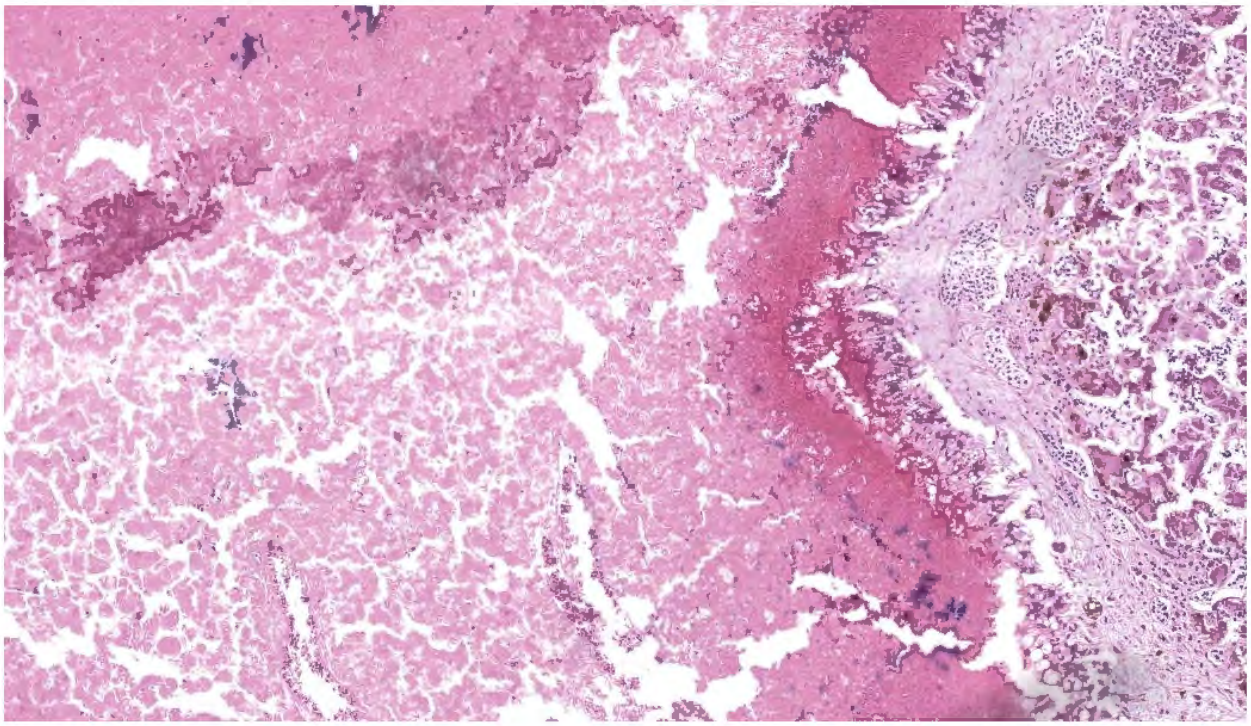

Figure 1-2: Liver, chicken. Areas of hepatocellular infarction contain large colonies of cocci, and are bounded by a thick eosinophilic rim of necrotic heterophils and cellular debris, and in turn by a layer of epithelioid and fewer foreign-body type macrophages and concentric lamellae of fibrous connective tissue. (HE, 125X)

(asa1), hemolysin activator (cylA), endocarditis antigen (efaA), surface protein (esp), gelatinase (gelE, and putative surface antigen EF0591.[5]

Enterococcus cecorum has become a significant disease in adult broiler chickens, causing femoral head necrosis, spondylitis, and arthritis. This disease is colloquially called "kinky back" when vertebral osteoarthritis occurs. The pathogenesis was recently described as requiring intestinal colonization that progressed to bacteriaemia prior to invading the skeletal tissue and demonstrated that intestinal disease itself was not required.[1,2]

In other species, Enterococci cause mastitis, enteritis, respiratory disease, endocarditis, and urinary tract disease as well as septicemia.[9] In humans, Enterococci cause 12% of nosocomial infections with E. faecalis and faecium being the most prevalent of the species.[6] Nosocomial infections frequently occurred through IV catheters, urinary catheters, aortic valve implantation, prosthetic joints, and other surgical sites. Occasionally, neurologic diseases, to include meningitis, do occur.[7]

Contributing Institution:
University of Connecticut Department of Pathobiology and Veterinary Sciences
Connecticut Veterinary Medical Diagnostic Laboratory
https://pathobiology.cahnr.uconn.edu/
https://cvmdl.uconn.edu/

JPC Diagnoses:
1. Liver: Hepatitis, necrotizing, heterophilic and granulomatous, chronic, multifocal to coalescing, severe, with numerous cocci.
2. Spleen: Splenitis, necrotizing, heterophilic and granulomatous, chronic, multifocal, moderate, with numerous cocci.

3. Liver: Extramedullary hematopoiesis, chronic, periportal, moderate.

JPC Comment:
The University of Pennsylvania's Dr. Nathan Helgert moderated this year's 11th conference. This is his first time moderating for the WSC, and participants thoroughly enjoyed his quick wit and engaged teaching style. He chose to focus on poultry and ruminant pathology, which participants are always grateful for. This first case was a classic entity with fantastic histologic lesions that, according to some conference goers, provided the perfect moment to make use of the term "geographic" to describe those dramatic areas of necrosis. They truly resemble some beautiful cartography.

Conference discussion focused on the diagnostic approach to cases like this one where additional diagnostics are required to "suss out" the etiologic agent. Participants were asked to take a figurative step back and develop a list of possible causes of bacterial sepsis in chickens that could lead to hepatic and splenic lesions like these. The list included *E. coli* (colibacillosis), *Salmonella typhimurium, Staphylococcus aureus, Enterococcus spp, Streptococcus spp., Erysipelothrix rhusiopathiae* (although this is more likely in turkeys and pheasants than in chickens), *Mycobacterium spp (*especially *M. avium),* and *Pasteurella multocida*, to name just a few. Some of these look nearly identical to one another both grossly and histologically, while others of these have more distinct features. Either way, culture and special stains will be needed.

As with every case of suspected bacterial infection, a simple Gram stain can provide crucial information. Of these above-mentioned

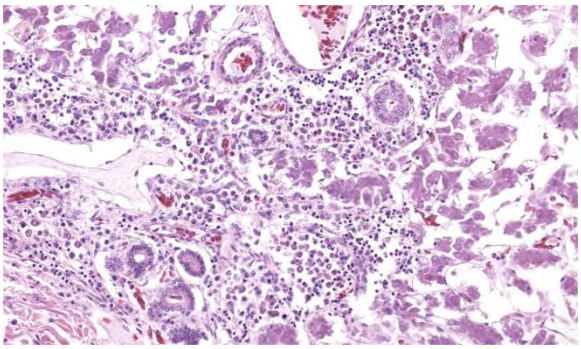

Figure 1-3: Liver, chicken. Portal areas are markedly expanded by extramedullary hematopoiesis. (HE, 406X)

organisms, several of them are gram-negative rods, which would make them less likely with the gram-positive staining seen in this case. *Mycobacterium spp*, which are best revealed with acid-fast stains due to the mycolic acid in their cell wall, were not present in this case. *Erysipelothrix rhusiopathiae* is a gram-positive rod, but the bacteria in this case were clearly cocci. Although it can sometimes be challenging to discern bacterial morphology, participants felt confident in this case calling these cocci both on the H&E and on the gram stain. This narrowed the field substantially to *Streptococcus, Staphylococcus,* or *Enterococcus*. The contributor was able to culture *Enterococcus faecalis* from an aerobic bacterial culture to confirm the identity of the offending organism in this case.

The contributor provides a succinct overview of *Enterococcus spp* in poultry, including the virulence factors that enable their pathogenesis. Infection by *Enterococcus spp* in chickens (and other birds) is considered opportunistic, and affected birds are generally older (>12wks) than those affected by *E.coli*, which typically affects younger birds. *Enterococcus faecalis* is normal flora of the chicken GI tract, whereas *Enterococcus cecorum,* which still requires intestinal colonization to occur prior

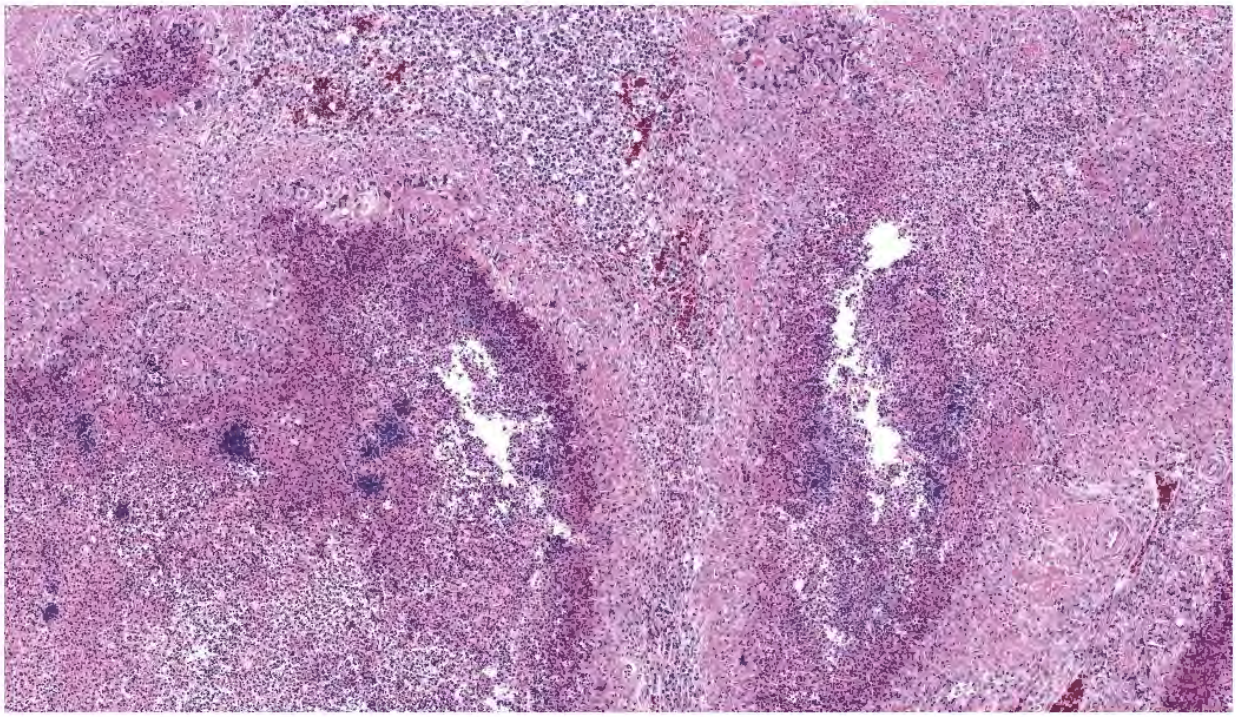

Figure 1-4: Spleen, chicken. Heterophilic granulomas, similar to those seen in the liver, are centered on areas of splenic necrosis with colonies of cocci.. (HE, 165X)

to septicemic spread, is not.[4,5] *E. cecorum* has a known predilection for bone, and primary sites of bone infection include the free thoracic vertebra (the synsacrum), the femoral head, and the hock.[2]

So why the free thoracic vertebrae? Predilection of *E. cecorum* for this site has been linked to osteochondrosis dissecans (OCD) of the free thoracic vertebrae, which is a common background lesion in broiler chickens.[2,4] The current hypothesis is that these OCD lesions result in clefts in the articular cartilage within these vertebrae that facilitate *E. cecorum* colonization and subsequent vertebral osteomyelitis.[2] Bacterial infection of bone results in a marked inflammatory response, coupled with edema and suppuration secondary to the actions of neutrophils and macrophages that are called in by pro-inflammatory cytokines. Additionally, there is subsequent osteoclast activation and bone resorption, which can result in pathologic fracture and collapse of the affected vertebrae.[2] This is one of the most common sequelae of this condition.[2,4] Following fracture, there is dorsal displacement of suppurative material and necrotic bone into the spinal canal, resulting in a sudden onset of ataxia and loss of proprioception to the hind limbs. Affected chickens will have a classic "motorcycle rider" or "hock-sitting" stance due to their inability to use their legs.[1,2.4] These birds will also have dirty wing edges due to "wing-walking" behavior as they attempt to ambulate with the support of their wings.

If you aren't sure what this "motorcycle rider" stance looks like in *Entercoccus*-infected birds, please do not google "motorcycle rider chicken" without the addition of "*Enterococcus*" unless you want to see photoshopped images of chickens riding actual motorcycles, or unless you want to learn all about "chicken

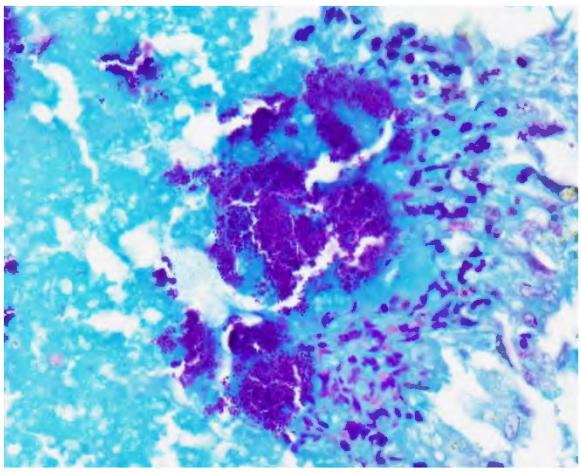

Figure 1-5: Liver, chicken. Colonies of cocci stain gram-positive. (Twort's, 400X) (Photo courtesy of: University of Connecticut Department of Pathobiology and Veterinary Sciences, Connecticut Veterinary Medical Diagnostic Laboratory, https://pathobiology.cahnr.uconn.edu/, https://cvmdl.uconn.edu/)

strips" in the motorcycle community, which refer to the unworn rubber on the outer edges of motorcycle tires. They are called "chicken strips" because they are usually seen on bikes of riders that are considered too nervous, or "chicken", to lean their bike over in sharp turns. Speaking from experience, being able to lean your bike over so far in a turn that you "get your knee down" to the pavement is considered to be an important rite of passage for motorcyclists, but one would have to imagine that chickens do not appreciate this comparison (*MAJ C. Culligan, personal communication*).

References:

1. Borst LB, Jung A, Chen LR, Suyemoto MM, Barnes, HJ. A Review of *Enterococcus* cecorum infection in Poultry. *Avian Dis*. 2018; 62: 261-271.

2. Borst LB, Suyemoto MM, Sarsour AH, et al. Pathogenesis of Enterococcal Spondylitis Caused by *Enterococcus cecorum* in Broiler Chickens. *Vet Path*. 2017; 54: 61-73.

3. Cao GT, et al. Effects of a probiotic, *Enterococcus faecium*, on growth performance, intestinal morphology, immune response, and cecal microflora in broiler chickens challenged with *Escherichia coli* K88. *Poult Sci*. 2013; 92(11): 2949-2955.

4. Dolka B, Chrobak-Chmiel D, Czopowicz M, Szeleszczuk P. Characterization of pathogenic Enterococcus cecorum from different poultry groups: Broiler chickens, layers, turkeys, and waterfowl. *PLoS One*. 2017;12(9):e0185199.

5. Jorgensen SL, et al. Characterization of *Enterococcus faecalis* isolated from the cloaca of fancy breeds and confined chickens. *J Appl Microbiol*. 2017; 122: 1149-1158.

6. Rehman MA, Yin X, Zaheer R, et al. Genotypes and Phenotypes of Enterococci Isolated from Broiler Chickens. *Front Sustain Food Sys*. 2018; 2: 1-28.

7. Said MS, Tirthani E, Lesho E. *Enterococcus Infections*. Treasure Island, FL; Stat Pearls [Internet]; 2022: 1-33

8. Streptococci. In: Quinn PJ, Markey BK, Carter, ME, Donnelly WJ, Leonard FC. *Veterinary Microbiology and Microbial Disease.* London, UK; Blackwell Science Ltd; 2002: 49-51.

9. The Genera *Streptococcus* and *Enterococcus*. In: Songer JG, Post KW. *Veterinary Microbiology: Bacterial and Fungal Agents of Animal Disease*. 1st ed. St. Louis, MO; Elsevier Saunders; 2005: 51-53.

10. Zheng A, Luo J, Meng K, Li J, Bryden WL, Chang W, Zhang S, Wang LX, Liu G, Yao B. Probiotic (*Enterococcus faecium*) induced responses of the hepatic proteome improves metabolic efficiency of broiler chickens (Gallus gallus). BMC Genomics. 2016;17:89.

CASE II:

Signalment:
78-day-old Chicken (*Gallus gallus*)

History:
The case is a chicken found dead on a Japanese native breed farm.

Gross Pathology:
The liver was enlarged and diffusely dark red. The spleen was moderately enlarged.

Laboratory Results:
DNA was extracted from the liver homogenate. PCR for detecting avian leukosis virus (ALV) subgroup B and endogenous subgroup E was positive.

Microscopic Description:
Round hematopoietic tumor cells strongly infiltrated the hepatic blood vessels and sinusoids. The hepatic sinusoids were diffusely expanded by tumor cell infiltration, with fewer normal erythrocytes and enlarged Kupffer cells which sometimes contained cellular debris. Most hepatocytes were shrunken. A few granulocytes were also found in the hepatic sinusoid. Small foci of granulocytic cells at different nuclear maturation stages were present around some hepatic triads. Tumor cells appeared round, oval, or polygonal in shape with a distinct cell border, amphophilic cytoplasm, anisocytosis, and anisokaryosis. Some tumor cells contained perinuclear pale areas known as halos. The nucleus was round and hyper

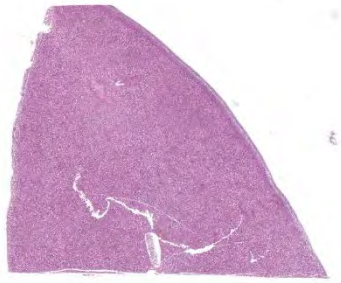

Figure 2-1: Liver, chicken. One section of liver is submitted for examination. (HE, 8X)

chromatic to pale, with one or two large nucleoli and coarsely clumped chromatin. Some binuclear tumor cells were also observed. There was significant mitosis and karyorrhexis of tumor cells. The cytoplasmic eosinophilic granules that are characteristic to myelocytic lineage cells were not present in tumor cells.

Immunohistochemical analysis revealed that tumor cells consistently exhibited cytoplasmic staining of hemoglobin antigen, with variable staining intensity, faint to strong, depending on the tumor cell. Hemoglobin was also detected in normal erythrocytes. Tumor cells were negative for CD3 (T cell marker), BAFF-R (B cell marker), and Iba-1 (macrophage/monocyte marker). Enlarged Kupffer cells were positive for Iba-1.

Tumor cells were observed in other organs, but only in the blood vessels. Some thrombi composed of necrotic tumor cells and fibrin were also observed in the vessels. The bone marrow was not histologically examined.

Contributor's Morphologic Diagnoses:
Avian erythroblastosis

Contributor's Comment:
Avian erythroblastosis (AE), also called erythroid leukosis, is a hematopoietic tumor of

Figure 2-2: Liver, chicken. Hepatic sinusoids are filled with innumerable immature and neoplastic chicken erythrocytes. (HE, 738X). Hepatocytes are diffusely and mildly atrophic. There are numerous rhectic neoplastic cells and Kupffer cells often contain cellular debris.

erythrocytic lineage cells in birds.[2,7,9] Spontaneous occurrence of this tumor is rare in commercial chickens,[2] although there are several experimental reports of AE in chickens inoculated with AE virus (AEV) and some other viral strains in the avian leukosis/sarcoma group.[3,4,10,11,14,16,17] Experimentally, the viruses can induce AE and often other types of tumors, depending on the experimental conditions, such as the strain and dose of virus, inoculation route, and various host factors.[3,4,10,11,14,16,17] Historically, AEV has been used in research on viral oncogene and erythrocytic differentiation.[7,8,9] The relationship between the occurrence of AE and exogenous ALV infection is unclear in this case.

On the basis of the histologic and IHC findings, the hematopoietic tumor was diagnosed as AE. The chicken exhibited findings suggestive of AE, such as an enlarged, cherry red liver, intravascular nature of tumor cells, and round hematopoietic tumor cells with occasional perinuclear halo.[2,14] In addition, IHC detection of hemoglobin antigens in tumor cells was conclusive evidence of AE.

Hemoglobin is one of the markers useful for diagnosing erythrocytic tumors in humans and other mammals.[6,15,18] Past studies have reported that hemoglobin is present in transformed AE cells of chickens inoculated with AEV.[1,5] In past related studies conducting immunofluorescence assays of cultured AE cells transformed by AEV infection, the cells expressed a variety of avian erythrocytic markers, including hemoglobin, histone-5, erythroblast surface antigen, and erythrocyte surface antigen.[3,8] A commercial rabbit monoclonal antibody (clone EPR3608) against the human hemoglobin can cross-react with chicken erythrocytes and erythrocytic precursors in the

bone marrow on paraffin sections without nonspecific reactions.

Histologic differential diagnosis includes myeloid, lymphoid, and histiocytic tumors.[2,13] In addition, a concurrent tumor of mixed AE and myelocytoma components has been described.[2] A myeloid tumor can be differentiated from AE in that myeloid tumor cells replicate in both extra and intravascular space and often contain cytoplasmic granules.[2,14] In our case, small foci consisting of granulocytic cells in the liver were considered by size, distribution, and cellular morphology as foci of extramedullary granulopoiesis, which are often found in avian tissue.[2] Lymphoma was ruled out by negative IHC results by using anti-human CD3 and anti-chicken BAFF-R antibodies, which are the most appropriate commercial antibodies for detecting chicken T and B lymphocytes on FFPE sections.[12] The negative IHC results with this anti-human Iba-1 antibody indicate that tumor cells in our case were not macrophage/monocyte lineage cells.

Contributing Institution:
National Institute of Animal Health, NARO.
https://www.naro.go.jp/english/laboratory/niah/index.html

JPC Diagnoses:
1. Liver: Intravascular round cell neoplasm.
2. Liver: Extramedullary hematopoiesis, chronic, periportal, moderate.

JPC Comment:
This case proved to be challenging for participants given that the condition is relatively obscure and requires IHCs for definitive diagnosis. Leukemia and leukemic lymphoma were the top diagnoses considered by conference participants prior to case discussion. The contributor provides an excellent overview of and

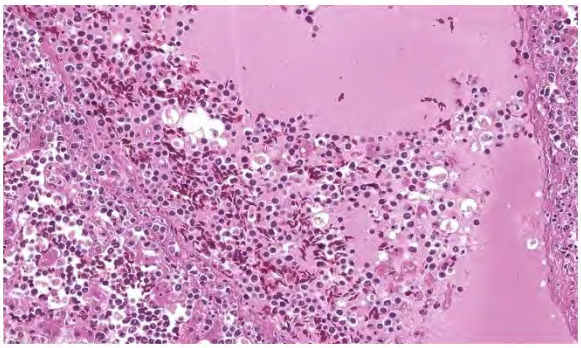

Figure 2-3: Liver, chicken. Neoplastic erythroblasts circulate within hepatic vessels. (HE, 738X).

a convincing diagnostic workup for the diagnosis of avian erythroblastosis in their comment. An in-house hemoglobin IHC at the JPC similarly revealed moderate cytoplasmic immunoreactivity for hemoglobin within the neoplastic cell population and no immunoreactivity of neoplastic cells for lymphocyte markers (CD3, CD20, PAX5, CD34). This entity, and its accompanying histologic findings, provided great discussion of oncogenic viruses and intravascular round cell neoplasms of avian species. “Intravascular round cell neoplasm” was ultimately the morphologic diagnosis that was favored by the JPC due to the inability to reach the diagnosis of erythroblastosis on the H&E slide alone (the JPC morphologic diagnosis is always based on the HE section, which is the only section provided in advance of the conference.)

Conference discussion focused largely on avian leukosis virus and its subtypes. Avian leukosis viruses (ALV) are alpharetroviruses that are usually slowly oncogenic. Subtype A is the most common, and subtypes A through E, as well as J, are known to infect chickens. Other subtypes affect numerous other species of birds. These viruses cause a variety of neoplasms by inserting themselves as promoters

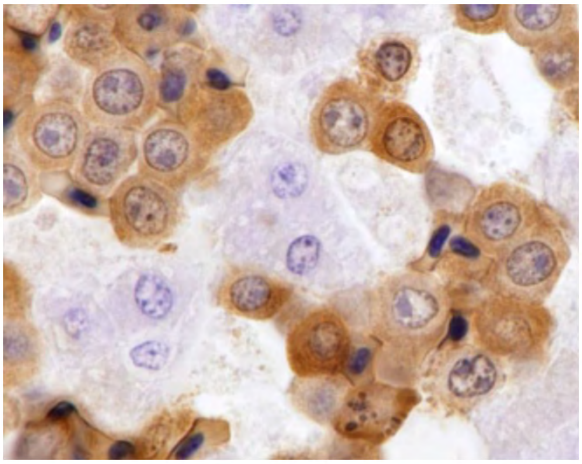

Figure 2-4: Liver, chicken. Neoplastic cells stain strongly positive for hemoglobin. (anti-HB, 1000X). (Photo courtesy of: Japanese National Institute of Animal Health, NARO, https://www.naro.go.jp/english/laboratory/niah/index.html)

into the affected chicken's genome near a cellular proto-oncogene, such as c-erbB, causing overexpression of the proto-oncogene. This overexpression leads to downstream dysregulation of cellular division and promotion of uncontrolled cell growth. *Et voila*, a neoplasm is produced! Such neoplasms include erythroblastosis, lymphomas (usually B-cell with IgM production), myelocytomatosis (subtype J), and various sarcomas.

Certain subtypes of ALV, such as subtype E, are endogenous to the DNA of chickens, where they live quietly and can be genetically inherited. These endogenous viral subtypes are considered to be non-oncogenic but can confound PCR results by producing false positives. As such, PCR for avian leukosis viruses is problematic and not generally reliable.

The subtypes of ALV that produce erythroblastosis, colloquially known as "avian erythroblastosis virus" (AEV), are unique among ALVs in that they stimulates rapid oncogenesis due to their genome containing its own potent oncogene (v-erbB).[11,13] This oncogene is a mutated and shortened version of the c-erbB proto-oncogene within chicken DNA that is associated with other ALVs.[13] The v-erbB oncogene results in the production of a mutated form of epidermal growth factor receptor (EGFR) protein, which is a type of tyrosine kinase receptor. This family of receptors is directly involved in cell signaling for growth and division. This receptor mutation results in loss of the ligand binding domain found in normal EGFR, as well as structural changes in its cytoplasmic regulatory regions. This enables the mutated EGFR to experience ligand-independent constitutive signaling activity and stimulate constant, transformative, cellular growth.[13] As such, this virus is able to directly cause erythroblastosis and fibrosarcomas, which have a much more rapid onset of disease, whereas most ALVs cause slow-growing neoplasms via an indirect route.[13] Chickens affected with avian erythroblastosis have a characteristically "cherry red" liver on gross examination.

Wrapping up the discussion of this fascinating and rare case was a quick review of other major oncogenic viruses in chickens, which included gallid herpesvirus-2 (causative agent of Marek's disease, which usually affects young birds and results in a classical T-cell lymphoma) and avian gammaretrovirus (causative agent of avian reticuloendotheliosis).

References:

1. Ambs E, Thorell B. On the type of hemoglobin in the neoplastic cell of virus-induced fowl erythroleukemia. *J Natl Cancer Inst*. 1960;25:685–695.
2. Barnes HJ, Fletcher OJ. Hemic system. In: Abdul-Aziz T, Fletcher OJ, Barnes HJ,

eds. *Avian histopathology.* 4th ed. Jacksonville, FL: American Association of Avian Pathologists. 2016:1–16.
3. Beug H, von Kirchbach A, D¨oderlein G, et al. Chicken hematopoietic cells transformed by seven strains of defective avian leukemia viruses display three distinct phenotypes of differentiation. *Cell* 1979:18:375–390.
4. Burmester BR, Adrian Gross M, Walter WG, et al. Pathogenicity of a viral strain (RPL12) causing avian visceral lymphomatosis and related neoplasms. II. Host-virus interrelations affecting response. *J Natl Cancer Inst*. 1959;22:103–127.
5. Cowles J, Saikkonen J, Thorell B. On the presence of hemoglobin in erythroleukemia cells. *Blood* 1958;13:1176–1184.
6. Edamoto H, Suwa K, Tamura K. Spontaneous erythroid leukemia in a 6-wk-old male Crlj: B6C3F1 mouse. *J Toxicol Pathol*. 2017;20:101–104.
7. Graf T, Beug H. Avian leukemia viruses interaction with their target cells in vivo and in vitro. *Biochim Biophys Acta*. 1978;516:269–299.
8. Graf T, Beug H, Royer-Pokora B, et al. In vitro transformation of hematopoietic cells by avian erythroid and myeloid leukemia viruses: a model system for the differentiation of normal and neoplastic cells. In: Clarkson B, Marks P, Till JE, eds. *Differentiation of normal and neoplastic hematopoietic cells*. New York, NY: Cold Spring Harbor Laboratory. 1978:625–639.
9. Hayman MJ, Beug H. Avian erythroblastosis: a model system to study oncogene co-operation in leukemia. *Cancer Surv*. 1992;15:53–68.
10. Hihara H, Yammamoto H, Ishino S, et al. Pathogenicity of some clones from field isolates of avian leukosis viruses. *Natl Inst Anim Health Q*. 1972;12:117–126.
11. Hihara H, Yamamoto H, Shimohira H, et al. Avian erythroblastosis virus isolated from chick erythroblastosis induced by lymphatic leukemia virus subgroup A. *J Natl Cancer Inst*. 1983;70:891–897.
12. Kurokawa A, Yamamoto Y. Immunohistochemical identification of T and B lymphocytes in formalin-fixed paraffin-embedded chicken tissues using commercial antibodies. *Vet Immunol Immunopathol*. 2020;228:110088.
13. Massoglia S, Gray A, Dull TJ, Munemitsu S, Kun HJ, Schlessinger J, Ullrich A. Epidermal growth factor receptor cytoplasmic domain mutations trigger ligand-independent transformation. *Mol Cell Biol.* 1990;10(6):3048-55.
14. Nair V. Leukosis/sarcoma group. In: Swayne DE, Boulianne M, Logue C, et al., eds. *Diseases of poultry,*14th ed. Hoboken, NJ: Wiley-Blackwell. 2020:587–625.
15. Ogasawara F, Kumagai Y, Mikami O, et al. Erythroblastic sarcoma in the thoracic cavity of a cow. *J Vet Med Sci*. 2019;81:134–137.
16. Purchase HG. The pathogenesis and pathology of neoplasms caused by avian leukosis viruses. In: de Boer GF, ed., *Avian leukosis*. Boston, MA: Martinus Nijhoff Publishing. 1986:171–196.
17. Venugopal K, Howes K, Flannery DM, et al. Isolation of acutely transforming subgroup J avian leukosis viruses that induce erythroblastosis and myelocytomatosis. *Avian Pathol*. 2000;29:327–332.

18. Wang W, Wang SA, Medeiros LJ, et al. Pure erythroid leukemia. *Am J Hematol*. 2017;92:292–296.

CASE III:

Signalment:
4.5-year-old, female, Holstein-cow, *Bos taurus*

History:
The animal was slaughtered. The owner observed swellings of the limbs (not further specified) for one year prior to slaughter. At the slaughterhouse, the referring veterinarian submitted pieces of kidney, heart, muscles of the brisket and flank region to the Institute of Veterinary Pathology for further investigations.

Gross Pathology:
In all submitted tissues, multifocal to coalescing, miliary to nodular, whitish, coarsely textured foci were noted on the cut surface.

Laboratory Results: N/A

Figure 3-1: Heart, ox. Cut section of the heart muscle (left ventricular wall) with miliary white foci bulging from the cut surface. (Photo courtesy of: Institut für Veterinärpathologie, Vetsuisse-Fakultät, Universität Zürich, https://www.vetpathology.uzh.ch)

Microscopic Description:

Myocardium (left ventricular wall) and striated muscle (brisket): Affecting approximately 10-20% of the myocardial and skeletal muscle tissue, there is a marked intraluminal, haphazardly arranged, often glomeruloid, highly cellular proliferation of plump spindeloid cells within medium to large-size arterioles with partial to complete occlusion of the vascular lumina accompanied by a pronounced thickening of the corresponding tunica media (medial hypertrophy). These spindeloid cells have abundant, slightly granular, eosinophilic, occasionally vacuolized cytoplasm with indistinct cell borders containing oval to cigar-like shaped nuclei with inconspicuous nucleoli and coarsely stippled chromatin. There is moderate anisokaryosis and anisocytosis with infrequent multinucleated cells being present. Mitotic figures are rare or absent (<1/HPF).

There are frequent perivascular accumulations of variable numbers of hemosiderinloaden macrophages intermingled with a low number of inflammatory cell infiltrates consisting of lymphocytes and plasma cells as well as fewer neutrophils with rare small aggregates of extravasated erythrocytes. Few affected arterioles are infiltrated by a small to moderate number of eosinophils (not present on all slides). These inflammatory infiltrates also extend occasionally into the adjacent myocardial interstitium. The glomeruloid proliferations in the heart are surrounded by a moderate to marked deposition of collagen fibers (fibrosis) along with edema. Occasionally and affecting less than 5% of cardiomyocytes, there are intrasarcoplasmic protozoal cysts of approximately 100-200 µm in diameter containing numerous crescent-shaped bradyzoites. Perilesional myocytes of the brisket often display

Figure 3-2: Skeletal muscle, ox. Similar gross changes are seen on a cut section of the brisket muscle. (Photo courtesy of: Institut für Veterinärpathologie, Vetsuisse-Fakultät, Universität Zürich, https://www.vetpathology.uzh.ch)

sarcoplasmic hypereosinophilia, swelling, loss of cross-striation and occasional fragmentation (hyaline degeneration and necrosis). Immunohistochemical labelling shows frequent cytoplasmic reactivity of the intralesional spindeloid cells for factor VIII/von Willebrand factor (vWF) and smooth muscle actin (SMA).

Contributor's Morphologic Diagnoses:
Myocardium of the left ventricular wall and striated muscle (brisket): Severe multifocal arteriolar intraluminal endothelial and pericyte proliferation with intraand perilesional hemosiderosis as well as hemorrhages accompanied by diffuse media hypertrophy (consistent with reactive angioendotheliomatosis) and mild eosinophilic arteriolitis Heart (myocardium): Moderate to marked, multifocal to coalescing interstitial lymphoplasmacytic myocarditis and myocardial fibrosis with occasional intrasarcoplasmic protozoal cysts (most likely *Sarcocystis sp*.) Striated muscle (brisket): Mild multifocal degeneration and necrosis of myocytes

Contributor's Comment:
In human medicine, the term angioendotheliomatosis includes either a malignant or a benign variant. The latter, also termed as reactive angioendotheliomatosis (RAE), is characterized by intravascular endothelial as well as pericyte proliferation and is mainly restricted to the skin.[9,16] Associations between this condition and type 2, 3, or 4 hypersensitivity diseases were hypothesized, including autoimmune diseases, such as thrombotic thrombocytopenic purpura (TTP), underlying subacute systemic infections, or organ transplantation.[8,11,14,16] The malignant angioendotheliomatosis (MAE) commonly refers to a rare type of angiotropic large cell lymphoma but may also apply to intravascular disseminated angiosarcoma.[9,16]

In veterinary medicine, cases of MAE in the form of intravascular angiotropic lymphoma have been documented in dogs and to a lesser extent in cats.[7,10] All previously published cases had concurrent involvement of the central nervous system and, to a lesser extent,

other organs of the digestive, endocrine, respiratory, and urogenital systems of which the liver, lung, small intestine, and kidney are frequently represented. The veterinary cases mostly resembled human reports except for humans mainly being affected by a B-cell lineage neoplasm.[10]

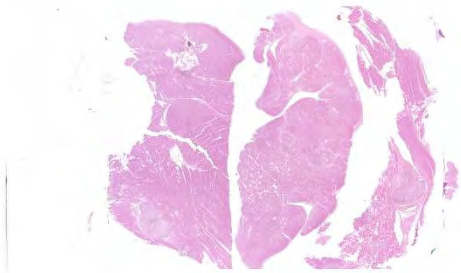

Figure 3-3: Heart, ox. Sections from various areas of the heart are submitted for examination and all are similar. Within each section, arteriolar walls are profoundly thickened. (HE, 10X)

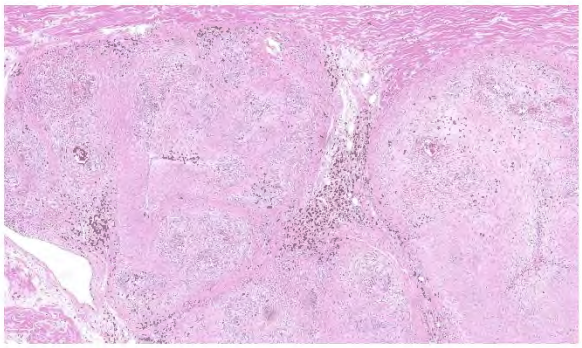

Figure 3-4: Heart, ox. Within the ventricular wall, arterioles are markedly tortuous with numerous small branches. Each arteriole has a markedly thickened wall which often compromises the lumen, and spindle cells profoundly expand the arteriolar wall. There is fibroplasia surrounding these arterioles which extends into the adjacent myocardium. At the periphery of some of the affected arterioles, there are numerous hemosiderin laden macrophages, indicating previous hemorrhages. (HE, 92X)

Contrary to humans in which RAE is mainly benign, the feline counterpart feline systemic reactive angioendotheliomatosis (FSRA) is a rare fatal multisystemic disease of unclear origin with few documented cases.[3,12,13,16] Affected animals often present with cardiorespiratory symptoms due to the heart being the main affected organ. Other organs in which lesions were frequently observed include the kidney, spleen, intestine, and lymph nodes, followed by others, but to a lower degree.[3,11] In most of these cases, the cause remained unidentified. One cat was diagnosed with TTP, to which the lesions were presumably attributed.[2]

Previously, there has been one report in which such proliferative lesions were observed in a 2-year-old Corriente steer. The lesions resembled FRSA and were termed systemic reactive angioendotheliomatosis-like syndrome.[2] The authors believed that the animal was persistently infected with the bovine viral diarrhea virus (BVDV) since they detected corresponding intralesional antigen by immunohistochemistry. The authors hypothesized that a TTP-like condition due to a BVDV infection was present.[2] Formalin-fixed paraffin-embedded tissues (FFPE) of this animal plus other species suffering from vascular proliferative disorders, including cats with FSRA, were subjected to molecular analysis yielding the isolation of *Bartonella sp*.-DNA in all specimens. In addition, the authors demonstrated in vitro evidence for *Bartonella vinsonii sp. berkhoffi* being capable of inducing the transcription factor hypoxia-induced factor-1 (HIL-1) with subsequent production of the endothelial mitogen vascular endothelial growth factor (VEGF) in human cells (HeLa 229).[1] The results led to the conclusion that there might be an association between *Bartonella sp*.-infections and the vascular proliferative disorders. However, these results need to be interpreted with caution as there is a likelihood of false-positive PCR results for *Bartonella spp*. in FFPE-specimens due to cross-contamination during necropsy or histology processing.[15]

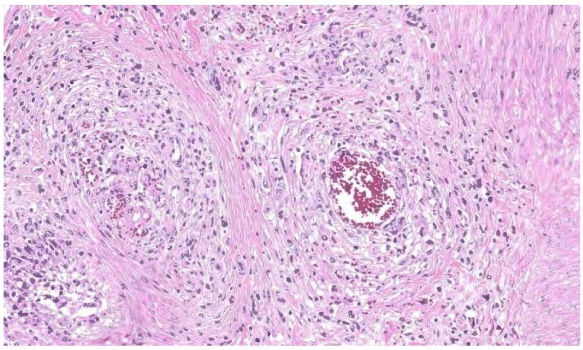

Figure 3-5: Heart, ox: High magnification of several affected arterioles demonstrating their tortuosity, proliferation of a variety of spindle cells (endothelium, smooth muscle and fibroblasts, luminal compromise, formation of numerous smaller arteriolar branches, wand in some areas, endothelial loss hemorrhage , and extrusion of plasma proteins into the wall. (HE 468X)

The findings of the present case are consistent with the case report of Breshears et al., and the diagnosis of a systemic reactive angioendotheliomatosis-like syndrome was made. The glomeruloid proliferation of endothelial cells and pericytes staining positive for factor VIII/von Willebrand factor (vWF) and smooth muscle actin (SMA), respectively, is in concordance with the previous literature on RAE and FSRA.[2,3,10,16,17] Without exception, these lesions were present in all submitted tissue samples including the kidney and flank muscle (not shown). No evidence for the presence of BVDV antigen was detected by immunohistochemical labeling using the C42 and 15C5 monoclonal antibodies against the viral protein Erns (envelope protein, RNase, secreted) of which one is specifically directed against BVDV while the other is detecting pestiviruses, respectively.[4] Furthermore, no intralesional argyrophilic microbial structures could be found.

The occasionally seen intra-sarcoplasmic protozoal cysts are most likely bradyzoites of a Sarcocystis sp. In brief, this is a highly prevalent heteroxenous coccidian parasite, including around 90 species, which can infect a wide range of species, including humans. Its lifecycle consists of gametogeny (sexual stages) in the definitive host and schizogony (asexual stages) in the intermediate host. Coincidentally, the schizogony partially takes place within endothelial cells of arterioles and capillaries before its final stage in the musculature.[6] On some slides, we noticed a mild eosinophilic intralesional inflammatory component which are most likely due to the protozoal infection. However, no additional investigation has been attempted in this case, as the significance of this infection is mostly clinically irrelevant.

Contributing Institution:
University of Zurich
Winterhurerstrasse 268
https://www.vetpathology.uzh.ch

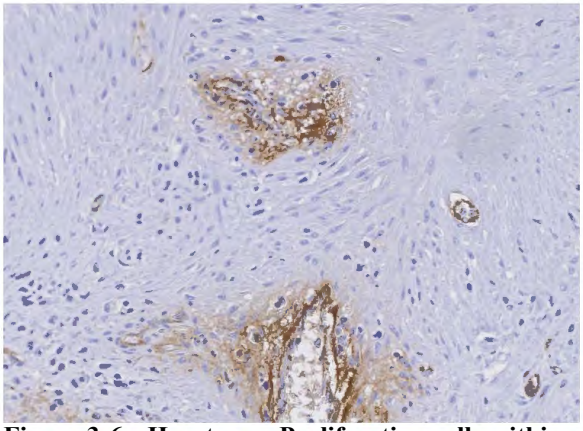

Figure 3-6: Heart, ox:. Proliferating cells within the walls of affected arterioles demonstrate moderate cytoplasmic immunoreactivity for von-Willebrand's factor. (anti-VWF, 400X). (Photo courtesy of: Institut für Veterinärpathologie, Vetsuisse-Fakultät, Universität Zürich, https://www.vetpathology.uzh.ch)

JPC Diagnoses:

1. Heart and skeletal muscle, arterioles: Atypical endothelial and pericyte proliferation (angioendotheliomatosis), chronic, diffuse, severe, with medial hypertrophy and mural and adventitial fibrosis.
2. Heart, myocytes: Sarcocysts, multiple. Another unique condition in its first WSC iteration in this species, this case also proved to be diagnostically challenging for participants. The contributor provided an excellent write-up summarizing the current literature on this condition across species. Similar cases of systemic reactive angioendotheliomatosis and SRE-like syndrome have been seen before in the WSC (Conference 21, Case 3, 2014, Conference 13, Case 4, 2019, and Conference 9, Case 1, 2020), all of which have had great write-ups and similar immunohistochemical staining patterns with vWF and smooth muscle actin (SMA) to those that were performed in this case, but were all in cats.
3. The contributor's comment covered all pertinent aspects of conference discussion, from the comparison between human and veterinary forms of this condition, to the current hypotheses on this syndrome's pathogenesis, to the possible associations of this condition with TTP and certain systemic infections (i.e. *Bartonella spp.* in cats and bovine pestivirus in cattle). Although this condition is rare, a recent 2024 paper found that systemic reactive angioendotheliomatosis in cats can mimic hypertrophic cardiomyopathy both clinically and on echocardiogram and should be considered as a differential for cats that have symmetrical left ventricular wall thickening.[5]

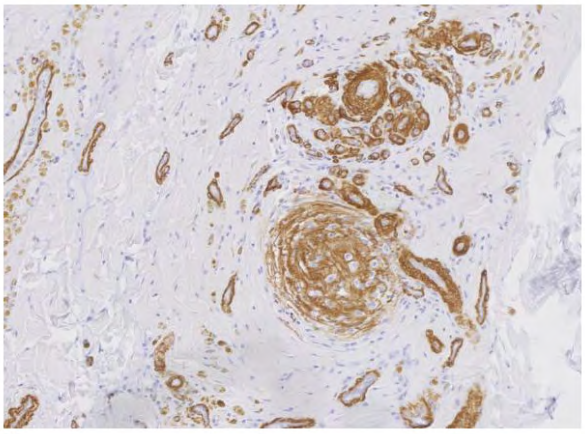

Figure 3-7: Heart, ox. Proliferating cells within the walls of affected arterioles demonstrate moderate cytoplasmic immunoreactivity for smooth muscle actin. (anti-SMA, 400X). (*Photo courtesy of:* Institut für Veterinärpathologie, Vetsuisse-Fakultät, Universität Zürich, https://www.vetpathology.uzh.ch)

JPC Comment:

Another unique condition in its first WSC iteration in this species, this case also proved to be diagnostically challenging for participants. The contributor provided an excellent write-up summarizing the current literature on this condition across species. Similar cases of systemic reactive angioendotheliomatosis and SRE-like syndrome have been seen before in the WSC (Conference 21, Case 3, 2014, Conference 13, Case 4, 2019, and Conference 9, Case 1, 2020), all of which have had great write-ups and similar immunohistochemical staining patterns with vWF and smooth muscle actin (SMA) to those that were performed in this case, but were all in cats.

The contributor's comment covered all pertinent aspects of conference discussion, from the comparison between human and veterinary forms of this condition, to the current hypotheses on this syndrome's pathogenesis, to the possible associations of this condition with TTP and certain systemic infections (i.e. *Bartonella spp.* in cats and bovine pestivirus in

cattle). Although this condition is rare, a recent 2024 paper found that systemic reactive angioendotheliomatosis in cats can mimic hypertrophic cardiomyopathy both clinically and on echocardiogram and should be considered as a differential for cats that have symmetrical left ventricular wall thickening.[5]

References:

1. Beerlage C, Varanat M, Linder K, Maggi RG, Cooley J, Kempf VA, Breitschwerdt EB. *Bartonella vinsonii subsp. berkhoffii* and *Bartonella henselae* as potential causes of proliferative vascular diseases in animals. *Med Microbiol lmmunol.* 2012;201(3):319-326.
2. Breshears MA, Johnson BJ. Systemic reactive angioendotheliomatosis-like syndrome in a steer presumed to be persistently infected with bovine viral diarrhea virus. *Vet Pathol.* 2008;45(5):645-649.
3. Fuji RN, Patton KM, Steinbach TJ, Schulman FY, Bradley GA, Brown TT, Wilson EA, Summers BA. Feline systemic reactive angioendotheliomatosis: eight cases and literature review. *Vet Pathol.* 2005;42(5): 608-617.
4. Herrold E, Schober K, Miller J, Jennings R. Systemic reactive angioendotheliomatosis mimicking hypertrophic cardiomyopathy in a domestic shorthair cat. *J Vet Cardiol.* 2024;56:65-71.
5. Hilbe, Camenisch, Braun, Peterhans, Stalder, P, Zlinszky, & Ehrensperger. Mucosal lesions in a sheep infected with the Border Disease Virus (BDV). *Schweizer Archiv für Tierheilkunde. 2009*;151(8), 391-396.
6. Jubb, Kennedy, and Palmer's Pathology of Domestic Animals. Vol 1. 6th ed. St. Louis, MO: Elsevier; 2016:235-6.
7. Lapointe JM, Higgins RJ, Kortz GD, Bailey CS, Moore PF. lntravascular malignant T-cell lymphoma (malignant angioendotheliomatosis) in a cat. *Vet Pathol.* 1997;34(3):247-250.
8. Lazova R, Slater C, Scott G. Reactive angioendotheliomatosis. Case report and review of the literature. *Am J Dermatopathol.* 1996;18(1):63-69.
9. Lin BT, Weiss LM, Battifora H. lntravascularly disseminated angiosarcoma: true neoplastic angioendotheliomatosis? Report of two cases. *Am J Surg Pathol.* 1997;21(10):1138-1143.
10. McDonough SP, Van Winkle TJ, Valentine BA, vanGessel YA, Summers BA. Clinicopathological and immunophenotypical features of canine intravascular lymphoma (malignant angioendotheliomatosis). *J Comp Pathol.* 2002;126(4):277-288.
11. McMenamin ME, Fletcher CD. Reactive angioendotheliomatosis: a study of 15 cases demonstrating a wide clinicopathologic spectrum. *Am J Surg Pathol.* 2002;26(6):685-697.
12. Rothwell TL, Xu FN, Wills EJ, Middleton DJ, Bow JL, Smith JS, Davies JS. Unusual multisystemic vascular lesions in a cat. *Vet Pathol.* 1985;22(5):510-512.
13. Straumann Kunz U, Ossent P, Lott-Stolz G. Generalized intravascular proliferation in two cats: endotheliosis or intravascular pseudoangiosarcoma? *J Comp Pathol.* 1993;109(1):99-102.
14. Umlas, J. Glomeruloid structures in thrombohemolytic thrombocytopenic purpura, glomerulonephritis, and disseminated intravascular coagulation. *Human Pathology*. 1972;3(3):437-441.

15. Varanat M, Maggi RG, Linder KE, Horton S, Breitschwerdt EB. Cross-contamination in the molecular detection of Bartonella from paraffin-embedded tissues. *Vet Pathol.* 2009;46(5):940-944.
16. Wick MR, Rocamora A. Reactive and malignant "angioendotheliomatosis": a discriminant clinicopathological study. *J Cutan Pathol*. 1988;15(5):260-271.
17. Yamamoto S, Shimoyana Y, Haruyama T. A case of feline systemic reactive angioendotheliomatosis. *J Fel Med Surg.* 2015.

CASE IV:

Signalment:
Five-month old, male, Japanese black, bovine (*Bos taurus*)

History:
The present calf was transferred to a farm for fattening at the age of 4-month old and vaccinated with the mixed live vaccines, including bovine infectious rhinotracheitis virus, bovine viral diarrhea virus (BVDV) type 1, bovine parainfluenza virus type 3, bovine respiratory syncytial virus, and bovine adenovirus (BAV) type 7. The calf developed respiratory signs such as coughing and was administered with florfenicol, cefazolin and dexamethasone. The calf died at the age of 5-month-old. The other calves in the farm did not show any apparent clinical signs.

Gross Pathology:
At necropsy, a small amount of bloody feces was attached to the anal area. The lung showed multiple consolidation with caseonecrotic foci. The abomasum had multiple erosions and ulcers in the pyloric part of mucosa. From the duodenum to rectum, the mucosa was dark red and covered with dark red, watery or fibrinous contents. The thymus, both the cervical and

Figure 4-1: Abomasum, Japanese black calf. The abomasum has multiple erosions and ulcers in the pyloric part of mucosa. (Photo courtesy of: National Institute of Animal Health, http://www.naro.affrc.go.jp/english/niah/index.html)

thoracic parts, was membranous, showing to be atrophic. The gallbladder was almost empty of bile and had streaks of dark red mucosa.

Laboratory Results:
No bacteria were isolated from liver, spleen, kidney, heart, lung, or brain. Neither *Salmonella* nor *Clostridium perfringens* were isolated from cecal and jejunal contents, respectively. PCR tested positive for *Mycoplasma bovis* from the lung, negative for BVDV from the kidney, and positive for BAV from the liver, kidney, heart, lung, and cecal content. BAV was isolated from the liver, kidney, heart, lung, and cecal content. The isolate was identified to be BAV type 5 by sequencing the hexon gene.

Microscopic Description:
In the abomasum, focally extensive hemorrhage and edematous swelling were present in the lamina propria mucosa and in the submucosa, respectively. In the lamina propria mucosa, the capillary blood vessels and small veins showed severe congestion and hemorrhage. The endothelial cells of these vessels and arterioles had basophilic to amphophilic

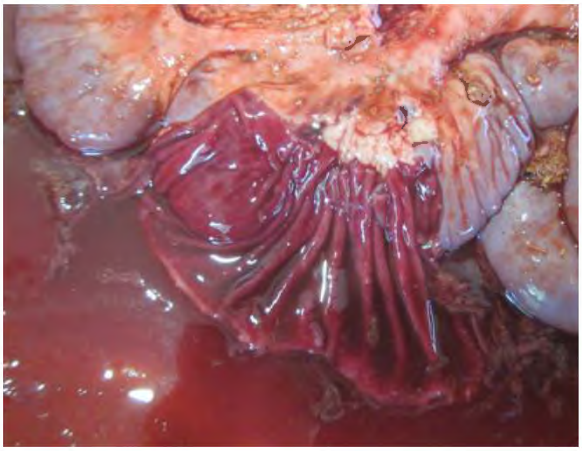

Figure 4-2: Abomasum, Japanese black calf. From the duodenum to rectum, the mucosa was dark red and covered with dark red, watery or fibrinous contents (Photo courtesy of: National Institute of Animal Health, http://www.naro.affrc.go.jp/english/niah/index.htm)

intranuclear inclusion bodies, of either full type or Cowdry type A. Occasionally, focal areas of necrotic mucosal epithelium were accompanied by neutrophil infiltration. In the submucosa, the endothelial cells of blood vessels had the same intranuclear inclusion bodies. Fibrinous and proteinous or serous materials were accumulated in some parts of the submucosal tissue. Neither bacteria nor fungi were detected by Gram and Giemsa stain, and by periodic acid-Schiff and Grocott methods, respectively.

Contributor's Morphologic Diagnoses:
Abomasum: abomasitis, hemorrhagic, focally extensive, with endothelial intranuclear inclusion bodies.

Contributor's Comment:
The present case was characterized pathologically by adenoviral hemorrhagic gastroenteritis and mycoplasmal caseonecrotic bronchopneumonia. The endothelial intranuclear inclusion bodies were detected histologically in the gastrointestinal tract (abomasum, duodenum, jejunum, ileum, cecum, colon, and rectum), liver, gallbladder, spleen, kidney and lung. The forestomach and brain contained no endothelial intranuclear inclusion bodies. In the abomasum, focal ulceration was associated with hemorrhagic abomasitis (No ulceration in the submitted sections). In the ileal Peyer's patch, lymphocytes were severely depleted. Epitheliotropic BAV inclusion bodies were not observed in any organs. By immunohistochemistry, the endothelial intranuclear inclusion bodies showed positive cross-reaction to anti-BAV type 7, weak cross-reaction to anti-BAV type 1, but negative for anti-BAV type 3 antisera. By transmission electron microscopy, the endothelial cells of hepatic sinusoids had paracrystalline arrays of adenovirus-like particles, 60-80 nm in diameter, in their nuclei.

BAV belong to the family *Adenoviridae*, genera *Mastadenovirus*, and *Atadenovirus*.[8] The serotypes of BAV-1, -2, -3, -9 and -10 belong to the genus *Mastadenovirus*, and the serotypes of BAV-4, -5, -6, -7, and -8 belong to the genus *Atadenovirus*.[1,2,3,4,5,6,7,10] Serotypes 3, 4, 7, 10 have been associated with enteric disease.[4,7,8] BAV, including serotypes 3, 7 and 10 has also been associated with respiratory disease.[2,4,5,6] BAV-5 was isolated from a calf

Figure 4-3: Abomasum, Japanese black calf. A section of abomasum with a focally extensive area of mucosal necrosis and hemorrhage is submitted for examination. There is marked edema and thickening of the submucosa. (HE, 12X).

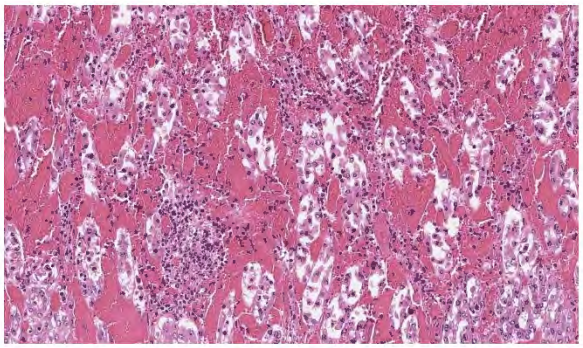

Figure 4-4: Abomasum, Japanese black calf. Higher magnification of the acute hemorrhage, glandular necrosis and aggregates of neutrophils within the mucosa. (HE, 381X).

with weak calf syndrome, but not have been fully associated with severe gastroenteric disease.[1]

Adenovirus infections in animals appear, in general, to be subclinical, and disease seems to occur more commonly in immunologically compromised individuals.[8] In the present calf, the stress and debilitation caused by transportation and by mycoplasmal pneumonia might have caused immunosuppression, followed by systemic BAV-5 infection and gastroenteritis.

The pathogenesis of adenoviral gastroenteritis in calves is not fully clarified. It appears that after an initial viremic stage, the virus localizes in the endothelial cells of vessels in a variety of organs, resulting in thrombosis with subsequent focal areas of ischemic necrosis.[8] Especially, in the bovine gastrointestinal tract, it appears that the endothelial cells of capillary and small veins are highly susceptible to cytopathic effect of the BAV-5 strain. Severely swollen and necrotic endothelial cells may impede the blood circulation through the lamina propria, leading to severe congestion, followed by hemorrhage per diapedesis and per rhexis.

Contributing Institution:
National Institute of Animal Health,
National Agriculture and Food Research Organization (NARO)
3-1-5Kannondai, Tsukuba, Ibaraki 3050856, Japan
(WSC ID95)
http://www.naro.affrc.go.jp/english/niah/index.html

JPC Diagnoses:
Abomasum: Abomasitis, necrohemorrhagic, acute, focally extensive, severe, with submucosal edema and endothelial intranuclear viral inclusions.

JPC Comment:
This was a beautiful example of a classic entity that served as a nice little dessert to wrap the conference up. The endothelial intranuclear viral inclusions (and their ubiquitous distribution) in this case are textbook-worthy (have you ever considered how many histologic images in veterinary pathology texts come from the WSC?)

As some participants struggled minimally with tissue identification in this case, a quick review of abomasal microanatomy is in order, as not all regions of the abomasum are identical. Chief and pyloric cells are only found in

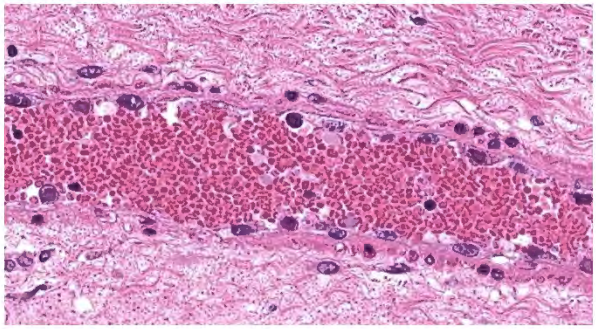

Figure 4-5: Abomasum, Japanese black calf. Endothelial cells lining a submucosal vein contain intranuclear adenocarcinoma inclusions. (HE,1181X).

the fundic portion of the abomasum, whereas the pylorus and cardia lack these. Additionally, there are no goblet cells. The lack of goblet cells in this section immediately rules out large intestine, Other helpful hints include the tortuosity of gastric pits, whereas intestinal crypts are straight. Adipose tissue is not found in the intestinal submucosa but can be seen in the submucosa of the ruminant abomasum and in the equine cecum. Lastly, the degree of autolysis can also be used as a clue. The intestines tend to have a high degree of autolysis due to the milieu of bacterial flora that reside within. The stomach, on the other hand, is a borderline sterile environment that very few bacteria can tolerate due to the level of acidity (unless you are *Helicobacter* spp…), so there is generally little autolysis.

The contributor's write-up of bovine adenoviruses covered much of what was discussed in conference about this ubiquitous and relevant viral family. While the pathogenesis is not well-understood, the abomasum in this case had a significant, wedge-shaped hemorrhagic infarct on the H&E slide that tied in well to the current hypothesis on the pathogenesis of this virus. It is thought that viral targeting of endothelial cells and subsequent endothelial viral inclusions may disrupt blood flow to some degree, leading to turbulence and increased incidence of thrombosis of smaller vessels that can lead to ischemic infarcts.[9] There was conversation on whether this should be morphed as an abomasitis or a vasculitis due to the endothelial targeting. It was ultimately the opinion of participants that this would not classify as true vasculitis due to the lack of inflammation in vessel walls.

Conference concluded with a quick review of the viruses that form paracrystalline arrays on

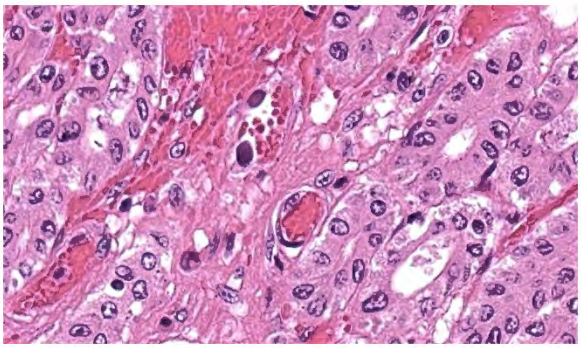

Figure 4-6: Abomasum, Japanese black calf. Adenoviral inclusions also are present within capillary endothelium within the hemorrhagic mucosa (HE, 1205X).

electron microscopy, which include adenovirus, polyomavirus, papillomavirus, picornavirus, circovirus, iridovirus, birnavirus, and flavivirus and a brief overview of a few pertinent adenoviruses in other species that would likely qualify as important boards-fodder. The main one on that list was canine adenovirus-1, which causes infectious canine hepatitis usually in puppies less than 10 days old and can also cause "blue eye" secondary to the corneal edema sometimes seen with this virus. The other notable mentions were avian adenovirus serovars 4 and 8, which cause inclusion body hepatitis and hydropericardium syndrome in poultry, and type II avian adenovirus, which causes hemorrhagic enteritis and marble spleen disease in turkeys.

References:

1. Coria MF, McClurkin AW, Cutlip RC, et al. Isolation and characterization of bovine adenovirus type 5 associated with "weak calf syndrome". *Arch Virol.* 1975;47:309-317.
2. Fent GM, Fulton RW, Saliki JT, et al. Bovine adenovirus serotype 7 infections in postweaning calves. *Am J Vet Res.* 2002;63(7):976-978.

3. Graham DA, Calvert V, Benkö M, et al: Isolation of bovine adenovirus serotype 6 from a calf in the United Kingdom. *Vet Rec.* 2005;156:82-86.
4. Lehmkuhl HD, Cutlip RC, DeBey BM. Isolation of a bovine adenovirus serotype 10 from a calf in the United States. *J Vet Diagn Invest.* 1999;11:485–490.
5. Narita M, Yamada M, Tsuboi T, et al. Immunohistopathology of calf pneumonia induced by endobronchial inoculation with bovine adenovirus 3. *Vet Pathol.* 2002;39:565–571.
6. Narita M, Yamada M, Tsuboi T, et al. Bovine adenovirus type 3 pneumonia in dexamethasone-treated calves. *Vet Pathol.* 2003;40:128–135.
7. Smyth JA, Benko M, Moffett DA, et al. Bovine adenovirus type 10 identified in fatal cases of adenovirus-associated enteric disease in cattle by in situ hybridization. *J Clin Microbiol.* 1996;34(5):1270–1274.
8. Uzal FA, Plattner BL, Hostetter JM. Alimentary system. In: Jubb, Kennedy, and Palmer's. Pathology of Domestic Animals. 6th ed. St. Louis, MO: Elsevier; 2016:143-144.
9. Werid GM, Ibrahim YM, Girmay G, Hemmatzadeh F, Miller D, Kirkwood R, Petrovski K. Bovine adenovirus prevalence and its role in bovine respiratory disease complex: A systematic review and meta-analysis. *Vet J.* 2025;310:106303.
10. Zhu Y-M, Yu Z, Cai H, et al. Isolation, identification, and complete genome sequence of a bovine adenovirus type 3 from cattle in China. *Virol J.* 2011;8:557-564.

Joint Pathology Center
Veterinary Pathology Services

WEDNESDAY SLIDE CONFERENCE 2025-2026

Conference #12 — 19 November 2025

CASE I:

Signalment:
Stillborn male Rocky Mountain bighorn sheep (*Ovis canadensis*) lamb, estimated gestational age of greater than 140 days

History:
This bighorn sheep lamb is a stillborn from a ewe that is part of a free-ranging population from Washington state. This ewe birthed a full-term healthy lamb during the previous lambing season; however, two different ewes in the same herd had aborted, and toxoplasmosis was diagnosed as the cause.

Gross Pathology:
Crown-rump length was 48.5 cm. No obvious gross abnormalities were seen within the examined organs.

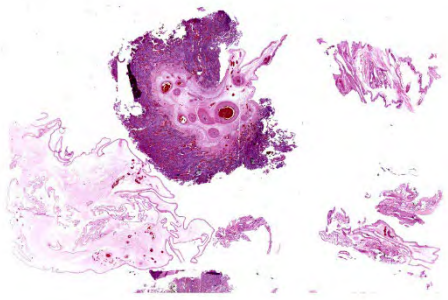

Figure 1-1: Placenta, lamb. One section of cotyledon and several sections of chorioallantoic membranes are submitted for examination. (HE, 6X)

Laboratory Results:
Neospora and *Toxoplasma* duplex PCR on paraffin-embedded brain tissue: *Toxoplasma* detected, *Neospora* not detected.

Microscopic Description:
Placenta: Trophoblasts are rarely expanded by single intracytoplasmic protozoal cysts up to 15 µm in diameter with thin, refractile, bright eosinophilic walls which surround dozens of elongate 2 x 1 µm bradyzoites. Multiple regions within the cotyledonary placenta comprising approximately 15% of the total examined area are effaced by hypereosinophilic cellular and pyknotic to karyorrhectic nuclear debris (lytic necrosis) and fibrillar to amorphous eosinophilic material (fibrin). Small caliber blood vessels within the cotyledonary placenta are occasionally occluded by dense fibrin coagula with loss of the subjacent endothelium (fibrin thrombi).

Contributor's Morphologic Diagnoses:
Placentitis, necrotizing, acute, multifocal, moderate with thrombosis and intralesional protozoal cysts morphologically consistent with *Toxoplasma gondii.*

Contributor's Comment:
Toxoplasma gondii is an obligate intracellular parasitic protozoan in the phylum Apicomplexa, and the cause of toxoplasmosis. Members of the *Felidae* family are definitive hosts of *T. gondii*. Following infection through ingestion of tissues containing *T. gondii* cysts,

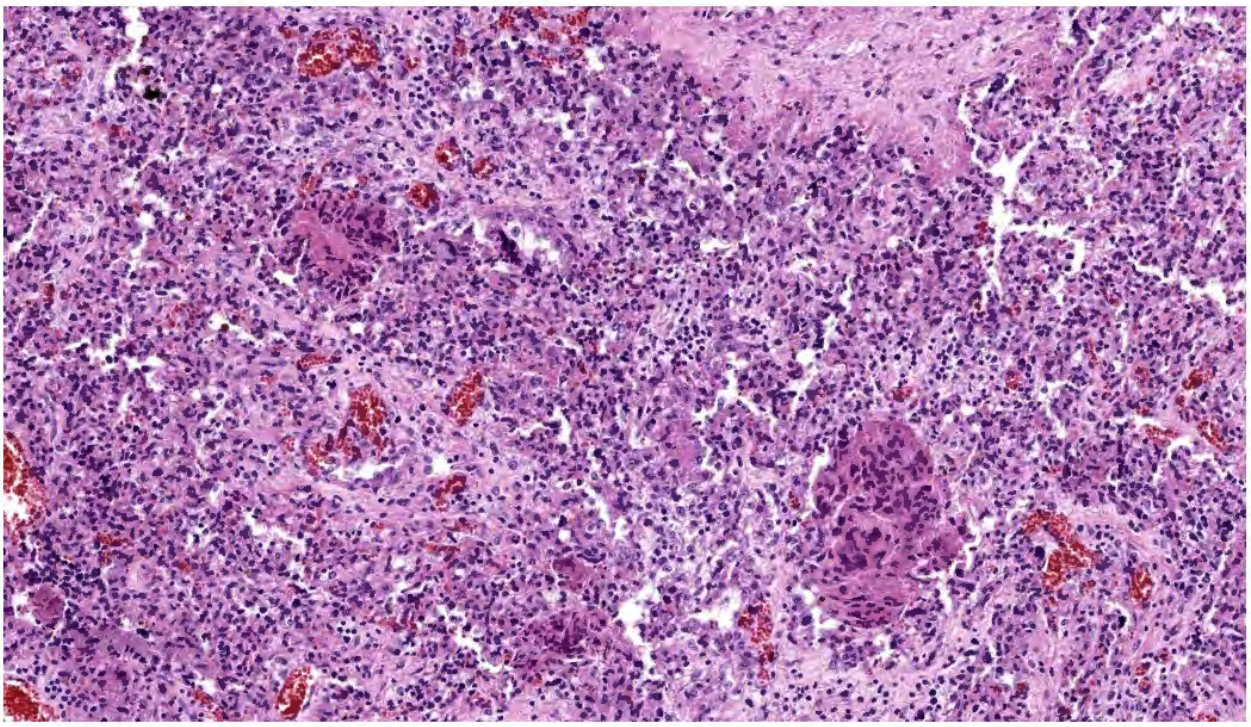

Figure 1-2: Placenta, lamb. There are multifocal areas of lytic necrosis that are scattered through the chorionic vili. (HE, 229X)

felids typically shed oocysts in their feces for one to two weeks. All other homeothermic vertebrate species are susceptible to infection and become intermediate hosts through ingestion of food, water, or soil contaminated with oocysts. Following ingestion, sporozoites are released from the oocyst and multiply asexually within the intestinal lamina propria as tachyzoites. Within hours, tachyzoites disseminate hematogenously or via lymphatics to other organs. *T. gondii* forms tissue cysts within the organs of intermediate hosts, with muscular and neural tissues preferentially affected. Tissue cysts persist for the life of the host and will perpetuate the life cycle if ingested by a felid.[3]

The outcome of infection is dependent upon individual host and parasite factors, including host susceptibility, immune status, parasite virulence, and parasitic life stage to which the host is exposed. Infected animals may remain subclinical or progress to systemic infection, abortion, and/or death.[5] Spread of tachyzoites to the placenta and fetus of a pregnant animal typically results in necrotizing lesions within the placenta and fetal brain, though other organs may also be involved.[2] In this case, protozoal cysts associated with mononuclear inflammation were also identified within the brain, lungs, and adipose tissue. Toxoplasmosis and neosporosis can cause similar lesions, and the tissue cysts of each species cannot be reliably distinguished using histology alone. Therefore, definitive diagnosis relies on ancillary testing such as PCR or immunohistochemistry.[6]

The reproductive consequences of *T. gondii* infection are well-studied in domestic sheep, with one meta-analysis reporting detection of *T. gondii* using molecular methods in 42% of aborted sheep fetuses from 11 countries.[7] However, its impact on wild sheep populations is poorly understood. Only one case of confirmed toxoplasmosis in a bighorn sheep has been published to date.[1]

Contributing Institution:
Washington Animal Disease Diagnostic Laboratory, Washington State University (https://waddl.vetmed.wsu.edu/)

JPC Diagnoses:
Placenta: Placentitis, necrotizing, subacute, multifocal to coalescing, moderate, with intratrophoblastic and intrahistiocytic apicomplexan zoites.

JPC Comment:
This year's 12th conference was moderated by the JPC's own MAJ Anna-Maria Travis, an enthusiast of reproductive pathology, who led participants through a "Call the Midwife"-themed conference, complete with a fancy English tea party. As participants donned bowties and/or fasteners, sipped hot tea out of fine bone china, and enjoyed scones with homemade clotted cream, this first case demonstrated a classic entity that is an absolute "must-know" for any diagnostic pathologist.

The contributor's comment gives a great overview of the life cycle of *Toxoplasma gondii*, which participants were asked to recount during conference. In many species, *Toxoplasma gondii* is known to cause disseminated disease, infections of the CNS (leukoencephalomalacia), and abortions (except in cattle). It is considered an economically important cause of abortions in sheep and goats, especially in late pregnancy, and generally results in classic gross lesions in the placental cotyledons. Affected cotyledons are bright red (in contrast to their normal deep purple color) and contain numerous 1-3mm white flecks/foci of necrosis and mineralization. The intercotyledonary chorioallantois is usually spared but may be edematous.

Fetal leukoencephalomalacia has been reported in fetal lambs infected with

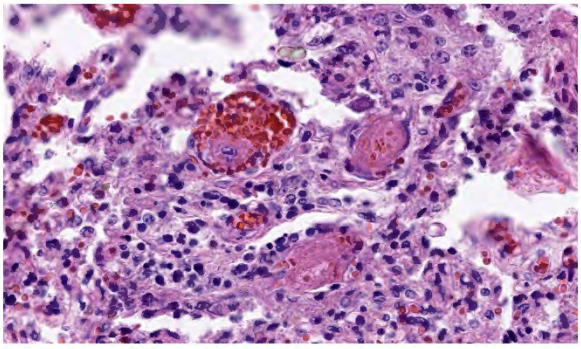

Figure 1-3: Placenta, lamb. Placental vessels occasionally are occluded by fibrin thrombi. (HE, 229X)

Toxoplasma gondii.[4] In fetuses with leukomalacia, histologic loss of oligodendrocytes and increased numbers of both astrocytes and microglia in areas of necrosis and the immediately-surrounding neuropil are common findings.[4] These lesions are similar to those seen in sheep used experimentally for inflammation syndrome and hypoxic models of periventricular leukomalacia in humans. It has been hypothesized that a fetal inflammatory syndrome resulting in hypoxia of the CNS may be involved in the pathogenesis of early abortion in ovine toxoplasmosis.[4]

Ewes do not typically show any signs of infection, and the effects on the fetus depend on the stage of gestation. In early gestation, fetal death with resorption or mummification is common. In mid-gestation, there can either be fetal death with resorption/mummification or there may be stillborn lambs. Occasionally, a fetus infected during this time frame may survive to term, but they are usually weak and do not survive long. In late gestation, the fetus will develop an immune response and may survive.

Important differentials to consider in ovine placentitis were included in conference discussion and covered: *Neospora caninum*, which causes similar lesions in the aborted placenta to *T. gondii* and requires PCR to differentiate; *Chlamydia abortus*, which causes a necrotizing placentitis with vasculitis that, in

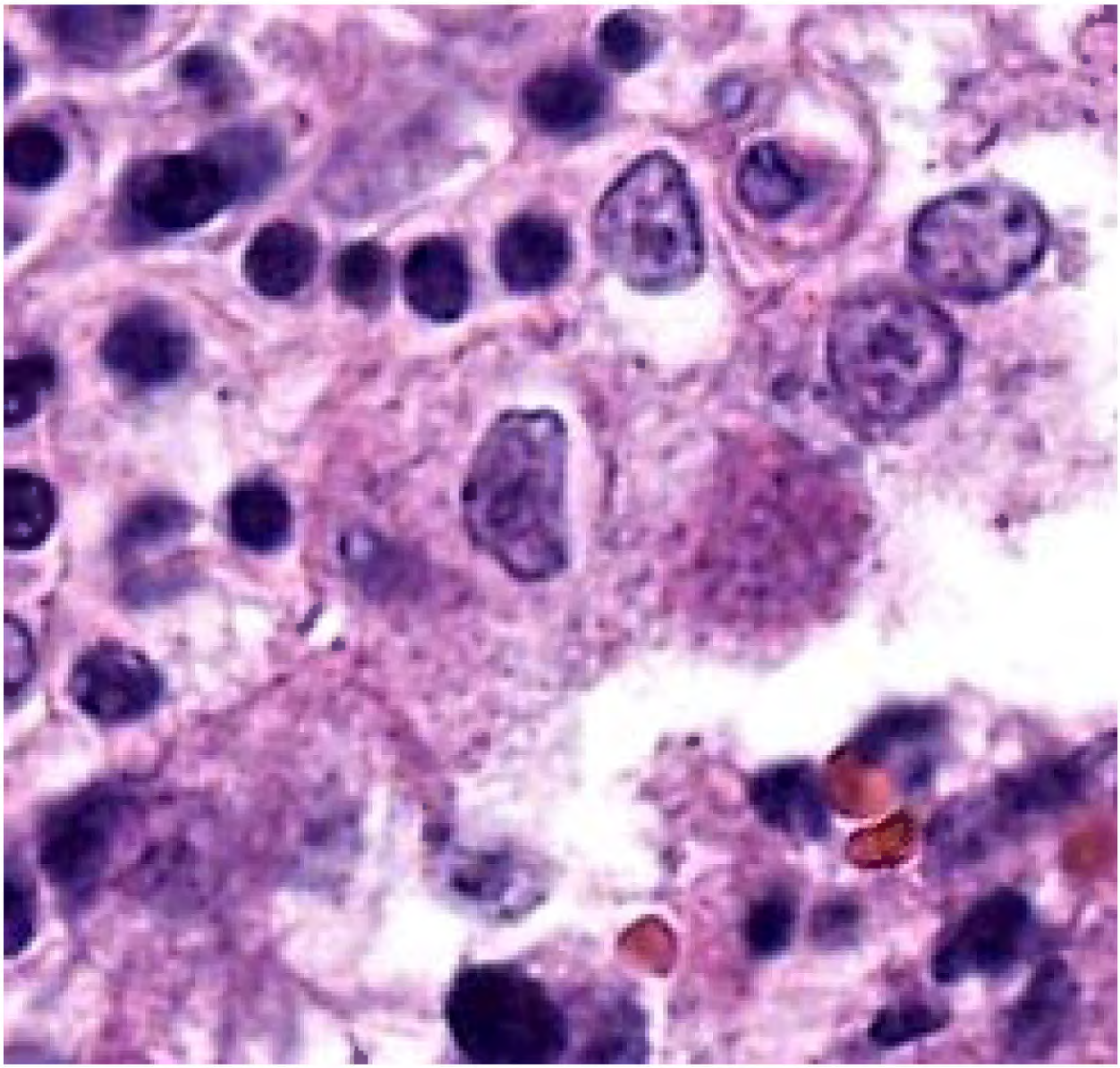

Figure 1-4: Placenta, lamb. Trophoblasts occasionally contain a 12-15um apicomplexan schizont consistent with Toxoplasma gondii (HE, 520X)

contrast to *T. gondii*, will affect the intercotyledonary areas and produce a leathery thickening of the placenta; *Coxiella burnetti*, which will cause similar lesions to *Chlamydia abortus*, but without vasculitis; *Brucella ovis*, which produces a thick, brown exudate that covers the chorionic surface of the placenta, causes leathery thickening of the intercotyledonary spaces, and is associated with vasculitis; *Campylobacter fetus*, which results in relatively non-specific edematous changes to the fetus, an exudative placentitis, and characteristic targetoid hepatic necrosis of the fetal liver; and, lastly, *Listeria monocytogenes*, which is associated with intratrophoblastic gram-positive bacilli and a necrotizing and suppurative placentitis of both the cotyledons and the intercotyledonary spaces.

Wrapping up this case's discussion, MAJ Travis touched on a few helpful tips regarding infectious ruminant abortions that pathologists should keep in mind when evaluating these

cases. These pointers can be summarized as follows: Bacterial and mycotic infections generally compromise the placenta and deprive the fetus of oxygen/nutrients, resulting in fetal death from placental insufficiency rather than direct infection of the fetus. Viral infections, however, tend to move right on through the placenta without causing it too much damage, but will go on to infect and kill the fetus via virus-induced organ damage. In general, mares get bacterial and mycotic placentitis via cervical infection, whereas cows get bacterial or mycotic placentitis via hematogenous spread. Finally, the most important organs to collect when working up an abortion case are the placenta, abomasum or stomach fluid, liver, lung, kidney, brain, eyelid (surface and palpebral conjunctiva) from bovine fetuses especially, and serum from the dam at the time of the abortion followed by another serum sample two weeks later to check for any rise in titers.

References:

1. Baszler, TV, Dubey, JP, Löhr, CV, et al. Toxoplasmic encephalitis in a free-ranging rocky mountain bighorn sheep from Washington. *J Wildl Dis.* 2000;36:752–754.
2. Buxton, D, Gilmour, JS, Angus, KW, et al. Perinatal changes in lambs infected with *Toxoplasma gondii*. *Res Vet Sci.* 1982; 32:170–176.
3. Dubey, JP, Lindsay, DS. Neosporosis, toxoplasmosis, and sarcocystosis in ruminants. *Vet Clin North Am Food Anim Pract.* 2006;22:645–671.
4. Gutiérrez-Expósito D, Arteche-Villasol N, Vallejo-García R, Ferreras-Estrada MC, Ferre I, Sánchez-Sánchez R, Ortega-Mora LM, Pérez V, Benavides J. Characterization of Fetal Brain Damage in Early Abortions of Ovine Toxoplasmosis. *Vet Pathol.* 2020;57(4):535-544.
5. Lindsay, DS, Dubey, JP. Neosporosis, toxoplasmosis, and sarcocystosis in ruminants: An Update. *Vet Clin North Am Food Anim Pract.* 2020;36:205–222.
6. Miller AD, Porter BF. Nervous System. In: McGavin, MD, Zachary, JF, eds. Pathologic Basis of Veterinary Disease. 7th ed. St. Louis, MO: Mosby Elsevier; 2022:930.
7. Nayeri, T, Sarvi, S, Moosazadeh, M, et al. Global prevalence of *Toxoplasma gondii* infection in the aborted fetuses and ruminants that had an abortion: A systematic review and meta-analysis. *Vet Parasitol.* 2021;290:109-370.

CASE II:

Signalment:
9-year-old FS Chihuahua (dog, *Canis lupus familiaris)*

History:
This dog was previously diagnosed with an intermediate grade mammary carcinoma.

Gross Pathology:
This was a 2 x 1.5 x 1.5 cm, tan, firm, subcutaneous mass from the left axilla. It was not overtly associated with a mammary gland.

Laboratory Results:
N/A

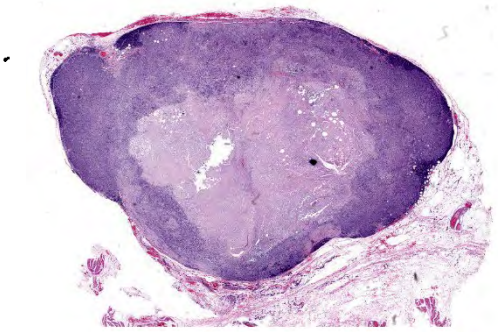

Figure 2-1: Lymph node, dog. A lymph node is effaced by a neoplasm – remnant lymph node is present beneath the capsular surface. Approximately 33% of the neoplasm is necrotic. (HE, 17X)

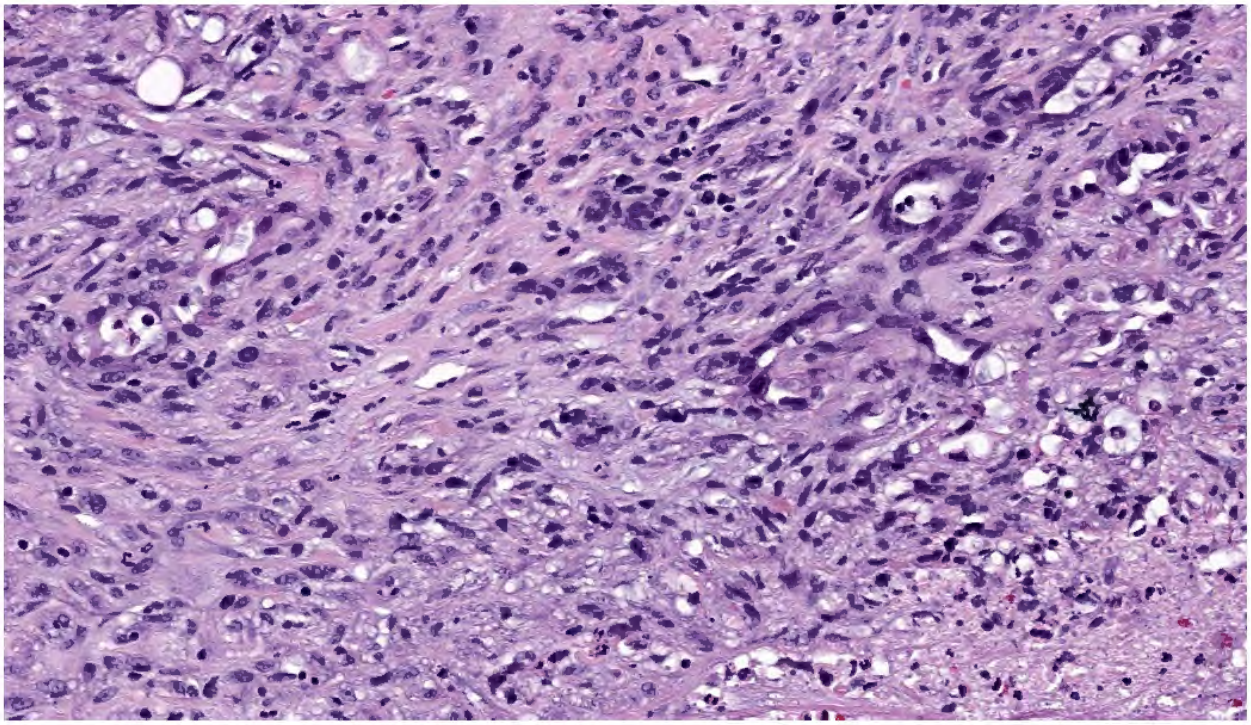

Figure 2-2: Lymph node, dog. There are two cell types within the neoplasm. The predominant cell type is myoepithelium arranged in long streams and bundles, and scattered throughout are cuboidal epithelium forming glands. (HE, 458X)

Microscopic Description:
Axillary mass: Examined are two sections of haired skin and mammary tissue containing an encapsulated structure rimmed by lymphocytes (lymph node, presumptive) that is 95% effaced by a large neoplasm composed of two cell populations. The first, and most numerous, population consists of spindle-shaped cells arranged in haphazard bundles and whorls immersed in a pale basophilic matrix and supported by a fine fibrovascular stroma. These cells have indistinct borders and a moderate amount of wispy to vacuolated pale basophilic cytoplasm. Nuclei are ovoid to elongate with evenly dispersed chromatin and 1-2 indistinct nucleoli. Anisokaryosis is moderate. The second population consists of polygonal cells arranged in tubules. This population has more abundant eosinophilic cytoplasm, but the nuclear morphology is nearly identical to the first population. Mitoses are 34 in 2.37 mm^2, including bizarre mitoses. There is extensive central necrosis of the mass, which abuts the surgical margin of the submitted tissues.

Immunohistochemistry results: The polygonal cell population exhibits strong, diffuse membranous and cytoplasmic positivity for MNF116 (pancytokeratin). This population is negative for smooth muscle actin (SMA), consistent with epithelial cells. The spindle cell population exhibits moderate to strong, predominantly membranous positivity for MNF116, as well as moderate to strong membranous and cytoplasmic positivity for SMA, consistent with myoepithelial cells. There is a smaller group of streaming spindle cells that are negative for MNF116 and positive for SMA, consistent with myofibroblasts (desmoplastic response). Controls stain appropriately.

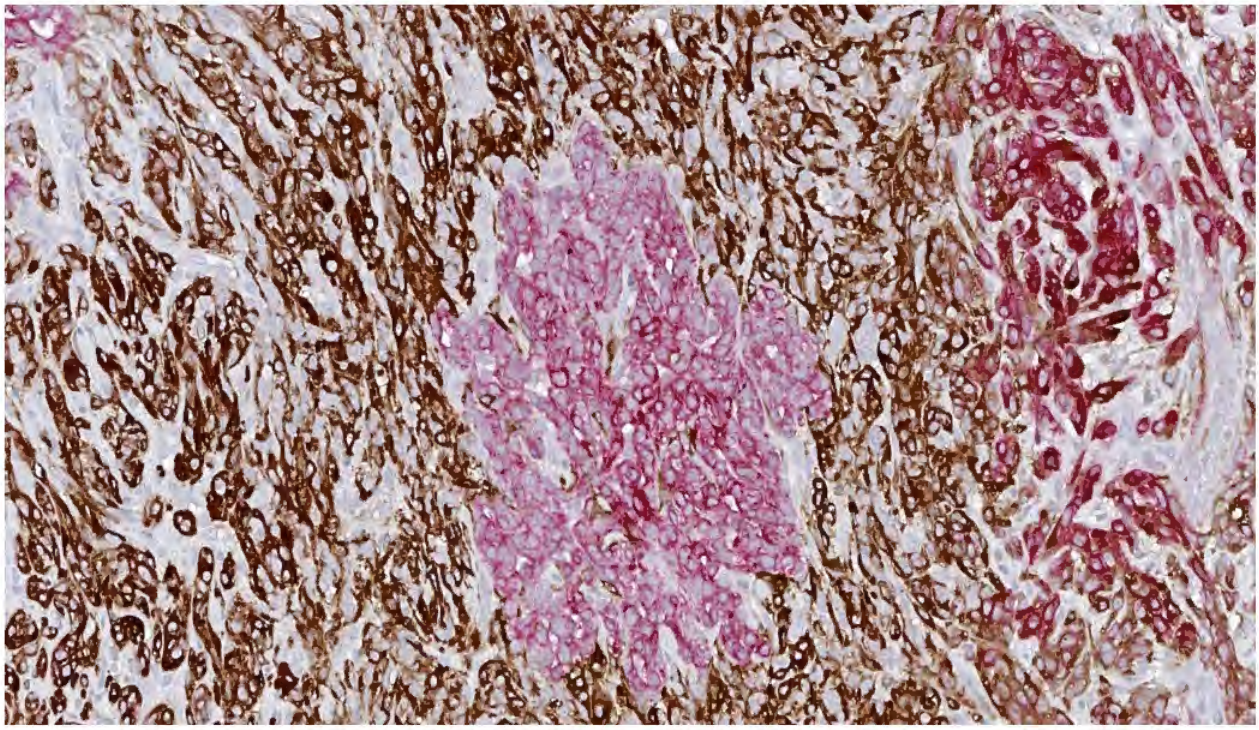

Figure 2-3: Lymph node dog. Neoplastic epithelial cells exhibit strong cytoplasmic positivity for cytokeratin (brown chromogen), and neoplastic myoepithelial cells exhibit moderate cytoplasmic positivity for smooth muscle myosin (red chromogen). (anti AE1/AE3 and SMMH, 400X).

Contributor's Morphologic Diagnoses:
Axillary mass: Mammary carcinoma and malignant myoepithelioma, grade II

Contributor's Comment:
The diagnosis of canine carcinoma and malignant myoepithelioma (CAMM) was first introduced in the review article *Classification and Grading of Canine Mammary Tumors* (2011) by M. Goldschmidt, et. al.[2] In previous classification systems for canine mammary tumors, any tumor containing both luminal epithelial and myoepithelial cells was considered either a complex tumor (without a mesenchymal component) or a mixed tumor (with a mesenchymal component), without differentiating between tumors whose myoepithelial population was benign and those with a malignant myoepithelial component.[3,4] Recognizing CAMM as a separate entity in the 2011 classification system required two major changes in our approach to mammary tumors. First, the use of immunohistochemistry (IHC) to accurately characterize and classify mammary tumors became widespread enough that consistently accurate classification of mammary tumors was possible, allowing the behavior of individual tumor types to be studied more closely.[2] Secondly, our definition of complex mammary carcinomas evolved to only include those tumors with a *benign* myoepithelial component, in recognition of the fact that mammary tumors in which both the epithelial and myoepithelial populations are malignant might behave differently than those in which the myoepithelial population is benign.[2-4] In fact, a follow-up 2-year prospective study of 229 dogs showed that dogs with CAMM were more than 10 times more likely to experience tumor-related death than dogs with complex carcinoma, validating the decision to separate these two entities.[5]

The myoepithelial cell population in canine complex mammary tumors is positive for

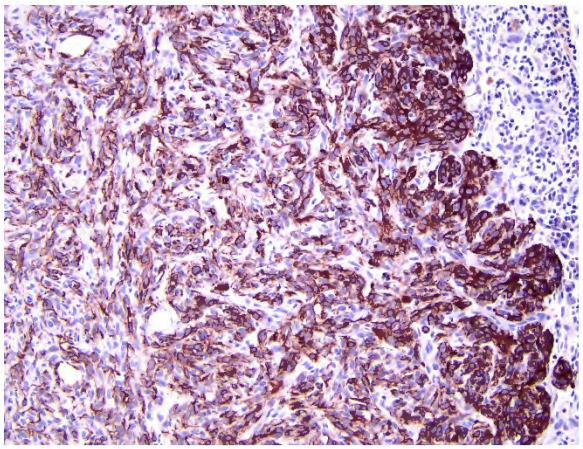

Figure 2-4: Lymph node, dog. Myoepithelial cells exhibit strong membranous positivity for MNF116. (anti- MNF116, 200X) (Photo courtesy of: Veterinary Medical Diagnostic Laboratory, University of Missouri, https://vmdl.missouri.edu/)

smooth muscle actin (SMA), calponin, vimentin, p63, and high molecular weight basal cytokeratins CK5, CK6, and CK14, while the epithelial population expresses luminal cytokeratins CK8, CK18, and CK19.[8] Interestingly, the myoepithelial population in CAMM has higher expression of CK5, CK14, SMA, calponin, and p63 (characterized as an "intermediary" or less well-differentiated phenotype), compared to the myoepithelial population in complex carcinoma (which is more similar to that of terminally differentiated myoepithelial cells).[6] CAMM myoepithelial cells also have significantly higher Ki67 expression than those in complex carcinoma, in accordance with their more aggressive biological behavior.[6] Conversely, the benign myoepithelial population in canine complex mammary carcinomas has been theorized to play a tumor suppressor role, accounting for the better prognosis of complex carcinoma when compared to simple carcinomas that have no myoepithelial component.[1,7] However, if this is true, the tumor suppressor activity appears to be a feature specific to terminally differentiated myoepithelial cells, rather than the malignant, intermediary-like myoepithelial population present in CAMM.[6]

The present neoplasm most likely represents metastasis of a primary mammary carcinoma to the axillary lymph node, which is supported by the patient history, anatomic location of the mass, and the presence of a compressed population of mature lymphocytes enclosed within a thin fibrous capsule, consistent with remnant nodal architecture. However, given the presence of mammary tissue in the adjacent subcutis, the possibility remains that this is a primary tumor arising from mammary tissue in an unusual location (i.e., the axilla). Either way, the morphologic features of the myoepithelial population (pleomorphism, anisokaryosis, and a high mitotic rate, including bizarre mitoses) are consistent with malignancy, supporting a diagnosis of CAMM over complex mammary carcinoma, in which the myoepithelial component is uniform with minimal anisocytosis and anisokaryosis.[2]

Definitive diagnosis of CAMM requires IHC to confirm the presence of both a myoepithelial and an epithelial component.[2] The present mass has three subpopulations of cells with differing immunophenotypes. The first is the luminal epithelial cell population, which is positive for MNF116 and negative for SMA.

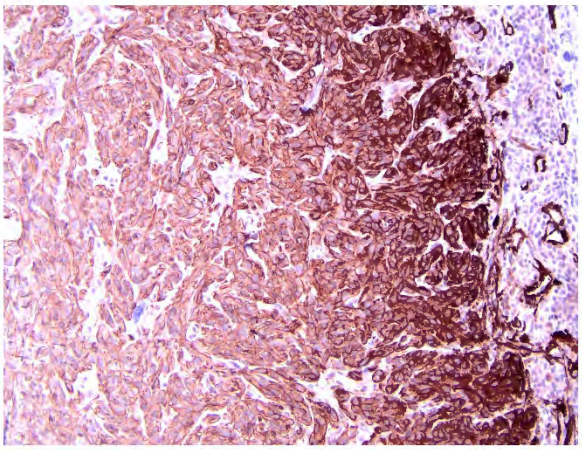

Figure 2-5: Lymph node, dog. Myoepithelial cells exhibit strong cytoplasmic positivity for smooth muscle actin. (anti- SMA, 200X) (Photo courtesy of: Veterinary Medical Diagnostic Laboratory, University of Missouri, https://vmdl.missouri.edu/)

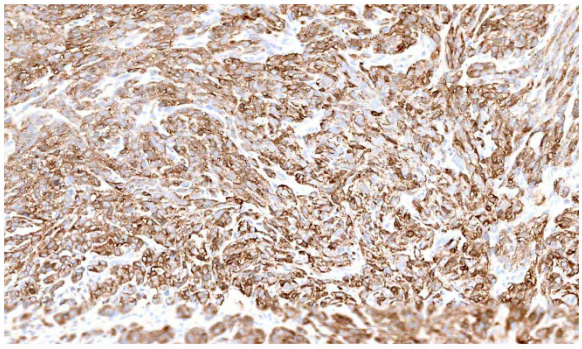

Figure 2-6: Lymph node, dog. Myoepithelial cells exhibit strong cytoplasmic positivity for calponin. (anti- calponin, 350X).

MNF116 is an antibody that reacts with cytokeratins 5, 6, 8, 17, and possibly 19; thus, it is expected to stain both luminal epithelial cells and myoepithelial cells. The second group of cells, the myoepithelial population, is positive for both MNF116 and SMA, as expected. However, there is a third population, which is composed of streaming spindle cells that are positive for SMA but not MNF116. These cells are consistent with a desmoplastic response characterized by myofibroblast proliferation, which is a feature shared with highly aggressive mammary carcinomas such as anaplastic carcinoma.[2]

Contributing Institution:
Veterinary Medical Diagnostic Laboratory
University of Missouri
https://vmdl.missouri.edu/

JPC Diagnoses:
Lymph node: Malignant epithelial and spindle cell neoplasm, metastatic.

JPC Comment:
This second case stimulated lively discussion amongst participants regarding both anatomic location and diagnosis. Some participants were successfully able to get to lymph node, while others hedged a bit more and felt comfortable with calling it subcutaneous tissue with a particularly immunogenic neoplasm. Either way, it was a tough call, but the presence of a capsule and subcapsular sinuses are what helped push participants off the fence and onto Team Lymph Node.

MAJ Travis led participants through a "Mammary Neoplasms 101" conversation, covering the major classifications of mammary tumors. These include ductular, simple (involve just neoplastic epithelium), complex (epithelium and myoepithelium), mixed (Epithelium, myoepithelium, and either bone, cartilage, and/or adipose tissue), and myoepithelial. Within each of these are subcategories, but those five main classifications are a "must-know" starting place when working up mammary neoplasms as a pathologist. Current criteria for histologic grading of canine mammary neoplasms includes evaluation of percentage of tubule formation, nuclear pleomorphism, and mitotic count.[2]

Dogs have the highest incidence of mammary neoplasms of any domestic species.[2] Luckily for dogs, the majority of these tumors are clinically benign, which contrasts with most other domestic species that have mostly malignant mammary neoplasms. In dogs, these are typically progressive, and development of neoplasia can proceed from ductular or lobular hyperplasia to dysplasia and onwards to neoplasia. Even within benign adenomas, there can be progression to non-invasive adenocarcinoma and further progression to metastatic mammary adenocarcinoma if these neoplasms are left to grow on the affected dog. Mammary sarcomas in dogs are much less common than epithelial neoplasms but are significantly more aggressive and metastatic when they do occur. Additionally, if a dog develops one mammary neoplasm, it is common for multiple others to develop over time. The prognosis for each mass may vary greatly, and different types of mammary

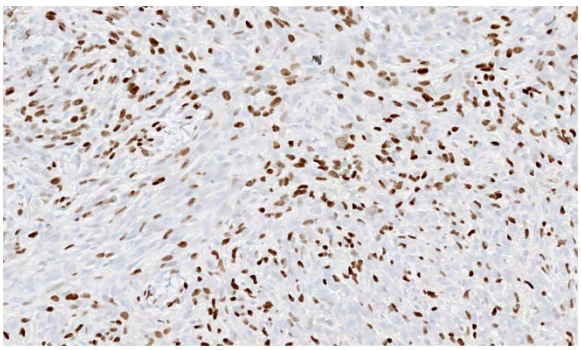

Figure 2-7: Lymph node, dog. 66% of myoepithelial cells exhibit strong nuclear positivity for P-63. (anti-P63, 350X).

tumors can be found in the mammary glands of an individual animal.[1,2]

On to the difficulty in providing an appropriate morphologic diagnosis. When deciding how to morphologically diagnose WSC cases, the JPC tries to provide a diagnosis that would be achievable from the H&E slide alone (as this is what is available to participants around the world before each conference). As such, and after much deliberation, participants ultimately decided on a diagnosis of metastatic malignant epithelial and spindle cell neoplasm, as there were no exclusively defining features of a mammary-specific neoplasm on the H&E slide. All agreed, however, that the IHC profile of this neoplasm is supportive of the contributor's diagnosis of canine mammary carcinoma and malignant myoepithelioma (CAMM), especially given the immunoreactivity of the neoplastic cells for calponin and the spindle cells to both p63 and smooth muscle myosin-heavy chain, which is more specific for myoepithelium than just smooth muscle actin.

Following these spirited discussions, Dr. Bruce Williams deployed some well-timed humor by asking attendees, "Having never been to a tea party before, is this what people *normally* talk about?" Probably not, Dr. Williams, probably not.

References:

1. Chang SC, Chang CC, Chang TJ, Wong ML. Prognostic factors associated with survival two years after surgery in dogs with malignant mammary tumors: 79 cases (1998-2002). J Am Vet Med Assoc. 2005;227:1625-1629.
2. Goldschmidt M, Peña L, Rasotto R, Zappulli V. Classification and grading of canine mammary tumors. Vet Pathol. 2011;48(1):117-131.
3. Hampe JF, Misdorp W. IX: Tumours and dysplasias of the mammary gland. Bull World Health Organ. 1974;50:111-133.
4. Misdorp W, Else RW, Hellmen E, Lipscomb TP. Histologic Classification of Mammary Tumors of the Dog and the Cat, 2nd ser., vol. 7. Armed Force Institute of Pathology and World Health Organization;1999.
5. Rasotto R, Berlato D, Goldschmidt MH, Zappulli V. Prognostic significance of canine mammary tumor histologic subtypes: an observational cohort study of 229 cases. Vet Pathol. 2017;54(4):571-578.
6. Rasotto R, Goldschmidt MH, Castagnaro M, Carnier P, Caliari D, Zappulli V. The dog as a natural animal model for study of the mammary myoepithelial basal cell lineage and its role in mammary carcinogenesis. J Comp Pathol. 2014;151(2-3):166-180.
7. Rasotto R, Zappulli V, Castagnaro M, Goldschmidt MH. A retrospective study of those histopathologic parameters predictive of invasion of the lymphatic system by canine mammary carcinomas. Vet Pathol. 2012;49:330-340.
8. Sorenmo KU, Rasotto R, Zappulli V, Goldschmidt MH. Development, anatomy, histology, lymphatic drainage, clinical features, and cell differentiation markers of canine mammary gland neoplasms. Vet Pathol. 2011;48:85-97.

~~CASE III:~~

Signalment:
2 year intact female cynomolgus macaque (*Macaca fascicularis*)

History:
A 2-year-old female cynomolgus macaque in a vehicle control group of a 3-month safety assessment study was necropsied per standard GLP procedures at the end of the study timeline.

Gross Pathology:
No gross lesions were noted at the time of necropsy.

Laboratory Results:
N/A

Microscopic Description:
Uterus: Regionally effacing the endometrium, displacing and disrupting the normal glandular and stromal architecture, is a poorly circumscribed, nonencapsulated, infiltrative proliferation of highly pleomorphic round to polygonal neoplastic cells arranged in sheets. The neoplastic proliferation is composed of a biphasic population of uninucleate or multinucleate cells with distinct cell borders, moderate to marked amounts of eosinophilic cytoplasm, and large round vesiculate to finely stippled nuclei and 1-4 variably prominent nucleoli, consistent with a trophoblastic (cytotrophoblasts and syncytiotrophoblasts, respectively) lineage. There are 2 mitotic figures in 10 high power fields (400x). Moderate numbers of lymphocytes and plasma cells are scattered throughout the adjacent endometrial stroma and outer myometrium. Dilated endometrial glands occasionally contain a variable amount of eosinophilic amorphous to basophilic flocculant debris and few macrophages or lymphocytes. Regional erosion of endometrial epithelium is present. The ovary lacks corpora lutea, consistent with sexual immaturity.

Figure 3-1: Uterus, cynomolgus monkey. A section of normal ovary (top) and uterus (bottom) are submitted for examination. At subgross magnification, there is multifocal dilation of endometrial glands. (HE, 10X)

Slides not provided:

Immunohistochemistry on the uterine neoplasm is performed using anti-human chorionic gonadotropin (hCG), anti-pancytokeratin AE1/AE3, anti-human placental lactogen (huPL), anti-p63, anti-CD10, anti-placental alkaline phosphatase (PLAPH), anti-progesterone receptor (PR), anti-estrogen receptor α (ERα), and anti-Ki67 antibodies and is visualized using 3,3′-diaminobenzidine or Fast Red as a chromogen. Occasional neoplastic cells with high degrees of atypia express cytoplasmic labeling for hCG. Neoplastic cells have strong cytoplasmic and membranous labeling for pancytokeratin AE1/AE3. Labeling for huPL and CD10 demonstrates rare neoplastic cells expressing moderate to strong cytoplasmic immunolabeling; however, the majority of neoplastic cells are negative. Few neoplastic cells have weak nuclear p63 labeling. Labeling for Ki67 demonstrates moderate to

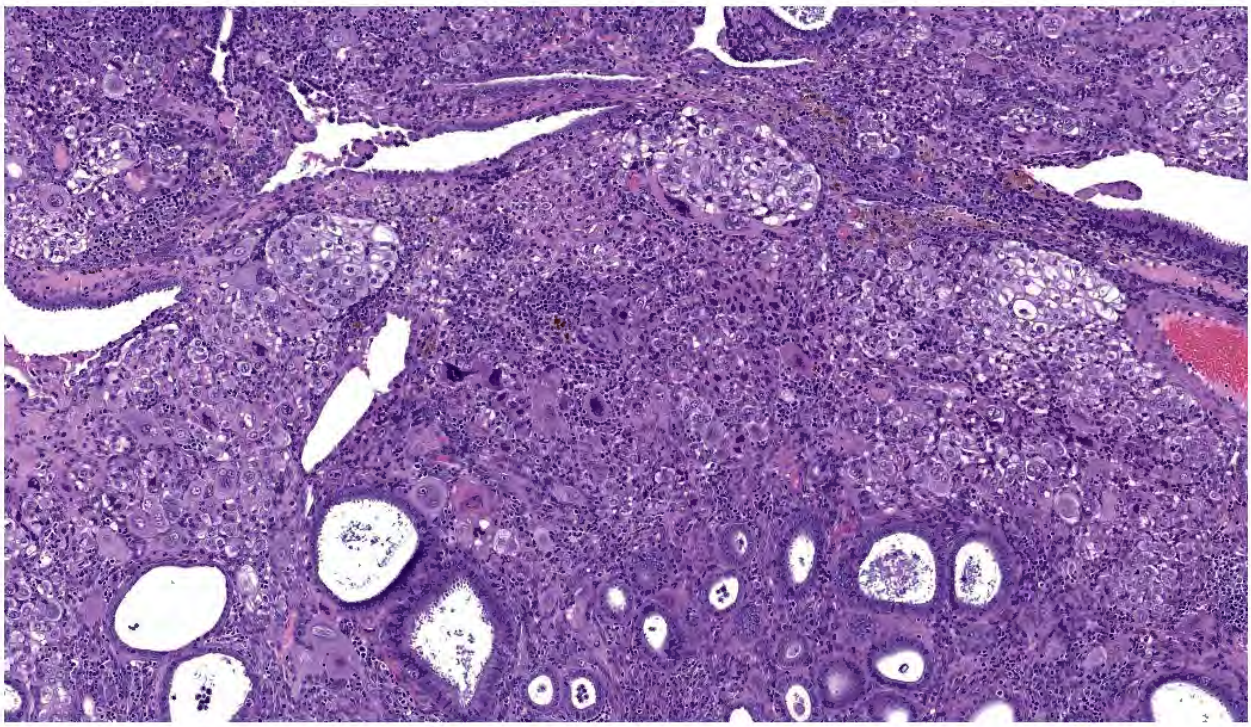

Figure 3-2: Uterus, cynomolgus monkey. Expanding the endometrium, there is a multilobular neoplasm which is composed of nests of uninucleate cells resembling trophoblasts and multinucleated cells resembling syncytiotrophoblasts. There are also numerous lymphocytes infiltrating this tissue. (HE, 150X)

high numbers of proliferative neoplastic cells regionally. Overall, PR and ERα expression is limited due to the immature age of the animal, but is present in the expected locations in the endometrial stroma and glandular epithelium, and absent in the neoplastic population. Neoplastic cells do not label for PLAPH. These immunohistochemical findings further support a diagnosis of choriocarcinoma.

Contributor's Morphologic Diagnoses:
Uterus: Choriocarcinoma

Contributor's Comment:
Choriocarcinoma is a neoplasm of trophoblastic lineage that most often arises in women following normal or abnormal pregnancies.[1] Diagnostic features include highly pleomorphic, polygonal to round cells with abundant cytoplasm that are both uninucleate (cytotrophoblast or intermediate trophoblast-like) and multinucleate (syncytiotrophoblast) cells, and often a high mitotic rate with metastasis. Morphologic features on histologic evaluation of hematoxylin and eosin-stained uterus from this sexually immature cynomolgus macaque were consistent with choriocarcinoma.

In human medicine, choriocarcinoma falls under the umbrella entity of gestational trophoblastic disease. Other neoplasms in this entity include placental site trophoblastic tumor (PSTT) and epithelioid trophoblastic tumor (ETT). PSTTs are composed of a monomorphic population of large, pleomorphic cells derived from implantation-type intermediate trophoblasts. Most cells are uninucleate, but it is not uncommon to see occasional scattered multinucleate cells. ETTs arise from chorionic-type intermediate trophoblasts and present as nests, cords, or solid masses with a monomorphic population of small, round cells.[1] Choriocarcinomas tend to have a distinct morphology compared to PSTT and ETT with the presence of uninucleate and multinu-

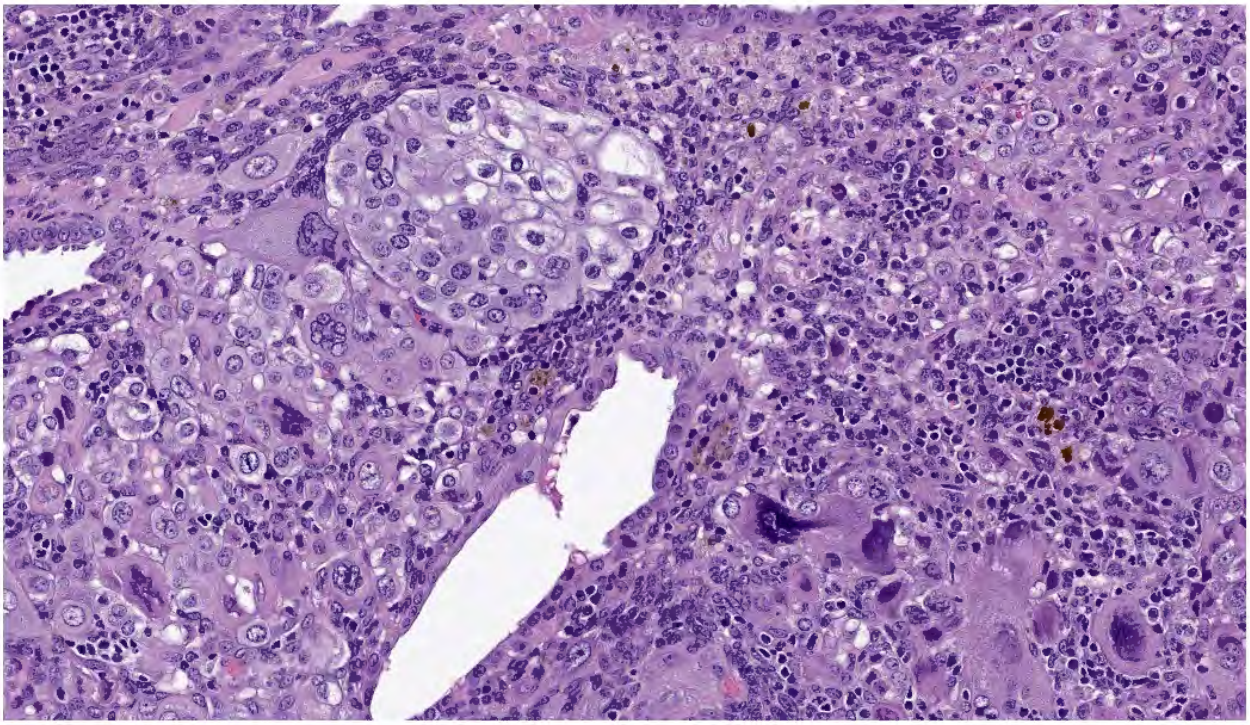

Figure 3-3: Uterus, cynomolgus monkey. Higher magnification of nests of uninucleate neoplastic cells resembling trophoblasts, and fewer multinucleated neoplastic cells resembling syncytiotrophoblasts. There are rare hemosiderin-laden macrophages scattered throughout. (HE, 381X)

cleate cells; however, a panel of immunohistochemical markers is commonly used to confirm diagnosis. Characterization with antibodies against hCG, pancytokeratin AE1/AE3, huPL, p63, CD10, PLAPH, and Ki67 provides further support for a diagnosis of choriocarcinoma. These immunohistochemical markers are helpful in distinguishing between PSTT, ETT, and choriocarcinoma (see table).[5]

Marker	PSTT	ETT	Choriocarcinoma	Lesion
hCG	+/-	+/-	+	+
huPL	+	+/-	+/-	Rare
p63	-	+	+/-	Rare weak
Pancytokeratin AE1/AE3	+	+	+	+
CD10	+/-	-	+/-	Rare
PLAPH	-	-	-	-
Inhibin-α	+	+	+	Not performed
Ki67 Index	Moderate	Moderate	High	High

This neoplasm has been reported in laboratory and domestic species and is noted in the International Harmonization of Nomenclature and Diagnostic Criteria (INHAND) for non-proliferative and proliferative lesions in non-human primates (NHP), mice, and rabbits.[2-4] In women, non-gestational choriocarcinoma can occasionally arise in the ovary and have only rarely been reported as a primary tumor in the uterus.[7] While non-gestational choriocarcinoma of the ovary has been reported in NHP, there are no published examples of a primary non-gestational choriocarcinoma of the uterus.

Spontaneous neoplasms in nonrodent species are rare in routine toxicology work due to the young age of animals used in nonclinical toxicity testing. Knowledge of spontaneous background lesions is necessary to distinguish from potential test article-related effects in any species.

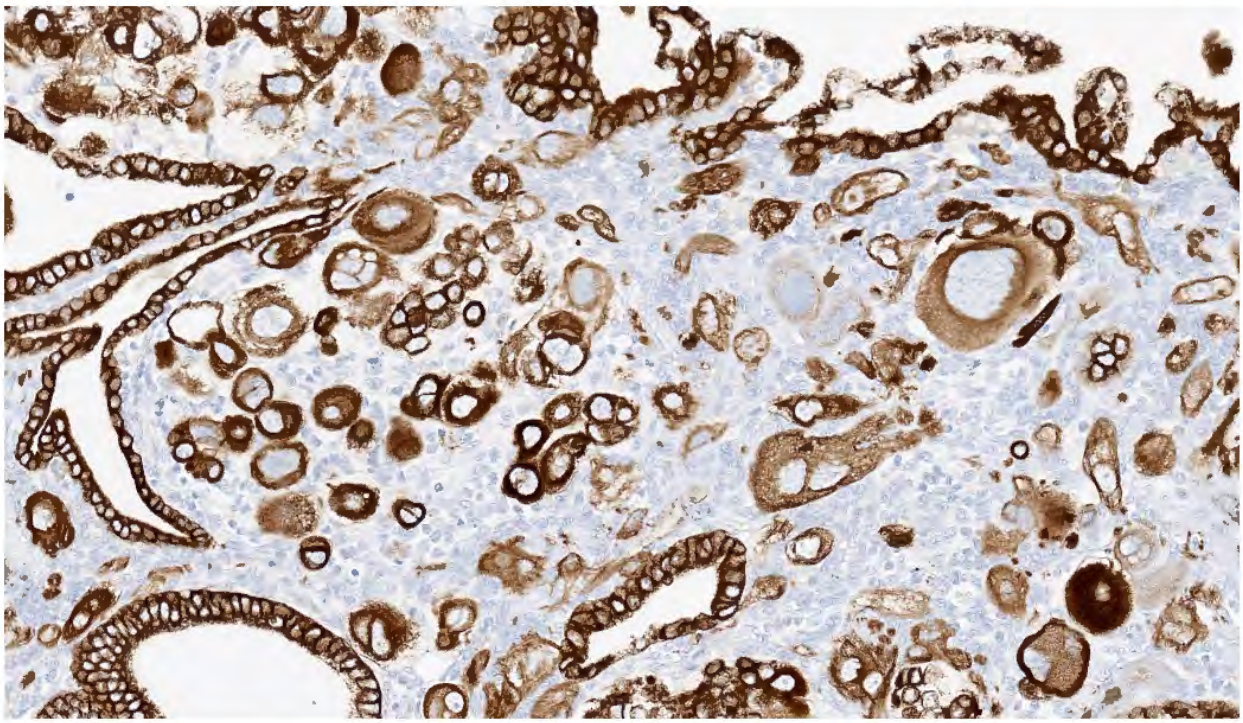

Figure 3-4: Uterus, cynomolgus monkey. The neoplastic cells (both uni- and multinucleated) demonstrate strong cytoplasmic immunopositivity. (anti-AE1/AE3, 381X)

Contributing Institution:
Charles River Laboratories – Mattawan, MI
criver.com

JPC Diagnoses:
Uterus: Choriocarcinoma.

JPC Comment:
The contributor of this case provides a great overview of choriocarcinomas, their main differentials, and the common immunohistochemical profiles expected with these neoplasms in their comment. These topics covered much of what was discussed in conference for this case.

The topic of the IHCs prompted a review of what each of the pertinent markers is for and what some of the IHC targets do physiologically. For example, choriocarcinomas are readily immunoreactive for human chorionic gonadotropin (hCG). In the body, hCG (or any of the species-specific CGs, for that matter), is produced by the placental trophoblasts (the cell of origin in choriocarcinoma) and stimulates the release of progesterone from the corpus luteum (CL) to maintain the pregnancy. Human placental lactogen (HPL) also functions as a marker for trophoblasts and is released by the placenta to, among other functions, stimulate growth of the mammary glands for lactation. CD10 marks endometrial stroma. Inhibin, released from granulosa cells (GC) to regulate production of follicle-stimulating hormone (FSH), will be immunoreactive in granulosa cells (including in some neoplastic GC populations). Although choriocarcinoma is classified as a germ cell tumor, it is weakly to not at all immunoreactive for placental-like alkaline phosphatase (PLAP), which is a marker of germ cells. This is thought to be due to the neoplastic choriocarcinoma cells being less well-differentiated or potentially even de-differentiated compared to regular syncytiotrophoblasts, which are usually immunoreactive for PLAP.[6] Lastly, p63, a member of the p53 "Guardian of the Genome" family of genes, will be immunoreactive in

myoepithelial cells, squamous epithelial cells, and a few others. The table provided by the contributor provides an excellent resource for cross-comparison of IHC profiles between these in choriocarcinomas and their differentials.[5]

Choriocarcinomas are categorized as gestational (associated with pregnancy) or non-gestational (formed in the absence of pregnancy). Some participants were astutely able to deduce from the types of follicles found in the accompanying ovary on the slide that this was very likely a juvenile animal. This, coupled with the lack of gestational change to the uterus, led some to make the jump to a non-gestational choriocarcinoma. Kudos are due to the participants that managed to reason through those subtleties! As mentioned in the contributor's comment, there are no published examples of primary non-gestational uterine choriocarcinoma in non-human primates.

While most participants were readily able to reach the diagnosis of "choriocarcinoma" from the H&E section in the absence of any immunomarkers,there was quite a bit of discussion on if this neoplasm would truly classify as a choriocarcinoma or if it would be considered "choriocarcinomatous differentiation" due to the young age of the animal. This is a term occasionally utilized in research settings, usually in the context of early choriocarcinoma-like changes seen with decidual reactions in NHPs. Although there was no evidence of decidual reaction in this case, we consulted with our JPC MD reproductive subspecialists, who agreed with the diagnosis of choriocarcinoma. The term "choriocarcinomatous change/differentiation" is not utilized in human medicine and is not listed in the NHP INHAND guide for terminology related to this neoplasm.[3] As such, the JPC refrains from the usage of this term.

References:

1. Benirschke K, Kaufmann P. Chapter 23: Trophoblastic Neoplasms. *Pathology of the Human Placenta.* 5th ed. New York: Springer-Verlag; 2006.
2. Bradley AE, Wancket LM, Rinke M, et al. International Harmonization of Nomenclature and Diagnostic Criteria (INHAND): Nonproliferative and Proliferative Lesions of the Rabbit. *J Toxicol Pathol*, 2021; 34(3 suppl): 183S-292S.
3. Colman K, Andrews RN, Atkins H, et al. International Harmonization of Nomenclature and Diagnostic Criteria (INHAND): Non-proliferative and Proliferative Lesions of the Non-human Primate (*M. fascicularis*). *J Toxicol Pathol*, 2021; 34(3 suppl): 1S-182S.
4. Dixon D, Alison R, Bach U, et al. Nonproliferative and Proliferative Lesions of the Rat and Mouse Female Reproductive System. *J Toxicol Pathol*, 2014; 27(3-4 suppl): 1S-107S.
5. Elmore SA, Carreira V, Labriola CS, et al. Proceedings of the 2018 National Toxicology Program Satellite Symposium. *J Toxicol Pathol*, 2018; 46(8): 865-897.
6. Lösch A, Kainz C. Immunohistochemistry in the diagnosis of the gestational trophoblastic disease. *Acta Obstet Gynecol Scand.* 1996;75(8):753-6.
7. Maesta I, Michelin OC, Traiman P, Hokama P, Rudge MVC. Primary non-gestational choriocarcinoma of the uterine cervix: A case report. *Gynecol Oncol*, 2005; 98(1): 146-50.

CASE IV:

Signalment:

2-years-old, female, rabbit, *Oryctolagus cuniculus domesticus*

History:

This rabbit was taken to the veterinary hospital with the main complaint of bleeding from the genitals. Because uterine bleeding was sus

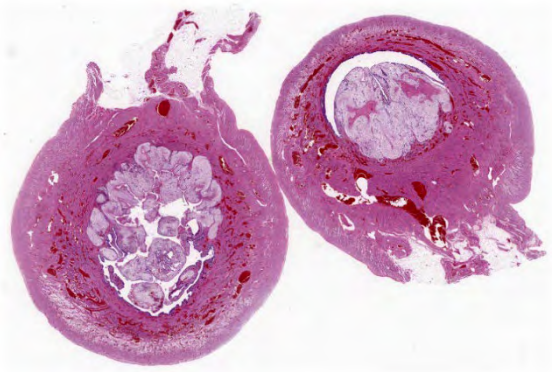

Figure 4-1: Uterus, rabbit. Two sections of the uterus demonstrate a polypoid multinodular thickening of the uterine mucosa predominantly on the mesometrial side. The endometrium in this area exhibits profound pallor. (HE, 12X)

pected, a total hysterectomy and oophorectomy were performed. A mass-like lesion was identified in the right uterine horn.

Gross Pathology:
The midbody of the right uterine horn had a circular lump (0.6 cm in diameter). The cut section of this lump appeared white and solid.

Laboratory Results:
N/A

Microscopic Description:
The endometrium on the mesometrial side of the uterus proliferated with the formation of large nodules and numerous polyps. The surface of the nodules and polyps was covered by endometrial epithelium, however, approximately 50% of the epithelium were eroded. The polyps and nodule contained numerous blood vessels with normal endothelium, along with cells that resembled large-vacuolated decidual cells, arranged in sheets. The decidual cells had distinct cell boundaries, a round shape, abundant transparent cytoplasm, and nuclei ranging from oval to irregular shapes. Mitotic figures were also occasionally observed. Just beneath the endometrial epithelium, the decidual cells exhibited a spindle-shaped morphology. (Fig.1 and 2)On the antimesometrial side of the uterine, endometrial hyperplasia was mild, decidual cells in the endometrial stroma were sparse, and proliferation of huge giant cells resembling trophoblast was prominent. The huge giant cells displayed a variety of morphologies, including round, spindle, to pleomorphic, with notably large, highly atypical nuclei and abundant cytoplasm. Multinucleated giant cells were also observed.

The immunohistochemical analysis demonstrated that normal endometrial epithelium is positive for progesterone receptor (PgR), keratin AE1/AE3, and CAM5.2, and negative for CD10, SMA and desmin. Normal endometrial stromal cell is positive for PgR and CD10, and negative for keratin AE1/AE3, CAM5.2, SMA and desmin. Decidual cell is positive for PgR and CD10, and negative for keratin AE1/AE3, CAM5.2, SMA and desmin. The huge giant cells exhibited positive for keratin AE1/AE3, CAM5.2 and CD10, and negative staining for PgR, SMA and desmin.

Contributor's Morphologic Diagnoses:
Uterus: Decidual reaction

Contributor's Comment:
Rabbits have a hemodichorial and bidiscoid type of placenta. Histologically, the placenta of rabbits is composed of the labyrinth zone, the junctional zone, the decidua zone, and the mesometrium.[3,6,7] In the labyrinth zone, there are two layers of trophoblasts, an outer and inner layer separating the maternal blood spaces from the fetal blood vessels. The outer trophectoderm is comprised of the syncytiotrophoblasts. The inner trophectoderm is one layer of cytotrophoblasts overlying fetal blood vessels. The junctional zone is composed of glycogen cells with eosinophilic cytoplasm

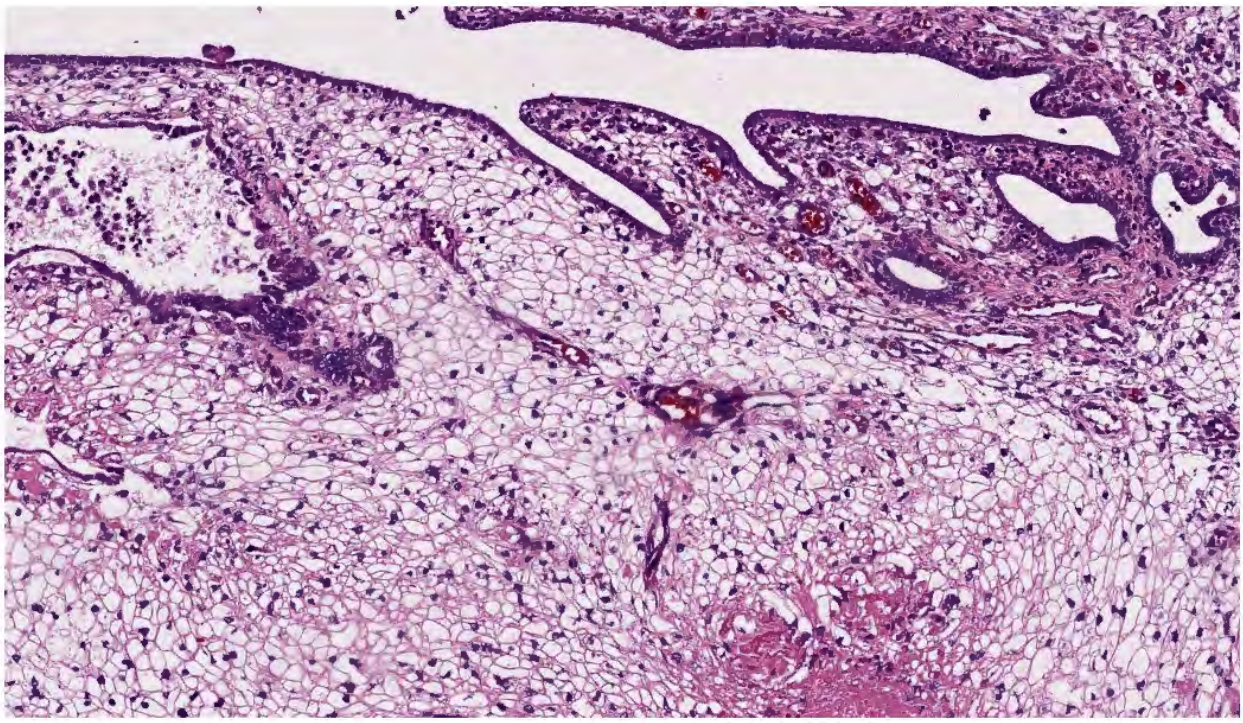

Figure 4-2: Uterus, rabbit. Endometrial stromal cells are swollen with clear cell change (decidual reaction) markedly separating tortuous endometrial glands. (HE, 230X)

containing PAS-positive substances and giant cells having often 2-3 number of nuclei. The decidua originates from stromal cells of the mesometrial endometrium. Before 11 days of pregnancy, it consists of proliferating spindle cells, subsequently, vacuolated cells known as decidual cells begin to appear. The proliferation of decidual cells continues, and from 13 days of pregnancy, necrosis of decidual cells begins to be observed. In mid-gestation, the decidual zone is divided into the zone of necrosis and the zone of separation.[3,6,7] The zone of necrosis develops with dilated blood vessels as pregnancy advances. This zone is detected under the junctional zone and is composed of necrotic tissue. The zone of separation, which is composed of the cells having large foamy cytoplasm, becomes thinner without necrosis as pregnancy advances.[3,6,7]
During pregnancy in rabbits, a characteristic feature is the presence of giant cells on the obplacental (antimesometrial) region. These giant cells are referred to as obplacental giant cells to distinguish them from certain cell populations of the definitive (chorioallantoic) placenta and decidua.[1] Immunocytochemistry shows that the giant cells are positive for cytokeratin and vimentin, but are negative for desmin and Factor VIII-related antigen. The cells are positive for cytokeratin from their inception, but only become vimentin-positive between Days 12 and 15 of pregnancy, a change seemingly related to their detachment from epithelial tissue to take on an independent existence.

The case was characterized by the proliferation of vacuolated cells in the endometrial stroma covered by normal endometrial epithelium. In the presence of an embryo and normal placental formation, trophoblasts attached to the outer surface of the endometrial epithelial cells.[3,6,7] However, in this case, the absence of trophoblast cell proliferation clearly indicates that normal placental formation has not occurred. It can thus be concluded that only vacuolated cells of maternal origin are

proliferating. The vacuolated cells exhibited a morphology similar to that of decidual cells during normal placental formation and frequently contained PAS-positive granules, further supporting this interpretation. Immunohistochemical staining revealed positivity for CD10, negativity for keratin and positivity for progesterone receptors. These findings are consistent with the staining pattern of endometrial stromal cells and provide further confirmation of the origin of these cells from the endometrial stroma. Sensitization by progesterone is necessary for the initiation of decidualization of the endometrial stroma, and stable progesterone activity is necessary for the stable existence of decidual cells.[2] In this case, the expression of progesterone in both the endometrial stroma and epithelium indicates that a decidual reaction has occurred overall.

In contrast, numerous giant cells were observed on the obplacental (antimesometrial) region. These giant cells are similar to obplacental giant cells formed in the pregnant uterus of rabbits with regard to both cell morphology and location. [1] The origin of these cells remains unclear. The absence of obvious trophoblasts and the formation of giant cells in the endometrial stroma beneath the normal endometrial epithelium suggest a uterine origin. However, immunostaining revealed positivity for CK and CAM5.2 (epithelial marker) and CD10 (positive for endometrial stromal cell), and negative for PgR (positive for both endometrial epithelial and stromal cell), which did not correspond with the staining patterns of endometrial epithelial or stromal cells. Consequently, it was not possible to ascertain their origin with any degree of certainty.

The decidual reaction is a well-documented phenomenon in rats, which can be categorized into two distinct types. The first type is characterized by the formation of nodules in the uterine cavity, exhibiting a high degree of structural organization and regional variation.

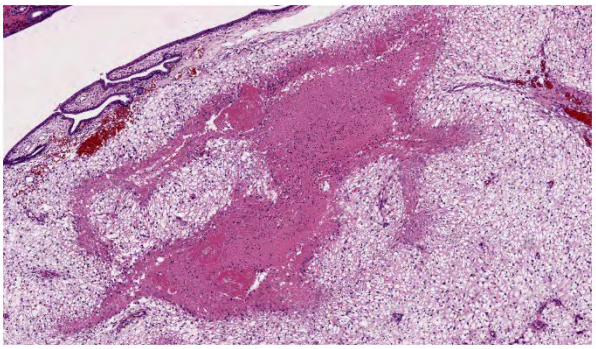

Figure 4-3: Uterus, rabbit. There are geographic areas of necrosis within the decidualized endometrial stroma. (HE, 103X)

The second type is referred to as focal decidualization, which is marked by the proliferation of decidual cells within a specific area of the endometrial stroma. Decidual cells in rats are large cells with oval nuclei and eosinophilic cytoplasm, characterized by PAS-positive small vacuolated cytoplasm. In the present case, although the lesions in rabbits corresponded to the focal decidualization observed in rats due to the absence of clear organization, the morphology of decidual cells differed, with rabbits exhibiting distinct vacuolated cells. The substantial disparities in placental formation among different animal species imply that the morphology of decidual reactions also exhibits considerable variation.

Contributing Institution:

Setusunan Univeristy, Laboratory of Pathology, Faculty of Pharmaceutical Sciences 45-1 Nagaotoge-cho, Hirakata, Osaka JAPAN 5730101

JPC Diagnoses:

Uterus, endometrial stroma: Decidual reaction, subacute, focally extensive, severe, with trophoblastic giant cells.

JPC Comment:

This final case provided a not-oft seen entity in diagnostic pathology, but one that is frequently encountered in research animals. Many thanks to the contributor for providing

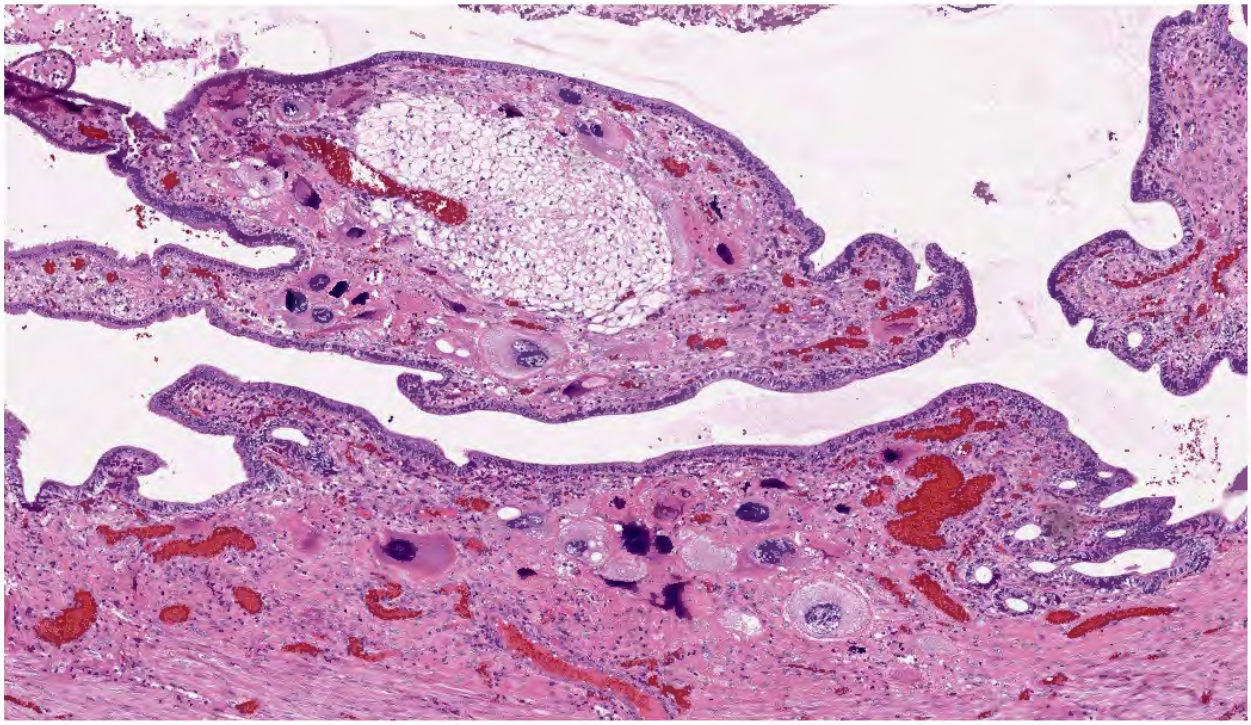

Figure 4-4: Uterus, rabbit. In one area of the section, adjacent to a nest of decidualized endometrial stroma, giant cells resembling trophoblasts and syncytiotrophoblasts infiltrate the endometrium. (HE, 121X)

this highly educational case, along with an excellent write-up on rabbit placentation and decidual reactions. Being able to identify a decidual reaction as such and not mistaking it for another lesion is an important part of understanding the normal reproductive physiology of species with a deciduate uterus. The degree of proliferation in this case caused some participants to pause a suggest possible diagnoses such as deciduoma vs focal decidualization, but the ultimate consensus following consultation with reproductive specialists was that this is consistent with the spectrum of decidual reaction in a rabbit. MAJ Travis used this case as an opportunity to review pertinent reproductive physiology, which encompassed much of this case's discussion and will be summarized here.

Ovarian follicle development starts with primordial follicles, which are surrounded by a single layer of squamous epithelial follicular cells. Primordial follicles then develop into primary follicles that are encircled by a single layer of plump cuboidal follicle cells.[10] In primary follicles, the zona pellucida, a thick, glycoprotein-rich layer, forms between the primary oocyte and the adjacent follicle cells. In the later developmental stages of the primary follicle, the follicular cells surrounding it undergo stratification into the stratum granulosum/membrana granulosa, which is avascular.[10] At this point, the follicle cells are now known as granulosa cells. Simultaneously, the stromal cells surrounding the late primary follicle form a sheath of connective tissue, known as the theca folliculi, that differentiates into the theca interna, which is an inner, highly vascularized layer containing cuboidal secretory cells, and the theca externa, composed of an outer layer of smooth muscle and collagen. The cells of the theca interna have many luteinizing hormone (LH) receptors and synthesize an androgen precursor to estrogen. However, without the help of granulosa cells, thecal calls cannot convert this androgen precursor into estrogen. The granulosa cells, under

Figure 4-5: Uterus, rabbit. High magnification of the pleomorphic giant cells. (HE, 121X)

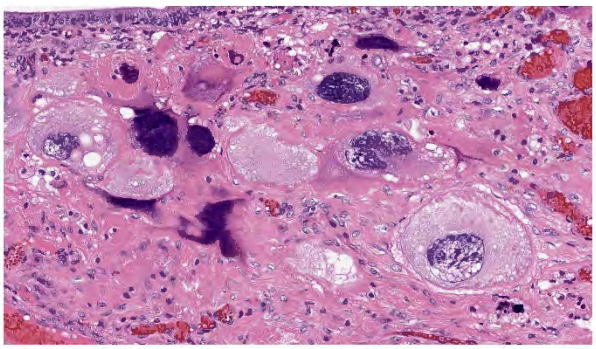

Figure 4-5: Uterus, rabbit. High magnification of the pleomorphic giant cells. (HE, 121X)

the influence of follicle stimulating hormone (FSH) from the anterior pituitary gland, catalyze the conversion of the precursor to estrogen, which enables further proliferation of granulosa cells.

Primary follicles develop into secondary (also called antral) follicles, which are characterized by a proliferation of granulosa cells that increase the follicle's size in the presence of sufficient FSH, growth factors, and calcium. Fluid-filled cavities appear among the granulosa cells and coalesce to form a single, crescent-shaped cavity (the antrum).[10] As this antrum enlarges, its lining of granulosa cells forms a thickened layer around the primary oocyte. This layer is called the "cumulus oophorous." These cells immediately surrounding the oocyte remain after ovulation and become known as the corona radiata.[8]

Finally, the mature/graafian follicle, housing a mature secondary oocyte, causes a bulge on the ovarian surface. Increased pressure in the antrum leads to attenuation of the granulosa cells and the development of the single layer of corona radiata cells around the secondary oocyte.[10] Approximately 24hrs prior to ovulation, the anterior pituitary releases a surge of FSH and LH in response to the rise in estrogen production from the follicle. Following this surge, LH receptors on the granulosa cells are downregulated and no longer produce estrogens, resulting in a decrease in estrogen that enables a subsequent rise in progesterone. During ovulation, the secondary oocyte is released from the mature follicle. Increased antral pressure effectively causes the oocyte, with its corona radiata, to explode out of the follicle. The peristaltic action of the theca externa's smooth muscle layer enables the freed oocyte to be propelled towards the fimbria of the oviduct. From there, the oocyte adheres to the fimbriae and is then actively transported into the uterus by ciliated cells that line the uterine tube.

Following the rather traumatic exit of the oocyte from the follicle during ovulation, the ruptured follicle experiences bleeding from the capillaries of the theca interna into the follicular lumen, earning it the name "corpus hemorrhagicum" (CH). The remaining follicular wall, composed of granulosa and thecal cells, is thrown into deep folds as the follicle collapses. The granulosa cells and the theca interna then differentiate into granulosa luteal and theca luteal cells through a process known as "luteinization" to form the "corpus luteum" (CL). Granulosa luteal cells are large and compose roughly 80% of the CL. They synthesize estrogen, progesterone, and inhibin (inhibin regulates production of FSH). By contrast, theca luteal cells are small and make up the remaining ~20% of the CL. They secrete androgens and progesterone. As the CL begins to form, blood vessels rapidly grow in to form a rich and complex vascular network. Progesterone and estrogen produced by the CL stimulate the growth and secretory activity of the endometrium to prepare for implantation of a fertilized oocyte. In cases where fertilization occurs, chorionic gonadotropin (CG) is produced by the early placenta, which stimulates consistent progesterone secretion from the CL to maintain the pregnancy. If no fertilization occurs, there is no CG production and the CL degenerates, leaving a scar known as the "corpus albicans" (CA). Over time, the CA shrinks and fades away.[10]

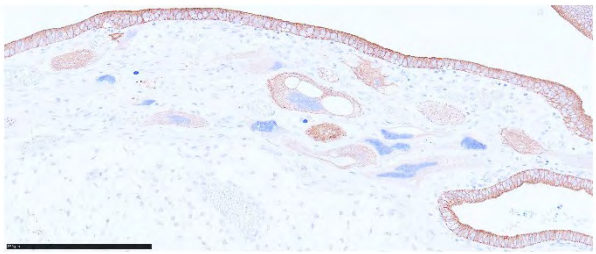

Figure 4-6: Uterus, rabbit. Giant cells demonstrate variably strong cytoplasmic immunoreactivity for cytokeratin. (anti-AE1/AE3, 121X)

Once ovulation has occurred, an oocyte has roughly 24hrs to be fertilized.[8] Sperm cells, upon contact with an oocyte, penetrate the oocyte by binding to zona pellucida receptors and releasing enzymes to degrade the corona radiata. Once a spermatozoon gains entry to the oocyte, the nucleus of the sperm's head is incorporated into the oocyte, where it will release its DNA and start the formation of the zygote. The fertilized oocyte then undergoes a series of changes while passing through the uterus, dividing many times to form a ball of cells called a morula (Latin for "mulberry"), which is still surrounded by a zona pellucida. Through subsequent cell divisions, the embryo loses its zona pellucida and forms a hollow sphere (blastocyst) with a centrally located cluster of cells called the "embryoblast", which will develop the amniotic sac, fetal yolk sac, and fetus. The embryoblast is surrounded by a layer of cells that will form trophoblasts, which ultimately become the placenta.

Trophoblasts, when they contact the uterine wall, begin to proliferate and invade the endometrium. Trophoblasts are biphasic and include cytotrophoblasts, which form the mitotically active inner cell layer, and syncytiotrophoblasts (which are a further differentiation of cytotrophoblasts) that form the outer layer, are not mitotically active, are frequently multinucleated, and actively invade the epithelium and underlying uterine stroma to facilitate implantation of the embryo.[8] Syncytiotrophoblasts secrete chorionic gonadotropin to support the CL and maintain the pregnancy in a sort of, "I'm still here and active, don't let me die," feedback loop.

Animals with a deciduate (meaning "falling off/shedding") uterus have a portion of the endometrium, primarily the antimesometrial portion, that undergoes morphologic changes that can be seen histologically. The maternal portion of the endometrium that undergoes these changes and ultimately tears away with the placenta is called the "decidua".[8] The decidua provides physical support, nutrition, immunological protection, and hormonal support to the developing embryo.[8] Species with a deciduate uterus include rabbits, humans, rodents, and non-human primates, and the histologic appearance of the decidual reaction varies between species.[3,7] Animals with a deciduate uterus shed their placenta at parturition and it includes all but the deepest layer of the endometrium. The process of decidualization involves stromal cells, also called "decidual cells", that become large and rounded in response to increased progesterone. There are three regions of the decidua named based on their relationship to the site of embryo implantation and include the decidua basalis (endometrium that underlies implantation site), the decidua capsularis (thin portion of the endometrium between the implantation site and the uterine lumen), and the decidua parietalis (the remaining endometrium of the uterus).

In the absence of pregnancy, a decidual reaction is thought to be a proliferative response of stromal endometrial cells that is histologically similar to decidual implantation sites. It is associated with pseudopregnancy and nonspecific physical stimuli. It requires both estrogen and progesterone to be present, and there must be some form of physical stimulus to induce the reaction.[2] In research, this can be done by scratching the endometrium and then supporting with estrogen and progesterone administration. In toxicological studies, the presence or absence of a decidual reaction is considered

a sensitive indicator of estrogenic or anti-estrogenic activity.[3,4,10]

References:

1. Blackburn DG, Osteen KG, Winfrey VP, Hoffman LH. Obplacental giant cells of the domestic rabbit: development, morphology, and intermediate filament composition. *J Morphol.* 1989;202:185-203.
2. Fischer B, Chavatte-Palmer P, Viebahn C, Navarrete Santos A, Duranthon V. Rabbit as a reproductive model for human health. *Reproduction*. 2012;144(1):1-10.
3. Furukawa K, Kuroda Y, Sugiyama A. A comparison of the histological structure of the placenta in experimental animals. *J Toxicol Pathol.* 2014;27:11-18.
4. Furukawa K, Tsuji N, Sugiyama A. Morphology and physiology of rat placenta for toxicological evaluation. *J Toxicol Pathol*. 2019;32:1-17.
5. Gnecco JS, Ding T, Smith C, Lu J, Bruner-Tran KL, Osteen KG. Hemodynamic forces enhance decidualization via endothelial-derived prostaglandin E2 and prostacyclin in a microfluidic model of the human endometrium. *Hum Reprod*. 2019;34(4):702-714.
6. Greaves P. Female genital tract. In: Histopathology of Preclinical Toxicity Studies: Interpretation and Relevance in Drug Safety Evaluation, 3rd ed., pp728-729. Elsevier, London, UK, 2007.
7. Kotera K. Histological observation of the chronological changes in the constituent zones of the rabbit placenta. *Jpn J Anim Reprod.* 1986;32: 69–77.
8. Schlafer DH, Foster RA. Female Genital System. In: Maxie MG, ed. Jubb, Kennedy & Palmer's Pathology of Domestic Animals. Vol 3. 6th ed. St. Louis, MO: Elsevier; 2016:358-464.
9. Yoshizawa K, Emoto Y, Kinoshita Y, Kimura A, Uehara N, et al. Histopathological and immunohistochemical characterization of spontaneously occurring uterine deciduomas in young adult rats. *J Toxicl Pathol.* 2013;26:61-66.
10. Zhang XK, Li X, Han XX, Sun DY, Wang YQ, Cao ZZ, Liu L, Meng ZH, Li GJ, Dong YJ, Li DY, Peng XQ, Zou HJ, Zhang D, Xu XF. Cadmium induces spontaneous abortion by impairing endometrial stromal cell decidualization. *Toxicology*. 2025;511:154069.

Joint Pathology Center
Veterinary Pathology Services

WEDNESDAY SLIDE CONFERENCE 2025-2026

Conference #13 — 26 November 2025

CASE I:

Signalment: 1.5-year-old male New Zealand white rabbit (*Oryctolagus cuniculus*)

History: This 1.5-year-old rabbit (R-857) was found dead in his cage on 4/25/2023. He was on a behavioral study with a high cholesterol diet. An autopsy was performed, and formalin fixed liver, heart, and kidney were submitted to the Michigan State University Veterinary Diagnostic Laboratory.

Gross Pathology: Veterinarian who performed the autopsy noted the liver was diffusely dark green and stomach contained food but was not distended.

Laboratory Results: Not applicable.

Microscopic Description: Approximately 60% of the hepatocytes in mostly periportal and centrilobular regions are markedly expanded by high numbers of microvesicular vacuolations (steatosis/lipid) and more rarely macrovesicular vacuolations or a mixture of the two. Sinusoids contain increased myofibroblasts (activated hepatic stellate cells) causing multifocal collapse of hepatocellular cord architecture. The myofibroblasts extend near portal areas, but distinct biliary hyperplasia is not appreciated. Occasionally hepatocytes are dissociated and composed of hypereosinophilic cytoplasm and lack a nucleus (necrosis). There are occasional binucleated hepatocytes. Canaliculi are multifocally, mildly expanded by tan

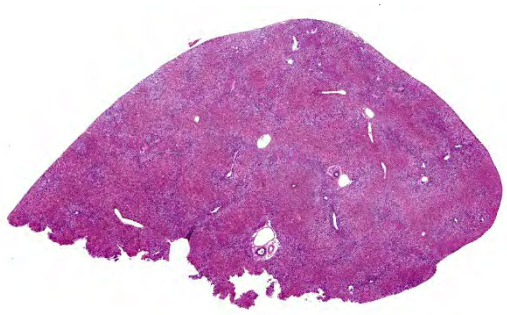

Liver, rabbit: One section of liver is submitted for examination. At subgross magnification, there are retiform patterns of pallor within the section. (HE, 21X)

to brown material (bile). Very rare lymphocytes are within sinusoids and in portal areas.

Contributor's Morphologic Diagnoses: Severe, chronic, multifocal to coalescing microvesicular and macrovesicular steatosis with sinusoidal fibrosis and cholestasis

Contributor's Comment: Hepatic steatosis or lipidosis is a common sequela to high cholesterol diets in rabbits, including New Zealand white rabbits.[6] Rabbits are highly susceptible to hypercholesterolemia and subsequent atherosclerosis and hepatic steatosis.[1,6] Hypercholesterolemia and hyperlipidemia also occur in rabbits affected by inflammatory processes and disease, without a high cholesterol diet.[9] In rabbits, hypercholesterolemia is accompanied by increased circulating very low-density lipoproteins (VLDL) and low-density lipoproteins (LDL).[1] The VLDL

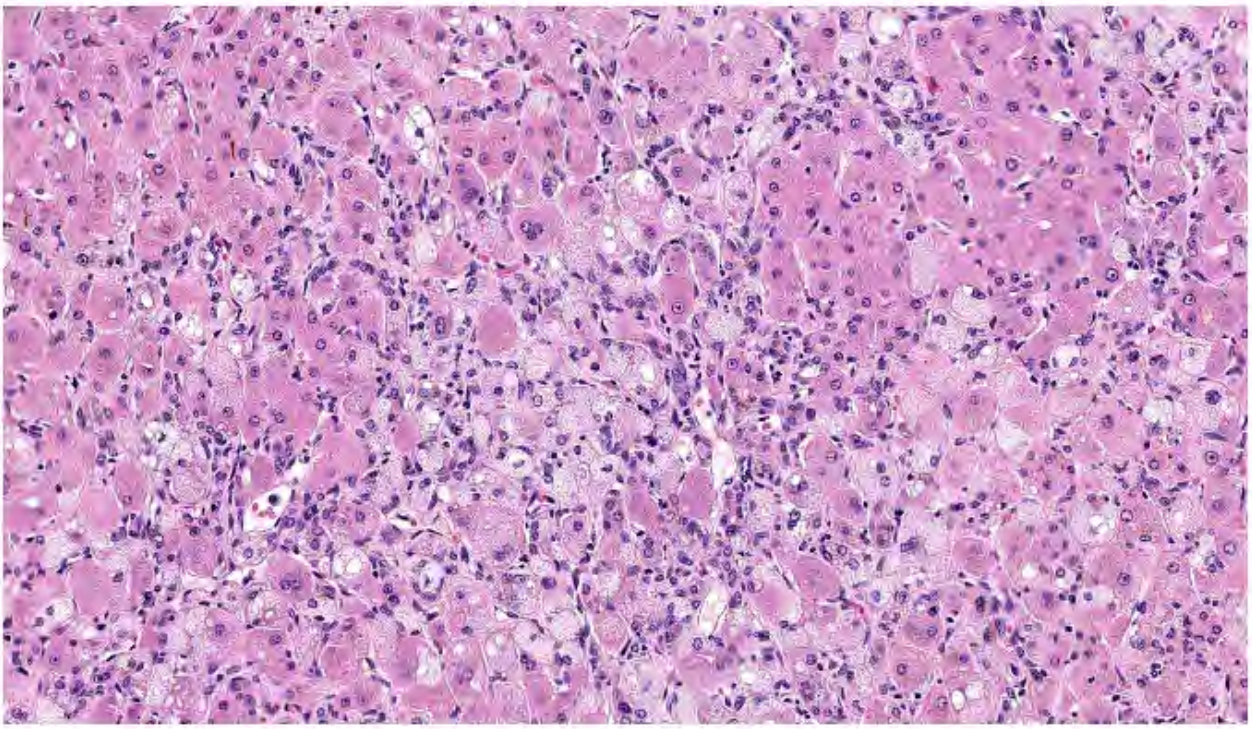

Liver, rabbit: There is diffuse loss of sinusoidal architecture. Within centrilobular and periportal areas of the lobule, hepatocytes are markedly swollen due to accumulation of vary ing sizes of lipid vacuoles within their cytoplasm. Hepatocytes are separated and surrounded by proliferating stellate cells and small amounts of collagen. (HE, 318X)

(specifically β- VLDL) lead to the lesions of atherosclerosis, and both VLDL and LDL are transported to and from hepatocytes via LDL receptors.[1,11] In rabbits and humans, hepatic steatosis can occur if cholesterol and triglycerides, in the form of VLDL and LDL, overload hepatocytes. In humans and animals with metabolic syndrome, ruminants, and cats, adipose tissue is broken down, releasing triglycerides or free fatty acids which go to the liver and similarly overload the hepatocytes.[3,11] Synthesis of VLDL in hepatocytes occurs in the endoplasmic reticulum (ER) and there is some mitochondrial oxidation normally. When overloaded, there can be ER stress and mitochondrial dysfunction associated with lipotoxic metabolites of fatty acids, thus leading to more steatosis.[5] Therefore, hepatic steatosis pathogenesis includes both the triglycerides themselves, as well as lipotoxic metabolites.

Steatosis occurs in a macrovesicular or microvesicular form. Macrovesicular steatosis is more often associated with hepatic lipidosis as seen in cats, ruminants, and animals with metabolic syndrome. Both macrovesicular and microvesicular steatosis are due to triglyceride accumulation. Microvesicular steatosis is also associated with mitochondrial dysfunction[4] and is most common in toxic hepatopathies, like Reye's syndrome in humans[3,4]. The mitochondrial dysfunction and lipotoxicity are likely why microvesicular steatosis has a poorer prognosis.

Hepatic steatosis in humans is referred to as non-alcoholic or metabolic dysfunction-associated fatty liver disease (NAFLD and MAFLD) and can lead to steatohepatitis (NASH or MASH)[7]. Metabolic dysfunction-associated steatohepatitis (MASH) is associated with steatosis, inflammation, hepatocellular degeneration, and fibrosis,

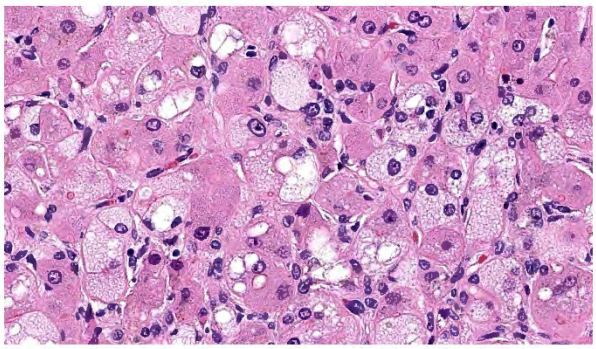

Liver, rabbit: Higher magnification of lipid-laden hepatocytes with small lipid vacuoles (microsteatosis) and larger lipid vacuoles (macrosteatosis). Hepatocytes often contain lipofuscin granules in their cytoplasm as well. Stellate cells proliferate along the sinusoids. (HE, 881X)

almost all clearly displayed in this rabbit and in a rabbit model[2]. This rabbit and humans with MASH often also have concurrent hypercholesterolemia and atherosclerosis[2].

The liver histopathology in this case also provided opportunity to review the classic lesions of liver repair. One group of progenitor cells in the liver (also termed oval cells in rodents) is located within the canals of Hering. When the liver is damaged, these cells are activated and lead to histopathologic "biliary duct hyperplasia", "ductular reaction", or "oval cell activation"[8]. In addition to this population of progenitor cells are hepatic stellate cells. Hepatic stellate cells reside in the space of Disse along the sinusoids and are activated from relatively quiescent cells into myofibroblasts when there is liver damage[3,8]. This case highlights early fibrosis within the sinusoids or space of Disse due to activation of hepatic stellate cells.

Contributing Institution:
Michigan State University Veterinary Diagnostic Laboratory
4125 Beaumont Road
Lansing, MI 48910-8104
https://cvm.msu.edu/vdl

JPC Diagnoses: Liver: Hepatocellular micro- and macrovesicular lipidosis, chronic, multifocal to coalescing, severe, with marked stellate cell hyperplasia and cholestasis.

JPC Comment: Conference 13 was moderated by the Dr. Louis Huzella, a previous graduate of this program during the AFIP years. As his conference was held the day before the Thanksgiving holiday here in the U.S., he selected cases that he felt were loosely in keeping with that theme. This made for an enjoyable and light-hearted conference to with which to wrap up the 2025 conferences.

The contributor in this case provided a well-thought and informative writeup of hepatic lipidosis and hyperlipidemia, and much of what was discussed in conference is covered in their comment. Conference participants were, for the most part, readily able to achieve the reach the correct morphologic diagnosis in this case, but there was some speculation on the origin of the hyperplastic spindle cell population on the H&E. As mentioned by the contributor, there are two main possibilities: oval cells or stellate cells. Oval cells are bipotential progenitors of both hepatocytes and biliary ductular epithelial cells. Hepatic stellate cells, also called Ito

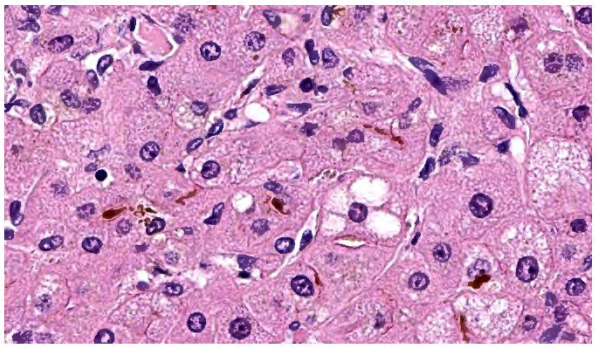

Liver, rabbit: Bile canaliculi are often expanded with bile. (HE, 921X)

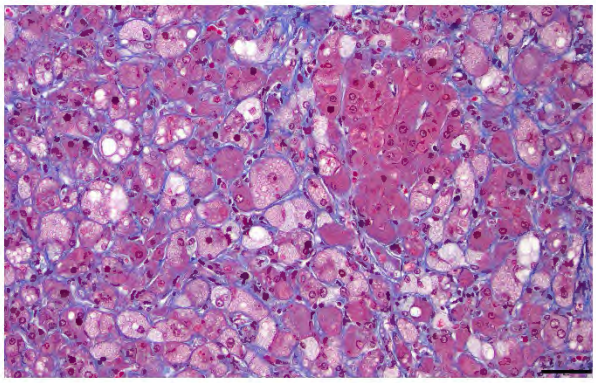

Liver, rabbit: A Masson's trichrome demonstrates the fibrous connective tissue lining sinusoids and surrounding occasional hepatocytes. (Masson's trichrome, 200X). (Photo courtesy of: Michigan State University Veterinary Diagnostic Laboratory, https:/cvm.msu.edu/vdl)

cells, live primarily in the space of Disse, store Vitamin A, and can be activated into myofibroblasts following injury that will produce connective tissue components.[3,8] Participants wondered if there was both oval cell and stellate cell hyperplasia in this case due to the presence of mild ductular reaction, cholestasis, and fibrosis, but unanimously agreed that there was at least stellate cell activation due to the fibrosis highlighted by a Masson's trichrome. This is a difficult distinction to make on H&E alone.

Of laboratory animal species, rabbits are more similar to humans in lipoprotein metabolism, atherosclerosis, and myocardial function than are rats and mice.[10] The Watanabe heritable hyperlipidemic (WHHL) rabbit is a specific strain of New Zealand White rabbit that was developed in Japan and is used as an animal model of familial hypercholesterolemia. Within the WHHL strain, there are two additional advanced strains used for specific hyperlipidemia-related diseases processes and include the coronary atherosclerosis-prone WHHL rabbit and the myocardial infarction-prone WHHL rabbit.[10] Hypercholesterolemia in the WHHL rabbit family is due to reduced LDL uptake by the liver.[10] Watanabe rabbits have played an important role in advancing these research areas and enabling a better understanding of these diseases in humans and animals alike. Additionally, studies in Watanabe rabbits have led to the development of a number of statins, which are inhibitors of cholesterol biosynthesis, to help treat hypercholesterolemia in humans.[10]

References:

1. Fan J, Kitajima S, Watanabe T, et al.. Rabbit models for the study of human atherosclerosis: from pathophysiological mechanisms to translational medicine. *Pharmacol Ther*. 2015;146:104-119.
2. Hayashi M, Kuwabara Y, Ito K, et al. Development of the Rabbit NASH Model Resembling Human NASH and Atherosclerosis. *Biomedicines*. 2023;11(2):384.
3. Maxie MG. Jubb, Kennedy, and Palmer's pathology of domestic animals Pathology of domestic animals). St. Louis, Missouri: Elsevier, 2016.
4. Natarajan SK, Eapen CE, Pullimood AB, Balasubramanian KA. Oxidative stress in experimental liver microvesicular steatosis: role of mitochondria and peroxisomes. *J Gastroenterol Hepatol*. 2006;21:1240-1249.
5. Neuschwander-Tetri BA. Hepatic lipotoxicity and the pathogenesis of nonalcoholic steatohepatitis: the central role of nontriglyceride fatty acid metabolites. *Hepatology*. 2010;52:774-788.
6. Percy DH, Barthold SW, Griffey SM. Pathology of laboratory rodents and rabbits. Ames, Iowa: John Wiley & Sons, Inc., 2016.
7. Pipitone RM, Ciccioli C, Infantino G, et al. MAFLD: a multisystem disease.

Ther Adv Endocrinol Metab. 2023;14:20420188221145549.
8. Roskams T. Relationships among stellate cell activation, progenitor cells, and hepatic regeneration. *Clin Liver Dis*. 2008;12:853-860,ix.
9. Sharma D, Hill AE, Christopher MM. Hypercholesterolemia and hypertriglyceridemia as biochemical markers of disease in companion rabbits. *Vet Clin Pathol.* 2018;47:589-602.
10. Shiomi M. The History of the WHHL Rabbit, an Animal Model of Familial Hypercholesterolemia (I) - Contribution to the Elucidation of the Pathophysiology of Human Hypercholesterolemia and Coronary Heart Disease. *J Atheroscler Thromb*. 2020;27(2):105-118.
11. Zhou F, Sun X. Cholesterol Metabolism: A Double-Edged Sword in Hepatocellular Carcinoma. *Frontiers in Cell and Developmental Biology.* 2021;9.

CASE II:

Signalment: Necropsy was performed on two male castrated pre-fattening pigs each of about 25 kg body weight (*Sus scrofa domesticus*).

History: The owner reported an increased mortality rate in a herd of pre-fattening pigs. Clinically affected animals showed yellowish to greyish, watery diarrhea with a sudden worsening of their general condition before they died spontaneously.

Gross Pathology: Both animals were in a moderate nutritional condition and showed severely sunk bulbi (dehydration). Multifocal to coalescing, yellowish, not removable plaques (fibrin) were observed on the mucosa of the stomach. The large intestine contained brown, fluid material and the mucosa of cecum and colon ascendens was multifocally to coalescing covered with yellowish, not removable plaques (fibrin/necrosis). The fibrin strands and necrotic areas were sometimes associated with the lymphatic tissue and band-like or sometimes appeared button-shaped. The rectum was empty.

Colon: Fibrinonecrotic plaques, both linear and button-shaped, are scattered throughout the colon. (Photo courtesy of: Institute of Veterinary Pathology, Vetsuisse-Faculty (University of Zurich), www.vetpathology.uzh.ch)

Laboratory Results: The bacteriological examination (culture) revealed the following result: *Salmonella enterica subsp. enterica serovar Typhimurium*

Microscopic Description: Large intestine (Colon ascendens): Multifocal to coalescing, a thick layer of fibrin, sometimes intermingled with degenerated neutrophils, and abundant coccoid to rod-shaped bacteria are attached to the mucosa. In these areas, the mucosa is diffusely destroyed (necrosis) and replaced by fibrin, cell debris and fewer coccoid to rod-shaped bacteria. The lamina propria and the submucosa show a moderate infiltration with neutrophils as well as fewer lymphocytes and histiocytes. The few remaining crypts are dilated and some of them contain neutrophils and cell debris. Some capillaries and venules contain fibrin thrombi or are dilated and filled with neutrophils.

Colon and colonic lymph nodes: At subgross magnification, there is pallor of the colonic mucosa. Within the colonic lymph nodes, there are no apparent germinal centers as well as a diminished paracortex. (HE, 17X)

Mandibular lymph node: Lymphoid follicles are indistinct as a result of a severe lymphocyte depletion and replacement by aggregates of epithelioid macrophages with abundant eosinophilic cytoplasm.

Immunohistochemistry examination: Immunohistochemistry using an antibody directed against PCV-2 antigen revealed positive labeling in the cytoplasm of the epithelioid macrophages.

Contributor's Morphologic Diagnoses:
Large intestine: fibrinous to necrotizing enteritis, severe, chronic, multifocal to coalescing

Mandibular lymph node: granulomatous lymphadenitis, mild, multifocal, with lymphoid depletion

Contributor's Comment: *Salmonella* spp. are gram-negative, aerobic or facultative anaerobic and motile bacteria. The route of bacterial entry is mostly fecal-oral. The bacteria are mainly detected in contaminated food, water and aerosols but flies and fomites can also act as transmission sources. Furthermore, transplacental infection is also possible. Salmonellosis is an important zoonotic disease and all known species are pathogenic. It is a significant cause of acute and chronic

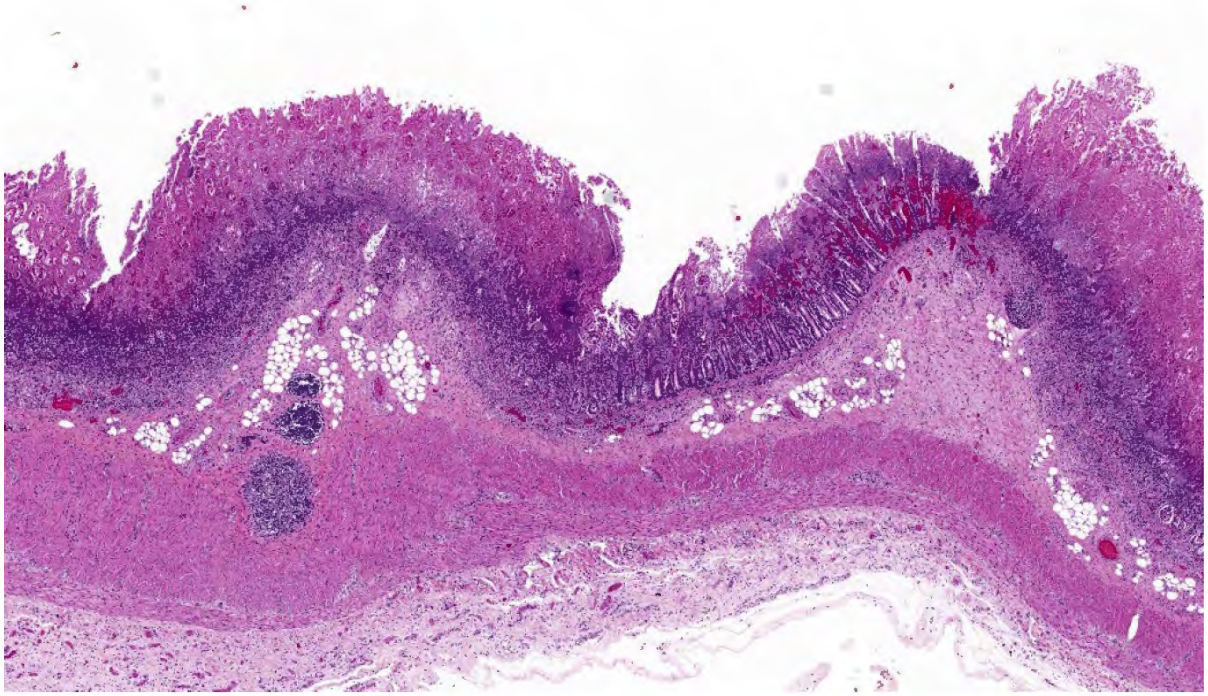

Colon, pig: There is partial to full-thickness necrosis of the colonic mucosa, multifocal hemorrhage, and depleted Peyer's patches. (HE, 47X)

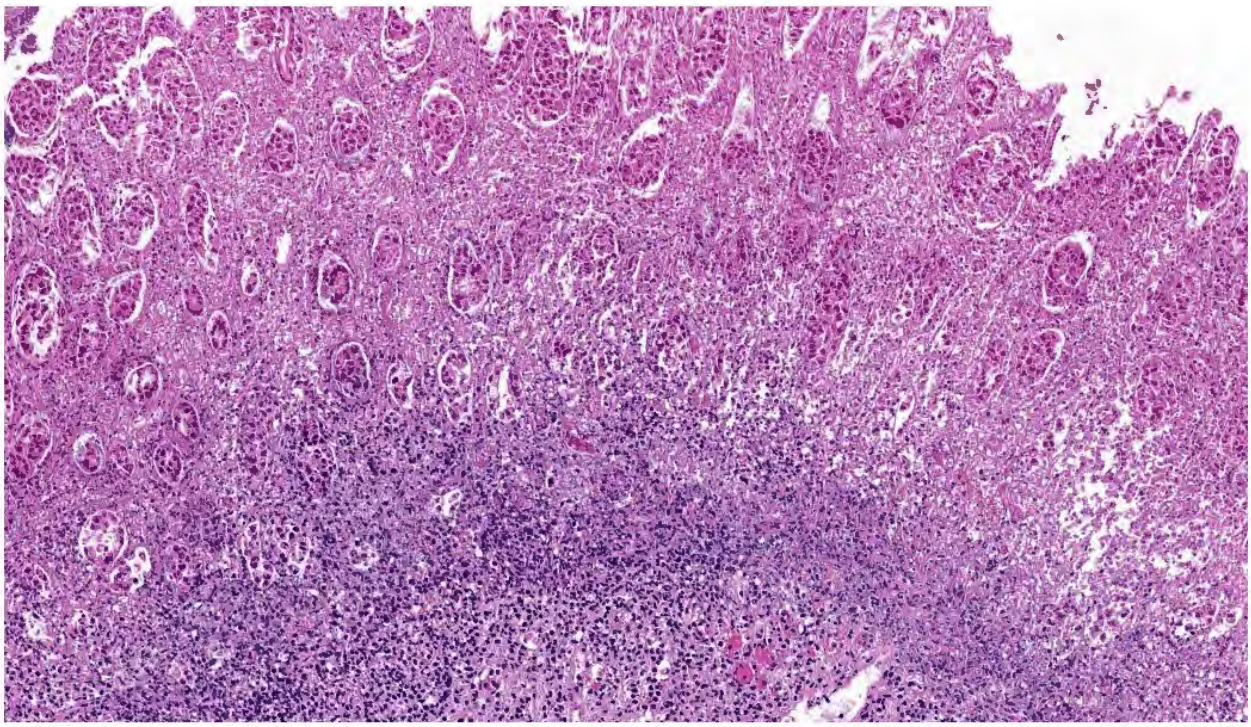

Colon, pig: There is coagulative necrosis of the superficial mucosa and lytic necrosis of the deep mucosa which effaces the muscularis mucosa and extends into the underlying submucosa (HE, 227X).

diarrhea and might even result in death of animals or humans. The most commonly isolated serovars in animals are *Salmonella Typhimurium, Salmonella Enterica, Salmonella Dublin, Salmonella Choleraesuis and Salmonella Typhosa*. Three forms of salmonellosis are reported: septicemic, acute enteric and chronic enteric. Which form occurs is depending on many factors such as infectious dose, previous exposure to the bacterium and stress (overcrowding, transport, cold temperatures, feed changes, pregnancy, parturition, surgery, anesthesia, antibiotic administration). It is possible that some of the recovered animals become carriers shedding the organism in their feces for at least 3-5 months.

Salmonella septicemia: The peracute Salmonella septicemia occurs in calves, foals and pigs and is mostly fatal. Younger animals get more frequently infected. This form of disease is usually caused by *Salmonella Choleraesuis*. Gross lesions are minimal or can present as fibrinous polyserositis and fibrinoid necrosis of blood vessels with microvascular thrombosis, which results in extensive petechiation and a blue discoloration of the extremities, ventrum, ears and tail in pigs due to endotoxemia. Furthermore, petechial hemorrhages can develop in many organs and tissues.

Acute enteric salmonellosis: The acute enteric form occurs in cattle, pigs, horses and rarely carnivores and is most frequently caused by *Salmonella Typhimurium*. A catarrhal enteritis with focal to diffuse fibrinonecrotic ileotyphlocolitis is the characteristic sign; the intestine is filled with mucus, fibrin, and occasionally blood. Moreover, multifocal hepatocellular necrosis, mesenteric lymphadenopathy and fibrinous cholecystitis are pathognomonic for the acute enteric salmonellosis.

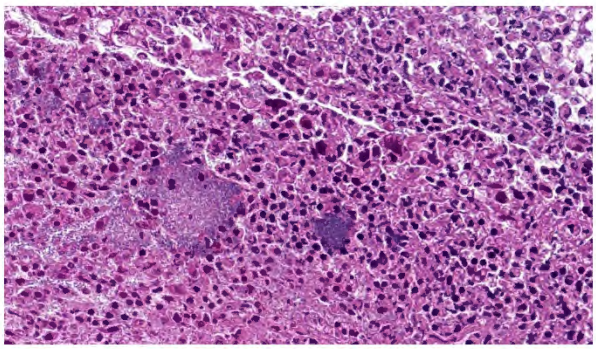

Colon, pig: There are scattered colonies of coccobacilli within the necrotic mucosa. (HE, 960X).

Chronic enteric salmonellosis: The chronic form occurs in pigs, cattle and horses. Multiple necrotizing and ulcerated foci are commonly seen in the cecum, colon and rectum ("button ulcers") of pigs. Rectal strictures can develop due to vascular thrombosis caused by the infection.

The co-infection with PCV-2 in this case is interpreted as an underlying disease leading to an immunosuppression and rendering the pigs more susceptible for secondary bacterial infection, in this case *Salmonella enterica* subsp. *enterica* Serovar t*yphimurium.*

Contributing Institution:

Institute of Veterinary Pathology
Vetsuisse-Faculty (University of Zurich)
Winterthurerstrasse 268, CH-8057 Zurich
www.vetpathology.uzh.ch

JPC Morphologic Diagnosis:

1. Colon: Colitis, necrotizing, subacute, diffuse, severe, with Peyer's patch depletion and numerous coccobacilli.
2. Lymph nodes: Lymphoid depletion, diffuse, severe.

JPC Comment:

What a fantastic case this is! It highlights some of the classic GI lesions in a severe case of salmonellosis, and the degree of lymphoid depletion present in both the GI-associated lymphoid tissue and the mandibular lymph nodes were excellent clues for the pathologist to suspect a primary cause of immune suppression as well. Many thanks to the contributor for providing this highly educational case to the WSC!

Due to the degree of necrosis and inflammationin the submitted section of colon. some participants had difficulty deciding in which segment of the GI tract this sample originated. The presence of occasional intact crypts and multiple lymphoid follicles were helpful in establishing an anatomic location of "intestine" (remember, there are no lymphoid follicles in the stomach except in severe cases of *Helicobacter spp* infection in some species), but it can be challenging to get further than "intestine" when a section is as inflamed and necrotic as the tissue is in this case.

There was discussion on the difference between lymphoid necrosis and lymphoid depletion, the former of which implies active targeting of lymphocytes while the latter can be an aftermath of lymphoid necrosis or can be a separate process secondary to any number of pathogeneses (i.e. SCID). The target cell for porcine circovirus-2 is macrophages, and a classic case of PCV-2 may result in

Colonic lymph nodes, pig: Colonic lymph nodes are markedly depleted, with no germinal centers and a sparse paracortex. (HE, 13X)

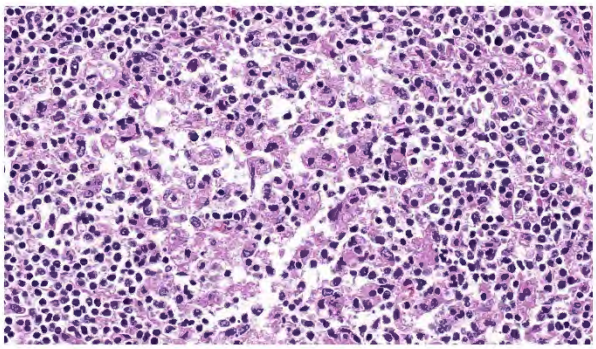

Colonic lymph nodes, pig: There are small aggregates of macrophages scattered throughout the nodes. (HE, 720X)

granulomatous lymphadenitis, an unusual result of most viral infections. Lymphocytes are not directly targeted in the pathogenesis of PCV-2 but are rather secondary victims to the inflammation from immune response to the virus, making this case a great example of lymphoid depletion. This is further exacerbated in cases of secondary bacterial infection when the offending bacteria colonize Peyer's patches, which is an important step in the pathogenesis of enteric salmonellosis.

Porcine circovirus-2 is a bit of a catch-all virus in that it causes a wide variety of clinical signs in affected pigs. It should *always* be on the differential list for sick pigs due to the many ways it manifests. PCV-2 is widely distributed in domestic pigs and wild boars, and has also been isolated from cattle, dogs, deer, chamois, mice, and various arthropods (i.e., ticks and mosquitoes). PCV-2 infection in swine can be either subclinical or cause numerous forms of illness that are collectively referred to as "PCV-associated diseases" (PCVAD). These includes post-weaning multisystemic wasting syndrome (PMWS), porcine respiratory disease complex, porcine dermatitis and nephropathy syndrome, and both reproductive and enteric diseases.[1] The immunosuppression associated with PCV-2 is characterized by lymphopenia, lymphoid cell (both B and T cell) depletion, and altered cytokine production.[1] Because of its immunosuppressive effects, PCV-2 is frequently diagnosed concurrently with various other pathogens, and these combinations often provoke more severe disease together than they would individually, as seen in this case with concurrent salmonellosis.

During the initial phase of enteric *Salmonella* infection, the bacteria invades intestinal epithelial cells by employing an SPI-1 Type III secretion system (T3SS). This induces alterations in intestinal folds and in actin structures of the intestinal epithelial cells, facilitating the uptake of *Salmonella* by these non-phagocytic cells.[4] Alternatively, *Salmonella* can invade M cells that cover Peyer's patches, enabling entry into lymphoid follicles.[4] From here, the bacteria are taken up by phagocytes such as dendritic cells and macrophages. Upon internalization by these cells, Salmonella forms its own specialized membrane-bound blebs known as "*Salmonella*-containing vacuoles" (SCVs). Once within these vacuoles, the expression of SPI-1 T3SS is down-regulated and the SPI-2 T3SS is up-regulated.[4] Where the SPI-1 system facilitates entry into host cells, the SPI-2 system promotes survivability and replication of the bacteria within host cells. Within these vacuoles, the bacteria can also deliver various effector proteins into the cytoplasm of phagocytes, triggering caspase-1 activation and subsequent apoptosis.[4] The lysis of these cells releases additional *Salmonella* bacteria into the host, further perpetuating infection.

Lastly, there was brief discussion during conference on host-adapted vs non-host-adapted *Salmonella* spp. and the histologic clues that may key the pathologist in to suspecting one versus the other - of course, morphology is not definitive, and culture and PCR are required for confirmation. That being said, the

targeting of blood vessels is a feature seen most often with host-adapted *Salmonella* infections (*S. cholerasuis* and *S. typhisuis* in swine). This feature is not generally seen in non-host-adapted *Salmonella* infections (*S. typhimurium,* as in this case, does not target vessels, and causes a necrotizing enterocolitis, as it does in many other mammalian species). All *Salmonella* spp. in swine will target lymphoid tissues as part of their pathogenesis. Wrapping up this case discussion was a quick reminder of the orientation of porcine lymph nodes…remember, they are "inside-out"; the medulla is on the outside!

References:

1. Fehér E, Jakab F, Bányai K. Mechanisms of circovirus immunosuppression and pathogenesis with a focus on porcine circovirus 2: a review. *Vet Q*. 2023;43(1):1-18.
2. Jubb, Kennedy, Palmer`s. Pathology of Domestic Animals. Volume 2. Sixth edition. St. Louis, Elsevier; 2016.
3. Zachary JF, McGavin MD. Pathologic Basis of Veterinary Disease. Fifth edition. St. Louis, MO:Elsevier Mosby; 2012.
4. Zhang Y, Xu M, Guo Y, Chen L, Vongsangnak W, Xu Q, Lu L. Programmed cell death and *Salmonella* pathogenesis: an interactive overview. *Front Microbiol*. 2024;14:1333500.

CASE III:

Signalment: A juvenile (<1 year old), male bald eagle (*Haliaeetus leucocephalus*)

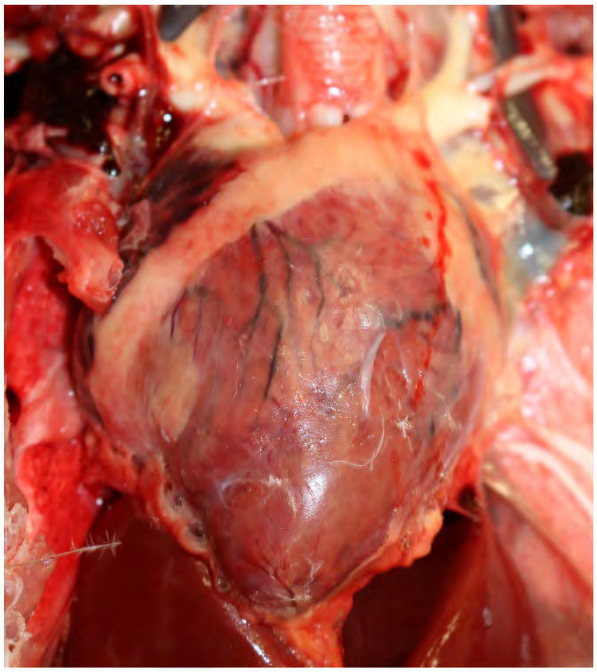

Heart, bald eagle: There are multifocal areas of pallor within the myocardium and a small amount of fibrin on the epicardium. (Photo courtesy of: University of Connecticut, Connecticut Veterinary Medical Diagnostic Laboratory, https://cvmdl.uconn.edu/)

History: The eagle was admitted to a local raptor rehabilitation center in Connecticut two days before death, The bird was reported to be 10% dehydrated, showing neurologic signs including seizures and ventral flexion of the neck. The lead level was 4 ug/dL. The eagle received subcutaneous fluid therapy of unreported volume every six hours. The eagle was fed with quail once with assistance but regurgitated all the stomach contents afterward. The eagle was found deceased in the cage on the day of the necropsy submission.

Gross Pathology: This eagle was in adequate nutritional condition, with intra-coelomic adipose stores. A small amount (2-3 mL) of mildly greenish seromucous nasal fluid was discharged from the nostrils, along with two bright red threadlike, 1 cm-long nematodes. The myocardium had multifocal pale areas.

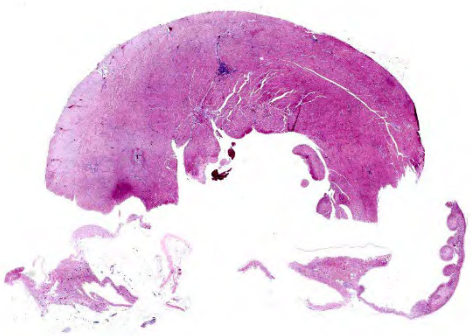

Heart, bald eagle. Three sections of heart, to include both ventricles and the interventricular septum. At subgross magnification, several foci of inflammation are visible in the myocardium. (HE, 15X)

Laboratory Results: Frozen brain tissue was positive for West Nile virus via real-time quantitative polymerase chain reaction (qPCR) performed by the Connecticut Veterinary Medical Diagnostic Laboratory. A cloacal swab sample was submitted for avian influenza virus (IAV) testing via PCR, and the result was not detected.

Microscopic Description: Heart: Multifocally infiltrating the myocardial interstitium are small to moderate numbers of lymphocytes, histiocytes, and fewer heterophils admixed with scattered cell debris. Adjacent cardiomyocytes are fragmented with loss of cross striation (myocardial necrosis). Occasionally, the myocardium contains protozoal cysts measuring up to 70 x 20 µm, containing numerous bradyzoites.

Contributor's Morphologic Diagnosis:

Lymphohistiocytic myocarditis, multifocal, moderate, with myocardial necrosis and protozoal cysts, heart.

Contributor's Comment: Additional histologic findings in this case included lymphohistiocytic encephalitis with perivascular cuffing. The histopathological findings in the heart and the brain are consistent with West Nile virus (WNV) infection, confirmed by the molecular testing of frozen brain tissue via qPCR. West Nile virus is an arthropod-borne, enveloped RNA virus of the family Flaviviridae, genus Flavivirus. The virus is primarily transmitted by mosquitoes, but direct contact with infected animals and via oral uptake of virus-infected tissues have also been reported.[1,3] WNV causes fatal diseases in humans, horses, and a wide variety of birds, including bald eagles.[7] Gross lesions caused by WNV in bald eagles included bilaterally symmetrical cerebral pan-necrosis with hydrocephalus ex vacuo, retinal scarring, myocardial pallor, and rounded heart apex.[7] Histologic lesions included lymphoplasmacytic encephalitis, myocarditis, pectenitis, and choroiditis.[7] Diagnosis of WNV requires a combination of detection of viral antigen and/or RNA or virus-specific antibodies in the cerebrospinal fluid.

Differential diagnoses for the protozoa observed in the cardiomyocytes included *Sarcocystis* and *Toxoplasma*. Protozoal encephalitis seemed to be unlikely based on the absence of protozoal organisms in the H&E-stained sections, although the co-existence of protozoal encephalitis cannot be ruled out entirely in this case.

The histological characteristics of the nematode in the trachea are consistent with tracheal worm (*Syngamus trachea*), and this finding is considered incidental in this case.

Contributing Institution:
University of Connecticut Veterinary Diagnostic Laboratory
61 N Eagleville Rd (yes, Eagleville), Storrs, CT 06269

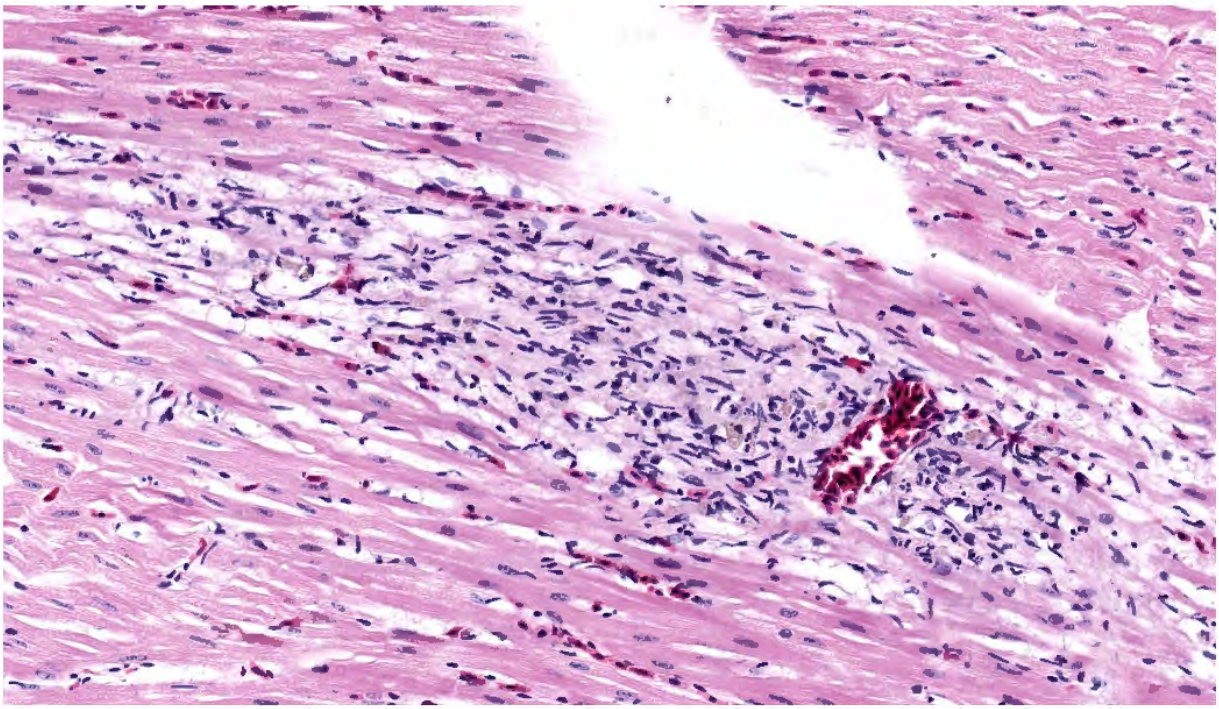

Heart, bald eagle. There are areas of myocardial necrosis and loss with infiltration of low to moderate numbers of macrophages and heterophils admixed with few siderophages edema and cellular debris. Cardiomyocytes are lost in this region – remnant cardiomyocytes are markedly shrunken and occasionally demonstrate karyorrhexis. There is hypertrophy of interstitial cell and fibroblast nuclei. (HE, 459X)

JPC Morphologic Diagnosis:

1. Heart: Myocarditis, lymphoplasmacytic and histiocytic, chronic, multifocal, moderate, with cardiomyocyte necrosis.
2. Heart, cardiomyocytes: Intrasarcoplasmic apicomplexan schizonts, multiple.

JPC Comment: This case was challenging due to the subtlety of the myocardial necrosis, but conference participants astutely managed to come up with a reasonable list of differentials, all of which must be considered in cases of myocardial necrosis in Bald eagles: lead toxicosis, highly pathogenic avian influenza (HPAI), and West Nile virus (WNV). All participants basically waved "Hello", to the protozoal bradyzoites in the myocardium and drove on, realizing that, although fun to look at, they were likely not the cause of this bird's lesions and are a common finding in wild avians.

WNV was first isolated in Uganda in 1937 but did not rise to notoriety until its relatively recent spread throughout Europe and the Americans.[2] Within the US, WNV broke onto the scene in the summer of 1999 in New York City as an unknown cause of high mortality in bird populations and an encephalitis of unknown origin in horses.[5] These cases in animals preceded the disease in humans, which ultimately resulted in 62 deaths in this initial outbreak. From the US outbreak, WNV spread to Canada and Mexico, where it was identified in both countries in 2002. WNV continues to cause occasional outbreaks with severe neurological disease in both humans and horses, and is maintained in the environment predominantly within wild bird and mosquito populations.[2,5]

Birds are the main vertebrate hosts of WNV.[2,5] They are usually asymptomatic, but

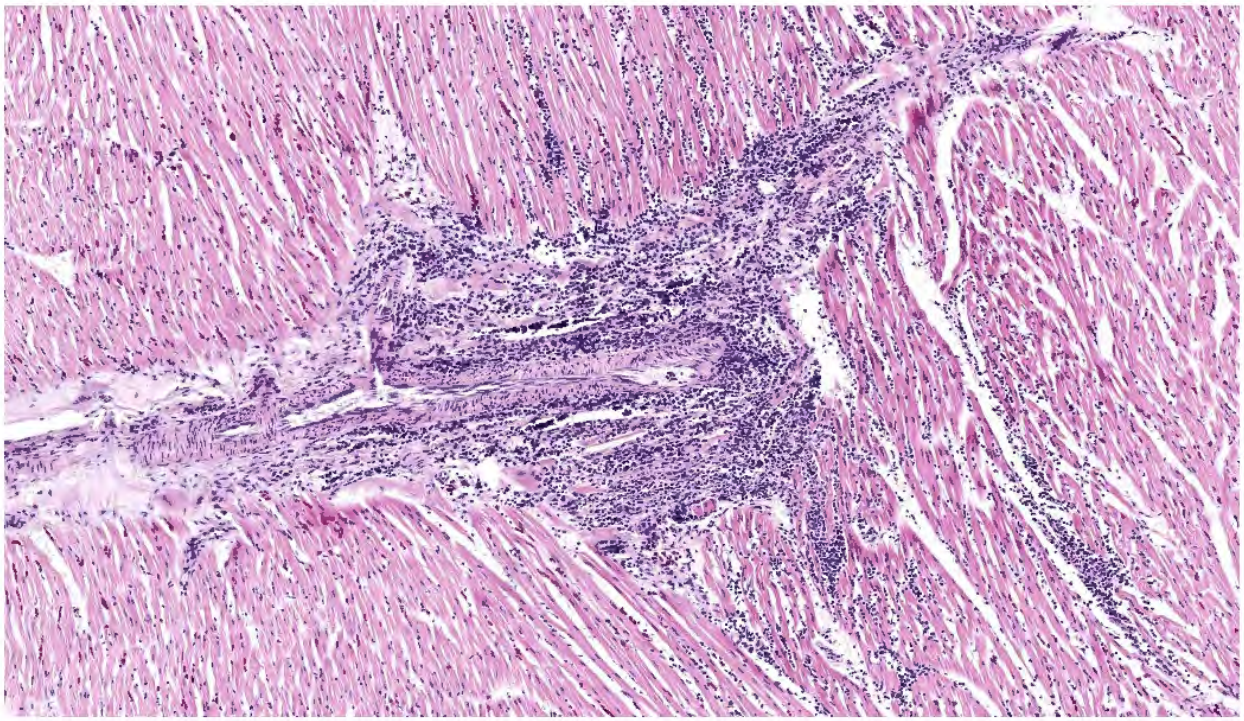

Heart, bald eagle. There is profound periarterial inflammation in one area of the left ventricle, with macrophages, lymphocytes and plasma cells extending into the adjacent myocardium. In areas in which the inflammation extends, there is degeneration and necrosis of cardimyocytes. (HE, 172X)

if clinical signs do manifest, they most commonly include ruffled feathers, lethargy, difficulty moving, and loss of appetite that can be severe enough to cause emaciation. Affected birds may also have profuse oronasal secretions, dehydration, head tremors, and/or seizures.[5] Death of infected birds typically occurs within 24hrs of the onset of clinical signs. Of bird species, corvids are exquisitely susceptible to WNV and the only sign of infection may be that they drop dead out of the sky. Histologically, the most common lesion of WNV in birds is necrosis +/- hemorrhages and the most frequently affected organs are the brain, liver, heart, kidney, and spleen.[5] There may also be ocular lesions (i.e., neuritis, retinal inflammation, iris degeneration) that can result in clinical blindness.[5]

Circling back to the two other primary differentials to consider in this case, the histologic lesions in this case are less consistent with lead toxicosis, but blood lead levels should be considered in any case of this nature. Histologic lesions of lead toxicity in bald eagles are those of a primary vascular injury and are classically characterized by fibrinoid necrosis of small to medium-caliber arteries in the heart, brain, and eyes.[4] Blood lead concentrations greater than 4ppm are associated with a higher likelihood of cardiac lesions in bald eagles.[4] In cases of HPAI in bald eagles, gross and histologic lesions are similar to those seen in WNV and PCR is required to achieve definitive diagnosis. Histologic lesions of HPAI in bald eagles include a leukocytoclastic and fibrinoid vasculitis, as well as necrotizing and hemorrhagic encephalitis, myocarditis, pancreatitis, adrenalitis, histiocytic splenitis, and anterior uveitis.[6]

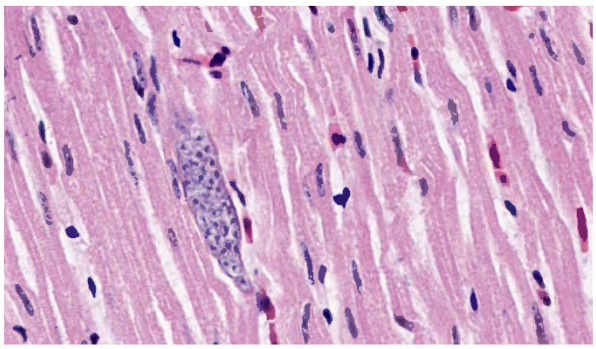

Heart, bald eagle. Multifocally, cardiomyocytes contain numerous round 2um zoites (HE, 1800X)

References:

1. Banet-Noach C, Simanov L, Malkinson M. Direct (nonvector) transmission of West Nile virus in geese. *Avian Pathol.* 2003;32:489–494.
2. Donadieu E, Bahuon C, Lowenski S, Zientara S, Coulpier M, Lecollinet S. Differential virulence and pathogenesis of West Nile viruses. *Viruses*. 2013;5(11):2856-80.
3. Komar N, Langevin S, Hinten S, et al. Experimental infection of North American birds with the New York 1999 strain of West Nile virus. *Emerg Infect Dis.* 2003;9:311–322.
4. Manning LK, Wünschmann A, Armién AG, Willette M, MacAulay K, Bender JB, Buchweitz JP, Redig P. Lead Intoxication in Free-Ranging Bald Eagles (Haliaeetus leucocephalus). *Vet Pathol.* 2019;56(2):289-299.
5. Saiz JC, Martín-Acebes MA, Blázquez AB, Escribano-Romero E, Poderoso T, Jiménez de Oya N. Pathogenicity and virulence of West Nile virus revisited eight decades after its first isolation. *Virulence*. 2021;12(1):1145-1173.
6. Wünschmann A, Franzen-Klein D, Torchetti M, Confeld M, Carstensen M, Hall V. Lesions and viral antigen distribution in bald eagles, red-tailed hawks, and great horned owls naturally infected with H5N1 clade 2.3.4.4b highly pathogenic avian influenza virus. *Vet Pathol.* 2024;61(3):410-420.
7. Wünschmann A, Timurkaan N, Armien AG, et al. Clinical, pathological, and immunohistochemical findings in bald eagles (*Haliaeetus leucocephalus*) and golden eagles (*Aquila chrysaetos*) naturally infected with West Nile virus. *J Vet Diagn Invest.* 2014;26:599–609.

CASE IV:

Signalment: Adult, female, *Antigone canadensis*, greater sandhill crane

History: Two lesser snow geese and two greater sandhill cranes were submitted for postmortem examination to investigate the

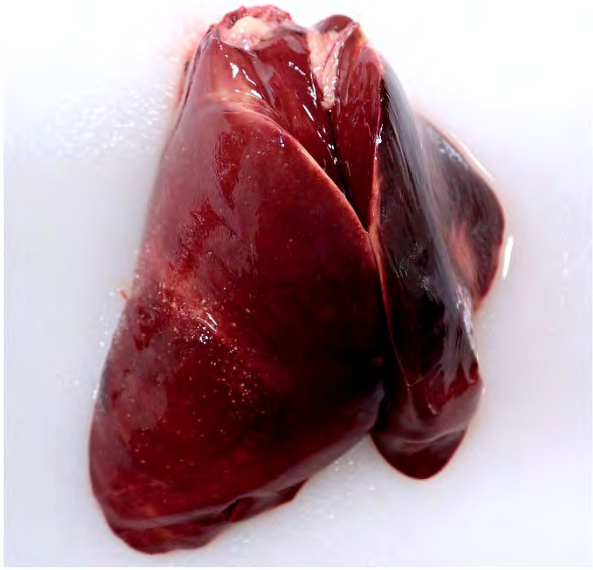

Liver, sandhill crane. The liver was enlarged, congested, and contained numerous random pinpoint tan foci. (Photo courtesy of: New Mexico Department of Agriculture Veterinary Diagnostic Services, https://nmdeptag.nmsu.edu/labs/veterinary-diagnostic-services.html

Spleen, sandhill crane. The spleen was enlarged and contained numerous coalescing pinpoint tan foci. (Photo courtesy of: New Mexico Department of Agriculture Veterinary Diagnostic Services, https://nmdeptag.nmsu.edu/labs/veterinary-diagnostic-services.html

death of at least 30 birds that included a variety of duck species, lesser snow geese and greater sandhill cranes at a waterfowl management area.

Gross Pathology: The crane was in good body condition and with minimal postmortem decomposition. The liver was enlarged, congested, and contained numerous random pinpoint tan foci. The spleen was enlarged and contained numerous coalescing pinpoint tan foci.

Laboratory Results

Pasteurella multocida was isolated from the liver and spleen.

PCR testing was negative for avian influenza virus and avian paramyxovirus.

Microscopic Description: The liver has multiple random foci of necrosis that are filled with necrotic debris, fibrin, variable numbers of intact and degenerate heterophils and macrophages, and variable numbers of Gram-negative coccobacilli. There are multiple sinusoids that contain coccobacilli with small numbers of sinusoids that contain fibrin thrombi. The hepatocytes adjacent to the sinusoids with fibrin thrombi are often necrotic. There are small numbers of perivascular aggregates of lymphocytes.

Contributor's Morphologic Diagnosis:

Liver – Hepatitis, necrotizing, heterophilic and histiocytic, random, multifocal with intralesional and intravascular Gram-negative coccobacilli and sinusoidal fibrin thrombi; etiology *Pasteurella multocida*.

Contributor's Comment: Fowl cholera is a disease of birds caused by the Gram-negative rod-shaped bacterium *Pasteurella multocida*.[3,4,6,7,8] The bacterium is known to infect numerous species of birds including but not limited to domestic poultry, wild waterfowl, birds of prey, and birds in zoological collections. Fowl cholera typically occurs as an acute fatal respiratory and septicemic disease with death occurring within 24-48 hours. Chronic and even benign infections with *P. multocida* can occur. Of the domestic poultry, turkeys are more susceptible to infection with *P. multocida* than chickens.[4,7] Adult chickens are most susceptible to infection with *P. multocida* that young chickens.[4,7] Among wild birds, outbreaks of fowl cholera typically occur in North American waterfowl in wetlands or nesting areas.[3,6,8]

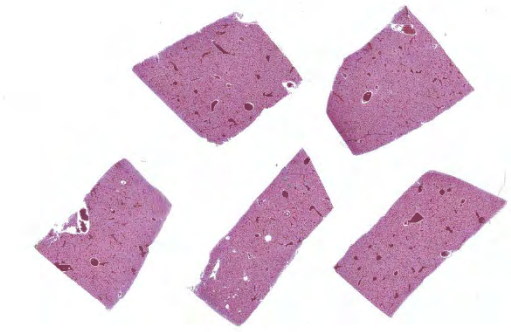

Liver, sandhill crane. Multiple sections of liver are submitted for examination. (HE, 10X)

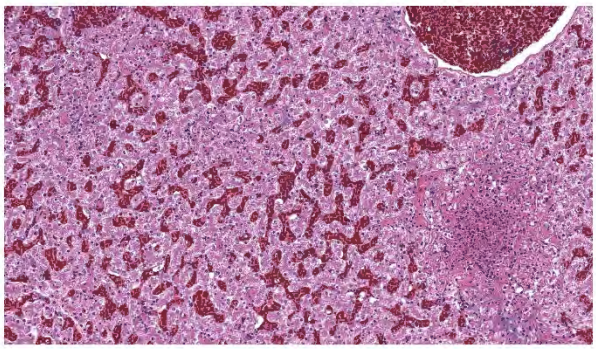

Liver, sandhill crane. Numerous foci of hepatocellular necrosis are scattered throughout the section. A small more recent area is at left, with a larger, more advanced lesion at right. (HE, 290X)

P. multocida is likely transmitted to susceptible birds from the contaminated environment or bird-to-bird contact.[3,6,8] Large numbers of *P. multocida* are shed in nasal, oral and ocular secretions of live sick birds, and large numbers of *P. multocida* contaminate the environment from the carcasses of dead birds.[3,4,6,7,8] Immediate removal of carcasses from the outbreak area is important for the management of avian cholera in wild birds as the bird carcasses will continually contaminant the environment with *P. multocida* if left to naturally decompose or be consumed by scavengers.[3,6,8] How *P. multocida* is transmitted between outbreak areas is not known, but it is believed that some lesser snow geese and Ross's geese can be carriers of *P. multocida*.[3,8,9] In some wetlands, an increase in the population of lesser snow geese has been associated with an increase in the incidence and mortality numbers of avian cholera.[2,3,8,9] The ability of *P. multocida* to persist in the environment has not been fully clarified.[3,6,8] However, there are some studies that show *P. multocida* cannot be isolated from the wetland environment after 7 weeks of an outbreak.[1,8] Thus, long term persistence of the bacterium in the environment is not likely the source of multiple outbreaks in the same area that occur years apart.

In acute fowl cholera, the most likely sign of disease first noticed is the death of large numbers of birds.[4,6,7,8] Clinical signs are only evident for a short period prior to death and include anorexia, ruffled feathers, depression, oral and nasal discharge, increased respiratory rate, diarrhea, and cyanosis of nonfeathered skin. Birds that die of acute fowl cholera are in good body condition and often will still have food in the esophagus and crop. These birds may have congestion of their organs with hemorrhages on serosal surfaces and in the heart, lungs, fat, and other organs. Birds dying acutely with fowl cholera can have multifocal random tan foci in an enlarged liver. The spleen can be enlarged and have multifocal random tan foci. Microscopically, the liver, spleen and lung can have random foci of necrosis filled with heterophils and bacteria. Lesions in the lung are most common in turkeys. There are often bacteria within numerous blood vessels.

Chronic *P. multocida* infections in birds are often localized infections in comparison to the fatal septicemia of acute fowl cholera.[4,7]

Localized infections of *P. multocida* most commonly occur in the respiratory tract. Any part of the respiratory tract can be involved

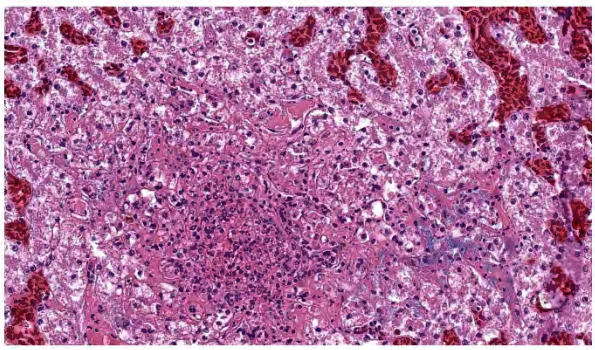

Liver, sandhill crane. High magnification of an area of hepatocellular lytic necrosis. Colonies of coccobacilli are entrapped in fibrin at right; there are small colonies within the sinusoids at the periphery of the necrotic focus. (HE, 619X)

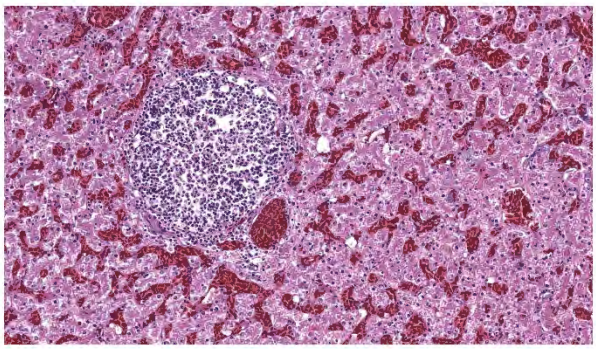

Liver, sandhill crane. Foci of extramedullary hematopoiesis abut portal areas. (HE, 318X).

including the lungs, sinuses, and pneumatic bones. A common chronic respiratory tract lesion in turkeys with *P. multocida* is pneumonia. Other chronic infections with P. multocida in birds include conjunctivitis, arthritis, pododermatitis, salpingitis, and otitis media. The microscopic lesions of chronic P. multocida infections in birds tend to be heterophilic inflammation mixed with macrophages and multinucleated giant cells.

Contributing Institution:
New Mexico Department of Agriculture Veterinary Diagnostic Services

https://nmdeptag.nmsu.edu/labs/veterinary-diagnostic-services.html

JPC Morphologic Diagnosis:

Liver: Hepatitis, necrotizing, acute, random, marked, with fibrin thrombi and numerous colonies of coccobacilli.

JPC Comment: Fowl cholera was last seen in the WSC in Conference 22, Case 1 of the 2014-2015 WSC. Sandhill cranes are not usually a species that comes to mind in a classic diagnosis of fowl cholera. However, *Pasteurella multocida* happens to be one of the leading bacterial causes of death for sandhill cranes in the U.S. and is commonly isolated from wild bird populations. There is some evidence that migratory bird populations may contribute to outbreaks.[3,7] The contributor's comment in this case provides a thorough overview of *P. multocida* in common avian species and is worth the read. Much of the discussion held in this case revolved around topics in their write-up.

P. multocida is associated with a wide range of diseases in several species of animals. Some of the major diseases in domestic species include hemorrhagic septicemia in ungulates, atrophic rhinitis in swine, and fowl cholera in wild and domestic birds. *P. multocida* sports a handful of key virulence factors that include a capsule, lipopolysaccharide (LPS), iron-regulated proteins, and outer membrane proteins OmpA, OmpH, sialylation of outer membrane components, and the adhesion protein filamentous hemagglutinin B2 (FhaB2).[5] The FhaB proteins are both surface-associated and secreted by the bacteria, the latter of which is necessary to establish infection in turkeys upon mucosal exposure.

It is thought that FhaB2 in *P. multocida* functions as an adherence molecule involved in colonization and invasion of respiratory mucosal surfaces in turkeys.[5] Due to the key role FhaB2 plays in the pathogenesis of fowl cholera, there have been vaccine trials using recombinant FhaB2 peptides that demonstrated anti-FhaB2 antibodies effectively protected turkeys against challenge with both homologous and heterologous strains of *P. multocida*.[5] This wide cross-protection is thought to be due to the high degree of conservation of *P. multocida* FhaB2 protein sequences.

References:

1. Blanchong JA, Samuel MD, Goldberg DR, Shadduck DJ and Lehr MA. Persistence of *Pasteurella multocida* in

wetlands following avian cholera outbreaks. *J Wildl Dis*. 2006;41(1):33-39.

2. Blanchong JA, Samuel MD, Mack G. Multi-species patterns of avian cholera mortality in Nebraska's rainwater basin. *J Wildl Dis*. 2006;41(1):81-91.

3. Botzler RG. Epizootiology of avian cholera in wildfowl. *J Wildl Dis*. 1991;27(3):367-395.

4. Christensen JP, Bojesen AM, Bisgaard M. Fowl cholera. In: Pattison M, McMullin PF, Bradbury JM, Alexander DJ, eds. *Poultry Diseases*. 6th ed. Saunders Elsevier; 2007.

5. Dassanayake RP, Briggs RE, Kaplan BS, Menghwar H, Kanipe C, Casas E, Tatum FM. Pasteurella multocida filamentous hemagglutinin B1 (fhaB1) gene is not involved with avian fowl cholera pathogenesis in turkey poults. *BMC Vet Res.* 2025;21(1):207.

6. Friend M. Avian cholera. In: Friend M, Franson JC, Ciganovich EA, eds. *Field Manual of Wildlife Diseases General Field Procedures and Diseases of Birds*. United States Geological Survey; 1999.

7. Glisson JR. Pasteurellosis and other respiratory bacterial infections. In: Saif YM, Fadly AM, Glisson JR, McDougald LR, Nolan LK, Swayne DE, eds. *Diseases of Poultry*. 12th ed. Wiley-Blackwell; 2008.

8. Samuel MD, Botzler RG, Wobeser GA. Avian cholera. In: Thomas NJ, Hunter DB, Atkinson CT, eds. *Infectious Diseases of Wild Birds*. Blackwell; 2007.

9. Samuel MD, Shadduck DJ, Goldberg DR, Johnson WP. Avian cholera in waterfowl: The role of lesser snow and Ross's geese as disease carriers in the Playa Lakes Region. *J Wildl Dis*. 2005;41(1):48-57.

Joint Pathology Center
Veterinary Pathology Services

WEDNESDAY SLIDE CONFERENCE 2025-2026

Conference #14 07 January 2026

CASE I:

Signalment:
9-year-old American Quarter Horse gelding (*Equus caballus*)

History:
This horse was acutely recumbent and depressed with severe colic, muscle fasciculations, and hyperhidrosis. A second horse from the same group had similar, more mild clinical signs, including depression and patchy sweating. A mule from the same pasture was found dead.

Gross Pathology:
Crown-rump length was 48.5 cm. No obvious gross abnormalities were seen within the examined organs.

Figure 1-1. Liver, horse: Stomach contents from the affected individual. (Photo courtesy of: University of Wyoming, Wyoming State Veterinary Laboratory).

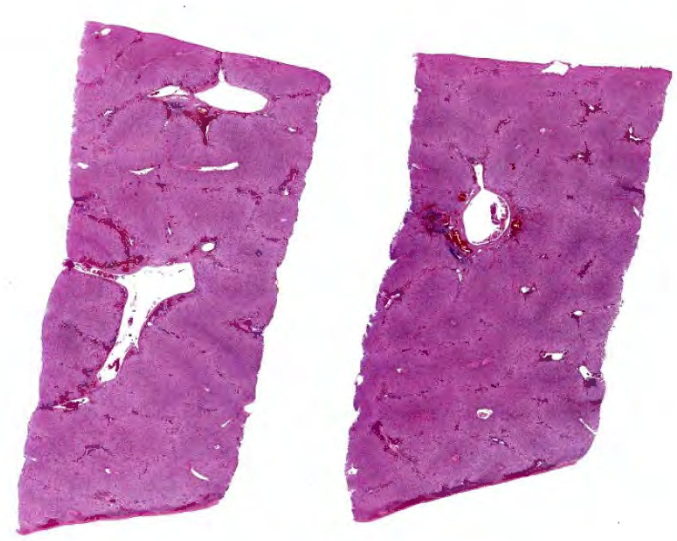

Figure 1-2. Liver, horse: Two sections of liver are submitted for examination. (HE, 10X).

Laboratory Results:
Phosphine gas was detected in the gastric contents of this horse and 3 of the 7 other horses in the same group.

Microscopic Description:
Liver: Diffusely, hepatocytes are moderately swollen and contain numerous small (~1µm) discrete to coalescing cytoplasmic vacuoles (microvesicular hepatopathy). Nuclei remain centrally located. Within the centrilobular interstitium, hepatocytes are occasionally individualized, rounded, shrunken, and/or hypereosinophilic with karyolysis (necrosis). There is mild, patchy periportal hemorrhage.

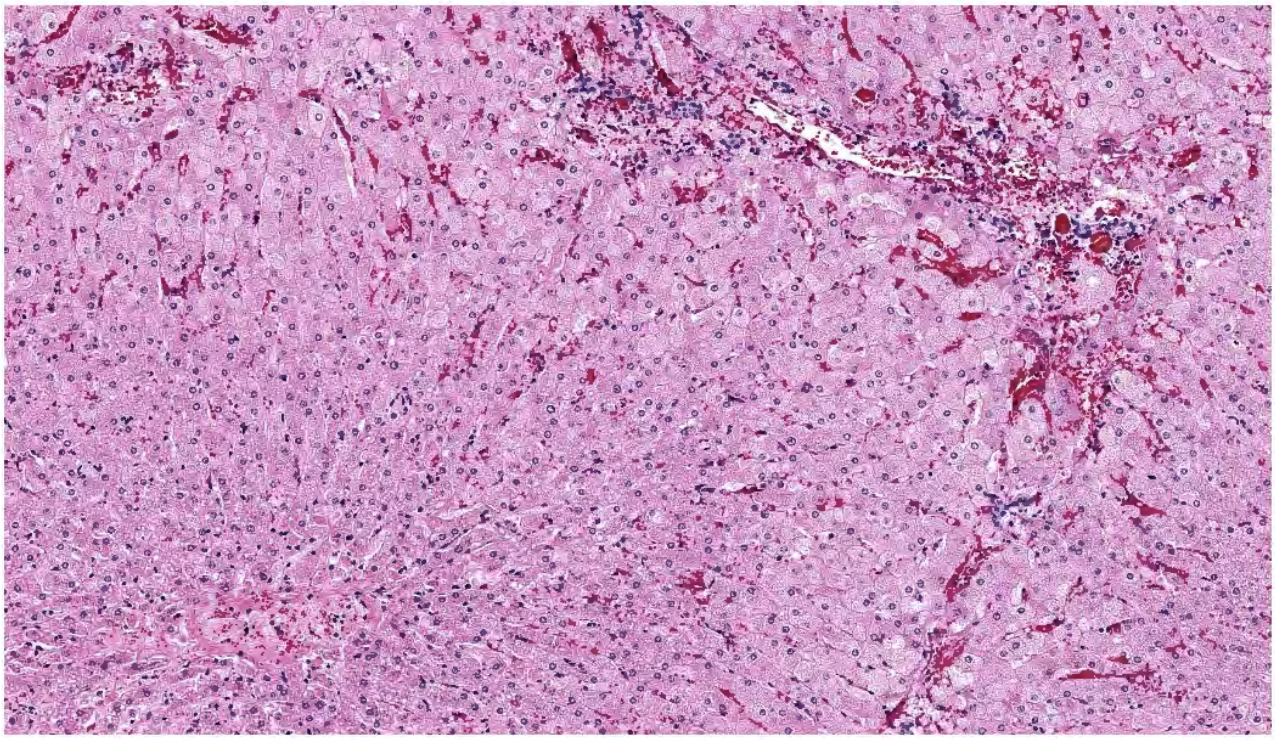

Figure 1-3. Liver, horse: Hepatocytes are diffusely swollen (and compress sinusoids) in all regions of the hepatic lobule by an accumulation of discrete lipid vacuoles. There is multifocal periportal hemorrhage. There is multifocal necrosis and loss of centrilobular hepatocytes. (HE, 195X)

Special stains:

- Osmium tetroxide post-fixation revealed prominent staining of microvesicular lesions, confirming the vacuoles as lipid droplets.
- Oil Red O revealed prominent staining of microvesicular lesions, again confirming the vacuoles as lipid droplets.

Contributor's Morphologic Diagnoses:

Liver: Microvesicular hepatopathy, moderate, acute, diffuse, with mild centrilobular hepatocellular necrosis.

Contributor's Comment:

Phosphine toxicosis was suspected based on recent use of grain-based zinc phosphide rodenticide to control a colony of black-tailed prairie dogs on a 200-hectare pasture. This suspicion was confirmed by the presence of phosphine gas in the stomach contents of this horse and 3 additional horses in the same group. Phosphine gas is a toxic metabolite of metallic phosphides, including zinc phosphide rodenticide and aluminum phosphide insecticide. It is readily produced in the acidic environment of the stomach and inhibits cytochrome C oxidase, thereby blocking mitochondrial oxidative phosphorylation and resulting in rapid energy depletion.[1] Metallic phosphides pose a threat to a wide variety of non-target mammalian and avian species, and are particularly dangerous to horses and other equids which cannot vomit.

Documented lesions of phosphine toxicosis are largely nonspecific and include disseminated congestion and hemorrhage, pulmonary edema, inconsistent myocardial, renal, and/or CNS pathology and recently described microvesicular hepatic steatosis.[2,3,4,5] Macrovesicular steatosis is seen in equine cases of

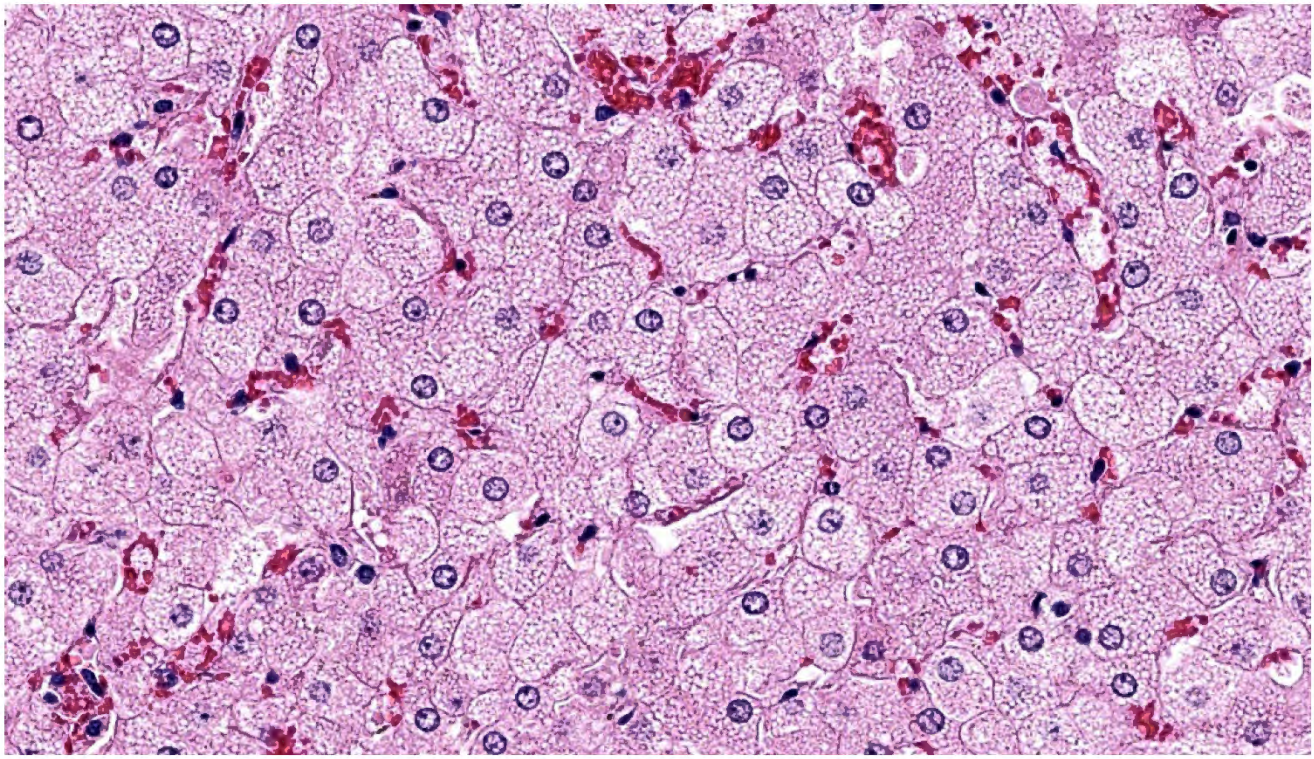

Figure 1-4. Liver, horse: High magnification of affected hepatocytes with numerous lipid vacuoles in their cytoplasm (HE, 705X).

longer duration, along with variable centrilobular hepatocellular necrosis.[3] While macrovesicular hepatic steatosis is a relatively common and nonspecific lesion, microvesicular steatosis has a shorter list of differentials. Defined as multiple lipid vacuoles smaller in size than hepatocyte nuclei[6], microvesicular steatosis is a feature of toxicants that inhibit fatty acid oxidation, including tetracycline, salicylates, hypoglycin A, and valporic acid, in addition to metallic phosphides.[6]

Phosphine gas is toxic to humans and poses a risk to medical professionals treating intoxicated patients.[7] The smell of decaying fish in gastrointestinal contents, either due to phosphine gas itself or contaminants in the pesticide, should raise suspicion on postmortem examination; importantly, pathologists should take care not to inhale the odor in attempt to distinguish the gas. Detection of phosphine gas in gastric contents can be accomplished via reaction with sulfuric acid, which produces a color change that signals a positive result as a rapid, qualitative diagnostic assay.[3] Gas-chromatography-mass spectrometry can be employed for confirmation.[8]

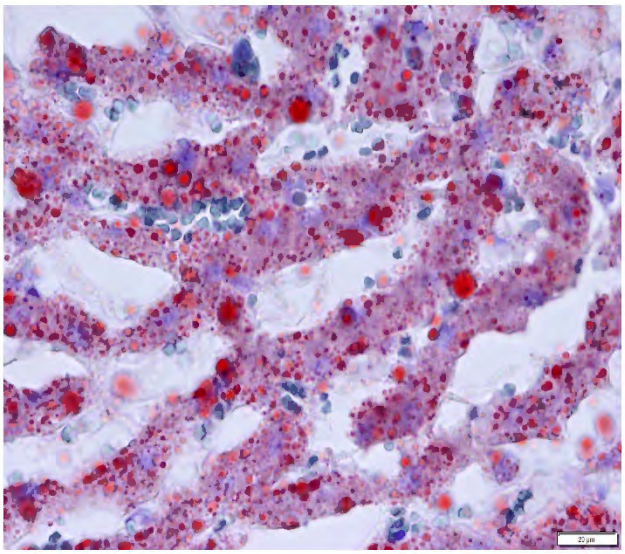

Figure 1-5. Liver, horse: An Oil Red O stain demonstrates lipid within hepatocellular cytoplasm. (Oil Red O, 400X). (Photo courtesy of: University of Wyoming, Wyoming State Veterinary Laboratory).

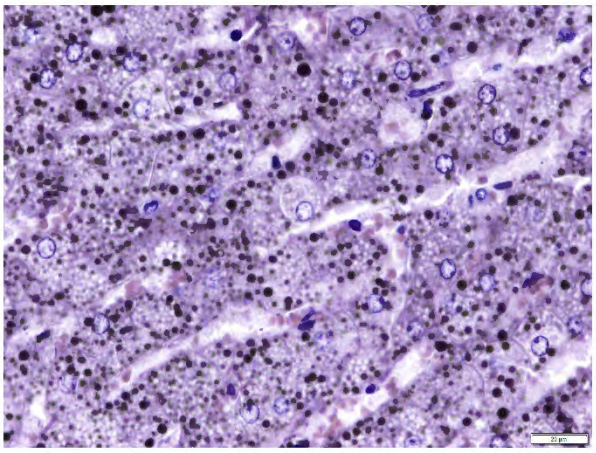

Figure 1-6. Liver, horse: An osmium tetraoxide stain demonstrates lipid within hepatocellular cytoplasm. (Osmium tetraoxide, 400X). (Photo courtesy of: University of Wyoming, Wyoming State Veterinary Laboratory).

Contributing Institution:
University of Wyoming
Wyoming State Veterinary Laboratory
1174 Snowy Range Road
Laramie, WY 82070

JPC Diagnoses:

Liver: Hepatocellular lipidosis, microvesicular, acute, diffuse, severe.

JPC Comment:
Welcome to the second half of WSC 2025-2026! This fourteenth conference was moderated by one of our treasured regulars: Dr. Julie Engiles from the University of Pennsylvania's New Bolton Center! Although Dr. Engiles specializes in equine orthopedic pathology, the JPC is currently lacking equine bone cases for the WSC (the team is not-secretly hoping for more orthopedic case submissions for next year, hint, hint). As such, she led participants through an excellent equine-focused, "squishy tissue" conference.

Discussion of this first case, never seen before in the WSC, covered the ins and outs of phosphine gas poisoning and other potential differentials for acute hepatotoxins in horses. The pattern of lesion distribution in this case was, unlike most toxins that whack the liver, not focused predominantly on centrilobular hepatocytes. Many hepatotoxins are metabolized to their toxic forms by CP450 in centrilobular regions, hence why those cells end up predominantly affected. Centrilobular hepatocytes are already living on the razor's edge of hypoxia as it is, they don't need much to be pushed over that edge. Few toxins, however, such as phosphorus, microcystin, and phosphine gas, do not need to be metabolized to cause serious damage. Instead, they are so directly toxic that they affect whatever they come across first. In the liver, this is the periportal areas, as those are the sites of first contact in the liver for products from systemic circulation.

Other differentials for acute hepatic necrosis in horses include equine parvovirus (Theiler's disease) and the newly described equine hepacivirus. This flavivrus is closely related to human hepatitis C virus and is currently being looked at as a potential model for Hep C studies.[9]

There are two main forms of phosphides that are globally available and commonly used as pesticides: aluminum phosphide (AlP) and zinc phosphide (ZnP). AlP is generally considered the more volatile of the two. It reacts violently and exothermically with any moisture/acid it comes into contact with to create highly toxic, flammable, and often spontaneously igniting phosphine gas (PH_3).[6] This reaction is what makes it such a potent fumigant, but also makes it extremely hazardous. It is most commonly utilized in pellet form for grain fumigation, stored food protection, and large-scale pest control. Despite its risks, it is still the most widely utilized fumigant for stored grains.[1] Ingestion is the most common method of exposure in humans and animals,

followed by inhalation and absorption, respectively.[6] Most case reports of phosphine poisoning are from India, with many reports also from Iran, Sri Lanka, Morocco, and numerous "developed" countries.[6] As recently as 2022, there was an incident of accidental phosphine gas poisoning in Delhi, where two persons died of phosphine gas exposure after sleeping in a warehouse containing AlP.[12]

ZnP, on the other hand, primarily reacts with acids rather than just any form of moisture like AlP does, enabling its use as a common bait rodenticide. As with any other form of bait rodenticide, it is not uncommon for other animals that are not the intended target to ingest the poison and end up dead. Upon ingestion by an animal, the ZnP reacts with hydrochloric acid in the stomach to produce lethal phosphine gas that is rapidly absorbed through the gastrointestinal tract, leading to systemic toxic effects that can manifest as acute, severe cardiac arrhythmias, shock, acidosis, hepatic lipidosis (as in this case), seizures, and/or pulmonary edema.[1,6]

In addition to directly corrosive actions, phosphine is a potent metabolic poison that functions similarly to cyanide, disrupting cellular energy production by targeting mitochondria and inhibiting cytochrome C oxidase.[1,2,6] The electron transport chain, the major producer of ATP via oxidative phosphorylation and a process in which cytochrome C oxidase is a key player, occurs on the inner mitochondrial membrane. Following their production via the Kreb's cycle, NADH molecules enter the transport chain and donate electrons to NADH dehydrogenase (also known as complex I). From here, the electrons are passed down a series of subsequent complexes like a relay race that ultimately produce a proton gradient across the mitochondrial membrane. Once an electron reaches complex IV (also known as cytochrome C oxidase), it is combined with an oxygen molecule and protons to form water, making oxygen the final electron acceptor and enabling the continued flow of the transport chain. The resultant proton gradient powers ATP synthase which, as protons flow back into the mitochondrial matrix, converts ADP to ATP in large quantities for use in energy-driven cellular functions. Basically, if cytochrome C oxidase is unable to do its job, electrons can't reach oxygen, which causes the chain to back up with "stuck" electrons, halting proton pumping, stopping ATP synthesis, and severely depleting cellular energy, which eventually leads to cell death. This effect is particularly potent in high-energy organs like the heart, lungs, liver, and brain.

As noted by the contributor, a "rotting fish" or "garlic" smell may accompany phosphine gas at autopsy. While pure PH_3 gas is odorless, the fishy smell associated with phosphine gas results from common contaminants in the gas, primarily diphosphane (P_2H_4) or other organic phosphine compounds. Either way, sniffing dead bodies to try and figure out, "What's that smell?" is strongly ill-advised.

References:

1. Alzahrani SM, Ebert PR. Pesticidal Toxicity of Phosphine and Its Interaction with Other Pest Control Treatments. *Current Issues in Molecular Biology*. 2023;45(3):2461-2473
2. Bumbrah GS, Krishan K, Kanchan T, Sharma M, Sodhi GS. Phosphide poisoning: a review of literature. Forensic science international. 2012 Jan 10;214(1-3):1-6.
3. Cullen JM, Stalker MJ. Liver and biliary system. In: Maxie MG, ed. Jubb, Kennedy, and Palmer's Pathology of Domestic Animals.6th ed. Vol. 2. Philadelphia, PA: Elsevier, 2016:273–278.

4. Drolet R, Laverty S, Braselton WE, Lord N. Zinc phosphide poisoning in a horse. *Equine Veterinary Journal.* 1996;28(2):161-2.
5. Fox JH, Porter BF, Easterwood L, Hildenbrand JR, Hélie P, Smylie J, O'Toole D. Acute hepatic steatosis: a helpful diagnostic feature in metallic phosphide–poisoned horses. *JVDI*. 2018;30(2):280-5.
6. Gurjar M, Baronia AK, Azim A, Sharma K. Managing aluminum phosphide poisonings. *J Emerg Trauma Shock*. 2011;4(3):378-84.
7. Nagy AL, Bolfa P, Mihaiu M, Catoi C, Oros A, Taulescu M, Tabaran F. Intentional fatal metallic phosphide poisoning in a dog—a case report. *BMC Veterinary Research.* 2015;11(1):158.
8. Olivares CP, Martínez RR, Daba MM, Thomsen JL. Zinc phosphide poisoning in a mare. *Veterinaria México.* 2002;33(3):343-6.
9. Pacchiarotti G, Nardini R, Scicluna MT. Equine Hepacivirus: A Systematic Review and a Meta-Analysis of Serological and Biomolecular Prevalence and a Phylogenetic Update. *Animals (Basel).* 2022;12(19):2486.
10. Plumlee KH. Pesticide toxicosis in the horse. *Vet Clin North Am Equine Pract*. 2001;17:491–500.
11. Robison WH, Hilton HW. Gas chromatography of phosphine derived from zinc phosphide in sugarcane. *J Agric Food Chem.* 1971;19:875–878.
12. Singh R, et al. Mysterious death due to accidental inhalation of phosphine – A unique case study. *Forensic Science International: Reports*. 2022;5:100264.

CASE II:

Signalment:

9-year-old male Arabian horse (*Equus ferus caballus)*

History:

A 9-year-old male Arabian horse from Lagoa Santa (State of Minas Gerais, Brazil), was admitted to the veterinary hospital of the Universidade Federal de Minas Gerais (UFMG) with history of acute ataxia, depression, incoordination and reluctance to move. The horse belonged to a riding school, where no other horses showed any neurological signs, and was dewormed with Ivermectin. Therapy with steroidal and non-steroidal anti-inflammatory drugs was instituted (unknow drugs and dosages) at the horse training site, and the animal was anesthetized with detomidine and ketamine for the transport to UFMG. At admission, the horse was still anesthetized. When no longer anesthetized, the horse made several unproductive attempts to stand. Neurological signs progressed over the next 24 hours to bilateral ventromedial strabismus and reduction of threat response.

Physical exam revealed hypothermia (36.1°C), dry mucous membranes, increased

Figure 2-1. Kidney, horse: Gross appearance of the kidney with multifocal nodules, elevated, white-yellowish in the center, red on the edges and firm. (Photo courtesy of: Escola de Veterinária, Universidade Federal de Minas Gerais – www.vet.ufmg.br).

capillary refill time, skin ulcers secondary to decubitus in the tuber coxae, head and limbs, as well as a superficial wound in the atlanto-occipital region, probably due to previous fall.

At the veterinary hospital, intravenous (IV) fluid therapy with 7.2% hypertonic saline solution, followed by Ringer's lactate solution dimethyl sulfoxide (IV), ceftiofur, and dexamethasone therapy was initiated. Skull radiograph showed no significant abnormalities. Due to poor prognosis and lack of response to therapy the horse was euthanized and subject to necropsy.

Gross Pathology:
The kidneys had multifocal nodules, ranging from 2 to 15 cm in diameter, elevated, white-yellowish in the center, red on the edges, and firm. In the right kidney the lesion replaced, approximately, fifty percent of the renal parenchyma, whereas in the left kidney there were multiple nodules ranging from 1 to 3 cm in diameter. Renal and internal iliac lymph nodes were moderately enlarged and firm, with undefined cortico-medullary distinction. Meninges and brain parenchyma were moderately hyperemic.

Laboratory Results:
Cerebrospinal fluid (CSF) revealed no change in color (clear), protein (34.02 mg / dL) and glucose (61.5 mg / dL). A mild increase in nucleated cells were observed (20 cells / µL, reference value: 5 cells / µL). No erythrocytes, eosinophils or parasitic structures were observed.

Microscopic Description:
Kidneys: Multifocal to coalescent areas of loss of normal parenchyma with replacement by severe lymphohistioplasmocytic inflammatory infiltrate, with epithelioid macrophages, multinucleated giant cells, and large numbers of intralesional nematodes. Parasites were elongated, with aproximately 80 to 90 µm long (most of them fragmented), cylindrical, with

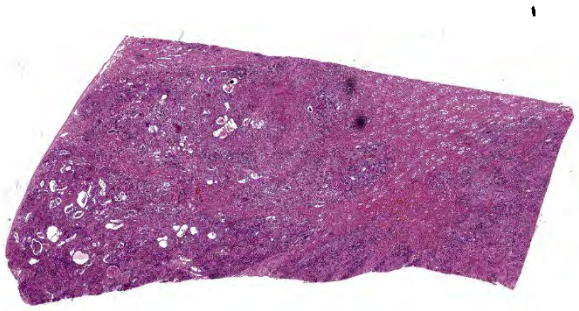

Figure 2-2. Kidney, horse. Within the submitted section of kidney, approximately 66% of the section is effaced by inflammatory changes. At subgross magnification, numerous severely ectatic tubules are present. (HE, 10X).

sharp ends, covered by smooth cuticle, platimiarian musculature and an evident elongated and central rhabditiform esophagus, occupying the initial third of the body (morphology consistent with *Halicephalobus gingivalis*). Associated with these lesions there were also fibroplasia, necrosis, vasculitis and the remaining renal tubules were dilated and filled with macrophages, neutrophils, cellular debris, and numerous sections of *H. gingivalis*.

Contributor's Morphologic Diagnoses:
Kidneys: multifocal to coalescent, severe, chronic, granulomatous nephritis associated to intralesional nematodes compatible with *Halicephalobus gingivalis* and multifocal, severe, vasculitis, horse.

Contributor's Comment:
H. gingivalis is a nematode, genus *Halicephalobus*, order Rhabditida, superfamily Rhabditoidea and family Rhabditidae that have a smooth and thin cuticle, with transverse striations, conical tail ending in fine point, elongated buccal cavity and a rhabditiform esophagus.[2] It is a free-living nematode, usually found in the soil and organic matter, but its life cycle and pathogenesis are still unknown. Apparently, skin or mucosal lesions are the port of entry from where the parasite spreads by

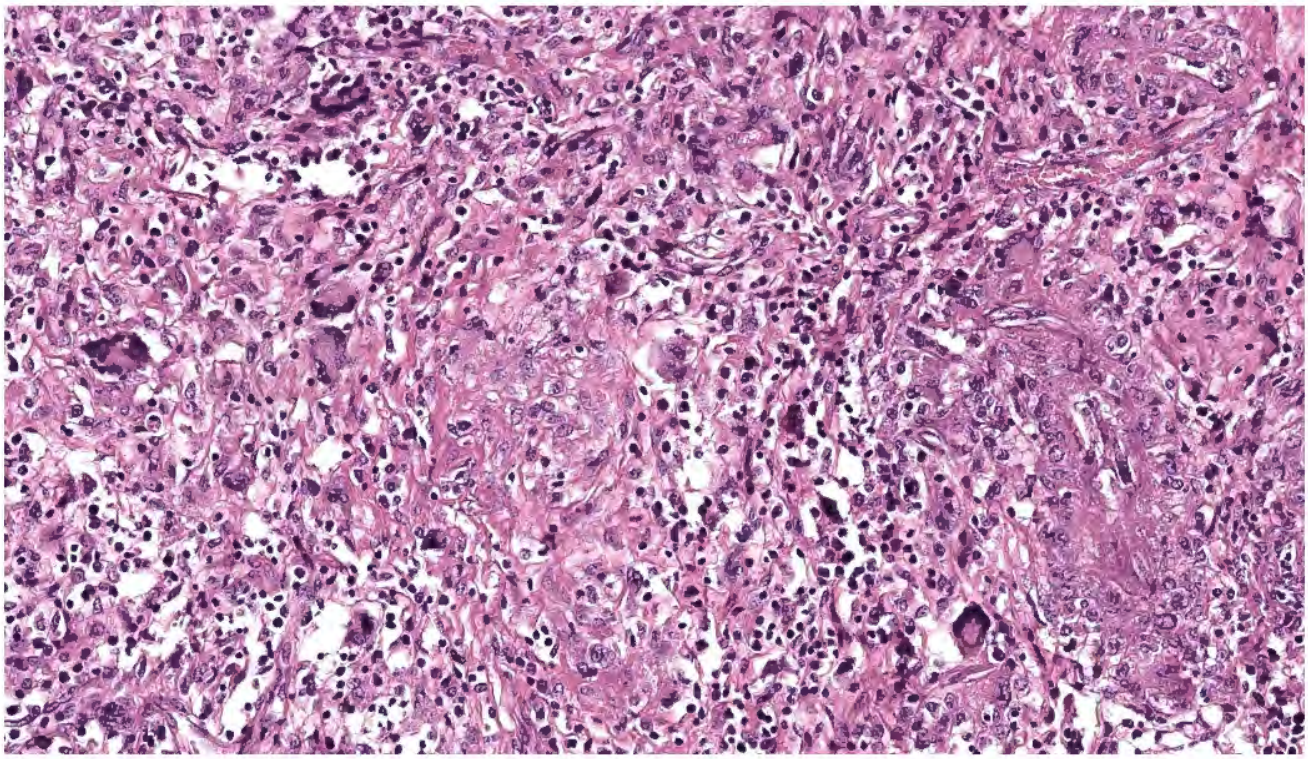

Figure 2-3. Kidney, horse. The renal parenchyma is effaced by granulomatoeus inflammation containing numerous epithelioid macrophages, multinucleated foreign body-type macrophages, fibrosis and cross and tangential sections of larval rhabditoid nematodes. (HE, 318X).

hematogenous or lymphatic route. Other possible ways of dissemination in organs are through the optic or trigeminal nerves, and the lacrimal duct.[3,7,9,10]

H. gingivalis often infects horses. However, there are reported infections affecting zebra, calves, and humans.[5,6,8] Most of the human and equine reported cases were from Europe, North America, and Northeast of Asia. Brazil have just three previously reported cases in horses, two of them with brain infection and one with granulomatous myocarditis.[4,11,13] Clinical signs in infected animals reflect the distribution and intensity of the lesions. The lesions observed on the organs of this horse are compatible with other reports.[6,11,13]

Diagnosis of *H. gingivalis* infection based on direct detection of larvae by CSF analysis has been previously reported.[1] However, there are no studies demonstrating a correlation between larval detection in CFS and the brain lesions. Detection of larvae in the urine of infected horses has been also reported, suggesting that it can be a route of elimination to the environment, which is compatible with the abundant amount of nematode inside renal tubules found in the histopathology of this horse.[7,12] This horse was dewormed with Ivermectin. Some reports suggest that this drug or the recommended dose to treat gastrointestinal parasites are not effective against *H. gingivalis,* and no other chemical therapies have been described for this infection.[3,9,11]

Contributing Institution:
Escola de Veterinária, Universidade Federal de Minas Gerais – www.vet.ufmg.br

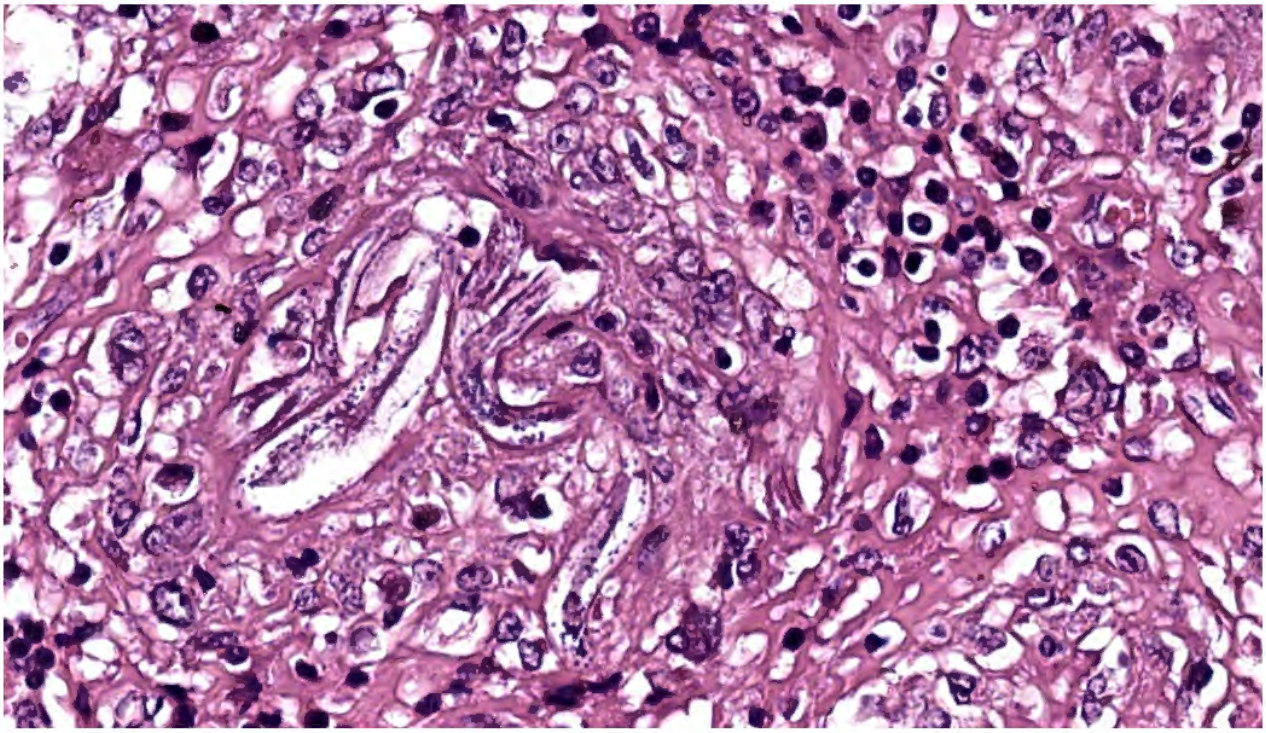

Figure 2-4. Kidney, horse. Higher magnification of larval rhabditoid nematodes embedded within an inflammatory focus. (HE, 1120X).

JPC Diagnoses:
Kidney: Nephritis, granulomatous, chronic-active, multifocal to coalescing, severe, with adult and larval rhabditid nematodes and eggs.

JPC Comment:
This is a great example of a classic entity in horses. The contributor's comment covers most of what was discussed regarding *H. gingivalis*. A few points of note from this conversation are that, as a reminder, the neutrophils most of our routine large animal species (equines and bovines, especially) are more eosinophilic that in small animals and can be mistaken for eosinophils. Remember, in horses, their eosinophils are prominent and look like raspberries! Additionally, *H. gingivalis*, although commonly associated with the oral cavity, facial bones, kidneys, and brain, can cause lesions anywhere throughout the body. Dr. Engiles told participants of a recent case she had of *H. gingivalis* infection in the cannon bone of a horse where the parasites had migrated into the bone hematogenously. The horse's presenting complaint was just "lameness." This was an important lesson in not pigeonholing oneself and remaining open-minded about possible diagnoses.

The genus *Halicephalobus* is derived from the Greek roots "*hyalinos*", "*kephalon*", and "*lobos*", meaning "transparent head lobe". This apparently refers to the clear, lobed head structure of the adult nematode seen on stereomicroscopy. You'll have to ask the parasitologists on that one. For *H. gingiavlis*, the specific species epithet originates from its initial identification in the oral cavity of a horse. Stefanski was the first person to describe the nematode in 1954 when he found worms in a gingival granuloma in a horse in Poland.[9] *H. gingivalis* has also been referred to as *Micronema deletrix* or *H. deletrix* over the years.[2,9]

In all cases of *H. gingivalis* in both humans and animals, only parasitic female adults, larvae, and eggs have been isolated from hosts. This strongly suggests that *H. gingivalis* can reproduce parthenogenetically, which is

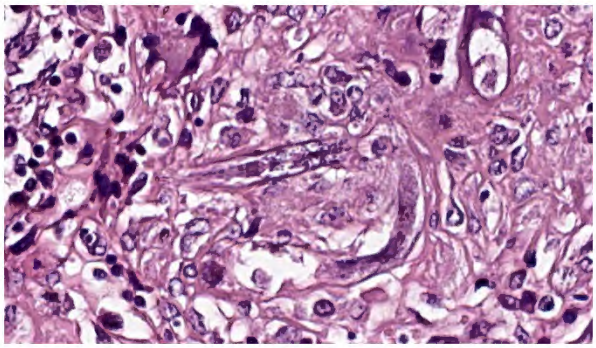

Figure 2-5. Kidney, horse. Higher magnification of the characteristic rhabditoid esophagus)corpus, isthmus, and buld) within a larval nematode. larval rhabditoid nematodes embedded within an inflammatory focus. (HE, 1120X)

known to occur in other rhabditid nematodes. *H. gingivalis* is primarily considered a pathogen of horses and other equids but is also known to affect humans and was recently reported in ruminants.[5,9] Transmammary infection from mare to foal has also been reported once.[9]

References:

1. Adedeji AO, Borjesson DL, Kozikowski-Nicholas TA, Cartoceti AN, Prutton J, Aleman M. What is your diagnosis? Cerebrospinal fluid from a horse. *Vet Clin Pathol.* 2015; 44(1):171-2.
2. Anderson RC, Under KE, Peregrine AS. *Halicephalobus gingivalis* (Stefanski, 1954) from a fatal infection in a horse in Ontario, Canada with comments on the validity of *H. deletrix* and a review of the genus. *Parasite*.1998; 5:255-61.
3. Brojer JT, Parsons DA, Linder KE, Peregrine AS, Dobson H. *Halicephalobus gingivalis* encephalomyelitis in a horse. *Can Vet J.* 2000;41:559-61.
4. Cunha BM, França TN, Miranda IC, Santos AM, Seixas JN, Pires APC, Santos BBN, Peixoto PV. Miocardite granulomatosa em cavalo por *Halicephalobus gingivalis* (*H. deletrix*) - Relato de caso. *Rev Braz Med Vet.* 2016;38(2):113-16.
5. Enemark HL, Hansen MS, Jensen TK, Larsen G, Al-Sabi MNS. An outbreak of bovine meningoencephalomyelitis with identification of *Halicephalobus gingivalis*. *Vet Parasitol.* 2016;218:82-6.
6. Isaza R, Schiller CA, Stover J, Smith PJ, Greiner EC. *Halicephalobus gingivalis* (nematoda) infection in a grevy's zebra (*Equus grevyi*). *J Zoo Wild Med.* 2000;31(1):77-81.
7. Kinde H, Mathews M, Ash L, Leger JSt. *Halicephalobus Gingivalis* (*H. Deletrix*) infection in two horses in southern California. *J Vet Diagn Invest*. 2000;12(2):162–5.
8. Lim CK, Crawford A, Moore CV, Gasser RB, Nelson R, Koehler AV, Bradbury RS, Speare R, Dhatrak D, Weldhagen GF. First human case of fatal *Halicephalobus gingivalis* meningoencephalitis in Australia. *J Clin Microbiol.* 2015;53:1768-74.
9. Onyiche TE, Okute TO, Oseni OS, Okoro DO, Biu AA, Mbaya AW. Parasitic and zoonotic meningoencephalitis in humans and equids: Current knowledge and the role of *Halicephalobus gingivalis*. Parasite Epidemiol Control. 2017 Dec 29;3(1):36-42.
10. Pearce SG, Bouré LP, Taylor JA, Peregrine AS. Treatment of a granuloma caused by *Halicephalobus gingivalis* in a horse. *J Am Vet Med Assoc.* 2001;219(12):1735-8.
11. Rames DS, Miller DK, Barthel R, Craig TM, Dziezyc J, Helman RG, Meale R. Ocular *Halicephalobus* (syn. *Micronema*) *deletrix* in a horse. *Vet Pathol.* 1995;32(5):540-2.
12. Sant'Ana FJF, Júnior JAF, Costa YL, Resende RM, Barros CSL. Granulomatous meningoencephalitis due to *Halicephalobus gingivalis* in a horse. *Braz J Vet Pathol.* 2012;5(1):12-5.
13. Taulescu MA, Ionicã AM, Diugan E, Pavaloiu A, Cora R, Amorim I, Catoi C, Roccabianca P. First report of fatal systemic *Halicephalobus gingivalis* infection in two Lipizzaner horses from Romania: clinical, pathological, and molecular characterization. *Parasitol Res.* 2015;115(3):1907-2103.
14. Vasconcelos RO, Lemos KR, Moraes JRE, Borges VP. *Halicephalobus gingivalis* (*H. deletrix*) in the brain of a horse. *Cienc Rural.* 2007;37(4):1185-7.

CASE III:

Signalment:
33-year-old, female intact donkey (jenny), *Equus asinus*)

History:
1-week history of weight loss. There was an acute decline over 24 hours with depression and anorexia. Physical exam revealed a heart rate of 88bpm, ileus, and delayed capillary refill time. ICU care was offered but, due to the poor prognosis, the owners opted to euthanize.

Gross Pathology:
Externally the animal was emaciated. There was 24.5L of red watery peritoneal fluid, and 500ml of red watery pleural fluid. There were multifocal to coalescing exophytic, papillary, white nodules ranging from pinpoint to 5x5x2cm on the abdominal and thoracic body walls, the diaphragm, the omentum, the mesentery, the lung, the liver, the spleen, the perirenal adipose tissue, and the ovary. The nodules were frequently associated with multifocal to coalescing hemorrhages.

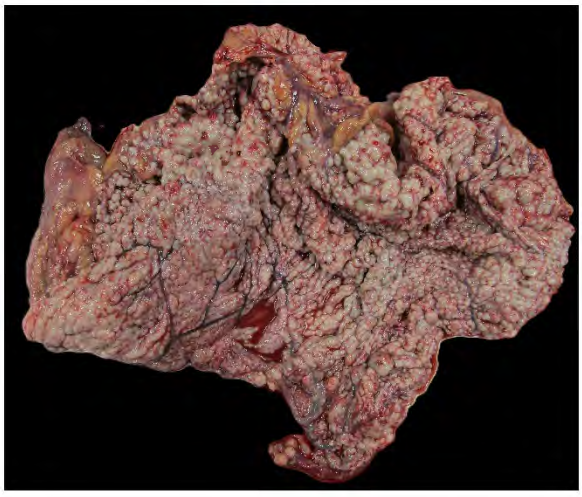

Figure 3-1. Omentum, donkey: The omentum is covered by multifocal to coalescing exophytic, papillary, white nodules ranging from pinpoint to 5x5x2cm in diameter. (Photo courtesy of: University of Nottingham, https://www.nottingham.ac.uk/vet/service-for-business/veterinary-pathology-service/index.aspx).

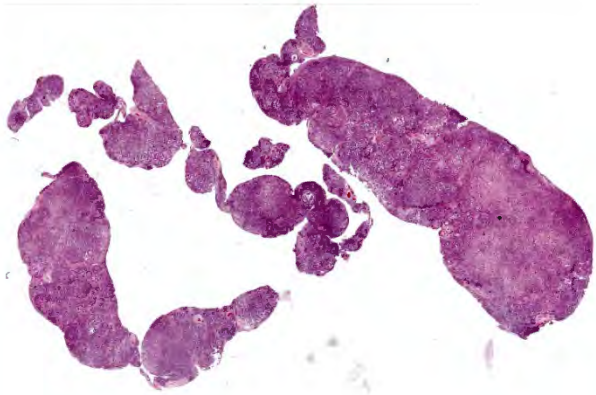

Figure 3-2. Omentum, donkey: One section of omentum is submitted for examination. The omental architecture is effaced by an infiltrative neoplasm. (HE, 6X).

Laboratory Results:
N/A

Microscopic Description:
Extending from and infiltrating the omentum is an unencapsulated, poorly demarcated, moderately cellular neoplasm composed of cuboidal to polygonal cells arranged in acini, tubules and nests, and more rarely micropapillary projections, on a moderate fibrovascular stroma. Neoplastic cells have variably distinct cell borders, an abundant amount of granular, eosinophilic and occasionally indistinctly vacuolated cytoplasm, and a pleomorphic, centrally placed nucleus with finely stippled to marginated chromatin and up to 3, occasionally very large distinct magenta nucleoli. There is marked anisocytosis and anisokaryosis, and 21 mitotic figures in 2.37mm2 – equivalent of 10 high power fields (40x obj); these are occasionally bizarre. There are occasional multinucleated neoplastic cells with up to 3 nuclei which occasionally compress and occasional apoptotic bodies are seen. Multifocally, neoplastic stroma contains minimal extravasations of erythrocytes (haemorrhage), and there are multifocal mild infiltrations of deform adjacent nuclei (nuclear molding).

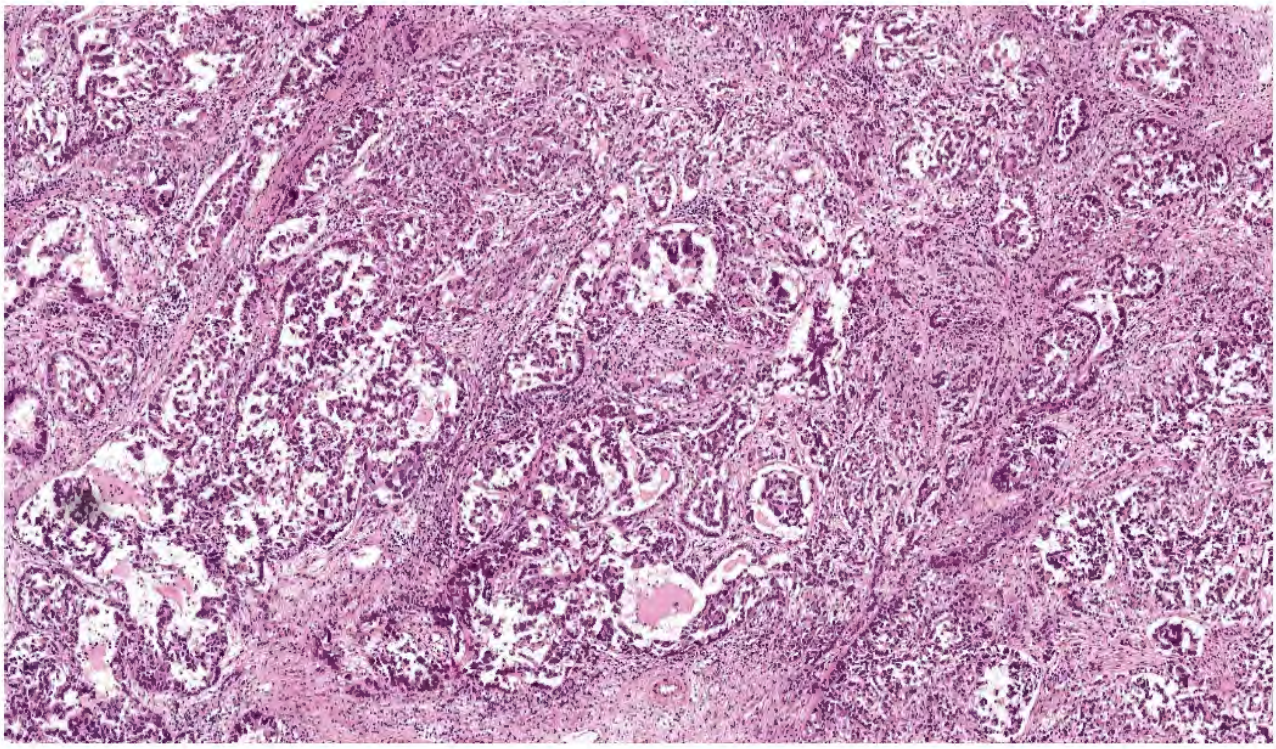

Figure 3-3. Omentum, donkey: The omentum is effaced by mesothelial cells forming large cystic spaces containing epithelioid mesothelial cells forming papillary and micropapillary projections on a dense fibrous stroma. (HE, 98X).

There is occasional single cell necrosis, and-mainly mature small lymphocytes, some plasma cells, and fewer neutrophils. Blood vessels are multifocally moderately congested and are often lined by plump (reactive) endothelium.

Immunohistochemistry: Neoplastic cells are diffusely strongly positive for vimentin. The majority of neoplastic cells are moderately positive for cytokeratin.

Contributor's Morphologic Diagnoses:
Pleural and peritoneal cavities: Mesothelioma, epithelioid subtype.

Contributor's Comment:
Postmortem examination revealed the presence of a neoplastic process within the pleural and peritoneal cavity, which on histopathology had a morphology most likely consistent with a mesothelioma.[3,12] Additionally, the immunopositivity of both cytokeratin and vimentin, is consistent with a mesothelial origin, although rarely this dual positivity can be present in metastatic ovarian or renal carcinomas, which were not identified in this case.[12]

Mesotheliomas are considered rare and affect many animal species; they are most commonly reported in cattle, which have a congenital form, and in canines.[4,8,9,17] They have also been reported in goats, cats, sheep, horses, jaguars, skunks, and amazon parrots.[5,6,11,13-15] They should be differentiated from mesothelial hyperplasia using the features in Table 1, taken from Husain et al., 2018.[3] This case displays a moderate amount of fibrovascular stroma with invasion, contains complex tubular and micropapillary structures with disorganized growth, and only a mild inflammation which is consistent with mesothelioma.[3]

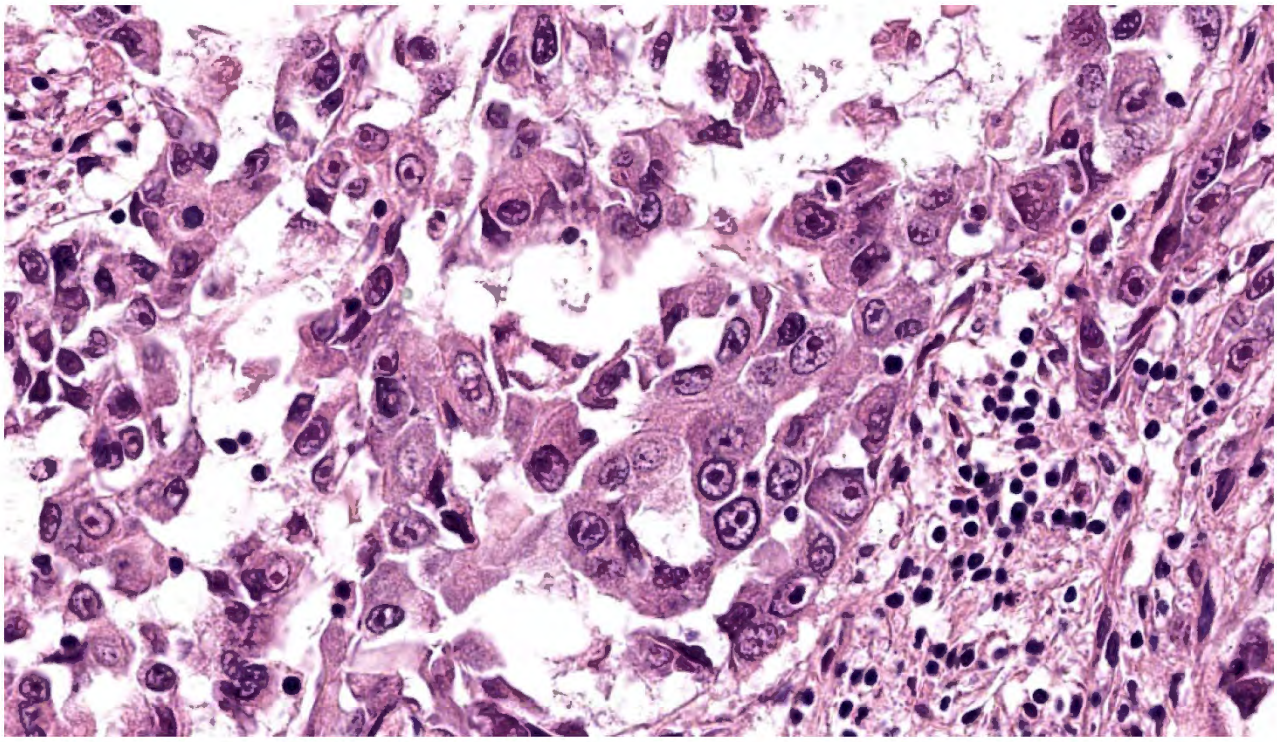

Figure 3-4. Omentum, donkey: Neoplastic mesothelial cells are moderately pleomorphic. (HE, 686X).

Confirmed cases are unreported in donkeys, however, there are suggested similarities in neoplastic diseases in donkeys and horses.[1] Most diagnoses are made postmortem.[12]
Mesotheliomas can be classified as:

- Epithelioid (most common, better prognosis): Small oval to cuboidal cells shape that connect often forming small tubular or papillary structures;
- Sarcomatoid or Fibrous: fusiform cells that do not connect or form structures and widely infiltrate surrounding tissue; or
- Mixed or Biphasic: contains at least 10% of each cell type (epithelioid and sarcomatoid cells).[3,12]

In humans and dogs further subclassification can be performed with 17 subtypes, and stroma can contain chondroid or osseous differentiation, due to the multipotency of mesothelial cells.[3,12] In humans, canines and bovines, mesothelioma has been associated with asbestos fiber inhalation.[2,4,8]

Calretinin, where commercially available, can be a useful addition to an immunohistochemistry panel for suspected mesothelioma in horses, and may be useful in the donkey, in addition to vimentin and cytokeratin.[16]

Looking at the ultrastructure may aid diagnosis, particularly where concern remains for malignant carcinomas. Neoplastic epithelioid

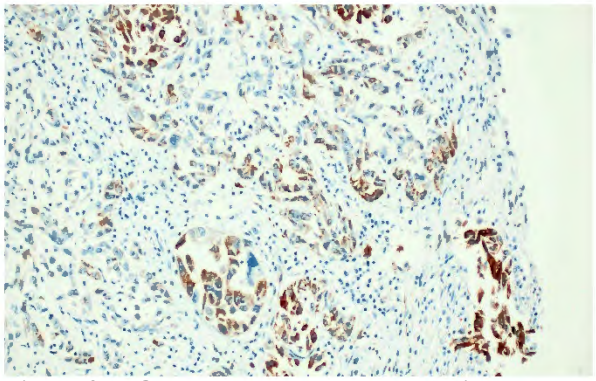

Figure 3-5. Omentum, donkey: Neoplastic mesothelial cells demonstrate moderate cytoplasmic immunoreactivity for cytokeratin. (anti-AE1/AE3, 400X) (Photo courtesy of: University of Nottingham, see weblink in Fig 3-1)

mesothelial cells have abundant, long, occasionally branching microvilli, and circumferential nuclear intermediate microfilaments.[3]

Table 1: Reactive Mesothelial Hyperplasia Versus Mesothelioma (taken from Husain et al., 2018)[3]

Mesothelial hyperplasia	**Mesothelioma**
Absence of stromal invasion (beware of entrapment and *en face* cuts)	Stromal invasion usually apparent (highlight with pancytokeratin staining)
Cellularity may be prominent but is confined to the mesothelial surface/ pleural space and is not in the stroma	Dense cellularity, including cells surrounded by stroma
Simple papillae, single cell layers	Complex papillae, tubules and cellular stratification
Loose sheets of cells without stroma	Cells surrounded by stroma (''bulky tumor'' may involve the mesothelial space without obvious invasion)
Necrosis rare	Necrosis present (occasionally)
Inflammation common	Inflammation usually minimal
Uniform growth (highlighted with cytokeratin staining)	Expansile nodules; disorganized growth (highlighted on cytokeratin staining)
Usually not useful	
Mitotic activity Mild to moderate cytology's atypia	

Contributing Institution:

Veterinary Pathology Service
University of Nottingham
Sutton Bonington Campus
College Road
Sutton Bonington
Leicestershire
United Kingdom
LE12 5RA
https://www.nottingham.ac.uk/vet/service-for-business/veterinary-pathology-service/index.aspx

JPC Diagnoses:

Omentum: Mesothelioma.

JPC Comment:

This third case was challenging due to the epithelioid nature of this mesothelioma. Most conference participants were readily able to reach a diagnosis of "carcinoma" or "adenocarcinoma" and many listed epithelioid mesothelioma as a differential. Tissue identification was challenging and only the most experienced participants felt confident calling it omentum based off the HE secttion. The features described by these participants that clued them in to "omentum" included a nodular "string of pearls" subgross appearance, the composition of a highly vascular fibroadipose tissue, and the wherewithal to remember that the omentum exists in the first place, which can be challenging in and of itself some days. The contributor provided a succinct, eloquent write-up on mesotheliomas and their classifications, which were covered during the conference discussion.

An interesting feature within the nuclei of some of the neoplastic cells caught the eye of a few of the participants. Infrequently, neoplastic mesothelial cells have what look like irregularly shaped, eosinophilic, intranuclear inclusion bodies (INIBs). This is an uncommon, but documented, feature of certain mesotheliomas in humans that can be seen both cytologically and histologically, particularly in adenomatoid and epithelioid forms.[5,6] INIBs have also been seen, albeit rarely, in laboratory hamsters and rats infected with SV40 that subsequently developed mesothelioma.[21] INIBs are reported, also rarely, in both cattle and dogs with mesothelioma associated with asbestos exposure, although the significance of those inclusions is unknown. Lastly, INIBs can be a rare feature of reactive mesothelial cells as well, making their presence challenging to interpret, but may prompt pathologists to assess for viral or asbestos-related causes.[21]

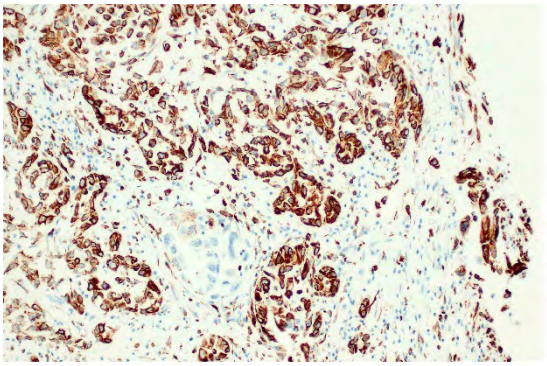

Figure 2-6. Omentum, donkey: Neoplastic mesothelial cells demonstrate strong cytoplasmic immunoreactivity for vimentin. (anti-vimentin, 400X) (Photo courtesy of: University of Nottingham, see weblink in Fig 3-1).

The last notable point in this case discussion focused on other possible differentials for this lesion in equids, which prompted a quick conversation on equine herpesvirus-5, the cause of equine multinodular pulmonary fibrosis in horses. In donkeys, asinine herpesvirus-5 causes a similar syndrome and, if this tissue had been from the lungs, this virus would have been a good differential to put on the list.

Mesothelioma was first described by Bichat in 1827. Mesothelial cells originate from the embryonic lateral plate mesoderm, forming a protective epithelial lining known as the mesothelium for the pleural, pericardial, and peritoneal spaces.[3] There are two layers to the lateral plate mesoderm that form during development. The dorsal layer, called the somatic mesoderm, is associated with the overlying ectoderm, while the ventral layer, termed the splanchnic mesoderm, is associated with the underlying endoderm.[3] The splanchnic mesoderm eventually forms the visceral mesothelium on organs, whereas the somatic mesoderm develops into the parietal mesothelium of the body wall.

Mesothelial cells are somewhat unique amongst cell types for their dual immunoreactivity to both pancytokeratin and vimentin. During development, mesothelial cells differentiate from their mesodermal precursors, developing features of both epithelial and mesenchymal cells. With certain stimuli, mesothelial cells can undergo epithelial-to-mesenchymal transition (EMT) into other cell types, such as myofibroblasts, smooth muscle cells, and/or endothelial cells.[3] This ability highlights their roles in repair and tissue formation following injury or inflammation.

While this immunohistochemistry (IHC) profile can be a useful feature for diagnosis, there are other neoplasms that can express dual positivity for pancytokeratin and vimentin when neoplastic cells undergo EMT. As mentioned by the contributor, this has been reported in metastases from both ovarian and renal carcinomas.[16] It has also been documented in melanomas and aggressive metaplastic mammary carcinomas in humans.[9] The absence of an additional primary neoplasm can help rule out other tumors, but there are other IHCs utilized in veterinary literature to assist in definitively diagnosing mesotheliomas. The JPC performed in-house calretinin and Wilms Tumor 1 (WT1) immunohistochemistry on this case post-conference, as both of these markers have been utilized in animal species to diagnose mesothelioma successfully.[20] Unfortunately, neither of these IHCs worked on the donkey tissue in this case.

References:

1. Davis CR, Valentine BA, Gordon E, McDonough SP, Schaffer PA, Allen AL, & Pesavento P. Neoplasia in 125 donkeys (*Equus asinus*): literature review and a survey of five veterinary schools in the United States and Canada. *JVDI*. 2016;28(6):662–670.
2. Glickman LT, Domanski LM, Mawire TG, Dumxzig RR, & Churgs A. Mesothelioma in Pet Dogs Associated with Exposure of Their Owners to Asbestos. *Environmental Research.* 1983;32.
3. Hiriart E, Deepe R, Wessels A. Mesothelium and Malignant Mesothelioma. *Journal of Developmental Biology*. 2019;7(2):7

4. Husain AN, et al. Guidelines for pathologic diagnosis of Malignant Mesothelioma: 2017 Update of the consensus statement from the International Mesothelioma Interest Group. *Archives of Pathology and Laboratory Medicine.* 2018;142(1):89–108)
5. Kadota K, Suzuki K, Colovos C, Sima CS, Rusch VW, Travis WD, Adusumilli PS. A nuclear grading system is a strong predictor of survival in epitheloid diffuse malignant pleural mesothelioma. *Mod Pathol.* 2012;25(2):260-71.
6. Kawai T, Kawashima K, Serizawa H, Miura H, Kyeongil K. Adenomatoid mesothelioma with intranuclear inclusion bodies: a case report with cytological and histological findings. *Diagn Cytopathol.* 2014;42(5):436-40.
7. Kim SM, Oh Y, Oh SH, & Han JH. Primary diffuse malignant peritoneal mesothelioma in a striped skunk (*Mephitis mephitis*). *Journal of Veterinary Medical Science.* 2016;78(3):485–487
8. Krametter R, Bago Z, Floeck M, Baumgartner W. Abdominal mesothelioma in a goat. *N Z Vet J.* 2004;52(5):293-6.
9. Kuburich NA, Kiselka JM, den Hollander P, Karam AA, Mani SA. The cancer chimera: Impact of vimentin and cytokeratin co-expression in hybrid epithelial/mesenchymal cancer cells on tumor plasticity and metastasis. *Cancers (Basel).* 2024;16(24):4158.
10. Lopez A, et al. Respiratory system, Thoracic Cavities, Mediastinum, and Pleurae. In: Zachary JF, ed. Pathologic Basis of Veterinary Disease. 6th ed. St. Louis, MO: Mosby Elsevier; 2016: 597-598.
11. McCleery B, Jones MP, Manasse J, Johns S, Gompf RE, Newman S. Pericardial Mesothelioma in a Yellow-naped Amazon Parrot (*Amazona auropalliata*). *J Avian Med Surg*. 2015;29(1):55-62.
12. Misdorp W. Congenital tumours and tumour-like lesions in domestic animals. 1. Cattle. A review. *Vet Q.* 2002;24(1):1-11.
13. Misdorp W. Tumours in calves: comparative aspects. *J Comp Pathol.* 2002;127(2-3):96-105
14. Moberg HL, Gramer I, Schofield I, Blackwood L, Killick D, Priestnall SL, Guillén A. Clinical presentation, treatment and outcome of canine malignant mesothelioma: A retrospective study of 34 cases. *Vet Comp Oncol*. 2022;20(1):304-312.
15. Movassaghi AR, Maleki M, & Khanzadi S. Primary pericardial mesothelioma in a sheep. *Comparative Clinical Pathology.* 2009;18(4):459–461.
16. Munday JS, Löhr CV, and Kiupel M. Tumors of the Alimentary tract - Tumors of the peritoneum and retroperitoneum. In: Meuten DJ, ed. Tumors in Domestic Animal, 5th Ames, IA: John Wiley and Sons Inc; 2017:592-595.
17. Passantino G, Sassi E, Filippi I, Serata V, Tinelli A, Zizzo N. Thoracic and Abdominal Mesothelioma in an Older Horse in Lazio Region. *Animals (Basel).* 2022;12(19):2560.
18. Schlueter AH, Dehghanpir SD, Boudreaux B, Robinson C, Menk P Lima JC, Langohr IM. Feline mesothelioma: case report and review of cytologic, immunocytochemical, histopathologic, and immunohistochemical findings. *J Vet Diagn Invest.* 2021;33(4):753-757.
19. Souza Fde A, de Carvalho CJ, de Almeida HM, Pires LV, Silva Ldos S, Costa FA, Silva SM. Peritoneal mesothelioma in a jaguar (*Panthera onca*). *J Zoo Wildl Med.* 2013;44(3):737-9.
20. Stoica G, Cohen N, Mendes O, Kim HT. Use of immunohistochemical marker calretinin in the diagnosis of a diffuse malignant metastatic mesothelioma in an equine. *J Vet Diagn Invest*. 2004;16(3):240-3.
21. Testa JR, Berns A. Preclinical Models of Malignant Mesothelioma. *Front Oncol.* 2020;10:101.
22. Uzal FA, Plattner BL, Hostetter JM. Alimentary system. In: Maxie MG, ed. Jubb, Kennedy, and Palmer's Pathology of Domestic Animals, Vol 2, 6th ed. St. Louis, MO: Elsevier; 2016:256-7.

CASE IV:

Signalment:
6 year-old female Merino sheep (*Ovis aries*)

History:
Six of 2,300 5-6 year old first cross ewes run on improved pastures in the Cowra district of NSW were noticed to be unusually thin in late October 2014. As ovine Johne's disease was considered a possibility, one of these ewes was euthanased and necropsied on the 26 November 2014.

Gross Pathology:
The serosa of the small intestine, caecum and colon was covered in miliary to focally extensive firm, white, raised plaques. In some areas, the plaques were as small as 1mm diameter, pinpoint lesions, whereas in others as much as 90 percent of the serosal surface was covered.

Laboratory Results:
N/A.

Microscopic Description:
Colon: The lamina propria, submucosa, muscularis mucosa and serosa are markedly expanded by a poorly demarcated, non-encapsulated, infiltrative neoplasm composed of two populations of neoplastic epithelial cells. The neoplastic cells occur singly and in loose packets, lobules and cords, and are supported by variable fibrous stroma containing fibrocytes, fibroblasts and a light basophilic matrix. The predominant neoplastic cell is round to ovoid, 20–50 µm in diameter, with distinct cell borders, abundant finely granular basophilic cytoplasm, peripherally located oval nuclei with lightly stippled pale chromatin and single nucleoli. The secondary type of neoplastic cell is round to oval; 15-30 µm in diameter; with distinct cell borders; moderate amounts of cytoplasm containing small eosinophilic granules; single, peripherally located, large nuclei with coarse chromatin and single nucleoli. Both sub-populations of neoplastic cells exhibit moderate anisocytosis and anisokaryosis. Mitoses are rare (< 1 per HPF). There is moderate expansion of the adventitia of large vessels with neoplastic cells. The lamina propria propria is diffusely expanded by moderate numbers of lymphocytes, plasma cells, occasional macrophages and rare eosinophils. Crypts are often ectatic, lined with attenuated epithelium and containing non-degenerate neutrophils, rare macrophages and lymphocytes (crypt abscess).

Figure 4-1. Sheep, jejunum: The serosa of the small intestine, caecum, and colon is covered in military to focally extensive firm, white, raised, plaques. (Photo courtesy of: Elizabeth Macarthur Agricultural Institute, Menangle, New South Wales.)

Figure 3-2. Sheep, jejunum: Plaques are white, and slightly raised. Lymphatics are mildly dilated. (Photo courtesy of: Elizabeth Macarthur Agricultural Institute, Menangle, New South Wales.)

Contributor's Morphologic Diagnoses:
1. Large intestine, colon: Intestinal adenocarcinoma, sheep (Ovis aries), ruminant.

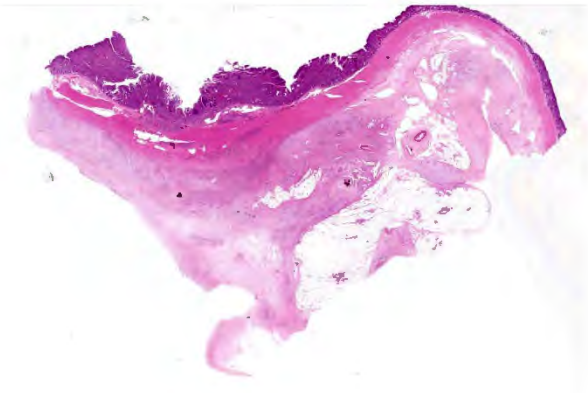

Figure 4-3. Sheep, ileocecal junction: One section of jejunum is submitted for examination. Centrally, there is an area of architectural loss within the mucosa, and an infiltrative neoplasm extending transmurally to the markedly fibrotic serosa. (HE, 7X).

2. Large intestine: Colitis, lymphoplasmacytic, chronic, diffuse, mild, with multifocal crypt abscesses.

Contributor's Comment:

Intestinal adenocarcinoma is a common gastrointestinal tumour of older sheep.[4,11] A wide range of neoplasms have been described in sheep, adenocarcinoma of the small intestine is reported to be the most common of these by far (Table 1).[2] Most are usually discovered at slaughter as incidental findings; if clinical signs are present, weight loss and occasionally ascites are usually the only signs. In an early report of the disease, Ross (1980) reported an overall prevalence of 0.272 percent in sheep examined at abattoirs in southern NSW, and McDonald and Leaver (1965) found that 0.4 percent of all sheep on a single property and 2 percent of sheep over 5 years of age had lesions consistent with intestinal adenocarcinoma.[5,12]

To date, only a limited number of studies have investigated factors associated with intestinal adenocarcinoma in sheep. According to Simpson (1972), intestinal adenocarcinoma in New Zealand is more common in British breeds than in "fine wool" breeds, and is associated with increased stocking density.[13] Ross (1980) reported that regional prevalence in NSW varied between 0.2 to 1.5 percent, however Simpson (1972) found that geographic variation in the prevalence of intestinal adenocarcinoma was not statistically significant.[12,13] Munday et al. (2009) found no association between intestinal adenocarcinoma and herpesviruses, *Helicobacter* spp., or *Mycobacterium avium* subspecies *paratuberculosis* in sheep in New Zealand.[9]

Intestinal adenocarcinomas have been reported in a wide range of animal species. [3] Ovine intestinal adenocarcinomas appear histologically similar to human colonic adenocarcinomas, although there are differences in site of primary growth, development of polyps, and site of metastasis.[6] Neoplastic ovine intestinal adenocarcinoma cells grown in vitro do not express fibronectin, and have altered expression of beta-catenin, E-cadherin, cycloxygenase-2, and p53 protein.[7,10] Mismatch repair protein defects do not appear to be associated with tumorigenesis.[8] Other differential diagnoses for chronic ill-thrift in sheep include ovine Johne's disease (OJD), malnutrition, balanoposthitis, cutaneous myiasis, peritonitis and pneumonia. [11] From a

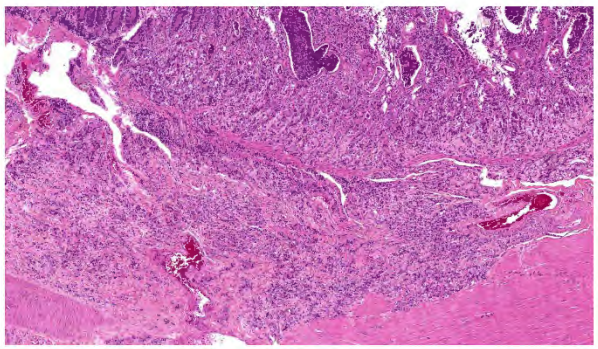

Figure 4-4. Sheep, ileocecal junction: The neoplasm extends from the overlying disordered mucosa through the muscularis mucosa into the submucosa. In the overlying mucosa, remnant crypts are markedly ectatic and filled with neutrophils and cellular debris. (HE, 105X).

production and biosecurity perspective, OJD is of the most concern. The two diseases appear markedly different grossly and histologically, although the simultaneous occurrence of both diseases has been reported by Bush et al. (2006).[1]

Table 1: Neoplasms in sheep described at the Ruakura Animal Health Laboratory from 1955 to 1968. Adapted from Cordes and Shortridge (1971)[2]

Site of neoplasm	No. of cases	Diagnosis
Small intestine	143	Mucous-gland adenocarcinoma
Liver	12	Hepatoma
	2	Adenocarcinoma - possibly primary in genitalia
Liver and/or pancreas	15	Ductal adenocarcinoma
Adrenal	1	Cortical adenoma
Pituitary	1	Adenocarcinoma of pars intermedia
Ovary	3	Granulosa tumour
Testicle	2	Seminoma
	1	Sertoli cell tumour
Kidney	1	Renal adenocarcinoma
	3	Embryonal nephroma
Epidermis	4	Papilloma of skin
	2	Squamous carcinoma of mouth
	1	Metastatic squamous carcinoma in liver and colon
	1	Squamous carcinoma of ear
Reticuloendothelial system	32	Lymphosarcoma - lymphoid
	7	Lymphosarcoma - reticulum cell
of	1	Thymoma
Blood vessel	8	Angiosarcoma of:
		brain (1)
		liver (5)
		stifle joint (1)
		hock joint (1)
Nerve	1	Neurofibroma of wall of thorax
Striated muscle	3	Rhabdomyoma of heart
Brain	1	Astrocytoma
Other connective tissues	4	Fibrosarcoma
	3	Myxosarcoma
	2	Osteogenic sarcoma
	1	Liposarcoma
	1	Synovioma

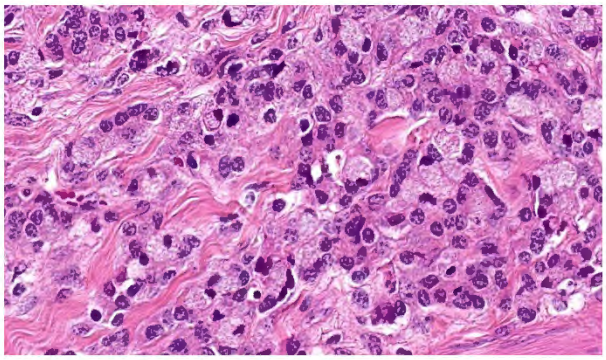

Figure 4-5. Sheep, ileocecal junction: High magnification of neoplastic cells. (HE, 1051X).

Contributing Institution:

State Veterinary Diagnostic Laboratory
Elizabeth Macarthur Agricultural Institute
Woodbridge Rd
Menangle
NSW 2568
Australia

JPC Diagnoses:

Ileocecal junction: Intestinal adenocarcinoma.

JPC Comment:

This last case is a classic! Many thanks to the contributor for a great submission and write-up. Most participants were readily able to reach a diagnosis of intestinal adenocarcinoma in this case due to the high mitotic rate, degree of invasion the neoplasm into abluminal tis-

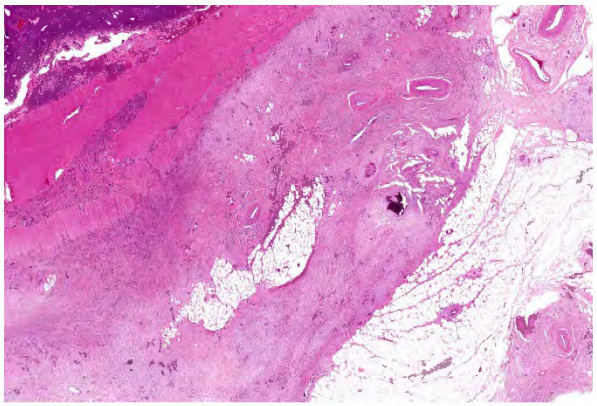

Figure 4-6. Sheep, ileocecal junction: The neoplasm extends through the markedly fibrotic serosa into the adjacent mesentery. (HE, 23X).

sue layers, and the striking desmoplastic response. The deep infiltration from the mucosa outwards allows for a strong argument of a primary intestinal adenocarcinoma rather than a metastatic carcinoma. Intestinal adenocarcinomas tend to invade from the mucosa deep into and run laterally through the submucosa and subsequent layers.

In sheep, the primary ruleout would be metastatic uterine adenocarcinoma, but this would more likely present on the serosal surface due to direct seeding of the abdomen (carcinomatosis) or via lymphatic spread rather than invading from the mucosa. Additionally, intestines are not a primary site for lymphatic metastases for uterine adenocarcinoma in most species; the lungs, liver, and mesentery, however, are.[3] Although generally considered an incidental finding at slaughter, previous studies have demonstrated an increased incidence of intestinal adenocarcinoma in sheep in New Zealand following exposure to feedstuffs sprayed with phenoxy and picolinic acid herbicides.[10]

Despite being able to reach a diagnosis, most participants struggled with the specific anatomic location for this tissue. After much back and forth, the consensus amongst conference-goers was that this is likely representative of the ileocecal junction or close to it, since there are features of both small and large intestine on opposite ends of the H&E slide. While there are crypts, mucus glands, and subcutaneous fat consistent with large intestine visible on one side, there are also villi on the other, most clearly seen associated with and around the neoplasm.

Lastly, there are notable mucosal erosions with regional neoplasia-associated architecture disruption that most participants felt was likely the cause of the inflammation present in the slide rather than an additional primary enteritis. As such, this is reflected in the JPC morphologic diagnosis, which focuses solely on the neoplasm and considers the other changes to be secondary.

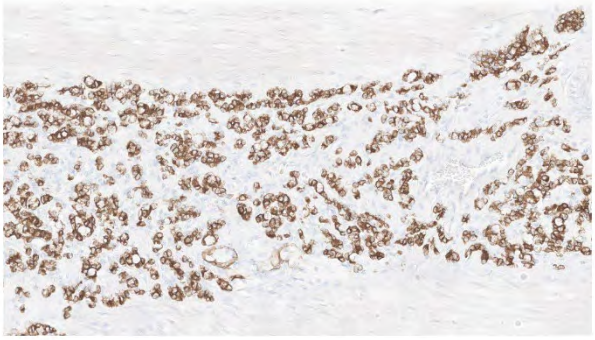

Figure 4-7. Sheep, ileocecal junction: Neoplastic cells demonstrate strong cytoplasmic immunoreactivity for cytokeratin. (anti-AE1/AE3, 321X).

References:

1. Bush RD, Toribio JA, Windsor PA: The impact of malnutrition and other causes of losses of adult sheep in 12 flocks during drought. *Aust Vet J.* 2006:84(7)**:**254-260.
2. Cordes D, Shortridge E: Neoplasms of sheep: a survey of 256 cases recorded at Ruakura Animal Health Laboratory. *NZ Vet J.* 1971:19(4)**:**55-64.
3. Hananeh WM, Ismail ZB, Daradka MH. Tumors of the reproductive tract of sheep and goats: A review of the current literature and a report of vaginal fibroma in an Awassi ewe. *Vet World.* 2019;12(6):778-782.
4. Lingeman CH, Garner F: Comparative study of intestinal adenocarcinomas of animals and man. *Journal of the National Cancer Institute.* 1972:48(2)**:**325-346.
5. Maxie G: Jubb, Kennedy & Palmer's Pathology of Domestic Animals: 3-Volume Set: Elsevier Health Sciences; 2007.
6. McDonald JW, Leaver DD: Adenocarcinoma of the small intestine of Merino sheep. *Australian Veterinary Journal.* 1965:41(9)**:**269-271.
7. Munday JS, Brennan MM, Jaber AM, Kiupel M: Ovine intestinal adenocarcinomas: histologic and phenotypic comparison with human

colon cancer. *Comp Med.* 2006:56(2)**:**136-141.
8. Munday JS, Brennan MM, Kiupel M: Altered expression of beta-catenin, E-cadherin, cycloxygenase-2, and p53 protein by ovine intestinal adenocarcinoma cells. *Vet Pathol.* 2006:43(5)**:**613-621.
9. Munday JS, Frizelle FA, Whitehead MR: Mismatch repair protein expression in ovine intestinal adenocarcinomas. *Vet Pathol.* 2008:45(1)**:**3-6.
10. Munday JS, Keenan JI, Beaugie CR, Sugiarto H: Ovine small intestinal adenocarcinomas are not associated with infection by herpesviruses, *Helicobacter* species or *Mycobacterium avium* subspecies *paratuberculosis. J Comp Pathol.* 2009:140(2-3)**:**177-181.
11. Newell KW, Ross AD, Renner RM. Phenoxy and picolinic acid herbicides and small-intestinal adenocarcinoma in sheep. *Lancet*. 1984;2(8415):1301-5.
12. Norval M, Head K, Else R, Hart H, Neill W: Growth in culture of adenocarcinoma cells from the small intestine of sheep. *British journal of experimental pathology.* 1981:62(3)**:**270.
13. Radostits OM, Gay CC, Hinchcliff KW, Constable PD: Diseases caused by bacteria *Veterinary Medicine: A Textbook of the Diseases of Cattle, Sheep, Pigs, Goats, and Horses*: Elsevier Saunders; 2007:920.
14. Ross AD: Small intestinal carcinoma in sheep. *Aust Vet J.* 1980:56(1)**:**25-33.
15. Simpson BH: The geographic distribution of carcinomas of the small intestine in New Zealand sheep. *New Zealand Veterinary Journal.* 1972:20(3)**:**24-28.

Joint Pathology Center
Veterinary Pathology Services

WEDNESDAY SLIDE CONFERENCE 2025-2026

Conference #15 — 14 January 2026

CASE I:

Signalment:
29 week old, intact female, C57BL/6NCrl mouse (*Mus musculus*)

History:
This animal was utilized in a study of chronic kidney disease and was euthanized at a pre-defined study endpoint.

Gross Pathology:
The body weight was 14 g and the mouse had decreased fat stores. Bilaterally the kidneys were diffusely pale-tan and shrunken with a pitted appearance and miliary white depressed foci.

Laboratory Results:
Serum chemistry demonstrated elevated BUN (94 mg/dL; ref 5-28), creatinine (0.54 mg/dL; ref 0.20-0.50), globulin (2.9 g/dL; ref 1.7-2.2), and phosphorous (15.4 mg/dL; ref 7.3-14.5).

Complete blood count demonstrated a microcytic, hypochromic, regenerative anemia (HCT 33.2%, ref 37.2-62.0; MCV 36.1 fL, ref 42.6-56.0; MCH 11.3 pg, ref 13-16.8; RET 603.8 K/uL, ref 294-444).

Automated leukocyte differential demonstrated leukopenia (3.26 K/uL, ref 3.9-13.96) characterized by a lymphopenia (0.82 K/uL, ref 2.88-10.92).

Urine specific gravity was low (1.015, ref 1.050-1.093).

Microscopic Description:
Kidney. The surface of the renal cortex is undulating with an irregular, scalloped appearance. Multifocally, renal tubules are dilated and have an attenuated epithelium. Dilated tubules are variably filled with an amorphous, pale basophilic material or abundant degenerate neutrophils, and less commonly contain brown to pale basophilic, spiculated, radiating birefringent crystalline material (2,8-dihydroxyadenine crystals) or dark basophilic coarsely granular material Occasionally, crystal-filled tubules are surrounded by neutrophils, macrophages, and multinucleated giant cells. Often, Bowman's spaces are mild to moderately dilated. Throughout the renal parenchyma, between tubules are streams of fibroblasts and collagen.

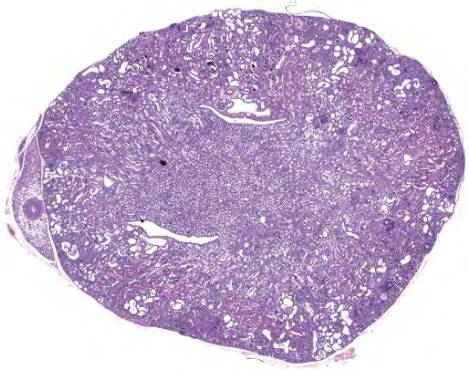

Figure 1-1. Kidney, mouse: At sub-gross magnification, groups of ectatic tubules are present in the cortex along with abundant mineral. The capsule has an undulant profile. (HE, 10X)

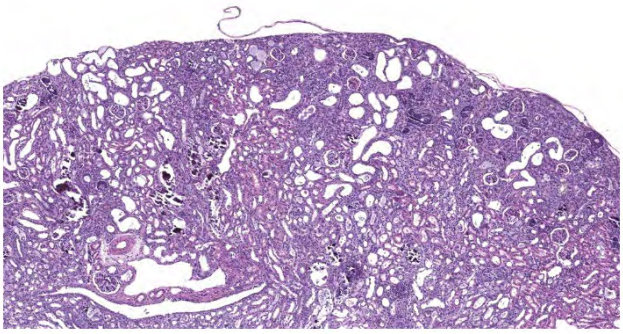

Figure 1-2. Kidney, mouse: Within the cortex, regional groups of tubules demonstrate ectasia with epithelial attenuation, loss of cytoplasmic eosinophilic eosinophilia, and mineralization. (HE, 94X)

Contributor's Morphologic Diagnoses:

Liver: Microvesicular hepatopathy, moderate, acute, diffuse, with mild centrilobular hepatocellular necrosis.

Contributor's Comment:

This mouse was administered 0.2% adenine in the diet for six weeks as part of a study on CKD. The animal was part of the control group and received no experimental manipulations except for adenine administration. The adenine diet model is a commonly utilized, well-established model of chronic kidney disease (CKD) in mice and rats.[9] This diet induces a tubulointerstitial nephritis secondary to the metabolism of adenine in the kidneys. Adenine is metabolized by the enzyme xanthine dehydrogenase into 2,8-dihydroxyadenine (DHA), which precipitates in renal tubules, resulting in crystal formation.[16] Injury of the tubules leads to tubulointerstitial inflammation which progresses over time to interstitial fibrosis.[15] The model mirrors some of the clinicopathologic findings observed in human and animal CKD, including azotemia, hyperphosphatemia, elevated parathyroid hormone (PTH), and anemia.[4,13,16] This model is well-established and reproducible in rodents, and while it has also been described in rabbits it is not well characterized in this species.[5]

Naturally occurring chronic renal disease in mammals typically results in non-regenerative anemia due to decreased production of erythropoietin, increased hepcidin, suppression of erythropoiesis, and decreased red blood cell lifespan.[11] Studies of the adenine diet model of chronic kidney disease in rodents have demonstrated variation in the nature of the resulting anemia. Some studies employing the adenine diet model to study anemia of CKD have demonstrated no difference in absolute reticulocyte count between anemic and non-anemic animals, consistent with a non-regenerative response that is expected in a model of CKD-associated anemia.[2, 17] However, others have demonstrated anemia with an increase in absolute reticulocyte count in rodents consuming a high-adenine diet.[1] In the course of this study, we have observed an apparent regenerative response characterized by increased reticulocytes in adenine-treated mice. The mechanism for reticulocytosis in the face of overt renal insufficiency is not yet understood.

Rodents consuming a high-adenine diet begin to demonstrate evidence of renal injury, including reduction in creatinine clearance and intraluminal crystals, starting on day 3 after diet initiation.[10] DHA crystals are brown, spiculated spheres which are birefringent in polarized light microscopy. Kidney lesions progresses as the diet is maintained, with tubular damage as the primary lesion. Crystals are primarily localized to proximal tubules and ascending limbs of the loops of Henle.[10] Glomeruli are not directly injured by DHA nephropathy; however, dilation of the Bowman's space is reported as a histologic finding of the adenine diet model.[9] Direct tubular injury is accompanied by inflammation characterized primarily by macrophages which accumulate around injured tubules.[10,15] Over time,

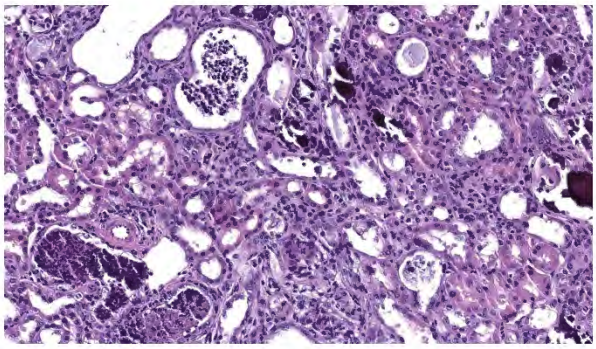

Figure 1-3. Kidney, mouse: Higher magnification of tubular changes with ectasia, collapse, proteinosis, mineralization, infiltration of tubular lumens with necrotic neutrophils, and expansion of the interstitium with macrophages and mild fibrosis. (HE, 381)

tubular injury and inflammation progresses to interstitial fibrosis.

In humans, an inherited defect in purine metabolism leads to the accumulation of DHA and subsequent DHA nephrolithiasis. This autosomal recessive disorder results from a mutation of the gene encoding the enzyme adenine phosphoribosyltransferase (APRT), which normally catalyzes the formation of 5'-adenosine monophosphate (AMP) from adenine.[3] Without this enzyme, adenine is instead metabolized to DHA which, as in the mouse model, precipitates within renal tubules and causes crystalline nephropathy. The mechanisms of the adenine diet in rodents closely recapitulate this human disease, making the adenine diet model a suitable preclinical model APRT deficiency.[10] While the currently reported prevalence of APRT deficiency in human populations is quite low, this may represent an under-reporting of disease frequency.[3] Biochemical stone analysis fails to differentiate DHA from uric acid, so stereomicroscopic analysis of urinary stones and infrared spectroscopy are preferable.[3]

DHA nephrolithiasis, likely caused by a similar genetic mutation, has been reported rarely in dogs.[6, 8] There is a breed predisposition for primitive-type breeds such as malamutes and Native American Indian dogs. The genetic mutation identified in affected dogs is a missense mutation of the *APRT* gene.[6] Clinically, affected animals have been documented to develop uroliths throughout the upper and lower urinary tract, which in some cases progress to obstructive renal failure. Treatment, as in humans, is administration of xanthine dehydrogenase inhibitors such as allopurinol.

Multiple drugs and toxins are capable of causing renal intratubular crystallization and subsequent damage. Ethylene glycol and melamine/cyanuric acid toxicosis are two examples of crystal nephropathy of veterinary importance. In contrast to DHA precipitation in the adenine diet model, ethylene glycol (EG) and melamine/cyanuric acid ingestion result in calcium oxalate monohydrate crystals or melamine-containing crystals, respectively. In EG toxicosis, EG metabolism results in the production of several end products, including oxalic acid. Oxalic acid binds to calcium within renal tubules and forms calcium oxalate crystals, which are directly cytotoxic and results in renal tubular epithelial cell death.[12] The mechanism of melamine renal toxicity is less clearly elucidated, but co-administration of melamine and cyanuric acid appears necessary to induce crystal formation.[14] Presence of melamine/cyanuric acid crystals within renal tubules is associated with tubular epithelial necrosis.[7]

Contributing Institution:
Laboratory of Comparative Pathology, Memorial Sloan Kettering Cancer Center, The Rockefeller University, Weill Cornell Medicine. https://www.mskcc.org/research/ski/core-facilities/comparative-medicine-pathology-0

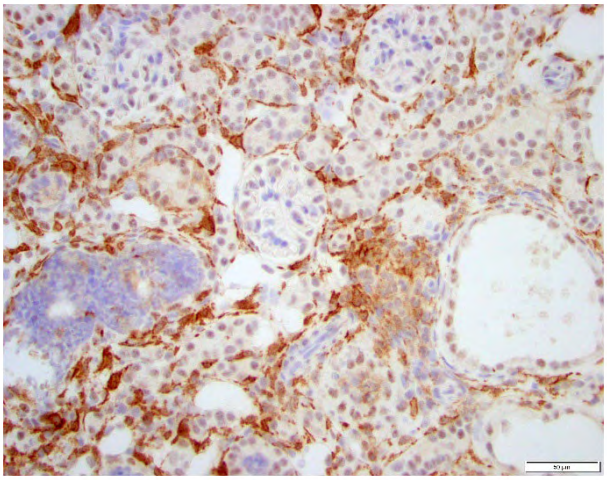

Figure 1-4. Kidney, mouse: There are moderate numbers of IBA-1 immunopositive macrophages withi the interstitium. (anti-IBA-1, 400X)) (Photo courtesy of: Laboratory of Comparative Pathology, Memorial Sloan Kettering Cancer Center, The Rockefeller University, Weill Cornell Medicine. https://www.mskcc.org/research/ski/core-facilities/comparative-medicine-pathology-0)

JPC Diagnoses:
Kidney, cortex: Tubular degeneration, necrosis, and regeneration, chronic, diffuse, marked, with intratubular and interstitial crystals, granular and hyaline casts, mineralization, and interstitial fibrosis.

JPC Comment:
Conference 15 was moderated by the globally renowned Dr. Cory Brayton, a top expert in mouse pathology from Johns Hopkins School of Medicine. This first case is one that has never been seen before in the WSC, and the contributor provided an outstanding write-up to accompany it.

Conference discussion covered multiple topics, some of which are covered in the provided write-up. Dr. Brayton spoke on numerous important features in the evaluation of a case such as this. These included knowing the history of the affected animal, understanding common background lesions in particular mice strains, and where the discerning pathologist should look for mineral in the kidneys (within tubules, in tubular basement membranes, and within vascular tunics). Additionally, emphasis was placed on ensuring one takes the time to evaluate the presence or absence of tubular degeneration, regeneration, and/or atrophy (all of which were present in this case as tubular damage is the primary lesion of adenine nephritis), and the histologic appearance of crystals. There was some speculation amongst participants on the presence of tubular regeneration in this slide, which is typically characterized by hypercellular, more basophilic tubules with a high N:C ratio in their epithelial cells. Ultimately, the presence of regenerative tubules was agreed upon, although it took the more experienced eyes in the room to point them out to less experienced participants. The Non-Neoplastic Lesion Atlas and Mouse INHAND guide both have excellent examples of tubular regeneration for those that may be unfamiliar.[6,16] There was discussion on how to discern atrophy of brown fat after one participant questioned if the adipose tissue in the slide was atrophic or just brown fat (it was brown fat), which is challenging, but best assessed around the salivary gland in mice. Atrophic brown fat has the appearance of being its own unidentifiable organ due to the degree of consolidation; don't be fooled!

There was significant discussion on the complete blood count (CBC) of this case, which demonstrated a microcytic, hypochromic, regenerative anemia. This struck conference participants as odd since most chronic kidney disease (CKD) patients have a normochromic, non-regenerative anemia due to the lack of erythropoietin production from the damaged kidneys. Additionally, the reticulocyte count was reportedly elevated, which should have

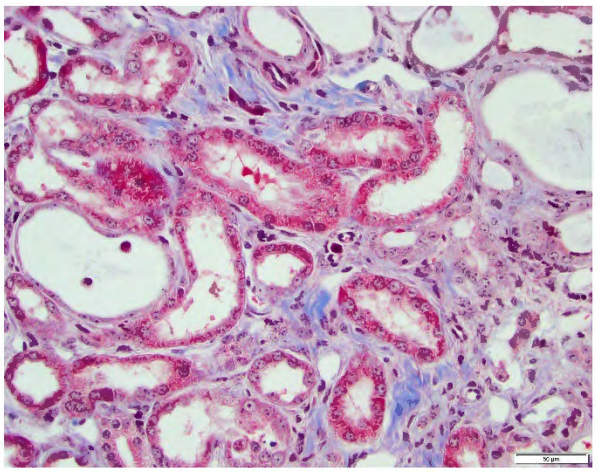

Figure 1-5. Kidney, mouse: A Masson's trichrome stain highlights the mild interstitial fibrosis. (Masson's, 400X) (Photo courtesy of: Laboratory of Comparative Pathology, Memorial Sloan Kettering Cancer Center, The Rockefeller University, Weill Cornell Medicine. https://www.mskcc.org/research/ski/core-facilities/comparative-medicine-pathology-0).

resulted in macrocytosis rather than microcytosis. The blood chemistry profile of this animal also revealed an elevated BUN, mildly elevated creatinine, mildly elevated globulin, and mild hyperphosphatemia. While these findings indicate an azotemia was present, the elevated globulin and phosphorus levels may suggest that this animal was dehydrated and had a pre-renal azotemia rather than renal azotemia. Urine specific gravity (USG) and total protein (TP) measurements would have helped tease this out further, but conference participants acknowledge that there are limitations in some cases. Additionally, most laboratories have their own reference ranges for different strains of mice that often differ from those used in other labs, so conference participants assumed that this contributor's lab knows their reference ranges in this particular mouse strain and deferred to their data in drawing these conclusions. It certainly made for excellent discussion!

While the history of an adenine diet in this mouse made for a straightforward diagnosis, other possible causes of brown crystals in kidneys include melamine cyanuric acid, bilirubin, calcium carbonate, and ammonium biurate, to name the most pertinent. Additional causes of proximal convoluted tubular (PCT) damage in other species that win honorable mentions from conference discussion include aminoglycosides (foals and humans), oxalates (ruminants), monensin (horses and poultry), and ethylene glycol (dogs, cats, and humans).

Lastly, wrapping up discussion was a quick mention by Dr. Brayton on the potential for Mouse Kidney Parvovirus (MKPV) to confound CKD studies in mice. In a recent study, it was found that MKPV-infected mice on an adenine diet for CKD study had more interstitial nephritis at one month and two months of diet consumption compared to those that did not have MKPV.[15] They also had less interstitial fibrosis at 2 months comparatively.[15] This virus, which makes for some stunning histologic images, by the way (please see the cover of the new Barthold book), can complicate grading and evaluation of CKD-associated lesions in mice that are infected during the study period and, as such, lesions should be interpreted with caution and contexts.

References:

1. Akchurin O, Patino E, Dalal V, et al. Interleukin-6 contributes to the development of anemia in juvenile CKD. *Kidney International Reports*. 2019;4:470-483.
2. Akchurin O, Sureshbabu A, Doty SB, et al. Lack of hepcidin ameliorates anemia and improves growth in an adenine-induced mouse model of chronic kidney disease. *Am J Physiol Renal Physiol*. 2016;311(5):F877-F889.

3. Bollee G, Harambat J, Bensman A, Knebelmann B, Daudon M, Ceballos-Picot I. Adenine Phosphoribosyltransferase Deficiency. *Clin J Am Soc Nephrol*. 2012;7:1521-1527.
4. deFrutos S, Luengo A, Garcia-Jerez A, et al. Chronic kidney disease induced by an adenine rich diet upregulates integrin linked kinase (ILK) and its depletion prevents the disease progression. *BBA Molecular Basis of Disease.* 2019;1865:1284-1297.
5. Florens N, Lemoine S, Pelletier CC, Rabeyrin M, Juillard L, Soulage CO. Adenine Rich Diet Is Not a Surrogate of 5/6 Nephrectomy in Rabbits. *Nephron*. 2017;135:307-314.
6. Frazier KS, Seely JC, Hard GC, et al. Proliferative and nonproliferative lesions of the rat and mouse urinary system. *Toxicol Pathol*. 2012;40(4 Suppl):14S-86S.
7. Furrow E, Pfeifer RJ, Osborne CA, Lulich JP. An APRT mutation is strongly associated with and likely causative for 2,8-dihydroxyadenine urolithiasis in dogs. *Mol Genet Metab.* 2014;111(3):399-403.
8. Hau AK, Kwan TH, Li PK. Melamine Toxicity and the Kidney. *J Am Soc Nephrol.* 2009;20:145-250.
9. Houston DM, Moore AE, Mendonca SZ, Taylor JA: 2,8-Dihydroxyadenine uroliths in a dog. *J Am Vet Med Assoc*. 2012;241:1348–1352.
10. Jia T, Olauson H, Lindberg K, et al. A novel model of adenine-induced tubulointerstitial nephropathy in mice. *BMC Nephrology.* 2013;14:116.
11. Klinkhammer BM, Djudjaj S, Kunter U, et al. Cellular and Molecular Mechanisms of Kidney Injury in 2,8-Dihydroxyadenine Nephropathy. *J Am Soc Nephrol.* 2020;31:799-816.
12. Lippi I, Perondi F, Lubas G, et al. Erythrogram patterns in dogs with chronic kidney disease. *Vet Sci*. 2021;8(7):123.
13. McMartin K. Are calcium oxalate crystals involved in the mechanism of acute renal failure in ethylene glycol poisoning? *Clinical Toxicology*. 2009;47(9):859-869.
14. Rahman A, Yamazaki D, Sufiun A, et al. A novel approach to adenine-induced chronic kidney disease associated anemia in rodents. *PLoS ONE*. 2018;13(2): e0192531.
15. Ritter AC, Arbona RRJ, Livingston RS, Monette S, Lipman NS. Effects of Mouse Kidney Parvovirus on Pharmacokinetics of Chemotherapeutics and the Adenine Model of Chronic Kidney Disease. *Comp Med*. 2023;73(2):153-172.
16. Sands JM, Verlander JW. Anatomy and physiology of the kidneys. In: Toxicology of the Kidney, 3rd ed (Tarloff JB, Lash LH, eds). CRC Press, Boca Raton, FL. 2005;3-56.
17. Son JY, Kang YJ, Kim KS, et al. Evaluation of Renal Toxicity by Combination Exposure to Melamine and Cyanuric Acid in Male Sprague-Dawley Rats. *Toxicol*. Res. 2014;30(2):99-107.
18. Tamura M, Aizawa R, Hori M, Ozaki H. Progressive renal dysfunction and macrophage infiltration in interstitial fibrosis in an adenine-induced tubulointerstitial nephritis mouse model. *Histochem Cell Biol*. 2009;131:483-490.

19. Tani T, Orimo H, Shimizu A, Tsuruoka S. Development of a novel chronic kidney disease mouse model to evaluate the progression of hyperphosphatemia and associated mineral bone disease. *Scientific Reports*. 2017;7:2233.
20. Thibodeau JF, Simard JC, Holterman CE, et al. PBI-4050 via GPR40 activation improves adenine-induced kidney injury in mice. *Clin Sci (Lond)*. 2019;133(14):1587-1602.

CASE II:

Signalment:
21-year-old, intact male, rhesus macaque, (*Macaca mulatta*)

History:
This Indian-origin rhesus macaque has a history of oral and dental disease. Approximately four months prior to necropsy, heavy dental calculus, gingivitis, and loose teeth necessitated cleaning and extraction of multiple teeth. The extraction sites did not heal despite several therapies. Radiographs revealed a retained tooth fragment and an oronasal fistula. The dental fragment was removed and this surgical site also failed to heal. Incisional biopsies of the palatine mucosa and buccal mucosa were collected and microscopic evaluation revealed an ameloblastoma. Euthanasia was elected.

Gross Pathology:
Well-muscled, aged, intact male rhesus monkey in excellent nutritional condition (body weight 11.8, body condition score 3/5). Expanding the buccal mucosa and gingiva adjacent to the dental extraction sites and invading the hard palate is a pale, white, glistening neoplasm that measures up to 3.6 cm in greatest dimension (tissue not submitted). The gastric mucosa is diffusely and moderately thickened

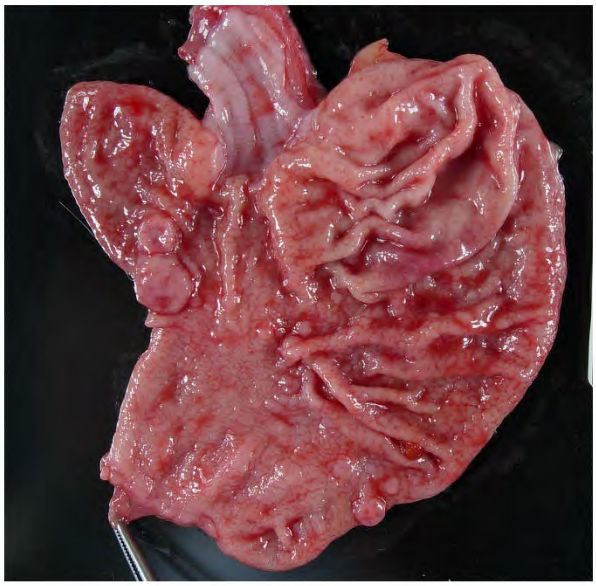

Figure 2-1. Stomach, rhesus macaque: Numerous round, fleshy, dark pink, sessile tumors protrude from the gastric mucosa into the lumen and measure up to 1 cm in diameter (Photo courtesy of: Oregon National Primate Research Center, https://www.ohsu.edu/onprc).

and exhibits a cobblestone pattern. Round, fleshy, dark pink, sessile tumors protrude from the gastric mucosa into the lumen and measure up to 1 cm in diameter. There are multiple outpouchings of the intestinal mucosa (diverticulosis). The free margins of the left atrioventricular valve are minimally thickened and nodular (endocardiosis). The aortic intima is multifocally thickened with raised white to yellow irregular plaques (atherosclerosis). Few cysts measuring up to 0.2 cm in diameter are present in both renal cortices.

Laboratory Results:
N/A.

Microscopic Description:
Focally elevating the attenuated, intact superficial epithelium and expanding the gastric mucosa and submucosa and displacing gastric

Figure 2-2. Stomach, rhesus macaque: Two full-thickness sections of stomach are submitted for examination. (HE, 9X)

glands are multiple, coalescing, partially encapsulated multilobulated neoplasms composed of nests and packets of neoplastic cells supported by a fine fibrovascular stroma.

)Some rosette formation with luminal blood is present and in other areas, there is pseudoglandular formation with entrapment of glands and foveolar epithelium. Neoplastic cells are round to polygonal with variably indistinct cell borders and amphophilic to pale eosinophilic, lightly granular cytoplasm. Nuclei are round to oval with usually one distinct nucleolus and finely dispersed to coarsely stippled chromatin. Occasionally, neoplastic cells contain up to three nuclei. There is moderate to marked anisocytosis and anisokaryosis and less than one mitotic figure/HPF. Submucosal vascular invasion is present. There is proprial edema overlying mucosal nodules. Moderate numbers of plasma cells and lymphocytes, fewer eosinophils, and occasional macrophages, neutrophils, and Mott cells are present within the lamina propria and multifocally traverse the muscularis mucosa and extend to the submucosa. Multifocally, there is foveolar hyperplasia and dysplasia and expansion of the mucosa-associated lymphoid tissue. The submucosa is variably edematous and lymphatic vessels are ectatic.

Contributor's Morphologic Diagnoses:

1. Stomach: Neuroendocrine tumor (carcinoid), multiple, mucosa and submucosa with vascular invasion.

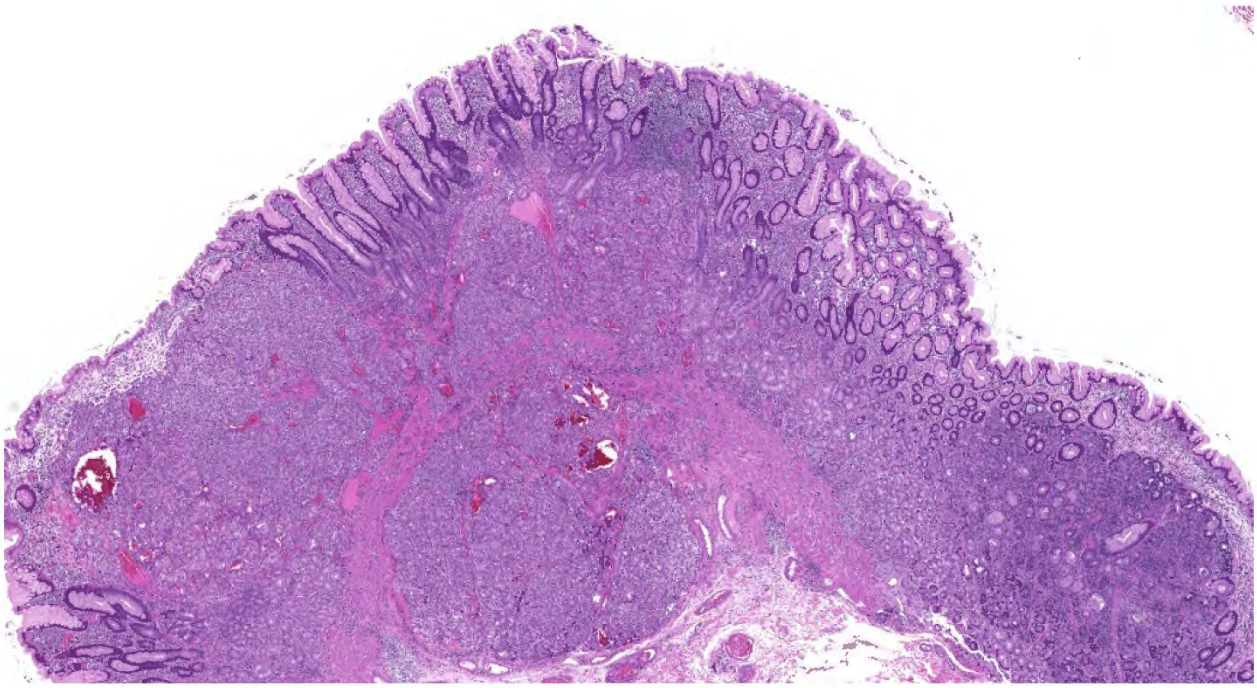

Figure 2-3. Stomach, rhesus macaque: There is a neoplasm infiltrating the gastric mucosa and underlying submucosa. (HE, 44X)

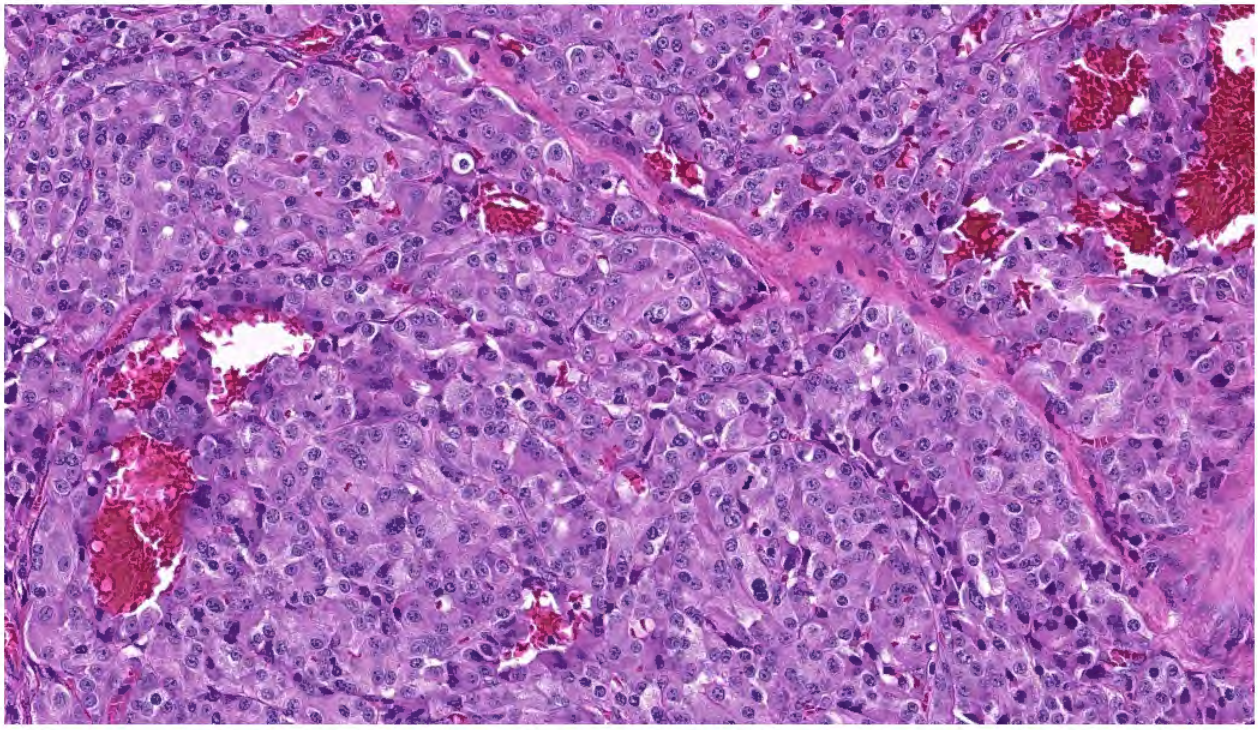

Figure 2-4. Stomach, rhesus macaque: Neoplastic cells are arranged in nests and packets. (HE, 306X)

2. Stomach: Gastritis, plasmacytic, lymphocytic, few eosinophils and occasional macrophages, neutrophils, and Mott cells, diffuse, moderate, with multifocal, mild foveolar hyperplasia and dysplasia.

Contributor's Comment:

This macaque had multiple malignant gastric carcinoids. Vascular invasion was evident in the vasculature of the submucosa; however, regional or distant metastases were not identified on microscopic examination of remaining tissues. A Churukian-Schenk histochemical stain highlighted argyrophilic granules within neoplastic cells, and neoplastic cells were also immunoreactive for chromogranin A, a neuroendocrine marker (fig. 3). The histologic features, immunohistochemical and special histochemical staining of these neoplasms were consistent with the diagnosis of carcinoids.

Gastric carcinoid tumors arise from the neuroendocrine cells of the mucosa and are rare in this large nonhuman primate colony. A retrospective review of pathology records spanning the last six decades at the center revealed only one other case of gastric carcinoid in an adult female rhesus macaque. A single, malignant carcinoid that exhibited lymphatic invasion was diagnosed. During a recent virtual conference, multiple neuroendocrine gastric neoplasms were reported in an aged rhesus macaque. (Ruivo, P. 2023, April 25. Gastric Neuroendocrine Tumor, NHPRC Virtual Slide Conference, California National Primate Research Center, UC Davis School of Veterinary Medicine.) A review of the literature revealed rare reports of carcinoid tumors involving sites other than the stomach in nonhuman primates and included hepatic carcinoid tumors in a baboon (Papio sp.) and a Japanese macaque (Macaca fuscata), the lung of a rhesus macaque (Macaca mulatta), and the duodenum of a cynomolgus macaque (Macaca fascicularis).[2,4,5,7]

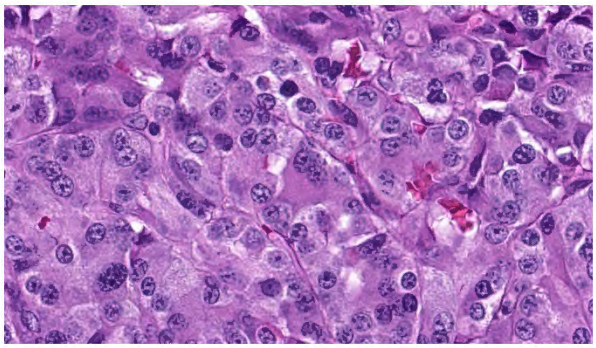

Figure 2-5. Stomach, rhesus macaque: High magnification of neoplastic cells, which have abundant granular cytoplasm, minimal atypia, and a low mitotic rate. (HE, 306X)

In humans, gastric carcinoids may be solitary or multiple and are placed in three categories. Type 1 presents with multiple, slow growing tumors. Local and distant metastases are rare. The pathogenesis is thought to involve chronic atrophic gastritis where there is parietal cell loss resulting in achlorhydria which causes excessive release of gastrin from G cells. Hypergastrinemia stimulates tumor formation and growth. Type 2 carcinoids are associated with gastrinomas; hypergastrinemia occurs because of a primary increase in gastric acid production. These carcinoids are associated with Zollinger-Ellison syndrome and generally occur in patients with MEN type I. Tumors are small, multiple, slow growing, and metastasize more often when compared to type 1. Type 3 carcinoids are usually solitary, rapidly growing, and exhibit frequent metastases to regional lymph nodes and the liver. They are not associated with chronic atrophic gastritis, gastrinomas, or MEN 1, and may be composed of multiple kinds of endocrine cells. Blood gastrin levels are normal. Atypical carcinoid syndrome characterized by flushing may be seen.[13] The classification scheme for human carcinoids could not be applied in this case. There were multiple tumors in this macaque. The functionality of the tumors is unknown. Clinical signs such as nausea, vomiting, diarrhea, and sustained weight loss consistent with Zollinger-Ellison syndrome were not reported. Chronic, atrophic gastritis was not evident on microscopic examination.

Spontaneous gastric neuroendocrine tumors are rare in domestic veterinary species.[1,12] Other species reported with spontaneous gastric neuroendocrine tumors include a ferret (Mustela putorius furo), an aged Sprague-Dawley Rat, and 7/135 striped field mice (Apodemus agrarius).[3,8,9] At least two species are an exception to the rarity of gastric carcinoids noted here. A retrospective study of neoplasia in the alimentary tract of bearded dragons (Pogona spp) reported that of 26 gastric neoplasms, 16 were neuroendocrine carcinomas. Metastases were observed in 14 of these cases most often to the liver and kidney reflecting an aggressive biologic behavior.[6] In another study involving bearded dragons, 5 of 5 tumors demonstrated immunolabeling for somatostatin.[10] Spontaneous gastric carcinoids were diagnosed on necropsies of 600 African rodents, Praomys (Mastomys) natalensis housed in a closed colony. Two-thirds of the aged males and one-third of the aged females were affected and exhibited regional and distant metastases.[11]

Contributing Institution:
Pathology Services Unit
Division of Animal Resources and Research Support
Oregon National Primate Research Center
505 NW 185th Avenue
Beaverton, OR 97006
https://www.ohsu.edu/onprc

JPC Diagnoses:
1. Stomach: Neuroendocrine tumor (carcinoid).
2. Stomach: Gastritis, lymphoplasmacytic, chronic, diffuse, moderate.

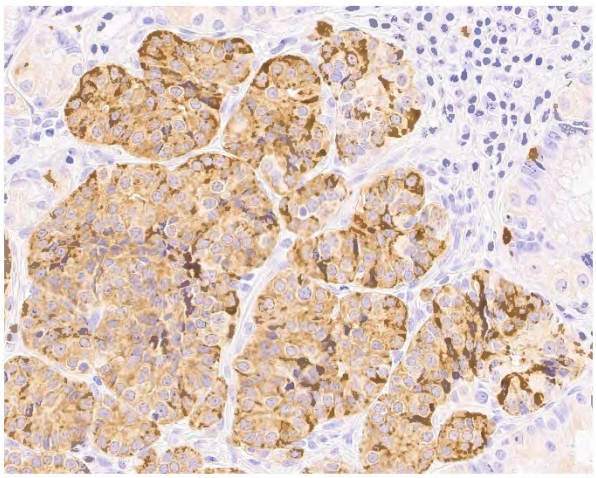

Figure 2-6. Stomach, rhesus macaque: Neoplastic cells demonstrate strong diffuse cytoplasmic immunopositivity for chromogranin A. (anti-chromogranin A, 400X) (Photo courtesy of: Oregon National Primate Research Center, https://www.ohsu.edu/onprc)

JPC Comment:

Another fantastic write-up! This case made for highly educational discussion on a classic entity. Many thanks to the contributor for providing this case, along with chromogranin A IHC images that supported the diagnosis. Chromogranin A is a great IHC to use for these types of cases, as it immunoreacts with dense granules in neuroendocrine cells. Other great IHC options for neuroendocrine neoplasms include synaptophysin or insulinoma-associated protein-1 (INSM-1).

Most participants were initially split on this diagnosis based on the H&E alone, with some confidently diagnosing a carcinoid and others wondering about an adenocarcinoma due to the formation of what appeared to be acini. The presence of nests, packets, pseudoglandular formation, and rosettes in the neoplasm's pattern should clue the pathologist into the possibility that this is a neuroendocrine neoplasm rather than an epithelial one. Participants engaged in spirited debate on the presence of vascular invasion in this digital-only case. Most participants were not sold on it and interpreted the nucleated cells within blood vessels as either histiocytes or other nucleated circulating cells. Ultimately, IHC would have been necessary to confirm this. As such, vascular invasion was left out of the JPC's morphologic diagnosis. Participants did agree that the gastritis should receive its own morphologic diagnosis, as most did not think it was simply a result of the neoplasm due to the prevalence of gastritis, enteritis, and colitis seen in captive nonhuman primates.

Although this case did not classify as such, diagnostic criteria for gastric neuroendocrine carcinoma (gNEC) were reviewed as part of the discussion due to the invasion into the underlying stroma seen on the slide. This feature should have put gNEC on any initial differentials list. Important criteria for gNEC include a single, large, ulcerated mass, usually in the cardia or antrum of the stomach, with poorly differentiated cells arranged in sheets or nests with extensive necrosis.[14] gNEC usually has a spicy mitotic rate (>20 per 1mm^2) and an high Ki67 proliferation index (always >20% and commonly above 70%).[14] The neoplasm in this case was not classified as a gNEC as, although it was invading into the submucosa, it did not have a high mitotic rate, was multifocal, and was not associated with necrosis.

Other gastric and intestinal neuroendocrine neoplasms were reviewed, along with a few important syndromes to keep in mind that are commonly associated with them. For example, gastrinomas that secrete gastrin can do so in such amounts that they stimulate hypersecretion of hydrochloric acid in the stomach, causing gastritis, esophagitis, and/or gastric and duodenal ulceration. This is known as Zollinger-Ellison syndrome. Additionally, carcinoids can be seen in Multiple Endocrine Neoplasia-1 Syndrome. MEN1 results from an autosomal dominant inactivating mutation of the menin gene. Normally, this gene produces menin, a scaffold protein that functions as a critical tumor suppressor, especially in endocrine glands, where it regulates cell growth,

division, DNA repair, and apoptosis.[9] The diagnosis of MEN1 in humans requires either demonstration of the genetic mutation OR least two of the following: parathyroid gland tumor, pituitary tumor, and either gastric, enteric, or pancreatic neuroendocrine tumor (pancreatic are the most common).[12] Alternatively, in humans, MEN1 can also be diagnosed with any one of the listed neoplasms along with demonstration that the affected person also has a first-degree relative with confirmed MEN1. Clinically, primary hyperparathyroidism is the first and most common manifestation of MEN1.[12] Other final points of discussion included the classification of gastric carcinoids (GNETs) into three different types, each of which was kindly covered in the contributor's comment.

References:

1. Albers TM, Alroy J, McDonnell JJ, Moore AS. A Poorly Differentiated Gastric Carcinoid in a Dog. *J Vet Diagn Invest*. 1998;10(1):116-118.
2. Aloisio, F, Dick EJ, Hubbard, GB. Primary hepatic neuroendocrine carcinoma in a baboon (*Papio sp*.). *J Med Primatol*. 2009;38:23-26.
3. Bousquet T, Bravo-Araya M, Davies JL. Gastric neuroendocrine carcinoma (carcinoid) in a ferret (*Mustela putorius furo*). *Can Vet J.* 2022;63(11):1109-1113.
4. Giddens WE, Dillingham LA. Primary Tumors of the Lung in Nonhuman Primates; Literature Review and Report of Peripheral Carcinoid Tumors of the Lung in a Rhesus Monkey. Vet Pathol. 1971;8(5-6):467-478.
5. Hirata A, Miyamoto Y, Kaneko A, Sakai H, Yoshizaki K, Yanai T, Miyabe-Nishiwaki T, Suzuki J. Hepatic neuroendocrine carcinoma in a Japanese macaque (*Macaca fuscata*). *J Med Primatol*. 2019;48(2):137-140.
6. LaDouceur EB, Argue A, Garner MM. Alimentary Tract Neoplasia in Captive Bearded Dragons (*Pogona* spp). *J Comp Pathol*. 2022;194:28-33.
7. Lau DT, Spinelli JS. A spontaneous carcinoid tumor in a cynomolgus monkey, *Macaca fascicularis*. *Lab Anim Care*. 1970;20(6):1145-8.
8. Majka JA, Sher S. Spontaneous gastric carcinoid tumor in an aged Sprague-Dawley rat. *Vet Pathol*. 1989;26(1):88-90.
9. Matkar S, Thiel A, Hua X. Menin: a scaffold protein that controls gene expression and cell signaling. *Trends Biochem Sci*. 2013;38(8):394-402.
10. Oh SW, Chae C, Jang D. Spontaneous gastric carcinoid tumors in the striped field mouse (*Apodemus agrarius*). *J Vet Med Sci*. 1997;59(8):703-6.
11. Ritter JM, Garner MM, Chilton JA, Jacobson ER, Kiupel M. Gastric Neuroendocrine Carcinomas in Bearded Dragons (*Pogona vitticeps*). Veterinary Pathology. 2009;46(6):1109-1116.
12. Singh G, Mulji NJ, Jialal I. Multiple Endocrine Neoplasia Type 1. [Updated 2023 Jul 10]. In: StatPearls [Internet]. Treasure Island (FL): StatPearls Publishing; 2025.
13. Snell KC, Stewart HL. Spontaneous diseases in a closed colony of *Praomys (Mastomys) natalensis*. *Bull World Health Organ*. 1975;52(4-6):645-50.
14. Uccella S, La Rosa S. Neuroendocrine neoplasms of the stomach. Update on diagnostic criteria, classification, and prognostic markers. *Virchows Arch*. Published online November 22, 2025.
15. Uzal FA, Plattner BL, Hostetter JM. Alimentary system. In: Maxie MG, ed. *Jubb, Kennedy and Palmer's Pathology of Domestic Animals.* Vol 2. 6th ed. St. Louis, MO: Elsevier; 2016:105-106.

Wardlaw R, Smith JW. Gastric carcinoid tumors. *Ochsner J*. 2008;8(4):191-6.

CASE III:

Signalment:
Adult female wild mouse (*Mus musculus*)

History:
This wild mouse was found dead in a primate enclosure.

Gross Pathology:
The aorta was lacerated at the level of T8-T9 where the spinal column was severely dislocated and the thoracic cavity contained a large blood clot.

Laboratory Results:
N/A

Microscopic Description:
Few acinar and stromal cells with markedly enlarged nuclei and abundant cytoplasm (cytomegaly) with 8-12 µm eosinophilic intranuclear inclusions were scattered throughout the submandibular salivary gland with accompanying lymphoplasmacytic infiltration in several regions.

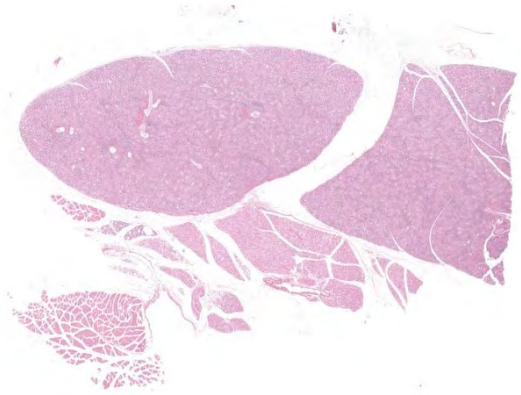

Figure 3-1. Mandibular salivary gland, mouse: One section of the mandibular gland, with associated brown fat and skeletal muscle, is submitted for examination. (HE, 20X)

Contributor's Morphologic Diagnoses:
Sialoadenitis, multifocal, subacute to chronic, mild with epithelial and stromal cytomegaly and intranuclear inclusions (cytomegalovirus)

Contributor's Comment:
Although traumatic laceration of the thoracic aorta with resultant hemothorax was considered the cause of death, infection with mouse cytomegalovirus (MCMV) was a prominent incidental finding in this wild mouse. Wild mice are commonly infected with MCMV, a DNA virus in the family *Herpesviridae*, subfamily *Betaherpesvirinae*, and genus *Muromegalovirus*.[6] Several genetically distinct strains of MCMV exist within wild mouse populations, and mixed infections of single mice are not uncommon. In fact, up to four genetically distinct strains of MCMV have been isolated from a single wild mouse.[3]

The most frequently encountered lesions occur in the submandibular salivary glands and rarely in the parotid glands, with excretion in saliva serving as the primary means of transmission through grooming and biting activities. Typical histological findings include eosinophilic intranuclear and intracytoplasmic inclusions in acinar epithelial cells with cytomegaly and interstitial lymphoplasmacytic inflammation.[6] Intranuclear inclusions result from viral DNA replication within the nuclei of infected cells, while intracytoplasmic inclusions represent replication processes that occur in the cytoplasm, including production of the capsid protein.[8]

As resistance typically evolves after weaning, overt disease and disseminated lesions occur

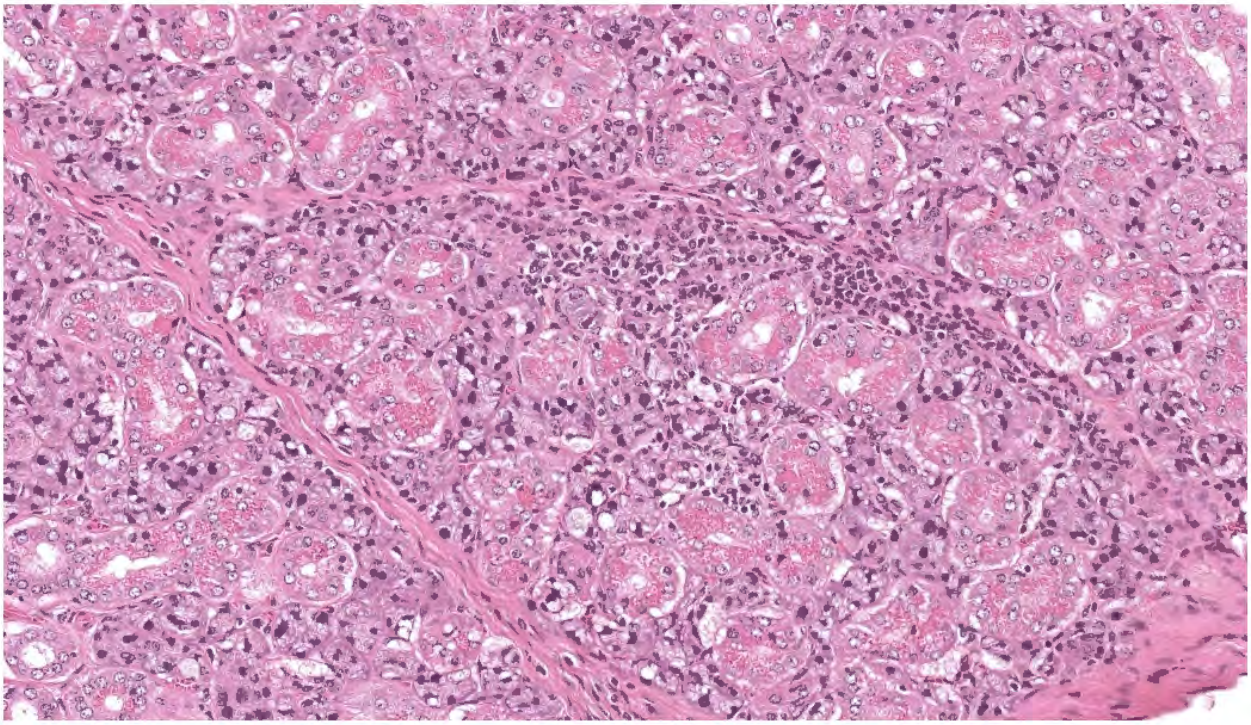

Figure 3-2. Mandibular salivary gland, mouse: The salivary gland interstitium is multifocally infiltrated by moderte numbers of lymphocytes, plasma cells and macrophages. (HE, 365X)

infrequently in naturally infected mice. Neonates are more susceptible to severe disease which may result in encephalitis,
retinitis, pneumonia, hepatitis, myocarditis, adrenalitis and haemopoietic failure. MCMV causes lifelong, persistent infections with intermittent reactivation and viral shedding at times of host immunosuppression. Latent virus in mice may be found in the salivary glands and in other tissues including lung, spleen, liver, kidney, heart, adrenal glands, and myeloid cells.[6]

The betaherpesviruses are highly host specific. Natural infections of cytomegalovirus occur in primates and guinea pigs as well as mice. Rhesus cytomegalovirus (macacine herpesvirus-3) is the most common opportunistic viral infection in rhesus macaques infected with simian immunodeficiency virus.[1] It causes multiorgan dysfunction, with interstitial pneumonia, encephalitis, gastroenteritis and lymphadenitis being most common.[2] In guinea pigs, lesions are largely regarded as incidental findings at necropsy and usually confined to the salivary ductal epithelial cells.[8]

As the course of MCMV infection in mice has similarities to the course of human cytomegalovirus (HCMV) infection, MCMV has been extensively studied and used as a model of the human disease. Credited as the “mother of cytomegalovirus,” M. G. Smith first isolated MCMV from the salivary glands of naturally infected laboratory mice in 1954 and propagated it in cell culture.[7] Most laboratory studies have utilized the original Smith strain of MCMV, or derivates thereof, which may not accurately reflect the natural biology of MCMV strains. Nevertheless, the intense scrutiny of MCMV as a model system has shed considerable light on disease pathogenesis.[6]

Investigations into the variable susceptibility of mouse strains to MCMV infection have

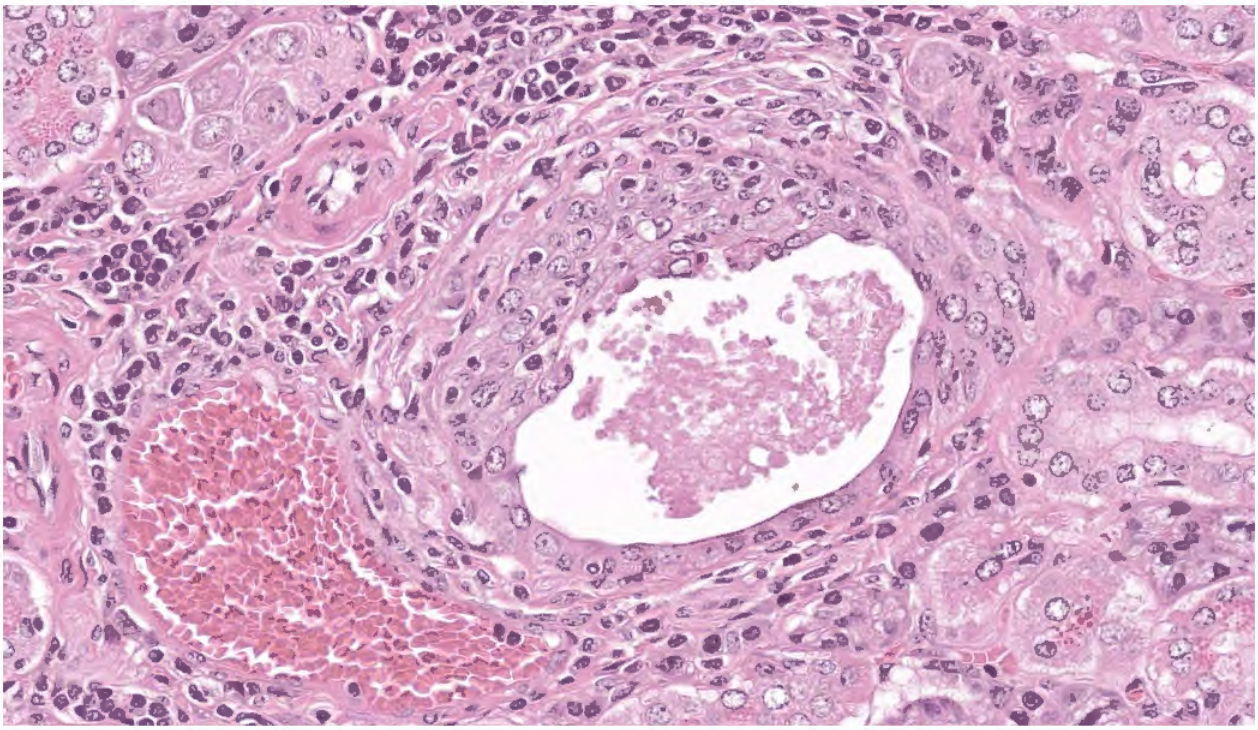

Figure 3-3. Mandibular salivary gland, mouse: There is multifocal necrosis of acinar epithelium with attenuation of remnant epithelium and accumulation of eosinophilic debris within the lumen. (HE, 650X)

shown that innate immune function, in particular the effectiveness of the natural killer (NK) cell response, is the key determinant of resistance to the initial infection and the suppression of viral replication. For example, C57BL/6 (B6) mice are generally considered resistant to MCMV due to the expression of Cmv-1 encoded Ly49H, an NK cell-activating receptor that recognizes the m157 viral protein at the surface of MCMV-infected cells. Activated NK cells suppress the infection by direct lysis of infected cells and by producing cytokines to mediate T-cell responses.[4] Other genetically resistant mouse strains include B10, CBA and C3H mice, while susceptible strains include BALB/c and A strain mice. Susceptibility of wild mice to MCMV strains that circulate in wild populations is attributed to m157 proteins that are unable to activate NK cells via Ly49H.[9] Humoral immunity is relatively unimportant in controlling MCMV infection.

Contributing Institution:
Wake Forest School of Medicine
Department of Pathology, Section on Comparative Medicine
Medical Center Boulevard, Winston-Salem, NC 27157
www.wakehealth.edu

JPC Diagnoses:
Salivary gland: Sialoadenitis, lymphoplasmacytic, chronic, multifocal, mild, with epithelial karyomegaly and intranuclear viral inclusions.

JPC Comment:
This case provided an excellent example of a truly classic lesion that every pathologist should be able to recognize and should come to the forefront of the mind when presented with a slide of murine salivary gland. The contributor provided a great comment on cytomegaloviruses and covered much of what was taught during this case in conference.

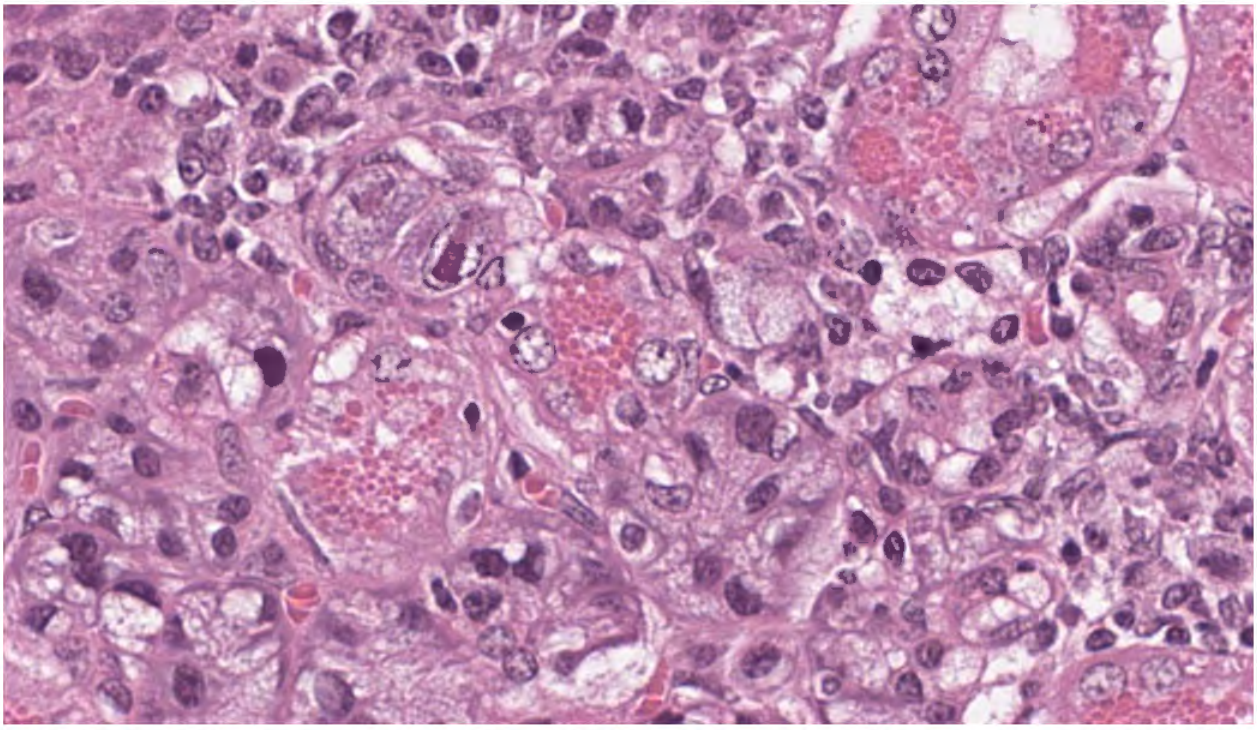

Figure 3-4. Mandibular salivary gland, mouse: Rare acinar cells demonstrate karyomegaly with a single oblong intranuclear cytomegaloviral inclusion which is surrounded by a clear halo. (HE, 1221X)

The submandibular salivary gland in mice (and multiple other species) is a mixed gland with both serous and mucinous glands. In male mice, the submandibular salivary glands are larger than those in female mice and contain brightly eosinophilic, prominent granules in the ductal epithelial cells. Don't forget, though, that those granules can also be seen in pregnant females. B6-strain mice are resistant to infection with CMV, but DBA2 and BALB/C mouse strains are susceptible due to their immune bias towards a Th2 (humoral) response. A subdued Th1 (cell-mediated) immune response results in less effective defense against intracellular pathogens, such as viruses. Th2 cells produce cytokines IL-4 and IL-10, which inhibit the development and function of Th1 cells and their key cytokines, which include interferon-gamma (IFN-γ). A strong IFN-γ response is essential for activating cell-mediated immunity and effectively eliminating virus-infected cells.

While the tissue identification and diagnosis in this case were straightforward, there were some other structures on the slide that served as an excellent reminder of mouse anatomy. Mammary tissue in mice is extensive and can be as far cranial as the submandibular area. Mammary glands are frequently seen in association with the submandibular salivary gland, often hanging out in the subcutaneous tissues. Another primary differential for viral inclusions in the salivary glands of mice is murine polyomavirus (MmusPyV-1). This double-stranded DNA virus is, as the name implies, associated with the development of multiple neoplasms in infected mice. While not all polyomaviruses cause neoplasm development, mouse polyomavirus is well-known to do so. Hamster polyomavirus is similar.

One other important betaherpesvirus of note from discussion is suid herpesvirus-2 (porcine

roseolovirus), which causes necrotizing rhinitis and abortions in swine and can be lethal to humans.[5]

References:

1. Assaf BT, Knight HL, Miller AD. Rhesus cytomegalovirus (Macacine herpesvirus 3)-associated facial neuritis in simian immunodeficiency virus-infected rhesus macaques (*Macaca mulatta*). *Vet Pathol.* 2015;52(1):217-223.
2. Baskin GB. Disseminated cytomegalovirus infection in immunodeficient rhesus monkeys. *Am J Pathol*. 1987;129(2):345-352.
3. Booth M, et al. "Molecular and Biological Characterization of New Strains of Murine Cytomegalovirus Isolated from Wild Mice." *Archives of Virology*. 1993:132(1-2);209–220.
4. Fodil-Cornu N, et al. "Ly49h-Deficient C57BL/6 Mice: A New Mouse Cytomegalovirus-Susceptible Model Remains Resistant to Unrelated Pathogens Controlled by the NK Gene Complex." *Journal of Immunology*. 2008:181(9);6394–6405.
5. Hansen S, Menandro ML, Franzo G, et al. Presence of porcine cytomegalovirus, a porcine roseolovirus, in wild boars in Italy and Germany. *Arch Virol*. 2023;168(2):55.
6. Lathbury LJ, et al. "Effect of Host Genotype in Determining the Relative Roles of Natural Killer Cells and T Cells in Mediating Protection against Murine Cytomegalovirus Infection." *Journal of General Virology*. 1996:77(10);2605–2613.
7. Percy DH, Barthold SW. *Pathology of Laboratory Rodents and Rabbits*. 3rd ed. Ames, IA: Blackwell Publishing; 2007:222.
8. Reddehase, MJ. "Margaret Gladys Smith, Mother of Cytomegalovirus: 60th Anniversary of Cytomegalovirus Isolation." *Medical Microbiology and Immunology*. 2015:204(3);239–241.
9. The Joint Pathology Center, Wednesday Slide Conference 2014-2015, Conference 14, Case: 01." *Askjpc.org*. 2015.
10. Voigt V, et al. "Murine Cytomegalovirus M157 Mutation and Variation Leads to Immune Evasion of Natural Killer Cells." *Proceedings of the National Academy of Sciences of the United States of America*. 2003:100(23);13483–13488.

CASE IV:

Signalment:

5-week-old, female, B6.129S4-C3^{tm1Crr}/J mouse

History:

This female targeting a mutation in the complement component C3 (C3 KO) was 5 weeks old, and she had shown an abnormal enlarged abdomen (homogenous, firm but not very hard to touch). Apart from that she was in normal general condition, with no signs of dehydration nor malnutrition and no signs of diarrhea. Pregnancy is excluded since the animal has been kept in a stock cage with other females.

Gross Pathology:

A fresh carcass was received. No external lesions were observed apart from an enlarged abdomen, which was firm upon palpation.
Abdominal cavity: The abdominal cavity contained a moderate amount of clear, pale-yellow fluid.

Kidney: The left kidney was markedly enlarged, measuring approximately 8x5x4mm, along with an associated diffuse dilation of the left ureter (appr. 5mm in diameter). The left ureter and left kidney were transparent and filled with clear fluid (interpreted as urine). Renal parenchyma was not evident. A hole of approximately 5mm in length was observed in the left renal capsule. Size, surface and color of the right kidney appeared unremarkable, but on cut section, a moderately dilated renal

Figure 4-1. Kidney and ureter, B6.129S4-C^{3tm1Crr}/J mouse: The left kidney is markedly enlarged and transparent, measuring approximately 8 x 5 x 4 mm, as is the left ureter (appr. 5 mm in diameter). These structures are filled with urine. (Photo courtesy of: Institute of Animal Pathology, Vetsuisse Faculty – University of Bern, www.itpa.vetsuisse.unibe.ch)

pelvis was noted. Other observed organs were macroscopically unremarkable.

Laboratory Results:
N/A.

Microscopic Description:
Left kidney: The left kidney is composed of multiple, largely dilated cavities that divide the kidney into numerous islands of parenchyma. These cavities are lined by 2–4 layers of cuboidal to highly columnar, eosinophilic epithelial cells with no mitotic activity (collecting ducts). Few sloughed epithelial cells and erythrocytes are present in the lumen of these ducts. The parenchyma contains islands of immature glomeruli with peripheral nuclei, poorly developed capillaries, and thickened Bowman's capsule (vimentin positive). Primitive tubules are lined by large basophilic cuboidal epithelial cells with minimal or absent lumina. Other areas within the parenchyma consist of mature tubules and glomeruli with some tubules showing mild dilation and intraluminal protein casts. Collecting duct-like structures are multifocally surrounded by loosely arranged mesenchymal tissue (primitive mesenchyme). The interstitium is multifocally expanded by fibrous connective tissue and some areas are infiltrated by low to intermediate numbers of lymphocytes, plasma cells, macrophages, and occasional neutrophils. Some arteries are very prominent (large) with thickened media, and they appear tortuous. A medium sized artery is surrounded and infiltrated by inflammatory cells predominantely macrophages, neutrophils and occasionally multinucleated giant cells within adventitia, media and intima (transmural). Diffuse proliferation of fibroblasts and deposition of fibrin within the vessel wall is observed. Occasionally, the tunica intima is disrupted. Endothelial cell proliferation is evident with clustering of endothelial cells attempting to recanalize the affected lumina.

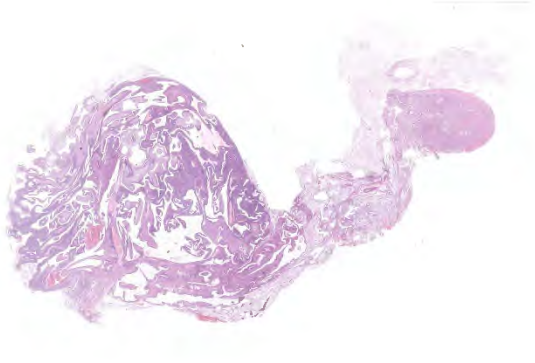

Figure 4-2. Kidney and ureter, B6.129S4-C^{3tm1Crr}/J mouse: One section of the kidney and ureter are submitted for examination. The kidney is a cystic mass (or mess, if you prefer) and has collapsed on itself in the cassette, resulting in the numerous cystic spaces within the parenchyma. A similar change is present in the markedly dilated ureter. (HE, 16X)

Left ureter: Multiple longitudinal and cross-sections of the ureter are present, consisting of urothelium, lamina propria, a smooth muscle layer, and an outer adventitial layer. The perirureteral mesenchymal tissue similar to persistent mesenchyme was observed surrounding left ureter and multifocally contains fibrin and exhibits multifocal moderate hemorrhage, and is infiltrated by inflammatory cells, predominantly neutrophils and macrophages, with the presence of hemosiderophages.

Contributor's Morphologic Diagnoses:
Left kidney:

1. Multicystic renal dysplasia with focal rupture of the capsule.
2. Mild to moderate multifocal chronic lymphoplasmacytic tubulointerstitial nephritis.
3. Severe diffuse chronic histiocytic arteritis

Contributor's Comment:
Here, we present an interesting case of unilateral renal dysplasia with unusual cystic dilation of the pelvis and collecting ducts in laboratory mice. Renal dysplasia is well-documented in domestic animals due to its clinical significance; however, the condition has been rarely reported in rodents. Among rodents, renal dysplasia has been reported in a Wistar rat, a Sprague Dawley rat and a Syrian hamster.[5,7,9] To the best of our knowledge, this is the first reported spontaneous occurring case of renal dysplasia in mice.

Renal dysplasia is a congenital or neonatal developmental anomaly of the kidney that results from disruption of the normal development of the collecting duct system.[3] The disease is often congenital, caused by alterations in the renal branching morphogenesis, which occur due to changes in transcription factors, growth factors, and cell surface signaling peptides.[3] It can also be caused by disease in the early neonatal period, before differentiation of the nephrogenic tissue is completed. This is true in species, which have an active subcapsular nephrogenic zone at birth such as cats, dogs, and pigs.[3] In mice, nephrogenesis begins before day 11 of gestation and is completed at birth, whereas in dogs nephrogenesis is completed by post-natal day 14, and even later by post-natal day 21 in pigs and rabbits.[4] This suggests that renal dysplasia in mice is more

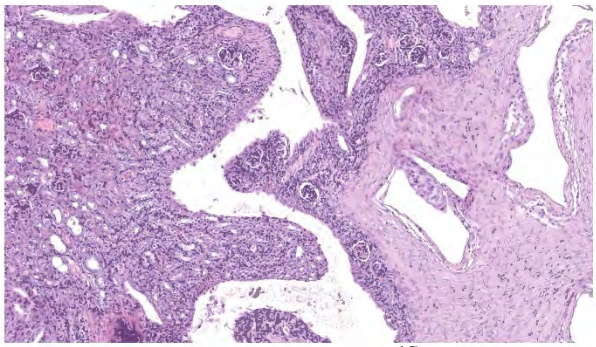

Figure 4-3. Kidney, B6.129S4-C3^{tm1Crr}/J mouse: The cystic nature of the kidney makes identification of normal architecture difficult. The cortex is easily identified due to the presence of glomeruli. As is typical in hydronephrosis, the medulla is markedly fibrotic, and likely represented at left in this distorted kidney. (HE, 163X)

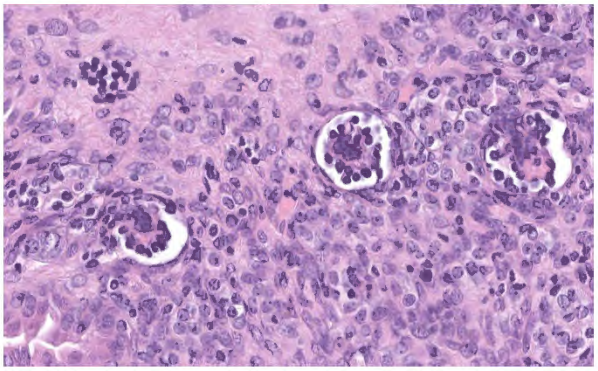

Figure 4-4. Kidney, B6.129S4-C3^{tm1Crr}/J mouse: Within the remnant cortex, numerous small glomeruli with peripheral nuclei (fetal glomeruli) are present.(HE, 663X)

likely to result from congenital anomalies rather than neonatal developmental abnormalities.

Grossly, dysplastic kidneys are usually misshapen, fibrosed with thick-walled cysts and dilated tortuous ureters.[3] One or both kidneys can be affected and the condition can be clinically silent if unilateral, or embryonically lethal when bilateral.[4] Key histological features of renal dysplasia include structures inappropriate to the stage of development or the presence of anomalous structures, in particular undifferentiated mesenchyme, metanephric blastema, immature glomeruli, blind ending collecting tubules, atypical tubular epithelium, metanephric ducts (lined by cuboidal or columnar epithelium), and metaplastic cartilage or bone (rare in domestic animals).[3,8] These alterations could be masked by compensatory, degenerative or inflammatory changes.[3]

This is a case of unilateral renal dysplasia, including immature glomeruli, primitive tubuli and extensively dilated collecting duct-like structures surrounded by primitive mesenchyme. The presence of proteinaceous casts, extensive fibrosis and interstitial nephritis display secondary changes related to impaired renal function. Defective metanephric differentiation results from abnormal interaction between the uretic bud and metanephric blastema leading to renal dysplasia. Complete failure of initiating ureteric bud induction can be diagnosed histologically by the presence of metanephric ducts surrounded by primitive mesenchyme and dysontogenic tissue formation6. As observed in this case, the presence of fetal glomeruli, persistent mesenchyme, and anomalous tubular structures suggests that induction of metanephric blastema was initiated but failed to progress to full differentiation. This is further supported by the immunohistochemistry findings, which demonstrate the persistence of mesenchymal markers (vimentin) in primitive tubules alongside epithelial differentiation (cytokeratin positivity) in more developed structures.[2]

Renal dysplasia may be accompanied by extrarenal abnormalities including segmental ureteral agenesis of the associated dysplastic kidney and imperforate anus.[3] Ureteral anomalies are frequently associated with renal dysplasia due to the close developmental relationship between the kidney and the collecting system. Reported ureteral abnormalities in cases of renal dysplasia include ectopic ureters, ureteral obstruction with hydronephrosis,

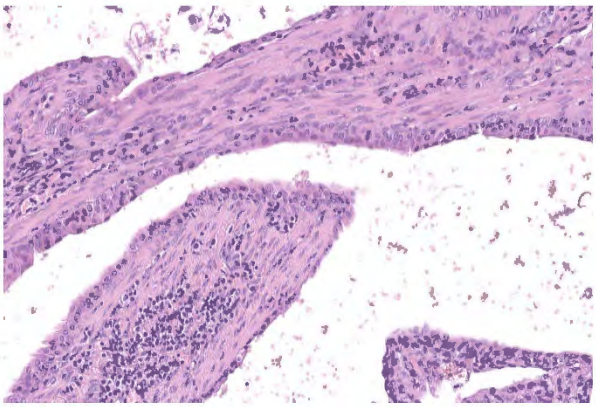

Figure 4-5. Kidney, B6.129S4-C3^{tm1Crr}/J mouse: The cysts are lined with one to multiple layers of urothelium, suggesting a markedly dilated renal pelvis. (HE, 381X)

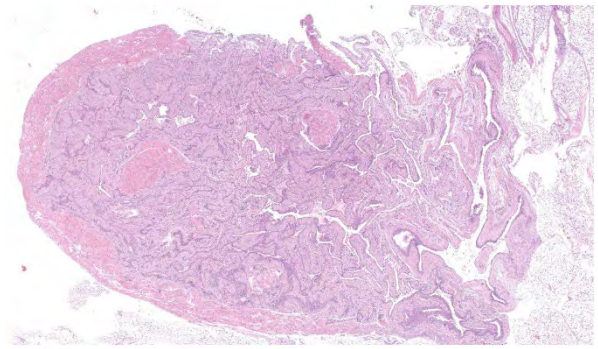

Figure 4-6. Ureter, B6.129S4-C3tm1Crr/J mouse: The collapse of the dilated bladder in the cassette prior to section has resulted in marked complexity in identification (HE, 40X)

hydroureter, and congenital urothelial cell hyperplasia.[10,11] In this case, the ureter associated with the dysplastic kidney is largely dilated and supposably tortuous. While no significant histopathological abnormalities were observed in the ureter itself, its tortuous nature may have impaired urine drainage, potentially leading to progressive renal dilation and rupture.

The observed arteritis in the left kidney is notable. While arteritis is not a common feature of renal dysplasia, it can occur secondary to chronic inflammation or immune-mediated processes such as anti-Glomerular Basement Membrane (GBM) disease.[6] In murine models, polyarteritis nodosa (PAN) is a recognized disease and is characterized by fibrinoid degeneration and necrosis of the tunica media and inflammation of medium and small arteries. This process is mostly associated with neutrophils with or without mononuclear leukocytes and thickening and fibrosis of the vessel wall.[1] Changes often involve arteries of the tongue, head, pancreas, heart, kidneys, mesentery, urinary bladder, uterus, testes, and gastrointestinal tract. Lesions are segmental and their etiology is unknown, but immune complexes have been found in affected vessels.[1] Polyarteritis is an incidental finding which can be associated with segmental infarction of the kidney and scarring.[1]

Although PAN has not yet been described as directly associated with renal dysplasia, chronic kidney injury may predispose to vascular inflammation. In addition, the knockout of C3 in this mouse is associated with defective antibody response to T cell dependent antigens, which might have contributed to disease development. However, arteritis was not observed in other examined organs. Additional investigations into the pathogenesis of arteritis in this case are therefore required.
This is the first case report of spontaneous renal dysplasia in mice. Possible causative relation of dysplastic changes and arteritis observed in this case remains unclear and requires further investigation to elucidate its etiology, particularly in the context of murine models of inflammation, such as C3 knockout.

Contributing Institution:
Institute of Animal Pathology
Vetsuisse Faculty – University of Bern
Länggassstrasse 122
CH-3012 Bern
Switzerland
www.itpa.vetsuisse.unibe.ch

JPC Diagnoses:

1. Kidney: Congenital hydronephrosis, severe, with tubular and glomerular atrophy, interstitial fibrosis, mild lymphoplasmacytic interstitial nephritis.
2. Kidney: Asynchronous maturation, with fetal glomeruli, rare primitive tubules, and primitive mesenchyme.
3. Kidney, arteries and arterioles: Arteritis, neutrophilic and histiocytic, proliferative and necrotizing, chronic, multifocal, severe.

JPC Comment:
This case was fascinating and provided substantial discussion amongst participants, particularly on how best to morph these lesions. The contributor's comment lays out many of the points of debate amongst participants and makes a strong argument for a congenital lesion with prominent secondary changes. The question most attendees were wondering was, "Which parts are congenital and which parts are secondary?"

The large number of fetal glomeruli, presence of few primitive tubules, and occasional primitive mesenchyme, especially in a 5-week old mouse, certainly suggest a degree of renal dysplasia. Mouse kidneys should be completely developed within 4 days of birth (no later than 7 days).[1,5] However, there was debate amongst conference attendees on whether this was a primary renal dysplasia or a secondary delay in maturation due to atrophy caused by congenital hydronephrosis/hydroureter. The fetal glomeruli were strikingly obvious in this case and are characterized by a reduction in the number of capillaries, the presence of podocyte nuclei that palisade around the periphery of a small glomerular tuft, decreased tuft segmentation, and a thick Bowman's capsule. Immature glomeruli are, in a not-so-convoluted kidney, usually best seen in the subcapsular cortex.[1,5] Glomeruli aside, however, while there were rare definitively primitive tubules, most participants thought that many of the tubules were atrophied in response to the severe hydronephrosis rather than truly dysplastic. This was further complicated by the complete lack of medullary distal convoluted tubules. Additionally, there were occasional glomeruli that were mature and the majority of the scant interstitium was relatively developed. As such, many conference participants preferred the term "asynchronous maturation" to describe the spectrum of development seen within the kidney.

Participants wholeheartedly agreed with the contributor regarding the arteritis and similarly diagnosed polyarteritis nodosa (PAN) due to the degree of subintimal proliferation, neutrophilic inflammation, disruption of the elastic laminae, fibrinoid necrosis, and tortuosity of the arteries. Although usually associated with hypertension and most commonly seen in the pancreas, mesentery, and testes, renal PAN is well-documented.[2,4] In this case, it is possible that the degree of hydronephrosis and subsequent pressure atrophy could have contributed to the development of hypertension-like lesions in the arteries, although this is purely speculative and could be a separate process entirely.
The flocculent, cystic spaces made definitive interpretation of this case challenging. The lining of the cystic spaces resembled either persistent metanephric ducts (ducts in the outer medulla lined by pseudostratified, ciliated, columnar epithelium), transitional urothelium, and/or serosa. Metanephric ducts in the medulla potentially represented persistent, incompletely differentiated ureteric bud branches that did not differentiate into normal collecting tubes as they are supposed to, further suggesting a congenital etiology in this condition.[5,10] The presence of serosa-lined spaces implies that some cysts had collapsed in on themselves during processing. Everyone unanimously agreed, however, that this was not polycystic kidney disease.

Differentiating between cystic renal dysplasia and polycystic kidney disease can be challenging, but there are some key differences to be aware of. Cystic renal dysplasia (CRD) is the

most common pediatric renal disease in humans (and is also more common in most animals). It typically has larger cysts that are variably sized and lined by flat-cuboidal epithelium. CRD usually results from urinary tract obstruction and is often unilateral. It occurs sporadically and does not have a defined inheritance pattern like PKD. The characteristic findings for renal dysplasia will be present (fetal glomeruli, primitive tubules, primitive loose mesenchyme, +/- cartilaginous metaplasia, +/- mesenchymal collarettes), and there may or may not be vascular changes.[4,10]

Polycystic kidney disease (PKD), on the other hand, is divided into two subtypes: autosomal dominant PKD (ADPKD) and autosomal recessive PKD (ARPKD). ADPKD is familial, bilateral, and usually does not present until adulthood.[4,10] There is no immature mesenchyme or cartilage present. ARPKD is also familial and bilateral but is generally present at birth.[4] The cysts in ARPKD arise from the collecting ducts and are typically uniform, radially arranged, and fusiform. There is similarly no immature mesenchyme or cartilage.

Due to the differing stages of maturation and the convolution of this case, the JPC consulted with Texas A&M's Dr. Rachel Cianciolo, one of the premier renal experts in veterinary pathology. Her conlusions matched those of some of our more experienced conference particpants in that, while there are abundant fetal glomeruli, there are some that are more mature, but smaller and atrophic. According to Dr. Cianiolo, this supports a diagnosis of a congenital hydronephrosis with delayed renal development, making this case an example of a congenital anomaly of the kidney and urinary tract. She also believes, as did many of our conference attendees, that the cysts are mostly irregular cuts of a severely dilated renal pelvis and calyceal diverticula rather than tubular cysts. Lastly, she stated that, in order to determine if this condition was truly destructive to the kidney and surrounding structures, imaging studies would be necessary. While cost certainly can dictate whether or not imaging will be done in a case, it should be considered in anomalalies like this where imaging could provide additional supportive evidence for a diagnosis, as well as scratch the academic itch to "know"! Many thanks Dr. Cianciolo for sharing her expertise on this interesting case!

References:

1. Baldock RA, Armit C. eHistology image and annotation data from the Kaufman Atlas of Mouse Development. *Gigascience*. 2018;7(2):gix131.
2. Barthold SW, Griffy SM, Percy DH. Pathology of Laboratory Rodents and Rabbits, Fourth Edition. 4th ed. (Barthold SW, Griffey SM, Percy DH, eds.). Wiley; 2016.
3. Carev D, Saraga M, Saraga-Babic M. Expression of intermediate filaments, EGF and TGF-alpha in early human kidney development. *J Mol Histol.* 2008;39(2):227-235.
4. Cianciolo R., Mohr F. Urinary system. In: Maxie M., ed. Jubb, Kennedy, and Palmer's Pathology of Domestic Animals. Vol 2. 6th ed. Elsevier; 2016:376-464.
5. Elmore SA, Kavari SL, Hoenerhoff MJ, et al. Histology atlas of the developing mouse urinary system with emphasis on prenatal days E10.5-E18.5. *Toxicol Pathol*. 2019;47(7):865-886.
6. Frazier KS. Species Differences in Renal Development and Associated Developmental Nephrotoxicity. *Birth Defects Res.* 2017;109(16):1243-1256.

7. Ikeyama Seiichi, Nishibe Tadayuki, Furukawa Satoshi, Goryo Masanobu, Okada Kosuke. Unilateral Renal Dysplasia in a Syrian Hamster. *J Toxicol Pathol.* 2001;14(4):309-312.
8. Jennette JC, Falk RJ, Bacon PA, et al. 2012 revised International Chapel Hill Consensus Conference Nomenclature of Vasculitides. *Arthritis Rheum*. 2013;65(1):1-11.
9. Lee Y-H, Kim D, Park SH, et al. Unilateral non-cystic renal dysplasia in a Sprague Dawley rat. *J Biomed Res*. 2014;15(2):92-95.
10. Picut CA, Lewis RM. Microscopic features of canine renal dysplasia. *Vet Pathol.* 1987;24(2):156-163.
11. Schorsch F, Pohlmeyer-Esch G, Lasserre-Bigot D. Unilateral Renal Agenesis/ Dysplasia associated with Contralateral End-Stage Kidney Disease in Two Wistar Rats. *Eur J Vet Pathol.* 2001;7(3):127-134.
12. The Joint Pathology Center (JPC). JPC Wednesday Slide Conference 2023-2024, Conference 5, Case 04. Published 2023.
13. Yoshida K, Takezawa S, Itoh M, et al. Renal Dysplasia with Hydronephrosis and Congenital Ureteral Stricture in Two Holstein-Friesian Calves. *J Comp Pathol*. 2022;193:20-24.

Joint Pathology Center
Veterinary Pathology Services

WEDNESDAY SLIDE CONFERENCE 2025-2026

Conference #16 21 January 2026

CASE I:

Signalment:
15-yr-old pony mare (*Equus caballus*)

History:
Ten-day history of colic and diarrhea with suspected peritonitis. Tested positive by PCR for equine coronavirus (antemortem), and received aggressive supportive care (IV fluids, antibiotics, anti-inflammatories, etc.), but became persistently painful and was euthanized. The submitting veterinarian was concerned about intestinal infarction or displacement.

Gross Pathology:
The carcass was in good nutritional condition, with adequate amount of fat reserves, well fleshed, moderately dehydrated, and mild to moderate state of postmortem decomposition.

Figure 2-1. Colon, horse: The serosa of the colon was multifocally hemorrhagic. (Photo courtesy of: California Animal Health and Food Safety Laboratory, Sa Bernardino Laboratory. https://cahfs.vetmed.ucdavis.edu/)

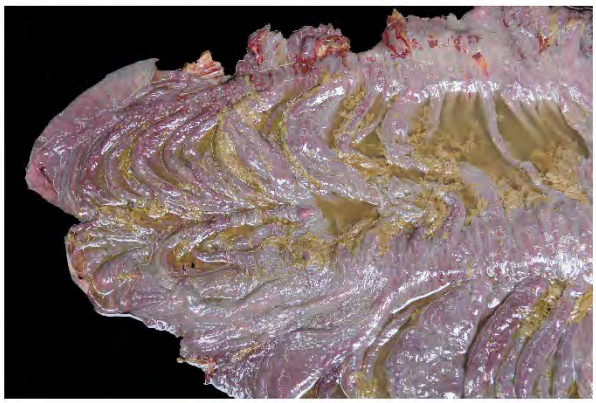

Figure 1-2. Colon, horse: There was clear liquid content throughout small and large intestine, and a pseudo membrane covering the mucosa of the right ventral colon and cecum. (Photo courtesy of: California Animal Health and Food Safety Laboratory, San Bernardino Laboratory. https://cahfs.vetmed.ucdavis.edu/)

About 10 liters of murky fluid were present in the abdomen. There were ~ 5 liters of clear thoracic fluid. The serosa of the colon was multifocally hemorrhagic. There was clear liquid content throughout small and large intestine, and a pseudo membrane covering the mucosa of the right ventral colon and cecum.

There was an~ 6 cm diameter jejunal diverticulum with very thick wall, that was adhered to the serosa of the cecum and the parietal peritoneum. The lungs were congested and edematous.

No other significant gross abnormalities were observed in the rest of the carcass.

Laboratory Results:
Clostridioides difficile and *Salmonella typhimurium* were isolated from small intestinal and colonic content. *S. typhimurium* was also isolated from the liver.

ELISA for toxins A and B of *C. difficile* was positive on small intestinal and colonic contents. ELISA for *Clostridium perfringens* alpha, beta and epsilon toxins was negative on the same specimens.

Mixed aerobic flora was isolated from small intestinal and colonic contents, liver and lung.

A heavy metal screen on liver revealed that copper and selenium were marginally below normal range. All other heavy metals were within normal range.

Microscopic Description:
Colon: There is severe, diffuse necrosis of the mucosa where the superficial epithelium and, less prominently, the crypt epithelium is lost and/or show hypereosinophilia, pyknosis, karyorrhexis and karyolysis. The lamina propria is diffusely eosinophilic and infiltrated by a large number of viable and degenerated neutrophils and fewer neutrophils, plasma cells and macrophages; this cellular infiltration extends to the submucosa. Multifocally, the mucosa is covered by a thick pseudo membrane composed of fibrin, cell debris, red blood cells, neutrophils and myriad mixed bacteria. Several blood vessels of the lamina propria show thrombosis. In areas where the superficial epithelium is still present, erosions are seen through which large number of neutrophils are seen exiting the lamina propria into the lumen (volcano lesions). The submucosa is severely dilated and edematous; there is vascular congestion and the lymphatic vessels are dilated. The serosa shows reactive mesothelial cells.

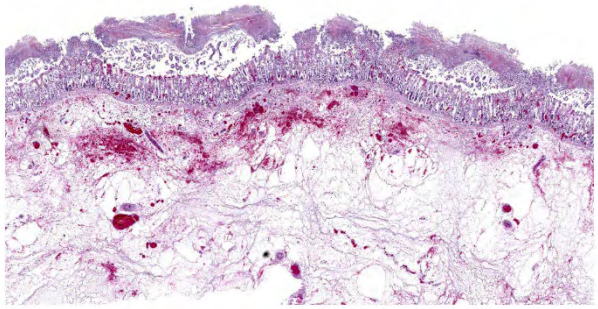

Figure 1-3. Colon, horse: The mucosa is covered by a serocellular crust and the submucosa is markedly expanded by edema and multifocal hemorrhage. (HE, 30X)

Contributor's Morphologic Diagnoses:
Colitis, fibrinonecrotizing, diffuse, with thrombosis, volcano lesions, submucosal edema and myriad intralesional mixed bacteria

Contributor's Comment:
This horse had severe colitis produced by a co-infection with *C. difficile* and *Salmonella* Typhimurium. Grossly and microscopically, there are several overlapping features in the lesions produced by these two microorganisms which make them impossible to differentiate based only on lesions.[3,7] An etiologic diagnosis cannot therefore be made without ancillary laboratory tests.[3,7]

In the case of *S. T*yphimurium, the infection was confirmed by PCR and culture followed by serotyping. Detection of this microorganism in intestinal content and liver suggests that the intestinal infection occurred before and there was systemic dissemination through the damaged intestinal mucosa, although intestinal mucosa damage is not a requirement for absorption and dissemination of this Salmonella spp.[5,7]

The diagnosis of *C. difficile* infection was confirmed by the detection of toxins A/B of this

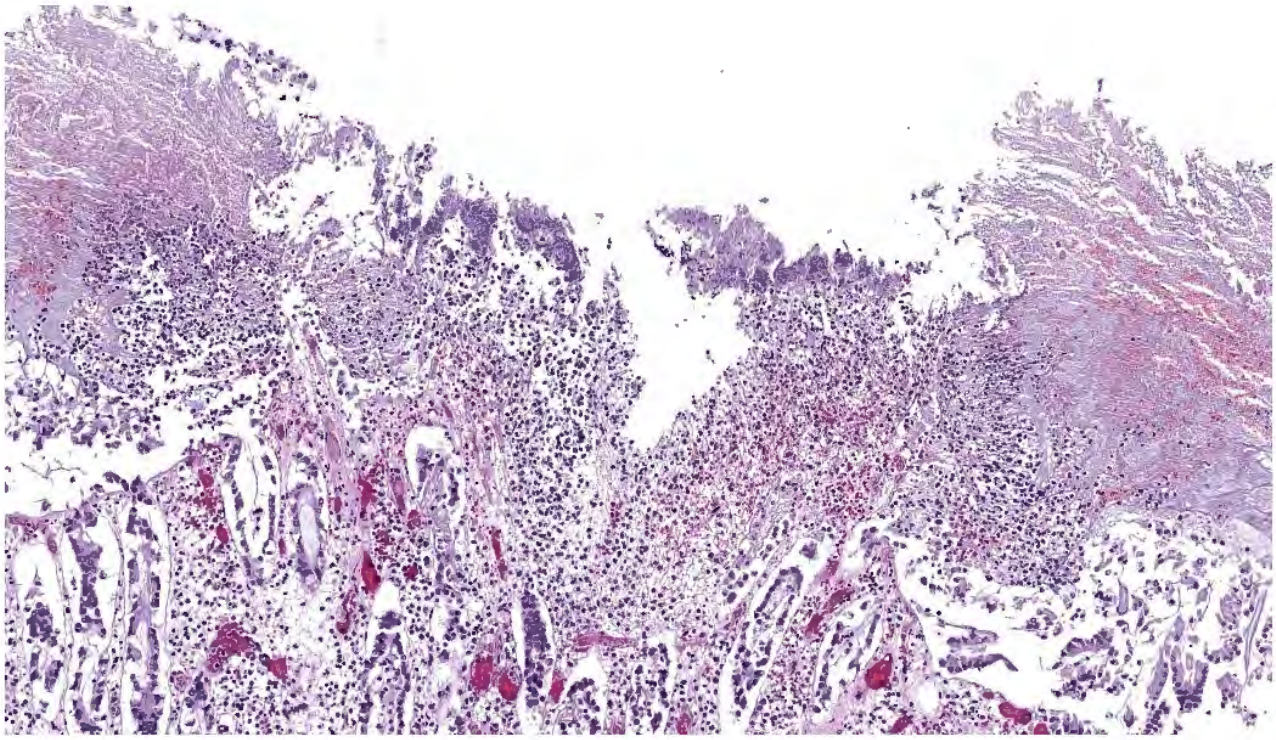

Figure 1-4. Colon, horse: Neutrophils extend vertically from the necrotic mucosa and peripherally within the overlying serocellular crust ("volcano ulcer") (HE, 180X)

microorganism in both small and large intestinal content. Because this ELISA test uses a cocktail of anti-toxin A and anti-toxin B antibodies, the positive result means that in the intestinal content there was one of the two toxins.[6] Isolation of *C. difficile* is suggestive of this microorganism involvement in the colitis, but not confirmatory as a number of clinically healthy horses can harbor *C. difficile* in the intestine.[4,5,6,7] Likewise, both gross and microscopic lesions are suggestive of, but not confirmatory, *C. difficile* infection. In particular, the volcano lesions are considered highly suggestive for *C. difficile* infection; this finding should, however, be interpreted with care, as other pathogens can also cause this lesion.[3,4,7]

The two main predisposing factors for *C. difficile* infection in horses are antibiotic therapy and hospitalization, both factors that were present in this case.[7] It is therefore speculated that salmonellosis occurred first and the attempts to control the disease with hospitalization and antibiotic treatment favored *C. difficile infection.*

No lesions suggestive of equine coronavirus were observed in the intestine of this horse; in particular, no intracytoplasmic inclusion bodies (the hallmark of such infection) were seen.[7] However, the necrosis of the mucosa was so extensive that if there were inclusion bodies, these may have been missed. Unfortunately, no post-mortem testing for equine coronavirus was performed.

This horse also had also a small intestine diverticulum, which was considered an incidental finding. Copper and selenium deficiency were also considered incidental findings, although a minor role in infection predisposition cannot be ruled out.

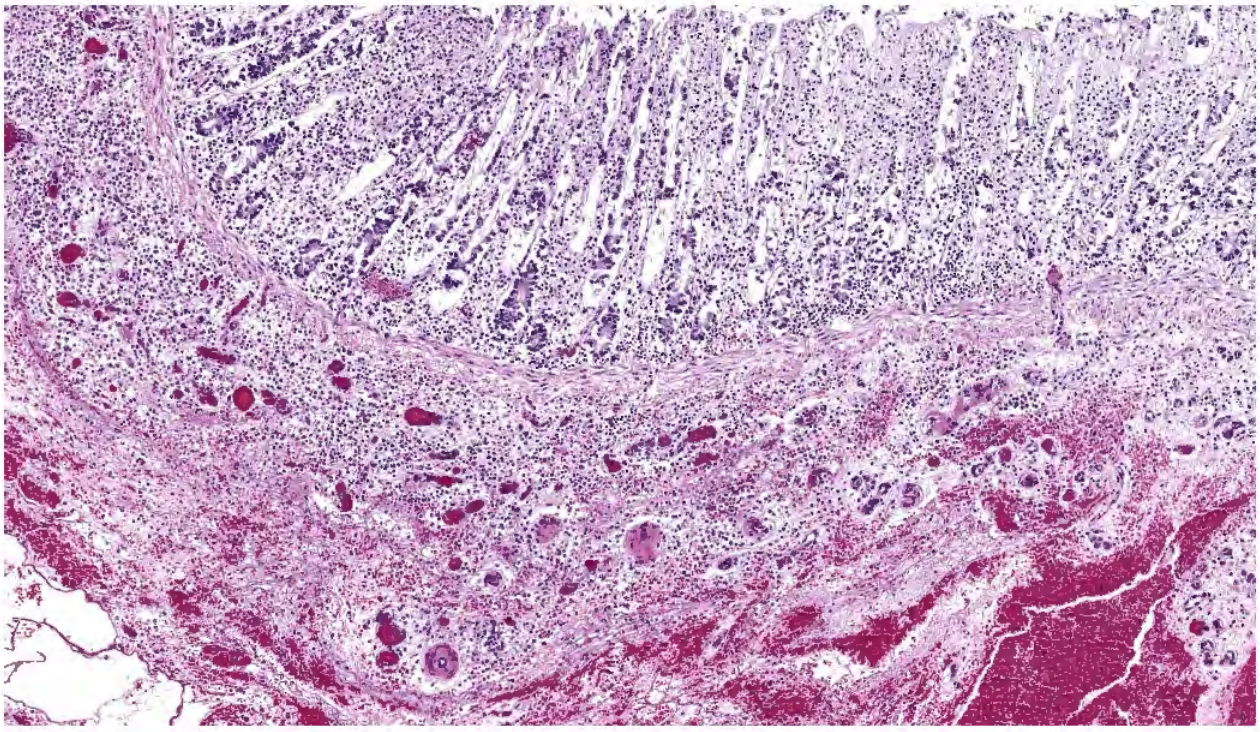

Figure 1-5. Colon, horse: The lamina propria and underlying submucosa are expanded by hemorrhage, edema, and numerous neutrophils. There are several thrombosed veins in the submucosa. (HE, 124X)

Contributing Institution:
California Animal Health and Food Safety Laboratory, Sa Bernardino Laboratory.
https://cahfs.vetmed.ucdavis.edu/

JPC Diagnoses:
Colon: Colitis, fibrinonecrotic, subacute, diffuse, marked, thrombosis, edema, and volcano lesions.

JPC Comment:
The JPC was thrilled to have the revered Dr. Paco Uzal, who needs no introduction, back again this year as a conference moderator. This first case provided a great example of an equine colitis case with multiple etiologies, something that is common in equine practice. The contributor provided an excellent write-up on this case and touched on many of the primary points of discussion during conference. Some participants struggled with determining if the tissue ID was small intestine or colon due to the degree of necrosis; this is reasonable and it can become incredibly difficult to differentiate the two when the architecture is lost. This horse also had a history of extensive NSAID administration and hospitalization, both of which are predisposing factors for both *C. difficile and Salmonella* infection. Grossly and histologically, *C. difficile*, *Salmonella* spp, and NSAID-induced ulceration can all look identical; culture and toxin typing are necessary for confirmatory diagnosis.[3] Participants agreed that the relevance of the previous equine coronavirus infection in this case could not be known.

Salmonella enterica var Typhimurium, thought to be the primary pathogen in this case by both the contributor and conference participants, is a non-host-adapted species of *Salmonella* that causes enteric disease in numerous species.[3] The overt lack of GI-associated lymphoid tissue (GALT) histologically should

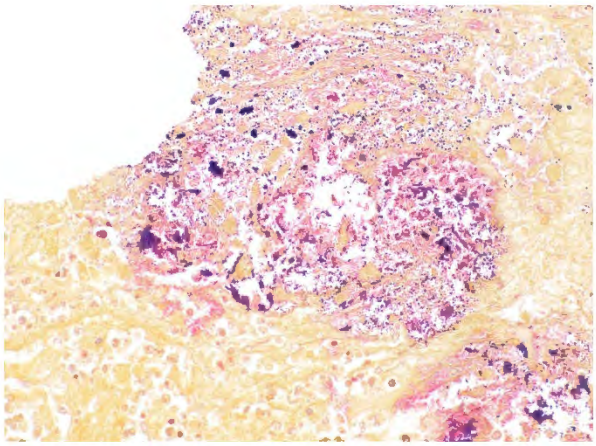

Figure 1-6. Colon, horse: There are colonies of mixed gram-positive and gram-negative bacilli within the necrotic mucosa. (Hucker Conn, 400X).

clue the pathologist in to the possibility for a *Salmonella* infection due to its tendency to infect the GALT first. *Salmonella* utilizes a Type 3 secretion system (T3SS) to stimulate phagocytosis and entry into M-cells and, subsequently, macrophages in the underlying lymphoid tissue. *Salmonella* inhibits fusion of the phagosome and lysosome to ensure its survivability within the macrophage and begins replicating safely within a Salmonella-containing vacuole (SCV). From there, it can be trafficked throughout the body hidden within macrophages. Later, using a Type 1 secretion system (T1SS), *Salmonella* stimulates apoptosis of the macrophage via activation of caspase 1, enabling each *Salmonella* to escape the host cell and infect additional cells. In this case, *Salmonella* Typhimurium was cultured from the small intestine, colon, and liver, indicating a septic process.

Clostridioides difficile (renamed in 2016 from *Clostridium difficile*) affects many species of all ages.[1,3] The primary clinical sign is profuse diarrhea. Histologically, "volcano lesions", as seen in this case, are a hallmark of *C. difficile* in the acute phase of infection.[3,4] Although other organisms (including *Salmonella*) can cause these lesions, they are considered classic for *C. difficile*. These lesions are characterized by micro-ulcerations of the mucosa with necrotic debris and neutrophils being "spat out" into the lumen, giving it the appearance of lava spewing from an erupting volcano. Following acute infection, volcano lesions become difficult to see histologically due to the progression to a full-blown necrotizing colitis, the lesions of which are non-specific and can be caused by a number of enteric pathogens (i.e. *Salmonella spp, Brachyspira spp*, etc.). As mentioned by the contributor, culture is a more suggestive method for confirming a diagnosis of *C. difficile*, but the results must be interpreted with caution as, according to Dr. Uzal, 3% of clinically normal horses will grow *C. difficile* on culture of enteric content.[4]

ELISA testing for *C. difficile* A/B toxin from the intestinal content/feces of affected animals, which was performed in this case, is considered confirmatory for a diagnosis of *C. difficile*. These toxins are the primary drivers of disease in *C. difficile* infection. TcdA (enterotoxin) binds to intestinal brush border receptors, while TcdB (cytotoxin) binds to receptors like LRP1. Both are internalized via receptor-mediated endocytosis, where they inactivate small GTP-binding proteins of the Rho/Ras family via mono-O-glucosylation.[2] These proteins play key roles in regulating the cytoskeletal dynamics of actin. Their inactivation leads to changes in the shape of the cell, retraction of cell processes, detachment from neighboring cells, and cell rounding.[1,2] This causes the cell to undergo apoptosis.[1,2] In the case of detachment-mediated stress, this form of apoptosis may be similar to anoikis, a form of apoptosis that occurs in "homeless", anchor-dependent cells that have become detached from the extracellular matrix and/or surrounding cells.

References:

1. Di Bella S, Ascenzi P, Siarakas S, Petrosillo N, di Masi A. *Clostridium difficile* Toxins A and B: Insights into Pathogenic Properties and Extraintestinal Effects. *Toxins (Basel)*. 2016;8(5):134.
2. Liu Z, et al. Structural basis for selective modification of Rho and Ras GTPases by *Clostridioides difficile* toxin B. *Sci Adv*. 2021;7:eabi4582.
3. Mendonça FS, Navarro MA, Uzal FA. The comparative pathology of enterocolitis caused by *Clostridium perfringens type C, Clostridioides difficile, Paeniclostridium sordellii, Salmonella enterica* subspecies *enterica* serovar Typhimurium, and non-steroidal anti-inflammatory drugs in horses. *J Vet Diagn Invest.* 2021;34:412-420.
4. Uzal FA, Diab SS, Blanchard P, Moore J, Anthenill L, Shahriar F, Garcia JP, Songer JG.. *Clostridium perfringens* type C and *Clostridium difficile* co-infection in foals. *Vet Microbiol.* 2012;156:395-340.
5. Uzal FA, Diab SS. Gastritis, enteritis, and colitis in horses. *Vet Clin North Am Equine Pract*. 2015;31:337-358.
6. Uzal FA, Navarro MA, Asin J, Henderson EE. Clostridial Diseases of Horses: A Review. Vaccines (Basel). 2022;10:318.
7. Uzal FA, Arroyo LG, Navarro MA, Gomez DE, Asín J, Henderson E. Bacterial and viral enterocolitis in horses: a review. *J Vet Diagn Invest.* 2022;34:354-375.

CASE II:

Signalment:

8-month-old, castrated male domestic shorthair cat (*Felis catus)*

History:

The cat was neutered and was recovering well until the evening following surgery. After then, the cat was inappetent and lethargic. He developed diarrhea the second day after surgery. The cat was found dead the third day after surgery.

Gross Pathology:

At postmortem examination, the cat was in good body condition with minimal postmortem decomposition. The skin of the scrotum, prepuce and perineum was swollen with large amounts of subcutaneous edema and emphysema. The right and left inguinal areas and medial aspect of the thighs were swollen by subcutaneous edema and emphysema, but the right rear leg was particularly swollen. The skin of the medial aspect of the thigh of the right rear leg was mottled red and green. The semitendinosus and semimembranosus muscles of the right and left rear legs were dark red to black, edematous and emphysematous with the most severe lesions in the right rear leg. There was marked subcutaneous edema consisting of light red fluid cloudy fluid in the skin of the dorsal lumbar area extending ventrally into the right and left flanks.

Figure 2-1. Skeletal muscle, cat: (Photo courtesy of: New Mexico Department of Agriculture Veterinary Diagnostic Services http://www.nmda.nmsu.edu/home/divisions/vds/)

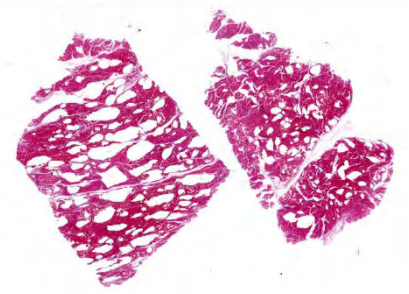

Figure 2-2. Skeletal muscle, cat: At subgross magnification, there is marked emphysema within the sections of skeletal muscle. (HE, 10X)

Laboratory Results:
Fluorescent antibody testing of the affected skeletal muscle was positive for *Clostridium novyi* and negative for *Clostridium chauvoei*, *Clostridium septicum* and *Clostridium sordellii*.

Moderate numbers of *Clostridium novyi* and rare *Clostridium perfringens* were isolated on anaerobic culture. There were no bacteria isolated on aerobic culture.

Microscopic Description:
The grossly affected skeletal muscle is necrotic with swollen, hypereosinophilic to pale staining myofibers that have lost their cross striations. The sarcoplasm of small numbers of myofibers is fragmented and replaced by eosinophilic flocculent material. The interstitium is emphysematous and contains small amounts of hemorrhage and edema that separate individual myofibers and the endomysium. There are also numerous large bacilli and a few perivascular to random multifocal infiltrates of small numbers of degenerate neutrophils in the interstitium. There are small numbers of arterioles and venules with necrosis of the vascular wall.

Contributor's Morphologic Diagnoses:
Skeletal muscle: Acute necrosis with emphysema, hemorrhage, mild suppurative myositis and numerous intralesional bacilli; etiology, *Clostridium novyi.*

Contributor's Comment:
Clostridium species are large, gram-positive, rod-shaped bacteria that produce endospores.[4] They are obligate anaerobes with some species being difficult to grow (*Clostridium novyi* and *C. haemolyticum*) because they can rapidly die (within fifteen minutes) after being exposed to oxygen. The pathogenic *Clostridium* can be divided into three general groups based on the disease they cause. The neurotoxic clostridia include *C. botulinum* and *C. tetani*. The histotoxic clostridia include *C. chauvoei*, *C. haemolyticum*, *C. novyi* types A and B, *C. perfringens* type A, *C. septicum* and *C. sordelli*. The enteric clostridium include *C. perfringens* types A-E, *C. difficile*, *C. spiroforme* and *C. colinum*. Some authors will placed *C. piliforme* in a group by itself and classify it as an atypial clostridium. The histotoxic clostridia produce toxins, are invasive, and are responsible for the various forms of clostridial myonecrosis (clostridial myositis) such as malignant edema, gas gangrene, blackleg, and pseudoblackleg.[2,5,6] Other than blackleg in ruminants being specifically caused by *C. chauvoei*, the other forms of clostridial myonecrosis are not specifically caused by any species of *Clostridium*. The clostridia causing myonecrosis are typically found in the soil or are part of the flora of the gastrointestinal tract. Clostridial myonecrosis can be the result of endogenous latent clostridial spores that reside in the skeletal muscle or exogenous bacteria that are introduced as wound contaminants. In both cases, the pathogenesis of myonecrosis is the same. Trauma to the skeletal muscle results in localized tissue hypoxia and anaerobic conditions allowing the clostridia to proliferate. As the pH and oxygen content of the traumatized skeletal

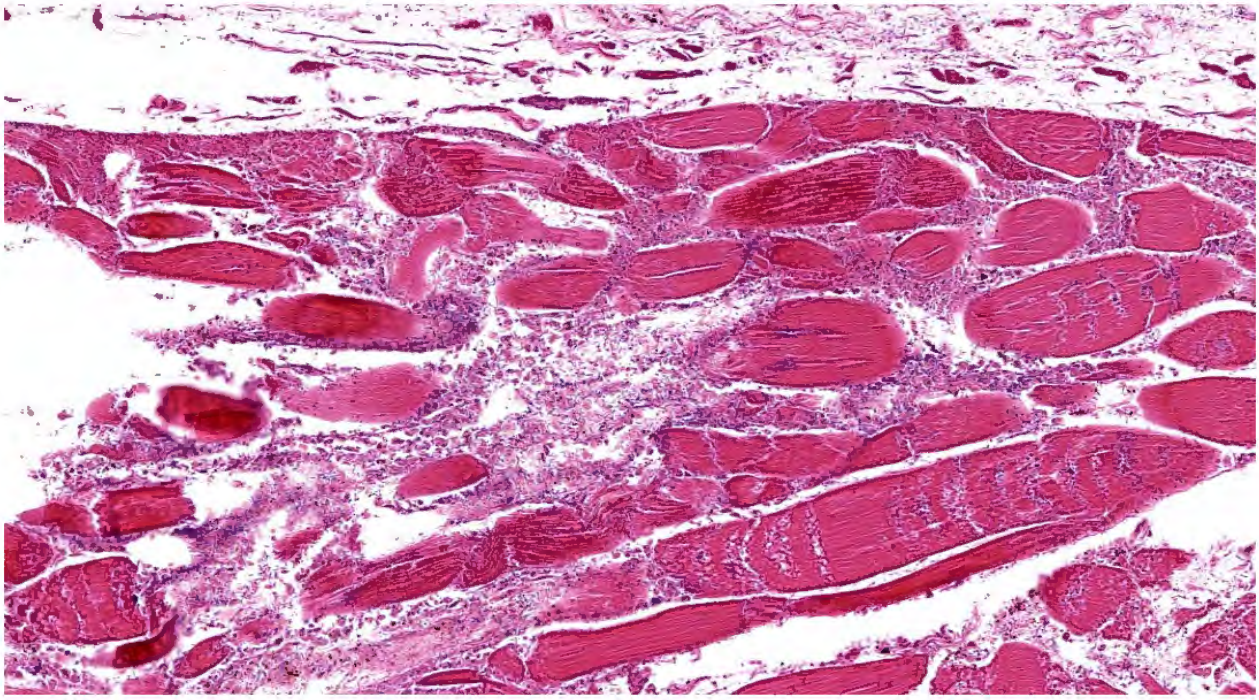

Figure 2-3. Skeletal muscle, cat: Necrotic fibers demonstrate contraction band formation, myofibrillolysis, and fragmentation. There are numerous robust bacilli within the necrotic myofibers and adjacent endo- and perimysium. (HE, 394X)

muscle decreases, the conditions for clostridial growth and toxin production become ideal. The clostridial toxins inhibit neutrophil infiltration into the lesion as well as weakening endothelial cell-to-cell contact. The clostridial toxin's effects on endothelial cells can result in vascular thrombosis causing further tissue hypoxia and necrosis. The clostridial toxins are eventually absorbed systemically and can result in hypovolemia, cavitary effusion, low cardiac output, low cardiac contractility, shock and death.

In the submitted case, the histotoxic clostridium *C. novyi* was detected in the skeletal muscle by fluorescent antibody testing as well as being isolated from the affected skeletal muscle. *Clostridium novyi* has three types.[2,4] *Clostridium novyi* type A produces alpha toxin (a cytotoxin) and causes clostridial myonecrosis. *Clostridium novyi* type B produces both the cytotoxic alpha toxin and a beta toxin (a phospholipase). *Clostridium novyi* type B causes infectious necrotizing hepatitis (black disease) following liver fluke infections in ruminants. *Clostridium novyi* type C does not produce toxins and is not pathogenic. The *C. novyi* alpha toxin as well as four other large clostridial cytotoxins function by glucosylating cellular GTPase proteins.[1,2] The clostridial cytotoxins have a particular affinity for the GTPase proteins that are involved in maintaining the cytoskeletal function. Inhibition of the cytoskeletal proteins results in loss of endothelial cell integrity that results in edema and thrombosis locally as well as hypovolemia, hypotension, organ failure and death systemically.

Clostridial myonecrosis can develop in multiple species, but is most common in ruminants, horses, and swine.[3] In all species, skeletal muscle necrosis in the primary lesion. The muscle necrosis is accompanied by edema, hemorrhage, and often emphysema. The hemorrhage and lysis of erythrocytes cause the affected skeletal muscle to be dark red to black.

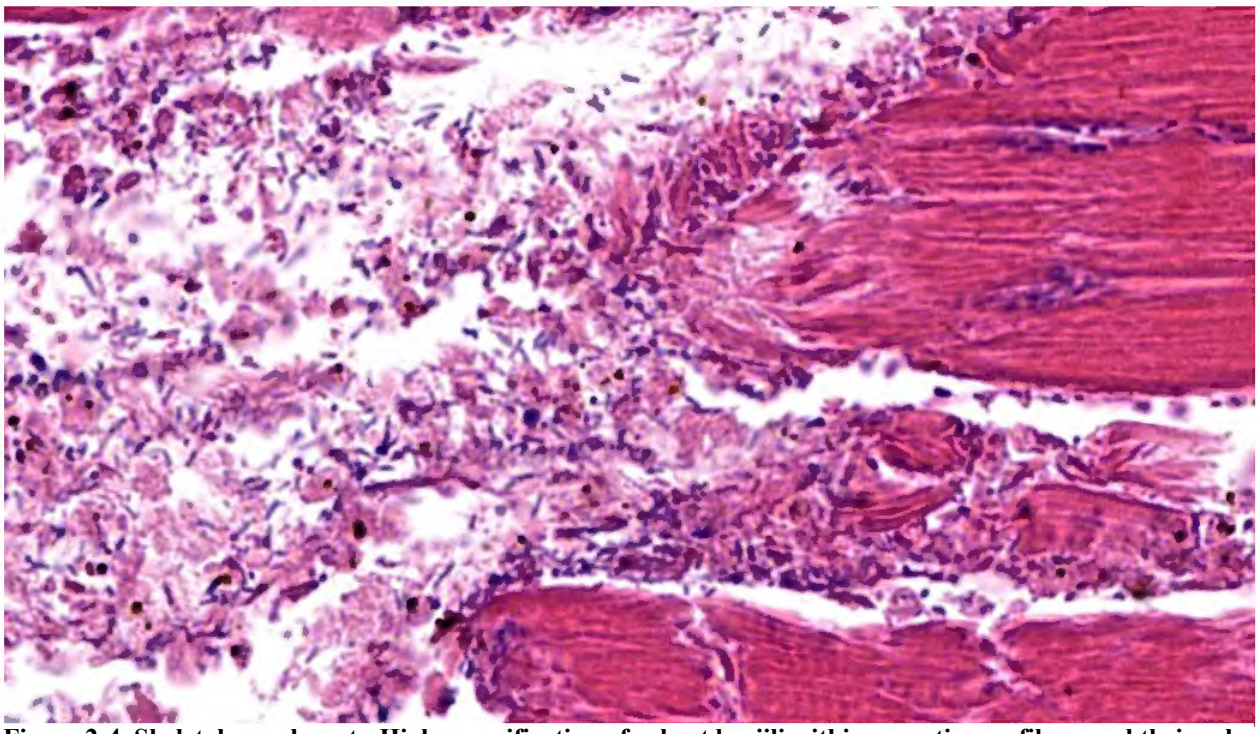

Figure 2-4. Skeletal muscle, cat: High magnification of robust baciili within necrotic myofibers and their cellular debris. (HE, 1800X)

The necrotic skeletal muscle often has a rancid odor. The microscopic lesions mirror the gross lesions. The primary microscopic lesion is necrotic myofibers that are separated by edema, hemorrhage and lysed erythrocytes. The skeletal muscle may be emphysematous. There typically are very few neutrophils within the lesion. The number of bacteria in the lesion varies widely with the lesions in some animals containing large numbers of bacteria with the lesions in other animals containing small numbers of bacteria. Most lesions have small numbers of bacteria. Fragmentation of the necrotic myofibers in the deeper aspects of the lesions may be present. The affected animals die quickly usually within twenty-four hours if not treated. The histotoxic clostridia spread quickly throughout the carcass postmortem resulting in rapid decomposition. Because these bacteria spread quickly throughout the carcass postmortem, one has to be careful in interpreting positive identification of histotoxic clostridia within muscle lesions as the *Clostridium* species identified may be a postmortem contaminant rather than the cause of the muscle necrosis.

Contributing Institution:
New Mexico Department of Agriculture
Veterinary Diagnostic Services
http://www.nmda.nmsu.edu/home/divisions/vds/

JPC Diagnoses:
Skeletal muscle: Myositis, necrotizing, acute, diffuse, severe, with emphysema and large, occasionally sporulating bacilli.

JPC Comment:
This contributor's outstanding comment pretty much covers it all! The few points from the conference discussion not covered in the write-up above focused on a review of some of the terminology utilized to describe degenerative and necrotic lesions in skeletal muscle ("loss of cross striations," "vacuolation,"

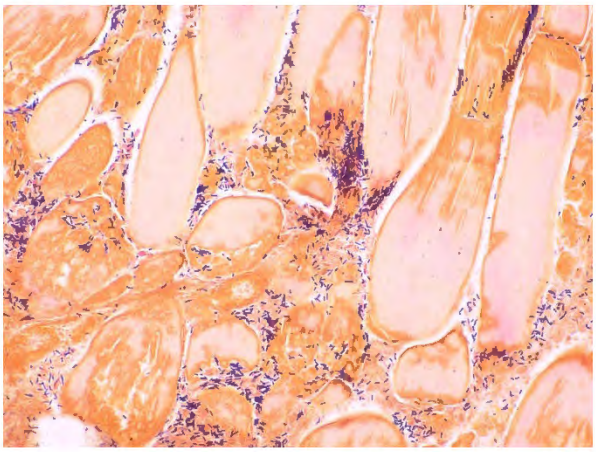

Figure 2-5. Skeletal muscle, cat: High magnification of robust gram-positive bacilli within areas of necrotic skeletal muscle. (Hucker Conn, 400X)

"fragmentation," "myofibrillolysis," "contraction bands", etc.). Contraction bands, in particular, take some practice to see on an H&E and are characterized by hypercontracted, intensely eosinophilic transverse bands within the sarcoplasm of myocytes. These represent focal myofibrillar disruption and are often seen in rhabdomyolysis, trauma, or ischemia.[7] They correspond to extremely shortened sarcomeres with obliterated I-bands and H-zones and are an indication of myocyte necrosis.[7] The contraction bands in these cases can be beautifully revealed with a PTAH stain. For both written and oral descriptions of slides in which a clostridial organism is suspected, Dr. Uzal additionally made a point to mention that there should be mention of whether the bacteria are sporulating or non-sporulating. In this case, there were a few sporulating bacteria present on the H&E; this is reflected in the JPC's morphologic diagnosis.

Dr. Uzal ran immunohistochemical stains on this case for multiple gas gangrene-causing clostridial species in his lab, as gas gangrene cases are frequently infected with multiple organisms. In this case, there was immunoreactivity for both *Clostridium novyi* and *Paraclostridium sordellii* (previously *C. sordellii*). Of the types of *C. novyi* listed by the contributor, type A was most likely the offender in this case. The Type A toxin of *C. novyi* behaves similarly to the A-B toxin of *C. difficile* discussed above in Case 1. Participants also took note that C. perfringens had been cultured by the contributor and speculated that the *C. perfringens* were present as bystanders and were not actively contributing to the infection in this cat.

References:

1. Aronoff DM. Clostridium novyi, sordellii, and tetani: mechanisms of disease. *Anaerobe*. 2013;24:98-101.
2. Aronoff DM and Kazanjian PH. Historical and contemporary features of infections due to Clostridium novyi. *Anaerobe*. 2018;50:80-84.
3. Cooper BJ and Valentine BA. Muscle and tendon. In: Maxie MG, ed. *Pathology of Domestic Animals*. 6th ed. vol. 1. St. Louis, MO: Elsevier; 2016:230-233.
4. Markey BK, Leonard FC, Archambault M, Cullinane A, Maguire D. Clostridium species. In: Markey BK, Leonard FC, Archambault M, Cullinane A, Maguire D, eds. *Clinical Veterinary Microbiology*. 2nd ed. St. Louis, MO: Mosby Elsevier; 2013:215-229.
5. Nagahama M, Takehara M, Rood JL. Histotoxic clostridial infections. *Microbiol Spectrum*. 2019;6(4):1-17.
6. Stevens DL, Aldape MJ, Bryant AE. Life-threatening clostridial infections. *Anaerobe*. 2012;18:254-259.
7. Venance SL, Burns KL, Veinot JP, Walley VM. Contraction bands in visceral and vascular smooth muscle. *Hum Pathol*. 1996;27(10):1035-1041.

CASE III:

Signalment:
9-month-old, female, spayed Bernese Mountain dog (*Canis lupus familiaris)*

History:
The dog presented for a 1-month history of severe ileus that was unresponsive to medical management. Abdominal radiographs showed a diffusely fluid and gas distended small intestine, with an intestinal diameter reaching 3.3 cm. Laparotomy to obtain biopsies of the gastrointestinal tract was performed. Due to poor prognosis and progressive clinical deterioration the patient was euthanized. A post-mortem examination was declined by the owners.

Gross Pathology:
During surgery, the gastrointestinal tract was reported to be diffusely distended and friable without any appreciable peristaltic movement.

Laboratory Results: N/A

Microscopic Description:
Duodenum, jejunum and ileum: Diffusely throughout the sections, there is partial to complete loss of the leiomyocytes of the outer and inner muscularis, which are multifocally replaced by loose fibrous connective tissue (fibrosis). The remaining smooth muscle is infiltrated by large numbers small and intermediate lymphocytes, few macrophages and neutrophils. The same inflammatory infiltrate is present throughout the muscularis mucosae. Remaining leiomyocytes have pale, frequently vacuolated cytoplasm. In the submucosa, muscularis and serosa there are small to moderate numbers of perivascular lymphocytes. Small lymphocytes, and infrequently neutrophils, surround or infiltrate the myenteric and submucosal ganglia, though neurons do not exhibit degenerative changes. The lamina propria contains a markedly increased number of lymphocytes, plasma cells and a mildly increased number of eosinophils. The epithelium is diffusely overlain by myriad bacterial rods. The serosa is mildly expanded by increased clear space (edema) and is lined multifocally by markedly hypertophied mesothelium. In the stomach a similar process is observed but restricted to the outer aspect of the muscularis with a patchy/multifocal distribution and sparing of the muscularis mucosae. (section not submitted)

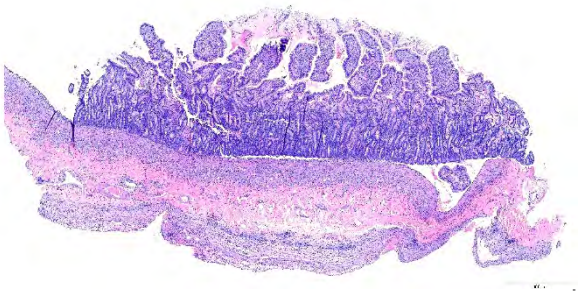

Figure 3-1. Jejunum, dog. The jejunal wall is markedly thinned and the muscularis propria and muscularis mucosae have a marked inflammatory infiltrate. (HE, 10X) (Photo courtesy of: Cummings School of Veterinary Medicine at Tufts University, Department of Biomedical Sciences, Section of Pathology, http://vet.tufts.edu/department-of-biomedical-sciences/research/pathology/)

Contributor's Morphologic Diagnoses:
Duodenum, jejunum and ileum: Severe, diffuse, chronic lymphocytic leiomyositis with severe muscularis atrophy; marked, diffuse, chronic lymphoplasmacytic enteritis.

Contributor's Comment:
Chronic intestinal pseudo-obstruction (CIPO) is a well-documented, rare gastrointestinal syndrome and represents a disorder leading to impaired intestinal motility that results in signs compatible with intestinal obstruction without occlusion of the intestinal lumen.[4,6,8,15]

Etiology of CIPO can be broadly considered primary (idiopathic), secondary or familial

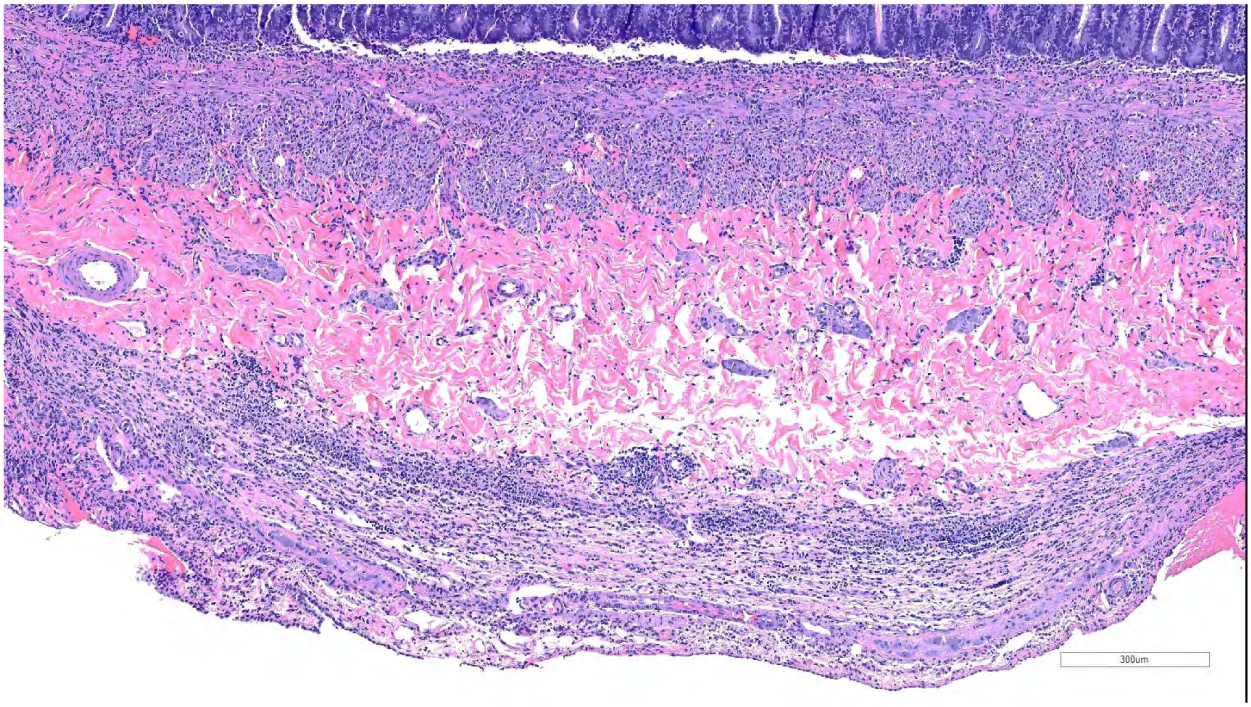

Figure 3-2. Jejunum, dog. Higher magnification showing the thinning of the muscularis with a marked lymphocytic inflammatory infiltrate that spares the submucosa. (HE, 100X) (Photo courtesy of: Cummings School of Veterinary Medicine at Tufts University, , Department of Biomedical Sciences, Section of Pathology, http://vet.tufts.edu/department-of-biomedical-sciences/research/pathology/)

where primary CIPO has no demonstrable etiopathologic cause, and secondary CIPO may be due to systemic pathology and thus, is more commonly seen in older human patients.[4] Regardless of the cause, CIPO is classified histologically in humans as myopathic, mesenchymopathic, and neuropathic groups, based on the involvement of the nerve pathways supplying the gastrointestinal tract, the interstitial cells of Cajal, and smooth muscle cells, respectively.[1,4,15]

The classic clinical presentation of affected dogs is marked gastric and small intestinal dilation with severe hypomotility and clinical signs of abdominal discomfort, vomiting, regurgitation, small bowel diarrhea, anorexia, and weight loss. Clinicopathologic changes are variable and nonspecific. Radiographic and ultrasonographic imaging of the abdomen shows variable involvement of the stomach, small intestine and colon in all dogs with diffuse dilatation of the small intestine, variable dilation of the stomach and large intestine.[15]

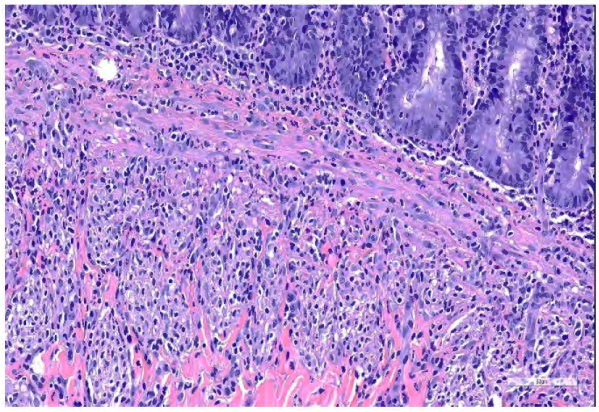

Figure 3-3. Jejunum, dog. Higher magnification showing the marked lymphocytic infiltrate affecting the muscularis mucosae and the mixed inflammatory infiltrate in the lamina propria. (HE, 400X) (Photo courtesy of: Cummings School of Veterinary Medicine at Tufts, , Department of Biomedical Sciences, Section of Pathology, http://vet.tufts.edu/department-of-biomedical-sciences/research/pathology/)

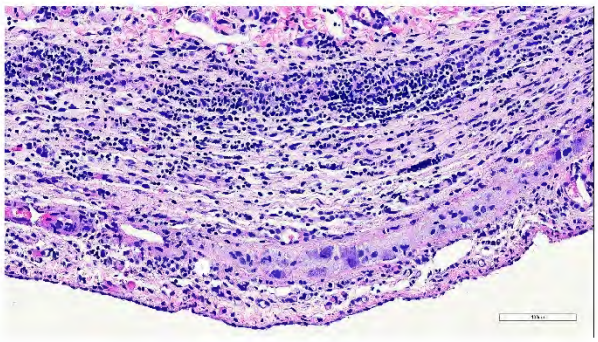

Figure 3-4. Jejunum, dog. There is marked loss of the smooth muscle of the muscularis with a marked lymphocytic infiltrate that spares the myenteric ganglia. (HE, 400X) (Photo courtesy of: Cummings School of Veterinary Medicine at Tufts University, Department of Biomedical Sciences, Section of Pathology, http://vet.tufts.edu/department-of-biomedical-sciences/research/pathology/)

CIPO in dogs is a rare disorder that is increasingly being diagnosed, and is attributed to intestinal leiomyositis.[10,15] Prior reports of leiomyositis have been described in large breed dogs and similar to this case, Bernese Mountain dogs are featured in several of these reports.[3,6,15] Other breeds reported in the literature include Portuguese Water dogs, Yorkshire Terrier, Border Collie, American Staffordshire Terrier, English Springer Spaniel, German Shepherd Dog, and mixed breed dogs.[6,8,15] The ages of affected dogs range from 6 months to 10 years old, which emphasizes that this disorder should be a differential in both young and older dogs.[15] In human pediatric patients, a similar idiopathic/autoimmune myositis restricted to the muscularis propria has been described as an isolated condition or arise as part of more generalized connective tissue disease.[9,13] This pattern differs from other congenital conditions in humans where smooth muscle from the urinary tract, particularly the urinary bladder, is also affected.[14]

Microscopic findings reported for this condition consist of mild to marked mononuclear infiltrate, myofiber degeneration and fibroplasia or fibrosis centered within the muscularis propria of the stomach, small and large intestinal wall with the jejunum being the most severely and chronically affected segment.[7,15] In early lesions the inflammation and smooth muscle degeneration are segmental, random between the outer and inner muscularis layers and sparing of the muscularis mucosae.[15] Concurrent cecal involvement leading to impaction has also been described.[5] Consistent histologic findings included T-lymphocyte inflammation within the muscularis propria with relative sparing of the mucosa, submucosa and neural plexuses.[14] In one case report the inflammatory infiltrate was predominantly of B-lymphocytes and featured extensive angiogenesis.[6] Leiomyocytes appear to be the target of the inflammation given the presence of various stages of degeneration leading to complete myofiber loss in chronic stages of the disease. Superficial inflammation is a frequent secondary finding in CIPO and has been associated with bacterial overgrowth, which were changes observed in this case.[6] Neuropathy has not been a feature in most reports of canine CIPO. Inflammatory cells obscuring the

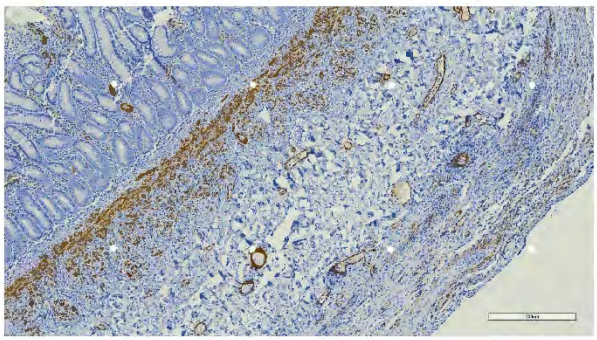

Figure 3-5. Jejunum, dog. Loss of smooth muscle is stressed by loss of smooth muscle actin immunoreactivity of the muscularis with relative sparing of the muscularis mucosae. (Anti-SMA, 400X) (Photo courtesy of: Cummings School of Veterinary Medicine at Tufts University, Department of Biomedical Sciences, Section of Pathology, http://vet.tufts.edu/department-of-biomedical-sciences/research/pathology/)

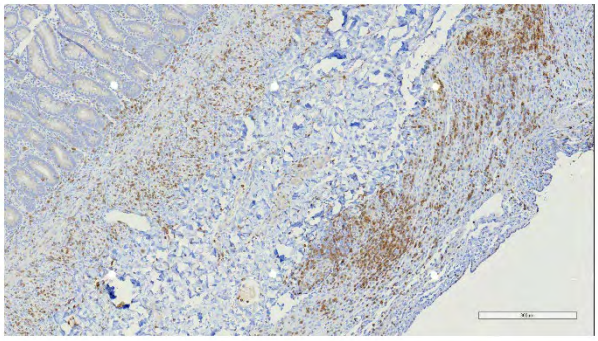

Figure 3-6. Jejunum, dog. The lymphocytic infiltrate in the muscularis is composed predominantly of lymphocytes showing strong cytoplasmic and membranous immunoreactivity for CD3, proving T-cell origin. Anti-CD3. (HE, 200X) (Photo courtesy of: Cummings School of Veterinary Medicine at Tufts University, Department of Biomedical Sciences, Section of Pathology, http://vet.tufts.edu/department-of-biomedical-sciences/research/pathology/)

myenteric and submucosal plexuses in this case were considered an extension from the neighboring inflammation as no degenerative changes were observed in the neurons. Myenteric ganglionitis has, however, been reported occurring concurrently with leiomyositis.[10]

The pathogenesis for this condition remains unclear, though the targeting of smooth muscle by T-lymphocytes is supportive of a cell-mediated inflammatory process suggestive of an immune-mediated process against intestinal smooth muscle.[11,14,15] In humans with intestinal leiomyositis, the inflammation is specific for the intestinal musculature as leiomyocytes of vessels or other tissues are unaffected.[15] Humans with intestinal leiomyositis can have autoimmune disease as a preexisting condition, including systemic lupus erythematosus, rheumatoid arthritis, scleroderma, and autoimmune hepatitis.[7] Neither the dog in this case nor those in the largest case series in dogs with leiomyositis had concurrent evidence of systemic autoimmune disease.[14] In few human cases, acute episodes of infectious gastroenteritis or diarrhea preceded the development of gastrointestinal distention.[7] Molecular mimicry has been proposed as a mechanism for the development of leiomyositis, although an explanation of restriction of the inflammation to the gastrointestinal tract was not elucidated.[7]

An important diagnostic consideration for cases of leiomyositis is mechanical obstruction secondary to foreign body. The combination of complementary imaging methods such as abdominal radiographs with ultrasonography is the most effective method to rule out the presence of a mechanical obstruction, though exploratory laparotomy is required for sampling when leiomyositis is suspected.[15]
The prognosis of dogs with intestinal leiomyositis is generally poor with survival times ranging from 10 days to 5 weeks after diagnosis.[14] Management of CIPO in humans is challenging and aimed at controlling symptoms and minimizing complications and typically involves immunomodulatory therapy.[12,15] Early diagnosis and treatment, results in a better long-term prognosis in humans. One case report in a dog described a favorable response to therapy after early diagnosis and treatment, suggesting better prognosis if the condition is identified before the onset of muscle atrophy.[11]

Contributing Institution:
Cummings School of Veterinary Medicine at Tufts University
Department of Biomedical Sciences, Section of Pathology
200 Westboro Rd.
North Grafton, MA. 01536
http://vet.tufts.edu/department-of-biomedical-sciences/research/pathology/

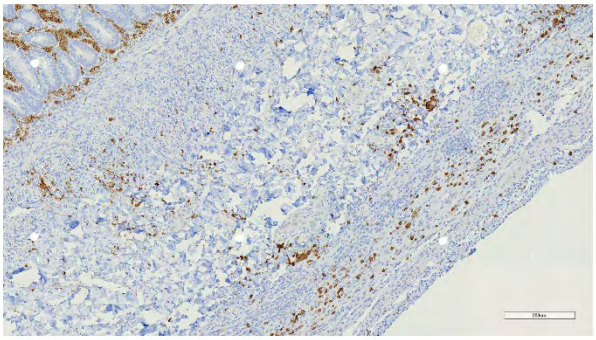

Figure 3-7. Jejunum, dog. A small percentage of the inflammatory infiltrate shows strong membranous and variable cytoplasmic immunoreactivity for CD20, consistent with B-cells. Anti-CD20. (HE, 400X) (Photo courtesy of: Cummings School of Veterinary Medicine at Tufts University, Department of Biomedical Sciences, Section of Pathology, http://vet.tufts.edu/department-of-biomedical-sciences/research/pathology/)

JPC Diagnoses:

Small intestine: Leiomyositis, lymphocytic, chronic, diffuse, severe, with marked smooth muscle loss and fibrosis.

JPC Comment:

Yet again, a fantastically written comment by the contributor that hits on the majority of conference discussion points! Chronic intestinal pseudo-obstruction (CIPO) has also been known by many names throughout its history, including fibrosing gastrointestinal leiomyositis, intestinal leiomyositis, idiopathic intestinal pseudo-obstruction, chronic intestinal dysmotility, and enteric myopathy. Many of these names are no longer in use, but intestinal leiomyositis and CIPO are most commonly utilized in the current literature. A good way to think about CIPO is that it is the clinical disease that can result from intestinal leiomyositis. This entity was last seen in the WSC in 2017 during Conference 4, Case 2. Histologically, the focus of lymphocytic inflammation on the smooth muscle cells of the intestine with replacement fibrosis and an absence of infectious organisms should make one think about this clinical syndrome, especially if the history fits.

The contributor thoroughly describes the syndrome in dogs, and differential diagnoses were mentioned in conference. These should include lymphocytic polymyositis, as some cases of this condition can have similar lesions in the esophagus and other areas of smooth muscle, and Chagas disease, caused by *Trypanosoma cruzi* (last seen in the WSC in 2024 during Conference 3, Case 3). T. cruzi can cause similar symptoms by causing chronic inflammation that leads to the destruction of the enteric nervous system (ENS), particularly the myenteric plexus.[13] This destruction results in severe neuromuscular dysfunction, leading to conditions like megaesophagus and megacolon.[13]

One participant brought up the possibility of a dysautonomia in this case, which is a great thought since CIPO may result from segmental or diffuse neuromuscular dysfunction in the gut. There are multiple forms of dysautonomia, such as specific autoimmune forms like autoimmune autonomic ganglionopathy (AAG) that involves autoantibodies attacking nerve cells.[2] Other forms arise secondary to other autoimmune disorders (i.e., Sjögren's, systemic lupus erythematosus).[2] However, in this case, the ganglia in the intestine looked great! This steered attendees away from considering a neuromuscular autoimmune condition. That being said, the pathogenesis of this condition has yet to be elucidated, and there is evidence that an autoimmune attack against smooth muscle cells could be at play.[12]

References:

1. Antonucci A, Fronzoni L, Cogliandro L, et al. Chronic intestinal pseudo-obstruction. *World J Gastroenterol.* 2008;14:2953–2961.
2. Blitshteyn S. Dysautonomia: a common comorbidity of systemic disease. *Immunol Res*. 2025;73(1):105.
3. Couraud L, Jermyn K, Yam PS, Ramsey IK, Philbey AW. Intestinal pseudo-obstruction, lymphocytic leiomyositis and atrophy of the muscularis externa in a dog. *Veterinary Record.* 2006;159:86–87.

4. Downes TJ, Cheruvu MS, Karunaratne TB, De Giorgio R, Farmer AD. Pathophysiology, Diagnosis, and Management of Chronic Intestinal Pseudo-Obstruction. *Journal of Clinical Gastroenterology.* 2018;52:477–489.
5. Eastwood JM, McInnes EF, White RN, Elwood CM, Stock G. Caecal Impaction and Chronic Intestinal Pseudo-Obstruction in a Dog. *Journal of Veterinary Medicine Series A*. 2005;52:43–44.
6. Gianella P, Tecilla M, Bellino C, et al. An unusual case of intestinal leiomyositis in a Bernese mountain dog. *Schweiz Arch Tierheilkd*. 2015;157:563–567.
7. Haas S, Bindl L, Fischer H-P. Autoimmune enteric leiomyositis: A rare cause of chronic intestinal pseudo-obstruction with specific morphological features. *Human Pathology*. 2005;36:576–580.
8. Johnson CS, Fales-Williams AJ, Reimer SB, Lotsikas PJ, Haynes JS. Fibrosing Gastrointestinal Leiomyositis as a Cause of Chronic Intestinal Pseudo-Obstruction in an 8-Month-Old Dog. *Veterinary Pathology.* 2007;44:106–109.
9. Kapur RP. Intestinal Motor Disorders. In: Pathology of Pediatric Gastrointestinal and liver disease. New York: Springer; 2014:249–316.
10. Kopke MA, Ruaux CG, Gal A. Myenteric ganglionitis and intestinal leiomyositis in a Jack Russell terrier: Myenteric ganglionitis and intestinal leiomyositis in a dog. Journal of Small Animal Practice. 2018: 1-4.
11. Murtagh K, Oldroyd L, Ressel L, Batchelor D. Successful management of intestinal pseudo-obstruction in a dog. *Veterinary Record Case Reports*. 2013: e000025
12. Oton E, Moreira V, Redondo C, et al. Chronic intestinal pseudo-obstruction due to lymphocytic leiomyositis: is there a place for immunomodulatory therapy?. *Gut*. 2005;54(9):1343–1344.
13. Pérez-Molina JA, Crespillo-Andújar C, Trigo E, et al. Chagas disease is related to structural changes of the gut microbiota in adults with chronic infection (TRIPOBIOME Study). *PLoS Negl Trop Dis*. 2023;17(7):e0011490.
14. Ruuska T, Karikoski R, Smith VV, Milla PJ. Acquired myopathic intestinal pseudo-obstruction may be due to autoimmune enteric leiomyositis. Gastroenterology. 2002;122:1133–1139.
15. Zacuto AC, Pesavento PA, Hill S, et al. Intestinal Leiomyositis: A Cause of Chronic Intestinal Pseudo-Obstruction in 6 Dogs. *Journal of Veterinary Internal Medicine.* 2016;30:132–140.

CASE IV:

Signalment:
6-week-old, female, New Zealand white rabbits (*Oryctolagus cuniculus*)

History:
A total of 15 rabbits arrived from the vendor and appeared in good health. Six days post-arrival, animal A was found dead in the cage, and B was found moribund. Animal B died before treatments could be commenced.

Gross Pathology:
The only obvious gross lesions in both animals were severely edematous large intestine which contained scant liquid feces..

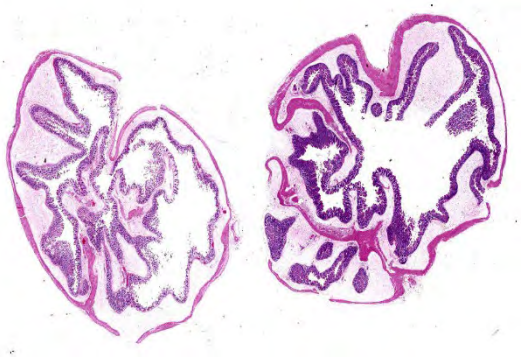

Figure 4-1. Colon, rabbit: Two sections of colon are submitted for examination. At subgross magnification, there is profound submucosal edema. (HE, 12X)

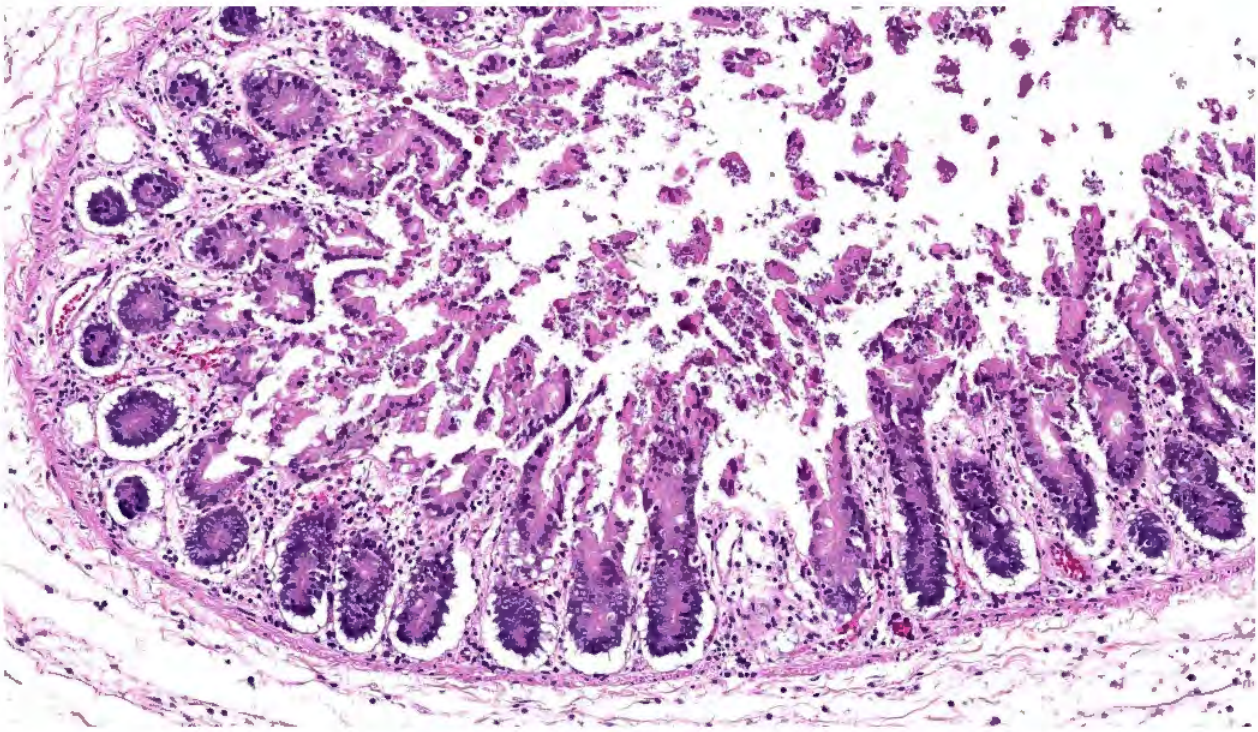

Figure 4-2. Colon, rabbit: There is ulceration of the colonic mucosa. (HE, 100X)

Laboratory Results:
Feces submitted to IDEXX yielded positive results for *Clostridium difficile* toxins A&B via ELISA.

Microscopic Description:
Cecum at ileocecocolic junction: One full-thickness cross sections of cecum at the ileocecocolic junction are examined from each animal (2 total). Diffusely, the submucosa is expanded by clear space (edema) and admixed inflammatory cells (neutrophils, macrophages, lymphocytes, and fewer plasma cells)(Fig 1). The lamina propria is multifocally expanded by edema, hemorrhage, the previously mentioned admixed inflammatory cells, and karyorrhectic debris (Fig 2). The overlying epithelium has multifocal erosions and ulcerations with surface necrotic debris and mixed bacterial colonies.

Contributor's Morphologic Diagnoses:
Typhlocolitis, acute, ulcerative, with edema and hemorrhage.

Contributor's Comment:
Clostridioides difficile (renamed from *Clostridium difficile* in 2016) is a toxin-producing, gram-positive, spore-forming anaerobe that affects humans and a variety of animal species.[4,9] When it was first identified from the feces of clinically normal babies in the 1930's it was named "the difficult clostridium" due to the fact that it was difficult to isolate and slow to grow in culture.[4,8] Sometimes called "pseudomembranous colitis", this entity causes classic histopathology lesion in humans and non-human primates including pseudomembrane formation on the intestinal surface.[2,8,13] In humans and animals, the pathogenesis involves disruption of commensal bacteria flora, colonization by C. difficile, and the release of toxins that cause significant mucosal damage.[4,8,13]

Rabbits are subject to a number of different clostridial diseases including enterotoxemia (*C. difficile, D. perfringens, C. spiroforme*), Tyzzer's disease (*C. piliforme*), dysautonomia

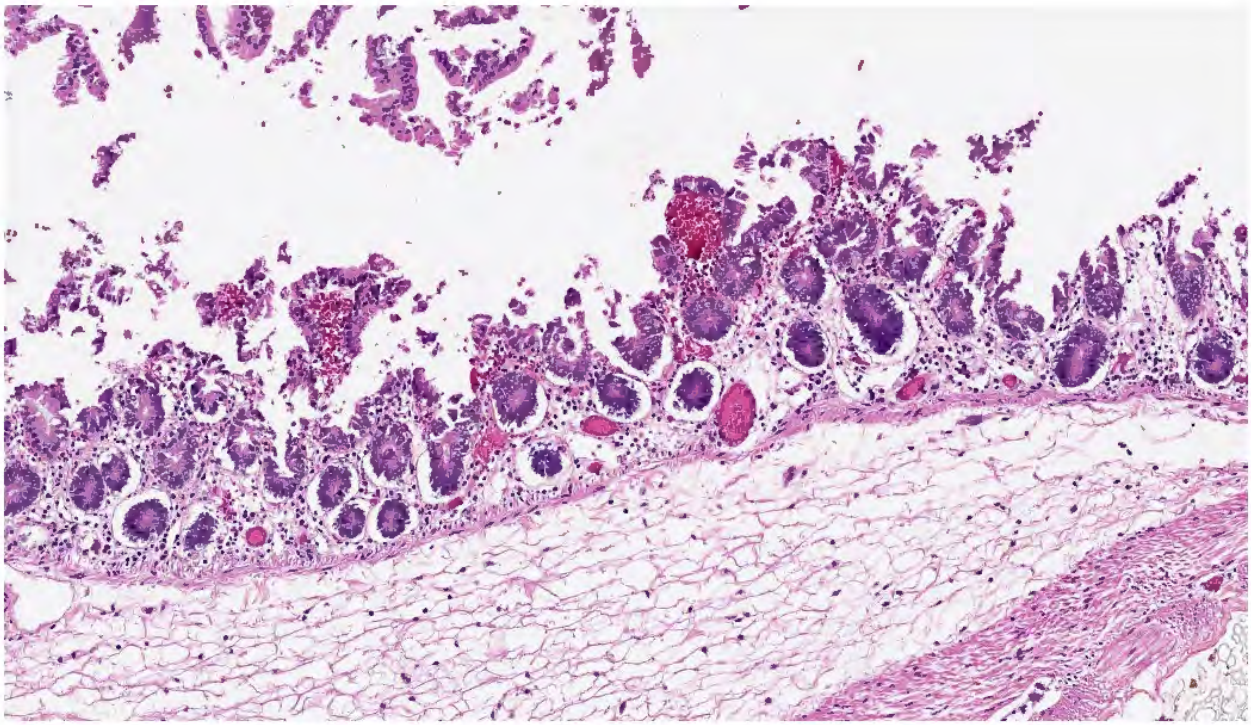

Figure 4-3. Colon, rabbit: There is multifocal hemorrhage of the colonic mucosa and marked submucosal edema. (HE, 200X)

(*C. botulinum*), and epizootic rabbit enteropathy (*C. perfringens* alpha toxin). Clostridial enterotoxemia has similar features in rabbits regardless of the species.[12] Chronicity can be acute or peracute.[6] In these cases, a peracute infection is likely since diarrhea, dehydration, or weight loss were not noted prior to death.

The primary virulence factors of *C. difficile* are two major exotoxins, toxin A and toxin B.[1-14] Both are enterotoxins, while Toxin B is both an endotoxin and cytotoxin. These toxins have the ability to glycosylate and inactivate Ras GTPases, disabling key cell signaling pathways, and glycosylate Rho and interfere with its regulation of cytoskeletal actin leading to apoptotic cell death of colonic epithelium.[1,13] Fecal ELISA is commonly used to identify these toxins and was used as a confirmation method in these rabbits to confirm the presence of *Clostridium difficile* A and B toxins in these rabbits. Fecal culture is the most sensitive method, but it is not very specific due to the possibility of isolating non-toxigenic isolates.[6] PCR detection of *C. difficile* is also highly sensitive and can discriminate between toxigenic and nontoxigenic strains of the organism by detecting its toxin-producing genes.[6]

As in humans, *C difficile* enterotoxemia in rabbits is associated with anything that disrupts the normal intestinal flora including antibiotic treatment.[1-14] These animals had not been treated with antibiotics, and it is suspected that stress from shipping was the primary factor leading to Clostridial disease in this case.

Although antibiotic treatment with metronidazole is considered the first choice of treatment in both humans and companion animals, treatment of *C. difficile*-associated disease has increasingly been associated with failure and recurrence.[3,11,14] In humans and marmosets, fecal transplantation shows promising results as a treatment for recurrent CDAD.[11,14] Additionally, a 2024 paper shows promising results

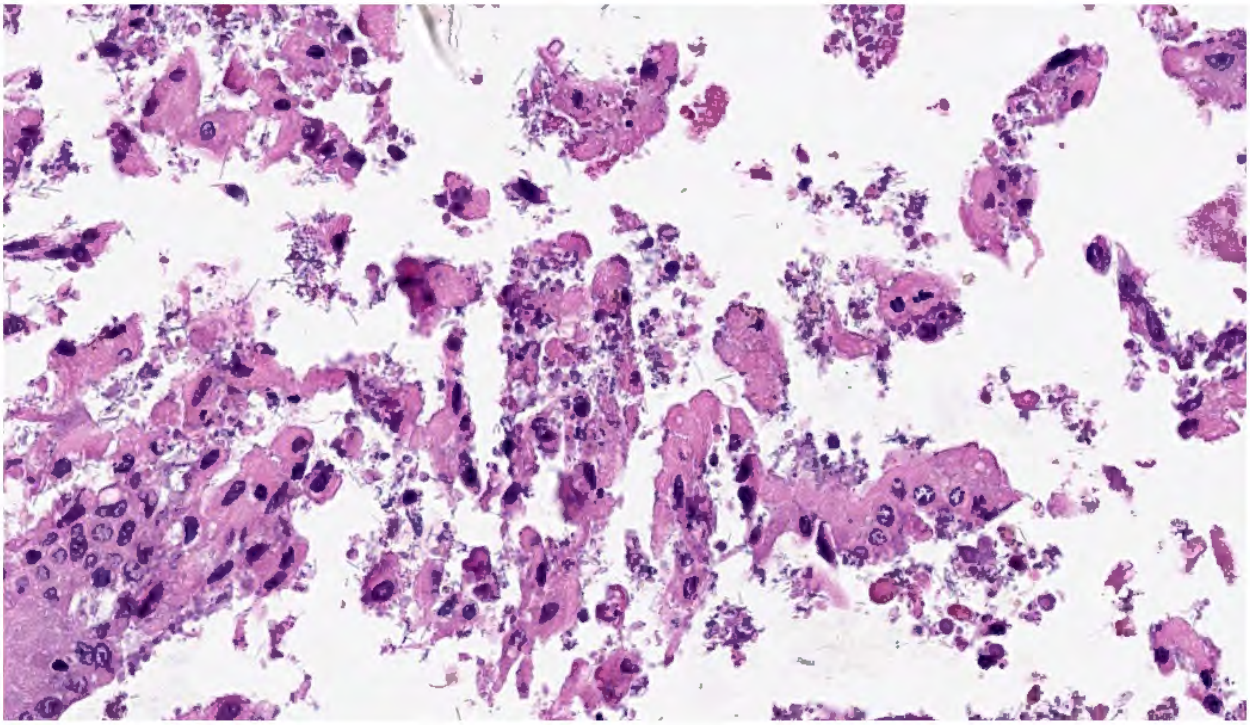

Figure 4-4. Colon, rabbit: Sloughed and necrotic enterocytes are admixed with numerous robust bacterial rods within the lumen (HE, 800X)

in the development of a *C. difficile* vaccine that uses metal-catalyzed oxidation (MCO) to inactivate toxins A & B after 2-3 intramuscular injections in rabbits.[1]

Contributing Institution:
Division of Laboratory Animal Resources
University of Pittsburgh
S1040 Thomas E. Starzl Biomedical Science Tower
200 Lothrop Street
Pittsburgh, PA 15261
http://www.dlar.pitt.edu/

JPC Diagnoses:
Colon: Colitis, necrotizing, subacute, multifocal, moderate, with volcano lesions, hemorrhage, and severe submucosal edema.

JPC Comment:
Wrapping up this conference is a classic example of another *C. difficile* infection, this time in a rabbit. Rabbits, along with hamsters and mice, are utilized in laboratory medicine in *C. difficile* studies. Rabbits specifically have been utilized because their gut tends to be colonized by heterogeneous *C. difficile* ribotypes, many of which are commonly isolated in humans.[6] As mentioned by the contributor, despite the lack of aggressive antibiotic therapy in the history, this animal had been recently transported and participants agreed that the stress of travel could have served as the predisposing factor for *C. difficile* overgrowth.

Similar to Case 1, due to the presence of volcano lesions coupled with mucosal ulceration/necrosis and heterophilic inflammation, Dr. Uzal says this is *C. difficile* until proven otherwise! This case had some solid examples of volcano lesions in which heterophils could be seen exploding out of tiny ulcers in the mucosa.

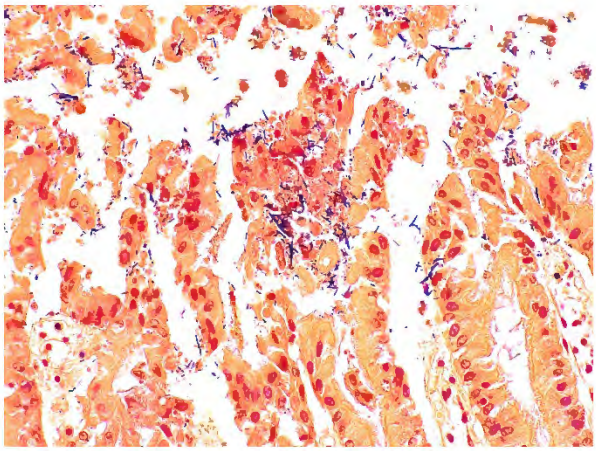

Figure 4-5. Colon, rabbit: Numerous robust gram-positive bacilli are present in the necrotic superficial mucosa. (Hucke , 400X)

Histologically, the colon was severely edematous and had gram-positive bacilli present within areas of mucosal necrosis that showed up beautifully on a Gram stain performed by Dr. Uzal's lab. A secondary bacterial infection was considered by conference participants in the markedly dilated sections of gut in this case, especially since rabbits frequently have multispecies enteric infections similar to cattle (i.e. coronavirus, rotavirus, *C. difficile, E. coli,* etc.), but there was no laboratory testing available to confirm this. *C. difficile*, however, was confirmed by the contributor via ELISA for A/B toxin.

References:

1. Aminzadeh A, et al. Immunogenicity and safety in rabbits of a *Clostridioides difficile* vaccine combining novel toxoids and a novel adjuvant. *Vaccine*. 2024;42(7):1582-1592.
2. Armstrong AR, Wünschmann A, Rigatti LH, Klein EC. *Clostridium difficile* enterocolitis in a captive Geoffroy's spider monkey (*Ateles geoffroyi*) and common marmosets (*Callithrix jacchus*). *Veterinary Pathology*. 2019;56(6):959-963.
3. Aslam S, Hamill RJ, Musher DM. Treatment of *Clostridium difficile*-associated disease: old therapies and new strategies. *Lancet Infect Dis*. 2005;5(9):549-57.
4. Czaepiel J, et al. *Clostridium difficile* infection: a review. *Europ J Clin Microbiol Inf Dis.* 2019;38:1211-1221.
5. Delmée M. Laboratory diagnosis of *Clostridium difficile* disease. *Clin Microbiol Infect*. 2001;7(8):411-6.
6. Drigo I, Mazzolini E, Bacchin C, et al. Molecular characterization and antimicrobial susceptibility of Clostridium difficile isolated from rabbits raised for meat production. *Vet Microbiol*. 2015;181(3-4):303-307.
7. Keel MK, Songer JG. The comparative pathology of *Clostridium difficile*-associated disease. *Vet Pathol.* 2006;43(3):225-40.

Joint Pathology Center
Veterinary Pathology Services

WEDNESDAY SLIDE CONFERENCE 2025-2026

Conference #17 — 28 January 2026

CASE I:

Signalment:
Female Indian ringneck parrot/parakeet (*Psittacula krameria*)

History:
Trouble breathing, wings out.

Gross Pathology:
There was moderate gelatinous hydrothorax and ascites. The lungs were congested and edematous.

Laboratory Results:
Transmission electron microscopy - lung: Intranuclear and intracytoplasmic herpesviral replication complexes

- Psittacine herpesvirus 1 PCR - lung: negative
- Herpesvirus PCR and sequencing: positive - Psittacid herpesvirus 5

Microscopic Description:
The bronchi and parabronchi contain numerous large syncytia with large amphophilic-to-eosinophilic intranuclear inclusions that marginalize the chromatin. Bronchi and parabronchi also often contain foamy macrophages, pale basophilic mucus, homogeneously eosinophilic edema fluid, fibrin, cellular debris, and sloughed necrotic epithelial cells.

Contributor's Morphologic Diagnoses:
Lung: Pneumonia, histiocytic, with syncytia and intranuclear inclusion bodies

Contributor's Comment:
Pulmonary lesions in this parrot were consistent with a herpetic pneumonia (cause: Psittacid alphaherpesvirus 5). *Herpesviridae* is a large family of double-stranded DNA viruses that can infect a wide variety of animal species, including fish, mollusks, reptiles, birds and mammals.[1,3] A hallmark of this family of viruses is persistent infection (or latency) with intermittent or continuous shedding. Herpesviruses can be sub-classified into alpha-, beta-, or gamma-herpesviruses. The subfamily *Alphaherpesvirinae* is further subdivided into the following genera: *Iltovirus*, *Scutavirus*, *Simplexvirus*, *Varicellovirus,* and *Mardivirus*.

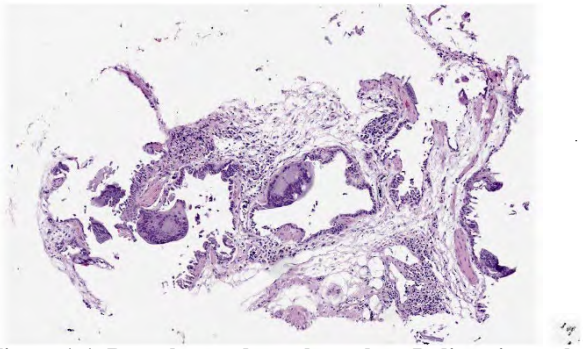

Figure 1-1. Bronchus and parabronchus, Indian ringneck parakeet: One section of mildly autolytic bronchus and parabronchus is submitted for examination. There are numerous cytomegalic multinucleated viral syncytia within the airway epithelium which project into the lumen of the airways. nucleated viral syncytia within the airway epithelium which project into the lumen of the airways. (HE, 188X)

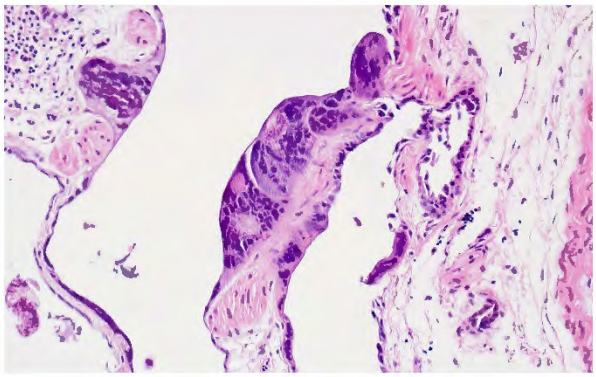

Figure 1-2. Bronchus and parabronchus, Indian ringneck parakeet: Higher magnification of viral syncytia. (HE, 188X) (Photo courtesy of: California Animal Health and Food Safety Laboratory, Sa Bernardino Laboratory. https://cahfs.vetmed.ucdavis.edu/)

The subfamily *Betaherpesvirinae* is further subdivided into the following genera: *Cytomegalovirus*, *Muromegalovirus*, *Proboscivirus*, *Quwivirus*, and *Roseolovirus*. Similarly, the subfamily, *Gammaherpesvirinae* is also subdivided into several genera – *Lymphocryptovirus*, *Bossavirus*, *Macavirus*, *Manticavirus*, *Patagivirus*, *Percavirus*, and *Rhadinovirus*.[1]

Herpesviruses of veterinary significance and their classification:[3]

- Subfamily *Alphaherpesvirinae*: Bovine herpesvirus 1 (Infectious bovine rhinotracheitis virus, Infectious pustular vulvovaginitis virus), Bovine herpesvirus 2 (Mammillitis, Pseudo-lumpy skin disease virus), Bovine herpesvirus 5 (Bovine encephalitis virus), Canid herpesvirus 1, Caprine herpesvirus 1, Cercopithecine herpesvirus 1 (B virus disease of macaques), Cercopithecine herpesvirus 9 (Simian varicella virus), Equid herpesvirus 1, Equid herpesvirus 3 (Equine coital exanthema virus), Equid herpesvirus 4 (Equine rhinopneumonitis virus), Felid herpesvirus 1 (Feline viral rhinotracheitis virus), Gallid herpesvirus 1 (Avian infectious laryngotracheitis virus), Gallid herpesvirus 2 (Marek's disease virus), Human herpesvirus 1, Human herpesvirus 2, Human herpesvirus 3 (Varicella-zoster virus), Saimiriine herpesvirus 1 (Herpesvirus tamarinus), Chelonid herpesvirus 5
- Subfamily *Betaherpesviriane*: Murid herpesvirus 1 and *2*, Elephantid herpesvirus (Endotheliotropic elephant herpesvirus), Suid herpesvirus (Porcine cytomegalovirus), Macacine herpesvirus 3 (Rhesus cytomegalovirus)

- Subfamily *Gammaherpesvirinae*: Malignant catarrhal fever (cause: Alcelaphine herpesvirus 1, Ovine herpesvirus 2), Bovine herpesvirus 4, Equid herpesvirus 2, Equid herpesvirus 5, Equid herpesvirus 7 (Asinine herpesvirus 2), Human herpesvirus 4 (Epstein-Barr virus), Saimiriine herpesvirus 2 (Herpesvirus saimiri), Otarine herpesvirus 1

There are a number of herpesviruses of significance in birds including *Gallid alphaherpesvirus 1* (GaAHV1; causative agent of infec

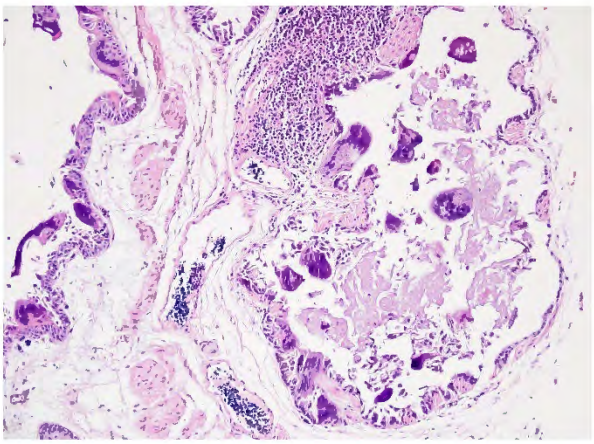

Figure 1-3. Bronchus and parabronchus, Indian ringneck parakeet: The lumen of the airway contains sloughed epithelium and viral syncytia, edema fluid, few histiocytes, and small amounts of cellular debris. (HE, 400X) (Photo courtesy of: California Animal Health and Food Safety Laboratory, Sa Bernardino Laboratory. https://cahfs.vetmed.ucdavis.edu/)

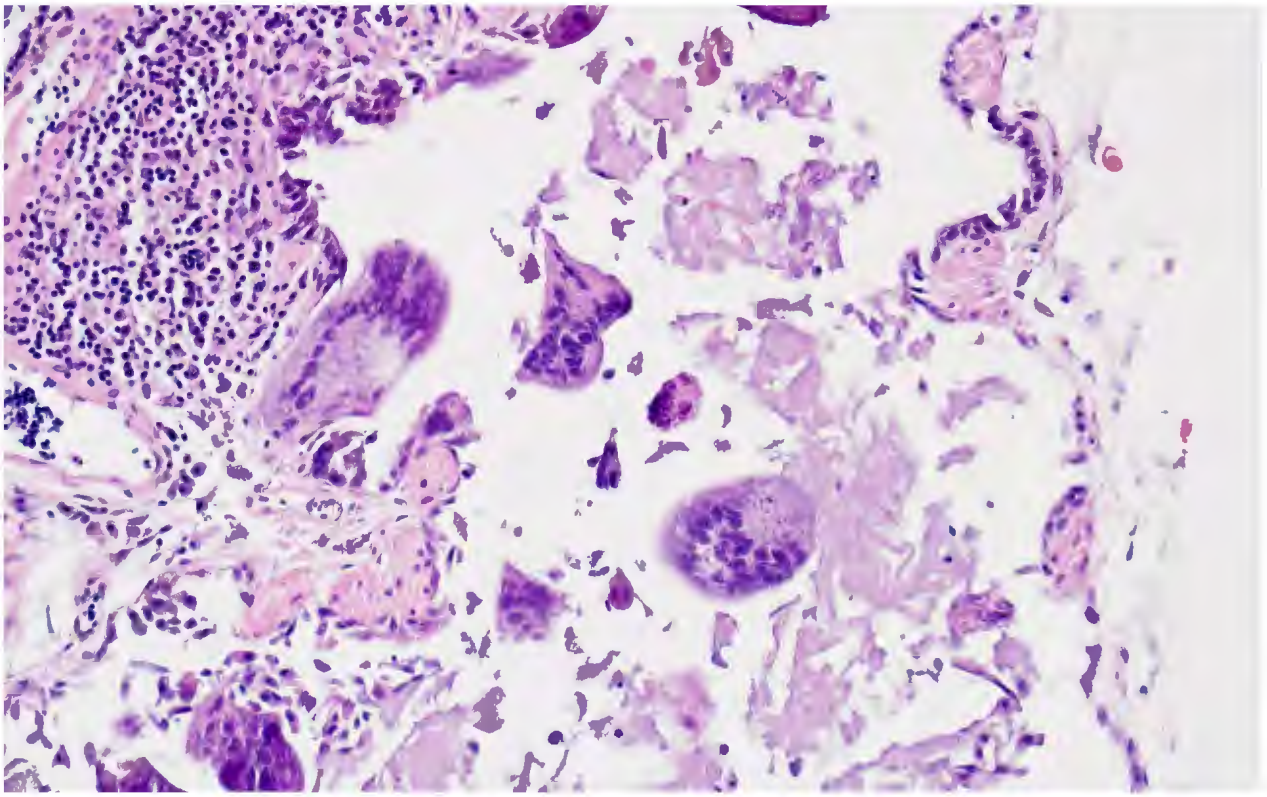

Figure 1-4. Bronchus and parabronchus, Indian ringneck parakeet: Higher magnification of luminal contents and viral syncytia. (HE, 400X) (Photo courtesy of: California Animal Health and Food Safety Laboratory, Sa Bernardino Laboratory. https://cahfs.vetmed.ucdavis.edu/)

tious laryngotracheitis), *Gallid alphaherpesvirus 2* (GaAHV2; causative agent of Marek's disease), *Anatid alphaherpesvirus 1* (AnAHV1; causative agent of duck viral enteritis), *Psittacid alphaherpesvirus 1* (PsAHV1; causative agent of Pacheco's disease and papillomatosis), and *Columbid alphaherpesvirus 1* (CoAHV1; pigeon herpesvirus; fatal disease in hawks, owls, and falcons). In psittacines, at least 5 herpesviruses have been named; all of the aforementioned viruses cluster in the genus *Iltovirus*.[2]

- *Psittacid alphaherpesvirus 1* (PsAHV1)
- Provisionally named Psittacid alphaherpesvirus 2 (PsAHV2)
- Provisionally named Cacatuid alphaherpesvirus 1
- Provisionally named Cacatuid alphaherpesvirus 2
- Provisionally named Psittacid alphaherpesvirus 3 (PsAHV3)
- Provisionally named Psittacid alphaherpesvirus 5 (PsAHV5)

Respiratory herpesviruses have been described in Indian ringneck parrots as early as the 1990s.[4,8] Similar gross and microscopic lesions have been reported in psittacines infected with PsAHV3 and PsAHV5, including the formation of large syncytia and intranuclear inclusions throughout the respiratory tract.[2,6,7] Thus far, PsAHV5 has been detected in Indian ringneck parakeets, Alexandrine parakeets, Bourke's parrots, and possibly eclectus parrots. Concurrent infections, such as Aspergillosis, are common.[2]

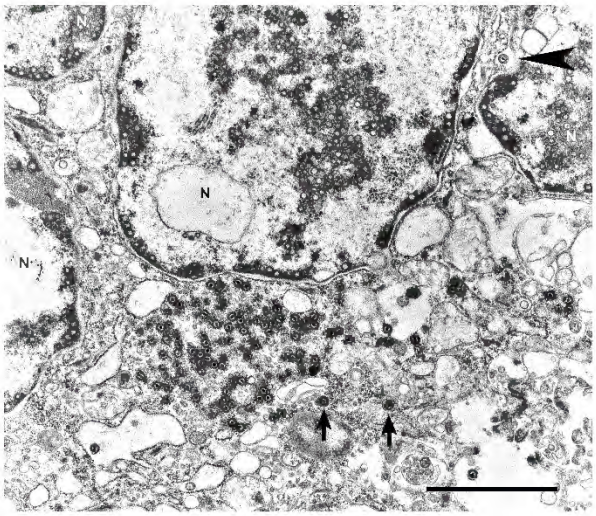

Figure 1-5. Bronchus and parabronchus, Indian ringneck parakeet: Syncytial cell with nuclear replication and assembly and cytoplasmic replication complexes. Note numerous nucleocapsids positioned at the nuclear membrane. A maturing enveloped virion is trafficking through the nuclear membrane (black arrowhead). Virions near cisterns (arrows) are gaining the final envelope and tegmental proteins. N = nuclei. Bar = 2µm.

Contributing Institution:

California Animal Health and Food Safety Laboratory (San Bernardino Branch)
https://cahfs.vetmed.ucdavis.edu/

JPC Diagnoses:

1. Tubular reproductive tract, air sac, lung: Epithelial necrosis, acute, multifocal, moderate, with intranuclear viral inclusions and numerous syncytia.
2. Liver: Hepatitis, necrotizing, acute, multifocal, random, moderate with microbes consistent with microsporidia.

JPC Comment:

The JPC's own Dr. Elise LaDouceur moderated this year's avian-focused seventeenth conference. This first case provided participants with a panoply/salmagundi/"dog's breakfast" of tissues to sort through to achieve a diagnosis. The characteristic intranuclear viral inclusion bodies of herpesvirus were best seen in the air sac respiratory epithelium, which also rewarded conference-goers with some exceptional viral syncytia. Of the potential herpesviral culprits, psittacine alphaherpesviruses (PsAHV) 1, 3, and 5 have been reported in psittacine species, including Indian ringneck parakeets, and PsAHV-5 was isolated by the contributor in this case. The contributor provided some beautiful electron microscopy (EM) photos from this bird that demonstrated intranuclear herpesviral virions, with some virions budding from the nuclear envelope to become enveloped themselves, and others hanging around the rough endoplasmic reticulum (RER) to acquire additional proteins. The JPC is grateful to the contributor for providing these excellent educational images!

In addition to the respiratory epithelium, a tubular structure adjacent to the ovary was also affected by PsAHV-5 (i.e., had syncytia and epithelial necrosis). The smooth muscle wall and cellularity of this structure is consistent with either oviduct or remnant Wolffian duct. This suggests that PsAHV-5 may have a broader epitheliotropism beyond respiratory epithelium.

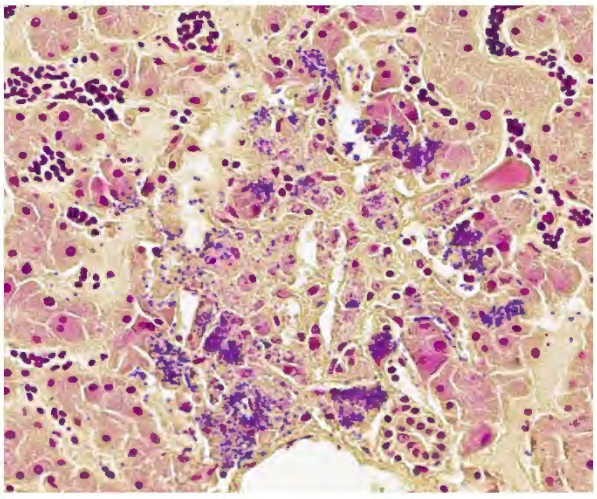

Figure 1-6. Liver, Indian ringneck parakeet: There are gram positive, round to oval, intracellular organism in regions of hepatocellular necrosis. Organisms have an eccentric clearing, most consistent with microsporidial spores. (Brown and Brenn (B&B) Gram stain, 400X)

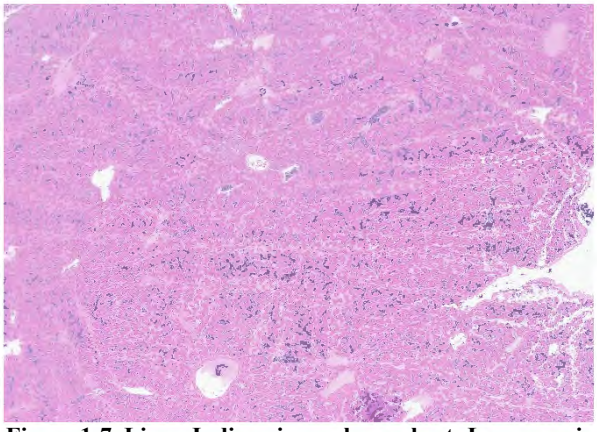

Figure 1-7. Liver, Indian ringneck parakeet: Low magnification of the liver demonstrates numerous, linear clefts filled with pale eosinophilic fluid typical of "freeze thaw" artifact. (HE, 188X)

The liver had multifocal, random hepatocellular necrosis centered on microbes that were intracellular (within hepatocytes), round to ovoid, and 1.5-2.5µm with an eccentric clearing. These organisms were gram-positive, argyrophilic on GMS, and positively staining on Giemsa; PAS and acid-fast stains were negative. Conference participants discussed at length the potential identity of these organisms. The primary differential is *Encephalitozoon hellum*, which is a microsporidian parasite in psittacines. *E. hellum* is an intracellular parasite that is ovoid, 1.5-2.5 µm, and has a predilection for the liver.[5] It is most common in immunosuppressed animals, which was likely in this case given the herpesvirus infection. Other differentials raised by participants included chlamydiosis, which can cause intracellular bacterial inclusions in the liver, but the individualized organisms were too large for chlamydiosis. Additionally, *Chlamydia spp.* would be expected to be gram-negative (unlike the gram-positive organisms in this case).[5] Candidiasis was also considered; however, yeasts should be positive for PAS (unlike the PAS negative organisms in this case) and is typically larger than 1.5µm.[5] Ultimately, confirmatory diagnosis of *E. hellum* would require molecular investigation or ultrastructural analysis (transmission electron microscopy) revealing polar filaments.[5]

Participants also noted the characteristic "freeze-thaw" artifact of the liver that is best appreciated at low magnification and causes acicular clefts filled with pale eosinophilic fluid. This is a classic artifact to be aware of!

References:

1. Gatherer D, Depledge DP, Harley CA, et al. ICTV virus taxonomy profile: *Herpesviridae* 2021. *J Gen Virol* 2021;102:001673.
2. Henderson EE, Streitenberger N, Asin J, et al. Psittacid alphaherpesvirus 5 infection in Indian ringneck parakeets in southern California. *J Vet Diagn Invest*. 2023;35(1):67-71.
3. Knowles DP. *Herpesvirales*. In: MacLachlan NJ, Dubovi EJ ed. Fenner's Veterinary Virology. 4th ed. Elsevier 2011:179-202.
4. Lazic T, Ackermann MR, Drahos JM, Stasko J, Haynes JS. Respiratory herpesvirus infection in two Indian Ringneck parakeets. *J Vet Diagn Invest*. 2008;20:235–238.
5. Schmidt RE, Struthers JD, Phalen DN. Liver. In: *Pathology of Pet and Aviary Birds*. 3rd ed. John Wiley & Sons; 2024: 197-238.
6. Shivaprasad HL, Phalen DN. A novel herpesvirus associated with respiratory disease in Bourke's parrots (*Neopsephotus bourkii*). *Avian Pathol*. 2012;41:531–539.
7. Sutherland M, Sarker S, Raidal SR. Molecular and microscopic characterisation of a novel pathogenic herpesvirus from Indian ringneck parrots (*Psittacula krameri*). *Vet Microbiol.* 2019;239:108428.

8. Tsai SS, Park JH, Hirai K, Itakura C. Herpesvirus infections in psittacine birds in Japan. *Avian Pathol.*1993;22:141–156.

CASE II:

Signalment:
2-wk-old domestic duck (*Anas platyrhynchos* var *domestic*a)

History:
The duck was intranasally inoculated with Asian H5N1 subtype highly pathogenic avian influenza (HPAI) virus isolated in 2008. Cloudy eyes appeared on the third day after inoculation. The duck died on day 6 post inoculation.

Gross Pathology:
Pancreatic focal necrosis and myocarditis were observed.

Laboratory Results:
N/A.

Microscopic Description:
The corneal stroma exhibited edema, scattered cellular debris, and inflammatory cell infiltrates that were predominantly located in the middle to deep layers of the stroma. Inflammatory cells were heterophils and foamy macrophages. Many corneal stromal spindle cells (keratocytes) became swollen. Corneal endothelium was diffusely lost, and the Descemet's membrane was exposed to the anterior chamber. Lymphoplasmacytic inflammation and focal loss of the muscular cells were observed in the iris. Inflammatory infiltrations were trapped in the pectinate ligament of the iridocorneal angle. Mild edema and inflammatory cells were observed in the conjunctiva.

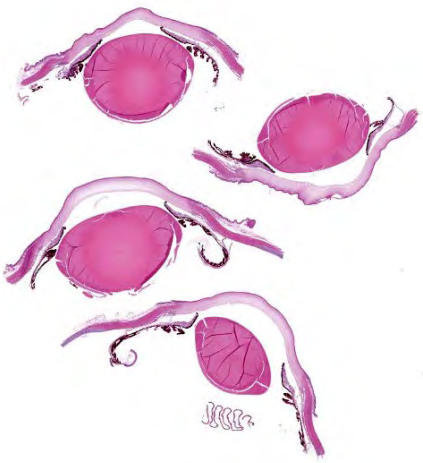

Figure 2-1. Eye, anterior segment, duckling: Multiple sections of the anterior segment, including the cornea, iris, ciliary body and lens are submitted for examination. (HE, 11X)

Contributor's Morphologic Diagnoses:
1. Keratitis, heterophilic, with edema and diffuse corneal endothelial loss.
2. Iritis, lymphoplasmacytic.

Contributor's Comment:
The H5Nx subtype HPAI virus is a global threat to the poultry industry and wild birds. The popular clinical signs of domestic ducks infected with the HPAI virus are depression, anorexia, decreased egg production, neurologic signs, and mortality. [9,10,17] In addition, corneal opacity (sometimes termed cloudy eye or blindness) is one of the characteristic and frequent findings in infected ducks. [1,6,9,13,18] Corneal ulceration and exophthalmos are rare findings in experimental infection.[17] Ocular change by HPAI has been recorded in some waterfowl species, including bar-headed geese, cracking geese, herring gulls, laughing gulls, mallard ducks (including domesticated breeds), swan geese, and wood ducks.[1-3,6,8,14,16]

The corneal opacity is probably attributed to keratitis caused by the H5N1 subtype HPAI virus. The diffuse to focal loss of corneal endothelial cells was consistently observed in ducks inoculated with the virus.[18] The corneal

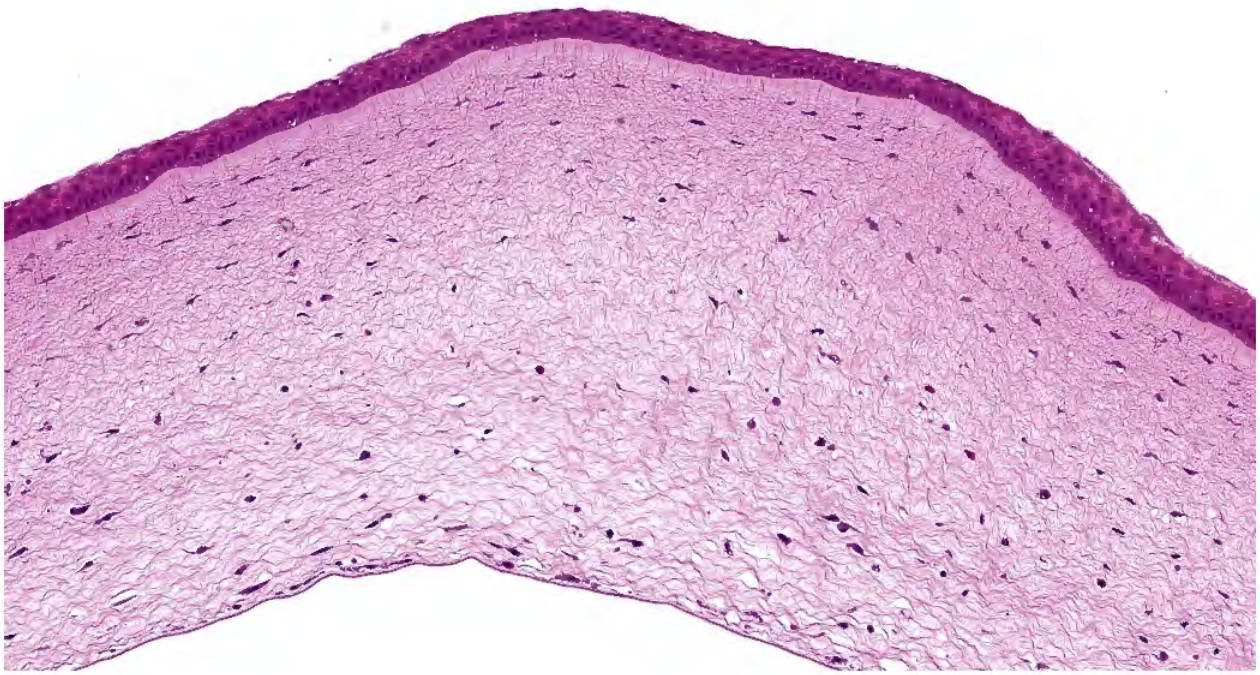

Figure 2-2. Cornea, duckling: There is marked edema of the corneal stroma, which is most profound on the inner 66% of the corneal stroma. There is scattered loss of corneal keratocyte nuclei. The endothelium is diffusely lost. (HE, 333X).

endothelium is a functional cell monolayer that maintains corneal transparency.[15] The corneal endothelium transports water from the stroma to the anterior chamber and functions as a physical barrier to water movement.[14] Although controversial, corneal endothelial cells are thought to have a limited capacity to regenerate.[5,12,15] Therefore, an extensive loss of these cells can lead to corneal stromal edema and inflammation resulting in corneal opacity. Recovery from the opacity has been reported in geese and ducks experimentally infected with the H5N1 HPAI virus.[8,18]

The H5N1 HPAI virus can replicate in various types of ocular cells in domestic ducks. The type A influenza viral antigen can be detected by immunohistochemistry in the corneal endothelial cells for short period before its loss.[18] The virus antigens can also be detected in the epithelial and stromal cells of the cornea, and cells of the iris, pectinate ligament, ciliary process, and pecten.[18]

Contributing Institution:
National Institute of Animal Health, NARO
3-1-5 Kannondai, Tsukuba, Ibaraki, Japan 3050856

JPC Diagnoses:
Eye (globe): Corneal endothelial and stromal necrosis, acute, diffuse, severe, with granulocytic and lymphocytic keratitis and anterior uveitis.

JPC Comment:
This case was an excellent example of how subtle lesions can clue a pathologist in to a specific etiology and how the evaluation of what is missing in a tissue is just as important as what is present. The lesions in this case were largely referrable to the necrosis and loss of corneal endothelium due to the HPAI infection. The corneal endothelium is responsible for removal of fluid from, and overall hydration of, the cornea. Its absence

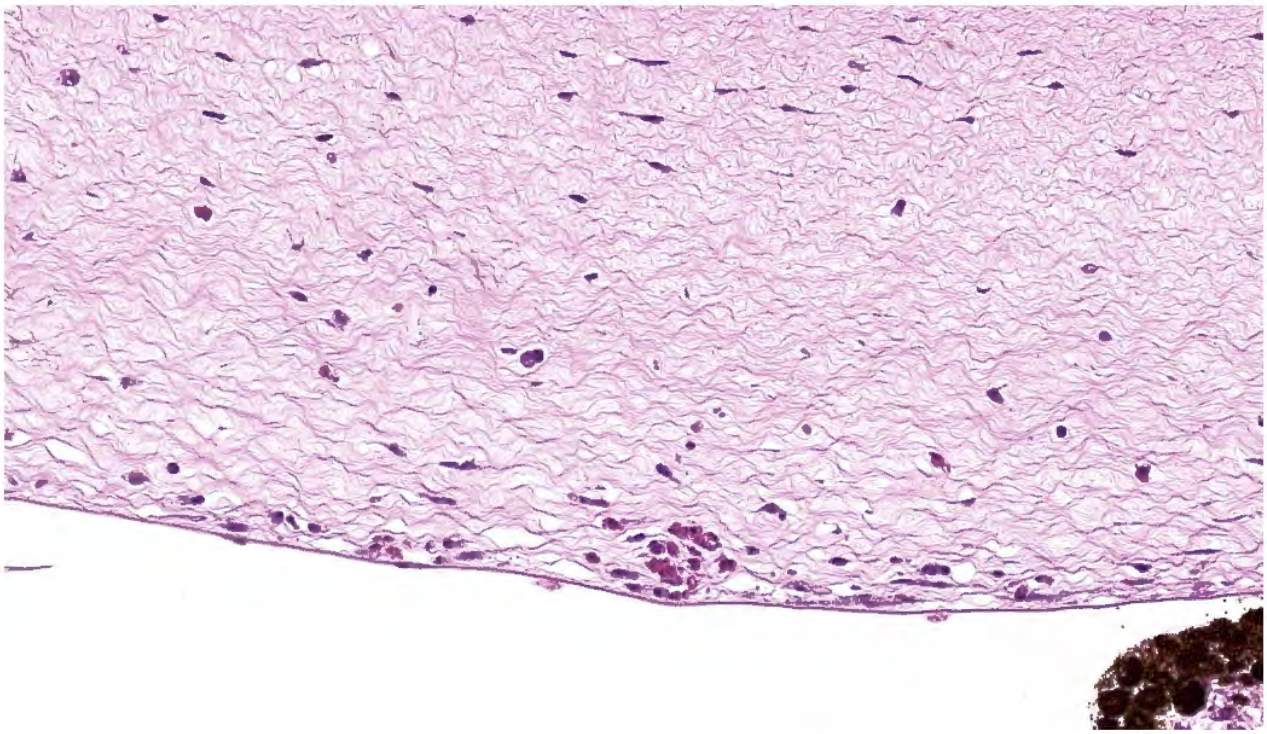

Figure 2-3. Cornea, duckling: There is diffuse loss of the corneal endothelium, marked stromal edema and infiltration of the inner layers of the cornea stroma by individualized and small groups of granulocytes. (HE, 681X).

contributed to marked corneal edema and subsequent stromal necrosis in this case. Stromal necrosis in the cornea can be a tricky diagnosis to make but is characterized by a lack of nuclei and slight tinctorial change to the stromal fibers of the cornea. These findings were most pronounced in the inner portions of the cornea (i.e., in the region closest to the corneal endothelium). While there are multiple causes of keratitis in Anseriformes (e.g., trauma, bacteria, fungi, WNV, immune-mediate disease), the specific loss of corneal endothelium appears to be unique to HPAI.[11]

HPAI viruses primarily derive their virulence from the hemagglutinin (HA) protein, which effectively enables entry into host cells. HPAIs are usually of the H5 or H7 subtypes. Influenza A viruses also make use of, amongst many other virulence factors, non-structural protein 1 (NS1), which suppresses innate immune responses by blocking type 1 interferon production and signaling. NS1 does this by binding viral RNA and sequestering it away from cytosolic pattern recognition receptors, such as RIG1 and MDA5, effectively preventing the downstream signaling pathways that would alert the cell to the presence of viral genetic material and subsequent interferon transcription.[7] This process is crucial to enabling the virus to replicate in large numbers early in an infection and cause a high viremia. These viruses demonstrate marked tropism for endothelial cells and cause multifocal hemorrhage, edema, and necrosis. In birds, meningoencephalitis and pancreatic necrosis are the two most common lesions. Less commonly, the spleen, heart, and lungs are also affected. These lesions arise due to the vascular damage, thrombosis, and dysregulated immune responses caused by the virus within the host, leading to tissue ischemia, necrosis, and, in severe cases, multiorgan failure.[1,2,3]

Conference participants also discussed the anatomy of the avian eye and how the lesions in this case were related to loss of corneal endothelial cells. Avian eyes have several unique

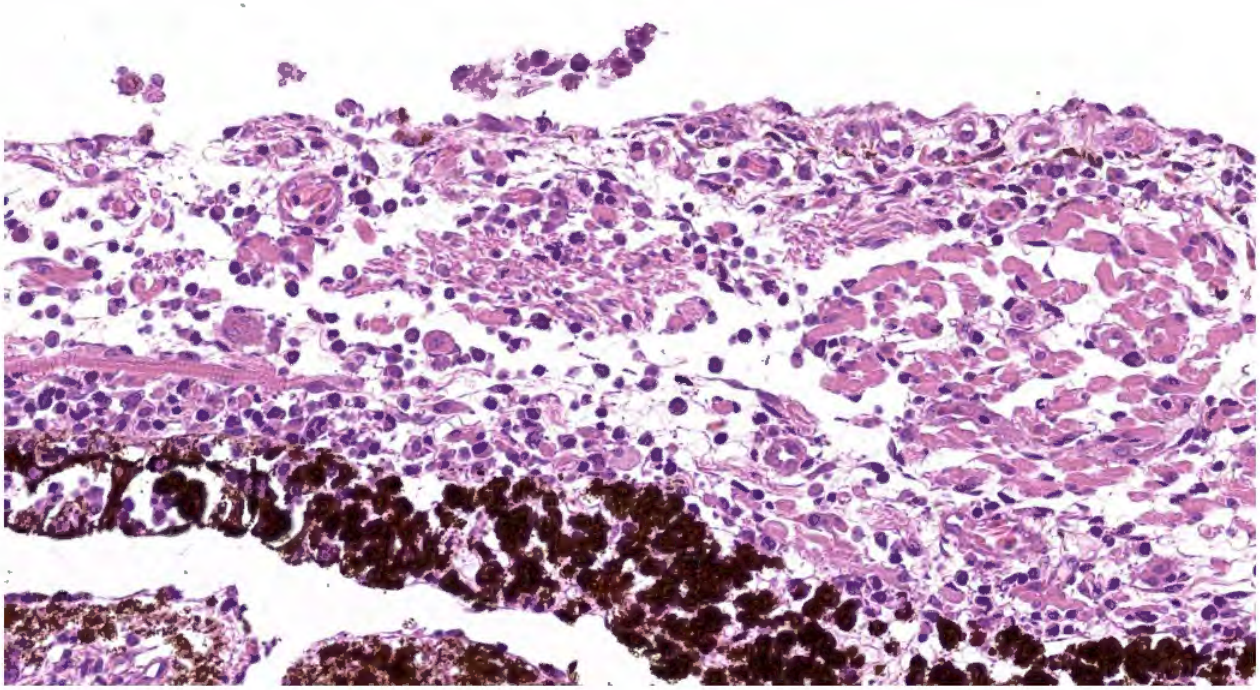

Figure 2-4. Iris, duckling: The iris is thickened and expanded by infiltration of moderate numbers of lymphocyte and plasma cells and edema which separates iridal myocytes. (HE, 811X).

anatomic features that are not present in their mammalian counterparts. The avian retina is avascular for enhanced visual acuity. Nutrition to the vitreous and retina is supplied by the pecten, which is a vascular plexus composed of small caliber blood vessels and pigmented cells. Recent research demonstrates that the inner retina receives glucose from the pecten, which also removes lactic acid.[4] Additionally, because of the pecten, trimming of an avian eye for histologic evaluation is slightly different than a mammalian eye. Rather than trimming the eye with a dorsoventral cut perpendicular to the scleral arteries at the back of the eye as is standard for mammals, avian eyes require the cut to be made parallel with the arteries to ensure that the pecten is in section. The avian sclera often entombs cartilage and/or bone, which is particularly prominent in birds of prey. In these species, the scleral ossicles are so thick that the eyes require decalcification prior to histologic processing. The iris also has various modifications depending on the species, perhaps the most striking of which is in Strigiformes (owls). Owls have xanthophores that occupy the majority of the iridial stroma and impart the dramatic yellow iridial coloration characteristic of many members of their species.[11]

References:

1. Brown JD, Stallknecht DE, Beck JR, et al. Susceptibility of North American ducks and gulls to H5N1 highly pathogenic avian influenza viruses. *Emerg Infect Dis*. 2006;12(11):1663–1670.
2. Brown JD, Stallknecht DE, Swayne DE. Experimental Infection of Swans and Geese with Highly Pathogenic Avian Influenza Virus (H5N1) of Asian Lineage. *Emerg Infect Dis*. 2008;14(1):136–142.
3. Brown JD, Stallknecht DE, Swayne DE. Experimental infections of herring gulls (*Larus argentatus*) with H5N1 highly pathogenic avian influenza viruses by intranasal inoculation of virus and ingestion

of virus-infected chicken meat. *Avian Pathol*. 2008;37(4):393–397.
4. Damsgaard C, Skøtt MV, Williams CJA, *et al.* Oxygen-free metabolism in the bird inner retina supported by the pecten. *Nature*. 2026.
5. Hirst LW, Bancroft J, Bi JQ, et al. Corneal endothelial response to induced myopia in the chicken. *Clin Experiment Ophthalmol*. 2001;29(4):244–247.
6. Kishida N, Sakoda Y, Isoda N, et al. Pathogenicity of H5 influenza viruses for ducks. *Arch Virol.* 2005;150(7):1383–1392.
7. Mok BW, Liu H, Chen P, et al. The role of nuclear NS1 protein in highly pathogenic H5N1 influenza viruses. *Microbes Infect*. 2017;19(12):587-596.
8. Nemeth NM, Brown JD, Stallknecht DE, Howerth EW, Newman SH, Swayne DE. Experimental infection of bar-headed geese (*Anser indicus*) and ruddy shelducks (*Tadorna ferruginea*) with a clade 2.3.2 H5N1 highly pathogenic avian influenza virus. *Vet Pathol*. 2013;50(6):961–970.
9. Pantin-Jackwood MJ, Swayne DE. Pathogenesis and pathobiology of avian influenza virus infection in birds. *Rev Sci Tech*.2009;28:113–136.
10. Rhyoo MY, Lee KH, Moon OK, W et al. Analysis of signs and pathology of H5N1-infected ducks from the 2010-2011 Korean highly pathogenic avian influenza outbreak suggests the influence of age and management practices on severity of disease. *Avian Pathol*. 2015;44(3):175–181.
11. Schmidt RE, Struthers JD, Phalen DN, eds. Special sense organs. In: *Pathology of Pet and Aviary Birds*. 3rd ed. John Wiley & Sons, Inc; 2024:439-464.
12. Schwartzkopff J, Bredow L, Mahlenbrey S, et al. Regeneration of corneal endothelium following complete endothelial cell loss in rat keratoplasty. *Mol Vis.* 2010;16:2368–2375.
13. Spackman E, Pantin-Jackwood MJ, Lee SA, Prosser D. The pathogenesis of a 2022 North American highly pathogenic clade 2.3.4.4b H5N1 avian influenza virus in mallards (*Anas platyrhynchos*). *Avian Pathol.* 2023;52(3):219–228.
14. Sturm-Ramirez KM, Hulse-Post DJ, Govorkova EA, et al. Are ducks contributing to the endemicity of highly pathogenic H5N1 influenza virus in Asia? *J Virol*. 2005;79(17):11269–11279.
15. Tuft SJ, Coster DJ. The corneal endothelium. *Eye*. 1990;4(3):389–424.
16. Yamamoto Y, Nakamura K, Yamada M, Mase M. Comparative pathology of chickens and domestic ducks experimentally infected with highly pathogenic avian influenza viruses (H5N1) isolated in Japan in 2007 and 2008. *J Agric Res Q*. 2010;44(1):73–80.
17. Yamamoto Y, Nakamura K, Okamatsu M, et al. Avian influenza virus (H5N1) replication in feathers of domestic waterfowl. *Emerg Infect Dis.* 2008;14(1):149–151.
18. Yamamoto Y, Nakamura K, Yamada M, Mase M. Corneal opacity in domestic ducks experimentally infected with H5N1 highly pathogenic avian influenza virus. *Vet Pathol*. 2016;53(1):65–76.

CASE III:

Signalment:
Adult carrion crow (*Corvus corone*) of unknown gender.

History:
An adult carrion crow was found dead in a humane trap. Only liver was submitted for examination.

Figure 3-1. Liver, crow: There are yellow, multifocal to coalescing granulomas within the liver. (Photo courtesy of: Division of Pathology, Public Health and Disease Investigation, College of Medical, Veterinary & Life Sciences, University of Glasgow, http://www.gla.ac.uk/schools/vet/).

Gross Pathology:
In a multifocal distribution, the liver contains numerous, cream/pale yellow, moderately firm, partially confluent nodules ranging from 1x1x1mm to 6x9x7mm.

Laboratory Results:
N/A

Microscopic Description:
Approximately 70% of normal hepatic parenchyma is replaced by heterogeneously sized, multifocal to coalescing, randomly distributed foci (up to 5 mm in diameter) characterized by large, central, variably eosinophilic regions admixed with nuclear debris (necrosis), which are surrounded by inflammatory infiltrates (granulomas).

The inflammatory infiltrates consist of an inner, in most cases single layer of very large cells (up to 90 µm in diameter) with numerous (4-20) nuclei in a random arrangement (foreign body giant cells) abutting the area of necrosis, followed by a wider zone mostly comprising large (epithelioid) macrophages with occasional foreign body giant cells. Further peripherally moderate numbers of lymphocytes and plasma cells, and rare heterophils are present, multifocally situated within concentrically arranged collagen with attendant spindle cells.

The areas of necrosis consist of variably intense eosinophilic amorphous central regions, which towards their periphery multifocally exhibit more distinct cellular outlines of homogenously eosinophilic (necrotic) cells and often small to moderately sized (10 – 30 µm) round clear spaces. Small numbers of granulomas contain short basophilic rods (length 3-5 µm) within the less densely arranged necrotic material. Additionally rare individual heterophils also are seen.

The intima of a large portal blood vessel which only contains a thin to moderately thick layer of smooth muscle tissue (interpreted as large vein) in a multifocal to coalescing distribution is moderately expanded by small numbers of macrophages admixed with larger numbers of lymphocytes and plasma cells, and rare heterophils, whilst the lumen of this vessel contains moderate to large numbers of monocytes, erythrocytes and heterophils and small numbers of lymphocytes and plasma cells. Focally, the mural lymphoplasmacytic infiltrates are associated with a small, well-defined accumulation of macrophages.

Additionally, the portal area described above contains small numbers of cavernous structures, which in small areas

Figure 3-2. Liver, crow: Approximately 50% of the section of liver is effaced by coalescing granulomas. (HE, 9X)

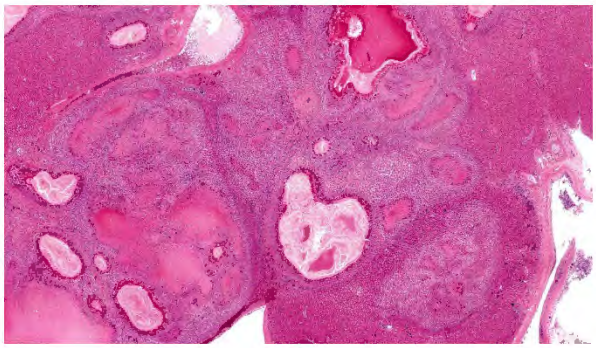

Figure 3-3. Liver, crow: Higher magnification of coalescing granulomas, with a central core of eosiiophilic cellular debris . (HE, 20X)

appears to be lined by cuboidal epithelium (interpreted as bile ducts) and contain small numbers of parasite profiles admixed with moderate numbers of desquamated epithelial cells and small numbers of macrophages and heterophils. The parasitic profiles are characterised by a thin (5-8µm) eosinophilic cuticle which lacks spines but occasionally appears ciliated, no apparent coelomic cavity, uteri containing numerous eggs and testes containing linear basophilic spermatids within the same profile (hermaphroditic organism), vitellaria containing cells with homogeneous intensely eosinophilic cytoplasm, and a ventral sucker. The eggs, measuring approximately 20 x 45 µm, are oval although often unilaterally flattened (operculated), with yellow to brown 3-5 µm thick walls and contain a miracidium (trematode, consistent with *Lyperosomum longicauda*). Small numbers of lymphocytes, plasma cells and heterophils are multifocally present in the wall of the bile ducts.

Contributor's Morphologic Diagnoses:

Liver: Hepatitis, granulomatous, multifocal to coalescing, subacute to chronic, marked to severe; with:

a) Intralesional bacilli consistent with *Mycobacterium* spp.; and
b) Phlebitis granulomatous, subacute to chronic, focal, moderate; and
c) Cholangitis pyogranulomatous, multifocal, chronic, minimal; with intralesional flukes consistent with *Lyperosomum longicauda*.

Contributor's Comment:

Histological examination of the crow liver submitted revealed extensive effacement of the liver parenchyma by numerous, variably sized granulomas, many of which contain large numbers of acid-fast short rods. Additionally, focally a large vascular profile interpreted as a large vein exhibits a predominantly lymphoplasmacytic, focally also granulomatous intramural inflammatory infiltrate, whilst small and moderately sized cavities associated with the same portal area, devoid of erythrocytes and partially lined by cuboidal epithelium (interpreted as bile ducts) contain small numbers of trematode sections.

Considering the paucity of pathological changes associated with the flukes, these very likely need to be considered incidental findings in this case. The cause of the phlebitis is not entirely clear, however, taking the nature of the inflammatory infiltrate into account, this process may need to be considered to be associated with the mycobacterial infection either via local extension or possibly also via extension from the lymphatics present within the vascular wall.

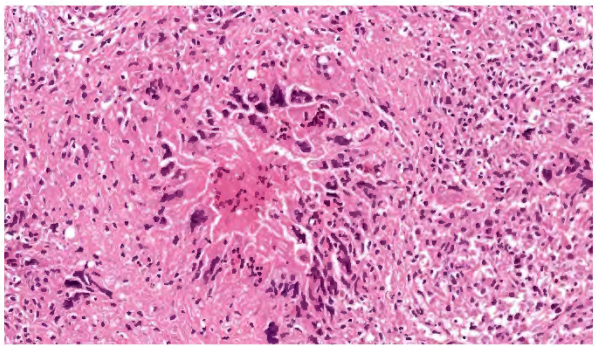

Figure 3-4. Liver, crow: High magnification of a granulomas, with a central core of eosiiophilic cellular debris, bounded by numerous epithelioid and foreign body-type macrophages. (HE, 537X)

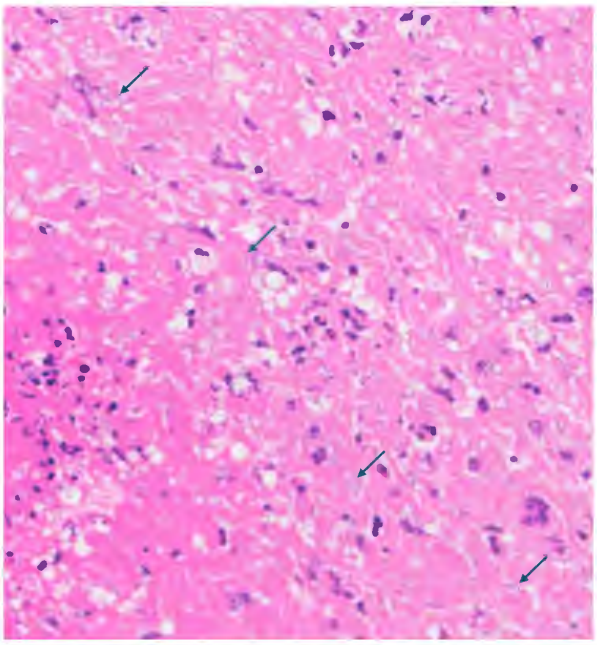

Figure 3-5. Liver, crow: There are faintly staining bacteria (arrows) within a granuloma, characteristic of mycobacteriosis. (HE, 400X)

Avian hepatic granulomas may be of viral, bacterial, fungal, protozoal or helminth aetiology, with such agents exhibiting a preference for the liver or infecting the liver in an opportunistic fashion.[13] Special stains revealed many of the hepatic granulomas in this bird to contain large numbers of short, acid-fast rods present both in macrophages and multinucleated giant cells and also extracellularly, which from their morphology and staining profile are most likely consistent with *Mycobacterium* spp.

Avian mycobacteriosis is primarily caused by *M. avium* (serotypes 1, 2, 3, and 6) and *M. genavense*, and is seen in found in many different birds including poultry, game, cage, wild and zoological species, predominantly of the North Temperate Zone. Less commonly *M. intracellulare, M. scrofulaceum*, *M. fortuitum*, *M. tuberculosis* and *M. bovis* are involved. The *M. avium* complex includes *M. avium* subsp. *avium*, *M. avium* subsp. *paratuberculosis*, *M. avium* subsp. *silvaticum* and *M. intracellulare.*[5]

Mycobacterium avium subsp. *paratuberculosis*, which causes Johne's disease in ruminants, has both been isolated from tissue and feces of Scottish carrion crows (*Corvus corone*). Additionally, histological lesions consistent with *M. avium* subsp. *paratuberculosis* were observed in these animals, albeit described to be much milder when compared to those present in this crow.[2] The infection of crows is surmised to be via the oral route, possibly from ingestion of infected rabbit or ruminant tissue. Experimentally, the contamination of livestock food by wildlife feces in turn has been determined as a possibility for the prevalence of paratuberculosis in the east of Scotland, and wild rabbits previously have been implicated as a possible wildlife reservoir for paratuberculosis.[4,12] Johne's disease is relatively commonly diagnosed in cattle of the southwest of Scotland and an increase of this disease in small ruminants in Scotland also has been reported.[10,11]

Considering crows (in experimental conditions) have also been infected with *M. bovis*, however, here only the intraperitoneal inoculation, not the oral infection, resulted in mycobacterial infection evident grossly, histologically or in pooled tissue cultures, *M. bovis* as a causative agent is considered less likely in this bird.[3] Ultimately, PCR would need to conducted to be able to confidently identify the mycobacterial (sub-) species involved.

Generally, stress, age, immune status and possible pre-existing disease are considered predisposing factors for the infection of birds with *Mycobacterium* spp; transmission may

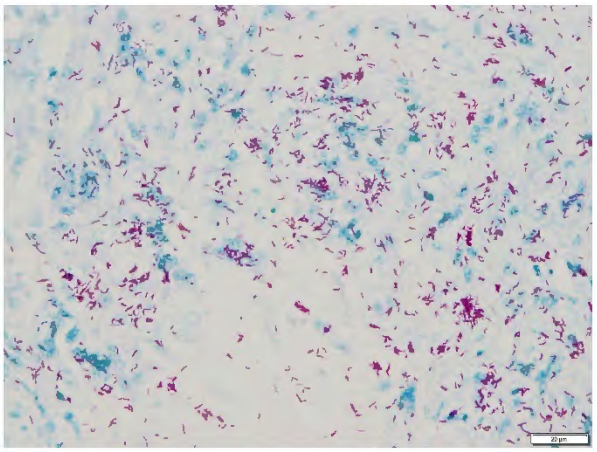

Figure 3-6. Liver, crow: Within the center of the granulomas, there are numerous acid-fast bacilli both within histiocytes and extracellularly. (Ziehl-Nielsen, 600X)(Photo courtesy of: Division of Pathology, Public Health and Disease Investigation, College of Medical, Veterinary & Life Sciences, University of Glasgow, http://www.gla.ac.uk/schools/vet/)

be oral or via aerosols. Usually, granulomatous disease is present in multiple organs, including liver, spleen, pleura, intestinal serosa, bone marrow and lung, however, previous examination of common crows with mycobacterial granulomas revealed a strong predisposition of the liver to lesions, with only rarely the spleen, peritoneum and lung affected.[9,13] To what extent other organs were involved in the crow submitted unfortunately remains unknown. However, depending on the extent and distribution of other organs involved, the mycobacterial infection may have contributed to or even caused the death of this bird.

Dicrocoeliidae, which are small, lancet-like flukes occurring in the biliary and pancreatic ducts of vertebrates, represent a large family of trematodes with over 400 species. Their life cycle usually include two (snails and arthropods) or three (snails, arthropods and amphibians/reptiles) intermediate hosts. The genera and species present with this family are distinguished from one another by the location and size of testes, ovary, vitellarium, suckers, caecum, genital pore, excretory vesicle and body form.

Lyperosomum longicauda of the genus *Lyperosomum* is the common fluke of carrion crows (*Corvus corone*) in Europe. They exhibit a relatively elongate body with a thin cuticle lacking spines. The pharynx is large, whilst the oesophagus is short. Two caeca are present. The testes are close to round, orientated slightly oblique to one another and are found close the ventral sucker, which is larger than the oral sucker. The ovary is present caudal to the testes, whilst the genital pore is located just caudal to the pharynx. The vitellaria are relatively short and the uterus contains dark brown, thick-shelled eggs approx. 32 x 21 µm in size.[7] Twenty species are present in the *Lyperosomum* genus, which may be found in intestines and livers of birds and mammals; the known life cycles include two hosts, namely terrestrial snails and insects.

Whilst most commonly trematodes in birds are present in the intestines, *Lyperosomum longicauda* is only found in the liver. This parasite also has been described in other birds including the song thrush (*Turdus philomelos*)

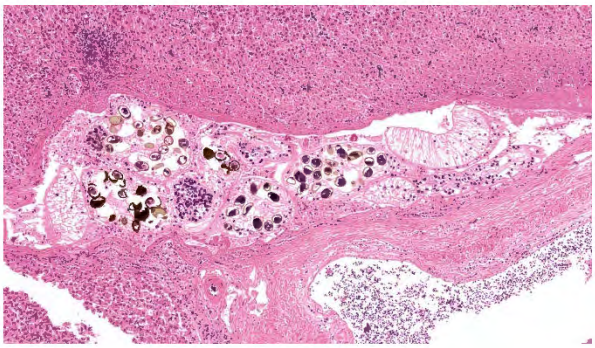

Figure 3-7. Liver, crow: A bile duct contains a tangential section of an elongate adult trematode with multiple oral suckers, a thin tegument, a parenchymatous body cavity and numerous cross sections of a uteus contain operculated eggs with miracidia. (HE,135X)

and the northern bald ibis (*Geronticus eremita*).[7] Canadian common crows (*Corvus brachyrhynchos*) exhibit *Conspicuum macroorchis* of the genus *Conspicuum*, and *Brachylecithum stunkardi* of the genus *Brachylecithum*/ *Lyperosomum* within gall bladders and bile ducts.[1]

Contributing Institution:
Division of Pathology, Public Health and Disease Investigation
School of Veterinary Medicine
College of Medical, Veterinary & Life Sciences
University of Glasgow
464 Bearsden road
G61 1QH
Glasgow, Scotland, United Kingdom
http://www.gla.ac.uk/schools/vet/

JPC Diagnoses:
1. Liver: Hepatitis, granulomatous, chronic, multifocal and random, severe, with faintly staining bacilli.
2. Liver: Adult trematodes.
3. Liver, large-caliber veins: Phlebitis, lymphoplasmacytic, chronic, multifocal, moderate.
4. Liver: Hepatitis, lymphoplasmacytic, chronic, multifocal and portal, mild.

JPC Comment:
This case was an excellent demonstration of mycobacteriosis in a bird. Many thanks to this contributor for providing this classic case. With careful scrutiny, the more recent granulomas contained numerous, faintly staining bacilli on H&E stain, which is typical of *Mycobacterium* spp. In many cases of paucibacillary mycobacteriosis, the bacilli can be seen at the center of "younger" granulomas, but they are characteristically poorly staining. This appearance can allow the pathologist to make a presumptive diagnosis of mycobacteriosis prior to confirmation with acid fast stains.

Paucibacillary mycobacteriosis is what is expected in most cases of *M. avium ssp avium, M. tuberculosis*, etc. due to these bacteria inciting a Th1 response with resultant strong T-cell immunity.[6] The stimulated Th1 cells produce cytokines such as IL-1 and interferon to classically activate macrophages (M1 response). This enables the formation of granulomas to wall off the invaders and creates "tuberculoid" inflammation.[6] Because the bacilli are predominantly seen only within the center of young granulomas rather than diffusely spread about, this form of mycobacteriosis is referred to as "paucibacillary." On the other than, multibacillary mycobacteriosis is characterized by diffuse, disorganized inflammation with numerous bacteria that are poorly contained.[6] This version of mycobacteriosis results from Th2 activation and subsequent production of IL-4 and IL-13. These interleukins result in alternative (M2) macrophage activation, resulting in "lepromatous" inflammation. *M. avium ssp pseudotuberculosis* (Johne's disease) and *M. leprae* (leprosy) are the classic examples of this type of mycobacteriosis, in which there are usually numerous acid-fast bacilli present throughout the inflamed tissue.[6]

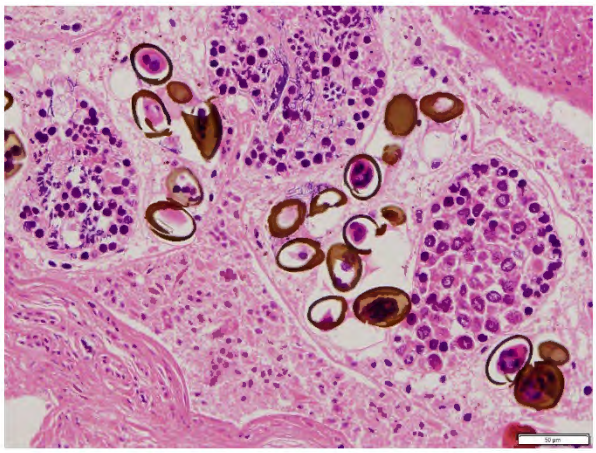

Figure 3-8. Liver, crow: High magnification of trematode eggs containing miracidia. (HE, 400X)(Photo courtesy of: Division of Pathology, Public Health and Disease Investigation, College of Medical, Veterinary & Life Sciences, University of Glasgow, http://www.gla.ac.uk/schools/vet/)

Conference participants discussed at length whether the trematodes were present within a bile duct or within a portal vein. Support for portal vein includes: the shape of the luminal structure was similar to portal veins in the surrounding liver, the lumen contained erythrocytes (along with trematodes), the animal had substantial phlebitis, and definitive epithelial lining was not identified. Phlebitis was particularly pronounced in the large portal vein profile next to the trematode. Phlebitis is an uncommon lesion of mycobacteriosis but can be seen in several other conditions in birds, including parasitism, aspergillosis, viral infection (e.g., WNV, HPAI, Paramyxovirus), sepsis, and (less commonly) immune mediated disease. Lead toxicity may also cause vasculitis, but it is typically fibrinoid vasculitis (unlikely the lymphocytic vasculitis seen in this case).[12]

Ultimately, participants were unable to definitively determine whether the trematodes were intravascular or within a bile duct. Immunohistochemistry for pancytokeratin (AE1/AE3) was attempted to look for an epithelial lining to rule in/out a bile duct as the luminal structure. Unfortunately, IHC was non-contributory (internal controls were negative), likely due to autolysis in the specimen. Dr. Chris Gardiner was consulted on this case regarding the identity of the trematodes. Dr. Gardiner confirmed that this is trematode, specifically a hermaphroditic trematode with operculated eggs. The fact that this trematode is hermaphroditic at least ruled out schistosomes, as that particular genus of trematodes are gonochoric and do not have operculated eggs. Per Dr. Gardiner, further determination of the trematode genus and species would require removal of whole specimens at necropsy and submission to a parasitologist.

References:

1. Andrews SE, Threlfall W. Parasites of Common Crow (*Corvus Brachyrhynchos)* in Insular Newfoundland. *Proceedings of the Helminthological Society of Washington.* 1975;42:24-28.
2. Beard PM, Daniels MJ, Henderson D, Pirie A, Rudge K, Buxton D, Rhind S, Greig A, Hutchings MR, McKendrick I, Stevenson K, Sharp JM. Paratuberculosis infection of nonruminant wildlife in Scotland. *J Clin Microbiol*. 2001;39:1517-1521.
3. Butler KL, Fitzgerald SD, Berry DE, Church SV, Reed WM, Kaneene JB. Experimental inoculation of European starlings (*Sturnus vulgaris*) and American crows (*Corvus brachyrhynchos*) with *Mycobacterium bovis*. *Avian Dis.* 2001;45:709-718.
4. Daniels MJ, Hutchings MR, Greig A. The risk of disease transmission to livestock posed by contamination of farm stored feed by wildlife excreta. *Epidemiol Infect*. 2003;130:561-568.
5. Dhama K, Mahendran M, Tiwari R, Dayal Singh S, Kumar D, Singh S, Sawant PM: Tuberculosis in Birds: Insights into the *Mycobacterium avium* Infections. *Vet Med Int.* 2011;2011:712369.
6. Frank KM and McAdam AJ. Infectious Disease. In: Robbins and Cotran, ed. *Pathologic Basis of Disease*. 10th ed. Philadelphia, PA: Elsevier; 2021:374.
7. Gonenc B, Oge H, Oge S, Emir H, Ozbakis G, Asti C. First record of *Lyperosomum longicauda Rudolphi*,1809 (Trematoda: *Dicrocoeliidae*) in Northern Bald Ibis (*Geronticus eremita*) in Turkey. *Ankara Universitesi Veteriner Fakultesi Dergisi.* 2012;59: 227-230.
8. Mettrick DF. Studies on the helminth parasites of British birds. In: Department of Parasitology. University of London. 1957.
9. Mitchell CA, Duthie RC. Tuberculosis of the Common Crow. *Can J Comp Med Vet Sci*. 1950;14:109-117.

10. SAC C VS. Increase in the prevalence of Johne's disease in sheep in Scotland. *Vet Rec*. 2011;168:13-16.
11. SAC S VS. Johne's disease commonly diagnosed in cattle in south-west Scotland. *Vet Rec*. 2009;164:256-259.
12. Schmidt RE, Struthers JD, Phalen DN. *Pathology of Pet and Aviary Birds*. 3rd ed. John Wiley & Sons; 2024.
13. Shaughnessy LJ, et al. High prevalence of paratuberculosis in rabbits is associated with difficulties in controlling the disease in cattle. *Vet J*. 2013;198:267-270.
14. Supartika IK, Toussaint MJ, Gruys E. Avian hepatic granuloma. A review. *Vet Q*. 2006;28:82-89.

CASE IV:

Signalment:
Four-month-old, male, Oriental magpie robin (*Copsychus saularis)*

History:
The carcass was submitted from a regional zoo to perform a necropsy of the animal. Carers and veterinarians reported no history of clinical disease. It was found dead inside the house.

Gross Pathology:
The bird was in poor body condition, as assessed by a moderate to severe reduction of the bulk of muscles throughout the body, including both deep and superficial pectoral muscles (muscle atrophy). There were numerous pinpoint white foci in the liver and spleen (moderate, multifocal, acute necrotizing hepatitis and splenitis). Transversal cuts of the left humerus revealed multifocal to coalescing, irregularly shaped, well demarcated, depressed areas filled with a green soft material (severe heterophilic necrotizing osteomyelitis).

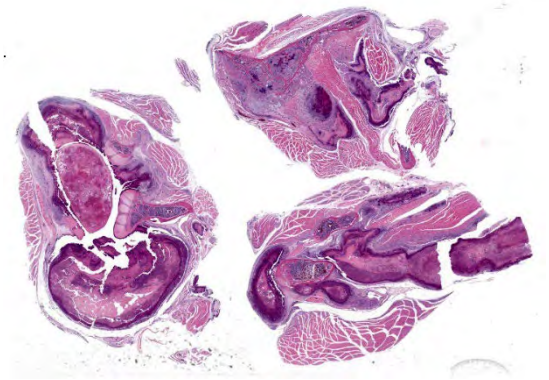

Figure 3-1. Humeroradial joint, Oriental magpie robin: Three sections of the humeroradial jointand associated soft tissues are submitted for examination. There is profound necrosis and inflammation affecting all tissues within and surrounding the joint. (HE, 12X)

Laboratory Results:
The bacteriological results revealed light growths of *Yersinia pseudotuberculosis* in the lungs and liver by using matrix-assisted laser desorption ionization time-of-flight (MALDI-TOF) mass spectrometry

Microscopic Description:
Bones and adjacent soft tissue. Multifocally throughout bone, synovial joint and muscle tissue and affecting approximately 60% of the tissue examined, there are severe, multifocal to coalescing inflammatory infiltrates. The inflammation is chiefly composed of degenerate heterophils, with fewer lymphocytes and plasma cells, embedded in eosinophilic material showing no cellular outlines (lytic necrosis) with nuclear fragmentation and loss (karyorrhexis and karyolysis); embedded within the necro-inflammatory process are common , up 100 micrometers in diameter, cocco-bacillary bacterial colonies; in some foci, the necro-inflammatory foci are bordered by macrophages forming multinucleated giant cells containing a 15-50 nuclei with a horse-shoe arrangement with occasional foamy cytoplasm. The inflamed bones show reduction of medullary bony trabeculae (osteolysis), with

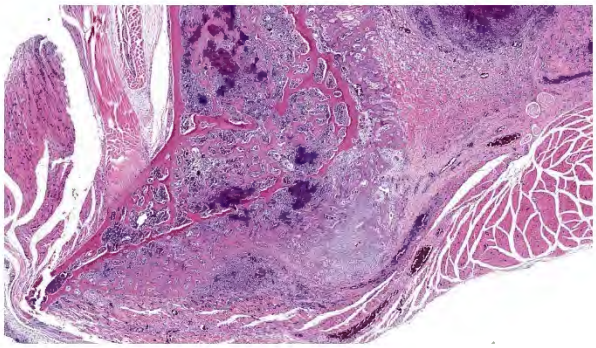

Figure 4-2. Humeroradial joint, Oriental magpie robin: There are multiple foci of necrosis within the medullary cavity of one of the bones, multifocal lysis of lamellar bone, and profound periosteal new bone formation. (HE, 55X)

multifocal scalloping and thinning of the remaining ones with an increased basophilic hue while other show empty lacunae and diffuse eosinophilia (osteonecrosis); the periosteum instead shows a common exophytic proliferation of the cortical bone with cartilage and woven bone formation (periosteal reaction).

The inflammatory infiltrate is also observed infiltrating and filling multifocal synovial joint lumina and capsules (arthro-synovitis), with a layer of fibrin embedding heterophils and covering multifocally the articular cartilage, which shows increase eosinophilia (cartilage degeneration).

The adjacent rhabdomyocytes exhibit multifocal reduction in size and diameter, with angular edges (muscular atrophy) with the closest one to the inflammation exhibiting an amphophilic sarcoplasm and linear arranged central nuclei (myotubes) and rare areas of endomysial fibrosis.

Contributor's Morphologic Diagnoses:

1. Bone: multifocal to coalescing, severe, subacute, heterophilic and necrotizing osteomyelitis, with osteolysis, periosteal reaction, osteonecrosis and with intralesional bacterial colonies.
2. Synovial joints: diffuse, severe, subacute, fibrinous and heterophilic arthro-synovitis with intralesional bacterial colonies.
3. Skeletal muscle: Severe, multifocal, subacute, heterophilic and necrotizing myositis with intralesional bacterial colonies.

Contributor's Comment:

Yersiniosis has been frequently reported in more than a hundred different species worldwide, including avian, mammals and reptiles, and it may act as a zoonotic pathogen.[3] Yersiniosis can be caused by *Yersinia pseudotuberculosis* and *Y.enterocolitica*, although the latter is more frequently involved in humans and primates cases. *Y. pseudotuberculosis* can be commonly isolated from wild animals and birds, but there are very few reports of cases of avian osteomyelitis sustained by *Y. pseudotuberculosis*.[4] A recent outbreak in a slaughter turkey flock was reported in Finland, while other older outbreaks were documented in the UK and California, still in turkeys.[1,6,8] In mammals, a Y. pseudotuberculosis osteomyelitis case was reported in a ring-tailed lemur in UK.[7]

We decided to submit this case due to the paucity of *Y. pseudotuberculosis* induced osteomyelitis in birds reported in literature. Such

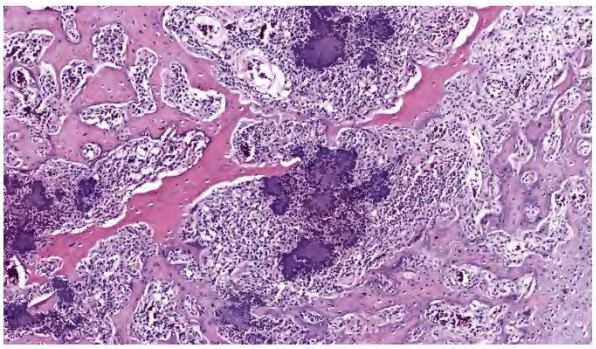

Figure 4-3. Long bone, humeroradial joint, Oriental magpie robin: Areas of bone necrosis contain large numbers of necrotic heterophils, abundant cellular debris, and large colonies of 1-2um coccobacilli. (HE, 254X)

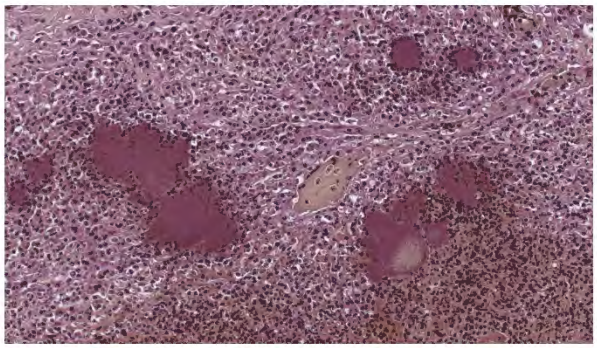

Figure 4-4. Long bone, humeroradial joint, Oriental magpie robin: Coccobacilli are gram-negative. (Brown-Hopps, 400X)

case is, to the best of our knowledge, the first pathological description of a *Y. pseudotuberculosis* induced osteomyelitis in an Oriental Magpie Robin. The present case was characterized by extensive inflammation with large bacterial colonies also spotted in other organs (spleen, liver, lung and large intestine), and therefore suggesting a systemic infection.

Yersinia pseudotuberculosis is a ubiquitous Gram-negative anaerobic coccobacillus bacterium from the Enterobacter family. The most common route of infection is oro-fecal thought contaminated food or water, although the epidemiology of the disease is considered multifactorial and highly complex. Therefore, the severity of the clinical signs and lesions would be highly variable and dependent on numerous environmental (e.g. management, temperature, etc.) and host (e.g. age, stress, parasitism and / or concomitant infections, etc.), conditions. No predisposing conditions to such infection were detected here.

Although the bacteriological culture isolated Yersinia pseudotuberculosis, other differential diagnosis for large colonies of bacteria would be: *Actinomyces sp., Actinobacillus sp. Arcanobacter sp., Corynebacterium sp., Staphylococcus sp. or Streptococcus sp.* (YACS acronym).

Contributing Institution:
University of Liverpool, Institute of Infection, Veterinary and Ecological sciences, Department of Veterinary anatomy, Physiology and Pathology.

JPC Diagnoses:
1. Wing: Osteomyelitis, tenosynovitis, myositis, and cellulitis, necrotizing and heterophilic, chronic, multifocal, severe, with pannus and large colonies of bacteria.
2. Skeletal muscle, adipose tissue: Atrophy, chronic, diffuse, severe.

JPC Comment:
The avian skeletal system has several unique functional adaptations. Birds have three types of bone: pneumatic, hematopoietic, and medullary.[5] Pneumatic bones have air sacs in the endosteum in place of bone marrow. The number and distribution of pneumatic bones varies by species, but most birds have pneumatic humeri, femurs, sternums, and skulls.[5] The remainder of the bones are hematopoietic and have bone marrow. Medullary bone is present in female birds prior to laying eggs when they deposit calcium on the endosteum, with deposits filling the marrow cavity of long bones.[5] Additionally, many bones are fused

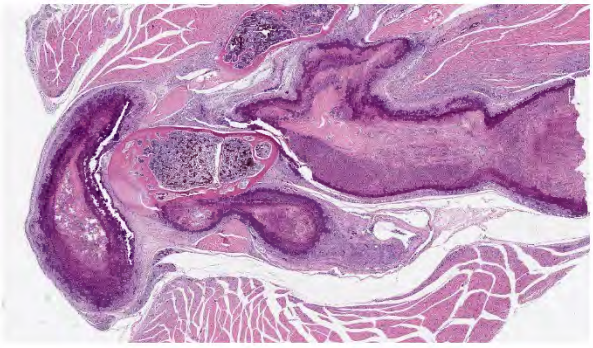

Figure 4-5. Joint space, humeroradial joint, Oriental magpie robin: The joint space is expanded and filled an inflammatory exudate, cellular debris, and bacterial colonies , which extends into the joint capsule. Bacterial colonies are present within the joint capsule (top). (HE, 34X).

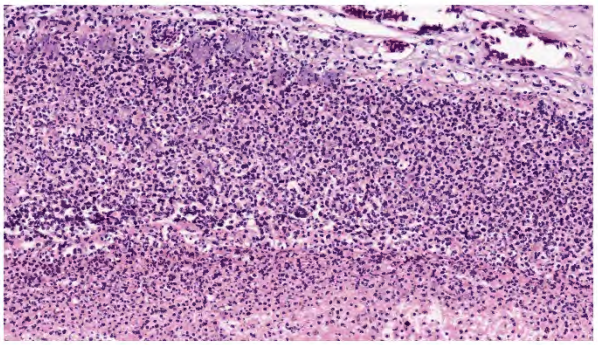

Figure 4-6. Skeletal muscle, Oriental magpie robin: Granulation tissue with inflammation and bacterial colonies extends into the adjacent, moderately atrophic skeletal muscle (HE, 380X)

(e.g., tibiotarsus, synsacrum, etc.). The slide in this case had a pneumatic bone that articulated with two hematopoietic long bones surrounded by abundant skeletal muscle; this consistent with wing where the humerus (pneumatic bone) articulates with the radius and ulna (hematopoietic bones). The leg (at the articular of the femur and tibiotarsus) was also considered, but the amount of skeletal muscle was deemed to be excessive for this location. Foci of inflammation and necrosis were present in both pneumatic and hematopoietic bone, suggestive of systemic bacterial sepsis.

Many classic features of bone and joint inflammation and healing were demonstrated in this case, including osteonecrosis and periosteal new bone formation (characterized by lattices of woven bone oriented perpendicularly to the bone's long axis). In addition to the excellent description provided by the contributor, conference participants also noted decreased basophilia of the articular cartilage. This is a common finding of arthritis and correlates to loss of proteoglycans in the chondroid matrix.[2] Additionally, one of the joints was overlain by a thin layer of fibrovascular tissue, consistent with pannus. Pannus is caused by proliferation of stromal cells in chronic arthritis and was nicely highlighted with a Masson's trichrome stain.[2]

Conference participants also discussed the cause of the severe skeletal muscle atrophy in this case. Skeletal muscle atrophy can be caused by disuse atrophy, which was presumably present in this animal. However, negative energy balance can also lead to primary skeletal muscle atrophy due to birds' high metabolic demands. Examination of body condition score in birds often involves palpation of the breast muscle, as muscling has direct cor-

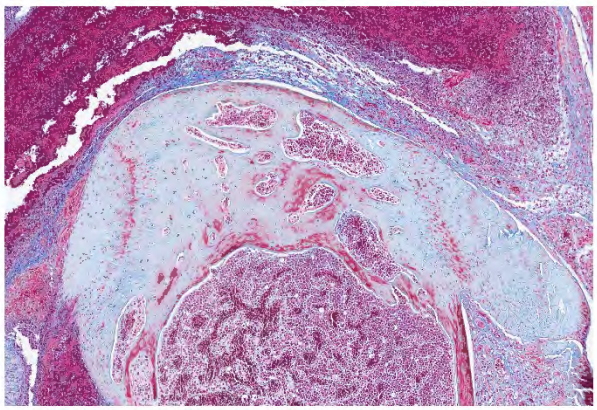

Figure 4-7. Joint space, humeroradial joint, Oriental magpie robin: The articular cartilage is covered by a thin band of fibrovascular tissue, consistent with pannus. (Masson's trichrome stain, 64X)

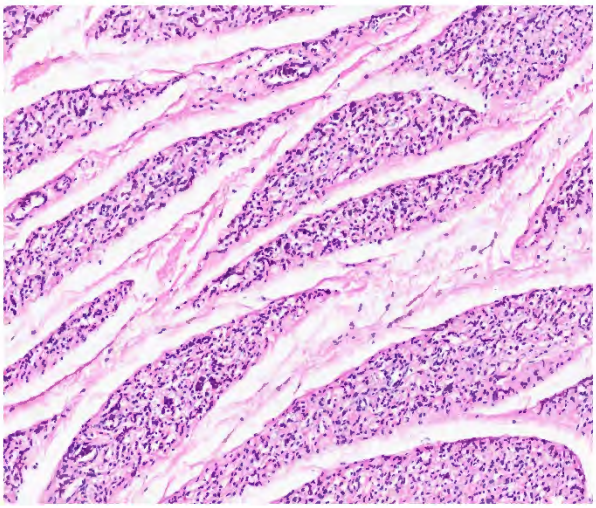

Figure 4-8. Periarticular adipose tissue, humeroradial joint, Oriental magpie robin: Markedly atrophic adipose tissue. (HE, 380X)

relation to overall nutritional status. This animal had severe adipose atrophy as well, indicative of negative energy balance, which likely also contributed to muscular atrophy.

References:

1. Blomvall L, et al. Osteomyelitis in a slaughter turkey flock caused by Yersinia pseudotuberculosis sequence type ST42. *Veterinary Microbiology*. 2022;269:109424.
2. Craig LE, Dittmer KE, Thompson KG. Bones and joints. In: Maxie MG, ed. *Jubb, Kennedy & Palmer's Pathology of Domestic Animals*. Vol 1. 7th ed. Saunders Ltd; 2026:16-163.
3. Fredriksson-Ahomaa, M, Joutsen S, Laukkanen-Ninios R. Identification of *Yersinia* at the species and subspecies levels is challenging. *Curr Clin Microbiol*. 2018;5:135–142.
4. Le Guern AS, Martin L, Savin C, Carniel E. Yersiniosis in France: overview and potential sources of infection. *Int J Infect Dis.* 2016;46:1-7.
5. Smith D. Anatomy and postmortem examination. In: Schmidt RE, Struthers JD, Phalen DN, eds. *Pathology of Pet and Aviary Birds*. 3rd ed. John Wiley & Sons; 2024:1-18.
6. Wallner-Pendleton E, Cooper, G. Several outbreaks of *Yersinia pseudotuberculosis* in California turkey flocks. *Avian Dis.* 1983;27:524–526.
7. Walker D, Gibbons J, Harris JD, et al. Systemic *Yersinia pseudotuberculosis* as a cause of osteomyelitis in a captive ringtailed lemur (*Lemur catta*). *J Comp Pathol*. 2018;164:27-31.
8. Wise DR, Uppal PK. Osteomyelitis in turkeys caused by *Yersinia pseudotuberculosis*. *J Med Microbiol*.1972;5:128–130.

Joint Pathology Center
Veterinary Pathology Services

WEDNESDAY SLIDE CONFERENCE 2025-2026

Conference #18 — 04 February 2026

CASE I:

Signalment:
Adult, female, breed unspecified sheep (*Ovis aries*)

History:
This sheep displayed progressive clinical signs of neurological disease over a three day period culminating in tetraparesis and lateral recumbency, despite treatment with antibiotics, vitamin B complex and corticosteroids.

Gross Pathology:
At necropsy, the cerebrospinal fluid was cloudy and contained strands of fibrin. No other abnormalities were noted.

Figure 1-1. Brain, sheep: Sections from the cervical spinal cord, brainstem, and cerebellum are submitted for examination. (HE, 9X)

Laboratory Results:
A replicate section was examined by immunohistochemistry using a rabbit polyclonal anti Listeria monocytogenes antibody (#DF2302-50-0, Fisher Scientific, Houston, TX, USA), at a dilution of 1:2000, using the Dako Envision system (Dako Ag-ilent Pathology Solutions, Carpinteria, CA, USA), via an indirect immunoperoxidase procedure. Within the microabscesses in the brain and cervical spinal cord, there were a low to moderate number of bacteria that bound to the primary antibody.

Microscopic Description:
Brain, cerebellum and brainstem: In the brainstem gray matter, there are random multifocal, mild to moderate, variably discrete, infiltrates of hypersegmented and fragmented neutrophils, admixed with fewer mononuclear cells, consistent with microabscesses. Brainstem neurons within and adjacent to the neutrophilic infiltrates are pale, with central chromatolysis, consistent with neuronal degeneration. There are scattered microglial cells, mild gray matter spongiosis and infrequent microhemorrhages. Scattered blood vessels are lined by plump endothelial cells and have perivascular mild infiltrates of predominantly lymphocytes, with fewer neutrophils (perivascular cuffs). The cerebellar leptomeninges are multifocally, mildly infiltrated by predominantly lymphocytes, with fewer admixed neutrophils.

Figure 1-2. Cervical spinal cord, sheep: While inflammatory lesions are present in all sections, they are most severe in the cervical spinal cord. (HE, 30X)

Cervical spinal cord: In the gray matter and white matter, there are scattered, variably discrete, random multifocal, mild to moderate, infiltrates of neutrophils and mononuclear cells, consistent with microabscesses. There is neuronal degeneration, spongiosis, microgliosis, and swollen axons. Blood vessels are lined by plump endothelial cells and have perivascular mild to moderate infiltrates of predominantly lymphocytes, with fewer admixed neutrophils and infrequent plasma cells. The leptomeninges are multifocally expanded by mild to moderate infiltrates of lymphocytes with infrequent admixed neutrophils.

Contributor's Morphologic Diagnoses:

1. Brain, cerebellum and brainstem: Meningoencephalitis, lymphocytic, multifocal, mild to moderate, with multiple brainstem neutrophilic microabscesses.
2. Cervical spinal cord: Meningomyelitis, lymphocytic, multifocal, moderate, with multiple neutrophilic microabscesses.

Contributor's Comment:

A replicate section was examined by tissue Gram stain. There were low numbers of gram-positive bacilli, some intracellular, within areas of inflammation. A replicate section was examined by immunohistochemistry, using a rabbit polyclonal anti *Listeria monocytogenes* antibody (#DF2302-50-0, Fisher Scientific, Houston, TX, USA), at a dilution of 1 :2000, using the Dako Envision system (Dako Agilent Pathology Solutions, Carpinteria, CA, USA), via an indirect immunoperoxidase procedure. Within the microabscesses in the brain and cervical spinal cord, there were a low to moderate number of bacteria that bound to the primary antibody. The microscopic findings in the central nervous system accounted for the clinical signs in this sheep. The microscopic findings were typical of listeric encephalitis in ruminant species and the diagnosis was confirmed by immunohistochemistry.

Listeria monocytogenes is a gram-positive, facultative, anaerobic bacillus common in the environment. The bacteria can multiply within wide temperature and pH ranges. They can tolerate conditions of acidity, salinity and low moisture. They can survive in soil for many months and can be isolated from the feces of healthy cattle. *Listeria monocytogenes* is an intracellular pathogen of macrophages, neutrophils and epithelial cells. The bacterial surface proteins, Type A and Type B internalins, are virulence determinants. These proteins internalize with E-cadherin, an adherens junction transmembrane glycoprotein, to enable bacteria to cross intestinal, placental and blood brain barriers.

In sheep and other ruminants, listeriosis can manifest as three different syndromes, with little or no overlap. They are likely to be separate clinical presentations. The three syndromes are infection of the pregnant uterus resulting in abortion, blood borne infection with septicemia and with disseminated abscesses, and an ascending encephalitis.

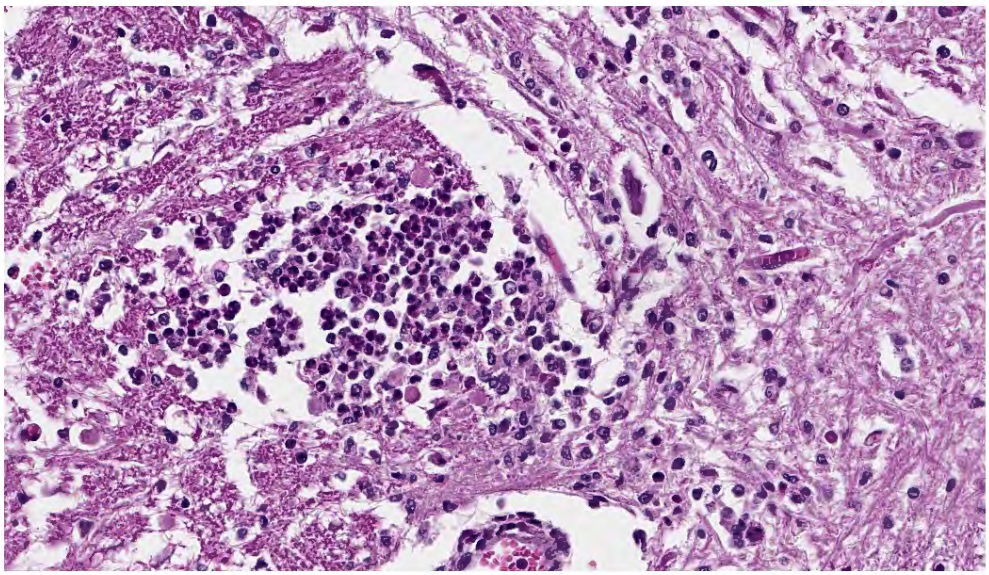

Figure 1-3. Cervical spinal cord: Within the grey matter (and scattered throughout the white matter), there are aggregates of intact and necrotic neutrophils (microabscesses). (HE, 691X)

Although listeric encephalitis has been associated with feeding of spoiled silage, environmental and fecal contamination are more common sources of infection than silage feeding in sheep and goats because many small rumi nants are never fed silage. The onset of the encephalitic form is usually very rapid. Death can ensue 24 to 48 hours after clinical signs appear. Clinical signs of listeric encephalitis in sheep and goats include lethargy, inappetence, loss of coordination, head pressing, circling, blindness, salivation, facial paralysis and culminate in recumbency, convulsions and death. This syndrome is more common in one to three-year-old small ruminants than in older animals.

There are few or no gross lesions in listeric encephalitis. Leptomeningeal opacity and cloudy cerebrospinal fluid may be the only findings seen at necropsy. Typically, microscopic lesions of listeric encephalitis are limited to the brainstem and cervical spinal cord. They include microabscesses, glial nodules, perivascular accumulation of lymphocytes and lymphocytic leptomeningitis. Gram-positive bacilli can be found within the microabscesses.

In listeric encephalitis, the likely route of infection of ingested *Listeria* bacilli is via breaks in the oral mucous membrane, with subsequent invasion of nerve endings of the trigeminal nerve branches. The bacteria travel via axonal flow to the central nervous system to infect neural cells, generally at the level of the brainstem and cervical spinal cord, where these nerve branches terminate. There may be a trigeminal ganglioneuritis. The bacteria multiply in neuronal cell bodies and then move to the inner side of the neuronal cell membrane via actin-filament mediated mobility. Aggregates of bacteria use a bacterial surface protein (surface protein actA) to move by actin polymerization. A pseudopod containing the bacteria invaginates randomly into an adjacent neural cell, forming a double-membrane bound endocytotic vesicle. This vesicle is lysed by listeriolysin 0, aided by a phospholipase and lecithinase, to release the bacteria into the cytoplasm of the newly invaded neural cell, as direct cell-to-cell extension of infection. Neural cell infection and endothelial damage lead to an inflammatory response and disruption of the blood-brain barrier with chemokine production and recruitment and activation of neutrophils.

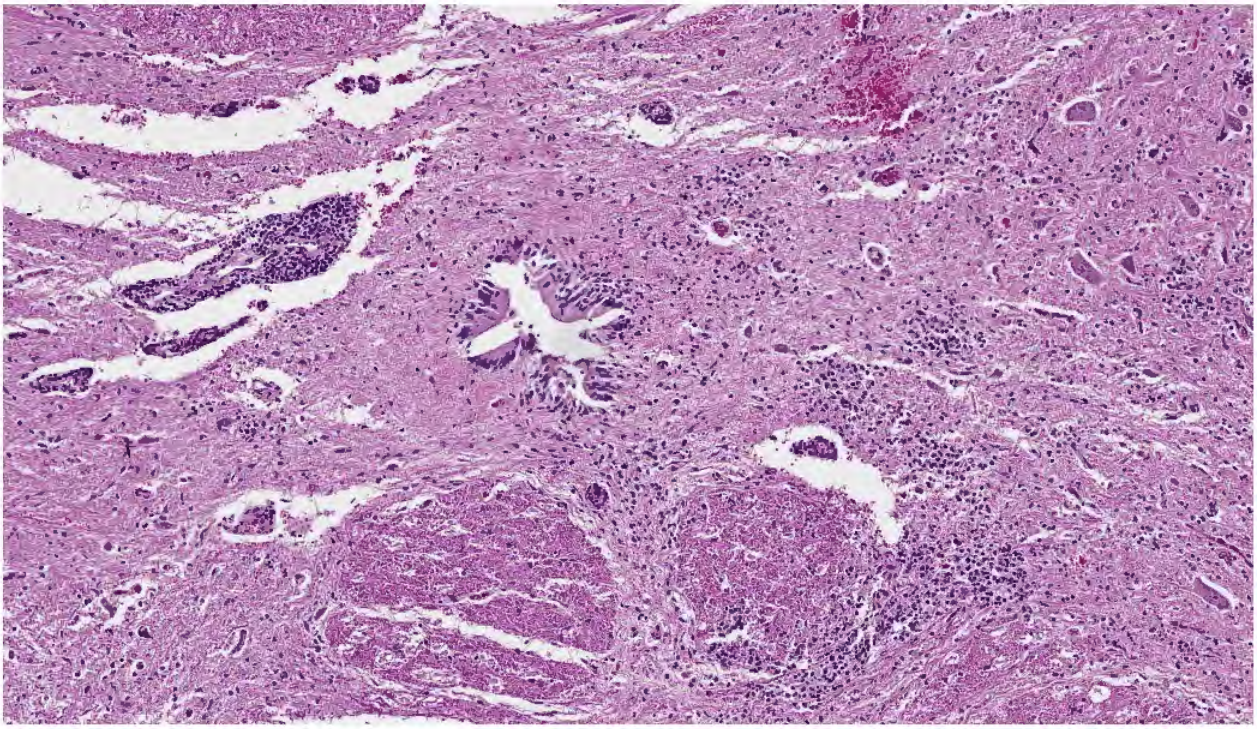

Figure 1-4. Cervical spinal cord: Throughout the section, in rarefied areas, there are microabscesses, perivascular cuffs of lymphocytes, plama cells, transmigrating neutrophils in Virchow-Robin spaces, and focal areas of hemorrhage. (HE, 171X)

Listeria monocytogenes is a zoonotic agent. Listeriosis in humans is a rare disease with high mortality (20-30%). Generally, it is a self-limiting foodborne illness. Certain risk groups (pregnant women, neonates, adults 65 years of age and over and individuals with compromised immune systems) may develop invasive disease one to four weeks following an episode of food borne illness. Invasive disease may include pregnancy complications (miscarriage, stillbirth, premature delivery due to *in utero* infection), life-threatening infection of the newborn, septicemia, meningitis and meningoencephalitis. Occasionally, it is an occupational disease of veterinarians and farmers, usually contracted from direct contact with infected livestock or their products of conception. To prevent contamination by *Listeria monocytogenes* in food processing establishments, cleaning and disinfection of facilities must be emphasized, with attention paid to proper maintenance and temperature control of food refrigeration equipment.

Contributing Institution:
United States Army Medical Research Institute of Infectious Diseases
https://www.usamriid.army.mil

JPC Diagnoses:
1. Cervical spinal cord: Meningomyelitis, suppurative, subacute, multifocal, moderate, with microabscesses.
2. Brainstem and cerebellar white matter: Leukoencephalitis, suppurative, subacute, multifocal, mild to moderate, with microabscesses and lymphohistiocytic meningitis.

JPC Comment:
This week's conference was moderated by MAJ Sarah Sulkosky, a former WSC Coordinator! *Listeria monocytogenes* has already

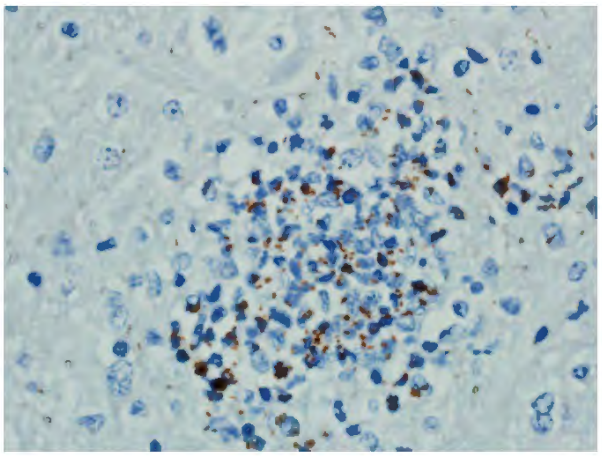

Figure 1-5. Brain: Within the microabscesses in the brain and cervical spinal cord, there were low to moderate numbers of bacteria that bound to anti-*Listeria monocytogenes* antibody. (Courtesy of United States Army Medical Research Insti-tute of Infectious Diseases; https://www.usamriid.army.mil)

been seen this year in a case of sepsis in a non-human primate (Conference 10, Case 3), but the CNS presentation of Listeriosis, particularly in a small ruminant, is worth its own conversation. The contributor provided a wonderful write-up on this entity, which contains most of what was discussed in conference. There was a quick discussion on the minimum histologic features of vasculitis, which include inflammatory cells (particularly neutrophils) AND cellular debris in the vessel wall, and extrusion of protein (which often polymerizes into fibrin) within the vessel wall.

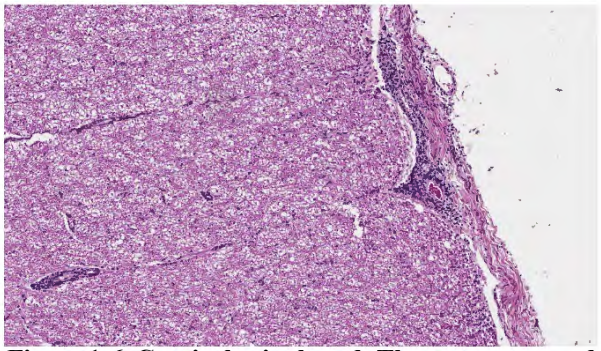

Figure 1-6. Cervical spinal cord: There are scattered aggregates of lymphocytes, plasma cells and fewer macrophages within the meninges and extending down along Virchow-Robin spaces. (HE, 189X)

Listeria monocytogenes was first described in 1926 by Murray as *Bacterium monocytogene*s after isolating it from the livers of diseased rabbits and guinea pigs.[1] A year later in 1927, Pirie isolated a similar organism from gerbils and proposed the genus name *Listerella* in 1930 to honor British surgeon and antiseptic technique frontman, Dr. Joseph Lister.[1] Dr. Lister discovered that sterilizing surgical instruments prior to use resulted in fewer post-operative infections. He is also the inspiration behind the name for one of our most popular antiseptic brands, “Listerine.” "Listerella", however, was a name previously used for a slime mold, so Pirie changed the name to *Listeria* in 1940.[1]

In cases of listeric encephalitis, *Listeria monocytogenes* is most classically associated with a rhombencephalitis, which is inflammation of the brainstem and cerebellum. These areas are most often affected due to the retrograde axonal transport *Listeria* makes along the trigeminal nerve. The sensory root for the trgimenal nerve emerges from the ventrolateral aspect of the pons, specifically the middle cerebellar peduncle, which connects the pons to the cerebellum.[3]

References:

1. Etymologia: *Listeria*. *Emerg Infect Dis*. 2016;22(4):633.
2. Maxie MG, Youssef S. Nervous System. In: Maxie MG, ed. *Jubb, Kennedy and Palmer's Pathology of Domestic Animals.* Vol I. 5th ed. Elsevier; 2007:405-408.
3. Ogino MH, Tadi P. Neuroanatomy, Trigeminal Reflexes. In: StatPearls [Internet]. Treasure Island (FL): StatPearls Publishing; 2025.
4. Zachary J. Mechanisms of Microbial Infections. In: Zachary J, McGavin MD, ed.

Pathologic Basis of Veterinary Disease. 5th ed. Elsevier, 2012:192-195.
5. Zachary J. Nervous System. In: Zachary J, McGavin MD, ed. *Pathologic Basis of Veterinary Disease.* 5th ed. Elsevier, 2012:845-846.
6. https://www.fda.gov/.../get-facts-about-listeria
7. https://www.cdc.gov/listeria/index.html.
8. https://www.canr.msu.edu/news/listeriosis-in-sheep-and-goats.

CASE II:

Signalment:
7-week-old, intact male, mixed breed dog (*Canis lupus familiaris*)

History:
This puppy came from a litter of 14 born to a rescued, unvaccinated dam. Half of the litter failed to thrive and was reportedly unable to latch; affected puppies were subsequently tube fed. There was concern for aspiration pneumonia and antibiotic treatment was initiated. The puppies had been dewormed and received the first of a vaccine series. This puppy was acutely anorexic, and was bottle fed prior to death.

Gross Pathology:
The liver was diffusely mottled yellow to red and had tens of pinpoint, flat, red discoloration randomly scattered across the capsular surface. The lungs were diffusely mottled tan to pink, slightly rubbery, and exuded a moderate amount of clear to yellow, watery to slightly viscous fluid on cut section. On cut surface of the brain, primarily within the thalamus, was a fairly well demarcated region of red to brown discoloration and there were pinpoint regions of red-brown discoloration throughout the adjacent parenchyma.

Figure 2-1. Cerebrum, dog: Multiple sections of cerebrum are submitted for examination. At subgross magnification, multiple hemorrhagic foci may be seen in the section at left. (HE, 9X)

Laboratory Results:
- Canine adenovirus-2 PCR: Positive
- Aerobic culture, lung: No growth
- Aerobic culture, liver: No growth
- Canine herpesvirus PCR: Negative

Microscopic Description:
Throughout the cerebral gray matter, small caliber vessel walls were frequently obscured by mild to moderate amounts of eosinophilic, fibrillar, proteinaceous material and hemorrhage. Endothelial cells frequently contained large, eosinophilic, intranuclear inclusions which peripheralize chromatin. Affected vessels were frequently cuffed by moderate numbers of macrophages and lymphocytes, and there were frequent, small areas of hemorrhage spilling into the adjacent tissue. The meninges overlying the cerebellum were moderately expanded by lymphocytes and macrophages, and endothelial cells frequently contained intranuclear inclusions similar to those found in the cerebral vessels.

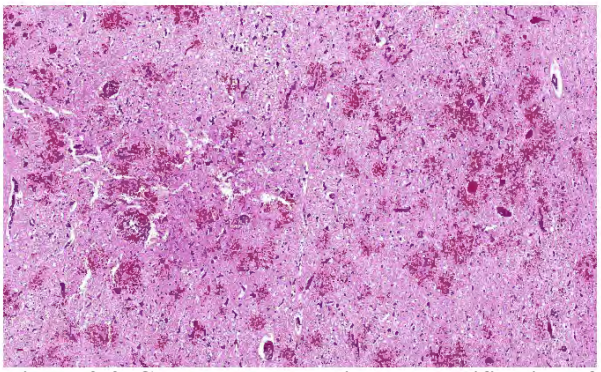

Figure 2-2. Cerebrum, dog: Higher magnification of the numerous foci of hemorrhage within the cerebrum (HE, 102X)

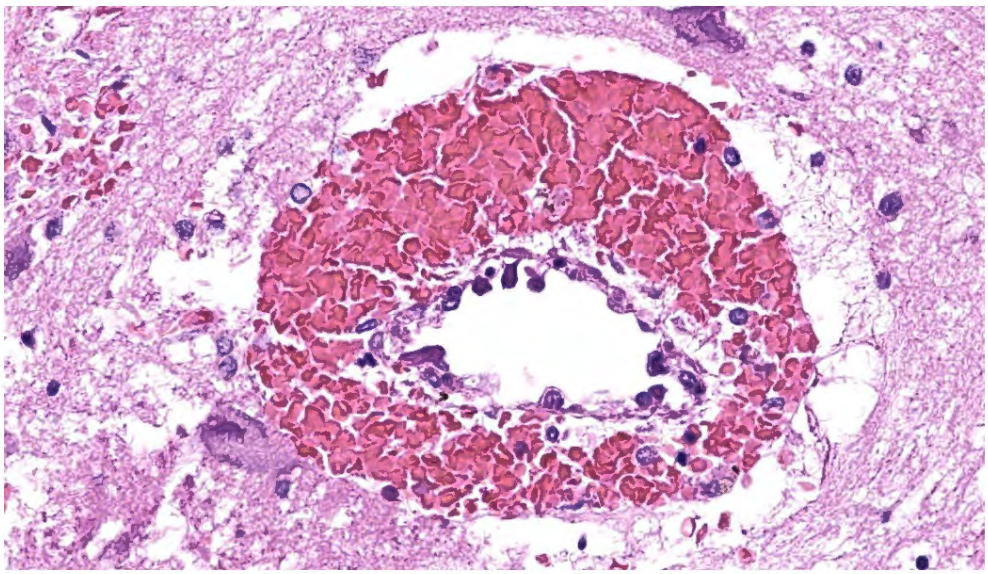

Figure 2-3. Cerebrum, dog: High magnification of an affected vessel with perivascular hemorrhage. (HE, 990X)

Contributor's Morphologic Diagnoses:
Severe, multifocal, acute, histiocytic vasculitis and meningitis with cerebral hemorrhage and intranuclear viral inclusions.

Contributor's Comment:
Adenoviruses are linear, double-stranded DNA, icosahedral viruses which are subdivided into four genera – *Mastadenovirus*, *Aviadenovirus*, *Atadenovirus*, and *Siadenovirus*. Mammalian adenoviruses generally belong to the *Mastadenovirus* genus and are categorized based on neutralization assays. This viral family replicates within nuclei, leading to the formation of characteristic intranuclear inclusions seen in a variety of cell types depending on the species and site of infection. Canine adenovirus-1 infection, colloquially known as infectious canine hepatitis, most often infects hepatocytes leading to acute hepatitis, but can infect the endothelium, causing disseminated intravascular coagulation and hemorrhage. Infection with canine adenovirus-2 is typically localized to the respiratory system, causing mild, non-specific signs of acute respiratory disease which eventually resolve.[8]

Although unusual, systemic infection with canine adenovirus-2 has previously been reported.[1] In one report, neurologic signs were noted in 3 of 4 puppies out of a litter of 9 who were diagnosed with CAV-2 systemic infection. Two of these puppies displayed concurrent, mild respiratory signs. Interestingly, as in the submitted case, these puppies were born to an unvaccinated dam. In contrast to the submitted case, despite the clinical presence of neurologic abnormalities prior to death, nervous system lesions were not present histologically, although virus was detected via PCR in the brain in one affected animal.[1]

While reports of CAV2-induced vasculitis are sparse, other species of adenovirus-associated vasculitis are more common. Perhaps the most similar syndrome of adenovirus-associated vasculitis is seen in adenovirus hemorrhagic disease of cervids. Clinically, this disease presents similarly to epizootic hemorrhagic disease, with histologic lesions including systemic vasculitis and petechiae, along with intranuclear inclusions which separate this disease from epizootic hemorrhagic disease. Affected animals have numerous intranuclear inclusion bodies found in the endothelial cells of a variety of organs, including the brain, which are occasionally associated with fibrin thrombi or fibrinoid necrosis, vasculitis, and/or perivascular cuffs.[2,9] In affected animals, lesions are most frequent in the lungs

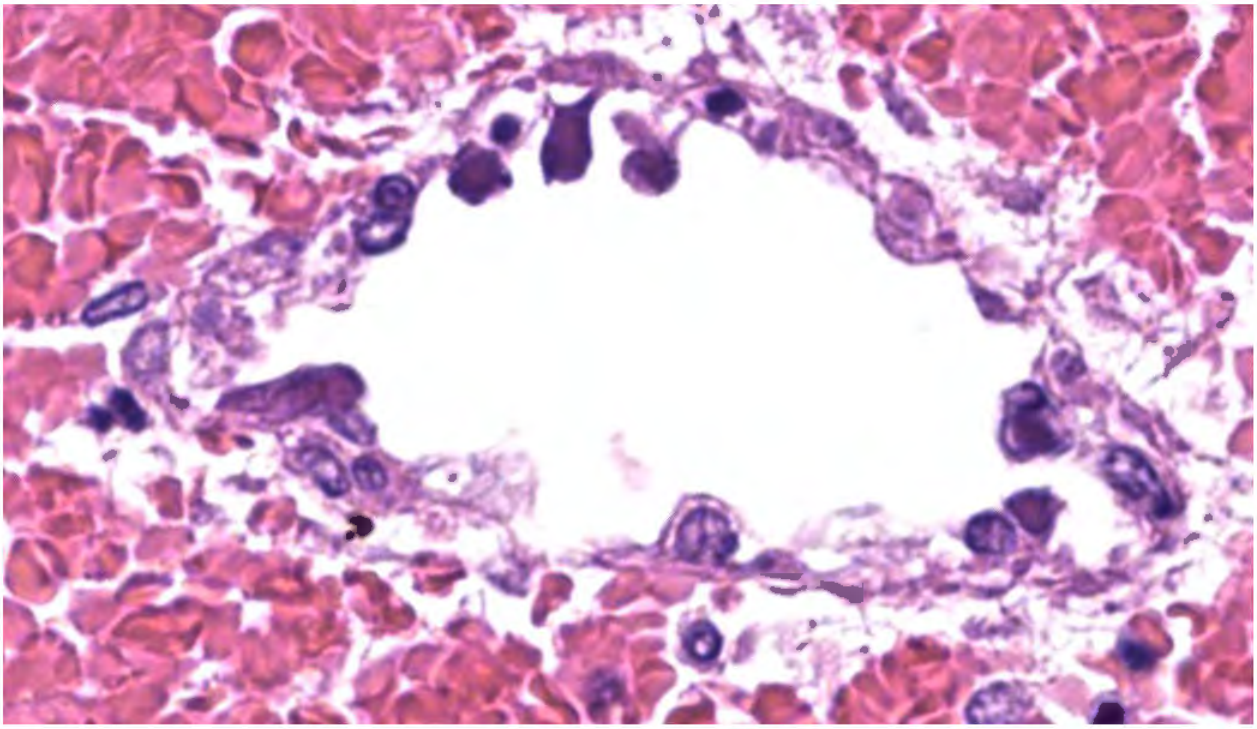

Figure 2-4. Cerebrum, dog: High magnification of endothelial cells which are swollen by karyomegalic intranuclear viral inclusions consistent with adenoviral inclusions. (HE, 2500X)

and brain, although hepatic lesions may also be seen, as in this case.[9]

Human adenovirus of an undetermined serotype has been reported as a cause of acute retinal necrosis due to occlusive vasculitis.[7] One study examining the presence of vasculitis associated with severe respiratory infections found uncommon reports of thrombosis or vasculitis associated with human respiratory adenovirus infections.[5] Following a variety of immunosuppressive therapies and stem cell transplant, adenovirus-associated vasculitis with microscopic regions of cortical necrosis and hemorrhage were seen in a human multiple myeloma patient. In this case, abundant viral inclusions were found in the endothelial cells, but not epithelial cells within the examined organs.[4]

In the current case, CAV-2 was detected via PCR and immunohistochemistry within the histologically observed cerebral and meningeal lesions associated with vasculitis. Previously reported cases of disseminated CAV-2 infection with vasculitis have been proposed to be associated with other infectious agents or diseases causing immunosuppression. There was not evidence of an underlying cause for immunosuppression in the current case, and there was no evidence of concurrent systemic disease. Thus, the vascular lesions associated with CAV-2 appear to be the primary cause of disease in this puppy. As in the above discussed previously reported case of CAV-2 infections associated with neurologic signs in a litter of puppies, it appears likely that the lack of maternal vaccination may have contributed to disease in this case.[1]

Contributing Institution:
National Institute of Health Comparative Biomedical Scientist Training Program

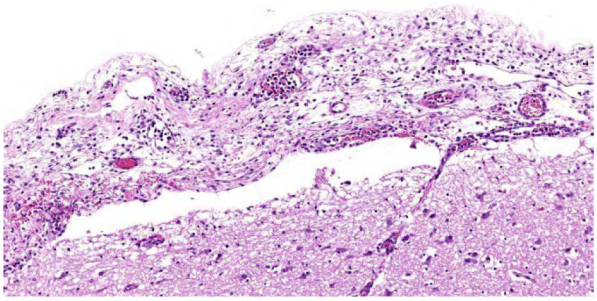

Figure 2-5. Cerebrum, dog: There is mild lymphoplasmacytic meningitis with edema. Vascular changes are present, but far less severe than in the underlying neuropil. (HE, 246X)

JPC Diagnosis:
Cerebrum: Vasculitis, neutrophilic and lymphocytic, subacute, multifocal to coalescing, marked, with fibrin thrombi, lymphohistiocytic meningitis, and endothelial intranuclear viral inclusions.

JPC Comment:
This case stimulated great discussion during conference and the WSC team would like to thank this contributor for sending in such an interesting submission and a fantastic write-ip! MAJ Sulkosky stated that, although the causative agent was diagnosed as CAV-2 by the contributor, this case should be considered classic for a CAV-1 infection in a puppy. CAV-1 has been seen a couple of times recently in the WSC in 2022, Conference 22, Case 3, and in 2019, Conference 16, Case 1.

Conference participants speculated as to why CAV-2 was isolated in this case, as there was no mention of testing for CAV-1 in the contributor's writeup, and wondered if there had potentially been cross-reactivity on the test. The papers that describe CAV-2 encephalitic disease in dogs lack supporting evidence to demonstrate that the lesions were caused exclusively by CAV-2, so attendees remained unconvinced.[1,3] Most wondered if this case was instead a CAV-1 encephalitis and the CAV-2 positivity was either a false positive, was showing as positive due to the recent history of a distemper combo vaccine in this puppy, or was due to a co-infection with CAV-1 that was just not tested for. It is still unclear if CAV-2 can truly cause vasculitis in the brains of puppies. CAV-2 is considered primarily a mild respiratory pathogen, and there are very rare reports of other organs affected.

There is one paper that describes 2 cases of fatal encephalitic CAV-1 infection in puppies, but the sequence of the pVII gene in that CAV-1 was more closely related to that seen in CAV-2, suggesting a possible recombinant strain.[10] The pVII gene in canine adenoviruses encodes an arginine-rich core protein (pre-VII) which is cleaved to form pVII. The pVII protein is responsible for condensing the viral DNA within the capsid, acting like a histone protein.[6] pVII plays a critical role in the virus's structure and, due to its nuclear localization, serves as a target for labeling in research studies.[6]

Wrapping up this spirited case discussion was a review of the viruses that form paracrystalline arrays that can be seen with electron microscopy. This list of viruses can be remembered using the acronym "PPPICCA," which stands for paramyxovirus, picornavirus, polyomavirus, iridovirus, circovirus, calicivirus, and adenovirus.

References:

1. Benetka V, Weissenböck H, Kudielka I, Pallan C, Rothmüller G, Möstl K. Canine adenovirus type 2 infection in four puppies with neurological signs. 2006;158(3):91–94.
2. Burek-Huntington K, Miller MM, Beckmen K. Adenovirus hemorrhagic disease in Moose (*Alces americanus gigas*) in Alaska, USA. *J Wildl Dis*. 2021;57(2):418–422.
3. Chander V, et al. Isolation and genetic characterization of canine adenovirus type

2 from a domestic dog showing neurological symptoms. *Braz J Microbiol*. 2021 Dec;52(4):2521-2528.
4. Claveau JS, LeBlanc R, Ahmad I, et al. Cerebral adenovirus endotheliitis presenting as posterior reversible encephalopathy syndrome after allogeneic stem cell transplantation. *Bone Marrow Transplantation*. 2017:52;1457–1459.
5. Dolby HW, Potey P, Wilder-Smith AB, et al. Histological evidence of pulmonary microthrombosis and vasculitis in life-threatening respiratory virus diseases. *Open Forum Infect Dis*. 2021;8(2).
6. Morrison MD, Onions DE, Nicolson L. Complete DNA sequence of canine adenovirus type 1. *J Gen Virol*. 1997;78(4):873-878.
7. Özdemir HB, Özdal PÇ. Human adenovirus: An unusual causative agent for acute retinal necrosis presented with central retinal vascular occlusion. *Ocul Immunol Inflamm*. 2020;28(5):749–753.
8. Quinn PJ, Markey BK, Leonard FC, Fitz-Patrick ES, Fanning S, Hartigan PJ. Adenoviridae. In: *Veterinary Microbiology and Microbial Disease, 2nd ed*. Blackwell Publishing; 2011:588-592.
9. Woods LW, Swift PK, Barr BC, et al. Systemic Adenovirus Infection Associated with High Mortality in Mule Deer (*Odocoileus hemionus*) in California. *Vet Pathol*. 1996;33.
10. Wong M, Woolford L, Hasan NH, Hemmatzadeh F. A Novel Recombinant Canine Adenovirus Type 1 Detected from Acute Lethal Cases of Infectious Canine Hepatitis. *Viral Immunol*. 2017;30(4):258-263.

CASE III:

Signalment:
1-year-old, intact female, pit bull dog (*Canis familiaris*)

History:
History of weight loss despite appetite and diarrhea. Animal became neurologic and blind for approximately one week until developing seizures. No reported bloodwork abnormalities (complete blood count, blood serum chemistry, and bile acids). Dog was euthanized and submitted for necropsy.

Gross Pathology:
The animal was emaciated with generalized muscle atrophy and scant visceral adipose. The pancreas was reduced to small, thin, red-grey lobules. In the small intestine, there was mild ancylostomiasis with segmental intraluminal hemorrhage. The feces in the distal colon were pale green and soft. The lateral ventricles of the brain were mildly dilated.

Laboratory Results:
- *Toxoplasma gondii* PCR: positive (CT brain: 25.4, heart: 21.4)

Figure 3-1. Cerebrum, dog: A section of cerebrum is submitted for examination. At subgross magnification, there is mild dilation of the lateral ventricle, and hypercellularity of the periventricular white matter is visible. (HE, 9X)

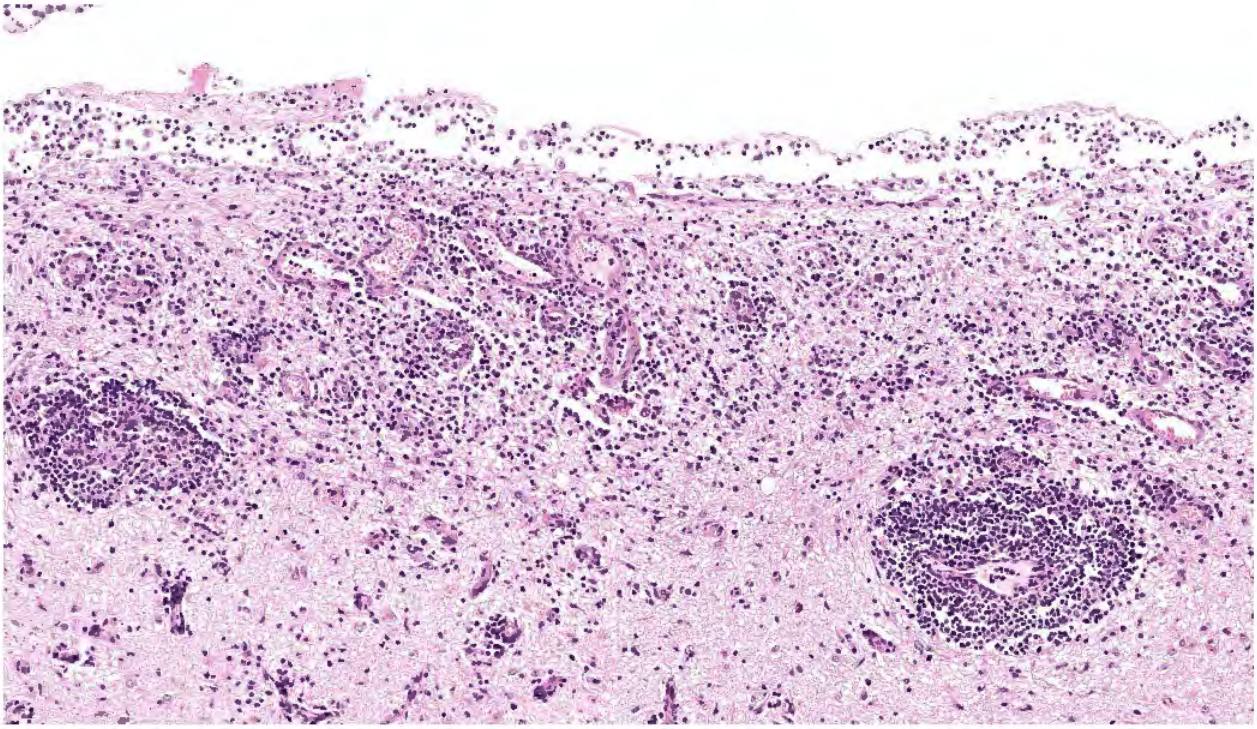

Figure 3-2. Cerebrum, dog: While there is inflammation throughout all layers of the cerebrum, to including both gray and white matter, inflammation is most prominent in the edematous periventricular white matter. This area is infiltrated by large numbers of of lymphocytes, macrophages, and fewer neutrophils and plasma cells. Cuffs of numerous lymphocytes and plasma cells, and fewer macrophages are present around blood vessels. (HE, 194X)

- *Neospora caninum* PCR: not detected
- Fecal testing: *Ancylostoma* spp. ova detected

Microscopic Description:
Brain: The meninges are moderately expanded by macrophages, plasma cells, and lymphocytes that surround and partially obscure reactive meningeal vessels. Inflammatory cells extend around vessels into the subtending parenchyma, filling and expanding Virchow Robin spaces up to 12-15 cell layers thick. There are focal areas of infiltration of macrophages, lymphocytes, and plasma cells into the surrounding parenchyma with associated vacuolation and necrosis of the parenchyma, neuronal satellitosis and necrosis, infiltration of gitter cells, gliosis, and astrocytosis. Isolated within the parenchyma and associated with areas of inflammation and necrosis are numerous 12 to 45-µm diameter protozoal cysts containing closely packed clusters of 1 to 2-µm wide, crescent-shaped bradyzoites. At the level of the corpus striatum, there is vacuolation of white matter tracts with occasional spheroids, digestion chambers, and numerous protozoa. Vessels adjacent to the lateral ventricle are obscured by macrophages, lymphocytes, plasma cells, and neutrophils with indistinct, hypereosinophilic vascular walls (necrosis) and perivascular exudation of fibrin and edema. The ependyma spanning the lateral ventricle is segmentally discontinuous with disruption by inflammatory cells and necrotic material that extend into the ventricular lumen.

Contributor's Morphologic Diagnoses:
Brain: Meningoencephalitis and ventriculitis, necrotizing and histiocytic to lymphoplasmacytic, subacute, multifocal, moderate,

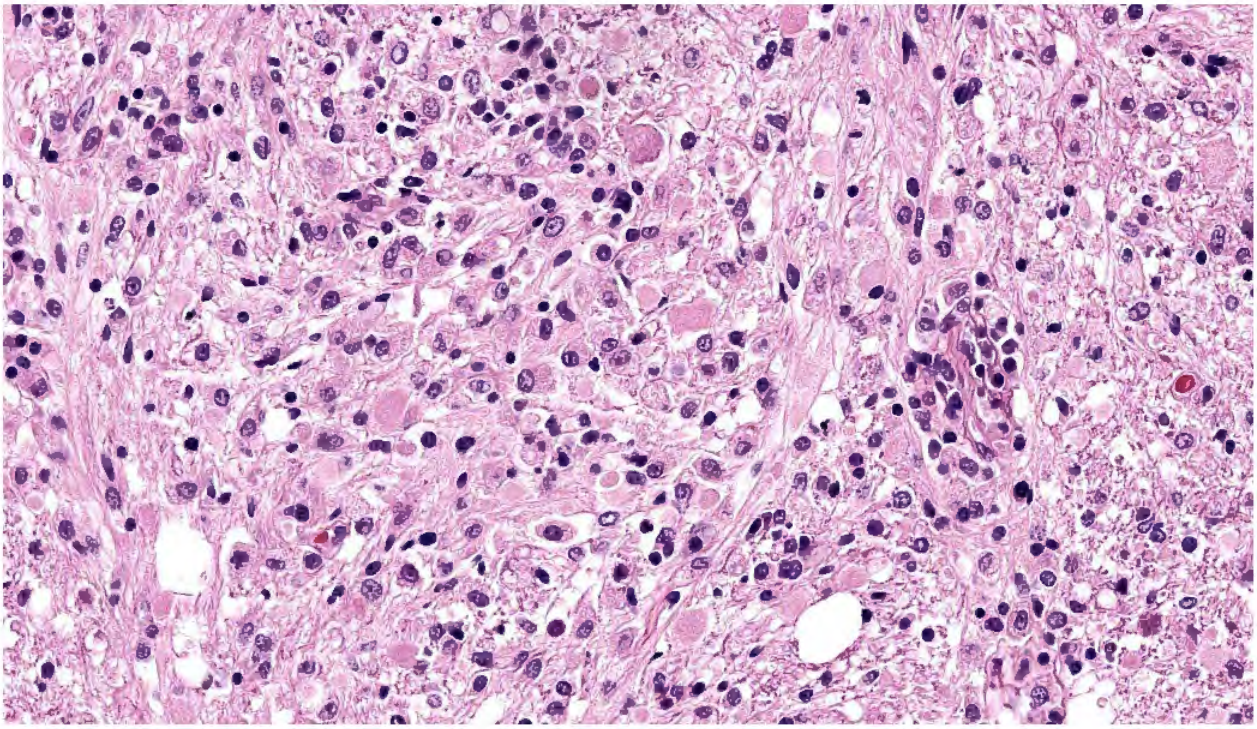

Figure 3-3. Cerebrum, dog: Within the area of rarefaction and inflammation within the internal capsule, there is infiltration of large number of lymphocytes, macrophages, and fewer plasma cells and numerous dilated axon sheaths and spheroids. (HE, 582X)

with protozoal cysts and zoites, vasculitis and vascular necrosis.

Contributor's Comment:

Toxoplasmosis is caused by the apicomplexan protozoan *Toxoplasma gondii*.[4] It can infect a variety of hosts including mammals and birds and causes a wide spectrum of disease.[3,4] Toxoplasmosis is an important zoonotic pathogen and cause of abortion in primates, prosimians, and ruminants.[6,7]

Infected felines may serve as definitive or intermediate hosts, while all other non-felids act as intermediate hosts.[3,4,7] In felines, enteroepithelial replication culminates in the release of unsporulated oocysts in the feces, which sporulate in the environment and become a source of infection for both definitive and intermediate hosts.[4,7] Oocysts are only produced in the definitive felid host.[3,4] Infection of intermediate hosts follows an extraintestinal replication cycle with rapid division of tachyzoites spread widely throughout multiple tissues.[6] A third infective form involves the deposition of latent tissue cysts in tissues containing slowly replicating bradyzoites.[3,4] Infection occurs following ingestion of sporulated oocysts shed from definitive host in the environment or via consumption of zoites or tissue cysts from infected prey. Alternatively, infection can occur transplacentally.[3]

Manifestation of clinical disease may vary given the wide distribution of protozoa within tissues. Systemic disease is classically characterized by interstitial pneumonia, hepatic necrosis, lymphadenitis, myocarditis, and meningoencephalitis.[7] Other lesions may include uveitis, adrenalitis, nephritis, myositis, and placental necrosis/placentitis.[3]

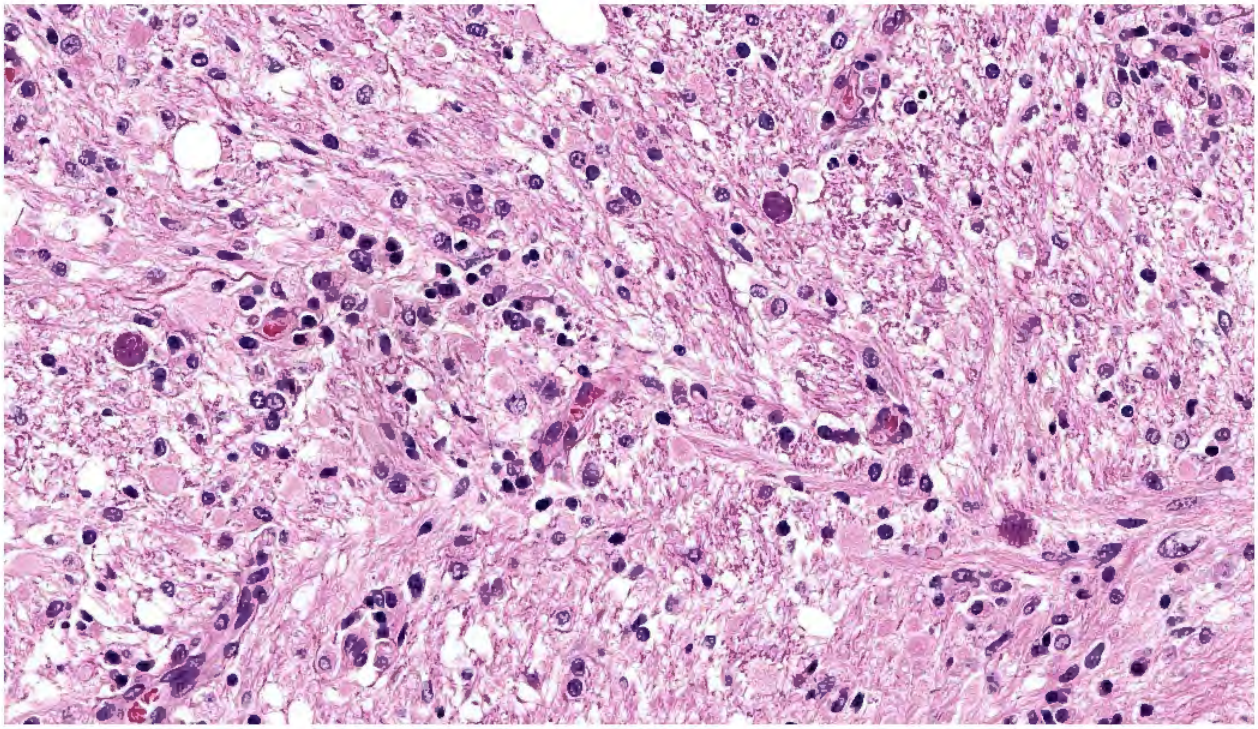

Figure 3-4. Cerebrum, dog: In areas of inflammation (including the internal capsule, pictured here), there are scattered 15-20um apicomplexan cysts containing numerous tachyzoites. (HE, 582X)

Central nervous system disease is more common in young or immunosuppressed individuals and is difficult to differentiate histologically from *Neospora caninum*, *Sarcocystis* spp., or *Encephalitozoon cuniculi*, thus requiring additional testing modalities (immunohistochemistry, PCR, and/or special histochemical staining) to differentiate.[4] However, observing necrosis in multiple organ systems associated with the presence of protozoal infective stages is most suggestive of toxoplasmosis.[7]

In dogs, toxoplasmosis is rarely a primary disease and often seen in conjunction with immunosuppression or comorbidities.[2] Immunosuppression was suspected in this dog. Although clinical data (i.e. serum trypsin-line immunereactivity) supportive of exocrine pancreatic insufficiency (EPI) was not available, the reported clinical signs of diarrhea and weight loss despite sufficient appetite are suggestive of EPI. This is further supported by postmortem lesions of pancreatic atrophy, pale stools, and emaciation. It is possible that EPI resulted in immunosuppression from chronic malnutrition, nutrient deficiency, and possible cobalamin deficiency from small intestinal bacterial overgrowth (SIBO). These factors may have predisposed this dog to the development of systemic toxoplasmosis.

Contributing Institution:
University of Georgia College of Veterinary Medicine, Department of Pathology, Tifton Veterinary Diagnostic and Investigational Laboratory, Tifton, Georgia, USA, www.vet.uga.edu/dlab

JPC Diagnoses:
Cerebrum: Meningoencephalitis, necrotizing and lymphohistiocytic, subacute, multifocal to

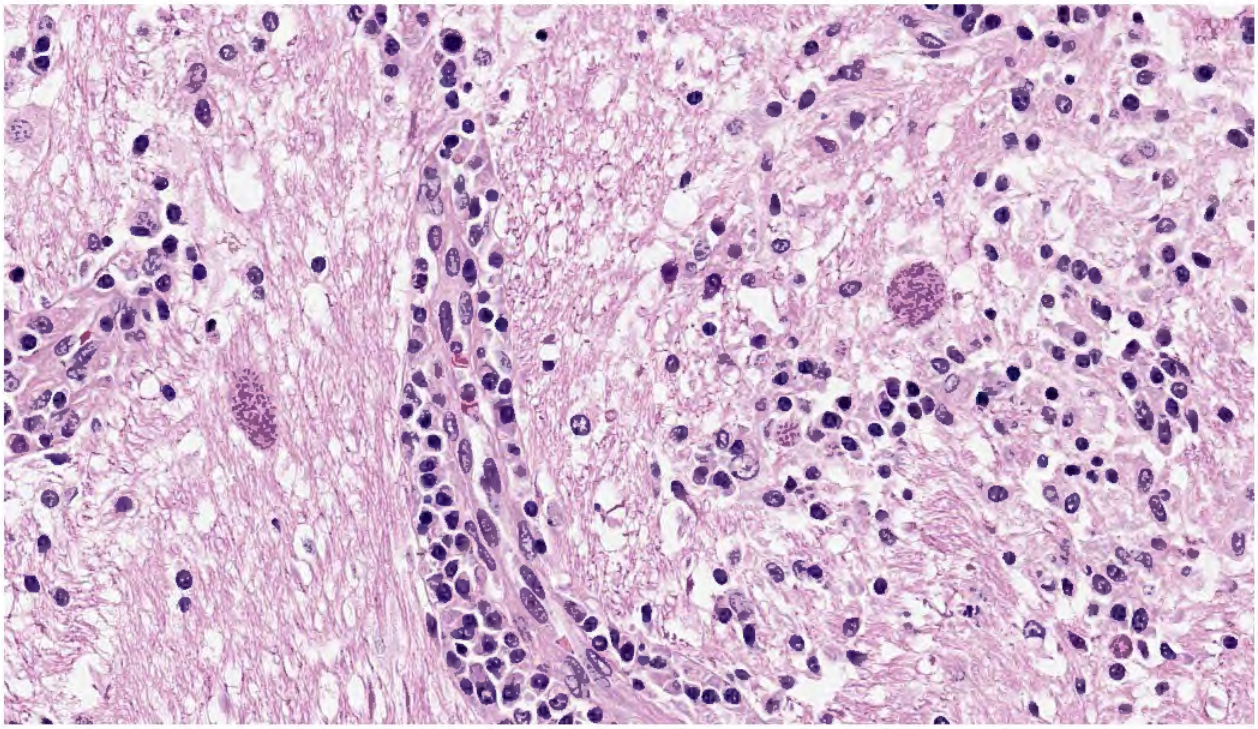

Figure 3-5. Cerebrum, dog: In areas of inflammation, there are scattered 15-20um apicomplexan cysts containing numerous zoites. (HE, 691X)

coalescing, marked, with vasculitis and apicomplexan cysts.

JPC Comment:
A classic and oft-seen entity in the WSC, *Toxoplasma gondii* makes another appearance this year in a fantastic canine case. Organisms were readily apparent within the neuropil of the periventricular grey matter on the H&E slide, prompting an excellent discussion of *T. gondii* and the zoonotic risk these infections pose. The contributor provided an excellent comment in this case and, once again, many of their points were mentioned in conference discussion.

Toxoplasma gondii is an obligate intracellular apicomplexan protozoal parasite that was named in 1908 by researchers Nicolle and Manceaux.[1] They the names comes from the Greek word "toxon*"* (meaning "bow" or "arc"), referring to the crescentic shape of the tachyzoite stage, and "gondii", chosen in honor of the North African gundi (*Ctenodactylus gundi*). This rodent is the host animal in which the parasite was first identified.[1] Since its initial discovery in the gundi, *T. gondii* has been identified in numerous mammalian species and in a wide range of tissue types.

The pathogenesis of *T. gondii* starts with penetration of the intestinal mucosa by a tachyzoite, sporozoite, or bradyzoite either from ingestion of an infected host, from transplacental transmission, or by consumption of oocysts from the environment. The zoites can then either be trafficked in leukocytes to other tissues (i.e., lymph nodes and liver) or remain free in the bloodstream. The tachyzoites replicate within host cells until the cell lyses, at which point the tachyzoites are free to infect other cells and cause additional tissue damage. Cell-mediated immunity eventually can control, but not eliminate, the infection, and the parasites form dormant tissue cysts filled with

bradyzoites within the heart, skeletal muscle, and brain in the chronic stages of infection.

Systemic toxoplasmosis is seen predominantly in neonates that were infected transplacentally or in immunocompromised animals that have low levels of interferon gamma and an inability to activate macrophages. In systemic "toxo", the hallmarks of infection include necrosis and the presence of zoites. These most often manifest as either interstitial pneumonia (most common), meningoencephalitis (with necrosis, malacia, vasculitis, and vascular necrosis), focal hepatic necrosis, lymphadenitis, and/or myocarditis.

In cases of meningoencephalitis, the parasites can enter the brain by breaching the blood–brain barrier (BBB) using three possible mechanisms: 1) infection of monocytes that then traverse the endothelium, 2) direct penetration and migration across the BBB, or 3) infection of and growth within endothelial cells and eventual exit into the neuropil.[5] Once inside the brain, *T. gondii* can infect multiple cell types, including astrocytes, microglia, and neurons, and form tissue cysts.[5]

The contributor mentioned that this dog also had histologic and gross evidence of pancreatic atrophy and atrophic lymphocytic pancreatitis. In dogs, juvenile pancreatic atrophy is an immune-mediated condition characterized by infiltration of T-cells (predominantly CD8+) into the pancreas.[2] Around 6-12mo of age, affected dogs start to demonstrate clinical signs of exocrine pancreatic insufficiency. Histologically, pancreatic ducts and connective tissue structures predominate in the later stages of this condition with fatty replacement and minimal exocrine tissue, little inflammation, and fibrosis.[2] Participants speculated on and agree with the contributor that the exocrine pancreatic insufficiency suspected in this dog may have led to immunocompromise and subsequent systemic toxoplasmosis infection.

References:

1. Black MW, Boothroyd JC. Lytic cycle of Toxoplasma gondii. *Microbiol Mol Biol Rev*. 2000;64(3):607-623.
2. Brenner K, Harkin KR, Andrews GA, Kennedy G. Juvenile pancreatic atrophy in Greyhounds: 12 cases (1995-2000). *J Vet Intern Med*. 2009;23(1):67-71.
3. Calero-Bernal R, Gennari SM. Clinical toxoplasmosis in dogs and cats: an update. *Front Vet Sci.* 2019;6:54.
4. Cantile C, Youssef S. Nervous System. In: Maxie MG, ed. *Jubb, Kennedy, and Palmer's Pathology of Domestic Animals. Vol. 1.* 6th ed. St. Louise, MO: Elsevier; 2016:387-389.
5. Courret N, Darche S, Sonigo P, Milon G, Buzoni-Gâtel D, Tardieux I. CD11c- and CD11b-expressing mouse leukocytes transport single Toxoplasma gondii tachyzoites to the brain. *Blood*. 2006;107(1):309-316.
6. McAloose D, Stalis IH. Prosimians. In: Terio KA, McAloose D, St. Leger J, eds. *Pathology of Wildlife and Zoo Animals*. San Diego, CA: Elsevier; 2018: 338.
7. Uzal FA, Plattner BL, Hostetter JM. Alimentary system. In: Maxie MG, ed. *Jubb, Kennedy, and Palmer's Pathology of Domestic Animals. Vol. 2.* 6th ed. St. Louise, MO: Elsevier; 2016:236-238.

CASE IV:

Signalment:
4-month-old, female, Angus cow (*Bos taurus*)

History:
Calf presented with history of ongoing generalised ataxia, wide-based stance, incoordination and intermittent head tremor. The calf was otherwise in good body condition. One other calf was similarly affected and there were 74 other unaffected calves in the herd.

Gross Pathology:
There was subjectively increased amount of CSF present upon removing the brain. A unilateral, focal, kidney cyst was also present.

Laboratory Results:

Test	Result
Blood lead	Negative
Chlamydia CFT	Negative
Pestivirus antigen capture ELISA	Negative
CBC & Biochemistry	Mild Elevation GLDH – 15.09 (6.14-13.34 U/L) Moderate Elevation CK – 2401 (43-580 U/L) Mild Elevation AST – 133 (58-125 U/L) Mild elevation Leukocytes – 13.46 (4.8-13.0 U/L) Otherwise unremarkable
CSF Analysis	Colour: Opaque white Transparency: cloudy Flocculation: none Microprotein: 0.515 g/L Total nucleated cell count (TNCC): 0.725 x 10^9/L Red cell count: 0.005 x 10^{12}/L Neutrophils: 22% Small mononuclear cells: 45% Large mononuclear cells: 33% Interpretation: Pleocytosis with elevated protein
Neimann-Pick Type C genotyping PCR	Non-carrier
Alpha-mannosidosis genotyping PCR	Affected

Microscopic Description:
Cerebellum: Multifocally, numerous Purkinje cells at the junction between the molecular and granule cell layer, as well as occasional neurons within the granular cell layer and cerebellar deep nuclei are moderately swollen, have pale granular eosinophilic to clear, finely vacuolated or foamy cytoplasm that often dis-places the nuclei towards the periphery. Neurons are multifocally lost within the Purkinje (empty baskets) and granular layers. Through-out the white matter tracts, there are numerous variably sized (up to 60µm in diameter) hypereosinophilic axonal swellings (spheroids) as well as less frequent dilation of peri-axonal spaces containing fragmented myelin debris (ellipsoids) and foamy macrophages (digestion chambers). Multifocally, few axonal swellings are also present within the granule cell layer (torpedoes).

Contributor's Morphologic Diagnoses:
Cerebellum: Neuronal vacuolation and loss, diffuse, severe with occasional neuronal intracellular granular eosinophilic material accumulation, torpedoes, spheroids and digestion chambers (Wallerian degeneration).

Figure 4-1. Cerebellum, calf: One section of cerebellum is submitted for examination. The cerebellar folia appears thinned. (HE, 9X)

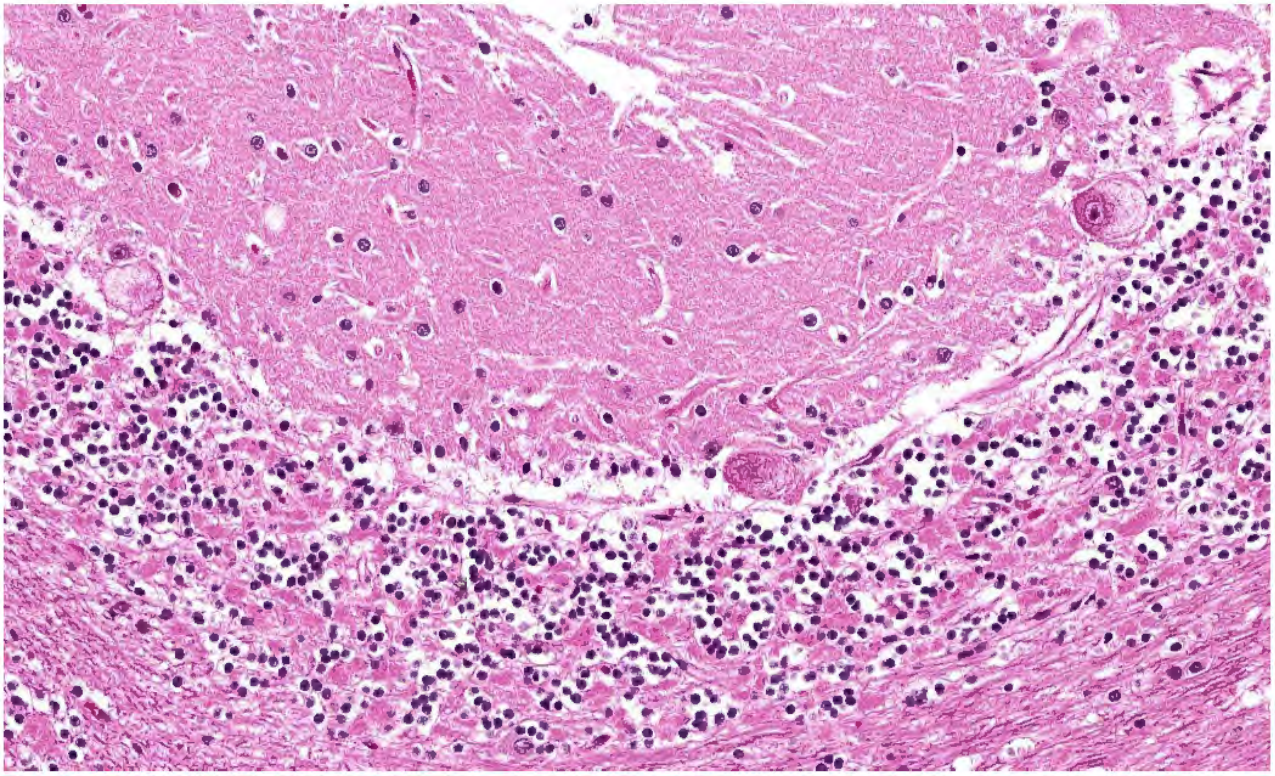

Figure 4-2. Cerebellum, calf: There is segmental loss of Purkinje cells with formation of "empty baskets." Remnant Purkinje cells are swollen due to the accumulation of numerous clear vacuoles within their cytoplasm. (HE, 381X)

Contributor's Comment:

Alpha-mannosidosis is a type of inherited lysosomal storage disease predominantly seen in cattle.[3] The condition is best characterized in Angus and Murray Grey cattle.[3] It has also been reported in Galloway cattle as well as Persian, domestic longhair, and shorthair cats.[2,7,12,15] The condition is rare in humans.

This storage disease was first described in Angus calves in Australia in 1957 and later extensively studied in New Zealand, becoming one of the earliest major investigations into lysosomal storage diseases in animals.[18,24] Due to high economic impact, characterization of the disease and detection of both affected and carrier animals became a priority within the livestock industry. Clinically, affected animals develop ill-thrift, ataxia, incoordination, head and intention tremors, often display a wide-based stance and can be abnormally aggressive.[16,24] These signs can be seen as young as 4 weeks of age, with some animals able to survive up to 18 months of age.[3,24]

Individuals affected with alpha-mannosidosis are deficient in lysosomal alpha-mannosidase activity, leading to accumulation and storage of mannose within vacuoles of affected cells.[3] Under light microscopy, these vacuoles are empty and expand the cytoplasm.[16] The condition affects all cells within the body except hepatocytes, though is generally most notice-able microscopically within the nervous system.[3] In this case, neuronal vacuolation was most prominent within the thalamus and in Purkinje cells of the cerebellum. Few renal tubular epithelial cells were also affected. In addition to neuronal vacuolation, dysfunction and death of neurons has led to other secondary changes such as Wallerian degeneration with prominent spheroid formation, as well as torpedoes.

Histologically, alpha-mannosidosis is typically indistinguishable from other forms of storage disease, however differentials can generally be

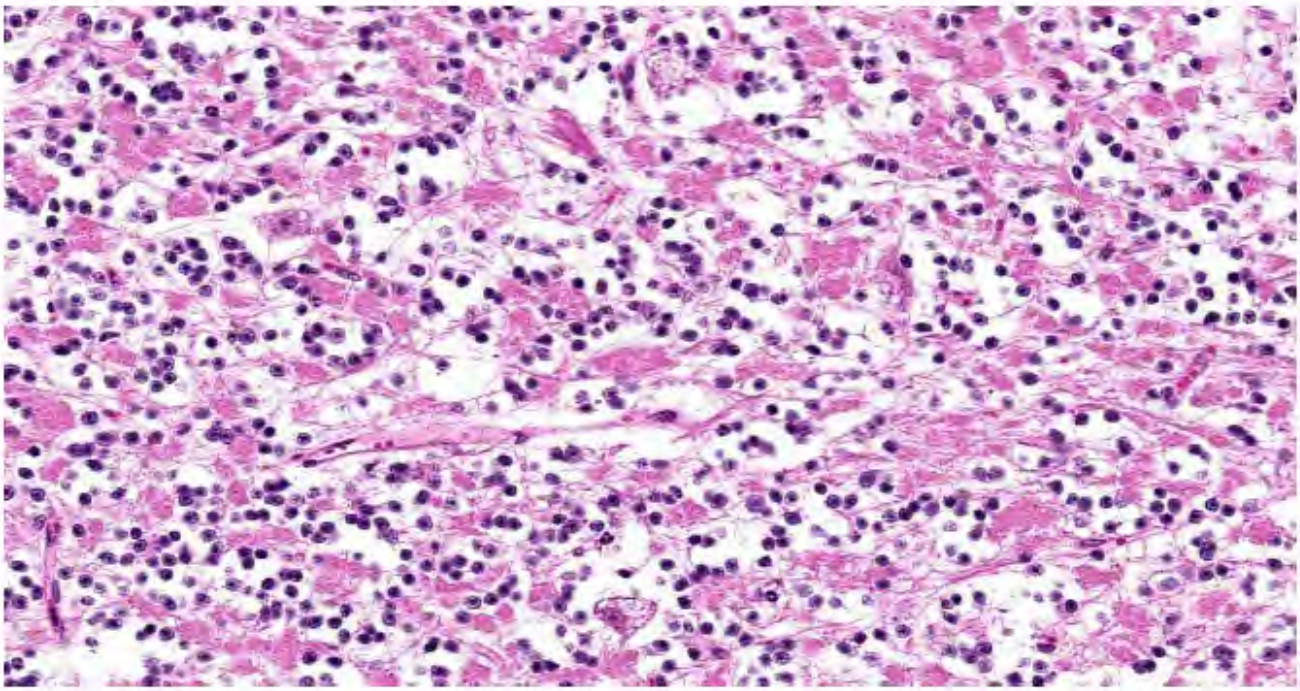

Figure 4-3. Cerebellum, calf: There is diffuse and mild loss of neurons within the granular layer and several neurons are also swollen due to cytoplasmic vacuolation. (HE, 580X)

narrowed down based on the breed affected. In this case, Neimann Pick Type C was also considered as a differential, given this lysosomal storage disease also affects Angus cattle.[25] However, this condition has only been reported in one herd in Australia between 2002 and 2005.[25] Other inherited storage diseases identified in cattle is summarized below (Table 1). While this case was confirmed to be inherited, acquired mannosidosis is also possible in herbivorous species, particularly livestock. Ingestion of plants containing the indolizidine alkaloid swainsonine can lead to inhibition of alpha-mannosidase, resulting in similar effects to the inherited con-dition.[5,6] Common swainsonine containing plants include *Swainsonia* spp. (Darling Pea and Swainson pea) mostly seen in Australia, as well as *Oxytropis* spp. and *Astragalus* spp. (locoweeds) found in areas of Africa, China and North America.[9,14]

Table 1: Inherited storage diseases reported in cattle.[4,8,12,1313,20,21,22,23,24,27]

Disorder	Breed/s affected
Alpha-mannosidosis	Angus, Galloway, Murray Grey
Beta-mannosidosis	Salers
GM, gangliosidosis	Holstein-Friesian
Glycogen storage disease type II (Pompe's disease)	Brahman, Droughtmaster, Shorthorn, Blanco Orejinegro
Sphingomyelinosis (Neimann Pick type C)	Angus
Neuronal ceroid lipofuscinosis*	Beefmaster, Devon, Holstein

*This condition is generally histologically distinct from other storage diseases, as the accumulation of storage material within neurons is pigmented (yellow-brown).

Contributing Institution:

Elizabeth Macarthur Agricultural Institute (EMAi), NSW, DPIRD

https://www.dpi.nsw.gov.au/about-us/science-and-research_old/centres/emai

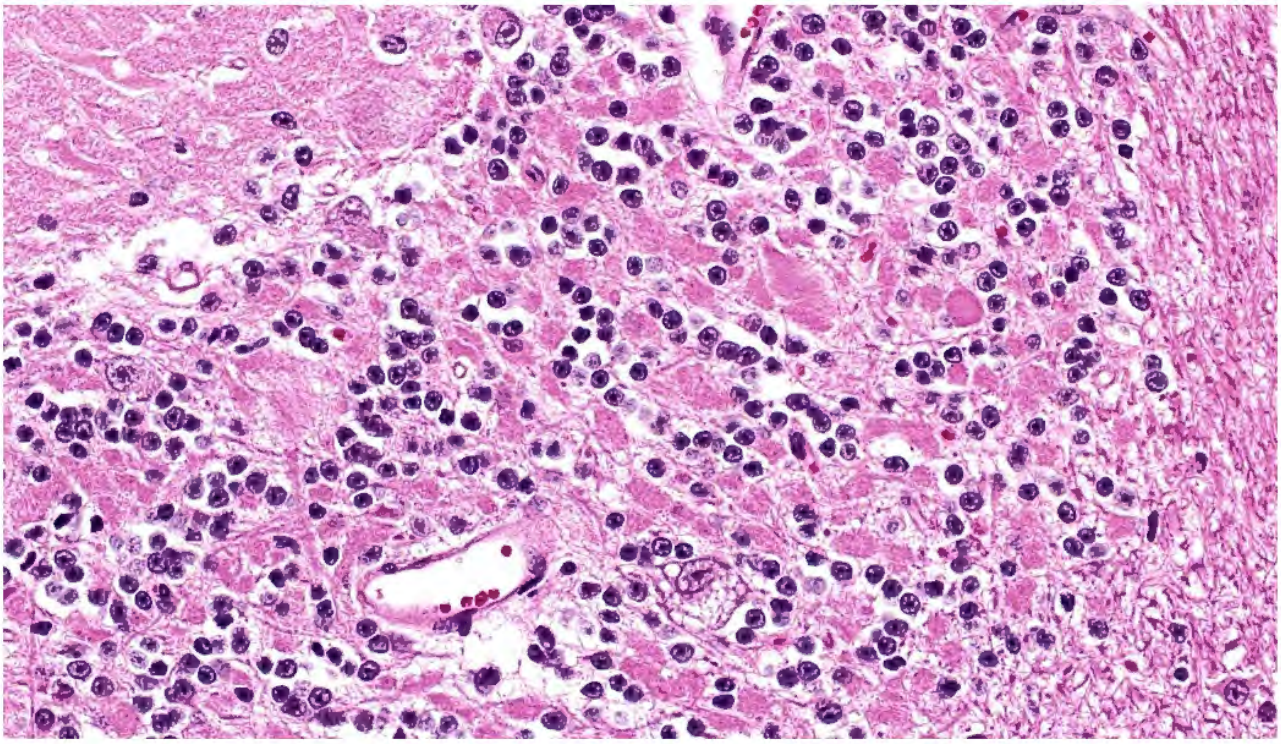

Figure 4-4. Cerebellum: There are numerous spheroids and torpedoes within the depleted granular cell layer. (HE, 590X)

JPC Diagnoses:
Cerebellum: Neuronal vacuolation and loss, chronic, diffuse, severe, with axonal swelling.

JPC Comment:
This case provided a wonderful example of a lysosomal storage disease (LSD) in a bovine. Cattle are the poster children for many different LSDs amongst our domestic species, as mentioned by the contributor in their excellent comment. Other species with known genetic predispositions for certain LSDs include: Nu-bian goats and German shepherd dogs (beta-mannosidosis), English Springer spaniel dogs (alpha-L-fucosidosis), and Persian cats (alpha-mannosidosis). Participants also learned a fun new term to describe the proliferation of microglia around Purkinje cells: "microglial shrubbery."

Cattle affected with alpha-mannosidosis typically are slow to grow, develop progressive ataxia, exhibit behavioral changes, and do not live longer than 18-mo.[3] Most of their cells are affected by this condition except for hepatocytes. However, there is a case report in Galloway calves that reported consistent, severe hepatocyte vacuolation in calves diagnosed with alpha-mannosidosis, so it is possible that a spectrum of severity exists.[11] In other species affected by alpha-mannosidosis, including cats, humans, and certain strains of mice, there is hepatocyte involvement. However, in bovine alpha-mannosidosis, the oligosaccharides that accumulate are similar to those seen in a partial deficiency of normal lysosomal alpha-mannosidase, meaning that they correspond to intermediates in the catabolic pathway.[10] This suggests that there might be some residual activity of alpha-mannosidase in affected cattle. In comparison, the oligosaccharides that accumulate in cats, who are usually more severely affected by alpha-mannosidosis than cattle, are representative of intact moieties rather than intermediates, indicating that there is no residual activity.[10]

This may explain why the liver is generally less affected in cattle compared to other species.

Top differentials in this case discussed during conference included other LSDs, swainsonine toxicosis, and perennial ryegrass toxicosis ("ryegrass staggers"). Of these, perennial ryegrass is the only one not discussed by the contributor in their comment. "Ryegrass staggers" is caused by ingestion of ryegrass containing the endophytic fungus *Epichloë festucae* var. *lolii* (formerly known as *Neotyphodium lolii*). This fungus, while it has been demonstrated to work symbiotically with the ryegrass to increase its hardiness and survivability, produces four indolic lolitrems that are tremorigenic neurotoxins. The most common of these neurotoxins is lolitrem B. These toxins bind and inhibit calcium-activated potassium channels that are responsible for stoppage of action potentials in depolarizing neurons.[3] Inhibition of these channels leads to prolonged cellular depolarization and sustained impulse transmission at the motor endplate, causing sustained tremors and spasms in affected animals. Histologically, there are limited findings, but these can be similar to some of the lesions seen in an LSD. These include proximal axonal swelling ("torpedo formation") in the granular and Purkinje cell layers of the cerebellum and vacuolar degeneration and loss of Purkinje cells.[3] However, there will not be accumulation of material within cytoplasmic vacuoles, as seen with LSDs.

The JPC's morphologic diagnosis for this case made use of the term "axonal swelling" to encompass the torpedoes, spheroids, and digestion chambers seen histologically, as all three of these are variations of axonal swelling at different portions of the neuron. Torpedoes are proximal swellings seen within the Purkinje and granular cell layers of the cerebellum; spheroids are swellings at the distal portions of the axons. Digestion chambers are the result of these swellings, where the axons are undergoing Wallerian degeneration and are fragmenting. The JPC acknowledged that it is not wrong to list these things out individually. Participants simply chose to group them for the sake of brevity.

References:

1. Bryan L, Schmutz S, Hodges SD, et al. Bovine β-mannosidosis: pathologic and genetic findings in Salers calves. *Veteri-nary Pathology.* 1993;30(2):130-9.
2. Burditt LJ, Chotai Kand Hirani Set al. Biochemical studies on a case of feline mannosidosis. *Biochemical Journal.* 1980;189(3):467-73.

1. Cantile C and Youssef S. Nervous System. In: *Jubb, Kennedy and Palmer's Pathology of Domestic Animals.* Vol 2. 6th Ed. St. Louis, MO. Elsevier; 2016: 286-293.
2. Caivio-Nasner S, Lopez-Herrera A and Gonzalez-Herrera LG et al. Frequency of genotypic markers for genetic disorders, colour, polledness, and major genes in Blanco Orejinegro cattle. *Tropical Animal Health and Production.* 2021;53:1-1.
3. Cholich LA, Martinez A and Micheloud JF et al. Alpha-mannosidosis caused by toxic plants in ruminants of Argentina. *Anais da Academia Brasileira de Ciencias.* 2021;93(suppl 3):e20191496.
4. Cook D, Gardner DR and Welch KD et al. A survey of swainsonine content in Swainsona species. *The Rangeland Journal.* 2017;39(2):213-8.
5. Cummings JF, Wood PA, De Lahunta A et al. The clinical and pathologic heterogeneity of feline alpha-mannosidosis. *Journal of veterinary internal medicine.* 1988;2(4):163-70.
6. Donnelly WJ and Sheahan BJ. GM1 gan-

gliosidosis of Friesian calves: a review. *Irish Veterinary Journal.* 1981; 35(3):45-48, 51-55.
7. Darling PR, Huxtable CR and Colegate SM. Inhibition of lysosomal alpha-mannosidase by swainsonine, an indolizidine alkaloid isolated from *Swainsona canescens*. *Biochemical Journal.* 1980;191(2):649.
8. DeGasperi R, al Daher S, Daniel PF, Winchester BG, Jeanloz RW, Warren CD. The substrate specificity of bovine and feline lysosomal alpha-D-mannosidases in relation to alpha-mannosidosis. *J Biol Chem*. 1991;266(25):16556-16563.
9. Embury DH and Jerrett IV. Mannosidosis in Galloway calves. *Veterinary pathology.* 1985; 22(6): 548-551.
10. Hafner S, Flynn Sand Harmon BG et al. Neuronal ceroid-lipofuscinosis in a Holstein steer. *Journal of veterinary diagnostic investigation.* 2005;17(2):194-7.
11. James LF, Kampen KR and Hartley WJ. Comparative pathology of Astragalus (locoweed) and *Swainsona* poisoning in sheep. *Pathologia veterinaria.* 1970;7(2):116-24.
12. Jezyk PF, Haskins ME and Newman LR. Alpha-mannosidosis in a Persian cat. *Journal of the American Veterinary Medical Association.* 1986;189(11):1483-5.
13. Jolly RD. The pathology of the central nervous system in pseudolipidosis of Angus calves. *Journal of Pathology.* 1971; 103:113-121.
14. Jolly RD. Mannosidosis and its control in Angus and Murray Grey cattle. *New Zealand Veterinary Journal.* 1978;26(8):194-8.
15. Jolly RD, Dittmer KE and Jones BR et al. Animal medical genetics: a historical perspective on more than 50 years of research into genetic disorders of animals at Mas-sey University. *New Zealand Veterinary Journal.* 2021;69(5):255-66.
16. Jolly RD, Martinus RD and Palmer ON. Sheep and other animals with ceroid-lipofuscinoses: Their relevance to Batten disease. *American journal of medical genetics.* 1992;42(4):609-14.
17. Jolly RD, Van-De-Water NS and Richards RB et al. Generalized glycogenosis in beef shorthorn cattle-heterozygote detection. *Australian Journal of Experimental Biology and Medical Science.* 1977;55(2):141-50.

    Lyons RE, Johnston DJ and McGowan MR et al. E7 (1057LHA) mutation of the acidic a-glucosidase gene causes Pompe's disease in Droughtmaster cattle. *Australian Veterinary Journal.* 2017;95(5):138-42.
18. O'Sullivan BM, Healy PJ and Fraser IR et al. Generalised glycogenosis in Brahman cattle. *Australian Veterinary Journal.* 1981;57(5):227-9.
19. Read WK and Bridges CH. Neuronal Lipodystrophy. Occurrence in an lmbred Strain of Cattle. *Pathologia veterinaria.* 1969;6(3):235-43.
20. Whittem JH, Walker D. "Neuronopathy" and" Pseudolipidosis" in Aberdeen-Angus calves. *Journal of Pathology and Bacteriology.* 1957; 74:281-288.
21. Woolley SA, Tsimnadis ER and Lenghaus C et al. Molecular basis for a new bovine model of Niemann-Pick type C disease. *Plos One.* 2020;15(9):e0238697.

Joint Pathology Center
Veterinary Pathology Services

WEDNESDAY SLIDE CONFERENCE 2025-2026

Conference #19 — 11 February 2026

CASE I:

Signalment:
Male, 408-gram, age unknown, Fischer 344 rat (*Rattus norvegicus*)

History:
The rat had telemetry placement surgery on 8 June 2015. Post-operative treatments included meloxicam, buprenex along with supplemental feeding. Animal recovered from surgery without complication and was acting normally during the initial post-surgery period. On the 26th of June, the rat appeared pale and lethargic and euthanasia was elected.

Gross Pathology:
This rat has a body score of 3/5 with adequate subcutaneous and visceral fat. The skin incisions over the skull and left thorax from the telemetry surgery have completely healed. The pocket over the left thorax holding the telemetry device contains 5 ml of milky serosanguinous fluid. There is a layer of fibrin coating the telemetry device. The lungs were collapsed and diffusely red. The spleen is enlarged measuring 6.5 x 2 x 1 cm, friable with a homogenous pale red area on one pole (infarct). The liver is diffusely pale (light brown) and friable and the thymus is mottled tan/brown. The pancreas is soft and tan and both kidneys have a brown/green appearance. There is a moderate amount of dry food contents in the stomach, small amount of normal digesta and gas in the small intestine, moderate amount of soft green contents in the cecum and many dry fecal pellets in the colon. There is no urine in the bladder.

Laboratory Results:
N/A.

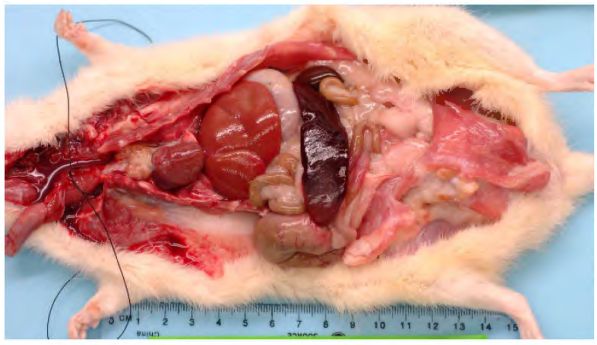

Figure 1-1. Abdominal cavity, rat: The liver and spleen are markedly enlarged. (Photo courtesy of: US Army Institute of Chemical Defense).

Figure 1-2. Liver, rat: The liver demonstrates marked pallor (normal control on left). (Photo courtesy of: US Army Institute of Chemical Defense).

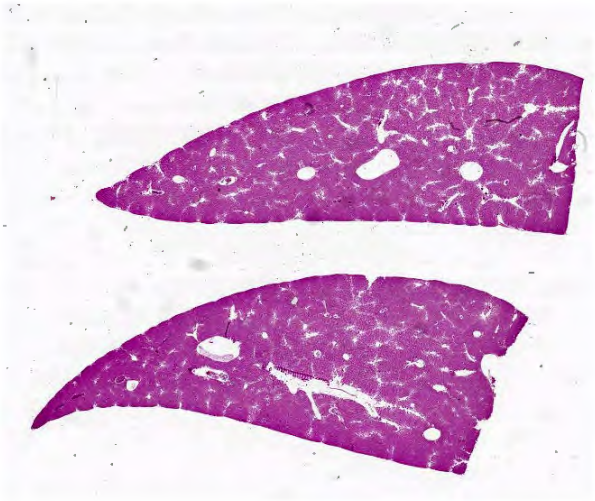

Figure 2-3. Liver, rat: Two sections of liver are submitted for examination. There are no changes at subgross magnification. (HE, 12X)

Microscopic Description:

Liver: Diffusely filling portal veins and expanding sinusoids is a neoplastic population composed of round cells with distinct cell borders, small amount of eosinophilic, granular cytoplasm, round to occasional reniform nucleus, clumped chromatin and indistinct nucleolus. Mitotic rate is <1 per hpf.

Diffusely centrilobular hepatocytes are lost, degenerating or necrotic. Diffusely there is lobular atrophy and sinusoids are expanded by previously described neoplastic cells admixed with eosinophilic cellular debris. Multifocally centrilobular kupffer cells and/or hepatocytes contain hemosiderin pigment. Multifocally within portal regions there is an increase in small bile duct profiles (ductular reaction). Rarely, bile duct epithelial cells are degenerative, necrotic or undergoing regeneration.

Contributor's Morphologic Diagnoses:

Liver: Leukemia, large granular lymphocytic

Contributor's Comment:

Large granular lymphocytic (LGL) leukemia, formally identified as mononuclear cell leukemia (MCL), is the main cause of death among Fischer 344 (F344) rats >20 months of age.[4] Reported frequency ranges from 10 - 35% with 50% of early deaths is some 2-year studies being caused by this disease.[6] LGL leukemia has been reported in other strains of rats.

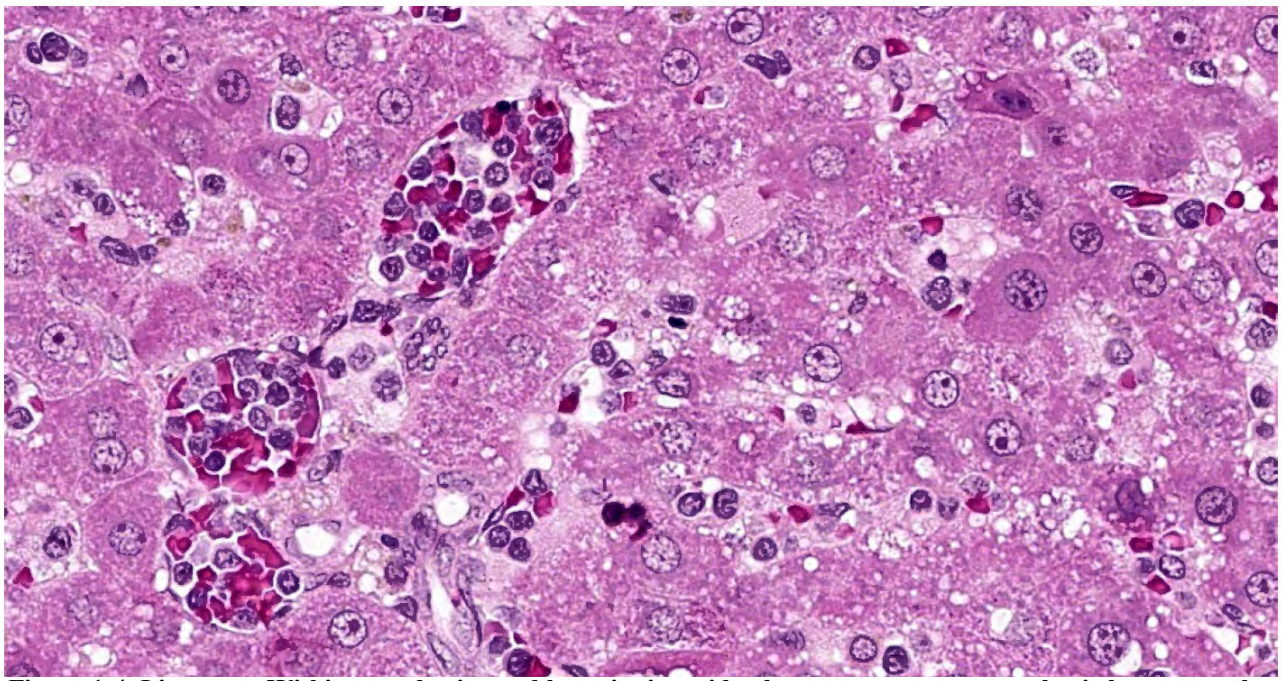

Figure 1-4. Liver, rat: Within portal veins and hepatic sinusoids, there are numerous neoplastic large granular lymphocytes. Few centrilobular hepatocytes are hypereosinophilic, contracted, and without nuclei (necrotic) (HE, 900X)

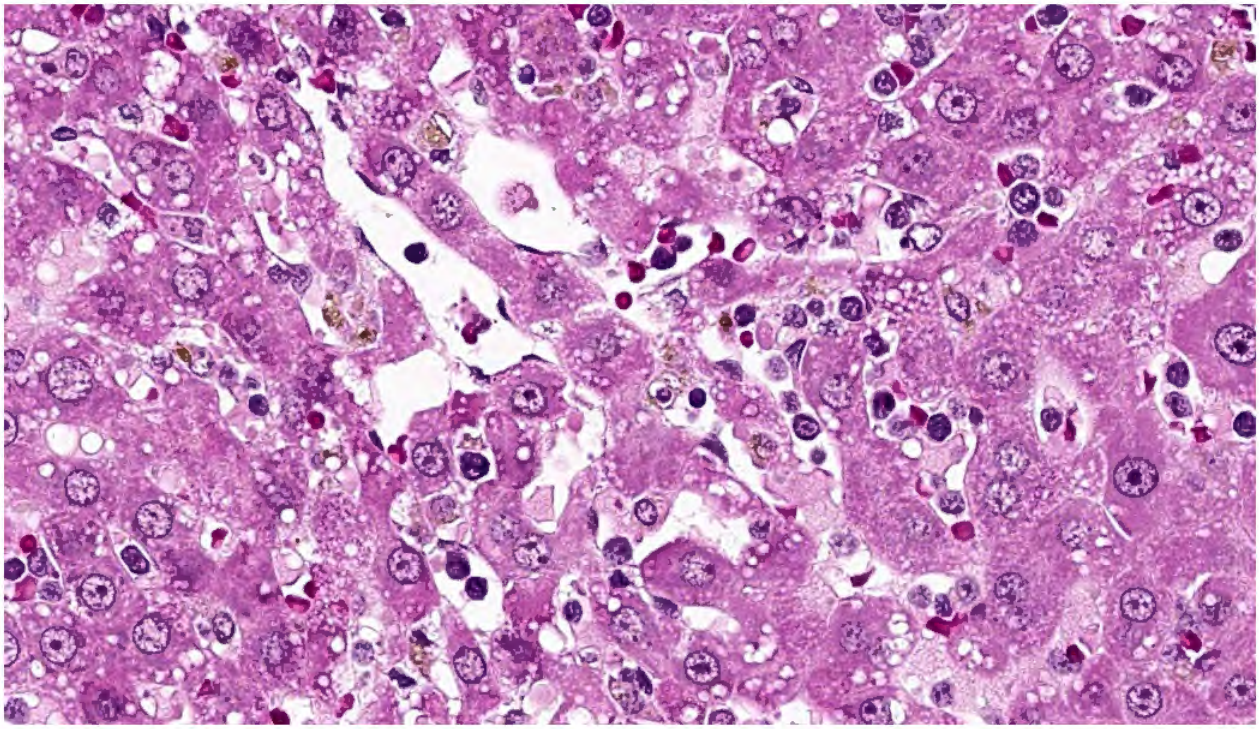

Figure 1-5. Liver, rat: There is loss of centrilobular hepatocytes resulting in enlarged centrilobular veins, and Kupffer cells in this area contain abundant lipofuscin granules. (HE, 900X)

Wistar-Furth rats have the next highest occurrence with an incidence rate of 15-22%, while the disease is rarely seen in Sprague-Dawley rats (0.6%).[7] Naturally occurring LGL leukemia has not been reported in mice.[7]

Clinical signs are characterized by weight loss, anemia, jaundice, and depression.[1] There is usually a concurrent, immune-mediated hemolytic anemia, with thrombocytopenia and clotting abnormalities suggestive of disseminated intravascular coagulation.[1] Splenomegaly is the most common characteristic macroscopic finding in rats afflicted with LGL leukemia.[4]

Histological findings, in general, include diffuse infiltration of the splenic red pulp sinusoids of variable density, infiltration of the hepatic sinusoids with variable centrilobular hepatocellular degeneration, and necrosis and atrophy of hepatic cords and infiltration of the alveolar septa of the lungs.[7] Other tissues affected include lymph nodes, adrenal gland, kidney, and bone marrow.

Contributing Institution:
U.S. Army Medical Research Institute of Chemical Defense
(https://usamricd.health.mil/)

JPC Diagnoses:
Liver: Large granular cell leukemia.

JPC Comment:
Conference 19 was moderated by the esteemed Dr. Kimberly Whitten, a veteran Department of Defense laboratory animal toxicological pathologist who works for USAMRICD. This first case was a classic entity in F344 rats and one that must be at the forefront of any pathologist's mind in this strain. LGL leukemia in F344 rats closely resembles the NK-cell leukemia seen in humans

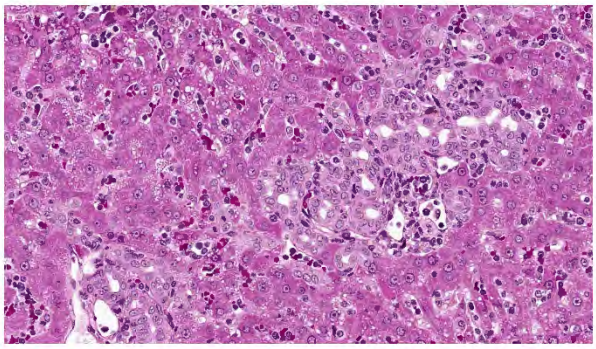

Figure 1-6. Liver, rat: There is moderate biliary hyperplasia. (HE, 750X)

and, as such, they are used as a research model for this aggressive disease.[7] Morphologically, the LGL leukemia cells resemble normal rat LGLs, but there are notable differences in cytotoxicity & surface antigens. Normal rat LGLs usually express surface markers such as CD8, CD2, CD56, and ASGM1, while leukemic LGLs tend to show abnormal or low-level expression of T-cell receptor (TCR) beta chains, may or may not express ASGM1, and can display heterogeneity in markers like CD56.[7,9] This suggests that these leukemias may be of a heterogeneous lymphocytic origin, although NK-cell markers predominate.[7,9]

Natural killer cells are vital, fast-acting lymphocytes of the innate immune system that, unlike most other lymphocytes, identify and destroy virally infected or cancerous cells without prior sensitization. Acting as a first line of defense, they utilize surface receptors to detect absent MHC-I molecules or "stressed" signals on target cells, prompting the NK cells to release cytotoxic granules containing pore-forming enzymes, such as granzyme B.[2]

Dr. Whitten quizzed participants on other common tumors in F344 rats, which included: testicular interstitial cell tumors, which occur in almost 100% of aged male Fischer rats; mesotheliomas of the tunica vaginalis of the testes, which occur in up to 5% of males and may spread to the peritoneal and pleural cavities; pituitary adenomas, which are seen in 30% of rats and may be prolactin producing, which can result in mammary hyperplasia; mammary gland tumors (primarily mammary fibroadenoma), which occur in roughly 40% of female and 20% of male rats; pheochromocytomas, seen in 30% of male rats in a recent study; and thyroid C-cell carcinomas, occurring in up to 10% of aged rats.[3]

References:

1. Barthold SW, Griffey SM, Percy DH. Rat. In: *Pathology of laboratory rodents and rabbits*. 4th ed. Ames, IA: John Wiley & Sons, Inc: 2016;166-167.
2. Mace EM. Human natural killer cells: Form, function, and development. *J Allergy Clin Immunol*. 2023;151(2):371-385.
3. Sass B, Rabstein LS, Madison R, Nims RM, Peters RL, Kelloff GJ. Incidence of spontaneous neoplasms in F344 rats throughout the natural life-span. *J Natl Cancer Inst*. 1975;54(6):1449-1456.
4. Shiga A, Narama I. Hepatic lesions caused by large granular lymphocytic leukemia in Fischer 344 rats: similar morphologic features and morphogenesis to those of nodular regenerative hyperplasia (NRH) in human liver. *Toxicol Pathol*. 2015;43:852-864.
5. Stefanski SA, Elwell MR, Stromberg PC. Spleen, lymph nodes, and thymus. In: Boorman GA, Eustis LS, Elwell MR, Montgomery CA, MacKenzie WF, ed. *Pathology of the Fischer rat: reference and atlas*. San Diego, CA: Academic Press;1990:374-379.

6. Stromberg PC, Vogtsberger LM. Pathology of the mononuclear cell leukemia of Fischer rats. *Vet Pathol*. 1983;20:698-708.
7. Thomas J, Haseman JK, Goodman JI, et al. A review of large granular lymphocytic leukemia in Fischer 344 rats as an initial step toward evaluating the implication of the endpoint to human cancer risk assessment. *Toxicol Sci*. 2007;99:3-19.
8. Ward JM, Reynolds CW. Large granular lymphocyte leukemia: a heterogeneous lymphocytic leukemia in F344 rats. *Am J Pathol*. 1983;111:1-10.
9. Watters RJ, Liu X, Loughran TP Jr. T-cell and natural killer-cell large granular lymphocyte leukemia neoplasias. *Leuk Lymphoma*. 2011;52(12):2217-2225.

CASE II:

Signalment:
7.5-year-old male cynomolgus macaque (*Macaca fasicularis*)

History:
This animal had undergone surgery six days previously to induce acute hepatic failure by ischemic liver injury and had concurrently received a xenographic transplant of swine hepatocytes into the spleen. It had been started on tacrolimus immunosuppressive therapy prior to manipulation. Two days post-operatively, the monkey began progressive clinical deterioration as well as developing diabetes. It was unresponsive to empirical supportive therapy and was euthanized.

Gross Pathology:
Kidneys were reported to be pale and reduced in size without additional specifications.

Laboratory Results:
N/A.

Figure 2-1. Kidney, rhesus macaque: A section of kidney is submitted for examination. At subgross magnification, numerous ectatic tubules are visible. (HE, 9X)

Microscopic Description:
Renal lesions involve primarily the tubular component and are characterized by a variety of morphological features. Swelling and vacuolar change are prominent within proximal renal tubular epithelium, especially in the straight portion of that segment. Many tubules contain prominent cast-structures, typically consisting of granular to globular eosinophilic material, frequently admixed with blueish-gray proteinaceous sheets. Exfoliated epithelial cells are occasionally incorporated into the cast structures with numerous tubules also containing aggregates of mixed, primarily granulocytic inflammatory cells. Individually necrotic renal tubular epithelium is occasional evident. Associated with obstruction created by these casts, there is extensive, widespread tubular dilatation. Although extremely infrequent, fibrin thrombi were noted within occasional glomerular capillary loops. However, other significant glomerular changes were uncommon at the light microscopic level.

Contributor's Morphologic Diagnoses:
1. Renal tubular vacuolization, patchy to focally extensive, primarily proximal tubules, moderate-marked.
2. Coarsely granular eosinophilic tubular casts with occasional proteinaceous sheets consistent with myoglobin and associated

myoglobinuric nephrosis, patchy, moderate, with associated marked tubular dilatation and epithelial cell thinning.
3. Acute tubular injury (ATI), patchy, mild, characterized by renal tubular epithelial cell exfoliation, individual cellular degeneration and patchy, primarily granulocytic inflammatory cell aggregates.
4. Focal glomerular capillary loop fibrin thrombi, minimal.

Contributor's Comment:
Despite administration at standard dosing levels, this animal's tacrolimus levels climbed at one point to 80 ng/ml (target range <16 ng/ml) and the monkey developed clinical signs of toxicity as well as diabetes. Unfortunately, renal function values were not available at the time of necropsy.

Tacrolimus, also known as FK506 is a macrolide immunosuppressive drug derived from the fungus *Streptomyces tsukubaensis*, approved by the FDA in 1994 to lower the risk of allogenic organ transplant rejection. Although not sharing molecular structural properties, it has similar therapeutic mechanisms and toxicity with its older immunosuppressive counterpart, cyclosporine. Both are classified as calcineurin inhibitors (CNI), affecting calcium-dependent events such as nitric oxide synthase activities, apoptosis, and cell degranulation.[13]

Renal toxicity is a well-recognized effect, both to transplanted kidneys as well as the native kidneys of patients receiving other organs. Early nephrotoxicity is primarily associated with acute arteriole vasoconstriction and is thought to be of multifactorial pathogenesis, including increasing vasoconstrictive factors, reducing vasodilator mechanisms and increasing the formation of free radicles.[3,4,6,7,14] Toxicity due to vasospasms can manifest in a so-

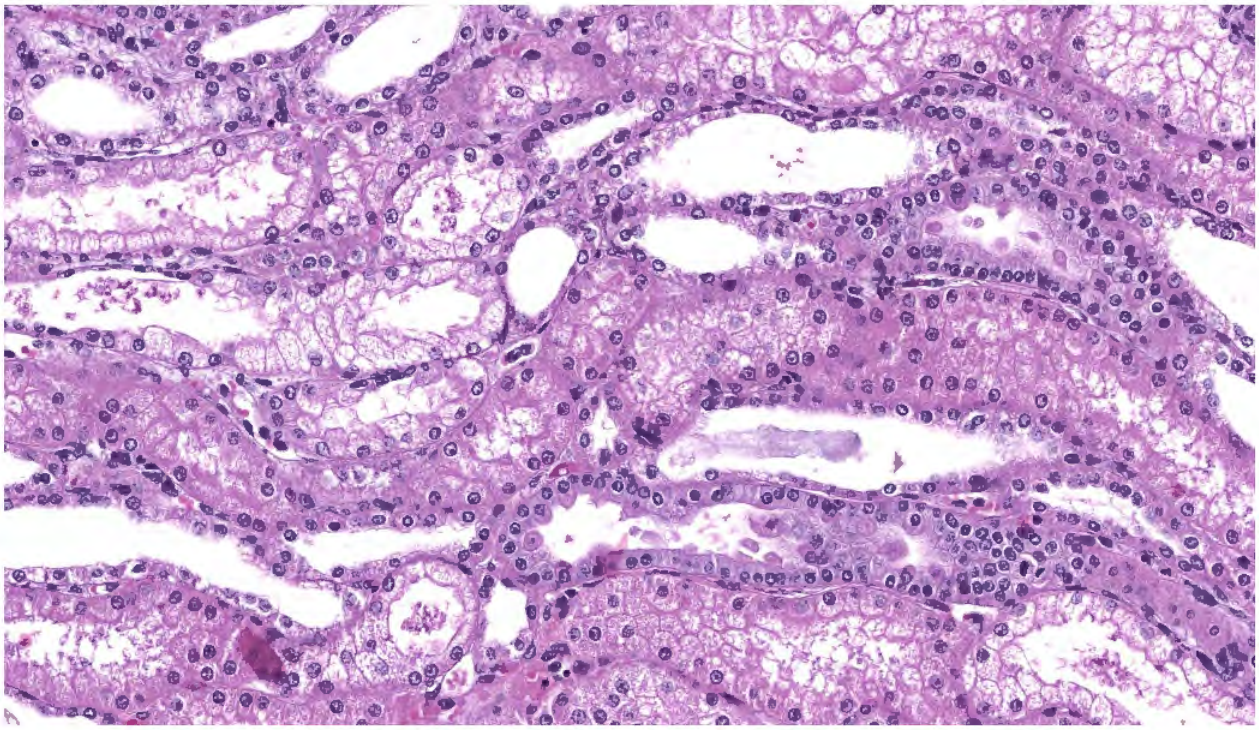

Figure 2-2. Kidney, rhesus macaque: Within the more distal nephron, numerous changes, including ectasia, swelling and cytoplasmic vacuolation, and regeneration are visible. (HE, 380X)

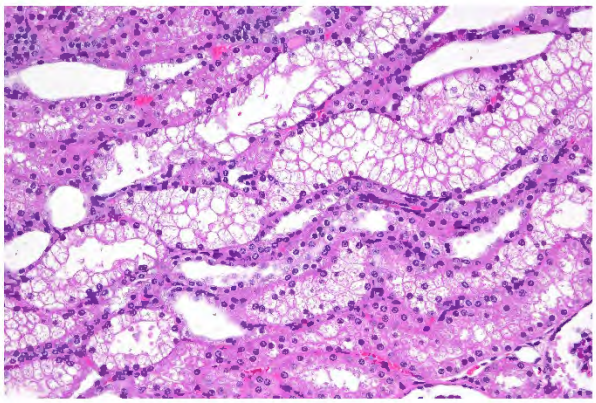

Figure 2-3. Kidney, rhesus macaque: Tubular epithelium is markedly vacuolated. (HE, 200X) (Photo courtesy of: Division of Laboratory Animal Resources, University of Pittsburgh, www.dlar.pitt.edu).

called "functional form" without any characteristic morphological changes, or with associated structural histological alterations, either acute or chronic.[13] The latter includes effects on both arterioles (especially afferent arterioles) and glomeruli, including smooth muscle cell swelling, endothelial cell injury/necrosis and fibrin thrombi, potentially resulting in thrombotic microangiopathy. Such changes were considered to be relatively modest in this case, although very mild mesangial matrix expansion and hypercellularity of the juxtaglomerular apparatus were occasionally noted. Tubular components of CNI injury can include the development of vacuolization leading to clear, aqueous fluid accumulation (the latter being associated ultrastructurally with dilated smooth endoplasmic reticulum and occur predominantly in the straight portion of the proximal tubules.) This process was prominent in this monkey. As vacuolar change is a common, non-specific lesion often seen with osmotic nephrosis due to agents such as mannitol, inulin, glucose, radiocontrast agents, chemicals that induce vacuolation through phagolysosomes and other causes of tubular ischemia correlation with other factors must be taken in ascribing its pathogenesis.[7]

Another form of renal tubular injury is occurring in this case – likely tacrolimus related as well, but of a more secondary mechanism. Since early after its therapeutic use, tacrolimus has been known to be associated with severe rhabdomyolysis, although the incidence is considered rare.[1,2] The role of calcineurin in skeletal muscles is complex, with both protective and detrimental effects.[14] CNI are potent CYP450 inhibitors and this may be related to an increased incidence of muscle toxicity in transplant recipients, especially associated with other drug interactions.[1]

Renal casts noted in this case (and often admixed with numerous dehisced epithelial cells) were suggestive of myoglobin origin. They are often comprised of round granules that line up in chains or aggregate in clusters. Tinctorially, there is variation between and even within different stains applied with a typical pink to red-brown appearance with H&E, pink to bright magenta with PAS, and often a gray-blue sheet containing fine red granules on Trichrome.[5,8] Immunostaining with antibody to myoglobin was strongly positive in

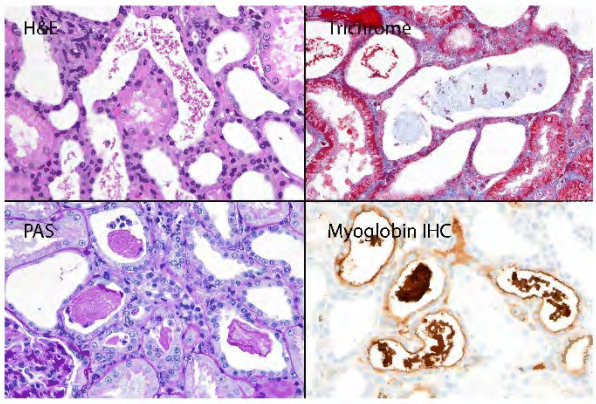

Figure 2-4. Kidney, rhesus macaque: There are eosinophilic tubular casts with occasional crystalline protein consistent with myoglobin and mild associated myoglobinuric nephrosis. (Photo courtesy of: Division of Laboratory Animal Resources, University of Pittsburgh, www.dlar.pitt.edu).

these casts, often with a prominent rope-like string to beaded appearance. Interestingly, the concept that acute kidney injury is triggered by myoglobin as a direct, sole toxin appears to be oversimplified and there is ample evidence that additional factors such as hypovolemia, renal vasoconstriction or urine acidification are required for nephrotoxicity.[9,12] Of these factors, certainly vasoconstriction directly associated with CNI effects would have likely been present. Again, in this case the myoglobinuric nephrosis present cannot be definitively ascribed to tacrolimus, but this is considered a likely pathogenesis, especially in the absence of other common pathogeneses such as severe trauma, dehydration, and other frequently associated comorbidities.[5]

Although both the direct and indirect effects of tacrolimus toxicity in this case were thought to be substantially responsible for lesions, the impact of the severe ischemic hepatic and biliary injury created prior to the transplant was also considered to have potentially played a role in some of the changes present.

Hepatorenal syndrome (HRS) involves the development of renal failure in patients with severe liver disease and while often seen in chronic cirrhosis, it can also occur in patients with acute liver disease.[10] The pathogenesis is associated with severe renal vasoconstriction resulting from complex changes in splanchnic and general circulations as well as systemic and renal vasoconstrictors and vasodilators.[10] This entity is mentioned only to emphasize the complexity and interconnectedness of the kidneys with other systemic functions.

In addition to renal effects, other common toxic complications associated with tacrolimus use in humans include neurological problems and diabetes, although numerous other clinical problems such as diarrhea, pruritus and alopecia are reported.[16]

Contributing Institution:
Division of Laboratory Animal Resources, University of Pittsburgh; (www.dlar.pitt.edu)

JPC Diagnoses:
Kidney: Tubular vacuolization, necrosis, and regeneration, acute, multifocal, marked, with granular casts and glomerular fibrin thrombi.

JPC Comment:
The contributor of this case provided an exceptional comment and covered much of what was discussed in conference. Hemoglobin and myoglobin were discussed as the two main rule-outs for the granular casts present in the kidney and special attention was drawn to the fact that, with tacrolimus toxicity, the vacuolation of the straight portion of the proximal convoluted tubules (PCT) is the primary process and is associated with dilation of the smooth endoplasmic reticulum of the PCT epithelial cells.[14] This kidney presented a couple of nice examples of tubular regeneration as well. Additional ruleouts in this case that were considered were aminoglycoside toxicity, which tends to appear more like a lysosomal storage disease with build-up of cytoplasmic material in the PCT epithelial cells, mannitol administration, which can cause osmotic nephrosis when given in high volume or over a prolonged period of time, and any other toxins that inhibit CYP450 that may have also resulted in tubular epithelial vacuolation.

CYP450 enzymes in the kidney are critical for maintaining fluid and electrolyte balance, regulating blood pressure, and metabolizing drugs or toxins. They function primarily in the PCTs to catalyze the oxidation of arachidonic acid into vasoactive substances, such as certain HETE molecules (vasoconstrictors) and epoxyeicosatrienoic acids (EETs; vasodilators), which all help to modulate vascular tone

and tubular sodium transport.[11] These potent signaling molecules act as protective, locally acting agents in the kidney to reduce blood pressure, decrease inflammation, and prevent tissue fibrosis.[11] When CYP450 is inhibited, these molecules are not produced effectively, resulting in kidney injury.

References:

1. Dopazo C, Bilbao I, Lazaro JL et al. Severe Rhabdomyolysis and Acute Renal Failure Secondary to Concomitant Use of Simvastatin With Rapamycin Plus Tacrolimus in Liver Transplant Patient. *Transplantation Proceedings*. 2009;41:1021–1024.
2. Hibi S, Misawa A, Tsunamoto K et al. Severe rhabdomyolysis associated with tacrolimus. *Lancet*. 1995;346(8976):70.
3. Issa N, Kukla A and Ibrahim HN. Calcineurin Inhibitor Nephrotoxicity: A Review and Perspective of the Evidence. *Am J Nephrolo*. 2013;37:602-612.
4. Kemper J and Kniska K. Pathophysiology and treatment of calcineurin inhibitor nephrotoxicity. *Kidney Centric*. 2014;1-6.
5. Liapis H, Boils CB, Hennigar R and Silva F. Myoglobin casts in renal biopsies: immunohistochemistry and morphologic spectrum. *Human Pathology*. 2016;54:25-30.
6. Myers BD. Cyclosporine nephrotoxicity. *Kidney International*. 1986;30:964-974.
7. Naesens M, Kuypers DR and Sarwal M. Calcineurin Inhibitor Nephrotoxicity. *American Society of Nephrology*. 2009;4:481-508.
8. Najafian B, Fogo AB, Lusco MA and Alpers CE. AJKD Atlas of Renal Pathology: Myoglobin Cast Nephropathy. Am J Kidney Dis. 2017;69(2):e7–e8.
9. Najafian B, Frankinn DB and Fogo AB. Acute Renal Failure and Myalgia in a Transplant Patient. *J Am Soc Nephrol*. 2007;18:2870–2874.
10. Ng C, Chan M, Morris HI et al. Hepatorenal Syndrome. *Clin Biochem Rev*. 2007;28:11-17.
11. Omata K, Abe K, Sheu HL, et al. Roles of renal cytochrome P450-dependent arachidonic acid metabolites in hypertension. *Tohoku J Exp Med*. 1992;166(1):93-106.
12. Petejova N and Martinek A. Acute kidney injury due to rhabdomyolysis and renal replacement therapy: a critical review. Critical Care. 2014;18:224.
13. Renal Transplantation Pathology. In: Jennette JC, Olson JL, Silva FG and D'Agati VD eds. *Hepinstall's Pathology of the Kidney Vol II*. 7th Ed. Philadelphia US: Wolters Kluwer; 2015:1321-1460.
14. Randhawa PS, Starzl TE and Demetris AJ. Tacrolimus (FK506)-Associated Renal Pathology. *Adv Anal Pathol*. 1997;4(4):265-276.
15. Sathyan S, Baskharoun R and Perlman AS. Prevention of Recurrent Episodes of Rhabdomyolysis With Tacrolimus in a Transplant Recipient With Myopathy. *American Journal of Therapeutics*. 2014;21:e171–e174.
16. Scott LJ, McKeage K, Keam SJ, *et al.* Tacrolimus: A further update of its use in the management of organ transplantation. *Drugs*. 2003;63:1247–1297.

CASE III:

Signalment:

A 2-year-old female spayed Pitbull (*Canis lupus familiaris*)

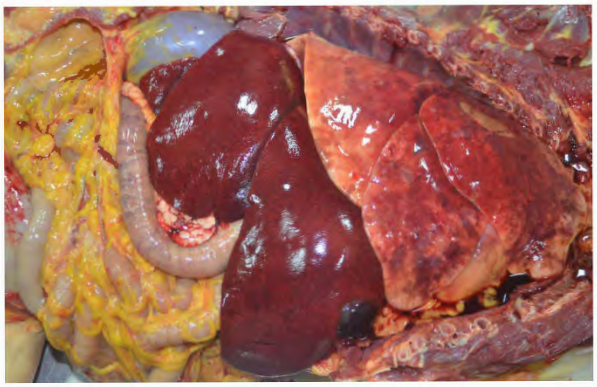

Figure 3-1. Liver, dog: There is icterus of the mesenteric adipose tissue and the liver is enlarged, dark red, and granular. (Photo courtesy of: Louisiana Animal Disease Diagnostic Laboratory (LADDL), School of Veterinary Medicine, Louisiana State University (http://www1.vetmed.lsu.edu/laddl/index.html))

History:

A two-year old pit bull was hospitalized for management of acute liver injury and coagulopathy two days after ingesting three bulbs of cycad palm. Despite aggressive treatment, the patient developed hepatic encephalopathy and shock. Due to a poor prognosis, humane euthanasia was elected.

Gross Pathology:

There was generalized icterus including the skin, mucus membranes, subcutaneous and mesenteric adipose tissue, fascia, and sclera, as well as petechiae and ecchymoses. The liver was enlarged, dark red and granular. There were multiple gastric mucosal ulcers, and melena throughout the gastrointestinal tract.

Laboratory Results:

The dog had hypoalbuminemia, hypocholesteremia, and hypoglycemia as well as unmeasurable PT and PTT, and severe thrombocytopenia. ALT, AST, GGT, ALP, and total bilirubin were all elevated.

Microscopic Description:

Liver: There is massive loss of hepatocytes in all examined sections with approximately 99% of the hepatic parenchyma affected. The portal regions contain scant numbers of remaining hepatocytes with large numbers of macrovesicular and microvesicular lipid vacuoles. Kupffer cells and occasional hepatocytes contain moderate amounts of yellow brown pigment (lipofuscin). There is moderate proliferation of oval cells, which have large open nuclei with a prominent nucleolus. There are increased numbers of circulating neutrophils and monocytes within the sinusoids.

Contributor's Comment:

Cycad palms are primitive palm-like plants that are native to tropical and subtropical regions of the world. All cycads belong to the class Cycadopsida and the order Cycadales. In the United States common cycads palms include *Dycas revoluta*, *Cycas circinalis*, and *Zaminia floridana* and are commonly referred to as sago palms. In addition to being native in some regions, they are also popular ornamental plants in non-native climates.[1,5] All parts of the cycad plant are toxic but the highest concentration of toxin is found in the seeds.[11]

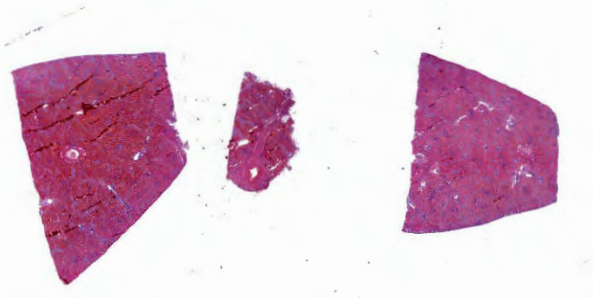

Figure 3-2. Liver, dog: Three sections of liver are submitted for examination; all are similar. At subgross magnification, normal hepatocellular architecture is lost and there is diffuse hemorrhage throughout the hepatic parenchyma (HE, 8X).

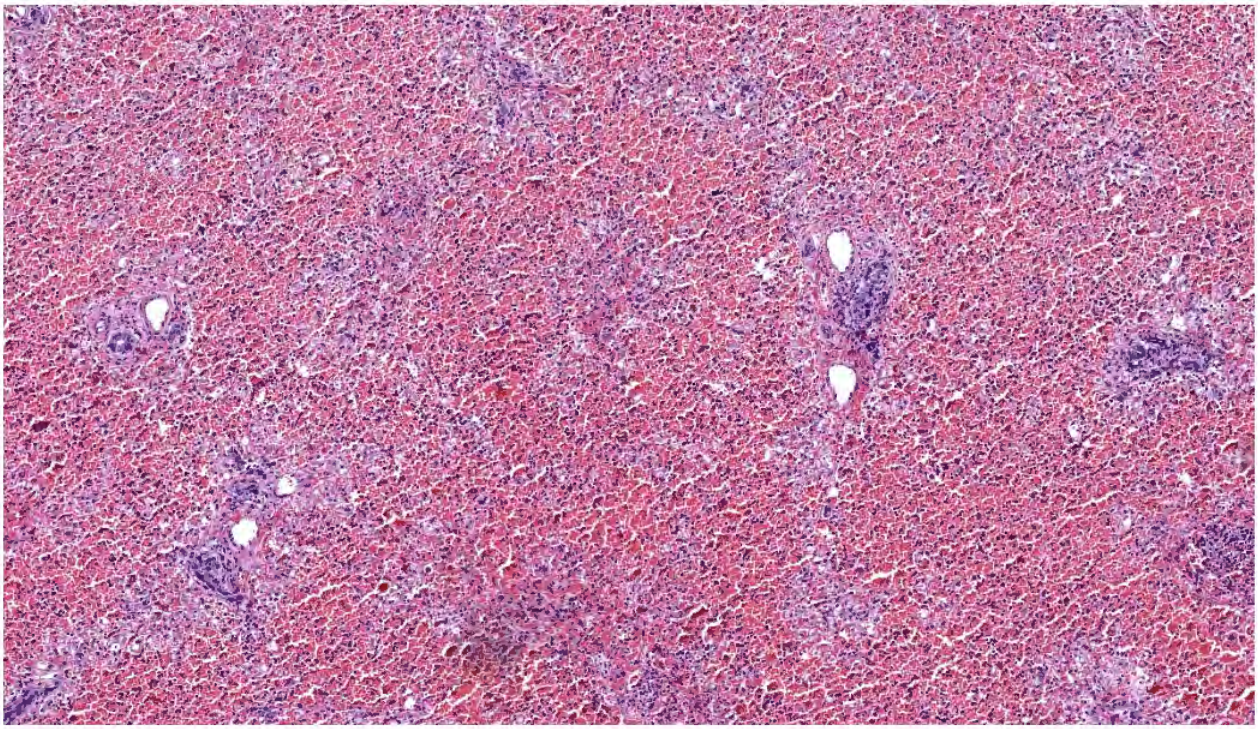

Figure 3-3. Liver, dog: There is massive necrosis of the hepatic lobule with diffuse hemorrhage. Portal areas remain. (HE, 115X)

Cycads contain three types of toxins: azoxyglycosides, of which cycasin is the most prominent member, β-methylamino-L-alanine (BMAA), and an unidentified high molecular weight compound.[1,11] Cycasin, the predominant toxin, is metabolized by intestinal bacteria into the toxic metabolite methylazoxymethanol (MAM). MAM is neurotoxic, carcinogenic, mutagenic, teratogenic, and hepatotoxic.[1,5,11] This carcinogen potential has been documented in rats where chronic exposure leads to cancer development in the liver, kidney, and intestinal tract of laboratory rodents and nonhuman primates.[8,14] Once metabolized in the intestine, MAM undergoes enterohepatic circulation and enters the liver via the portal vein where it is metabolized by hepatic cytochrome P450 (CYPs).

Cycad ingestion in dogs leads to gastrointestinal and hepatic disease caused by methylazoxymethanol (MAM). Common clinical signs in dogs include vomiting, diarrhea occasionally with melena, abdominal pain, anorexia, icterus, hypersalivation, depression, and neurological signs secondary to hepatic encephalopathy. Common clinical pathology findings include hyperbilirubinemia, elevated alanine aminotransferase (ALT), elevated alkaline phosphatase, hypocholesterolemia, hypoalbuminemia, elevated prothrombin time (PT), elevated partial thromboplastin time (PTT), and thrombocytopenia.[1,2,5,11,13]

There are multiple retrospective studies on cycad poisoning in dogs with survival rates ranging from 32 to 64%.[1,3,5] Severe liver injury leads to decreased synthesis of coagulation factors, decreased production of albumin, and disrupted bile acid circulation leading to decreased intestinal absorption of vitamin K.[5,11] All of these lead to the observed clinical abnormalities. Increased vascular permeability also leads to albumin loss through intestinal

and renal losses. Thrombocytopenia may occur due to coagulopathy and gastrointestinal bleeding.

MAM is oxidized by hepatic cytochrome P450 (CYPs) leading to centrilobular necrosis as the most common finding in acute toxicosis. Subacute changes include severe centrilobular coagulative necrosis with some regeneration as well as portal fibrosis and bile duct proliferation. Chronic changes include diffuse hepatocellular necrosis, hepatic degeneration and regeneration with extensive stromal collapse, bridging fibrosis with nodular regeneration, and biliary hyperplasia.[5] There are multiple retrospective studies on cycad poisoning in dogs with survival rates ranging from 32 to 64% and even with recovery chronic hepatic disease can persist.[1,3,5]

Cycad intoxication also occurs in domestic ruminants where it manifests as two distinct syndromes: neurologic and hepato-gastrointestinal.[6,7,8,12] The hepatic-gastrointestinal syndrome causes hepatocellular megalocytosis, centrilobular necrosis, and biliary duct hyperplasia. These may be similar to other hepatic toxicoses such as aflatoxin, pyrrolizidine alkaloids, *Lantana* species, and spordesmin. As in dogs, cycasin and its metabolites have been linked to hepatic-gastrointestinal syndrome in ruminants, and the hepato-gastrointestinal syndrome is more common in sheep compared to the neurologic syndrome which is more common in cattle.[1]

Cycads also contain the neurotoxin beta-methylamino-L-alanine (BMAA) and an unidentified neurotoxin. This unidentified neurotoxin is thought to be the cause of neurologic disease in cattle with chronic cycad poisoning, where progressive proprioception deficits in the hindlegs are attributed to axonal degeneration in the dorsal funiculus and the spinocerebellar and corticospinal tracts.[7,8,12]

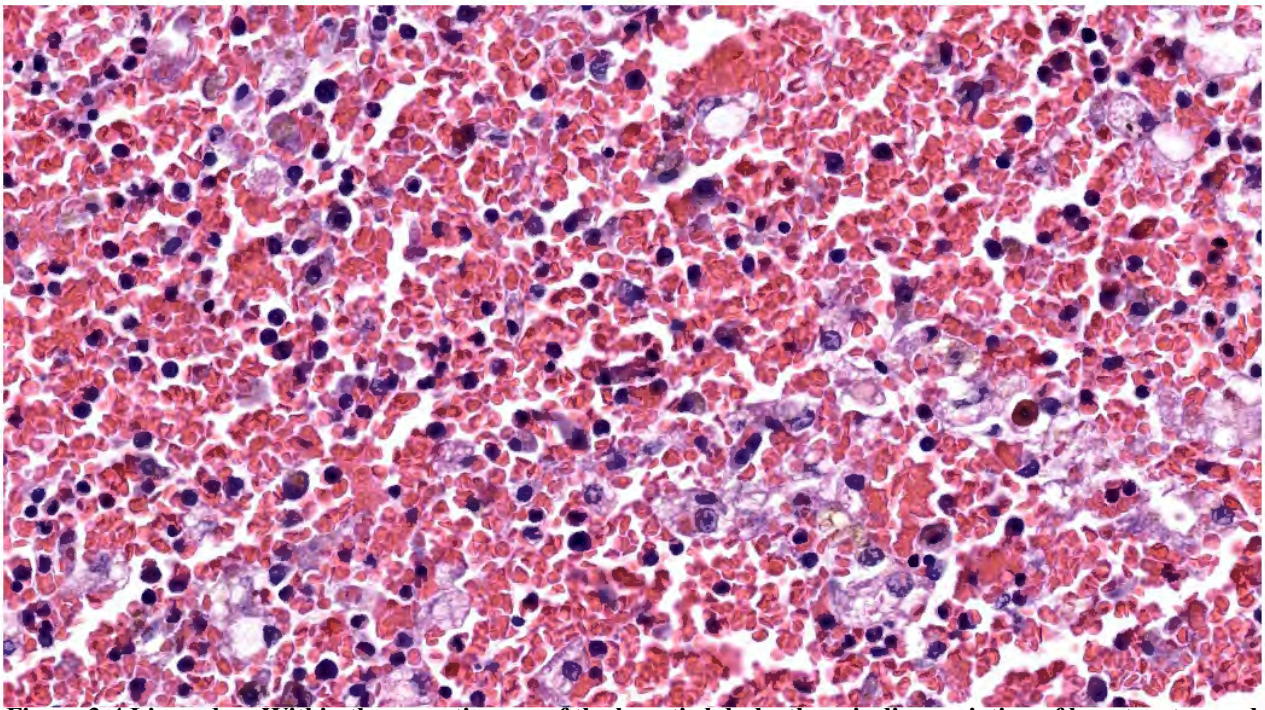

Figure 3-4 Liver, dog: Within the necrotic area of the hepatic lobule, there is disassociation of hepatocytes, and many discernible hepatocytes are pyknotic and fragmented. There is diffuse hemorrhage and infiltrating debris and hemosiderin-laden macrophages. (HE, 731X)

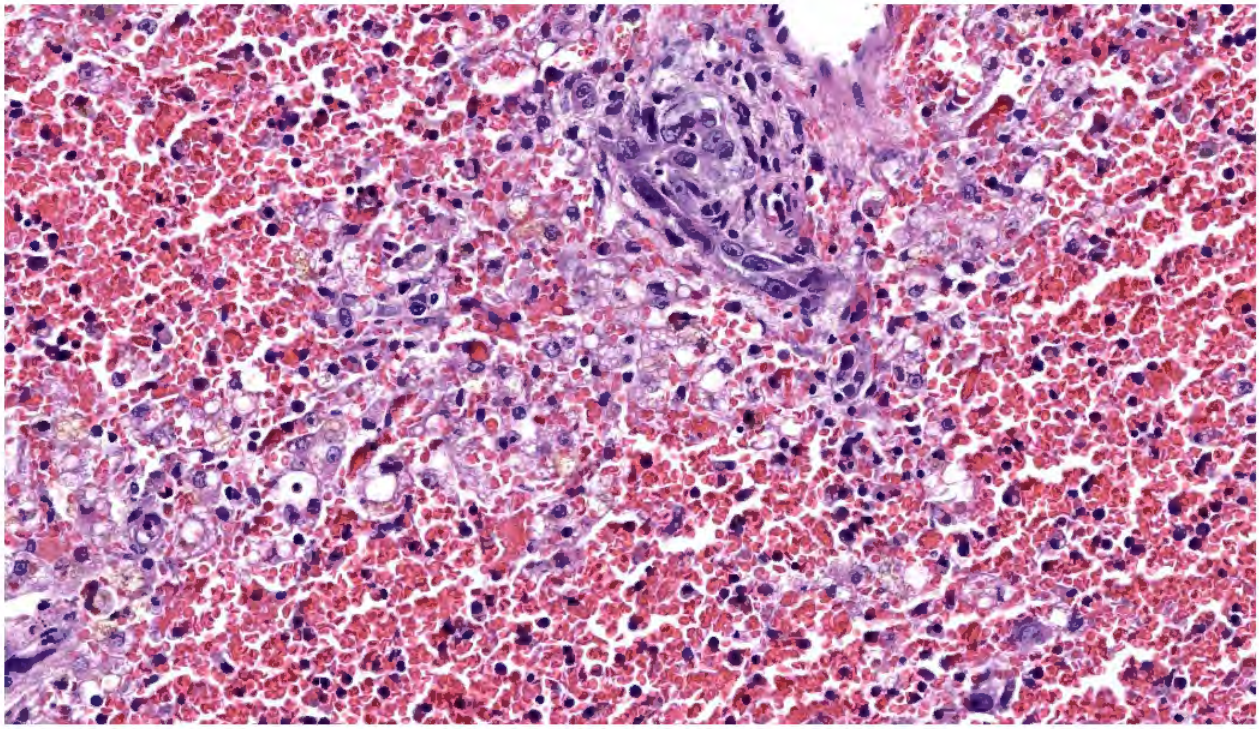

Figure 3-5. Liver, dog: In some lobules, degenerating hepatocytes remain with numerous lipid vacuoles in their cytoplasm. Few fibroblasts are proliferating around/within portal areas. (HE, 481X)

Cycad intoxication is associated with severe disease and fatalities in multiple domestic species caused primarily by hepatotoxicity which leads to secondary effects of hepatic failure including hepatic encephalopathy, coagulopathy, and hypoproteinemia.[1-5,11,13] In the cattle, cycad intoxication can also cause neurologic disease due to axonal degeneration.[7,8,12]

Contributing Institution:
Louisiana Animal Disease Diagnostic Laboratory (LADDL), School of Veterinary Medicine, Louisiana State University (http://www1.vetmed.lsu.edu/laddl/index.html)

JPC Diagnoses:
Liver: Hepatocellular necrosis, acute, massive, diffuse, with hemorrhage and stromal collapse.

JPC Comment:
This contributor also provides an outstanding comment on this entity, which represents a case of acute hepatic necrosis secondary to a toxin in a dog. Much of what was discussed in conference for this case is covered in their write-up. Hepatic damage by cycad palm is progressive and dose-dependent.[9] Dr. Whitten discussed the acute changes seen in toxicity cases such as this, which include centrilobular hemorrhage & massive hepatocellular coagulative necrosis, vacuolar degeneration, hepatic venous congestion, pigmentary bile duct distention, bile duct plugging, and intracanalicular cholestasis.

Participants were also asked about various other potential causes of of massive hepatic necrosis across numerous species. Other toxic and chemical causes discussed included heavy metals, such as copper toxicity in sheep and young cattle, arsenic, and iron; medications/drugs, with specific mention of high-

dose ivermectin, some antibiotics, halothane, and phenobarbital; plants, fungi, and algae, such as *Amanita spp*. toadstools, *Senecio spp.* and *Crotalaria spp.* (pyrrolizidine alkaloids), *Aspergillus spp*. (aflatoxins), *Fusarium spp.* (fumonisins), and blue-green algae (cyanobacteria); and industrial chemicals like carbon tetrachloride, chlorinated hydrocarbons, and pesticides (i.e., paraquat).[4] Infectious causes included canine adenovirus-1 (canine infectious hepatitis), canine herpesvirus-1, rabbit calicivirus (rabbit hemorrhagic disease virus), *Clostridium novyi* (Black Disease), and *Salmonella spp*. A variety of ischemic and metabolic causes were mentioned and, in summary, covered shock/hypoxia, thromboembolisms, heat stroke, and DIC.[4] A brief mention of liver flukes, such as *Fasciola hepatica*, was made due to their contribution to the development of Black Disease via creation of migration tracks that enable a hypoxic environment for *Clostridium novyi* to proliferate. Lastly, there was brief discussion on the massive hepatic necrosis seen with Theiler's disease in horses (caused by equine parvovirus) and the lesions of inherited copper storage disease in Bedlington Terrier and Doberman dogs.

In cases of cycad palm in dogs, cattle, and rodents, lesions of the CNS have been reported in addition to the gastro-hepatic syndrome.[6,7,8,12] The primary lesions seen in the CNS include vacuolation of the neuropil, demyelination, and spongiform change to the brain and spinal cord.[8,12] While sago palm is known to produce BMAA neurotoxin, Dr. Whitten speculated that some of the brain lesions (i.e., astrocyte swelling and cytotoxic edema) may also be secondary to hepatic encephalopathy from severe hepatic necrosis.

References:

1. Albretsen JC, Khan SA, Richardson JA. Cycad palm toxicosis in dogs: 60 cases (1987-1997). *J Am Vet Med Assoc*. 1998;213: 99-101.
2. Botha CJ, Naude TW, Swan GE, Ashton MM, van der Wateren JF. Suspected cycad (*Cycas revoluta*) intoxication in dogs. *J S Afr Vet Assoc*. 1991;62: 189-190.
3. Clarke C, Burney D. Cycad Palm Toxicosis in 14 Dogs from Texas. *J Am Anim Hosp Assoc*. 2017;53: 159-166.
4. Cullen JM, Stalker MJ. Liver and Biliary System. In: Maxie MG, ed. *Jubb, Kennedy & Palmer's Pathology of Domestic Animals.* Vol 2. 6th ed. St. Louis, MO: Elsevier; 2016:258-352.
5. Ferguson D, Crowe M, McLaughlin L, Gaschen F. Survival and prognostic indicators for cycad intoxication in dogs. *Journal of veterinary internal medicine*. 2011;25: 831-837.
6. Gabbedy BJ, Meyer EP, Dickson J. Zamia palm (*Macrozamia reidlei*) poisoning of sheep. *Aust Vet J*. 1975;51: 303-305.
7. Hall WT. Cycad (zamia) poisoning in Australia. *Aust Vet J*. 1987;64: 149-151.
8. Hooper PT, Best SM, Campbell A. Axonal dystrophy in the spinal cords of cattle consuming the cycad palm, Cycas media. *Aust Vet J*. 1974;50: 146-149.
9. Lake BB, Edwards T, Atiee G, Stone R, Scott L. The characterization of cycad palm toxicosis and treatment effects in 130 dogs. *Aust Vet J*. 2020;98(11):555-562.
10. Laqueur GL, Matsumoto H. Neoplasms in female Fischer rats following intraperitoneal injection of methylazoxy-methanol. *J Natl Cancer Inst*. 1966;37: 217-232.
11. Milewski LM, Khan SA. An overview of potentially life-threatening poisonous plants in dogs and cats. *Journal of Veterinary Emergency and Critical Care*. 2006;16:25-33.
12. Reams RY, Janovitz EB, Robinson FR, Sullivan JM, Rivera Casanova C, Mas E. Cycad (*Zamia puertoriquensis*) toxicosis

in a group of dairy heifers in Puerto Rico. *J Vet Diagn Invest*. 1993;5:488-494.
13. Senior D, Sundlof S, Buergelt C, Hines S, O'Neil-Foil C, Meyer D. Cycad intoxication in the dog. *The Journal of the American Animal Hospital Association (USA)*. 1985.
14. Sieber SM, Correa P, Dalgard DW, McIntire KR, Adamson RH. Carcinogenicity and hepatotoxicity of cycasin and its aglycone methylazoxymethanol acetate in nonhuman primates. *Journal of the National Cancer Institute*. 1980;65: 177-189.

CASE IV:

Signalment:
Mouse (*Mus musculus*), female, 129S/SvEv background, >6 months of age

History:
These transgenic mice are from a 129S/SvEv genetic background. The colony is showing a high {>50%) incidence of ocular lesions manifesting clinically as crusted eyes with conjunctival swelling and ocular discharge.

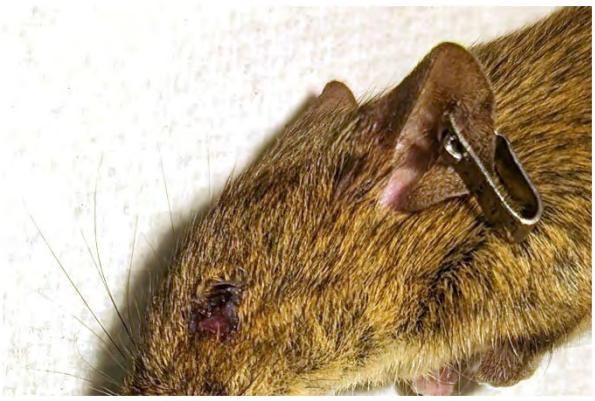

Figure 4-1. Head, 129S/SvEv mouse: Affected animals demonstrated crusted eyes with conjunctival swelling and ocular discharge. (Photo courtesy of: In Vivo Animal Core, Unit for Laboratory Animal Medicine University of Michigan, https://animal-care.umich.edu/ business-services/vivo-animal-core).

Gross Pathology:
Both mice showed serous ocular discharge, porphyrin staining, medial canthus swelling, and blepharospasm bilaterally. No experimental history of eye manipulation was reported. One mouse had been treated with an ocular antibiotic ointment.

Laboratory Results:
N/A.

Microscopic Description:
Bilaterally or unilaterally*, the eyelids contained locally extensive epidermal acanthosis and ortho to parakeratotic hyperkeratosis of varying severity. This was accompanied by epithelial erosion and mild serocellular crusting. There was mild to moderate mixed neutrophilic to lymphocytic inflammation within the conjunctiva and eyelid sebaceous glands (Meibomian glands). Focally there was occasional dilation and mild degeneration of Meibomian gland acini or ductules. The cornea, lens, iris, retina, optic nerve and other interior structures of the eyes were normal.

The Harderian gland was mildly enlarged (section plane-dependent) and glandular lumens contained occasional brown pigmented inspissated material (porphyrin secretions). Glandular epithelium lacked atypia and there was no compression or invasion as might be seen with adenoma or carcinoma.

**Grossly, the lesion was present bilaterally in affected mice but, due to section plane and variable severity, it is microscopically more evident unilaterally in the submitted examples.*

Contributor's Morphologic Diagnoses:
1. Eyelids: Blepharoconjunctivitis, neutrophilic, with epidermal acanthosis, erosions, and ortho to parakeratotic hyperkeratosis, unilateral to bilateral, moderate, chronic.

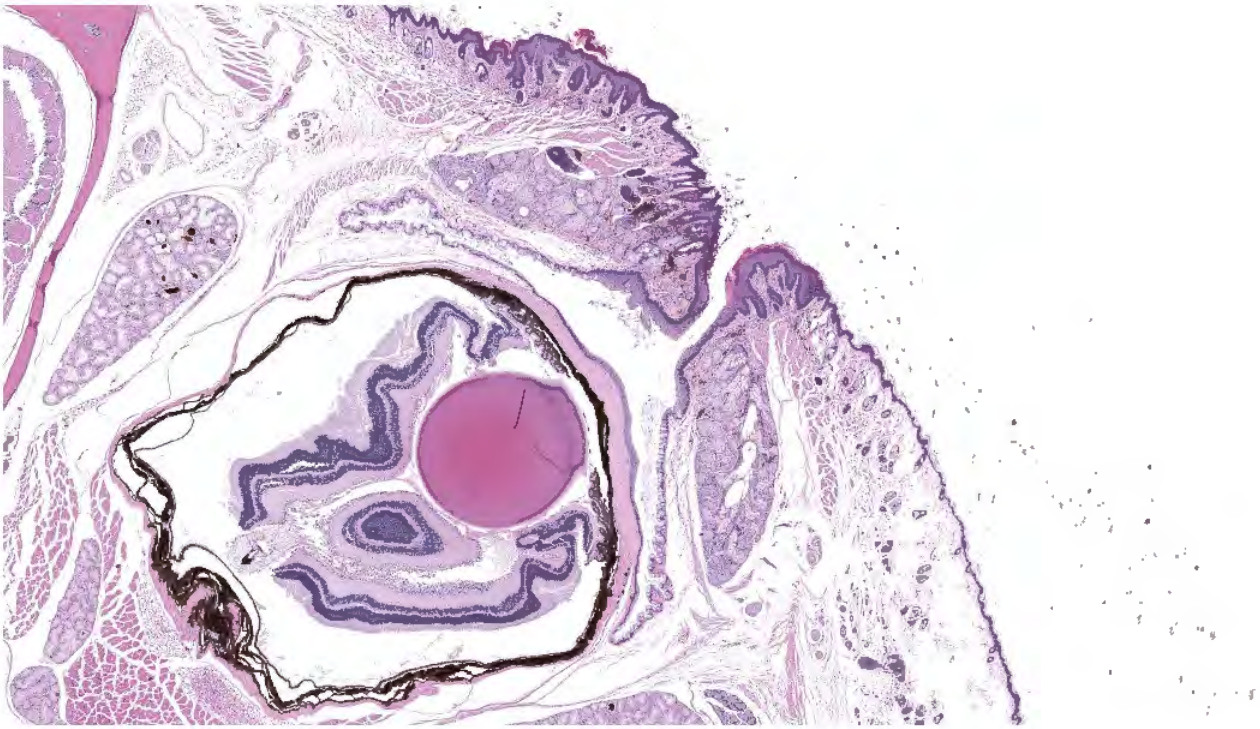

Figure 4-2. Eye, 129S/SvEv mouse: Unilaterally, there is blepharitis and conjunctivitis with epidermal hyperplasia of the eyelid and conjunctiva and overlying serocellular crusting of the eyelid. There is moderate accumulation of porphyrin pigment in the Harderian gland. (HE, 40X)

2. Harderian gland: Hyperplasia with inspissated porphyrin secretions, bilateral, mild, chronic.

Contributor's Comment:

Blepharoconjunctivitis occurs with high frequency in aging 129S/SvEv, 129P, and other 129 origin substrains.[2,3] An incidence of >90% was reported in one lifetime survey of pathology in 129S6/SvEvTac mice (older nomenclature for 129S/SvEv). Findings ranged from suppurative to mononuclear inflammation and epidermal changes included acanthosis and focal erosion or ulceration.[2] In this submission, the epidemiology of the lesion presentation and its similarity to the literature descriptions of blepharoconjunctivitis supported that its occurrence was related to the underlying background strain and not to the knockout gene.

The underlying cause for blepharitis or blepharoconjunctivitis in 129S substrains is unknown. Underlying age-related structural and functional changes in the position and function of lacrimal glands are believed to play a role, possibly by impacting mucocutaneous barrier function. Age-associated anterior migration of the palpebral mucocutaneous junction in mice has been cited as contributing to eyelid laxity and poor Meibomian gland function.[2] *Corynebacterium* species biochemically similar to C. *urealyticum,* C. *pseudodiphtheriticum,* and C. *bovis* have been cultured from affected eyelids. However, these agents were not identified in all affected animals and are also commensally found on the eyelids of normal mice. Additionally, rederivation into SPF housing was not sufficient to prevent occurrence.[2] In the submitted case, the attending clinical veterinarian reported that treatment with topical ocular antibiotic ointment appeared to decrease lesion severity and prolong

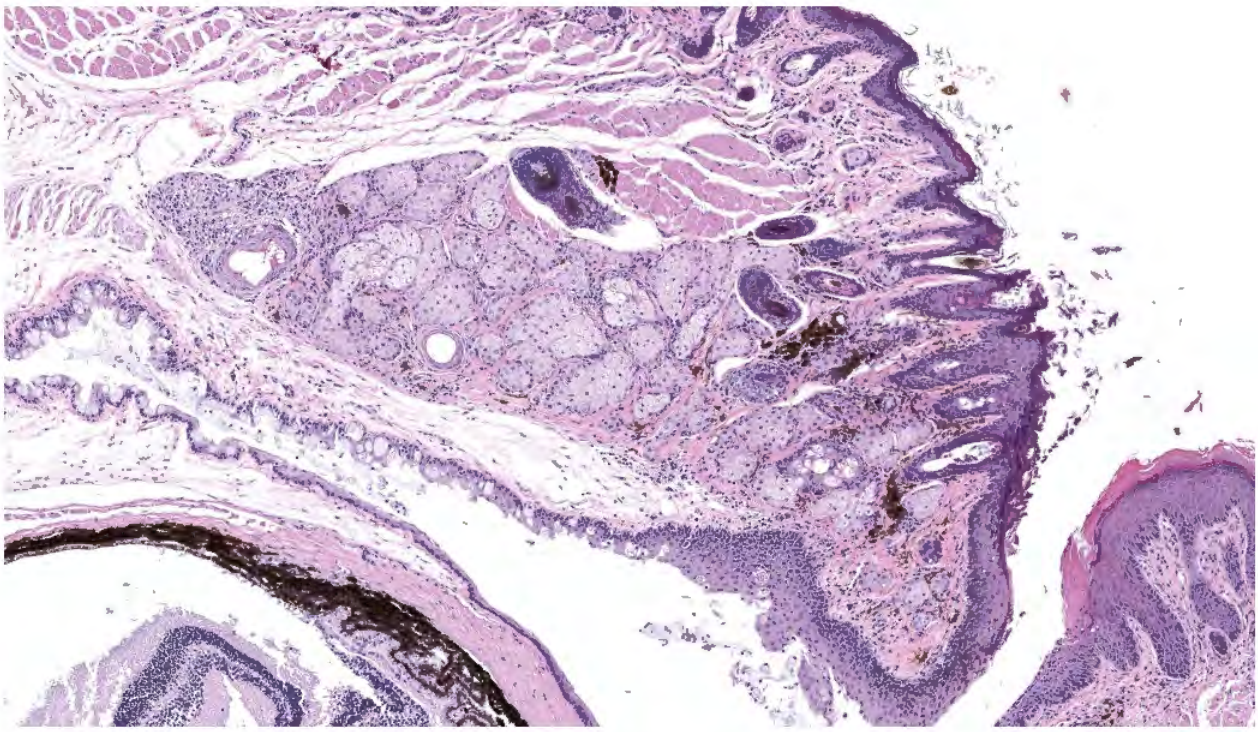

Figure 4-3. Eyelid, 129S/SvEv mouse: The eyelid has hyperplasia of the epidermis extending down into hair follicles, overlying serocellular crust, and mild dermal lymphoplasmacytic inflammation which infiltrates the subjacent Meibomian glands. (HE, 123X)

the time until the animal reached humane endpoints for euthanasia, but did not fully resolve the lesion.

Harderian gland adenomas have been linked to blepharoconjunctivitis in 129S6/SvEvTac mice, but these were believed to be a concurrent aging lesion that played an exacerbating rather than a causative role.[2]

Nomenclature of 129 mice can be confusing. 129 mice are made up of 3 major subfamilies with enough genetic variation between them that they are considered separate strains. As such, these subfamilies have been designated as the parental strain (129P), the Steel strain (129S), and the teratoma strain (129T). There are also several substrains within each of these three. 129S/SvEv mice, the strain in this submission, are widely commercially available and are frequently utilized to generate embryonic stem cells (ESCs) for the production of mice with targeted mutations (knockouts). They were originally bred from 129S mice received from Dr. Martin Evans, giving them their substrain designation.[4]

Contributing Institution:
In Vivo Animal Core, Unit for Laboratory Animal Medicine
University of Michigan
2800 Plymouth Road
Ann Arbor, Ml 48109
(https ://animal care .um ich .edu/ business-services/vivo-animal-core)

JPC Diagnoses:
1. Eyelid: Blepharoconjunctivitis, unilateral, lymphocytic and neutrophilic, chronic, diffuse, mild, with epidermal hyperplasia and erosion.
2. Eyelid, Meibomian gland: Adenitis, lymphoplasmacytic, chronic, focal, mild.

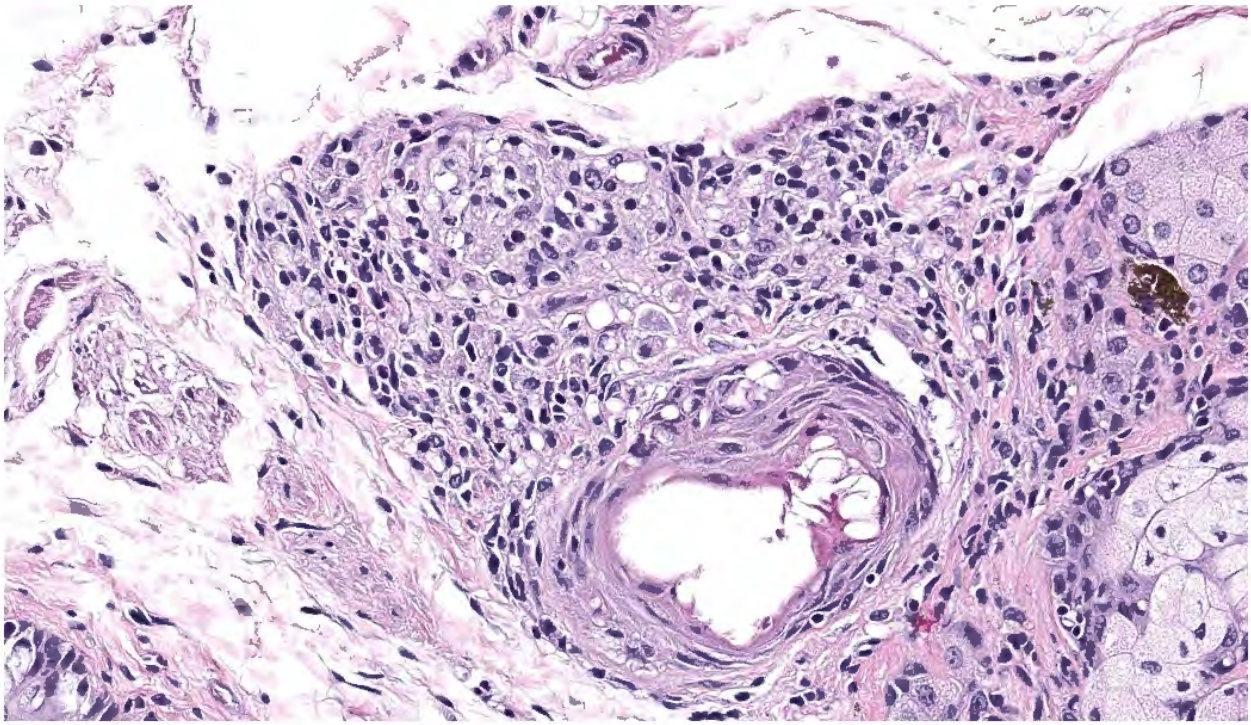

Figure 4-4. Eyelid, 129S/SvEv mouse: There is focal loss of Meibomian gland architecture and infiltration by lymphocytes and plasma cells. (HE, 381X)

JPC Comment:

Although seemingly a not-so-exciting lesion, this is one that needs to be able to be recognized by the pathologist, especially in 129 mice. It is a common finding in 129 substrains! The contributor did a great job discussing this lesion in their comment which, again, covered most of this case's conversation. Some participants were thrown off initially by the size discrepancy between the two lenses, but this is largely due to a function of cut during processing and is not a lesion. The contributor mentioned that this was a grossly bilateral lesion but did acknowledge that this is not seen histologically due to sectioning. In short, don't be thrown off if the lesion isn't obvious on both eyelids despite the gross description.

Although not in the contributor's description, a few participants astutely perceived the presence of a sequestrum characterized by necrotic bone with surrounding osteoclastic activity within the right side of the maxillary bone. This sequestrum is surrounded by moderate inflammation and fibrosis, and there is an underlying neutrophilic and lymphocytic gingivitis. Most participants thought this may have been related to some form of oral trauma that resulted in a penetrating injury to the hard palate. Gingivitis is a common background lesion in laboratory mice, and the sequestrum was a neat secondary lesion to find! The JPC did not include the sequestrum and gingivitis in the morphologic diagnoses, however, to ensure clarity on the primary blepharoconjunctivitis lesion in this case.

Conference attendees were also quizzed on additional common background lesions of 129 mice, which include a reduced or absent corpus callosum (can be up to 80% in some groups of 129 mice), spontaneous testicular teratomas and lung tumors, eosinophilic crystalline pneumonia (also known as acidophilic macrophage pneumonia), hyalinosis of the

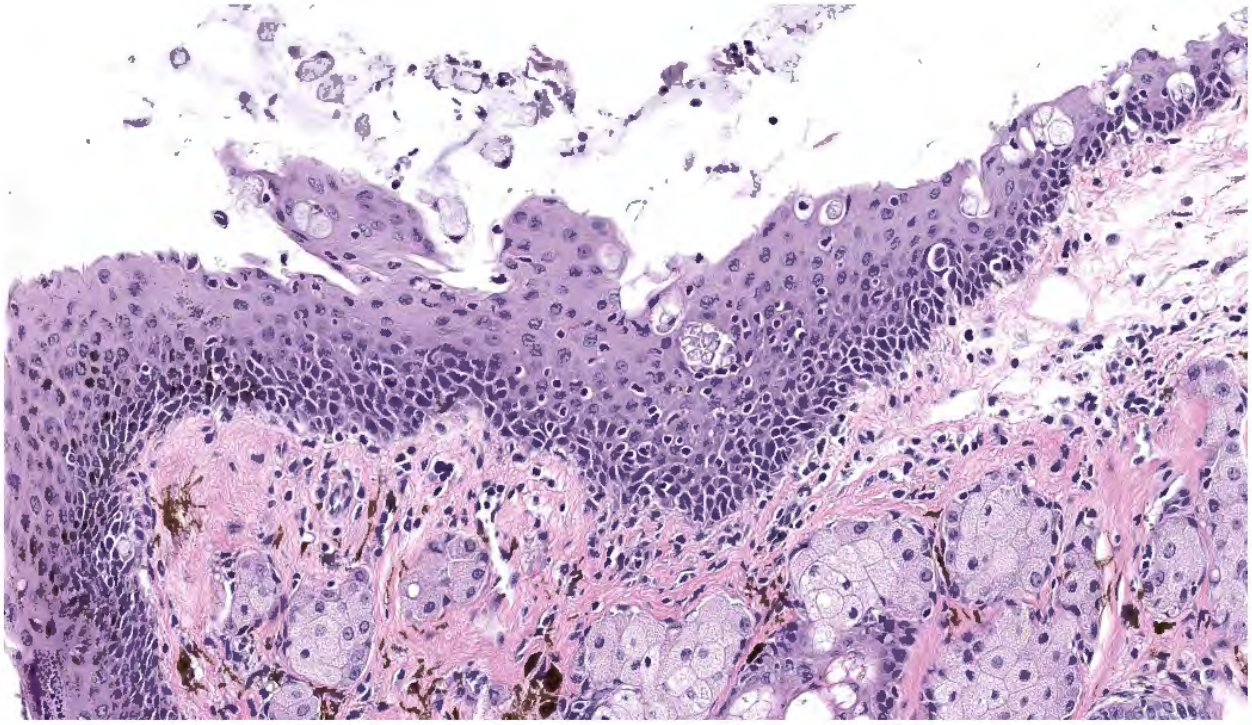

Figure 4-5. Eyelid, 129S/SvEv mouse: The conjunctival epithelium is infiltrated by low numbers of neutrophils and lymphocytes. (HE, 381X)

glandular stomach, respiraoty tract, and gallbladder, urolithiasis, megaesophagus, polyarteritis, and age-related hearing loss in 129P3/J mice. This particular lesion is caused by a Cdh23ahl mutation that results in progressive hearing loss by 3 months of age.[1] In contrast, 129S/SvEv mice are resistant to noise-related hearing loss.[5]

References:

1. Burghard AL, Morel NP, Oliver DL. Mice heterozygous for the Cdh23/Ahl1 mutation show age-related deficits in auditory temporal processing. *Neurobiol Aging*. 2019;81:47-57.
2. Radaelli E, Castiglioni V, Recordati C, et al. The pathology of aging 129S6/SvEv-Tac mice. *Vet Pathol.* 2016;53(2):477-92.
3. Sundberg JP, Brown KS, Bates R, Cunliffe-Beamer TL, Bedigian H. Suppurative conjunctivitis and ulcerative blepharitis in 129/J mice. *Lab Anim Sci.* 1991;41:516-18.
4. Mouse strain 129 substrain nomenclature. Mouse Genome Informatics Database at the Jackson Laboratory, Bar Harbor, ME. Accessed September 13, 2023.
5. Yoshida N, Hequembourg SJ, Atencio CA, Rosowski JJ, Liberman MC. Acoustic injury in mice: 129/SvEv is exceptionally resistant to noise-induced hearing loss. *Hear Res*. 2000;141(1-2):97-106.

Joint Pathology Center
Veterinary Pathology Services

WEDNESDAY SLIDE CONFERENCE 2025-2026

Conference #20 — 25 March 2026

CASE I:

Signalment:

Adult, castrated male, wild donkey (*Equus africanus asinus*)

History:

Seven wild donkeys died over the course of a week following a history of respiratory signs. Two of the donkeys were submitted for postmortem examination and diagnostic workup. Tissues from one of these animals are included here.

Gross Pathology:

The lungs are diffusely swollen with a lobular pattern. On the cut surface, red areas of pulmonary consolidation are seen in a lobular pattern, separated by unaffected lung lobules. Moderate amounts of thick tan exudate are noted in the airways. The trachea contains moderate amounts of stable foam. The tracheobronchial lymph nodes are enlarged.

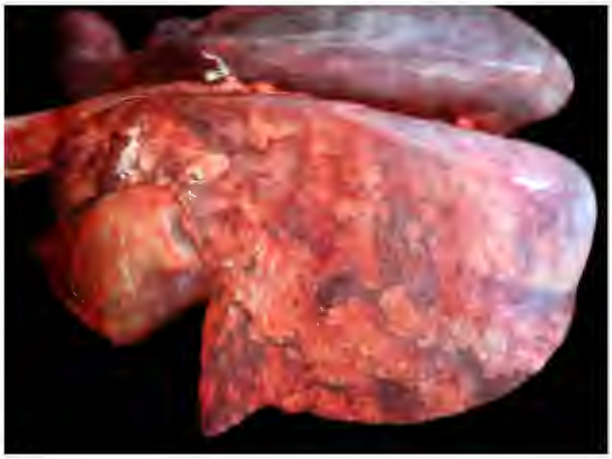

Figure 1-1. Lung, donkey: The lungs fail to collapse and are diffusely swollen with a lobular pattern (*Photo courtesy of*: California Animal Health and Food Safety Laboratory System (CAHFS), San Bernardino Laboratory, https://cahfs.vetmed.ucdavis.edu/locations/san-bernardino-lab)

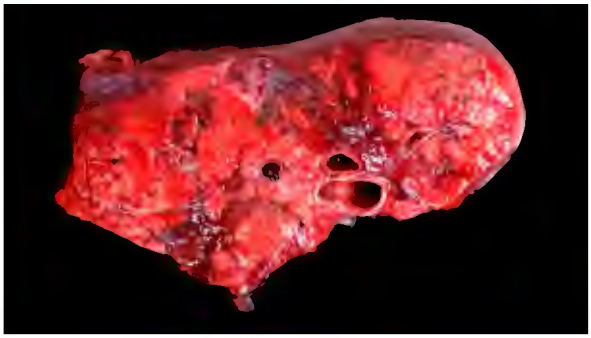

Figure 1-2. Lung, donkey. On the cut surface, there is pulmonary consolidation in a lobular pattern separated by unaffected or overinflated lung lobules. (*Photo courtesy of*: California Animal Health and Food Safety Laboratory System (CAHFS), San Bernardino Laboratory, https://cahfs.vetmed.ucdavis.edu/locations/san-bernardino-lab) .

Laboratory Results:

Virology: Influenza A virus was detected in nasal and bronchial swabs, as well as in the lung. Whole genome sequencing successfully recovered 16% (2.1 kb) of the entire equine influenza virus genome. The strain was highly similar (>99.7% nucleotide identity) to multiple strains (H3N8) from the United States and Chile.

-Equine herpesvirus 1 and 4 (EHV-1 and EHV-4) were not detected by PCR.

-No viral particles were detected by virus isolation (nasal and bronchial swabs and lung).

Bacteriology: Mixed flora was isolated form the lung.

Electron microscopy: No viral particles were detected in the lung.

Contributor's Comment:

Equine influenza virus A (EIV) is an enveloped, single-segmented, negative-sense RNA virus belonging to the Orthomyxoviridae family and Influenza A genus.[8] In equids, two main subtypes have been described: H7N7 (extinct since 1979) and H3N8.[1] H3N8 infects and causes disease in horses, donkeys, dogs, pigs, and camels, and there is evidence that it occasionally infects humans.[7,14,15] Outbreaks of H3N8 in donkeys have been identified in several regions and countries, including the United States, Brazil, Chile, Europe, China, Senegal, Pakistan, Turkey, West and Central Africa, Egypt, and India.[1] Only a few countries such as New Zealand and Iceland are free of equine influenza.[3] H3N8 strains have been considered emerging in donkeys in Colorado, California, and China.[1,14] Outbreaks of H3N8 show

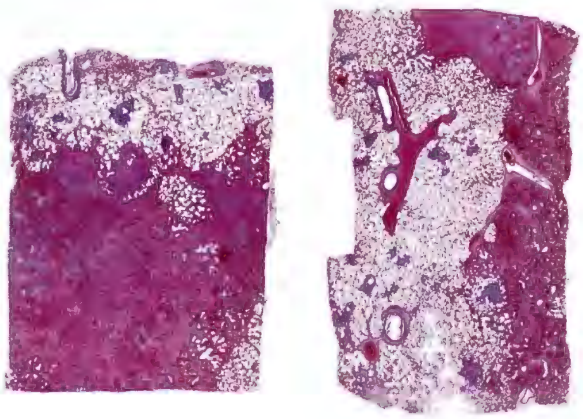

Figure 1-3. Lung, donkey: In the submitted sections of lung, over 50% of the pulmonary parenchyma is consolidated. (HE, 10X)

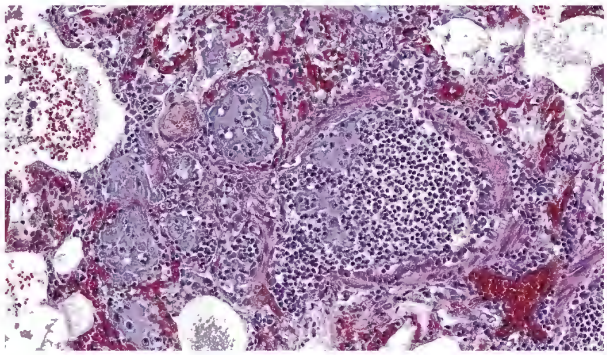

Figure 1-4. Lung, donkey: Throughout the section, airways are filled with large numbers of neutrophils, macrophages, mucin, and cellular debris. There is segmental necrosis and loss of airway epithelium. The inflammatory exudate extends into and fills adjacent alveoli.

no age predilection; morbidity is often high (81%) and mortality is low, although it can reach up to 20%, particularly in donkeys.[8,11,14] Donkeys are more susceptible to EIV infection compared to horses,[3,12] possibly due to a higher propensity for bacterial bronchopneumonia or recurrent coinfections with *Dictyocaulus arnfieldii*.[3]

EIV is extremely contagious and transmission occurs by direct contact with infected animals or fomites, as well as via aerosols. It can effectively travel through the air over distances of up to 1-2 km.[12] The incubation period ranges from 1 to 3 days.[12] EIV primarily infects respiratory tract epithelial cells through receptor-mediated endocytosis. The spike glycoprotein, HA, attaches to sialic acid receptors on the host cell surface.[10,12] Viral replication leads to epithelial cell death, mostly through apoptosis, and subsequent chemotaxis of immune cells, causing inflammation and reducing mucociliary clearance.[10]

Uncomplicated cases of EIV infection are typically mild and self-limiting. In equids, clinical signs include nasal serous or mucopurulent discharge, dry cough, pyrexia, loss of appetite, weakness, poor performance,

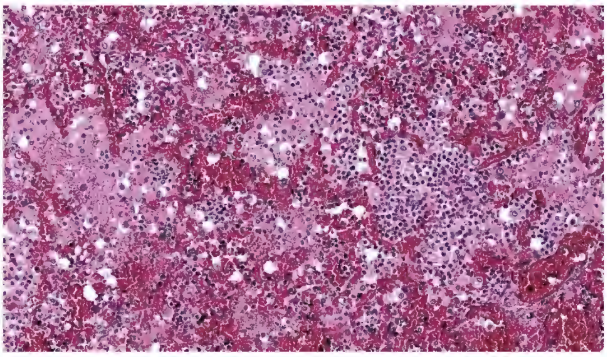

Figure 1-5. Lung, donkey: In inflamed areas, alveoli septa are filled with numerous neutrophils, alveolar macrophages, edema, hemorrhage, and polymerized fibrin. Alveolar septa are markedly congested with mild edema, increased numbers of circulating neutrophils, and occasional Type II pneumocyte hyperplasia.

and hyperemia of nasal and conjunctival mucosae.[9] Clinical signs are generally milder in horses and mules compared to donkeys.[12] Fatal cases may occur with complications from pulmonary bacterial infections such as those caused by *Streptococcus equi* subsp. *zooepidemicus*, *Streptococcus* spp., *Klebsiella pneumoniae*, and *Actinobacillus* spp.[5,6,11,14] Rare complications include myocarditis, chronic obstructive pulmonary diseases, and encephalitis.[9,12]

Typical pathological changes in equids with viral pneumonia include pulmonary consolidation in a lobular pattern separated by unaffected or overinflated lung lobules, or less commonly, a diffuse pattern of pneumonia.[1] EIV infections complicated by secondary bacterial infections are characterized by fibrinosuppurative exudate and pulmonary consolidation, mostly restricted to the cranioventral pulmonary lobes (bronchopneumonia).[1,12,13] Histologically, acute stages typically reveal rhinitis and tracheitis with epithelial necrosis and infiltrates of lymphocytes in the lamina propria. Subacute to chronic lesions consist of epithelial hyperplasia and squamous metaplasia.[6,11] Affected lungs exhibit bronchointerstitial pneumonia with hyaline membranes in the alveoli, type II pneumocyte hyperplasia, and necrotizing bronchitis/bronchiolitis. Secondary bacterial bronchopneumonia may also develop.[4,6,12]

Other viral upper respiratory infections such as Equine Herpesvirus 1 (EHV-1) and Equine Herpesvirus 4 (EHV-4) produce similar lesions and should be considered as differential diagnoses in donkeys.[2] Confirmation of the etiology in cases of EIV infection should involve fluorescent antibody testing (FAT), immunohistochemistry (IHC), virus isolation, molecular testing, and/or partial genetic and phylogenetic analysis of the virus.[10]

Contributing Institution:

California Animal Health and Food Safety Lab
105 W Central Ave, San Bernardino, CA 92408, USA.
https://cahfs.vetmed.ucdavis.edu/

JPC Morphologic Diagnosis:

Lung: Pneumonia, bronchointerstitial, necrotizing and fibrinosuppurative, acute, multifocal to coalescing, marked, with thrombosis, edema, and hyaline membranes.

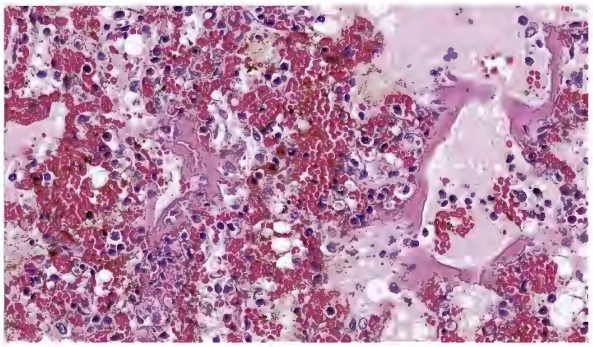

Figure 1-6. Lung, donkey: Compacted fibrin lines alveolar septa (hyaline membranes). (HE, 773X)

JPC Comment:

The 20th conference of the 2025-2026 Wednesday Slide Conference was moderated by the wonderful Dr. Patty Pesavento, from the University of California, Davis. This first case was a fantastic example of equine influenza with a secondary bacterial infection, and the contributor provided a fantastic writeup for this entity.

Determining differentials in a case of viral pneumonia in any species requires a working knowledge of viral pathogenesis and target cells to refine the list of potential offenders. In this case, the most striking hallmarks for influenza virus include the end-airway epithelial necrosis and patchy areas of hemorrhage. Influenza is both endotheliotropic and epitheliotropic and, while it affects epithelial cells in the upper airways, it has unique tropism for the type I and type II pneumocytes of the alveoli as well. It causes significant destruction to end-airways as a result. This key difference can help separate an influenza infection from other pneumotropic viruses, such as calicivirus in cats. (Feline calicivirus infection of the lung can look nearly identical to an H5N1 influenza virus infection in a cat, but the state of the end airways can help clue in the pathologist to which virus is most likely and can assist in decision-making for next testing steps. The more virulent strains of feline calicivirus can cause severe interstitial pneumonia, but they do not cause necrosis of end airways the way that influenza does.)

Grossly, an influenza-infected lung has a "checkerboard" appearance with random, alternating areas of dark red atelectasis and light pink, aerated lung. This pattern manifests because influenza does not uniformly infect every cell it comes into contact with due to varied densities of sialic acid receptors on the host cells. Dark red to purple areas of consolidation represent collapsed alveoli whose airway has been clogged by exudate and which can no longer pass air through to the alveoli.. These solidified, dark red sections contrast sharply with the lighter-colored, air-filled alveoli.

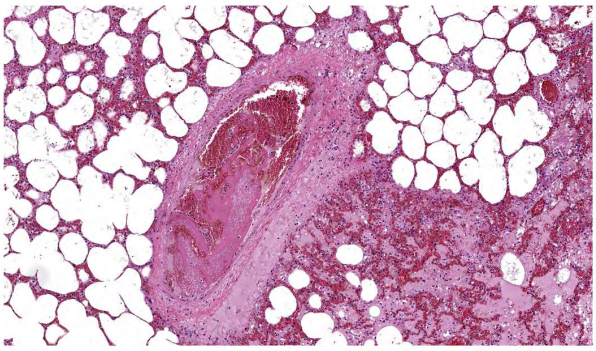

Figure 1-7. Lung, donkey: A pulmonary vein contains a large occlusive fibrin thrombus (HE, 162X)

As stated by the contributor, donkeys are more susceptible to equine influenza virus than horses, although both species primarily develop respiratory disease with influenza.[1] This is true in pigs and humans, as well, where the lung is the main target of influenza.

In cats, however, the primary presentation of influenza, especially H5N1, is encephalitis. Cats are also susceptible to cerebral infarcts from influenza targeting vascular endothelium. Swine can also be infected with neurotropic strains of influenza A, including H5N1. One of the main mechanisms for infection with H5N1 influenza in cats is consumption of contaminated cow's milk.[9]

In cattle, the primary targets for influenza are the mammary glands due to high tropism for and concentration of the virus in bovine mammary gland epithelium with subsequent shedding of the virus into milk.[9] It is unclear if this is true in other species, but it has been definitively demonstrated that, in humans, the virus does not target the mammary glands.[9] Additionally, modern pasteurization

and homogenization methods used in most commercial dairies completely kills any influenza virus that may be present in cow milk, so milk from dairies that use these methods is still very much safe for human consumption.[9] In birds, the primary cellular targets for influenza, especially highly pathogenic avian influenza, are the brain and pancreas. Avian influenza was discussed more in depth in this year's Conference #17, Case 2.

All participants considered the bacterial infection to be secondary and due to aerogenous introduction of bacteria into an already virus-infected lung. This ruled out *Streptococcus spp,* including *S. equi* or *S. zooepidemicus,* as contributing to the bacterial infection, as these spread hematogenously.

References:

1. Ahearne MM, Pentzke-Lemus LL, Romano AM, Larsen ED, Watson AM, O'Fallon EA, Landolt GA. Disease progression, pathologic, and virologic findings of an equine influenza outbreak in rescue donkeys. *J Vet Intern Med*. 2022; 36(6):2230-2237.

2. Boyle AG, Timoney JF, Newton JR, Hines MT, Waller AS, Buchanan BR. Streptococcus equi Infections in Horses: Guidelines for Treatment, Control, and Prevention of Strangles-Revised Consensus Statement. *J Vet Intern Med*. 2018;32 (2):633-647.

3. Câmara RJF, Bueno BL, Resende CF, Balasuriya UBR, Sakamoto SM, Reis JKPD. Viral Diseases that Affect Donkeys and Mules. *Animals* (Basel). 2020;25;10(12):2203.

4. Carvallo FR, Stevenson VB. Interstitial pneumonia and diffuse alveolar damage in domestic animals. *Vet Pathol*. 2022;59 (4):586-601.

5. Carvallo FR, Uzal FA, Diab SS, Hill AE, Arthur RM. Retrospective study of fatal pneumonia in racehorses. *J Vet Diagn Invest*. 2017;29(4):450-456.

6. Chambers TM. Equine Influenza. *Cold Spring Harb Perspect Med*. 2022; 4;12 (1):a038331.

7. Crawford PC, Dubovi EJ, Castleman WL, Stephenson I, Gibbs EP, Chen L, Smith C, Hill RC, Ferro P, Pompey J, Bright RA, Medina MJ, Johnson CM, Olsen CW, Cox NJ, Klimov AI, Katz JM, Donis RO. Transmission of equine influenza virus to dogs. *Science*. 2005; 21;310(5747):482-5.

8. Dionísio L, Medeiros F, Pequito M, Faustino-Rocha AI. Equine influenza: a comprehensive review from etiology to treatment. *Anim Health Res Rev*. 2021; 22(1):56-71.

9. Landolt GA. Equine influenza virus. *Vet Clin North Am Equine Pract*. 2014; 30 (3):507-22.

10. Rahman A, Uzal FA, Hassebroek AM, Carvallo FR. Retrospective study of pneumonia in non-racing horses in California. *J Vet Diagn Invest*. 2022; 34 (4):587-593.

11. Singh RK, Dhama K, Karthik K, Khandia R, Munjal A, Khurana SK, Chakraborty S, Malik YS, Virmani N, Singh R, Tripathi BN, Munir M, van der Kolk JH. A Comprehensive Review on Equine Influenza Virus: Etiology, Epidemiology, Pathobiology, Advances in Developing Diagnostics, Vaccines, and Control Strategies. *Front Microbiol*. 2018; 6(9):1941.

12. Timoney PJ. Equine influenza. *Comp Immunol Microbiol Infect Dis*. 1996; 19 (3):205-11.

13. Yang H, Xiao Y, Meng F, Sun F, Chen M, Cheng Z, Chen Y, Liu S, Chen H. Emergence of H3N8 equine influenza virus in donkeys in China in 2017. *Vet Microbiol.* 2018; 214:1-6.

14. Xie T, Anderson BD, Daramragchaa U, Chuluunbaatar M, Gray GC. A Review of Evidence that Equine Influenza Viruses Are Zoonotic. *Pathogens*. 2016; 12;5 (3):50.

CASE II:

Signalment:

4-year-old, male, Balinese cat, (*Felis silvestris catus)*

History:

Sudden death**,** after one month in which the subject manifested increased appetite.

Gross Pathology:

At necropsy, multiple organs were affected:

Abdominal cavity: in the cavity there was an effusion (approx. 30 ml) of pale, yellow, and transparent fluid which contained scattered strands of white, elastic, and insoluble material (fibrin).

On the serosal surfaces of the major abdominal and thoracic organs (spleen, kidneys, intestine, pancreas, lungs and heart) there were multifocal, well defined, irregularly round, raised, white, and compact plaques that varied in size from few millimeters to a centimeter in major diameter. Some of these lesions extended into the parenchyma of organs and presented poorly defined and irregular edges.

Thoracic cavity: the same fluid (approx. 10 ml) was found in the thoracic cavity.

Trachea: There was moderate intraluminal white-pink foam (edema). Lungs: multifocal, white, solid, slightly protruding lesions up to few millimeters in diameter were present under the pleura. At cut surface, they showed irregular well-defined margins and white coloration.

Liver: The serosal surface of the organ was covered by extensive and abundant yellow, firm material, with a granular superficial appearance. On cut surface, the material did not extend into the parenchyma. Many multifocal friable yellow adhesions were present between the liver and the wall of the abdominal cavity.

Lymph nodes: Thoracic and abdominal lymph nodes were enlarged, dark red, and firm. At cut surface, they presented a diffuse homogenous dark red coloration. The macroscopic morphological diagnosis was therefore: diffuse and severe fibrinous peritonitis and pleuritis with generalized severe hemorrhagic lymphadenitis.

Laboratory Results: N/A

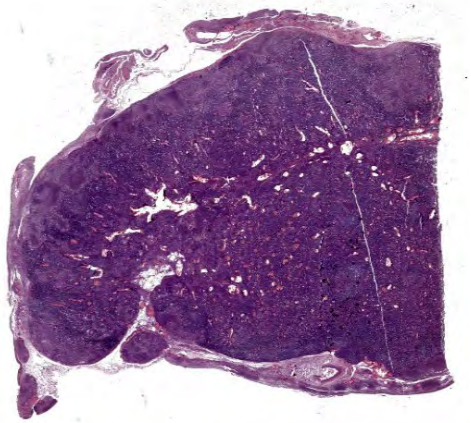

2-1. Lymph node, cat. A partial section of a markedly enlarge lymph node is submitted for examination. There is loss of the normal nodal architecture. (HE, 9X)

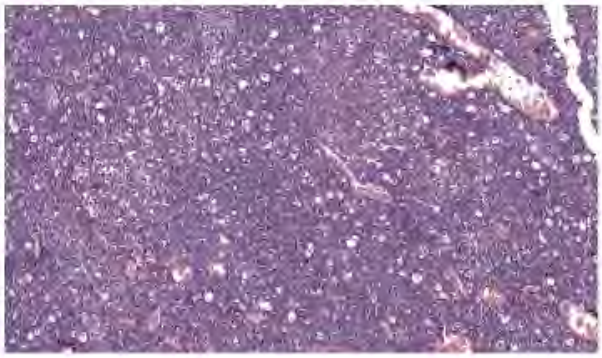

2-2. Lymph node, cat. There is marked expansion of the paracortex with loss of germinal centers. Numerous tingible body macrophages and apoptotic lymphocytes give the node a "starry sky"

Microscopic Description:

Abdominal lymph node: Multifocal, severe cellular infiltrates with undefined margins are randomly distributed within the lymph node parenchyma especially in the subcapsular areas. They extend into the serosal expanding and effacing the mesothelial lining. The infiltrates are characterized by a severe mixed inflammatory population with large-numbers of both viable and lytic neutrophils surrounded by occasional large macrophages with abundant cytoplasm and rare lymphocytes and plasma cells. In the center of almost each infiltrate the neutrophils population shows karyolysis, pyknosis, karyorrhexis and the accumulation of extensive amount of amorphous eosinophilic, proteinaceous material admixed with cellular debris (lytic necrosis).

Immunohistochemical (IHC) staining of lymph node sections using a mouse anti-Feline Coronavirus antibody (clone FIPV3-70 Serotec, Oxford UK) demonstrates strong positivity for many elements within the inflammatory infiltrates, suggestive of presence of viral antigen.

Contributor's Morphologic Diagnosis: Multifocal severe necrotizing and piogranulomatous lymphadenitis and peritonitis associated with Feline Coronavirus antigen. Feline infectious peritonitis.

Additional findings:

- Diffuse severe peritonitis
- Multifocal severe piogranulomatous hepatitis, pneumonia, pancreatitis, nephritis,myocarditis and enteritis.
- Lung: Mild diffuse edema and mild diffuse emphysema
- Liver: Diffuse, severe hepatic hydropic degeneration.

Contributor's Comment:

Feline infectious peritonitis (FIP) is an uncommon, fatal, progressive, and immune-mediated disease of cats caused by feline coronavirus (FCoV) infection. At present, despite decades of research on its etiology, pathogenesis, transmission, and prevention, FIP is still one of the most frequent fatal and infectious feline disease for which there is, so far, no effective cure.[1]

Infection with FCoV is common in cats throughout the world, although, in most cats, the virus causes no clinical signs. However, in some cats, FCoV infection is associated with the development of the progressive and fatal disease manifestation of FIP.[3]

Figure 2-3. Lymph node, cat. Lymph node, cat There are numerous coalescing areas of lytic necrosis within the expanded paracortex. (HE, 114X)

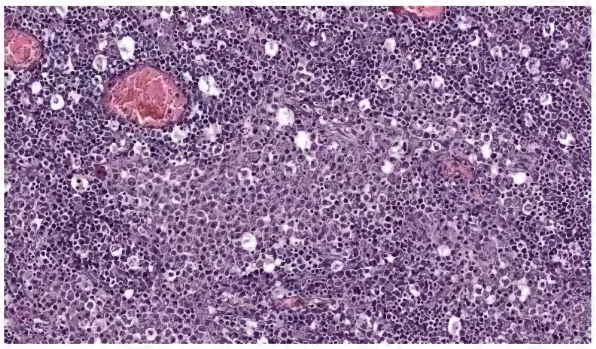

Figure 2-4. Lymph node, cat. There are extensive areas of granulomatous inflammation scattered throughout the cortex. (HE, 381X)

The current knowledge of genetic differences between feline enteric coronaviruses (FECV) and feline infectious peritonitis virus (FIPV) has been mainly based on comparative sequence analyses that revealed "discriminatory" mutations that are present in FIPVs but not in FECVs.[6] Most of these mutations result in amino acid substitutions in the S protein and these may have a critical role in the switch from FECV to FIPV.[1] In most cases, the precise roles of these mutations in the molecular pathogenesis of FIP have not been tested experimentally in the natural host, mainly due to the lack of suitable experimental tools including genetically engineered virus mutants.[6]

Cats that do not clear FIPV develop either dry or wet forms of the disease depending on whether ineffective cell-mediated or humoral immunity dominates the clinical disease. Although often described as distinct entities, the effusive and non-effusive forms of FIP are the farthest of a continuum of syndromes, characterized by vasculitis and pyogranulomatous inflammation. Effusive disease is more common than the non-effusive form, and mixed forms are common.[6] In our case clear indication of vasculitis was not present and necrosis was diffusely associated with the pyogranulomatous infiltrate, therefore IHC was needed to confirm the etiology.

Contributing Institution:

Dept. Comparative Biomedicine and Food Science (BCA) -
Veterinary Medicine - University of Padua
AGRIPOLIS - Viale dell'Università 16
35020 Legnaro (PD) - Italy
http://www.bca.unipd.it/en/

JPC Morphologic Diagnosis:

Lymph node: Lymphadenitis and capsulitis, necrotizing and granulomatous, chronic, multifocal to coalescing, marked, with paracortical hyperplasia.

JPC Comment:

This case was an excellent representation of a real-life manifestation of FIP, as classic vasculitis was not a significant part of this lesion (although areas of necrosis within the node suggested the presence of vascular damage. The top differentials for participants included FIP, *Francisella tularensis*, and *Yersinia pestis* (causative agent of bubonic plague) and other "hot" gram-negatives, and less commonly, and rare cases of feline parvovirus infection. The Pesavento Laboratory confirmed the positive

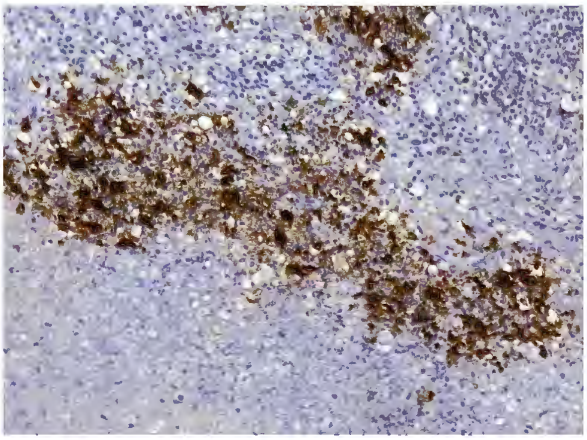

Figure 2.5. Lymph node, cat. Areas of granulomatous inflammation demonstrate strong immunostaining against coronaviral antigen (anti-FIPV3-70, 200X) (*Photo courtesy of*: Dept. Comparative Biomedicine and Food Science (BCA), Veterinary Medicine - University of Padua, http://www.bca.unipd.it/en/).

immunohistochemical identification of coronavirus in this case using a canine coronavirus antibody which cross reacts with many other related coronaviruses.

FIP is globally distributed and fatal if untreated. Today, however, antiviral treatment is over 80% effective.[4] Certain breeds are more susceptible to infection, but the gene association in the host has not yet been identified.[8] FIPV can cause disease in exotic big cat species as well, and has been reported in lions, servals, cheetahs, mountain lions, and others.[2,5,7,9,10]

Dr. Pesavento discussed how much we still have to learn about FIP, including the triggers of viral activation, how FIP persists in a host, the host range, susceptibility factors, and how variable manifestations of infection affect the outcome for the individual. While 98% of cats infected with FeCoV never develop FIP, what exactly causes or triggers the genetic mutations that result in FIP is still unknown. The general cause of FIP is enteric persistence of FeCoV within a host, specifically within the colon, coupled with systemic access and mutation of the virus into a pathogenic FIPV. There are multiple mutations and multiple genes involved in this transformation of FeCoV into FIPV, many of which are not fully understood.

Additionally, a phenomenon known as "antibody-dependent enhancement" has been demonstrated in cats that are re-infected with an identical serotype of FIPV.[11] Antibody-dependent enhancement (ADE) is a phenomenon in which non-neutralizing or weak antibodies bind to a virus but fail to neutralize it. Instead, the antibody actually facilitates the virus' entry into cells, resulting in increased viral replication and more severe disease.[11] This makes this disease particularly challenging for vaccine development. Currently vaccine development targets the nucleocapsid (N) protein. This N protein is well-conserved across coronaviral strains, unlike the spike (S) protein that is prone to significant variation. The N protein can trigger a longer-lasting antibody response, but, perhaps more importantly, an N-specific cytotoxic T lymphocyte response. This elegant targeting of a cell-mediated, rather than a humoral, response may help avoid antibody-dependent enhancement in FIPV.

References:

1. Brown MA, Troyer JL, Pecon-Slattery J, Roelke ME, O'Brien SJ. Genetics and Pathogenesis of Feline Infectious Peritonitis Virus. *Emerg Infec Dis*. 2009;15 (9):1445-1452

2. Evermann JF, Heeney JL, Roelke ME, McKeirnan AJ, O'Brien SJ. Biological and pathological consequences of feline infectious peritonitis virus infection in the cheetah. *Arch Virol*. 1988;102(3-4):155-171.

3. Giordano A, Paltrinieri S, Bertazzolo W, Milesi E, Parodi M. Sensitivity of Trucut and fine-needle aspiration biopsies of liver and kidney for diagnosis of feline infectious peritonitis. *Vet Clin Path*. 2005;34(4):368-374.

4. Kipar A, Meli ML. Feline Infectious Peritonitis: Still an Enigma? *Vet Path*. 2014;51 (2):505-526.

5. Juan-Sallés C, Domingo M, Herráez P, Fernández A, Segalés J, Fernández J. Feline infectious peritonitis in servals (Felis serval). *Vet Rec*. 1998;143(19):535-536.

6. Kipar A, Meli ML. Feline Infectious Peritonitis: Still an Enigma? *Vet Path*. 2014;51 (2):505-526.

7. Mwase M, Shimada K, Mumba C, Yabe

J, Squarre D, Madarame H. Positive immunolabelling for feline infectious peritonitis in an African lion (Panthera leo) with bilateral panuveitis. *J Comp Pathol*. 2015;152(2-3):265-268.

8. Pesteanu-Somogyi LD, Radzai C, Pressler BM. Prevalence of feline infectious peritonitis in specific cat breeds. *J Feline Med Surg*. 2006;8(1):1-5.

9. Stephenson N, Swift P, Moeller RB, Worth SJ, Foley J. Feline infectious peritonitis in a mountain lion (Puma concolor), California, USA. *J Wildl Dis*. 2013;49(2):408-412.

10. Stout AE, André NM, Whittaker GR. Feline coronavirus and feline infectious peritonitis in nondomestic felid species. *J Zoo Wildl Med*. 2021;52(1):14-27.

11. Takano T, Kawakami C, Yamada S, Satoh R, Hohdatsu T. Antibody-dependent enhancement occurs upon re-infection with the identical serotype virus in feline infectious peritonitis virus infection. *J Vet Med Sci*. 2008;70 (12):1315-1321.

CASE III:

Signalment:

5-month-old, female black-winged starling (*Acridotheres melanopterus*)

History:

This was a parent-raised bird hatched in a mixed species aviary. It was found dead in the habitat with no previous clinical history.

Gross Pathology:

Postmortem and body condition were good with mild autolysis and moderate fat stores. The liver was enlarged filling much of the coelomic cavity and mottled shades of tan and brown. The spleen was enlarged at 3 x 0.5 x 0.5 cm. The upper gastrointestinal tract was empty and the small and large intestinal loops were diffusely mildly dilated.

Laboratory Results:

In-house cPCR assays with sequencing (frozen lung and duodenum):

- Isospora-specific cytochrome *c* oxidase: *Isospora serini* (BLAST Accession ON584773), 96.7-96.9% identical
- Trichomonas 18S rRNA: *Cochlosoma anatis* (BLAST Accession AY247745), 92.7% identical

Electron microscopy, California Animal Health and Food Safety Lab in Davis, CA (formalin-fixed liver):

- Free organisms- family *Trichomonadidae* flagellates with 5 apical flagella (one recurrent)
- Lymphocytes- Intracytoplasmic *Isospora*

Microscopic Description:

Liver: Surrounding portal regions and occasionally coalescing are infiltrates of moderate numbers of lymphocytes and histiocytes that disrupt the hepatic architecture. Within the lymphocytes and histiocytes are numerous, 2um in diameter, basophilic protozoal organisms surrounded by a thin, clear halo that peripheralizes the nucleus. The inflammatory cells separate and individualize the hepatocytes, which display mild karyomegaly and frequent binucleation. Free within the sinusoidal lumina and within portal and central veins are numerous, approximately 5 um diameter, pyriform flagellate protozoa with a single, variably distinct nucleus. Occasional large lymphocytes and rare plasma cells circulate throughout the sinusoids.

Duodenum: The mucosal lamina propria is

markedly infiltrated and expanded by numerous lymphocytes and histiocytes with rare plasma cells. The inflammatory cells broaden and occasionally fuse the villi and separate the intestinal crypts. Within the mononuclear cells are abundant 2um diameter, basophilic protozoal organisms surrounded by a thin, clear halo that peripheralizes and indents the nucleus. The crypt epithelial cells are often pyknotic and sloughed into the lumen. Epithelial cells at the crypt bases are often hyperplastic, piling three to four cells thick with increased numbers of mitotic figures. The coelomic fat surrounding the duodenum has small, multifocal aggregates of lymphocytes.

Cloaca, colon, and bursa of Fabricius: The lamina propria of the colon is infiltrated and expanded by moderate numbers of lymphocytes and plasma cells that separate colonic crypts. Multifocal crypts are filled with numerous, approximately 5 um diameter, pyriform flagellates with a single, variably distinct nucleus. Similar flagellates are also identified in large numbers within the lumen. Within the bursa of Fabricius, there are similar trichomonad flagellates as well as approximately 2-3 um diameter, round, protozoal organisms that are often adhered to the superficial surface of the epithelial cells.

3-1. Abdominal viscera, starling: Sections from the gastrointestinal tract to include liver, duodenum, pancreas, cloaca and bursa are submitted for examination.

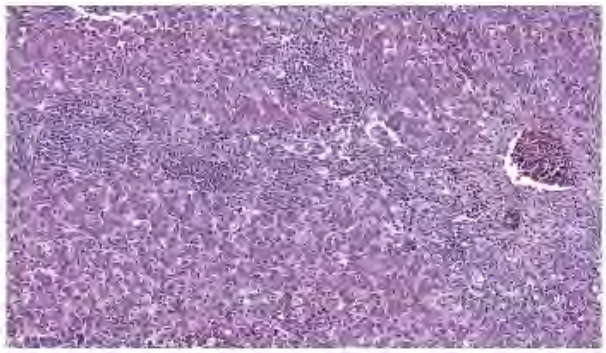

Figure 3-2. Liver, starling: There is marked inflammation centered on portal areas, which is composed of large numbers of macrophages, lymphocytes and plasma cells which crosses the limiting plate and extends into the adjacent hepatic parenchyma. (HE, 279X).

Contributor's Morphologic Diagnosis:

Liver: Moderate, multifocal, chronic, lymphohistiocytic hepatitis with intracellular protozoa (consistent with isosporosis, *Isospora* sp) and sinusoidal flagellates
Duodenum: severe, chronic, segmental, histiocytic enteritis, with abundant intracellular protozoa (consistent with isosporosis, *Isospora* sp.)
Cloaca and bursa of Fabricius: moderate, chronic, proliferative and lymphoplasmacytic cloacitis and bursitis with superficial mucosal protozoa, consistent with cryptosporidiosis, *Cryptosporidium* sp.
Colon and cloaca: myriad crypt and luminal flagellates

Contributor's Comment:

This young black-winged starling had two clinically significant systemic protozoal infections, confirmed by PCR assays and electron microscopy, that likely led to its death. A third suspected protozoal infection was seen histologically in the cloaca and bursa of Fabricius but not confirmed with ancillary testing. Gizzard candidiasis completed the picture of a bird with an immature or deficient immune system despite its apparently

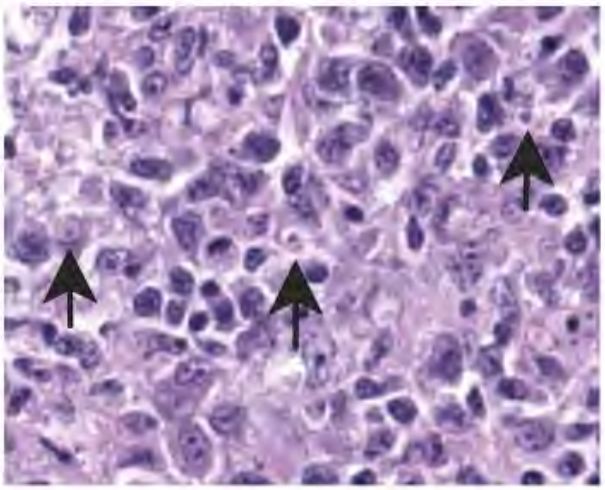

3-3. Liver, starling: Macrophages and lymphocytes occasionally contain a single cytoplasmic protozoal zoite consistent with *Sarcocystis spp.* which measures 2-3um and often peripheralizes or compresses the nucleus. (HE, 1793X).

adequate nutritional status.

Systemic isosporosis was identified histologically and cytologically in histiocytes and lymphocytes of an inflammatory response affecting small intestine, liver, spleen, and other tissues. Isosporosis is well-described in captive and free-range passerines. Formerly known as atoxoplasmosis, the pathogenesis of systemic isosporosis remains uncertain but involves extraintestinal invasion of mononuclear cells by sporozoites that undergo asexual reproduction. It is endemic in populations of passerines with fatal infections associated with stress, concurrent infections, or immunosuppression.[3] Mortality due to *Isospora sp* in wild birds is low, however, mortality in captive birds is significantly higher. Stress due to captivity and increased shedding of infective oocysts have been proposed as possible causes for the higher mortality observed in captive passerines.[3] As seen in this case, isosporosis is most commonly seen in the proximal segments of the small intestine and is accompanied by infiltration by mononuclear cells. Compromise to the intestinal mucosa as a result of the severe inflammation in this case could have led to invasion by the second protozoal infection.

Present in often very large numbers throughout the vasculature were extracellular protozoa consistent with flagellates that could have contributed to the inflammation in some tissues. Using a trichomonad PCR assay, sequences with a closest match to *Cochlosoma anatis* were obtained from both lung and intestine, although identity was only ~93%. Electron microscopy of liver tissue confirmed intracellular protozoa consistent with *Isospora*, and extracellular flagellates consistent with tetratrichomonads based on the presence of 5 undulipodia at the apical pole with one recurrent. In contrast, *Cochlosoma* sp. have six flagella, one of which is recurrent. Both *Cochlosoma* and *Trichomonas* have a single nucleus, a parabasal apparatus, a tubular axostyle, and a crescent-shaped pelta.[6] Prior studies have identified via sequence analysis of the 16S rRNA gene that *Cochlosoma* and *Trichomonas* are genetically similar, which likely accounts for the 93% identity match.[4] *Tetratrichomonas* and *C. anatis* are often identified with other intestinal pathogens and their pathogenicity as a sole pathogen remains uncertain.[1,4] Both have been documented as the cause of fulmi-

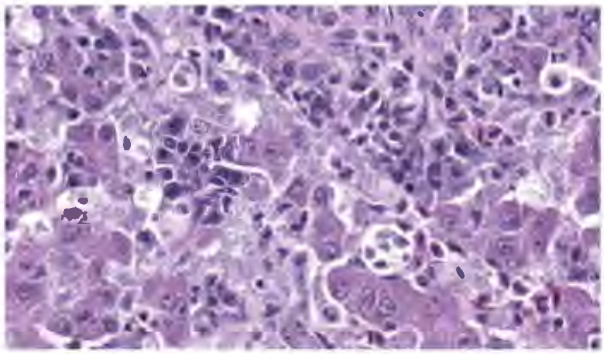

Figure 3-4. Liver, starling: Within portal areas, macrophages also contain multiple 2-4um pyriform flagellates within their cytoplasm. (HE, 1493X)

nant disease in a variety of birds. Tetratrichomoniasis has been identified as the causative agent of acute typhlohepatitis in ducks, a necrotizing hepatitis and splenitis in a Waldrapp ibis and necrotizing hepatitis in a free-ranging white pelican.[1,2] *Cochlosoma anatis* is linked to enteritis in turkeys, as well as increased dehydration, malabsorption, and mortality in young finches.[4] However, prior studies have failed to document clinical signs or histologic lesions in experimental infections with *Trichomonas* and coinfections of *Cochlosoma* with other intestinal pathogens have demonstrated greater pathogenicity than with either pathogen alone.[1,4]

Flagellates were also present in the colonic and cloacal lumen, including deep in the crypts. In this location, their visualization was complicated by suspected cryptosporidiosis, the third protozoal infection, which was best seen in the bursa of Fabricius. The cryptosporidiosis within the bursa of Fabricius was not confirmed via ancillary diagnostics, but the appearance in this location was typical, though less common than proventricular cryptosporidiosis in passerines. The colonization of the bursa by the *Cryptosporidium*

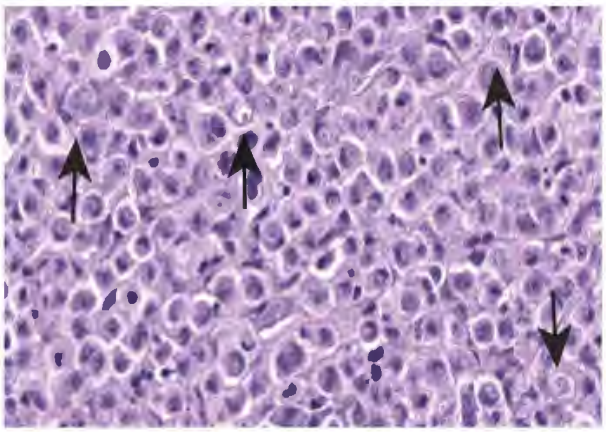

Figure 3-5. Duodenum, starling: The lamina propria is expanded by large numbers of macrophages which surround, separate, and often efface crypts. (HE, 279X)

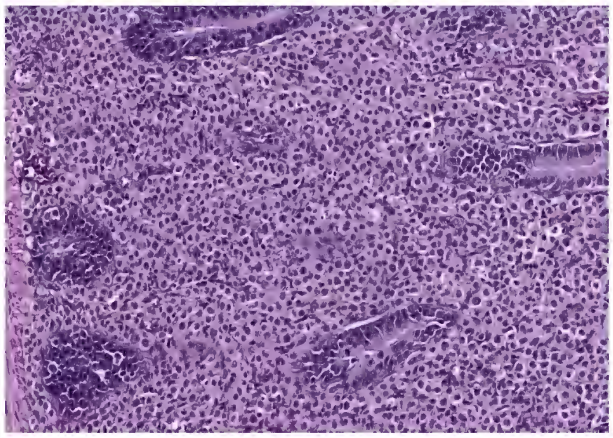

Figure 3-6. Duodenum, starling; Macrophages occasionally contain a single cytoplasmic protozoal zoite consistent with *Sarcocystis spp.* which measures 2-3um and often peripheralizes or compresses the nucleus. (HE, 1793X).

and the resulting bursitis may have impaired the humoral immune response, further predisposing the starling to the multiple concurrent protozoal infections.

Contributing Institution:

Disease Investigations
San Diego Zoo Wildlife Alliance
PO Box 120551
San Diego, CA 92112
https://science.sandiegozoo.org/disease-investigations

JPC Morphologic Diagnosis:

1. Liver: Cholangiohepatitis, histiocytic and lymphoplasmacytic, chronic, diffuse, marked, with intrahistiocytic apicomplexan zoites and sinusoidal flagellates.
2. Duodenum: Enteritis, histiocytic, chronic, diffuse, severe, with intrahistiocytic apicomplexan zoites.
3. Cloaca: Cloacitis, proliferative and histiocytic, chronic, diffuse, marked, with numerous luminal flagellates.
4. Bursa of Fabricius: Bursitis, necrotizing, chronic, multifocal, mild, with intraluminal flagellates.

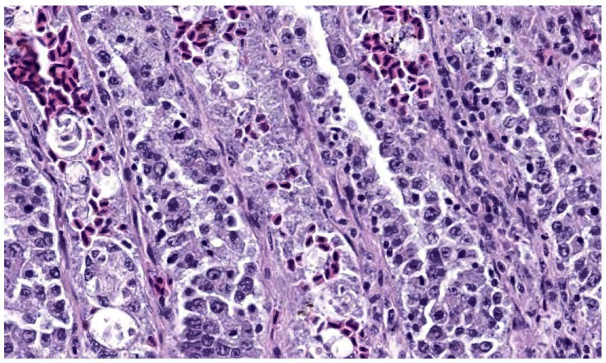

Figure 3-7. Cloaca: There are numerous 2-4um pyriform protozoa within the glands and occasionally with macrophages cytoplasm. (HE 864X)

JPC Comment:

Many thanks to this contributor for an interesting case and well-written comment! It has been a while since the WSC saw a case of atoxoplasmosis (WSC 2009, Conf 18, Case 3), and this case provided some excellent discussion points. This was a challenging slide for many participants due to the lymphoproliferative nature of this protozoal infection, which, depending on the severity of the infection and the species affected, can be confused with lymphoma caused by gallid herpesvirus-2 (Marek's disease), and avian retrovirus (lymphoid leukosis), etc.[3] This was true in this conference, and some participants wondered about a lymphoma as the primary disease with the protozoa being secondary. The *Isospora serini* were easier for the participants to find in this collection of tissue, but finding the flagellates, (*Cochlosoma anatis*) proved more difficult on the HE section (however, once the first flagellate were identified, participants were able to find them with ease.) Flagellates have a small, pinpoint nucleus and piriform shape, which differentiates them from mucin and debris. The group decided that there was not definitive evidence of cryptosporidia on the section of bursa, but only a very limited area of bursal epithelium (which cryptosporidia invade) was present in the section, so sampling was extremely limited.

This case provided a nice example of granulopoiesis in the liver, characterized by granulocytes that lacked a bilobed nucleus and clustered with hematopoietic precursors. It is easy to overlook or over-interpret extramedullary hematopoiesis, but knowing which species it is normally and commonly seen in is important. Birds, reptiles, and some rodents can routinely have foci of EMH in their livers. There was additionally some beautiful tertiary lymphoid follicle development in this case secondary to the chronic inflammation!

Evaluation of the bursa of Fabricius proved to be an important point of discussion. The bursa naturally involutes as birds age and should be a synchronous process.[7] In chickens, the Bursa begins involution around 8-10 weeks of age and is generally heavily involuted by 6-7mo old.[7] In this case, however, there was asynchronous depletion of the Bursa, indicating that this was not natural involution. There were some follicles that exhibited lytic central necrosis and lymphocytolysis, demonstrating an active insult to the Bursa that may have contributed to this

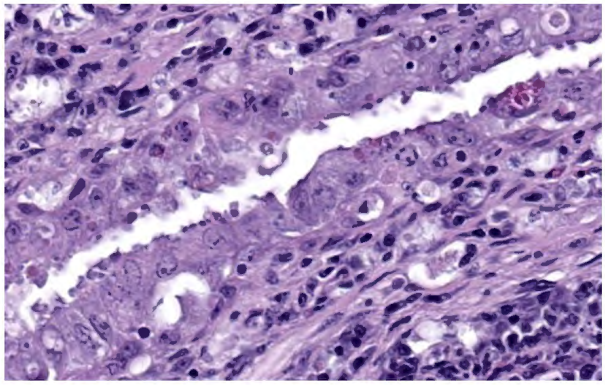

Figure 3-8. Bursa of Fabricius, starling: There are numerous cryptosporidial meronts and gamonts within the apical cytoplasm (intracellular, extracytoplasmic) of epithelial cells. (HE, 1072X)

bird's immunosuppression. Whether this was viral or parasitic could not be determined. Although participants were not convinced about *Cryptosporidium spp.*, the bursal epithelium are good places to hunt for them since the bursa of Fabricius is a continuation of the intestine. In trying to put a pathogenesis together in this case, participants thought that the most likely primary cause of this bird's demise was nutritional malabsorption due to the marked histiocytic enteritis with epithelial necrosis and crypt separation.

Finally, Dr. Pesavento quizzed participants on the ultrastructural images from this case, which was an appreciated, succinct review for many attendees. Key takeaways from this discussion included trusting your anchors (i.e. erythrocytes, nuclei, etc.), determining the number of cell profiles in the EM image, and knowing what normal looks like so you can evaluate the abnormal. The protozoal organisms on EM had some key characteristics to look for, as well, including the flagella on the trichomonads with their classic microtubule 9+2 arrangement, and the apicomplexan conoid, rhoptries, and micronemes within the *Isospora*.[5,6] Her last piece of wisdom in this case regarded microvilli on EM: don't call them microvilli unless you can see the actin microfilaments holding them up. If not, they are termed "cellular projections."

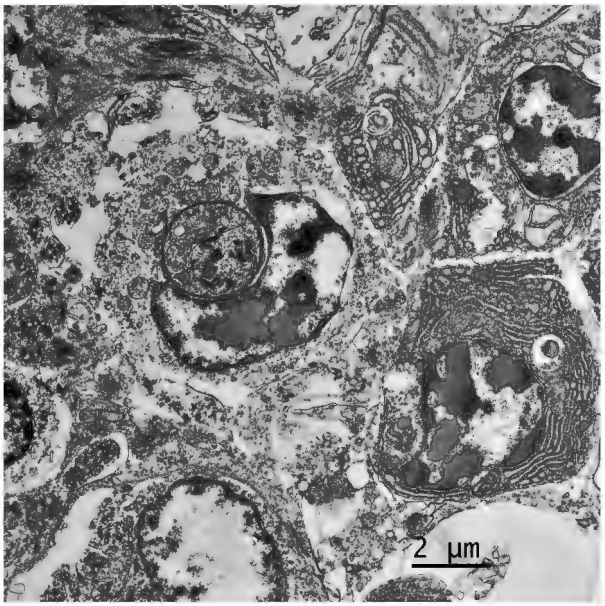

Figure 3-9. Liver, starling: An ultrastructural photomicrograph demonstrates a single apicomplexan schizont with the cytoplasm of a macrophage. A plasma cell is at right. (Photo courtesy of Disease Investigations, San Diego Zoo Wildlife Alliance, https://science.sandiegozoo.org/disease-investigations)

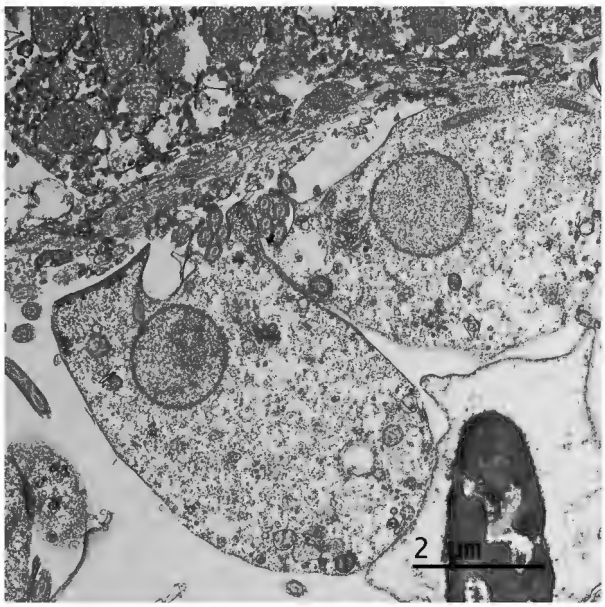

Figure 3-10. Cloaca, starling: An ultrastructural photomicrograph demonstrates two flagellates within the lumen of the cloaca. Numerous cross sections of flagella may be seen at th periphery of the flagellates. (Photo courtesy of Disease Investigations, San Diego Zoo Wildlife Alliance, https://science.sandiegozoo.org/disease-investigations)

References:

1. Amin A, Bilic I, Liebhardt D, Hess M. Trichomonads in birds – a review. *Parasitol*. 2014;141(6):733-747.

2. Burns RE, Braun J, Armien AG, Rideout BA. Hepatitis and splenitis due to systemic tetratrichomoniasis in an American white pelican (*Pelecanus erythrorhynchos*). *J Vet Diagn Invest*. 2013;2(4):511-4.

3. Cushing TL, Schat KA, States SL, Grodio JL, O'Connell PH, Buckles EL.

Characterization of the host response in systemic Isosporosis (Atoxoplasmosis) in a colony of captive American goldfinches (*Spinus tristis*) and house sparrows (*Passer domesticus*). *Vet Pathol.* 2011;48(5):985-992.

4. Evans NP, Evans RD, Fitz-Coy S, Pierson FW, Robertson JL, Lindsay DS. Identification of new morphological and life-cycle stages of *Cochlosoma anatis* and experimental transmission using pseudocyst. *Avian Dis*. 2006;50(1):22-27.

5. Udoumoh AF, Nwaogu IC, Igwebuike UM, Obidike IR. Pre-hatch and post-hatch development of the bursa of Fabricius in broiler chicken: a morphological study. Vet Res Forum. 2022 Sep;13 (3):301-308.

6. Pecka Z, Nohýnková E, Kulda J. Ultrastructure of *Cochlosoma anatis* (Kotlán, 1923) and taxonomic position of the family Cochlosomatidae (parabasala: Trichomonadida). *Eur J Protistol*. 1996;32(2):190-201.

7. Udoumoh AF, Nwaogu IC, Igwebuike UM, Obidike IR. Pre-hatch and post-hatch development of the bursa of Fabricius in broiler chicken: a morphological study. Vet Res Forum. 2022 Sep;13 (3):301-308.

CASE IV:

Signalment:

5-year-old, female-spayed , mixed-breed dog (*Canis familiaris*)

History:

The patient presented to a veterinary medical teaching hospital with left-sided hemiparesis, acute onset of bilateral blindness and circling to the right. Bloodwork revealed no significant abnormalities. Upon hospital admission, the patient's obtundation progressed to stupor so euthanasia was elected . The owners reported that the patient had no significant clinical history other than diagnosis of and recovery from canine distemper at 1-year-old.

Gross Pathology:

No significant gross abnormalities were appreciated.

Laboratory Results:

Canine distemper virus (Brain): Neurons and, less frequently, astrocytes exhibit strong cytoplasmic immunoreactivity.

Special stains: Luxol fast blue (Brain): Decreased positive staining supports demyelination of the cortical white matter.

Microscopic Description:

The slide contains one section of cerebrum at the level of the basal nuclei and corpus callosum. The white matter and, to a lesser extent, grey matter are moderately vacuolated and hypercellular. Vacuolation is defined by clear, well-demarcated vacuoles that reach up to 50 um diameter

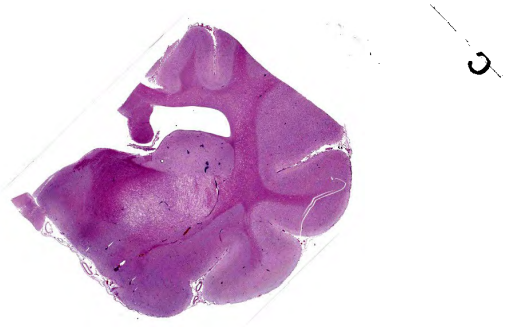

Figure 4-1. Cerebrum, dog: A section of cerebrum through the corpus callosum and thalmusis submitted for examination. At subgross magnification perivascular cuffing of thalamic vessels is visible. (HE, 8X)

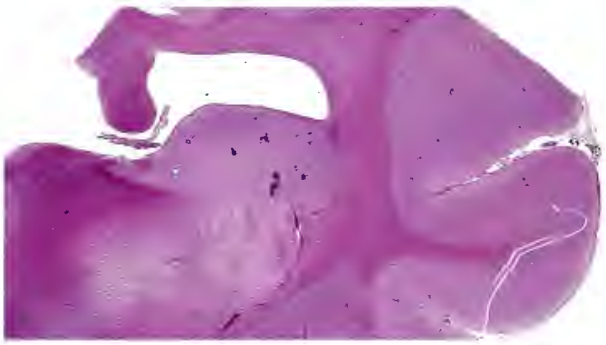

Figure 4-2. Cerebrum, dog: At low magnification, marked spongiosis of the thalamic white matter and to a lesser extent, the internal capsule is visible. (HE, 12X)

(spongiosis). The neuropil is additionally disrupted by increased numbers of proliferating glial cells (gliosis). Parenchymal vacuolation and gliosis of the grey matter is less severe than that described within the white matter. Neurons and astrocytes occasionally contain round intranuclear inclusion bodies that are approximately 5 um diameter and brightly eosinophilic. Morphologically-similar, intracytoplasmic inclusions are rare. Perivascular cuffing throughout the grey and white matter is characterized by mild to marked expansion of Virchow-Robbins space by small numbers of densely-packed lymphocytes and fewer plasma cells.

Contributor's Morphological Diagnosis:

Brain: Severe multifocal demyelination with lymphoplasmacytic perivascular encephalitis, gliosis and neuronal and astrocytic, intranuclear and intracytoplasmic inclusion bodies.

Contributor's Comment:

This case highlights an excellent example of canine distemper virus infection in the brain of a dog. Astrocytes and neurons contain both intracytoplasmic and intranuclear viral inclusion bodies, which are characteristic of Canine Distemper Virus (CDV) and other Paramyxoviruses including Newcastle Disease Virus, Measles Virus and Rinderpest Virus. The first supplementary image illustrates immunoreactivity for CDV within a neuron. The second supplementary image highlights demyelination and status spongiosis of the white matter, which has been proposed to be consequent to the direct effect of the virus on oligodendrocytes. Interestingly, there is no ultrastructural evidence of viral infection of oligodendrocytes.[5] However, studies over the past decade have suggested that an axonopathy precedes demyelination, therefore promoting speculation that CDV encephalopathy is not a primary demyelinating disease.[4]

Four distinct presentations of CDV within the central nervous system have been characterized: classic canine distemper, multifocal distemper encephalomyelitis in mature dogs, old dog encephalitis and post-vaccinal canine distemper encephalitis.

Despite discrepancies in clinical presentation, initial disease pathogenesis remains similar across all four presentations. Upon inhalation, viral particles gain access to macrophages and epithelial cells through the signaling lymphocyte activation molecule (SLAM) and nectin-4 receptor, respectively. The virus travels within these infected leukocytes to regional lymph nodes and the tonsils, where viral replication occurs over the

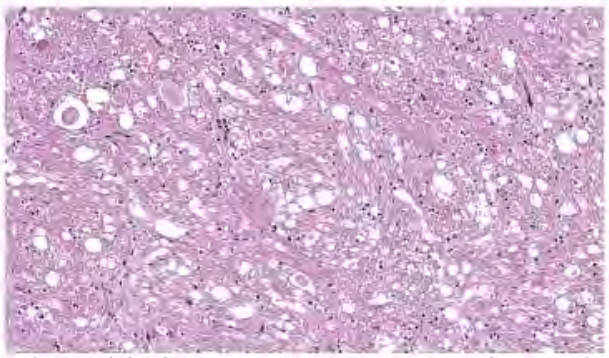

Figure 4-3. Cerebrum, dog: In areas of thalamic spongiosis, there is marked dilation of myelin sheaths with spheroid formation. (HE, 273X)

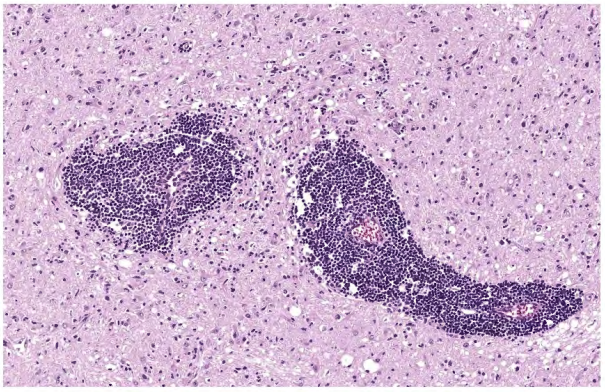

Figure 4-4. Cerebrum, dog: There is marked expansion of Virchow-Robin's spaces within the thalamus by numerous lymphocytes and plasma cells. (HE, 212X)

first twenty four hours of infection. Cell-associated viremia follows and the virus spreads to all lymphoid tissues and blood lymphocytes by five days post-infection. Viral infection of lymphoid tissues and lymphocytes results in lymphocytolysis and leukopenia, which ultimately leads to immunosuppression. Following initiation of immunosuppression, the clinical course depends largely on the host immune response, namely whether there is adequate, delayed/ intermediate or a failure of humoral/cellular immunity.

Within the presented case, the patient's advanced age and reported history of canine distemper are most consistent with old dog encephalitis (ODE). Old dog encephalitis is rarely reported and therefore its pathogenesis remains poorly understood. Nonetheless, ODE is believed to develop within immunocompetent individuals with a subclinical, persistent infection. A replication-defective virus is suspected to persist within neurons of the central nervous system.[2] Notably, a recent study provided evidence that non-cytolytic, cell-to-cell viral transmission occurs within astrocytes through a third receptor that is independent of SLAM and nectin-4.[1]

Although ODE appears to be a chronic disease, clinical presentation may be acute with sudden onset of neurologic abnormalities. This form of the canine distemper progresses over several months until the patient becomes comatose and eventually dies. At the time of this patient's workup, no effective treatment or preventative for ODE had been identified.

Contributing Institution:

University of California, Davis Veterinary Medical Teaching Hospital
https://www.vetmed.ucdavis.edu/hospital

JPC Morphologic Diagnosis:

Cerebrum: Demyelination, multifocal to coalescing, severe, with gliosis, perivascular cuffing, and neuronal and glial intranuclear and intracytoplasmic viral inclusions.

JPC Comment:

Wrapping up this conference was a stunning case of canine morbillivirus with readily identifiable viral inclusions. Canine distemper virus is a top infectious cause of demyelinating injury in dogs. This is due to direct infection and destruction of glial cells, such

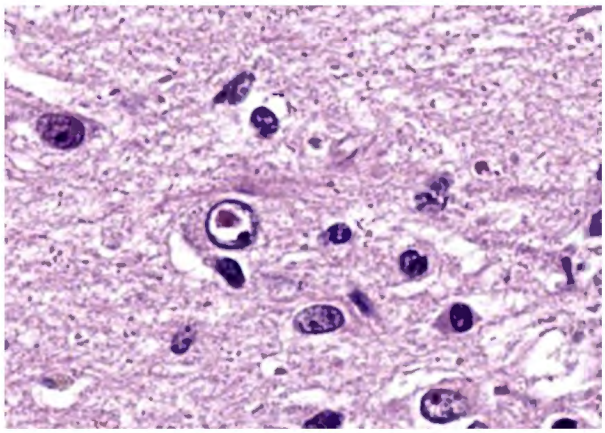

Figure 4-5. Cerebrum, dog: Rare thalamic neurons contain large 4-5um eosinophilic intranuclear viral inclusions. (HE, 565X)

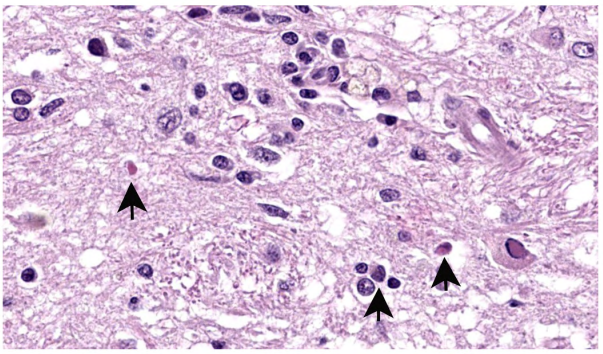

Figure 4-6. Cerebrum, dog: Rare thalamic glial cells contain smaller 2-3um eosinophilic intracytoplasmic viral inclusions (arrows). A neuron with an intranuclear inclusion is at right. (HE, 565X)

as oligodendrocytes (primary myelinating cell of the CNS), astrocytes, and microglia.[3,5] CDV can also infect neurons, including Purkinje's cells and granular cells.[3] The cerebellum is consistently affected in cases of CDV, with demyelinating lesions in the cerebellar white matter. Other common sites for similar lesions include the periventricular white matter (especially around the 4th ventricle) and the optic pathways.[3] Occasionally, the white matter of the spinal cord may be involved. The Pesavento Lab also performed IHC on this case and was able to readily demonstrate the virus within glial cells and neurons in this case.

In acute and subacute cases of CDV, astrocytes and oligodendrocytes are infected in the early demyelinating phase. This manifests predominantly as vacuolation and/or dilation of myelin sheaths, demyelination, and axonal swelling (spheroids), +/- digestion chambers. The distribution is frequently multifocal but is usually concentrated in the caudal brainstem and cerebellum. The viral inclusion bodies of CDV (known as "Lentz bodies") can be seen either in the nucleus or cytoplasm of infected cells both within the brain and in other tissues.[3,5]

"Old dog encephalitis" (ODE) is a controversial condition. The paper that describes this condition had eight dogs total in the study, with one being experimentally infected.[2] ODE is a disease of neurons and grey matter, especially in the cerebral cortex and thalamus, which contrasts starkly with the caudal brain predilection of acute/subacute CDV infection.[2] Although viral antigen was densely expressed in neurons in the ODE paper, the demyelinating component of this disease was less pronounced.[2] In cases of ODE, the cerebellum and caudal brainstem are comparatively spared.[2] As such, there is still room for interpretation on the cause of ODE and the correlation, or lack thereof, with replication-deficient CDV infection.

CDV manifests in a variety of other ways outside of the CNS due to remarkable pleocellular tropism. These include pustular dermatitis and nasodigital hyperkeratosis/ parakeratosis (also known as "hard pad disease"), enamel hypoplasia/dysplasia, ocular manifestations, myocardial necrosis, and metaphyseal osteosclerosis. Metaphyseal osteosclerosis occurs as CDV infects osteoclasts directly, causing a growth retardation lattice (also known as a "double line") within the bony trabeculae due to lack of trabecular resorption during bone maturation. Currently, it is unknown which tissue sample is the most sensitive for testing due to CDV's incredibly broad cellular tropism.

Another historical ruleout for spongiosis in the white matter of a dog that was mentioned by one participant (old enough to remember when it was banned by the FDA is hexachlorophene, which also results in a similar spongiotic and demyelinating injury).

References:

1. Alves L, Khosravi M, Avila M, et al. SLAM- and nectin-4-independent non-

cytolytic spread of canine distemper virus in astrocytes. *Journal of Virology.* 2015;89:5724-5733.

2. Axthelm M, Krakowka D. Experimental old dog encephalitis (ODE) in a gnotobiotic dog. *Veterinary Pathology.* 1998;35:527-534.

3. Carvalho OV, Botelho CV, Ferreira CG, Scherer PO, Soares-Martins JA, Almeida MR, Silva Júnior A. Immunopathogenic and neurological mechanisms of canine distemper virus. Adv Virol. 2012;2012:163860.

4. Lempp C, Spitzbath I, Puff C, et al. New aspects of the pathogenesis of canine distemper leukoencephalitis. *Viruses.* 2014;6:571-601.

5. Vandevelde M, Zurbriggen A. The neurobiology of canine distemper virus. *Veterinary Microbiology.* 1995;44:271-280.

Joint Pathology Center
Veterinary Pathology Services

WEDNESDAY SLIDE CONFERENCE 2025-2026

Conference #21 08 April 2026

Case 1:

Signalment:

5-year-old, neutered male, domestic ferret (*Mustela putorius furo*)

History:

The patient was presented to the Exotics Service for evaluation of acute non-ambulatory paraparesis. The patient had a more prolonged history of lethargy and diarrhea. Neurolocalization was to the T3-L3 spinal cord. On abdominal palpation, the bladder was markedly distended and turgid; the spleen was severely enlarged, and multiple abdominal lymph nodes were enlarged. Cytology of the spleen showed moderate plasmacytosis and extramedullary hematopoiesis. The owners elected euthanasia due to concerns for quality of life.

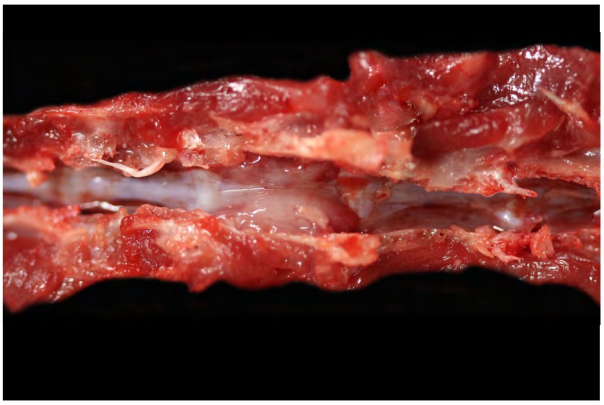

Figure 1-1: Spinal column, ferret: A 0.6cm long, soft, light purple grey, bilobed mass arises from the ventral vertebral body of T11 and protrudes into the spinal canal. (*Photo courtesy of*: Schwarzman Animal Medical Center, 510 East 62nd St. New York, NY 10065. http://www.amcny.org)

Gross Pathology:

Associated with the vertebral body and the ventral aspects of the pedicles of T11 and protruding into the vertebral canal was a 0.6 cm long, soft, light purple grey, bilobed mass that surrounded and compressed the local segment of spinal cord. With examination of the external surface, an approximately 1.4 cm long segment of the regional spinal cord was streaked white, red, and dark red (hemorrhages). After formalin fixation and decalcification, the T11-L1 vertebrae was sectioned serially. The cut surfaces of the T11 vertebral body and portions of the pedicles were expanded and replaced by a poorly demarcated, soft, shiny, white tissue inconsistently mantled by an irregular brown rim that filled the medullary cavity with loss of the trabecular architecture. The regional cortical bone was irregular and multifocally thinned.

In addition, the spleen was severely enlarged (95.6 g; 6.8% of the body weight) with dozens of randomly distributed sharply demarcated, pinpoint to 0.6 cm in diameter, oval to spherical, soft, white foci and nodules.

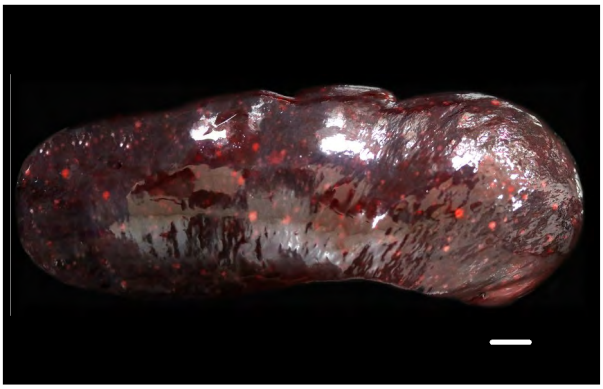

Figure 1-2: Spleen, ferret: There is marked splenomegaly and the parenchyma contains numerous cellular foci ranging up to 0.6cm in diameter. (*Photo courtesy of*: Schwarzman Animal Medical Center, 510 East 62nd St. New York, NY 10065. http://www.amcny.org)

Laboratory Results:

Pertinent Hematology and Biochemistry:

RBC - 11.94 M/µL (*6.60 - 12.20 M/µL*)
Calcium - 11.5 mg/dL (*7.6 - 10.4 mg/dL*)
Total Protein - 8.7 g/dL (*4.8 - 8.3 g/dL*)
Albumin - 3.6 g/dL (*2.6 - 4.0 g/dL*)
Globulin - 5.1 g/dL (*2.2 - 4.3 g/dL*)
Albumin: Globulin Ratio - 0.7
Cholesterol - 126 mg/dL (*100 - 300 mg/dL*)

Urine Protein Electrophoresis:

At the time of euthanasia, urine protein electrophoresis (IDEXX Diagnostic Laboratories) was pending. The following day, a large peak in the beta fraction (284.74 mg/dL) that appears relatively narrow supporting a possible monoclonal gammopathy was reported. Urine electrophoretograms are best interpreted in correlation with serum electrophoresis to confirm monoclonal gammopathy.

Urine Protein - 340.6 mg/dL
Albumin (EPH) - 11.24 mg/dL
Alpha Globulin % - 27.59 mg/dL
Beta Globulin - 284.74 mg/dL
Gamma Globulin - 17.03 mg/dL

Postmortem Cytology:

Vertebral foramen mass Touch imprints of the surface of the T11 vertebral canal mass are composed of sheets of markedly pleomorphic neoplastic round cells. Round cells have moderate to large amounts of deep to pale blue cytoplasm with variable nuclear-to-cytoplasmic ratio. These cells typically contain a single, eccentrically marked cellular and nuclear pleomorphism. There are rare atypical mitotic figures.

Microscopic Description:

T11 Vertebra: Replacing and effacing the medullary cavity and multifocally infiltrating and destroying the cortical bone to extend into the vertebral foramen and local paravertebral stroma is a densely cellular, unencapsulated, poorly demarcated, infiltrative mass comprised of closely packed round cells arranged in sheets supported by a fine, fibrovascular stroma. Neoplastic round cells have distinct cell borders, moderate amounts of pale eosinophilic cytoplasm with inconsistent perinuclear clearing (Golgi apparatus), and single nucleus. Nuclei are round, paracentral to eccentric, and have coarse to clumped chromatin and up to one prominent nucleolus. Anisocytosis and anisokaryosis are marked, with up to 6-fold difference in nuclear side, as well as occasional megakaryocytic cells and bi- and multinucleated neoplastic cells. Fifteen mitotic figures are seen in 10 [40x x FN22] HPF. Infrequent individual necrotic neoplastic cells are scattered throughout the tumor. Approximately 40**%** of the vertebral cortical bone is lytic due to tumor infiltration and is multifocally replaced by reactive fibroblasts and a fibrocol-

lagenous stroma. The retained cortical bone is multifocally thinned and there is resorption and remodeling characterized by scalloped surfaces and shelves of woven bone bordered by neoplastic cells and reactive fibroblasts. At the periphery of the tumor and within regions of bone resorption there are minimal hemorrhages.

Contributor's Morphologic Diagnoses:

T11 VERTEBRA, MASS REGION: Malignant plasma cell tumor (multiple myeloma/ plasma cell myeloma) with regional cortical bone, skeletal muscle, and adipose tissue invasion; bone loss, resorption, and remodeling; and myelophthisis [mitotic count = 15 mitotic figures in 10 [40x x FN22] HPF]
SPINAL CORD, T11 REGION (slide not included):

1. Hemorrhages, acute, multifocal to coalescing, moderate
2. Axonal degeneration, multifocal to coalescing (ventral and lateral funiculi), severe with markedly dilated myelin sheaths, multifocal intravacuolar fragmented myelin and macrophages (ellipsoids/ digestion chambers); multifocal swollen axons (spheroids); and marked reactive glial cells [compression myelopathy]

SPLEEN (slide not included):

1. Multifocal to coalescing malignant plasma cell tumors (multiple myeloma/plasma cell myeloma), multifocal with atypia [mitotic count = 11 mitotic figures in 10 [40x x FN22] HPF]
2. Extramedullary hematopoiesis, chronic, multifocal, moderate

Contributor's Comment:

The submitted ferret's presentation of acute non-ambulatory paraparesis and distended urinary bladder with large residual urine volume, along with reported neurolocalization, supported a T3-L3 myelopathy of unclear origin. Potential differentials for this ferret's clinical presentation of acute paresis included metabolic disease (i.e., insulinoma, hyperadrenocorticism, prolonged estrus), neoplasia (i.e., plasma cell tumor (solitary osseous plasmacytoma, multiple myeloma), lymphoma, chordoma, osteoma, osteosarcoma), Aleutian disease, intervertebral disc disease, vertebral congenital malformations, and primary myelitis.[11] Autopsy confirmed a mass originating within the T11 vertebra associated with marked osteolysis and extension into the vertebral canal, as well as extension into the surrounding fibrous and adipose tissue stroma. Compressive myelopathy secondary to tumor growth was confirmed. Consistent with the antemortem abdominal ultrasound, the spleen was severely enlarged with multi-

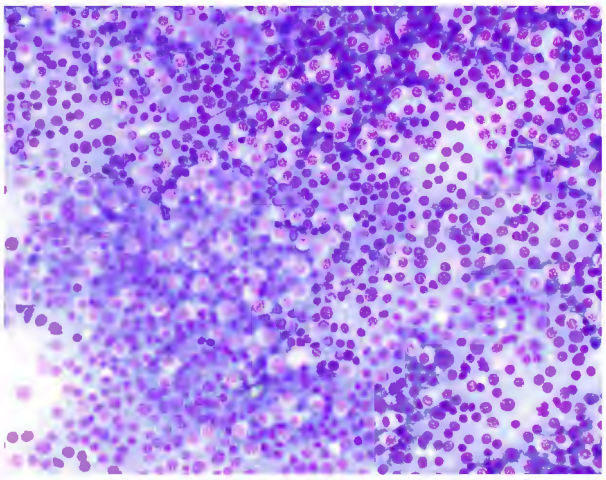

Figure 1-3: Vertebral mass, ferret. A touch impression demonstrates numerous round cells with excentric moderately anisokaryotic nuclei. (*Photo courtesy of*: Schwarzman Animal Medical Center, 510 East 62nd St. New York, NY 10065. http:// www.amcny.org) (Wright-Giemsa 1000X)

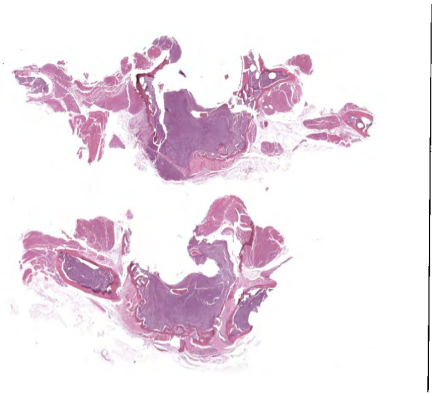

Figure 1-4: Thoracic vertebra, ferret: At subgross magnification, an infiltrative neoplasm effaces the medullary cavity and cortex of the ventral vertebral body, and extends into the underlying epaxial muscle and soft tissue and into the overlying spinal canal. (HE, 10X)

ple white foci and nodules. Microscopic examination confirmed a neoplastic population of plasma cells in both the vertebrae and spleen suggestive of multiple myeloma/ plasma cell myeloma. After gross postmortem examination, findings of the previously submitted urine electrophoresis reported a relatively narrow, large peak in the beta fraction supportive of a possible monoclonal gammopathy. An additional finding in this patient of unclear clinical significance was a single pancreatic neuroendocrine tumor, which was confirmed as an insulinoma with immunohistochemistry for insulin.

Tumors originating from plasma cells include extramedullary plasmacytoma, solitary osseous plasmacytoma, and multiple myeloma (plasma cell myeloma). Plasmacytomas are the most common plasma cell tumors in dogs, and are described frequently in cats and uncommonly in other species.[15,32] Plasmacytomas are typically solitary and are most commonly described in the skin/ subcutis, oral cavity, gastrointestinal tract (particularly colorectal region), but can occur in any organ.[7,9,18,24,30,32,33] Plasmacytomas are typically benign and surgical excision is generally considered curative.[5,7,9,24,32,33] However, infrequent reports of plasmacytomas displaying relatively more aggressive behavior have been described in both dogs and cats.[6,9,32] Cutaneous plasmacytomas over the face can display local tissue invasion, including into the underlying bone.[33] Rare cases of plasmacytoma with associated monoclonal gammopathies are reported in dogs but multiple myeloma should be favored in cases of plasma cell tumor with monoclonal gammopathy.[7,15,32] Solitary osseous plasmacytomas are rare neoplasia reported in people, dogs, and ferrets,[15,25,29] and in humans may represent an early stage of multiple myeloma.[22,25,29] Solitary osseous plasmacytomas represent lytic, locally destructive tumors affecting a single site and not associated with gammopathy,[15,22,25,29] and have been reported in the vertebrae, jaw, carpus, long bones, and ribs of dogs.[25] Multiple myeloma (plasma cell myeloma) is a rare neoplasm of malignant plasma cells arising in the bone marrow or extramedullary sites (i.e., spleen and liver) associated with hyperglobulinemia.[5-8,14-16,20,23,26,29,31-33] Extramedullary site involvement is more common in the cat.[13,29,32,33] The term myeloma-related diseases (MRD) has been adopted in humans and cats, to describe a group of plasma cell or immunoglobulin-secreting B-cell tumors, of which multiple myeloma is one.[1,8,13,14,15,22,32] Multiple myeloma is more commonly reported in dogs and to a lesser extent in cats, including a non-domestic feline.[6,7,13,20,24,26,29,32] Multiple myeloma represents approximately 0.3-1**%** and <1% of all malignancies in dogs and cats, respectively.[1,6,7,14,21,23,26,29,31,34] Cases in other species (horses, cows, pigs, rabbits) are uncommon.[5,7,12,20,23,24,32] Multiple myeloma is more common in middle aged to older animals1,[5,16,22,23,26,29,34]; however, an atypical

presentation in three juvenile dogs have been reported.[22,34] There is no breed or sex predilection in dogs.[31,32] In cats, a male predominance has been reported.[6,14,23,29] In dogs, altered cell cycle protein cyclin C expression may be associated with tumor development.[32]

A common, but not consistent, feature of multiple myeloma is the production of immunoglobulin (Ig) or Ig fragments (paraprotein or M-protein) leading to a gammopathy on electrophoresis, which is most typically monoclonal and less commonly biclonal.[5-8,14,16,21-23,26,29,31-33,36] Light-chain fragments, unattached to heavy chain portions, are filterable though the glomeruli leading to Bence-Jones proteinuria.[6-8,21,22,29,32] Evaluation of densitometric M-protein concentration can be used to evaluate response to therapy.[21,22] Non-secretory myeloma, lacking a gammopathy, is seen in small percentage of cases.[32,33] Other conditions that can be associated with monoclonal gammopathies include chronic infections (i.e., ehrlichiosis and other tick-borne disease, leishmaniasis, chronic pyoderma, and FIP) and other neoplastic processes (i.e., B-CLL, B-cell lymphoma).[7,23,32-33] The most common clinical signs seen with multiple myeloma are non-specific and include pallor, lethargy, listlessness/weakness, inappetence, anorexia, weight loss, and intermittent vomiting.[14,23,26,29] More specific clinical signs depend on distribution of bone lesions and visceral organ involvement, as well as the clinical ramifications of hyperglobulinemia and hypercalcemia. Pain and lameness are common complaints in dogs due to bone lesion(s).[7,8,32,33] With vertebral column involvement, spinal pain, proprioceptive ataxia, paraplegia, and other neurologic manifestations can be seen.[6,29,33,36] Osteolytic lesions are less common in cats.[1,14,19,22,31,32] CBC and biochemical changes include anemia (most commonly non-regenerative, normocytic, normochromic), thrombocytopenia, various leukopenias, hypercalcemia (related to osteolysis and/or PTHrP production), hyperglobulinemia, hypoalbuminemia, hypercholesterolemia, elevated ALP, and azotemia.[6,8,14,16,23,26,29,31-34,36] Circulating neoplastic cells are rarely reported with multiple myeloma.[7,16,23,29,32] Thrombocytopenia, as well as altered platelet function due to paraproteins, can lead to bleeding diathesis.[23,26,32,33] Precipitation of the paraprotein and immunoglobulins (cryoglobulinemia) at cold temperatures can lead to ischemia damage, as well as bleeding tendencies.[7,28] Polyuria and polydipsia can be seen secondary to hypercalcemia, light-chain proteinuria, or amyloidosis.[33] Associated disease manifestations attributed to hyperglobulinemia, paraproteinemia, and biochemical alterations include hyperviscosity syndrome, renal disease (including glomerulonephritis and nephrotic syndrome), light chain deposition disease, extra-tumoral amyloidosis, hypertension, heart failure, immunosuppression, and retinopathy or retinal hemorrhages.[5,7,14,19,23,26,28,29,31,32,36] Myelomatous pleural effusion is a rare clinical manifestation described in people and cats.[1,14] When present,

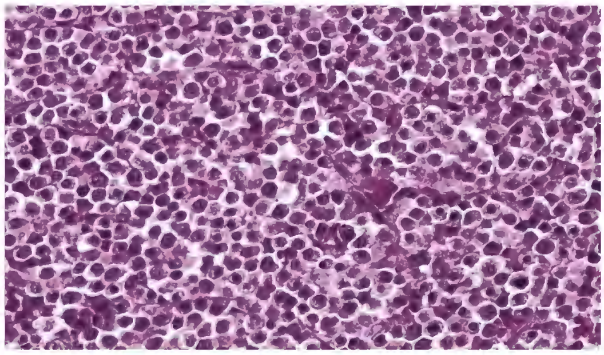

Figure 1-5 Thoracic vertebra, ferret: High magnification of neoplastic cells closely mirrors the cytologic presentation of sheets of round cells with moderate anisokaryosis and excentric nuclei. (HE, 1127X)

osteolytic bone lesions tend to involve areas of active hematopoiesis.[13,29] In small animals, the vertebra (particularly thoracolumbar), femur, pelvis, humerus, skull, and ribs are the most common sites.[6,8,29,34] On imaging, bone lesions are classified most commonly as discrete, "punched out" lytic lesions, typically in multiple bones, with variable sclerotic margins and periosteal reactions.[6,8,16,23,29] Less common imaging patterns include permeative lysis, small lytic foci, homogenous, soft tissue attenuating intramedullary masses, and generalized osteoporosis.[8,29] Pathologic fractures can be seen.[6-8,14] In one case series of bone lesions of computed tomography (CT) in dogs, all the studied dogs had axial skeleton involvement and 69% had concurrent appendicular skeleton lesions.[8]

On gross examination of affected bones, the trabecular bone/medullary cavity are replaced and filled by a soft, fleshy to gelatinous, dark red to grey-pink nodules and masses.[6,29] Histology shows focal or locally extensive solid tumors of densely packed neoplastic plasma cells arranged in sheets, cords, and packets that replace the hematopoietic cells and adipose tissue of the medullary cavity and are supported by a fine fibrous stoma.[6,7,16,29,32] Cortical bone destruction with/or without local soft tissue invasion can be seen.[29] Cellular features of plasma cell differentiation include round cells with moderate to large amounts of amphophilic to basophilic cytoplasm with perinuclear clearing (Golgi apparatus).[7,9,16,18,22,30,32] Nuclei are paracentral to eccentrically placed with clumped chromatin that aggregate in the center or along the nuclear membrane ("clockface" pattern).[7,9,16,18,22,32] Mott cells with prominent cytoplasmic vacuoles (Russel bodies) containing immunoglobulins and may result from altered intracellular protein transport.[18,22,32] Due to differences in stain protocols, these vacuoles can range from semi-clear, to light blue, to pink.[22,32] "Flame cells" are characterized by an outer rim of densely purple or eosinophilic cytoplasm,[32] with light to bright pink projections/blebs or fringe due to accumulation of immunoglobulins.[7,22,23,29] Less well-differentiated tumors display a wider range of cellular and nuclear pleomorphism, variable nuclear-to-cytoplasmic ratio, increased numbers of binucleate and multinucleated cells, and lack of Golgi perinuclear clearing.[29,32] Plasma cell tumors infrequently have intratumoral light chain amyloid (AL-amyloid).[6,7,18,19,22,24,30,32] Erythrophagocytic plasma cell tumors have been described.[3,26] With less differentiated forms, immunohistochemistry (IHC) can be useful to rule-out other round cells tumors. In dogs, MUM1 is the most specific marker for plasma cell tumors.[6,7,9,16,24,26,31-34] Multiple myeloma oncogene 1 (MUM1) is an interferon regulatory transcription factor involved in immunoglobulin light-chain re-arrangement and production of plasma cells.[16,22,24,31,32] Additional tumors that can infrequently be immunoreactive to MUM1 include B-cell lymphoma and anaplastic lymphoma.[24,32] Less consistently plasma cell tumors will stain with λ and κ light chains, Ig heavy chains, CD79a, and CD20.[9,19,22,24,32,33] In one study of canine plasmacytomas, 93.5% of tumors were immunoreactive to MUM1, while only 56.2% and 19.4% of tumors were reactive with CD79a and CD20, respectively.24 In a case series in cats, 32% of MRDs were immunoreactive to CD79+.[19] Methyl green pyronine histochemical stain inconsistently highlight plasma cells.[9]

Traditionally, the presence of multiple osteolytic lesions was strongly suggestive

of multiple myeloma in dogs; however, disease manifestation in cats are different than those reported in both dogs and humans where cats with MRDs typically present with paraproteinemia and have less frequent bone marrow involvement.[1,14,19,22,31,32] In two retrospective studies of MRDs in cats, only a percentage of cats displayed osteolytic lesions (58.3% of studied cats) or bone marrow plasmacytosis (63% of studied cats), and most cats had non-cutaneous, extramedullary plasma cell tumors, typically in the liver and/or spleen in those evaluated for them.[14,23] Thus, extramedullary neoplastic transformation may be more common in cats with MRD than other species,[1, 19, 22, 31] but it is unknown in feline MRD affecting both compartments concurrently arise initially in extramedullary sites with later bone marrow infiltration or extramedullary tumors represent metastases.[14,19] Historically, the diagnostic criteria of multiple myeloma required the presence of two or more of the following features: 1) bone marrow with >20% of plasma cells, 2) osteolytic lesions, 3) serum or urine monoclonal gammopathy, and 4) light-chain proteinuria (Bence-Jones proteinuria).[1,5,7,8,14,16,17,21-24,29,31,33,34,36] Recent studies show the diagnostic criteria of Bence-Jones proteinuria can be fulfilled by documenting free light-chains (fLCs) in urine and/or serum.[8,22,34] Recently, the diagnostic criteria in humans has been updated to add weight to each criteria, as well as incorporate advanced imaging findings, signs of organ-damage, presence of "myeloma-defined events" (hypercalcemia, renal disease, anemia, and bone lysis), and biomarkers of malignancy; and in this updated criteria the threshold of plasmacytosis can be lowered to >10% depending on the clinical picture.[22,23,28] Based on newer information, the threshold for plasmacytosis could be lowered (>10%) in feline cases with visceral organ involvement, presenting hyperglobulinemia or paraproteinemia, and with atypical plasma cell morphologies.[1,14,16,23,29,33] In a retrospective study of multiple myeloma in 16 cats, bone marrow plasmacytosis, ranging from 13-99%, was present in 93.3% of the examined cats, and the majority of these cases (83.3%) had immature and atypical morphologies.[23] The authors advocated for a modified diagnostic criteria in cats to include consideration of plasma cell morphology and visceral organ involvement.[23] In a multi-institutional retrospective study of feline MRDs, of 17 cats with bone marrow involvement 64.7% of cats had plasmacytosis of >10% and 35.3% of cats had bone marrow plasmacytosis ranging from 5-10% with marked cytonuclear atypia.[14] In this series, bone marrow plasmacytosis was rarely seen in cats without splenic or liver involvement (9% of the study population).[14] The authors of this study emphasized the importance of extramedullary involvement and bone marrow cellular atypia as part of the criteria of diagnosis in cats, even when bone marrow plasmacytosis between 5-10%.[14] Current recommendations in cats include at least two of the following: 1) >10% bone marrow plasmacytosis or >5% atypical plasma cells, 2) paraproteinemia, 3) osteolytic lesions, 4) light chain proteinuria, and 5) visceral organ involvement.[14,23,33]

The two most common neoplasms in domestic ferrets arise in the endocrine system (i.e., pancreatic neuroendocrine tumors and adrenal cortical tumors).[2,27,35] The most common hematologic malignan-

cy in ferrets is lymphoma, and spinal lymphoma can present with neurologic dysfunction similar to the submitted case.[11,27,35] Chordomas are the most common neoplastic process in the musculoskeletal system of ferrets, they are low grade malignancies derived from the notochord and can be associated with locally destructive lesions in the vertebral body at any segment of the spinal column and be associated corresponding neurologic symptoms.[27,35] Like the submitted case which had concurrent plasma cell tumors and insulinoma, multiple distinct, synchronous tumors are common in ferrets and up to 20% of ferrets are diagnosed with multiple simultaneous tumors.[27] Like the submitted case, reports of malignant plasma cell tumors, including plasma cell myeloma/multiple myeloma, in ferrets are limited, but in reports hindlimb ataxia and paresis were common clinical complaints and association with vertebral bone tumors was confirmed in multiple cases.[5,17,20,35] Plasma cell tumors have been reported in the bone (most commonly the vertebrae), spleen, liver, lymph node, as well as multicentric disease in ferrets.[2,5,17,20] In addition, a case report of a solitary osseous plasmacytoma associated with secondary vertebral fracture and without gammopathy and extramedullary involvement has been reported in a ferret that presented with non-ambulatory paraparesis, decreased postural reactions, upper motor neuron bladder, and pain.[15] In one case series of malignant plasma cells tumors in six ferrets, clinical signs included hindlimb ataxia and paresis (most common), urinary system signs (either primary or neurologic), and pain.[5] Reported hematologic alterations were variable among the reported ferrets but included anemia, neutrophilia, leukocytopenia, hyperglobulinemia, hyperphosphatemia, hypoglycemia, and hypercalcemia; however, concurrent disease processes may have been a contributing factor in the study cohort (i.e., adrenal disease, inflammatory bowel disease, lymphoma, hemangiosarcoma, insulinoma).[5] In this study population, hyperglobulinemia was most common and monoclonal gammopathy was confirmed in one ferret.[5,35] At the time of diagnosis in this cohort, extramedullary disease was identified in 5/6 cases and dissemination to more than four locations was seen in majority of these.[5] Based on this patient population, malignant plasma cell tumors are aggressive in ferrets and rapidly progressive with a median survival time of 107 days following diagnosis.5 In two single case reports of multiple myeloma/plasma cell myeloma in ferrets, a similar presentation of paraparesis and hind limb paralysis, related to vertebral plasma cells tumors were documented and one of these cases had confirmed extramedullary tumors including in the liver, spleen, lymph nodes, kidney, and thyroid glands.[17,20]

Contributing Institution:

Schwarzman Animal Medical Center, 510 East 62nd St. New York, NY 10065
http://www.amcny.org

JPC Morphologic Diagnosis:

Vertebra, spinal canal, and epaxial musculature: Malignant hematopoietic round cell tumor.

JPC Comment:

Dr. Derron "Tony" Alves, a former Director of the JPC's Veterinary Pathology Service and retired U.S. Army colonel, moderated

this year's 21st conference, providing participants with some fascinating lab animal case selections. This first case sparked an excellent discussion on species-specific pathology in ferrets. Ferrets are notorious for developing a variety of neoplasms, including islet cell tumors, adrenocortical tumors, and lymphoma, all of which should come to the top of the pathologist's mind when approaching ferret cases (especially in the age group of the ferret in this case. This case indeed had a concurrent insulinoma, highlighting the species' tendency toward multiple synchronous neoplasms.

Participants immediately recognized a round cell neoplasm replacing the vertebral marrow cavity. Because participants had only the H&E slide to review prior to conference, and because the neoplastic cells displayed atypia without uniformly classic plasma cell morphology, conference goers agreed that they could not definitively diagnose a plasma cell tumor from the slide alone. As such, the JPC elected to diagnose a malignant hematopietic round cell tumor which would cover both lymphoma (the most common malignancy in this species) as well as myeloma (also a hematopoetic malignancy, but which arises from the bone marrow rather than the lymph nodes or spleen). However, when the full clinical, gross, and laboratory context was revealed, including vertebral osteolysis, splenic involvement, monoclonal gammopathy, classic cytologic findings, and systemic plasma cell proliferation, the case aligned well with multiple myeloma as the final diagnosis. This contrast between what can be stated from the H&E slide alone and what can be concluded from a more comprehensive data set provided an excellent teaching moment on the importance of a full diagnostic work-up in cases such as this.

Participants reviewed the different plasma

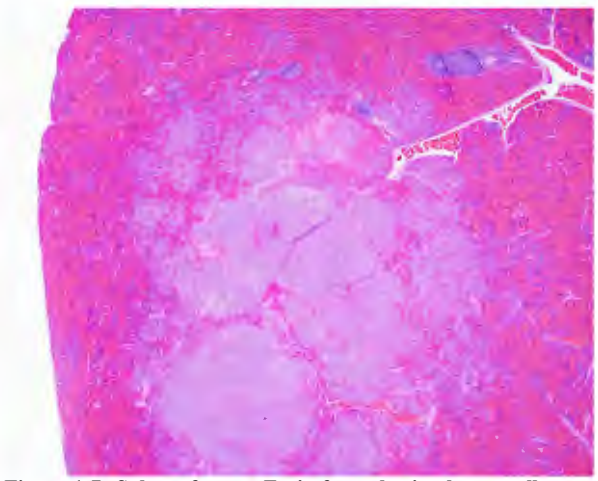

Figure 1-7: Spleen, ferret: Foci of neoplastic plasma cells are scattered throughout the splenic parenchyma. (HE, 100X) : Schwarzman Animal Medical Center, 510 East 62nd St. New York, NY 10065. http://www.amcny.org)

cell tumors, including solitary osseous plasmacytoma. This form serves as a "between" diagnosis that is neither a benign cutaneous plasmacytoma nor a fully systemic multiple myeloma. Osseous plasmacytomas are typically single, isolated bone lesions without gammopathy or visceral involvement, which did not match the full case once ancillary findings were revealed.

The slide also contained several key osseous features, including resting and reversal lines, microfractures, reactive fibrosis, and numerous osteoclasts. All of these are consistent with an aggressive, lytic bone process. Although not present on the H&E slide, the contributor provided some excellent gross and additional histologic images that showed compression myelopathy of the affected area of thoracic spinal cord, serving as a correlation to the pathogenesis of the clinical presentation in this case.

The gross image of marked a markedly enlarged spleen with multifocal, pale tan nodules prompted a strong reminder from Dr. Alves that this pattern should raise suspicion for necrotizing splenitis across species lines. The marked splenic enlargement in this spe-

cies is a common finding in older ferrets and typically associated with extramedullary hematopoesis (noted by the contributor in this case).

The group revisited the clinicopathologic hallmarks of multiple myeloma, which are covered in the contributor's excellent comment.[14,23,33] One participant provided a fantastic reminder that globulins bind calcium in the blood and, when globulins are elevated, this can produce a falsely elevated total calcium on chemistry panels. An ionized calcium is required to confirm true hypercalcemia in such cases. Participants also reviewed other causes of increased gammaglobulins across species lines, such as ehrlichiosis, leishmaniasis, FIP, and chronic pyodermas.

Participants reviewed the different plasma cell tumors, including solitary osseous plasmacytoma. This form serves as a "between" diagnosis that is neither a benign cutaneous plasmacytoma nor a fully systemic multiple myeloma. Osseous plasmacytomas are typically single, isolated bone lesions without gammopathy or visceral involvement, which did not match the full case once ancillary findings were revealed.

The slide also contained several key osseous features, including resting and reversal lines, microfractures, reactive fibrosis, and numerous osteoclasts. All of these are consistent with an aggressive, lytic bone process. Although not present on the H&E slide, the contributor provided some excellent gross and additional histologic images that showed compression myelopathy of the affected area of thoracic spinal cord, serving as a correlation to the pathogenesis of the clinical presentation in this case.

The gross image of marked a markedly enlarged spleen with multifocal, pale tan nodules prompted a strong reminder from Dr. Alves that this pattern should raise suspicion for necrotizing splenitis across species lines. The marked splenic enlargement in this species is a common finding in older ferrets and typically associated with extramedullary hematopoesis (noted by the contributor in this case).

The group revisited the clinicopathologic hallmarks of multiple myeloma, which are covered in the contributor's excellent comment.[14,23,33] One participant provided a fantastic reminder that globulins bind calcium in the blood and, when globulins are elevated, this can produce a falsely elevated total calcium on chemistry panels. An ionized calcium is required to confirm true hypercalcemia in such cases. Participants also reviewed other causes of increased gammaglobulins across species lines, such as ehrlichiosis, leishmaniasis, FIP, and chronic pyodermas.

References:

1. Amalbert T, Canonne AM, and Beguin J. Myelomatous pleural effusion in a cat diagnosed with multiple myeloma. *Journal of Feline Medicine and Surgery Open Reports.* 2023;9 (1):20551169221134094.
2. Avallone G, Forlani A, Tecilla M, et al. Neoplastic diseases in the domestic ferret (*Mustela putorius furos*) in Italy: Classification and tissue distribution of 856 cases (2000-2010). *BMC Veterinary Research*. 2016;12:275.
3. Barger AM, Skowronski MC, and MacNeill AL. Cytologic identification of erythrophagocytic neoplasms in dogs. *Veterinary Clinical Pathology*. 2012;41(4):587-

589.
4. Cantile C and Youssef S. Nervous System. In: Maxie MG, ed. *Jubb, Kennedy and Palmer's Pathology of Domestic Animals*. Vol 1. 6th ed. Philadelphia, PA: Elsevier Saunders; 2016:403.
5. Clagett DO, Johnston MS, and Han S. Malignant plasma cell neoplasia in ferrets: A review of 6 cases. *Journal of Exotic Pet Medicine*. 2017;26:36-46.
6. Craig LE, Dittmer KE, and Thompson KG. Bones and Joints. In: Maxie MG, ed. *Jubb, Kennedy and Palmer's Pathology of Domestic Animals*. Vol 1. 6th ed. Philadelphia, PA: Elsevier Saunders; 2016:123.
7. Durham AC and Boes KM. Bone Marrow, Blood Cells, and the Lymphoid/Lymphatic System. In: Zachary JF and McGavin MD, eds. *Pathologic Basis of Veterinary Disease*. 7th eds. St Louis, MO: Elsevier. 2022;842-843,869.
8. Harris RA, Miller M, Donaghy D, et al. Light chain myeloma and detection of free light chains in serum and urine of dogs and cats. *JVIM*. 2021;35:1031-1040.
9. Hendrick MJ. Mesenchymal Tumors of the Skin and Soft Tissue. In: Mueten DJ, ed. *Tumors in Domestic Animals*. 5th ed. Ames, Iowa: John Wiley and Sons Inc; 2017:171-172.
10. Hoim SE, Fitzgerald E, Mapletoft E, et al. Computed tomographic findings in dogs with multiple myeloma. *Vet Med Sci*. 2023;9:660-669.
11. Ingrao JC, Eschar D, Vince A, et al. Focal Thoracolumbar spinal cord lymphosarcoma in a ferret (*Mustela putorius furo*). *Can Vet J.* 2014;55:667-671.
12. Kameyama M, Ishikawa Y, Shibahara T, et al. Plasma cell myeloma producing IgG, IgM, and IgA immunoglobulins in a cow. *JVDI*. 2003;15:166-169.
13. Kappeli U, Eulenberger U, Nitzl D, et al. Clinical challenge. Multiple myeloma. *Journal of Zoo and Wildlife Medicine*. 2009;40(4):398-401.
14. Lecot L, Desmas-Bazelle I, Benjamin S, et al. Descriptive analysis and prognostic factors in cats with myeloma-related disorders: A multicenter retrospective study of 50 cases. *JVIM.* 2024;38:1693-1705.
15. Liatis T, Gardini A, Marcal VS, et al. Surgical treatment of a vertebral fracture caused by osseous plasmacytoma in a domestic ferret (*Mustela putorius furo*). *Journal of Exotic Pet Medicine*. 2019;29:200-206
16. Marchegiani A, Palumbo Piccionello A, Salvaggio A, et al. What Is Your Diagnosis? J Am Vet Med Assoc. 2016;249(1):47-9
17. Marks AL, Gaschen L, Tully TN, et al. What is your diagnosis? Plasma cell neoplasia. J Am Vet Med Assoc. 2010;237(9):1033-4.
18. Mauldin EA and Peters-Kennedy J. Integumentary System. In: Maxie MG, ed. *Jubb, Kennedy and Palmer's Pathology of Domestic Animals*. Vol 1. 6th ed. Philadelphia, PA: Elsevier Saunders; 2016:735.
19. Mellor PJ, Haugland S, Smith KC, et al. Histopathologic, Immunohistochemical, and Cytologic Analysis of Feline Myeloma-Related Disorders: Further Evidence for Primary Extramedullary Development in the Cat. *Vet Pathol.* 2008;45:159-173.

BK, et al. Solitary osseous plasmacytoma in dogs: 13 cases (2004-2019). *JSAP.* 2021;62:1114-1121.
26. Romanelli P, Recordati C, Rigamonti P, et al. Erythrophagocytic multiple myeloma in a dog. JVDI. 2022;34(4):718-722.
27. Schoemaker NJ. Ferret Oncology: Diseases, Diagnostics, and Therapeutics. *Vet Clin Exot Anim*. 2017;20:183-208.
28. Spyropoulou M, Montanes-Sancho I, Gow AG, et al. Cryoglobulinemia associated with multiple myeloma in dog presenting with epistaxis and skin lesions. *Veterinary Medicine and Science*. 2024;10:e70084.
29. Thompson KG and Dittmer KE. Tumors of Bone. In: Mueten DJ, ed. *Tumors in Domestic Animals*. 5th ed. Ames, Iowa: John Wiley and Sons Inc;2017:412-414.
30. Uzal FA, Plattner BL, and Hostetter JM. Alimentary System. In: Maxie MG, ed. *Jubb, Kennedy and Palmer's Pathology of Domestic Animals*. Vol 2. 6th ed. Philadelphia, PA: Elsevier Saunders;2016:27-28.
31. Valente PCLG, Peleteiro MC, Dias MJ, et al. Multiple myeloma in dogs: Use of the cell block technique as a new diagnostic tool. Vet Clin Pathol. 2024;53(1):93-98.
32. Valli VE, Bienzle D, Meuten DJ, and Linder KE. Tumors of the Hemolymphatic System. In: Mueten DJ, ed. *Tumors in Domestic Animals*. 5th ed. Ames, Iowa: John Wiley and Sons Inc;2017:218-225.
33. Valli VEO, Kiupel M, and Bienzle D. Hematopoietic System. In: Maxie MG, ed. *Jubb, Kennedy and Palmer's Pathology of Domestic Animals*. Vol 3. 6th ed. Philadelphia, PA: Elsevier Saunders;2016:137,226-228.
34. Wachowiak IJ, Moore AR, Avery A, et al. Atypical multiple myeloma in 3 young dogs. *Veterinary Pathology*. 2022;59 (5):787-791.
35. Williams BH and Wyre NR. Neoplasia in Ferrets. *Ferrets, Rabbits, and Rodents*. 2020;92-108.
36. **Wyatt S, De Risio L, Driver C, et al. Neurologic signs and MRI findings in 12 dogs** with multiple myeloma. *Vet Radiol Ultrasound*. 2019;60:409-415.

CASE II:

Signalment:

Adult male Fischer 344 (F344) rat (*Rattus norvegicus*)

History:

This rat was part of a research study and was exposed to a chemical on 10/20/2014. He was then found dead on 11/28/2024.

Gross Pathology:

Received for autopsy is a 389g, adult, male Fischer 344 rat with a body condition score of 3/5, adequate subcutaneous and visceral fat, and in full rigor mortis. There is mild autolysis. There is multifocal, patchy thin-

Figure 2-1: Abdominal viscera, rat: The markedly and irregularly distended urinary bladder is ruptured with an adherent blood clot. (*Photo courtesy of:* Comparative Pathology Department at the Institute of Chemical Defense, https://usamricd.health.mil/)

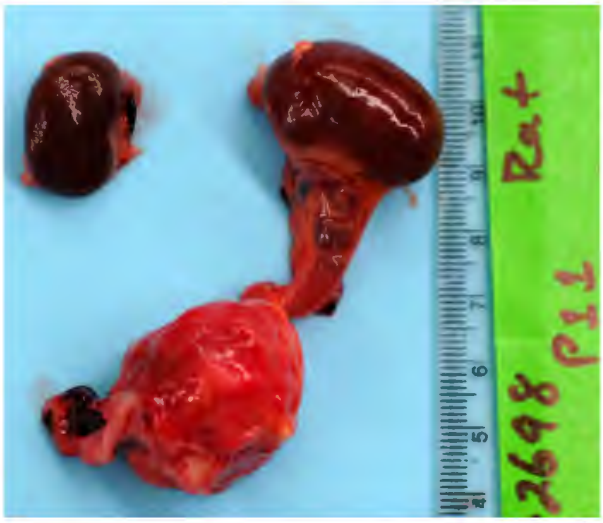

Figure 2-2: Kidneys, ureter, urinary bladder, rat: The left kidney is 3 x 2 x 1.5 cm and the left ureter is 5 mm in diameter (hydronephrosis and hydroureter). The urinary bladder is expanded by a 2.5 cm, round, firm, mass. (*Photo courtesy of:* Comparative Pathology Department at the Institute of Chemical Defense, https://usamricd.health.mil/)

ning of the haircoat along the dorsum with multifocal scabs; a section is taken for histology. The abdominal cavity feels doughy. Upon incising the abdominal cavity, there is approximately 10 mL of serosanguineous fluid in the abdomen (uroperitoneum). The lungs collapse when the diaphragm is cut; they are inflated with 10 mL of 10% NBF. The stomach is full of yellow-gray ingesta. There is scant to moderate amounts of green-brown digesta in the moderately autolyzed small intestines. The cecum is full of dry, green-gray digesta. The distal colon in empty and the proximal colon contains few fecal pellets. The urinary bladder is ruptured with clotted blood adhered to the edges of the rupture. On the dorsal left side of the urinary bladder is a 2.5 cm, round, firm, mass that is pale white and homogenous with central necrosis on cut section. The left kidney is 3 x 2 x 1.5 cm and the left ureter is 5 mm in diameter (hydronephrosis and hydroureter). There are multifocal red-orange, 1-3 mm foci of neoplasia in the right testicle (suspect interstitial cell tumor). All other organs examined appear grossly normal.

Laboratory Results:

Cytologic findings (touch impression of the mass): This fair quality, highly cellular cytologic specimen is composed of a mixture of rafts of tightly adherent polygonal epithelial cells, smaller clusters of epithelial cells, and occasional individualized epithelial cells. There is marked anisocytosis and anisokaryosis with cells measuring 3-12 erythrocytes in diameter and nuclei measuring 2-8 erythrocytes in diameter. Cells have abundant light blue, occasionally vacuolated cytoplasm. Nuclei have reticulated chromatin and occasional prominent nucleoli. Many cells exhibit high nuclear:cytoplasm ratio. There are occasional bi- and multi-nucleated cells. This is on a background of abundant cellular debris, viable and degenerate neutrophils, cocci and coccobacilli bacteria, macrophages, stain precipitate, and naked and streaming nuclei.

Microscopic Description:

Urinary bladder: Arising from urothelium, infiltrating and expanding the lamina propria, and surrounding the ureter is a non-

Figure 2-3: Urinary bladder and kidney, rat A section of urinary bladder with a large transmural neoplasm (left) and a concave section of hydronephrotic kidney are submitted for examination. (HE, 9X)

encapsulated, well demarcated, moderately cellular neoplasm composed of polygonal cells arranged in nests on a fibrovascular stroma. Each neoplastic cell has indistinct cell borders, a moderate amount of pale basophilic cytoplasm, with a single misshapen nucleus with finely stippled chromatin and 1 -3 distinct nucleoli. Anisocytosis and anisokaryosis are moderate. There are 2 mitotic figures per 2.37mm^2. The neoplastic nests are often separated by a robust scirrhous response. Multifocally the neoplastic cells are replaced by eosinophilic, amorphous material (necrosis).

Prostate gland: Multifocally, prostatic glands are filled with cellular debris and degenerate neutrophils.

Kidney: There is severe dilation of the renal pelvis with marked thinning of the renal medulla and cortex.

Contributor's Morphologic Diagnosis:

Urinary bladder: Urothelial cell carcinoma, *Rattus norvegicus*.

Kidney: Hydronephrosis, severe.

Prostate gland: Prostatitis, neutrophilic, mild.

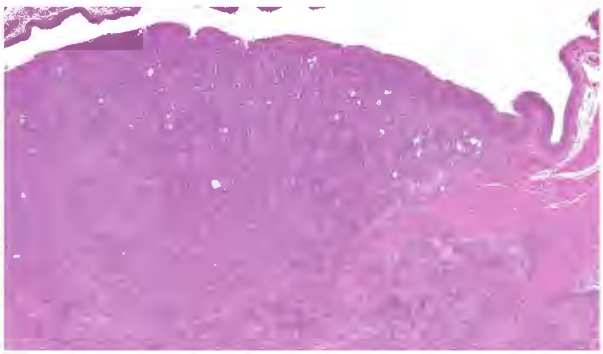

Figure 2-4: Urinary bladder, rat. A transmural neoplasm extends downward from the ulcerated epithelium and effaces the wall of the bladder. (HE, 58X)

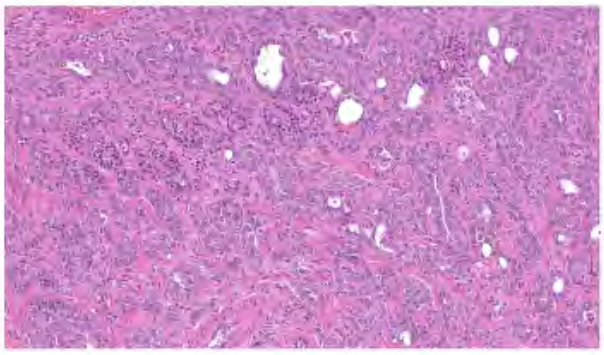

Figure 2-5: Urinary bladder, rat. Neoplastic epithelial cells are arranged in trabeculae and occasional glands on a dense fibrous stroma. (HE, 278X)

Contributor's Comment:

The cause of death in this animal is a ruptured urinary bladder secondary to outflow obstruction from a urinary tumor. The tumor observed both grossly and microscopically is consistent with a urothelial cell carcinoma of the urinary bladder epithelium. Spontaneous urothelial cell carcinomas of the urinary bladder are rare in rats. Although they may be locally invasive, they rarely metastasize. In this case, both the size of the tumor and the strong scirrhous response contributed to the outflow tract obstruction (and therefore an inability to urinate) and urinary inflow tract obstruction from the left kidney (resulting in unilateral hydronephrosis and hydroureter).

This case lacks Melamed-Wolinksi (MW) bodies, which are not listed as a feature in rats[(1)]. MW bodies were first described in 1961 by Melamed and Wolinska while studying 500 urine cytology specimens[(2)] and are defined as single to many round red-or green cytoplasmic inclusions seen in degenerated urothelial cells; however, MW bodies are not always round.[(3)] Cells with MW bodies when noted in body fluids (e.g., pleural fluid, ascitic fluid) signify urothelial origin and suggest metastasis. Recent studies suggest MW bodies are enlarged lysosomes occur-

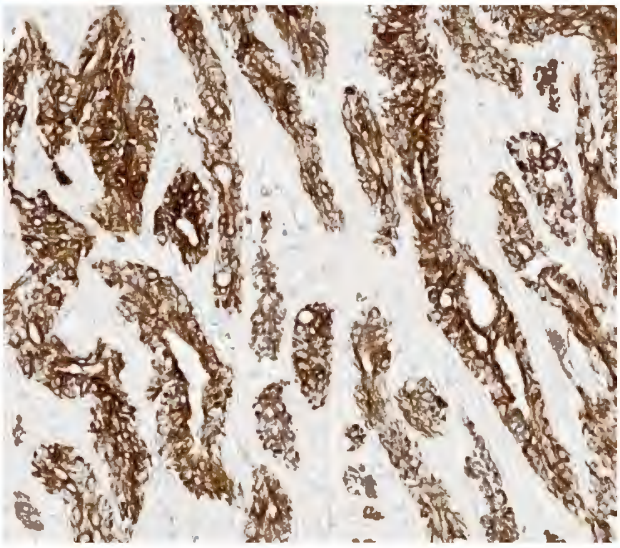

Figure 2-6: Urinary bladder, rat: Neoplastic cells demonstrate strong cytoplasmic immunoreactivity for cytokeratin (anti-AE1/AE3, 400X)

ring in degenerating urothelial cells.[2]

In addition to the urinary bladder tumor, this case provides a great example of what happens upstream of the urinary bladder when it is blocked. At www.medicinepoems.com, there is an 8-stanza ode to hydronephrosis. The second stanza reads as follows:

Hydronephrosis, the name it bears in pain,

A flood within the kidney's fragile frame,

Where once smooth flow of life's essential stream,

Is halted now, a blocked and troubled dream.

Contributing Institution:

Comparative Pathology Department at the Institute of Chemical Defense

https://usamricd.health.mil/

JPC Morphologic Diagnosis:

1. Urinary bladder: Urothelial cell carcinoma.
2. Kidney: Hydronephrosis, chronic, diffuse, severe.

JPC Comment:

First of all, if you missed the poem above, go read it now. It is a blessing for the WSC to have been graced by an ode to hydronephrosis such as this.

This case generated rich discussion on the importance of strain-specific background pathology. As is true for most laboratory rat strains, the Fischer 344s come with genetic baggage. They are predisposed to large granular lymphocytic leukemia, testicular mesothelioma (typically the epithelioid variant), and testicular interstitial cell tumors, the last of which can induce hypercalcemia in this strain. While none of these were primary considerations in this case, the reminder served as a useful anchor for approaching pathology in this particular strain.

Differential diagnoses for this urinary bladder mass included urothelial cell carcinoma, prostatic carcinoma, and renal carcinoma, with the latter two included largely to ensure that metastatic or locally invasive disease was not being overlooked. The histologic architecture of an infiltrative epithelial neo-

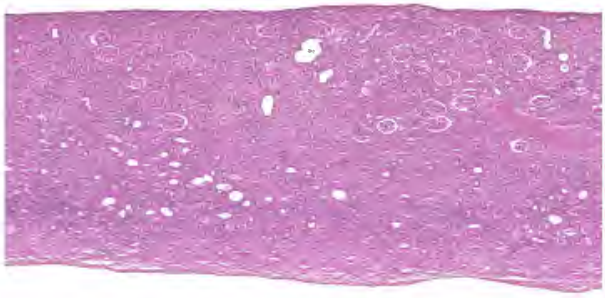

Figure 2-7: Kidney, rat. The urinary pelvis is markedly dilated, resulting in a concave appearance to the kidney (hydronephrosis). The medulla (bottom), and to the lesser extent, cortex (top) are compressed with marked loss of nephrons, occasional ectasia of remnant tubules and fibrosis. (HE, 86X)

plasm seemingly arising from the bladder wall favored a urothelial origin, but immunohistochemistry provided an additional layer of information. The neoplastic cells were diffusely immunoreactive for CK7, a cytokeratin expressed in most primary urinary bladder carcinomas.[4] They were negative for GATA3, a transcription factor involved in urothelial differentiation, which may suggest prostatic carcinoma instead.[5] However, Dr. Alves noted that GATA3 is most reliable in well-differentiated urothelial carcinomas, and its absence here is also consistent with less well-differentiated UCCs, as in this case.[5] The tumor was also negative for PAX8, a marker of renal tubular epithelium, which helped exclude renal carcinoma.[2] Uroplakin, a highly specific marker for urothelial cell carcinoma, unfortunately did not work in this case.[7] Participants also discussed the glandular differentiation present within the tumor, which can be seen in both urothelial cell and prostatic carcinomas. In humans, glandular differentiation in urothelial carcinoma is associated with invasion and poorer differentiation.[8] While extrapolating across species is something to be avoided, the same pattern was evident here.

One of the most instructive aspects of this case was the hydronephrosis, which was beautifully captured on the H&E slide. Dr. Alves emphasized not to overlook this lesion: the upstream consequences of urinary outflow obstruction (pelvic dilation, cortical and medullary thinning, tubular atrophy) were classic! The obstruction in this rat was likely caused by the combination of the tumor's size and its pronounced desmoplastic response, which occluded the bladder outlet.

References:

1. Ayra P, Khalbuss WE, Monaco SE, Pantanowitz L. Melamed-Wolinska bodies. *Diagn Cytopathol*. 2012;40:150-1.

2. Barr ML, Jilaveanu LB, Camp RL, Adeniran AJ, Kluger HM, Shuch B. PAX-8 expression in renal tumours and distant sites: a useful marker of primary and metastatic renal cell carcinoma?. *J Clin Pathol*. 2015;68(1):12-17.

3. Frazier KS, Seely JC, Hard GC, et al. Proliferative and Nonproliferative Lesions of the Rat and Mouse Urinary System. *Toxicologic Pathology*. 2012;40(4_suppl):14S-86S.

4. Jiang J, Ulbright TM, Younger C, et al. Cytokeratin 7 and cytokeratin 20 in primary urinary bladder carcinoma and matched lymph node metastasis. *Arch Pathol Lab Med*. 2001;125(7):921-923.

6. Liang Y, Heitzman J, Kamat AM, Dinney CP, Czerniak B, Guo CC. Differential expression of GATA-3 in urothelial carcinoma variants. *Hum Pathol*. 2014;45(7):1466-1472.

7. Rashidi B, Tongson-Ignacio JE. Melamed-Wolinska bodies in urine cytology an interesting aggregate in a degenerated urothelial cell. *Diagn Cytopathol*. 2011;39:117.

8. Tian W, Guner G, Miyamoto H, et al. Utility of uroplakin II expression as a marker of urothelial carcinoma. *Hum Pathol*. 2015;46(1):58-64.

9. Zhao G, Wang C, Tang Y, et al. Glandular differentiation in pT1 urothelial carcinoma of bladder predicts poor prognosis. *Sci Rep*. 2019;9(1):5323.

CASE III:

Signalment:

14-month-old female intact common mar

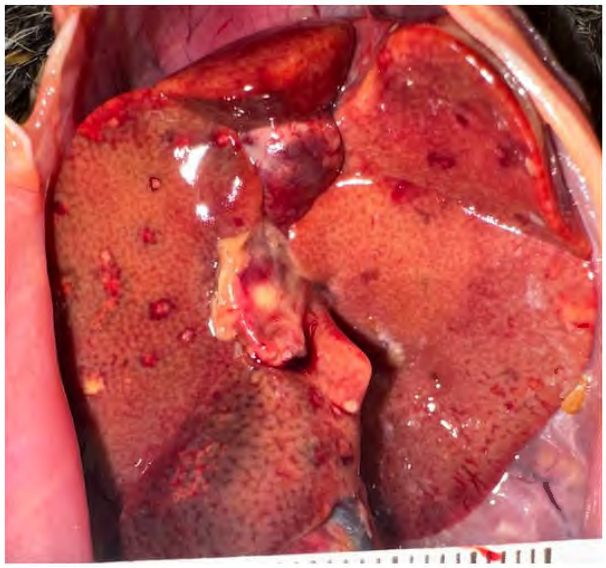

Figure 3-1: Liver, marmoset: The liver is diffusely yellow orange and contains distributed throughout all liver lobes were randomly dispersed yellow-white and red rimmed, ~0.5 cm diameter, foci that extended into the parenchyma on cut section. (*Photo courtesy of:* Laboratory of Comparative Pathology; Memorial Sloan Kettering Cancer Center, https://www.mskcc.org/research/ski/core-facilities/comparative-medicine-pathology-0)

moset (*Callithrix jacchus*)

History:

This marmoset was presented with a sudden onset of lethargy and anorexia. The marmoset died approximately 18 hours post clinical evaluation and initiation of medical treatment.

Gross Pathology:

Examined was a female marmoset in fair nutritional condition (2.5/5) with mild post-mortem autolysis. Distributed throughout all liver lobes were yellow-white and red rimmed, ~0.5 cm diameter, randomly dispersed foci that extended into the parenchyma on cut section. The parenchyma was diffusely orange with an enhanced reticular pattern (Fig. 1). The lungs were diffusely bright red and atelectatic. Sections from all pulmonary lobes floated in formalin. There was marked diffuse gas dilation of the stomach. All segments of the small intestine were moderately to markedly distended by air and contained small amounts of digesta. The pancreatic lymph node adjacent to the duodenum was approximately 3x the size of normal. The cecum and colon had multifocal white to pale tan, circular areas of serosal discoloration. There were formed feces in the colon.

Laboratory Results:

Bacterial species identification confirmed by MALDI-TOF mass spectrometry:

Liver, aerobic culture: 3+ *P. aeruginosa* and <1+ *K. pneumoniae*

Liver, anaerobic culture: *Clostridium barattii* on thiglycolate

Lung, aerobic culture: 3+ *P. aeruginosa*, 1+ *K. pneumonia* and *Ligilactobacillus rauteri*

Cecum, aerobic culture: 3+ Mixed bacterial sps. included: *Pseudomonas aeruginosa*, *Proteus mirabilis*, *Klebsiella pneumonia, Citrobacter freundii* and *Citrobacter farmer*

K. pneumonia string test: negative

P. aeruginosa ISH of liver: bacteria strongly positive, located diffusely within sinusoids and concentrated around vessels (Fig. 3 & 4).

Gram stain: Gram-negative rod-shaped bacteria associated with areas of inflammation and necrosis in the liver and gallbladder and presence of Gram-negative bacteria in circulation

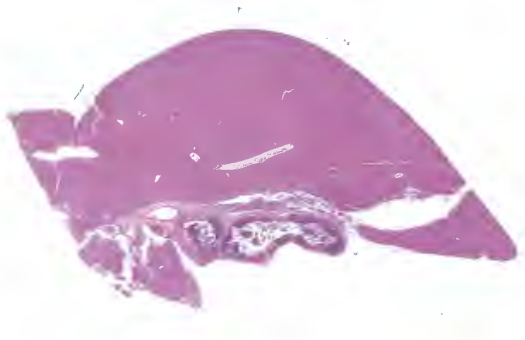

Figure 3-2: Liver and gallbladder, marmoset: A section of liver and gallbladder are submitted for examination. The wall of the gallbladder is effaced by necrosis and inflammation. (HE, 10X).

in the glomeruli and pulmonary vasculature

Microscopic Description:

Gallbladder and liver: The gallbladder and adjacent portal tracts are effaced by multifocal to coalescing areas of coagulative and lytic necrosis admixed with foci of suppurative inflammation. The gallbladder is transmurally severely expanded by numerous neutrophils, scattered lymphocytes and histiocytes, abundant polymerized fibrin, necrotic debris eosinophilic proteinaceous fluid (edema), extravasated red blood cells (hemorrhage), and mats of extracellular rod-shaped bacteria (bacilli). Multifocally, blood vessels in the gallbladder are distorted by endothelial and/or mural necrosis and innumerable bacilli. Some vessels are partially occluded by fibrin and bacterial thrombi. Remaining intact vessels are congested. There is marked loss of gallbladder epithelium characterized by hypereosinophilia and loss of nuclear detail (necrosis), occasionally seen sloughing into the lumen admixed with neutrophils, fibrin, and red blood cells. Throughout the liver, bile ducts and portal vasculature undergo similar changes of varying severity (Fig 2). Bacilli are located extracellularly within portal areas and within sinusoids or intracellularly within macrophages. There are moderate, acute, multifocal loss of hepatocellular detail admixed with areas of fragmented chromatin and karyolytic debris (coagulative and lytic necrosis). Remaining hepatocytes are mildly to moderately swollen by small to medium-sized, round, clear, cytoplasmic vacuoles.

Contributor's Morphologic Diagnosis:

1. Gallbladder: Severe, acute, multifocal to coalescing, necrotizing and suppurative, transmural cholecystitis with hemorrhages, congestion, polymerized fibrin, edema, and intralesional bacilli
2. Vasculature, gallbladder and liver: Marked, acute, multifocal endothelial necrosis with mural bacterial colonization, bacteremia, and fibrin thrombi
3. Liver: Severe, acute, multifocal, necrotizing and suppurative cholangiohepatitis with multifocal hemorrhages, acute random hepatic necrosis, and intralesional bacilli
4. Liver: Mild to moderate, multifocal, microvesicular steatosis

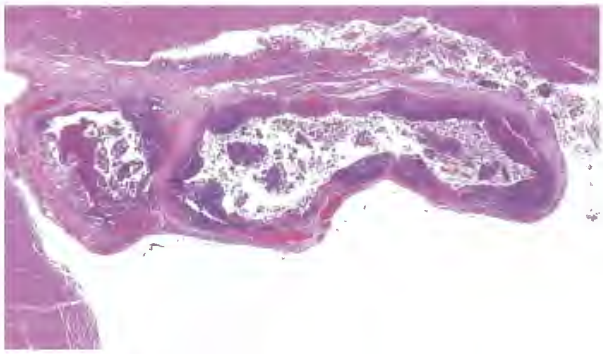

Figure 3-3: Gallbladder, marmoset: The wall of the gallbladder is transmurally necrotic with infiltration of innumerable neutrophils and hemorrhage. The lumen contains abundant cellular debris. (HE, 27X).

Contributor's Comment:

The cause of death of this marmoset was due systemic bacterial infection that likely originated in the upper small intestine, resulting in an ascending biliary tree infection and translocation into the blood supply. Intravascular bacteria were identified in the heart, lung, kidneys, liver, gallbladder, duodenum, mesentery, cecum, and adrenal glands. Necrotic foci and hemorrhage were identified in the stomach, cecum, and mid-colon; these lesions lacked leukocytic cell infiltrates and were therefore considered peracute and secondary to sepsis/toxemia. Bacterial translocation across these lesions resulting in bacteremia cannot be ruled out.

In the case presented here, both *P. aeruginosa* and *K. pneumoniae* were isolated from the liver and lung. Given the gross and microscopic findings of acute hepatic necrosis and strong positive *P. aeruginosa* ISH, *P. aeruginosa* was determined to be the most likely primary pathogen. *K. pneumoniae* infections in non-human primates tend to form abscesses, which is not a feature of this infection.[12] Additionally, we did not observe clear halos surrounding the bacilli when associated with leukocytes, which is a microscopic feature when dealing with hypervirulent *K. pneumoniae* outbreaks in NHPs. This marmoset also had a mild to moderate chronic lymphoplasmacytic enteritis with the duodenum most affected. Microbiome studies comparing healthy and sick captive marmosets affected by IBD or duodenal strictures/dilatation syndrome from different facilities demonstrated significant alterations in the diversity and shifts in their bacterial flora in the small intestine in sick marmosets.[19,20] We cannot rule out the possibility that IBD may have contributed to alterations in the normal bacterial flora and facilitating the translocation of pathogenic bacteria in this case.

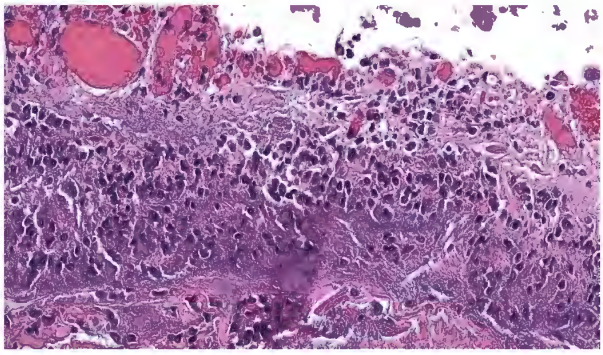

Figure 3-4: Gallbladder, marmoset: Within the necrotic wall, there are innumerable bacilli. (HE,696X).

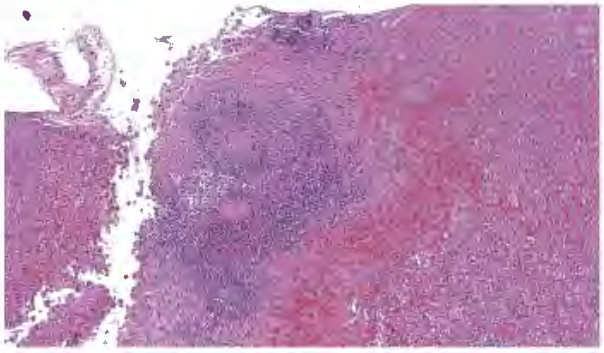

Figure 3-5: Liver, marmoset: Areas of necrosis and hemorrhage, with bacilli, are scattered within the hepatic parenchyma. (HE, 273X).

Pseudomonas species are motile, gram negative, bacillary, opportunistic pathogens of humans, animals, and plants. *P. aeruginosa* is associated with various diseases in veterinary species that include, but are not limited to, the following: septicemia in newly-hatched chickens and late stage embryos;[11] mastitis in cattle, sheep, and goats;[5,14] fleece rot in sheep;[6] pyoderma, otitis externa, and ulcerative keratitis in in dogs and cats;[8,17,18] hemorrhagic pneumonia in mink;[1] metritis in mares;[7] mouth rot (necrotic stomatitis) in snakes;[4] otitis media, pneumonia, septicemia enteritis, and sudden death chinchillas;[9] and wound infections in many species. In hu-

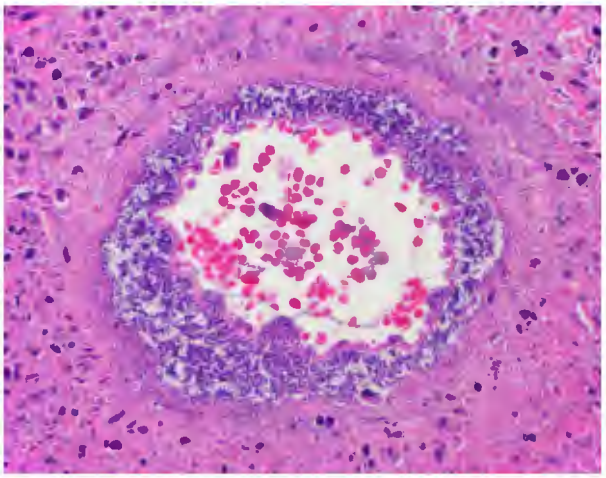

Figure 3-6: Liver, marmoset: Hepatic vessel surrounded by numerous bacilli indicates sepsis. (HE, 400X). (*Photo courtesy of:* Laboratory of Comparative Pathology; Memorial Sloan Kettering Cancer Center, https://www.mskcc.org/research/ski/core-facilities/comparative-medicine-pathology-0)

mans, this bacterium is often associated with infections in critically ill and immunocompromised patients. Over many years, *P. aeruginosa* isolates from hospital-acquired infections in humans have become increasingly antimicrobial resistant, and treatment options are limited.[2]

P. aeruginosa contains an array of virulence factors, allowing it to cause a wide variety of clinical diseases.[10] The outer membrane contains lipopolysaccharide, which modulates adherence to epithelial cells, evasion of phagocytosis, and activation of host immune response leading to dysregulated cytokine production. Biofilm formation is modulated by production of alginate and other exopolysaccharides. The flagellum allows for bacterial dispersion through aqueous and low-viscosity environments, relying on chemotaxis to swim toward epithelial cells. Pili are primarily used for epithelial cell adherence. A type III secretion system injects several cytotoxins and exotoxins that cause rapid host cell death. Several extracellular proteolytic enzymes, such as alkaline proteases and elastases, can cause significant host tissue damage and subsequent invasion. Because iron is required for bacterial growth, the bacteria has siderophores to scavenge this nutrient.[10,22]

P. aeruginosa has been isolated from squirrel monkeys with meningitis, pododermatitis and cellulitis, and abscesses; an African green monkey with pneumonia and myocarditis; and from a chimpanzee with suppurative nephritis.[21] Though *P. aeruginosa* is rarely a primary pathogen in marmosets a recent case series reported necrosuppurative cholangiohepatitis and necrotizing typhlitis in 7 indoor housed marmosets common.[16] Infection was attributed to *Pseudomonas* contamination of the water supply. Though *P. aeruginosa* was frequently isolated from lesions in these cases, a subset of lesions recovered both *E. coli* and *P. aeruginosa.*[16]

Contributing Institution:

Laboratory of Comparative Pathology; Memorial Sloan Kettering Cancer Center, Weill Cornell Medicine, Hospital for Special Surgery, and The Rockefeller University
417 E. 68th St., ZRC-940
New York, NY 10065
https://www.mskcc.org/research/ski/core-facilities/comparative-medicine-pathology-0

JPC Morphologic Diagnosis:

1. Gallbladder: Cholecystitis, necrosuppurative, acute, diffuse, severe, with vasculitis and innumerable bacilli.
2. Liver: Cholangiohepatitis, necrosuppurative, acute, multifocal to coalescing, severe, with portal vein thrombi, random hepatocellular necrosis, and

innumerable bacilli.

JPC Comment:

This case, along with the outstanding contributor comment, provided an excellent opportunity to discuss necrotizing hepatitis in marmosets. Dr. Alves emphasized that necrotizing hepatitis in New World primates should immediately bring alphaherpesviruses to mind, including human herpes simplex virus (human alphaherpesvirus-1), macacine herpesvirus 1 (Herpes B), and saimariine herpesvirus 1 (formely known as *Herpesvirus tamarinus* or Herpes T).[13] Other major differentials to consider include lymphocytic choriomeningitis virus (LCMV), and a wide array of "hot gram-negative bacteria" such as *Francisella tularensis*, *Pseudomonas aeruginosa*, and other fulminant septicemic organisms.[13] To foot-stomp this point, participants received a firm reminder to know their alphaherpesviruses, as these agents remain among the most devastating and diagnostically urgent pathogens in Old and New World primates.[13]

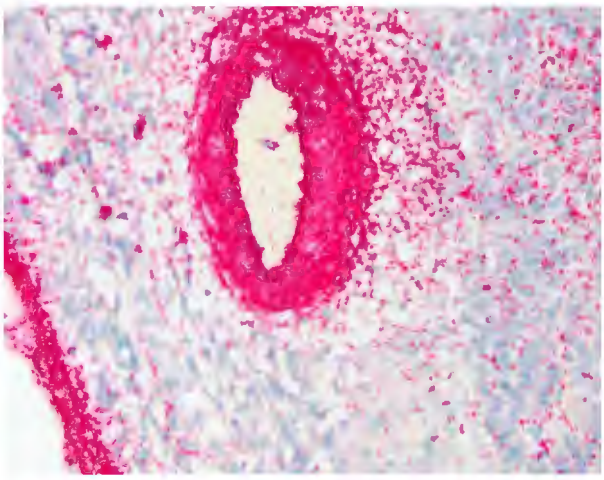

Figure 3-7: Liver, marmoset: Bacilli within the perivascular areas in the liver are positive on ISH for *P. aeruginosa*. (ISH, 400X). (*Photo courtesy of:* Laboratory of Comparative Pathology; Memorial Sloan Kettering Cancer Center, https://www.mskcc.org/research/ski/core-facilities/comparative-medicine-pathology-0)

The hepatic necrosis in this case was acute, and participants noted that cholestasis, which is generally considered a lesion of chronicity, was absent. The lack of viral inclusions also argued against many of the viral pathogens on the differential list. However, Dr. Alves cautioned against prematurely dismissing viruses simply because bacteria are abundant; many viral infections create the perfect environment for secondary bacterial invasion, and the presence of bacteria does not automatically identify the primary pathogen.

In this case, however, the evidence strongly supported *Pseudomonas aeruginosa* as the primary agent, with *Klebsiella pneumoniae* acting as a secondary invader. The bacteria are gram-negative and argyrophilic, and both were cultured from affected tissues. *Klebsiella pneumoniae* infections often produce overt abscessation, "turkey egg" kidneys, and acute renal tubular necrosis.[15] The absence of these lesions further supported the role of *Klebsiella pneumoniae* as a secondary pathogen, although it is more than capable of causing disease on its own.[15]

Participants discussed the most likely pathogenesis of infection as having ascended from the gastrointestinal tract, traveled up the common bile duct, and seeded the gallbladder and liver, producing the necrotizing cholangiohepatitis observed. This concurs with the contributor's proposed cause of death. The ascending route is well-documented in marmosets, particularly in the context of intestinal dysbiosis or chronic enteritis, and is a common route of infection for many enteric gram-negative bacterial pathogens.

Dr. Alves concluded the discussion with a concise review of the pathogenesis of

gram-negative septicemia, emphasizing how rapidly this cascade can overwhelm animals. Circulating endotoxin (LPS) first binds to LPS-binding protein. This complex then engages CD14 on leukocytes. After dissociation of the binding protein, the CD14–LPS complex binds to TLR4, triggering a MyD88-dependent signaling cascade that drives NF-κB and interferon activation.[3] The result is widespread macrophage stimulation with release of cytokines and nitric oxide, followed by endothelial activation and the induction of tissue factor. Tissue factor stimulates the extrinsic coagulation cascade. Once the coagulation cascade is initiated, endothelial injury accelerates, leading to consumptive coagulopathy and, ultimately, the risk of disseminated intravascular coagulation.[3] This mechanistic walkthrough tied together the hepatic necrosis, vascular injury, and multiorgan involvement seen in the case, reinforcing why gram-negative septicemia remains such a devastating process.

References:

1. Bai J, Wang X, Zhang Z, et al. Overview of Mink Immunity and Resistance to *Pseudomonas aeruginosa*. *Vet Med Int*. 2023;(1):6158844.
2. Bassetti M, Vena A, Croxatto A, et al. How to manage *Pseudomonas aeruginosa* infections. *Drugs in context*. 2018;7.
3. Bochud PY, Calandra T. Pathogenesis of sepsis: new concepts and implications for future treatment. *BMJ*. 2003;326 (7383):262-266.
4. Ciobotaru E, Tudor L, Constantinescu CM, et al. *Pseudomonas spp*. induced lesions in non-venomous snakes. *J Comp Path.* 2009;141(4):283.
5. Dapgh AN, Hakim HS. Abouelhag HA, et al. Detection of virulence and multi-drug resistance operons in *Pseudomonas aeruginosa* isolated from Egyptian Baladi sheep and goat. *Vet World*. 2019:12(10):1524.
6. Denmann S, Tellam R, Vuocolo T, et al. Fleece rot and dermatophilosis (lumpy wool) in sheep: opportunities and challenges for new vaccines. *Anim Prod Sci*. 2021;62(4); 301-320.
7. Ferrer MS, & Palomares R. Aerobic uterine isolates and antimicrobial susceptibility in mares with post-partum metritis. *EVJ.* 2018;50(2):202-207.
8. Hillier A, Alcorn JR, Cole LK, et al. Pyoderma caused by *Pseudomonas aeruginosa* infection in dogs: 20 cases. *Vet Derm.* 2006;17(6);432-439.
9. Hirakawa Y, Sasaki H, Kawamoto E, et al. Prevalence and analysis of *Pseudomonas aeruginosa* in chinchillas. *BMC Vet Res*. 2010;6:1-10.
10. Jurado-Martín I, Sainz-Mejías M, & McClean S. *Pseudomonas aeruginosa*: an audacious pathogen with an adaptable arsenal of virulence factors. *Int J Mol Sci.* 2021;22(6);3128.
11. Kebede F. *Pseudomonas* infection in chickens. *J Vet Med Anim Health*. 2010;2(4):55-58.
12. Keesler RI, Colagross-Schouten A, Reader JR. Clinical and pathologic features of spontaneous *Klebsiella pneumoniae* infection in 9 rhesus macaques (*Macaca mulatta*). *Comp Med.* 2020;70 (2):183-9.
13. Mätz-Rensing K, Bleyer M. Viral Diseases of Common Marmosets. *The Common Marmoset in Captivity and Biomedical Research*. 2019;251-264.

14. Park H, Hong M, Hwang S, et al. Characterisation of *Pseudomonas aeruginosa* related to bovine mastitis. *Acta Vet Hung*. 2014;62(1):1-12.

15. Pisharath HR, Cooper TK, Brice AK, et al. Septicemia and peritonitis in a colony of common marmosets (Callithrix jacchus) secondary to Klebsiella pneumoniae infection. *Contemp Top Lab Anim Sci*. 2005;44(1):35-37.

16. Powers SJ, Castell N, Vistein R, et al. Bacterial Cholecystitis and Cholangiohepatitis in Common Marmosets (*Callithrix jacchus*). *Comp Med.* 2023;73 (2):173-180.

17. Pye C. *Pseudomonas* otitis externa in dogs. *CVJ*. 2018;59(11):1231.

18. Santos TM, Ledbetter RC, Caixeta LS, et al. Isolation and characterization of two bacteriophages with strong in vitro antimicrobial activity against *Pseudomonas aeruginosa* isolated from dogs with ocular infections. *Am J Vet Res*. 2011;72 (8):1079-1086.

19. Sheh A, Artim SC, Burns MA, et al. Alterations in common marmoset gut microbiome associated with duodenal strictures. *Sci Rep*. 2022;12(1):5277.

20. Sheh A, Artim SC, Burns MA, et al. Analysis of gut microbiome profiles in common marmosets (*Callithrix jacchus*) in health and intestinal disease. *Sci Rep*. 2022;12(1):4430.

21. Simmons J, Gibson S. Bacterial and mycotic diseases of nonhuman primates. *Nonhuman Primates in Biomedical Research*. 2012:105-72.

22. Rocha AJ, Barsottini MRDO, Rocha RR, et al. *Pseudomonas aeruginosa*: virulence factors and antibiotic resistance genes. *Brazi Arch Biol Techn*. 2019;62, e19180503.

CASE IV:

Signalment:

19 year old, female, African green monkey (*Chlorocebus aethiops sabaeus*).

History:

A 19-year-old, multiparous, fourth-generation colony-bred female African green monkey (*Chlorocebus aethiops sabaeus*) developed a swelling in the lateral aspect of the right thigh region over the course of 5 years. The animal was maintained exclusively for breeding and was not involved in any experimental procedures.

While housed in an outdoor breeding group, the monkey was observed by caretakers to be limping and unable to bear weight on her right hind limb. Upon closer inspection, the lateral thigh region appeared swollen and bruised.

The monkey was treated with multiple doses of nonsteroidal anti-inflammatory drugs and dexamethasone with only partial regression of the swelling. On palpation, the lateral thigh was firm and warm, with no additional abnormalities noted on physical examination.

Gross Pathology:

On postmortem examination, the carcass weighed 3.83 kg and had a body condition of 2 out of 5. The swollen area on the right pelvic limb exhibited mild alopecia and crusting.

Postmortem radiographs showed an extensive, multilocular radiopaque mass within

Figure 4-1: Hindlimb, African green monkey: A multilocular radiopaque mass is present within soft tissues surrounding the latero-caudal aspect of the right hip and stifle. (*Photo courtesy of*: Ross University School Of Veterinary Medicine, https://veterinary.rossu.edu/research/pathology-training-program)

soft tissues surrounding the latero-caudal aspect of the right hip and stifle, extending from the level of the greater trochanter to approximately 10 cm distal to the tibiofemoral joint. The mass did not invade long bones.

Dissection revealed a multilobulated, non-encapsulated, crepitant, yellow to red mass measuring 11 × 5 × 4 cm, infiltrating and replacing the subcutaneous tissue and skeletal muscles of the right thigh.

The mass contained numerous hard, white spicules, suggesting mineralization. The periosteum of the right femur was focally and extensively irregular. No gross pathological alterations were observed in the internal organs.

Laboratory Results:

Laboratory data was not available for this case.

Microscopic Description:

The affected skeletal muscle and subcutis were infiltrated and expanded by abundant, irregular, globoid amphophilic to basophilic material, consistent with mineralization. This mineralized material was surrounded by extensive fibrous connective tissue proliferation (fibrosis), admixed with numerous macrophages, lymphocytes, and fewer multinucleated giant cells containing phagocytosed mineral material. Scattered throughout the mass, rare foci of osteoid formation were observed, characterized by a low number of empty lacunae and necrotic osteoid undergo-

Figure 4-2: Hindlimb, African green monkey: A multilobulated, non-encapsulated, crepitant, yellow to red mass measuring 11 × 5 × 4 cm, infiltrating and replaces the subcutaneous tissue and skeletal muscles of the right thigh. (*Photo courtesy of*: Ross University School Of Veterinary Medicine, https://veterinary.rossu.edu/research/pathology-training-program)

Figure 4-3: Hindlimb, African green monkey: Two sections of a multifocally mineralized bony mass within the subcutaneous fat (left) and skeletal muscle (right) are submitted for examination. (HE, 10X)

ing remodeling. Multifocally within the mineralized soft tissue lesions, multiple tortuous blood vessels with thickened tunica media were observed. Additionally, there were areas of extensive hemorrhage, neovascularization, and granulation tissue formation infiltrating and replacing the surrounding adipose tissue.

Contributing Institution:

Pathology Department, Ross University School Of Veterinary Medicine
https://veterinary.rossu.edu/research/pathology-training-program

Contributor's Morphologic Diagnosis:

Skeletal muscle: Granulomatous myositis and steatitis with soft tissue mineralization, chronic, focally extensive, severe, with fibrosis and rare osseous metaplasia.

Contributor's Comment:

Soft tissue mineralization is broadly categorized into three types based on underlying pathophysiologic mechanisms: dystrophic, metastatic, and idiopathic calcification.[5,7]

Dystrophic calcification is characterized by the deposition of mineral in areas of tissue injury, occurring despite normal serum levels of calcium and phosphate. It is often associated with prior injury, necrosis, inflammation, or neoplasia, and has been reported following chronic inflammatory conditions. Metastatic calcification occurs primarily in humans and is associated with disturbances in calcium or phosphate metabolism, most commonly hypercalcemia, hyperphosphatemia or a combination of both. It is typically observed in conditions such as chronic renal failure, end-stage kidney disease, or vitamin D toxicosis. Idiopathic calcification occurs without identifiable tissue injury or underlying metabolic abnormality. No specific cause is evident, although breed or familial predisposition may be present.[5,7]

In humans, Hyperphosphatemic Familial Tumoral Calcinosis (HFTC) results from either a deficiency of intact FGF23 or impaired FGF23 signaling, most oftenin-herited in an autosomal recessive pattern. Mutations in GALNT3, FGF23, KL (encoding KLOTHO), as well as the presence of autoantibodies targeting FGF23, disrupt FGF23 production or activity. This disruption results in hyperphosphatemia with high-normal calcium levels, leading to an

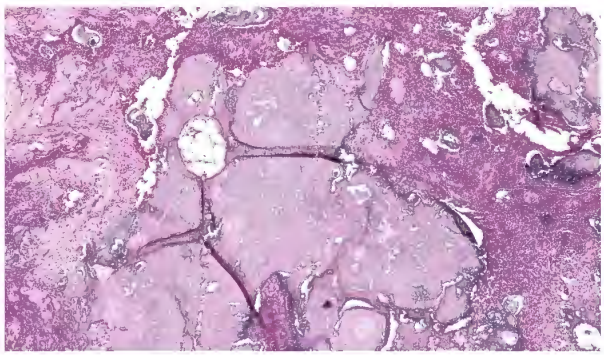

Figure 4-4: Hindlimb, African green monkey: The mass is composed of disorganized foci of mineral, fibrous connective tissue, osteoid matrix, and woven bone. (HE 176X)

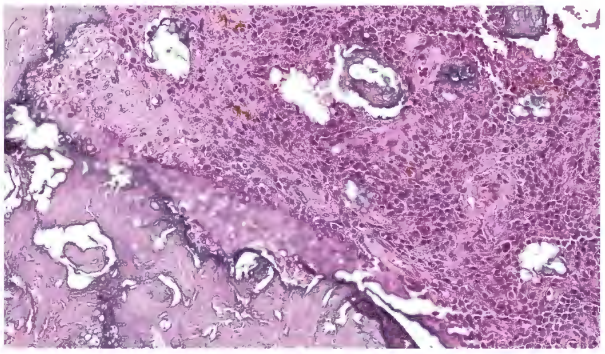

Figure 4-5: Hindlimb, African green monkey: The mass is surrounded by loosely arranged fibrous connective tissue containing numerous epithelioid macrophages. (HE, 378X)

elevated calcium-phosphate product, which is believed to play a key role in the development of ectopic calcification.[1]

In animals, gross lesions associated with calcinosis circumscripta have been documented in a variety of anatomical locations, including the tongue, margins of the pinnae, spine, salivary glands, aorta, mammary glands, small intestine, footpads, paravertebral soft tissues, cheeks, and both right and left hind limbs.[4,5,7]

In dogs, cats, and horses, the lesions typically present as bulging, fluctuant, or cystic masses that may be variably ulcerated and contain chalky white mineralized material.[4] In a study comprising 77 canine cases, lesion diameters ranged from 2 to 13 cm, with the majority measuring between 0.5 and 3 cm. Lesions were solitary in 82% of cases and multiple in 18%, with no apparent symmetry in the latter. Grossly, lesions varied from small, firm, white nodules to large cystic masses filled with abundant chalky white material. Some lesions were freely movable, whereas others were firmly adherent to the surrounding tissues. On cut surface, most lesions exhibited multifocal nodules containing gritty, chalky white material.[7]

In a documented case involving a cynomolgus macaque (*Macaca fascicularis*), multiple raised, nodular masses of variable size were observed on both, the left and right feet. On cross-section the lesions consisted of firm subcutaneous nodules containing white, chalk-like material, and no gross pathological abnormalities were identified in the internal organs.[5]

Histologically, calcinosis circumscripta is characterized by aggregates of amorphous to granular, lightly to deeply basophilic mineralized material. These deposits are typically surrounded by macrophages, multinucleated giant cells, and occasional lymphocytes, and are delineated by fibrous connective tissue bands. As the lesion progresses, mineralization becomes more extensive and is accompanied by pronounced fibrosis. The associated inflammatory response may diminish over time, and areas of osseous or cartilaginous metaplasia may develop. In certain cases, epidermal sequestration or transepidermal elimination of mineralized material may lead to ulceration.[2,3,4]

In this case, the lesions were confined to the right pelvic limb, with no evidence of involvement of other organ systems. A diagnosis of *calcinosis circumscripta* (tumoral calcinosis) was established based on the morphological, histopathological and immuno-

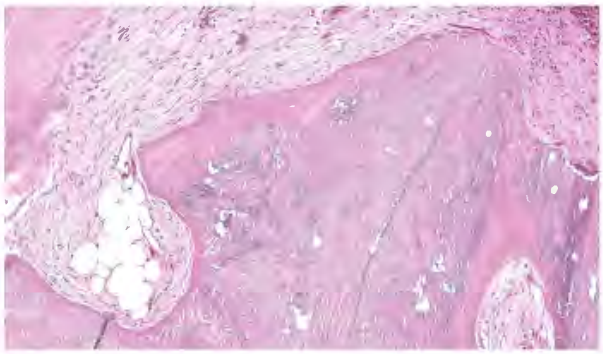

Figure 4-6: Hindlimb, African green monkey: In some areas, the mass contains woven bone. (HE, 233X)

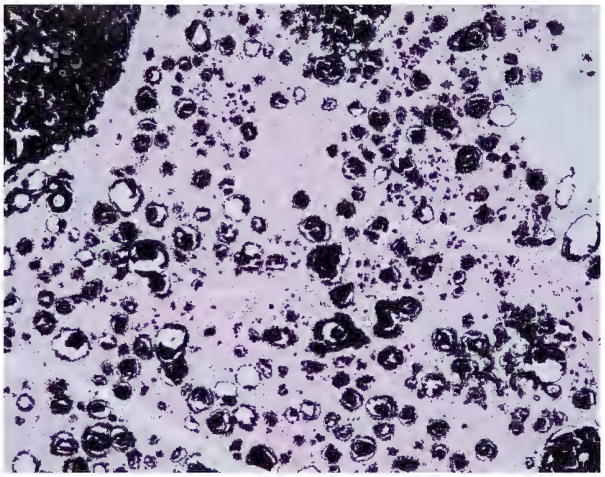

Figure 4-7: Hindlimb, African green monkey: A Von Kossa stain highlights mineral within the mass. (*Photo courtesy of*: Ross University School Of Veterinary Medicine, https://veterinary.rossu.edu/research/pathology-training-program) (Von Kossa, 100X)

histochemical characteristics of the lesion. Mason trichrome, Von Kossa and Perl's Prussian blue stains were performed and were positive for the fibrous connective tissue (the first one) and the globular amorphous mineral (the last two). The presence of iron within the mineralized material is intriguing. Anecdotally, the African Green Monkeys on this facility tend to present hepatic iron overload and multifocal organ hemosiderosis. Extraskeletal osteosarcoma was considered as a potential differential. However, the cellular infiltrate was immunopositive for IBA-1 (histiocytes/macrophages) and immunonegative for SATB2 (osteoblastic origin, osteosarcoma), α-SMA38 (mature myofibroblast, smooth muscle tumor), SOX10 (neural crest origin, melanoma and certain soft tissue neoplasms), and S100 (amelanotic melanoma and certain soft tissue neoplasms). Based on clinical history of this animal, the lesion in this case most likely represents dystrophic calcification secondary to prior traumatic injury, as has been described in other nonhuman primates. To date, neither metastatic nor idiopathic calcification has been reported in this species.

JPC Morphologic Diagnosis:

Subcutaneous fat and skeletal muscle: Mineralization, chronic, focally extensive, severe, with granulomatous inflammation and osseous metaplasia.

JPC Comment:

The lesions in this fascinating case, while most consistent with calcinosis circumscripta, also shared histologic overlap with a condition known as myositis ossificans (also known as myositis ossificans traumatica). Myositis ossificans (MO) presents as a focal mass in the skeletal muscle, most commonly associated with the limbs, such as the biceps or thigh muscles.[8] The pathogenesis of MO is speculative, but is believed to occur due to trauma and the resulting granulomatous inflammation, fibrosis, mineralization, and ossification that occur over months. Myositis ossificans is rarely reported in veterinary species, with several case reports in dogs, horses, cats, and a vampire bat.[3]

There is substantial histologic overlap between MO and calcinosis circumscripta; both lesions can have a mass effect due to mineral, fibrosis, granulomatous inflammation, and, occasionally, bone. Calcinosis circumscripta typically has a larger proportion of mineral and tends to occur in the skin and subcutis, often over pressure points. In contrast, MO has a variable amount of mineral versus bone depending on the stage of the lesion and occurs primarily within the skeletal muscle.[2] In this case, participants agreed that there were features of both present, but could not land squarely on one or the other. It is possible that the chronicity of this lesion represents a continuum between these two in

this particular case.

Participants reviewed the three main types of pathologic calcification (dystrophic, metastatic, and idiopathic) and how each relates to systemic calcium status. Dystrophic calcification occurs in necrotic or damaged tissues and is typically associated with normal serum calcium.[6] Metastatic calcification, by contrast, reflects hypercalcemia, and preferentially affects tissues involved in acid-base exchange, including the gastric lamina propria, kidneys, lungs, and blood vessels.[6] Finally, idiopathic calcification is caused by unknown metabolic triggers, but is associated with excess endogenous or exogenous corticosteroids in both veterinary and human medicine.[6]

A valuable discussion was held on the functional differences between M1 and M2 macrophages and the role of CD4+ T-helper cells in driving this differentiation. M1 macrophages, associated with pro-inflammatory responses, express CD68 and CD80, whereas M2 macrophages, associated with tissue repair and remodeling, express CD163 and CD206. Dr. Alves' lab ran these markers for this case, and the immunophenotype confirmed a predominance of M2 macrophages within the lesion. This finding aligned well with the chronicity of the process and the extensive remodeling present.
Overall, this case served as an excellent review of the mechanisms and morphologic patterns of tissue mineralization, the role of macrophage differentiation in chronic lesions, and the importance of integrating lesion distribution, chronicity, and tissue context in cases of mineralization.

References:

1. Boyce AM, Lee AE, Roszko KL, Gafni RI. Hyperphosphatemic Tumoral Calcinosis: Pathogenesis, Clinical Presentation, and Challenges in Management. *Front Endocrinol (Lausanne)*. 2020;11:293.
2. De Paolo M, Gracis M, Lacava G, Vapniarsky N, Arzi B. Management of bilateral pterygoid myositis ossificans-like lesion in dogs. Front Vet Sci. 2022 Oct 10;9:992728.
3. Hausmann JC, Manasse J, Churgin S, Steinberg H, Clyde VL, Wallace R. Myositis ossificans traumatica in a vampire bat (*Desmodus rotundus*). J Zoo Wildl Med. 2016 Sep;47(3):895-899.
4. Mauldin EA, Peters-Kennedy J. Integumentary system. In: Maxie MG, ed. *Jubb, Kennedy & Palmer's Pathology of Domestic Animals*. Vol 1. 6th ed. St. Louis: Elsevier. 2016: 509–736.
5. Radi ZA, Sato K. Bilateral dystrophic calcinosis circumscripta in a cynomolgus macaque (*Macaca fascicularis*). *Toxicol Pathol*. 2010;38(4):637-641.
6. Sakals S, Peta HG, Fernandez NJ, Allen AL. Determining the cause of hypercalcemia in a dog. *Can Vet J*. 2006;47(8):819-821.
7. Tafti AK, Hanna P, Bourque AC. Calcinosis circumscripta in the dog: a retrospective pathological study. J Vet Med A Physiol Pathol Clin Med. 2005;52(1):13-7.
8. Vilar JM, Ramirez G, Spinella G, Martinez A. Kinematic characteristics of myositis ossificans of the semimembranosus muscle in a dog. Can Vet J. 2010 Mar;51 (3):289-92.

Joint Pathology Center
Veterinary Pathology Services

WEDNESDAY SLIDE CONFERENCE 2025-2026

Conference #22 16 April 2026

CASE I:

Signalment:

A 2.5 year old primiparous Holstein Friesian cow *(bos taurus).*

History:

This dairy cow was from a herd of 360 animals, and had been exhibiting clinical signs consistent with toxic mastitis within the previous three weeks. Initially, this cow was treated with broad spectrum antibiotics, non-steroidal anti-inflammatories, and oral fluids, but failed to improve and was euthanized on welfare grounds.

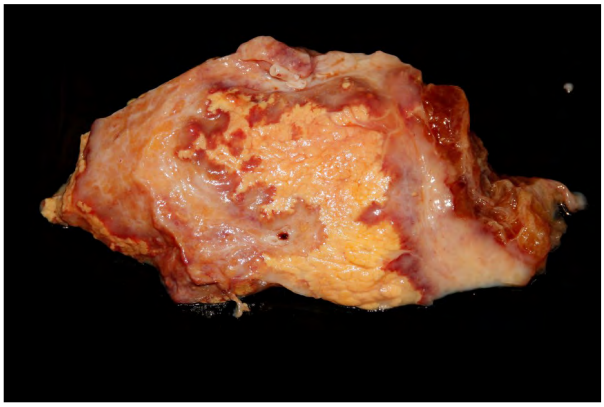

Figure 1-1. Mammary gland, ox: The mammary gland is enlarged and fibrotic, and on cut surface there is a distinct area of pallor (sequestrum) surrounded by a hyperemic halo.. (*Photo courtesy of*: University of Nottingham, https://www.nottingham.ac.uk/vet/service-for-business/veterinary-pathology-service/index.aspx)

Gross Pathology:

The right cranial mammary gland is enlarged and firm, and on the cut surface there is locally extensive fibrosis, with a distinct area of pallor (sequestrum) surrounded by a hyperemic halo. Within the teat cistern there is pale yellow, watery, fibrinosuppurative content. There is a focal, ~1-2cm diameter, capsulated abscess within the parenchyma as well. There is marked subcutaneous oedema surrounding the affected quarter.

Diagnostic Testing:

The aerobic bacteriology of the affected mammary gland identified *Klebsiella pneumoniae*, which was resistant to Ampicillin and sensitive to Neomycin, Streptomycin, Amoxicillin/Clavulanic acid, Cefpodoxime, Trimethoprim/Sulphamethoxazole, Enrofloxacin, Tetracycline. The culture and PCR-denaturing gradient gel electrophoresis (DGGE) testing for *Mycoplasma* was unrewarding.

Microscopic Description:

Mammary Gland - Right cranial quarter
The mammary gland is effaced in a focally extensive manner by moderately well demarcated palely eosinophilic parenchyma with partial loss of differential staining and cellular detail whilst retaining preservation of the overall architecture (coagulative necrosis - sequestrum). Within the necrotic ar-

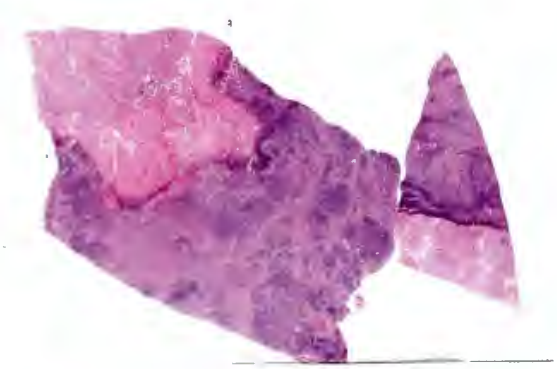

Figure 1-2. Mammary gland, ox: Two sections of mammary gland are submitted for examination. Both sections contain extensive areas of coagulative necrosis (infarcts, sequestra) which are bounded by a dense area of cellular debris. There is loss of architecture and hypercellularity of the remnant mammary gland. (HE, 0.7X).

ea, there are scattered pale basophilic, 2-3 micron in length, coccobacilli. The necrosed area is bordered by a thick rim of granulation tissue and nascent fibrosis. Throughout the remaining parenchyma, the mammary gland is multifocally effaced by extensive areas of abundant lytic and karyorrhectic leucocytes and debris (lytic necrosis) with abundant fibrin, alongside abundant granulation tissue, and a marked inflammatory infiltrate comprising of lymphocytes and plasma cells, often forming small clusters. Multifocally, there are small numbers of compressed and distorted interlobular ducts, remnants of compressed and atrophic mammary alveoli or basophilic mineral concretions of proteins and salts, that are sometimes accompanied by macrophages or very rare multinucleated giant cells (foreign body type). Within the inflamed granulation tissue, a small number of ducts are dysplastic, and scattered throughout the parenchyma are a moderate number of round optically empty spaces (lipid). Within some ducts, there are accumulations of lytic leucocytes and necrotic debris. A small number of mammary alveoli multifocally contain viable, degenerated and lytic neutrophils as well as necrotic debris that is bordered, dissected, and compressed by collars of fibrosis.

Morphological Diagnosis:

Mammary Gland: Severe, chronic-active, multifocal to coalescing neutrophilic, necrotizing and lymphoplasmacytic mastitis with intralesional bacteria, granulation tissue and sequestrum formation

Disease: Coliform mastitis

Aetiology: *Klebsiella pneumoniae*

Contributor's Comment:

The post-mortem findings are compatible with the history of mastitis. Based on the gross post-mortem appearance of the mammary glands, a coliform mastitis was considered most likely, with *E. coli, Klebsiella spp.,* and *Enterobacter spp.* considered as the top differentials. Furthermore, the macroscopic and histopathological findings of necrosis and inflammation within the mammary parenchyma were compatible with coliform mastitis.

Bovine mastitis is one of the most prevalent and consequential diseases of dairy cows globally, carrying significant detrimental welfare and financial implications (1). Mastitis in dairy cows is caused by a wide varie-

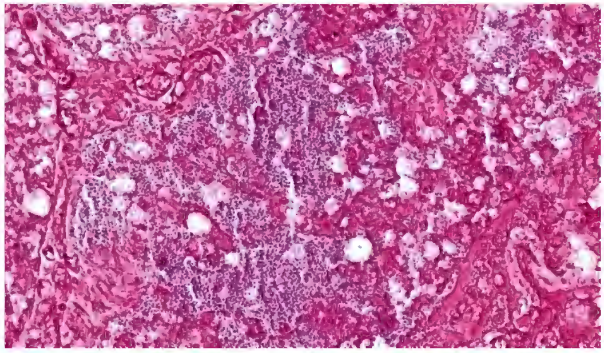

Figure 1-3. Mammary gland, ox: High magnification of tissue within the sequestrum. There is a diffuse loss of staining affinity. Scattered throughout this area, there are numerous individualized 2um bacilli. (HE, 915X).

ty of pathogens, including gram-positive cocci, gram-negative bacilli, *Mycoplasma bovis*, and the *Prototheca* species. Among these, gram-positive cocci and gram-negative bacilli are the main agents and the pathogenesis encompasses ascending infection. *Streptococcus agalactiae* and some types of *Staphylococcus aureus* are obligate parasites of the gland and inevitable pathogens, but the great majority of infections are opportunistic and environmental (see JPC 1210466).

Coliform bacteria such as *Escherichia coli* (the most common), and other Enterobacteriaceae *(Enterobacter, Klebsiella, Citrobacter, Serratia, and Proteus).* are ubiquitous in the environment and have the capacity to cause severe environmental mastitis via ascending infection from the teat.[1] Coliforms produce endotoxins causing hemorrhage, oedema, thrombosis, and vascular damage, subsequently damaging tissues and potentially leading to death. Lactating cows are more likely to succumb to the effects of the endotoxins, as their response is determined by their reproductive cycle.[5] The typical coliform mastitis in cows presents clinically with a sudden drop in milk production, watery or bloody milk, and a swollen, hot, and painful udder. Affected cows often show systemic signs such as fever, depression, dehydration, and, in severe cases, may become recumbent or die rapidly due to endotoxemia. As seen in this case, if the cow survives this acute and toxic stage, the affected mammary gland is then likely to sequester and slough off due to necrosis of the glandular tissue secondary to chronic coliform mastitis.[12]

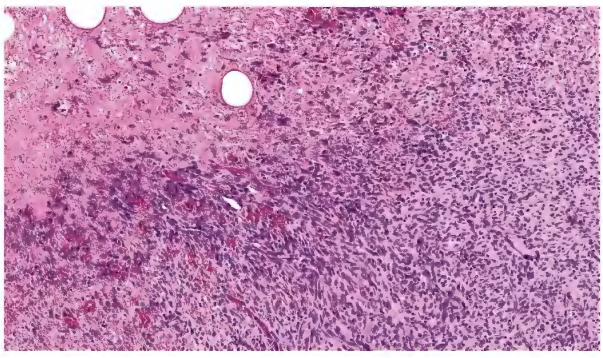

Figure 1-4 Mammary gland, ox: Areas of infarction are also bounded by maturing granulation tissue, which forms dense bands of fibrous connective tissue effacing the adjacent alveolar tissue. ERE. (HE, 468X).

Extensive investigations on the virulence profile of the *E coli* associated mastitis did not identify a clear set of virulence genes, and some authors prefer the use of mastitis associated *E. coli* (MAEC), with MAEC being more an "ecotype" rather than a "pathotype" .[6, 16]

Klebsiella pneumoniae is one of the most common coliforms causing clinical bovine mastitis, but has been found to be one of the most damaging when considering milk production, treatment costs, and mortality rate. *K. pneumoniae* mastitis has a poor cure rate after antimicrobial treatment, and although it is commonly an environmental opportunist, lateral spread from diseased to healthy cattle is possible.[11, 12]

The pathogenicity of *K. pneumoniae* is related to its virulence factors, with the primary factors being capsular polysaccharide (CPs), lipopolysaccharides, siderophores, and fimbriae. Furthermore, *Klebsiella* species are a known reservoir for antibiotic resistance genes, which can spread to other Gram-negative bacteria.[12, 16, 17] In vitro infection of bovine mammary epithelial cells with *K. pneumoniae* resulted in, showing rapid adherence to, and invasion of, mammary epithelial (milk-producing) cells by *K. pneumoniae* leading to cellular damage and apoptosis. *K. pneumoniae* was shown to promote the production of the following cytokines:

IL8, IL-1β, and Tumor Necrosis Factor-α (TNF-α), as well as promoting the transcriptional expression of the pro-inflammatory genes for IL-6, IL-8, IL-1β, and TNF-α.[10]

Contributing Institution:

Veterinary Pathology Service
University of Nottingham
Sutton Bonington Campus
College Road
Sutton Bonington
Leicestershire
United Kingdom
LE12 5RA
https://www.nottingham.ac.uk/vet/service-for-business/veterinary-pathology-service/index.aspx

JPC Morphologic Diagnosis:

Mammary gland: Mastitis, necrosuppurative, chronic-active, multifocal to coalescing, severe, with infarction and innumerable coccobacilli.

JPC Comment:

The one and only Dr. Corrie Brown, livestock infectious disease expert extraordinaire from the University of Georgia, moderated the JPC's 22nd conference this year before presenting the keynote lectures at the Northeastern Veterinary Pathology Conference in Washington, D.C. She put WSC participants through their paces with a quartet of excellent ruminant cases, starting off with this classic, but deceptively nuanced, case of coliform mastitis. This served as a springboard to review the anatomy, immunology, and epidemiology of mastitis in dairy cattle. One participant astutely reminded everyone that, in the lactating mammary gland, the term "acinus" should be substituted in favor of the term "alveolus" to help differentiate between the stages. This is a small but important distinction when describing the functional unit of milk production.

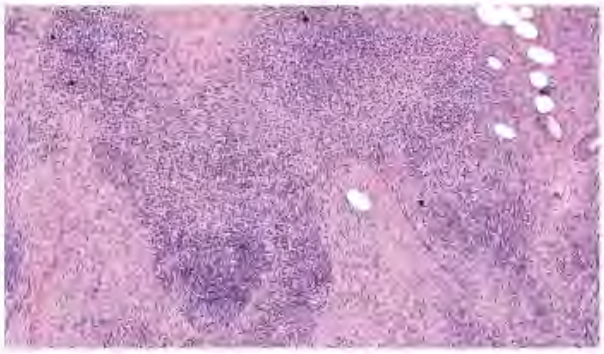

Figure 1-5. Mammary gland, ox. Within the remaining mammary gland, there is effacement of alveolar tissue by fibrous connective tissue and a diffuse infiltrate of macrophages, fewer neutrophils, and aggregates of lymphocytes and plasma cells. Remnant alveoli and ducts are shrunken and infiltrated by inflammatory cells and occasionally contain corpora amylaceae and few neutrophils. (HE, 121X)

Participants initially considered *Staphylococcus aureus* as a potential cause in this case. However, the absence of Splendore–Hoeppli material and the overwhelming necrosuppurative characteristic of the lesion made this etiology less likely. *Trueperella pyogenes* was also suggested as a differential, but its hallmark abscess formation was not present. Instead, presentation of overwhelming necrosis pointed towards coliforms, which, as the contributor mentioned in their comment, include *E. coli, Enterobacter, Klebsiella, Citrobacter, Serratia,* and *Proteus*.[1,2]

Dr. Brown emphasized that mastitis is primarily a disease of dairy cattle, not because other animals don't get mastitis, but because dairy cows experience far more teat trauma through repeated hand- or machine-milking. The teat canal and cistern normally provide excellent immune protection, but chronic mechanical stress compromises this barrier. This is why pre- and post-milking teat dipping remains one of the most effective mas-

titis prevention strategies in modern dairy management.

A key teaching point was that effectively all mastitis pathogens enter the mammary gland through the teat with one important exception: highly pathogenic avian influenza.[14,15] This virus is currently the only virus known to infect the bovine mammary gland. HPAI was recently seen in the WSC this year during Conference 17, Case 2.

Dr. Brown contrasted the clinical behavior of the major mastitis pathogens as important clues to assist the pathologist in narrowing down differentials. *Staphylococcus aureus* and *Streptococcus spp.* typically cause subclinical or mild clinical mastitis — the cow feels fine, but the milk looks and smells abnormal. Dry cow therapy has nearly eradicated *Streptococcus* mastitis in the United States, although *Staphylococcus* continues to be one of the most common mastitis pathogens affecting dairy cattle.[7] Coliform mastitis, however, is entirely different. Cows become acutely, profoundly ill, often immediately postpartum, with systemic endotoxemia driving the severity of disease.[2] Recovery rates are poor even with aggressive therapy.[2,11,12]

Participants differed in opinion regarding the use of the term "sequestrum." While the contributor provides a cogent explanation for why this term may be used in cases of mastitis - due to the body walling off the affected quarter and eventually sloughing it - some participants opined that the sharply demarcated, devitalized region of mammary tissue was better described as an infarct given the endotoxin-induced thrombosis that is characteristic of coliform mastitis. This distinction mattered, they argued, because the pathogenesis is vascular, not traumatic.

Discussion then turned to *Klebsiella pneumoniae*, the major pathogen in this case. *Klebsiella* thrives in wood products such as sawdust and shavings, making bedding a common source of exposure.[8] While sometimes described as "contagious," Dr. Brown clarified that transmission is environmental, not cow to cow.[11] Participants debated whether *Klebsiella* can enter mammary epithelial cells; while *Salmonella* and *Shigella* are well-established as intracellular pathogens, the evidence for *Klebsiella* is less clear.[4] There are, however, some in-vitro studies that suggest possible invasion, although whether this translates in-vivo has yet to be fully elucidated.[4]

One participant noted that the bacterial morphology in this case did not match their mental image of *Klebsiella*, which is typically produces a capsule. The capsule of *Klebsiella* is one of its most important virulence factors.[10,17] The organisms here appear to lack a capsule on H&E, which contributed to diagnostic hesitation. Others wondered whether a *Staphylococcus aureus* co-infection might be present, which is certainly possible given that there were several gram-positive bacteria present on a Gram stain. However, capsule production by *Klebsiella* may be downregulated secondary to certain host factors, such as increased extracellular iron as occurs with severe tissue damage, so reliance on capsule presence may be deceptive.[10]

References:

1. Bianchi RM, Schwertz CI, de Cecco BS, Panziera W, De Lorenzo C, Heck LC, Snel GGM, Lopes BC, da Silva FS, Pavarini SP, Driemeier D. Pathological and microbiological characterization of mastitis in dairy cows. *Trop Anim Health Prod.* 2019 Sep;51(7):2057-2066.

2. Burvenich C, Van Merris V, Mehrzad J, Diez-Fraile A, Duchateau L. Severity of E. coli mastitis is mainly determined by cow factors. Vet Res. 2003;34(5):521-564.

3. Cheng J, Zhang J, Han B, Barkema HW, Cobo ER, Kastelic JP, Zhou M, Shi Y, Wang J, Yang R, Gao J. Klebsiella pneumoniae isolated from bovine mastitis is cytopathogenic for bovine mammary epithelial cells. J Dairy Sci. 2020 (4):3493-3504.

4. Clegg S, Murphy CN. Epidemiology and Virulence of Klebsiella pneumoniae. Microbiol Spectr. 2016;4(1):10.1128/microbiolspec.UTI-0005-2012.

5. Foster, R.A., 2017. Female reproductive system and mammae. In: J.F. Zachary (ed), Pathologic basis of veterinary disease, 6th ed, (Elsevier, St. Louis, MO), p. 1147–1193.

6. Germon P, Foucras G, Smith DGE, Rainard P. Invited review: Mastitis Escherichia coli strains-Mastitis-associated or mammo-pathogenic? J Dairy Sci. 2025 May;108(5):4485-4507.

7. Keefe GP. Streptococcus agalactiae mastitis: a review. *Can Vet J*. 1997;38 (7):429-437.

8. Morales-Ubaldo AL, Rivero-Perez N, Valladares-Carranza B, Velázquez-Ordoñez V, Delgadillo-Ruiz L, Zaragoza -Bastida A. Bovine mastitis, a worldwide impact disease: Prevalence, antimicrobial resistance, and viable alternative approaches. *Vet Anim Sci*. 2023 Jul 24;21:100306.

9. Munoz MA, Welcome FL, Schukken YH, Zadoks RN. Molecular epidemiology of two Klebsiella pneumoniae mastitis outbreaks on a dairy farm in New York State. *J Clin Microbiol*. 2007;45 (12):3964-3971.

10. Paczosa MK, Mecsas J. Klebsiella pneumoniae: Going on the Offense with a Strong Defense. *Microbiol Mol Biol Rev*. 2016;80(3):629-661. Published 2016 Jun 15.

11. Pollock J, Foster G, Henderson K, Bell J, Hutchings MR, Paterson GK. Antimicrobial resistance profiles and molecular epidemiology of Klebsiella pneumoniae isolates from Scottish bovine mastitis cases. *Epidemiol Infect*. 2025 Jan 17;153:e15

12. Schlafer, D.H., Foster, R.A. 2016 Female genital system. In: M.G. Maxie (ed|), Jubb, Kennedy, and Palmer's Pathology of Domestic Animals, 6th ed, vol. 3, (Elsevier, St. Louis, MO), 358–464.

13. Schukken Y, Chuff M, Moroni P, Gurjar A, Santisteban C, Welcome F, Zadoks R. The "other" gram-negative bacteria in mastitis: Klebsiella, serratia, and more. Vet Clin North Am Food Anim Pract. 2012 Jul;28(2):239-56.

14. Shi J, Kong H, Cui P, et al. H5N1 virus invades the mammary glands of dairy cattle through 'mouth-to-teat' transmission. *Natl Sci Rev*. 2025;12(9):nwaf262.

15. Sordillo LM, Streicher KL. Mammary gland immunity and mastitis susceptibility. *J Mammary Gland Biol Neoplasia*. 2002;7(2):135-146.

16. Tong X, Barkema HW, Nobrega DB, Xu C, Han B, Zhang C, Yang J, Li X, Gao J. Virulence of Bacteria Causing Mastitis in Dairy Cows: A Literature Review. *Microorganisms*. 2025 Jan 15;13(1):167.

17. Wusiman, M., Zuo, J., Yu, Y. et al. Mo-

lecular characterization of Klebsiella pneumoniae in clinical bovine mastitis in 14 provinces in China. *Vet Res Commun*. 2025;49(18).

CASE II:

Signalment:

Four-year-old Holstein cow (*Bos taurus taurus*).

History:

A 5-year-old Holstein cow was presented with a history of breathing difficulty, and progressive weight loss before calving. The cow was treated with tetracycline, dipyrone, and flunixin meglumine for approximately two weeks; however, the doses were not recorded by the farmer. After calving, weight loss worsened and muffled heart sounds were noticed 3 days before the animal died.

Gross Pathology:

A five-year-old Holstein cow was submitted for necropsy examination presenting a poor body condition and markedly pale mucous membranes. Grossly, extensive areas of hemorrhage were observed in the pericardium, epicardium, extending to the pulmonary artery. Examination of the heart cavities demonstrated a friable, irregular, mottled white, brown and red vegetative mass of approximately 5.0 x 3.0 x 2.0 cm firmly adhered to all cusps of the pulmonary valve (Figure 1). In the lungs, multifocal to coalescent areas of consolidation were observed in all pulmonary lobes, and these were characterized by firm consistency, reddish color, and were associated with interlobular edema. Additionally, multiple yellowish, firm structures were observed occluding blood vessels (thrombi) (Figure 2). The abomasum was markedly distended and filled with free non coagulated blood, associated with severe multifocal mucosal ulcerations. Hemorrhagic content was seen throughout the intestinal tract. No other lesions were observed in the remaining organs.

Figure 2-1. Pulmonary valve, ox: A friable vegetative mass of approximately 5.0 x 3.0 x 2.0 cm firmly adhered to all cusps of the pulmonary valve (*Photo courtesy of:* Faculdade de Veterinária, Universidade Federal do Rio Grande do Sul, Setor de Patologia Veterinária, http://www.ufrgs.br/

Figure 2-2. Pulmonary valve, ox: The lungs are multifocally consolidated firm, and were associated with interlobular edema. Yellow thrombi are present within vessels. (*Photo courtesy of:* Faculdade de Veterinária, Universidade Federal do Rio Grande do Sul, Setor de Patologia Veterinária, http://www.ufrgs.br/patologia)

Laboratory Results:

Refrigerated samples of the lungs and valve were cultured and submitted to the 16S

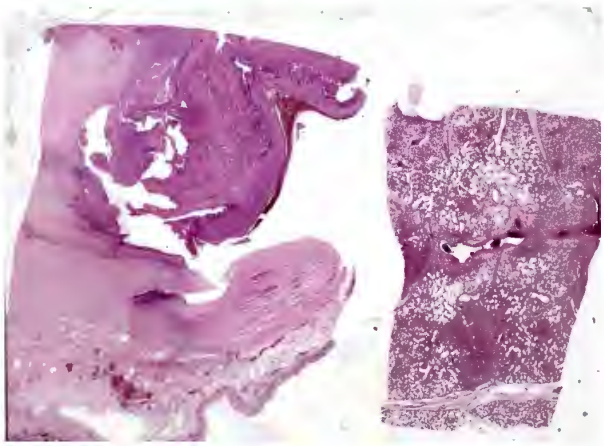

Figure 2-3. Pulmonary valve and lung. ox: A markedly remodeled section of the pulmonary valve with a large thrombus on the dorsal surface is submitted as well as a section of markedly consolidated lung.

rRNA gene sequencing that revealed *Helcococcus ovis* in the valve sample. No bacterial growth was obtained from the lung sample. Gram stain was performed in the lungs and valve showing abundant Gram-positive coccoid bacterial aggregates inside arterioles in the lungs and in the vegetative structures in the heart.

Microscopic Description:

The submitted slides present one section of heart and one section of lung (Figure 3). In the heart, severe thickening of the pulmonary valve endocardium is observed, characterized by marked proliferation of fibrovascular tissue, inflammatory infiltrate of non-degenerate and degenerate neutrophils, as well as macrophages, deposition of eosinophilic material (fibrin), cellular debris, and an abundant number of coccoid basophilic bacterial colonies. The lung exhibits multifocal severe thrombosis characterized by large amounts of fibrin deposition inside large and small arterioles, associated with Gram-positive bacterial colonies (Figure 4), similar to those seen in the pulmonary valve (not all slides contain bacterial colonies in the lungs). Adjacent to these areas, in the alveolar space, a moderate inflammatory infiltrate of neutrophils, areas of necrosis, edema, and fibrosis, as well as free erythrocytes (hemorrhage), and a moderate number of macrophages are observed. Interlobular septa are thickened by fibrous connective tissue and inflammatory infiltrate of non-degenerate and degenerate neutrophils, as well as fibrin deposition. There is also a moderate thickening of the visceral pleura, characterized by the proliferation of fibrous connective tissue.

Contributor's Morphologic Diagnosis:

Heart: Valvulitis and Endocarditis, fibrinosuppurative, diffuse, severe, with intralesional coccoid bacterial aggregates.
Lung: Pneumonia, suppurative, thromboembolic, multifocal to coalescent, severe, with intralesional coccoid bacterial aggregates.

Contributor's Comment:

The gross and microscopic findings observed in this case were compatible with vegetative valvular endocarditis and thromboembolic pneumonia caused by a bacterial agent, that was confirmed through culture and molecular analysis as *Helcococcus ovis*. This bacterium is a gram-positive coccus

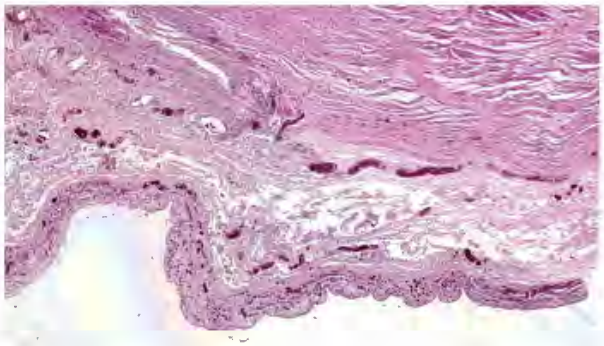

Figure 2-4. Pulmonary valve, ox: The valve is markedly remodeled by abundant edema, moderate suppurative inflammation, granulation tissue and fibrosis. (HE, 32X)

that has been associated with multiple clinical presentations, such as mastitis in sheep, endocarditis and abortion in cattle, and pulmonary abscesses in horses.[2,6] Reports in Germany suggest that *H. ovis* is an emerging pathogen that can lead to valvular endocarditis.[5] Differential diagnoses must include other bacterial agents, such as *Streptococcus* sp. and *Trueperella pyogenes*, which are the most common agents associated to endocarditis in cattle.[1] Besides bacteria, occasionally mycotic or parasitic infection can lead to endocarditis, as a result of systemic mycotic disease caused by zygomycetes or *Aspergillus* sp., or larvae of *Strongylus vulgaris*.[7]
Endocarditis is the inflammation of endocardium, and even though any part of this tissue layer may be affected, lesions usually affect primarily the valves.[7] In cattle, the tricuspid valve, followed by the mitral valve are more commonly involved in endocarditis, and the pulmonary valve is considered to be an uncommon presentation.[1,5] Usually, endocarditis in cattle is associated with traumatic lesions, followed by bacterial infection, with sustained or recurrent bacteremia, such as in cases of peritoneal abscesses, hepatic abscesses, mastitis and metritis.[7] It is not well understood how *H. ovis* enters the bloodstream or its original habitat; however, Rothschild suggested that the possible source of

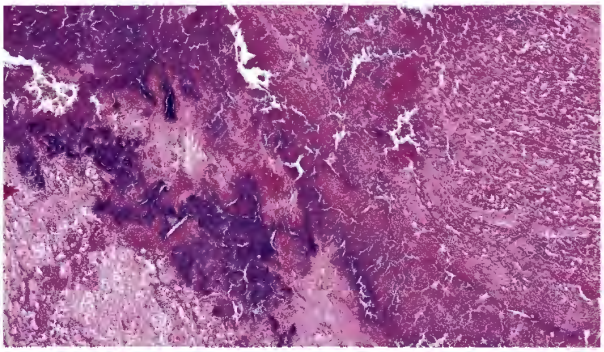

Figure 2-5. Pulmonary valve, ox: Adherent to the valve is a large fibrin thrombus with entrapped colonies of cocci. (HE, 387X)

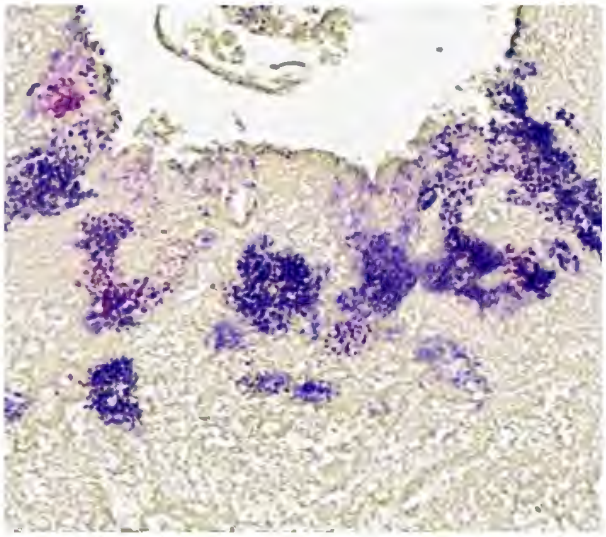

Figure 2-6. Pulmonary valve, ox: Numerous colonies of gram-positive cocci are embedded within the fibrin thrombus. (Brown-Brenn, 1350X)

infection could be the skin.[8] Bacteria from the skin can enter into the systemic circulation due to lesions that break the skin barrier, leading to bacteremia, and may adhere to heart valves.[7] In the present case, no surgical procedure was done, nor open wound or history of previous diseases, including mastitis or metritis, were observed or reported. Even though the cow presented abomasal ulcers at the time of necropsy, those were considered to be acute as a result of anti-inflammatory treatment and not related to the endocarditis.

Post reported a case of valvular endocarditis by *H. ovis* in the right atrioventricular valve of a bull in the state of North Carolina (USA), and the microscopic findings, such as severe inflammatory infiltrate and areas of necrosis, were similar to those observed in this case.[6] Similar patterns of chronic endocarditis caused by *H. ovis* were described by Kutzer, which consisted of valvular emboli characterized by a luminal zone showing unorganized fibrinous exudate.[5]

Common clinical signs of endocarditis in cows are reported as progressive weight loss,

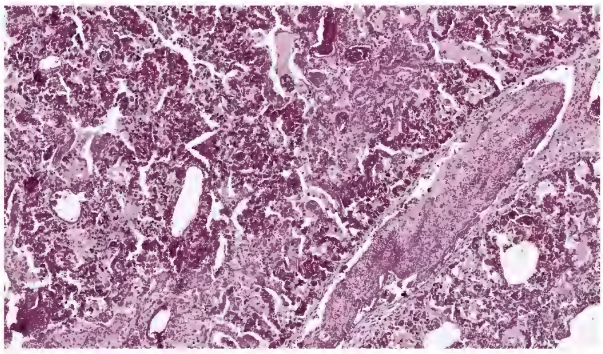

Figure 2-7. Lung, ox: In areas of consolidation, septa are markedly congested, and alveoli contain abundant edema, hemorrhage, and polymerized fibrin. Intralobular septa are markedly expanded by edema and lymphatics contain occlusive fibrin thrombi. (HE, 220X)

drop in milk production, lameness, tachycardia with auscultation of heart murmur, fever, and consequent respiratory distress.[1,7] In the case here described, the owners noticed weight loss, milk drop and fever, however, these clinical signs were thought to be associated with other infectious diseases, including tick fever. Valvular endocarditis is usually fatal, and valvular damage and embolism are common sequelae.[4,7] Some portions of the vegetative lesion can detach and be carried through the blood circulation as emboli and, in some cases such as the one described here, those emboli are also septic, carrying the bacterial agent involved in the endocarditis. Emboli that arise from the right heart usually produce pulmonary abscessation or pulmonary thrombosis, as observed in this case.[7] The lung lesions were consistent with pulmonary thromboembolism due to the right heart endocarditis. Surrounding the thrombi areas in the lungs, areas of coagulative necrosis with inflammatory cells and hemorrhage could be observed.

In the case here described, it was only possible to culture the bacteria from the heart sample (affected valve), and not from the lungs. This difference may be caused by several features related to the location of bacterial aggregates, bacteria behavior, selection of sampling area and previous antibiotic treatment. One of the main characteristics of *H.ovis* is that it shows growth in satellites, and the lack of inoculation with other bacteria (e.g. Staphylococcus aureus) may have disadvantaged the isolation of the agent.[5] The methods used in classical bacteriology are unable to reach the definitive diagnosis of infection by *H.ovis,* and molecular analysis is necessary to identify this bacterium.

Contributing Institution:

Setor de Patologia Veterinária, Universidade Federal do Rio Grande do Sul, Brazil Faculdade de Veterinária

Universidade Federal do Rio Grande do Sul
Setor de Patologia Veterinária
http://www.ufrgs.br/patologia

JPC Morphologic Diagnosis:

Pulmonary valve: Valvulitis, fibrinosuppurative, chronic-active, focally extensive, severe, with remodeling and colonies of cocci.

Lung: Pneumonia, embolic, fibrinosuppurative, chronic-active, diffuse, severe with marked edema and septic thrombi.

JPC Comment:

This case challenged participants right from the start with tissue identification. Several attendees initially thought they were looking at the aorta or another large elastic artery. Only after it was revealed in conference to be heart valve did many realize the tissue in question was pulmonic valve. This tissue ID, which very few participants managed to get to before conference, could be aided by a small region of cardiac muscle (likely at the valve root, with central nuclei and fibrosis, a subtle but critical clue. This set the tone for a case that required attention to anatomic

context and lesion distribution.

Once oriented, participants quickly recognized the hallmarks of valvular endocarditis with septic thromboembolic pneumonia, a classic pairing when emboli originate from the right heart. A separate case in a non-human primate was seen in this year's Conference 5, Case 2. Dr. Brown emphasized this point: right-sided endocarditis causes pulmonary emboli, whereas left-sided endocarditis produces systemic infarcts (especially in the kidneys). The lung lesions in this cow (fibrinosuppurative embolic pneumonia with septic thrombi) were textbook examples of this pathogenesis.

Differentials for bovine endocarditis were reviewed, with *Streptococcus bovis* and *Trueperella pyogenes* topping the differential list for many participants. These two bacteria remain the most common etiologies for this disease in cattle.[1] However, the contributor identified the culprit as *Helcococcus ovis*. There is also a recently described related species that is able to cause human disease called *Helcococcus bovis,* which is closely related to *H. ovis*.[3] This organism is becoming recognized as an emerging pathogen in ruminants, though it is still unfamiliar to many diagnosticians.[3,4,5] Dr. Brown noted that *Helcococcus ovis* and *H. bovis* are believed to be part of the skin microbiome, gaining access to the bloodstream through minor breaches in the integument.[5] *H. ovis* has also demonstrated widespread resistance to tetracyclines.[3]

A particularly interesting point mentioned in conference was the organism's growth behavior. *Helcococcus bovis* demonstrates satellite growth, requiring the presence of *Staphylococcus* spp. on blood agar to grow robustly.[5] This helps to explain why the organism was isolated from the valve, where bacterial load was highest, but not from the lungs, despite clear histologic evidence of septic emboli. Dr. Brown reminded participants that failure to culture an organism does not exclude its presence, especially when dealing with fastidious bacteria.

This cow also had abomasal ulcers, which prompted a brief review of NSAID-associated ulceration. Dr. Brown walked participants through the mechanism: NSAIDs inhibit prostaglandin synthesis, which among other deleterious processes, leads to decreased bicarbonate secretion. A lack of bicarbonate results in increased abomasal acidity, leading to mucosal injury and ulcer formation. These lesions were considered acute and unrelated to the endocarditis by the contributor.

References:

1. Buczinski S, Tsuka T, Tharwat M: The diagnostic criteria used in bovine bacterial endocarditis: A meta-analysis of 460 published cases from 1973 to 2011. *Vet J*. 2012;193(2):349–357.
2. Colins MD, Falsen E, Foster G, Monasterio LR, Dominguez L, Fernandez-Garazabal JF: *Helcococcus ovis* sp. nov., a Gram-positive organism from sheep. *Int J Syst Bacteriol*. 1999;49 (4):1429-1432.
3. Cunha F, Zhai Y, Casaro S, et al. Pangenomic and biochemical analyses of *Helcococcus ovis* reveal widespread tetracycline resistance and a novel bacterial species, *Helcococcus bovis*. *Front Microbiol*. 2024;15:1456569.
4. Kemper RT, Lopes BC, Rosa RB, et al: Valvular endocarditis associated with *Helcococcus ovis* in a cow in Southern Brazil. *Cienc Rural*. 2020. In press.
5. Kutzer P, Schulze C, Engelhardt A, Wieler LH, Nordhoff M: *Helcococcus*

ovis, an emerging pathogen in bovine valvular endocarditis. *J Clin Microbiol*. 2008;46(10):3291-3295.

6. Post KW, Rushton SD, Billington SJ: Valvular endocarditis associated with *Helcococcus ovis* infection in a bovine. *J Vet Diagn Invest*. 2003;15(5):473-475.
7. Robinson WF, Robinson NA. Cardiovascular system. In: MAXIE MG, ed. *Pathology of Domestic Animals-Volume 3*. 6th ed. St. Louis, USA: Elsevier; 2016:16-101.
8. Rothschild CM, Oaks JL, Schaupp JK, Rurangirwa FR, Sellon DC, Hines MT: *Helcococcus ovis* isolated from a pulmonary abscess in a horse. *J Clin Microbiol*. 2004;42(5):2224-2226.

CASE III:

Signalment:

Angus feeder calf (*Bos Taurus)* less than one year of age. Unknown gender.

History:

Acute onset of severe respiratory distress with cough and expiratory noise. The calf was afrebrile (102.6 °F). When the calf was removed from its pen to administer treatment, it died in the chute.

Gross Pathology:

No gross lesions were reported.

Laboratory Results:

PCR on lung tissue was negative for *Pasteurella multocida, Histophilus somni, Mannheimia haemolytica, Mycoplasma bovis,* Bovine herpesvirus 1, Bovine viral diarrhea virus, Bovine coronavirus, and Bovine respiratory syncytial virus.

Aerobic culture of lung yielded no bacterial pathogens.

Microscopic Description:

Lung: Sections of lung display a severe diffuse proliferative and exudative inflammatory process. Alveolar spaces contain variable amounts of homogenous eosinophilic fluid (edema fluid) mixed with fibrin and leukocytes. There is diffuse type II pneumocyte hyperplasia. Alveoli are lined by hyaline membranes (variability in the severity of hyaline membranes is observed among the sections submitted). Bronchi and bronchioles in some locations appear within normal limits whereas in other regions they are lined by attenuated epithelial cells and contain edema mixed with macrophages and sloughed epithelial cells within their lumina. There is pleural, peribronchiolar, and interlobular edema. Alveolar septa are thickened and severely congested.

Contributor Morphologic Diagnosis:

Lung; pneumonia, interstitial, histiocytic, subacute, diffuse, severe, with hyaline membrane formation, type II pneumocyte hyperplasia, and edema

Contributor Comment:

Atypical interstitial pneumonia (AIP) repre-

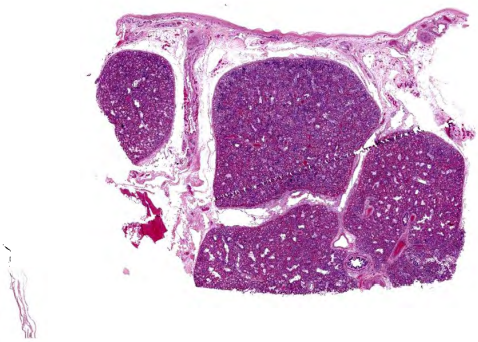

Figure 3-1. Lung, ox: A section of lung is submitted for examination. At subgross magnification, the interlobular septa and pleura is markedly expanded by clear space, and the pulmonary parenchyma is consolidated. (HE, 10X)

sents a sporadic disease of cattle that has traditionally been known by a number of names including "fog fever", "dust pneumonia", and "acute bovine pulmonary emphysema and edema", among others.[5,7] A number of causes have been proposed in the literature including ingestion of compounds toxic to pneumocytes, poor air quality, inhalation of foreign material, as well as parasites and viruses, most notably BRSV.[4]

The metabolic activation and accumulation of 3-methyl indole (3-MI), a metabolite of tryptophan is the most widely accepted cause and is traditionally seen in cattle moved to lush green pastures in the early fall. Animals affected with AIP have been shown to have significantly higher plasma levels of 3-MI compared to unaffected animals.[1] Additionally, a syndrome mimicking AIP was experimentally reproduced in cattle and goats after the administration of 3-MI.[3]

Within the rumen, L-tryptophan is converted first to indoleacetic acid and subsequently to 3-MI by *Lactobacillus* spp. of bacteria.[2] Within the lung, nonciliated epithelial cells called Club cells (formerly called Clara cells) further metabolize 3-MI resulting in a compound that is toxic to pneumocytes and endothelial cells.[4] The resulting vascular and epithelial cell damage results in large

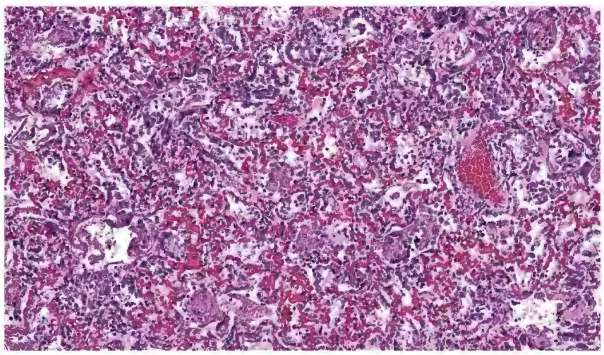

Figure 3-2. Lung, ox: Diffusely, alveolar spaces contain abundant edema fluid, polymerized fibrin, and moderate numbers of alveolar macrophages and fewer neutrophils. HE, 256X)

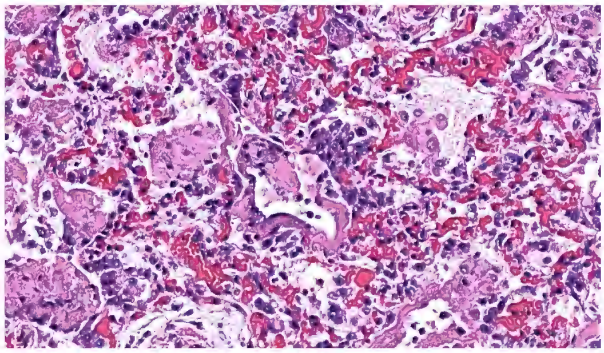

Figure 3-3. Lung, ox: Multifocally, polymerized fibrin occasionally compacts at the periphery of alveoli to form hyaline membranes (center). (HE, 556X)

amounts of high protein content edema fluid that polymerizes forming the hallmark histologic feature of hyaline membranes. The lining of alveolar walls with hyaline membranes decreases oxygen exchange efficiency leading to the severe respiratory distress and ultimately death in these animals.

Further complicating the etiologic component behind AIP is the fact that the disease also occurs in feedlot animals who are not fed lush grasses but instead a more concentrated ration. Potential AIP causes or inciting factors unique to feedlot environments that have been proposed are discussed in a recent review and include melengestrol acetate (MGA), BRSV infection, bacterial respiratory disease, heat, and dusty conditions.[9]

Response to treatment for AIP is traditionally very poor.[4] In the contributor's experience, feedlot cases of AIP tend to happen in fat cattle (most often heifers) at the end of the feeding period during the late summer months with high daytime temperatures. Experiencing sudden deaths due to AIP the week, or even the day of shipment to slaughter is not uncommon, making the economic losses even greater on a per case basis. The contributor has observed numerous cases with a history like this case where the stress of movement in these respiratory compro-

mised animals proves too much and they often die on the way to, or within the chute when treatment is attempted.

Contributing Institution:

University of Nebraska – Lincoln
Nebraska Veterinary Diagnostic Center
Lincoln, NE
https://vbms.unl.edu/nvdls

JPC Morphologic Diagnosis:

Lung: Pneumonia, interstitial, necrotizing, subacute, diffuse, severe, with hyaline membranes, type II pneumocyte hyperplasia, and interlobular and pleural emphysema and edema.

JPC Comment:

This case illustrates a classic picture of acute interstitial pneumonia (AIP) in cattle. This condition has been historically known by a few different names, including "atypical interstitial pneumonia," "acute bovine pulmonary emphysema and edema" (ABPEE) or "fog fever." The names "fog fever" and ABPEE are still widely used clinically. Participants were reminded that this syndrome fits under the clinical umbrella of acute respiratory distress syndrome (ARDS), whereas pathologically it is best described as diffuse alveolar damage (DAD). It is important to note that DAD is a pattern rather than a single disease entity. Dr. Brown discussed with participants the five major causes of DAD in cattle that are worth having as a mental list: Lush pasture/L tryptophan (3 MI ("fog fever")), moldy sweet potatoes (4-ipomeanol), perilla mint toxicity, high oxygen exposure ("oxygen toxicity"), and radiation/certain chemotherapeutics.

On histology, the lung showed the expected constellation of hyaline membranes, type II pneumocyte hyperplasia, and interlobular and subpleural emphysema that are consistent with DAD. The group focused temporarily on the interlobular septa, where the clear spaces were debated as edema versus emphysema. Several participants emphasized that, in this context, the expansion of the interstitium and septa are far more likely to be emphysema from ruptured alveoli rather than just edema, especially when accompanied by the clear space dissecting along septa and into the pleura. This correlates well with the most reported gross findings for AIP in cattle, which include interlobular emphysema, a "checkerboard" appearance to the lungs of alternating firm, dark red areas and fluffy, pink areas, and overinflated lobes. [8]

The pathogenesis discussion centered on the classic pasture-associated form of AIP, which is covered by the contributor in their comment. The resulting vascular and epithelial injury leads to protein-rich edema, hyaline membrane formation, and interstitial emphysema, all of which were seen in this case. The feedlot form of AIP received special attention because, as noted by the contributor, its pathogenesis differs. Unlike the well-characterized pasture-associated 3-MI form, the etiology of AIP in feedlot cattle remains unclear. While 3-MI toxicity is central to the disease in pastured cattle, evidence for the same mechanism in feedlot animals is lacking.[6] Other factors mentioned by the contributor, including dietary composition, ruminal microbiome, concurrent respiratory disease, heat, dust, MGA administration in heifers, and management stressors, are all under consideration in the literature and were discussed in conference.[6,8]

Finally, conference goers addressed the chronicity (or lack thereof) of this case, which puzzled many participants. One participant remarked that, in subacute DAD, one expects fibrin and hyaline membranes

whereas, in more chronic stages, type II pneumocyte hyperplasia predominates as the lung attempts repair. It is unusual, but not impossible, to see prominent hyaline membranes and marked type II pneumocyte hyperplasia together. When they do coexist, it likely reflects a lesion in transition, with ongoing injury superimposed on early repair.[8] Both lesions together have been reported in cases of AIP in cattle.[8] In fact, in a recent review, the most consistent histologic features in cases of AIP included hyaline membranes, type II pneumocyte hyperplasia, obliterative bronchiolitis, and interlobular emphysema.[8] This nuance helped reconcile the features seen histologically with the clinical history of acute, severe respiratory distress.

References:

1. Ayroud M, Popp JD, VanderKop MA, et al. Characterization of acute interstitial pneumonia in cattle in southern Alberta feedyards. *Can Vet J.* 2000;41(7):547-554.
2. Carlson JR, Breeze RG. Ruminal metabolism of plant toxins with emphasis on -dolic compounds. *J Anim Sci* .1984;58 (4):1040–9.
3. Carlson J, Yokoyama M, Dickinson, EO. Induction of Pulmonary Edema and Emphysema in Cattle and Goats with 3-Methylindole. *Science.* 1972;176:298-299.
4. Doster AR. Bovine atypical interstitial pneumonia. *Vet Clin North Am Food Anim Pract*. 2010;26(2):395-407.
5. Doster AR, Mitchell FE, Farrell RL, Wilson BJ. Effects of 4-ipomeanol, a product from mold-damaged sweet potatoes, on the bovine lung. *Vet Pathol.* 1978;15(3):367-75.
6. Haydock LAJ, Fenton RK, Sergejewich L, Squires EJ, Caswell JL. Acute interstitial pneumonia and the biology of 3-methylindole in feedlot cattle. Anim Health Res Rev. 2022 Jun;23(1):72-81.
7. Maxie MG, Jubb KVF. Jubb, Kennedy, and Palmer's Pathology of Domestic Animals. 2016:574.
8. Schmidt PH, White BJ, Woolums AR, Larson RL. Scoping review of clinical signs, etiologies, pathology findings, risk factors, and treatments of acute interstitial pneumonia in North American feedlot cattle. JVDI. 2026:10406387261419913.
9. Woolums AR. Feedlot Acute Interstitial Pneumonia. *Vet Clin North Am Food Anim Pract*. 2015;31(3):381-9.

CASE IV:

Signalment:

Four-year-old Texel ewe, sheep (*Ovis aries*)

History:

In January 2018, a farm owner reported clinical signs of blindness and stumbling gait in three sheep. These sheep were part of a flock of 96 Texel sheep, ranging from 5 months to 7 years old. The sheep were raised in a semi-intensive grazing system. Sheep from different origins were purchased and introduced into the flock without any testing for infectious agents. The clinical course lasted approximately 2 months, and other clinical signs included anorexia and progressive weight loss. Due to poor prognosis, these three sheep were humanely euthanized and submitted for postmortem examination. One of the sheep is represented in this conference.

Gross Pathology:

At the gross examination, the ewe was in poor body condition. Sections of the cerebrum revealed multifocal to coalescing, irregular, yellow to brown, soft areas delimiting the periventricular region. The lungs were heavy and non-collapsed, with rib impressions, with a pale gray to pink color, and a diffusely rubbery texture. On the cut surface, multiple white and firm foci, measuring 0.1 to 0.5 cm in diameter were observed, mainly around bronchi. The mammary gland was mildly hardened. No significant lesions were observed in other organs, including multiple joints (stifle, carpi, and tarsi).

Laboratory Results:

The macerated brain and lungs of each animal were pooled, proviral DNA was isolated using a standard phenol-chloroform protocol (Sambrook and Russel, 2001), and the nested PCR was performed using a protocol that amplifies a 460 bp of 5'LTR region of proviral SRLV DNA (Ryan et al., 2000). The nested PCR for VMV was positive on the sheep's tissue pool (brain and lung).

Microscopic Description:

Cerebrum: In the white matter of the cerebrum, adjacent to the lateral ventricles, there is a well-demarcated, focally extensive area of marked neuropil rarefaction and liquefactive necrosis with numerous gitter cells and reactive astrocytes, including gemistocytes. Amidst this area, multifocal, marked inflammatory infiltrate of foamy macrophages and lymphocytes is observed, predominantly surrounding perivascular spaces, sometimes forming nodule-like structures. A similar inflammatory component is observed infiltrating, expanding, and partially effacing the adjacent ependymal epithelium. Additionally, cholesterol clefts, multifocal hemorrhage, multifocal white matter vacuolation, and mineral deposits are observed amidst this periventricular area of necrosis. The choroid plexus of the lateral ventricles (present in some slides) is expanded by abundant fibrin deposition, a small number of macrophages, and moderate to marked infiltrate composed mainly of lymphocytic aggregates forming lymphoid follicle-like structures. In the brainstem, the leptomeninges is moderately expanded by similar areas of perivascular infiltrate (not shown in the slides).

Contributor's Morphologic Diagnosis:

Cerebrum: Leukoencephalitis and ependymitis, necrotizing, lymphohistiocytic, focally extensive, marked, with demyelination, Texel, ovine.

Figure 4-1. Cerebrum, sheep: At subgross magnification, the lateral ventricle is dilated and the cerebral gyri are flattened. There is profound pallor of the periventricular white matter. (HE, 7X)

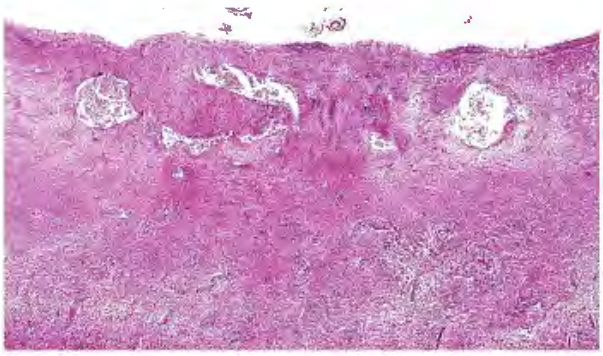

Figure 4-2. Cerebrum, sheep: There is segmental loss of the ependyma. The periventricular white matter is markedly rarefied with foci of liquefactive necrosis and extensive infiltration with inflammatory cells. (HE, 42X)

Choroid plexus: Choroid plexitis, lymphohistiocytic, multifocal, marked, Texel, ovine.

Contributor's Comment:

Small ruminant lentiviruses (SRLV) are non-oncogenic retroviruses that infect sheep and goats, leading to diseases known as visna-maedi (VM; also known as ovine progressive pneumonia) and caprine arthritis and encephalitis (CAE).[2] The etiological agents of VM and CAE are Visna-maedi virus (VMV) and caprine arthritis encephalitis virus (family *Retroviridae*, genus *Lentivirus*). The major tropism of SRLVs is for monocyte/macrophages and dendritic cells.[2,9] Both diseases (VM and CAE) are multisystemic, progressive, and degenerative, with the establishment of persistent viral infection via viral genomic integration into the host's genome.[1,9]

Sheep infected with VMV develop a chronic wasting syndrome characterized by persistent infection in several organs, including lungs, central nervous system, mammary gland, and joints.[1,10] The respiratory form (maedi) is characterized by lymphocytic interstitial pneumonia, smooth muscle hyperplasia and is the most common form of the disease.[2] Clinical signs consist of progressive weight loss and dyspnea.[1,2,10] Chronic progressive arthritis of the carpus or tarsus is seen in SRLV-infected animal, with a higher incidence in goats.[2] A large proportion of sheep and goats infected by this virus present a non-suppurative, indurative mastitis.[2] The neurologic form of the disease (visna) is sporadic and was first described in Iceland as non-suppurative demyelinating encephalitis clinically characterized by a chronic progressive paralytic disease of adult sheep.[10] Different from other studies that describe that the lesions of the nervous form are mainly located in the white matter of the cerebellar peduncles, pons, and the medulla oblongata[1]. In our study the lesions were commonly observed extending from the periventricular areas, and choroid plexus. The occurrence of visna can be related to the involvement of neurotropic strains of VMV, and the severity of the lesions suggests that highly pathogenic strains of the virus are a probability.[1]

Clinical signs of visna are not pathognomonic; therefore, pathological and ancillary laboratory testing is necessary to differentiate this condition from those caused by other pathogens. Differential diagnoses for neurological disease in sheep include listeriosis, Border disease, rabies, louping-ill, polioencephalomalacia, coenurosis, and scrapie.[4,7,8]

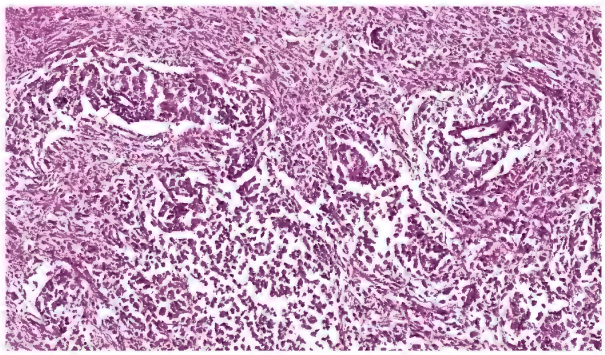

Figure 4-3. Cerebrum, sheep: The rarified periventricular white matter is infiltrated by large numbers of gitter cells which also form thick cuffs around vessels. (HE, 221X)

The clinical features of rabies can be mistaken with the neurologic form of SRLV, as described in our cases, in which the sheep demonstrated similar neurologic signs. Nonetheless, the time lapse between the onset of clinical signs and death significantly differs between the two diseases. Rabies has acute clinical progression (approximately 5 days); visna is instead a chronic and progressive disease that can last for weeks or months.[1,7]

Contributing Institution:

Faculdade de Veterinária
Universidade Federal do Rio Grande do Sul
Setor de Patologia Veterinária
http://www.ufrgs.br/patologia

JPC Morphologic Diagnosis:

Cerebrum: Periventricular demyelination, diffuse, severe, with liquefactive necrosis, hydrocephalus ex vacuo, and histiocytic leukoencephalitis and ependymitis.

JPC Comment:

This last case highlighted the classic neuropathologic presentation of the "visna" form of small ruminant lentivirus (SRLV) infection, and it prompted a rich discussion on lesion distribution, viral tropism, and breed susceptibility. "Maedi" is Icelandic for

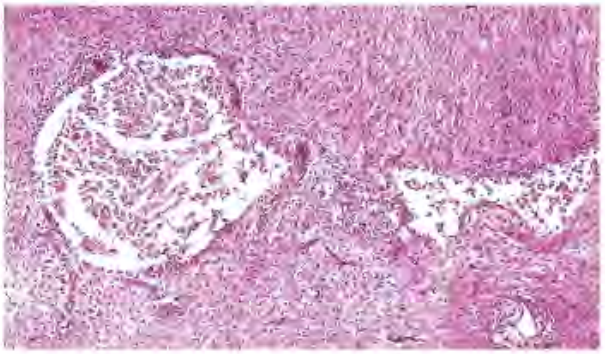

Figure 4-4. Cerebrum, sheep: Gitter cells also fill areas of liquefactive (cavitary) necrosis. (HE, 164X)

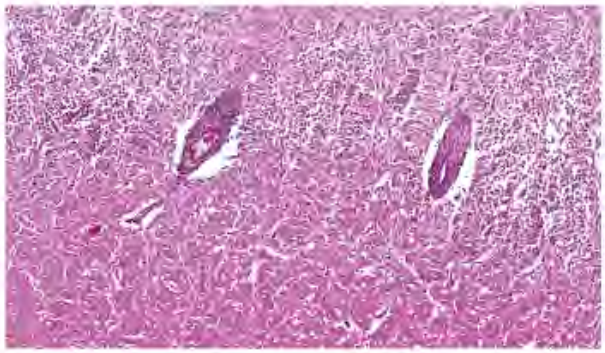

Figure 4-5. Cerebrum, sheep: Vichow-Robins' spaces at the interface of the gray (bottom) and white matter (top) are expanded by numerous macrophages, lymphocytes, and plasma cells. (HE, 125X)

"dyspnea", referring to the respiratory form of SRLV infection, while "visna" means "shrinkage", describing the progressive neurologic wasting syndrome first recognized in Icelandic sheep. In the United States, the pulmonary form is more commonly known as ovine progressive pneumonia (OPP). Regardless of the clinical manifestation, the underlying agent is still SRLV, a non-oncogenic retrovirus with a major tropism for monocytes, macrophages, and dendritic cells.[5,9]

The histologic features in this case were striking. The dominant lesion was massive demyelination of the periventricular white matter, with relative sparing of the internal capsule. The presence of choroid plexus epithelium and lateral ventricle placed this section in the posterior telencephalon, consistent with the known predilection of small SRLV lesions for periventricular regions. Participants noted the flattened gyri and marked ventricular dilation, which are consistent with hydrocephalus *ex vacuo*. This is a form of hydrocephalus seen secondary to a loss of significant amounts of neuroparenchyma, which expands the ventricular system.

Dr. Brown emphasized that SRLV exempli-

fies a lifelong infection. Viral integration into the host genome allows the virus to persist silently for years before clinical disease emerges.[5] Transmission patterns differ somewhat between syndromes: caprine arthritis encephalitis virus (CAE) is classically associated with ingestion of colostrum and milk transmission from infected ewes, whereas MVV is associated with spread via respiratory secretions among adult sheep.[2] However, both viruses can use either route, and both establish chronic infection of macrophages.[5] This macrophage tropism correlates well with the prominent histiocytic infiltrates in the CNS in this case.

The group briefly reviewed the clinical and epidemiologic implications of SRLV infection. Because infected animals remain lifelong carriers, seropositive sheep should be culled in control programs, and flock management must focus on preventing both respiratory spread and milk-borne transmission. The interplay between viral strain and host genetics determines whether an infected animal develops pulmonary "maedi", neurologic "visna", indurative mastitis, or chronic arthritis, and this Texel ewe exemplified the severe neurotropic form of the disease.

Texel sheep, as in this case, are among the breeds reported to be more susceptible to SRLV-associated disease. The reasons are not fully understood, but host genetics are thought to influence both viral replication and lesion severity.[3] Texels have repeatedly been implicated in flocks with high disease burdens.[3] Corriedales and Valais blacknose sheep are also reported to be more susceptible.[3,6]

References:

1. Benavides J, Gómez N, Gelmetti D, Ferreras MC, García-Pariente C, Fuertes M, Gárcia-Marín JF, Pérez V. Diagnosis of the nervous form of maedi-visna infection with a high frequency in sheep in Castilla y León, Spain. *Vet Rec.* 2006;158:230-235.
2. Blacklaws B. Small Ruminant Lentiviruses: Immunopathogenesis of visna-maedi and caprine arthritis and encephalitis virus. *Comp Immunol Microbiol Infect Dis.* 2012;35:259-269.
3. de Miguel R, Arrieta M, Rodríguez-Largo A, Echeverría I, Resendiz R, Pérez E, Ruiz H, Pérez M, de Andrés D, Reina R, de Blas I, Luján L. Worldwide Prevalence of Small Ruminant Lentiviruses in Sheep: A Systematic Review and Meta-Analysis. Animals (Basel). 2021 Mar 11;11(3):784.
4. Guedes KMR, Riet-Correa F, Dantas AFM, Simões SVD, Miranda Neto EG, Nobre VMT, Medeiros RMT. Diseases of the central nervous system in goats and sheep of the semiarid. *Pesq Vet Bras.* 2007;27(1):29-38.
5. Kalogianni AI, Stavropoulos I, Chaintoutis SC, Bossis I, Gelasakis AI. Serological, Molecular and Culture-Based Diagnosis of Lentiviral Infections in Small Ruminants. Viruses. 2021 Aug 27;13(9):1711.
6. Letko A, Bützberger C, Hirter N, Paris JM, Abril C, Drögemüller C. Genetic evaluation of small ruminant lentivirus susceptibility in Valais blacknose sheep. Anim Genet. 2021 Oct;52(5):781-782.
7. Rissi DR, Pierezan F, Kommers GD, Barros CSL. Occurrence of rabies in sheep in Rio Grande do Sul, Brazil. *Pesq Vet Bras.* 2008;28(10):495-500.
8. Rissi DR, Pierezan F, Oliveira Filho JC, Fighera RA, Irigoyen LF, Kommers GD, Barros CSL. Diseases of sheep from central Rio Grande do Sul State, Brazil: 361 cases. *Pesq Vet Bras.* 2010;30(1):21-28.
9. Ryan S, Tiley L, McConnell I, Black-

laws B. Infection of dendritic cells by the Maedi-Visna Lentivirus. *J Virol.* 2000;74(21):10096-10103.

10. Sigurdsson B, Pálsson PA, Grímsson H. Visna, a demyelinating transmissible disease of sheep. *J Neuropathol Exp Neurol.* 1957;16:389-403.

Joint Pathology Center
Veterinary Pathology Services

WEDNESDAY SLIDE CONFERENCE 2025-2026

Conference #23 — 22 April 2026

CASE I:

Signalment:

2-year-old, neutered male, German shepherd dog, *Canis lupus familiaris*, canine

History:

This dog presented to the referring veterinarian for a three-month history of lethargy and neurologic signs, including a hypermetric gait and ataxia. Spinal radiographs and bloodwork were within normal limits. Given prior medical history of testing positive for Lyme borreliosis and anaplasmosis, doxycycline was prescribed, and the dog was referred to a neurologist. Neurological examination revealed hypermetria of the right forelimb, combined vestibular and sensory ataxia, and a broad-based stance. There were "slightly increased cells" in the cerebrospinal fluid and an MRI of the brain was within normal limits. The dog was treated with clindamycin and prednisone for suspected encephalitis. Three weeks later, a urine sample was negative for *Blastomyces dermatitidis* antigen, and a cervical MRI was within normal limits; treatment with doxycycline, clindamycin, and prednisone was continued. One month following the initial presentation, the dog's energy level and appetite had improved, but the dog continued to exhibit mild hypermetria in all four limbs. A recheck cerebrospinal fluid tap was within normal limits. Antemortem diagnostics for infectious diseases including *Toxoplasma gondii*, *Neospora caninum*, *Cryptococcus neoformans*, and *Blastomyces dermatitidis* all yielded negative results. Nerve and muscle biopsies were performed, and the nerve biopsies indicated possible increased fat droplets with a "possible suggestion of carnitine deficiency." The dog was started on gabapentin and enrofloxacin and was continued on prednisone and clindamycin. The dog continued to decline despite treatment, and was euthanized approximately three months after the initial presentation and submitted for necropsy.

Gross Pathology: After fixation and trimming, the cross sections of the entire length of the spinal cord exhibited well-demarcated, wedge or V-shaped, off-white pallor of the dorsal funiculi.

Laboratory Results: None.

Immunohistochemistry (IHC):

The following IHC preparations were performed:

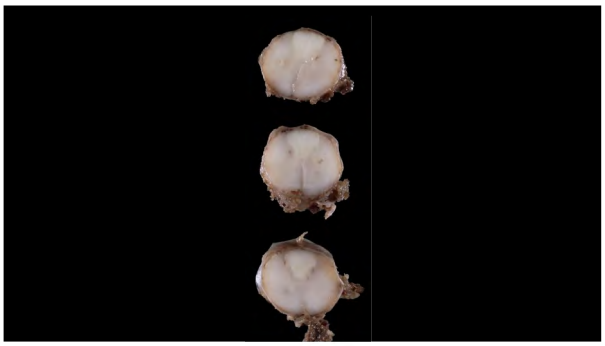

Figure 1-1. Spinal cord, dog: The dorsal funiculi are bilaterally pale along the length of the spinal cord. (*Photo courtesy of*: University of Minnesota Veterinary Diagnostic Laboratory, https://www.vdl.umn.edu/)

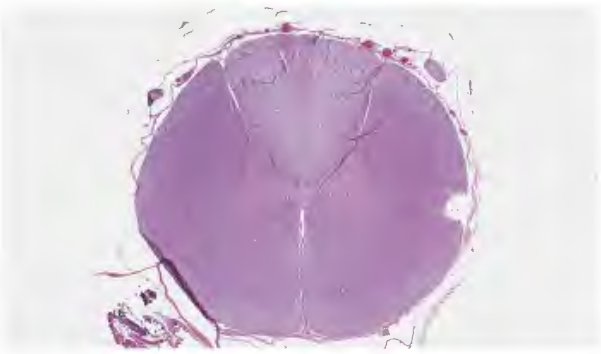

Figure 1-2. Spinal cord, dog: At subgross magnification, there is rarefication of the white matter of the dorsal funiculi. (HE, 23X).

Canine distemper virus antigen: There was no immunoreactivity (negative).

Borrelia burgdorferi antigen: The results were equivocal with mild nonspecific immunoreactivity.

Brain:

Canine distemper virus antigen: There was no immunoreactivity (negative).

Canine herpesvirus antigen: There was no immunoreactivity (negative).

Canine adenovirus (CAV-1 and CAV-2) antigen: There was very little immunoreactivity (equivocal result).

Microscopic Description:

Spinal cord (thoracic segments): In all of the examined cross sections, the white matter of the dorsal funiculi is diffusely and moderately to markedly vacuolated with myelin disruption and loss and axonal degeneration (Wallerian degeneration). Multifocally throughout the white matter of the dorsal funiculi, there are moderately to markedly dilated myelin sheaths, some of which contain gitter cells or eosinophilic cellular debris (ellipsoids); degenerate axons (spheroids); mild to moderate gliosis; and small to moderate numbers of lymphocytes and macrophages. Additionally, there are perivascular cuffs consisting of small numbers of lymphocytes surrounding small- and medium-caliber blood vessels within the dorsal funiculi. These lesions are in marked contrast to the lateral and ventral funiculi, which are within normal limits. There are small numbers of basophilic bacilli scattered throughout all sections (interpreted as postmortem overgrowth/cadaveric bacilli).

Special Stains:

The following special stains were applied to sections of the spinal cord (thoracic segments):

Hematoxylin & eosin/Luxol fast blue: Throughout the dorsal funiculi, there is extensive and marked myelin loss and disruption. These regions contain numerous astrocytes that exhibit haphazard arrangement of the eosinophilic fibrillary acidic proteins of their processes, as well as multifocal accumulations of eosinophilic cellular debris. Extensively scattered throughout the dorsal funiculi, there is rarefaction with vacuolation of the neuropil. Within one of the examined cross sections, there is a dorsal spinal nerve root which exhibits diffuse loss of myelin.

Bielschowsky silver: In all of the examined sections, there is a regionally extensive, marked decrease in axonal density throughout the dorsal funiculi. The axons that remain in this region are frequently shrunken or fragmented.

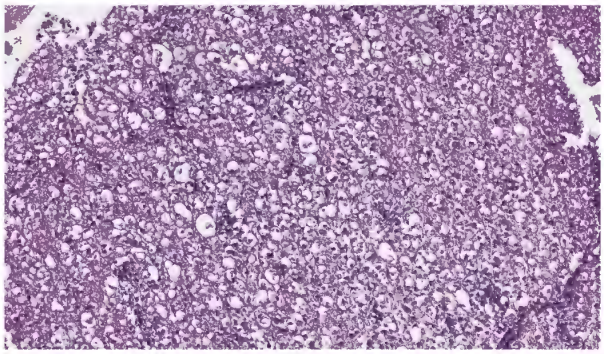

Figure 1-3. Spinal cord, dog: Within affected funiculi, myelin sheaths are diffusely dilated, and contain variably swollen axons, cellular debris, or Gitter cells. Vessels are cuffed by one or more layers of Gitter cells. (HE, 241X).

Contributor's Morphologic Diagnosis: Spinal cord (dorsal funiculi) – myelin loss and disruption with axonal degeneration (Wallerian degeneration), diffuse, moderate to marked, subacute to chronic, with mild lymphocytic and histiocytic infiltration, lymphocytic perivascular cuffs, and gliosis

Contributor's Comment:

The gross and microscopic lesions observed in this case, particularly the diffuse Wallerian degeneration of the dorsal funiculi throughout the entire length of the spinal cord, are suggestive of canine ganglioradiculitis, also known as sensory neuropathy or sensory neuronopathy. Canine ganglioradiculitis is described as a rare, idiopathic disease of adult dogs characterized by various degrees of inflammation within the peripheral ganglia, dorsal root ganglia, dorsal spinal nerve roots, and dorsal funiculi of the spinal cord.[1,3,5-9] On histopathology, the characteristic features of the disease include nonsuppurative inflammation of the dorsal root spinal ganglia and cranial sensory ganglia with secondary, extensive Wallerian degeneration in the dorsal funiculi throughout the entire length of the spinal cord.[5] In the case presented here (but not included in the submitted sections), there were variable degrees of mononuclear inflammation, gliosis, myelin loss, and neuronal degeneration within select dorsal nerve roots and dorsal root ganglia; however, the most striking gross and histopathologic lesions involved the dorsal funiculi throughout the entire length of the spinal cord (as exhibited on the submitted slide). These lesions included marked Wallerian degeneration characterized by myelin disruption and loss, with axonal degeneration. Mononuclear infiltration, both in the form of perivascular cuffing as well as throughout the dorsal funiculi, was also an important feature in this case.

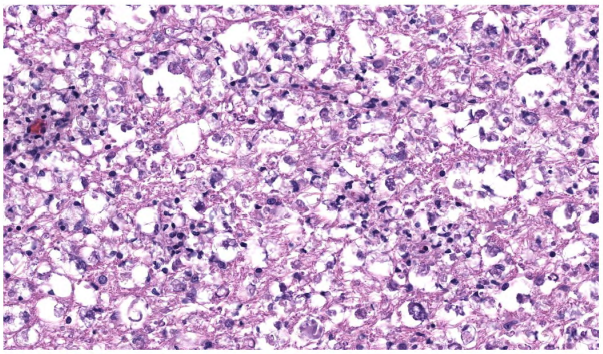

Figure 1-4. Spinal cord, dog: Higher magnification of axonal degeneration within the dorsal funiculi. (HE, 241X).

Canine ganglioradiculitis has been reported to be a sporadic disease usually affecting adult dogs with no breed or sex predilections.[5] This condition is considered a general proprioceptive disorder without involvement of the motor system.[3] The clinical signs associated with this condition are usually abrupt in onset and slowly progressive (over several months) and can be asymmetrical. In this case, the dog initially presented with hypermetria of the right forelimb and the signs progressed toward sensory ataxia and a hypermetric gait in all four limbs. The clinical signs of canine ganglioradiculitis are variable, but often include generalized sensory ataxia, hypermetria, base-wide stance, depression or loss of spinal reflexes, reduced postural reactions, facial hypalgesia, dysphagia, masticatory muscle wasting, and megaesophagus.[5] Additionally, cerebrospinal fluid findings can be normal or exhibit increases in both cells and proteins, as was reported in this case.[8]

Hereditary sensory neuropathies have been reported in Long-haired Dachshund dogs and in Pointer dogs.[2,4] In the case of Long-haired Dachshunds, the clinical signs include loss or reduction of proprioception, reduced

or absent pain sensation, and urinary and fecal incontinence. Histologically, there is a decrease in the number of myelinated nerve fibers in numerous peripheral nerves (including the radial and saphenous nerves) as well as axonal degeneration, particularly of unmyelinated C fibers.[4] With Pointer dogs, the condition is clinically characterized by acral mutilation and insensitivity and is histologically characterized by reduction in the number of neurons within ganglia; however, neuronal degeneration and degenerating myelinated axons within the ganglia are considered rare in these cases.[2] A decrease in the density of myelinated fibers within the dorsolateral fasciculus of the spinal cord has been associated with the hereditary condition in Pointer dogs.[2] An additional clinical differential to be considered is Coonhound paralysis or idiopathic polyradiculitis; however, the pathologic changes of this neuropathy are usually concentrated at the ventral roots and associated clinically with motor deficits such as tetraplegia.[5]

The cause of canine ganglioradiculitis remains unknown. Hypotheses concerning the cause of this condition include an immune-mediated pathogenesis (with cell-mediated and/or humoral components), a viral infection, or a toxic etiology. Autoantibody detection using indirect immunofluorescence assay on the sera from two dogs did not detect autoantibodies against canine ganglion tissues.[5]

Contributing Institution:

University of Minnesota Veterinary Diagnostic Laboratory
College of Veterinary Medicine
244 VDL, 1333 Gortner Ave.
St. Paul, MN 55108
https://www.vdl.umn.edu/

JPC Morphologic Diagnosis:

Thoracic spinal cord, dorsal funiculi: Axonal degeneration and loss, chronic, diffuse, marked, with mild lymphocytic perivascular leukomyelitis.

JPC Comment:

Dr. Jey Koehler, from Auburn University's School of Veterinary Medicine (and our Department consultant on all things neuropathological), moderated this year's 23rd conference with a lineup of neuro cases that integrated anatomy, histology, and clinical neurology. Before diving into this first case, there was a review of the three true forms of ataxia: cerebellar, vestibular, and proprioceptive. Understanding the differences can help clinicians and pathologists localize neurologic disease, and it is common to have more than one type play a role. Cerebellar ataxia is characterized by ataxia and dysmetria or hypermetria of all four limbs, a "goose-stepping" gait, wide-based stance, truncal sway, and intention tremors, but with normal strength and proprioception. Vestibular ataxia can also have a wide based stance, but affected animals have more of a "crab-walking" or "wall-walking" gait, have lateralized lesions (i.e., head tilt, leaning or circling to one side, etc.), falling/stumbling, and a loss of balance when the head is lifted

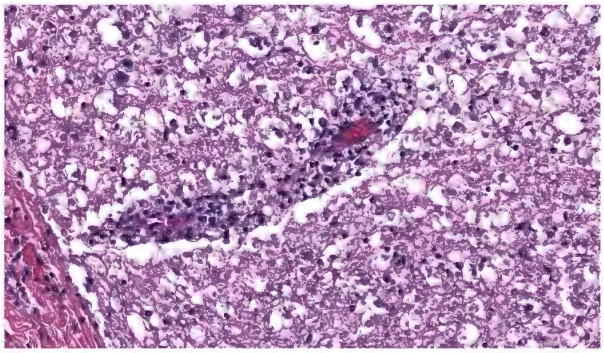

Figure 1-5. Spinal cord, dog: Vessels are cuffed by moderate numbers of Gitter cells and lymphocytes. (HE, 574X).

or the eyes are covered. Lastly, animals with a proprioceptive ataxia show scuffing of the toes when walking, knuckling, crossing over of the limbs, truncal sway, "abnormal stance", and exaggerated circumduction, abduction, and adduction. This dog's history suggested combined vestibular and proprioceptive ataxias. In vestibular ataxia, there is a dysfunction of the vestibular reflex pathways that maintain eye, head, and body position, while proprioceptive ataxia is secondary to loss of neural input from proprioceptors (i.e., muscle spindles, ligaments, joint receptors, etc.). This ataxia review emphasized why a good history is crucial for interpretation of neurologic lesions.

Participants were encouraged to always pay attention to neuroanatomic location when evaluating the nervous system and to be as specific as possible. This was a theme that ran through all four cases in this conference, and Dr. Koehler shared tips on how to determine precisely at which level of the spinal cord a particular histology section may have been taken from, based on the shape of the cord, gray-to-white matter ratio, and the presence of specific tracts. The cervical spinal cord characteristically is either top-heavy (especially pronounced at the level of C1) or is symmetrically oval with a high proportion of white matter. She emphasized how caudal cervical and proximal lumbar segments can look deceptively similar on histology, and how careful attention to the dorsal columns, particularly the medially located fasciculus gracilis (pelvic limb input) and more lateral fasciculus cuneatus (thoracic limb input), can help orient the pathologist. She shared a clever mnemonic to make the distinction between their functions memorable: "If you want to be a graceful dancer, you need legs; if you want to write in cuneiform, you need arms."

The thoracic spinal cord, by comparison, is more spherical and has very little grey matter compared to the other segments. Here, there may be lateral horns (intermediate column) that are composed of visceral motor neurons. In the lumbar segment, the spinal cord becomes bottom-heavy with large ventral horns and a dorsal "caterpillar" shape. The lumbar cord also has a higher proportion of grey matter compared to the cervical segment. Lastly, the sacral cord, is comparatively small with a high proportion of grey matter and usually can be relied upon to have several "nerve friends" nearby. As cited by Dr. Koehler during conference, the University of Minnesota's online "Spinal Cord Anatomy Lab" is an excellent resource for learning the distinguishing histologic features of each cord segment.

Then on to this particular case - many of the major features of sensory neuropathy/ ganglioradiculitis discussed during conference are covered in the contributor's excellent write-up. One of the central discussions during this case was whether it should be given a morphologic diagnosis of leukomyelitis, axonal degeneration, or as demyelination. The inflammation in this particular section was minimal, leading some participants to balk at the idea of using the "-itis" terminology. Dr. Koehler emphasized that, while she views this condition as fundamentally inflammatory since current literature points to the pathogenesis likely being immune-mediated with predominant T-lymphocyte infiltrates, this case lacked the histologic features necessary to truly label it as leukomyelitis.[7] Additionally, inflammation in cases of sensory neuropathy is often

minimal in the cord itself, but may be prominent in the dorsal ganglia.[7] As such, the primary lesion is thought to occur in the ganglia with secondary degeneration of the central projections in the dorsal columns.[7] Without the dorsal root ganglia in section, the group was left to interpret the pattern of a disease restricted to the ascending sensory tracts (white matter), with Wallerian-like degeneration.[6,7] This was reflected in the JPC's morphologic diagnosis, which prioritized the axonal degeneration and loss as the primary process in this slide, with a secondary leukomyelitis.

References:

1. Cantile C, Youssef S. Nervous System. In: Maxie MG, ed. *Jubb, Kennedy, and Palmer's Pathology of Domestic Animals.* Vol. 1. 6th ed. St. Louis, MO: Elsevier; 2016:395.
2. Cummings JF, de Lahunta A, Winn SS. Acral mutilation and nociceptive loss in English pointer dogs. *Acta Neuropathol*. 1981;53(2):119-127.
3. De Lahunta A, Glass E, Kent M. *Veterinary Neuroanatomy and Clinical Neurology.* St. Louis, MO: Elsevier Saunders; 2015:252-253.
4. Duncan ID, Griffiths IR, Munz M. The pathology of a sensory neuropathy affecting Long haired Dachshund dogs. *Acta Neuropathol*. 1982;58(2):141-151.
5. Funamoto M, Nibe K, Morozumi M, et al. Pathological features of ganglioradiculitis (sensory neuropathy) in two dogs. *J Vet Med Sci*. 2007;69(12):1247-1253.
6. Hamzianpour, N, Eley, TS, Kenny, PJ, et al. Magnetic resonance imaging findings in a dog with sensory neuronopathy. *J Vet Intern Med*. 2015;29(5):1381-1386.
7. Porter B, Schatzberg S, McDonough S, et al. Ganglioradiculitis (sensory neuronopathy) in a dog: Clinical, morphologic, and immunohistochemical findings. *Vet Pathol*. 2002;39(5):598-602.
8. Summers BA, Cummings JF, de Lahunta A. *Veterinary Neuropathology*. St. Louis, MO: Mosby-Year Book, Inc; 1995.
9. Wouda W, Vandevelde M, Oettli P, et al. Sensory neuronopathy in dogs: A study of four cases. *J Comp Pathol*. 1983;93 (3):437-450.

CASE II:

Signalment:

Male, European Badger *(Meles meles),* Mustelidae

History:

Two badgers were found by walkers at the edge of the forest and were brought to the Zagreb Zoo. The animals very quickly developed neurological signs similar to epileptiform seizures. They were treated with fenbendazole, but within a few days they stopped responding to the therapy and were euthanized.

Gross Pathology:

Animals were in good nutritional condition. No significant pathological changes were observed macroscopically. Blood vessels of meninges and brain cortex were moderately congested.

Laboratory Results:

lmmunofluorescence test for Rabies Virus Antigen: Negative.

PCR testing for Herpesvirus was positive

and sequencing showed the virus to be of badger *Gammaherpesvirus.* PCR testing for Flaviviridae was negative.

Microscopic Description:

Cerebrum; multifocally affecting the meninges, the gray matter, and to a lesser extent the white matter, there is perivascular cuffing with low to moderate numbers of lymphocytes, plasma cells and fewer macrophages, that expand Virchow-Robin space up to four times normal. Within gray matter, neurons are occasionaly swollen with eosinophilic cytoplasm (degeneration), or are shrunken and angular with hypereosinophilic cytoplasm and nuclear pyknosis (necrosis). Affected neurons are occasionally surrounded by glial cells (satellitosis). Multifocally, there are small areas of hemorrhage.

Contributor Morphologic Diagnosis:

Cerebrum; Meningoencephalitis, perivascular, lymphoplasmacytic, multifocal, mild to moderate, with neuronal degeneration and necrosis, and mild hemorrhage.

Contributor Comment:

The European badger *(Meles meles*), also known as the Eurasian badger, is a badger species in the family Mustelidae native to almost all of Europe and some parts of Western Asia. Literature data about diseases in this species are generally limited and mostly related to selected infections, such as bovine tuberculosis, canine distemper and rabies.[1,5,9] It is also afflicted with a wide range of parasites that are mostly just a random finding and have no major impact on the badger population health.[10]

Figure 2-1. Cerebrum, badger: One section of cerebrum is submitted for examination. Other than a slight flattening of the gyri, there are no discernable lesions at subgross magnification. (HE, 7X)

In recent years, it has been found that *Mustelid gammaherpesvirus 1* (MusGHV-1) is circulating in the badger population in Europe.[2,11,12,15] Phylogenetic analysis of sequence data demonstrates that MusHV-1 is a member of the *Rhadinovirus* genus within *Gammaherpesvirinae* closely related to equine herpesvirus 2 and 5.[2,12] For the first time, it was isolated from pulmonary fibroblasts cultures established from a European badger that additionally had eosinophilic, probably verminous pneumonia, but no other obvious association to disease.[2] Few later studies found high prevalence of MsGHV-1 in the genital tracts of European badgers.[11,12,15] It is highly prevalent amongst wild badgers in the UK and Ireland, where MusGHV-1 DNA isolation from blood shows near 100% infection rate at some localities.[14] Badgers have a highly promiscuous, polygynandrous mating system, characterized by repeated mating behavior, likely putting them at a particular risk of contracting sexually transmitted infections that possibly includes also MusGHV-1.[7,13.15]

Regarding meningoencephalitis, except the previously mentioned distemper and rabies, we found no data on herpesviruses as a possible cause of meningoencephalitis in badgers. In domestic animals, encephalitic her-

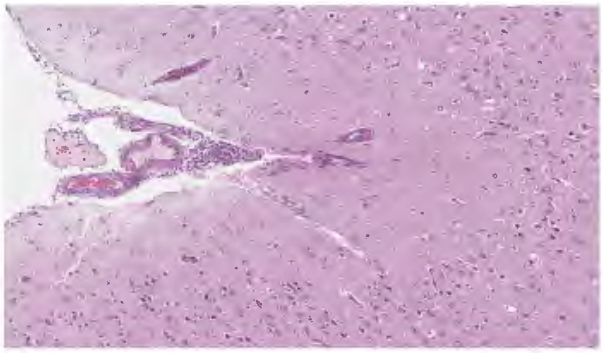

Figure 2-2. Cerebrum, badger: There is mild multifocal lymphoplasmacytic inflammation within the meninges. (HE, 217X)

pesviruses are mostly members of the subfamily Alphaherpesvirinae, and cause cell injury through necrosis of infected neurons and glial cells, necrosis of infected endothelial cells and secondary effects of inflammation, cytokines and chemokines. However, some gammaherpesviruses can also cause lesions in the nervous system such as e.g. murid gammaherpesvirus 4, rhesus macaque rhadinovirus, ovine herpesvirus 2 in cows, and several gammaherpesviruses exist in ursine species and cause neurological lesions.[3] Herpesviruses enter the CNS principally by retrograde axonal transport; however, entry by hematogenous spread via viremia and leukocytic trafficking may occur. These viruses also have a unique survival mechanism that allow them to hide in a latent form in nervous tissue, such as the trigeminal ganglion. Stress or other factors can activate latent virus, resulting in encephalitis.

Contributing Institution:

Department of Veterinary Pathology
Faculty of Veterinary Medicine
University of Zagreb
Heinzelova 55
10000 Zagreb
Croatia.
http://www.vef.unizg.hr/

JPC Morphologic Diagnosis:

Cerebrum: Meningoencephalitis, lymphoplasmacytic, subacute, diffuse, mild, with neuronal necrosis, gliosis, and rare intranuclear viral inclusion bodies.

JPC Comment:

This case challenged participants with both neuroanatomic orientation and its identification as a viral meningoencephalitis, as the submitted slides varied in their anatomic level. Dr. Koehler began by anchoring everyone to two reliable landmarks on the slide that she received: the olfactory stria and the olfactory tubercle, the latter memorably described as "the wiggly bits." Conference participants, however, received a slide that included cerebrum with hippocampus and thalamus rather than the olfactory stria and tubercle. Despite variation in tissue cuts among slides, the lesions were consistent and included a multifocal lymphoplasmacytic meningoencephalitis with neuronal necrosis, edema, and perivascular cuffing, although intranuclear viral inclusions were more readily identified on the section containing thalamus.

The inflammatory pattern prompted discussion of reactive astrocytes, with Dr. Koehler

Figure 2-3. Cerebrum, badger: Lymphoplasmacytic inflammation extends down along Virchow-Robin's spaces within the grey matter. (HE, 381X)

emphasizing that the umbrella term "reactive astrocytes" is now preferred over attempting to subtype astrocytic morphologies.[8] The constellation of dead neurons, edema, and perivascular lymphoplasmacytic cuffs strongly supported an inflammatory etiology, and herpesvirus rose quickly to the top of the differential list, along with canine distemper virus (canine morbillivirus), as this has also been reported in American badgers.[4,10]

Participants reviewed the biology of Mustelid gammaherpesvirus-1 (MusGHV-1), also known as Badger herpesvirus, a gammaherpesvirus in the genus Percavirus that is highly prevalent in European badgers.[6] Several studies have demonstrated near-universal infection rates in some populations, with high viral loads in the genital tract.[15] Combined with the badger's polygynandrous mating system, this supports sexual transmission as a major route of spread.[7,15]

While MusGHV-1 is widespread in European badger populations, its role in neurologic disease is less well-defined. PCR alone cannot distinguish latent from active infection, which is a key point when interpreting herpesvirus-associated lesions. Dr. Koehler noted that more definitive attribution of the lesions to MusGHV-1 would require in-situ hybridization (ISH) or virus-specific immunohistochemistry. She and other participants felt, however, that the striking eosinophilic intranuclear viral inclusions in neurons and glial cells in this case support active infection.

Participants also discussed mustelid herpesvirus-2, an alphaherpesvirus identified in sea otters that is primarily associated with ulcerative oral lesions and skin plaques, particularly in Alaskan populations.[6,16] This virus is closely related to badger herpesvirus and serves as a reminder that mustelids host multiple herpesviruses with differing tissue tropisms and pathogenic potential.

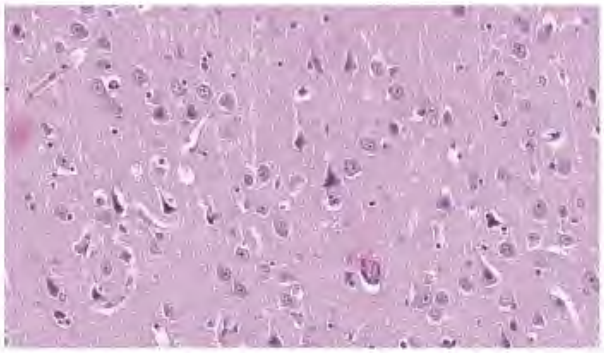

Figure 2-4. Cerebrum, badger: Scattered gray matter neurons are contracted and necrotic. (HE, 496X)

References:

1. Akdesir E, Origgi FC, Wimmershoff J, et al. Causes of mortality and morbidity in free-ranging mustelids in Switzerland: necropsy data from over 50 years of general health surveillance. *BMC Vet Res.* 2018;14:195-214.
2. Banks M, King DP, Daniells C, et al. Partial characterization of a novel gammaherpesvirus isolated from a European badger (*Meles meles*). *J GenVirol.* 2002; 83:1325-1330.
3. Black W, Troyer RM, Coutu J, et al. Identification of gammaherpesvirus infection in free-ranging black bears (*Ursus americanus). Virus* Res. 2019; 259:46-53.
4. Di Sabatino D, Di Francesco G, Zaccaria G, et al. Lethal distemper in badgers (*Meles meles*) following epidemic in dogs and wolves. *Infect Genet Evol*. 2016;46:130-137.
5. Donnelly CA, Wei G, Johnston WT, et al. Impacts of widespread badger culling on cattle tuberculosis: concluding analyses from a large-scale field trial. *Int J Infect Dis.* 2007; 11:

300-308.

6. Dotto-Maurel A, Arzul I, Morga B, Chevignon G. Herpesviruses: overview of systematics, genomic complexity and life cycle. *Virol J.* 2025;22(1):155.
7. Dugdale HI, Macdonald OW, Pope LC, et al. Polygynandry, extra-group paternity and multiple-paternity litters in European badger (*Meles meles*) social groups. *Mol Ecol.* 2007;16:5294-5306.
8. Escartin C, Galea E, Lakatos A, et al. Reactive astrocyte nomenclature, definitions, and future directions. *Nat Neurosci*. 2021;24(3):312-325.
9. Hammer AS, Dietz HH, Andersen TH, et al. Distemper virus as a cause of central nervous disease and death in badgers *(Meles meles*) in Denmark. *Vet Rec.* 2004; 154:527-530.
10. Hancox M. Parasites and infectious diseases of the Eurasian badger *(Meles meles*): a review. *Mammal Rev.* 1980;10(4):151-162.
11. Kent A, Ehlers B, Mendum T, et al. Genital Tract Screening Finds Widespread Infection with Mustelid Gammaherpesvirus 1 in the European Badger (*Meles* meles). *J Wildl Dis.* 2018;54(1):133-137.
12. King DP, Mutukwa N, Lesellier S, et al. Detection of mustelid herpesvirus -1 infected European Badgers (*Meles meles*) in the British Isles. *J Wildl Dis.* 2004;40(1):99-102.
13. Kokko H, Ranta E, Ruxton G, et al. Sexually transmitted disease and the evolution of mating systems. *Evolution.* 2002;56(6):1091-1100.
14. Miller AD, Zachary JF. Nervous System. In: Zachary JF ed. *Pathologic Basis of Veterinary Disease.* 6th ed. St. Louis, MO: Elsevier; 2017:805-907.
15. Tsai M, Fogarty U, Byrne AW, et al. Effects of mustelid gammaherpesvirus-1 (MusGHV-1) reactivation in European Badger (*Meles meles*) genital tracts on reproductive fitness. *Pathogens.* 2020;769.
16. Tseng M, Fleetwood M, Reed A, et al. Mustelid herpesvirus-2, a novel herpes infection in northern sea otters (*Enhydra lutris kenyoni*). *J Wildl Dis*. 2012;48(1):181-185.

CASE III:

Signalment:

1-year-old, intact male (stud colt), American Quarter Horse, *Equus caballus,* horse.

History:

The animal was presented to the large animal teaching hospital for progressive lameness of the hind limbs and a possible pelvic injury after a collision with another horse in pasture six months prior resulted in a fall. Lameness examination revealed a marked grade three lameness of the left hind limb and limited flexion of the stifles with both hind toes worn down from dragging. On neurologic examination, he circumducted his outside hind limb when turning in tight circles. When his head was lifted and he was walked forward, his forelimbs hovered for a prolonged period before he placed them back on the ground. He had mild difficulty backing up and stumbled when walking down the grass hill. Radiographs of the cervical spinal cord revealed severe dorsal deviation of C3 relative to the caudal endplate of C2 and severe stenos is of the spinal canal at C2-C3. The owners elected for euthanasia and an autopsy was performed the same day.

Gross Pathology:

The 2nd and 3rd cervical vertebral joints were stiff and fixed in a flexed position with minimal manual flexion available. The flexed position resulted in a narrow cervical spinal canal at the level of the 2nd and 3rd cervical vertebrae with dorsal compression and flattening of the underlying spinal cord.

Laboratory Results: N/A

Microscopic Description:

Cervical spinal cord: Most severely affecting the white matter of the ventral and lateral funiculi, and to a lesser extent the dorsal funiculus, is extensive axonal degeneration in which 60% of myelin sheaths are markedly dilated and occasionally coalesce to form up to 80-um diameter clear spaces. The dilated myelin sheaths frequently contain swollen, eosinophilic axons (spheroids) or fragments of cellular debris with occasional axonophages (digestion chambers).

Contributor's Morphologic Diagnosis:

Cervical spinal cord: Axonal degeneration, locally extensive, marked, chronic with spheroids and digestion chambers (Wallerian degeneration).

Contributor's Comment:

The clinical course of the disease paired with the gross and histopathologic findings are consistent with cervical vertebral stenotic myelopathy (CVSM) with static stenosis. CVSM (also called cervical vertebral malformation-malarticulation or colloquially referred to and cited in older text as wobbler syndrome) is a common cause of spinal cord compression in horses and dogs.[1,4,5] The

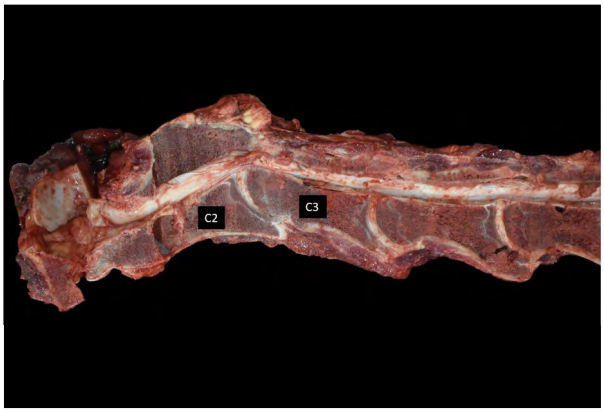

Figure 3-1. Cervical spine, horse: The 2nd and 3rd cervical vertebral joints were fixed in a flexed position resulting in narrowing of the cervical spinal canal and compression of the cord. (*Photo courtesy of*: Auburn University, https://www.vetmed.auburn.edu/academic-departments/dept-of-pathobiology/)

condition is characterized by a stenotic cervical vertebral canal and secondary extramedullary compression of the cervical spinal cord.[1,2,4] Microscopically, lesions within the affected spinal cord are typical of compressive injury to the spinal cord with extensive axonal degeneration leading to demyelination at the compression site.[1,4] White matter degeneration rostral to the compression is typically limited to the ascending tracts of the dorsal funiculi, while caudal is limited to the descending tracts of the ventral funiculi.[1]

In horses, two manifestations of the condition include cervical vertebral instability (dynamic stenosis) and cervical vertebral malformation (static stenosis). Dynamic compression occurs intermittently when the neck is flexed and typically occurs at C3-C5 vertebrae in horses 8 to 18 months of age.[1,4,5] In contrast, static stenosis is a constant compression regardless of neck position and typically occurs in horses 1-4 years of age and older, with dorsal or dorsolateral narrowing of the canal most commonly at C5-C7 vertebrae.[1,4] Lesions thought to contribute to stat-

Figure 3-2. Cervical spinal cord, horse: At subgross magnification, there are numerous dilated-myelin sheaths within the ventral and lateral funiculi. (HE, 16X)

ic stenosis include thickening of the ligamentum flavum, thickening of the dorsal lamina, or osteophytosis or osteochondrosis of the articular processes.[4,5] Bone cysts of the articular processes have also been reported, but further investigation is needed to determine their significance and correlation/causation.[2] The time required for development of lesions may account for the older age of onset seen with static stenosis. For this case, changes to the articular facets were not appreciated and a section of the ligamentum flavum was histologically unremarkable.

The pathogenesis of CVSM remains incompletely understood and is thought to be multifactorial with proposed pathways including disordered bone and cartilage maturation or abnormal biomechanical forces and altered vertebral structure.[2,5] Predisposing factors are thought to include rapid growth rates, nutritional over supplementation, and genetic predisposition.[1,2,4] Males and large breeds (thoroughbreds, Tennessee Walking Horses, and Warmbloods) have been shown to be at greatest risk for development.[1,3,4]

An interesting component of this case history is the worsening of lameness immediately following a traumatic incident (collision with another horse and fall). As the severity of CVSM is considered dependent on the speed and extent of spinal cord compression, one can speculate that the incident likely induced rapid compression of the damaged axons and secondary damage that the tissue was unable to accommodate for, in contrast to the slowly progressive compression induced by the static stenosis alone.[1]

Contributing Institution:

166 Greene Hall
College of Veterinary Medicine
Auburn University, AL 36849
https://www.vetmed.auburn.edu/academic-departments/deptof-pathobiology/

JPC Morphologic Diagnosis:

Cervical spinal cord, ventral and ventrolateral funiculi: Axonal degeneration and loss, subacute, regionally extensive, severe.

JPC Comment:

This case provided an excellent opportunity to revisit the neuroanatomic significance behind cervical vertebral stenotic myelopathy (CVSM) and the characteristic ventral white

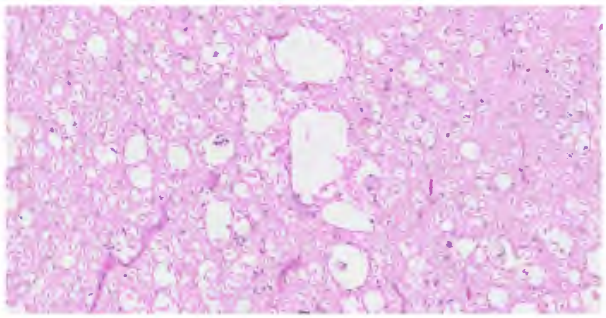

Figure 3-3: Cervical spinal cord, horse: In the ventral funiculi, 60% of myelin sheaths are markedly dilated and occasionally coalesce to form up to 80-um diameter clear spaces (HE, 100X) (*Photo courtesy of*: Auburn University, https://www.vetmed.auburn.edu/academic-departments/dept-of-pathobiology/)

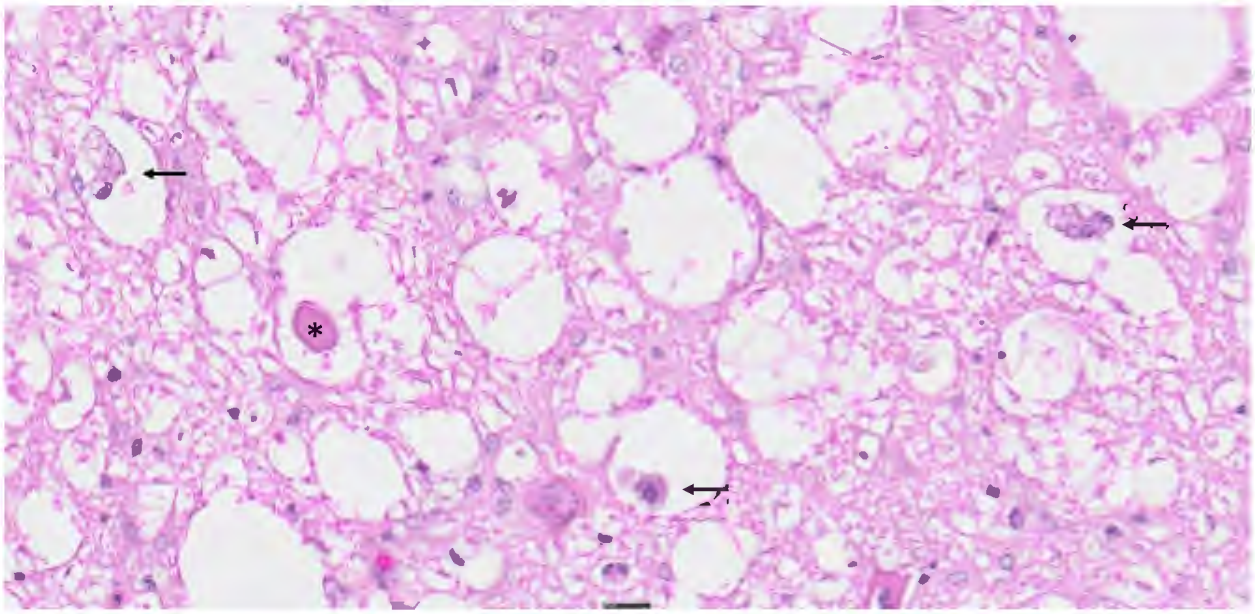

Figure 3-4. Cervical spinal cord, horse: Dilated myelin sheaths frequently contain swollen, eosinophilic axons (spheroids) (asterisk) or fragments of cellular debris with occasional axonophages (digestion chambers) (arrows). (HE, 200X) (*Photo courtesy of*: Auburn University, https://www.vetmed.auburn.edu/academic-departments/dept-of-pathobiology/)

matter degeneration that results from chronic spinal cord compression. This case was classic for this disease in almost all aspects. The clinical presentation and provided imaging correlated beautifully with the histologic pattern of ventral funiculus-predominant Wallerian-like degeneration, with spheroids, digestion chambers, and myelin loss. Many thanks to our contributor for providing fantastic supplemental images!

Participants reviewed the organization of spinal cord tracts, noting that descending motor pathways—including the lateral and ventral corticospinal tracts, reticulospinal tracts, and vestibulospinal tracts—are concentrated in the ventral and ventrolateral funiculi. In contrast, the dorsal and dorsolateral funiculi are dominated by ascending sensory tracts. This distinction is crucial because a lesion that selectively affects ventral white matter is almost always a descending motor tract problem. In horses, the spinal cord compression that occurs in this condition results in the proprioceptive ataxia that earns the condition the colloquial name of "Wobbler's disease."[6] The contributor provides a well-written overview of the two manifestations of this syndrome in horses.[1,4,6]

The age and breed in this case were somewhat atypical, prompting discussion about how trauma, growth rate, genetics, and vertebral conformation can result in differences in the expected presentation.[2] Regardless of the initiating factors, the histologic result is the same: chronic compression leading to Wallerian-like axonal degeneration.

Dr. Koehler highlighted the distinction between Wallerian degeneration and Wallerian -like degeneration, a nuance that often confuses trainees. True Wallerian degeneration was originally defined in the context of acute, severe, transecting injury to the spinal cord, where axons undergo rapid fragmentation distal to the site of injury.[2] In contrast,

Wallerian-like degeneration describes the same morphologic process, but arising from chronic, progressive insults such as compression, ischemia, or metabolic injury.[2] Histologically, the two are nearly indistinguishable; the difference lies in the tempo and mechanism of axonal injury. In this case, the chronicity of the lesion supports the use of the term "Wallerian-like". Similar to case 1, the JPC's morph reflects the participants' view that axonal degeneration and loss are the primary lesions in this case and encompass many of the other findings, including spheroids, digestion chambers, and demyelination since these are all considered manifestations of or sequalae to axonal degeneration/loss.

References:

1. Craig LE, Dittmer KE, Thompson KG. Nervous System. In: Zachary JF. *Pathologic Basis of Veterinary Disease.* St. Louis, MO: Elsevier; 2021: 952-954
2. Janes JG, et al. Cervical vertebral lesions in equine stenotic myelopathy. *Veterinary Pathol.* 2015; 52:919-27.
3. Levine JM, Ngheim PP, Levine GJ, Cohen, ND. Associations of sex, breed, and age with cervical vertebral compressive myelopathy in horses: 811 cases (1974-2007). *Journal of the American Veterinary Medical Association.* 2018; 233: 1453-1458.
4. Miller AD, Porter BF. Developmental Diseases of Joints. In: Maxie, MG. *Jubb, Kennedy, and Palmer's Pathology of Domestic Animals.* 6th ed, vol. 1. St. Louis, MO: Elsevier; 2016: 136.
5. Powers BE, Stashak TS, Nixon AJ, Yovich JV, Norrdin RW. Pathology of the Vertebral Column of Horses
6. Woodie B, Johnson AL, Grant B. Cervical Vertebral Stenotic Myelopathy. *Vet Clin North Am Equine Pract*. 2022;38 (2):225-248.

CASE IV:

Signalment:

5-year-old female spayed Blue Heeler Mix, Canis lupus familiaris, Canine.

History:

Figure 4-1: Hypothalamus, dog. A neoplasm obscures the pituitary gland and optic nerve. (*Photo courtesy of*: National Institutes of Health Comparative Biomedical Scientist Training Program (CBSTP) in collaboration with Colorado State University Veterinary Diagnostic Laboratory https.//nih-cbstp.nci.nih.gov/; https.// vetmedbiosci.colostate.edu/vdl/)

Figure 4-2. Skull base, dog. A neoplasm fills the sella turcica and extends along the right caudal cranial fossa and sellar region, accompanied by hemorrhage.. (*Photo courtesy of*: National Institutes of Health Comparative Biomedical Scientist Training Program (CBSTP) in collaboration with Colorado State University Veterinary Diagnostic Laboratory https.//nih-cbstp.nci.nih.gov/; https.//vetmedbiosci.colostate.edu/vdl/)

The patient had a two-week history of progressive clinical signs, initially presenting with bilateral elevation of the third eyelids, corneal ulcer in the right eye, coughing, leaving the tongue out of the mouth, and declining demeanor. Upon presentation to Colorado State University Urgent Care Service for evaluation of dysphagia and lethargy, dull mentation was noted. Neurological examination revealed absent palpebral and menace responses, as well as absent nasal sensation bilaterally. A negative direct and consensual pupillary light reflex was noted in the right eye. Due to quality-of-life concerns and an uncertain prognosis, humane euthanasia was elected.

Gross Pathology:

Along the ventral aspect of the brain, obscuring the optic nerve and pituitary gland, is a poorly demarcated region of soft white material surrounded by hemorrhage. Similar material is identified filling the sella turcica and extending along the right caudal cranial fossa and sellar region.

On the right eye there is a focal, centrally located, corneal ulcer measuring approximately 5mm X 3mm. Within the oral cavity, along the caudal right buccal mucosa there are multiple regions of ulceration, which sometimes align with adjacent dentition, ranging in size from 0.5cmX0.9cm to 0.7cmX1.2cm.

Laboratory Results:

Not performed.

Microscopic Description:

Captured in section is the optic chiasm, infundibulum, and pituitary. Effacing the pituitary and extending dorsally within hypothalamus, invading the surrounding leptomeninges, and infiltrating the piriform lobe is a poorly circumscribed, expansile and variably invasive, densely cellular neoplasm subdivided in lobules and packets by fibrovascular stroma. There are three neoplastic cell populations that haphazardly intermix, forming the mass effect. The predominate cell type (80%) consists of small, poorly differentiated polygonal cells with scant granular eosinophilic cytoplasm, indistinct cellular borders, and round nuclei with coarse chromatin arranged in nests and packets. Anisocytosis and anisokaryosis are mild with 17 mitotic figures per 10HPF (2.37mm^2). The second cellular population is comprised of round to polygonal cells with indistinct cellular borders, scarce eosinophilic cytoplasm

Figure 4-3. Hypothalamus, dog: A neoplasm infiltrates the hypothalamus. There are multifocal areas of thrombosis, necrosis and hemorrhage. (HE, 10X)

with prominent clear cytoplasmic vacuoles arranged in nests and packets. Nuclei are round to ovoid, eccentrically placed with finely stippled chromatin and prominent nucleolus. Anisocytosis and anisokaryosis are mild to moderate with rare mitotic figures identified. Finally, the third population are clusters of columnar cells with abundant amphophilic cytoplasm and indistinct cellular borders occasionally arranged in acini scattered throughout the mass**.** Nuclei are centrally placed, ovoid with finely stippled to vesicular chromatin. Anisocytosis and anisokaryosis are moderate with few scattered mitotic figures. Acini structures occasionally encircle granular basophilic to amphophilic material which sometimes has cellular debris. Throughout the neoplasm there are large regions of necrosis characterized by loss of tinctorial cellular staining, infiltrating viable and degenerate neutrophils, karyorrhectic debris, as well as hemorrhage and fibrin. Hemorrhage and neoplastic cells extend within the adjacent neuropil which exhibits spongy change. Multiple vessels are moderately to markedly ectatic and variably occluded by poorly organized fibrin and sometimes erythrocytes, platelets, and circulating leukocytes (thrombi). A few blood vessels are lined by hypertrophied endothelial cells and surrounded by cuffs of lymphocytes and plasma cells. There is rarefaction adjacent to the third ventricle as well as infiltration of Gitter cells.

Contributor's Morphologic Diagnosis:

Cerebrum: Malignant mixed germ cell tumor – suspect suprasellar germ cell tumor.

Contributor's Comment:

Masses in the pituitary and sellar region include primary pituitary neoplasia (e.g., adenoma or carcinoma), metastatic neoplasia (e.g., lymphoma, melanoma, mammary adenocarcinoma), meningioma, craniopharyngioma, and suprasellar germ cell tumor.[1,5,8,13,15] In this case, the absence of systemic disease lowered the likelihood of primary pituitary or metastatic neoplasms. Histopathologic examination further excluded these differentials, revealing neoplastic cells with varied morphology – predominantly poorly differentiated germ cells, along with hepatoid and epithelial components. Based on the location, mixed neoplastic morphology, as well as marked local invasion and destruction, a diagnosis of suprasellar germ cell tumor was made.

Mixed germ cell tumors are rare in domestic

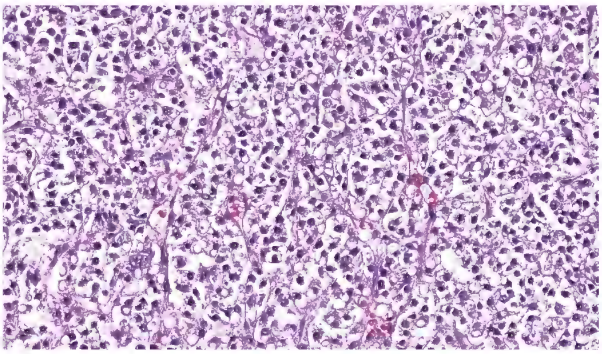

Figure 4-4. Hypothalamus, dog: The predominant morphology of the cells in the neoplasm are polygonal cells in nests and packets with moderate amounts of finely granular cytoplasm. (HE, 528X)

species, most frequently occurring in the gonads.[4,13,16] Extragonadal germ cell tumors are thought to arise from ectopic embryonic germ cells that become widely distributed.[1] In dogs, extragonadal tumors have been commonly reported in the suprasellar region with isolated cases also reported in the spinal cord and eye.[2,3,5,8,9,11,18] Key features of suprasellar germ cell tumors include: a midline mass effect above the sella turcica and dorsal to the pituitary gland; pleomorphic histomorphology with the tumor being composed of several distinct cell types including populations which resemble seminoma/dysgerminoma as well as secretory glandular and/or squamous elements (teratomatous differentiation); and positive immunoreactivity for alpha-fetoprotein (AFP).[18] In this case, all three criteria for a suprasellar germ cell tumor could not be met as AFP immunohistochemistry was unavailable at the laboratory.

Given the overlapping location, another differential considered in this case was craniopharyngioma. These tumors are presumed to arise from remnants of Rathke's pouch and are histologically characterized by sheets of round to polygonal neoplastic cells and clumps of palisading epithelial cells support-

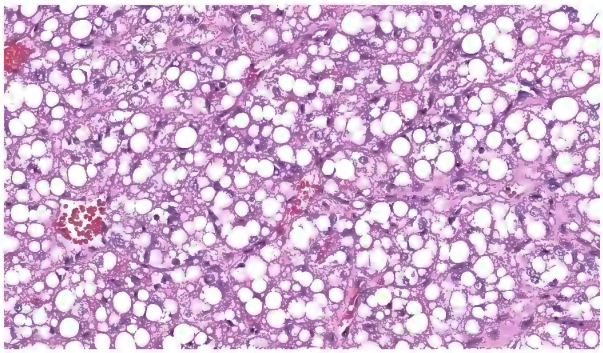

Figure 4-5. Hypothalamus, dog: The predominant cell type in the neoplasm are polygonal cells in nests and packets with moderate amounts of finely granular cytoplasm. (HE, 528X)

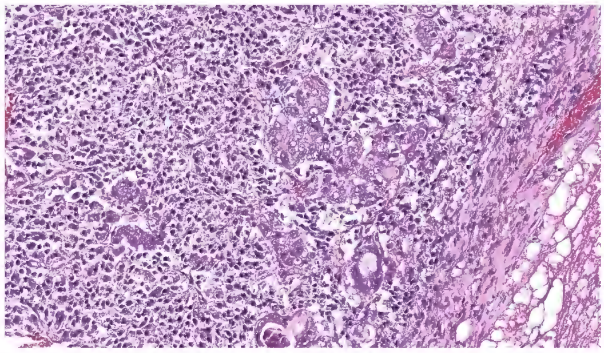

Figure 4-6. Hypothalamus, dog: A third, but far least common morphology of the neoplastic cells are cuboidal polygonal cells forming acini. (HE, 381X)

ed on a collagenous stroma[1,13] Distinguishing between craniopharyngioma and suprasellar germ cell tumors can be challenging, and differentiation often relies on the assessment of AFP immunoreactivity. AFP is produced by the yolk sac of a developing fetus and serves as a useful marker for germ cell tumors in both humans and dogs.[10,18] Neoplastic cells of suprasellar germ cell tumors exhibit AFP immunoreactivity, whereas craniopharyngiomas lack such reactivity. Further complicating differentiation between these neoplasms, the diagnosis of a suprasellar germ cell tumor is not precluded with weak or absent AFP immunoreactivity.[2]

Clinical signs associated with tumors in the pituitary region often include altered pituitary hormone secretion (e.g., hyperadrenocorticism) and can progress to deficits in cranial nerve function as well as central nervous system dysfunction caused due to tumor extension.[15] In the present case, clinicopathologic data were unavailable, and there was no history of underlying endocrinopathy. The intensifying cranial nerve deficits and declining mentation were attributed to the tumor's expansive growth and broad regions of necrosis.

Contributing Institution:

National Institutes of Health Comparative Biomedical Scientist Training Program (CBSTP) in collaboration with Colorado State University Veterinary Diagnostic Laboratory https.//nih-cbstp.nci.nih.gov/

https.//vetmedbiosci.colostate.edu/vdl/

JPC Morphologic Diagnosis:

Cerebrum, thalamus: Suprasellar germ cell tumor.

JPC Comment:

This final case provided an excellent opportunity for discussion of the complexities of midline embryologic tumors and for a brief review of cranial nerve anatomy. This helped participants understand how a midline suprasellar mass might disrupt multiple cranial nerve pathways either through direct compression, distortion of the diencephalon, or secondary effects on the brainstem.

Anatomic orientation was, as with all four of these cases, the next challenge. This cerebral section included thalamus with optic chiasm, third ventricle, and paleocortex, placing this tumor squarely in the suprasellar region. As mentioned by the contributor, the most common locations for extragonadal germ cell tumors in dogs include the suprasellar region, mediastinum, eye, and spinal cord.[10] They are often seen in young to middle-aged dogs, sometimes causing neurological or visual deficits.[10]

Immunohistochemistry plays a central role in the diagnosis. Participants were cautioned that pancytokeratin can cross react with GFAP, a pitfall that can mislead pathologists when evaluating tumors of the CNS.[7] In this case, the neoplasm exhibited weak to moderate immunoreactivity for alpha-fetoprotein (AFP), supporting germ cell differentiation.

The differential diagnoses discussed in this case included craniopharyngioma, teratoma, and pituitary carcinoma, all of which can arise in or near the sella turcica. However, the combination of midline location, mixed cellular morphology, and AFP immunoreactivity align best with a mixed germ cell tumor under the 2021 WHO classification guidelines. Among the listed suprasellar neoplasms, this was the diagnosis that participants agreed best fit the morphologic and immunophenotypic profile.

Dr. Koehler also emphasized the developmental significance of the midline. This region is a crossroads of embryologic migration, fusion, and differentiation, making it a hotspot for tumors derived from ectopic germ cells. The presence of multiple divergent cell populations within the tumor further supported this developmental origin.

Finally, the group discussed the contributor's use of the term "malignant." Some participants preferred not to use that term, noting that primary brain tumors can be fatal due to location alone, even when their biological behavior is histologically benign. While this neoplasm did show histologic invasion and necrosis, there is no established prognostic literature for canine suprasellar germ cell tumors and applying the term "malignant" risks implying a known clinical course. Dr. Koehler framed this as a bit of a philosophical issue for the intents and purposes of conference, however, because, in neuro-oncology, "malignancy" is often a function of where a tumor is, not just what it is.[12]

References:

1. Cantile C., Youssef S. Nervous System. In: Jubb, Kennedy, and Palmer's Pathology of Domestic Animals, ed. Maxie M.G. 6th edition. Philadelphia, USA: Elsevier, vol 1, p403-404.
2. Cook L, Tensley M, Drost WT, et. al. MRI findings of suprasellar germ cell tumors in two dogs. *J Am Animal Hosp Assoc.* 2018;54(3):167-172.
3. Ferreira AJ, Peleteiro MC, Carvalho T, Correia JM, Schulman FY, Summers BA. Mixed germ cell tumour of the spinal cord in a young dog. *J Small Anim Pract.* 2003;44(2):81–84.
4. Foster RA. Male Genital System. In: Jubb, Kennedy, and Palmer's Pathology of Domestic Animals, ed. Maxie M.G. 6th edition. Philadelphia, USA: Elsevier, vol 3:495-496.
5. Hare WR. Primary suprasellar germ cell tumor in a dog. *J Am Vet Med Assoc.* 1993;203(10):1432–1433.
6. Higgins RJ, Bollen AW, Dickinson RJ, Siso-Llonch S. Tumors of the Nervous System. In: Tumors in Domestic Animals, ed. Meuten DJ. 5th edition. Newark, USA: Wiley, p834-891.
7. Kriho VK, Yang HY, Moskal JR, Skalli O. Keratin expression in astrocytomas: an immunofluorescent and biochemical reassessment. *Virchows Arch*. 1997;431 (2):139-47.
8. Miller MA, Bruyette DS, Scott-Moncrieff JC, et al. Histopathologic Findings in Canine Pituitary Glands. *Vet Pathol.* 2018;55(6):871–879.
9. Nyska A, Harmelin A, Baneth G, et al. Suprasellar differentiated germ cell tumor in a male dog. *J Vet Diagn Invest*. 1993;5(3):462-467.
10. Patterson-Kane JC, Schulman FY, Santiago N, McKinney L, Davis CJ. Mixed germ cell tumor in the eye of a dog. *Vet Pathol*. 2001;38(6):712-714.
11. Rech RR, Souza SF, Silva MC. et al. Suprasellar germ cell tumor in a dog. *Ciência rural.* 2008;38(3):830-832.
12. Rees JH. Diagnosis and treatment in neuro-oncology: an oncological perspective. *Br J Radiol*. 2011;84 Spec No 2 (Spec Iss 2):S82-S89.
13. Rissi DR. A retrospective study of skull base neoplasia in 42 dogs. *J Vet Diagn Invest*. 2015;27(6):743-748.
14. Robinson NA, Manivel JC, Olson EJ. Ovarian mixed germ cell tumor with yolk sac and teratomatous components in a dog. *J Vet Diagn Invest*. 2013;25 (3):447-452.
15. Rosol TJ, Gröne A. Endocrine Glands. In: Jubb, Kennedy, and Palmer's Pathology of Domestic Animals, ed. Maxie M.G. 6th edition. Philadelphia, USA: Elsevier, vol 3, p287-288.
16. Rosol TJ, Meuten DJ. Tumors of the Endocrine Glands. In: Tumors in Domestic Animals, ed. Meuten DJ. 5th edition. Newark, USA: Wiley, p766-833.
17. Schlafer DH, Foster RA. Female Genital System. In: Jubb, Kennedy, and Palmer's Pathology of Domestic Animals, ed. Maxie M.G. 6th edition. Philadelphia, USA: Elsevier, vol 3, p377-378.
18. Valentine BA, Summers BA, de Lahunta A, White CL 3rd, Kuhajda FP. Supra-

sellar germ cell tumors in the dog: a report of five cases and review of the literature. *Acta Neuropathol*. 1988;76(1):94-100.

Joint Pathology Center
Veterinary Pathology Services

WEDNESDAY SLIDE CONFERENCE 2025-2026

Conference #24 29 April 2026

CASE I:

Signalment:

9 years, castrated male, domestic shorthair, *Felis catus*, cat

History:

The cat had a history of respiratory disease diagnosed as asthma. The respiratory disease had gotten worse for two weeks prior to death. The cat had an episode of respiratory distress the evening it was taken to an emergency clinic. When placed in the carrier to be transported to the emergency clinic, the cat become extremely agitated, distressed, and was thrashing in the carrier. The cat's thrashing in the carrier eventually stopped, and the cat was dead on arrival at the emergency clinic.

Figure 1-1. Heart, cat: The myocardium of the left ventricle and interventricular septum of the heart were diffusely thickened with a small slit-like left ventricular lumen (*Photo courtesy of* New Mexico Department of Agriculture Veterinary Diagnostic Services , https://www.nmda.nmsu.edu/nmda-homepage/divisions/vds/)

Figure 1-2. Trachea, cat: The cranial 1/3 of the ventral and lateral aspects of the trachea were thickened by a light tan and firm mass that was firmly attached to both the right and left lobes of the thyroid gland. (*Photo courtesy of* New Mexico Department of Agriculture Veterinary Diagnostic Services, https://www.nmda.nmsu.edu/nmda-homepage/divisions/vds/)

Gross Pathology:

The cat was in good body condition with mild postmortem decomposition. There were small amounts of blood in the mouth, larynx, trachea and esophagus. The cranial 1/3 of the ventral and lateral aspects of the trachea were thickened by a light tan and firm mass that was firmly attached to both the right and left lobes of the thyroid gland (Figure 1).

Figure 1-3. Trachea, cat: A neoplasm transmurally infiltrates the wall of the trachea and extends into the adjacent skeletal muscle and lymph node. (HE, 8X).

The right and left lobes of the thyroid gland were enlarged. The lungs were congested, heavy and wet. The heart was enlarged and weighed 24.0 grams. The myocardium of the left ventricle and interventricular septum of the heart were diffusely thickened with a small slit-like left ventricular lumen (Figure 2). The myocardium of the right ventricle of the heart was variably thickened.

Laboratory Results: There was no additional testing performed.

Microscopic Description:

The mucosal epithelium of the grossly affected trachea is multifocally eroded to ulcerated. The eroded and ulcerated tracheal mucosa is covered by a coagulum of fibrin, cellular debris and neutrophils. Where it is intact, there is multifocal squamous metaplasia of the tracheal mucosal epithelium (not present in every slide) (Figure 3). Clusters and trabeculae of neoplastic squamous epithelial cells suspended in a proliferative fibrovascular stroma variably thicken the submucosa deep to the intact tracheal mucosal epithelium (Figure 4). There are small numbers of clusters that have clear centers filled with variable amounts of cellular and necrotic debris resembling tubules. The neoplastic cells are round to polygonal with distinct cell borders, lightly eosinophilic cytoplasm and a large round nucleus. There is mild cellular and nuclear pleomorphism. There are three mitotic figures per ten high power fields. There is multifocal necrosis of the tracheal cartilage rings (not present in every slide). The peritracheal fat and skeletal muscle contain a large invasive mass of neoplastic squamous epithelial cells that encircle the right and left vagus nerves (not present in every slide). The neoplastic cells are arranged in clusters and trabeculae suspended in a dense and proliferative fibrovascular stroma. There are foci of necrosis in the mass. The cervical lymph nodes in the area contain neoplastic cells (not present in every slide) (Figure 5).

Contributor Comment:

Neoplasia of the trachea in cats is rare with most reports of neoplasia in the upper respiratory tract being in the larynx rather than the trachea.[1,2,3,4,5,6] The most commonly reported tracheal neoplasms in cats are lymphoma and carcinomas.[1,3] The reported tracheal carcinomas in cats include adenocarcinoma, squamous cell carcinoma, seromucinous carcinoma, tracheobronchial neuroendocrine carcinoma and carcinoma.[1,3] Squamous cell carcinomas were the most common tracheal carcinoma in one study of tracheal neoplasia in cats, but lymphoma was the most com-

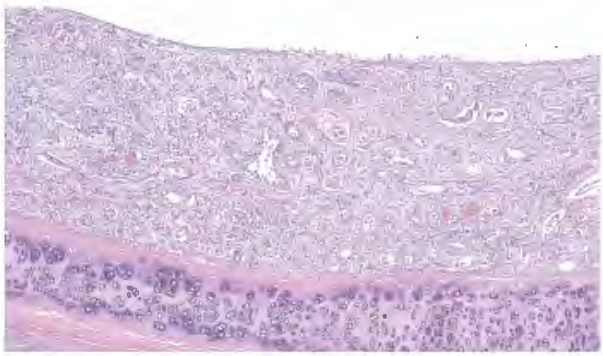

Figure 1-4. Trachea, cat: The tracheal submucosa is expanded by nests and tubules of non-keratinizing epithelium on a dense fibrous stroma. (HE, 140X).

mon tracheal neoplasia.[3] Tracheal neoplasia tends to occur in middle age to older cats with median ages reported as 9 years and 12 years of age.[1,3] In one study, more female cats had tracheal neoplasia than male cats.[3] In the same study, Siamese cats were predisposed to develop tracheal lymphoma.

Domestic longhair cats were predisposed to develop tracheal lymphoma and adenocarcinoma. However, there are so few cats with reported tracheal neoplasia that these findings may not be accurate.

Cats with tracheal neoplasia typically have nonspecific clinical signs of airway obstruction including dyspnea, wheezing, coughing, gagging, and stridor.[1,3,4,5] These clinical signs are not specific for tracheal neoplasia and are common with a variety of respiratory diseases including feline asthma, which was the initial diagnosis for the respiratory disease in this cat.[4,5] Because they are rare and the clinical signs are not specific, the diagnosis of tracheal neoplasia is often not made until the disease is advanced.[1,3] Thus, cats diagnosed with tracheal neoplasia often have short survival times with reported overall median survival times of 15.5 days and 121 days with therapy.[3] In this case, the diagnosis of tracheal neoplasia was not made until the postmortem examination. The cat also had hypertrophic cardiomyopathy that based on the clinical history was likely to have contributed greatly to the death of the cat with the potential development of a fatal cardiac arrhythmia.

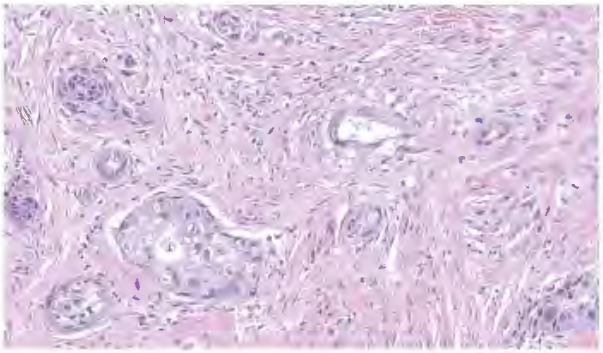

Figure 1-5. Trachea, cat: The neoplastic cells infiltrate the adjacent mediastinal tissue. is expanded by nests and tubules of non-keratinizing epithelium on a dense fibrous stroma. (HE, 348X).

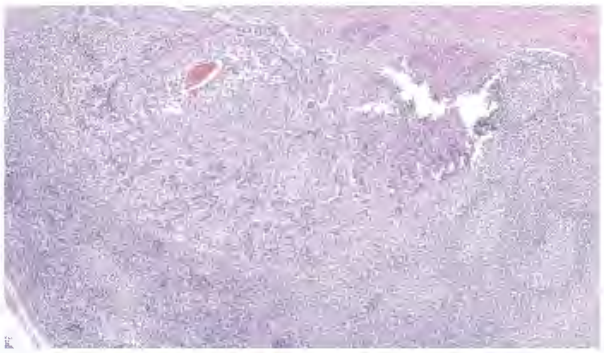

Figure 1-6. Mediastinal lymph node, cat: Neoplastic cells form nests and tubules within the paracortex and sinuses of a mediastinal lymph node. (HE, 98X)

Contributing Institution:

New Mexico Department of Agriculture Veterinary Diagnostic Services

https://www.nmda.nmsu.edu/nmda-homepage/divisions/vds/

JPC Morphologic Diagnosis:

Trachea: Adenosquamous carcinoma.

JPC Comment:

This year's 24th conference was moderated by Dr. Francisco Carvallo, a respiratory and infectious disease expert from the Virginia-Maryland College of Veterinary Medicine and a first-time moderator for the WSC! Following an excellent pre-conference lecture on the specifics and updated terminology of interstitial pneumonia, participants were treated to a respiratory-focused conference that opened with this surprisingly controversial case!

Diagnoses amongst participants on the pecise origin of this tumor (from the mucosal epithelium or the submucosal glandular

epithelium were varied due to the significant formation of tubules and acini by this neoplasm with only rare individual cell dyskeratosis. An Alcian blue stain was underwhelming due to significant background staining of tracheal mucus and ground substance, but there were some neoplastic acini that contained strongly Alcian blue-positive luminal material, indicating that neoplastic cells may be producing mucin. Additionally, the neoplastic cells lacked immunoreactivity for p63 and p40, making a diagnosis of squamous cell carcinoma less likely. Based on the morphology of the neoplasm and the suggestive results of the Alcian blue stain, the JPC decided on a diagnosis of adenosquamous carcinoma. Adenosquamous carcinoma is a rare, aggressive epithelial neoplasm that demonstrates both malignant squamous epithelial differentiation and a malignant glandular component within the same tumor.[7] Adenosquamous carcinomas tend to be highly infiltrative in the organs in which they arise and carry a poor prognosis.[7]

This neoplasm induced an impressive desmoplastic response in the surrounding connective tissue. Dr. Carvallo reviewed the pathogenesis of desmoplasia with conference attendees, talking through tumor cell signaling leading to activation of "cancer-associated fibroblasts" (CAFs) within the tumor microenvironment. Activation of CAFs induces signal transduction of pro-growth pathways that upregulate profibrotic genes, leading to production and remodeling of the extracellular matrix (ECM).[1] The increased density of the ECM can physically impede the delivery of therapeutic drugs, make it more difficult for T lymphocytes and NK cells to access the tumor (immune evasion), and enable tumor growth via sequestration of growth factors.[1] Additionally CAFs promote angiogenesis and epithelial-to-mesenchymal transition (EMT) to facilitate migration, invasion, and metastasis.[1]

References:

1. Asif PJ, Longobardi C, Hahne M, Medema JP. The Role of Cancer-Associated Fibroblasts in Cancer Invasion and Metastasis. *Cancers (Basel)*. 2021;13 (18):4720.
2. Carlisle CH, Biery DN, Thrall DE. Tracheal and laryngeal tumors in the dog and cat: literature review and 13 additional patients. *Vet Radiol*. 1991;32 (5):229-235
3. Caswell JL, Williams KJ. Respiratory system. In: Maxie MG, ed. *Pathology of Domestic Animals*. 6th ed, vol. 2. St. Louis, MO: Elsevier; 2016:480-483
4. Jakubiak MJ, Siedlecki CT, Zenger E, *et al*. Laryngeal, laryngotracheal, and tracheal masses in cats: 27 cases (1998-2003). *J Am Anim Hosp Assoc*. 2005;41:310-316
5. Jelinek F, Vozkova D. Carcinoma of the trachea in a cat. *J Comp Path*. 2012;147:177-180
6. Lobetti RG, Williams MC. Anaplastic tracheal squamous cell carcinoma in a cat. *Tydskr S Afr vet Ver*. 1992;63(3):132 -133
7. Mehrad M, Trinkaus K, Lewis JS Jr. Adenosquamous Carcinoma of the Head and Neck: A Case-Control Study with Conventional Squamous Cell Carcinoma. *Head Neck Pathol*. 2016;10(4):486-493.
8. Wilson DW. Tumors of the respiratory tract. Meuten DJ, ed. *Tumors in Domestic Animals*. 5th ed. Ames, IA: Wiley Blackwell; 2017:479.

CASE II:

Signalment:

Cat, domestic shorthair, 12 years-old, neutered male.

History: The cat was euthanized and the body was transferred to the necropsy service without any medical history.

Gross Pathology: The body was well preserved. The animal was in good body condition with abundant fat. About 150 ml of a latescent thoracic effusion (suspected chylous effusion) was present and associated to a white diffuse and moderate thickening of the pleura with occasional strands of fibrin (suspected chronic fibrosing pleuritis). No obvious cardiac anomaly was observed but alterations due to euthanasia with barbiturates prevented an optimal gross examination of the heart. Pulmonary lobes were slightly rounded and had a slightly thickened pleura. The left cranial pulmonary lobe was twisted at approximatively 180° around its hilus (lung lobe torsion), and was markedly and diffusely red, with blood oozing after sectioning (venous infarction).

Figure 2-1. Lung, cat: The left cranial pulmonary lobe was twisted at approximatively 180° around its hilus (lung lobe torsion), and was markedly and diffusely red, with blood oozing after sectioning (venous infarction) (*Photo courtesy of* Unité d'Histologie et d'Anatomie pathologique, Ecole Nationale vétérinaire d'Alfort (EnvA). https://www.vet-alfort.fr/)

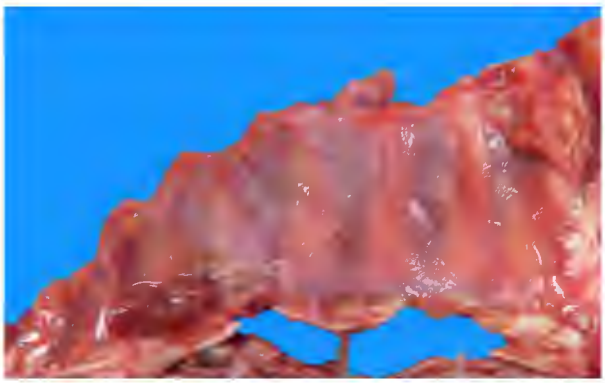

Figure 2-2. Lung, cat: There is moderate thickening of the pleura with occasional strands of fibrin (suspected chronic fibrosing pleuritis) (*Photo courtesy of* Unité d'Histologie et d'Anatomie pathologique, Ecole Nationale vétérinaire d'Alfort (EnvA). https://www.vet-alfort.fr/)

Other organs did not show significant gross lesions.

Laboratory Results:

Cytological analysis of the effusion was performed:

- gross aspect: lactescent (persistent after centrifugation)
- cellularity: 1380 nucleated cells per mm^3;
- protein concentration: 45 g/l (determined by refractometry)
- cells: numerous small lymphocytes and fewer foamy macrophages and neutrophils. No neoplastic cells or infectious agent were identified.

In cats, these findings are suggestive of a chylous effusion and/or an effusion secondary to cardiac insufficiency (although no gross cardiac anomaly was observed). Cholesterol and triglycerides concentrations were not assessed.

Figure 2-3. Lung, cat: Three sections of lung (two from the left cranial lobe and one from the left caudal lobe (at right) are submitted for examination. (HE, 10X)

Microscopic Description:

Heart (not submitted): No significant histological findings

Lungs: Three sections are submitted. Two are from the left cranial lobe (twisted lobe), the third one is from the left caudal lobe. Sections from the left cranial lobe show extensive and severe alveolar hemorrhages and marked vascular congestion. Alveolar walls are often diffusely eosinophilic with loss of basophilia (necrosis).

The left caudal lobe section shows occasional foci of fibrin exudation within the alveoli.

All three sections show a moderate to marked thickening of the pleura by a fibrovascular tissue, resembling granulation tissue, containing a variable amount of mature collagen and occasionally covered with fibrin. The underlying pleural tissue shows a slight to moderate infiltration with lymphocytes.

Prussian blue stain is negative on all sections.

Contributor's Morphologic Diagnosis:

Lungs :

Left cranial lobe: acute, severe, diffuse hemorrhagic necrosis (venous infarction) secondary to lobe torsion

Left caudal lobe: acute, minimal, multifocal, fibrinous alveolitis

Left cranial and caudal lobes: Chronic, moderate to marked, diffuse fibrinous and fibrosing pleuritis

Contributor's Comment: This case is a nice example of lung lobe torsion secondary to a chylothorax. Chylous effusions are composed of chyle. Chyle is a chylomicron-rich lymph fluid originating from the intestinal lacteals and circulating through the intestinal and mesenteric lymphatic vessels, the cisterna chyli and the thoracic duct that ultimately terminates in the left external jugular vein or jugulo-subclavian angle.[10,14] Chyle has a typical opaque white, milky (lactescent) to slightly pink color that persists after centrifugation. Cytologically, it is mainly composed of small lymphocytes and fewer foamy macrophages. Neutrophils may be present following repeated thoracocenteses. Chylous effusion can be confirmed biochemically by measurement of triglycerides and cholesterol concentrations in the effusion and in the serum: triglyceride concentration is typically higher in the effusion compared

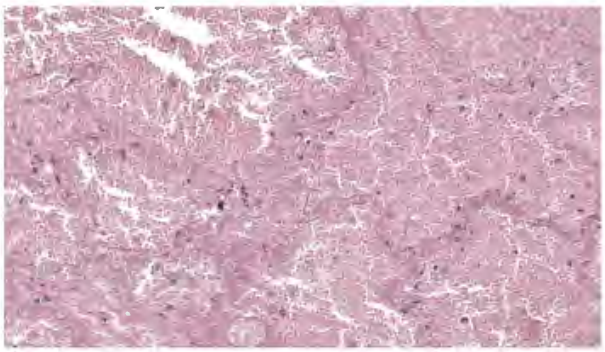

Figure 2-4. Lung, cat: High magnification of intra-alveolar hemorrhage and septal necrosis. (HE, 574X)

to serum, whereas the reverse is true for cholesterol concentration.[14]

The majority of chylous effusions are in the thorax (chylothorax). Most chylothorax are idiopathic, as suspected in this case.[10,14] Known causes of chylothorax are traumatic rupture of the thoracic duct, cardiomyopathy, right-sided heart failure, vena caval thrombosis, heart worms (dirofilariasis), thoracic neoplasia (thymoma, lymphoma, lymphangiosarcoma) or inflammatory lesions that cause obstruction of the thoracic duct.[6,10,14] Lung lobe torsion is also reported to cause chylothorax although the real sequence of events is not always clear in affected animals (see later).[12,14] Chyloabdomen is much less common than chylothorax. A study reported that almost half of chyloabdomens in dogs and cats occur in association with chylothorax and that in these cases the most common underlying cause is neoplasia.[5]

Although chyle is considered to be non-irritant, chronic chylothorax may lead to pleural fibrosis (fibrosing pleuritis), especially in cats, as illustrated in this case.[2,13,14] Macroscopically, lungs may be shrunken, rounded, and covered by a thick pleura.[2] This may lead to reduced pulmonary expansion and dyspnea even with minimal residual effusion.[2,10]

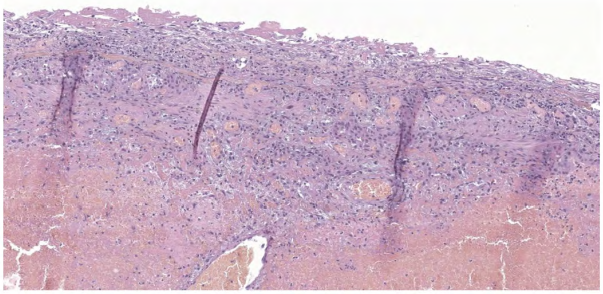

Figure 2-5. Lung, cat: There is marked thickening of the pleural surface by maturing granulation tissue, fibrous tissue and an overlying mat of fibrin. (HE, 221X)

In lung lobe torsion, affected lobes are deeply congested due to compression of veins at the site of torsion, preventing blood return to the heart and leading to severe congestion, hemorrhages and necrosis (venous infarction).[9] The compression does not affect arteries that have a thicker wall and higher hydrostatic pressure. As a consequence, blood may still penetrate the tissue.

The treatment of choice for lung lobe torsion is surgery after medical stabilization of the animal. Of note, the affected lobe should not be untwisted in order to avoid the release by hypoxic tissues of inflammatory cytokines, endotoxins, hypoxanthine and free radicals, as in the phenomenon of ischemia-reperfusion.[3,8,9]

Pleural effusion is often present in association with lung lobe torsion.[10,12,14] The effusion varies in nature (transudate, chyle, exudate, blood). There seems to be a debate regarding the pathogenesis of these effusions because some consider it to be a cause while others see it as a consequence of the lobe torsion.[8,12,14] Both cases might happen. In the present case, the lung torsion appears to be a recent event based on the lack of hemosiderin in the hemorrhagic parenchyma. On the contrary, the fibrosing pleuritis suggests that the chylothorax is chronic and should therefore be considered as the most likely cause for the lung lobe torsion in this cat.

Torsions can affect other organs such as hepatic lobes (pigs, cats, dogs, horses, rabbits), testes (horses, dogs), urinary bladder (dogs), uterus (especially in mares and cows) and caecum (cattle).[4,14] Hepatic lobe torsion has recently been described in three dromedary camels.[7]

Contributing Institution:

Unité d'Histologie et d'Anatomie pathologique, Ecole Nationale vétérinaire d'Alfort (EnvA). France

https://www.vet-alfort.fr/

JPC Morphologic Diagnosis:

1. Lung: Alveolar necrosis and hemorrhage, regionally extensive, severe (lobar torsion).
2. Lung, pleura: Pleuritis, fibrosing, chronic-active, diffuse, moderate.

JPC Comment:

The WSC has not seen a lung lobe torsion case since 1983! This second case also proved challenging and resulted in a variety of diagnoses from participants. There were some features on the slide that contributed to the confusion, including a lack of thrombosis, very little inflammation, and minimal fibrin within the lung coupled with significant edema and pleural changes (mesothelial hyperplasia, fibrosis, and fibrin). The primary supporting finding for the diagnosis of lung lobe torsion was the abundant congestion, intra-alveolar hemorrhage, and multifocal septal necrosis. The pleural changes threw participants for a loop when settling on a diagnosis. The changes were indicative of an acute-on-chronic process which, as mentioned by the contributor in their write-up, can occur with chronic chylothorax.[2,13,14] However, another primary cause for pleuritis in cats that was not tested for in this particular case is feline infectious peritonitis (FIP).[1] Although there were other features of FIP lacking in this case, it is always something to keep on the differential list for cases of pleural effusion of any kind in feline patients.[1]

A crucial contributor to the pathogenesis of lung lobe torsions is the dual blood supply to the lung, which has low and high-pressure systems. The pulmonary circulation, the low-pressure system, is where gas exchange occurs in the lung.[11] The bronchiolar circulation is the high-pressure system responsible for providing oxygen to the lung tissue itself.[11] When a lung lobe torsion occurs, the low-pressure system collapses, leading to venous infarction and coagulative necrosis of the alveoli.[9] The high-pressure system continues to pump oxygenated blood, leaving the bronchioles relatively intact.

Dr. Carvallo wrapped up this case with a discussion on a rarely mentioned topic in the lungs: the lymphatic circulation.[9] The lung does have a significant lymphatic network that drains from the interstitium to the mediastinal lymph nodes and back into the venous circulation. Lymphatic vessels are present throughout the parenchyma and subpleural spaces, but are absent within the alveolar capillary beds. They extend only as far as the respiratory bronchioles and alveolar ducts, leaving the gas exchange surfaces free of additional structures. However, in disease states, lymphatics can sprout in the alveolar interstitium, highlighting the need for a fine balance in disease between drainage of excess fluid, proteins, cells, etc. and ensuring adequate gas exchange can still occur.

References:

1. Beatty J, Barrs V. Pleural effusion in the cat: a practical approach to determining aetiology. *J Feline Med Surg*. 2010;12 (9):693-707.
2. Fossum T. Chylothorax in Cats: Is There a Role for Surgery? *J Feline Med Surg*. 2001;**3**(2):73–79.

3. Gicking JC, Aumann M. Lung lobe torsion. *Compendium*. 2011:E1–E6.
4. Graham J, Basseches J. Liver Lobe Torsion in Pet Rabbits: Clinical Consequences, Diagnosis, and Treatment. *Vet Clin North Am: Exot Anim Prac*. 2014;**17**(2):195–202.
5. Hatch A, Jandrey KE, Tenwolde MC, Kent MS. Incidence of chyloabdomen diagnosis in dogs and cats and corresponding clinical signs, clinicopathologic test results, and outcomes: 53 cases (1984–2014). *J Am Vet Med Assoc*. 2018;**253**(7):886–892.
6. Hinrichs U, Puhl S, Rutteman GR. Lymphangiosarcomas in Cats: A Retrospective Study of 12 Cases. *Vet Pathol*. 1999.
7. Ibrahim A, El-Ghareeb WR, Aljazzar A, Al-Hizab FA, Porter BF. Hepatic lobe torsion in 3 dromedary camels. *J VET Diagn Invest*. 2021;**33**(1):136–139.
8. Monnet E. Lungs. In: Vol. 2, *Veterinary Surgery Small Animal*. Tobias K & Johnston S, ed. 1st ed. St Louis, MO: Elsevier Mosby; 2012:1762–1763.
9. Mosier DA. Vascular disorders and thrombosis. In: *Pathologic Basis of Veterinary Disease*. Elsevier Mosby 2022:98–100.
10. Radlinsky MG. Thoracic cavity. In: Vol. 2, *Veterinary Surgery Small Animal*. Tobias K & Johnston S, ed. 1st ed. St Louis, MO: Elsevier Mosby; 2012:1787–1812.
11. Suresh K, Shimoda LA. Lung Circulation. *Compr Physiol*. 2016;6(2):897-943.
12. Tindale C, Cinti F, Cantatore M, et al. Clinical characteristics and long-term outcome of lung lobe torsions in cats: a review of 10 cases (2000–2021). *J Feline Med Surg*. 2022;**24**(10):1072–1080.
13. Valenciano AC, Arndt TP, Rizzi TE. Effusions: Abdominal, Thoracic and Pericardial. In: *Cowell and Tyler's Diagnostic Cytology and Hematology of the Dog and Cat*. Elsevier Mosby; 2014:259–260.
14. *Jubb, Kennedy, and Palmer's Pathology of Domestic Animals*. Maxie MG, ed. 6th ed. St Louis, MO: Elsevier; 2016.

CASE III:

Signalment:

12-day-old, male, Pit bull, *Canis familiaris*, canine

History: This was the fourth puppy from the litter to develop sudden-onset dyspnea and die within hours over the past week. All the affected puppies were in excellent body condition. The dam was obtained from a county shelter, and no medical history was available. Only one puppy was submitted for postmortem examination.

Gross Pathology: The lungs were mottled dark to light red, non-collapsing, rubbery, and wet on cut section. The right middle lung lobe sank in formalin. The liver contained multifocal, pinpoint (<1.0 mm) pale red to tan foci scattered throughout all lobes. Bilaterally, both kidneys had multifocal to coalescing hemorrhagic foci (0.1–0.2 cm in diameter) within the cortex, which extended

Figure 3-1. Kidneys, puppy. Distributed randomly throughout the cortex are numerous, 1-2.0 mm, red, foci. (*Photo courtesy of:* Midwestern University College of Veterinary Medicine, Diagnostic Pathology Center, https://www.mwuanimalhealth.com/diagnostic-pathology-center)

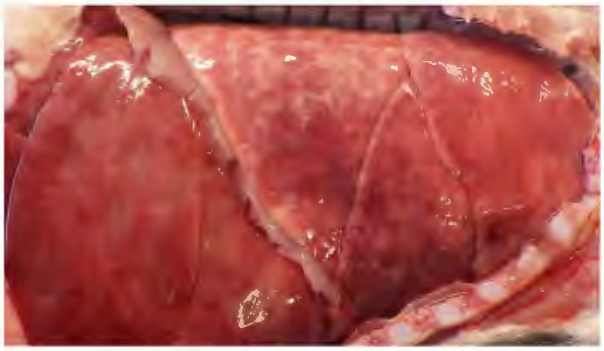

Figure 3-2. Lung and liver, puppy. Lung and liver, dog. The lungs are diffusely rubbery, firm, and fail to collapse. Throughout all liver lobes are numerous, subtle, multifocal, randomly distributed pinpoint (<1.0 mm) red to tan foci. (*Photo courtesy of:* Midwestern University College of Veterinary Medicine, Diagnostic Pathology Center, https://www.mwuanimalhealth.com/diagnostic-pathology-center)

into the corticomedullary junction on cut section.

Microscopic Description:

Kidney: Multifocally throughout the section, involving approximately 40% of the parenchyma, primarily within the cortex and extending to the corticomedullary junction, there are variably sized areas of necrosis. Affected tubules and occasional glomeruli are pale and eosinophilic, with loss of differential staining and absent to karyorrhectic nuclei, accompanied by interstitial hemorrhage and edema. Rarely, individual epithelial cell nuclei contain a single, round, eosinophilic intranuclear inclusion body that marginates the chromatin.

Lung: Multifocally throughout the section, alveolar septa are frequently and variably expanded, up to fourfold, by abundant fibrin, necrotic cellular debris, and very low numbers of neutrophils. Adjacent alveolar spaces contain similar material, along with small amounts of hemorrhage and foamy macrophages. Rarely, small eosinophilic intranuclear inclusion bodies are present within macrophages and pneumocytes at the margins of necrotic areas. The interstitium surrounding bronchi and the tunica adventitia of arteries is often expanded by a moderate amount of clear space (edema).

Contributor's Morphologic Diagnosis: Kidney, liver, brain, and lung: Nephritis, hepatitis, encephalitis, and interstitial pneumonia, necrotizing, multifocal, marked, with rare eosinophilic intranuclear inclusion bodies.

Contributor's Comment:

Canine herpesvirus type 1 (CHV-1) is an enveloped, double-stranded DNA virus in the *Alphaherpesvirinae* subfamily of the *Herpesviridae* family. First identified in the 1960s, it remains a significant cause of perinatal mortality in dogs.[2,4] The virus replicates most efficiently at subnormal body temperatures (34–36°C), which helps explain why neonatal puppies, who cannot yet regulate their body temperature well, are particularly susceptible. CHV-1 is inactivated at temperatures above 40°C, underscoring the importance of external heat support in managing suspected cases.[4]

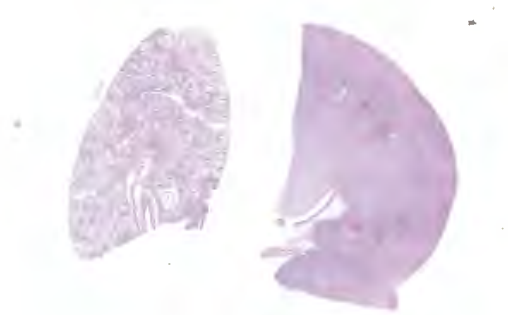

Figure 3-3. Lung and kidney, puppy: A section of lung and liver are submitted for examination. At subgross magnification, the lung is hypercellular with multifocal alveolar consolidation. There are multifocal areas of hemorrhage within the kidney and clusters of hypereosinophilic tubules. (HE, 10X)

The clinical course of infection is strongly age-dependent. Typically, puppies less than three weeks of age are at risk, often developing a fulminant, systemic infection characterized by viremia, multisystemic necrosis, and high mortality. In contrast, older puppies and adult dogs typically develop localized infections affecting the upper respiratory tract, eyes, or genital mucosa.[3,4] Infection during pregnancy in a naive bitch can result in fetal loss, abortion, or neonatal death. Surviving dogs may become latent carriers, harboring the virus in sensory ganglia with potential for reactivation during periods of stress, illness, or immunosuppression.[2,3]

Transmission in neonates occurs in utero, during passage through the birth canal, or postnatally via oronasal secretions from the dam or littermates. Fomites and caretakers may also contribute. In older dogs, aerosol transmission is more common. After local replication in the nasal mucosa and tonsils, the virus spreads to regional lymph nodes and subsequently disseminates to visceral organs and the central nervous system via infected leukocytes.[2,4]

The incubation period ranges from 6 to 10 days, and affected litters may experience mortality rates approaching 100% within a week of onset. Clinical signs include crying,

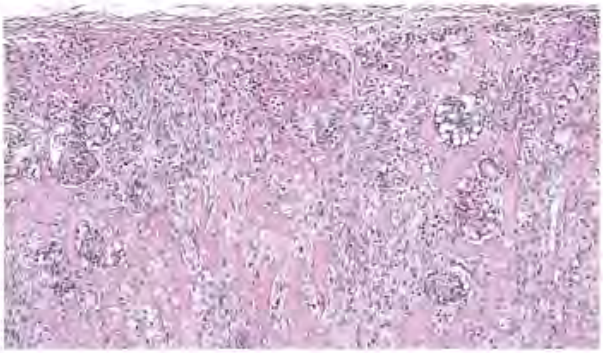

Figure 3-4. Kidney, puppy. Clusters of proximal convoluted tubules have undergone coagulative necrosis. (HE 311X)

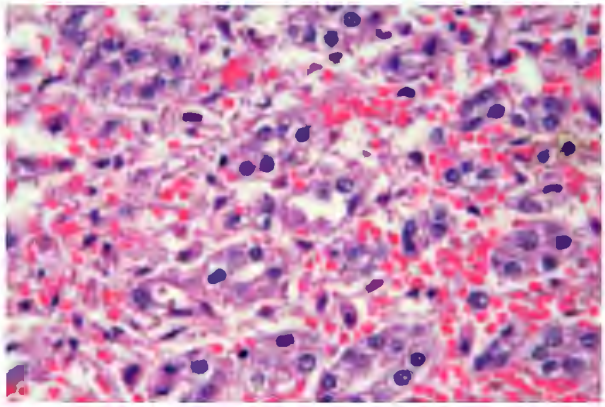

Figure 3-5. Kidney, puppy: Tubular epithelial cells at the edge of necrotic foci rarely contain an eosinophilic intranuclear inclusion body (arrow). (HE, 630X) (*Photo courtesy of:* Midwestern University College of Veterinary Medicine, Diagnostic Pathology Center, https://www.mwuanimalhealth.com/diagnostic-pathology-center)

anorexia, abdominal pain, hypothermia, and ataxia; some puppies may die suddenly with minimal premonitory signs.[3]

At necropsy, affected neonates often show characteristic gross and microscopic lesions, including multifocal hemorrhage and pallor in the liver, kidneys, lungs, spleen, and gastrointestinal tract, typically with minimal inflammation. Enlarged lymph nodes and nonsuppurative meningoencephalitis are also common. These findings are considered highly suggestive of systemic CHV-1 infection in puppies less than three weeks old.[3,4]

Contributing Institution:

Midwestern University College of Veterinary Medicine
Diagnostic Pathology Center
5725 West Utopia Rd.
Glendale, AZ 85308
https://www.mwuanimalhealth.com/diagnostic-pathology-center

JPC Morphologic Diagnosis:

1. Kidney: Nephritis, necrotizing, acute,

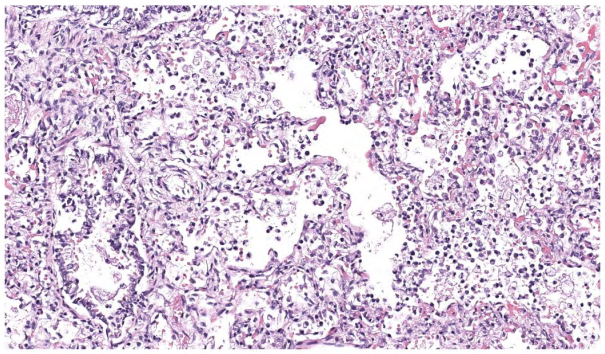

Figure 3-6. Lung, puppy: Alveolar septa are diffusely expanded by edema inflammatory cells, and cellular debris. Alveoli contain varying amounts of edema fluid, fibrin, alveolar macrophages, and cellular debris. There is multifocal necrosis and loss of airway epithelium, which often contain refluxed alveolar contents. (HE, 361X)

multifocal, moderate, with rare intranuclear viral inclusions.

2. Lung: Pneumonia, necrotizing, acute, multifocal to coalescing, moderate, with rare intranuclear viral inclusions.

JPC Comment:

What a classic case! The contributor provides a thorough, well-written comment on this entity that has been seen several times throughout the years of the WSC due to its continued relevance. Dr. Carvallo made a point to mention how pathologists should use all the clues at their disposal to help them gather as much information as possible. In this case, the size of the organs was sufficiently small that one could assume they were from a very young animal. Most would diagnose the changes in the lung as consistent with an interstitial pneumonia, but Dr. Carvallo stated that the preferred term in current veterinary literature would be "interstitial lung disease." This term is currently being added into the pathology lexicon as a broad term for cellular damage +/- leukocyte infiltration that mainly targets the interstitium, including the alveolar septa and adjacent bronchioles.[1] The term "interstitial pneumonia" is now being classified as a subtype of interstitial lung disease characterized by an increased number of leukocytes thickening the alveolar septa and vascular adventitia as seen with such diseases as ovine progressive pneumonia (OPP), porcine reproductive and respiratory syndrome (PRRS), sepsis, or parasitic larval migrations.[1]

References:

1. Carvallo-Chaigneau FR, Caswell JL. Special section on interstitial lung disease in domestic animals. *Journal of Veterinary Diagnostic Investigation*. 2026;0(0).
2. Decaro N, Martella V, Buonavoglia C. Canine adenoviruses and herpesvirus. *Vet Clin North Am Small Anim Pract*. 2008;38(4):799–814. doi:10.1016/j.cvsm.2008.02.006.
3. Evermann JF, Ledbetter EC, Maes RK. Canine reproductive, respiratory, and ocular diseases due to canine herpesvirus. *Vet Clin North Am Small Anim Pract*. 2011;41(6):1097–1110. doi:10.1016/j.cvsm.2011.08.007.
4. Greene CE. Canine herpesvirus infection. In: Greene CE, ed. *Infectious Diseases of the Dog and Cat*. 4th ed. Philadelphia, PA: WB Saunders; 2012:48–54

CASE IV:

Signalment:

3-year-old intact male Rocky Mountain bighorn sheep (Ovis canadensis canadensis).

History:

One of a group of 17 rams from a provincial park. Over a period of ~1 month several rams were observed coughing and 5 were found dead. Several animals within this group were collared allowing monitoring of movements and recovery of carcasses. Movement monitoring revealed recent proximity to a flock of domestic sheep. At the time of euthanasia, this individual appeared lethargic and had been observed coughing. This animal was euthanized by gunshot to the head and submitted for necropsy to allow for further evaluation of respiratory disease for herd management. The carcass was stored outside in -20°C temperatures for ~12 hours prior to necropsy examination.

Gross Pathology:

At necropsy examination, the distal trachea contained a small volume of stable tan foam. Approximately 20% of both left and right cranial lung lobes were firm, dark pink and well-demarcated from the surrounding parenchyma (Figure 1). On cut section, these areas exuded frothy white fluid and thin sections sank slightly in formalin before floating to the surface. Within the caudodorsal lung lobes there were ~5 indistinct multifocal firm nodules that ranged in size from 0.3 to 1.0 cm in diameter. On cut section these nodules were pale tan and merged with the surrounding parenchyma (Figure 2). Similar lung lesions were observed in other necropsied sheep from this cohort. One of the additional sheep also had unilateral suppurative mucoid yellow white fluid within the nasal passages and sinuses with diffuse reddening and slight thickening of the associated mucosa.

Laboratory Results :

Bacterial Culture Results: Lung grew 2+ *Bibersteinia trehalose*

PCR Results: *Mycoplasma ovipneumoniae* detected in lung tissue and by nasal swabs and confirmed through sequencing. Lung tissue was negative for bovine parainfluenza 3 virus, ovine progressive pleuropneumonia virus (Maedni Visna) and bovine respiratory syncytial virus.

Microscopic Description:

Two distinct patterns were observed within the examined sections of lung. Within caudodorsal regions (not apparent in submitted sections), there were large multifocal foci of mild histiocytic inflammation associated with nematodes of various life stages (adult, larval and eggs) (Figure 4 and 5). Adult

Figure 4-1. Lung, bighorn sheep. Approximately 20% of both left and right cranial lung lobes were firm, dark pink and well-demarcated from the surrounding parenchyma. (*Photo courtesy of*: Diagnostic Services Unit (DSU), University of Calgary. https://vet.ucalgary.ca/; https://vet.ucalgary.ca/departments-units/dsu/home)

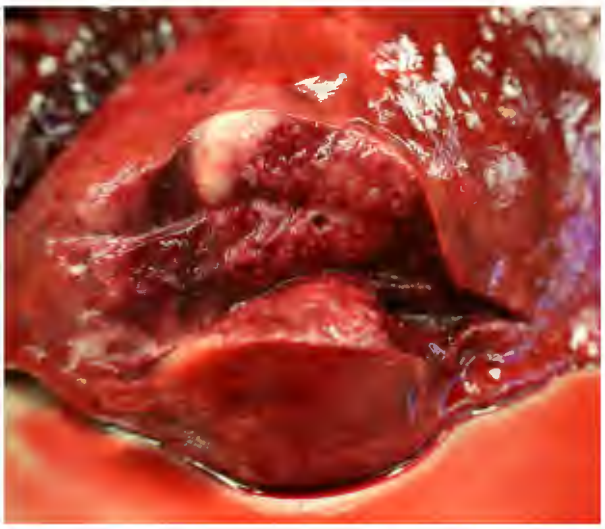

Figure 4-2. Lung, bighorn sheep. Within the caudodorsal lung lobes there were ~5 indistinct multifocal firm nodules that ranged in size from 0.3 to 1.0 cm in diameter. On cut section these nodules were pale tan and merged with the surrounding parenchyma Diagnostic Services Unit (DSU), University of Calgary. https://vet.ucalgary.ca/; https://vet.ucalgary.ca/departments-units/dsu/home)

nematodes are ~80 mm in diameter and characterized by a thick outer eosinophilic cuticle, pseudocoelom, gastrointestinal tract lined by cuboidal epithelium with a brush border and reproductive tract that is often paired. Larvae are coiled and ~15 mm in diameter. Eggs are ~50mm in diameter and surrounded by a clear capsule containing eosinophilic granular material and variable numbers of nucleated cells. Nematodes fill the alveoli and are associated with small numbers of histiocytes, lymphocytes, and plasma cells. Lymphocytes and plasma cells sometimes form small aggregates or cuffs around blood vessels. Rare adult nematodes are observed within the larger airways. Minimal inflammation extends into the surrounding parenchyma.

The second pattern (apparent in the submitted sections), observed within cranioventral sections of lung, is marked inflammation targeted towards small and large airways. Small terminal airways are most markedly affected and contain large numbers of luminal neutrophils. The surrounding respiratory epithelium is often hyperplastic and occasionally necrotic with sloughing into the airway lumen. Surrounding alveoli contain large numbers of luminal histiocytes with fewer neutrophils and occasionally are lined by cuboidal type II pneumocytes. There are rare multifocal areas of fibrin exudation into airways. Larval parasites resembling those described above are frequently seen individually within alveoli. Larger airways are often only minimally affected. Occasionally the lumen of smaller airways is compressed by nodular submucosal aggregates of inflammation (Figure 6). There are multifocal areas of acute hemorrhage throughout the lung (gunshot euthanasia associated).

Contributor's Morphologic Diagnosis:

Lung: Moderate, subacute, neutrophilic and histiocytic bronchopneumonia with epithelial hyperplasia

Lung, caudodorsal lobes: Mild, chronic multifocal histiocytic pneumonia with abundant intralesional nematodes and mild BALT hyperplasia

Contributor's Comment:

Histologic examination of the lungs confirmed a moderate bronchopneumonia as well as a mild lung worm infestation within the caudal lung lobes. A mild lymphoplasmacytic tracheitis was also present. Lung worms are ubiqui-

tous in this bighorn sheep population and are most likely *Protostrongylus stilesi*, although *P. rushii* are also observed. Bacterial culture of the lung grew a mixed population including 2+ *Bibersteinia trehalose*, a bacterial respiratory pathogen capable of causing bronchopneumonia in bighorn sheep. PCR testing of the lung was positive for *Mycoplasma ovipneumoniae* (Movi). Due to the potential for cross reaction with other *Mycoplasma spp*. sequencing was also performed for confirmation. Lung tissue was also tested and was negative for common respiratory viruses including parainfluenza 3 virus, ovine progressive pleuropneumonia virus (Maedni Visna) and bovine respiratory syncytial virus. Due to the small size of this herd, the history of other animals coughing, and the potential for transmission to a larger nearby group of ewes and lambs, culling of the remaining rams was initiated. The majority of the additional rams that were necropsied exhibited bronchopneumonia similar to that already described.

Epizootic outbreaks of pneumonia have been a population limiting problem in bighorn sheep likely since the early 20th century and the expansion of humans and domestic small ruminants west across North America.[3] Although pneumonia was recognized early as an important disease in wild bighorn sheep, and outbreaks were known to occur following exposures to domestic small ruminants, determining a definitive etiology took many years. Often, multiple potential respiratory pathogens were detected and therefore bighorn sheep pneumonia was discussed as a disease complex.[1] Associated etiologies that were explored included lungworms (both *P. rushii* and *P. stilesi*), leukotoxin producing members of the *Pasteurellaceae* family (*Mannheimia haemolytica*, *Bibersteinia trehalose* and *Pasteurella multocida*) and *Mycoplasma ovipneumoniae*. Viral respiratory pathogens including parainfluenza virus 3 and respiratory syncytial virus were also occasionally detected, but less commonly.

Advanced molecular techniques and careful experimental infections eventually lead to the identification of Movi as the most significant and essential pathogen in epizootic pneumonia of bighorn sheep.[2] Within domestic small ruminants, Movi is known as a cause of generally mild chronic bronchopneumonia in lambs, also known as atypical pneumonia or chronic non-progressive pneumonia.[9] Movi can affect several non-domestic species of the *Caprinae* subfamily including bighorn sheep, Dall's sheep, mountain goats and muskox, and is often carried in the nasal passages of healthy domestic sheep and goats. [5,10] Outbreaks in bighorn sheep can often be traced to contact with domestic small ruminants, more often sheep than goats. Movi associated outbreaks in bighorn sheep occur in two distinct forms. The first introduction of a novel strain of Movi to a naïve population leads to a slowly

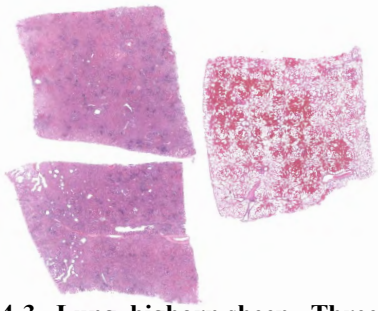

Figure 4-3. Lung, bighorn sheep. Three sections of lung are submitted for examination, with two of three being diffusely consolidated. (HE, 10X)

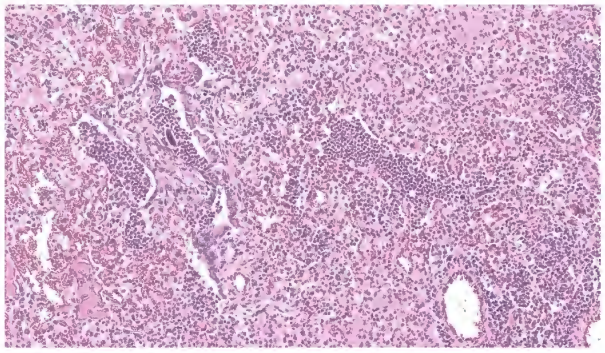

Figure 4-4. Lung, bighorn sheep. Diffusely alveoli and airways are filled with large numbers of neutrophils admixed with varying amounts of fibrin, edema and cellular debris. There are rare larval nematodes within both. (HE, 249X)

progressing pneumonia that affects all age classes and often results in high morbidity and mortality rates of 30-90%.[1] Reported clinical signs include coughing, nasal discharge, head shaking and ear drooping. The resultant pneumonia is frequently made more severe by secondary bacterial involvement often with members of the *Pasteurellaceae* such as the *Bibersteinia trehalose* observed in this case. Recurring outbreaks in subsequent years affect primarily lambs due to transmission from carrier ewes, and lead to low lamb recruitment and poor population growth. The outcome of infection in a population can be quite variable depending on complex interactions between host immunity, bacterial strain and environmental factors. Currently there are no vaccines or antibiotic therapies that have been found to be effective. [4]

Movi pneumonia bears some resemblance to the atypical pneumonia of pigs caused by *M. hyopneumoniae* and shares several histologic and pathogenic features with other members of the *Mycoplasma* genus. *Mycoplasma spp.* target and destroy the cilia of airways impeding mucocilliary clearance and predisposing the lungs to secondary bacterial infection.[1] Characteristic histologic features include hyperplasia of bronchiolar and alveolar epithelium, lymphoid (BALT) hyperplasia around airways and blood vessels, bronchiolar mucous metaplasia and more chronically, formation of distinct hyaline scars.[7] Hyaline scars are a unique feature that bear some resemblance to bronchiolitis obliterans observed in chronic bovine pneumonias, including those with *Mycoplasma bovis*. Hyaline scars are described as nodular broad-based accumulations of brightly eosinophilic poorly cellular material below the respiratory epithelium that result in compression and distortion of the airway lumen.[9] Unfortunately, depending on chronicity, many cases, including the current one, lack these characteristic histologic features and PCR testing and sequencing is necessary to confirm the diagnosis. In addition to bronchopneumonia, other Movi associated lesions include tracheitis, rhinitis, sinusitis and otitis media. [1]

Management of these outbreaks requires an adaptive approach and can be quite challenging depending on the timing of detection and many other factors. [4] Preventative management should focus on minimizing contact between bighorn sheep and domestic small ruminants. In first incursion outbreaks, or when only a small herd is affected, complete

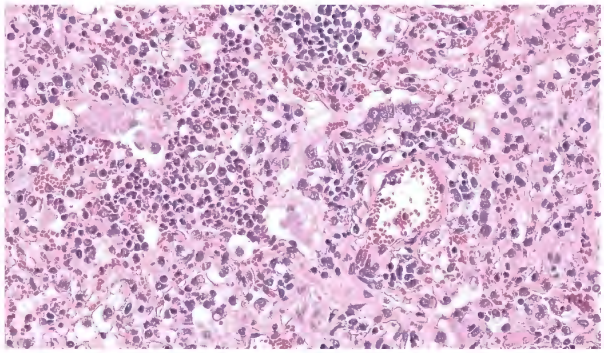

Figure 4-5. Lung, bighorn sheep. Higher magnification of the ninfalmmatory exudate. There is scattered type II pneumocyte hyperplasia. (HE, 594X)

depopulation may be an effective strategy given the short survival of the bacteria in the environment; Movi bacteria persist for only minutes outside of the host.[4] In more chronically affected populations, management may focus on testing and removal of carrier individuals. In this particularly outbreak, culling of the small affected herd seems to have been effective in preventing spread to the surrounding populations.

Contributing Institution:

Diagnostic Services Unit (DSU) within the Faculty of Veterinary Medicine, University of Calgary.

https://vet.ucalgary.ca/

https://vet.ucalgary.ca/departments-units/dsu/home

JPC Morphologic Diagnosis:

Lung: Bronchopneumonia, suppurative and histiocytic, subacute, diffuse, marked, with mild BALT hyperplasia, early obliterating bronchiolitis, and numerous metastrongyle larvae.

JPC Comment:

This case was an excellent example of a real-world diagnostic case with multiple pathogens. This contributor provided a fantastic comment on *Mycoplasma ovipneumonae* (Movi) and *Bibersteinia trehelosi*, as well as gave an honorable mention to the ubiquitous lungworms *Protostrongylus spp*, in their write-up. Movi is the #1 infectious disease of Bighorn sheep.[1] In cases of "bighorn sheep pneumonia", Movi is frequently the primary initiator of outbreaks and lays the foundation for a polymicrobial pneumonia.[1]

Bibersteinia trehelosi, previously *Pasteurella trehelosi*, is a common nasal commensal that is opportunistic in cases of bighorn

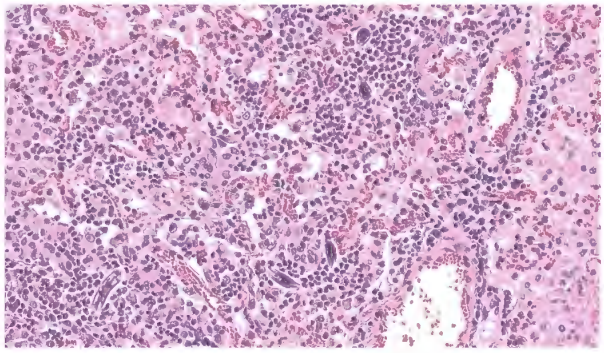

Figure 4-6. Lung, bighorn sheep. There are scattered cross- and tangential sections of nematode larva within the alveolar exudate. (HE, 471X)

sheep pneumonia.[1,6] It is best known for its role in systemic pasteurellosis in 4-9mo lambs and is also considered one of the pathogens within the ovine respiratory complex.[6]

Participants discussed the potential identity of the nematodes and considered *Dictyocaulus filaria, Muellerius capillaris, or Protostrongylus spp*. *Dictyocaulus spp* were quickly ruled out as they are larger lungworms that usually reside in the upper airways.[8] *Muellerius capillaris* was similarly discounted as they tend to accumulate in subpleural nodules.[8] *Protostrongylus spp*, however, are small and tend to disperse diffusely throughout the pulmonary parenchyma, as seen in this case.[8]

The lungs here also highlighted nice examples of early obliterating bronchiolitis (also representing the continuing evolution of terminology, having been previously referred to as "bronchiolitis obliterans"), characterized by organizing aggregates of fibrin that are covered by bronchiolar epithelial cells within bronchiolar lumens.

References:

1. Besser TE, Cassirer EF, Highland MA, Wolff P, Justice-Allen A, Mansfield K, Davis MA, Foreyt W. Bighorn sheep pneumonia: Sorting out the cause of a polymicrobial disease. *Preventive Veterinary Medicine.* 2013:108(2-3)**:**85-93.
2. Besser TE, Cassirer EF, Potter KA, Lahmers K, Oaks JL, Shanthalingam S, Srikumaran S, Foreyt WJ. Epizootic pneumonia of bighorn sheep following experimental exposure to *Mycoplasma ovipneumoniae*. *PLOS ONE.* 2014:9(10).
3. Cassirer EF, et al. Pneumonia in bighorn sheep: Risk and resilience. *Journal of Wildlife Management.* 2018:82(1)**:**32-45.
4. Garwood TJ, Lehman CP, Walsh DP, Cassirer EF, Besser TE, Jenks JA. Removal of chronic *Mycoplasma ovipneumoniae* carrier ewes eliminates pneumonia in a bighorn sheep population. *Ecology and Evolution.* 2020:10(7)**:**3491-3502.
5. Handeland K, Tengs T, Kokotovic B, Vikoren T, Ayling RD, Bergsjo B, Sigurdardottir OG, Bretten T. *Mycoplasma ovipneumoniae* - a primary cause of severe pneumonia epizootics in the norwegian muskox (*Ovibos moschatus*) population. *PLOS ONE.* 2014:9(9).
6. Jiang H, Yang L, Duan S, et al. Analysis of nasopharyngeal microbiota revealing microbial disturbance associated with ovine respiratory complex. *Res Vet Sci*. 2024;179:105383.
7. Maxie MG. *Jubb, Kennedy & Palmer's Pathology of Domestic Animals*: Elsevier, 2016. 2:563-564.
8. Miller DS, Weiser GC, Aune K, et al. Shared Bacterial and Viral Respiratory Agents in Bighorn Sheep (*Ovis canadensis*), Domestic Sheep (*Ovis aries*), and Goats (*Capra hircus*) in Montana. *Vet Med Int*. 2011;2011:162520.
9. Sheehan M, Cassidy JP, Brady J, Ball H, Doherty ML, Quinn PJ, Nicholas RAJ, Markey BK. An aetiopathological study of chronic bronchopneumonia in lambs in Ireland. *Veterinary Journal.* 2007:173 (3)**:**630-637.
10. Wolff PL, et al. Detection of *Mycoplasma ovipneumoniae* in pneumonic mountain goat (*Oreamnos americanus*) kids. *Journal of Wildlife Diseases.* 2019:55 (1)**:**206-212.

Joint Pathology Center
Veterinary Pathology Services

WEDNESDAY SLIDE CONFERENCE 2025-2026

Conference #25 06 May 2026

Case I:

Signalment: 26 y 9 m, male, *Tiliqua scincoides intermedia*, northern blue-tongued skink

Figure 1-1. Liver, blue-tongued skink: Approximately 70% of the liver was expanded and replaced by numerous white, well-demarcated, soft nodules up to 14mm in diameter. (*Photo courtesy of* Smithsonian's National Zoo and Conservation Biology Institute, Wildlife Health Sciences https://nationalzoo.si.edu/animals/veterinary-care)

History: Physical exam performed due to continued lethargy, complete anorexia, weight loss noted by keeper staff. Physical exam showed a lethargic, weak, pale 6-10% dehydrated blue-tongue skink. No masses noted on coelomic palpation, but significant muscle catabolism noted. Bloodwork showed increasing serum phosphorus, and uric acid indicative of renal disease. Due to quality of life concerns euthanasia performed via IV injection in the tail vein of Euthasol (pentobarbital/phenytoin solution) and potassium chloride mixed 1:1.

Gross Pathology:

Body condition was reduced with minimal coelomic fat and only remnants of shrunken, orange fat bodies. There was a moderate amount of clear coelomic fluid.

Approximately 70% of the liver was expanded and replaced by numerous white, well-demarcated, soft nodules up to 14 mm in diameter. The spleen was mottled with tan nodules up to 3 mm in diameter. There were white, chalky areas within both kidneys, up to 1.5 cm in diameter expanding

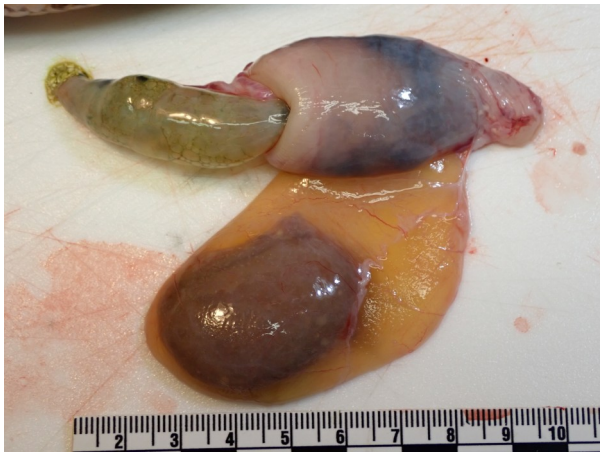

Figure 1-2. Colon, blue-tongued skink: Approximately 1.5 cm of the colon telescoped within the distal colon, and the intussusceptum was reddened, thickened, and not easily reduced, (*Photo courtesy of* Smithsonian's National Zoo and Conservation Biology Institute, Wildlife Health Sciences https://nationalzoo.si.edu/animals/veterinary-care)

and compressing the surrounding tissue. The urinary bladder contained a soft, grey, free-floating urocystolith.

Approximately 1.5 cm of the colon telescoped within the distal colon, and the intussusceptum was reddened, thickened, and not easily reduced.

Laboratory Results:

Urocystolith confirmed to be 100% urate crystals in a protein matrix.

Microscopic Description:

The slide contains two sections of colon. Expanding the lamina propria and invading and disrupting all layers of the colon wall is an unencapsulated, poorly demarcated, highly cellular neoplasm. The edges of the neoplasm have an exophytic to polypoid growth habit that protrudes into the colonic lumen. Neoplastic cells are arranged in sheets, trabeculae, acini, and nests within a variably dense fibrovascular to myxomatous matrix. Acinar lumina and some nests frequently contain degenerate and non-degenerate heterophils and abundant karyorrhectic debris. Nests often have keratinized inner layers of cells which have sloughed and laminated into keratin pearls. Neoplastic cells are polygonal, ranging from cuboidal to squamous, with distinct cell borders and moderate amounts of amphophilic cytoplasm. Anisocytosis and anisokaryosis are moderate to marked. Nuclei are oval with vesicular chromatin and 1-2 distinct, magenta nucleoli. Mitotic rate is 5-10 per 40x HPF. Bizarre mitotic figures and occasional multinucleation are noted. Individual cell necrosis and individual cell keratinization are common. Neoplastic cells often surround vasculature and occasional neoplastic cells are noted in vascular lumina.

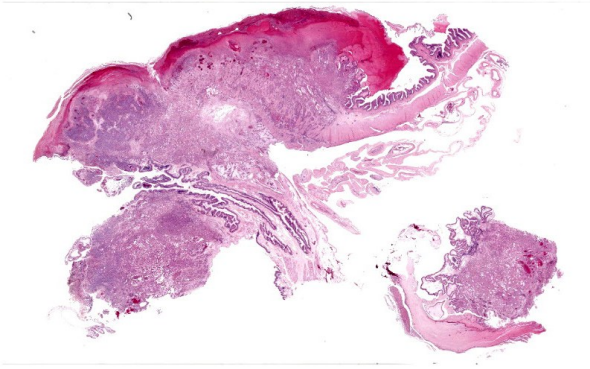

Figure 1-3. Colon, blue-tongued skink: The colon is transmurally infiltrated by a neoplasm with a segmentally ulcerated surface (HE, 10X).

Multifocally, the tumor is infiltrated by heterophils and lower numbers of lymphocytes and plasma cells. Superficial/luminal portions of the mass are broadly necrotic and overlain by a fibrinohemorrhagic pseudomembrane. Some portions of the luminal surface are keratinized and laminated (slide variability). The pseudomembrane and necrotic portions of the mass are heavily colonized by rod bacteria, and there is occasional mineralization within the necrotic tissue.

Adjacent non-neoplastic mucosa has marked lymphoid hyperplasia within the lamina propria and scattered goblet cell hyperplasia of the epithelium. Lymphatics and veins in the serosa are markedly dilated.

Contributor Morphologic Diagnosis:

Colon: Colonic adenosquamous carcinoma with ulceration, necrosis, and colonies of rod bacteria.

Colon: Intussusception, chronic (not apparent in slide submitted).

Liver, spleen, lungs, heart, urinary bladder, pancreas, fat bodies (slides not submitted): Metastatic adenocarcinoma.

Contributor Comment:

Gastrointestinal adenosquamous carcinomas are rare malignancies in mammals and even less commonly reported in the alimentary tract of reptiles. A tumor is considered adenosquamous if it exhibits significant rep-

resentation of both glandular and squamous differentiation.[5,6,8] Adenosquamous is a descriptor that is most commonly used in respiratory, alimentary, and mammary tumors with mixed glandular and squamous features and is not specific to any one cell of origin. The malignancy in this case clearly demonstrates glandular formations common in colonic adenocarcinomas, but some areas show nesting, keratinization, and even keratin pearl formation characteristic of squamous cell carcinomas. This tumor was highly metastatic – most likely due to hematogenous spread – and established itself in the liver, spleen, lungs, heart, urinary bladder, pancreas, and fat bodies of the animal. Tumor cells at metastatic sites did not maintain squamous differentiation and only occasionally formed vaguely glandular arrangements, with the vast majority of metastases composed of sheets of malignant cells.

Colonic malignancies of any type are uncommon in reptiles. In a 2004 retrospective of 5353 reptile submissions by Garner et al., neoplasia was not uncommon, with a prevalence of 9.8% across all species submitted (527 tumors).[1] Lizards (n= 1909) had a neoplastic prevalence of 8.5%. No cases of colonic adenocarcinoma were reported in any lizard, chelonian, or crocodilian. Only in snakes were cases reported, and in that taxon only 6/325 tumors were diagnosed as colonic adenocarcinomas, indicating these tumors are quite uncommon at ~1.1% of reptile tumors in the retrospective. There was one case of intestinal carcinoma in lizards (0.6% of lizard tumors), but it was small intestine.

In records from the Smithsonian's National Zoo and Conservation Biology Institute, seven cases of colonic adenocarcinoma were identified in lizards (contributor's unpublished research). Three species were represented: 1 blue-tongued skink (*Tiliqua* spp., this case), 4 Gila monsters (*Heloderma* spp), and 2 African plated lizards (*Gerrhosaurus validus*). While these are all heavy-bodied arid-environment lizards, they are not taxonomically closely related, and the overrepresentation should be interpreted in light of their long lifespans and popularity in zoo collections. Interestingly, the cases represent a prominent proportion of adult necropsy findings in these species (1/6 blue-tongued skinks, 2/5 plated lizards, and 4/12 Gila monsters). No cases of colonic adenosquamous carcinoma were described in the National Zoo's records for any species, though an adenosquamous carcinoma was described on the hemipenis of a Mexican lance-headed rattlesnake (*Crotalus polystictus*) and the esophagus of a wood duck (*Aix sponsa*).

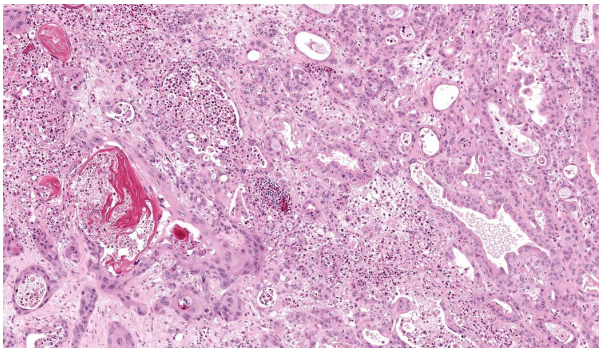

Figure 1-4. Colon, blue-tongued skink: The neoplasm is composed of moderately pleomorphic epithelial cells arranged in variably ectatic glands, trabeculae and nests. Some nests contain brightly eosinophilic lamellae of keratin, and acini often contain necrotic debris and sloughed cells. (HE, 160X)

Grossly, the section of colon including the tumor had an identifiable intussusception. Intussusception is the telescoping of a section of bowel (the intussusceptum) within an adjacent segment (the intussuscipiens), generally due to abnormal motility of the bowel smooth muscle. Intussusception is most common in young animals, where it is frequently associated with parasitism or inflam-

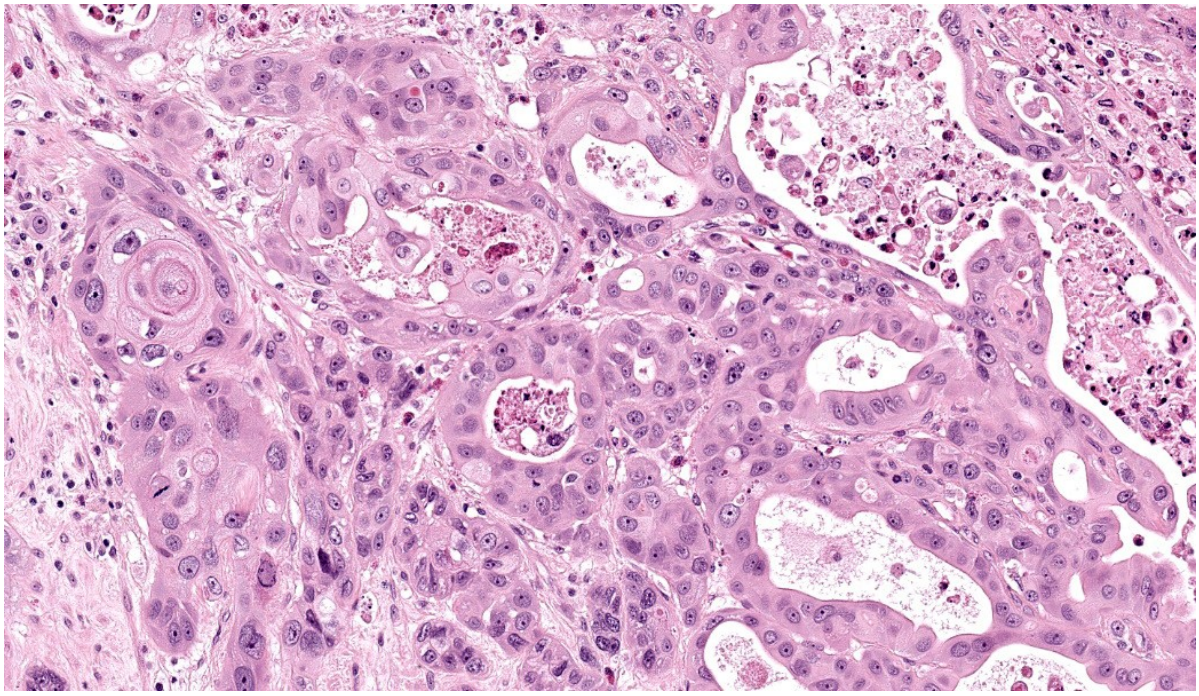

Figure 1-5. Colon, blue-tongued skink: High magnification of pleomorphic neoplastic cells. While most neoplastic cells are arranged in acini, here is central keratinization of nests of epithelium (center left) (HE, 381X).

mation. In the less frequent adult cases, tumors are often contributory. In humans, a retrospective of adult intestinal intussusception found that over 77% of cases were associated with a tumor, and nearly 60% of the intussusceptions were associated with a malignancy (74% of the tumors).[2] In the case presented here, the adenosquamous carcinoma is presumed to be the inciting cause of the grossly identified intussusception.

Contributing Institution:

Smithsonian's National Zoo and Conservation Biology Institute, Wildlife Health Sciences https://nationalzoo.si.edu/animals/veterinary-care

JPC Morphological Diagnosis:

Colon: Adenosquamous carcinoma

JPC Comment:

We crossed the finish line of this year's conferences with the amazing Dr. Kali Holder from the Smithsonian National Zoo! Dr. Holder brought her signature passion for pathology and exceptional comedic timing, setting the tone for a highly entertaining discussion on this first case. The neoplasm in this skink was diagnosed as an adenosquamous carcinoma, likely arising from the colon, with clear areas of both glandular and squamous differentiation. One participant noted that squamous differentiation in reptiles can also be due to hypovitaminosis A and chronic irritation,[7] postulating whether this could represent an adenocarcinoma with secondary squamous metaplasia rather than a true adenosquamous carcinoma. The organization of the squamous and glandular components convinced most attendees to support the ultimate diagnosis, however. When considering the disseminated metastasis of the primary carcinoma seen in this skink, Dr. Holder boldly exclaimed, "Don't put butt cancer in your heart! That's no way to run a skink!" Indeed.

The gross photographs, which are not provided to participants prior to conference, were crucial to diagnosing the intussusception in this case. Although uncommon in reptiles, intussusception is a well-recognized sequela to intestinal masses in numerous species, as they disrupt the coordinated peristaltic rhythm required to keep the bowel moving in a single direction.[4] Dr. Holder reviewed the pathophysiology of intussusception, which starts when a small fold of bowel telescopes into the adjacent segment, narrowing the lumen and causing partial or complete obstruction.[4] This leads to proximal distension, vascular compromise, edema, congestion, and inflammation. As the process worsens, fibrin accumulates on the serosa of the intussusceptum, which may cause adhesions between the intussusceptum and intussuscipiens. Severe cases progress to segmental necrosis, or even sloughing of the affected intestine.[4]

The difference between "intussusceptum" and "intussuscipiens" is a common sticking point for residents. A good way to differentiate between the two is making a mental connection between the word "recipient" and "intussuscipiens", which is the "recipient" of the intussusceptum. "Recipient" is basically part of the word "intussuscipiens!"

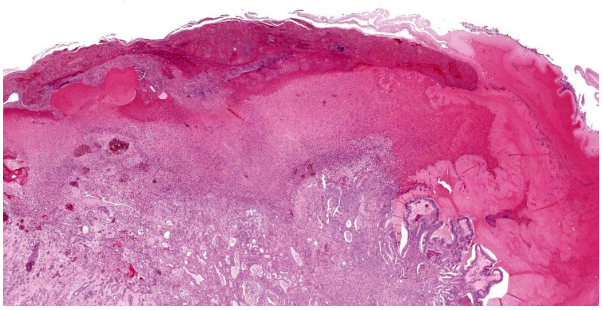

Figure 1-6. Colon, blue-tongued skink: The surface of the neoplasm is necrotic and covered with a serocellular crust. (HE, 29X).

In this skink, the neoplasm likely initiated a cascade of necrosis, inflammation, and mechanical disruption, culminating in the intussusception. This combination would likely have caused anorexia which, in reptiles, rapidly leads to dehydration.[2] Dehydration, in turn, causes renal stress and the precipitation of urate crystal deposition (gout). [2] Increased uric acid and urolithiasis were reported in this animal. This combination of unpleasantness likely contributed to this animal's clinical decline.

Dr. Holder closed this case with a discussion on how intestinal carcinomas in reptiles may be more common than currently recognized as improvements in husbandry, veterinary care, and pathology understanding allow more reptiles to reach ages where neoplasia becomes more prevalent.[1] Among reptiles, intestinal carcinomas are most common in snakes, less common in lizards, and rare in chelonians.[1]

Dr. Holder closed this case with a discussion on how intestinal carcinomas in reptiles may be more common than currently recognized as improvements in husbandry, veterinary care, and pathology understanding allow more reptiles to reach ages where neoplasia becomes more prevalent.[1] Among reptiles, intestinal carcinomas are most common in snakes, less common in lizards, and rare in chelonians.[1]

References:

1. Garner MM, Hernandez-Divers SM, Raymond JT. Reptile neoplasia: a retrospective study of case submissions to a specialty diagnostic service. *Vet Clin North Am Exot Anim Pract*. 2004 Sep 1;7:653–671.
2. Halán M, Kottferová L, Račka K, Lam A. The Amount of Food Ingested and Its Impact on the Level of Uric Acid in the

Blood Plasma of Snakes. *Animals (Basel)*. 2022;12(21):2959.

3. Honjo H, Mike M, Kusanagi H, Kano N. Adult Intussusception: A Retrospective Review. *World J Surg*. 2015 Jan 6 [cited 2021 Jul 29];39:134–138.
4. Marsicovetere P, Ivatury SJ, White B, Holubar SD. Intestinal Intussusception: Etiology, Diagnosis, and Treatment. *Clin Colon Rectal Surg*. 2017;30(1):30-39.
5. Munday JS, Löhr C V., Kiupel M. Tumors of the Alimentary Tract. In: Meuten DJ, ed. *Tumors in Domestic Animals*. Hoboken, NJ, USA: John Wiley & Sons, Inc.; 2016:499–601.
6. Sunkara T, Caughey ME, Makkar P, John F, Gaduputi V. Adenosquamous Carcinoma of the Colon. *Case Rep Gastroenterol*. 2017 Sep 1 [cited 2021 Jul 19];11:791.
7. Sykes JM 4th, Trupkiewicz JG. Reptile neoplasia at the Philadelphia Zoological Garden, 1901-2002. *J Zoo Wildl Med*. 2006;37(1):11-19.
8. Toumi O, Hamida B, Njima M, et al. Adenosquamous carcinoma of the right colon: A case report and review of the literature. *Int J Surg Case Rep*. 2018 Jan 1;50:119–121.

CASE II:

Signalment:

Juvenile female striped skunk (*Mephitis mephitis)*

History:

none

Gross Pathology:

The skunk was in good body condition with normal fat stores, and in good post-mortem condition. There were small numbers of fleas in the fur. There was a small amount of cloudy pink nasal discharge bilaterally. The cranioventral lung lobes were bilaterally dark red, wet, heavy, and firm. The right cranial lung lobe was mildly enlarged. All lung lobes contained small numbers of slender white worms up to 2cm in length. There were 16 ascarids in the gastrointestinal tract, 10 of which were in the stomach.

Laboratory Results:

Aerobic culture of the lung yielded a heavy growth of a *Pseudomonas* bacteria. Another colony type grew as well, but could not be separated from the heavy *Pseudomonas* growth.

Microscopic Description:

Pulmonary architecture is diffusely mildly to severely distorted by necrosis and inflammatory infiltrates. Bronchiolar submucosa is markedly expanded by dense infiltrates of neutrophils and macrophages, which often infiltrate surrounding alveoli. Diffusely, alveolar septa

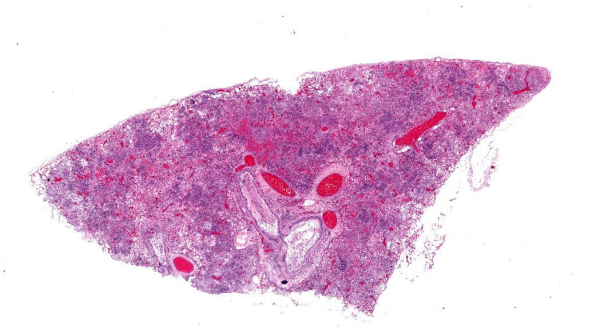

Figure 2-1. Lung, skunk: The submitted section of lung is diffusely consolidated with areas of parenchymal hypercellularity. (HE, 10X).

are undergoing fibrinoid necrosis, and protein-rich edema, sometimes with fibrin strands, fills alveoli**.** The walls of small arteries are infiltrated by neutrophils and macrophages and segments are undergoing fibrinoid necrosis. There are mild to severe hemorrhages scattered throughout the lung. There are large numbers of slender rod-type bacteria throughout most of the examined section, occasionally forming dense colonies that line vessels, alveolar walls, or bronchial and bronchiolar epithelium. There are smaller numbers of coccoid bacteria arranged in doublets or clusters, with small colonies generally found in close proximity to each other. Where bronchial and bronchiolar epithelium is present, there are moderate numbers of eosinophilic intracytoplasmic and rarely intranuclear inclusion bodies ranging from 2-6um diameter. Segmental bronchi are surrounded by marked interstitial edema, and there is mild to marked pleural edema and hemorrhage. Some sections have moderate numbers of larval nematodes which are 12-20um in diameter and up to 100um long, and lack a body cavity. These parasites have a slender serrated cuticle 1-2um thick and lateral alae. They are rarely abutted by multinucleated giant cells, and there are occasional elongate hyperchromatic basophilic structures suggestive of degenerating nematodes.

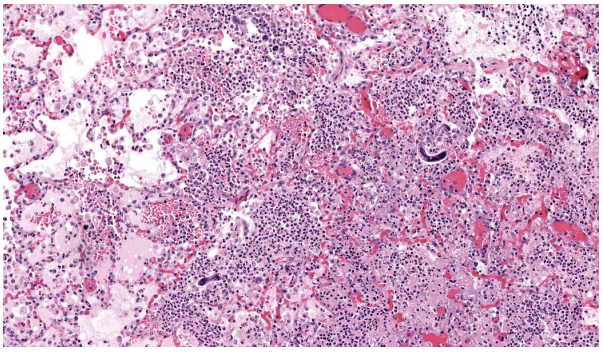

Figure 2-2. Lung, skunk: Areas of hypercellularity correspond to alveoli filled with neutrophils, eosinophilic, macrophages, and cross and tangential sections of metastrongyle larvae. There is multifocal septal necrosis. (HE, 290X).

Contributor's Morphologic Diagnosis:

Lung: Pneumonia, bronchointerstitial, necrotizing, acute, diffuse, severe, with growth of multiple bacterial species, and eosinophilic intracytoplasmic and intranuclear viral inclusions in epithelia, etiology consistent with canine distemper virus**;** and regional pulmonary larval nematodiasis

Contributor's Comment:

Canine distemper virus (CDV) is an enveloped, negative sense, single-stranded RNA virus in the family Paramyxoviridae, genus Morbillivirus.[3] The virus causes disease in both wild and domestic canids, as well as many other carnivores including seals, raccoons, weasels and the domestic ferret, skunks, and large cats such as lions and leopards; occasional outbreaks in populations of endangered large cats can have devastating population-level effect.[1,5,7,8,11,18] Dogs and raccoons are the most common reservoir populations. Other closely related viruses include phocine distemper virus and the morbilliviruses that cause disease in cetaceans, measles virus, Hendra virus that infects horses and humans, and peste des petits ruminants viruses.[3] Rinderpest, another morbillivirus that causes severe to fatal disease in cattle, was eradicated in 2011 with the help of vaccines.[20]

Initial replication of CDV occurs in tissue macrophages. The virus then spreads to tonsils and bronchial lymph nodes, spleen, lymphoid follicles in the lamina propria of the stomach and small intestines, other lymph nodes, and Kupffer cells; fever and leukopenia ensue. The virus is spread hematoge-

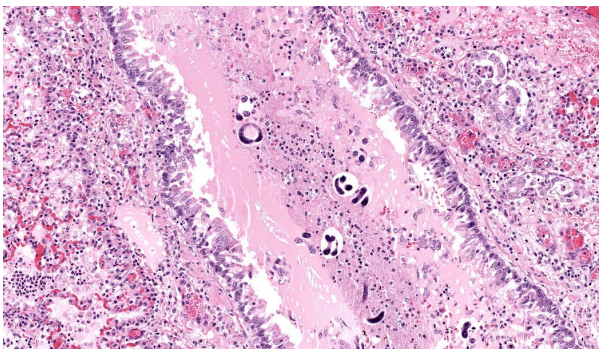

Figure 2-3. Lung, skunk: Airways contain refluxed alveolar contents. The airway epithelium is hyperplastic with individual epithelial cell necrosis. (HE, 281X).

nously to epithelia and to the central nervous system; once the virus begins replicating in epithelia, shedding ensues. Virus is most abundant in respiratory secretions and is commonly spread by droplets, but it can also be isolated from urine, and can be spread transplacentally. Shedding ceases once the immune system controls the virus, but can persist in some animals up to 90 days. Approximately 25-75% of dogs infected with CDV will have a strong humoral and cell-mediated immune response. Their signs may be entirely subclinical or limited to a brief fever, and the virus is cleared within two weeks of infection. Where dogs fail to develop a strong immune response, initial clinical signs are conjunctivitis and fever, followed by vomiting and diarrhea, anorexia, cough, increased respiratory effort, and secondary infections.[3] Some patients may then resolve the CDV infection, while others develop neurologic signs, which are almost always progressive. Neurologic signs include ataxia, tremors, myoclonus, seizures, coma, and death.[2]

Canine distemper virulence is associated with immunosuppression and neurotropism. Viral H protein binds to CD150 (signaling lymphocyte activation molecule), which is found on dendritic cells and activated monocytes, as well as both B- and T-cells. Early infection in monocytes and dendritic cells may interfere with normal antigen presentation, and upregulation of CD150 in infected animals may further enhance spread of the virus amongst lymphocytes.[14,17] CD4 (+) lymphocytes are first infected and lysed[6], and viral depletion combined with lack of cytokine stimuli from CD4 (+) cells combine to markedly reduce B-cells as well. Severe immunosuppression predisposes infected animals to secondary viral and bacterial infections, as with the bacterial pneumonia seen in this skunk.[2]

One to three weeks after recovery from systemic illness, some dogs develop neurologic disease. Virus is spread both anterograde up the axon and via circulating lymphocytes. Once in the brain, replication in the ependymal and choroid plexus epithelium allows virus to circulate in the CSF.[16] Acute encephalitis is a result of direct viral replication and injury in the central nervous system, with minimal inflammation. Virus is first detected in astrocyte foot processes and then neurons, and occasionally neuronal necrosis can lead to foci of polioencephalomalacia.[13] Historically, CDV infection has been thought of as a demyelinating disease. Though oligodendrocytes are seldom infected, infection of surrounding astrocytes and

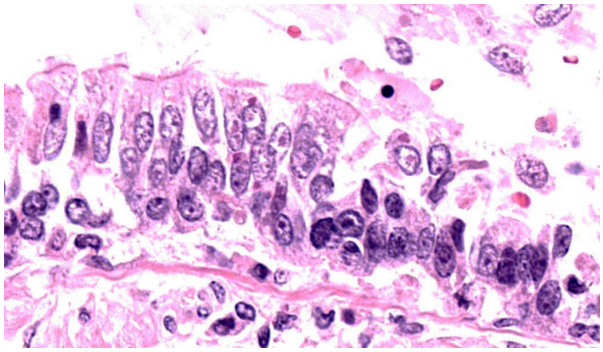

Figure 2-4. Lung, skunk: Airway epithelium contains both internuclear and intracytoplasmic viral inclusion. (HE, 1792X).

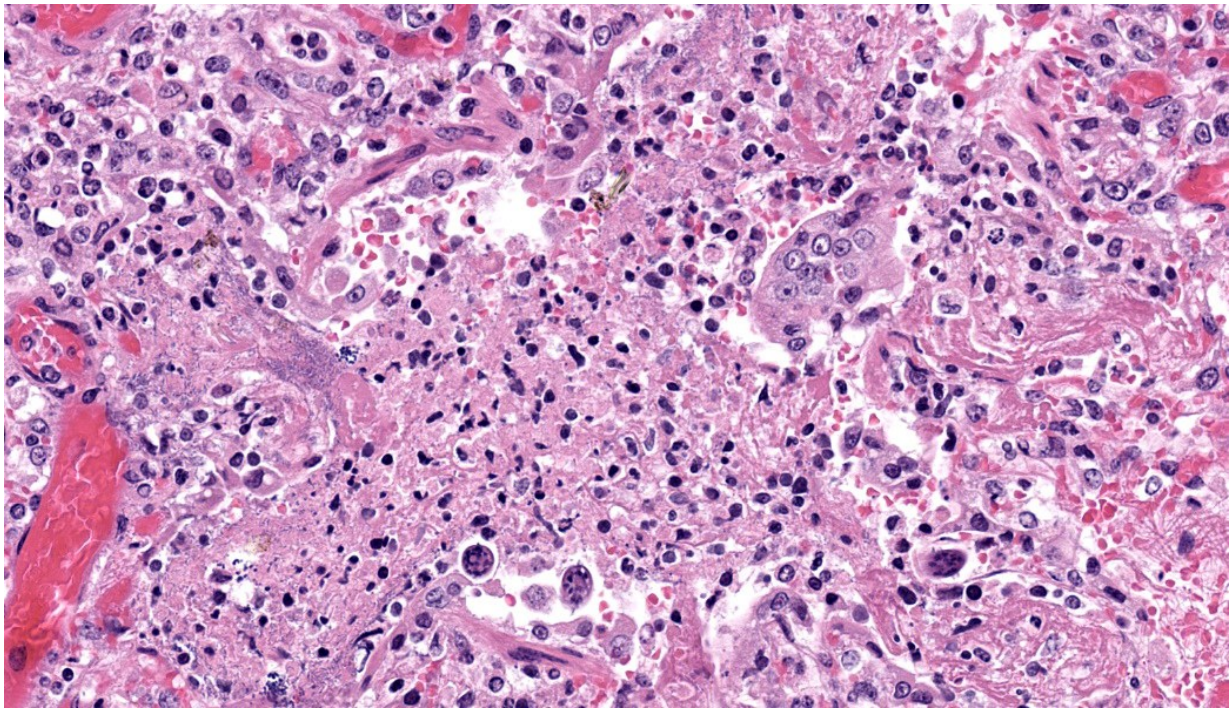

Figure 2-5. Lung, skunk: Within alveolar spaces there are bacterial colonies (left), multinucleated viral syncytia with intracytoplasmic viral inclusions (center right), and cross sections of larval ascarids with lateral alae. (HE, 701X)

microglia are thought to lead to oligodendrocyte dysfunction. However, other studies have demonstrated axonopath prior to demyelination.[12] Whether axonopathy is due primarily to neuronal infection or to bystander damage from infected astrocytes and microglia is uncertain. In patients that survive distemper virus infection, with or without associated neural signs, a replication-deficient form of the virus may persist in the brain and can re-emerge years later to cause neural signs in a condition termed "Old Dog Encephalitis".[3]

Suspicion for canine distemper virus infection is based on noting clinical signs in a susceptible animal. Antemortem testing includes serologic assays and PCR, and observation of distemper inclusions in circulating erythrocytes. Common findings on histology of tissues collected post-mortem are atrophy of lymph nodes, splenic white pulp, and other lymphoid organs; and during the systemic phase of disease, secondary bacterial infection may be present in the lungs and gastrointestinal tract. Lesions in the brain are usually leukoencephalomalacia with marked spongiosis. Mononuclear infiltrate is variable; there may be digestion chambers and large numbers of gitter cells. Caracteristic eosinophilic cytoplasmic viral inclusions can be found in lungs, brain, adrenal gland, gastric mucosa, and urinary bladder to varying degrees in any infected carnivore.[4] Nuclear inclusions are more common in neurons. If inclusions are not obvious, immunohistochemistry for the virus is elucidative.[3]

At necropsy, this skunk had severe cranioventral pneumonia. Lung submitted for aerobic culture grew a Pseudomonas; this bacterium may have inhibited growth of other organisms seen histologically. Bacterial infection was secondary to severe canine distemper virus infection. Inclusions are readi-

ly apparent in the lung, but were confirmed with immunohistochemistry. The skunk tested negative for rabies on DFA, and distemper inclusions were absent from the brain: as the skunk was still in the systemic phase of disease, intracranial infection may have been yet to be established. Regional infection of the lung by larval nematodes was an incidental finding; these may be *Filaroides milksi* or *Crenosoma mephiditis*.

Contributing Institution:

University of Connecticut Department of Pathobiology and Veterinary Science
http://www.patho.uconn.edu/

JPC Morphologic Diagnosis:

Lung: Pneumonia, bronchointerstitial, necrotizing and neutrophilic, subacute, diffuse, marked, with bronchiolar epithelial hyperplasia, viral syncytia, intraepithelial and intrahistiocytic intracytoplasmic and intranuclear viral inclusions, larval nematodes, and mixed bacteria.

JPC Comment:

What an excellent write-up by this contributor! Dr. Holder set the stage for this case with a quick skunk taxonomy review. Their scientific name, *Mephitis mephitis*, basically translates to "stinky stinky." As if that wasn't enough, their family name, Mephitidae, also means "stinky." Taxonomists really wanted to make sure no one missed the point there. With that poignantly olfactory context established, discussion advanced.

The lung sections showcased classic morbillivirus pathology, including syncytia in both epithelial cells and macrophages. However, because this skunk also had a secondary bacterial pneumonia, participants found themselves squinting at multinucleated cells wondering, "Is this a viral syncytial cell or just an enthusiastic giant cell macrophage?" Dr. Holder pointed out that using viral inclusions when visible within multinucleated cells can help tip the pathologist one way or the other, but she encouraged participants to accept that, without IHCs, not every multinucleated Joe on a slide is going to confess to its villain origin story.

One of the most interesting features in this case was the prominence of pulmonary megakaryocytes, which appear as large, basophilic, "ink blot" cells lounging around in the septal capillaries like they own the place. One participant pointed out that the lungs have their own megakaryocytes separate from those in the bone marrow and are a major site of platelet production in many mammalian species. Pulmonary megakaryocytes have important immune functions, as well. In humans, pulmonary megakaryocytes can become significantly more noticeable in severe disease states, and, in SARS-CoV-2 infections, they're considered a poor prognostic indicator.[15]

Regarding the bacterial infection that set up shop after morbillivirus did its damage and immunosuppressed this skunk, there were two distinct bacterial morphologies within areas of necrotic airways. Because tissue preservation was good in this case, these organisms were interpreted as true pathogens rather than postmortem freeloaders.

The group briefly discussed the nematodes present in the lung. Some larvae had lateral alae, prompting speculation *about Baylisascaris columnaris*, but the overall appearance favored metastrongyles as discussed by the contributor. Dr. Holder summed it up with characteristic flair by proclaiming, "A wild animal without parasites is a stadium with-

out fans."

Dr. Holder shared that she is convinced if we ever get a zombie apocalypse, it's going to be due to a morbillivirus. She wrapped up this case discussion with morbillivirus immunopathology, including lymphotropism, immunosuppression, and "immune amnesia." Morbilliviruses target lymphocytes via CD150 (SLAM). When a dendritic cell gets infected and traffics to regional lymph nodes, it can transmit virus to memory T cells, which are subsequently destroyed. Memory B cells are also depleted, and morbilliviruses can wipe out up to 70% of preexisting immune memory cells.[10] The result is a long-lasting vulnerability to other infections and reduced vaccine effectiveness.[10] Bummer

References:

1. Appel MJ, Yates RA, Foley GL, Bernstein JJ, Santinelli S, Spielman LH, Miller LD, Arp LH, Anderson M, Barr M, Pearce-Kelling S, Summers BA. Canine distemper virus epizootic in lions, tigers, and leopards in North America. *J. Vet. Diagn. Invest.* 1994; 6(3): 277–288
2. Beineke, A, Puff, C, Seehuesen, F, Baumgärtner. Pathogenesis and immunopathology of systemic and nervous canine distemper. *Vet Immunol Immunopathol.* 2009; 127(1-2): 1-18.
3. Greene, CE and Appel, MJ. Infectious Diseases of the Dog and Cat. 3rd Ed. Philadelphia, PA: Elsevier; 2006: 25-4
4. Greene, RG. A comparative study of distemper inclusions. *Am J Epidemiol.* 1939; 2: 73-87
5. Habermann, RT, Herman, CM, Williams Jr., FP. Distemper in raccoons and foxes suspected of having rabies. *JAVMA*. 1958; 132(1): 31-35.
6. Iwatsuki, K, Okita, M, Ochikubo, F, Gemma, T, Shin, YS, Miyashita, N, Mikami, T, Kai, C. Immunohistochemical analysis of the lymphoid organs of dogs naturally infected with canine distemper virus. *J. Comp. Pathol*. 1995; 113(2): 185-190
7. Kennedy, S, Kuiken, T, Jepson, PD, Deaville, R, Forsyth, M, Barrett, T, van de Bildt, MWG, Osterhaus, ADME, Eybatov, T, Duck, C, Kydyrmanov, A, Mitrofanov, I, Wilson, S. Mass die-off of Caspian seals caused by canine distemper virus. *Emerg. Infect. Dis*. 2000; 6(6): 637-639.
8. Kilham, L, Habermann, RT, Herman, CM. Jaundice and bilirubinemia as manifestation of canine distemper in raccoons and ferrets. *Am J Vet Res*. 1956; 17(62): 144-148.
9. Lemp, C, Spitzbarth, I, Puff, C, Cana, A, Kegler, K, Techangamsuwan, S, Baumgärtner, W, Seehusen F. New aspects of the pathogenesis of canine distemper leukoencephalitis. Virus. 2014; 6 (7): 2571-2601.
10. Morales GB, Muñoz MA. Immune amnesia induced by measles and its effects on concurrent epidemics. *J R Soc Interface*. 2021;18(179):20210153.
11. Roelke-Parker ME, Munson L, Packer C, Kock R, Cleaveland S, Carpenter M, O'Brien SJ, Pospischil A, Hofmann-Lehmann R, Lutz H, Mwamengele GL, Mgasa MN, Machange GA, Summers BA, Appel MJ. A canine distemper virus epidemic in Serengeti lions (*Panthera leo*). *Nature*. 1996; 379:441–445.
12. Seehusen, F, Baumgärtner, W. Axonal Pathology and Loss Precede Demyelination and Accompany Chronic Lesions in a Spontaneously Occurring Animal Model of Multiple Sclerosis *Brain Pathol.* 2010; 20(3): 551-559
13. Summers, BA, Greisen, HA, Appel, MJG. Early events in canine distemper encephalomyelitis. *Acta Neuropathol.*

1979; 46(1-2): 1-10.

14. Tatsuo, H, Ono, N, Yanagi, Y. Morbilliviruses use signaling lymphocyte activation molecules (CD150) as cellular receptors. *J. Virol*. 2001; 75(13): 5842-5850.
15. Vendevelde, M, Zurbriggen, A, Higgins, RJ, Palmer, D. Spread and distribution of viral antigen in nervous canine distemper. Acta Neuropathol. 1985; 67(3-4): 211-218.
16. Wenzlow, N, Plattet, P, Wittek, R, Zubriggen, A, Grone, A. Immunohistochemical demonstration of the putative canine distemper virus receptor CD150 in dogs with and without distemper. *Vet Pathol.* 2007; 44(6): 943-948.
17. Valdivia-Mazeyra MF, Salas C, Nieves-Alonso JM, et al. Increased number of pulmonary megakaryocytes in COVID-19 patients with diffuse alveolar damage: an autopsy study with clinical correlation and review of the literature. *Virchows Arch.* 2021;478(3):487-496
18. Woolf, A, Gremillion-Smith, C, Evans, RH. Evidence of canine distemper virus infection in skunks negative for antibody against rabies virus. *JAVMA.* 1986; 189 (9): 1086-1088.
19. Wünschmann, A, Kremmer, E, Baumgärtner, W. Phenotypical characterization of T and B cell areas in lymphoid tissues of dogs with spontaneous distemper. *Vet Immunol Immunopathol*. 2000; 73(1): 83-98.
20. Yadugiri, VT. Rinderpest: The fall of a virus. *Curr Sci.* 2011; 101(8): 990-993.

Case III:

Signalment:

Adult, female, Atlantic stingray, *Hypanus sabinus*

History:

This aquarium-housed Atlantic stingray initially presented to veterinary staff for a single, nodular mass on the ventral aspect of the left pectoral fin. Within one week, a second mass was noted. Excisional biopsy was elected and, at the time of surgery, multiple raised, hyperpigmented masses were found along the ventral surfaces of both pectoral fins. White purulent material was expressed from an excised nodule. Aerobic bacterial culture of the material yielded *Aeromonas* and *Staphylococcus spp*; however, no infectious agents were identified on cytology or histology. The animal was euthanized 13 months later due to a non-healing wound on the ventral pectoral girdle and progression of the nodular skin lesions along the pectoral fins.

Gross Pathology:

At necropsy, there were numerous (>50) firm-to-hard, well-demarcated, pale tan nodules on the ventral aspects of the pectoral and anal fins, ranging from 1-10 mm in diameter. On cut section, the nodules exuded thick, pale tan fluid. Other gross findings included a roughly 3 cm diameter cutaneous ulcer on the ventral the pectoral girdle, transudative coelomic effusion (15 ml), and multiple, 1-3 mm, firm, light tan nodules within the gill arches and along the ventral aspect of the spinal column. The liver was diffusely dark brown in color and sections sank in formalin (consistent with depleted hepatic lipid stores).

Laboratory Results:

Cytology: Unstained smears of fluid collected from the skin nodules showed numerous, variably-sized, round, birefringent crystals. No infectious organisms were identified on Diff-Quik stained slides.

Microscopic Description:

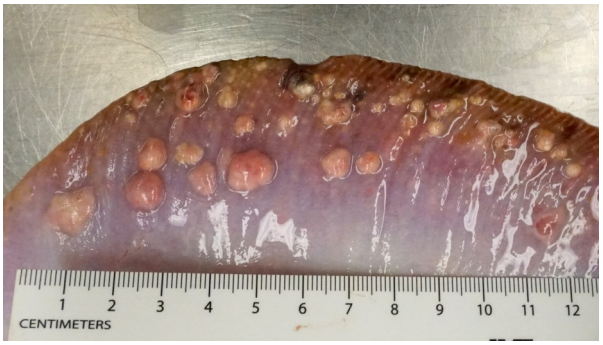

Figure 3-1. Pectoral fin, Atlantic stingray: There are numerous hard, well-demarcated, pale tan nodules on the ventral aspects of the pectoral and anal fins, ranging from 1-10 mm in diameter. (*Photo courtesy of:* Johns Hopkins University, School of Medicine Department of Molecular and Comparative Pathobiology, http://mcp.bs.jhmi.edu/)

Two, full-thickness sections of pectoral fin including skin, skeletal muscle, and radial cartilage: Markedly expanding the hypodermis are multiple, variably-sized (up to 7mm diameter) nodules comprising aggregates of amorphous to finely granular, lightly to darkly-basophilic mineralized material surrounded by fibroblasts and narrow zones of dense, fibrous collagen. Both the mineralized deposits and surrounding fibrous tissue are infiltrated by variable numbers of inflammatory cells including macrophages, lymphocytes, and eosinophilic granulocytes. Occasionally, larger nodules extend into and disrupt underlying skeletal muscle and radial cartilage. There is also multifocal mineralization of the radial cartilage without associated inflammation or deformation. In the epidermis overlying the nodules there is moderate intra- and extracellular edema. Multifocal separation and loss of the epidermis may be artefactual given the lack of associated hemorrhage and inflammation.

Contributor Morphologic Diagnosis:

Skin and skeletal muscle (pectoral fin): mineralization, chronic, multifocal to coalescing, severe with fibrosis, lymphohistiocytic and granulocytic inflammation

Contributor Comment:

Gross, cytologic, and histopathologic findings in this Atlantic stingray were consistent with widespread soft tissue mineralization. In addition to the skin, nodular foci of mineralization with associated chronic inflammation and fibrosis were found within connective tissue of the gill arches and surrounding to the vertebrae. Mild, multifocal mineralization was also evident in the kidneys, liver, and choroid plexus.

Soft tissue mineralization has been reported in multiple elasmobranch species including cownose rays, a bowmouth ray, a coral catshark, and a swell shark.[3,8] The diagnostic veterinary pathology service at Johns Hopkins has identified similar, but less severe, lesions in two other Atlantic stingrays from the same collection. Clinically, rays often present with firm, tan skin nodules lesions along the pectoral fins, tail, dorsal midline, and ventrum.[8] The condition is progressive and can affect multiple internal organs in-

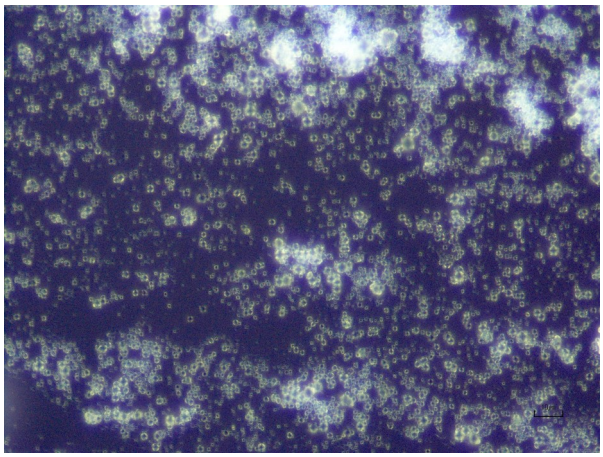

Figure 3-2. Pectoral fin, Atlantic stingray: Unstained smears of fluid collected from the skin nodules demonstrate numerous, variably sized, round, birefringent crystals. (*Photo courtesy of:* Johns Hopkins University, School of Medicine Department of Molecular and Comparative Pathobiology, http://mcp.bs.jhmi.edu/)

Figure 3-3. Pectoral fin, Atlantic stingray: Expanding the hypodermis, there are numerous areas of coalescing foci of mineralization. (HE, 10X)

cluding heart, vessels, kidneys, smooth muscle of the gills, intestines, and reproductive organs. Clinical signs include weight loss and death, likely as a result of the changes in the gills and cardiovascular system.

The pathogenesis of soft tissue mineralization in elasmobranchs is poorly understood. Gross and histomorphologic features of the nodular skin lesions closely resemble calcinosis circumscripta, which, in mammals, most commonly occurs over bony prominences and is thought to represent dystrophic mineralization related to previous trauma.[5] However, involvement of internal organs in elasmobranchs is more suggestive of metastatic mineralization secondary to calcium/ phosphorus imbalance. Inappropriate calcium supplementation, either in the water or diet, and underlying renal disease have been suggested as potential contributors.[8] In the present case, there were histologic changes indicative of chronic kidney disease including tubular atrophy and loss, glomerulosclerosis, and interstitial fibrosis.

Though skeletal anatomy and function vary greatly among elasmobranch species, the endoskeleton generally consists of chondrocytes within an uncalcified extracellular matrix, surrounded by a fibrous perichondrium. Within the axial and appendicular skeleton, mineralized units (called "tesserae") form between the cartilage center and the outer perichondrium.[1,2] In this stingray, the areas of mineralization within the cartilaginous radials of the pectoral fin (without associated deformation or inflammation) may be a variation of expected mineralization for the species.

Contributing Institution:

Johns Hopkins University, School of Medicine
Department of Molecular and Comparative Pathobiology
Broadway Research Building, #811
733 N. Broadway
Baltimore, MD 21205
Phone: 443-287-2953
Fax: 443-287-5628
http://mcp.bs.jhmi.edu/

JPC Morphologic Diagnosis:

Fin, hypodermis and joint space: Mineralization, chronic, multifocal to coalescing,

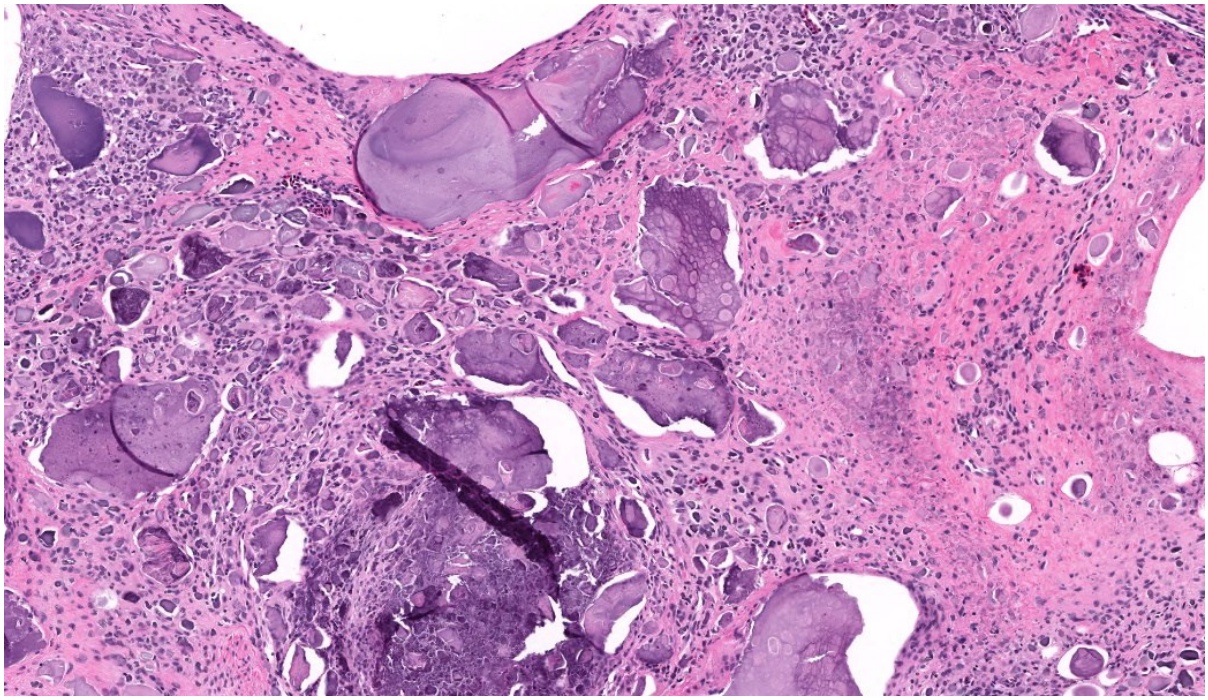

Figure 3-4. Pectoral fin, Atlantic stingray: Foci of mineral are admixed and surrounded with moderate numbers of macrophages, and fewer granulocytes and lymphocytes on a dense fibrous stroma. (HE, 151X)

marked, with granulomatous inflammation.

JPC Comment:

This case took participants into the world of elasmobranch pathology. Dr. Holder emphasized that the primary process in this lesion was mineralization; not dermatitis, inflammation, or infection - just good, old-fashioned calcium being in places where calcium should not be.

Participants noted mineral deposition not only in the soft tissues, but also within joint spaces. Rays normally possess mineralized skeletal elements called tesserae, which may extend to articular surfaces, but the intra-articular mineral in this case was prominent enough to catch the eyes of participants. However, as mentioned by the contributor, this could be a normal variant. The literature lacks information on what degenerative tesserae look like because elasmobranch skeletal remodeling is essentially thought to be nonexistent - just tesserae…forever.

The discussion then shifted to the relevance of the stingray's liver, which was grossly described as dark brown and sank in formalin. Elasmobranchs rely on hepatic lipid stores for buoyancy and a healthy liver should float.[7] A sinking liver indicates profound negative energy balance, and underscores how sick this ray was.

Tumoral calcinosis is a well-recognized but poorly understood condition in elasmobranchs. Two major forms occur - hydroxyapatite deposition disease (HADD) and calcium pyrophosphate deposition disease (CPDD).[4] HADD is extremely common in reptiles, so much so that this is almost exclusively the form they get. HADD in reptiles is often accompanied by urate deposition. Crystals are granular, rounded, and have

Figure 3-5. Pectoral fin, Atlantic stingray: There is mineralization of the cartilage of the fin as well. (HE, 151X)

minimal, soft birefringence, as in this case.[4] HADD is also associated with osteoarthritis in humans.[4] CPDD, on the other hand, is most common in mammals and birds. Crystals are rhomboid to spicular with bright blue to yellow birefringence.

As a final fun fact, Dr. Holder noted that elasmobranchs can be aged (by people who have this skill) by counting the layers of tesserae in their vertebrae.[5] This sounds like a sort of elasmobranch tree ring system, but sharks have the audacity to do it in cartilage instead of wood.

References:

1. Dean MN, Ekstroma L, Monsonego-Ornan E, et al. Mineral homeostasis and regulation of mineralization processes in the skeletons of sharks, rays and relative (Elasmobranchii). *Seminars in Cell & Develop Biology*. 2015; 46: 51-67.
2. Dean MN, Summers AP. Mineralized cartilage in the skeleton of chondrichthyan fishes. *Zoology*. 2006; 109: 164-168.
3. Garner, M. M. A retrospective study of disease in elasmobranchs. *Veterinary Pathology.* 2013; 50(3):377–389.
4. Hegazi T. Hydroxyapatite Deposition Disease: A Comprehensive Review of Pathogenesis, Radiological Findings, and Treatment Strategies. Diagnostics (Basel). 2023;13(16):2678.
5. Mauldin EA, Peters-Kennedy J. Integumentary System. In: Maxie G, ed. *Jubb, Kennedy, and Palmer's Pathology of Domestic Animals*. 6th ed (Vol 1). St. Louis, MO. Elsevier; 2016: 509-736
6. Seidel R, Lyons K, Blumer M, et al. Ultrastructural and developmental features of the tessellated endoskeleton of elasmobranchs (sharks and rays). J Anat. 2016;229(5):681-702.
7. Speers-Roesch B, Treberg JR. The unusual energy metabolism of elasmobranch fishes. *Comp Biochem Physiol A Mol Integr Physiol*. 2010;155(4):417-434.
8. Stedman NL, Garner MM. Chondrichthyes. In: Terio, McAloose, and St. Jeger eds. Pathology of Wildlife and Zoo Animals. London, UK: Academic Press; 2018: 995-1010.

Case IV:

Signalment:

27 y.o female Philippine crocodile *(Crocodylis mindorensis)*

History:

Adult female Philippine crocodile presented with blepharospasm and palpebral edema of left eye. Physical exam with ultrasound revealed retrobulbar mass of soft tissue. Fine needle aspirate cytology report revealed mesenchymal cells assessed as potentially neoplastic. A prolonged course of meloxicam and long-acting antibiotic was initiated, but eye did not improve. Two weeks later, CT revealed mass invading posterior chamber *at* the eye as well as widespread pulmonary consolidation and fibrosis. Repeated ocular ultrasound confirmed invasion of posterior chamber. Later enucleation of eye with as much retrobulbar tissue as possible was

performed, and bulb and adnexa were submitted to pathology as a biopsy. The animal was found dead the morning after enucleation and was submitted to pathology for necropsy.

Gross Pathology:

The dorsomedial aspect of the globe is expanded by a rounded tan soft tissue mass that rises approximately 3 mm from the scleral surface and infiltrates through the fibrous tunic of the eye. Upon sectioning the eye, the entire posterior chamber is occupied by a multinodular tan soft tissue mass with multifocal hemorrhage. The mass anteriorly displaces the lens, and the anterior chamber is partially collapsed.

Philippine crocodile, left globe, bisected. The posterior chamber is filled by a multilobular white mass with multifocal hemorrhage.

Laboratory Results:

> Fungal 18S rRNA PCR sequencing identified *Purpureocil/ium lilacinum* in tracheal wash samples from this animal

Microscopic Description:

Left eye. Disrupting the fibrocartilaginous tunic of the eye, infiltrating and obliterating the choroid, anteriorly displacing the retina, and filling >80% of the posterior chamber is a multilobular mass of coalescing granulomas, necrotic and cellular debris, and hemorrhage. Granulomas are characterized by central cores of densely eosinophilic protein, necrotic debris, degranulated heterophils, and negative-staining hyphal filaments. These cores are surrounded by abundant multinucleated giant cells and epithelioid to foamy macrophages, many with large, clear vacuoles. Individual lobules are separated by variable amounts of fibrous tissue infiltrated by lymphocytes, plasma cells, and intact heterophils.

Fungal hyphae are nonpigmented, 2-4 um in diameter, parallel-walled, and septate, with dichotomous branching. Portions of the retina are adhered to the posterior surface of the ciliary body. The remaining retina is fragmented, vacuolated, and infiltrated by heterophils. Granulomas focally extend into anteriorly displace the ciliary body. The remaining vitreous humor is multifocally coagulated and contains heterophils, detached retinal pigmented epithelium and erythrocytes. The anterior surface of the lens capsule is multifocally adered by fibrin to pigmented epithelial cells consistent with those on the posterior surface of the iris and ciliary body, which also display accumulations of fibrin (posterior synechae). The iris is anteriorly displaced, the iridocorneal angle is collapsed, and the anterior chamber is reduced. The iris is infiltrated by low numbers of lymphocytes, macrophages and heterophils. The cornea has reduced stromal separation artifact (corneal edema).

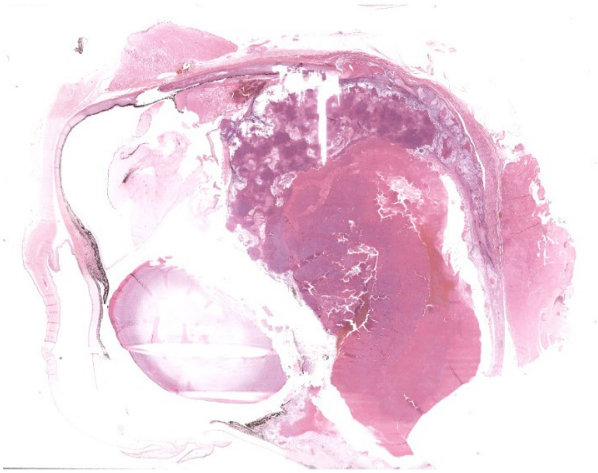

Figure 4-1. Eye, crocodile. The posterior uvea, from the caudal aspect of the ciliary body to the choroid is lined by numerous coalescing heterophilic granulomas and an heterophilic exudate fills the posterior chamber is filled with abundant brightly eosinophilic cellular debris. (HE, 9X).

Contributor's Morphologic Diagnosis: Left eye (OS): Panophthalmitis, granulomatous and heterophilic, severe, with abundant nonpigmented fungal hyphae.

Contributor's Comment:

The origin of the intra-ocular mycosis is presumed dissemination of fungi from a granulomatous pneumonia, which was found on necropsy the day following this enucleation. The pulmonary granulomas contained abundant morphologically identical fungal hyphae and widespread *Pseudomonas aeruginosa* colonies. Tracheal exudate cultured a fungus that was identified via 18S rRNA PCR as *Purpureocillium lilacinum* (formerly *Paecilomyces lilacinus).*

The ocular lesions in this case are not particular to a specific fungal organism. Indeed, ocular dissemination is a well-reported manifestation of systemic aspergillosis in German shepherd dogs. Anatomically, the retina of crocodilians is largely avascular, relying almost entirely on the richly vascular choroid layer just below.[7] The expansile granulomas visible in this case clearly show that they originated in this vascular layer, displacing the retina anteriorly and deforming and infiltrating the sclera.

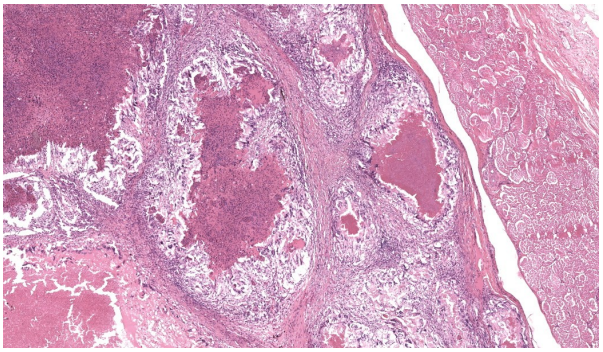

Figure 4-2. Eye, crocodile: Heterophilic granulomas contain a central area of degenerate heterophils surrounded by a layer of epithelioid and foreign body-type macrophages, in turn surrounded by concentric lamellae of fibrous connective tissue containing lymphocytes and plasma cells. (HE, 83X).

Hematogenous spread of fungal pathogens is a potential complication of any angioinvasive fungal infection, and in domestic animal veterinary medicine *Aspergillus, Fusarium,* and the Mucorales are often implicated.[7] In addition to saprophytic fungi such as *Aspergillus,* in reptiles, systemic mycoses are often caused by entomopathogenic fungi, such as *Purpurocilleum* or *Metarhizium.*[3,9] *P. lilacinum* is well reported as a cause of fatal systemic mycoses in turtles, crocodilians, and snakes.[3,6,8,9] Rapidly-growing opportunists such as *P. lilacinum* are a particular danger to reptiles under high stocking density, cold stress, or unsanitary environmental conditions.[8] In this case, *P. aeruginosa,* a bacterium fully capable of acting as a primary pathogen in an immunocompetent host, may have initiated the pneumonia and *P. lilacinum* was a secondary invader that subsequently seeded the eye. It is also plausible that there was an undetected stressor that resulted in *P. lilacinum* pneumonia with a secondary *Pseudomonas* co-infection.

This fungus is not solely a reptile pathogen. *P. lilacinum* has also been reported as a cause of fungal keratitis in humans, and general or local immunosuppression was a risk factor.[2] A recent paper from Louisiana identified 21 fungal pneumonia cases in wild Virginia opossums, a subset of which were successfully identified via fungal isolation and/or PCR as *P. lilacinum.*[5] The genus *Purpurocilleum* has recently been found to contain another species, *P. lavendulum,* closely related to *P. lilacinum,* which has been reported in fibrinous pneumonias of a green tree python and a panther chameleon.[10] *P. Javendulum* replicates more readily below 35°C than *P. macinum* and is thus of poten-

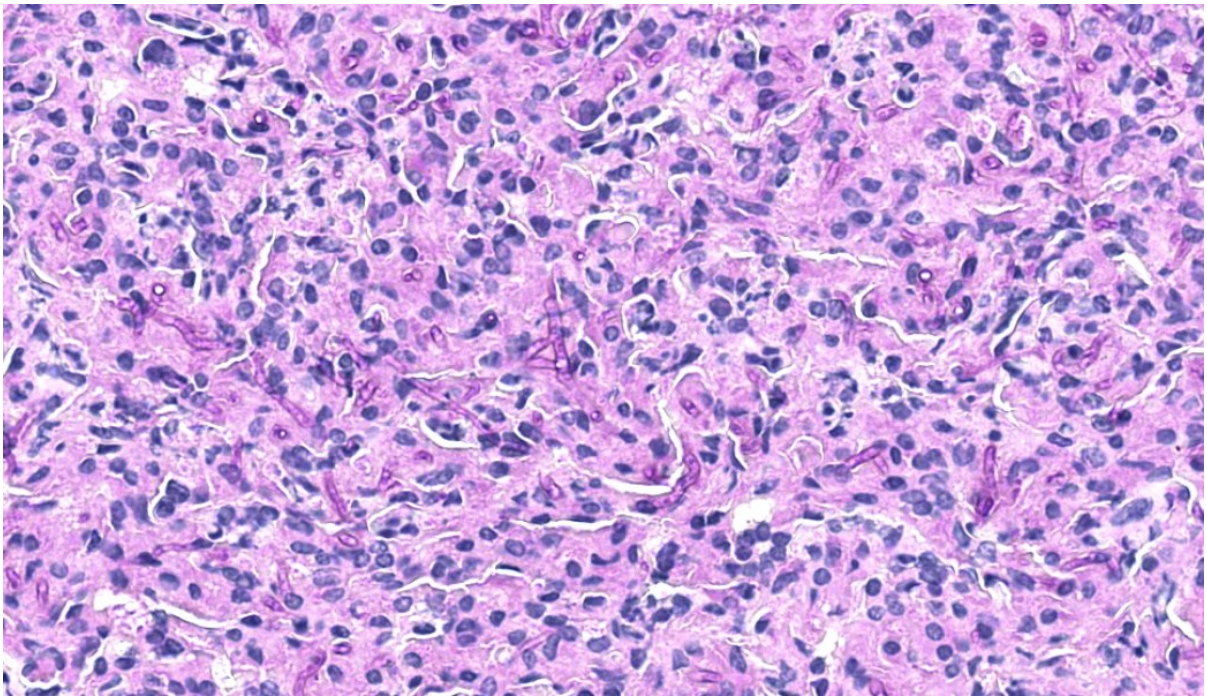

Figure 4-3. Eye, crocodile: Granulomas extend around to the posterior aspect of the degenerating ciliary body. (HE, 83X)

tial importance as a reptile pathogen though of less concern for mammals or birds.

Contributing Institution:

Smithsonian's National Zoo and Conservation Biology Institute
P.O. Box 37012, MRC 5501, Washington, DC 20013-7012

https://nationalzoo.si.edu/animals/veterinary-care

JPC Morphologic Diagnosis:

Globe: Panophthalmitis, heterophilic and granulomatous, chronic, diffuse, severe, with anterior and posterior synechiae, retinal detachment and degeneration, anterior lens luxation, and numerous fungal hyphae.

JPC Comment:

Dr. Holder opened the final case of the year by ranking crocodilians on the "Holder Scale of Spiciness." The Philippine crocodile, she explained, is "low spicy per unit mass", which translates to a contextually polite, manageable reptile compared to, say, the saltwater crocodile, which is "high spicy." The Cuban crocodile, however, she described as "the ultimate spicy." With longer legs set more underneath the body, Cuban crocs can gallop and (kind of) jump, and they do so with a raging bad attitude. With that energy established, the group turned to the eye.

One of the first questions raised during the discussion of this case was the increased cellularity of the lens. Participants wondered whether this represented a degenerative change; however, reptiles and birds possess an annular pad, which is a more densely cellular structure which supports visual accommodation.[4] It is not a degenerative change like one might see in other species, but rather is normal and a direct result of reptile evolution.

The cornea also caused some double takes. The eye had what appeared to be a "double cornea", but participants astutely presumed that the outer "cornea" was the nictitating membrane, which crocodilians use as both protection and as built-in "swim goggles."[4] This structure allows them to see underwater without risking their corneal integrity or visual acuity.[4]

Participants also noted lymphoid follicles in the conjunctiva. These were initially mistaken by some as small foci of lymphoplasmacytic inflammation, but crocodilians have normal conjunctival lymphoid tissue.[4] These follicles were a bit hyperplastic, however, in response to the raging fungal panophthalmitis. On H&E, the fungal hyphae stained negatively, appearing as faint, ghostly outlines that Dr. Holder described as "haunting the slide." A PAS stain brought them out into the light. This led to a broader discussion about fungal diagnostics and how temperature can profoundly affect fungal morphology.[9] For this reason, fungi may have different appearances in tissue between mammals and reptiles. And a reminder to all - appearance alone on histology should not be considered definitive for speciation[9] - accurate identification requires molecular testing, supported by morphology, for any fungus.

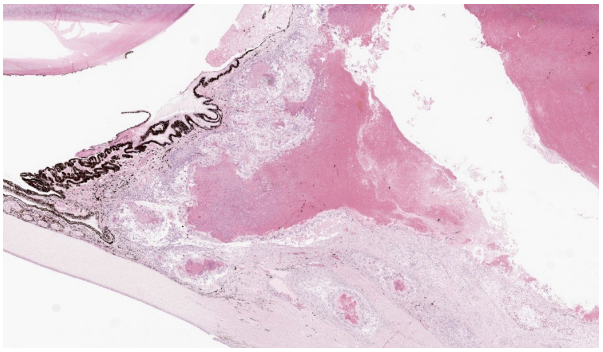

Figure 4-4. Eye, crocodile: Granulomas extend around to the posterior aspect of the degenerating ciliary body. (HE, 83X)

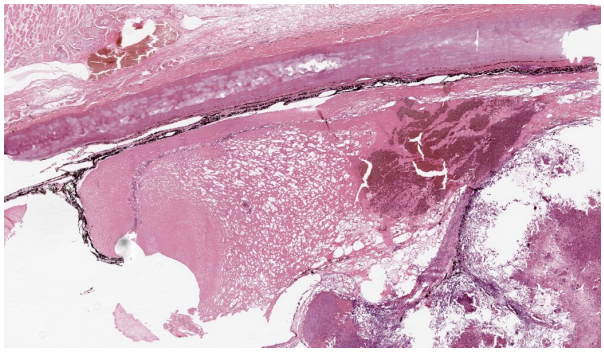

Figure 4-5. Eye, crocodile: The drainage angle is filled with hemorrhage and fibrin. (HE, 48X)

The culprit in this case, *Purpureocillium lilacinum*, is a saprophytic fungus that thrives in humid environments where meat is used as a food source. Basically, crocodile enclosures are its dream home. Fat from food creates a film on the water, which deposits on the floor of the tank and serves as an organic substrate for the fungus to grow.[7] *Purpureocillium lilacinum* gets its name from the formation of purple to rosy fungal mats, both in culture and in tissue, making it one of few fungi with built-in aesthetics.[1] Dr. Holder noted that *Purpureocillium spp* are also associated with pneumonia in opossums, whose lower body temperature makes them "step-reptiles" in terms of fungal susceptibility.[5] She also emphasized that stocking density plays a major role in *Purpureocillium* outbreaks, and crowded enclosures create ideal conditions for fungal spread.[10]

References:

1. Chen W, Hu Q. Secondary Metabolites of *Purpureocilliumlilacinum*. *Molecules*. 2021;27(1):18.
2. Chew R, Dorman A, Woods ML. *Purpureocillium lilacinum* keratitis: a case series and review of the literature. Canadian *Journal of Ophthalmology.* 2016;1;51(5):382-5.

3. Heard DJ, Cantor GH, Jacobson ER, Purich B, Ajello L, Padhye AA. Hyalohyphomycosis caused by *Paecilomyces lilacinus* in an Aldabra tortoise. *JAVMA*. 1986;189(9):1143-5.

4. Holmberg BJ. Ophthalmology of Exotic Pets. *Slatter's Fundamentals of Veterinary Ophthalmology*. 2008;427-441.

5. Falconnier N, Mitchell MA, et al. Pulmonary lesions in Virginia opossums (*Didelphis virginiana):* Characterizing fungal pneumonia associated with *Purpureocillium lilacinum*. *Veterinary Pathology*. 2025:03009858251338845.

6. Lafortune M, Wellehan JF, Terrell SP, Jacobson ER, Heard D, Kimbrough JW. Shell and systemic hyalohyphomycosis in Fly River turtles (*Carettochelys insculpta*) caused by *Paecilomyces lilacinus*. *Journal of Herpetological Medicine and Surgery*. 2005;15(2):15-9.

7. Martinez PS, Plummer CE. Ophthalmology of Crocodilia: Alligators, Crocodiles, Caimans, and Gharials. in: Montiani-Ferreira F. Wild and Exotic Animal Ophthalmology: Volume 1: Invertebrates, Fishes, Amphibians, Reptiles, and Birds. Cham: Springer International Publishing AG; 2022.

8. Meyer J, Loncaric I, Richter B, Spergser J. Fatal *Purpureocillium lilacinum* pneumonia in a green tree python. *JVDI*. 2018;30(2):305-9.

9. Pare JA, Conley KJ. Mycotic diseases of reptiles. In: Infectious diseases and pathology of reptiles. CRC Press; 2020

10. Schmidt V, Klasen L, Schneider J, Hubel J, Cramer K. Pulmonary fungal granulomas and fibrinous pneumonia caused by different hypocrealean fungi in reptiles. *Veterinary Microbiology*. 2018;1;225:58-63.